CHM 320: ADVANCED INORGANIC CHEMISTRY



staff
Kutztown University of Pennsylvania



CHM 320 Advanced Inorganic Chemistry textbook

This text is disseminated via the Open Education Resource (OER) LibreTexts Project (https://LibreTexts.org) and like the thousands of other texts available within this powerful platform, it is freely available for reading, printing, and "consuming."

The LibreTexts mission is to bring together students, faculty, and scholars in a collaborative effort to provide an accessible, and comprehensive platform that empowers our community to develop, curate, adapt, and adopt openly licensed resources and technologies; through these efforts we can reduce the financial burden borne from traditional educational resource costs, ensuring education is more accessible for students and communities worldwide.

Most, but not all, pages in the library have licenses that may allow individuals to make changes, save, and print this book. Carefully consult the applicable license(s) before pursuing such effects. Instructors can adopt existing LibreTexts texts or Remix them to quickly build course-specific resources to meet the needs of their students. Unlike traditional textbooks, LibreTexts' web based origins allow powerful integration of advanced features and new technologies to support learning.



LibreTexts is the adaptable, user-friendly non-profit open education resource platform that educators trust for creating, customizing, and sharing accessible, interactive textbooks, adaptive homework, and ancillary materials. We collaborate with individuals and organizations to champion open education initiatives, support institutional publishing programs, drive curriculum development projects, and more.

The LibreTexts libraries are Powered by NICE CXone Expert and were supported by the Department of Education Open Textbook Pilot Project, the California Education Learning Lab, the UC Davis Office of the Provost, the UC Davis Library, the California State University Affordable Learning Solutions Program, and Merlot. This material is based upon work supported by the National Science Foundation under Grant No. 1246120, 1525057, and 1413739.

Any opinions, findings, and conclusions or recommendations expressed in this material are those of the author(s) and do not necessarily reflect the views of the National Science Foundation nor the US Department of Education.

Have questions or comments? For information about adoptions or adaptions contact info@LibreTexts.org or visit our main website at https://LibreTexts.org.

The LibreTexts name, logo, and book covers are trademarked by LibreTexts, Inc. (a 501(c)(3) not-for-profit organization) and protected against unauthorized use.

This text was compiled on 10/23/2026

TABLE OF CONTENTS

Licensing

1: Introduction to Inorganic Chemistry

1.1: Inorganic vs Organic Chemistry

1.2: History of Inorganic Chemistry

1.3: Perspectives

2: Atomic Structure

2.1: Historical Development of Atomic Theory

2.1.1: The Periodic Table

2.1.2: Discovery of Subatomic Particles and the Bohr Atom

2.2: The Schrödinger equation, particle in a box, and atomic wavefunctions

2.2.1: Particle in a Box

2.2.2: Quantum Numbers and Atomic Wave Functions

2.2.3: Aufbau Principle

2.2.4: Shielding

2.3: Periodic Properties of Atoms

2.3.1: Ionization energy

2.3.2: Electron Affinity

2.3.3: Covalent and Ionic Radii

2.4: Problems

3: Simple Bonding Theory

3.1: Lewis Electron-Dot Diagrams

3.1.1: Formal Charge

3.1.2: Resonance

3.1.3: Breaking the octet rule with higher electron counts (hypervalent atoms)

3.1.4: Lewis fails to predict unusual cases- Boron and Beryllium

3.2: Valence Shell Electron-Pair Repulsion

3.2.1: Lone Pair Repulsion

3.2.2: Multiple Bonds

3.2.3: Electronegativity and Atomic Size Effects

3.2.4: Ligand Close Packing

3.3: Molecular Polarity

3.4: Hydrogen Bonding

4: Molecular Orbitals

4.1: Formation of Molecular Orbitals from Atomic Orbitals

4.1.1: Molecular Orbitals from s Orbitals

4.1.2: Molecular Orbitals from p Orbitals
4.1.3: Molecular orbitals from d orbitals
4.1.4: Nonbonding Orbitals and Other Factors
4.2: Homonuclear Diatomic Molecules
4.2.1: Molecular Orbitals
4.2.2: Orbital Mixing
4.2.3: Diatomic Molecules of the First and Second Periods
4.2.4: Photoelectron Spectroscopy
4.3: Heteronuclear Diatomic Molecules
4.3.1: Polar bonds
4.3.2: Ionic Compounds and Molecular Orbitals
4.P: Problems
5: Coordination Chemistry I - Structure and Isomers
5.1: History
5.2: Nomenclature and Ligands
5.3: Isomerism
5.4: Coordination Numbers and Structures
5.5: Coordination Frameworks
5.6: Hard and Soft Acids and Bases
5.6.1: Quantitative Measures of Hardness, Softness, and Acid-Base Interactions from a Hard Soft Acid-Base Principle perspective involve orbital energies and or apportioning acid-base bonding in terms of electrostatic and covalent factors
5.6.2: Hard-Hard and Soft-Soft preferences may be explained and quantified in terms of electrostatic and covalent and electronic stabilization on the stability of Lewis acid-base adducts
6: Symmetry and Group Theory
6.1: Symmetry Elements and Operations
6.2: Successive Operations
6.3: Significance of Recognizing Symmetry Elements
6.4: Point Groups
6.4.1: Groups of Low and High Symmetry
6.4.2: Other Groups
6.5: Character Tables - An Introduction
6.6: Character Tables
6.7: Properties and Representations of Groups
6.7.1: Matrices
6.7.2: Representations of Point Groups
6.8: Examples and Applications of Symmetry
6.8.1: Chirality
6.8.2: Molecular Vibrations
6.8A: Vibrational Spectroscopy

6.8C: Vibrational Spectroscopy of Linear and Bent triatomic Molecules

6.9: Larger (Polyatomic) Molecules

6.9.1: CO_2 (Revisted with Projection Operators)

6.9.2: BF_3

6.9.3: Bifluoride anion

6.9.4: Carbon Dioxide

6.9.5: H_2O

6.9.6: NH_3

6.10: MO Theory Applied to Polyatomic Molecules BH_3, NH_3, and CH_4

6.10A: BH_3

6.10B: NH_3

6.10C: CH_4

6.10D: A Comparison of MO and VB Bonding Models

6.P: Problems (under construction)

7: Ligand Field Theory (LFT) and Crystal Field Theory (CFT) of Octahedral Complexes

7.1: Introduction to Crystal Field Theory (Octahdral complexes)

7.2: Introduction to Ligand Field Theory (Octahedral complexes)

7.3: Ligand Field Stabilisation Energy (LFSE)

7.4: The Effect of the Metal Ion on d-Orbital Splitting

7.5: The Effect of Ligands and the Spectrochemical Series

8: LFT for Other Geometries / Spectroscopic Properties

8.1: The d-orbital splitting patterns for non-octahedral complexes

8.1.1: Tetrahedral and Octahedral Geometries

8.1.2: The Jahn-Teller Effect

8.1.3: Summary of the three most common geometries

8.2: Absorption Spectra and Magnetic Properties

8.2.1: Colors of Coordination Compounds (Electronic Absorption Spectra)

8.2.2: Predicting UV-visible Absorption

9: Spectroscopic and Magnetic Properties

9.1: Quantum Numbers of Multielectron Atoms

9.2: Electronic Spectra of Coordination Compounds

9.3: Tanabe-Sugano Diagrams

9.4: Magnetic Properties of Coordination Compounds

9.5: Magnetic Properties of Materials

10: Thermodynamics, Trends in Metal Complex Stability

10.1: Introduction to Substitution Reactions

10.2: Metal-Ligand Association Constants

10.3: Trends in M-L stability (Thermodynamics)

11: Kinetics, Trends in Kinetic Lability

11.1: Trends in Kinetic Lability

11.2: The Kinetic Chelate Effect

11.3: The Eigen-Wilkins Mechanism

11.4: Mechanisms of Substitution

11.5: The trans-effect

11.6: Redox Mechanisms

11.6.1: Outer Sphere Electron Transfer

11.6.2: Inner Sphere Electron Transfer

12: Structures and Energetics of Metallic and Ionic solids

12.1: Alloys and Intermetallic Compounds

12.1A: Substitutional Alloys

12.1B: Interstitial Alloys

12.1C: Intermetallic Compounds

12.2: Bonding in Metals and Semicondoctors

12.2A: Electrical Conductivity and Resistivity

12.2B: Band Theory of Metals and Insulators

12.2C: The Fermi Level

12.2D: Band Theory of Semiconductors

12.3: Ionic Lattices

12.3A: Structure - Rock Salt (NaCl)

12.3B: Structure - Caesium Chloride (CsCl)

12.3C: Structure - Fluorite (CaF_2)

12.3D: Structure - Antifluorite

12.3E: Structure - Zinc Blende (ZnS)

12.3F: Structure - β-Cristobalite (SiO_2)

12.3H: Structure - Rutile (TiO_2)

12.3I: Structure - Layers (CdI_2 and $CdCl_2$)

12.3J: Structure - Perovskite ($CaTiO_3$)

12.4: Lattice Energy - The Born-Haber Cycle

12.5: Defects in Solid State Lattices

12.5.E: Defects in Solid State Lattices (Exercises)

12.5A: Schottky Defect

12.5B: Frenkel Defect

12.5C: Experimental Observations of Schottky and Frenkel Defects

12.5D: Non-Stoichiometric Compounds

12.5E: Color Centers (F-Centers)

12.5F: Thermodynamic Effects of Crystal Defects

12.6: Introduction

12.7: Packing of Spheres
12.7A: Cubic and Hexagonal Closed Packing
12.7B: The Unit Cell of HPC and CCP
1.1: The Unit Cell
12.7C: Interstitial Holes in HCP and CCP
12.7D: Non-closed Packing- Simple Cubic and Body Centered Cubic
12.8: The Packing of Spheres Model Applied to the Structures of Elements
12.8A: Group 18 Elements in the Solid State
12.8B: H_2 and F_2 Solids
12.8C: Solid Metallic Elements
12.9: Polymorphism in Metals
12.9A: Polymorphism - Phase Changes in the Solid State
12.9B: Phase Diagrams
12.10: Metallic Radii
12.11: Melting Points and Standard Enthalpies of Atomization of Metals
12.12: Size of Ions
12.12A: Ionic Radii
12.12B: Periodic Trends in Ionic Radii
12.13: Crystal Structure of Semiconductors
13: Introduction to Organometallic Complexes
13.1: What is Organometallic Chemistry?
13.2: Historical Background
13.3: The 18 Electron Rule
13.4: Reactions Involving Gain or Loss of Ligands
13.5: Organometallic Catalysts
14: Experimental Techniques
14.1: Introduction
14.2: Separation and Purification Techniques
14.2A: Gas Chromatography (GC)
14.2B: Liquid Chromatography (LC)
14.2C: High-Performance Liquid Chromatography (HPLC)
14.2D: Recrystallization
14.3: Elemental Analysis
14.3A: CHN Analysis by Combustion
14.3B: Atomic Absorption Spectroscopy (AAS)
14.4: Computational Analysis - Thermogravimetry (TG)
14.5: Mass Spectrometry
14.5A: Electron Ionization (EI)

14.5B: Fast Atom Bombardment (FAB)
14.5C: Matrix-Assisted Laser Desorption Ionization Time-of-Flight (MALDI-TOF)
14.5D: Electrospray Ionization (ESI)

14.6: Infrared and Raman Spectroscopies
14.6A: Energies and Wavenumbers of Molecular Vibrations
14.6B: The Fourier Transform Infrared (FT-IR) Spectrometer and Sample Preparation
14.6C: Diagnostic Absorptions
14.6D: Deuterium/Hydrogen Exchange
14.6E: Raman Spectroscopy

14.7: Electronic Spectroscopy
14.7A: UV-VIS Absorption Spectroscopy
14.7B: Types of Absorption
14.7C: Absorbance and the Beer-Lambert Law
14.7D: Emission Spectroscopy

14.8: Nuclear Magnetic Resonance (NMR) Spectroscopy
14.8A: NMR Active Nuclei and Isotope Abundance
14.8B: Which Nuclei are Suitable for NMR Spectroscopic Studies
14.8C: Resonance Frequencies and Chemical Shifts
14.8D: Chemical Shift Ranges
14.8E: Solvents for Solution Studies
14.8F: Integration of Signals and Signal Broadening
14.8G: Homonuclear spin-spin coupling - $^{1}H - ^{1}H$
14.8H: Heteronuclear spin-spin coupling - $^{13}C - ^{1}H$
14.8I: Case Studies
14.8J: Stereochemically Non-Rigid Species
14.8K: Exchange Processes in Solution

14.9: Electron Paramagnetic Resonance (EPR) Spectroscopy
14.9A: What is EPR Spectroscopy?
14.9B: The Zeeman Electronic Effect
14.9C: EPR Spectra

14.10: Mossbauer Spectroscopy
14.10A: The Technique of Mossbauer Spectroscopy
14.10B: What Can Isomer Shift Data Tell Us?

14.11: Structure Determination - Diffraction Methods
14.11A: X-Ray Diffraction (XRD)
14.11B: Single Crystal X-Ray Diffraction
14.11C: Powder X-Ray Diffraction
14.11D: Single Crystal Neutron Diffraction
14.11E: Electron Diffraction

14.11F: Low-Energy Electron Diffraction (LEED)
14.11G: Structural Databases
14.12: Photoelectron Spectroscopy (PES, UPS, XPS, ESCA)
14.13: Computational Methods
14.13A: Hartree-Fock Theory
14.13B: Density Functional Theory
14.13C: Hückel MO Theory
14.13D: Molecular Mechanisms (MM)
14.14: Magnetism
14.14.1: example magnetic moment data and their interpretation
14.14.2: Magnetic Moments
14.14.3: Magnetic Moments 1
14.14.4: Magnetic Susceptibility Measurements
14.14.5: Magnetism
Tanabe Sugano Diagrams
Index
Glossary
Detailed Licensing

This page titled CHM 320: Advanced Inorganic Chemistry is shared under a license and was authored, remixed, and/or curated by LibreTexts.

Licensing

A detailed breakdown of this resource's licensing can be found in ***Back Matter/Detailed Licensing***.

This page titled Licensing is shared under a license and was authored, remixed, and/or curated by LibreTexts.

1: INTRODUCTION TO INORGANIC CHEMISTRY

This chapter introduces some history and context about the field of Inorganic Chemistry.

1.1: Inorganic vs Organic Chemistry

1.2: History of Inorganic Chemistry

1.3: Perspectives

This page titled 1: Introduction to Inorganic Chemistry is shared under a license and was authored, remixed, and/or curated by LibreTexts.

- 1: Introduction to Inorganic Chemistry by Kathryn Haas is licensed CC BY-NC-SA 4.0.

1.1: Inorganic vs Organic Chemistry

The division between the fields of Inorganic and Organic chemistry has become blurred. For example, let's look at one of the major classes of catalysts used for organic synthesis reactions: organometalic catalysts (Figure 1.1.1). Organometallic catalysts like these, and all organometallic compounds, contain metals that are bonded to carbon or carbon-containing molecules. So, are they "inorganic" because they contain metals, or "organic" because they contain carbon? These illustrate that clear divisions between organic and inorganic chemistry do not exist. Further, metal ions are common in biology and so the idea that metals are "inorganic" and thus classed as "non-living or non-biological" is incorrect. A canonical example is the organometallic catalyst adenosylcobalbumin, which is an important biological cofactor containing a cobalt (Co) ion (Figure 1.1.1, right) and a cobalt-carbon bond.

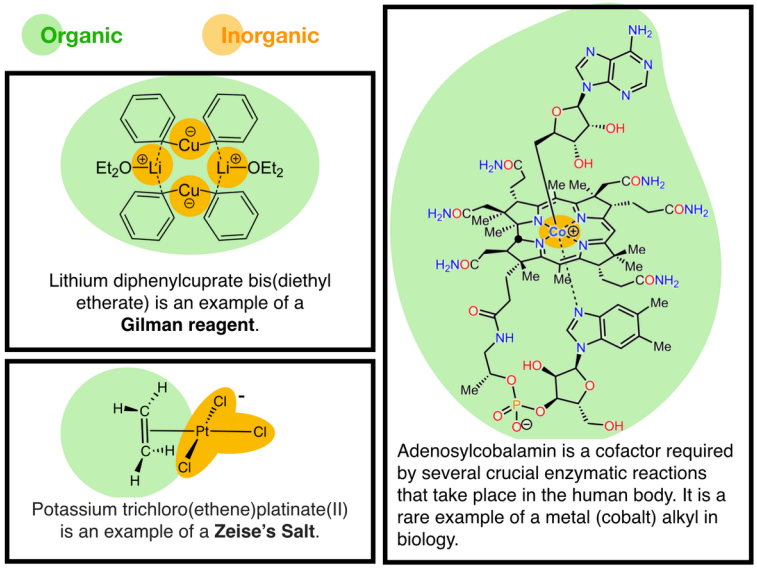
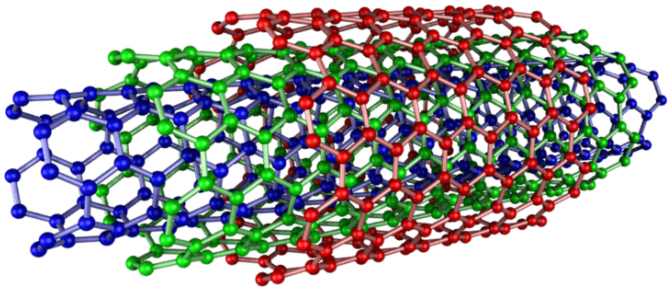


Figure 1.1.1: Some examples of organometallic catalysts. These compounds catalyze organic reactions or biochemical reactions and they are compounds that contain both carbon and metals. These compounds are examples of molecules that cannot be defined only as organic molecules or only as inorganic molecules. Adenosylcobalbumin is an example of an organometallic catalyst that is present in biology, further illustrating that "inorganic" metals are important cofactors in biology. This image is based on information on the Wikipedia article on Organometallic Chemistry and is created from images found there; attribution to images created by Alsosaid1987, AdoCbl-ColorCoded, CC BY-SA 4.0 and Smokefoot, Zeise'sSalt, CC BY-SA 3.0. (Kathryn Haas; CC-BY-SA)

Some of the subfields of Inorganic Chemistry focus on electrical conductivity of inorganic materials (i.e., conduction, superconduction, and semiconduction) and on the study of optical and electronic properties of inorganic nanomaterials. Electrical conductivity is a canonical property of metals, but carbon-based materials also demonstrate electrical conductivity. For example, carbon nanotubes conduct electricity through their extended conjugated π systems. Fullerenes, of which the most famous is Buckminsterfullerene, or Buckeyball (C_{60}), demonstrate interesting properties that are similar to nanoparticles, and when combined with metals and crystallized can demonstrate superconductivity.



Buckminsterfullerene is a type of fullerene with the formula C_{60}



Triple-walled armchair **carbon nanotube**

Figure 1.1.2: This figure is created from information found on the Wikipedia articles for Buckmisterfullerene and carbon nanotubes. Attribution Eric Wieser, Multi-walled Carbon Nanotube, CC BY-SA 3.0. (Kathryn Haas; CC-BY-SA)

Although carbon nanotubes and fullerenes are allotropes of carbon, their material properties are somewhat foreign to many organic chemists, who traditionally have focused on smaller organic molecules having very different properties. However, these properties are familiar to inorganic chemists. Thus, inorganic chemists have embraced these molecules as "inorganic" due to the fact that they behave more like inorganic materials than smaller organic molecules. This class of carbon-based molecules serves as another example of molecules that are not perfectly matched to the traditional definitions of "organic" and "inorganic" chemistry. Certainly, the future will hold more and more examples of molecules that do not fit into the traditional disciplines of chemistry.

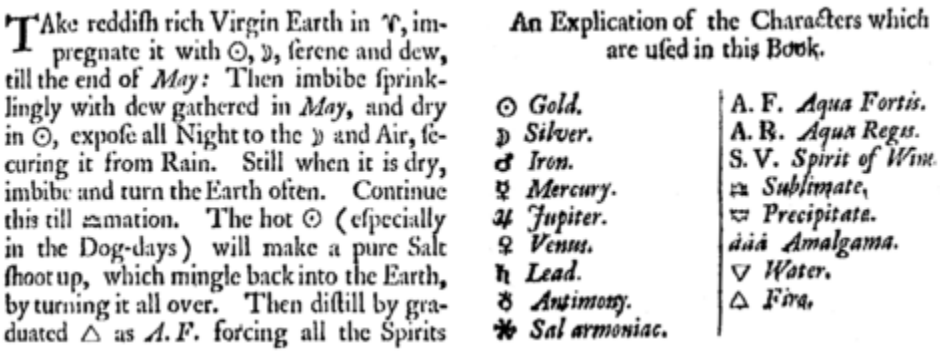
This page titled 1.1: Inorganic vs Organic Chemistry is shared under a license and was authored, remixed, and/or curated by Kathryn Haas.

- 1.2: Inorganic vs Organic Chemistry by Kathryn Haas is licensed CC BY-NC-SA 4.0.

1.2: History of Inorganic Chemistry

Metals serve an essential role in many aspects of human civilization and have defined ages of human history. The period of time from about 3300 BC to 1200 BC is often referred to as the Bronze Age. During this period our ancestors first started using metal and learned to mix various elements with copper to make a strong alloy, called bronze. This age yielded significant advancement in the crafting of sharper knives and stronger weapons out of metal instead of rock, wood and bone. Around 1200 BC the human race found an even harder metal and discovered a much stronger alloy called steel. This period is known as the Iron Age. More recently, periods of time known as Gold Rushes have caused huge changes in population distributions and wealth in some countries. Metal has obvious importance in our modern way of life. Today, iron and steel are used for making buildings, machines, automobiles, jewelry, cooking pots, tools, weapons, vehicles, electronics, surgical instruments and symbolic structures like the Eiffel Tower and the Statue of Liberty. Gold, silver, and copper still serve as currency for trade and exchange of goods and services.

The existence of chemistry as a field of study owes much to the fact that gold was a valuable commodity throughout our history. In both the ancient Egyptian society and during the Roman Empire, gold mines were the property of the state, not an individual or group. So there were few ways for most people to legally get any gold for themselves. The Alchemists were a varied group of scholars and charlatans who aimed to solve this problem by creating the **Philosopher's Stone** (which caused the transmutation of lead into gold). Three major streams of alchemy are known: Chinese, Indian, and European, with all three streams having some factors in common. Techniques developed in the European stream ultimately influenced the development of the science of chemistry.



TAke reddiſh rich Virgin Earth in ♈, impregnate it with ☉, ☽, ſerene and dew, till the end of *May*: Then imbibe ſprinklingly with dew gathered in *May*, and dry in ☉, expoſe all Night to the ☽ and Air, ſecuring it from Rain. Still when it is dry, imbibe and turn the Earth often. Continue this till ♎mation. The hot ☉ (eſpecially in the Dog-days) will make a pure Salt ſhoot up, which mingle back into the Earth, by turning it all over. Then diſtill by graduated △ as *A. F.* forcing all the Spirits

An Explication of the Characters which are uſed in this Book.

☉ *Gold.*	A. F. *Aqua Fortis.*
☽ *Silver.*	A. R. *Aqua Regis.*
♂ *Iron.*	S. V. *Spirit of Wine.*
☿ *Mercury.*	♎ *Sublimate.*
♃ *Jupiter.*	♍ *Precipitate.*
♀ *Venus.*	♎♎♎ *Amalgama.*
♄ *Lead.*	▽ *Water.*
♁ *Antimony.*	△ *Fire.*
✻ *Sal armoniac.*	

Figure 1.2.1. Alchemist recipe. Many of the specific approaches that alchemists used when they tried changing lead into gold are vague and unclear. Each alchemist had his own code for recording his data. The processes were kept secret so others could not profit from them. Different scholars developed their own set of symbols as they recorded the information they came up with. Many alchemists were not very honest, taking money from a nobleman by claiming to be able to make gold from lead, then leaving town in the middle of the night. Sometimes the nobleman would detect the fraud and have the alchemist hung. By the 1300's, several European rules had declared alchemy to be illegal and set out strict punishments for those practicing the alchemical arts.

Although alchemists were never successful in changing lead into gold, they made several contributions to modern-day chemistry. Strong acids and bases were discovered, including nitric acid ($ceHNO3$), sulfuric acid ($\mathrm{H_2SO_4}$), and hydrochloric acid (HCl), as well as sodium hydroxide (NaOH). Glassware for running chemical reactions was developed, as were methods for distillation, crystallization, and sublimation. Alchemy helped improve the study of metallurgy and the extraction of metals from ores. More systematic approaches to research were developed that allowed the discovery of atoms and laid the groundwork for development of the periodic table. For more about the History of Chemistry in general, try the LibreText page A Brief History of Chemistry.

Inorganic compounds have been known and used since antiquity; probably the oldest is the deep blue pigment called Prussian blue ($\mathrm{Fe_4[Fe(CN)_6]_3}$). However, the chemical nature of these substances was unknown until the late nineteenth and early twentieth century when the modern field of coordination chemistry emerged. Much of what we know about inorganic chemistry is based largely on the work of and debates between Alfred Werner (1866–1919; Nobel Prize in Chemistry in 1913) and Sophus Mads Jørgensen (1837 –1914). After Werner succeeded in these debates, the field of inorganic chemistry declined in popularity until the mid-twentieth century, when the second world war stimulated renewed interest. During the post-war era, several important discoveries and theories were developed. For example, important theories of bonding in coordination compounds were developed.

Soon after World War II, Crystal Field Theory (CFT) and Ligand Field Theory (LFT) were developed. These are two critical and complimentary theories that provide explanations of spectroscopic, chemical, and structural properties of inorganic coordination compounds, CFT being more simple, and LFT more accurate. In the 1950's, organometallic catalysts were discovered that catalyzed important organic reactions and the Haber-Bosch Process was discovered. The Haber-Bosch Process is catalyzed by an inorganic oxide catalyst and is one of the world's most important industrial reactions. It provides for the synthesis of ammonia directly from elemental nitrogen, N_2, and hydrogen, H_2.

$$\mathrm{N_2\,(g) + 3\,H_2\,(g)\ \rightleftharpoons 2\,NH_3\,(g)} \tag{1.2.1}$$

Since its development in the early twentieth century, it has led to the production of an enormous quantity of fertilizer, vastly increasing global food production. As a result, it is estimated that a significant fraction of the nitrogen content in the typical human body is ultimately derived from this process. Yet while the reaction must be run at high temperatures and pressures in the industrial setting, the nitrogenase enzyme in the roots of plants can carry out this reaction at the mild conditions within the soil. Intense investigations were then aimed at improving inorganic catalysts through understanding the metal cofactors in enzymes. The link between the Haber-Bosch industrial process and the nitrogenase enzyme was an early bridge between the fields of organometallic chemistry and biochemistry.

Contributions

Part of this page is adapted from K.Haas Ph.D. dissertation

Part of this page is adapted from the following LibreTexts pages

- Alchemy contributed by CK-12 Foundation by Sharon Bewick, Richard Parsons, Therese Forsythe, Shonna Robinson, and Jean Dupon.
- Werner's Theory of Coordination Compounds
- The Haber-Bosch Process Worksheet

This page titled 1.2: History of Inorganic Chemistry is shared under a CC BY-NC-SA 4.0 license and was authored, remixed, and/or curated by LibreTexts.

- 1.3: History of Inorganic Chemistry by Kathryn Haas is licensed CC BY-NC-SA 4.0.

1.3: Perspectives

The field of inorganic chemistry stands on the shoulders of giants (or in this case, many talented and dedicated scientists). If you are lucky enough to have journal access, peruse the titles and pages of the first issues of Inorganic Chemistry. You will find some lively debate about the puzzles of determining inorganic structure and reactivity. The scientists that made early discoveries in this field practiced elegant science.

The inorganic chemists who built our field are diverse. They are the ones who discovered new elements, developed new materials, characterized the fundamental principles of reactions, and developed the theories that we use to understand and predict metal structure and reactivity. And, there are people who are still working on these things today.

To gain more perspective on Inorganic Chemistry, compare the topics in the very first issue (Feb 1, 1962) to the most recent issue or the current most popular articles using the links below.

- The very first issue of Inorganic Chemistry from 1962: https://pubs.acs.org/toc/inocaj/1/1
- The latest issue of Inorganic chemistry: https://pubs.acs.org/toc/inocaj/current
- The most popular Inorganic Chemistry articles from the past month and the past year: https://pubs.acs.org/action/showMostReadArticles?journalCode=inocaj

This page titled 1.3: Perspectives is shared under a license and was authored, remixed, and/or curated by LibreTexts.

- 1.4: Perspectives by Kathryn Haas is licensed CC BY-NC-SA 4.0.

2: ATOMIC STRUCTURE

2.1: Historical Development of Atomic Theory

2.1.1: The Periodic Table

2.1.2: Discovery of Subatomic Particles and the Bohr Atom

2.2: The Schrödinger equation, particle in a box, and atomic wavefunctions

2.2.1: Particle in a Box

2.2.2: Quantum Numbers and Atomic Wave Functions

2.2.3: Aufbau Principle

2.2.4: Shielding

2.3: Periodic Properties of Atoms

2.3.1: Ionization energy

2.3.2: Electron Affinity

2.3.3: Covalent and Ionic Radii

2.4: Problems

This page titled 2: Atomic Structure is shared under a license and was authored, remixed, and/or curated by LibreTexts.

- 2: Atomic Structure by Kathryn Haas is licensed CC BY-NC-SA 4.0.

2.1: HISTORICAL DEVELOPMENT OF ATOMIC THEORY

Notes about this page

The page below is a brief overview on the history of atomic theory. It contains lots of video media.

Alternatives pages on the history of atomic theory are:

- A more detailed overview that includes practice problems is here (click).
- Another brief overview is here (click).

Skills to Develop

By the end of this section, you will be able to:

- State the postulates of Dalton's atomic theory
- Use postulates of Dalton's atomic theory to explain the laws of definite and multiple proportions
- Outline milestones in the development of modern atomic theory
- Summarize and interpret the results of the experiments of Thomson, Millikan, and Rutherford

A Video Introduction to Atomic Theory through the Nineteenth Century From Crash Course Chemistry

YouTube Video

This interactive element is not available in this format. Visit the link or scan the QR code to access it online.

View this YouTube Video online

Video 2.1.1**: Lavoisier's discovery of The Law of Conservation of Matter led to the Laws of Definite and Multiple Proportions and eventually Dalton's Atomic Theory.**

Atomic Theory through the Nineteenth Century

The earliest recorded discussion of the basic structure of matter comes from ancient Greek philosophers, the scientists of their day. In the fifth century BC, Leucippus and Democritus argued that all matter was composed of small, finite particles that they called *atomos*, a term derived from the Greek word for "indivisible." They thought of atoms as moving particles that differed in shape and size, and which could join together. Later, Aristotle and others came to the conclusion that matter consisted of various combinations of the four "elements"—fire, earth, air, and water—and could be infinitely divided. Interestingly, these philosophers thought about atoms and "elements" as philosophical concepts, but apparently never considered performing experiments to test their ideas.

The Aristotelian view of the composition of matter held sway for over two thousand years, until English schoolteacher John Dalton helped to revolutionize chemistry with his hypothesis that the behavior of matter could be explained using an atomic theory. First published in 1807, many of Dalton's hypotheses about the microscopic features of matter are still valid in modern atomic theory. Here are the postulates of Dalton's atomic theory.

1. Matter is composed of exceedingly small particles called atoms. An atom is the smallest unit of an element that can participate in a chemical change.
2. An element consists of only one type of atom, which has a mass that is characteristic of the element and is the same for all atoms of that element (Figure 2.1.1). A macroscopic sample of an element contains an incredibly large number of atoms, all of which have identical chemical properties.
3. Atoms of one element differ in properties from atoms of all other elements.
4. A compound consists of atoms of two or more elements combined in a small, whole-number ratio. In a given compound, the numbers of atoms of each of its elements are always present in the same ratio (Figure 2.1.2).
5. Atoms are neither created nor destroyed during a chemical change, but are instead rearranged to yield substances that are different from those present before the change (Figure 2.1.3).

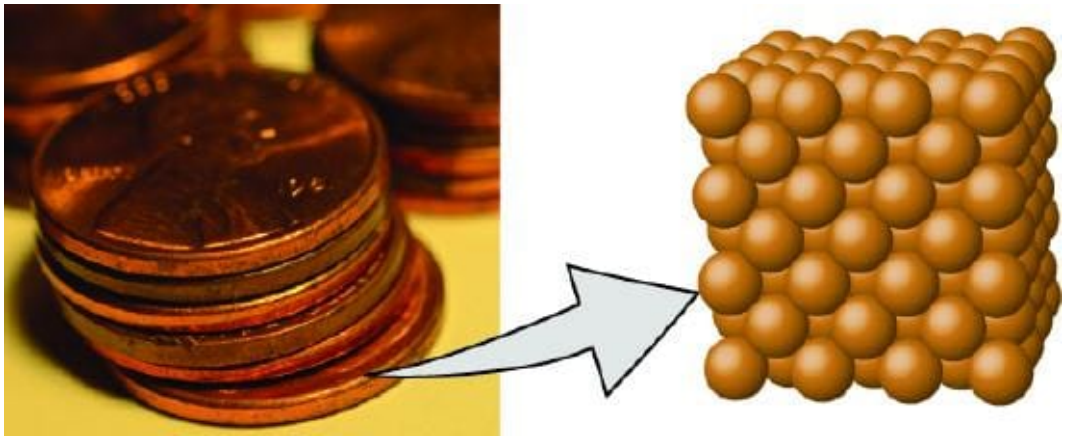


***Figure** 2.1.1: A pre-1982 copper penny (left) contains approximately 3×10^{22} copper atoms (several dozen are represented as brown spheres at the right), each of which has the same chemical properties. (credit: modification of work by "slgckgc"/Flickr)*

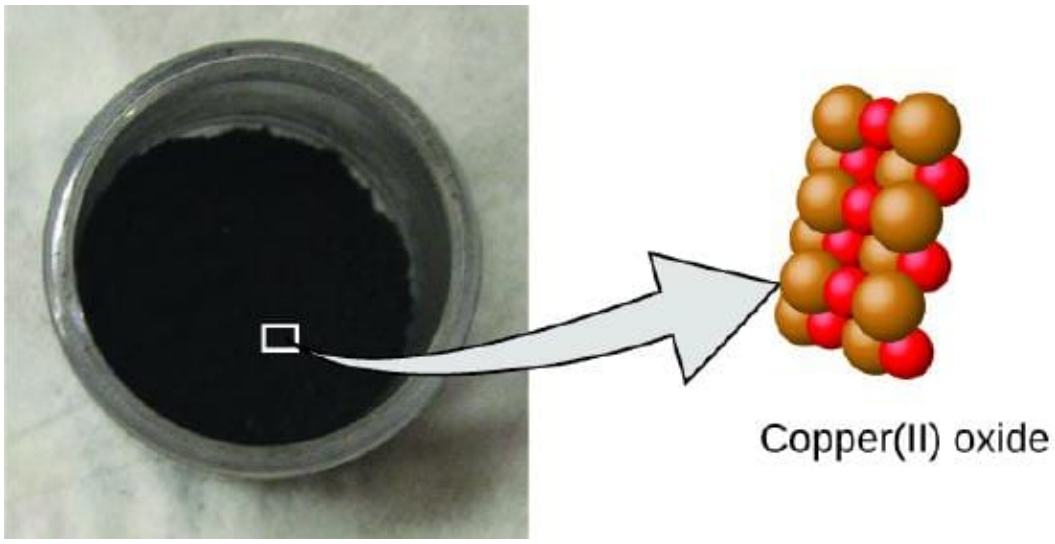


***Figure** 2.1.2: Copper(II) oxide, a powdery, black compound, results from the combination of two types of atoms—copper (brown spheres) and oxygen (red spheres)—in a 1:1 ratio. (credit: modification of work by "Chemicalinterest"/Wikimedia Commons)*

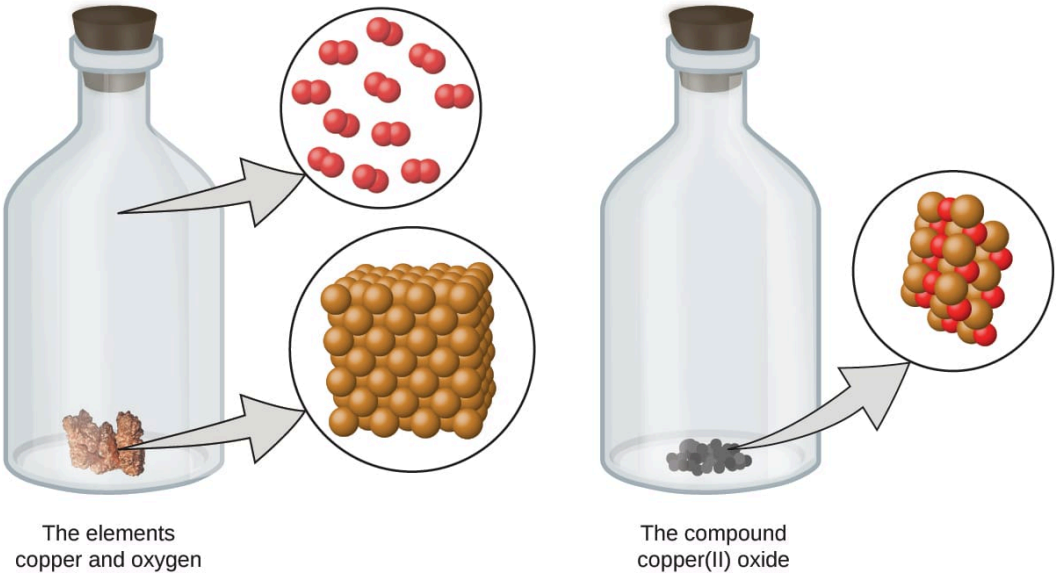


Figure 2.1.3*: When the elements copper (a shiny, red-brown solid, shown here as brown spheres) and oxygen (a clear and colorless gas, shown here as red spheres) react, their atoms rearrange to form a compound containing copper and oxygen (a powdery, black solid). (credit copper: modification of work by http://images-of-elements.com/copper.php).*

Dalton's atomic theory provides a microscopic explanation of the many macroscopic properties of matter that you've learned about. For example, if an element such as copper consists of only one kind of atom, then it cannot be broken down into simpler substances, that is, into substances composed of fewer types of atoms. And if atoms are neither created nor destroyed during a chemical change, then the total mass of matter present when matter changes from one type to another will remain constant (the law of conservation of matter (or mass)).

Want to learn more about the Law of Conservation of Mass?

YouTube Video

This interactive element is not available in this format. Visit the link or scan the QR code to access it online.

View this YouTube Video online

Video 2.1.2***: "We are made of star stuff" - Carl Sagan.***

Example 2.1.1: Testing Dalton's Atomic Theory

In the following drawing, the green spheres represent atoms of a certain element. The purple spheres represent atoms of another element. If the spheres touch, they are part of a single unit of a compound. Does the following chemical change represented by these symbols violate any of the ideas of Dalton's atomic theory? If so, which one?

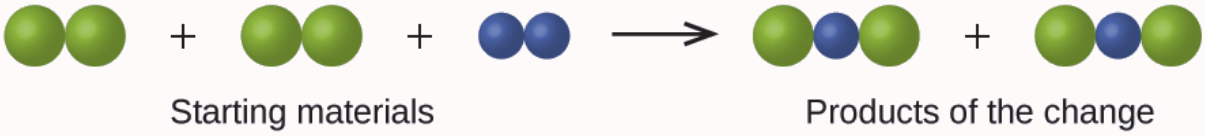


Solution

The starting materials consist of two green spheres and two purple spheres. The products consist of only one green sphere and one purple sphere. This violates Dalton's postulate that atoms are neither created nor destroyed during a chemical change, but are merely redistributed. (In this case, atoms appear to have been destroyed.)

Exercise 2.1.1

In the following drawing, the green spheres represent atoms of a certain element. The purple spheres represent atoms of another element. If the spheres touch, they are part of a single unit of a compound. Does the following chemical change represented by these symbols violate any of the ideas of Dalton's atomic theory? If so, which one



Answer

The starting materials consist of four green spheres and two purple spheres. The products consist of four green spheres and two purple spheres. This does not violate any of Dalton's postulates: Atoms are neither created nor destroyed, but are redistributed in small, whole-number ratios.

Dalton knew of the experiments of French chemist Joseph Proust, who demonstrated that *all samples of a pure compound contain the same elements in the same proportion by mass*. This statement is known as the law of definite proportions or the law of constant composition. The suggestion that the numbers of atoms of the elements in a given compound always exist in the same ratio is consistent with these observations. For example, when different samples of isooctane (a component of gasoline and one of the standards used in the octane rating system) are analyzed, they are found to have a carbon-to-hydrogen mass ratio of 5.33:1, as shown in Table 2.1.1.

Table 2.1.1*: Constant Composition of Isooctane*

Sample	Carbon	Hydrogen	Mass Ratio
A	14.82 g	2.78 g	$\frac{14.82\ \text{g carbon}}{2.78\ \text{g hydrogen}} = \frac{5.33\ \text{g carbon}}{1.00\ \text{g hydrogen}}$
B	22.33 g	4.19 g	$\frac{22.33\ \text{g carbon}}{4.19\ \text{g hydrogen}} = \frac{5.33\ \text{g carbon}}{1.00\ \text{g hydrogen}}$
C	19.40 g	3.64 g	$\frac{19.40\ \text{g carbon}}{3.63\ \text{g hydrogen}} = \frac{5.33\ \text{g carbon}}{1.00\ \text{g hydrogen}}$

It is worth noting that although all samples of a particular compound have the same mass ratio, the converse is not true in general. That is, samples that have the same mass ratio are not necessarily the same substance. For example, there are many compounds other than isooctane that also have a carbon-to-hydrogen mass ratio of 5.33:1.00.

Dalton also used data from Proust, as well as results from his own experiments, to formulate another interesting law. The law of multiple proportions states that *when two elements react to form more than one compound, a fixed mass of one element will react with masses of the other element in a ratio of small, whole numbers*. For example, copper and chlorine can form a green,

crystalline solid with a mass ratio of 0.558 g chlorine to 1 g copper, as well as a brown crystalline solid with a mass ratio of 1.116 g chlorine to 1 g copper. These ratios by themselves may not seem particularly interesting or informative; however, if we take a ratio of these ratios, we obtain a useful and possibly surprising result: a small, whole-number ratio.

$$\frac{\frac{1.116\ \text{g Cl}}{1\ \text{g Cu}}}{\frac{0.558\ \text{g Cl}}{1\ \text{g Cu}}} = \frac{2}{1} \tag{2.1.1}$$

This 2-to-1 ratio means that the brown compound has twice the amount of chlorine per amount of copper as the green compound.

This can be explained by atomic theory if the copper-to-chlorine ratio in the brown compound is 1 copper atom to 2 chlorine atoms, and the ratio in the green compound is 1 copper atom to 1 chlorine atom. The ratio of chlorine atoms (and thus the ratio of their masses) is therefore 2 to 1 (Figure 2.1.4).

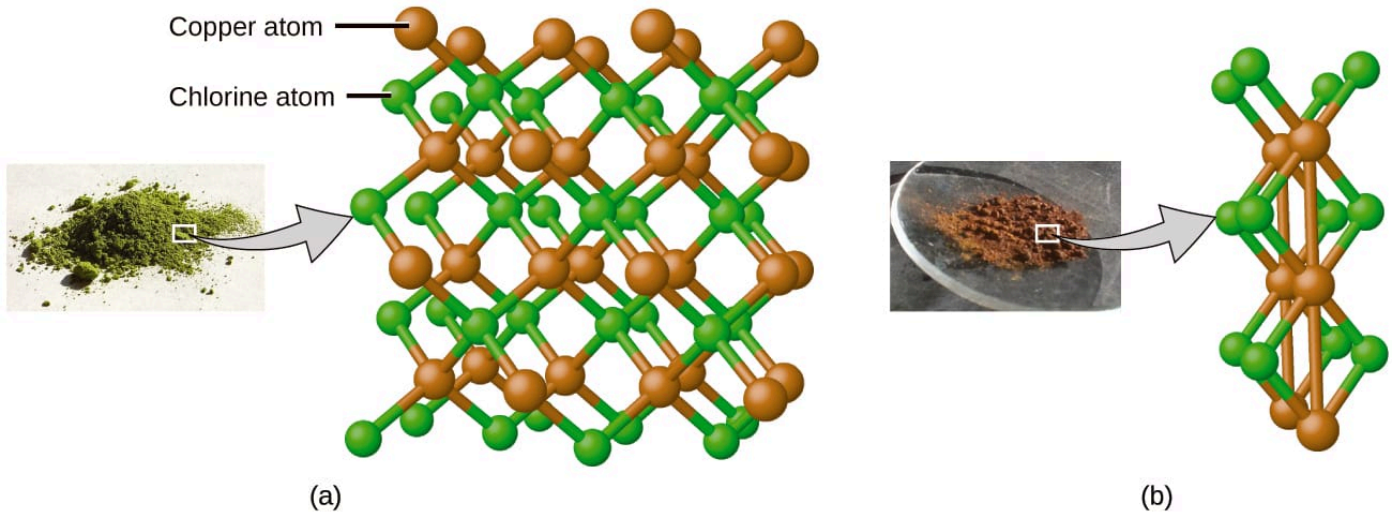


Figure 2.1.4*: Compared to the copper chlorine compound in (a), where copper is represented by brown spheres and chlorine by green spheres, the copper chlorine compound in (b) has twice as many chlorine atoms per copper atom. (credit a: modification of work by "Benjah-bmm27"/Wikimedia Commons; credit b: modification of work by "Walkerma"/Wikimedia Commons)*

Example 2.1.2: Laws of Definite and Multiple Proportions

A sample of compound A (a clear, colorless gas) is analyzed and found to contain 4.27 g carbon and 5.69 g oxygen. A sample of compound B (also a clear, colorless gas) is analyzed and found to contain 5.19 g carbon and 13.84 g oxygen. Are these data an example of the law of definite proportions, the law of multiple proportions, or neither? What do these data tell you about substances A and B?

Solution

In compound A, the mass ratio of carbon to oxygen is:

$$\frac{1.33\ \text{g O}}{1\ \text{g C}}$$

In compound B, the mass ratio of carbon to oxygen is:

$$\frac{2.67\ \text{g O}}{1\ \text{g C}}$$

The ratio of these ratios is:

$$\frac{\frac{1.33\ \text{g O}}{1\ \text{g C}}}{\frac{2.67\ \text{g O}}{1\ \text{g C}}} = \frac{1}{2}$$

This supports the law of multiple proportions. This means that A and B are different compounds, with A having one-half as much carbon per amount of oxygen (or twice as much oxygen per amount of carbon) as B. A possible pair of compounds that would fit this relationship would be A = CO_2 and B = CO.

Exercise 2.1.2

A sample of compound X (a clear, colorless, combustible liquid with a noticeable odor) is analyzed and found to contain 14.13 g carbon and 2.96 g hydrogen. A sample of compound Y (a clear, colorless, combustible liquid with a noticeable odor that is slightly different from X's odor) is analyzed and found to contain 19.91 g carbon and 3.34 g hydrogen. Are these data an example of the law of definite proportions, the law of multiple proportions, or neither? What do these data tell you about substances X and Y?

Answer

In compound X, the mass ratio of carbon to hydrogen is $\frac{14.13\ \text{g C}}{2.96\ \text{g H}}$.

In compound Y, the mass ratio of carbon to oxygen is $\frac{19.91\ \text{g C}}{3.34\ \text{g H}}$.

The ratio of these ratios is

$$\frac{\frac{14.13\ \text{g C}}{2.96\ \text{g H}}}{\frac{19.91\ \text{g C}}{3.34\ \text{g H}}} = \frac{4.77\ \text{g C/g H}}{5.96\ \text{g C/g H}} = 0.800 = \frac{4}{5}.$$

This small, whole-number ratio supports the law of multiple proportions. This means that X and Y are different compounds.

In the two centuries since Dalton developed his ideas, scientists have made significant progress in furthering our understanding of atomic theory. Much of this came from the results of several seminal experiments that revealed the details of the internal structure of atoms. Here, we will discuss some of those key developments, with an emphasis on application of the scientific method, as well as understanding how the experimental evidence was analyzed. While the historical persons and dates behind these experiments can be quite interesting, it is most important to understand the concepts resulting from their work.

Atomic Theory after the Nineteenth Century

If matter were composed of atoms, what were atoms composed of? Were they the smallest particles, or was there something smaller? In the late 1800s, a number of scientists interested in questions like these investigated the electrical discharges that could be produced in low-pressure gases, with the most significant discovery made by English physicist J. J. Thomson using a cathode ray tube. This apparatus consisted of a sealed glass tube from which almost all the air had been removed; the tube contained two metal electrodes. When high voltage was applied across the electrodes, a visible beam called a cathode ray appeared between them. This beam was deflected toward the positive charge and away from the negative charge, and was produced in the same way with identical properties when different metals were used for the electrodes. In similar experiments, the ray was simultaneously deflected by an applied magnetic field, and measurements of the extent of deflection and the magnetic field strength allowed Thomson to calculate the charge-to-mass ratio of the cathode ray particles. The results of these measurements indicated that these particles were much lighter than atoms (Figure 2.1.1).

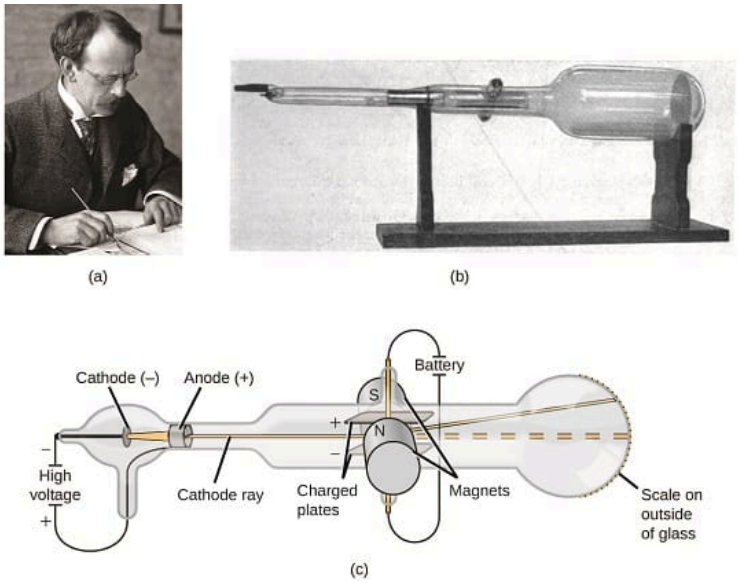
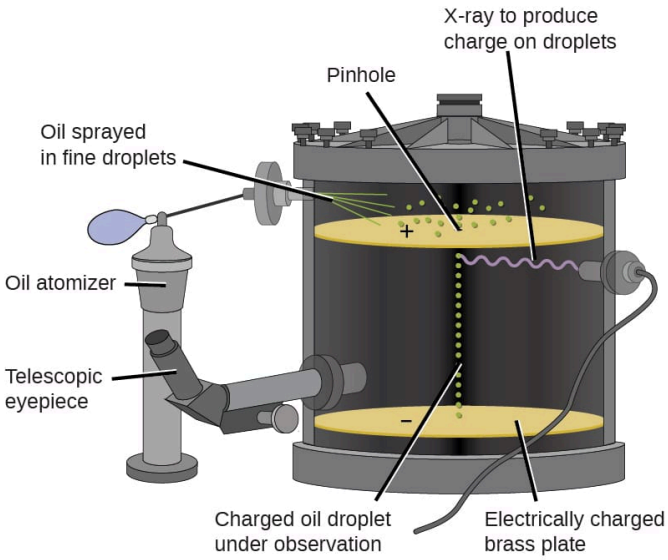


Figure 2.1.5*: (a) J. J. Thomson produced a visible beam in a cathode ray tube. (b) This is an early cathode ray tube, invented in 1897 by Ferdinand Braun. (c) In the cathode ray, the beam (shown in yellow) comes from the cathode and is accelerated past the anode toward a fluorescent scale at the end of the tube. Simultaneous deflections by applied electric and magnetic fields permitted Thomson to calculate the mass-to-charge ratio of the particles composing the cathode ray. (credit a: modification of work by Nobel Foundation; credit b: modification of work by Eugen Nesper; credit c: modification of work by "Kurzon"/Wikimedia Commons).*

Based on his observations, here is what Thomson proposed and why: The particles are attracted by positive (+) charges and repelled by negative (–) charges, so they must be negatively charged (like charges repel and unlike charges attract); they are less massive than atoms and indistinguishable, regardless of the source material, so they must be fundamental, subatomic constituents of all atoms. Although controversial at the time, Thomson's idea was gradually accepted, and his cathode ray particle is what we now call an electron, a negatively charged, subatomic particle with a mass more than one thousand-times less that of an atom. The term "electron" was coined in 1891 by Irish physicist George Stoney, from "*electr*ic i*on*."

In 1909, more information about the electron was uncovered by American physicist Robert A. Millikan via his "oil drop" experiments. Millikan created microscopic oil droplets, which could be electrically charged by friction as they formed or by using X-rays. These droplets initially fell due to gravity, but their downward progress could be slowed or even reversed by an electric field lower in the apparatus. By adjusting the electric field strength and making careful measurements and appropriate calculations, Millikan was able to determine the charge on individual drops (Figure 2.1.2).



Oil drop	Charge in coulombs (C)
A	4.8×10^{-19} C
B	3.2×10^{-19} C
C	6.4×10^{-19} C
D	1.6×10^{-19} C
E	4.8×10^{-19} C

Figure 2.1.6***:*** *Millikan's experiment measured the charge of individual oil drops. The tabulated data are examples of a few possible values.*

Looking at the charge data that Millikan gathered, you may have recognized that the charge of an oil droplet is always a multiple of a specific charge, 1.6×10^{-19} C. Millikan concluded that this value must therefore be a fundamental charge—the charge of a single electron—with his measured charges due to an excess of one electron (1 times 1.6×10^{-19} C), two electrons (2 times 1.6×10^{-19} C), three electrons (3 times 1.6×10^{-19} C), and so on, on a given oil droplet. Since the charge of an electron was now known due to Millikan's research, and the charge-to-mass ratio was already known due to Thomson's research (1.759×10^{11} C/kg), it only required a simple calculation to determine the mass of the electron as well.

$$\text{Mass of electron} = 1.602 \times 10^{-19} \cancel{\text{C}} \times \frac{1 \text{ kg}}{1.759 \times 10^{11} \cancel{\text{C}}} = 9.107 \times 10^{-31} \text{ kg} \tag{2.3.1}$$

Scientists had now established that the atom was not indivisible as Dalton had believed, and due to the work of Thomson, Millikan, and others, the charge and mass of the negative, subatomic particles—the electrons—were known. However, the positively charged part of an atom was not yet well understood. In 1904, Thomson proposed the "plum pudding" model of atoms, which described a positively charged mass with an equal amount of negative charge in the form of electrons embedded in it, since all atoms are electrically neutral. A competing model had been proposed in 1903 by Hantaro Nagaoka, who postulated a Saturn-like atom, consisting of a positively charged sphere surrounded by a halo of electrons (Figure 2.1.3).

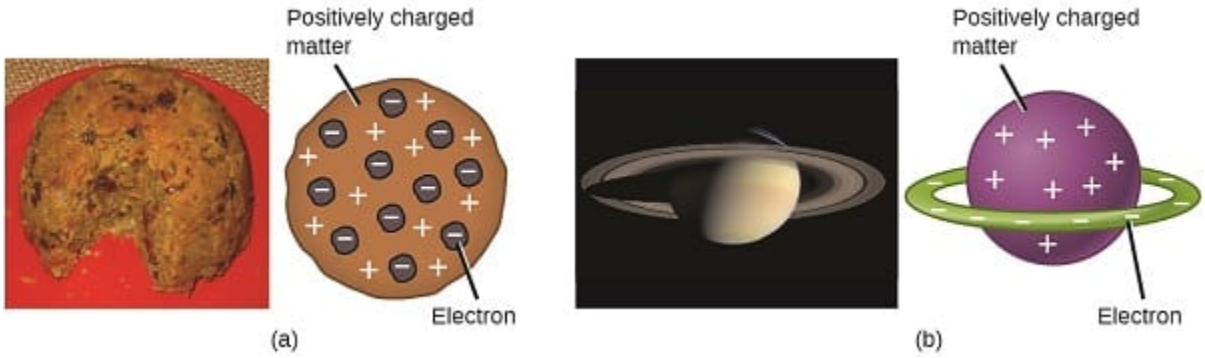


Figure 2.1.7*: (a) Thomson suggested that atoms resembled plum pudding, an English dessert consisting of moist cake with embedded raisins ("plums"). (b) Nagaoka proposed that atoms resembled the planet Saturn, with a ring of electrons surrounding a positive "planet." (credit a: modification of work by "Man vyi"/Wikimedia Commons; credit b: modification of work by "NASA"/Wikimedia Commons).*

The next major development in understanding the atom came from Ernest Rutherford, a physicist from New Zealand who largely spent his scientific career in Canada and England. He performed a series of experiments using a beam of high-speed, positively charged alpha particles (α particles) that were produced by the radioactive decay of radium; α particles consist of two protons and two neutrons (you will learn more about radioactive decay in the chapter on nuclear chemistry). Rutherford and his colleagues Hans Geiger (later famous for the Geiger counter) and Ernest Marsden aimed a beam of α particles, the source of which was embedded in a lead block to absorb most of the radiation, at a very thin piece of gold foil and examined the resultant scattering of the α particles using a luminescent screen that glowed briefly where hit by an α particle.

What did they discover? Most particles passed right through the foil without being deflected at all. However, some were diverted slightly, and a very small number were deflected almost straight back toward the source (Figure 2.1.4). Rutherford described finding these results: "It was quite the most incredible event that has ever happened to me in my life. It was almost as incredible as if you fired a 15-inch shell at a piece of tissue paper and it came back and hit you"[1] (p. 68).

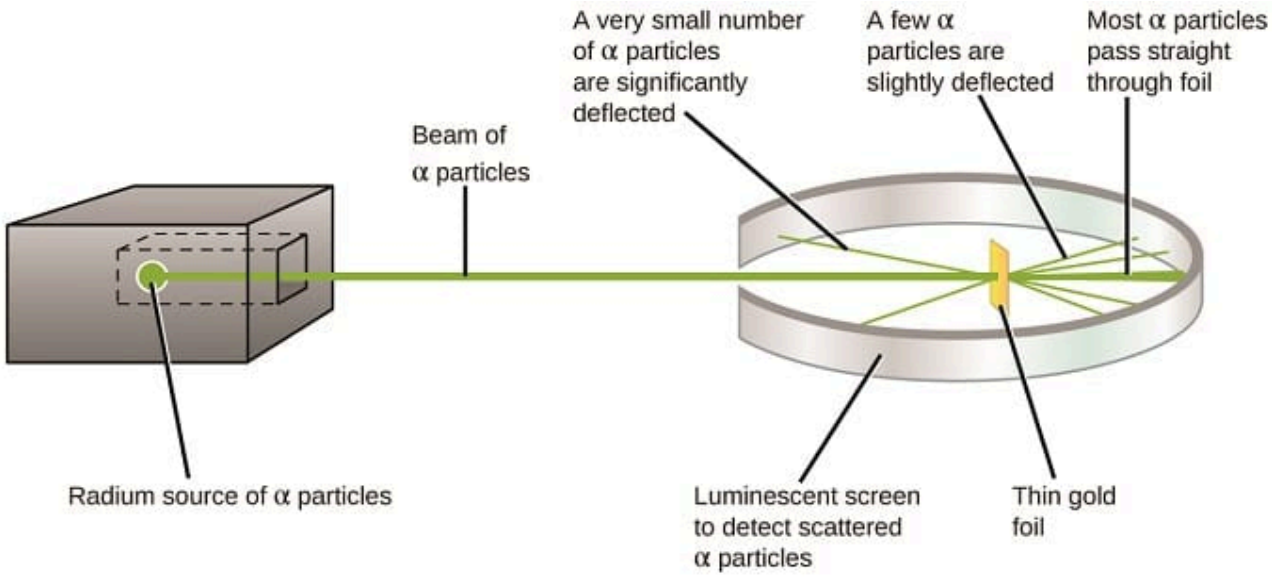


Figure 2.1.8***:*** *Geiger and Rutherford fired α particles at a piece of gold foil and detected where those particles went, as shown in this schematic diagram of their experiment. Most of the particles passed straight through the foil, but a few were deflected slightly and a very small number were significantly deflected.*

Here is what Rutherford deduced: Because most of the fast-moving α particles passed through the gold atoms undeflected, they must have traveled through essentially empty space inside the atom. Alpha particles are positively charged, so deflections arose when they encountered another positive charge (like charges repel each other). Since like charges repel one another, the few positively charged α particles that changed paths abruptly must have hit, or closely approached, another body that also had a highly concentrated, positive charge. Since the deflections occurred a small fraction of the time, this charge only occupied a small amount of the space in the gold foil. Analyzing a series of such experiments in detail, Rutherford drew two conclusions:

1. The volume occupied by an atom must consist of a large amount of empty space.
2. A small, relatively heavy, positively charged body, the nucleus, must be at the center of each atom.

This analysis led Rutherford to propose a model in which an atom consists of a very small, positively charged nucleus, in which most of the mass of the atom is concentrated, surrounded by the negatively charged electrons, so that the atom is electrically neutral (Figure 2.1.5).

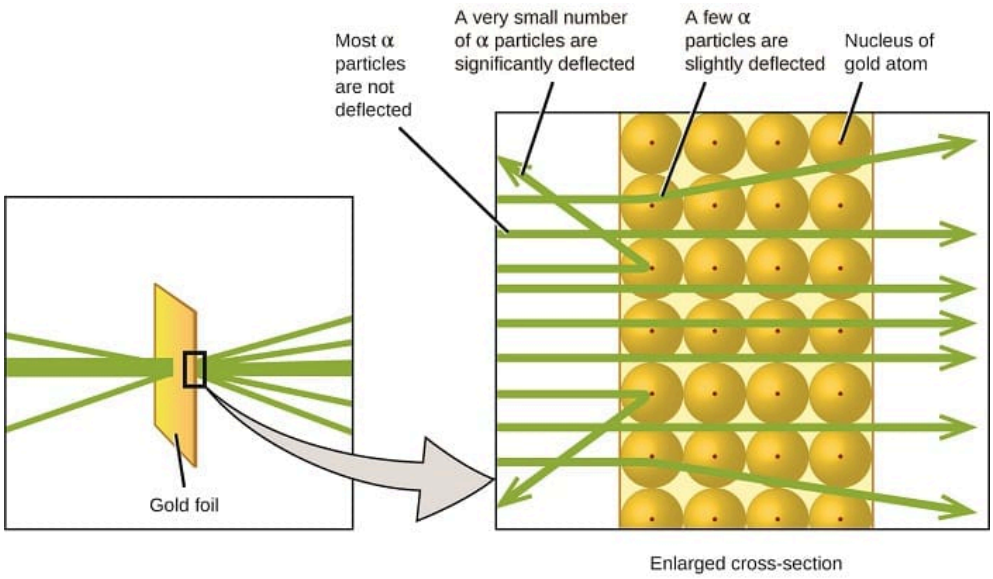


Figure 2.1.9*: The α particles are deflected only when they collide with or pass close to the much heavier, positively charged gold nucleus. Because the nucleus is very small compared to the size of an atom, very few α particles are deflected. Most pass through the relatively large region occupied by electrons, which are too light to deflect the rapidly moving particles.*

After many more experiments, Rutherford also discovered that the nuclei of other elements contain the hydrogen nucleus as a "building block," and he named this more fundamental particle the proton, the positively charged, subatomic particle found in the nucleus. With one addition, which you will learn next, this nuclear model of the atom, proposed over a century ago, is still used today.

Another important finding was the discovery of isotopes. During the early 1900s, scientists identified several substances that appeared to be new elements, isolating them from radioactive ores. For example, a "new element" produced by the radioactive decay of thorium was initially given the name mesothorium. However, a more detailed analysis showed that mesothorium was chemically identical to radium (another decay product), despite having a different atomic mass. This result, along with similar findings for other elements, led the English chemist Frederick Soddy to realize that an element could have types of atoms with different masses that were chemically indistinguishable. These different types are called isotopes—atoms of the same element that differ in mass. Soddy was awarded the Nobel Prize in Chemistry in 1921 for this discovery.

One puzzle remained: The nucleus was known to contain almost all of the mass of an atom, with the number of protons only providing half, or less, of that mass. Different proposals were made to explain what constituted the remaining mass, including the existence of neutral particles in the nucleus. As you might expect, detecting uncharged particles is very challenging, and it was not until 1932 that James Chadwick found evidence of neutrons, uncharged, subatomic particles with a mass approximately the same as that of protons. The existence of the neutron also explained isotopes: They differ in mass because they have different numbers of neutrons, but they are chemically identical because they have the same number of protons. This will be explained in more detail later in this unit.

YouTube Video

This interactive element is not available in this format. Visit the link or scan the QR code to access it online.

View this YouTube Video online

Video 2.1.2***: An Introduction to Subatomic Particles***

Summary

YouTube Video

This interactive element is not available in this format. Visit the link or scan the QR code to access it online.

View this YouTube Video online

Video 2.1.3***:*** *A summary of discoveries in atomic theory.*

YouTube Video

This interactive element is not available in this format. Visit the link or scan the QR code to access it online.

View this YouTube Video online

Video 2.1.4***:*** *A different summary of discoveries in atomic theory.*

The ancient Greeks proposed that matter consists of extremely small particles called atoms. Dalton postulated that each element has a characteristic type of atom that differs in properties from atoms of all other elements, and that atoms of different elements can combine in fixed, small, whole-number ratios to form compounds. Samples of a particular compound all have the same elemental proportions by mass. When two elements form different compounds, a given mass of one element will combine with masses of the other element in a small, whole-number ratio. During any chemical change, atoms are neither created nor destroyed.

Although no one has actually seen the inside of an atom, experiments have demonstrated much about atomic structure. Thomson's cathode ray tube showed that atoms contain small, negatively charged particles called electrons. Millikan discovered that there is a fundamental electric charge—the charge of an electron. Rutherford's gold foil experiment showed that atoms have a small, dense, positively charged nucleus; the positively charged particles within the nucleus are called protons. Chadwick discovered that the nucleus also contains neutral particles called neutrons. Soddy demonstrated that atoms of the same element can differ in mass; these are called isotopes.

Footnotes

1. Ernest Rutherford, "The Development of the Theory of Atomic Structure," ed. J. A. Ratcliffe, in *Background to Modern Science*, eds. Joseph Needham and Walter Pagel, (Cambridge, UK: Cambridge University Press, 1938), 61–74. Accessed September 22, 2014, https://ia600508.us.archive.org/3/it...e032734mbp.pdf.

Glossary

Dalton's atomic theory
: set of postulates that established the fundamental properties of atoms

law of constant composition
: (also, law of definite proportions) all samples of a pure compound contain the same elements in the same proportions by mass

law of multiple proportions
when two elements react to form more than one compound, a fixed mass of one element will react with masses of the other element in a ratio of small whole numbers

law of definite proportions
(also, law of constant composition) all samples of a pure compound contain the same elements in the same proportions by mass

alpha particle (α particle)
positively charged particle consisting of two protons and two neutrons

electron
negatively charged, subatomic particle of relatively low mass located outside the nucleus

isotopes
atoms that contain the same number of protons but different numbers of neutrons

neutron
uncharged, subatomic particle located in the nucleus

proton
positively charged, subatomic particle located in the nucleus

nucleus
massive, positively charged center of an atom made up of protons and neutrons

Contributors

- Paul Flowers (University of North Carolina - Pembroke), Klaus Theopold (University of Delaware) and Richard Langley (Stephen F. Austin State University) with contributing authors. Textbook content produced by OpenStax College is licensed under a Creative Commons Attribution License 4.0 license. Download for free at http://cnx.org/contents/85abf193-2bd...a7ac8df6@9.110).

- Adelaide Clark, Oregon Institute of Technology
- Crash Course Chemistry: Crash Course is a division of Complexly and videos are free to stream for educational purposes.
- TED-Ed's commitment to creating lessons worth sharing is an extension of TED's mission of spreading great ideas. Within TED-Ed's growing library of TED-Ed animations, you will find carefully curated educational videos, many of which represent collaborations between talented educators and animators nominated through the TED-Ed website.

Feedback

Have feedback to give about this text? Click here.

Found a typo and want extra credit? Click here.

2.1.1: The Periodic Table

2.1.2: Discovery of Subatomic Particles and the Bohr Atom

This page titled 2.1: Historical Development of Atomic Theory is shared under a license and was authored, remixed, and/or curated by LibreTexts.

- 2.1: Historical Development of Atomic Theory is licensed CC BY-NC-SA 4.0.

2.1.1: The Periodic Table

Learning Objectives

- To become familiar with the history of the periodic table.

The modern periodic table has evolved through a long history of attempts by chemists to arrange the elements according to their reactivity and other properties as an aid in predicting chemical behavior. Now that we have arranged the table according to electronic structure, it makes sense to go back and look at earlier efforts in the light of what we know about electronic structure.

One of the first to suggest such an arrangement was the German chemist Johannes Dobereiner (1780–1849), who noticed that many of the known elements could be grouped in triads, sets of three elements that have similar properties—for example, chlorine, bromine, and iodine; or copper, silver, and gold. Dobereiner proposed that all elements could be grouped in such triads, but subsequent attempts to expand his concept were unsuccessful. We now know that portions of the periodic table—the *d* block in particular—contain triads of elements with substantial similarities. The middle three members of most of the other columns, such as sulfur, selenium, and tellurium in group 16 or aluminum, gallium, and indium in group 13, also have remarkably similar chemistry.

By the mid-19th century, the atomic masses of many of the elements had been determined. The English chemist John Newlands (1838–1898), hypothesizing that the chemistry of the elements might be related to their masses, arranged the known elements in order of increasing atomic mass and discovered that every seventh element had similar properties (Figure 3.4.1). Newlands therefore suggested that the elements could be classified into octaves: a group of seven elements (not counting the noble gases, which were unknown at the time) that correspond to the *horizontal* rows in the main group elements. Unfortunately, Newlands's "law of octaves" did not seem to work for elements heavier than calcium, and his idea was publicly ridiculed. At one scientific meeting, Newlands was asked why he didn't arrange the elements in alphabetical order instead of by atomic mass, since that would make just as much sense! Actually, Newlands was on the right track—with only a few exceptions, atomic mass does increase with atomic number, and similar properties occur every time a set of ns^2np^6 subshells is filled. Despite the fact that Newlands's table had no logical place for the *d*-block elements, he was honored for his idea by the Royal Society of London in 1887.

John Newlands (1838–1898)

Newlands noticed that elemental properties repeated every seventh (or multiple of seven) element, as musical notes repeat every eighth note.

No.	No.	No.	No.	No.	No.	No.	No.
H 1	F 8	Cl 15	Co & Ni 22	Br 29	Pd 36	I 42	Pt & Ir 50
Li 2	Na 9	K 16	Cu 23	Rb 30	Ag 37	Cs 44	Tl 51
G 3	Mg 10	Ca 17	Zn 25	Sr 31	Bd [sic-Cd] 38	Ba & V 45	Pb 54
Bo 4	Al 11	Cr 19	Y 24	Ce & La 33	U 40	Ta 46	Th 56
C 5	Si 12	Ti 18	In 26	Zr 32	Sn 39	W 47	Hg 52
N 6	P 13	Mn 20	As 27	Di & Mo 34	Sb 41	Nb 48	Bi 55
O 7	S 14	Fe 21	Se 28	Ro & Ru 35	Te 43	Au 49	Os 51

NOTE. Where two elements happen to have the same equivalent, both are designated by the same number.

Figure 3.4.1 The arrangement of the elements into octaves as proposed by **Newlands:** *The table shown here accompanied a letter from a 27-year-old Newlands to the editor of the journal Chemical News in which he wrote: "If the elements are arranged in the order of their equivalents, with a few slight transpositions, as in the accompanying table, it will be observed that elements belonging to the same group usually appear on the same horizontal line. It will also be seen that the numbers of analogous elements generally differ either by 7 or by some multiple of seven; in other words, members of the same group stand to each other in the same relation as the extremities of one or more octaves in music. Thus, in the nitrogen group, between nitrogen and phosphorus there are 7 elements; between phosphorus and arsenic, 14; between arsenic and antimony, 14; and lastly, between antimony and bismuth, 14 also. This peculiar relationship I propose to provisionally term the Law of Octaves. I am, &c. John A. R. Newlands, F.C.S. Laboratory, 19, Great St. Helen's, E.C., August 8, 1865."*

The periodic table achieved its modern form through the work of the German chemist Julius Lothar Meyer (1830–1895) and the Russian chemist Dimitri Mendeleev (1834–1907), both of whom focused on the relationships between atomic mass and various physical and chemical properties. In 1869, they independently proposed essentially identical arrangements of the elements. Meyer aligned the elements in his table according to periodic variations in simple atomic properties, such as "atomic volume" (Figure 3.4.2), which he obtained by dividing the atomic mass (molar mass) in grams per mole by the density of the element in grams per cubic centimeter. This property is equivalent to what is today defined as molar volume, the molar mass of an element divided by its density (measured in cubic centimeters per mole):

$$\frac{molar\ mass\ \left(\not{g}/mol\right)}{density\ \left(\not{g}/cm^3\right)} = molar\ \ volume\ \left(cm^3/mol\right)$$

As shown in Figure 3.4.2 , the alkali metals have the highest molar volumes of the solid elements. In Meyer's plot of atomic volume versus atomic mass, the nonmetals occur on the rising portion of the graph, and metals occur at the peaks, in the valleys, and on the down slopes.

Dimitri Mendeleev (1834–1907)

When his family's glass factory was destroyed by fire, Mendeleev moved to St. Petersburg, Russia, to study science. He became ill and was not expected to recover, but he finished his PhD with the help of his professors and fellow students. In addition to the periodic table, another of Mendeleev's contributions to science was an outstanding textbook, *The Principles of Chemistry*, which was used for many years.

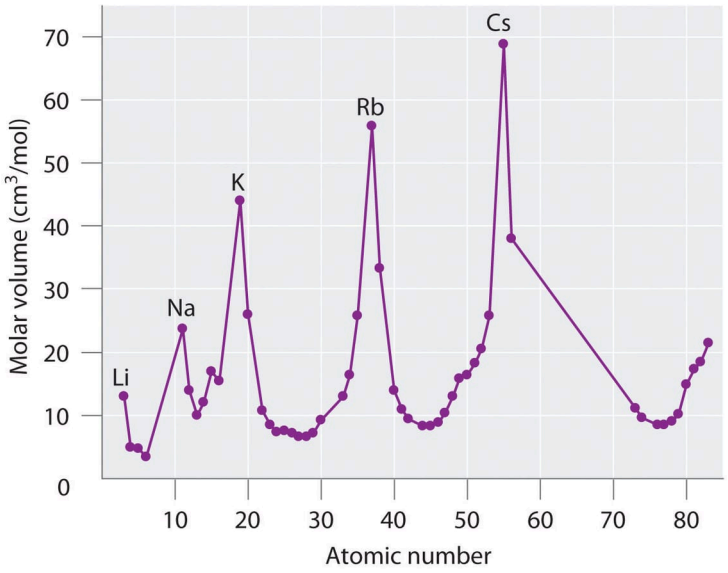


Figure 3.4.2 Variation of atomic volume with atomic number, adapted from Meyer's plot of **1870:** *Note the periodic increase and decrease in atomic volume. Because the noble gases had not yet been discovered at the time this graph was formulated, the peaks correspond to the alkali metals (group 1).*

Mendeleev's Periodic Table

Mendeleev, who first published his periodic table in 1869 (Figure 3.4.3), is usually credited with the origin of the modern periodic table. The key difference between his arrangement of the elements and that of Meyer and others is that Mendeleev did not assume that all the elements had been discovered (actually, only about two-thirds of the naturally occurring elements were known at the time). Instead, he deliberately left blanks in his table at atomic masses 44, 68, 72, and 100, in the expectation that elements with those atomic masses would be discovered. Those blanks correspond to the elements we now know as scandium, gallium, germanium, and technetium.

Reihen	Gruppe I. — R^2O	Gruppe II. — RO	Gruppe III. — R^2O^3	Gruppe IV. RH^4 RO^2	Gruppe V. RH^3 R^2O^5	Gruppe VI. RH^2 RO^3	Gruppe VII. RH R^2O^7	Gruppe VIII. — RO^4
1	H=1							
2	Li=7	Be=9,4	B=11	C=12	N=14	O=16	F=19	
3	Na=23	Mg=24	Al=27,3	Si=28	P=31	S=32	Cl=35,5	
4	K=39	Ca=40	— =44	Ti=48	V=51	Cr=52	Mn=55	Fe=56, Co=59, Ni=59, Cu=63.
5	(Cu=63)	Zn=65	— =68	— =72	As=75	Se=78	Br=80	
6	Rb=85	Sr=87	?Yt=88	Zr=90	Nb=94	Mo=96	— =100	Ru=104, Rh=104, Pd=106, Ag=108.
7	(Ag=108)	Cd=112	In=113	Sn=118	Sb=122	Te=125	J=127	
8	Cs=133	Ba=137	?Di=138	?Ce= 40	—	—	—	— — — —
9	(—)	—	—	—	—	—	—	
10	—	—	?Er=178	?La=180	Ta=182	W=184	—	Os=195, Ir=197, Pt=198, Au=199.
11	(Au=199)	Hg=200	Tl=204	Pb=207	Bi=208	—	—	
12	—	—	—	Th=231	—	U=240	—	— — — —

Figure 3.4.3 Mendeleev's periodic table, as published in the German journal *Annalen der Chemie und Pharmacie* in 1872: *The column headings "Reihen" and "Gruppe" are German for "row" and "group." Formulas indicate the type of compounds formed by each group, with "R" standing for "any element" and superscripts used where we now use subscripts. Atomic masses are shown after equal signs and increase across each row from left to right.*

The groups in Mendeleev's table are determined by how many oxygen or hydrogen atoms are needed to form compounds with each element. For example, in Group I, two atoms of hydrogen (H), lithium (Li), sodium (Na), and potassium (K) form compounds

with one atom of oxygen. In Group VII, one atom of fluorine (F), chlorine (Cl), and bromine (Br), reacts with one atom of hydrogen. Notice how this approach has trouble with the transition metals. Until roughly 1960, a rectangular table developed from Mendeleev's table and based on reactivity was standard at the front of chemistry lecture halls.

The most convincing evidence in support of Mendeleev's arrangement of the elements was the discovery of two previously unknown elements whose properties closely corresponded with his predictions (Table 3.4.1). Two of the blanks Mendeleev had left in his original table were below aluminum and silicon, awaiting the discovery of two as-yet-unknown elements, *eka*-aluminum and *eka*-silicon (from the Sanskrit *eka*, meaning "one," as in "one beyond aluminum"). The observed properties of gallium and germanium matched those of *eka*-aluminum and *eka*-silicon so well that once they were discovered, Mendeleev's periodic table rapidly gained acceptance.

YouTube Video

This interactive element is not available in this format. Visit the link or scan the QR code to access it online.

View this YouTube Video online

Table 3.4.1 Comparison of the properties predicted by Mendeleev in 1869 for *eka*-aluminum and *eka*-silicon with the properties of gallium (discovered in 1875) and germanium (discovered in 1886)

Property	*eka*-Aluminum (predicted)	Gallium (observed)	*eka*-Silicon (predicted)	Germanium (observed)
atomic mass	68	69.723	72	72.64
element	metal	metal	dirty-gray metal	gray-white metal
	low mp*	mp = 29.8°C	high mp	mp = 938°C
	d = 5.9 g/cm^3	d = 5.91 g/cm^3	d = 5.5 g/cm^3	d = 5.323 g/cm^3
oxide	E_2O_3	Ga_2O_3	EO_2	GeO_2
	d = 5.5 g/cm^3	d = 6.0 g/cm^3	d = 4.7 g/cm^3	d = 4.25 g/cm^3
chloride	ECl_3	$GaCl_3$	ECl_4	$GeCl_4$
	volatile	mp = 78°C bp* = 201°C	bp < 100°C	bp = 87°C
***mp = melting point; bp = boiling point.**				

When the chemical properties of an element suggested that it might have been assigned the wrong place in earlier tables, Mendeleev carefully reexamined its atomic mass. He discovered, for example, that the atomic masses previously reported for beryllium, indium, and uranium were incorrect. The atomic mass of indium had originally been reported as 75.6, based on an assumed stoichiometry of InO for its oxide. If this atomic mass were correct, then indium would have to be placed in the middle of the nonmetals, between arsenic (atomic mass 75) and selenium (atomic mass 78). Because elemental indium is a silvery-white *metal*, however, Mendeleev postulated that the stoichiometry of its oxide was really In_2O_3 rather than InO. This would mean that indium's atomic mass was actually 113, placing the element between two other metals, cadmium and tin.

One group of elements absent from Mendeleev's table was the noble gases, all of which were discovered more than 20 years later, between 1894 and 1898, by Sir William Ramsay (1852–1916; Nobel Prize in Chemistry 1904). Initially, Ramsay did not know where to place these elements in the periodic table. Argon, the first to be discovered, had an atomic mass of 40. This was greater than chlorine's and comparable to that of potassium; so Ramsay, using the same kind of reasoning as Mendeleev, decided to place the noble gases between the halogens and the alkali metals.

The Role of the Atomic Number in the Periodic Table

Despite its usefulness, Mendeleev's periodic table was based entirely on empirical observation supported by very little understanding. It was not until 1913, when a young British physicist, H. G. J. Moseley (1887–1915), while analyzing the frequencies of x-rays emitted by the elements, discovered that the underlying foundation of the order of the elements was the *atomic number*, not the atomic mass. Moseley hypothesized that the placement of each element in his series corresponded to its atomic number *Z*, which is the number of positive charges (protons) in its nucleus. Argon, for example, although having an atomic mass greater than that of potassium (39.9 amu versus 39.1 amu, respectively), was placed *before* potassium in the periodic table. While analyzing the frequencies of the emitted x-rays, Moseley noticed that the atomic number of argon is 18, whereas that of potassium is 19, which indicated that they were indeed placed correctly. Moseley also noticed three gaps in his table of x-ray frequencies, so he predicted the existence of three unknown elements: technetium (Z = 43), discovered in 1937; promethium (Z = 61), discovered in 1945; and rhenium (Z = 75), discovered in 1925.

H. G. J. Moseley (1887–1915)

Moseley left his research work at the University of Oxford to join the British army as a telecommunications officer during World War I. He was killed during the Battle of Gallipoli in Turkey.

Example 3.4.1

Before its discovery in 1999, some theoreticians believed that an element with a Z of 114 existed in nature. Use Mendeleev's reasoning to name element 114 as *eka*-_____; then identify the known element whose chemistry you predict would be most similar to that of element 114.

Given: atomic number

Asked for: name using prefix *eka*-

Strategy:

A Using the periodic table locate the n = 7 row. Identify the location of the unknown element with Z = 114; then identify the known element that is directly above this location.

B Name the unknown element by using the prefix *eka*- before the name of the known element.

Solution:

A The n = 7 row can be filled in by assuming the existence of elements with atomic numbers greater than 112, which is underneath mercury (Hg). Counting three boxes to the right gives element 114, which lies directly below lead (Pb). **B** If Mendeleev were alive today, he would call element 114 *eka*-lead.

Exercise

Use Mendeleev's reasoning to name element 112 as *eka*-_____; then identify the known element whose chemistry you predict would be most similar to that of element 112.

Answer: *eka*-mercury

Summary

The periodic table arranges the elements according to their electron configurations, such that elements in the same column have the same valence electron configurations. Periodic variations in size and chemical properties are important factors in dictating the types of chemical reactions the elements undergo and the kinds of chemical compounds they form. The modern periodic table was based on empirical correlations of properties such as atomic mass; early models using limited data noted the existence of **triads** and **octaves** of elements with similar properties. The periodic table achieved its current form through the work of Dimitri Mendeleev and Julius Lothar Meyer, who both focused on the relationship between atomic mass and chemical properties. Meyer arranged the elements by their atomic volume, which today is equivalent to the **molar volume**, defined as molar mass divided by

molar density. The correlation with the electronic structure of atoms was made when H. G. J. Moseley showed that the periodic arrangement of the elements was determined by atomic number, not atomic mass.

Key Takeaways

- The elements in the periodic table are arranged according to their properties, and the periodic table serves as an aid in predicting chemical behavior.

Conceptual Problems

1. Johannes Dobereiner is credited with developing the concept of chemical triads. Which of the group 15 elements would you expect to compose a triad? Would you expect B, Al, and Ga to act as a triad? Justify your answers.

2. Despite the fact that Dobereiner, Newlands, Meyer, and Mendeleev all contributed to the development of the modern periodic table, Mendeleev is credited with its origin. Why was Mendeleev's periodic table accepted so rapidly?

3. How did Moseley's contribution to the development of the periodic table explain the location of the noble gases?

4. The *eka*- naming scheme devised by Mendeleev was used to describe undiscovered elements.

    1. Use this naming method to predict the atomic number of *eka*-mercury, *eka*-astatine, *eka*-thallium, and *eka*-hafnium.
    2. Using the *eka*-prefix, identify the elements with these atomic numbers: 79, 40, 51, 117, and 121.

Numerical Problem

1. Based on the data given, complete the table.

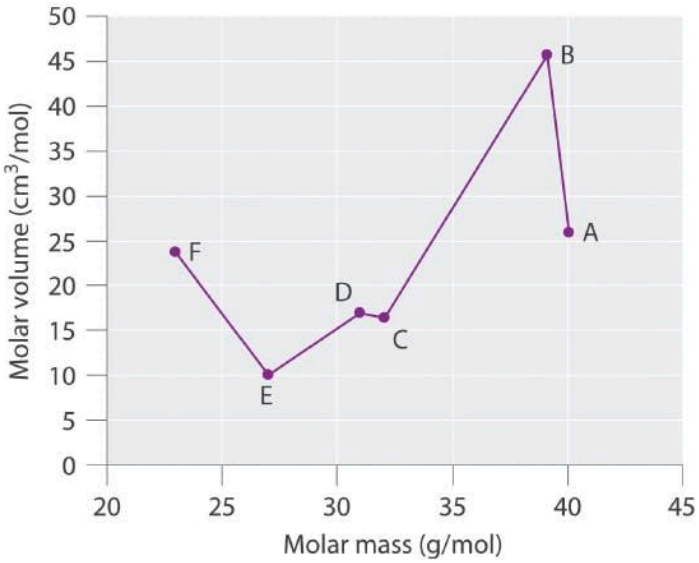
Species	Molar Mass (g/mol)	Density (g/cm^3)	Molar Volume (cm^3/mol)
A	40.078		25.85
B	39.09	0.856	
C	32.065		16.35
D		1.823	16.98
E	26.98		9.992
F	22.98	0.968	

Plot molar volume versus molar mass for these substances. According to Meyer, which would be considered metals and which would be considered nonmetals?

Answer

1.

Species	Molar Mass (g/mol)	Density (g/cm^3)	Molar Volume (cm^3/mol)
A	**40.078**	1.550	**25.85**
B	**39.09**	**0.856**	45.67
C	**32.065**	1.961	**16.35**
D	30.95	**1.823**	**16.98**
E	**26.98**	2.700	**9.992**
F	**22.98**	**0.968**	23.7



Meyer found that the alkali metals had the highest molar volumes, and that molar volumes decreased steadily with increasing atomic mass, then leveled off, and finally rose again. The elements located on the rising portion of a plot of molar volume versus molar mass were typically nonmetals. If we look at the plot of the data in the table, we can immediately identify those elements with the largest molar volumes (A, B, F) as metals located on the left side of the periodic table. The element with the smallest molar volume (E) is aluminum. The plot shows that the subsequent elements (C, D) have molar volumes that are larger than that of E, but smaller than those of A and B. Thus, C and D are most likely to be nonmetals (which is the case: C = sulfur, D = phosphorus).

Contributors and Attributions

- Anonymous

Modified by Joshua Halpern

Video from TED-Ed Lou Serocp

This page titled 2.1.1: The Periodic Table is shared under a license and was authored, remixed, and/or curated by LibreTexts.

- 2.1.1: The Periodic Table is licensed CC BY-NC-SA 4.0.

2.1.2: Discovery of Subatomic Particles and the Bohr Atom

Hydrogen Absorption and Emission Spectra

When a high-voltage electrical discharge is passed through a sample of hydrogen gas (H_2) at low pressure, the result is individual isolated hydrogen atoms that emit a red light. Unlike blackbody radiation, the color of the light emitted by the hydrogen atoms does not depend greatly on the temperature of the gas in the tube. When the emitted light is passed through a prism, only a few narrow lines of particular wavelengths, called a line spectrum, are observed rather than a continuous range of wavelengths (Figure 2.1.2.1). The light emitted by hydrogen atoms is red because, of its four characteristic lines, the most intense line in its spectrum is in the red portion of the visible spectrum, at 656 nm.

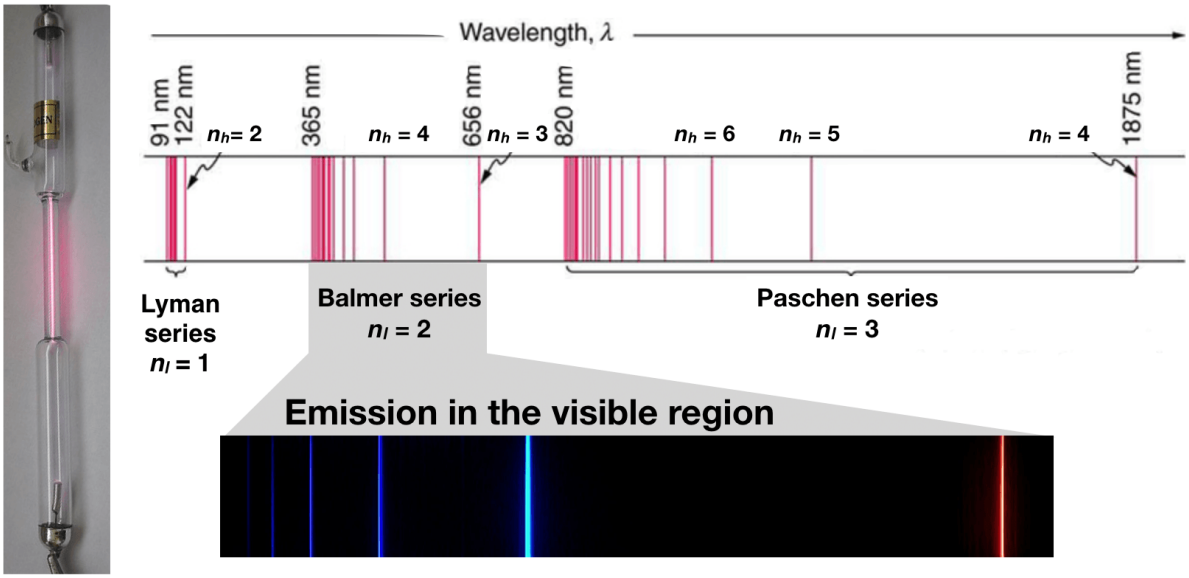


Figure 2.1.2.1: The emission of light by hydrogen atoms. (left) A sample of excited hydrogen atoms emits a characteristic red light. (bottom) When the light emitted by a sample of excited hydrogen atoms is split into its component wavelengths by a prism, four characteristic violet, blue, green, and red emission lines can be observed, with the most intense at 656 nm. (top) A diagram showing extended regions of the electromagnetic spectrum and the hydrogen line spectra that are observed. (Kathryn Haas; CC-BY-SA)

The Balmer Series

In 1885, a Swiss mathematics teacher, Johann Balmer (1825–1898), showed that the frequencies of the lines observed in the visible region of the hydrogen line spectrum fit a simple equation that can be expressed as follows:

$$u = constant\ \left(\frac{1}{2^2} - \frac{1}{n^2}\right) \tag{2.1.2.1}$$

where *n* = 3, 4, 5, 6. As a result, these lines are known as the *Balmer series*. The Swedish physicist Johannes Rydberg (1854–1919) subsequently restated and expanded Balmer's result in the *Rydberg equation*:

$$\frac{1}{\lambda} = R_H\ \left(\frac{1}{n_l^2} - \frac{1}{n_h^2}\right) \tag{2.1.2.2}$$

,

where n_l and n_h are positive integers, $n_h > n_l$, and R_H, the *Rydberg constant*, has a value of 1.09737 × 10^7 m^{-1}. Like Balmer's equation, Rydberg's simple equation described the wavelengths of the visible lines in the emission spectrum of hydrogen (with $n_l = 2, n_h = 3, 4, 5, ...$). More importantly, Rydberg's equation also predicted the wavelengths of other series of lines that would be observed in the emission spectrum of hydrogen: one in the ultraviolet ($n_l = 1, n_h = 2, 3, 4, ...$) and one in the infrared ($n_l = 3, n_h$

$= 4, 5, 6$).

Other Series

The results given by Balmer and Rydberg for the spectrum in the visible region of the electromagnetic spectrum start with $n_h = 3$, and $n_l = 2$.

Is there a different series with the following formula (e.g., $n_l = 1$)?

$$\frac{1}{\lambda} = R_{\mathrm{H}} \left(\frac{1}{1^2} - \frac{1}{n^2} \right) \tag{2.1.2.3}$$

The values for n_h and wavenumber u for this series would be:

Table 2.1.2.1*: The Lyman Series of Hydrogen Emission Lines* ($n_l = 1$)

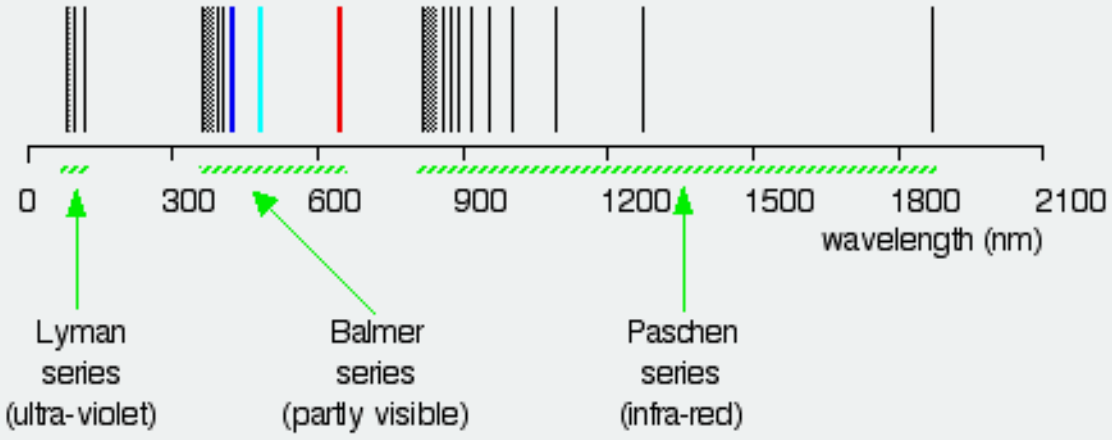
n_h	2	3	4	5
λ **(nm)**	121	102	97	94
$\tilde{u}$ **(cm^{-1})**	82,2291	97,530	102,864	105,332

Do you know what region of the electromagnetic radiation these lines are in? Of course, these lines are in the UV region, and they are not visible, but they are detected by instruments; these lines form a **Lyman series**. The existences of the Lyman series and Balmer's series suggest the existence of more series. For example, the series with $n_2^2 = 3$ and n_1^2 = 4, 5, 6, 7, ... is called the **Pashen series**.

Multiple series

The spectral lines are grouped into series according to n_1 values. Lines are named sequentially starting from the longest wavelength/lowest frequency of the series using Greek letters within each series. For example, the ($n_1 = 1/n_2 = 2$) line is called "Lyman-alpha" (Ly-α), while the ($n_1 = 3/n_2 = 7$) line is called "Paschen-delta" (Pa-δ). The first six series have specific names:

- Lyman series with $n_1 = 1$
- Balmer series with $n_1 = 2$
- Paschen series (or Bohr series) with $n_1 = 3$
- Brackett series with $n_1 = 4$
- Pfund series with $n_1 = 5$
- Humphreys series with $n_1 = 6$



The spectral series of hydrogen based on the Rydberg Equation (on a logarithmic scale).

Example 2.1.2.1: The Lyman Series

The so-called Lyman series of lines in the emission spectrum of hydrogen corresponds to transitions from various excited states to the *n* = 1 orbit. Calculate the wavelength of the lowest-energy line in the Lyman series to three significant figures. In what region of the electromagnetic spectrum does it occur?

Given: lowest-energy orbit in the Lyman series

Asked for: wavelength of the lowest-energy Lyman line and corresponding region of the spectrum

Strategy:

A. Substitute the appropriate values into Equation $Ref2.1.2.2$ (the Rydberg equation) and solve for λ.
B. Locate the region of the electromagnetic spectrum corresponding to the calculated wavelength.

Solution:

We can use the Rydberg equation (Equation $Ref2.1.2.2$ to calculate the wavelength:

$$\frac{1}{\lambda} = R_H \left(\frac{1}{n_l^2} - \frac{1}{n_h^2} \right)$$

A For the Lyman series, $n_1 = 1$.

$$\begin{aligned} \frac{1}{\lambda} &= R_H \left(\frac{1}{n_l^2} - \frac{1}{n_h^2} \right) \\ &= 1.097 \times m^{-1} \left(\frac{1}{1} - \frac{1}{4} \right) \\ &= 8.228 \times 10^6 \; m^{-1} \end{aligned}$$

Spectroscopists often talk about energy and frequency as equivalent. The cm^{-1} unit (wavenumbers) is particularly convenient. We can convert the answer in part A to cm^{-1}.

$$\begin{aligned} \tilde{u} &= \frac{1}{\lambda} \\ &= 8.228 \times 10^6 \; \cancel{m^{-1}} \left(\frac{\cancel{m}}{100 \; cm} \right) \\ &= 82,280 \; cm^{-1} \end{aligned}$$

and

$$\lambda = 1.215 \times 10^{-7} \; m = 122 \; nm$$

This emission line is called Lyman alpha and is the strongest atomic emission line from the sun; it drives the chemistry of the upper atmosphere of all the planets producing ions by stripping electrons from atoms and molecules. It is completely absorbed by oxygen in the upper stratosphere, dissociating O_2 molecules to O atoms, which react with other O_2 molecules to form stratospheric ozone (O_3).

B This wavelength is in the ultraviolet region of the spectrum.

Exercise 2.1.2.1: The Pfund Series

The Pfund series of lines in the emission spectrum of hydrogen corresponds to transitions from higher excited states to $n_1 = 5$. Calculate the wavelength of the *second* line in the Pfund series to three significant figures. In which region of the spectrum does it lie?

Answer available at the end of this section.

The above discussion presents only a phenomenological description of hydrogen emission lines. Balmer and Rydberg could predict where emission lines could occur, but they could not explain why lines followed this pattern using any useful theory. For an explanation of why atoms demonstrate discrete emission spectra, quantum theories were developed.

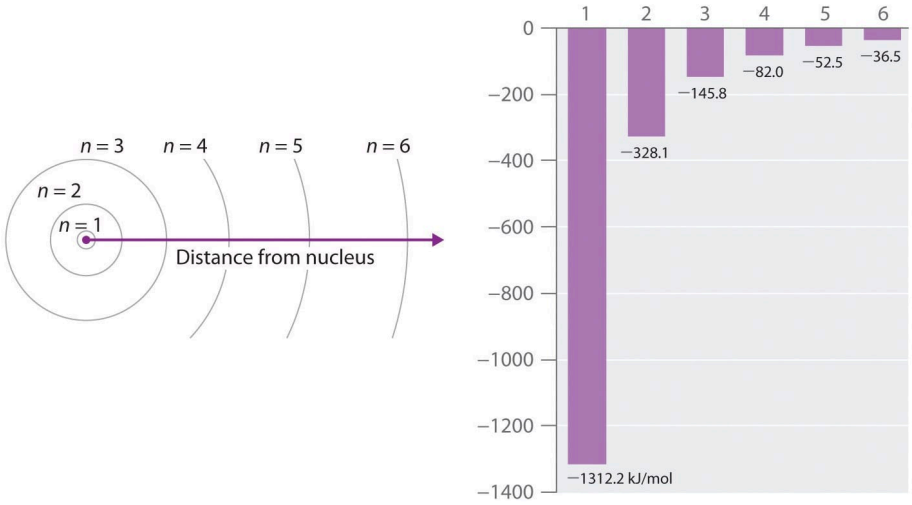
The Bohr Model

In 1913, a Danish physicist, Niels Bohr (1885–1962; Nobel Prize in Physics, 1922), proposed a theoretical model for the hydrogen atom that explained its emission spectrum. Bohr's model required only one assumption: *The electron moves around the nucleus in circular orbits that can have only certain allowed radii.* Rutherford's earlier model of the atom had also assumed that electrons moved in circular orbits around the nucleus and that the atom was held together by the electrostatic attraction between the positively charged nucleus and the negatively charged electron. Although we now know that the assumption of circular orbits was incorrect, Bohr's insight also posited that *the electron could occupy only certain regions of space*.

Using classical physics, Niels Bohr showed that the energy of an electron in a particular orbit is given by

$$E_n = \frac{-R_H hc}{n^2} \tag{2.1.2.4}$$

where R_H is the Rydberg constant, *h* is Planck's constant, *c* is the speed of light, and *n* is a positive integer corresponding to the number assigned to the orbit, with *n* = 1 corresponding to the orbit closest to the nucleus. In this model *n* = ∞ corresponds to the level where the energy holding the electron and the nucleus together is zero. In that level, the electron is unbound from the nucleus and the atom has been separated into a negatively charged (the electron) and a positively charged (the nucleus) ion. In this state the radius of the orbit is also infinite. The atom has been ionized.



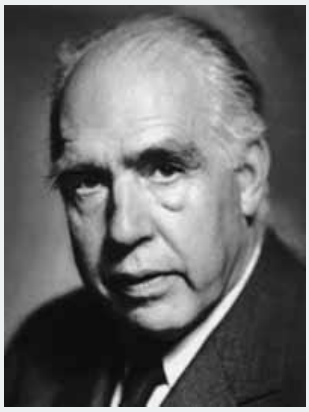
(a) Hydrogen orbits (Bohr model). Orbits are not drawn to scale.

(b) Hydrogen orbit energy (kJ/mol) vs. *n*

Figure 2.1.2.2: *The Bohr Model of the hydrogen atom (a) The distance of the orbit from the nucleus increases with increasing n. (b) The energy of the orbit becomes increasingly less negative with increasing n.*

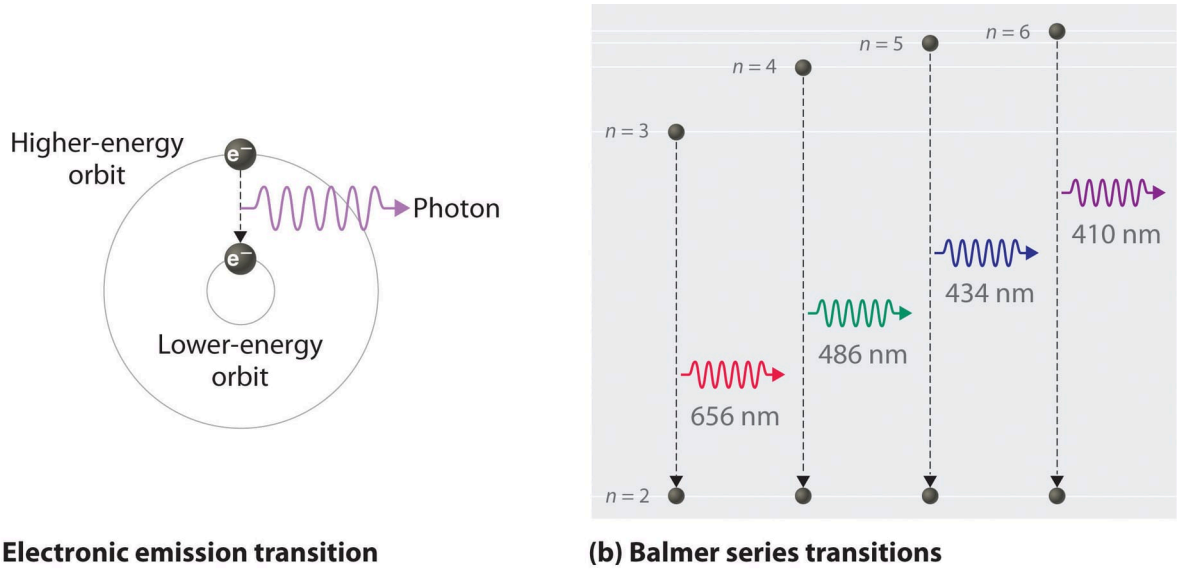
Niels Bohr (1885–1962)

During the Nazi occupation of Denmark in World War II, Bohr escaped to the United States, where he became associated with the Atomic Energy Project.



In his final years, he devoted himself to the peaceful application of atomic physics and to resolving political problems arising from the development of atomic weapons.

As n decreases, the energy holding the electron and the nucleus together becomes increasingly negative; the radius of the orbit shrinks and more energy is needed to ionize the atom. The orbit with n = 1 is the lowest lying and most tightly bound. The negative sign in Equation ??? indicates that the electron-nucleus pair is more tightly bound (i.e. at a lower potential energy) when they are near each other than when they are far apart. Because a hydrogen atom with its one electron in this orbit has the lowest possible energy, this is the **ground state** (the most stable arrangement of electrons for an element or a compound) for a hydrogen atom. As n increases, the radius of the orbit increases; the electron is farther from the proton, which results in a less stable arrangement with higher potential energy (Figure 2.1.2.2a). A hydrogen atom with an electron in an orbit with n > 1 is therefore in an **excited state**, defined as any arrangement of electrons that is higher in energy than the ground state. When an atom in an excited state undergoes a transition to the ground state in a process called decay, it loses energy by emitting a photon whose energy corresponds to the *difference* in energy between the two states (Figure 2.1.2.1).



(a) Electronic emission transition **(b) Balmer series transitions**

Figure 2.1.2.3: *The emission of light by a hydrogen atom in an excited state. (a) Light is emitted when the electron undergoes a transition from an orbit with a higher value of n (at a higher energy) to an orbit with a lower value of n (at lower energy). (b) The Balmer series of emission lines is due to transitions from orbits with n ≥ 3 to the orbit with n = 2. The differences in energy between these levels correspond to light in the visible portion of the electromagnetic spectrum.*

So the difference in energy (Δ*E*) between any two orbits or energy levels is given by $\Delta E = E_{n_l} - E_{n_h}$, where n_l is the final orbit and n_h the initial orbit. Substituting from Bohr's equation (Equation 2.1.2.4) for each energy value gives

$$\Delta E = E_{final} - E_{initial} = -\frac{R_H hc}{n_h^2} - \left(-\frac{R_H hc}{n_l^2}\right) = -R_H hc\left(\frac{1}{n_h^2} - \frac{1}{n_l^2}\right) \tag{2.1.2.5}$$

If $n_h > n_l$, the transition is from a higher energy state (larger-radius orbit) to a lower energy state (smaller-radius orbit), as shown by the dashed arrow in part (a) in Figure 2.1.2.3. Substituting *hc*/λ for Δ*E* gives

$$\Delta E = \frac{hc}{\lambda} = -R_H hc\left(\frac{1}{n_h^2} - \frac{1}{n_l^2}\right) \tag{2.1.2.6}$$

Canceling *hc* on both sides gives

$$\frac{1}{\lambda} = -R_H\left(\frac{1}{n_h^2} - \frac{1}{n_l^2}\right) \tag{2.1.2.7}$$

Except for the negative sign, this is the same equation that Rydberg obtained experimentally. The negative sign in Equations 2.1.2.6 and 2.1.2.7 indicates that energy is released as the electron moves from orbit n_h to orbit n_l because orbit n_h is at a higher energy than orbit n_l. Bohr calculated the value of R_H from fundamental constants such as the charge and mass of the electron and Planck's constant and obtained a value of 1.0974 × 10^7 m^{-1}, the same number Rydberg had obtained by analyzing the emission spectra.

We can now understand the physical basis for the Balmer series of lines in the emission spectrum of hydrogen ($2.1.2.3b$); the lines in this series correspond to transitions from higher-energy orbits (n > 2) to the second orbit (n = 2). Thus, the hydrogen atoms in the sample have absorbed energy from the electrical discharge and decayed from a higher-energy excited state (n > 2) to a lower-energy state (n = 2) by emitting a photon of electromagnetic radiation whose energy corresponds exactly to the difference in energy between the two states (Figure $2.1.2.3a$). The n = 3 to n = 2 transition gives rise to the line at 656 nm (red), the n = 4 to n = 2 transition to the line at 486 nm (green), the n = 5 to n = 2 transition to the line at 434 nm (blue), and the n = 6 to n = 2 transition to the line at 410 nm (violet). Because a sample of hydrogen contains a large number of atoms, the intensity of the various lines in a line spectrum depends on the number of atoms in each excited state. At the temperature in the gas discharge tube, more atoms are in the n = 3 than the n ≥ 4 levels. Consequently, the n = 3 to n = 2 transition is the most intense line, producing the characteristic red color of a hydrogen discharge (Figure $2.1.2.1a$). Other families of lines are produced by transitions from excited states with n > 1 to the orbit with n = 1 or to orbits with n ≥ 3. These transitions are shown schematically in Figure $2.1.2.4$:

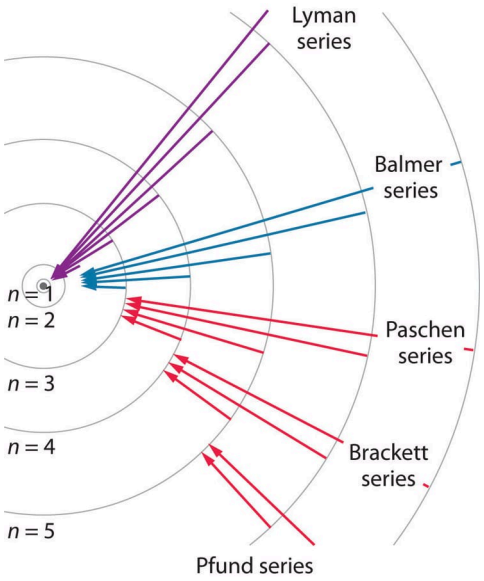


Figure 2.1.2.4: Electron transitions responsible for the various series of lines observed in the emission spectrum of hydrogen. The Lyman series of lines is due to transitions from higher-energy orbits to the lowest-energy orbit (n = 1); these transitions release a great deal of energy, corresponding to radiation in the ultraviolet portion of the electromagnetic spectrum. The Paschen, Brackett, and Pfund series of lines are due to transitions from higher-energy orbits to orbits with n = 3, 4, and 5, respectively; these transitions release substantially less energy, corresponding to infrared radiation. (Orbits are not drawn to scale.)

Using Atoms to Time

In contemporary applications, electron transitions are used in timekeeping that needs to be exact. Telecommunications systems, such as cell phones, depend on timing signals that are accurate within a millionth of a second per day; the same goes for the devices that control the US power grid. Global positioning system (GPS) signals must be accurate within a billionth of a second per day, which is equivalent to gaining or losing no more than one second in 1,400,000 years. Quantifying time requires finding an event with an interval that repeats on a regular basis.

To achieve the accuracy required for modern purposes, physicists have turned to the atom. The current standard used to calibrate clocks is the cesium atom. Supercooled cesium atoms are placed in a vacuum chamber and bombarded with microwaves whose frequencies are carefully controlled. When the frequency is exactly right, the atoms absorb enough energy to undergo an electronic transition to a higher-energy state. Decay to a lower-energy state emits radiation. The microwave frequency is continually adjusted, serving as the clock's pendulum.

In 1967, the second was defined as the duration of 9,192,631,770 oscillations of the resonant frequency of a cesium atom, called the *cesium clock*. Research is currently under way to develop the next generation of atomic clocks that promise to be even more accurate. Such devices would allow scientists to monitor vanishingly faint electromagnetic signals produced by nerve pathways in the brain and allow geologists to measure variations in gravitational fields, which cause fluctuations in time, that would aid in the discovery of oil or minerals.

Example 2.1.2.1: The Lyman Series

The so-called Lyman series of lines in the emission spectrum of hydrogen corresponds to transitions from various excited states to the n = 1 orbit. Calculate the wavelength of the lowest-energy line in the Lyman series to three significant figures. In what region of the electromagnetic spectrum does it occur?

Given: lowest-energy orbit in the Lyman series

Asked for: wavelength of the lowest-energy Lyman line and corresponding region of the spectrum

Strategy:

A. Substitute the appropriate values into Equation 2.1.2.4 (the Rydberg equation) and solve for λ.
B. Use Figure 2.2.1 to locate the region of the electromagnetic spectrum corresponding to the calculated wavelength.

Solution:

We can use the Rydberg equation to calculate the wavelength:

$$\frac{1}{\lambda} = -R_H \left(\frac{1}{n_h^2} - \frac{1}{n_l^2} \right)$$

A For the Lyman series, /(n_l = 1\). The lowest-energy line is due to a transition from the *n* = 2 to *n* = 1 orbit because they are the closest in energy.

$$\frac{1}{\lambda} = -R_H \left(\frac{1}{n_h^2} - \frac{1}{n_l^2} \right) = 1.097 \times m^{-1} \left(\frac{1}{1} - \frac{1}{4} \right) = 8.228 \times 10^6 \; m^{-1}$$

It turns out that spectroscopists (the people who study spectroscopy) use cm^{-1} rather than m^{-1} as a common unit. Wavelength is inversely proportional to energy but frequency is directly proportional as shown by Planck's formula, E=hu.

Spectroscopists often talk about energy and frequency as equivalent. The cm^{-1} unit is particularly convenient. The infrared range is roughly 200 - 5,000 cm^{-1}, the visible from 11,000 to 25,000 cm^{-1} and the UV between 25,000 and 100,000 cm^{-1}. The units of cm^{-1} are called wavenumbers, although people often refer to the unit as inverse centimeters. We can convert the answer in part A to cm^{-1}.

$$\tilde{u} = \frac{1}{\lambda} = 8.228 \times 10^6 \; \cancel{m^{-1}} \left(\frac{\cancel{m}}{100 \; cm} \right) = 82,280 \; cm^{-1}$$

and

$$\lambda = 1.215 \times 10^{-7} \; m = 122 \; nm$$

This emission line is called Lyman alpha. As the strongest atomic emission line from the sun, it drives the chemistry of the upper atmosphere of all the planets, producing ions by stripping electrons from atoms and molecules. It is completely absorbed by oxygen in the upper stratosphere, dissociating O_2 molecules to O atoms which react with other O_2 molecules to form stratospheric ozone.

B This wavelength is in the ultraviolet region of the spectrum.

Exercise 2.1.2.1: The Pfund Series

The Pfund series of lines in the emission spectrum of hydrogen corresponds to transitions from higher excited states to the *n* = 5 orbit. Calculate the wavelength of the *second* line in the Pfund series to three significant figures. In which region of the spectrum does it lie?

Answer available at the end of this section.

Bohr's model of the hydrogen atom gave an exact explanation for its observed emission spectrum. The following are his key contributions to our understanding of atomic structure:

- Electrons can occupy only certain regions of space, called *orbits*.
- Orbits closer to the nucleus are lower in energy.
- Electrons can move from one orbit to another by absorbing or emitting energy, giving rise to characteristic spectra.

Unfortunately, Bohr could not explain *why* the electron should be restricted to particular orbits. Also, despite a great deal of conjecturing, such as assuming that orbits could be ellipses rather than circles, his model could not quantitatively explain the emission spectra of any element other than hydrogen (Figure 2.1.2.5). In fact, Bohr's model worked only for species that contained

just one electron: H, He^{+}, Li^{2+}, and so forth. Scientists needed a fundamental change in their way of thinking about the electronic structure of atoms to advance beyond the Bohr model.

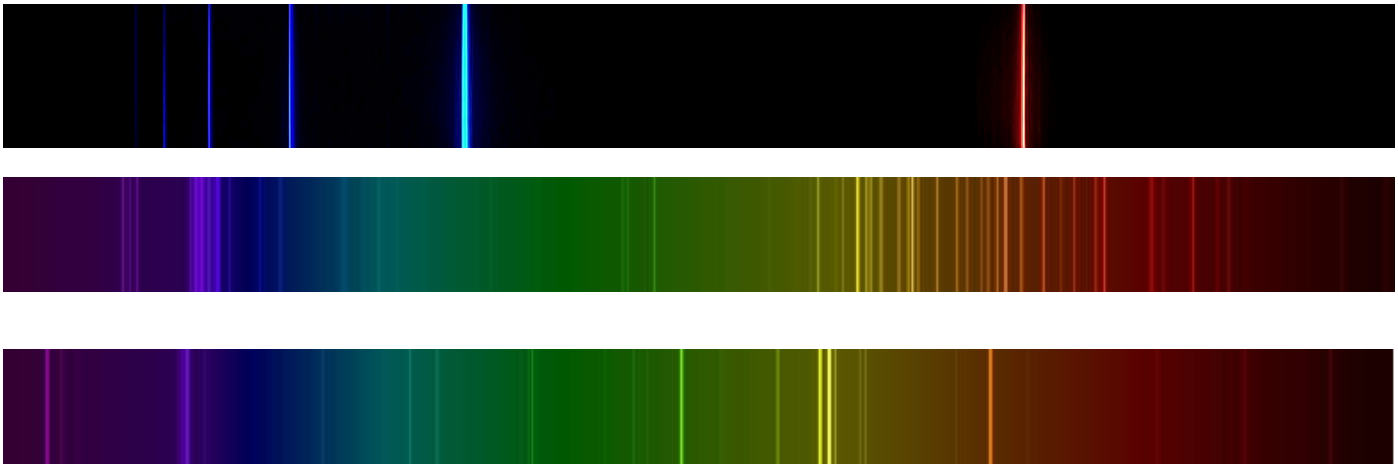


Figure 2.1.2.5: The emission spectra of elements compared to hydrogen. **Top:** hydrogen gas (atomized to hydrogen atoms in the discharge tube). **Middle:** neon. **Bottom:** mercury. The strongest lines in the hydrogen spectrum are in the far UV Lyman series starting at 124 nm and below. The strongest lines in the mercury spectrum are at 181 and 254 nm, also in the UV. These are not shown. Attribution: Hydrogen (Jan Homann / CC BY-SA); Neon (Teravolt at en.Wikipedia / Public domain); Mercury (Teravolt at en.Wikipedia / Public domain)

The Energy States of the Hydrogen Atom

Thus far, we have explicitly considered only the emission of light by atoms in excited states, which produces an emission spectrum (a spectrum produced by the emission of light by atoms in excited states). The converse, absorption of light by ground-state atoms to produce an excited state, can also occur, producing an absorption spectrum (a spectrum produced by the absorption of light by ground-state atoms).

> When an atom emits light, it decays to a lower energy state; when an atom absorbs light, it is excited to a higher energy state.

If white light is passed through a sample of hydrogen, hydrogen atoms absorb energy as an electron is excited to higher energy levels (orbits with $n \geq 2$). If the light that emerges is passed through a prism, it forms a continuous spectrum with *black* lines (corresponding to no light passing through the sample) at 656, 468, 434, and 410 nm. These wavelengths correspond to the $n = 2$ to $n = 3$, $n = 2$ to $n = 4$, $n = 2$ to $n = 5$, and $n = 2$ to $n = 6$ transitions. Any given element therefore has both a characteristic emission spectrum and a characteristic absorption spectrum, which are essentially complementary images.

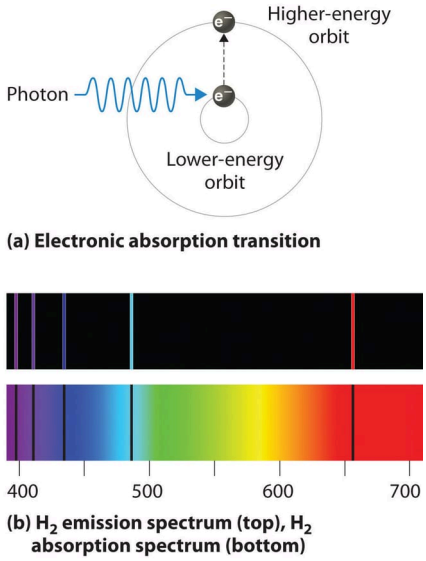


Figure 2.1.2.6: Absorption and emission spectra. Absorption of light by a hydrogen atom. (a) When a hydrogen atom absorbs a photon of light, an electron is excited to an orbit that has a higher energy and larger value of n. (b) Images of the emission and absorption spectra of hydrogen are shown here.

Emission and absorption spectra form the basis of *spectroscopy*, which uses spectra to provide information about the structure and the composition of a substance or an object. In particular, astronomers use emission and absorption spectra to determine the composition of stars and interstellar matter. As an example, consider the spectrum of sunlight shown in Figure 2.1.2.7. Since the sun is very hot, it emits light in the form of a continuous emission spectrum. Superimposed on the spectrum, however, is a series of dark lines primarily resulting from the absorption of specific frequencies of light by cooler atoms in the outer atmosphere of the sun. By comparing these lines with the spectra of elements measured on Earth, we now know that the sun contains large amounts of hydrogen, iron, and carbon, along with smaller amounts of other elements. During the solar eclipse of 1868, the French astronomer Pierre Janssen (1824–1907) observed a set of lines that did not match those of any known element. He suggested that they were due to the presence of a new element, which he named *helium*, from the Greek *helios*, meaning "sun." Helium (He) was finally discovered in uranium ores on Earth in 1895. Alpha particles are helium nuclei. Alpha particles emitted by radioactive uranium nuclei pick up electrons from the rocks to form helium atoms.

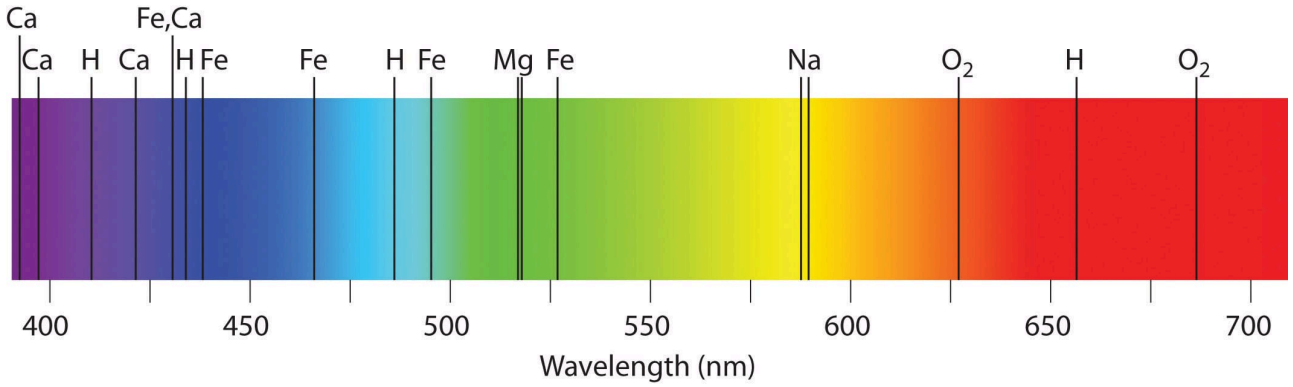


Figure 2.1.2.7: *The visible spectrum of sunlight. The characteristic dark lines are mostly due to the absorption of light by elements that are present in the cooler outer part of the sun's atmosphere; specific elements are indicated by the labels. The lines at 628 and 687 nm, however, are due to the absorption of light by oxygen molecules in Earth's atmosphere.*

The familiar red color of neon signs used in advertising is due to the emission spectrum of neon shown in part (b) in Figure 2.1.2.5 . Similarly, the blue and yellow colors of certain street lights are caused, respectively, by mercury and sodium discharges. In all these cases, an electrical discharge excites neutral atoms to a higher energy state, and light is emitted when the atoms decay to the ground state. In the case of mercury, most of the emission lines are below 450 nm, which produces a blue light (part (c) in Figure 2.1.2.5). In the case of sodium, the most intense emission lines are at 589 nm, which produces an intense yellow light.

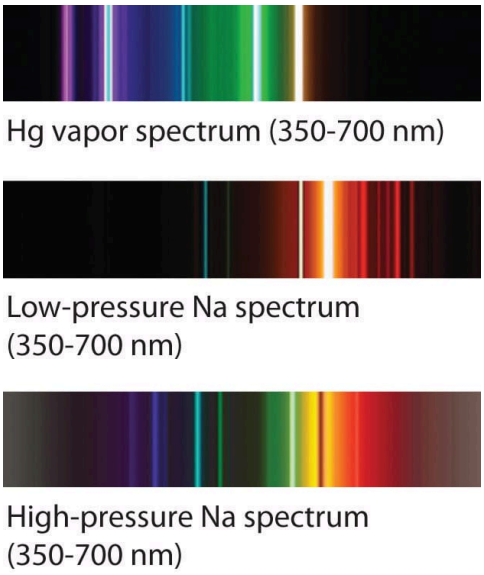


Figure 2.1.2.8: *The emission spectra of sodium and mercury. Many street lights use bulbs that contain sodium or mercury vapor. Due to the very different emission spectra of these elements, they emit light of different colors. The lines in the sodium lamp are broadened by collisions. The dark line in the center of the high pressure sodium lamp where the low pressure lamp is strongest is caused by absorption of light in the cooler outer part of the lamp.*

Summary

There is an intimate connection between the atomic structure of an atom and its spectral characteristics. Atoms of individual elements emit light at only specific wavelengths, producing a **line spectrum** rather than the continuous spectrum of all wavelengths produced by a hot object. Niels Bohr explained the line spectrum of the hydrogen atom by assuming that the electron moved in circular orbits and that orbits with only certain radii were allowed. Lines in the spectrum were due to transitions in which an electron moved from a higher-energy orbit with a larger radius to a lower-energy orbit with smaller radius. The orbit closest to the nucleus represented the **ground state** of the atom and was most stable; orbits farther away were higher-energy **excited states**. Transitions from an excited state to a lower-energy state resulted in the emission of light with only a limited number of wavelengths. Atoms can also absorb light of certain energies, resulting in a transition from the ground state or a lower-energy excited state to a higher-energy excited state. This produces an **absorption spectrum**, which has dark lines in the same position as the bright lines in the **emission spectrum** of an element. Bohr's model revolutionized the understanding of the atom but could not explain the spectra of atoms heavier than hydrogen.

Contributors and Attributions

- Modified by Joshua Halpern (Howard University)

Answers

Exercise 2.1.2.1: The Pfund Series

$4.65 \times 10^3\ nm$; infrared

Exercise 2.1.2.1: The Pfund Series

4.65 × 10^3 nm; infrared

This page titled 2.1.2: Discovery of Subatomic Particles and the Bohr Atom is shared under a license and was authored, remixed, and/or curated by LibreTexts.

- 2.1.2: Discovery of Subatomic Particles and the Bohr Atom is licensed CC BY-NC-SA 3.0.

2.2: THE SCHRÖDINGER EQUATION, PARTICLE IN A BOX, AND ATOMIC WAVEFUNCTIONS

Considering the failures of the Bohr model, Erwin Schrödinger and Werner Heisenberg proposed a major change in the paradigm regarding the electron. In several breakthrough papers (1925-1927) they attributed wave properties to electrons and they each received Nobel prizes for developing the theories of Wave Mechanics (or the "New Quantum Mechanics"). This approach treated electrons as having "dual" nature: possessing properties of *both* waves and particles.

Schrödinger's Equation describes the behavior of the electron (in a hydrogen atom) in three dimensions. It is a mathematical equation that defines the electron's position, mass, total energy, and potential energy. The simplest form of the Schrödinger Equation is as follows:

$$\hat{H}\psi = E\psi$$

where $\hat{H}$ is the **Hamiltonian operator**, E is the **energy of the electron**, and ψ is the **wavefunction**.

The Hamiltonian, $\hat{H}$

The Hamiltonian operator is like a set of instructions that tells us what to do with the function that follows it. A Hamiltonian operator is a function over three-dimensional space that corresponds to the sum of kinetic energies and potential energies of the particles in a system, one electron and its nucleus in this case. The Hamiltonian operator for a one-electron system is:

$$\hat{H} = \frac{-h^2}{8\pi^2 m_e}\left(\frac{\partial^2}{\partial x^2} + \frac{\partial^2}{\partial y^2} + \frac{\partial^2}{\partial z^2}\right) - \frac{Ze^2}{4\pi\epsilon_0 r},$$

where h is Planck's constant, m_e is the mass of the electron, e is the charge of the electron, r is the distance from the nucleus ($r = \sqrt{x^2+y^2+z^2}$), Z is the charge of the nucleus, and $4\pi\epsilon_0$ is the permittivity of a vacuum.

Kinetic Energy

The first part of the Hamiltonian written above, $\frac{-h^2}{8\pi^2 m_e}\left(\frac{\partial^2}{\partial x^2} + \frac{\partial^2}{\partial y^2} + \frac{\partial^2}{\partial z^2}\right)$ describes the kinetic energy of the electron. This is the energy due to motion of the electron.

Potential energy

The second part written above, $\frac{-Ze^2}{4\pi\epsilon_0 r}$, describes the potential energy of the electron, and is commonly written as $V(r)$ or $V(x,y,z)$.

$$V(x,y,x) = \frac{-Ze^2}{4\pi\epsilon_0 r} = \frac{-Ze^2}{4\pi\epsilon_0\sqrt{x^2+y^2+z^2}}$$

The potential energy depends on the attractive electrostatic force between the electron and the nucleus. You might notice that this attraction is essentially the same as the electrostatic force defined by Coulomb's law. And, just as in Coulomb's law, when two opposite charges are attracted to one another, the potential energy of the force is negative. Thus, when an electron is close to the nucleus, the potential energy is a large negative number corresponding to a strong attractive force. When an electron is farther from the nucleus, the potential energy is still negative but with a smaller magnitude, corresponding to a weaker attractive force. If the electron is very far from the nucleus ($r = \infty$) then the attractive force, and the potential energy, is zero.

The Wavefunction, ψ

In simple terms, the wavefunction (ψ) of an electron describes the electron's position in space, relative to the nucleus. The square of the ψ describes an atomic orbital. We can't define the position too exactly because we would violate the Heisenberg Uncertainty principle, but we can define its wave. A simple example of a ψ is described in the next section: Particle in a Box. Here, we will describe the ψ in general terms. Generally, in a one-electron atom, the electron ψ is defined by the wave's distance from the nucleus and its angle with respect to the x, y, and z axes of the atom's Cartesian coordinates (the nucleus is at the origin). The general form of the (ψ) for an electron in a hydrogen atom can be written as follows:

$$\psi_{n,l,m_l} = R_{n,l}(r) + Y_{l,m_l}(\theta, \phi)$$

Quantum Numbers define ψ

The (ψ) is defined by three of the quantum numbers: n, l, and m_l. These quantum numbers will be discussed more in a later section (2.2.2) The radial variation, R, depends on the electron's distance from the nucleus. The quantum numbers n (energy level) and l (orbital type) define R. Since n must be an integer, there are only certain allowed values for the solution to the wavefunction.

The angular variation, Y, depends on the angle with respect to the x, y, and z coordinates, and depends on the quantum numbers l (the orbital type) and m_l (the angular momentum, or the specific orbital). For example p_x lies along the x axis, while p_y points in a different direction in space.

For review, a list of the quantum numbers, their values, and meanings are in the table below.

SYMBOL	NAME	VALUES	MEANING
n	principal	$1, 2, 3...$(any integer)	energy level, shell
l	angular momentum	$0 \rightarrow n-1$	subshell, $0 = s, 1 = p, 2 = d, 3 = f...$ this is the angular dependence of the orbital, shape of the orbital *letters have historical meaning, sharp, principle, diffuse, fundamental
m_l	magnetic	$+l \rightarrow -l$	orientation of angular momentum in space, orbital
m_s	spin	$+\frac{1}{2}, -\frac{1}{2}$	the imaginary property we call "spin", up or down

---

Some important considerations and limitations

Although it might seem like there could be any value of x, y, and z for the Hamiltonian, these values are limited by the allowed positions of electrons according to ψ, which is limited by integer values of n. In other words the allowed solutions are *quantized*. However, there are an infinite number of values for n from $n = 1 \rightarrow \infty$, so there are also infinite solutions to the Schrödinger equation.

The ψ describes the wave properties of an electron. The probability of finding the electron somewhere in space is the square of the wavefunction (ψ^2 or $\psi\psi^*$). In other words, ψ^2 describes the shape and size of an electron's orbital (the shapes you already know).

There are some requirements for a physically realistic and meaningful solution for ψ, and thus ψ^2.

1. There is only one possible value for ψ for any set of the three quantum numbers n, l, m_l.
2. The ψ approaches zero as r approaches infinity, and so ψ^2 also approaches zero as $r \rightarrow \infty$.
3. The wavefunction must be normalized. In other words, the total probability of finding the electron in all of space must be 1.

$$\int_{\text{all space}} \psi_A \psi_A^* d\tau = 1$$

4. Any two orbitals must not occupy the same space. In other words, any two orbitals in an atom are orthogonal. If ψ_A and ψ_B

are wavefunctions for different orbitals in the same atom,

$$\int_{\text{all space}} \psi_A \psi_B^* d\tau = 0$$

5. The probability of finding the electron anywhere in infinite space must be defined. This means that the wave functions and their first derivatives must be continuous (i.e. not change abruptly from one point to the next).

Awesome Sources for further reading

- +Plus: https://plus.maths.org/content/schrodinger-1

2.2.1: Particle in a Box

2.2.2: Quantum Numbers and Atomic Wave Functions

2.2.3: Aufbau Principle

2.2.4: Shielding

This page titled 2.2: The Schrödinger equation, particle in a box, and atomic wavefunctions is shared under a CC BY-NC-SA 4.0 license and was authored, remixed, and/or curated by Kathryn Haas.

- 2.2: The Schrödinger equation, particle in a box, and atomic wavefunctions by Kathryn Haas is licensed CC BY-NC-SA 4.0.

2.2.1: Particle in a Box

The particle in the box is a model that can illustrate how a wave equation works. Although it does not represent a real situation, we can limit our model to just one dimension (the x-dimension, for instance) such that the Schrödinger equation becomes significantly simplified. Despite being unrealistic, this simplification is quite useful for gaining an understanding of the Schrödinger equation.

The model of a particle in a box

The particle in the box is a hypothetical situation with a particle trapped in a one-dimensional "box". Let's not get hung-up on the fact that the common object called a "box" is typically an object with three dimensions instead of just one dimension. And let's also not get hung up on the word "particle". This is a particle that has properties of a wave...so it is unlike the macroscopic particle that you're probably imagining. This "box" is more like a line, or an x-axis; it is just a one-dimensional space in which a particle-wave is trapped.

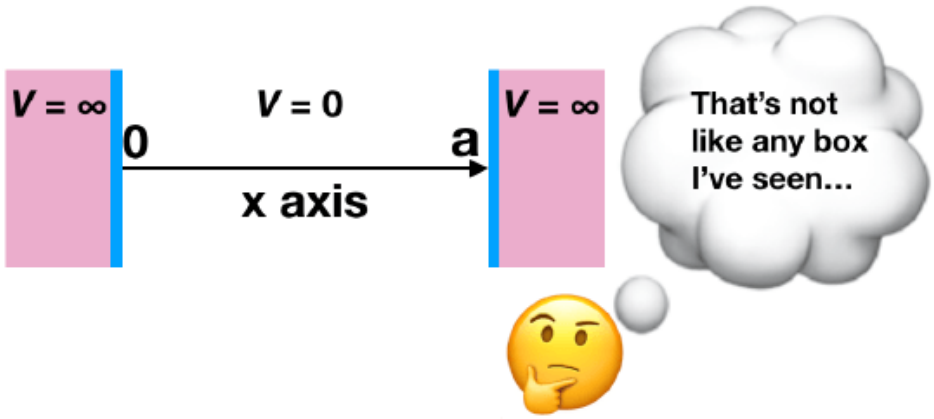


Figure 2.2.1.1. An illustration of the particle in the box model (particle not shown). The box is actually just a one-dimensional space, often assigned to the x-dimension (the x-axis). The particle has wave properties and is trapped in the box. Since no forces act on the particle inside the box, the particle's potential energy inside the box is zero ($V = 0$) and its potential energy outside the box is infinite ($V = \infty$). (CC-BY-NC-SA; Kathryn Haas)

The particle-wave can only exist inside the walls (where $0 < x < a$), along the x axis in the figure shown above. In terms of energy, the potential energy is zero ($V = 0$) because the particle is in an energetically-favorable position here. On the other hand, outside the box, the particle cannot exist and the potential energy is infinitely large ($V = \infty$) outside the walls (where $x < 0$ or $x > a$). This means that it is infinitely unfavorable for the particle-wave to exist outside the box, and so it never does. The particle-wave is trapped between the walls, along the 1-dimensional x axis, and there are no forces acting on the particle-wave inside this "box".

The Schrödinger wave equation for a particle in a box

The particle in a box model lets us consider a simple version of the Schrödinger equation. Before we simplify, let's take another look at the full Hamiltonian for a particle-wave in three dimensions (see equation 2.2.2) and the simplest form of the Schrödinger equation (see equation 2.2.1). Both of these equations are described in the previous section and are written below for convenience.

The Schrödinger Equation (from equation 2.2.1): $\hat{H}\psi = E\psi$

The Hamiltonian in three dimensions (from equation 2.2.2):

$$\hat{H} = \frac{-h^2}{8\pi^2 m_e}\left(\frac{\partial^2}{\partial x^2} + \frac{\partial^2}{\partial y^2} + \frac{\partial^2}{\partial z^2}\right) - \frac{Ze^2}{4\pi\epsilon_0 r}$$

In the particle in a box model, there is only one dimension, x. Because the y and z values are zero, we can drop y and z out of our

Hamiltonian equation. And, since $V = 0$ inside the box, we can drop the whole part of the Hamiltonian equation that describes the potential energy ($\frac{-Ze^2}{4\pi\epsilon_0 r}$). This leaves us with a much simplified Hamiltonian operator, which we can then use to write the Schrödinger wave equation for a particle moving in one dimension. One last thing we'll do is use a more general value m for the mass of the particle, rather than m_e that specifically represents the mass of an electron. The Schrödinger equation for a particle-wave in a one-dimensional box is:

$$\frac{-h^2}{8\pi^2 m}\left(\frac{\partial^2\psi(x)}{\partial x^2}\right) = E\psi \tag{2.2.1.1}$$

Exercise 2.2.1.1

Follow the steps that were described in the last paragraph to find Equation 2.2.1.1 from equation 2.2.1 and 2.2.2. In other words, derive the Schrödinger Equation for the particle in a box given the three-dimensional Hamiltonian and Schrödinger Equations.

Answer available at the end of this section.

The wavefunction of a one-dimensional wave

Although we've simplified the Schrödinger Equation by considering the particle in the box, Equation 2.2.1.1 may still look mysterious to you. But it's simpler than you might realize. Let's unpack it! Here we'll go through the steps of deriving the 1-dimensional wavefunction for the particle in a box. We won't try to derive a three-dimensional wavefunction for a "real" electron, but when you understand how to find the 1-dimensional wavefunction, and what it tells us, then you can conceptually extend this to understand what the wavefunction tells us about electrons in three dimensions.

Let's dissect Equation 2.2.1.1. Here it is again for reference:

$$\frac{-h^2}{8\pi^2 m_e}\left(\frac{\partial^2\psi(x)}{\partial x^2}\right) = E\psi$$

The expression $\frac{-h^2}{8\pi^2 m_e}$ is just a negative constant. This negative constant is multiplied by the second derivative of the wavefunction in the expression above. And E is a constant multiplied by that same function. We can rearrange this equation as follows:

$$\frac{\partial^2\psi(x)}{\partial x^2} = \frac{-8\pi^2 m_e E}{h^2}\psi = -C\psi \tag{2.2.1.2}$$

where C is just the constant; $C = \frac{8\pi^2 m_e E}{h^2}$

To an expert in the mathematical field of Differential Equations, this expression 2.2.1.1 follows a familiar pattern that makes it easy to translate. If you're not an expert in differential equations, that is OK; you'll just have to bear with this while things get a little "hand-wavy" and try Exercise 2.2.1.2 to prove it to yourself that the following "hand waviness" is true. An expert in differential equations could tell you that when the second derivative of a function is equal to a negative constant times that same function, the function can be written in terms of sin and cos, as shown in Equation 2.2.1.3 (that was the hand-wavy part...see, not so bad):

$$\psi = A\sin(rx) + B\cos(sx) \tag{2.2.1.3}$$

A, B, r, and s are constants in Equation 2.2.1.3. This expression is useful because it is in a form that we could plot with a graphing program (or calculator). However, to do so we must know the constants A, B, r, and s.

What are r and s?

If we substitute expression 2.2.1.3 into Equation 2.2.1.1 and solve for r and s, we find the expressions below.

$$r = s = \sqrt{2m_e E}\left(\frac{2\pi}{h}\right) \tag{2.2.1.4}$$

This shows us that r and s are equal and constant; we know the values for $\pi, h,$ and m_e, and we can solve for the constant E.

Exercise 2.2.1.2: Prove that Equation 2.2.1.3 is true

Show that Equation 2.2.1.3 is true in the case that Equation 2.2.1.2 ($\frac{\partial^2\psi(x)}{\partial x^2} = -C\psi$) is true. Also consider Equation 2.2.1.4 (r, s are constants and $r = s$) and explain why the constant r must equal s.

To do this problem, you'll also need to know the basic differentiation rules of $\sin$ and $\cos$ functions, given below for convenience.

Differentiation Rules for sin and cos:

$\frac{d}{dx}\Big(\sin(rx)\Big) = r\cos(rx)$, where r is a constant.

$\frac{d}{dx}\Big(\cos(rx)\Big) = -r\sin(rx)$, where r is a constant.

Answer available at the end of this section.

Exercise 2.2.1.4

*Complete Exercise 2.2.1.2 before attempting this one.

Derive the expression for r below (from Equation 2.2.1.4) using the 1-D wavefunction (2.2.1.3: $\psi = A\sin(rx) + B\cos(sx)$) and the 1-D Schrödinger equation (2.2.1.1: $\left(\frac{-h^2}{8\pi^2 m_e}\left(\frac{\partial^2\psi(x)}{\partial x^2}\right) = E\psi\right)$).

$r = \frac{2\pi}{h}\sqrt{2m_eE}$

Answer available at the end of this section.

What are A and B?

We can find the possible values of A and B by looking at the possible extremes for the value of x. In our model in Figure 2.2.1.1 , we can see that x can have values from $0 \rightarrow a$. The two extremes, where $x = 0$ and $x = a$, lie at the walls of the box. The electron cannot exist beyond these values because it is trapped inside the walls, so its wavefunction must be zero at $x = 0$ and $x = a$.

The case where $x = 0$ can help us find the value of B. We just said that the wavefunction must be zero where $x = 0$. This means:

$$\psi_{x=0} = A\sin(rx) + B\cos(sx) = A\sin(0) + B\cos(0) = 0$$

Because $A\sin(0) = 0$, the expression can be simplified to:

$$\psi_{x=0} = B\cos(0) = B(1) = 0$$

Now we can see that there is only one possible value for the constant, B, that would allow this expression to be true, $B = 0$. And since B is constant then it will always be zero despite the value of x. This simplifies our 1-D wavefunction:

$$\psi = A\sin(rx) \tag{2.2.1.5}$$

The case where $x = a$ can help us find the value for A. Since the wavefunction must be zero where $x = a$:

$$\psi_{x=a} = A\sin(rx) = A\sin(ra) = 0$$

In this case, A cannot be zero because if both A and B are zero, the wavefunction is zero at all values of x, and so our wavefunction would not exist inside the box. So, let's assume A is not zero. Then, it must be the case that

$$\sin(ra) = 0$$

and then because of the way that $\sin$ functions work, the quantity ra must be an integer value of π if $\sin(ra) = 0$.

$$ra = \pm n\pi$$

where $n = 1, 2, 3...$ any non-zero integer. We can ignore negative values here since both positive and negative values of r will give the same value for $\sin(ra)$. We can then solve for r:

$$r = \frac{n\pi}{a} \tag{2.2.1.6}$$

and substitute the value $r = \frac{n\pi}{a}$ into Equation 2.2.1.5 to get:

$$\psi = A \sin\left(\frac{n\pi x}{a}\right) \tag{2.2.1.7}$$

Recall that the square of the wavefunction (ψ^2) gives the probability of finding the electron anywhere in space. In our model, the probability of finding the particle-wave inside the box is unity (it is 1). Mathematically, this is the normalizing requirement (expressed as $\int \psi_A \psi_A^* d\tau = 1$), which can be solved to find the value of A.

$$A = \sqrt{\frac{2}{a}}$$

Now, we can substitute the value of A into expression 2.2.1.7, and we have a wavefunction that can be visualized using any graphing program/calculator!

$$\psi = \sqrt{\frac{2}{a}} \left(\sin\left(\frac{n\pi x}{a}\right)\right) \tag{2.2.1.8}$$

What is the energy (E) of a particle in the box?

So, now you can see how a 1-D wavefunction can be solved. But how do we find the E of the electron from this? Well, in order to not distract you earlier, we skipped over a very simple way to do this. The E falls right out of the equations you just saw. We can set the two expressions we found above for the constant r, (equations 2.2.1.4 and 2.2.1.6) equal to one another and then solve for E:

$$r = \frac{n\pi}{a} = \sqrt{2mE}\left(\frac{2\pi}{h}\right)$$

$$E = \frac{n^2 h^2}{8ma^2} \tag{2.2.1.9}$$

Expression 2.2.1.9 can be used to calculate the energy of a particle in a one-dimensional box of length a, given its integer energy level, n. Here we can see that the energy is quantized because n is an integer ($n = 1, 2, 3...$). In other words, n is a **quantum number**.

Making sense of the particle in a box: plotting the 1-D ψ and ψ^2.

No matter whether you're dealing with a 1-dimensional or 3-dimensional wave equation, the wavefunction itself (ψ) describes the particle's wave properties. This ψ doesn't have actual physical meaning, so it's hard to imagine what it "looks like" other than just plotting its function. However, the probability of finding the particle-wave at any specific position along the x-axis between $x = 0$ and $x = a$ is more physically meaningful. The probability of finding the particle is proportional to the square of the wave function, which is represented by either ψ^2 or, sometimes, $\psi\psi^*$. The plots of the functions for ψ and ψ^2 for the first three possible values of n are shown below in Figure 2.2.1.2. You could create plots similar to these simply by plotting the function shown in Equation 2.2.1.8 . To plot, you just need to assign a value of n, and it is convenient to assign the length of the box as $a = 1$. The plot generated would have the general ratio of $\frac{x}{a}$ on the x axis, and thus would be relevant for any length box.

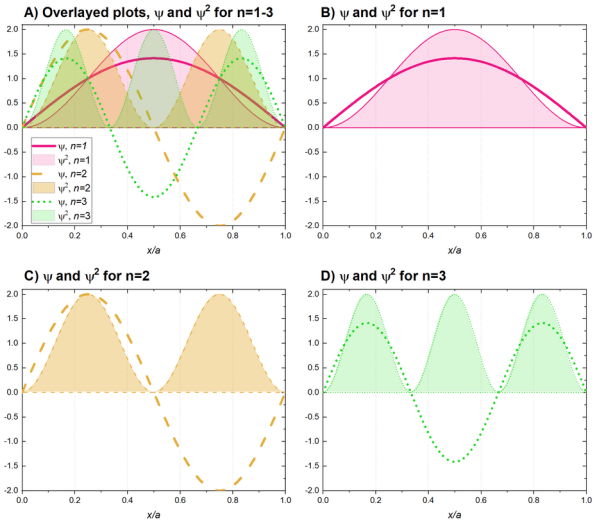


Figure 2.2.1.2. Plots of the 1-D ψ and ψ^2 for $n = 1$, $n = 2$, and $n = 3$ of a box of length a. The wavefunction (ψ) is plotted as a thick solid, dashed, or dotted line. The square of the wavefunction (ψ), which represents the probability of finding the particle at position x, is plotted as the thinner lines and is shaded. Solid lines represent $n = 1$, dashed lines represent $n = 2$, and dotted lines represent $n = 3$. (CC-BY-NC-SA; Kathryn Haas)

The graphs above represent "solutions" to the wave function. For example, the solution $n = 1$ gives the plot shown in Figure 2.2.1.2 B. The solution of $n = 2$ is plotted in Figure 2.2.1.2 C, and so on. These values for n are some of the possible solutions to the 1-dimensional ψ, and they yield descriptions of the wave behavior and probability of finding a particle in 1-dimensional space.

How does this apply to atoms?

The 1-dimensional particle in a box does not represent a real situation; but rather, it is a simple model that we can use to understand a more complex system, like a electron orbiting the nucleus in three dimensions. It's useful to recognize the analogies here that might represent something familiar in a real situation.

$x = 0$ is analogous to the nucleus in an atom. Here in the particle in a box model, $\psi = 0$ and there is zero probability of finding an electron. When this is extended to an atom, this position is analogous to the nucleus (at the origin of a coordinate system where $x = y = z = 0$. A 3-dimensional ψ is also zero at the nucleus and the electron cannot exist there; also, ψ approaches zero as it approaches this position in both the particle in a box model and in a more realistic case of an electron in an atom.

$x = a$ is analogous to a boundary surface far from the nucleus. In the particle in a box model, the 1-dimensional ψ is zero at $x = a$. This is analogous to an electron's ψ approaching zero as it gets further from the nucleus. There will be a more in depth description of boundary surface in the next section (2.2.2). You already know this as the outermost surface of an electron orbital. One minor but notable difference between the 1-dimensional particle in a box and the case of a real atom is that the ψ in three dimensions approaches but never quite reaches zero as distance from the nucleus increases, while $\psi = 0$ for $x = a$ in the more simple case of a 1-dimensional particle in a box.

A change in sign of the ψ (and where both $psi = 0$ and $\psi^2 = 0$) is a node. In both the 1-dimensional particle in a box model and in the more realistic 3-dimensional case, a node is found where the ψ changes sign. At this point, $\psi = \psi^2 = 0$; in other words there is zero probability of finding the particle or electron at these points. It is easy to spot these points in the plots above because the wave function crosses the x-axis and the ψ^2 meets zero.

Exercise 2.2.1.4

Identify the points on plots B, C, and D in Figure 2.2.1.2 that are nodes. How many nodes are there for $n = 1, n = 2$, and $n = 3$?

Answer available at the end of this section.

Exercise 2.2.1.5

Use a graphing program to plot the 1-dimensional ψ and ψ^2 for $n = 1, 2, 3, 4$. How many nodes are there for $n = 4$? Is this expected? Predict how many nodes we should expect for $n = 5$.

You can use any plotting program to do this, and if you aren't familiar with any, try this one: Desmos

Answer available at the end of this section.

In the next section, we will extend these ideas qualitatively to three dimensions. While there is only one quantum number in one dimension, there are three quantum numbers in three dimensions that (when combined) give discrete descriptions of an electron in three-dimensional space (plus a fourth quantum number that explains other properties of the electron).

Answers

Exercise 2.2.1.1

Here is the Hamiltonian Equation for in three dimensions.

$$\hat{H} = \frac{-h^2}{8\pi^2 m}\left(\frac{\partial^2}{\partial x^2} + \frac{\partial^2}{\partial y^2} + \frac{\partial^2}{\partial z^2}\right) - \frac{Ze^2}{4\pi\epsilon_0 r}$$

There are two parts to this equation: the kinetic energy contribution and the potential energy contribution. While the first part of this expression, $\frac{-h^2}{8\pi^2 m}\left(\frac{\partial^2}{\partial x^2} + \frac{\partial^2}{\partial y^2} + \frac{\partial^2}{\partial z^2}\right)$, is the **kinetic energy** contribution, the second part of the expression, $-\frac{Ze^2}{4\pi\epsilon_0 r}$, is the **potential energy (V)** contribution.

(1) Simplify the expression for kinetic energy

Your particle-wave is moving in only one dimension. We can arbitrarily choose the dimension x. This means that x is a variable and will have some value from 0 to a. On the other hand, the particle does not move in the other two dimensions, y and z. You can assign the position of the particle along x and y axes as zero or you can just understand that they do not exist in any significant capacity in our 1-D space. Either way, you can just drop them out of the kinetic energy part of the Hamiltonian, as so:

When $y = z = 0$ and the particle-wave only exists/moves in the x dimension, $\frac{-h^2}{8\pi^2 m}\left(\frac{\partial^2}{\partial x^2} + \frac{\partial^2}{\partial y^2} + \frac{\partial^2}{\partial z^2}\right) = \frac{-h^2}{8\pi^2 m}\left(\frac{\partial^2}{\partial x^2}\right)$

And the overall Hamiltonian is simplified:

$$\hat{H} = \frac{-h^2}{8\pi^2 m}\left(\frac{\partial^2}{\partial x^2}\right) - \frac{Ze^2}{4\pi\epsilon_0 r}$$

(2) Simplify the expression for potential energy (V).

The particle's potential energy inside the box is zero ($V = 0$). Therefore, $V = -\frac{Ze^2}{4\pi\epsilon_0 r} = 0$. We can simply drop the potential energy portion from the Hamiltonian because its value is zero.

The simplified Hamiltonian is now:

$$\hat{H} = \frac{-h^2}{8\pi^2 m}\left(\frac{\partial^2}{\partial x^2}\right)$$

(3) Substitute the simplified Hamiltonian into the Schrödinger Equation.

The Schrödinger is: $\hat{H}\psi = E\psi$

When the simplified Hamiltonian is substituted into this equation, the result is the 1-D Schrödinger Equation 2.2.1.1.

$$\left(\frac{-h^2}{8\pi^2 m}\left(\frac{\partial^2\psi(x)}{\partial x^2}\right)\right) = E\psi$$

Exercise 2.2.1.2**: Prove that Equation** 2.2.1.3 **is true**

You can show that 2.2.1.3 is true by substituting 2.2.1.3 back into Equation 2.2.1.2; in other words take the second derivative of the function, $\psi = A\sin(rx) + B\cos(sx)$ to show that $\frac{\partial^2\psi(x)}{\partial x^2} = -C\psi$. C, r, and s are arbitrary constants, and $r = s$. The actual value of these constants is irrelevant for this problem. Here is one way to approach the problem:

(1) Substitute $\psi = A\sin(rx) + B\cos(sx)$ into $\frac{\partial^2\psi(x)}{\partial x^2} = -C\psi$.

$$\frac{\partial^2}{\partial x^2}\left(A\sin(rx) + B\cos(sx)\right) = -C\psi$$

(2) Take the first and second derivative of $A\sin(rx) + B\cos(sx)$.

The result of taking the first derivative...

$$\frac{\partial}{\partial x}\left(rA\cos(rx) - sB\sin(sx)\right) = -C\psi$$

...and the second derivative...

$$-r^2 A\sin(rx) - s^2 B\cos(sx) = -C\psi$$

This is where we see that the only way $\psi = A\sin(rx) + B\cos(sx)$ is if we can factor the values r^2 and s^2 out of the left side. We have a hint that $r = s$ from the discussion above and Equation 2.2.1.4. Now we see that this is a necessary condition for the expression $-r^2 A\sin(rx) - s^2 B\cos(sx) = -C\psi$ to be true.

(3) Simplify

If $r = s$, then $r^2 = s^2$ and we can replace s with r in the equation above, as so...

$$-r^2 A\sin(rx) - r^2 B\cos(sx) = -C\psi$$

Now, we can factor the constant, $-r^2$ out of the left side of this expression,

$$-r^2\left(A\sin(rx) + B\cos(sx)\right) = -C\psi$$

Now we see that $\psi = A\sin(rx) + B\cos(sx)$ when $-C = -r^2$. In other words, we have shown that $\psi = A\sin(rx) + B\cos(sx)$ is true.

Why is this a useful exercise?

Although it is difficult to explain the derivation of the expression $\psi = A\sin(rx) + B\cos(sx)$ without differential equations and only knowing that $\frac{\partial^2\psi(x)}{\partial x^2} = -C\psi$, to show this is true is as simple as solving this exercise. This exercise is here to help you review your calculus and to show you that the "hand waving" in the text above is not magic, but it is coming from math that you have seen in your calculus courses. Math is crucial for explaining the nature of the universe! Eat your vegetables and practice your math.

Exercise 2.2.1.4

The steps below could be carried out in a different sequence:

(1) Rearrange

Let's move **all constants** to the right side of 2.2.1.1 so that we arrive at the expression that is shown in part of Equation 2.2.1.2 .

$\frac{\partial^2\psi(x)}{\partial x^2} = \frac{-8\pi^2 m_e E}{h^2}\psi$

(2) Take the second derivative of ψ, which we found in Exercise 2.2.1.2.

$\frac{\partial^2\psi(x)}{\partial x^2} = -r^2\left(A\sin(rx) + B\cos(sx)\right) = \frac{-8\pi^2 m_e E}{h^2}\psi$

And since $\psi = A\sin(rx) + B\cos(sx)$, we can simplify this by dividing both sides by ψ (or by $A\sin(rx) + B\cos(sx)$).

**recall that $s = r$. So, you could have substituted r for s in the expression above, and you'd still be on the right track.*

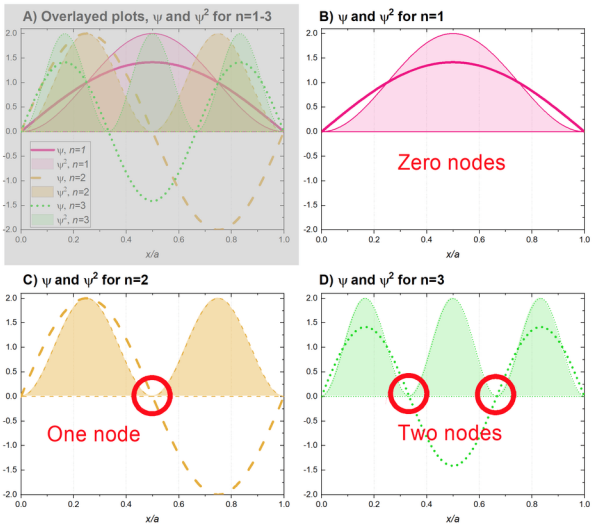
$-r^2 = \frac{-8\pi^2 m_e E}{h^2}$

(3) Solve for r (*we already showed $r = s$ in the Exercise 2.2.1.2).

$r = \sqrt{\frac{8\pi^2 m_e E}{h^2}} = \frac{2\pi}{h}\sqrt{2m_e E}$

Exercise 2.2.1.4

The nodes are annotated with red circles on the figure below. **Panel B** ($n = 1$) has zero nodes. There are two points where $\psi = 0$ in the case of $n = 1$, but these points are at the walls of the box and they are not nodes. The walls of the box are analogous to the nucleus and the boundary surface of an electron orbital. **Panel C** ($n = 2$) has one node where the ψ crosses zero. **Panel D** ($n = 3$) shows two nodes.



Exercise 2.2.1.5

You can use any plotting program to do this. This is the function you should plot (it is Equation 2.2.1.8):

$\psi = \sqrt{\frac{2}{a}}\left(\sin\left(\frac{n\pi x}{a}\right)\right)$

For n=1: Assign a value of $n = 1$, as stated in the problem. In the text above, it also states that it is convenient to assign a value of $a = 1$. Assigning these values results in the following function:

$\psi = \sqrt{\frac{2}{1}}\left(\sin\left(\frac{1\pi x}{1}\right)\right)$ and simplifying leads to $\psi = \sqrt{2}\left(\sin\left(\pi x\right)\right)$

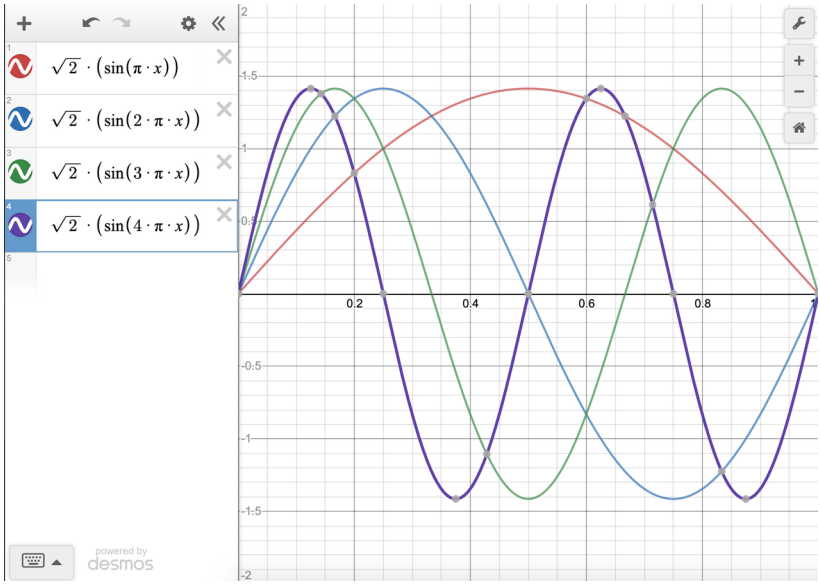
For n=2,3,4 you would repeat the process above. You will get the following functions:

For n=2: $\psi = \sqrt{2}\left(\sin\left(2\pi x\right)\right)$

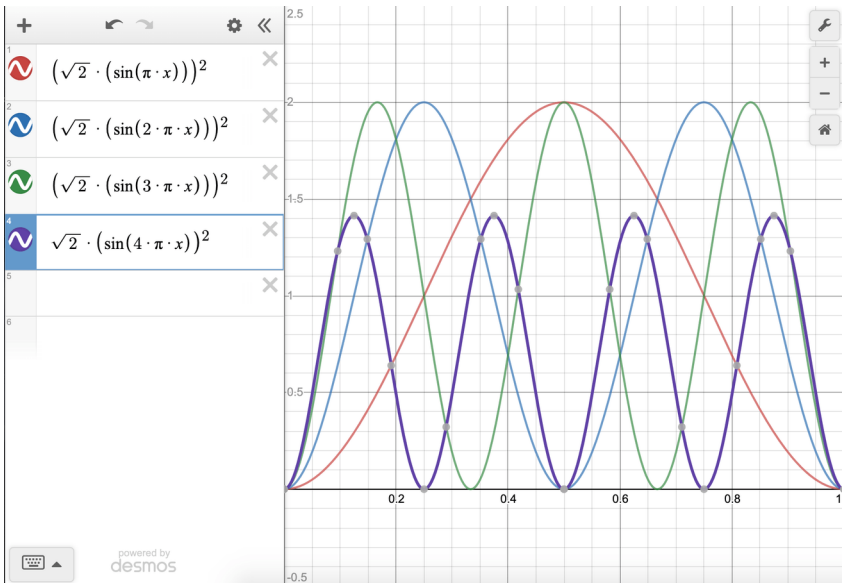
For n=3: $\psi = \sqrt{2}\left(\sin\left(3\pi x\right)\right)$

For n=4: $\psi = \sqrt{2}\left(\sin\left(4\pi x\right)\right)$

In a program like Desmos, you need to input the function correctly. It's useful to know the code for at least one graphing program. For Desmos, and most others, you can find help online. For example, the correct input for Desmos for the n=4 case is sqrt(2)*(sin(4*pi*x)). But, you have to type it in because copy/paste doesn't work. You'll also want to display your graph only from $x = 0$ to $x = 1$ by hitting the settings button (a little wrench in the upper right corner) and changing the x scale. Go ahead and change the y scale too, to $y = -2$ to $y = 2$. If you do this, you should get something that looks like this:



To graph the square of each wavefunction, you'd just square the functions that we just plotted:



In both the case of ψ and ψ^2, the $n = 4$ function shows three nodes (see the bolded purple line, where nodes are tiny grey spots on the axis). This follows a pattern that you might have noticed with the cases of $n = 1, 2,$ and 3 where the number of nodes is $n - 1$ (nodes = $n - 1$). We should expect three nodes for $n = 4$ based on this pattern, and four nodes for $n = 5$.

This page titled 2.2.1: Particle in a Box is shared under a CC BY-NC-SA 4.0 license and was authored, remixed, and/or curated by Kathryn Haas.

- 2.2.1: Particle in a Box by Kathryn Haas is licensed CC BY-NC-SA 4.0.

2.2.2: Quantum Numbers and Atomic Wave Functions

The one-dimensional particle in a box model from the previous section shows us how a wavefunction works in one dimension (the x- dimension). In one dimension, the wavefunction requires only one quantum number, n. A full explanation of the three-dimensional wavefunction for an electron is outside of the scope of this course. Instead, we will focus on gaining a conceptual understanding by extending knowledge of the one-dimensional wavefunction to a three-dimensional space.

Quantum numbers

Extending the wavefunction to three dimensions requires a total of three quantum numbers. In addition to n, which we saw in the one-dimensional case, we also need l and m_l to express the wavefunction in three dimensions. A complete solution to the Schrödinger equation, both the three-dimensional wavefunction and energy, includes a set of three quantum numbers (n, l, m_l). The wavefunction describes what we know as an atomic orbital; it defines the region in space where the electron is located. Additionally, there is a fourth quantum number, m_s. The m_s quantum number accounts for the observed interaction of electrons with an applied magnetic field; it is an additional postulate that is not part of the wavefunction. These four quantum numbers are described below.

The quantum number, n: This is the principle quantum number. This number represents the shell, including both the overall energy of the electron in that shell and the size of that shell. An allowed value for n is any non-zero, positive integer (1, 2, 3, 4, ... etc are allowed, but 4.1 is not allowed).

The quantum number, l: This is the angular momentum quantum number that corresponds to the subshell and its shape. It represents the angular dependence of the subshell, or the "shape" of the orbitals within a subshell. The allowed values of l depend on n. The allowed values of l for an electron in shell n are integer values between 0 to $n-1$, or $l = 0 \rightarrow n-1$. These values correspond to the orbital shape where $l = 0$ is an s-orbital, $l = 1$ is a p-orbital, $l = 2$ is a d-orbital, and $l = 3$ is an f-orbital.

The quantum number m_l: This is the magnetic quantum number. Its possible values give the number of orbitals within a subshell and its specific value gives the orbital's orientation in space. The allowed values of m_l depend on the value of l. The value of m_l is allowed to be any positive or negative integer between $+l$ and $-l$. In other terms, $m_l = +l \rightarrow -l$. For example, if the electron is in a 3-p-orbital, then $n = 3, l = 1$, and the possible values of m_l are $-1, 0,$ and $+1$. Since there are three possible values of m_l there are three orbitals in the p subshell. The specific m_l value defines in which of the three possible p-orbitals (p_x, p_y, or p_z) the electron exists. In the case of the s subshell, there is only one value, $m_l = 0$ because $l = 0$. The one value corresponds to the fact that there is only one s orbital in any shell.

The quantum number m_s: This quantum number accounts for the electron's "spin". In short, electrons interact with magnetic fields in a way that is similar to how a tiny bar magnet would interact with a magnetic field. The allowed values for m_s are $+\frac{1}{2}$ and $-\frac{1}{2}$.

Table 2.2.2.1. Quantum Numbers

SYMBOL	NAME	VALUES	MEANING
n	principal	$1, 2, 3$...(any integer)	energy level, shell
l	angular momentum	$0 \rightarrow n-1$	subshell, $0 = s, 1 = p, 2 = d, 3 = f$... this is the angular dependence of the orbital, shape of the orbital *letters have historical meaning, sharp, principle, diffuse, fundamental
m_l	magnetic	$+l \rightarrow -l$	orientation of angular momentum in space, orbital
m_s	spin	$+\frac{1}{2}, -\frac{1}{2}$	the imaginary property we call "spin", up or down

1-Electron Wavefunctions (Atomic orbitals)

One simplified representation of the three-dimensional wavefunction is shown below. This representation breaks the wavefunction into two parts: the **radial contribution** ($R_{n,l}(r)$) and the **angular contribution** ($Y_{l,m_l}(\theta,\phi)$).

$$\psi_{(n,l,m_l)} = R_{n,l}(r) \times Y_{l,m_l}(\theta,\phi) \tag{2.2.2.1}$$

Allowed Energies

From the wavefunction, we can find the allowed energies of an electron in an atom. We have not given you the more complex form of the wavefunction where you'd need to derive 2.2.2.2 from 2.2.2.1 because it is outside the scope of this course. Instead, consider the process that we used to derive the energy of a particle in a one-dimensional box in the previous section. A similar process can be used to find the energy of an electron in three dimensions, shown in 2.2.2.2.

$$E_n = -\frac{hcRZ^2}{n^2} = -(13.607\,eV)\left(\frac{Z}{n}\right)^2, \tag{2.2.2.2}$$

where n is the principle quantum number, h is Planck's constant, c is the speed of light, R is the Rydberg constant, and Z is the charge of the nucleus. It is useful to know that the value of $hcR = 13.6eV$. This is also the value of the ionization energy of an electron in a hydrogen atom. This equation only works for **hydrogenic atoms** (atoms or ions that are "like" hydrogen in that they have only one electron).

Exercise 2.2.2.1

The energy that it takes to eject a ground-state electron from a hydrogen atom (its ionization energy, IE) is measured to be approximately 13.6 eV, while the IE energy of a He^+ ion is four times greater at 54.4 eV. These values can be predicted using both Equation 2.2.2.2 and the Rydberg equation.

a. Using Equation 2.2.2.2 for allowed energies of electrons in a hydrogen atom, derive the energy of the ground state electron in H. Then repeat this process for a He^+ ion. What do the values indicate about the relative attraction between an electron and the nuclei of these two hydrogenic atoms?
b. Show that the IE of H's 1s electron can also be predicted by the Rydberg formula (equation 2.1.2.2).

Answer a available at the end of this section.

Answer) available at the end of this section.

Exercise 2.2.2.2

Which of the following are hydrogenic atoms? H, H^+, H^-, He, He^{2+}, He^+, He^-, Li, Li^{3+}, Li^{2+}, Li^+, Li^- .

Answer available at the end of this section.

Radial and Angular contributions to the wavefunction:

Radial contribution, $R_{n,l}(r)$

The radial part of the wavefunction, $R_{n,l}(r)$ gives the radial variation of ψ. In other words, $R_{n,l}(r)$ defines how the wavefunction depends on the distance of the electron from the nucleus (the radius). The $R_{n,l}(r)$ parts of the wavefunction for a hydrogenic atom are listed in Table 2.2.2.2, and they are plotted in Figure 2.2.2.1. Notice that the $R_{n,l}(r)$ of all s-orbitals (solid lines) reaches a maximum at $r = 0$. This is unique to the s-orbitals' $R_{n,l}(r)$. The $R_{n,l}(r)$ of p- and d-orbitals orbitals approaches zero as r approaches zero. This has important consequences for how closely an electron in these orbitals can approach the nucleus.

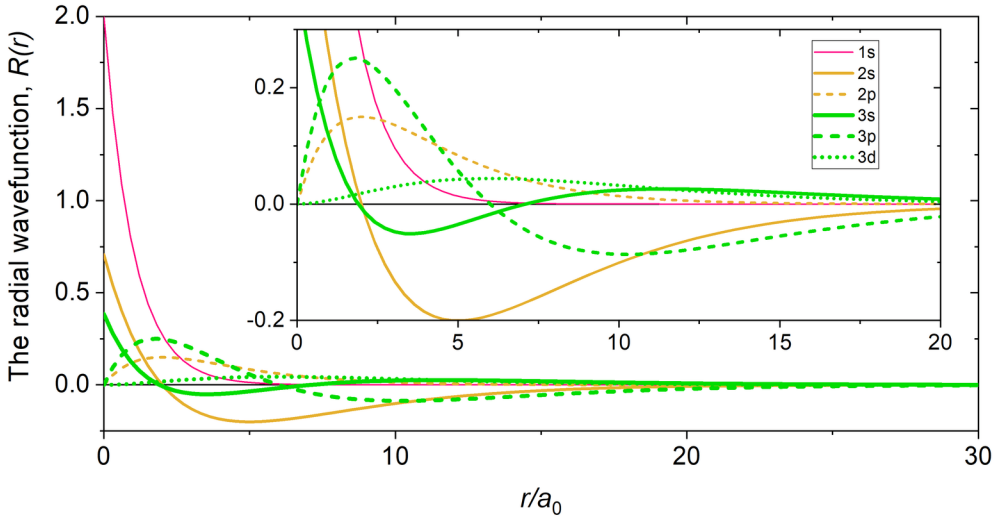


Figure 2.2.2.1. Plots of the radial wavefunction, $R_{n,l}(r)$, for the first three shells. The wavefunctions are plotted relative to $\frac{r}{a_0}$, where $a_0 = 52.9pm = 0.529\mathring{A}$ is the Bohr Radius (the radius of a hydrogen 1s orbital). The expressions for these radial wavefunctions ($R_{n,l}(r)$) are shown in Table 2.2.2.2. (Kathryn Haas; CC-NC-BY-SA)

Table 2.2.2.2. Radial wavefunctions ($R(r)$) for the first three shells of a hydrogen atom. Z is the nuclear charge, and $a_0 = 52.9pm = 0.529\mathring{A}$ is the Bohr radius (the radius of a hydrogen 1s orbital). For the H atom, $Z = 1$ (the nuclear charge of hydrogen). Plotting of the functions can be simplified if we set $a_0 = 1$ and plot the functions with respect to r/a_0, which was done to find the plots shown in Figure 2.2.2.1.

Orbital	n	l	$R_{n,l}(r)$
1s	1	0	$2\left[\frac{Z}{a_0}\right]^{3/2} e^{-Zr/a_0}$
2s	2	0	$2\left[\frac{Z}{2a_0}\right]^{3/2}\left(2-\frac{Zr}{a_0}\right) e^{-Zr/2a_0}$
2p	2	1	$\frac{1}{\sqrt{3}}\left[\frac{Z}{3a_0}\right]^{3/2}\left(\frac{Zr}{a_0}\right) e^{-Zr/2a_0}$
3s	3	0	$\frac{2}{27}\left[\frac{Z}{3a_0}\right]^{3/2}\left(27-18\frac{Zr}{a_0}-2(\frac{Zr}{a_0})^2\right) e^{-Zr/3a_0}$
3p	3	1	$\frac{1}{81\sqrt{3}}\left[\frac{2Z}{a_0}\right]^{3/2}\left(6-\frac{Zr}{a_0}\right)(\frac{Zr}{a_0}) e^{-Zr/3a_0}$
3d	3	2	$\frac{1}{81\sqrt{15}}\left[\frac{2Z}{a_0}\right]^{3/2}\left(\frac{Zr}{a_0}\right)^2 e^{-Zr/3a_0}$

Radial probability function, $4\pi r^2(R_{n,l}(r))^2$

Just like in the particle-in-a-box model, the square of the wavefunction is proportional to the probability of finding a particle (electron) at some point in space. The square of the radial part of the wavefunction is called the radial distribution function $4\pi r^2(R_{n,l}(r))^2$, and it describes the probability of locating the electron at some distance r away from the nucleus. When we normalize the probability functions by dividing the function by its integral over all space, we get the plots shown in Figure 2.2.2.2. The normalized probability functions are compared to the original radial part of the wavefunctions in Figure 2.2.2.3. The most probable distance for finding an electron is shown by the maximum value of the function. For an electron in the 1s orbital of H, the most probable distance from the nucleus occurs at $r = 1a_0$. This is the Bohr Radius, and it has a value of $a_0 = 52.9pm = 0.529\mathring{A}$. It is convenient to plot the functions of the hydrogen atomic orbitals relative to the size of its smallest orbital, the 1s orbital; this is the reason we plot $R_{n,l}(r)$ and $4\pi r^2(R_{n,l}(r))^2$ relative to $\frac{r}{a_0}$.

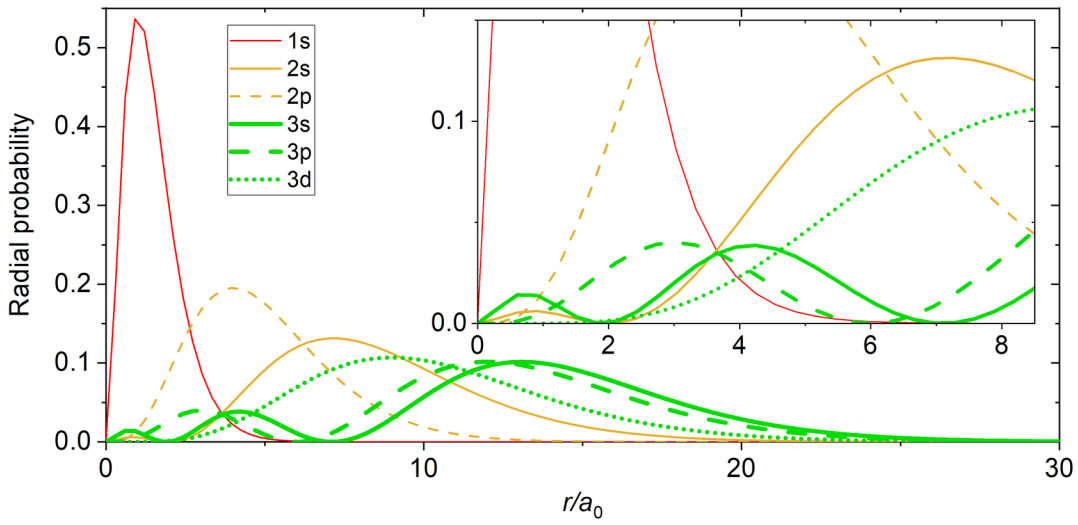


Figure 2.2.2.2: Plots of the normalized radial probability functions for the first three shells. The radial wavefunctions ($R_{n,l}(r)$) are shown in Table 2.2.2.2. (Kathryn Haas; CC-NC-BY-SA)

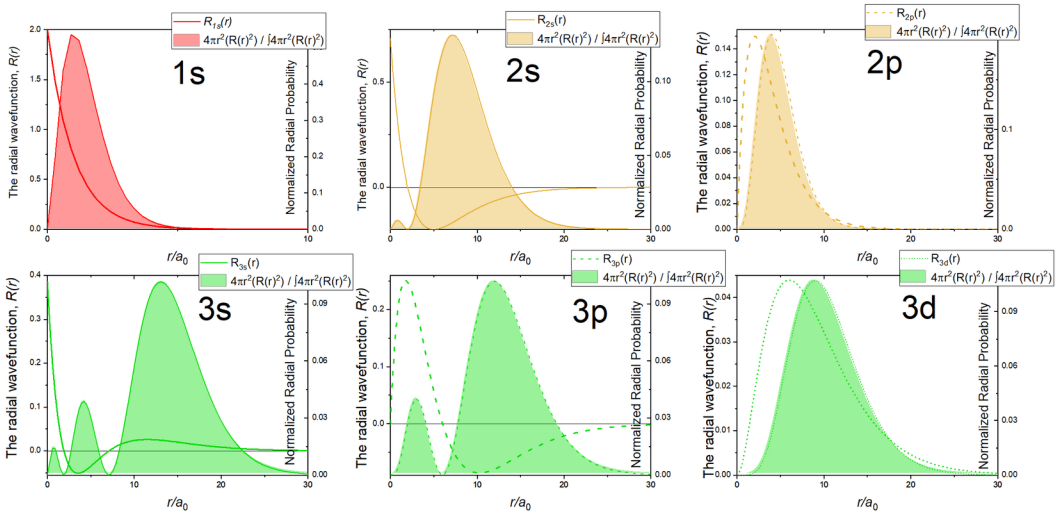


Figure 2.2.2.2. Plots of the normalized radial probability function for each orbital in the first three shells (shaded curves). The radial wavefunctions are also shown (Table 2.2.2.2). The y-axis on the left of each plot corresponds to the radial wavefunction (line); the y-axis on the right of each plot corresponds to the radial probability function (shaded). (Kathryn Haas; CC-NC-BY-SA)

Radial nodes

From the discussion of the 1-dimensional particle in a box, we learned that nodes exist where $\psi = 0$. In the case of the 3-dimensional wavefunction, there are two different types of nodes: radial nodes and angular nodes. **Radial nodes occur where the radial part of the wavefunction is zero ($R(x) = 0$).** These are easy to find by plotting the radial part of the wavefunction and finding where the radial part of the wavefunction (and the radial probability function) is zero (where $R_{n,l}(r) = 0$) and where $4\pi r^2 (R_{n,l}(r))^2 = 0$. These nodes are spherical in shape and depend on the energy level and subshell (the values of n and l). **The number of radial nodes is** $n - l - 1$. An example of a radial node is the single node that occurs in the $2s$ orbital ($2 - 0 - 1 = 1$ node). In contrast, the 1s orbital has zero radial nodes ($1 - 0 - 1 = 0$ nodes). Where there is a node, there is zero probability of finding an electron.

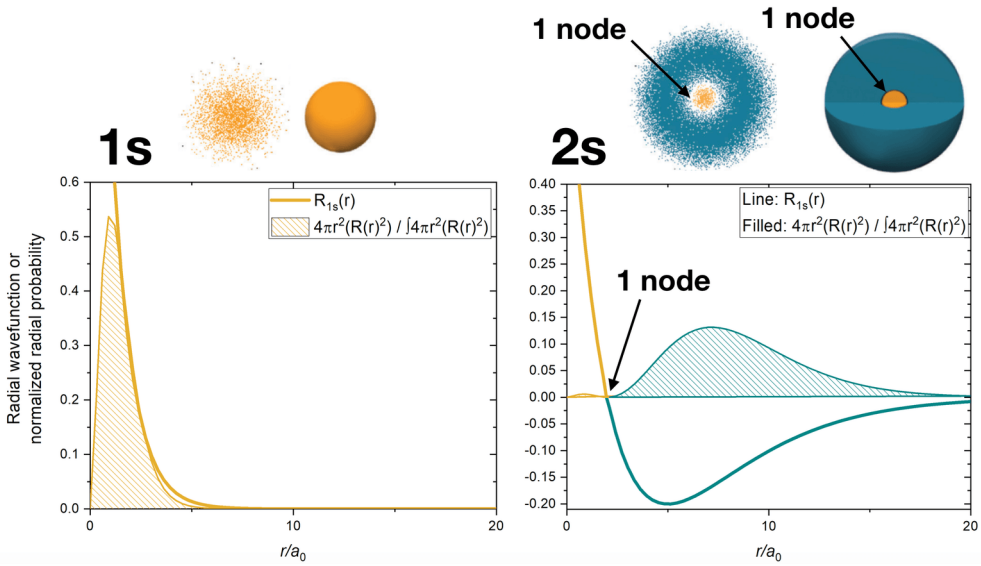


Figure 2.2.2.3: Visualization of the 1s and 2s atomic orbitals. Each orbital is shown as both an electron probability density plot and a contour plot above its wavefunction and probability density function. The 1s orbital has zero radial nodes. The 2s orbital has one radial node where its wavefunction changes sign and its radial probability function is zero. (Kathryn Haas; CC-BY-SA)

Boundary surfaces

A true node occurs where the probability of finding an electron is zero. Nodes occur where $\psi = \psi^2 = 0$. Far from the nucleus, the probability of finding the electron rapidly approaches zero, but is never *exactly* zero. What this means is that it is rather improbable to find the electron at far distances from the nucleus, but it's not impossible. The rapid fall of probability creates a boundary surface rather than a node. The boundary surface represents the area around the nucleus where the electron exists most of the time.

Exercise 2.2.2.1

How many radial nodes are in the s, p, d, and f orbitals in the first four shells? $n = 1, 2, 3, 4$?

Answer available at the end of this section.

Exercise 2.2.2.1

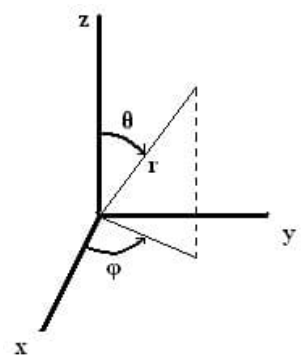
Draw a rough plot of the following:

a. The radial wavefunction, $R_{n,l}(r)$ and the probability density function, $4\pi r^2 (R_{n,l}(r))^2$, for the 1s orbital.
b. The radial wavefunction, $R_{n,l}(r)$ and the probability density function, $4\pi r^2 (R_{n,l}(r))^2$, for the 4s orbital.

Answer, 1s available at the end of this section.

Answer, 4s available at the end of this section.

Angular contribution, $Y_{l,m_l}(\theta,\phi)$, and angular probability function, $(Y_{l,m_l}(\theta,\phi))^2$



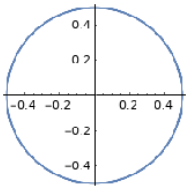
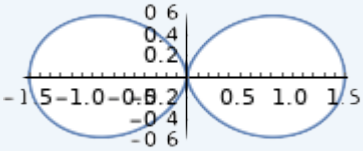
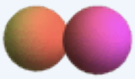
The angular contribution to the wavefunction, $Y_{l,m_l}(\theta,\phi)$, describes the wavefunction's shape, or the angle with respect to a coordinate system. To describe the direction in space, we use spherical coordinates that tell us distance *and* orientation in 3-dimensional space. There are three spherical coordinates: r, ϕ, and θ. r is the radius, or the actual distance from the origin. ϕ and θ are angles. ϕ is measured from the positive x axis in the xy plane and may be between 0 and 2π. θ is measured from the positive z axis towards the xy plane and may be between 0 and π.

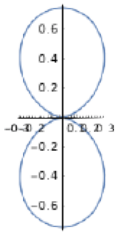
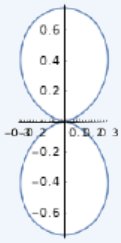
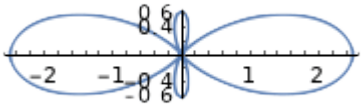
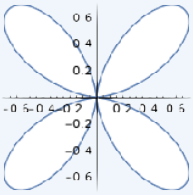
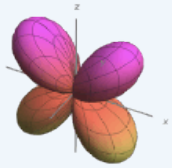
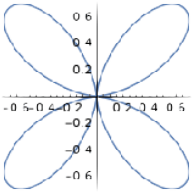
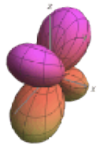
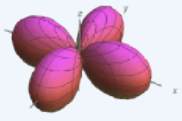
$$Y_{l,m_l}(\theta,\phi) = \left(\frac{1}{4\pi}\right)^{1/2} y(\theta,\phi)$$

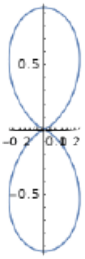
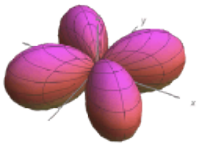
$Y_{l,m_l}(\theta,\phi)$, is slightly more difficult to describe than the radial contribution was. This is partly because $Y_{l,m_l}(\theta,\phi)$ contains imaginary numbers, which have no real, physical meaning. However, the angular part of the wavefunction becomes more "real" when you square it to get angular probability density, a more tangible concept described as the **shapes of orbitals**.

The values of θ, ϕ, and $y(\theta,\phi)$ for orbitals in the hydrogen atom are listed in Table 2.2.2.3. But $Y_{l,m_l}(\theta,\phi)$ is only a mathematical function and has no real physical meaning. The square of the radial wavefunction, $Y_{l,m_l}(\theta,\phi)^2$, gives the probability of finding the electron at a point in space on a ray described by (ϕ,θ). Thus $Y_{l,m_l}(\theta,\phi)^2$ describes the shape of the orbital.

Table 2.2.2.3. Components of the angular wavefunction and the resulting orbital shapes. The plots in the two right hand columns were created using Desmos and Mathematica: specifically "Spherical Harmonics" from the Wolfram Demonstrations Project, http://demonstrations.wolfram.com/SphericalHarmonics/ and "Visualizing Atomic Orbitals" demonstrations.wolfram.com/Vi...tomicOrbitals/.

subshell	m_l (orbital)	θ	ϕ	Plots of θ^2	orbital shapes
$l=0$, s	$m_l=0$	$\frac{1}{\sqrt{2}}$	$\frac{1}{\sqrt{2\pi}}$		
$l=1$, p	$m_l=0$	$\frac{\sqrt{6}}{2}\cos\theta$	$\frac{1}{\sqrt{2\pi}}$		

subshell	m_l (orbital)	θ	ϕ	Plots of θ^2	orbital shapes
$l = 1$, p	$m_l = +1$	$\frac{\sqrt{3}}{2}\sin\theta$	$\frac{1}{\sqrt{2\pi}}e^{i\phi}$		
$l = 1$, p	$m_l = -1$	$\frac{\sqrt{3}}{2}\sin\theta$	$\frac{1}{\sqrt{2\pi}}e^{-i\phi}$		
$l = 2$, d	0	$\frac{\sqrt{10}}{4}\left(3\cos^2\theta - 1\right)$	$\frac{1}{\sqrt{2\pi}}$		
$l = 2$, d	$m_l = +1$	$\frac{\sqrt{15}}{2}\sin\theta\cos\theta$	$\frac{1}{\sqrt{2\pi}}e^{i\phi}$		
$l = 2$, d	$m_l = -1$	$\frac{\sqrt{15}}{2}\sin\theta\cos\theta$	$\frac{1}{\sqrt{2\pi}}e^{-i\phi}$		
$l = 2$, d	$m_l = +2$	$\frac{\sqrt{15}}{4}\sin^2\theta$	$\frac{1}{\sqrt{2\pi}}e^{i2\phi}$		

subshell	m_l (orbital)	θ	ϕ	Plots of θ^2	orbital shapes
$l = 2$, d	$m_l = -2$	$\frac{\sqrt{15}}{4}\sin^2\theta$	$\frac{1}{\sqrt{2\pi}}e^{-i2\phi}$		

Angular nodes

Angular nodes exist where $(Y_{l,m_l}(\theta,\phi))^2 = 0$. These nodes are planar in shape, and they depend on the value of l. The number of angular nodes in any orbital is equal to l. This means that s-orbitals ($l = 0$) have zero angular nodes, p-orbitals ($l = 1$) have one angular node, d-orbitals ($l = 2$) have two angular nodes, and so on. Planar nodes can be flat planes (like the nodes in all p orbitals) or they can have a conical shape, like the two angular nodes in the d_{Z^2} orbital. Angular nodes in some p and d orbitals are shown in Figure 2.2.2.4.

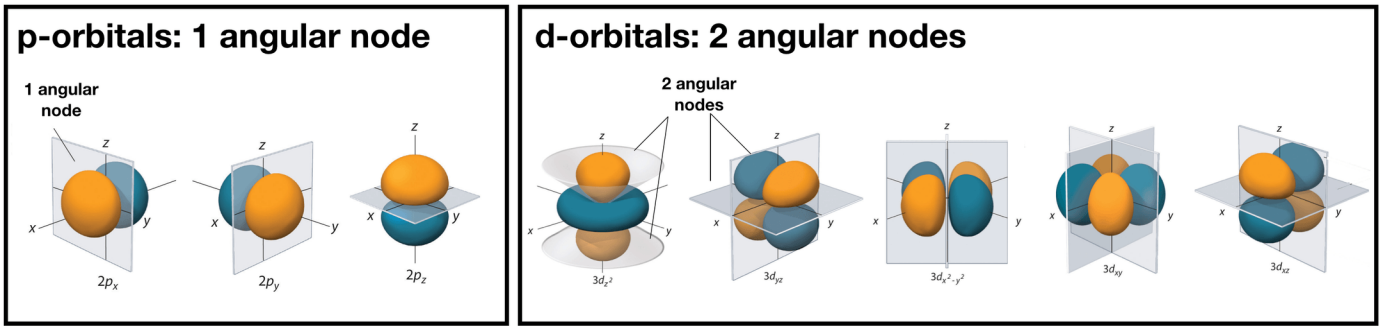
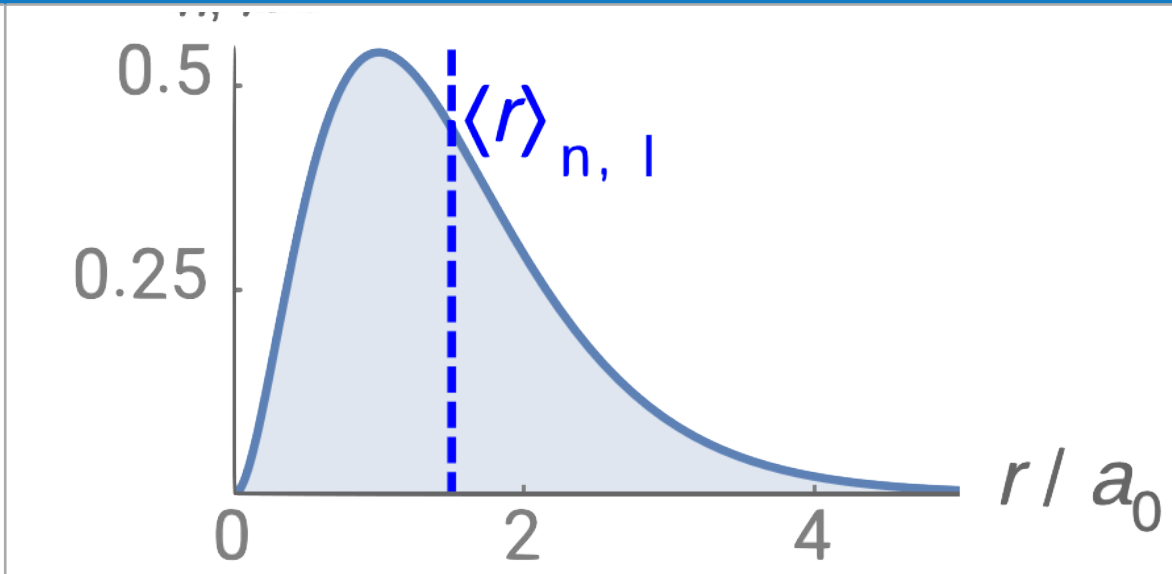
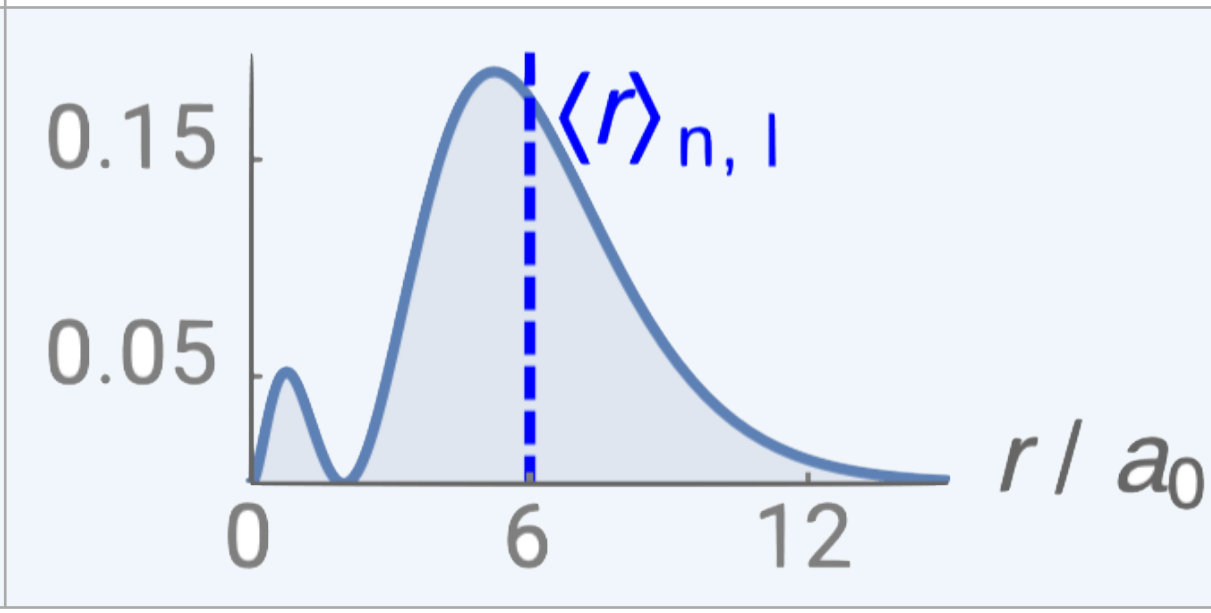


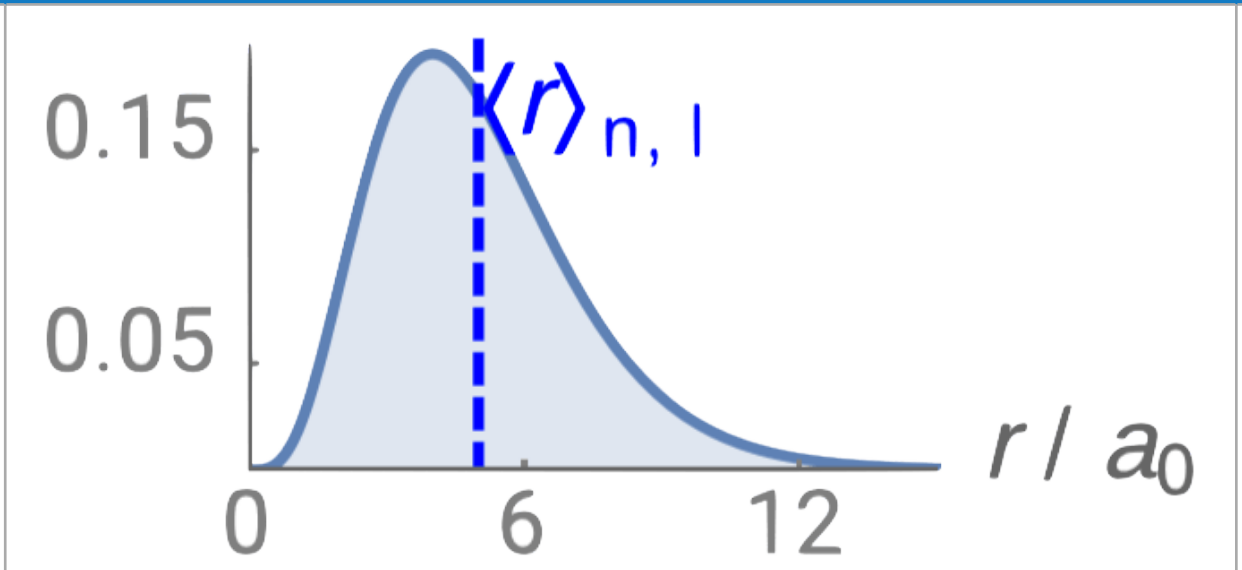
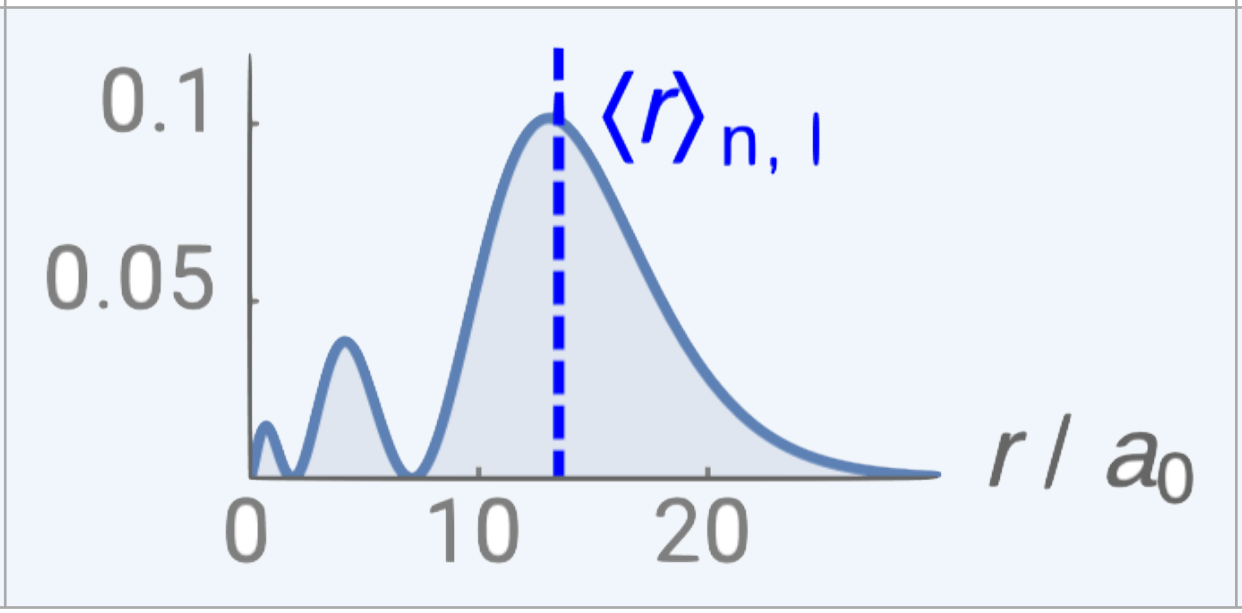
Figure 2.2.2.4: The angular nodes in p-orbitals and d-orbitals are shown. Every p orbital has one angular node, and every d orbital has two angular nodes. The number of angular nodes in any orbital is equal to the value of the quantum number, l. (CC BY-NC-SA; anonymous by request)

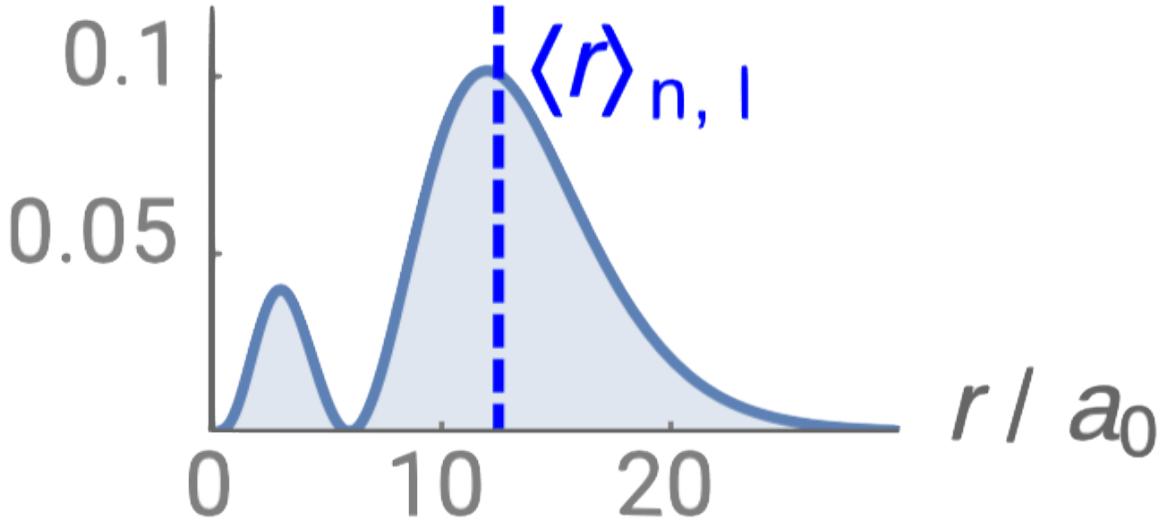
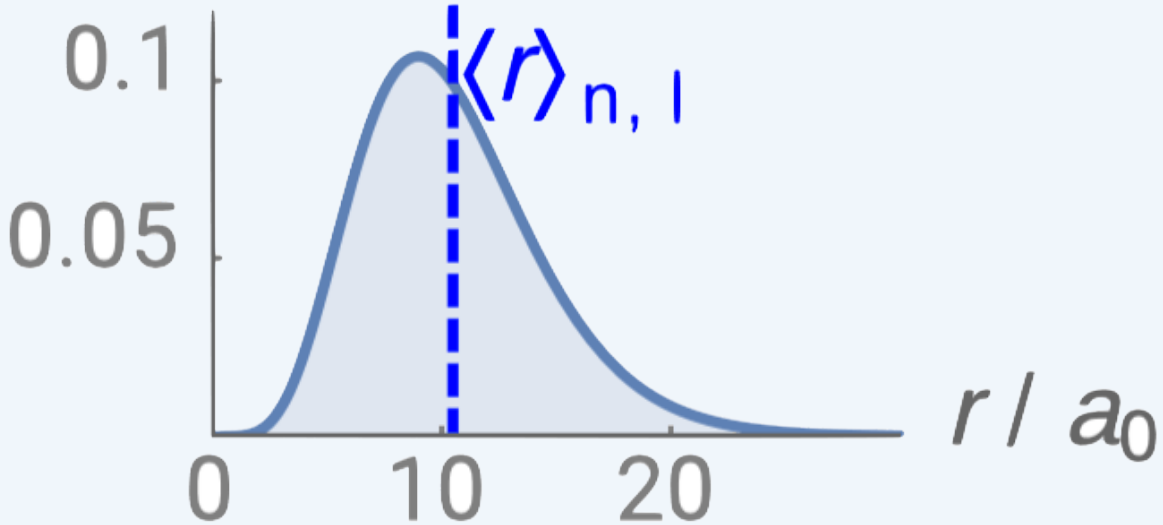
Atomic Orbitals

Atomic orbitals result from a combination of both the radial and angular contributions of the wavefunction. Atomic orbitals can have both angular nodes and radial nodes, depending on the values of n and l.

The chart below compares the radial variation, angular variation, and their combinations (orbitals).

Orbital	Radial Probability	Radi Nod
1s		0
2s		1

Orbital	Radial Probability	Radi Node
2p		0
3s		2

Orbital	Radial Probability	Radi Nod
3p		1
3d		0

Answers

Exercise 2.2.2.1

Use Equation 2.2.2.2 . For a hydrogen atom with one proton, $Z = 1$, and the ground state energy level is the lowest energy level, $n = 1$. Therefore, the energy of an electron in the ground state of a H atom is:

$E_n = -\frac{hcRZ^2}{n^2} = -13.607\ eV(\frac{1}{1})^2 = -13.607\ eV$, or *approximately* $-13.6\ eV$. Thus, the IE (energy necessary to remove that electron) is +13.6 eV.

We can use the same process to find the ground state energy of an electron in He^+. This time, $Z = 2$ because helium has two protons in its nucleus, and as before, the ground state is $n = 1$.

$E_n = -\frac{hcRZ^2}{n^2} = -13.607\ eV(\frac{2}{1})^2 = -54.428eV$, or *approximately* $-54.4\ eV$. Thus, the IE is +54.4 eV.

These ground-state energies are the same as the energy required to remove the ground state electron from H and He^+. In other words, these are the predicted ground state IE values for one electron in H and He^+. The *measured* IEs for these two species are in fact 13.6 eV and 54.4 eV, respectively.

The He^+ ion has a more negative value for its ground state energy with a magnitude four times greater than that of the ground state H electron. This means that

the He^+ electron is more strongly attracted to the (+2) nucleus than the H electron is attracted to the (+1) nucleus, and more energy is required to eject the He^+ electron than the H electron. It takes more energy to remove the electron from He^+ than from H. This makes sense in light of Coulomb's law: The attractive force between the H nucleus (+1) and an electron (-1) would be weaker than that of a He nucleus (+2) and an electron (-1) because the positive charge of the He nucleus has a greater magnitude.

Exercise 2.2.2.1

The Rydberg equation is: $\frac{1}{\lambda} = E(cm^{-1}) = R_H \left(\frac{1}{n_l^2} - \frac{1}{n_h^2}\right)$ where n_l and n_h are positive integers, $n_h > n_l$, and the *Rydberg constant* (R_H), has a value of 1.09737 × $10^7 m^{-1}$. We should set $n_l = 1$ to represent the initial ground state, and $n_h = \infty$ to represent the removal of the electron from the atom.

Step 1.

Calculate Energy (in m^{-1}) using the Rydberg equation:

$E = R_H \left(\frac{1}{n_l^2} - \frac{1}{n_h^2}\right) = 1.09737 \times 10^7 m^{-1} \left(\frac{1}{1^2} - \frac{1}{\infty^2}\right) = 1.09737 \times 10^7 m^{-1} (1 - 0) = 1.09737 \times 10^7 m^{-1}$

Ultimately, we want a value of energy in units of eV so we can compare it to the answers in part (a), but our value here is in units of inverse meters (m^{-1}). A quick internet search can tell you the conversion between inverse centimeters (cm^{-1}) and eV is $1eV = 8065.6cm^{-1}$.

Step 2.

Convert from m^{-1} to cm^{-1} to eV so that we can compare to the answer in part (a):

$1.09737 \times 10^7 \frac{1}{m} \times \frac{1m}{100cm} \times \frac{1eV}{8065.6 \frac{1}{cm}} = 13.6056eV$, or approximately 13.6 eV.

Exercise 2.2.2.2

Hydrogenic atoms are atoms or ions that contain only one electron. H, He^+, and Li^{2+} are hydrogenic atoms/ions that contain only one electron.

Exercise 2.2.2.1

You can approach this answer by using the mathematical relationship between the number of radial nodes and the values of n and l: **number of radial nodes is** $n - 1 - l$. You could also notice the pattern that the first orbital of any type (1s, 2p, 3d...) has zero radial nodes, the second orbital of a type (2s, 3p, 4d...) has one radial node, the third orbital of a type has two radial nodes (3s, 4p, 5d...)...etc.

A full list of all of the orbitals in the first four shells and their number of radial nodes is below. It's a good idea to prove to yourself that the numbers given below are consistent with the plots of the orbitals' wavefunctions for those orbitals in the first three shells:

s-orbitals:

1s: $n - 1 - l = 1 - 1 - 0 = 0$, zero radial nodes

2s: $n - 1 - l = 2 - 1 - 0 = 1$, one radial node

3s: $n - 1 - l = 3 - 1 - 0 = 2$, two radial nodes

4s: $n - 1 - l = 4 - 1 - 0 = 3$, three radial nodes

p-orbitals

2p: $n - 1 - l = 2 - 1 - 1 = 0$, zero radial nodes

3p: $n - 1 - l = 3 - 1 - 1 = 1$, one radial node

4p: $n - 1 - l = 4 - 1 - 1 = 2$, two radial nodes

d-orbitals

3d: $n - 1 - l = 3 - 1 - 2 = 0$, zero radial nodes

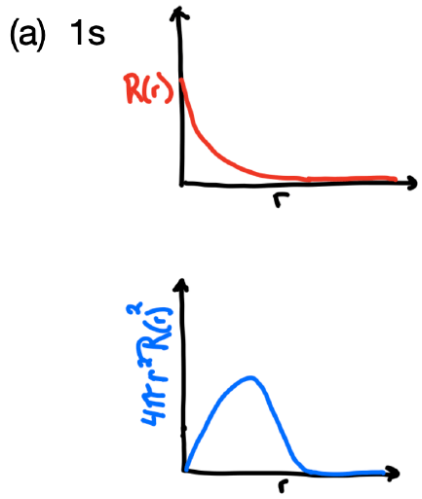
4d: $n - 1 - l = 4 - 1 - 2 = 1$, one radial nodes

f-orbital

4f: $n - 1 - l = 4 - 1 - 3 = 0$, zero radial nodes

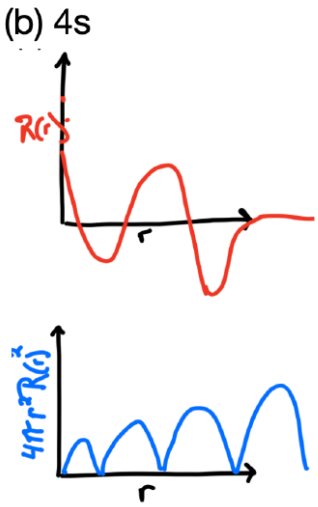
Exercise 2.2.2.1

The 1s orbital's $R_{n,l}(r)$ reaches a maximum near the origin and approaches zero far from the nucleus. The $4\pi r^2 (R_{n,l}(r))^2$ approaches zero at the origin, has a maximum intensity at the Bohr radius, and approaches zero far from the nucleus (its boundary surface).



Exercise 2.2.2.1

Like all s orbitals, the 4s orbital's $R_{n,l}(r)$ reaches a maximum near X=0, but it would be less intense than the function of the 1s, 2s, and 3s orbitals. It should have three radial nodes and so its wavefunction would change sign three times. This would give four regions of electron density in the probability function while the function would approach zero (boundary surface) far from the nucleus.



This page titled 2.2.2: Quantum Numbers and Atomic Wave Functions is shared under a CC BY-NC-SA 4.0 license and was authored, remixed, and/or curated by Kathryn Haas.

- 2.2.2: Quantum Numbers and Atomic Wave Functions by Kathryn Haas is licensed CC BY-NC-SA 4.0.

2.2.3: Aufbau Principle

Introduction

The **Aufbau Principle** (also called the **building-up principle** or the **Aufbau rule**) states that, in the ground state of an atom or ion, electrons fill atomic orbitals of the lowest available energy level before occupying higher-energy levels. In general, an electron will occupy an atomic orbital with the lowest value of n, l, m_l, in that order of priority. The value of m_s for an unpaired electron is conventionally assigned a value of $+\frac{1}{2}$. Each electron in an atom/ion must have a unique set of values for all four quantum numbers.

The Ground State of Hydrogenic Atoms/Ions

In a hydrogenic atom/ion, there is only one electron. In this case, the *only factor determining energy is the value of* n. The ground state will always be the 1s orbital ($n = 1, l = 0, m_l = 0, m_s = +\frac{1}{2}$).

The Ground State of Multi-electron Atoms/Ions

In atoms/ions with two or more electrons, the ground state electron configuration (1) minimizes the total energy of the electrons, (2) obeys the Pauli exclusion principle, (3) obeys Hunds rule of maximum multiplicity, and (4) considers the exchange interaction. These "rules" are described below.

---

(1) Electrons will occupy the lowest energy orbitals in order to minimize the total energy. The two quantum numbers that are related to energy in multi-electron atoms are n, and l. Thus, orbitals with the lowest values of n and l will fill first.

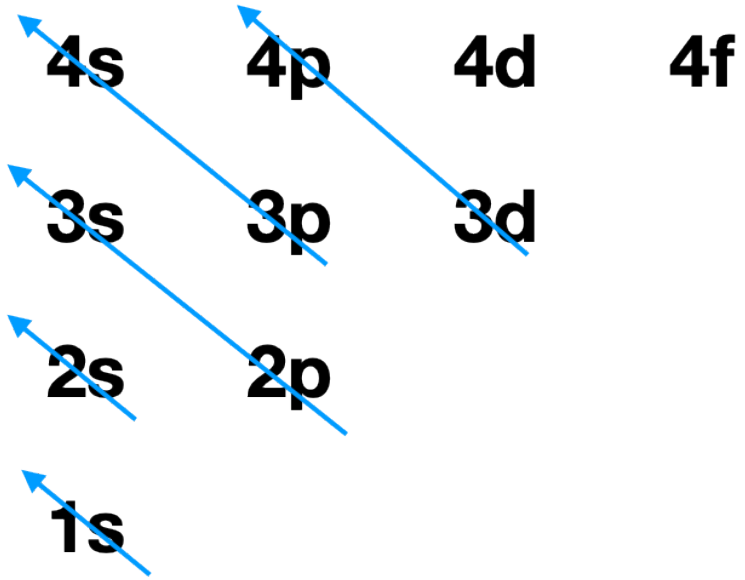
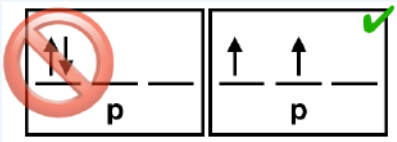


Figure 2.2.3.1. The order of filling of ground state electron orbitals is 1s, 2s, 2p, 3s, 3p, 4s, 3d, 4p, etc... (CC-BY-NC-SA; Kathryn Haas)

(2) Hund's rule of maximum multiplicity states that for a given electron configuration, the lowest energy arrangement of electrons in degenerate orbitals is the one with the greatest "multiplicity," where multiplicity is the number of unpaired electrons (n) plus 1 (multiplicity = n + 1). This rule is used to predict the ground state of an atom or molecule with one or more open electronic shells.

Hund's rule is based on empirical observation of atomic spectra, and it is a consequence of the energy required to pair two electrons in the same orbital. This energy of repulsion between two electrons in the same orbitals is a Coulombic energy of repulsion, Π_c, caused by two electrons with like charge sharing the same area of space (an orbital). When more than one electron occupies a set of degenerate orbitals, the most favorable arrangement is one where the number of paired electrons is minimized.

A simplified definition of Hund's rule is that **the lowest energy arrangement is the one with the greatest number of unpaired electrons**. This implies that if two or more orbitals of equal energy are available, electrons will occupy them singly before filling them in pairs. Examples of ground state arrangements of electrons in three degenerate p-orbitals is given in the figure shown here.



# of electrons in a p-subshell	Arrangement (unpaired electrons, n)	Spin Multiplicity (n + 1)
1	(n = 1)	2
2	(n = 2)	3
3	(n = 3)	4
4	(n = 2)	3
5	(n = 1)	2
6	(n = 0)	1

Figure 2.2.3.2**.** Hund's rule is that spin multiplicity must be maximized in the ground state. (Kathryn Haas; CC-NC-BY-SA)

(3) The Pauli exclusion principle states that it is impossible for two electrons of a multi-electron atom to have the same set of values for all four quantum numbers. Two electrons in different orbitals will have a different set of n, l, and m_l values. When two electrons reside in the same orbital, they posses the same n, l, and m_l values, therefore their m_s must be different. Thus, two electrons in the same orbital must have opposite half-integer spin projections of $+\frac{1}{2}$ and $-\frac{1}{2}$.

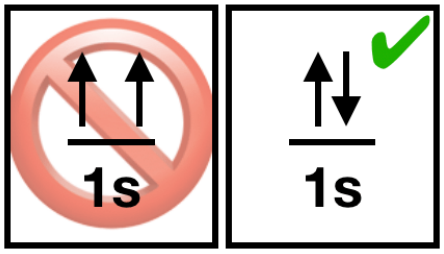


Figure 2.2.3.3**.** Pauli's principle tells us that paired electrons must have opposite spin. (Kathryn Haas; CC-NC-BY-SA)

(4) The exchange interaction is sometimes called the *exchange energy* or *exchange force*. However, it is not a true energy or force. Rather, it is a quantum mechanical effect that takes place between identical particles. The exchange interaction results in a ground state electron configuration with unpaired electrons all being of the same spin. Unpaired electrons are conventionally written in the "spin up" direction.

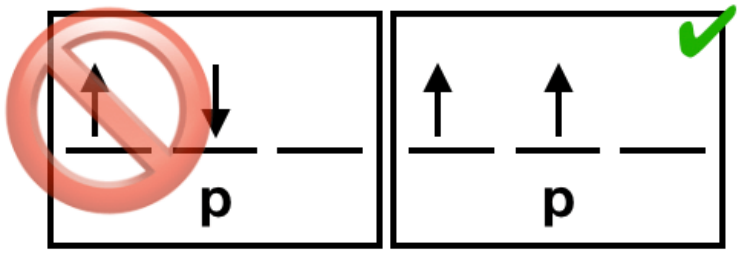


Figure 2.2.3.4**.** Unpaired electrons should have identical spins due to the exchange interaction. (Kathryn Haas; CC-NC-BY-SA)

Trends in Expected Electron Configuration

The four "rules" above can be used as guidelines to predict the ground state electron configuration of atoms, the filling of subshells, and the configuration of electrons in degenerate orbitals. However, the utility of these guidelines for predicting actual electron configurations requires more nuanced knowledge of the relative energy levels of orbitals.

Generally, orbital energy levels directly correspond to their shell number. Additionally, orbitals within a shell generally follow the energetic trend where s<p<d<f. Although these general trends for relative orbital energy levels hold true for most of the main block elements (the s - and p-blocks), there are important exceptions in the orbital energy levels of transition metal atoms and ions of the d- and f-blocks.

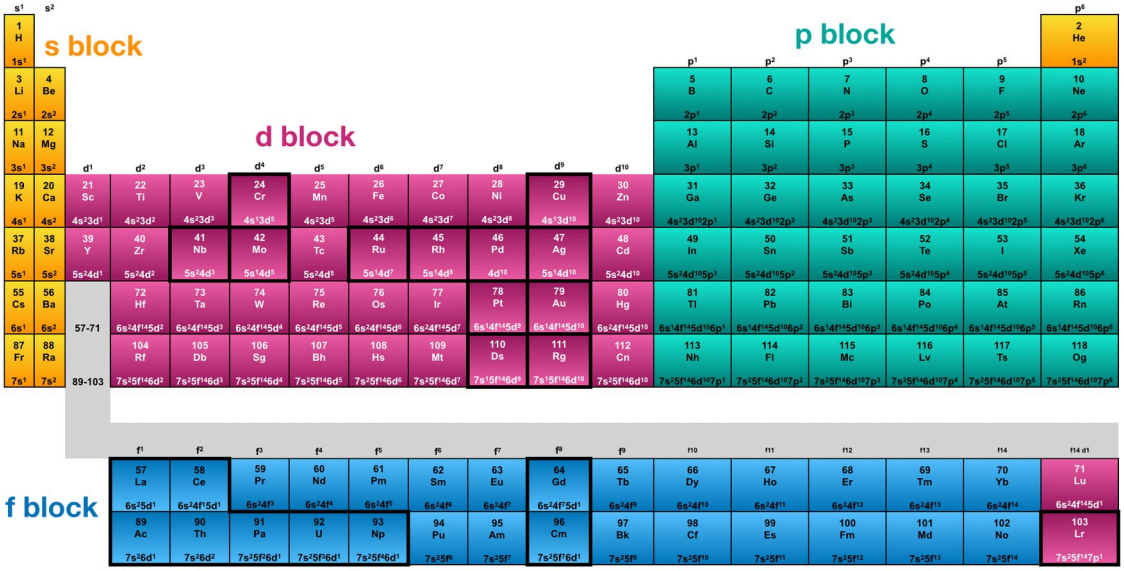


Figure 2.2.3.5. This is a depiction of the periodic table that highlights the s-, p-, d-, and f- blocks in different colors. Violations of the expected trend in electron configurations are outlined in a heavy black line. Several elements of the d block and f block violate the general trends in electron configuration because their orbital energy levels do not follow *general* trends. (CC-BY-NC-SA; Kathryn Haas)

Elements that violate general trends in electron configuration are outlined with a dark line in Figure 2.2.3.5. All of the exceptions are within the d- and f- blocks, and the violations are caused by an unexpected order of the orbital energy levels.

In the next section you will learn why the orbital energy levels correlate with shell number and why subshells within a shell usually follow the trend that s<p<d<f. You will also learn why there are occasional exceptions to this trend and how these exceptions

influence elemental properties.

References

1. Miessler, Gary L., and Donald A. Tarr. *Inorganic Chemistry*. Upper Saddle River, NJ: Pearson Prentice Hall, 2010. Print.
2. Brown, Ian David. *The Chemical Bond in Inorganic Chemistry the Bond Valence Model*. Oxford: Oxford UP, 2006. Print.

This page titled 2.2.3: Aufbau Principle is shared under a Public Domain license and was authored, remixed, and/or curated by Kathryn Haas.

- 2.2.3: Aufbau Principle by Kathryn Haas is licensed CC BY-NC-SA 4.0.

2.2.4: Shielding

Introduction

Coulomb's Law is from classical physics; it tells us that particles with opposite electrostatic charge are attracted to each other, and the larger the charge on either particle or the closer the distance between them, the stronger the attraction. Coulomb's law explains why atomic size decreases as the charge on the nucleus increases, but it can't explain the nuances and variations in size as we go across the periodic table. Coulomb's Law also explains why electrons in different shells (*n*), at different distances from the nucleus, have different energies. But on its own, Coulomb's law doesn't quite explain why electron subshells within a shell (like 2s vs. 2p) would have different energies. To explain these things, we need to consider how both electron **shielding** and **penetration** result in variations in effective nuclear charge (Z*) that depend on shell and subshell.

Effective Nuclear Charge (Z*)

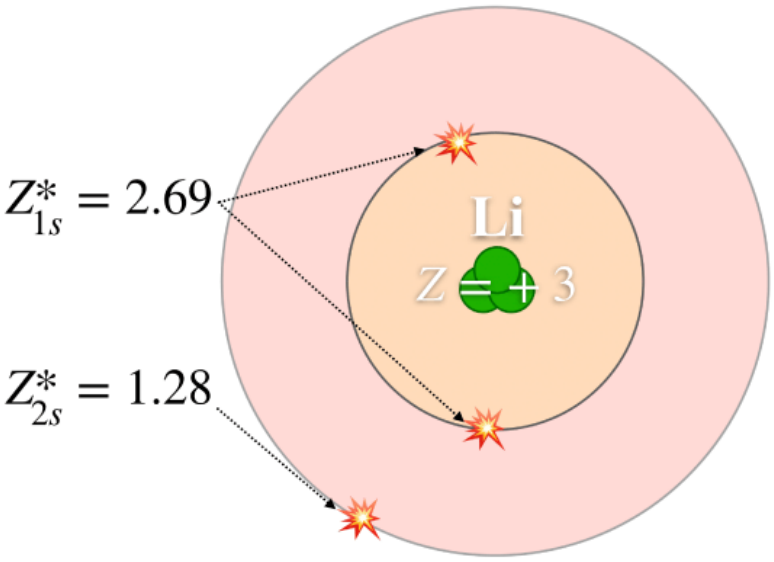


Figure 2.2.4.1. In a lithium atom, the nuclear charge (Z) is +3. 1s electrons experience an effective nuclear charge (Z*) of +2.69, and 2s electrons experience an Z* of +1.28. (CC-BY-NC-SA; Kathryn Haas)

Coulombs' law works well for predicting the energy of an electron in a hydrogen atom (because H has only one electron). It also works for hydrogen-like atoms: any nucleus with exactly one electron (a He^+ ion, for example, has one electron). However, Coulomb's law is insufficient for predicting the energies of electrons in multi-electron atoms and ions.

Electrons within a multi-electron atom interact with the nucleus and with all other electrons. Each electron in a multi-electron atom experiences both attraction to the nucleus and repulsion from interactions with other electrons. The presence of multiple electrons decreases the nuclear attraction to some extent. Each electron in a multi-electron atom experiences a different magnitude of (and attraction to) the nuclear charge depending on what specific shell and subshell the electron occupies. The amount of positive nuclear charge experienced by any individual electron is the **effective nuclear charge (Z*)**.

For example, in lithium (Li), none of the three electrons "feel" the full +3 charge from the nucleus (see Figure 2.2.4.1). Rather, each electron "feels" a Z* that is less than the actual Z and that depends on the electron's orbital. The actual nuclear charge in Li is $Z = +3$; the 1s electrons experience a $Z^* = +2.69$, and the 2s electron experiences a $Z^* = +1.28$. In general, core electrons (or the electrons closest to the nucleus), "feel" a Z* that is close to, but less than, Z. On the other hand, outer valence electrons experience a Z* that is much less than Z.

In summary:

- Core electrons: $Z^* \lessapprox Z$
- Valence electrons: $Z^* \ll Z$

Shielding:

Shielding is the reduction of true nuclear charge (Z) to the effective nuclear charge (Z*) by other electrons in a multi-electron atom or ion. Shielding occurs in all atoms and ions that have more than one electron. H is the only atom in which shielding does not occur.

Explanation of shielding: Electrons in a multi-electron atom interact with the nucleus and all other electrons in the atom. To describe shielding, we can use a simplified model of the atom: we will choose an electron-of-interest in a multi-electron atom and treat all the "other" electrons as a group of spherically-distributed negative charge. Classical electrostatics allows us to treat spherical distribution of charge as a point of charge at the center of the distribution. Thus, we consider all the "other" electrons in our atom as a point of negative charge in the center of the atom. While the positive charge of the nucleus provides an attractive force toward our electron, the negative charge distribution at the center of the atom would provide a repulsive force. The attractive and repulsive forces would partially cancel each other; but since there are less "other" electrons than there are protons in our atom, the nuclear charge is never completely canceled. The "other" electrons partially block, or shield, part of the nuclear charge so that our electron-of-interest experiences a partially-reduced nuclear charge, the Z*.

In reality, there is not a one-for-one "canceling" of the nuclear charge by each electron. Partly due to *penetration*, no single electron can completely shield a full unit of positive charge. Core electrons shield valence electrons, but valence electrons have little effect on the Z* of core electrons. The ability to shield, and be shielded by, other electrons strongly depends the electron orbital's average distance from the nucleus and its *penetration*; thus shielding depends on both shell (n) and subshell (l).

Shielding depends on electron penetration

Coulomb's law shows us that distance of an electron from its nucleus is important in determining the electron's energy (its attraction to the nucleus). The shell number (n) determines approximately how far an electron is from the nucleus *on average*. Thus, all orbitals in the same shell (s,p,d) have similar sizes and similar average distance of their electrons from the nucleus. But there is another distance-related factor that plays a critical role in determining orbital energy levels: *penetration*. **Penetration** describes the ability of an electron in a given subshell to penetrate into other shells and subshells to get close to the nucleus. Penetration is the **extent to which an electron can approach the nucleus**. Penetration depends on both the shell (n) and subshell (l).

The penetration of individual orbitals can be visualized using the radial probability functions. For example, Figure $2.2.4.2$ below shows plots of the radial probability function of the 1s, 2s, and 2p orbitals. From these plots, we can see that the 1s orbital is able to approach the closest to the nucleus; thus it is the most penetrating. While the 2s and 2p have most of their probability at a farther distance from the nucleus (compared to 1s), the 2s orbital and the 2p orbital have different extents of penetration. Notice that the 2s orbital is able to penetrate the 1s orbital because of the central 2s lobe. The 2p orbital penetrates somewhat into the 1s, but it cannot approach the nucleus as closely as the 2s orbital can. While the 2s orbital penetrates more than 2p (the 2s orbital can approach closer to the nucleus), the 2p is slightly *closer on average* than 2s. The order of Z* in 2s and 2p subshells depends on which factor (average distance or penetration) is more important. In the first two rows of the periodic table, penetration is the dominant factor that results in 2s having a lower energy than 2p (see Figure $2.2.4.4$ for values).

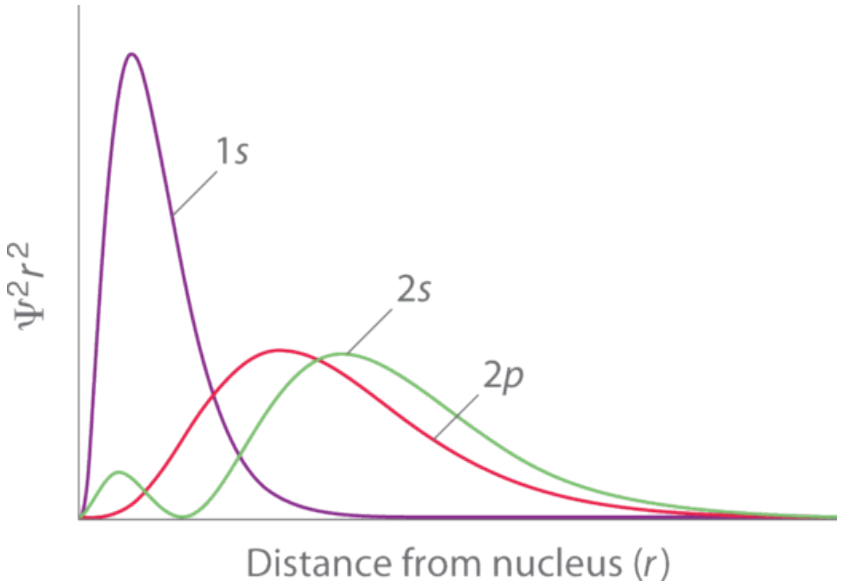


Figure 2.2.4.2. Orbital Penetration. A comparison of the radial probability distribution of the 2s and 2p orbitals for various states of the hydrogen atom shows that the 2s orbital penetrates inside the 1s orbital more than the 2p orbital does. Consequently, when an electron is in the small inner lobe of the 2s orbital, it experiences a relatively large value of Z*, which causes the energy of the 2s orbital to be lower than the energy of the 2p orbital.

An electron orbital's penetration affects its ability to shield other electrons and affects the extent to which it is shielded by other electrons. In general, electron orbitals that have greater penetration experience stronger attraction to the nucleus and less shielding by other electrons; these electrons thus experience a larger Z*. Electrons in orbitals that have greater penetration also shield other electrons to a greater extent.

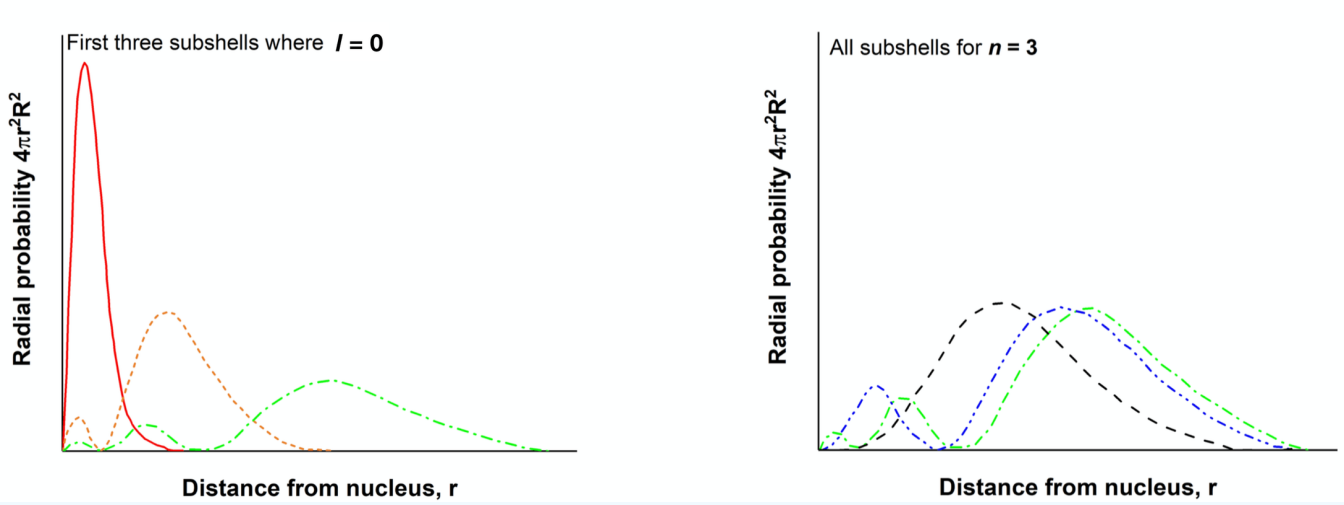
Within the same shell value (n), the penetrating power of an electron follows this trend in subshells (m_l):

s>p>d>f

Exercises

Exercises

1. Compare the 2s and 2p orbitals:
   (a) Which is closer to the nucleus on average?
   (b) Which is more penetrating?
   (c) Which orbital experiences a stronger Z* and is thus lower in energy (consider your experience, but also inspect Figures 1.1.2.3 and 1.1.2.4 from the previous page)? Please explain.
2. Peruse the Hyperphysics page (click) that shows radial probability functions of several orbitals (click around on various orbitals). Compare the 2p and 3s orbitals:
   (a) Which is farther from the nucleus on average?
   (b) Which is more penetrating?
   (c) Which orbital is lower in energy?
3. Which atom, Li, or N, has a stronger valence Z*? Explain why.
4. Explain why 2s and 2p subshells are completely degenerate in a hydrogen atom.
5. Which atom has a smaller radius: Be or F? Explain.
6. Which electrons shield others more effectively: 3p or 3d?
7. Use the clues given in the figures below to label the radial distribution functions shown.



8. Examine the plots on the right in the previous question, above. Note that this is a plot showing the probability density for the 3s, 3p, and 3d subshells.
(a) For which of these three functions is the highest probability density at the smallest r value (which is closest to the nucleus on average)? Is this the same subshell that penetrates most?
(b) Use this example to describe how penetration and shielding result in a splitting of subshell energy level in multi-electron atoms.

9. Explain why the ground state (most energetically favorable) electron configuration of Be is $1s^2 2s^2$ rather than alternative configurations like $1s^2 2s^1 2p^1$ or $1s^2 2p^2$.

Answer 1 available at the end of this section.

Slater's rules for estimating Z*

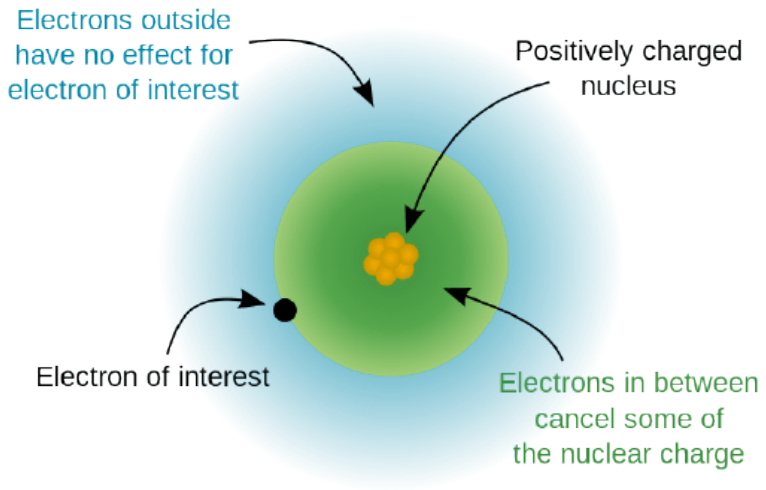


Figure 2.2.4.3. Diagram illustrating effective nuclear charge according to Slater's rules.

The Z* can be estimated using a number of different methods; probably the best known and most commonly used method is known as **Slater's Rules**. Slater developed a set of rules to estimate Z* based on how many other electrons exist in the atom and on the orbital location of the electron-of-interest. These two factors are important determinants in shielding, and they are used to calculate a **shielding constant (S)** used in Slater's formula:

$$Z* = Z - S$$

where Z is the actual nuclear charge (the atomic number) and Z* is the effective nuclear charge.

In the calculation of S, it is assumed that electrons closer to the nucleus than our electron-of-interest cancel some of the nuclear charge; those farther from the nucleus have no effect. To calculate S, all the relevant orbitals in an atom are written out in order of increasing energy, separating them into in "groups". Each change in shell number is a new group; s and p subshells are in the same group but d and f orbitals are their own group. You write out all the orbitals using parentheses until you get to the group of the electron-of-interest, like this:

(1s)(2s,2p)(3s,3p)(3d)(4s,4p)(4d)(4f)(5s,5p) etc.

**Critical: The orbitals must be written in order of increasing energy!

1. **Electrons in the same Group():** Each other electron (not counting the electron-of-interest) in the same group () as the chosen electron, contributes 0.35 to S.
   Conceptually, this means electrons in the same group shield each other 35%.
2. **Electrons in Groups() to the left:**
   - If the electron-of-interest is in a d or f subshell, every electron in groups () to the left contributes 1.00 to S.
     Conceptually, this means that d and f electrons are shielded 100% by all electrons in the same shell with a smaller value of l, as well as all electrons in lower shells (n).
   - If the electron-of-interest is in an s or p subshell, all electrons in the next lower shell (n - 1) contribute 0.85 to S. And all the electrons in even lower shells contribute 1.00 to S.
     Conceptually, this means that s and p electrons are shielded 85% by the electrons one shell lower, and 100% by all electrons in shells n - 2 or lower.
3. ***1s electrons:*** *S of a 1s electron is just S=0.3, no matter the element.*

A video explaining how to use Slater's Rules

Example 2.2.4.1: Fluorine, Neon, and Sodium

What is the Z* experienced by the valence electrons in the three isoelectronic species: fluorine anion (F^-), neutral neon atom (Ne), and sodium cation (Na^+)?

Solution

Each species has 10 electrons, and the number of core electrons is 2 (10 total electrons - 8 valence), but the effective nuclear charge varies because each has a different atomic number (Z). The approximate Z* can be found with Slater's Rules. For all of these species, we would calculate the same sigma value:

Calculating S: (1s)(2s,2p), $S = 2(0.85) + 7(0.35) = 1.7 + 2.45 = 4.15$

Fluorine anion: $Z* = 9 - S = 9 - 4.15 = 4.85$

Neon atom: $Z* = 10 - S = 10 - 4.15 = 5.85$

Sodium Cation: $Z* = 11 - S = 11 - 4.15 = 6.85$

So, the sodium cation has the greatest effective nuclear charge.

Exercise 2.2.4.1

Calculate Z* for a 3d-electron in a zinc (Zn) atom.

Answer available at the end of this section.

"Best" values for Z*

Slater's rules are a set of simple rules for predicting S and Z* based on empirical evidence from quantum mechanical calculations. In other words, the Z* calculated from Slater's rules are approximate values. The values considered to be the most accurate are derived from quantum mechanical calculations directly. You can find these values in a nice chart on the Wikipedia article of Effective Nuclear Charge. The chart is recreated here in Figure 2.2.4.3 for convenience:

Z or Z_{eff}	H																	He
Z	1.00																	2.00
1s	1.00																	1.69
	Li	Be											B	C	N	O	F	Ne
Z	3.00	4.00											5.00	6.00	7.00	8.00	9.00	10.00
1s	2.69	3.69											4.68	5.67	6.67	7.66	8.65	9.64
2s	1.28	1.91											2.58	3.22	3.85	4.49	5.13	5.76
2p													2.42	3.14	3.83	4.45	5.10	5.76
	Na	Mg											Al	Si	P	S	Cl	Ar
Z	11.00	12.00											13.00	14.00	15.00	16.00	17.00	18.00
1s	10.63	11.61											12.59	13.58	14.56	15.54	16.52	17.51
2s	6.57	7.39											8.21	9.02	9.83	10.63	11.43	12.23
2p	6.80	7.83											8.96	9.95	10.96	11.98	12.99	14.01
3s	2.51	3.31											4.12	4.90	5.64	6.37	7.07	7.76
3p													4.07	4.29	4.89	5.48	6.12	6.76
	K	Ca	Sc	Ti	V	Cr	Mn	Fe	Co	Ni	Cu	Zn	Ga	Ge	As	Se	Br	Kr
Z	19.00	20.00	21.00	22.00	23.00	24.00	25.00	26.00	27.00	28.00	29.00	30.00	31.00	32.00	33.00	34.00	35.00	36.00
1s	18.49	19.47	20.46	21.44	22.43	23.41	24.40	25.38	26.37	27.35	28.34	29.33	30.31	31.29	32.28	33.26	34.25	35.23
2s	13.01	13.78	14.57	15.38	16.18	16.98	17.79	18.60	19.41	20.21	21.02	21.83	22.60	23.37	24.13	24.89	25.64	26.40
2p	15.03	16.04	17.06	18.07	19.07	20.08	21.08	22.09	23.09	24.10	25.10	26.10	27.09	28.08	29.07	30.07	31.06	32.05
3s	8.68	9.60	10.34	11.03	11.71	12.37	13.02	13.68	14.32	14.96	15.59	16.22	17.00	17.79	18.60	19.40	20.22	21.03
3p	7.73	8.66	9.41	10.10	10.79	11.47	12.11	12.78	13.44	14.09	14.73	15.37	16.20	17.01	17.85	18.71	19.57	20.43
4s	3.50	4.40	4.63	4.82	4.98	5.13	5.28	5.43	5.58	5.71	5.84	5.97	7.07	8.04	8.94	9.76	10.55	11.32
3d			7.12	8.14	8.98	9.76	10.53	11.18	11.86	12.53	13.20	13.88	15.09	16.25	17.38	18.48	19.56	20.63
4p													6.22	6.78	7.45	8.29	9.03	9.34
	Rb	Sr	Y	Zr	Nb	Mo	Tc	Ru	Rh	Pd	Ag	Cd	In	Sn	Sb	Te	I	Xe
Z	37.00	38.00	39.00	40.00	41.00	42.00	43.00	44.00	45.00	46.00	47.00	48.00	49.00	50.00	51.00	52.00	53.00	54.00
1s	36.21	37.19	38.18	39.16	40.14	41.13	42.11	43.09	44.08	45.06	46.04	47.03	48.01	48.99	49.97	50.96	51.94	52.92
2s	27.16	27.90	28.62	29.37	30.13	30.88	31.63	32.38	33.16	33.88	34.63	35.39	36.12	36.86	37.60	38.33	39.07	39.80
2p	33.04	34.03	35.00	35.99	36.98	37.97	38.94	39.95	40.94	41.93	42.92	43.91	44.90	45.89	46.87	47.86	48.85	49.84
3s	21.84	22.66	23.55	24.36	25.17	25.98	26.79	27.60	28.44	29.22	30.03	30.84	31.63	32.42	33.21	34.00	34.79	35.58
3p	21.30	22.17	23.09	23.85	24.62	25.47	26.38	27.22	28.15	29.02	29.81	30.69	31.52	32.35	33.18	34.01	34.84	35.67
4s	12.39	13.44	14.26	14.90	15.28	16.10	17.20	17.66	18.58	18.99	19.87	20.87	21.76	22.66	23.54	24.41	25.30	26.17
3d	21.68	22.73	25.40	25.57	26.25	27.23	28.35	29.36	30.41	31.45	32.54	33.61	34.68	35.74	36.80	37.84	38.90	39.95
4p	10.88	11.93	12.75	13.46	14.08	14.98	15.81	16.44	17.14	17.72	18.56	19.41	20.37	21.27	22.18	23.12	24.03	24.96
5s	4.99	6.07	6.26	6.45	5.92	6.11	7.23	6.49	6.64	(empty)	6.76	8.19	9.51	10.63	11.62	12.54	13.40	14.22
4d			15.96	13.07	11.24	11.39	12.88	12.81	13.44	13.62	14.76	15.88	16.94	17.97	18.97	19.96	20.93	21.89
5p													8.47	9.10	10.00	10.81	11.61	12.43

Figure 2.2.4.4. This chart shows Z* values calculated by Clementi et al. in 1963 and 1967 that are consistent with SCF Calculations. This chart was created using data from the Wikipedia article on Effective Nuclear Charge. (Kathryn Haas; CC-NC-BY-SA)

Z* modulates attraction

When valence electrons experience less nuclear charge than core electrons, different electrons experience different magnitudes of attraction to the nucleus. A modified form of Coulomb's Law is written below, where e is the charge of an electron, Z* is the effective nuclear charge experienced by that electron, and r is the radius (distance of the electron from the nucleus).

$$F_{eff} = k\frac{Z * e^2}{r^2}$$

This formula suggests that if we can estimate Z*, then we can predict the attractive force experienced by, and the energy of, an electron in a multi-electron atom (ex. Li).

The attraction of the nucleus to valence electrons determines the atomic or ionic size, ionization energy, electron affinity, and electronegativity. The stronger the attraction, and the stronger Z*, the closer the electrons are pulled toward the nucleus. This in turn results in a smaller size, higher ionization energy, higher electron affinity, and stronger electronegativity.

General Periodic Trends in Z*

Close inspection of Figure 2.2.4.3 and analysis of Slater's rules indicate that there are some predictable trends in Z*. The data from Figure 2.2.4.3 is plotted below in Figure 2.2.4.4 to provide a visual aid to the discussion below.

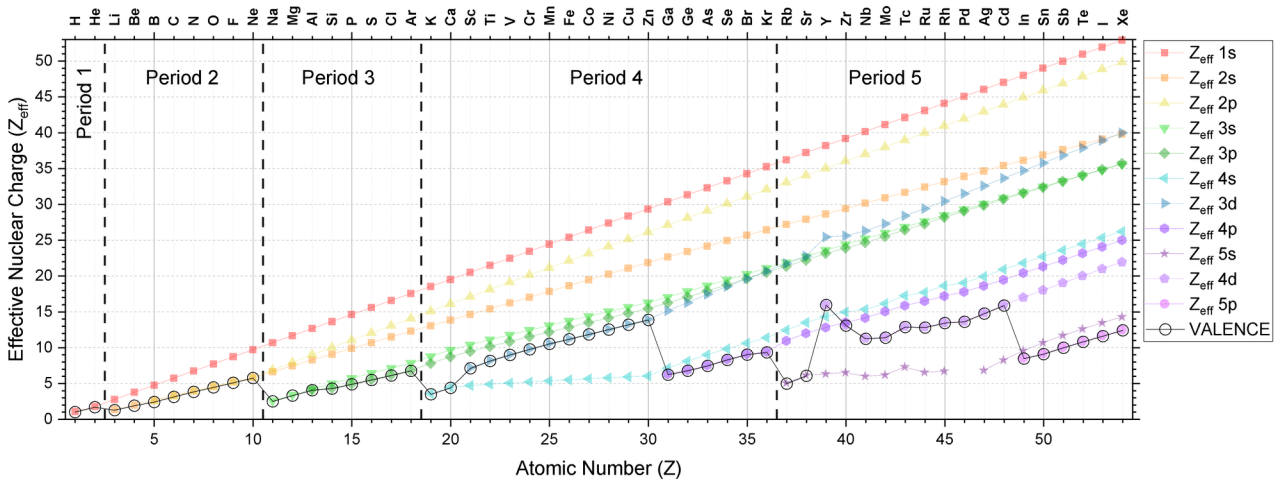


Figure 2.2.4.5: The Z* values for electrons in each subshell of the first 54 elements (H to Xe). Each subshell is plotted as a different series (see legend) and the valence shell is highlighted by a solid black line with open circles. (Kathryn Haas; CC-NC-BY-SA)

Trends in Z* for electrons in a specific shell and subshell

The Z* for electrons in a given shell and subshell generally increases as atomic number increases; this trend holds true going across the periodic table and down the periodic table. Convince yourself that this is true for any subshell by examining Figure 2.2.4.4. (CC-BY-NC-SA; Kathryn Haas)

Do you notice any exceptions to this general trend?

Inspection of Figure 2.2.4.4 should confirm for you that the Z* increases as Z increases for electrons in any subshell (like the 1s subshell for example, which is plotted above as a red line with square points). You can see this trend as the positive slope in each series. There is one obvious exception in Period 5 in elements 39 (Y) to 41 (Nb; the Z* of 4s actually decreases across these three elements as atomic number increases. There is also an exception between Y and Zr in the 3d subshell, and between Tc and Ru in the 5s subshell.

For valence electrons:

It is useful to understand trends in valence Z* because the valence Z* determines atomic/ionic properties and chemical reactivity. The trends in the valence Z* are not simple because as atomic number increases, the valence shell and/or subshell also changes. The valence Z* is indicated in Figure 2.2.4.4 as a black line with open circles.

Down the table: As we go down a column of the periodic table, the valence Z* increases. This is a simple trend because type of subshell is consistent and there is an increase only in shell and in atomic number, Z. This trend is best illustrated by inspection of Figure 2.2.4.3.

Across the table: the trend depends on shell and subshell, but generally Z* increases across a period.

Periods 1-3 (s and p only): As we go across the table in periods 1-3, the shell stays constant as Z increases and the subshell changes from s to p. In these periods, there is a gradual increase in valence Z* as we move across any of the first three periods.

Periods 4 and 5 (s, p, and d): Now we have some more complex trends because valence subshell and shell are changing as we increase in atomic number. Notice that the valence Z* generally increases going across a period as long as the subshell isn't changing; the exception is within the 4d subshell (elements 39-44 or Y-Ru). In general, going from an $(n)s$ subshell to an $(n-1)d$ subshell, there a relatively large increase in valence Z*. And in going from an $(n-1$d\) subshell to an $(n)p$ subshell, there is a relatively large decrease in Z*.

From one period to another: From Figure 2.2.4.4, we can see that as we increase Z by one proton, going from one period to the next, there is a relatively large decrease in Z* (from Ne to Na, for example). This is because as Z increases by a small

interval, the shell number increases, and so the electrons in the valence shell are much farther from the nucleus and are more shielded by all the electrons in the lower shell numbers.

Exercises

Exercise 2.2.4.2

1. Compare trends in Z* and atomic size. Explain how and why atomic size depends on Z*.
2. Compare trends in Z* and ionization energy. Explain how and why ionization energy depends on Z*.

Answer available at the end of this section.

References

1. Petrucci, Ralph H., William S. Harwood, F. Geoffrey Herring, and Jeffry D. Madura. General Chemistry: Principles and Modern Applications, Ninth Edition. Pearson Education Inc. Upper Saddle River, New Jersey: 2007.
2. Raymond Chang. Physical Chemistry for Biological Sciences. Sausalito, California: University Science Books, 2005
3. R. S. Mulliken, Electronic Structures of Molecules and Valence. II General Considerations, Physical Review, vol. 41, pp. 49-71 (1932)
4. Anastopoulos, Charis (2008). *Particle Or Wave: The Evolution of the Concept of Matter in Modern Physics*. Princeton University Press. pp. 236–237. ISBN 0691135126. http://books.google.com/?id=rDEvQZhpltEC&pg=PA236.

Contributors and Attributions

- Sidra Ayub (UCD), Alan Chu (UCD)
- Emily V Eames (City College of San Francisco)
- Curated or created by Kathryn Haas

Answers

Exercises

(a) The 2s orbital is closer to the nucleus on average.

(b) The 2s orbital is more penetrating than 2p.

(c) You might "know" that the 2s orbital is lower in energy than 2p because 2s fills first. But a close inspection of Figures 1.1.2.3 and 1.1.2.4 from the previous page indicates that while the 2s and 2p elements are degenerate in Ne (element 10), for elements with atomic number 11 and greater 2p has a higher Z* than 2s! This example illustrates that both average distance and penetration are factors in determining Z*, and the factor that is more important may change as we increase in atomic number.

(a) The 3s orbital reaches farther away from the nucleus and is on average farther from the nucleus than 2p.

(b) The 3s orbital is more penetrating than 2p, even though 3s is farther on average!

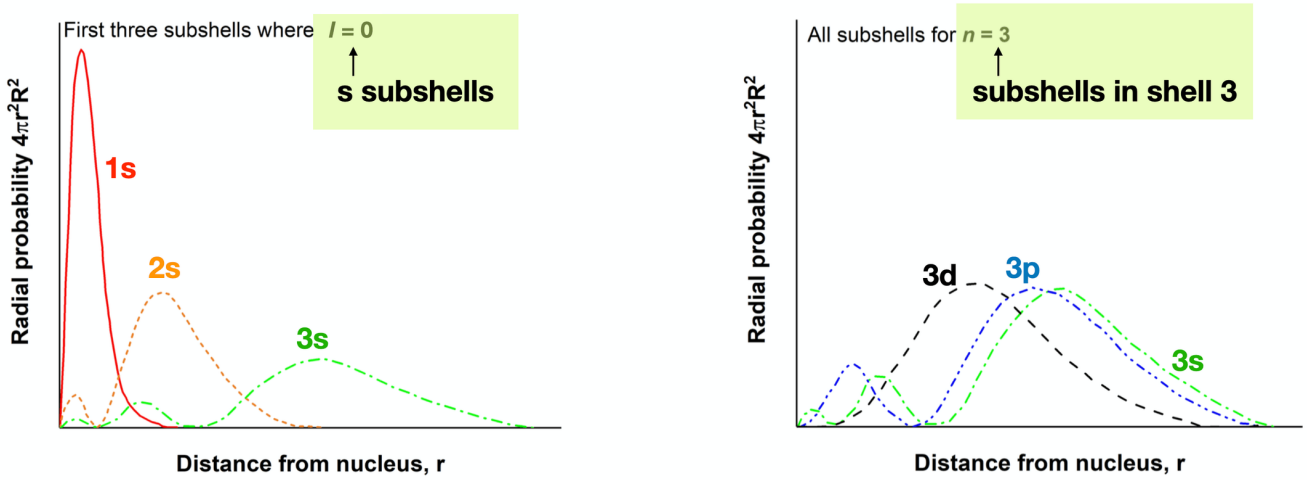
(c) The 2p orbital is lower in energy than 3s; this is because 2p is still significantly closer to the nucleus on average and experiences a stronger Z*. (Penetration is not the only consideration!)

A nitrogen atom has a stronger effective nuclear charge (Z*) than lithium due to its greater number of protons; even though N also has more electrons that would shield the nuclear charge, each electron only partially shields each proton. This means that atoms with greater atomic number always have greater Z* for any given electron.

The hydrogen atom has only one electron; thus there is no shielding to consider. When there are not other electrons to shield the nucleus, penetration and shielding are irrelevant, and subshells within a shell are degenerate.

Fluorine has a smaller radius than beryllium because F has a greater valence Z* and therefore pulls the valence electrons closer to the nucleus and provides a smaller atomic radius.

3p shields better than 3d because p orbitals penetrate more than d orbitals within the same shell.



3d is closest on average, but 3s penetrates most. The three subshells of $n = 3$ differ in their average distance and in their ability to penetrate; these factors result in differences in the Z* experienced by electrons in each orbital. We would expect 3s to be lowest in energy followed by 3p and then 3d.

This question is asking why the 2s orbital fills in Be before 2p is occupied. This is a multi-electron atom, therefore core electrons shield the 2s and 2p orbitals to different extents. In Be we expect the 2s orbital to fill before 2p because 2s penetrates more and experiences a higher Z*.

Exercise 2.2.4.1

Write out the relevant orbitals: (1s)(2s,2p)(3s,3p)(3d) ~~(4s)~~

Notice that although 4s is fully occupied, we don't include it because in Zn, 4s is higher in energy than 3d. Therefore, 4s is to the right of the d electrons we are considering. The electron-of-interest is in 3d, so the other nine electrons in 3d each contribute 0.35 to the value of S. The other 18 electrons each contribute 1 to the value of S.

$S = 18(1) + 9(0.35) = 21.15$

$Z* = 30 - 21.15 = 8.85$

So, although the nuclear charge of Zn is 30, the 3d electrons only experience a $Z* \approx 8.85$!

Exercise 2.2.4.2

1. On the periodic table, atomic radius generally decreases across the periods (left to right) and increases down the groups. As atomic number increases across the periodic table, nuclear charge (Z) increases and Z* increases. In turn, the atomic radius decreases because the higher nuclear charge (and thus higher Z*) pulls electrons closer to the nucleus. Atomic radius increases down the periodic table because the shell number increases. Despite an increase in Z* going down the periodic table, larger atomic radii result from electrons occupying higher shells.

2. Ionization energies (IE) are inversely related to atomic radius; IE increases across the periods and decreases down the groups. Since the nucleus holds valence electrons more strongly (due to higher Z*) across the periods, IE increases because valence electrons are harder to remove. Down the periodic table, larger atomic radii cause electrons in valence orbitals to be shielded by core electrons. Recall that shielding reduces the nuclear charge available to electrons in higher orbital levels, resulting in a lower Z*. With more shielding and lower Z*, the valence electrons are held less tightly by the nucleus such that ionization energy decreases (i.e., valence electrons are easier to remove).

This page titled 2.2.4: Shielding is shared under a CC BY-NC-SA 4.0 license and was authored, remixed, and/or curated by LibreTexts.

- 2.2.4: Shielding by Kathryn Haas is licensed CC BY-NC-SA 4.0.

2.3: PERIODIC PROPERTIES OF ATOMS

General periodic trends are specific patterns that are present within the periodic table; these are patterns in properties like electronegativity, ionization energy, electron affinity, atomic radius, melting point, and metallic character. General periodic trends provide chemists with an invaluable tool to quickly predict an element's properties. These trends exist because of the similar atomic structure of the elements within their respective group families or periods, and because of the periodic nature of the elements. Some of the general periodic trends are described in this section.

2.3.1: Ionization energy

2.3.2: Electron Affinity

2.3.3: Covalent and Ionic Radii

References

1. Russo, Steve, and Mike Silver. Introductory Chemistry. San Francisco: Pearson, 2007.
2. Petrucci, Ralph H, et al. General Chemistry: Principles and Modern Applications. 9th Ed. New Jersey: Pearson, 2007.
3. Atkins, Peter et. al, *Physical Chemistry*, 7th Edition, 2002, W.H Freeman and Company, New York, pg. 390.
4. Alberty, Robert A. et. al, *Physical Chemistry*, 3rd Edition, 2001, John Wiley & Sons, Inc, pg. 380.
5. Kots, John C. et. al, *Chemistry & Chemical Reactivity*, 5th Edition, 2003, Thomson Learning Inc, pg. 305-309.

This page titled 2.3: Periodic Properties of Atoms is shared under a license and was authored, remixed, and/or curated by LibreTexts.

- 2.3: Periodic Properties of Atoms by Kathryn Haas is licensed CC BY-NC-SA 4.0.

2.3.1: Ionization energy

Ionization energy (IE) is the energy required to **remove an electron from a neutral atom or cation in its gaseous phase**. IE is also known as *ionization potential*.

$$A_{(g)}^{n+} \longrightarrow A_{(g)}^{(n+1)+} + e^- \qquad IE = \Delta U$$

Conceptually, ionization energy is the affinity of an element for its outermost electron (an electron it already has in its valence shell).

1st, 2nd, and 3rd Ionization Energies

The symbol I_1 stands for the ***first ionization energy*** (energy required to take away an electron from a neutral atom, where $n = 0$). The symbol I_2 stands for the ***second ionization energy*** (energy required to take away an electron from an atom with a +1 charge, $n = 2$.)

- **First Ionization Energy,** I_1 (general element, A):

$$A_{(g)} \rightarrow A_{(g)}^{1+} + e^-$$

- **Second Ionization Energy,** I_2 (general element, A):

$$A_{(g)}^{1+} \rightarrow A_{(g)}^{2+} + e^-$$

- **Third Ionization Energy,** I_3 (general element, A):

$$A_{(g)}^{2+} \rightarrow A_{(g)}^{3+} + e^-$$

Each succeeding ionization energy is larger than the preceding energy. This means that $I_1 < I_2 < I_3 < ... < I_n$ will always be true. For example, ionization energy increases as succeeding electrons are taken away from Mg.

$$Mg_{\,(g)} \rightarrow {Mg^+}_{\,(g)} + e^- \quad I_1 = 738\,kJ/mol$$

$${Mg^+}_{\,(g)} \rightarrow {Mg^{2+}}_{\,(g)} + e^- \quad I_2 = 1451\,kJ/mol$$

Ionization energy is correlated with the strength of attraction between the positively-charged nucleus and the negatively-charged valence electrons. The higher the ionization energy, the stronger the attractive force between nucleus and valence electrons, and the more energy is required to remove a valence electron. The lower the ionization energy, the weaker the attractive force between nucleus and valence electrons, and the less energy required to remove a valence electron.

General periodic trends in electron affinity

In general, ionization energies increase from left to right and decrease down a group; however, there are variations in these trends that would be expected from the effects of penetration and shielding. The trends in **first ionization energy** are shown in Figure $2.3.1.1$ and are summarized below.

- **Across a period:** As Z* increases across a period, the ionization energy of the elements generally increases from left to right. However there are breaks or variation in the trends in the following cases:
  - IE is especially low when removal of an electron creates a newly empty p subshell (examples include I_1 of B, Al, Sc)
  - IE energy is especially low where removal of an electron results in a half-filled p or d subshell (examples include I_1 of O, S)
  - IE increases more gradually across the d- and f-subshells compared to s- and p- subshells. This is because d- and f-electrons are weakly penetrating and experience especially low Z*.
- **From one period to the next:** There is an especially large decrease in IE with the start of every new period (from He to Li or from Ne to Na for example). This is consistent with the idea that IE is especially low when removal of an electron creates a newly empty s-subshell.

- **Noble gases:** The noble gases posses very high ionization energies. Note that helium has the highest ionization energy of all the elements.
- **Down a group:** Although Z* increases going down a group, there is no reliable trend in IE going down any group; in some cases IE increases going down a group, while in other cases IE decreases going down a group.

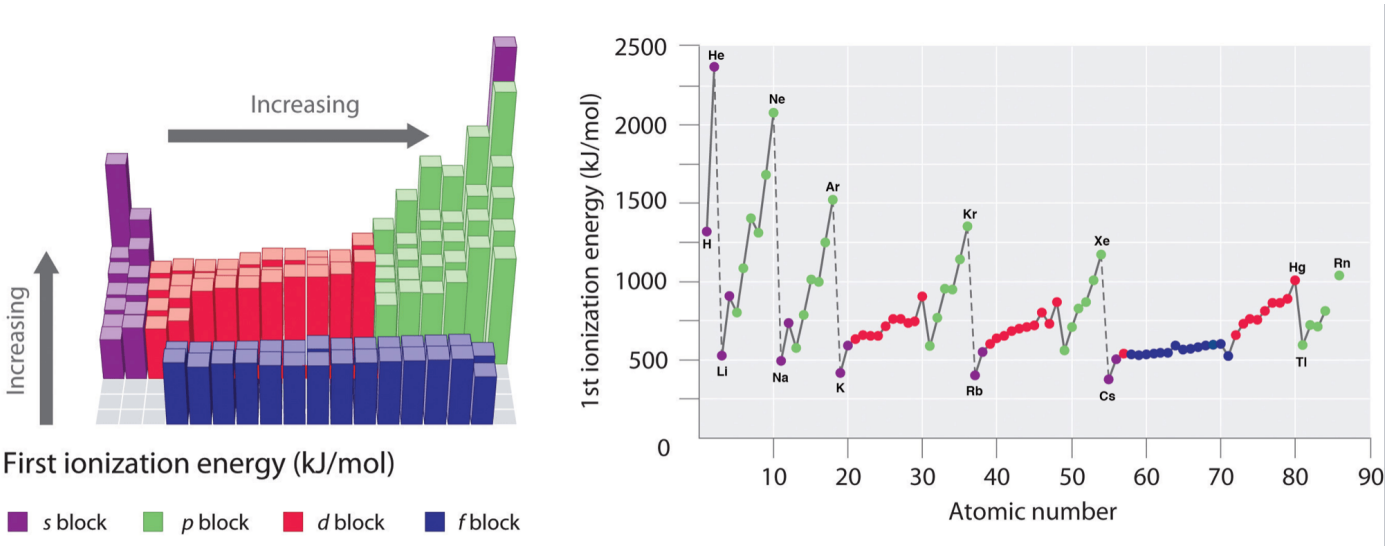


Figure 2.3.1.1: Graph showing the First Ionization Energy of the Elements. Left: ionization energies are mapped onto the periodic table, where the magnitude of ionization energy is depicted as a bar graph. Right: the first ionization energy is plotted against atomic number. In both panels the elements of the s-block are shown in purple, p-block are shown in green, d-block are shown in red, and f-block are shown in blue. (CC BY-NC-SA 3.0; anonymous)

Plots of the I_1, I_2, and I_3 of elements from hydrogen to krypton (first four periods) are shown in Figure 2.3.1.2. Notice that $I_3 > I_2 > I_1$. Also notice that trends mentioned above for I_1 hold true for subsequent ionizations when electron configurations are considered!

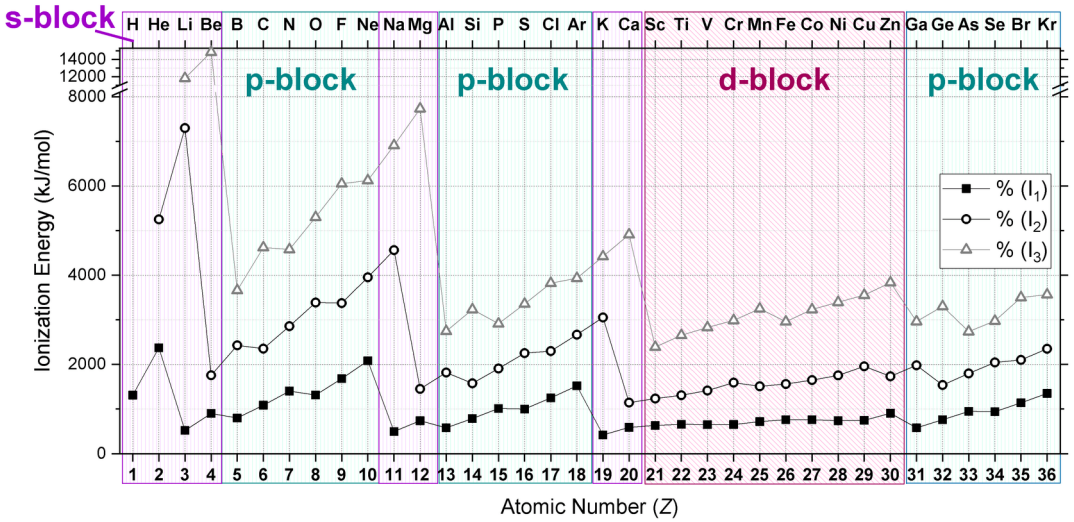


Figure 2.3.1.2. The first (I_1), second (I_2), and third (I_3) ionization energies plotted for elements with Z = 1 to 36 (H to Kr). The position of each element in its atomic form is indicated as s- p- or d-block. (CC-BY-NC-SA; Kathryn Haas)

This page titled 2.3.1: Ionization energy is shared under a license and was authored, remixed, and/or curated by LibreTexts.

- 2.3.1: Ionization energy by Bingyao Zheng, Emily Nguyen, Kathryn Haas, Swetha Ramireddy is licensed CC BY-NC-SA 3.0.

2.3.2: Electron Affinity

Definitions of Electron Affinity

According to IUPAC, there are two different, but equivalent, definitions of **electron affinity (EA)**.[1]

Definition: Electron Affinity defined as removal of an electron

Electron affinity can be defined as the energy *required* when an electron is removed from a gaseous anion. The reaction as shown in equation 2.3.2.1 is *endothermic* (positive ΔU) for elements except noble gases and alkaline earth metals. Under this definition, the more positive the EA value, the higher an atom's affinity for electrons.

$$A^-_{(g)} \longrightarrow A_{(g)} + e^- \qquad EA = \Delta U \tag{2.3.2.1}$$

The reaction shown in Equation 2.3.2.1 is similar those that define ionization energy. For this reason, the EA is also described as the *zeroth ionization energy*.

Definition: Electron Affinity defined as addition of an electron

An alternate and more common definition is the microscopic reverse of Equation 2.3.2.1. This more common definition states that electron affinity is the energy *released* when an electron is added to a gaseous atom, as shown in Equation 2.3.2.2. The reaction as shown in equation 2.3.2.2 is *exothermic* (negative ΔU) for elements except noble gases and alkaline earth metals. The more negative this EA value, the higher an atom's affinity for electrons.

$$A_{(g)} + e^- \longrightarrow A^-_{(g)} \qquad EA = \Delta U \tag{2.3.2.2}$$

Conceptually, this second definition is quite similar to the concept of electronegativity; but unlike electronegativity, EA is a well-defined quantitative measurement.

Trends in Electron Affinity

For this discussion, we will use the definition of EA that is consistent with it being a *zeroth ionization energy:* a more positive (larger) value means that the EA is higher (meaning stronger affinity toward an electron).

- **Across a period**: Similar to ionization energy, EA generally increases across a row of the periodic table; this observation is consistent with the increase in effective nuclear charge (Z*) from left to right across a period. However, there are variations across a period that are similar to variations in ionization energy and that can be explained by shielding, penetration, and electron configuration.
- **Down a group**: Like the case of ionization energy trends, EA does not consistently decrease going down a column of the periodic table despite the fact that Z^* increases down a group.

The trend in EA follows a zig-zag pattern similar to the one seen with ionization energies, except that it is displaced by one unit from the trend in I_1, two units from I_2, and so on. For example, EA peaks at F, while I_1 peaks at Ne, I_2 peaks at Na, and I_3 peaks at Mg. A plot of EA for the first 13 elements is shown overlaid on plots of I_1, I_2 and I_3 in Figure 2.3.2.1., where the shifts in the peaks and valleys within each zig-zag trend are indicated.

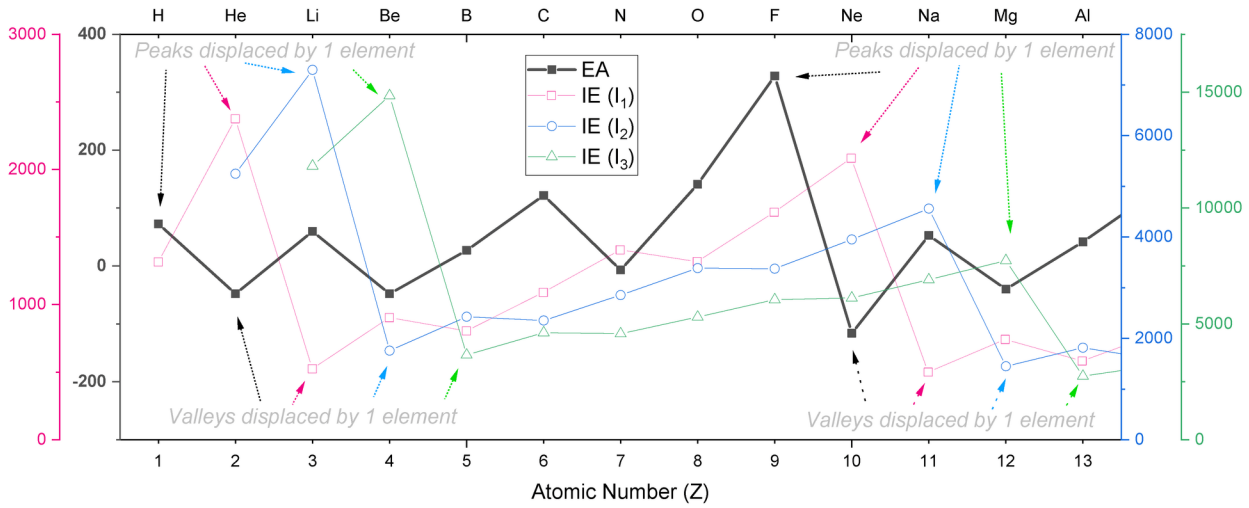


Figure 2.3.2.1. A plot of electron affinity (the zeroth ionization energy) is overlaid on plots of the first (I_1), second (I_2), and third (I_3) ionization energies. Each plot is shown using separate y-axes. Trends in EA are similar to those in ionization energies, except that the peaks and valleys of the trends are shifted by one unit, as indicated. These plots are shown in units of kJ/mole. (CC-BY-NC-SA; Kathryn Haas)

Sources

1. IUPAC. Compendium of Chemical Terminology, 2nd ed. (the "Gold Book"). Compiled by A. D. McNaught and A. Wilkinson. Blackwell Scientific Publications, Oxford (1997). Online version (2019-) created by S. J. Chalk. ISBN 0-9678550-9-8. doi.org/10.1351/goldbook.
2. Electron Affinity (data page), Wikipedia. en.Wikipedia.org/wiki/Electron_affinity_(data_page) Accessed 12/3/19.

This page titled 2.3.2: Electron Affinity is shared under a license and was authored, remixed, and/or curated by LibreTexts.

- 2.3.2: Electron Affinity by Kathryn Haas is licensed CC BY-NC-SA 4.0.

2.3.3: Covalent and Ionic Radii

Measurement of Radius

There are several methods that can be used to determine radii of atoms and ions:

- **Nonpolar atomic radii:** The radius of an atom is derived from the bond lengths within nonpolar molecules; one-half the distance between the nuclei of two atoms within a covalent bond.
- **van der Waals radius:** The radius of an atom is determined by collision with other atoms.
- **Crystal radii**: The atomic or ionic radius is determined using electron density maps from X-ray data.

The measurement of atomic or ionic size will depend on a number of factors, including the covalent character of bonding in any particular molecule, coordination number, physical state (liquid, solid, gas), the identity of nearby atoms/ions, variation in crystal structure, and distortions within regular crystal structures. You should keep in mind that the size of an atom or ion is a "fuzzy" measure, and the radius under a different set of conditions will probably change slightly.

Regardless, measured atomic and ionic radii reveal obvious trends across the periodic table and between atoms and ions. The relative atomic sizes shown in Figure 2.3.3.1 were derived from crystallographic data.[1]

Trends in Atomic Radius

Atomic size generally decreases gradually from left to right across a period of elements. As nuclear charge (Z) increases, we expect the effective nuclear charge (Z*) of the valence electrons to also increase. Increasing Z pulls electrons closer to the nucleus. However, with each additional unit of Z, there is also an additional electron. The change in size is a balance of a compression caused by increasing Z and an expansion in the number of electrons. As a result, the atomic radius decreases *gradually* across a period.

Atomic size generally increases going down a group. As valence electrons occupy higher level shells due to the increasing quantum number (n), size increases despite the fact that Z and Z* are increasing going down the group.

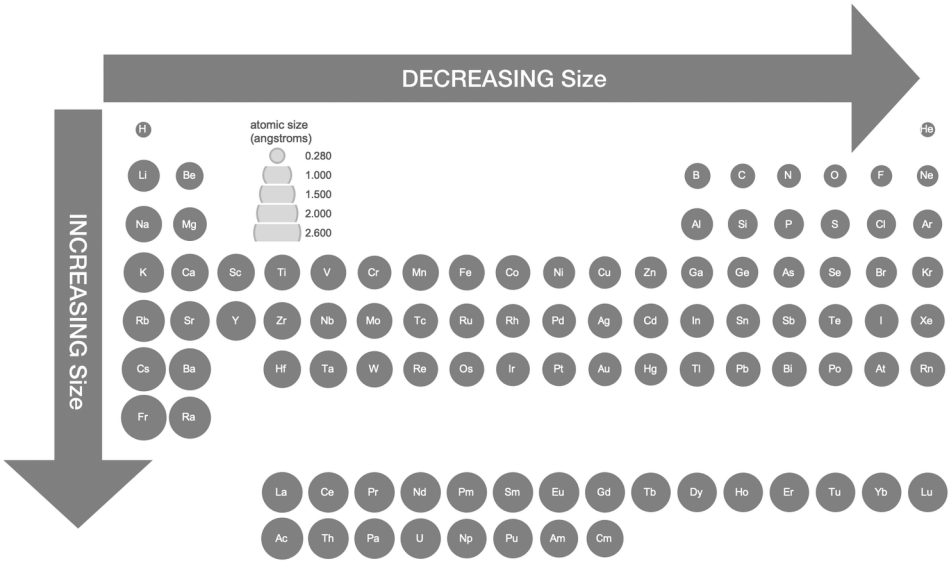


Figure 2.3.3.1. *Atomic Radii Calculated from Crystalographic Data. Data from Cordero, Beatriz, Veronica Gomez, Ana E. Platero-Prats, Marc Reves, Jorge Echeverria, Eduard Cremades, Flavia Barragan, and Santiago Alvarez. "Covalent Radii Revisited." Dalton Transactions, no. 21 (2008): 2832–38. doi:10.1039/b801115j.* (Kathryn Haas; CC-NC-BY-SA)

Trends in Ionic Radius

Trends in ionic radius follow general trends in atomic radius for ions of the same charge. Ionic radius varies with the charge of the ion (and number of electrons) and the electron configuration (e.g. high spin or low spin).

Cations

Compared to their atoms, cations have the same Z but fewer electrons. Removal of electrons from an atom to form a cation results in a significant increase in effective nuclear charge, resulting in all other electrons being more strongly attracted to the nucleus, and having a lower energy level. The result is a contraction in size from the atom to cation. Figure 2.3.3.2 visually illustrates the relative size of atoms and some cations of the first four periods; the data is available in tabular format in Figure 2.3.3.3.

Anions

Compared to their atoms, anions have the same Z but more electrons. Addition of electrons to an atom to form an anion results in a decrease in effective nuclear charge, which corresponds to a decrease in attractive force between the nucleus and electrons. Lower attractive force leads to expansion, where the size of the atom becomes larger in the formation of an anion. Figure 2.3.3.2 visually illustrates the relative size of atoms and some anions of the first four periods, while the data is available in tabular format in Figure 2.3.3.3.

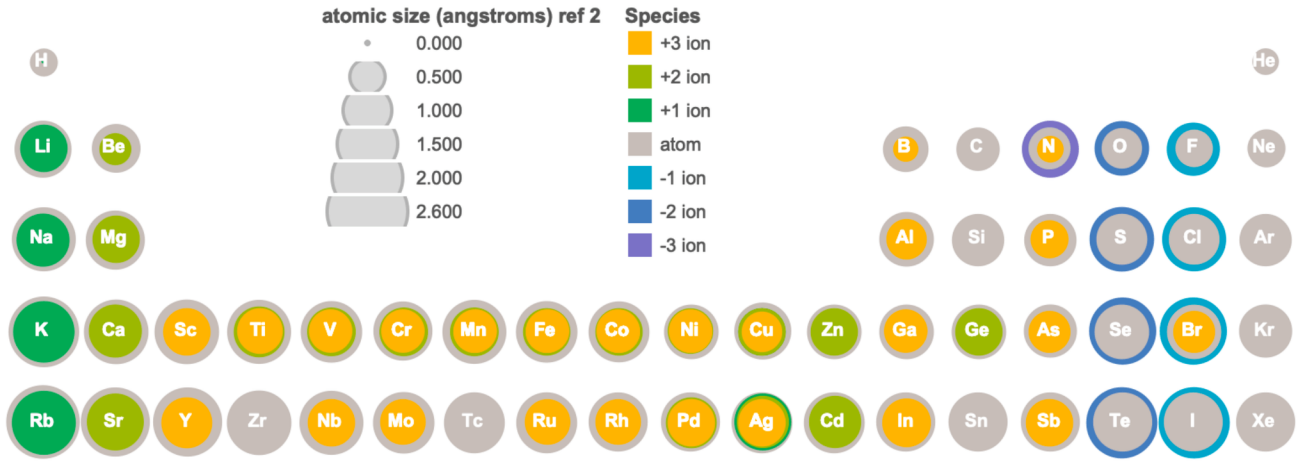


Figure 2.3.3.2. This figure illustrates relative size of atoms and ions of the first four periods of the periodic table. Atomic radius is indicated by grey circles. Radius of cations is shown in green (+1), lime (+2), and yellow (+3) circles. Radius of anions are shown as aqua (-1), blue (-2), and purple (-3) circles. Data from sources 1-3. (Kathryn Haas; CC-NC-BY-SA)

H 0.31 (atom) 0 (+1)																	He 0.28 (atom)
Li 1.28 (atom) 0.9 (+1) - -	Be 0.96 (atom) 0.41 (+2) - -											B 0.84 (atom) 0.25 (+1)	C 0.76 (atom) 0.29 (+4)	N 1.32 (-3) 0.71 (atom) 0.3 (+3) 0.27 (+5)	O 1.21 (-2) 0.66 (atom)	F 1.145 (-1) 0.57 (atom)	Ne 0.58 (atom)
Na 1.66 (atom) 1.16 (+1)	Mg 1.41 (atom) 0.86 (+2)											Al 1.21 (atom) 0.675 (+3)	Si 1.11 (atom) 0.4 (+4)	P 1.07 (atom) 0.58 (+3) 0.31 (+5)	S 1.7 (-2) 1.05 (atom) 0.51 (+4) 0.26 (+6)	Cl 1.67 (-1) 1.02 (atom)	Ar 1.06 (atom)
K 2.03 (atom) 1.52 (+1)	Ca 1.76 (atom) 1.14 (+2)	Sc 1.7 (atom) 0.885 (+3)	Ti 1.6 (atom) 1 (+2) 0.81 (+3) 0.745 (+4)	V 1.53 (atom) 0.93 (+2) 0.78 (+3) 0.72 (+4)	Cr 1.39 (atom) 0.94 (+2 hs) 0.87 (+2 ls) 0.7555 (+3) 0.69 (+4) 0.63 (+5) 0.58 (+6)	Mn 1.61 (atom) 0.97 (+2 hs) 0.81 (+2 ls) 0.785 (+3 hs) 0.72 (+3 ls) 0.67 (+4) 0.47 (+5) 0.395 (+6) 0.39 (+7)	Fe 1.52 (atom) 0.92 (+2 hs) 0.785 (+3 hs) 0.75 (+2 ls) 0.725 (+4) 0.69 (+3 ls) 0.39 (+6)	Co 1.5 (atom) 0.885 (+2 hs) 0.79 (+2 ls) 0.75 (+3 hs) 0.685 (+3 ls) 0.67 (+4 hs)	Ni 1.24 (atom) 0.83 (+2) 0.74 (+3 hs) 0.7 (+3 ls) 0.62 (+4)	Cu 1.32 (atom) 0.91 (+1, cn6) 0.87 (+2, cn6) 0.68 (+3, cn6)	Zn 1.22 (atom) 0.88 (+2)	Ga 1.22 (atom) 0.76 (+3)	Ge 1.2 (atom) 0.87 (+2) 0.67 (+4)	As 1.19 (atom) 0.72 (+3) 0.6 (+5)	Se 1.84 (-2) 1.2 (atom) 0.64 (+4) 0.56 (+6)	Br 1.82 (-1) 1.2 (atom) 0.73 (+3) 0.53 (+7) 0.45 (+5)	Kr 1.16 (atom)
Rb 2.2 (atom) 1.66 (+1)	Sr 1.95 (atom) 1.32 (+2)	Y 1.9 (atom) 1.04 (+3)	Zr 1.75 (atom) 0.86 (+4)	Nb 1.64 (atom) 0.86 (+3) 0.82 (+4) 0.78 (+5)	Mo 1.54 (atom) 0.83 (+3) 0.79 (+4) 0.75 (+5) 0.73 (+6)	Tc 1.47 (atom) 0.785 (+4) 0.74 (+5) 0.7 (+7)	Ru 1.46 (atom) 0.82 (+3) 0.76 (+4) 0.705 (+5) 0.52 (+7) 0.5 (+8)	Rh 1.42 (atom) 0.805 (+3) 0.74 (+4) 0.69 (+5)	Pd 1.39 (atom) 0.73 (+1) 1 (+2) 0.9 (+3) 0.755 (+4)	Ag 1.45 (atom) 1.29 (+1) 1.08 (+2) 0.89 (+3)	Cd 1.44 (atom) 1.09 (+2)	In 1.42 (atom) 0.94 (+3)	Sn 1.39 (atom) 0.83 (+4)	Sb 1.39 (atom) 0.9 (+3) 0.74 (+5)	Te 2.07 (-2) 1.38 (atom) 1.1 (+4) 0.7 (+6)	I 2.06 (-1) 1.39 (atom) 1.09 (+5) 0.67 (+7)	Xe 1.4 (atom) 0.62 (+8)

Figure 2.3.3.3.

This figure shows radii (in Angstroms) of atoms and ions of the first four periods of the periodic table. Radii from each element are listed from largest to smallest, ionic charge indicated in parentheses (); hs = high spin, ls = low spin, cn6 = coordination number is 6. Data from sources 1-3. (Kathryn Haas; CC-NC-BY-SA)

References

1. Cordero, Beatriz, Veronica Gomez, Ana E. Platero-Prats, Marc Reves, Jorge Echeverria, Eduard Cremades, Flavia Barragan, and Santiago Alvarez. *"Covalent Radii Revisited." Dalton Transactions, no. 21 (2008): 2832–38. doi:10.1039/b801115j.*
2. R. D. Shannon (1976). "Revised effective ionic radii and systematic studies of interatomic distances in halides and chalcogenides". *Acta Crystallogr A.* **32** (5): 751–767. Bibcode:1976AcCrA..32..751S. doi:10.1107/S0567739476001551.
3. Wikipedia articles on Atomic Radius and Ionic Radius.

This page titled 2.3.3: Covalent and Ionic Radii is shared under a license and was authored, remixed, and/or curated by LibreTexts.

- 2.3.3: Covalent and Ionic Radii by Bingyao Zheng, Emily Nguyen, Kathryn Haas, Swetha Ramireddy is licensed CC BY-NC-SA 4.0.

2.4: Problems

Example Exercises

The following series of problems reviews general understanding of the aforementioned material.

Exercises

1. Based on the periodic trends for ionization energy, which element has the highest ionization energy?

2. Which has a larger atomic radius: nitrogen or oxygen?

3. Which element is more electronegative, sulfur (S) or selenium (Se)?

4. Why is the electronegativity value of most noble gases zero?

5. Rewrite the following list in order of decreasing electron affinity: fluorine (F), phosphorous (P), sulfur (S), boron (B).

6. Which of these elements has a smaller atomic radius than sulfur (S): O, Cl, Ca, Li

Answer 1 available at the end of this section.

Answers

Exercises

Helium (He).

Atomic radius increases from right to left on the periodic table. Therefore, nitrogen is larger than oxygen.

Sulfur (S). Note that sulfur and selenium share the same column. Electronegativity increases up a column. This indicates that sulfur is more electronegative than selenium.

Because of their full valence electron shell, the noble gases are extremely stable and do not readily lose or gain electrons.

Fluorine (F)>Sulfur (S)>Phosphorous (P)>Boron (B). Explanation: Electron affinity generally increases from left to right and from bottom to top.

Oxygen (O) is the only element in the list with a smaller atomic radius than S. Periodic trends indicate that atomic radius increases down a group (from top to bottom) and from left to right across a period.

This page titled 2.4: Problems is shared under a license and was authored, remixed, and/or curated by LibreTexts.

- 2.4: Problems by Kathryn Haas is licensed CC BY-NC-SA 4.0.

3: SIMPLE BONDING THEORY

3.1: Lewis Electron-Dot Diagrams

3.1.1: Formal Charge

3.1.2: Resonance

3.1.3: Breaking the octet rule with higher electron counts (hypervalent atoms)

3.1.4: Lewis fails to predict unusual cases- Boron and Beryllium

3.2: Valence Shell Electron-Pair Repulsion

3.2.1: Lone Pair Repulsion

3.2.2: Multiple Bonds

3.2.3: Electronegativity and Atomic Size Effects

3.2.4: Ligand Close Packing

3.3: Molecular Polarity

3.4: Hydrogen Bonding

This page titled 3: Simple Bonding Theory is shared under a license and was authored, remixed, and/or curated by LibreTexts.

- 3: Simple Bonding Theory by Kathryn Haas is licensed CC BY-NC-SA 4.0.

3.1: LEWIS ELECTRON-DOT DIAGRAMS

In 1916, Gilbert Lewis Newton introduced a simple way to show the bonding between atoms in a molecule though Lewis electron dot diagrams. Creating Lewis diagrams is rather simple and requires only a few steps and some accounting of the valence electrons on each atom. Valence electrons are represented as dots. When two electrons are paired (lone pairs), they are represented by two adjacent dots located on an atom, and when two paired electrons are shared between atoms (bonds), they are shown as lines. For example, below are the electron dot structures of atoms and the Lewis electron dot structures of the molecules.

These diagrams are helpful because they allow us to show how atoms are connected, and when coupled with Valence Shell Electron Repulsion Theory (VSEPR), we can use Lewis structures to predict the shape of the molecule.

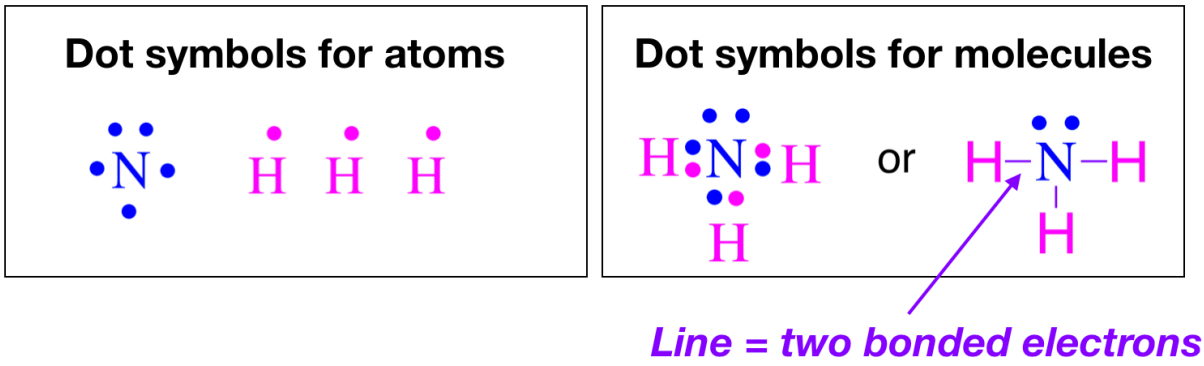


Figure 3.1.1: Lewis dot structure of atoms comprising ammonia and the dot structure of the molecule. (Kathryn Haas; CC-NC-BY-SA)

The drawing of Lewis electron-dot structures is guided largely by the **octet rule**: that atoms form bonds to achieve eight electrons in their valence shell. For many elements, a full valence shell has an electron configuration of s^2p^6, or eight electrons. A common exception to this rule is the first row elements, H and He. These two elements have $n = 1$ as their valence shell, and so they have only two electrons in a full valence shell ($1s^2$ electron configuration). Although H and He are exceptions to the "octet rule", they still form bonds to achieve a full valence shell. It may be better to think of this as the "full valence" rule of bonding. We will see many more violations to the "octet" rule as we progress through this course. In the case of metals and metalloids, breaking of the rules is particularly common. (CC-BY-NC-SA; Kathryn Haas)

Common violations of the octet rule

- **Less than eight electrons (hypovalency)**: H and He are examples of elements that cannot have more than two electrons in their full valence shell. Additionally, there are cases where a valid Lewis structure contains atoms with ***hypovalency:*** *partially-filled valence shells*. An example of this is a *carbocation, a positively charged carbon with only six electrons in its valence shell.* Carbocations are important intermediates in organic chemistry, and they are highly reactive (unstable) Lewis acids (electrophiles). Another example of hypovalency is the Lewis structure for BH_3, which shows boron with three bonds, and only six electrons in its valence shell. Boron hydride is a strong Lewis Acid. (Side note: the actual chemical form of BH_3 is not well-predicted by the Lewis structure and we'll see more about this in Section 3.1.4.)
- **More than eight electrons (hypervalency)**: This is a case where an element has more than eight electrons in its valence shell. It is common for larger atoms ($n \geq 3$), and it is discussed further in Section 3.1.2.

Pitfall alert! There are different rules for counting electrons depending on the purpose of the counting. These are the rules for counting for "octets". The rules for counting for calculation of an atom's formal charge are !!different!! and are described in Section 3.1.1. When an atom is part of a molecule, all electrons that are associated with the atom are counted as contributing to the atom's valence. This includes electrons that are lone pairs on the atoms, and *all* electrons that are shared in bonds. If four electrons are shared between two atoms, it is a double bond. If six electrons are shared between atoms, it is a triple bond.

Electrons in valence (octet) = total unbonded electrons on the atom + total bonded electrons (2 electrons per bond)

Even if you're an old pro at drawing Lewis structures, it's a good idea to polish up. Please complete the practice exercises below. You should get out an actual piece of paper (I know...just do it. It's good for you.) and a writing tool and try to complete each problem before checking the answer.

Exercise 3.1.1

Draw the Lewis structures for H_2O, CO_2, and N_2.

Answer available at the end of this section.

Exercise 3.1.2

Draw the Lewis structures for H_2, BH_3 and BF_3.

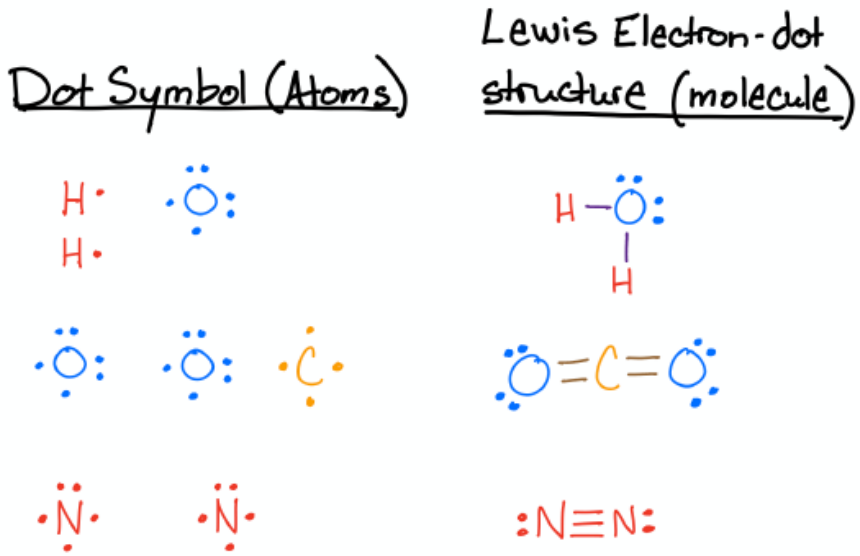
Answer available at the end of this section.

Outside Links

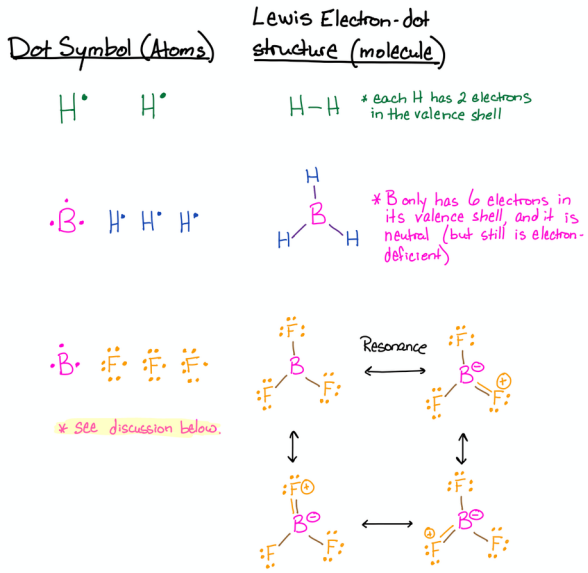
- en.Wikipedia.org/wiki/Lewis_structures
- http://www.ausetute.com.au/lewisstr.html
- cost.georgiasouthern.edu/chem...cule/lewis.htm

Answers

Exercise 3.1.1



Exercise 3.1.2



These three examples include atoms that have less than eight electrons in their valence shell. In the case of H, it is satisfied with only two electrons in its valence, as was discussed earlier in this section. The case of BH_3 was also discussed above. In the Lewis structure of BH_3, the boron can only have six electrons in its octet and it is neutral in charge. The boron is electron deficient even though it has neutral charge.

The case of BF_3 deserves a discussion: If you are unfamiliar with resonance and formal charge, see Sections 3.1.1 (Resonance) and 3.1.3 (Formal Charge) first and come back to this afterward. You might have drawn the BF_3 structure similar to the one that is drawn for BH_3, where boron has three bonds and only six electrons in its valence shell. If you did that, then you are correct; but if you only gave this structure, then your answer is not complete. There are three other correct ways to draw the structure. Since F has lone pairs of electrons, other valid Lewis structures would each have a double bond to one of the fluorines (three total). All of these structures are called resonance structures, and based on the four of them, we could predict that BF_3 would have B-F bonds that have some double-bond character. If fact, this is the case for BF_3; it has bond lengths that are shorter than single bonds, but longer than double bonds. Read more about it on its Wikipedia page here (click).

3.1.1: Formal Charge

3.1.2: Resonance

3.1.3: Breaking the octet rule with higher electron counts (hypervalent atoms)

3.1.4: Lewis fails to predict unusual cases- Boron and Beryllium

This page titled 3.1: Lewis Electron-Dot Diagrams is shared under a license and was authored, remixed, and/or curated by Kathryn Haas.

- 3.1: Lewis Electron-Dot Diagrams by Kathryn Haas is licensed CC BY-NC-SA 4.0.
- 2.1B: Lewis Structures by Andrew Iskandar is licensed CC BY 4.0.

3.1.1: Formal Charge

The formal charge of an atom in a molecule is the *hypothetical* charge the atom would have if we could redistribute the electrons in the bonds evenly between the atoms. Another way of saying this is that formal charge results when we take the number of valence electrons of a neutral atom, subtract the nonbonding electrons, and then subtract the number of bonds connected to that atom in the Lewis structure.

Calculating Formal Charges

We calculate the formal charge of an atom in a molecule or polyatomic ions as follows:

Formal Charge = (valence electrons of the "free" element) - (unshared electrons) - (bonds).

We can double-check formal charge calculations by determining the sum of the formal charges for the whole structure. The sum of the formal charges of all atoms in a molecule must be zero; the sum of the formal charges in an ion should equal the charge of the ion.

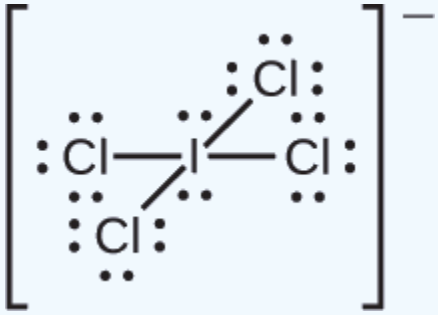
We must remember that the formal charge calculated for an atom is not the *actual* charge of the atom in the molecule. Formal charge is only a useful bookkeeping procedure; it does not indicate the presence of actual charges.

Calculating Formal Charge from Lewis Structures

Assign formal charges to each atom in the interhalogen ion $\mathrm{ICl_4^-}$.

Solution

We divide the bonding electron pairs equally for all $\mathrm{I{-}Cl}$ bonds:



We assign lone pairs of electrons to their atoms. Each Cl atom now has seven electrons assigned to it, and the I atom has eight.

Subtract this number from the number of valence electrons for the neutral atom:

- I: 7 – 8 = –1
- Cl: 7 – 7 = 0

The sum of the formal charges of all the atoms equals –1, which is identical to the charge of the ion (–1).

Exercise 3.1.1.1

Calculate the formal charge for each atom in the carbon monoxide molecule:



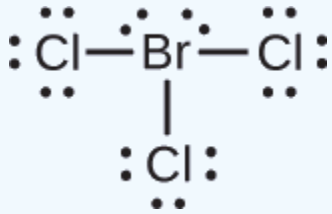
Answer available at the end of this section.

Example: Calculating Formal Charge from Lewis Structures

Assign formal charges to each atom in the interhalogen molecule $\mathrm{BrCl_3}$.

Solution

Assign one of the electrons in each Br–Cl bond to the Br atom and one to the Cl atom in that bond:



Assign the lone pairs to their atom. Now each Cl atom has seven electrons and the Br atom has seven electrons.

Subtract this number from the number of valence electrons for the neutral atom. This gives the formal charge:

- Br: 7 – 7 = 0
- Cl: 7 – 7 = 0

All atoms in $\mathrm{BrCl_3}$ have a formal charge of zero, and the sum of the formal charges totals zero, as it must in a neutral molecule.

Exercise 3.1.1.2

Determine the formal charge for each atom in $\mathrm{NCl_3}$.

Answer available at the end of this section.

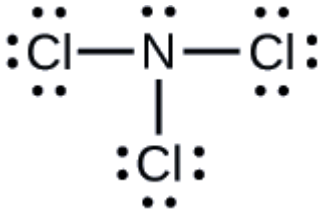
Answers

Exercise 3.1.1.1

C –1, O +1

Exercise 3.1.1.2

N: 0; all three Cl atoms: 0



This page titled 3.1.1: Formal Charge is shared under a license and was authored, remixed, and/or curated by LibreTexts.

- 7.5: Formal Charges and Resonance by OpenStax is licensed CC BY 4.0. Original source: https://openstax.org/details/books/chemistry-2e.

3.1.2: Resonance

Learning Objectives

- To understand the concept of resonance.

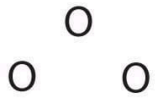
Resonance structures are a set of two or more Lewis Structures that collectively describe the electronic bonding of a single polyatomic species including fractional bonds and fractional charges. Resonance structures are capable of describing delocalized electrons that cannot be expressed by a single Lewis formula with an integral number of covalent bonds.

Sometimes one Lewis Structure is not Enough

Sometimes, even when formal charges are considered, the bonding in some molecules or ions cannot be described by a single Lewis structure. Resonance is a way of describing delocalized electrons within certain molecules or polyatomic ions where the bonding cannot be expressed by a single Lewis formula. A molecule or ion with such delocalized electrons is represented by several contributing structures (also called resonance structures or canonical forms). Such is the case for ozone (O_3), an allotrope of oxygen with a V-shaped structure and an O–O–O angle of 117.5°.

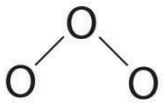
Ozone (O_3)

1. We know that ozone has a V-shaped structure, so one O atom is central:



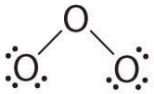
2. Each O atom has 6 valence electrons, for a total of 18 valence electrons.

3. Assigning one bonding pair of electrons to each oxygen–oxygen bond gives



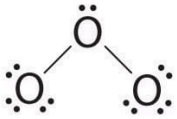
with 14 electrons left over.

4. If we place three lone pairs of electrons on each terminal oxygen, we obtain



and have 2 electrons left over.

5. At this point, both terminal oxygen atoms have octets of electrons. We therefore place the last 2 electrons on the central atom:

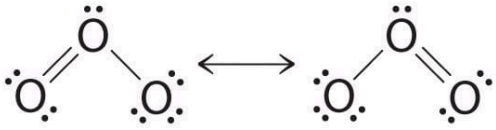


6. The central oxygen has only 6 electrons. We must convert one lone pair on a terminal oxygen atom to a bonding pair of electrons—but which one? Depending on which one we choose, we obtain either



Which is correct? In fact, neither is correct. Both predict one O–O single bond and one O=O double bond. As you will learn, if the bonds were of different types (one single and one double, for example), they would have different lengths. It turns out, however, that both O–O bond distances are identical, 127.2 pm, which is shorter than a typical O–O single bond (148 pm) and longer than the O=O double bond in O_2 (120.7 pm).

Equivalent Lewis dot structures, such as those of ozone, are called **resonance structures**. The position of the *atoms* is the same in the various resonance structures of a compound, but the position of the *electrons* is different. Double-headed arrows link the different resonance structures of a compound:



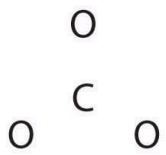
The double-headed arrow indicates that the actual electronic structure is an *average* of those shown, not that the molecule oscillates between the two structures.

> When it is possible to write more than one equivalent resonance structure for a molecule or ion, the actual structure is the average of the resonance structures.

The Carbonate (CO_3^{2-}) Ion

Like ozone, the electronic structure of the carbonate ion cannot be described by a single Lewis electron structure. Unlike O_3, though, the actual structure of CO_3^{2-} is an average of *three* resonance structures.

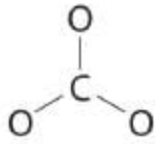
1. Because carbon is the least electronegative element, we place it in the central position:



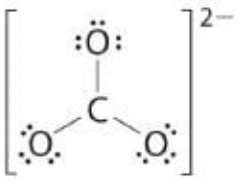
The three oxygens are drawn in the shape of a triangle with the carbon at the center of the triangle.

2. Carbon has 4 valence electrons, each oxygen has 6 valence electrons, and there are 2 more for the –2 charge. This gives 4 + (3 × 6) + 2 = 24 valence electrons.

3. Six electrons are used to form three bonding pairs between the oxygen atoms and the carbon:



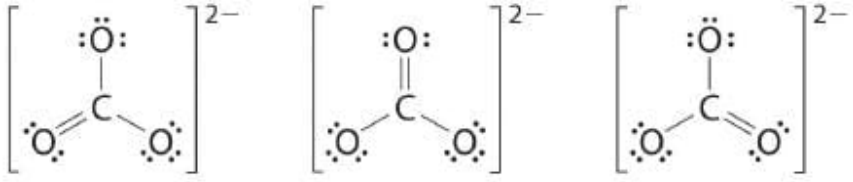
4. We divide the remaining 18 electrons equally among the three oxygen atoms by placing three lone pairs on each and indicating the –2 charge:



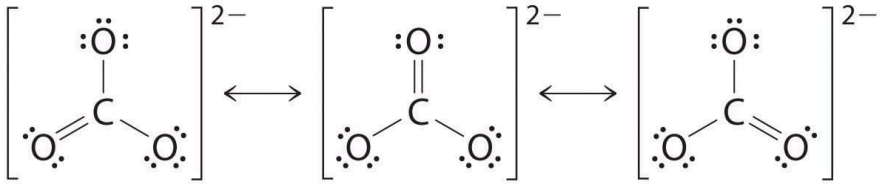
The Lewis dot structure has a central carbon that is bonded to 3 oxygens. Each oxygen has 3 lone pairs. The molecule is inside square brackets and has a charge of minus 2.

5. No electrons are left for the central atom.

6. At this point, the carbon atom has only 6 valence electrons, so we must take one lone pair from an oxygen and use it to form a carbon–oxygen double bond. In this case, however, there are *three* possible choices:



As with ozone, none of these structures describes the bonding exactly. Each predicts one carbon–oxygen double bond and two carbon–oxygen single bonds, but experimentally all C–O bond lengths are identical. We can write resonance structures (in this case, three of them) for the carbonate ion:



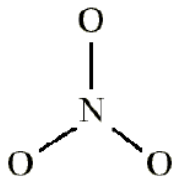
The resonance structure includes all three Lewis dot structures with double headed arrows between them.

The actual structure is an average of these three resonance structures.

The Nitrate (NO_3^-) ion

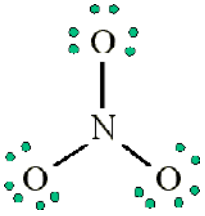
1. Count up the valence electrons: (1*5) + (3*6) + 1(ion) = **24** electrons

2. Draw the bond connectivities:

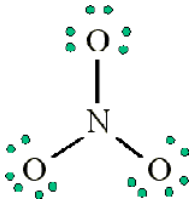


The three oxygens are drawn in the shape of a triangle with the nitrogen at the center of the triangle.

3. Add octet electrons to the atoms bonded to the center atom:

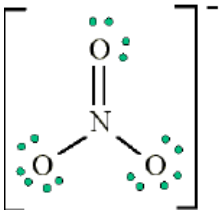


4. Place any leftover electrons (24-24 = **0**) on the center atom:



5. Does the central atom have an octet?

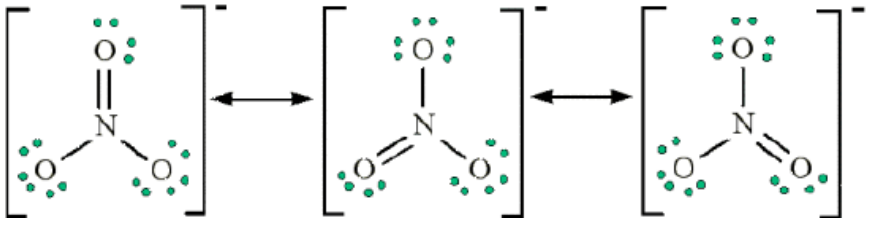
- **NO**, it has 6 electrons
- Add a multiple bond (first try a double bond) to see if the central atom can achieve an octet:



A double bond is added between one oxygen and the central nitrogen. The molecule has a negative charge.

6. Does the central atom have an octet?

- YES
- Are there possible resonance structures? YES



Note: We would expect that the bond lengths in the NO_3^- ion to be somewhat shorter than a single bond.

YouTube Video

This interactive element is not available in this format. Visit the link or scan the QR code to access it online.

View this YouTube Video online

Example 3.1.2.1: Benzene

Benzene is a common organic solvent that was previously used in gasoline; it is no longer used for this purpose, however, because it is now known to be a carcinogen. The benzene molecule (C_6H_6) consists of a regular hexagon of carbon atoms, each of which is also bonded to a hydrogen atom. Use resonance structures to describe the bonding in benzene.

Given: molecular formula and molecular geometry

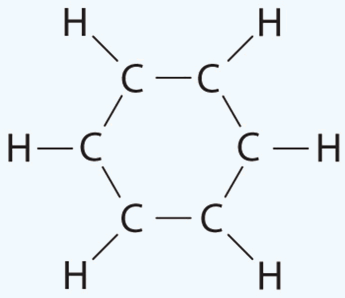
Asked for: resonance structures

Strategy:

A. Draw a structure for benzene illustrating the bonded atoms. Then calculate the number of valence electrons used in this drawing.
B. Subtract this number from the total number of valence electrons in benzene and then locate the remaining electrons such that each atom in the structure reaches an octet.
C. Draw the resonance structures for benzene.

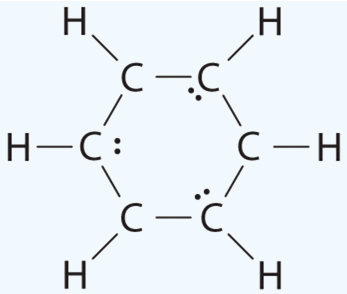
Solution:

A Each hydrogen atom contributes 1 valence electron, and each carbon atom contributes 4 valence electrons, for a total of (6 × 1) + (6 × 4) = 30 valence electrons. If we place a single bonding electron pair between each pair of carbon atoms and between each carbon and a hydrogen atom, we obtain the following:



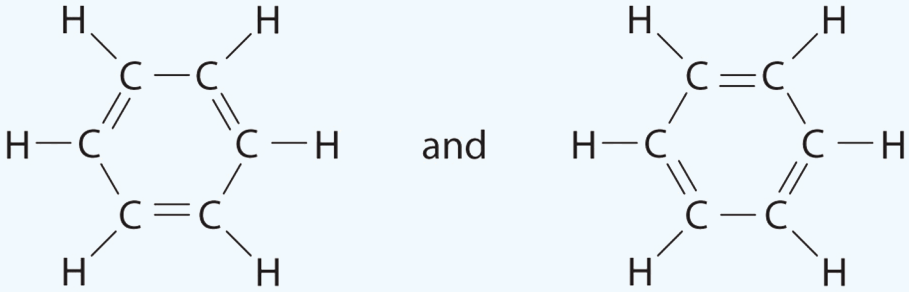
Each carbon atom in this structure has only 6 electrons and has a formal charge of +1, but we have used only 24 of the 30 valence electrons.

B If the 6 remaining electrons are uniformly distributed pairwise on alternate carbon atoms, we obtain the following:

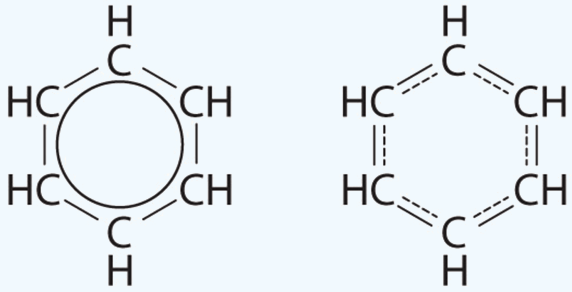


Three carbon atoms now have an octet configuration and a formal charge of –1, while three carbon atoms have only 6 electrons and a formal charge of +1. We can convert each lone pair to a bonding electron pair, which gives each atom an octet of electrons and a formal charge of 0, by making three C=C double bonds.

C There are, however, two ways to do this:



Each structure has alternating double and single bonds, but experimentation shows that each carbon–carbon bond in benzene is identical, with bond lengths (139.9 pm) intermediate between those typically found for a C–C single bond (154 pm) and a C=C double bond (134 pm). We can describe the bonding in benzene using the two resonance structures, but the actual electronic structure is an average of the two. The existence of multiple resonance structures for aromatic hydrocarbons like benzene is often indicated by drawing either a circle or dashed lines inside the hexagon:



Benzene

Exercise 3.1.2.1: Nitrite Ion

The sodium salt of nitrite is used to relieve muscle spasms. Draw two resonance structures for the nitrite ion (NO_2^-).

Answer available at the end of this section.

Warning

If several reasonable resonance forms for a molecule exists, the "actual electronic structure" of the molecule will probably be intermediate between all the forms that you can draw. The classic example is benzene in Example 3.1.2.1. One would expect the double bonds to be shorter than the single bonds, but if one overlays the two structures, you see that one structure has a single bond where the other structure has a double bond. The best measurements that we can make of benzene do not show two bond lengths - instead, they show that the bond length is intermediate between the two resonance structures.

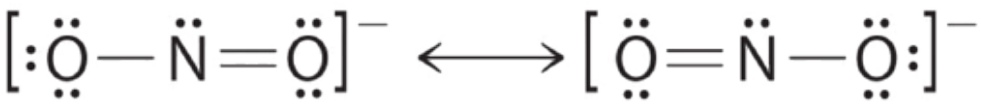
Resonance structures is a mechanism that allows us to use all of the possible resonance structures to try to predict what the actual form of the molecule would be. Single bonds, double bonds, triple bonds, +1 charges, -1 charges, these are our limitations in explaining the structures, and the true forms can be in between - a carbon-carbon bond could be mostly single bond with a little bit of double bond character and a partial negative charge, for example.

Summary

Some molecules have two or more chemically equivalent Lewis electron structures, called resonance structures. Resonance is a mental exercise and method within the Valence Bond Theory of bonding that describes the delocalization of electrons within molecules. These structures are written with a **double-headed arrow** between them, indicating that none of the Lewis structures accurately describes the bonding but that the actual structure is an average of the individual resonance structures. Resonance structures are used when one Lewis structure for a single molecule cannot fully describe the bonding that takes place between neighboring atoms relative to the empirical data for the actual bond lengths between those atoms. The net sum of valid resonance structures is defined as a resonance hybrid, which represents the overall delocalization of electrons within the molecule. A molecule that has several resonance structures is more stable than one with fewer. Some resonance structures are more favorable than others.

Answers

Exercise 3.1.2.1: Nitrite Ion



There is a double bond between one oxygen and the nitrogen, It can be found on the left oxygen or the right oxygen.

Resonance structures are particularly common in oxoanions of the *p*-block elements, such as sulfate and phosphate, and in aromatic hydrocarbons, such as benzene and naphthalene.

This page titled 3.1.2: Resonance is shared under a license and was authored, remixed, and/or curated by LibreTexts.

- 8.6: Resonance Structures is licensed CC BY-NC-SA 3.0.

3.1.3: Breaking the octet rule with higher electron counts (hypervalent atoms)

The octet rule applies well to atoms in the second row of the periodic table, where a full valence shell includes eight electrons with an electron configuration of s^2p^6. Even elements in the third and fourth row are known to follow this rule *sometimes*, but not always. In larger atoms, where $n \geq 3$ the valence shell contains additional subshells: the $d, f, g...$ subshells. Therefore, atoms with $n \geq 3$ can have higher valence shell counts by "expanding" into these additional subshells. When atoms contain more than eight electrons in their valence shell, they are said to be **hypervalent**. Hypervalency allows atoms with $n \geq 3$ to break the octet rule by having more than eight electrons. This also means they can have five or more bonds; something that is nearly unheard of for atoms with $n \leq 2$. Complete the exercises below to see examples of molecules containing hypervalent atoms.

Exercise 3.1.3.1

Draw the Lewis structures for sulfur hexafluoride ($\mathrm{SF_6}$).

Answer available at the end of this section.

Exercise 3.1.3.1

Draw the Lewis structure for chlorine trifluoride ($\mathrm{ClF_3}$.

Answer available at the end of this section.

Is hypervalency real? Not exactly. Hypervalency is a concept associated with hybrid orbital theory and Lewis theory. It's useful for some simple things, like predicting how atoms are connected and predicting molecular shape. But the idea that the d-orbitals are involved in bonding isn't accurate according to wave mechanics.

For main group molecules, chemists (like Pauling) thought a long time ago that hypervalence is due to expanded s^2p^6 octets. The consensus is now clear that d orbitals are NOT involved in bonding in molecules like SF_6 any more than they are in SF_4 and SF_2. In all three cases, there is a small and roughly identical participation of d-orbitals in the wavefunctions. This has been established in both MO and VB theory. However, using hybrid orbitals with d-orbital contributions equips us with a language which can pragmatically describe the geometries of highly coordinated substances.

While hybrid orbitals are a powerful tool to describe the geometries and shape of molecules and metal complexes, in "real" molecules their significance may be debated. Often a more realistic molecular orbitals approach is needed. However, from an epistemologically simple point of view, bonding theories can only be judged by their predictions. To the extent that hybridization can explain the shapes of PF_5 and SF_6, valence bond theory is a perfectly good theory. To the extent that if you write out the valence bond wavefunction using hybridized orbitals and calculate energies and other properties à la Pauling (i.e., ionization energy and electron affinities) and find them to be off from experimental results (by tens of kcals/mol), then valence bond theory is not accurate.

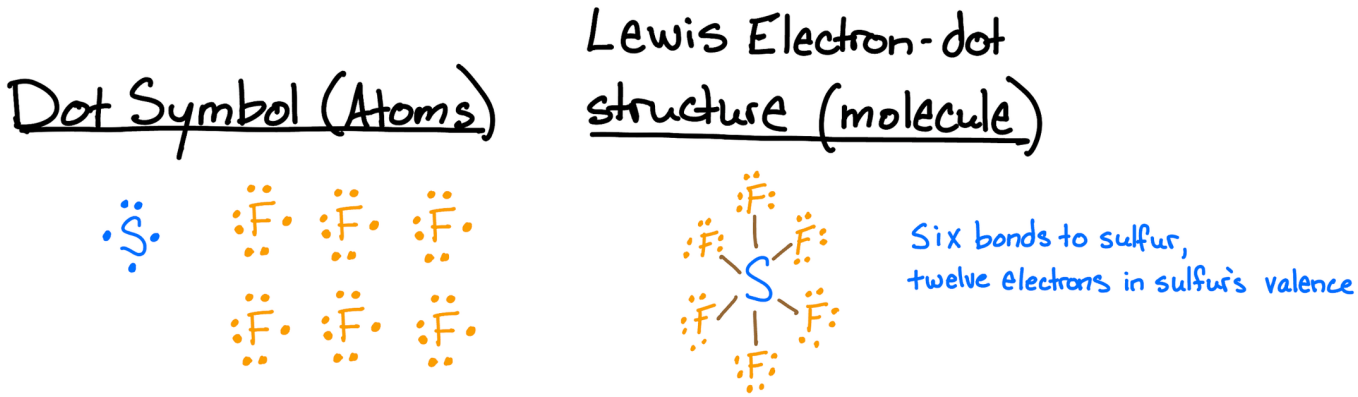
> Bonding theories can only be judged by their predictions.

A simple explanation that can be given is that molecular wavefunctions constructed out of hybridized atomic orbitals are accurate enough to predict some things, but not others. Predictions of any theory must be compared with empirical evidence to assess when they work and when they fail. When a theory gives the wrong answer, at least one assumption must not hold. In this case, the valence bond wavefunction is not accurate enough to capture some important features of a system's electronic structure. It may not be the most intellectually satisfying answer, but to say more would result in a much more complicated answer and certainly far beyond the level reasonably expected from general chemistry discussions.

Answers

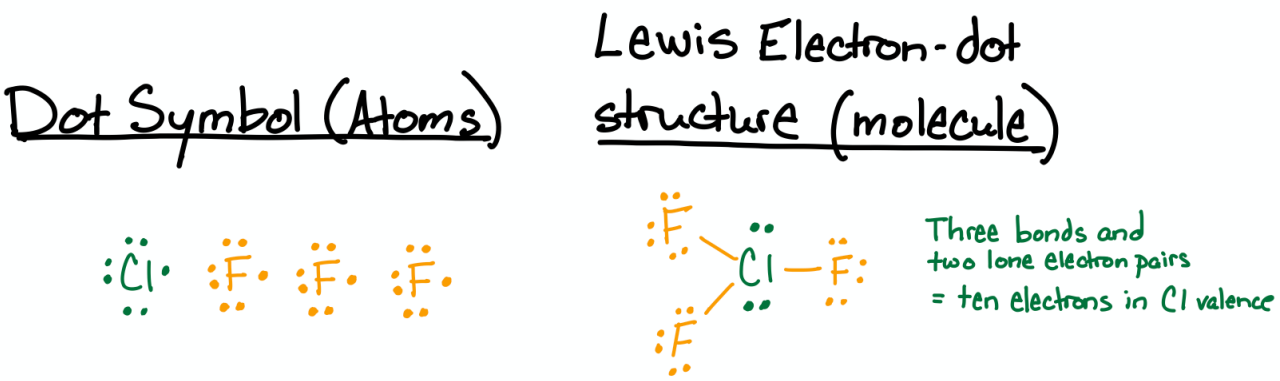
Exercise 3.1.3.1

Each fluorine atom has one valence electron and will make one bond each. The sulfur has six valence electrons, and must make six bonds to form a molecule with the six fluorine atoms. The molecular structure has six bonds to sulfur, with twelve valence electrons. The sulfur is hypervalent.



Exercise 3.1.3.1

All atoms are halogens and each has seven valence electrons. Chlorine is capable of hypervalency because it is in the third row of the periodic table; however fluorine cannot have more than eight valence electrons in its valence because it is in the second row. The structure has the three fluorine atoms bonded to a central chlorine atom. The chlorine has a valence of ten electrons due to its three bonds and two lone pairs.



This page titled 3.1.3: Breaking the octet rule with higher electron counts (hypervalent atoms) is shared under a license and was authored, remixed, and/or curated by Kathryn Haas.

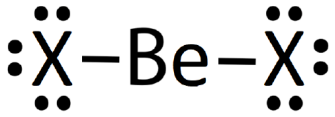
- 3.1.2: Breaking the octet rule with higher electron counts (hypervalent atoms) by Kathryn Haas is licensed CC BY-NC-SA 4.0.

3.1.4: Lewis fails to predict unusual cases- Boron and Beryllium

Two notable cases where Lewis theory fails to predict structure are the cases of beryllium (Be) and boron (B). These two atoms are in period 2 ($n = 2$) of the periodic table and their atoms have the valence electron configurations of $2s^2$ and $2s^2 2p^1$, respectively.

Beryllium

The Lewis electron dot structures are shown below for $\mathrm{BeX_2}$, where X is one of the halogens, F or Cl.



Each of the structures above would predict a linear geometry for the $\mathrm{BeX_2}$ molecule. Together the three resonance structures suggest partial double-bond character in the Be-X bond, which results in an intermediate bond length between a single and double bond.

There are issues with each of these resonance structures. The structure on the left would predict only four electrons around Be ; thus, the atom does not fulfill the octet rule. The structure on the left suggests multiple bonds for the halogen (X) and high separation of charge with formal charge on each atom. The structure in the middle is a mix of these problems. None of these situations is ideal according to Lewis theory. Further, experimental data is not consistent with any of these structures or their resonance hybrid (except in the case of $\mathrm{BeCl_2}$ at very high temperatures).

It turns out that the monomer of $\mathrm{BeX_2}$ does exist, but only at very high temperatures and low pressures. Even under extreme conditions, the monomer is not particularly stable due to the electron deficiency around Be.

BeF_2

At ambient temperature and pressure, BeF_2 is a solid that looks similar to quartz (Figure $3.1.4.1$) The Be is four-coordinate with tetrahedral geometry; each F is two-coordinate and the Be-F bond length is 1.54 Å. This structure is possible due to an extended 3-dimensional network in the solid where adjacent BeF_2 units are bonded to one another, as shown in Figure $3.1.4.1$.

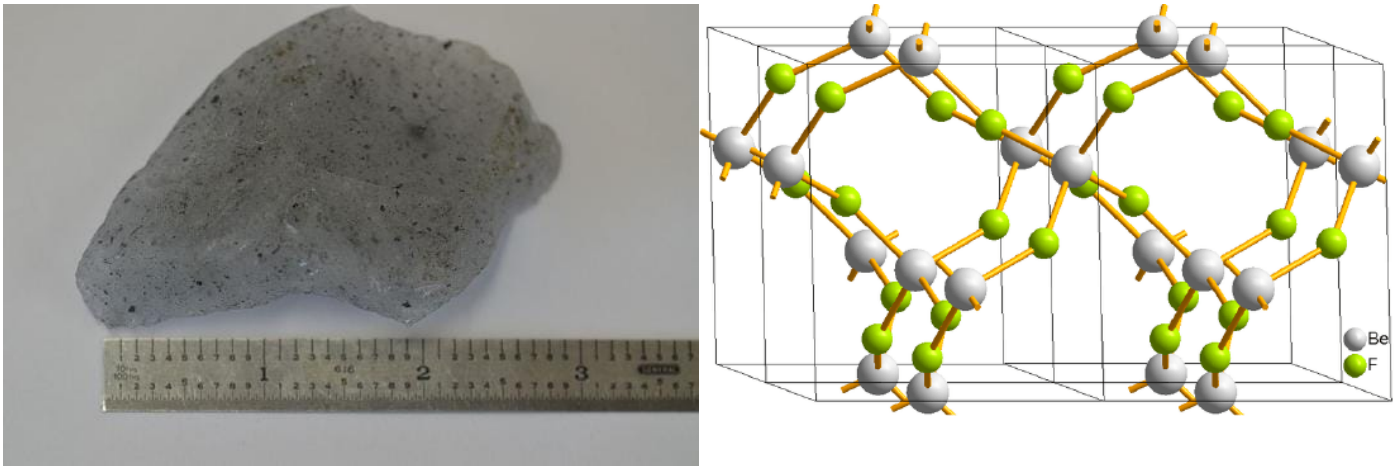


Figure $3.1.4.1$: (left) A nugget of beryllium fluoride obtained from Materion. Black spots are carbon (CC BY-SA 3.0; Bckelleher via Wikipedia). (right) BeF2 structure (CC BY-SA 3.0 Unported; Materialscientist via Wikipedia)

In the liquid phase, $\mathrm{BeF_2}$ has a fluctuating tetrahedral structure where Be and F ions exchange. The vapor phase is reached at temperatures higher than 1000 °C (at ~ 1 atm). In the vapor phase, $\mathrm{BeF_2}$ exists as a monomer with linear geometry and a bond length of 1.43 Å, consistent with a double bond between Be and F.

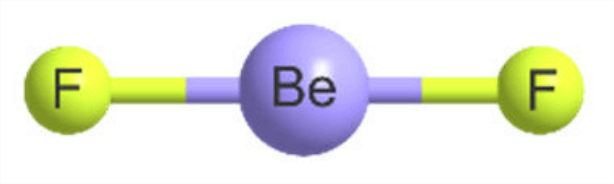


Figure 3.1.4.2: Geometries of $\mathrm{BeF_2}$. (CC BY; Ibon Alkorta and Anthony C. Legoe via Inorganics)

$\mathrm{BeCl_2}$

At ambient temperature and pressure, $\mathrm{BeCl_2}$ is a solid. As in $\mathrm{BeF_2}$ described above, $\mathrm{BeCl_2}$ has four-coordinate, tetrahedral Be and two-coordinate Cl. In contrast to $\mathrm{BeF_2}$, solid $\mathrm{BeCl_2}$ is a 1-dimensional polymer consisting of edge-shared tetrahedral.

In the gas phase, $\mathrm{BeCl_2}$ exists as a dimer with two chlorine atoms bridging two Be atoms. In the dimer, the Be atoms are 3-coordinate. Bridging Cl atoms are two-coordinate, while terminal Cl atoms are one-coordinate. At higher temperatures in the vapor phase, the linear monomer also exists.

Boron ($2s^2 2p^1$)

Prediction based on Lewis structures:

Lewis structures of $\mathrm{BH_3}$ and $\mathrm{BF_3}$ were described in Exercise 3.1.2, and are drawn again below for convenience.

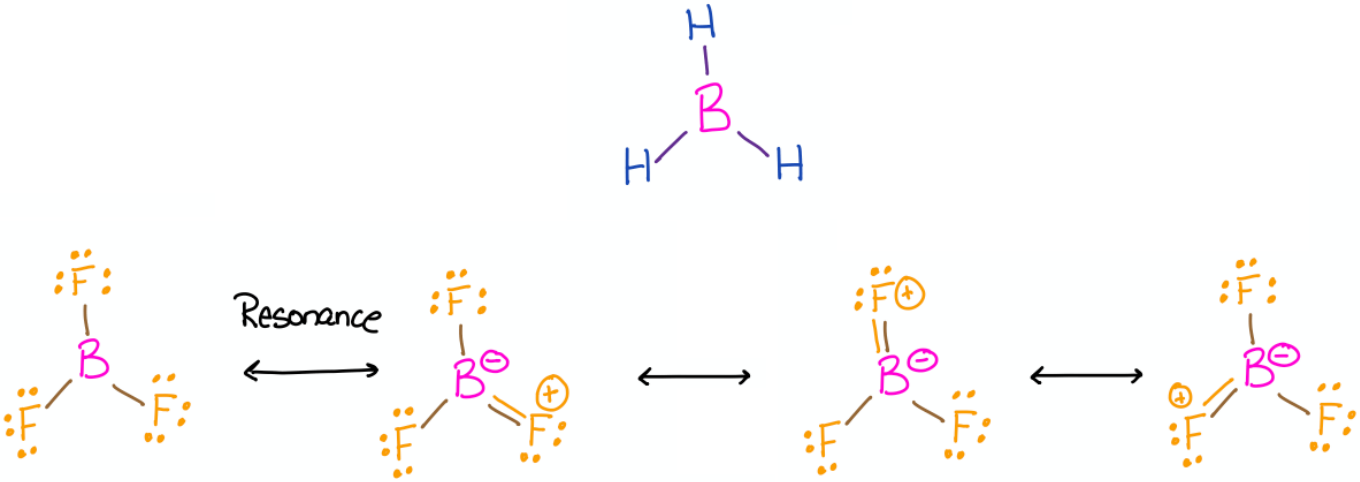


Figure 3.1.4.2: Lewis structures of $\mathrm{BH_3}$ and $\mathrm{BF_3}$. (Kathryn Haas; CC-NC-BY-SA)

Boron trihalides

Boron trihalides, like $\mathrm{BF_3}$, have properties that are largely predicted by Lewis structures and VSEPR theory. The Lewis structure for $\mathrm{BF_3}$ includes several resonance structures. The structure with only single bonds is the most common representation for this molecule because the charge separation shown in the other structures is considered to be unfavorable. The highly polarized B-F bond has a dipole moment that lies opposite to the indicated formal charges shown in the resonance structures with double bonds between boron and fluorine.

The resonance hybrid of $\mathrm{BF_3}$ predicts partial double bond character between boron and fluorine, thus a bond length shorter than a single bond. Using the Lewis structures and VSEPR theory, we would predict a trigonal planar geometry around boron. In fact, the actual structure of $\mathrm{BF_3}$ is a monomer with trigonal planar geometry and with bond length that is shorter than a single bond.

The case is similar to structures of other boron trihalides as well.

Boron trihalides are electron deficient at the boron center and react readily with Lewis bases. In other words they are strong Lewis acids (electrophiles).

Boron trihydride (BH_3 is really B_2H_6)

The properties of boron trihydride (BH_3) are not predicted by the simple predictions made through Lewis structures and VSEPR. The monomer, BH_3, is not stable, but when dissolved in the presence of a Lewis base, BH_3 can form a stable acid-base adduct. In its pure form, the compound actually exists as a dimeric gas with a molecular unit of B_2H_6 (try drawing a valid Lewis structure for that!). Its unexpected structure includes two H's that bridge the two boron atoms in 3-center-2-electron bonds. You can read more about B_2H_6 on the Wikipedia page for Diborane(6). The unique bonding observed for boron is described more in Chapter 8 and Chapter 15.

This page titled 3.1.4: Lewis fails to predict unusual cases- Boron and Beryllium is shared under a license and was authored, remixed, and/or curated by Kathryn Haas.

- 3.1.4: Lewis Fails to Predict Unusual Cases - Boron and Beryllium by Kathryn Haas is licensed CC BY-NC-SA 4.0.

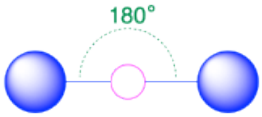
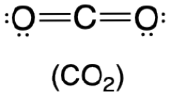
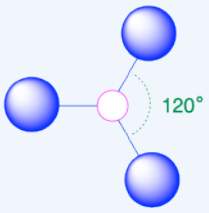
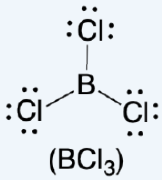
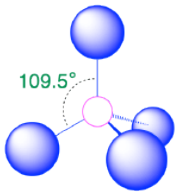
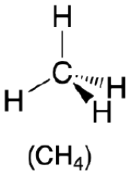
3.2: VALENCE SHELL ELECTRON-PAIR REPULSION

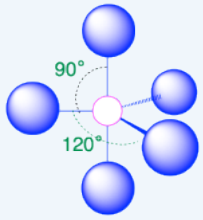
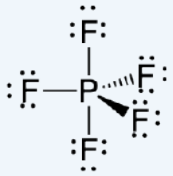
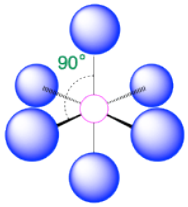
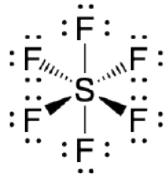
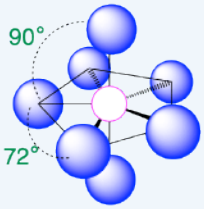
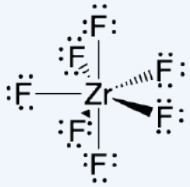
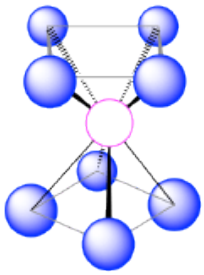
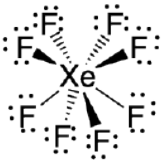
Introduction to VSEPR

The **Valence Shell Electron Repulsion (VSEPR)** model can predict the structure of most molecules and polyatomic ions in which the central atom is a nonmetal; it also works for some structures in which the central atom is a metal. VSEPR builds on Lewis electron dot structures (discussed in Section 3.1); Lewis structures alone predict only connectivity while the Lewis structure and VSEPR together can predict the geometry of each atom in a molecule. The main idea of VSEPR theory is that pairs of electrons (in bonds and in lone pairs) repel each other. The pairs of electrons (in bonds and in lone pairs) are called "groups". Because electrons repel each other electrostatically, the most stable arrangement of electron groups (i.e., the one with the lowest energy) is the one that minimizes repulsion. Groups are positioned around the central atom in a way that produces the molecular structure with the lowest energy. In other words, the repulsion between groups around an atom favors a geometry in which the groups are as far apart from each other as possible. Although VSEPR is simplistic because it does not account for the subtleties of orbital interactions that influence molecular shapes, it accurately predicts the three-dimensional structures of a large number of compounds.

We can use the VSEPR model to predict the geometry around the atoms in a polyatomic molecule or ion by focusing on the number of electron pairs (groups) around a *central atom* of interest. Groups include bonded and unbonded electrons; a single bond, a double bond, a triple bond, a lone pair of electrons, or even a single unpaired electron each count as one group. The molecule or polyatomic ion is given an $\mathbf{AX}_m\mathbf{E}_n$ designation, where **A is the central atom**, **X is a bonded atom**, **E is a nonbonding** valence electron group (usually a lone pair of electrons), and m and n are integers. The number of groups is equal to the sum of m and n. Using this information, we can describe the molecular geometry around a central atom, that is, the arrangement of the *bonded atoms* in a molecule or polyatomic ion. The geometries that are predicted from VSEPR when a central atom has only bonded groups ($n = 0$) are listed below in Table 3.2.1. The cases where lone pairs contribute to the total groups ($n \geq 1$) are discussed in the next section about lone pair repulsion.

Table 3.2.1. Geometries predicted using VSEPR theory (bonded groups only).

Groups around central atom ($m + n$)	Geometry Name	Geometry Sketch	Predicted bond Angle	Example
2	linear		180°	 (CO_2)
3	trigonal plane		120°	 (BCl_3)
4	tetrahedron		109.5°	 (CH_4)

Groups around central atom (m + n)	Geometry Name	Geometry Sketch	Predicted bond Angle	Example
5	trigonal bipyramid		90° and 120°	 (PF_5)
6	octahedron		90°	 (SF_6)
7	pentagonal bipyramid		90° and 72°	 ($[ZrF_7]^{3-}$)
8	square antiprism		70.5°, 99.6° and 109.5°	 ($[XeF_8]^{2-}$)

Practice

VSEPR to predict Molecular Geometry

You can follow these four steps to predict the geometry around an atom using VSEPR:

1. Draw the Lewis electron structure of the molecule or polyatomic ion.
2. For the central atom of interest, assign the AX_mE_n designation and the total number of groups (m+n).
3. Determine the electron group arrangement around the central atom that minimizes repulsions.
4. Describe the molecular geometry.

Use the procedure above to complete the exercises below

Exercise 3.2.1

Predict the geometry around the central atom in BeH_2 and CO_2.

Answer BeH2 available at the end of this section.

Answer CO2 available at the end of this section.

2. The carbon atom forms two double bonds. Each double bond is counted as one group, so there are two groups around the central atom. Once again, both groups around the central atom are bonds, so CO_2 is designated as AX_2.

3. Like BeH_2, the arrangement that minimizes repulsions places the groups 180° apart.

4. VSEPR only recognizes groups around the *central* atom (the carbon). Thus the lone pairs on the oxygen atoms do not influence the molecular geometry. With two bonded groups on the central atom and no lone pairs, the molecular geometry of CO_2 is linear (Table 3.2.1). The structure of CO_2 is shown in Table 3.2.1.

Exercise 3.2.2

Predict the geometry around the central atom in BCl_3 and CO_3^{2-}.

Answer BCl3 available at the end of this section.

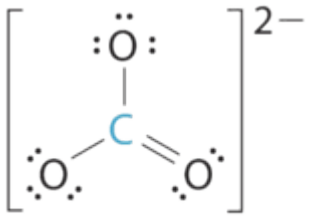
2. There are three groups around the central atom and all are single bonds. The structure is designated as AX_3.

3. To minimize repulsions, the groups are placed 120° apart (Table 3.2.1).

4. From Table 3.2.1 we see that with three bonding pairs around the central atom, the molecular geometry of BCl_3 is *trigonal planar*.

Answer CO_3^{2-}

1. The central atom, carbon, has four valence electrons, and each oxygen atom has six valence electrons. The Lewis electron structure of one of three resonance forms is represented as

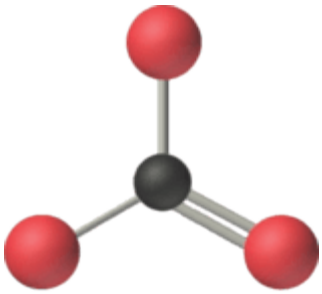


Lewis structure

2. The structure of CO_3^{2-} is a resonance hybrid. It has three identical bonds, each with a bond order of $1\frac{1}{3}$. All electron groups are bonds. With three bonding groups around the central atom, the structure is designated as AX_3.

3. We minimize repulsions by placing the three groups 120° apart (Table 3.2.1).

4. We see from Table 3.2.1 that the molecular geometry of CO_3^{2-} is trigonal planar with bond angles of 120°.



Molecular geometry
(trigonal planar)

In our next example we encounter the effects of lone pairs and multiple bonds on molecular geometry for the first time.

Exercise 3.2.3

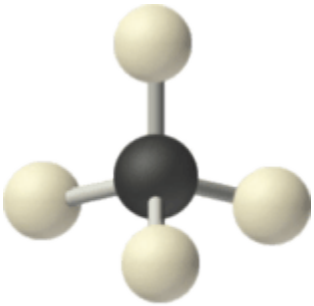
Predict the geometry around the central atom in CH_4, PCl_5 and SF_6.

Answer CH4 available at the end of this section.

2. There are four electron groups around the central atom. All electron groups are bonding pairs, so the structure is designated as AX_4.

3. As shown in Table 3.2.1, repulsions are minimized by placing the groups in the corners of a tetrahedron with bond angles of 109.5°.

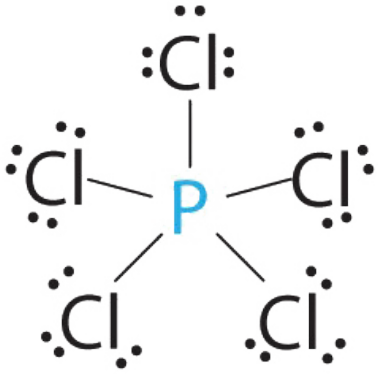
4. With four bonding pairs, the molecular geometry of methane is *tetrahedral* (Table 3.2.1).



Molecular geometry
(tetrahedral)

Answer PCl_5

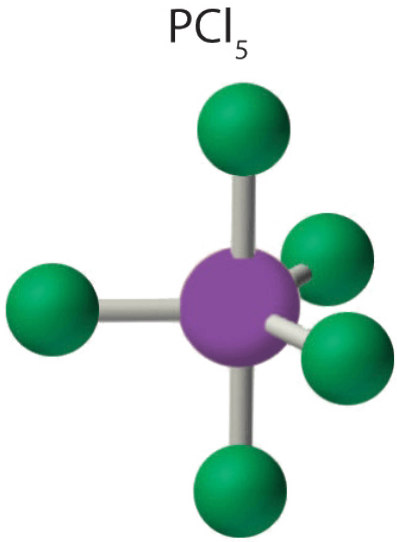
1. Phosphorus has five valence electrons and each chlorine has seven valence electrons, so the Lewis electron structure of PCl_5 is



2. There are five bonding groups around phosphorus, the central atom. All electron groups are bonds, so the structure is designated as AX_5.

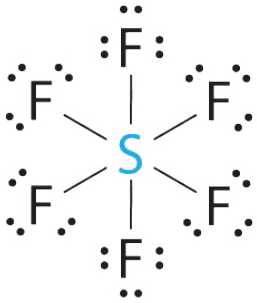
3. The structure that minimizes repulsions is a *trigonal bipyramid*, which consists of two trigonal pyramids that share a base (Table 3.2.1).

4. The molecular geometry of PCl_5 is *trigonal bipyramidal*, as shown below. The molecule has three atoms in a plane in *equatorial* positions and two atoms above and below the plane in *axial* positions. The three equatorial positions are separated by 120° from one another, and the two axial positions are at 90° to the equatorial plane. The axial and equatorial positions are not chemically equivalent.



Answer SF_6

1. The central atom, sulfur, contributes six valence electrons, and each fluorine atom has seven valence electrons, so the Lewis electron structure is



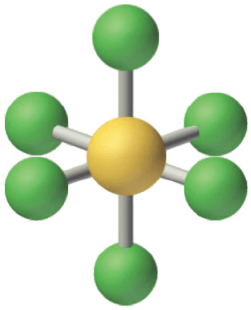
Lewis structure

With an expanded valence, this species is an exception to the octet rule.

2. There are six electron groups around the central atom, each a bonding pair. We see from Figure 3.2.2 that the geometry that minimizes repulsions is *octahedral*.

3. With only bonding pairs, SF_6 is designated as AX_6. All positions are chemically equivalent, so all electronic interactions are equivalent.

4. There are six nuclei, so the molecular geometry of SF_6 is octahedral.



Molecular geometry
(octahedral)

Answers

Exercise 3.2.1

1. The central atom, beryllium, contributes two valence electrons, and each hydrogen atom contributes one. The Lewis electron structure is



Lewis structure

2. There are two groups around the central atom, and both groups are single bonds. Thus BeH_2 is designated as AX_2.
3. We see from Table 3.2.1 that the arrangement that minimizes repulsions places the groups 180° apart.
4. From Table 3.2.1 we see that with two bonding pairs, the molecular geometry that minimizes repulsions in BeH_2 is *linear*.

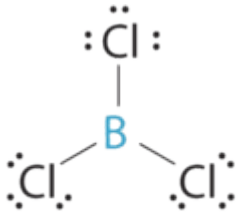
Exercise 3.2.1

1. The central atom, carbon, contributes four valence electrons, and each oxygen atom contributes six. The Lewis electron structure is



Exercise 3.2.2

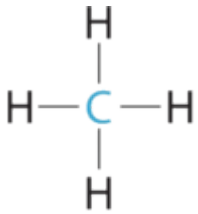
1. The central atom, boron, contributes three valence electrons, and each chlorine atom contributes seven valence electrons. The Lewis electron structure is



Lewis structure

Exercise 3.2.3

1. The central atom, carbon, contributes four valence electrons, and each hydrogen atom has one valence electron, so the full Lewis electron structure is



Lewis structure

3.2.1: Lone Pair Repulsion

3.2.2: Multiple Bonds

3.2.3: Electronegativity and Atomic Size Effects

3.2.4: Ligand Close Packing

This page titled 3.2: Valence Shell Electron-Pair Repulsion is shared under a CC BY-NC-SA 4.0 license and was authored, remixed, and/or curated by Kathryn Haas.

- 3.2: Valence Shell Electron-Pair Repulsion by Kathryn Haas is licensed CC BY-NC-SA 4.0.

3.2.1: Lone Pair Repulsion

In the previous section, we saw how to use VSEPR to predict the geometry around a central atom based on the number of groups attached to a central atom. However, our previous discussion was limited to the simple cases where all of the groups were bonded groups (i.e., in the designation $\mathbf{AX_mE_n}$, n=0). When all of the groups are bonds, the geometries can be predicted using information in Table 3.2.1 in the previous section. Now we will consider cases where one or more of these groups are lone pairs.

Lone pairs have stronger repulsive forces than bonded groups.

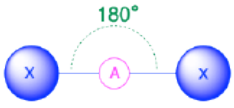
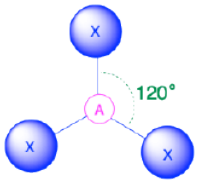
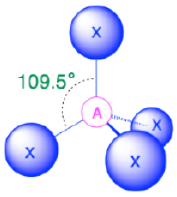
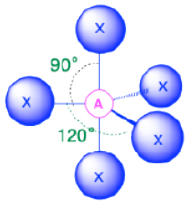
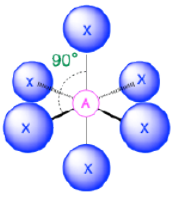
When one or more of the groups is a lone pair of electrons (non-bonded electrons), the experimentally-observed geometry around an atom is slightly different than in the case where all groups are bonds. The actual bond angles are similar, but not exactly the same, as those predicted based on the *total number of groups* (the "parent" geometry). When there is a mixture of group types (**lone pairs (E)** ***and*** **bonded groups (X)**) there are three different types of angles to consider: bond angles between two bonded atoms (**X-X** angles), angles between a bonded atom and a lone pair (**X-E** angles), and angles between two lone pairs (**E-E** angles). Empirical evidence shows the following trend in the degree of bond angles around atoms with a mixture of group types:

Trend in bond angles:

E-E >**X-E** >**X-X**

Using empirical evidence as a guide, we can predict that lone pairs repel other electron groups more strongly than bonded pairs. The molecular geometry of molecules with lone pairs of electrons is better predicted when we consider that electronic repulsion created by lone pairs is stronger than the repulsion from bonded groups. It is difficult to predict the exact bond angle based on this principle, but we can predict approximate angles, as described and summarized below in Table 3.2.1.1.

Table 3.2.1.1: Predictions of molecular geometry and bond angles around atoms with a mixture of bonded (X) and unbonded (E) electron groups.

	Electron Groups (m + n)				
	2 **(steric number = 2)**	**3** **(steric number = 3)**	**4** **(steric number = 4)**	**5** **(steric number = 5)**	**6** **(steric number = 6)**
Parent Geometry **(0 lone pairs)** **AX_m**	 **AX_2**, linear 180°	 **AX_3**, trig. plane 120°	 **AX_4**, tetrahedron 109.5°	 **AX_5**, trig. bipyramid 90°, 120°	 **AX_6**, octahedron 90°

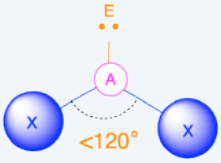
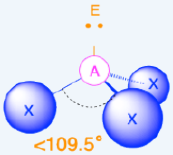
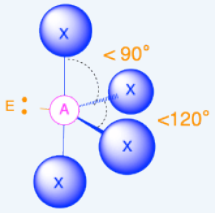
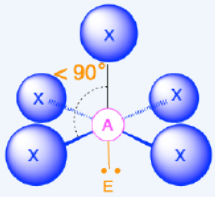
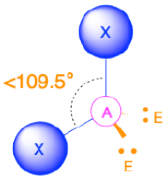
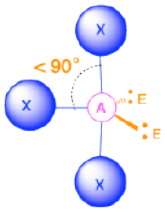
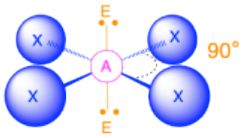
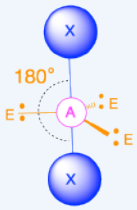
	Electron Groups (m + n)				
	2 (steric number = 2)	3 (steric number = 3)	4 (steric number = 4)	5 (steric number = 5)	6 (steric number = 6)
1 lone pair **AX_mE_1**		 **AX_2E_1**, bent <120°	 **AX_3E_1**, trig. pyramid <109.5°	 **AX_4E_1**, see-saw <90°, <120°	 **AX_5E_1**, square pyramid 90°, <90°
2 lone pairs **AX_mE_2**			 **AX_2E_2**, bent <109.5°	 **AX_3E_2**, T-shape <90°	 **AX_4E_2**, square plane 90°
3 lone pairs **AX_mE_3**				 **AX_2E_3**, linear 180°	

Table 3.2.1.1 summarizes the geometries and bond angles predicted for nearest-neighbor bonded groups on central atoms with a mixture of lone pairs and bonded groups. The table does not cover all possible situations; it only includes cases where there are two bonded groups in which an X-X angle is measurable between nearest-neighbors. A more detailed description of some selected cases is given below.

Two Electron Groups (m + n = 2)

(Steric number = 2) In the case that there are only two electron groups around a central atom, those groups will lie 180° from one

another. This results in a linear molecular geometry with 180° bond angles.

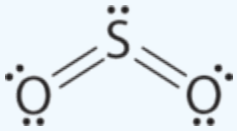
Three Electron Groups (m + n = 3)

(Steric number = 3) In the case that there are three electron groups around a central atom, those groups will lie approximately 120° from one another in space. This results in an electronic geometry that is approximately **trigonal planar**. There are two different molecular geometries that are possible in this category:

- When all of the electron groups are bonds (m = 3 or AX_3), the molecular geometry is a ***trigonal plane*** with **120°** bond angles.
- When there is one lone pair (m=2, n=1 or AX_2E_1), the molecular geometry is ***bent*** with a bond angle that is slightly **less than 120°**.

AX_2E Molecules: Example SO_2

1. The central atom, sulfur, has 6 valence electrons, as does each oxygen atom. With 18 valence electrons, the Lewis electron structure is shown below.



2. There are three electron groups around the central atom: two double bonds and one lone pair. We initially place the groups in a trigonal planar arrangement to minimize repulsions (Table 3.2.1.1).

3. With two bonding pairs and one lone pair, the structure is designated as AX_2E. This designation has a total of three electron pairs, two X and one E. The lone pair occupies more space around the central atom than a bonding pair (even double bonds!). Bonding pairs and lone pairs repel each other electrostatically in the order BP–BP < LP–BP < LP–LP. In SO_2, we have one BP–BP interaction and two LP–BP interactions.

4. The molecular geometry is described only by the positions of the nuclei, *not* by the positions of the lone pairs. Thus, with two nuclei and one lone pair the shape is *bent*, or *V shaped*, which can be viewed as a trigonal planar arrangement with a missing vertex. The O-S-O bond angle is expected to be *less than* 120° because of the extra space taken up by the lone pair.

Four Electron Groups (m + n = 4)

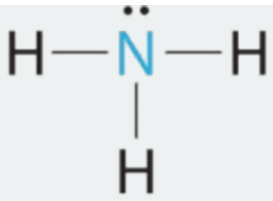
(Steric number = 4) In the case that there are four electron groups around a central atom, those groups will lie approximately 109.5° from one another in space. This results in an electronic geometry that is approximately **tetrahedral**. There are three different molecular geometries that are possible in this category:

- When all electron groups are bonds (m=4 or AX_4), the molecular geometry is a ***tetrahedron*** with bond angles of **109.5°**.
- When there is one lone pair (m=3, n=1 or AX_3E_1), the molecular geometry is a ***trigonal pyramid*** with bond angles of **slightly less than 109.5°**.
- When there are two lone pairs (m=2, n=2 or AX_2E_2), the molecular geometry is ***bent*** with bond angles of **slightly less than 109.5°**.

AX_3E Molecules: Example NH_3

One of the limitations of Lewis structures is that they depict molecules and ions in only two dimensions. With four electron groups, we must learn to show molecules and ions in three dimensions.

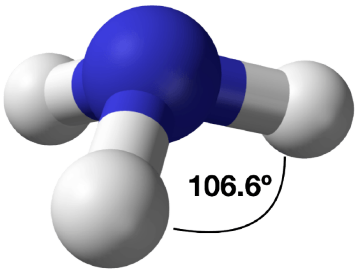
1. In ammonia, the central atom, nitrogen, has five valence electrons and each hydrogen donates one valence electron, producing the Lewis electron structure



Lewis structure

2. There are four electron groups around nitrogen, three bonding pairs and one lone pair. Repulsions are minimized by directing each hydrogen atom and the lone pair to the corners of a tetrahedron.

3. With three bonding pairs and one lone pair, the structure is designated as AX_3E. This designation has a total of four electron pairs, three X and one E. We expect the LP–BP interactions to cause the bonding pair angles to deviate significantly from the angles of a perfect tetrahedron.



The Difference in the Space Occupied by a Lone Pair of Electrons and by a Bonding Pair

As with SO_2, this composite model of electron distribution and negative electrostatic potential in ammonia shows that a lone pair of electrons occupies a larger region of space around the nitrogen atom than does a bonding pair of electrons that is shared with a hydrogen atom.

4. There are three nuclei and one lone pair, so the molecular geometry is *trigonal pyramidal*. In essence, this is a tetrahedron with a vertex missing. However, the H–N–H bond angles are less than the ideal angle of 109.5° because of LP–BP repulsion. The bond angles in ammonia are 106.6°.

AX_2E_2 Molecules: Example H_2O

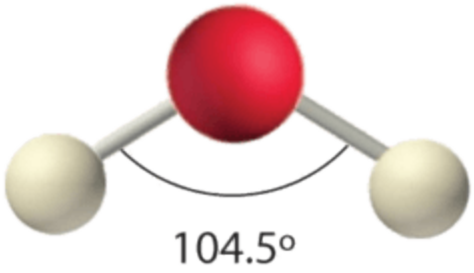
1. Oxygen has six valence electrons and each hydrogen has one valence electron, producing the Lewis electron structure



2. There are four groups around the central oxygen atom, two bonding pairs and two lone pairs. Repulsions are minimized by directing the bonding pairs and the lone pairs to the corners of a tetrahedron.

3. With two bonding pairs and two lone pairs, the structure is designated as AX_2E_2 with a total of four electron pairs. Due to LP–LP, LP–BP, and BP–BP interactions, we expect a significant deviation from idealized tetrahedral angles.

4. With two hydrogen atoms and two lone pairs of electrons, the structure has significant lone pair interactions. There are two nuclei about the central atom, so the molecular shape is *bent*, or *V shaped*, with an H–O–H angle that is even less than the H–N–H angles in NH_3, as we would expect because of the presence of two lone pairs of electrons on the central atom rather than one. This molecular shape is essentially a tetrahedron with two missing vertices.



Five Electron Groups (m + n = 5)

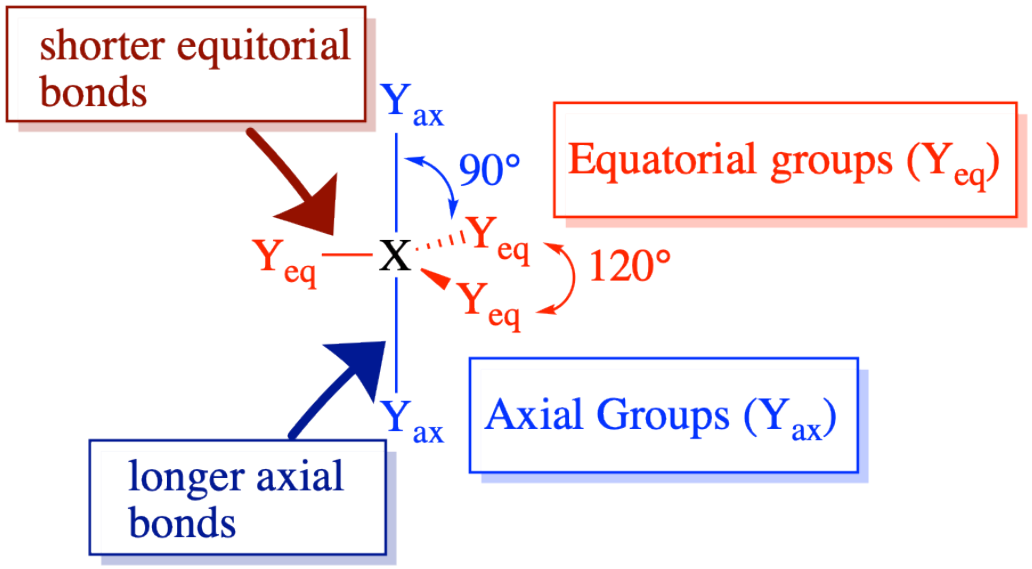


Figure: Trigonal pyramidal molecules (steric number 5) possess different bond angles and lengths for axial (ax) and equatorial (eq) pendant atoms. (CC-BY-NC-SA; Kathryn Haas).

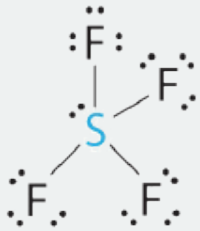
(Steric number = 5) In the case that there are five electron groups around a central atom, there are two different types of positions around the central atom: equatorial positions and axial positions. The three equatorial ligands are 120° from one another and are 90° from each of the two axial ligands. The axial positions have three adjacent groups oriented 90° away in space. Axial groups are thus more crowded than the equatorial positions with only two adjacent groups at 90°. The crowding of axial positions results in slight differences in bond distances; crowded axial groups have longer bonds than the less crowded equatorial groups. Lone pairs of electrons generally prefer to occupy equatorial positions rather than axial positions. The justification for this preference, according to VSEPR theory, is that the lone electron pairs are more repulsive than bonding electron pairs, and thus the lone pairs prefer the less crowded equatorial positions.

The arrangement of five groups around a central atom results in a **trigonal bipyramidal** electronic geometry. There are four different molecular geometries that are possible in this category, depending upon the number of bonded groups and lone pairs of electrons:

- When all electron groups are bonds (m=5 or AX_5), the molecular geometry is a ***trigonal bipyramid*** with bond angles of **120°** and **90°** between adjacent ligands.
- When there is one lone pair (m=4, n=1 or AX_4E_1), the lone pair occupies one of the equatorial positions. The molecular geometry is called a ***see saw*** with bond angles of **slightly less than 120°** and **slightly less than 90°**.
- When there are two lone pairs (m=3, n=2 or AX_3E_2), each lone pair occupies one of the three equatorial positions. The molecular geometry is ***T-shaped*** with bond angles of **slightly less than 120°** and **slightly less than 90°**.
- When there are three lone pairs (m=1, n=3 or AX_3E_2), the lone pairs occupy the three equatorial positions. The molecular geometry is ***linear*** with bond angles of **180°**.

AX_4E Molecules: SF_4

1. The sulfur atom has six valence electrons and each fluorine has seven valence electrons, so the Lewis electron structure is



Lewis structure

With an expanded valence, this species is an exception to the octet rule.

2. There are five groups around sulfur, four bonding pairs and one lone pair. With five electron groups, the lowest energy arrangement is a trigonal bipyramid.

3. We designate SF_4 as AX_4E; it has a total of five electron pairs. However, because the axial and equatorial positions are not chemically equivalent, where do we place the lone pair? If we place the lone pair in the axial position, we have three LP–BP repulsions at 90°. If we place it in the equatorial position, we have two 90° LP–BP repulsions at 90°. With fewer 90° LP–BP repulsions, we can predict that the structure with the lone pair of electrons in the *equatorial position is more stable than the one with the lone pair in the axial position*. We also expect a deviation from ideal geometry because a lone pair of electrons occupies more space than a bonding pair.

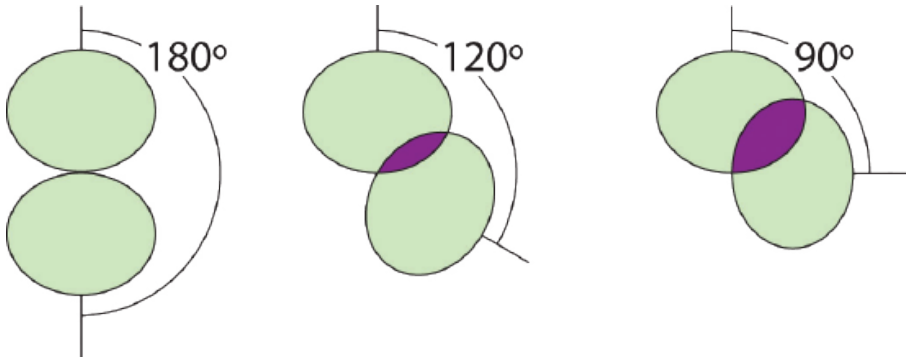
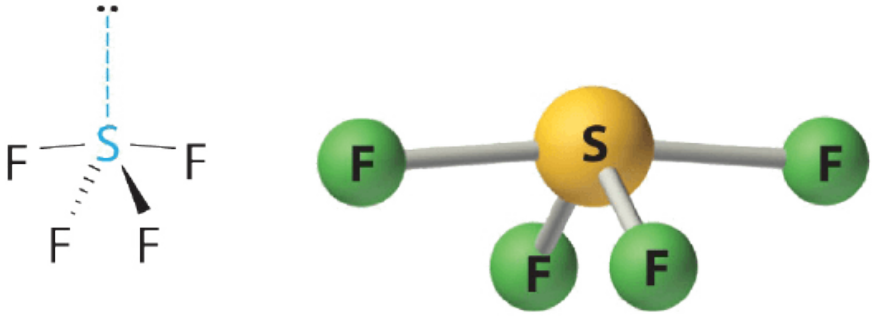


Illustration of the Area Shared by Two Electron Pairs versus the Angle between Them

At 90°, the two electron pairs share a relatively large region of space, which leads to strong repulsive electron–electron interactions.

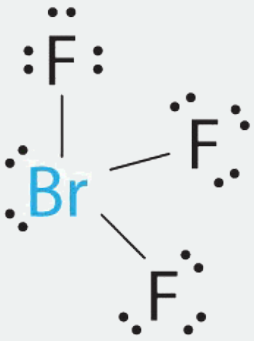
4. With four nuclei and one lone pair of electrons, the molecular structure is based on a trigonal bipyramid with a missing equatorial vertex; it is described as a *seesaw*. The F_{axial}–S–F_{axial} angle is 173° rather than 180° because of the lone pair of electrons in the equatorial plane.



Molecular geometry (seesaw)

AX_3E_2 Molecules: BrF_3

1. The bromine atom has seven valence electrons, and each fluorine has seven valence electrons, so the Lewis electron structure is

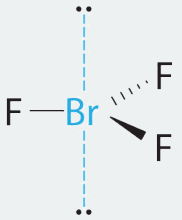


Lewis structure

Once again, we have a compound that is an exception to the octet rule.

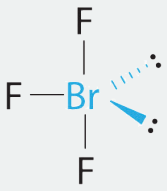
2. There are five groups around the central atom, three bonding pairs and two lone pairs. We again direct the groups toward the vertices of a trigonal bipyramid.

3. With three bonding pairs and two lone pairs, the structural designation is AX_3E_2 with a total of five electron pairs. Because the axial and equatorial positions are not equivalent, we must decide how to arrange the groups to minimize repulsions. If we place both lone pairs in the axial positions, we have six LP–BP repulsions at 90°. If both are in the equatorial positions, we have four LP–BP repulsions at 90°. If one lone pair is axial and the other equatorial, we have one LP–LP repulsion at 90° and three LP–BP repulsions at 90°:



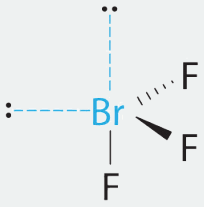
Lone pairs axial

(a)



Lone pairs equatorial

(b)



Lone pairs axial and equatorial

(c)

Interactions			
90° LP–LP	0	0	1
90° LP–BP	6	4	3

Structure (c) can be eliminated because it has a LP–LP interaction at 90°. Structure (b), with fewer LP–BP repulsions at 90° than (a), is lower in energy. However, we predict a deviation in bond angles because of the presence of the two lone pairs of electrons.

4. The three nuclei in BrF_3 determine its molecular structure, which is described as *T shaped*. This is essentially a trigonal bipyramid that is missing two equatorial vertices. The F_{axial}–Br–F_{axial} angle is 172°, less than 180° because of LP–BP repulsions.

Because lone pairs occupy more space around the central atom than bonding pairs, electrostatic repulsions are more important for lone pairs than for bonding pairs.

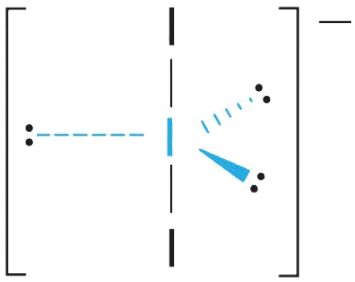
AX_2E_3 Molecules: I_3^-

1. Each iodine atom contributes seven electrons and the negative charge one, so the Lewis electron structure is



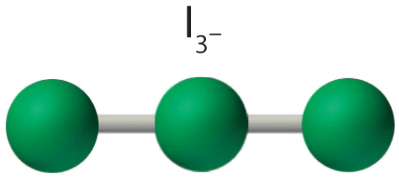
2. There are five electron groups about the central atom in I_3^-, two bonding pairs and three lone pairs. To minimize repulsions, the groups are directed to the corners of a trigonal bipyramid.

3. With two bonding pairs and three lone pairs, I_3^- has a total of five electron pairs and is designated as AX_2E_3. We must now decide how to arrange the lone pairs of electrons in a trigonal bipyramid in a way that minimizes repulsions. Placing them in the equatorial positions eliminates 90° LP–LP repulsions and minimizes the number of 90° LP–BP repulsions.



The three lone pairs of electrons have equivalent interactions with the three iodine atoms, so we do not expect any deviations in bonding angles.

4. With three nuclei and three lone pairs of electrons, the molecular geometry of I_3^- is linear. This can be described as a trigonal bipyramid with three equatorial vertices missing. The ion has an I–I–I angle of 180°, as expected.



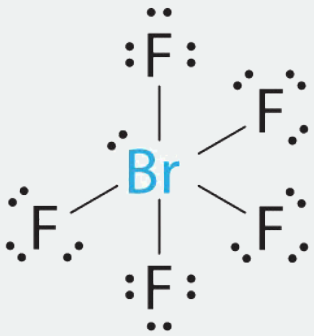
Six Electron Groups (m + n = 6)

(Steric number = 6) In the case that there are six electron groups around a central atom, the nearest groups will lie approximately 90° from one another in space. This results in an electronic geometry that is approximately **octahedral**. There are three relevant molecular geometries in this category:

- When all electron groups are bonds (m=6 or AX_6), the molecular geometry is an ***octahedron*** with bond angles of **90°** between adjacent bonds.
- When there is one lone pair (m=5, n=1 or AX_5E_1) we now distinguish between the axial and equitorial positions; the lone pair is considered to be in one of the axial positions, while the bond directly opposite of the lone pair is the axial bond. The molecular geometry is a ***square pyramid*** with bond angles of **90°** between adjacent equatorial bonds and **slightly less than 90°** between the axial bond and equatorial groups.
- When there are two lone pairs (m=4, n=2 or AX_4E_2), the lone pairs are opposite of one another and each occupy an axial position. The molecular geometry is ***square planar*** with bond angles of **90°**.

AX_5E Molecules: BrF_5

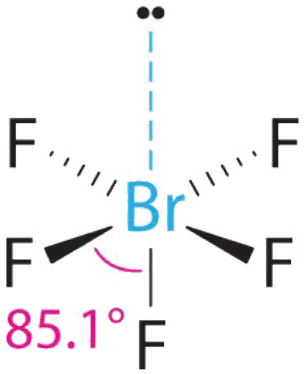
1. The central atom, bromine, has seven valence electrons, as does each fluorine, so the Lewis electron structure is



Lewis structure

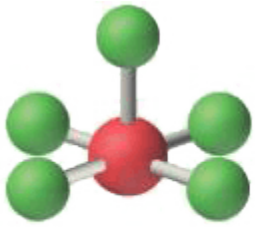
With its expanded valence, this species is an exception to the octet rule.

2. There are six electron groups around the Br, five bonding pairs and one lone pair. Placing five F atoms around Br while minimizing BP–BP and LP–BP repulsions gives the following structure:



3. With five bonding pairs and one lone pair, BrF_5 is designated as AX_5E; it has a total of six electron pairs. The BrF_5 structure has four fluorine atoms in a plane in an equatorial position and one fluorine atom and the lone pair of electrons in the axial positions. We expect all F_{axial}–Br–$F_{equatorial}$ angles to be less than 90° because of the lone pair of electrons, which occupies more space than the bonding electron pairs.

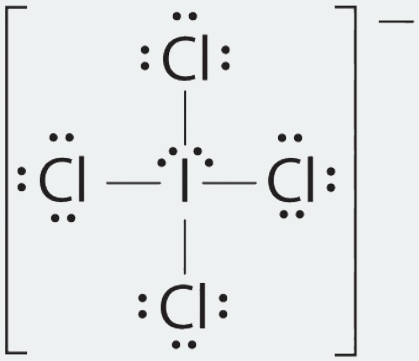
4. With five nuclei surrounding the central atom, the molecular structure is based on an octahedron with a vertex missing. This molecular structure is *square pyramidal*. The F_{axial}–B–$F_{equatorial}$ angles are 85.1°, less than 90° because of LP–BP repulsions.



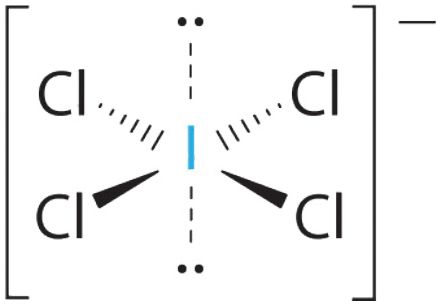
Molecular geometry
(square pyramidal)

AX_4E_2 Molecules: ICl_4^-

1. The central atom, iodine, contributes seven electrons. Each chlorine contributes seven, and there is a single negative charge. The Lewis electron structure is

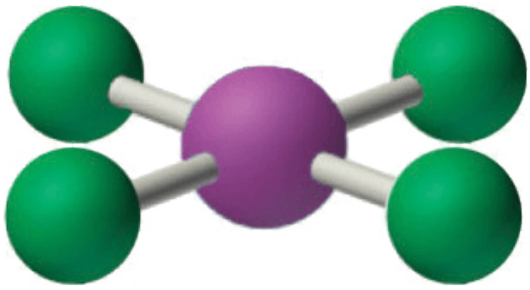


2. There are six electron groups around the central atom, four bonding pairs and two lone pairs. The structure that minimizes LP–LP, LP–BP, and BP–BP repulsions is



3. ICl_4^- is designated as AX_4E_2 and has a total of six electron pairs. Although there are lone pairs of electrons, with four bonding electron pairs in the equatorial plane and the lone pairs of electrons in the axial positions, all LP–BP repulsions are the same. Therefore, we do not expect any deviation in the Cl–I–Cl bond angles.

4. With five nuclei, the ICl4– ion forms a molecular structure that is s*quare planar*, an octahedron with two opposite vertices missing.



Summary

The arrangement of bonded atoms in a molecule or polyatomic ion is crucial to understanding the chemistry of a molecule, but Lewis electron structures give no information about **molecular geometry**. The **valence-shell electron-pair repulsion (VSEPR) model** allows us to predict which of the possible structures is actually observed in most cases. VSEPR is based on the assumption that pairs of electrons occupy space, and the lowest-energy structure is the one that minimizes repulsions between electron pairs. In the VSEPR model, the molecule or polyatomic ion is given an AX_mE_n designation, where A is the central atom, X is a bonded atom, E is a nonbonding valence electron group (usually a lone pair of electrons), and m and n are integers. Each group around the central atom is designated as a bonding pair (BP) or lone (nonbonding) pair (LP). From the BP and LP interactions we can predict both the relative positions of the atoms and the angles between the bonds, called the **bond angles**. From this we can describe the **molecular geometry**. The VSEPR model can be used to predict the shapes of many molecules and polyatomic ions, but it gives no information about bond lengths and the presence of multiple bonds. A combination of VSEPR and a bonding model, such as Lewis electron structures, is necessary to understand the presence of multiple bonds.

The relationship between the number of electron groups around a central atom, the number of lone pairs of electrons, and the molecular geometry is summarized in Table 3.2.1.1.

Example Excercises

Example 3.2.1.1

Using the VSEPR model, predict the molecular geometry of each molecule or ion.

1. PF_5 (phosphorus pentafluoride, a catalyst used in certain organic reactions)
2. H_3O^+ (hydronium ion)

Given: two chemical species

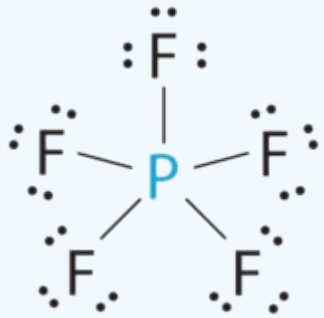
Asked for: molecular geometry

Strategy:

A. Draw the Lewis electron structure of the molecule or polyatomic ion.
B. Determine the electron group arrangement around the central atom that minimizes repulsions.
C. Assign an AX_mE_n designation; then identify the LP–LP, LP–BP, or BP–BP interactions and predict deviations in bond angles.
D. Describe the molecular geometry.

Solution:

1. **A** The central atom, P, has five valence electrons and each fluorine has seven valence electrons, so the Lewis structure of PF_5 is



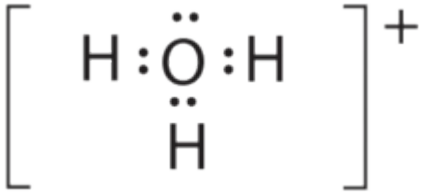
B There are five bonding groups about phosphorus. The structure that minimizes repulsions is a trigonal bipyramid.

C All electron groups are bonding pairs, so PF_5 is designated as AX_5. Notice that this gives a total of five electron pairs. With no lone pair repulsions, we do not expect any bond angles to deviate from the ideal.

D The PF_5 molecule has five nuclei and no lone pairs of electrons, so its molecular geometry is trigonal bipyramidal.



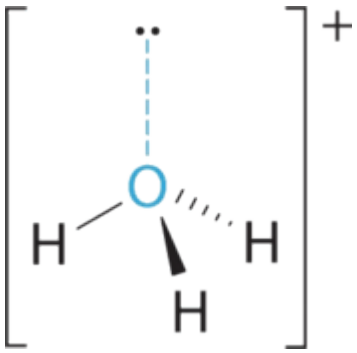
- **A** The central atom, O, has six valence electrons, and each H atom contributes one valence electron. Subtracting one electron for the positive charge gives a total of eight valence electrons, so the Lewis electron structure is



B There are four electron groups around oxygen, three bonding pairs and one lone pair. Like NH_3, repulsions are minimized by directing each hydrogen atom and the lone pair to the corners of a tetrahedron.

C With three bonding pairs and one lone pair, the structure is designated as AX_3E and has a total of four electron pairs (three X and one E). We expect the LP–BP interactions to cause the bonding pair angles to deviate significantly from the angles of a perfect tetrahedron.

D There are three nuclei and one lone pair, so the molecular geometry is *trigonal pyramidal*, in essence a tetrahedron missing a vertex. However, the H–O–H bond angles are less than the ideal angle of 109.5° because of LP–BP repulsions:



Exercise 3.2.1.1

Using the VSEPR model, predict the molecular geometry of each molecule or ion.

a. XeO_3
b. PF_6^-
c. NO_2^+

Answer a available at the end of this section.

Example 3.2.1.2

Predict the molecular geometry of each molecule.

1. XeF_2
2. $SnCl_2$

Given: two chemical compounds

Asked for: molecular geometry

Strategy:

Use the strategy given in Example3.2.1.1.

Solution:

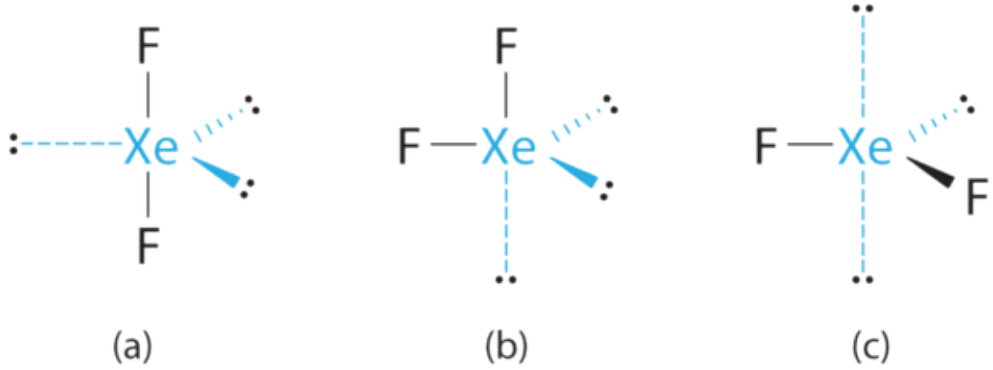
1. **A** Xenon contributes eight electrons and each fluorine seven valence electrons, so the Lewis electron structure is



B There are five electron groups around the central atom, two bonding pairs and three lone pairs. Repulsions are minimized by placing the groups in the corners of a trigonal bipyramid.

C From B, XeF_2 is designated as AX_2E_3 and has a total of five electron pairs (two X and three E). With three lone pairs about

the central atom, we can arrange the two F atoms in three possible ways: both F atoms can be axial, one can be axial and one equatorial, or both can be equatorial:

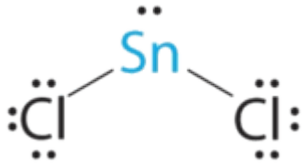


Interactions			
90 LP–LP	0	2	2

The structure with the lowest energy is the one that minimizes LP–LP repulsions. Both (b) and (c) have two 90° LP–LP interactions, whereas structure (a) has none. Thus both F atoms are in the axial positions, like the two iodine atoms around the central iodine in I_3^-. All LP–BP interactions are equivalent, so we do not expect a deviation from an ideal 180° in the F–Xe–F bond angle.

D With two nuclei about the central atom, the molecular geometry of XeF_2 is linear. It is a trigonal bipyramid with three missing equatorial vertices.

- **A** The tin atom donates 4 valence electrons and each chlorine atom donates 7 valence electrons. With 18 valence electrons, the Lewis electron structure is



B There are three electron groups around the central atom, two bonding groups and one lone pair of electrons. To minimize repulsions the three groups are initially placed at 120° angles from each other.

C From B we designate $SnCl_2$ as AX_2E. It has a total of three electron pairs, two X and one E. Because the lone pair of electrons occupies more space than the bonding pairs, we expect a decrease in the Cl–Sn–Cl bond angle due to increased LP–BP repulsions.

D With two nuclei around the central atom and one lone pair of electrons, the molecular geometry of $SnCl_2$ is bent, like SO_2, but with a Cl–Sn–Cl bond angle of 95°. The molecular geometry can be described as a trigonal planar arrangement with one vertex missing.

Exercise 3.2.1.2

Predict the molecular geometry of each molecule.

a. SO_3
b. XeF_4

Answer a available at the end of this section.

Answers

Exercise 3.2.1.1

trigonal pyramidal

octahedral

linear

Exercise 3.2.1.2

trigonal planar

square planar

This page titled 3.2.1: Lone Pair Repulsion is shared under a license and was authored, remixed, and/or curated by Kathryn Haas.

- 3.2.1: Lone Pair Repulsion by Kathryn Haas is licensed CC BY-NC-SA 4.0.
- 3.2.2: Multiple Bonds by Kathryn Haas is licensed CC BY-NC-SA 4.0.

3.2.2: Multiple Bonds

In the previous sections, we saw how to predict the approximate geometry around an atom using VSEPR theory, and we learned that lone pairs of electrons slightly distort bond angles from the "parent" geometry. This page discusses the effect of multiple (double and triple) bonds between bonded atoms.

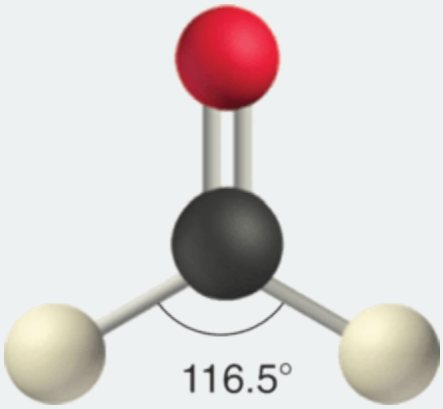
Double and triple bonds are more repulsive than single bonds

VSEPR theory predicts that double and triple bonds have stronger repulsive forces than single bonds. Like lone pairs of electrons, multiple bonds occupy more space around the central atom than a single bond. The result is that bond angles are slightly distorted compared to the parent geometry. Since a multiple bond has a higher electron density than a single bond, its electrons occupy more space than those of a single bond. Double and triple bonds distort bond angles in a way similar to what lone pairs do. Due to the stronger repulsion, double and triple bonds occupy positions similar to those of lone pairs in groups with 5 and 6 electron groups.

Examples 3.2.2.1

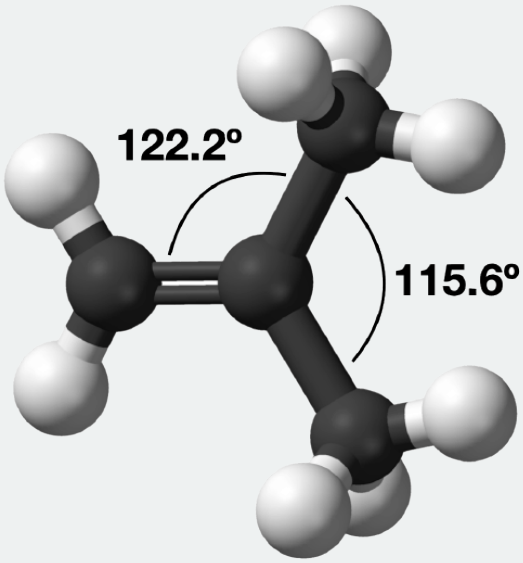
CH_2O

In a molecule such as CH_2O (AX_3), whose structure is shown below, the double bond repels the single bonds more strongly than the single bonds repel each other. This causes a deviation from ideal geometry (an H–C–H bond angle of 116.5° rather than 120°).



2-methybutene

In the molecule, $CH_2C(CH_3)_2$, the methyl—C—methyl bond angle is 115.6°, which is less than the 120° bond angle that would be expected of the parent geometry. On the other hand, the acetyl—C—methyl bond angle is greater than 120°, with an actual bond angle of 122.2°.



Atoms with both lone pairs and multiple bonds

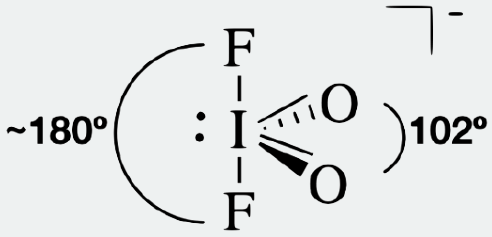
In general, we expect that a lone pair has slightly greater repulsive force than a multiple bond, and that a multiple bond has slightly greater repulsive force than a single bond. The **order of expected repulsive force** is:

$$\text{lone pair} > \text{double or triple bond} > \text{single bond}$$

Examples3.2.2.1

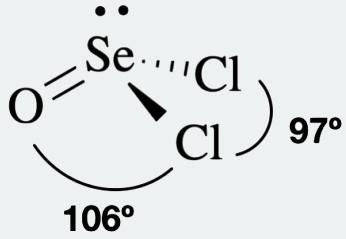
$IO_2F_2^-$

With five electron groups, the IO_2F_2 molecule has an approximately trigonal bipyramidal electronic (parent) geometry. The central iodine atom has a single bond to each of the fluorine atoms, a double bond to each oxygen, and a lone pair. The lone pair and the double bonds will occupy more space around iodine than each of the single bonds. Thus, we expect the lone pair and double bonds to occupy equatorial positions around the central iodine. The O=I=O bond angle is 102° (*much* smaller than the 120° angle expected from the parent geometry). This dramatically smaller angle is a result of the increased repulsion between the lone pair and the double bond.



$SeOCl_2$

With four electron groups, the $SeOCl_2$ molecule has four electron groups and approximately tetrahedral electronic (parent) geometry. It has both a lone pair and a double bond on the central selenium atom. The two chlorine atoms are singly bonded to selenium, while the oxygen is double bonded. The lone pair is most repulsive, followed by the double bonded oxygen, and then the chlorine bonds. This gives a Cl—Se—Cl bond angle of 97° and a Cl—Se—O bond angle of 106°; both angles are less than the 109.5° angles expected for the ideal tetrahedral geometry.



Practice

Exercise 3.2.2.1

Use VSEPR theory to predict the geometries and draw the structures of the following.

a. $XeOF_4$
b. NO_2^-
c. $SOCl_2$
d. IOF_3^-

Answer a available at the end of this section.

Answer b available at the end of this section.

Answer c available at the end of this section.

Answer d available at the end of this section.

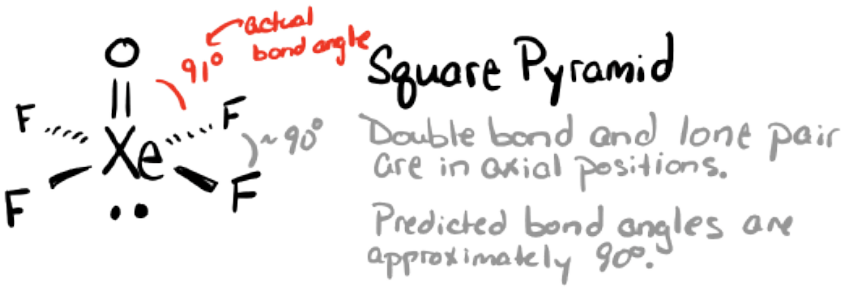
References

- Miessler, G.; Fischer, P.J.; Tarr, D. (2014). Inorganic Chemistry. New Jersey: Prentice-Hall. pp. 55

Answers

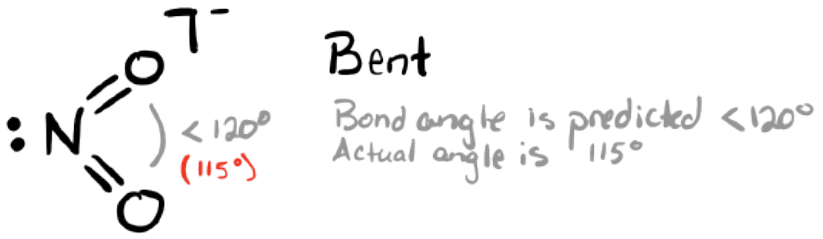
Exercise 3.2.2.1

This molecule has six electron groups around the central Xe atom (steric number 6), and thus has an approximately octahdral electronic (parent) geometry. There is a double bond to O and a lone pair, both of which are more strongly repulsive than the single bonds to F. The double bond and lone pair will be directly opposite to each other, designated as axial positions. The result is a square pyramidal molecular geometry. VSEPR theory predicts F—Xe—F bond angles of 90°. As a general rule, lone pairs are slightly more repulsive than multiple bonds, and so we might expect the O—Xe—F bond angles to be <90°; *however in this case the actual O—Xe—F bond angle is observed to be 91°* (you could not have predicted the latter).



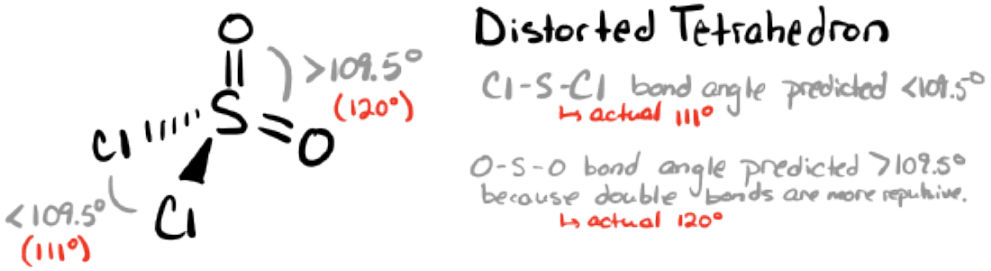
Exercise 3.2.2.1

This molecule has three electron groups around the central atom: one lone pair and two double bonds to oxygen atoms. This results in an approximately trigonal planar electronic (parent geometry). We expect the lone pair to be slightly more repulsive than double bonds, and so we expect the O—N—O bond angle to be slightly less than 120°. *The actual O—N—O angle is 115°.*



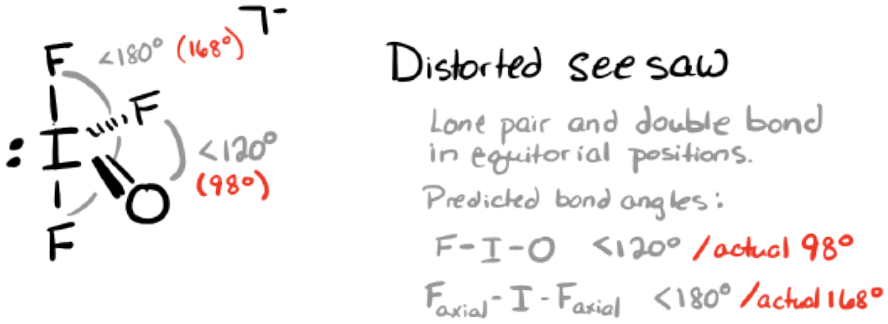
Exercise 3.2.2.1

This molecule has four electron groups (steric number 4) with an approximately tetrahedral electronic (parent) geometry. Each double bonded oxygen will take up more space around the central S than the single bonded Cl atoms. We should expect the double bonds to repel each other more strongly than they repel each single bond, with the least repulsive interaction being between the two single bonds. The bond angle for Cl—S—Cl is expected to be <109.5° according to VSEPR theory (however, it is actually 111°). We would expect the bond angle for O—S—O to be larger than the angle for Cl—S—Cl and for Cl—S—O. The O—S—O bond angle is predicted to be >109.5° (and the actual bond angle is 120°). The molecular geometry is a distorted tetrahedron.



Exercise 3.2.2.1

This molecule has five electron groups (steric number 5) with an approximately trigonal bipyramidal electronic (parent) geometry. There is one lone pair, a double bond to O, and three single bonds to F atoms around the central I atom. The lone pair and double bond are most repulsive, and should occupy the less crowded equatorial positions rather than the more crowded axial positions. This results in a seesaw molecular geometry. With the more repulsive lone pair and the strongest equatorial repulsive force being between the double bond and lone pair, we should expect the $F_{equatorial}$—I—O bond angle to be less than the 120° angle expected for the parent geometry (*it is actually much less, at 98°*). Due to repulsion between the axial F atoms and both the lone pair and double bond, we should expect the F—S—F bond angles to be compressed. The F_{axial}—I—F_{axial} is actually 168°.



This page titled 3.2.2: Multiple Bonds is shared under a license and was authored, remixed, and/or curated by Kathryn Haas.

- 3.2.2: Multiple Bonds by Kathryn Haas is licensed CC BY-NC-SA 4.0.

3.2.3: Electronegativity and Atomic Size Effects

Introduction

We saw in previous sections how lone pairs of electrons and multiple bonds distort bond angles between non-central atoms (ligands) around a central atom. This section describes how ligand **electronegativity and size also influence bond angles and molecular geometry**. Electronegativity is generally correlated with atomic size going down any group of the periodic table. There are some cases where bond angles can be predicted by these correlations. However, size and electronegativity can also work as competing factors in determining bond angles.

Definitions of Electronegativity

Linus Pauling introduced the first electronegativity scale in 1932 in order to explain the extra stability of molecules with polar bonds.[1] The electronegativity of an atom, represented by the Greek letter χ (chi), can be defined as the tendency of an atom to draw electrons to itself in a chemical bond. On the Pauling scale, the electronegativity difference between two atoms A and B was defined in terms of the dissociation energies E_d of the A-A, B-B, and A-B bonds:

$$\chi_A - \chi_B = \sqrt{E_d(AB) - [E_d(AA) + E_d(BB)]/2}$$

where the energies are expressed in electron volts. Pauling's scale of electronegativity ranges from Fluorine (most electronegative = 4.0) to Francium (least electronegative = 0.7). [2,3] The polarity of bonds and assignment of formal charges is predicted by electronegativity differences.

Periodic table of electronegativity using the Pauling scale

→ Atomic radius decreases → Ionization energy increases → Electronegativity increases →

Group →	1	2	3	4	5	6	7	8	9	10	11	12	13	14	15	16	17	18
↓ Period																		
1	H 2.20																	He
2	Li 0.98	Be 1.57											B 2.04	C 2.55	N 3.04	O 3.44	F 3.98	Ne
3	Na 0.93	Mg 1.31											Al 1.61	Si 1.90	P 2.19	S 2.58	Cl 3.16	Ar
4	K 0.82	Ca 1.00	Sc 1.36	Ti 1.54	V 1.63	Cr 1.66	Mn 1.55	Fe 1.83	Co 1.88	Ni 1.91	Cu 1.90	Zn 1.65	Ga 1.81	Ge 2.01	As 2.18	Se 2.55	Br 2.96	Kr 3.00
5	Rb 0.82	Sr 0.95	Y 1.22	Zr 1.33	Nb 1.6	Mo 2.16	Tc 1.9	Ru 2.2	Rh 2.28	Pd 2.20	Ag 1.93	Cd 1.69	In 1.78	Sn 1.96	Sb 2.05	Te 2.1	I 2.66	Xe 2.60
6	Cs 0.79	Ba 0.89	*	Hf 1.3	Ta 1.5	W 2.36	Re 1.9	Os 2.2	Ir 2.20	Pt 2.28	Au 2.54	Hg 2.00	Tl 1.62	Pb 1.87	Bi 2.02	Po 2.0	At 2.2	Rn 2.2
7	Fr 0.7	Ra 0.9	**	Rf	Db	Sg	Bh	Hs	Mt	Ds	Rg	Cn	Uut	Fl	Uup	Lv	Uus	Uuo

* Lanthanoids	La 1.1	Ce 1.12	Pr 1.13	Nd 1.14	Pm 1.13	Sm 1.17	Eu 1.2	Gd 1.2	Tb 1.1	Dy 1.22	Ho 1.23	Er 1.24	Tm 1.25	Yb 1.1	Lu 1.27
** Actinoids	Ac 1.1	Th 1.3	Pa 1.5	U 1.38	Np 1.36	Pu 1.28	Am 1.13	Cm 1.28	Bk 1.3	Cf 1.3	Es 1.3	Fm 1.3	Md 1.3	No 1.3	Lr 1.3

Figure 3.2.3.1: Table of Pauling electronegativities from Wikipedia's Electronegativity page (click).

While directly relevant to the strength of chemical bonds, the Pauling definition of electronegativity has a significant limitation: calculating each value requires data from several compounds in which specific atoms are bonded. This means that the scale cannot be successfully applied to all situations. To overcome this limitation, alternative electronegativity scales were developed based on different thermochemical measurements or calculations. These other scales are listed in the table below. More thorough descriptions of how values in each scale are calculated are described on Wikipedia's Electronegativity page (click) and a concise history of electronegativity scales is summarized in ref 4.

Scale Developer	Year first described	Characteristics
Linus Pauling[1]	1932	Based on bond energies
Robert S. Mulliken[5,6]	1934	Based on valence electron properties of atoms (electron affinity and ionization energy)
Louis Allred & Eugene G. Rochow[7]	1958	Based on electrostatic force (effective nuclear charge)
Robert T. Sanderson[8]	1983	Based on atomic electron density
Ralph G. Pearson[9]	1985	Related to Hard-Soft Acid-Based theory
Leland C. Allen, Joseph Mann, Terry L. Meek[10,11,12]	1989, 2000	Average ionization energies of valence shell electrons, configuration energies (CE) $$\mathrm{CE} = \frac{n\varepsilon_s + m\varepsilon_p}{n+m}$$ $n = \text{number of s electrons}$ $m = \text{number of p electrons}$ $\varepsilon_s, \varepsilon_p = \text{experimental 1-electron s and p energies}$

The primary advantage to this scale developed by Mann, Meek, and Allen[12] is that it is based on configuration energy (CE), the average ionization energies of valence electrons in ground state free atoms. A scale based on ionization energies can be calculated more directly for any element. However, a critique of all electronegativity scales, including this one, is that they are all based on assumptions that fail in some cases.

There is a relationship between electronegativity and atomic size because both are related to ionization energy. Like ionization energy, there is a general trend across the periodic table for both electronegativity and atomic size; in general, smaller atoms toward the top right-hand side of the periodic table have greater electronegativity values and smaller atomic size. We will see below that both electronegativity and atomic size influence bond angles and absolute molecular geometry around a central atom. In some cases, the size and electronegativity affects are aligned; in some cases these effects compete.

Electronegativity and Size Influence Bond Angles

Let's begin by examining the bond angles of several trigonal pyramidal molecules. The molecules shown in Figure 3.2.3.2 each have three identical "pendant groups" on the central atom (Figure 3.2.3.2). *Pendant atoms* or *pendant groups* are the atoms, or groups of atoms, that are bonded directly to the central atom. The molecules shown here are arranged according to the size of the central and pendant atoms. Central atoms increase in size going down this figure, and pendant atoms increase in size going across from left to right. The bond angles and bond lengths are labeled in each case.

What trends can you identify?

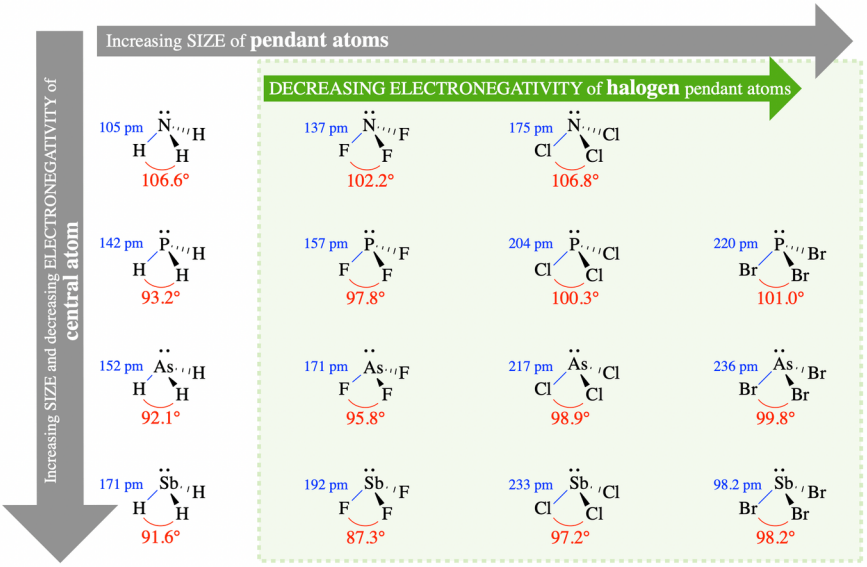


Figure 3.2.3.2: Several molecules with trigonal pyramidal electronic geometry are shown arranged according to size of the central atom (increasing size of central atom from top to bottom) and pendant atom (increasing size of pendant atoms from left to right). Bond angles and bond lengths are indicated. (Kathryn Haas; CC-NC-BY-SA)

Trends in Size

First, let's examine how the size of the central and pendant groups might influence bond angle. In VSEPR theory, **the size of atoms (or groups of atoms) will affect bond angles due to changes in steric interactions between pendant groups.**

Size of the central atom

Examine the relationship between the size of the central atom and the bond angles in Figure 3.2.3.2 (go down any column in the figure). For example, compare NH_3, PH_3, AsH_3, and SbH_3, with bond angles 106.6°, 93.2°, 92.1°, and 91.6°, respectively. In this series, the size of the central atom increases from N to Sb while the size of the pendant atom (hydrogen) remains constant. *As the size of the central atom increases, the bond angles decrease; thus, we observe a negative relationship between size of the central atom and the bond angle in these molecules*. This relationship is explained by sterics. As the central atom increases in size, the bond lengths also increase and the pendant atoms are farther from each other in space. In VSEPR theory, this will reduce steric interactions between the pendant groups. Since the lone pair on these molecules is more repulsive than bonded groups, the decrease in steric interactions between bonded groups results in a decrease in bond angles.

Size of the pendant atoms (or groups)

Examine the relationships between size of the halogen pendant atoms and bond angle in Figure 3.2.3.2 (go across any row within the shaded region). For example, compare PF_3, PCl_3, and PBr_3, with bond angles 97.8°, 100.3°, and 101.0°, respectively. In this series, the size of the pendant atom increases from F to Br while the central atom remains constant (phosphorous). *As the size of pendant atoms increases, the bond angle increases; thus, we observe a direct relationship between size of the pendant group and the bond angle in these molecules*. Again, we can explain this using sterics. As the size of the pendant atoms increases, sterics between the pendant groups will increase (despite small changes in bond length). Increased steric interactions between pendant groups will prefer larger bond angles between the groups.

This trend fails, however, if we consider the molecules with hydrogen as the pendant atoms. Notice, for example, that H is the smallest pendant atom. If we consider the trend described above, we should assume that XH_3 (where X is a variable atom) would have the smallest bond angle in the series of XH_3, XF_3, XCl_3, and XBr_3. However this is not the case of NH_3, NF_3, and NCl_3, with bond angles 106.6°, 102.2°, and 106.8°, respectively. To explain the variation in these bond angles, we need to consider electronegativity.

Trends in Electronegativity

Now let's examine how electronegativity influences bond angles around a central atom. In VSEPR theory, **electronegativity of atoms/groups will affect bond angles due to changes in the distribution of electron pairs around the central atom (and thus changes in the severity of electron pair repulsion).** This really comes down to bond polarity caused by the difference in electronegativity between the central atom and pendant groups (bond polarity in the context of valence bond theory). In a polar bond, the more electronegative atom will pull electron density towards itself. When a pendant atom is more electronegative, it will pull the bonded electron pair towards itself and away from the central atom; this will reduce the electron pair repulsion between bonded electron pairs on the central atom. A decrease in electron pair repulsion on the central atom should decrease bond angles between the groups (Figure 3.2.3.3).

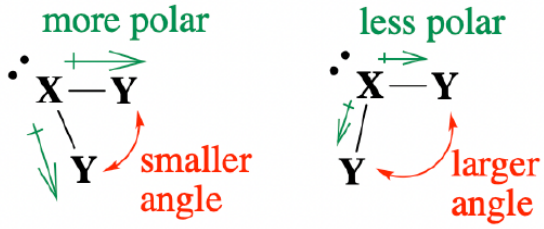


Figure 3.2.3.3. When electron pairs are distributed away from the central atom, repulsions are decreased, allowing smaller bond angles. (Kathryn Haas; CC-NC-BY-SA)

Electronegativity is an alternative explanation to the trends we already examined above in Figure 3.2.3.2 . For example, when we compare the halogen pendant atoms (shaded region in Figure 3.2.3.2) , the electronegativity of pendant groups decreases, bond polarity of the bonds decreases, and bond angles increase going from left to right and from F to Br. As more electron density remains on the central atom, electron repulsion between the bonded pairs increases and bond angles increase.

The electronegativity argument can also be used to explain the fact that NH_3 (106.6°) has a larger bond angle than NF_3 (102.2°). This particular case illustrates how electronegativity and size can be competing factors. While electronegativity differences seem to dominate in the case of NH_3 (106.6°) compared to NF_3 (102.2°), size differences still dominate in the cases of other XH_3 and XF_3 examples in Figure 3.2.3.2).

Exercise 3.2.3.1

Predict the geometry and approximate bond angles. Then put the molecules in each series in order of smallest to largest bond angle. Defend your answer.

a. The X-S-X bond angle in OSF_2, $OSCl_2$, $OSBr_2$
b. H_2O, H_2S, H_2Se, H_2Te
c. H_2O, OF_2, OCl_2

Answer (a) available at the end of this section.

Group Electronegativities

You probably heard the terms "electron donating group" and "electron withdrawing group" from your coursework in Organic Chemistry. For example, the acid trifluoroacetic acid (TFA) is more acidic than acetic acid due to the electron withdrawing effects of the CF_3 group compared to CH_3. CF_3 is an electron withdrawing group, while CH_3 is an electron donating group. In other words, CF_3 is more electronegative than CH_3.

The electron withdrawing ability (electronegativity) of groups can be estimated and compared, just as they are with atoms. Although there is no one scale that is used for group electronegativities, and published values even for the same groups vary widely, there are reliable trends within similar groups. The same size and electronegativity factors discussed above that affect bond angles for *pendant atoms*, also can be used to rationalize distorted bond angles for *pendant groups* around a central atom.

Exercise 3.2.3.2

Consider the relative electronegativities and sizes of the pendant atoms/groups in the following examples. Is the trend in bond angles what you would expect from the relative group electronegativities and relative sizes? What, if any, is the more dominant factor in determining the trend?

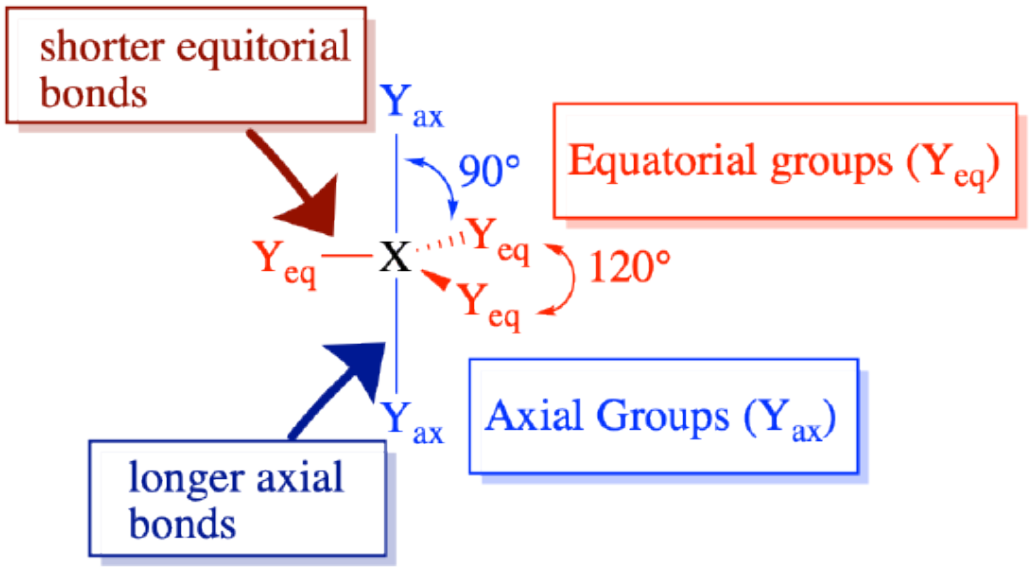
a. $N(CH_3)_3$ has an C-N-C bond angle of 110.9°, while $N(CF_3)_3$ has a bond angle of 117.9°.
b. The X-S-X bond angles in molecules of the form $SO_2(X)_2$ are: $SO_2(OH)_2$ 101.3°; $SO_2(CF_3)_2$ 102.0°; $SO_2(CH_3)_2$ 102.6°.

Answer (a) available at the end of this section.

Answer (b) available at the end of this section.

Special case of electronegativity and size in steric number 5 (trigonal bypyramid)

Molecules with steric number 5 are interesting because they posses two different types of positions (equatorial and axial). These positions have unique bond angles and bond lengths. Pendant atoms/groups have different preferences for the axial and equatorial positions that depend somewhat on their electronegativity.



Molecules with steric number 5 possess different bond angles and lengths for axial (ax) and equatorial (eq) pendant atoms. (CC-BY-NC-SA; Kathryn Haas)

In a previous section, we discussed the preference of lone pairs and multiple bonds for the equatorial positions in trigonal bipyramidal molecules. VSEPR theory rationalizes this by assuming that lone pairs and multiple bonds are more repulsive than the electron pairs in single bonds. Equatorial positions are less crowded (with only two closest neighbors at 90°, and two farther neighbors at 120°) compared to axial positions (with three closest neighbors at 90°), thus the more repulsive groups prefer the less crowded equatorial positions.

Pendant groups that are more electronegative result in weaker electron pair repulsion around the central atom, while groups that are less electronegative result in stronger electron-pair repulsion around the central atom (as described above). The result for steric number 5: **bonding pairs to *less electronegative elements* are *more repulsive*, and *generally prefer equatorial* positions.** Still, lone pairs and multiple bonds are more repulsive than single bonds and would show a stronger preference for equatorial positions.

Examples and Nuances

Exercise 3.2.3.3

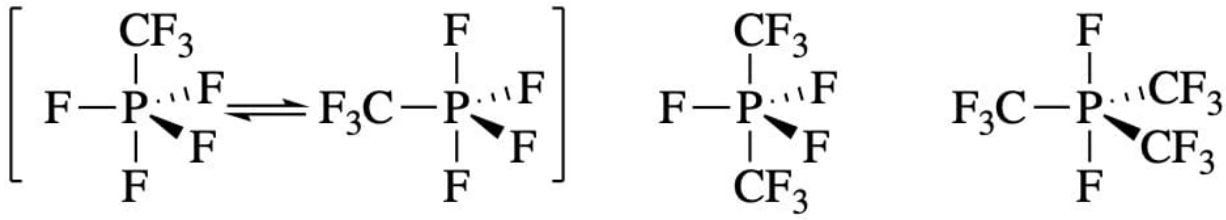
Some examples of molecule that demonstrate the equatorial preference of less electronegative groups are below. Predict (draw) their structures.

a. PF_4Cl, PF_3Cl_2, and PF_2Cl_3
b. $PF_4(CH_3)$ $PF_3(CH_3)_2$, and $PF_2(CH_3)_3$

Answer (a) available at the end of this section.

Answer (b) available at the end of this section.

In the exercise above, the structures can be explained by the electronegativity of the pendant groups; less electronegative groups prefer the equatorial positions. There are other similar molecules for which explanations (or predictions) are difficult. For example, the series of molecules below seems to have completely random placement of F and CF_3 groups. **These structures could not be predicted based on VSEPR theory.** It seems that in this case, the more symmetrical arrangements of pendant groups is preferred.



References and resources

1. Pauling, L. (1932). "The Nature of the Chemical Bond. IV. The Energy of Single Bonds and the Relative Electronegativity of Atoms". *J. Am. Chem. Soc.* **54**(9): 3570–3582. doi:10.1021/ja01348a011.
2. Housecroft, Catherine E. et. al. "Inorganic Chemistry" 3rd Edition. Pearson Education Limited 2008. Chapter 2.5 "Electronegativity Values" pgs. 42-44
3. International Union of Pure and Applied Chemistry. "Electronegativity". goldbook.iupac.org/E01990.html.
4. Pearson, R.G. *Acc. Chem. Res.* 1990, 23, 1, 1–2. https://doi.org/10.1021/ar00169a001
5. Mulliken, R. S. (1934). "A New Electroaffinity Scale; Together with Data on Valence States and on Valence Ionization Potentials and Electron Affinities". *J. Chem. Phys.***2** (11): 782–793. doi:10.1063/1.1749394.
6. Mulliken, R. S. (1935). "Electronic Structures of Molecules XI. Electroaffinity, Molecular Orbitals and Dipole Moments". J. Chem. Phys. **3** (9): 573–585. doi:10.1063/1.1749731.
7. Allred, A. L.; Rochow, E. G. (1958). "A scale of electronegativity based on electrostatic force". *Journal of Inorganic and Nuclear Chemistry*. **5** (4): 264–268. doi:10.1016/0022-1902(58)80003-2
8. Sanderson, R. T. (1983). "Electronegativity and bond energy". *Journal of the American Chemical Society*. **105** (8): 2259–2261. doi:10.1021/ja00346a026
9. Pearson, R. G. (1985). "Absolute electronegativity and absolute hardness of Lewis acids and bases". J. Am. Chem. Soc. 107 (24): 6801. doi:10.1021/ja00310a009.
10. Allen, Leland C. (1989). "Electronegativity is the average one-electron energy of the valence-shell electrons in ground-state free atoms". Journal of the American Chemical Society. 111 (25): 9003–9014. doi:10.1021/ja00207a003.
11. Mann, Joseph B.; Meek, Terry L.; Allen, Leland C. (2000). "Configuration Energies of the Main Group Elements". Journal of the American Chemical Society. 122 (12): 2780–2783. doi:10.1021/ja992866e.
12. Mann, Joseph B.; Meek, Terry L.; Knight, Eugene T.; Capitani, Joseph F.; Allen, Leland C. (2000). "Configuration energies of the d-block elements". Journal of the American Chemical Society. 122 (21): 5132–5137. doi:10.1021/ja9928677

Acknowledgment

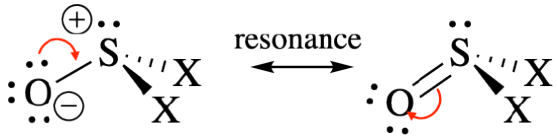
- Matthew Salem (UC Davis) (Pauling Electronegativity)
- Introduction to Inorganic Chemistry Wikibook (https://chem.libretexts.org/Bookshel..._Bond_Strength)

- Curated or created by Kathryn Haas

Answers

Exercise 3.2.3.1

Geometry and predicted bond angles: These are molecules with steric number 4. They can be written as two different resonance structures, and the resonance hybrid would have double bond character between S and O.



We would expect a trigonal pyramidal geometry with all bond angles <109.5° because the lone pair is more repulsive than bonds. Because the double bond is more repulsive than single bonds, we should also expect the O-S-X bond angles to be greater than the X-S-X bond angles.

Trend: This is a series of molecules that varies in the identity of the pendant atoms; the variation is within the halogens. The size of the halogens increases, and the electronegativity decreases in the order F, Cl, Br. Both size and electronegativity would lead us to conclude that the X-S-X bond angles would increase in the order $OSF_2 < OSCl_2 < OSBr_2$

Explanation: (1) Increasing electonegativity of the pendant atom (F > Cl > Br) increases the polarity of the bond and reduces the electron density of the bonded pair on the central atom. This reduces the e-e repulsions of adjacent bonded electron pairs on S, allowing the halogens to become closer. The more electronegative pendant atoms can have smaller bond angles. (2) Increasing size of pendant atoms (F < Cl < Br) increases steric repulsions and increases bond angle. Both explanations lead to the same predicted trend.

The actual measured X-S-X bond angles are OSF_2 (92.3°) / $OSCl_2$ (96.2°) / $OSBr_2$ (98.2°). The trend in these bond angles is consistent with the prediction.

Geometry and predicted bond angles: These are molecules with steric number 4, bent molecular geometry, with predicted bond angles <109.5° because the two lone pairs are each more repulsive than the bonds. There are two lone pairs and two single bonds to H around each central atom.

Trend: This is a series of molecules that varies in the identity of the central atom. The central atom increases in the order O < S < Se < Te, where Te is the largest element and O is the smallest. Arguments based on size would lead us to predict that the pendant groups of H_2Te would be less sterically crowded and thus have a smaller bond angle than the pendant groups of H_2O. The electronegativity decreases in the order O > S > Se > Te, where O is the most electronegative element and Te is the least. Thus, we expect the bonding electro pairs to be closer to the central atom on O than they would be on Te; we should expect H_2Te to have the least electron pair repulsions and thus smallest bond angle in this series, while H_2O would have the strongest electron pair repulsions and largest bond angles.

Both arguments lead to the same conclusion, that the order of increasing bond angle is $H_2Te < H_2Se < H_2S < H_2O$.

The actual measured bond angles are H_2Te (90.2°) / H_2Se (90.6°) / H_2S (92.1°) / H_2O (104.5). The trend in these bond angles is consistent with prediction.

Geometry and predicted bond angles: These are molecules with steric number 4, bent molecular geometry, with predicted bond angles <109.5° because the two lone pairs are each more repulsive than the bonds. There are two lone pairs and two single bonds to H around each central atom. (This is similar to the case in (b)).

Trend: This is a series of molecules that varies in the identity of the pendant atoms; two of the molecules have halogens, and the other has hydrogen pendant atoms. This is a case where size and electronegativity will be conflicting factors because trends in electronegativity do not mirror the trend in size.

- *Size:* The size of pendant atoms increases in the order H < F < Cl where H is smallest and Cl is largest. Prediction of bond angles based on size alone would lead to the predicted order of increasing bond angle $H_2O < OF_2 < OCl_2$.
- *Electronegativity*: The electronegativity decreases in the order F > Cl > H where F has the greatest electronegativity and H has the least. Since we expect the most electronegative pendant atoms to have the smallest bond angles, prediction based on electronegativity alone would lead to the predicted order of increasing bond angle $OF_2 < OCl_2 < H_2O$.

The points above illustrate how the two different arguments would lead to different predictions about the trend in bond angle. This makes it difficult to predict the actual order of increasing bond angle. However, we saw above in the example of NH_3 vs NF_3 that electronegativity is more important than size; yet in the case of NH_3 vs NCl_3, the much larger size of the pendant atom is more important. If we apply this lesson to the current problem, we might predict the order $OF_2 < H_2O < OCl_2$, and in fact this more nuanced prediction, based on a similar case, matches the actual order for measured bond angles: OF_2 (103.3°) < H_2O (104.5°) < OCl_2 (110.9°).

Exercise 3.2.3.2

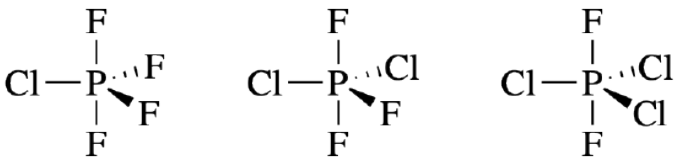
Add texts here. Do not delete this text first.

Exercise 3.2.3.2

Add texts here. Do not delete this text first.

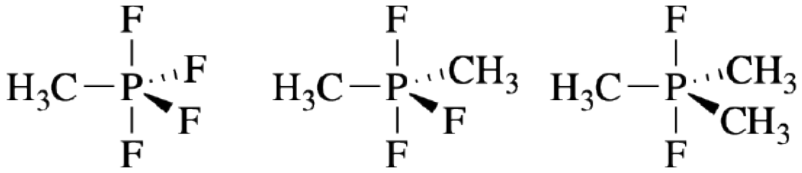
Exercise 3.2.3.3

Cl is less electronegative than F; thus we expect Cl to have stronger preference for the equatorial positions.



Exercise 3.2.3.3

CH_3, an electron donating group, is less electronegative than F. We expect CH_3 to have a stronger preference for the equatorial positions.



This page titled 3.2.3: Electronegativity and Atomic Size Effects is shared under a license and was authored, remixed, and/or curated by Kathryn Haas.

- 3.2.3: Electronegativity and Atomic Size Effects by Kathryn Haas is licensed CC BY-NC-SA 4.0.

3.2.4: Ligand Close Packing

Introduction

Ligand Close Packing (LCP) theory is complimentary to VSEPR, except that LCP focuses on repulsions between pendant *atoms* ("outer" atoms that are not directly bonded to one another), rather than focusing on the chemical environment around the central atom in a molecule. Both LCP and the VSEPR models were developed by Robert Gillespie.

The LCP model assumes that ligands (or pendant atoms) "pack" as closely as possible around a central atom. A given ligand will have a specific atomic radius when bound to a central atom. The distance between two ligands around the same central atom is simply the sum of the atomic radii of the pendant atoms. Therefore for a specific set of ligands around a specific central atom, the ligand-ligand distances are constant despite the coordination number or bond angles. In other words, for a series of similar molecules with the same central atom, while bond angles and bond distances of pendant atoms may change, the distances between two pendant atoms remain the same.

Ligand Close Packing Theory

According to LCP, distances between two pendant atoms are similar...

- even when steric number changes
- even when bond angles change
- Reason: pendant atoms "pack" around the central atom.

Ligand Close Packing and Bond Distances

If the distance between non-bonded atoms remains constant even while bond angles change, then the bond length between the pendant and central atom must change to accommodate. For example, PF_4^+ and PF_3O have almost identical $F-F$ distances of 238 and 237 pm, respectively. As expected from VSEPR, the $F-P-F$ bond angle in PF_4^+ is 109.5°. The $F-P-F$ bond angle in PF_3O (101.1°) is smaller due to the increased repulsion of the oxygen double bond. Therefore the P-F bond lengths must be different. In fact, the P-F bond distances are 145.7 pm in PF_4^+ and 154 pm in PF_3O.

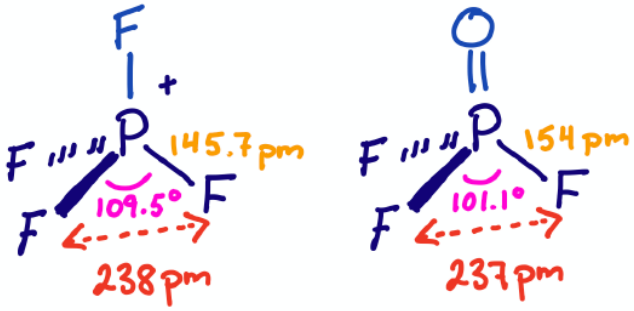


Figure 3.2.4.1: The molecular structures of PF_4^+ and PF_3O. The distances between neighboring F atoms are similar in the two molecules, while bond lengths and angles differ. The PF_4^+ ion has a $P-F$ bond length of 145.7 pm, an $F-P-F$ bond angle of 109.5°, and a distance of 238 pm between neighboring F atoms. The PF_3O molecule has a $P-F$ bond length of 154 pm, an $F-P-F$ bond angle of 101.1°, and a distance of 237 pm between neighboring F atoms. (CC-BY-NC-SA; Kathryn Haas)

The relationship between bond angles, bond lengths, and close-packing distance is described by right angle trigonometry (recall SOA-CAH-TOA). In a right triangle, the hypotenuse is the longest side, opposite to the right angle. For either of the other two angles in the triangle, the angle (θ) and lengths of the sides (*opposite* and *adjacent* to θ) are related by the trigometric functions shown in Figure 3.2.4.2 .

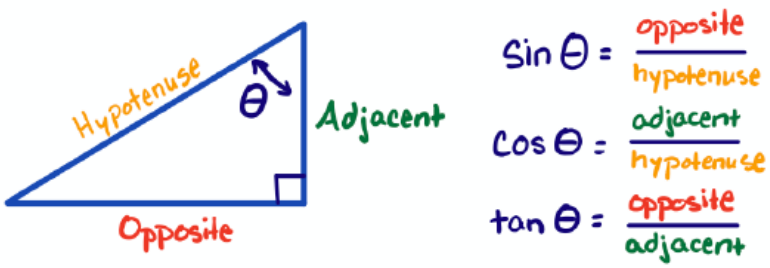


Figure 3.2.4.2: Visual depiction of SOA-CAH-TOA. (CC-BY-NC-SA; Kathryn Haas)

In the case of a molecule, we can apply right angle trigonometry by imagining that the bond angle is divided into two right angles, as illustrated in Figure 3.2.4.2. The hypotenuse of the triangles is the bond length, the opposite side is one half of the close-packing distance, and θ is one half the bond angle.

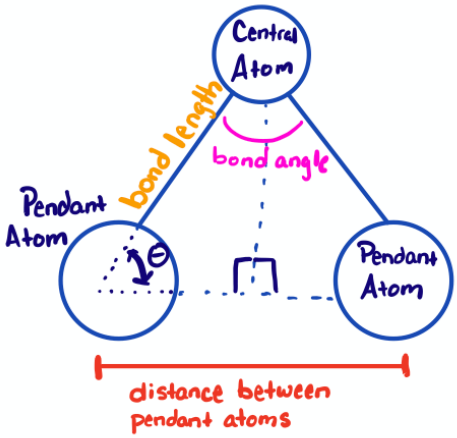


Figure 3.2.4.1: Illustration of how right angle trigonometry can be applied to determine bond angle, bond length, or distance between neighboring atoms: any bond angle can be divided into two right angles where the bond length is the hypotenuse, the distance between neighbors is twice the opposite side, and the bond angle is twice θ. (CC-BY-NC-SA; Kathryn Haas)

Exercise 3.2.4.1

The distance between F atoms is 212 pm in both NF_4^+ and NF_3. The bond angles are 109.5° and 102.3°, respectively. What are the expected $N-F$ bond lengths?

Answer available at the end of this section.

Sources and Resources

- https://en.Wikipedia.org/wiki/LCP_th...ieNyholm1957-3

Answers

Exercise 3.2.4.1



The actual measured bond lengths are 130 pm for $\mathrm{NF_4}^+$ and 136.5 pm for $\mathrm{NF_3}$.

This page titled 3.2.4: Ligand Close Packing is shared under a license and was authored, remixed, and/or curated by Kathryn Haas.

- 3.2.4: Ligand Close Packing by Kathryn Haas is licensed CC BY-NC-SA 4.0.

3.3: Molecular Polarity

Dipole moments occur when there is a separation of charge. They can occur between two ions in an ionic bond or between atoms in a covalent bond; dipole moments arise from differences in electronegativity. The larger the difference in electronegativity, the larger the dipole moment. The distance between the charge separation is also a deciding factor in the size of the dipole moment. The dipole moment is a measure of the polarity of the molecule.

Introduction

When atoms in a molecule share electrons unequally, they create what is called a dipole moment. This occurs when one atom is more electronegative than another, resulting in that atom pulling more tightly on the shared pair of electrons, or when one atom has a lone pair of electrons and the difference of electronegativity vector points in the same way. One of the most common examples is the water molecule, made up of one oxygen atom and two hydrogen atoms. The differences in electronegativity and lone electrons give oxygen a partial negative charge and each hydrogen a partial positive charge.

Dipole Moment

When two electrical charges, of opposite sign and equal magnitude, are separated by a distance, an electric dipole is established. The size of a dipole is measured by its dipole moment (μ). Dipole moment is measured in Debye units, which is equal to the distance between the charges multiplied by the charge (1 Debye equals $3.34 \times 10^{-30}\ C\ m$). The dipole moment of a molecule can be calculated by Equation 3.3.1:

$$\vec{\mu} = \sum_i q_i \vec{r}_i \tag{3.3.1}$$

where

- $\vec{\mu}$ is the dipole moment vector
- q_i is the magnitude of the ith charge, and
- $\vec{r}_i$ is the vector representing the position of ith charge.

The dipole moment acts in the direction of the vector quantity. An example of a polar molecule is $\mathrm{H_2O}$. Because of the lone pair on oxygen, the structure of $\mathrm{H_2O}$ is bent (via VSEPR theory), which means that the vectors representing the dipole moment of each bond do not cancel each other out. Hence, water is polar.

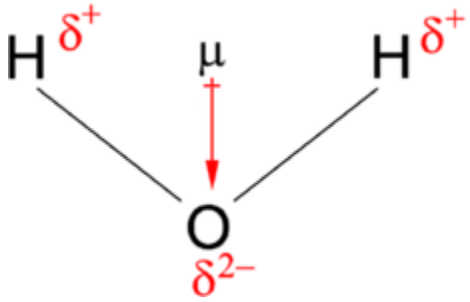


Figure 3.3.1: Dipole moment of water. The convention in chemistry is that the arrow representing the dipole moment goes from positive to negative. Physicist tend to use the opposite orientation.

The vector points from positive to negative, on both the molecular (net) dipole moment and the individual bond dipoles. Table A2 shows the electronegativity of some of the common elements. The larger the difference in electronegativity between the two atoms, the more electronegative that bond is. To be considered a polar bond, the difference in electronegativity must be large. The dipole moment points in the direction of the vector quantity of each of the bond electronegativities added together.

It is relatively easy to measure dipole moments: just place a substance between charged plates (Figure 3.3.2); polar molecules increase the charge stored on the plates, and the dipole moment can be obtained (i.e., via the capacitance of the system).

Nonpolar CCl_4 is not deflected; moderately polar acetone deflects slightly; highly polar water deflects strongly. In general, polar molecules will align themselves: (1) in an electric field, (2) with respect to one another, or (3) with respect to ions (Figure 3.3.2).

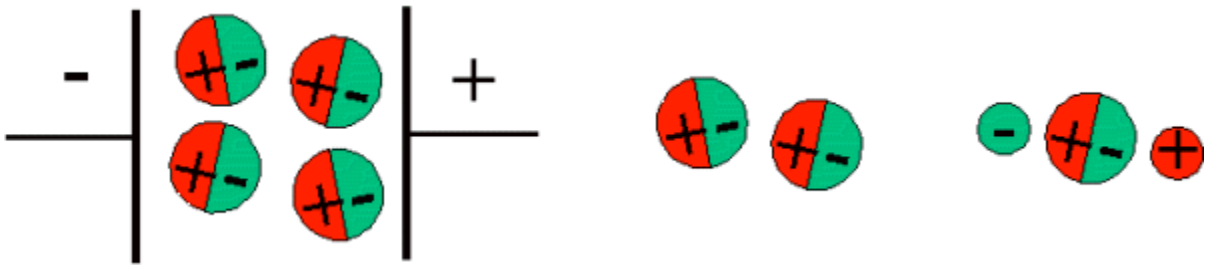


Figure 3.3.2: Polar molecules align themselves in an electric field (left), with respect to one another (middle), and with respect to ions (right)

Equation 3.3.1 can be simplified for a simple separated two-charge system like diatomic molecules or when considering a bond dipole within a molecule

$$\mu_{diatomic} = Q \times r \tag{3.3.2}$$

This bond dipole is interpreted as the dipole from a charge separation over a distance r between the partial charges Q^+ and Q^- (or the more commonly used terms δ^+ - δ^-); the orientation of the dipole is along the axis of the bond. Consider a simple system of a single electron and proton separated by a fixed distance. When the proton and electron are close together, the dipole moment (degree of polarity) decreases. However, as the proton and electron get farther apart, the dipole moment increases. In this case, the dipole moment is calculated as (via Equation 3.3.2):

$$\begin{aligned} \mu &= Qr \\ &= (1.60 \times 10^{-19}\, C)(1.00 \times 10^{-10}\, m) \\ &= 1.60 \times 10^{-29}\, C \cdot m \end{aligned}$$

The Debye characterizes the size of the dipole moment. When a proton and electron are 100 pm apart, the dipole moment is 4.80 D:

$$\begin{aligned} \mu &= (1.60 \times 10^{-29}\, C \cdot m)\left(\frac{1\ D}{3.336 \times 10^{-30}\, C \cdot m}\right) \\ &= 4.80\ D \end{aligned}$$

$4.80\ \ D$ is a key reference value and represents a pure charge of +1 and -1 separated by 100 pm. If the charge separation is increased then the dipole moment increases (linearly):

- If the proton and electron are separated by 120 pm:

$$\mu = \frac{120}{100}(4.80\ D) = 5.76\, D \tag{3.3.3}$$

- If the proton and electron are separated by 150 pm:

$$\mu = \frac{150}{100}(4.80\ D) = 7.20\, D \tag{3.3.4}$$

- If the proton and electron are separated by 200 pm:

$$\mu = \frac{200}{100}(4.80\ D) = 9.60\, D \tag{3.3.5}$$

Example 3.3.1: Water

The water molecule in Figure 3.3.1 can be used to determine the direction and magnitude of the dipole moment. From the electronegativities of oxygen and hydrogen, the difference in electronegativity is 1.2e for each of the hydrogen-oxygen bonds. Next, because the oxygen is the more electronegative atom, it exerts a greater pull on the shared electrons; it also has two lone pairs of electrons. From this, it can be concluded that the dipole moment points from between the two hydrogen atoms

toward the oxygen atom. Using the equation above, the dipole moment is calculated to be 1.85 D by multiplying the distance between the oxygen and hydrogen atoms by the charge difference between them and then finding the components of each that point in the direction of the net dipole moment (the angle of the molecule is 104.5°).

The bond moment of the O-H bond =1.5 D, so the net dipole moment is

$$\mu = 2(1.5)\cos\left(\frac{104.5^\circ}{2}\right) = 1.84\ D$$

Polarity and Structure of Molecules

The shape of a molecule and the polarity of its bonds determine the OVERALL POLARITY of that molecule. A molecule that contains polar bonds might not have any overall polarity, depending upon its shape. The simple definition of whether a complex molecule is polar or not depends upon whether its overall centers of positive and negative charges overlap. If these centers lie at the same point in space, then the molecule has no overall polarity (and is non polar). If a molecule is completely symmetric, then the dipole moment vectors on each molecule will cancel each other out, making the molecule nonpolar. A molecule can only be polar if the structure of that molecule is not symmetric.

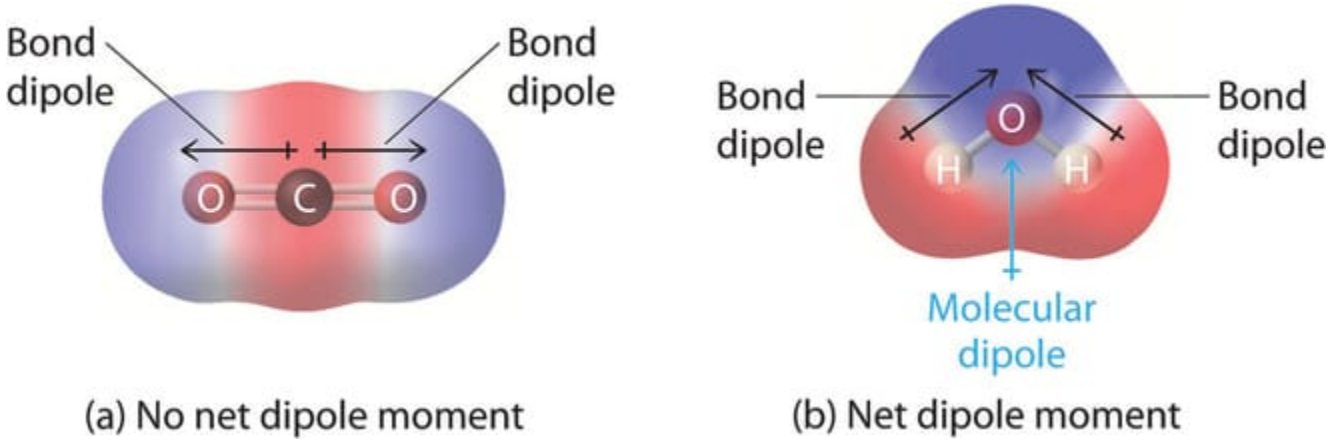


Figure 3.3.3: Charge distributions of CO_2 and H_2O\). Blue and red colored regions are negatively and positively signed regions, respectively. (CC BY-SA-NC 3.0; anonymous)

A good example of a nonpolar molecule that contains polar bonds is carbon dioxide (Figure $3.3.3a$). This is a linear molecule and each C=O bond is, in fact, polar. The central carbon will have a net positive charge, and the two outer oxygen atoms a net negative charge. However, since the molecule is linear, these two bond dipoles cancel each other out (i.e. the vector addition of the dipoles equals zero) and the overall molecule has a zero dipole moment ($\mu = 0$).

> Although a polar bond is a prerequisite for a molecule to have a dipole, not all molecules with polar bonds exhibit dipoles

For AB_n molecules, where A is the central atom and B are all the same types of atoms, there are certain molecular geometries which are symmetric. Therefore, they will have no dipole even if the bonds are polar. These geometries include linear, trigonal planar, tetrahedral, octahedral and trigonal bipyramid.

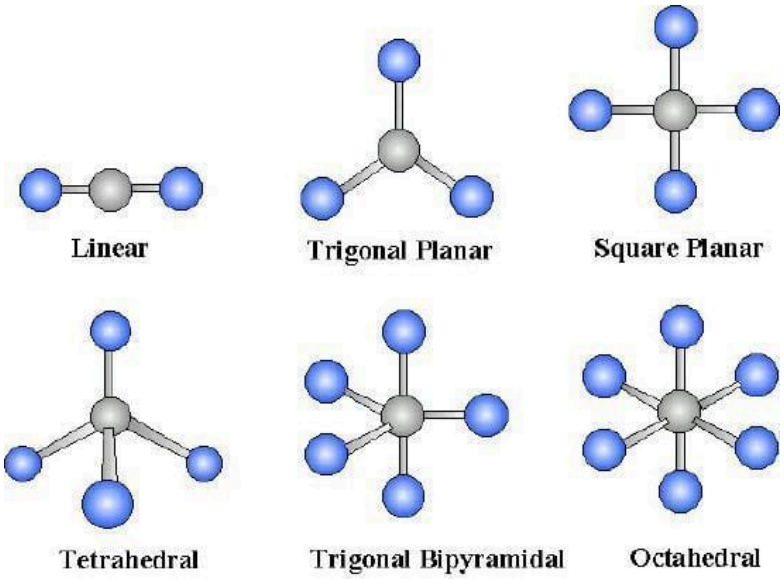
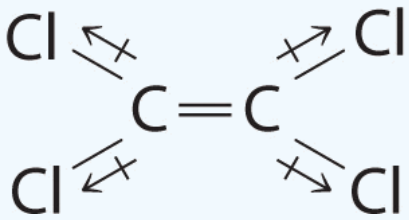


Figure 3.3.4: Molecular geometries with exact cancellation of polar bonding to generate a non-polar molecule ($\mu = 0$)

Example 3.3.3: C_2Cl_4

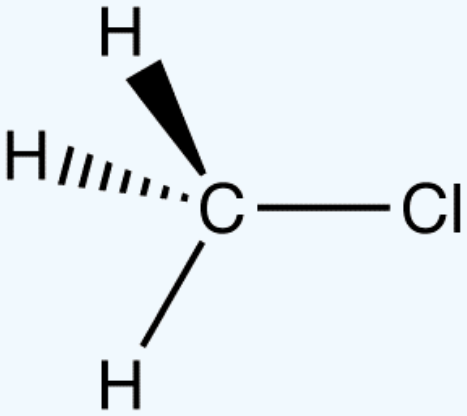
Although the C–Cl bonds are rather polar, the individual bond dipoles cancel one another in this symmetrical structure, and $Cl_2C{=}CCl_2$ does not have a net dipole moment.



Example 3.3.3: CH_3Cl

C-Cl, the key polar bond, is 178 pm. Measurement reveals 1.87 D. From this data, % ionic character can be computed. If this bond were 100% ionic (based on proton & electron),

$$\mu = \frac{178}{100}(4.80\ D)$$
$$= 8.54\ D$$



Although the bond length is ***increasing***, the dipole is ***decreasing*** as you move down the halogen group. The electronegativity decreases as we move down the group. Thus, the greater influence is the electronegativity of the two atoms (which influences the ***charge*** at the ends of the dipole).

Table 3.3.1: Relationship between Bond length, Electronegativity and Dipole moments in simple Diatomics

Compound	Bond Length (Å)	Electronegativity Difference	Dipole Moment (D)
HF	0.92	1.9	1.82
HCl	1.27	0.9	1.08
HBr	1.41	0.7	0.82
HI	1.61	0.4	0.44

References

1. *Housecroft, Catherine E. and Alan G. Sharpe. Inorganic Chemistry. 3rd ed. Harlow: Pearson Education, 2008. Print. (Pages 44-46)*
2. *Tro, Nivaldo J. Chemistry: A Molecular Approach. Upper Saddle River: Pearson Education, 2008. Print. (Pages 379-386)*

This page titled 3.3: Molecular Polarity is shared under a license and was authored, remixed, and/or curated by LibreTexts.

- Dipole Moments by Delmar Larsen, Mike Blaber is licensed CC BY 4.0.

3.4: Hydrogen Bonding

A hydrogen bond is an intermolecular force (IMF) that forms a special type of dipole-dipole attraction when a hydrogen atom bonded to a strongly electronegative atom exists in the vicinity of another electronegative atom with a lone pair of electrons. Intermolecular forces (IMFs) occur between molecules. Other examples include ordinary dipole-dipole interactions and dispersion forces. Hydrogen bonds are are generally stronger than ordinary dipole-dipole and dispersion forces, but weaker than true covalent and ionic bonds.

The evidence for hydrogen bonding

Many elements form compounds with hydrogen. If you plot the boiling points of the compounds of the group 14 elements with hydrogen, you find that the boiling points increase as you go down the group.

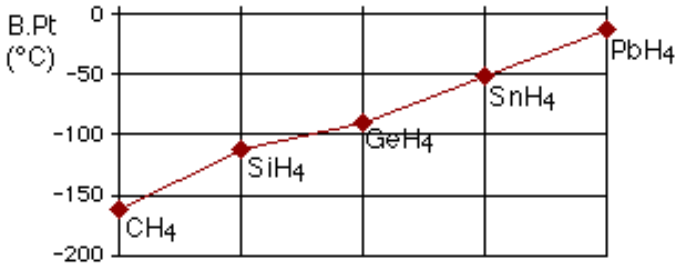


Figure 1: Boiling points of group 14 elemental halides.

The increase in boiling point happens because the molecules are getting larger with more electrons, and so van der Waals dispersion forces become greater. If you repeat this exercise with the compounds of the elements in groups 15, 16, and 17 with hydrogen, something odd happens.

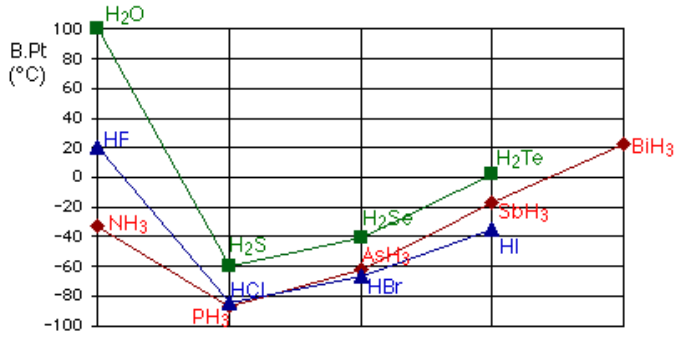


Figure 2: Boiling points of group 15-17 elemental halides.

Although the same reasoning applies for group 4 of the periodic table, the boiling point of the compound of hydrogen with the first element in each group is abnormally high. In the cases of NH_3, H_2O and HF there must be some additional intermolecular forces of attraction, requiring significantly more heat energy to break the IMFs. These relatively powerful intermolecular forces are described as hydrogen bonds.

Origin of Hydrogen Bonding

The molecules capable of hydrogen bonding include the following:

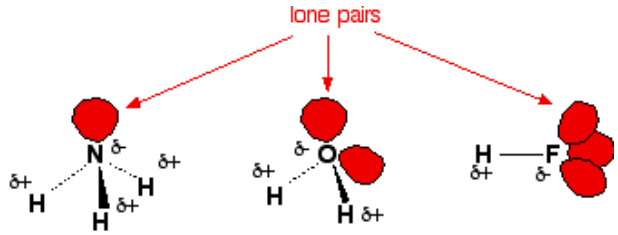


Figure 3: The lone pairs responsible for hydrogen bonding in NH_3, H_2O, and HF. The solid line represents a bond in the plane of the screen or paper. Dotted bonds are going back into the screen or paper away from you, and wedge-shaped ones are coming out towards you.

Notice that in each of these molecules:

- The hydrogen is attached directly to a highly electronegative atoms, causing the hydrogen to acquire a highly positive charge.
- Each of the highly electronegative atoms attains a high negative charge and has at least one "active" lone pair. Lone pairs at the 2-level have electrons contained in a relatively small volume of space, resulting in a high negative charge density. Lone pairs at higher levels are more diffuse and, resulting in a lower charge density and lower affinity for positive charge.

If you are not familiar with electronegativity, you should follow this link before you go on.

Consider two water molecules coming close together.

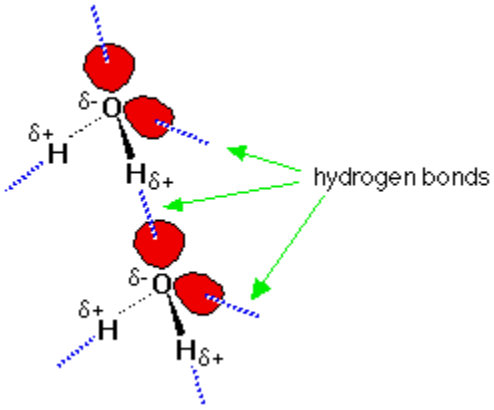


Figure 4: Hydrogen bonding in water

The δ^+ hydrogen is so strongly attracted to the lone pair that it is almost as if you were beginning to form a co-ordinate (dative covalent) bond. It doesn't go that far, but the attraction is significantly stronger than an ordinary dipole-dipole interaction. Hydrogen bonds have about a tenth of the strength of an average covalent bond, and are constantly broken and reformed in liquid water. If you liken the covalent bond between the oxygen and hydrogen to a stable marriage, the hydrogen bond has "just good friends" status.

Water is an ideal example of hydrogen bonding. Notice that each water molecule can potentially form four hydrogen bonds with surrounding water molecules: two with the hydrogen atoms and two with the with the oxygen atoms. There are exactly the right numbers of δ^+ hydrogens and lone pairs for every one of them to be involved in hydrogen bonding.

This is why the boiling point of water is higher than that of ammonia or hydrogen fluoride. In the case of ammonia, the amount of hydrogen bonding is limited by the fact that each nitrogen only has one lone pair. In a group of ammonia molecules, there are not enough lone pairs to go around to satisfy all the hydrogens. In hydrogen fluoride, the problem is a shortage of hydrogens. In water, two hydrogen bonds and two lone pairs allow formation of hydrogen bond interactions in a lattice of water molecules. Water is thus considered an ideal hydrogen bonded system.

More complex examples of hydrogen bonding

The hydration of negative ions

When an ionic substance dissolves in water, water molecules cluster around the separated ions. This process is called hydration.

Water frequently attaches to positive ions by co-ordinate (dative covalent) bonds. It bonds to negative ions using hydrogen bonds.

> If you are interested in the bonding in hydrated positive ions, you could follow this link to co-ordinate (dative covalent) bonding.

The diagram shows the potential hydrogen bonds formed with a chloride ion, Cl-. Although the lone pairs in the chloride ion are at the 3-level and would not normally be active enough to form hydrogen bonds, they are made more attractive by the full negative charge on the chlorine in this case.

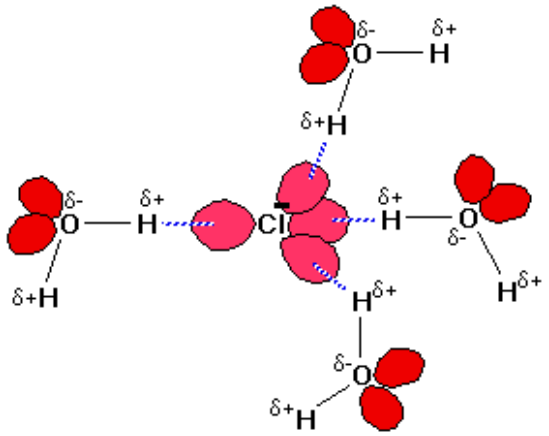


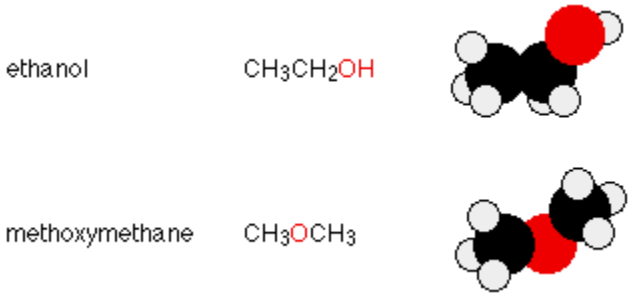
Figure 5: Hydrogen bonding between chloride ions and water.

However complicated the negative ion, there will always be lone pairs that the hydrogen atoms from the water molecules can hydrogen bond to.

Hydrogen bonding in alcohols

An alcohol is an organic molecule containing an -OH group. Any molecule which has a hydrogen atom attached directly to an oxygen or a nitrogen is capable of hydrogen bonding. Hydrogen bonds also occur when hydrogen is bonded to fluorine, but the HF group does not appear in other molecules. Molecules with hydrogen bonds will always have higher boiling points than similarly sized molecules which don't have an -O-H or an -N-H group. The hydrogen bonding makes the molecules "stickier," such that more heat (energy) is required to separate them. This phenomenon can be used to analyze boiling point of different molecules, defined as the temperature at which a phase change from liquid to gas occurs.

Ethanol, $\mathrm{CH_3CH_2{-}O{-}H}$, and methoxymethane, $\mathrm{CH_3{-}O{-}CH_3}$, both have the same molecular formula, $\mathrm{C_2H_6O}$.



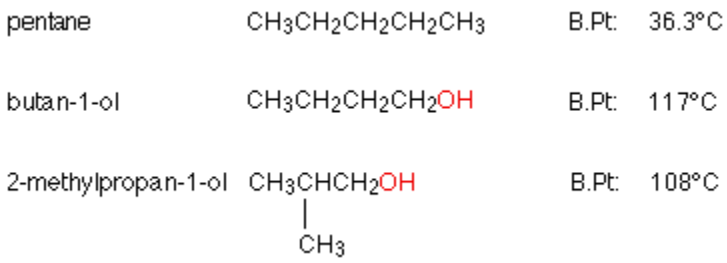
They have the same number of electrons, and a similar length. The van der Waals attractions (both dispersion forces and dipole-dipole attractions) in each will be similar. However, ethanol has a hydrogen atom attached directly to an oxygen; here the oxygen still has two lone pairs like a water molecule. Hydrogen bonding can occur between ethanol molecules, although not as effectively as in water. The hydrogen bonding is limited by the fact that there is only one hydrogen in each ethanol molecule with sufficient δ+ charge.

In methoxymethane, the lone pairs on the oxygen are still there, but the hydrogens are not sufficiently δ+ for hydrogen bonds to form. Except in some rather unusual cases, the hydrogen atom has to be attached directly to the very electronegative element

for hydrogen bonding to occur. The boiling points of ethanol and methoxymethane show the dramatic effect that the hydrogen bonding has on the stickiness of the ethanol molecules:

ethanol (with hydrogen bonding)	78.5°C
methoxymethane (without hydrogen bonding)	-24.8°C

The hydrogen bonding in the ethanol has lifted its boiling point about 100°C. It is important to realize that hydrogen bonding exists in addition to van der Waals attractions. For example, all the following molecules contain the same number of electrons, and the first two have similar chain lengths. The higher boiling point of the butan-1-ol is due to the additional hydrogen bonding.



Comparing the two alcohols (containing -OH groups), both boiling points are high because of the additional hydrogen bonding; however, the values are not the same. The boiling point of the 2-methylpropan-1-ol isn't as high as the butan-1-ol because the branching in the molecule makes the van der Waals attractions less effective than in the longer butan-1-ol.

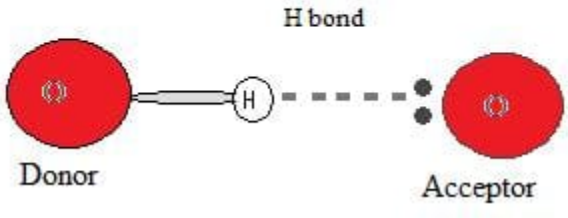
Hydrogen bonding in organic molecules containing nitrogen

Hydrogen bonding also occurs in organic molecules containing N-H groups; recall the hydrogen bonds that occur with ammonia. Examples range from simple molecules like CH_3NH_2 (methylamine) to large molecules like proteins and DNA. The two strands of the famous double helix in DNA are held together by hydrogen bonds between hydrogen atoms attached to nitrogen on one strand, and lone pairs on another nitrogen or an oxygen on the other one.

Donors and Acceptors

In order for a hydrogen bond to occur there must be both a hydrogen donor and an acceptor present. The donor in a hydrogen bond is usually a strongly electronegative atom such as N, O, or F that is covalently bonded to a hydrogen bond.

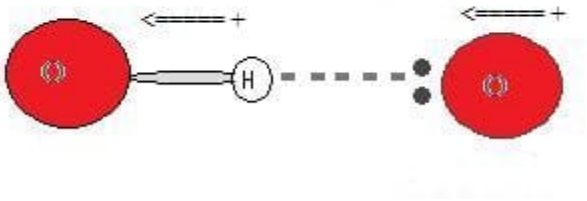
The hydrogen acceptor is an electronegative atom of a neighboring molecule or ion that contains a lone pair that participates in the hydrogen bond.



Why does a hydrogen bond occur?

Since the hydrogen donor (N, O, or F) is strongly electronegative, it pulls the covalently bonded electron pair closer to its nucleus, and away from the hydrogen atom. The hydrogen atom is then left with a partial positive charge, creating a dipole-dipole

attraction between the hydrogen atom bonded to the donor and the lone electron pair of the acceptor. This results in a hydrogen bond.(see Interactions Between Molecules With Permanent Dipoles)

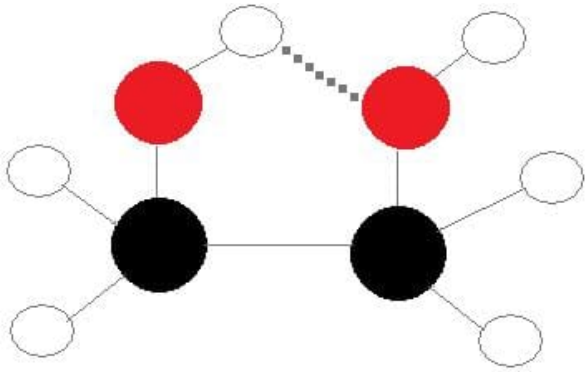


Types of hydrogen bonds

Although hydrogen bonds are well-known as a type of IMF, these bonds can also occur within a single molecule, between two identical molecules, or between two dissimilar molecules.

Intramolecular hydrogen bonds

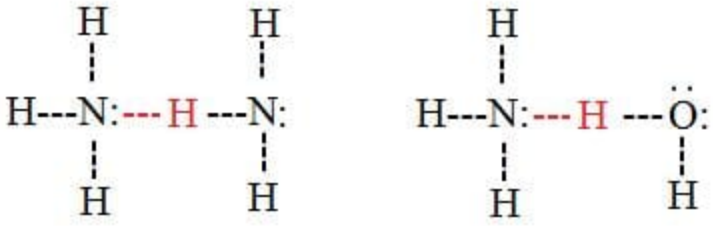
Intramolecular hydrogen bonds are those which occur *within* one single molecule. This occurs when two functional groups of a molecule can form hydrogen bonds with each other. In order for this to happen, both a hydrogen donor a hydrogen acceptor must be present within one molecule, and they must be within close proximity of each other in the molecule. For example, intramolecular hydrogen bonding occurs in ethylene glycol ($C_2H_4(OH)_2$) between its two hydroxyl groups due to the molecular geometry.



Intramolecular h-bonding in Ethylene Glycol molecule

Intermolecular hydrogen bonds

Intermolecular hydrogen bonds occur *between* separate molecules in a substance. They can occur between any number of like or unlike molecules as long as hydrogen donors and acceptors are present in positions where they can interact with one another. For example, intermolecular hydrogen bonds can occur between NH_3 molecules alone, between H_2O molecules alone, or between NH_3 and H_2O molecules.



Properties and effects of hydrogen bonds

On Boiling Point

When we consider the boiling points of molecules, we usually expect molecules with larger molar masses to have higher normal boiling points than molecules with smaller molar masses. This, without taking hydrogen bonds into account, is due to greater dispersion forces (see Interactions Between Nonpolar Molecules). Larger molecules have more space for electron distribution and thus more possibilities for an instantaneous dipole moment. However, when we consider the table below, we see that this is not always the case.

Compound	Molar Mass	Normal Boiling Point
H_2O	18 g/mol	373 K
HF	20 g/mol	292.5 K
NH_3	17 g/mol	239.8 K
H_2S	34 g/mol	212.9 K
HCl	36.4 g/mol	197.9 K
PH_3	34 g/mol	185.2 K

We see that H_2O, HF, and NH_3 each have higher boiling points than the same compound formed between hydrogen and the next element moving down its respective group, indicating that the former have greater intermolecular forces. This is because H_2O, HF, and NH_3 all exhibit hydrogen bonding, whereas the others do not. Furthermore, H_2O has a smaller molar mass than HF but partakes in more hydrogen bonds per molecule, so its boiling point is higher.

On Viscosity

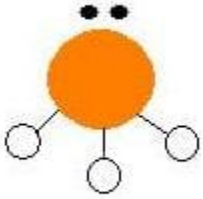
The same effect that is seen on boiling point as a result of hydrogen bonding can also be observed in the viscosity of certain substances. Substances capable of forming hydrogen bonds tend to have a higher viscosity than those that do not form hydrogen bonds. Generally, substances that have the possibility for multiple hydrogen bonds exhibit even higher viscosities.

Factors preventing Hydrogen bonding

Electronegativity

Hydrogen bonding cannot occur without significant electronegativity differences between hydrogen and the atom it is bonded to. Thus, we see molecules such as PH_3, which do not participate in hydrogen bonding. PH_3 exhibits a trigonal pyramidal molecular geometry like that of ammonia, but unlike NH_3 it cannot hydrogen bond. This is due to the similarity in the electronegativities of phosphorous and hydrogen. Both atoms have an electronegativity of 2.1, and thus, there is no dipole moment. This prevents the hydrogen atom from acquiring the partial positive charge needed to hydrogen bond with the lone electron pair in another

molecule. (see Polarizability)



Atom Size

The size of donors and acceptors can also affect the ability to hydrogen bond. This can account for the relatively low ability of Cl to form hydrogen bonds. When the radii of two atoms differ greatly or are large, their nuclei cannot achieve close proximity when they interact, resulting in a weak interaction.

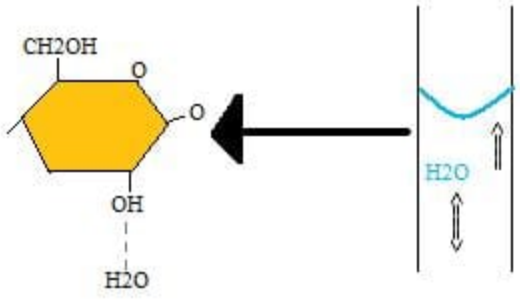


Hydrogen Bonding in Nature

Hydrogen bonding plays a crucial role in many biological processes and can account for many natural phenomena such as the Unusual properties of Water. In addition to being present in water, hydrogen bonding is also important in the water transport system of plants, secondary and tertiary protein structure, and DNA base pairing.

Plants

The cohesion-adhesion theory of transport in vascular plants uses hydrogen bonding to explain many key components of water movement through the plant's xylem and other vessels. Within a vessel, water molecules hydrogen bond not only to each other, but also to the cellulose chain that comprises the wall of plant cells. Since the vessel is relatively small, the attraction of the water to the cellulose wall creates a sort of capillary tube that allows for capillary action. This mechanism allows plants to pull water up into their roots. Furthermore, hydrogen bonding can create a long chain of water molecules, which can overcome the force of gravity and travel up to the high altitudes of leaves.



Proteins

Hydrogen bonding is present abundantly in the secondary structure of proteins, and also sparingly in tertiary conformation. The secondary structure of a protein involves interactions (mainly hydrogen bonds) between neighboring polypeptide backbones which contain nitrogen-hydrogen bonded pairs and oxygen atoms. Since both N and O are strongly electronegative, the hydrogen atoms bonded to nitrogen in one polypeptide backbone can hydrogen bond to the oxygen atoms in another chain and vice-versa. Though they are relatively weak, these bonds offer substantial stability to secondary protein structure because they repeat many times and work collectively.

In tertiary protein structure, interactions are primarily between functional R groups of a polypeptide chain; one such interaction is called a hydrophobic interaction. These interactions occur because of hydrogen bonding between water molecules around the hydrophobe that further reinforces protein conformation.

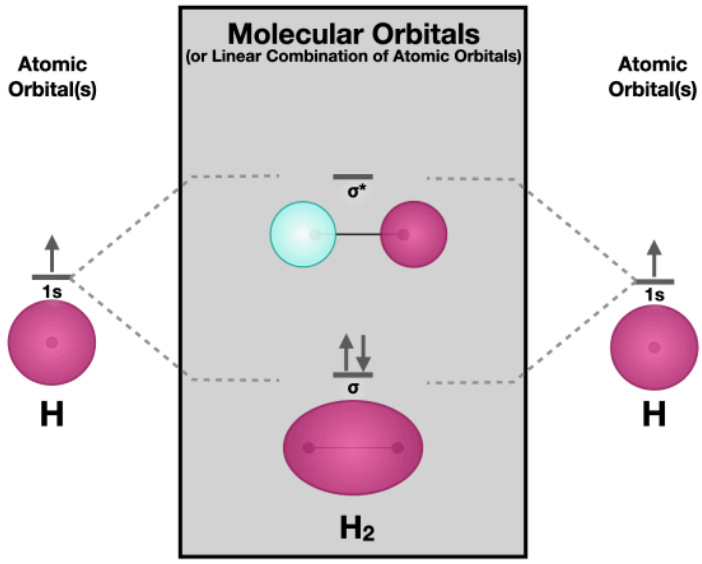
References

1. Brown, et al. Chemistry:The Central Science. 11th ed. Upper Saddle River, New Jersey: Pearson/Prentice Hall, 2008.
2. Chang, Raymond. General Chemistry:The Essential Concepts. 3rd ed. New York: Mcgraw Hill, 2003
3. Petrucci, et al. General Chemistry: Principles & Modern Applications. 9th ed. Upper Saddle River, New Jersey: Pearson/Prentice Hall, 2007.

This page titled 3.4: Hydrogen Bonding is shared under a license and was authored, remixed, and/or curated by LibreTexts.

- Hydrogen Bonding by Jim Clark, Jose Pietri is licensed CC BY-NC-SA 4.0.

4: MOLECULAR ORBITALS



Molecular Orbital Theory

Molecular Orbital (MO) Theory is a sophisticated bonding model. It is generally considered to be more powerful than *Lewis* and *Valence Bond Theories* for predicting molecular properties, however this power comes at the price of complexity. In its full development, MO Theory requires complex mathematics, though the ideas behind it are simple. Atomic orbitals (AOs) that are localized on individual atoms combine to make molecular orbitals (MOs) that are distributed over the molecule. The simplest example is the molecule, dihydrogen (H_2), in which two independent hydrogen 1s orbitals combine to form the sigma bonding and antibonding orbitals of the dihydrogen molecule (see figure). The MO's are also called Linear Combinations of Atomic Orbitals (LCAO).

4.1: Formation of Molecular Orbitals from Atomic Orbitals

4.1.1: Molecular Orbitals from s Orbitals

4.1.2: Molecular Orbitals from p Orbitals

4.1.3: Molecular orbitals from d orbitals

4.1.4: Nonbonding Orbitals and Other Factors

4.2: Homonuclear Diatomic Molecules

4.2.1: Molecular Orbitals

4.2.2: Orbital Mixing

4.2.3: Diatomic Molecules of the First and Second Periods

4.2.4: Photoelectron Spectroscopy

4.3: Heteronuclear Diatomic Molecules

4.3.1: Polar bonds

4.3.2: Ionic Compounds and Molecular Orbitals

4.P: Problems

This page titled 4: Molecular Orbitals is shared under a CC BY-NC-SA 4.0 license and was authored, remixed, and/or curated by Kathryn Haas.

- 5: Molecular Orbitals by Kathryn Haas is licensed CC BY-SA 4.0.

4.1: FORMATION OF MOLECULAR ORBITALS FROM ATOMIC ORBITALS

Molecular orbital theory extends from quantum theory and the atomic orbital wavefunctions (ψ) described by the Schrödinger equation. While the Schrödinger equation defines a Ψ for electrons in individual atoms, we can approximate the molecular wavefunction (what Ψ would look like if we combined the ψ of individual atoms). The addition or subtraction of wavefunctions is termed **linear combination of atomic orbitals** (LCAO). Molecular orbital theory is applied to LCAO to describe bonding.

The LCAO for the wavefunction of two atoms (ψ_a and ψ_b) is represented by the general expression below. The coefficients c_a and c_b quantify the contribution of each atomic ψ to the molecular Ψ.

$$\Psi = c_a\psi_a + c_b\psi_b$$

For two atomic ψs to form a bond, three conditions must be satisfied:

- First, the **distance between the atoms** must be small enough to provide good overlap. This is because the two orbitals must be able to overlap using regions of ψ^2 where the probability of finding electrons is significant. If atoms are not close enough, ψ_a and ψ_b cannot interact productively. At the same time, the atoms must be far enough apart that their nuclei do not repel each other.
- The **symmetry of the orbitals** must be compatible such that regions of ψ_a and ψ_b with the same sign constructively interfere more than regions with opposite sign destructively interfere. In other words, for a productive interaction, there must be a relatively high probability of finding an electron between the two nuclei, and this depends on the symmetry (and sign of the ψ) of the atomic orbitals.
- Third, the **energies of the atomic orbitals** must be similar. Orbitals with similar energy combine to make the most stable bonding molecular orbitals. Atomic orbitals with very different energies form less stable bonding interactions, and the larger the difference in the atomic orbitals, the weaker the bonding interaction will be.

Atomic orbitals combine to form molecular orbitals when these three conditions are met. The result is a set of bonding molecular orbitals that are lower in energy than the original atomic orbital energies.

4.1.1: Molecular Orbitals from s Orbitals

4.1.2: Molecular Orbitals from p Orbitals

4.1.3: Molecular orbitals from d orbitals

4.1.4: Nonbonding Orbitals and Other Factors

This page titled 4.1: Formation of Molecular Orbitals from Atomic Orbitals is shared under a CC BY-NC-SA 4.0 license and was authored, remixed, and/or curated by Kathryn Haas.

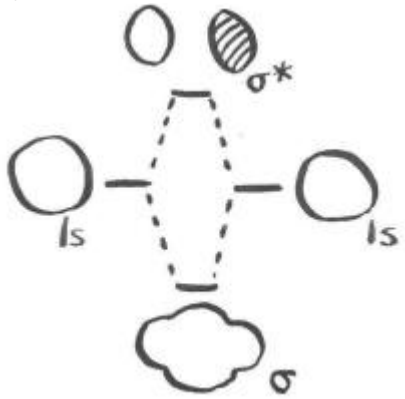
- 5.1: Formation of Molecular Orbitals from Atomic Orbitals by Kathryn Haas is licensed CC BY-SA 4.0.

4.1.1: Molecular Orbitals from s Orbitals

In the case of the hydrogen molecule, we took two atomic orbitals and combined them to form two molecular orbitals. These new molecular orbitals had different wavelengths than the two atomic orbitals: one had a longer wavelength and was a little lower in energy, while the other had a shorter wavelength and was a little higher in energy. If we take into account the energy of the two original atomic wavefunctions, and compare them to the total energy of the two new molecular wavefunctions, there is no change overall.

We started with two atomic orbitals, and by combining them we produced two molecular orbitals. Both of these ideas are useful in considering the formation of more complex molecules from individual atoms.

- ◦ The average energy of the orbitals has remained almost constant.
  ◦ Also, the number of wavefunctions has remained constant.



◦

Of course, from the point of view of the two real electrons, some remarkable changes have occurred. Both of these electrons have adopted a longer wavelength and a lower energy and that has made all the difference. There is an occupied molecular orbital and an unoccupied molecular orbital; only the occupied orbital makes a real energetic contribution to the overall stability of the molecule. The unoccupied orbital is completely imaginary.

A bonding picture of He_2 would look exactly the same, because it would also involve the overlap of 1s electrons on one atom with 1s electrons on the other atom. There would be a different electronic energy, however. That difference would affect the prospects of helium-helium bond formation.

- The electrons have lower kinetic energy in the bond than they had before bonding.
- Electronic energy has decreased. A stable bond has formed.

Exercise 4.1.1.1

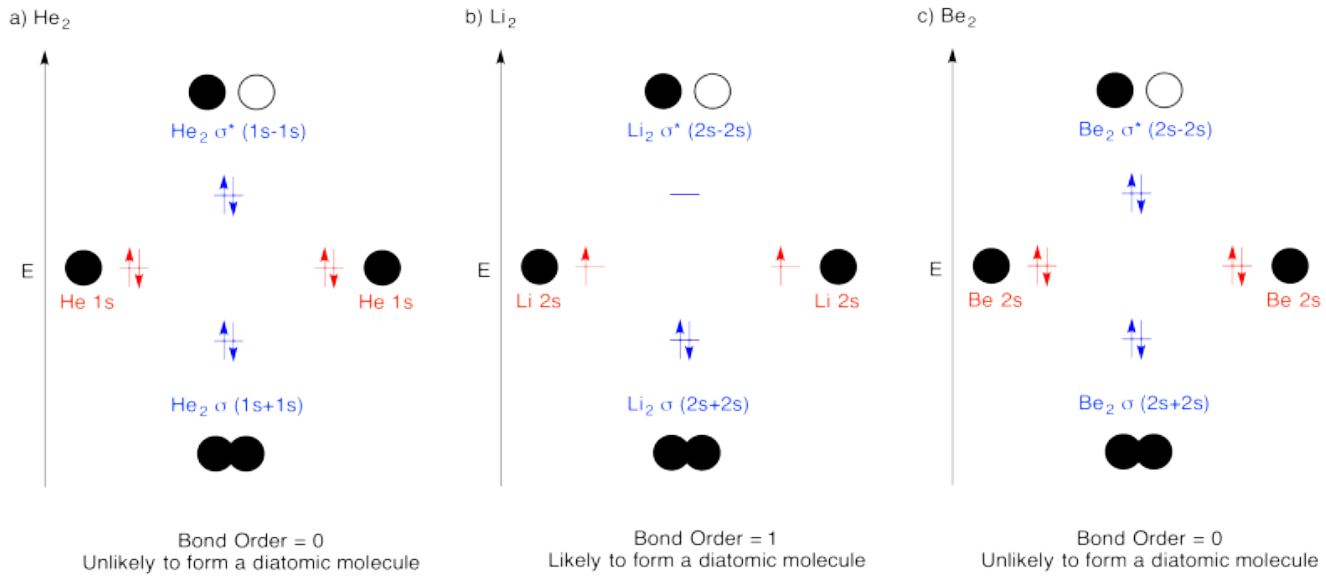
Construct molecular orbital diagrams for the following diatomic species and discuss the likelihood of bond formation in each case.

a. He_2.
b. Li_2.
c. Be_2.

Answer available at the end of this section.

Answers

Exercise 4.1.1.1



This page titled 4.1.1: Molecular Orbitals from s Orbitals is shared under a CC BY-NC-SA 4.0 license and was authored, remixed, and/or curated by Chris Schaller.

4.1.2: Molecular Orbitals from p Orbitals

Bonding with P-orbitals

Sigma bonding with p-orbitals

Other diatomic molecules in the upper right corner of the periodic table can be constructed in a similar way. Look at dinitrogen, N_2.

We can think about how dinitrogen would form if two nitrogen atoms were placed close enough together to share electrons. Nitrogen has more electrons than hydrogen, so this interaction is more complicated.

In our qualitative examination of bonding in main group diatomics, we will take the approach used in Lewis structures and just look at the valence electrons. A quantitative molecular orbital calculation with a computer would not take this shortcut, but would include all of the electrons in the atoms that are bonding together.

Nitrogen has five valence electrons, and these electrons are found in the 2s and 2p levels. There are three possible atomic orbitals in the 2p level where some of these electrons could be found: p_x, p_y and p_z. We need to look at the interaction between the s and p_x, p_y and p_z orbitals on one nitrogen atom with the s and p_x, p_y and p_z orbitals on the other nitrogen. That process could be extremely complicated, but:

- Orbital interactions are governed by symmetry.

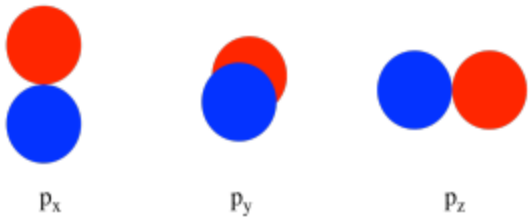
Orbitals interact most easily with other orbitals that have the same element of symmetry. For now, we can simplify and say that orbitals on one atom only interact with the same type of orbitals on the other atom.

- s orbitals interact with s orbitals. We can already see how that will work out in dinitrogen, because that is what happened in dihydrogen.
- p_x orbitals interact with p_x orbitals.
- p_y orbitals interact with p_y orbitals.
- p_z orbitals interact with p_z orbitals.

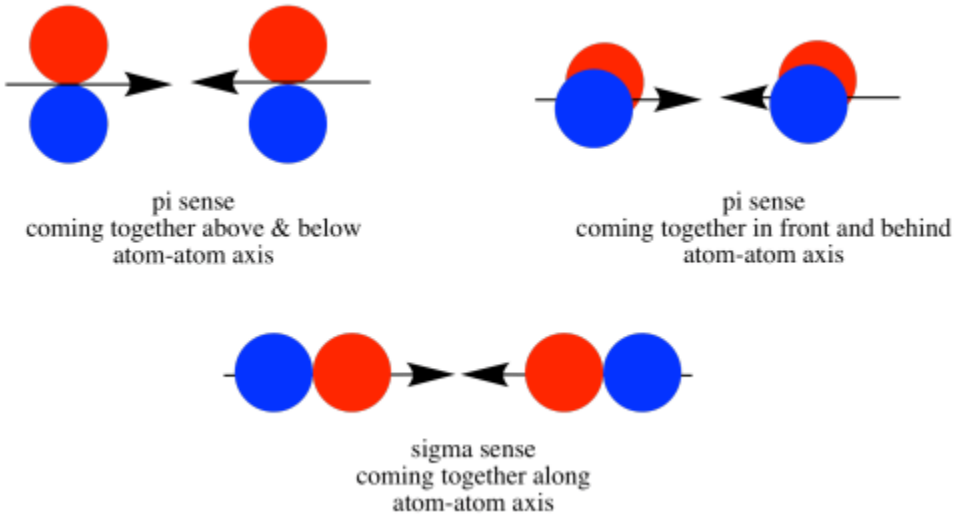
Another complication here is that the s and p orbitals do not start out at the same energy level. When the orbitals mix, one combination goes up in energy and one goes down. Does the s antibonding combination go higher in energy than the combinations from p orbitals? Do the p bonding combinations go lower in energy than the combinations from s orbitals? We will **simplify** and **assume** that the s and p levels remain completely separate from each other. This is not always true, but the situation varies depending on what atoms we are dealing with.

- The combination of one s orbital with another is just like in hydrogen. Two original orbitals will combine and rearrange to produce two new orbitals.
- There is a bonding combination in which the orbitals are in phase. The new orbital produced has a longer wavelength than the original orbital. It is lower in energy.
- There is an antibonding combination in which the orbitals are out of phase. The new orbital produced has a shorter wavelength than the original orbital. It is higher in energy.

In considering the interaction of two p orbitals, we have to keep in mind that p orbitals are directional. A p orbital lies along a particular axis: x, y or z. The three p orbitals on nitrogen are all mutually perpendicular (or orthogonal) to each other. That situation is in contrast to s orbitals, which are spherical and thus look the same from any direction.

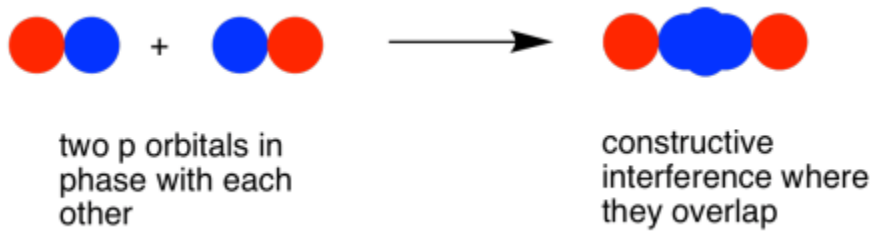


We first need to define one axis as lying along the N-N bond. It does not really matter which one. We arbitrarily say the N-N bond lies along the z axis. The p_z orbitals have a different spatial relationship to each other compared to the p_y and p_x. The p_z orbitals lie along the bond axis, whereas the p_y and p_x are orthogonal to it.

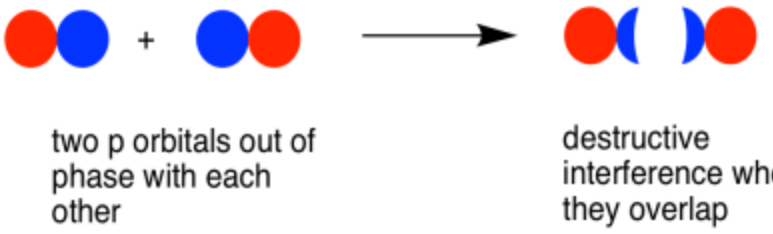


As the nitrogen atoms are brought together, one lobe on one p_z orbital overlaps strongly with one lobe on the other p_z orbital. The other lobes point away from each other and do not interact in any obvious way.

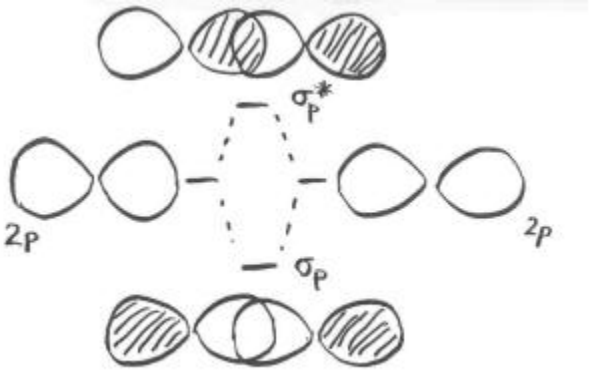
As with the s orbital, the p_z orbitals can be in-phase or out-of-phase. The in-phase combination results in constructive interference. (Here, "in-phase" means the lobes that overlap are in-phase; for that to happen the two p orbitals are actually completely out-of-phase with each other mathematically, so that one orbital is the mirror image of the other.) This combination is at a longer wavelength than the original orbital. It is a lower energy combination.



The out-of-phase combination (meaning in this case that the overlapping lobes are out-of-phase) results in destructive interference. This combination is at shorter wavelength than the original orbital. It is a higher energy combination.



As a result, we have two different combinations stemming from two different p orbitals coming together in two different ways. We get a low-energy, in-phase, bonding combination and a high-energy, out-of-phase, antibonding combination.



What about those other p orbitals, the ones that do not lie along the bond axis? We'll take a look at that problem on the next page.

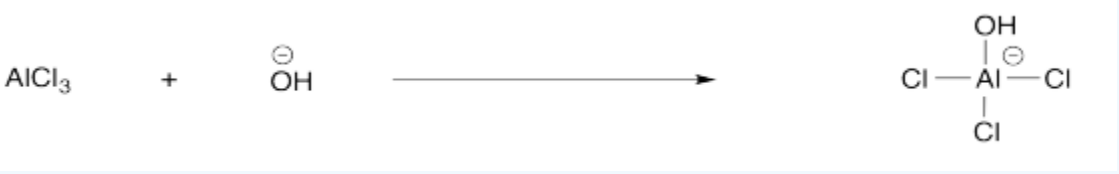
Exercise 4.1.2.2

Draw an MO cartoon of a sigma bonding orbital formed by the overlap of two p orbitals between two oxygen atoms. Label the positions of the oxygen nuclei with the symbol "O". Label the O-O bond axis.

Answer available at the end of this section.

Exercise 4.1.2.3

Chemical reactions can be described by MO diagrams too! Consider the following reaction in which a new sigma bond is formed.



Draw an MO diagram for the reaction above. In other words, start from the one frontier MO on each reactant to build the MO's of the new sigma bond in the product.

- Draw the orbital from the base (hydroxide) that is likely to donate its electrons.
- Draw the orbital from the acid (aluminum chloride) that is likely to accept electrons.
- Complete the MO mixing diagram of these two orbitals:

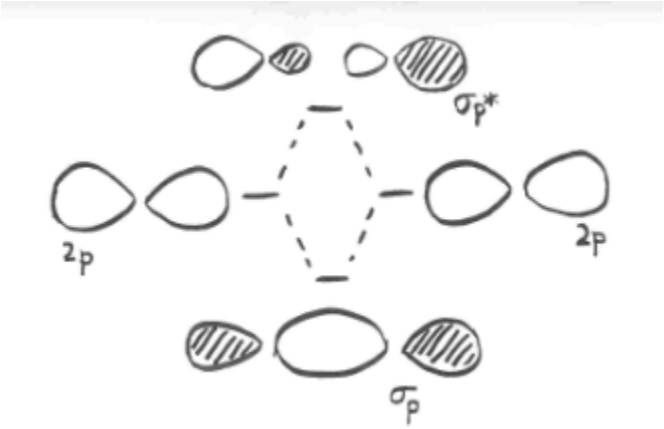
- Label the electron donating orbital
- Label the electron accepting orbital
- Populate the MO mixing diagram with electrons

o Draw a cartoon showing each reactant and product MO that contributes to the bonding interaction.

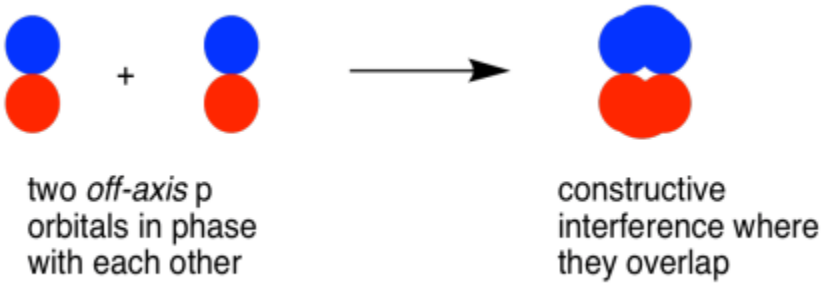
Answer available at the end of this section.

Pi-bonding with p-orbitals

Earlier, we saw that p orbitals that lie along the same axis can interact to form bonds.



Parallel, but not collinear, p orbitals can also interact with each other. They would approach each other side by side, above and below the bond axis between the two atoms. They can be close enough to each other to overlap, although they do not overlap as strongly as orbitals lying along the bond axis. They can make an in-phase combination, as shown below.

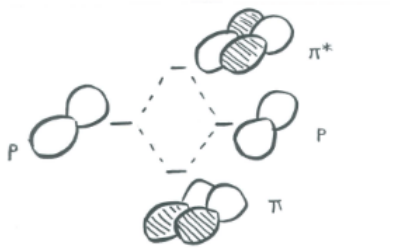


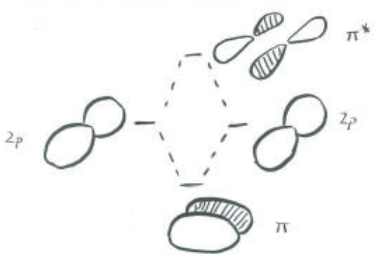
They could also make an out-of-phase combination, as shown below.



- parallel p orbitals can overlap to produce bonding and antibonding combinations.
- the resulting orbitals contain nodes along the bond axis.
- the electron density is found above and below the bond axis.
- this is called a p (pi) bond.

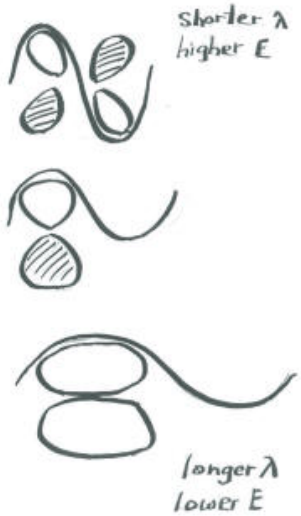
The illustration above is for one set of p orbitals that are orthogonal to the bond axis. The second picture shows the result of the constructive (or destructive) interference. A similar picture could be shown for the other set of p orbitals.



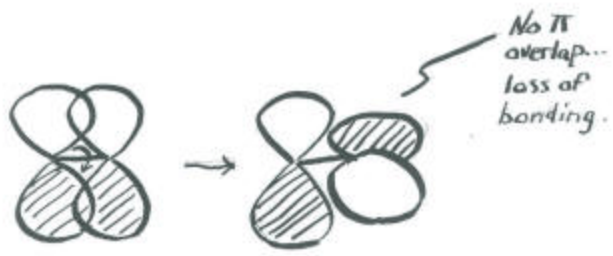


In a main group diatomic species like dinitrogen, one p orbital lying along the bond axis can engage in s bonding. The two p orbitals orthogonal to the bond axis can engage in p bonding. There will be both bonding and antibonding combinations.

Just as the sigma-bonding orbitals display progressively shorter wavelengths along the bonding axis as they go to higher energy, so do the pi bonding orbitals. In other words, there are more nodes in the higher-energy orbitals than in the lower-energy ones.



An important consequence of the spatial distribution or "shape" of a p orbital is that it is not symmetric with respect to the bond axis. An s orbital is not affected when the atom at one end of the bond is rotated with respect to the other. A p orbital is affected by such a rotation. If one atom turns with respect to the other, the p orbital would have to stretch to maintain the connection. The orbitals would not be able to overlap, so the connection between the atoms would be lost.



Exercise 4.1.2.4

The combinations of _____ atomic orbitals leads to σ orbitals.

Draw pictures.

Answer available at the end of this section.

Exercise 4.1.2.5

The combinations of _____ atomic orbitals leads to π orbitals.

Draw pictures.

Answer available at the end of this section.

Exercise 4.1.2.6

Which molecular orbital is typically the highest in energy?
a. p
b. σ
c. π*
d. π
e. σ*

Answer available at the end of this section.

Exercise 4.1.2.7

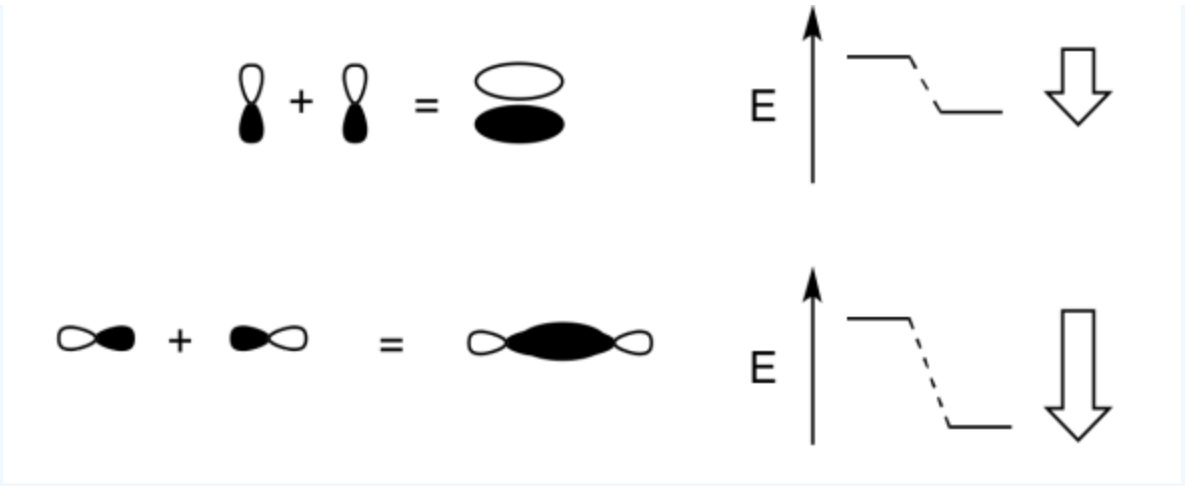
Why would a *core* 1s orbital not interact with a *valence* 2s orbital?

Hint: Why is a Li_2O bond stronger than a K_2O bond?

Answer available at the end of this section.

Exercise 4.1.2.8

Add a few words to explain the ideas conveyed in these drawings.



Answer available at the end of this section.

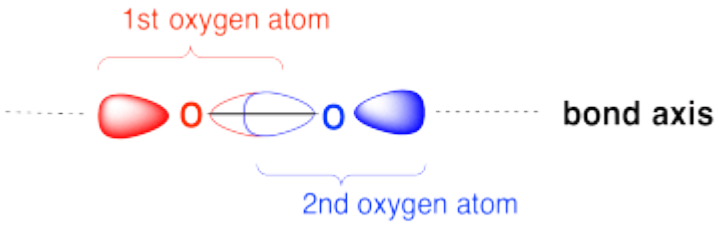
Attribution

Chris P Schaller, Ph.D., (College of Saint Benedict / Saint John's University)

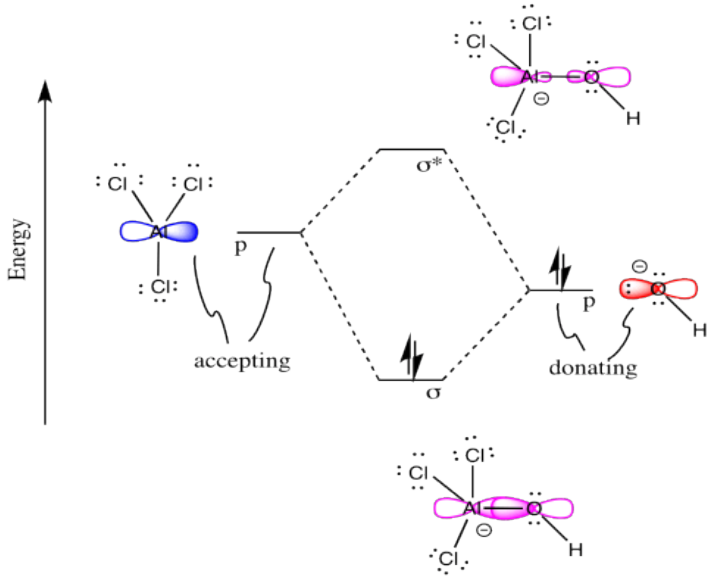
Curated or created by Kathryn Haas

Answers

Exercise 4.1.2.2

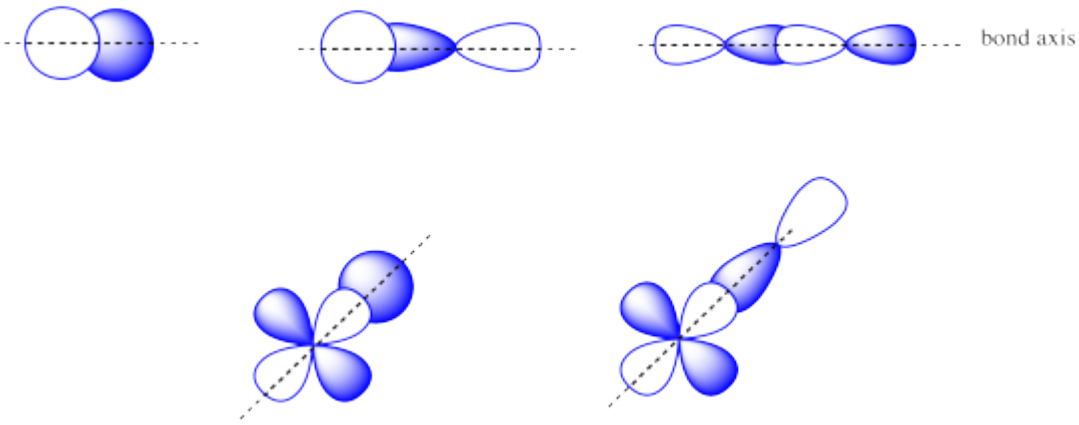


Exercise 4.1.2.3



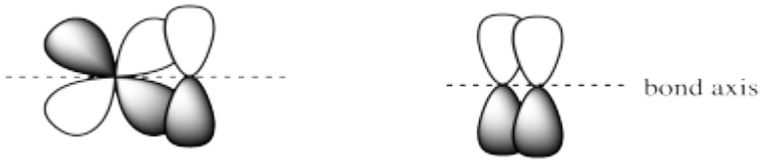
Exercise 4.1.2.4

The combinations of ***s* + *s*** OR ***s* + *p*** OR ***p* + *p*** OR ***s* + *d*** OR ***p* + *d*** atomic orbitals can lead to σ orbitals.



Exercise 4.1.2.5

The combinations of side by side p + p or p + d atomic orbitals leads to π orbitals.



Exercise 4.1.2.6

e) σ*

Exercise 4.1.2.7

Li^+ and O^{2-} are more similar in size than K^+ and O^{2-}, so the bond between Li^+ and O^{2-} is stronger.

The energy difference between any core orbitals and valence orbitals is too large, so they cannot interact. In order for orbitals to interact, the orbitals need to have the same symmetry, be in the same plane, and be similar in energy.

Exercise 4.1.2.8

When two parallel p orbitals combine out-of-phase, destructive interference occurs.

There is a node between the atoms.

The energy of the electrons increases.

When two parallel p orbitals combine in-phase, constructive interference occurs.

There is no node between the atoms; the electrons are found above and below the axis connecting the atoms.

The energy of the electrons decreases.

This page titled 4.1.2: Molecular Orbitals from p Orbitals is shared under a CC BY-NC-SA 4.0 license and was authored, remixed, and/or curated by Chris Schaller.

- 5.1.2: Molecular Orbitals from p Orbitals by Chris Schaller is licensed CC BY-SA 3.0.

4.1.3: Molecular orbitals from d orbitals

In transition metals and other heavier elements, the d orbitals may combine with other orbitals of compatible symmetry (and energy) to form molecular orbitals. Generally, there are three types of bonding and antibonding interactions that may occur with d orbitals: sigma (σ), pi (π), and delta (δ) bonds.

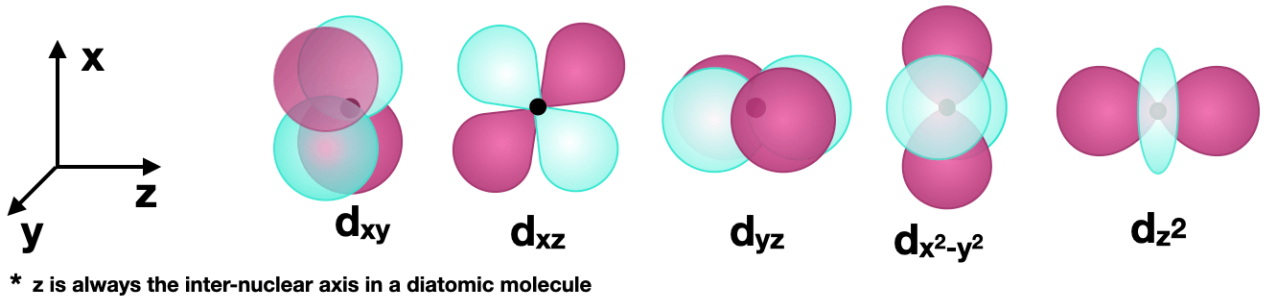


Figure 4.1.3.1: The five $3d$ orbitals are shown. The orientation of the axes is consistent and the z axis is horizontal for convenience in drawing bonding along the z axis (see examples below). (CC-BY-SA; Kathryn Haas)

Sigma (σ) bonding with d orbitals

σ bonds are symmetric with respect to the inter-nuclear axis (in a diatomic molecule, this is the z axis). An example of a σ bond formed by d orbitals is that of two d_{z^2} orbitals (see Figure 4.1.3.2). If a bonded atom is in a position other than on the z axis (in an octahedral geometry, for example), σ bonds can also form. For example, two $d_{x^2-y^2}$ orbitals on atoms bonded along the x or y axes could also form a σ bond.

d orbitals can also form σ bonds with other types of orbitals with the appropriate symmetry. Examples of orbitals with appropriate symmetry are the s orbital and certain p orbitals on another atom, as shown below in Figure 4.1.3.2.

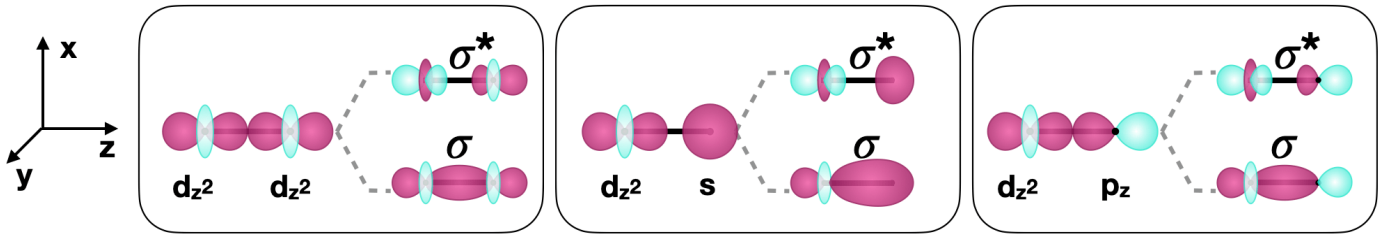


Figure 4.1.3.2: Selected examples of σ bonds involving d orbitals along the z internuclear axis (shown as a bold horizontal line) between two atoms. (CC-BY-SA; Kathryn Haas)

Pi (π) bonding with d orbitals

π bonds are those with one node that is in-plane with the internuclear axis. A π bond can form between two d orbitals or between d orbitals and other types of orbitals with comparable symmetry. An example of a π bond between two d orbitals is that formed by two d_{xz} orbitals along the z axis (shown in Figure 4.1.3.3). d orbitals can also form π bonds using p orbitals with compatible symmetry, as shown in Figure 4.1.3.3.

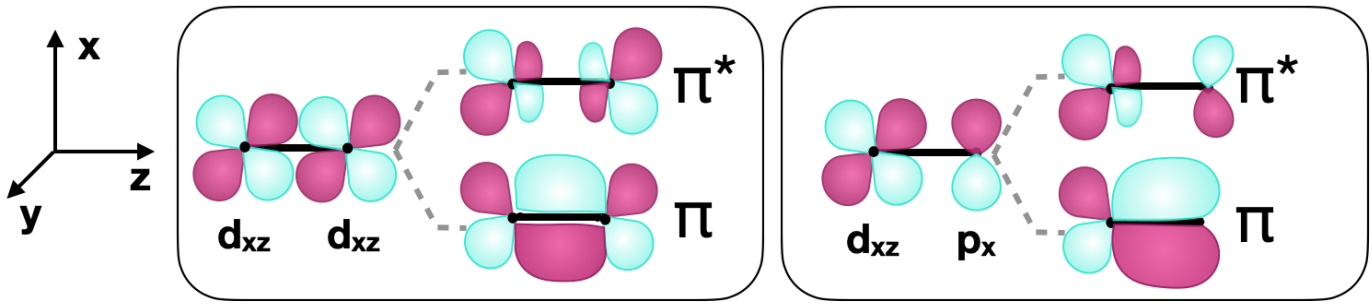


Figure 4.1.3.3: Selected examples of π bonds involving d orbitals along the z internuclear axis (shown as a bold horizontal line) between two atoms. (CC-BY-SA; Kathryn Haas)

Delta (δ) bonding with d orbitals

δ bonds are those with two nodes that are in-plane with the internuclear axis. δ bonds can form between two d orbitals with appropriate symmetry. For example, when two atoms bond along the z axis, the d_{xy} orbitals and the two $d_{x^2-y^2}$ orbitals can form δ bonds (Figure 4.1.3.4).

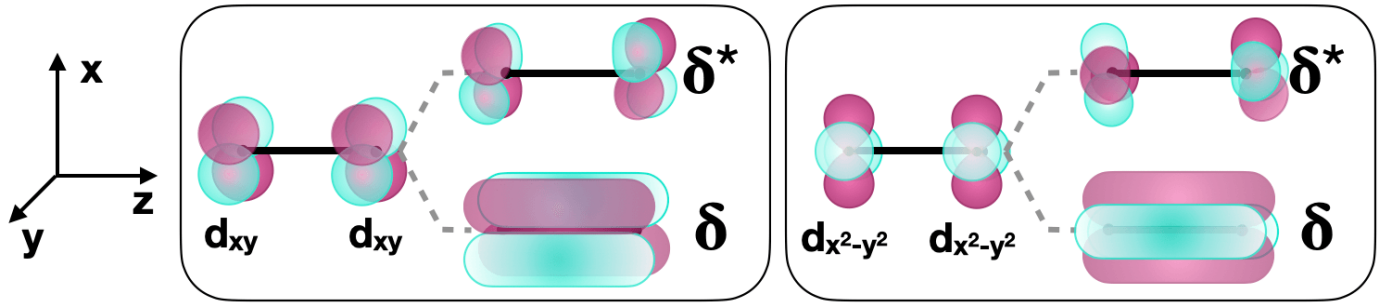


Figure 4.1.3.4: Selected examples of δ bonds involving d orbitals along the z internuclear axis (shown in bold horizontal line) between two atoms. (CC-BY-SA; Kathryn Haas)

Incompatible orbitals

In the descriptions above, we focused on how bonds (and antibonds) can be formed with d orbitals. All bonding and non-bonding interactions require that orbitals have compatible symmetry to form productive interactions. It is worth mentioning that orbitals with symmetry that is incompatible with the d orbitals will not have bonding or antibonding interactions with d orbitals. The figure below shows several sets of orbitals that are incompatible for bonding.

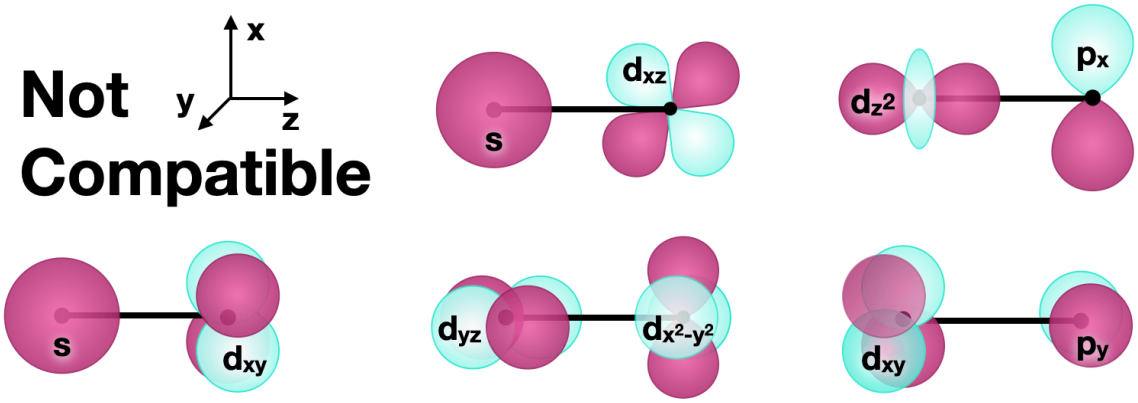


Figure 4.1.3.5: Several incompatible pairs of orbitals. (CC-BY-SA; Kathryn Haas)

Curated or created by Kathryn Haas

This page titled 4.1.3: Molecular orbitals from d orbitals is shared under a CC BY-NC-SA 4.0 license and was authored, remixed, and/or curated by Kathryn Haas.

- 5.1.3: Molecular orbitals from d orbitals by Kathryn Haas is licensed CC BY-SA 4.0.

4.1.4: Nonbonding Orbitals and Other Factors

The simplest case is when there is an even number of atomic orbitals that all combine to form strong bonding and antibonding orbitals. But what if there is an uneven number of atomic orbitals? Or what if there are some orbitals that don't meet the criteria for bonding? Or what if the bonding interactions are weak? In these cases, there will be molecular orbitals on the molecule that have non-bonding character.

It is important to note that the bonding, non-bonding, and antibonding nature of orbitals exist on a spectrum. Some bonding and anti-bonding orbitals may have some non-bonding character depending on where their energies lie with respect to the original atomic orbital energies. When molecular orbitals have energies similar to their original atomic orbitals, they will have some non-bonding character. The closer the energies of atomic and molecular orbitals, the more non-bonding the molecular orbitals.

Two major factors to consider

Uneven number of atomic orbitals: In the case that there is an uneven number of atomic orbitals with compatible symmetry, orbitals with non-bonding character will form. For example, in the case where three atomic orbitals combine, the most common result is formation of a low-energy bonding orbital, a high energy antibonding orbital, and a non-bonding orbital of intermediate energy (Figure 4.1.4.1).

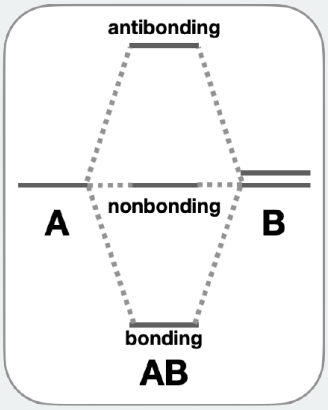


Figure 4.1.4.1. This figure illustrates the most common case for three atomic orbitals that combine to form three molecular orbitals; formation of one low-energy bonding, one high-energy antibonding, and one intermediate energy non-bonding molecular orbital. (CC-BY-NC-SA, Kathryn Haas)

Differences in energy: Combination of orbitals with different energies may lead to orbitals with non-bonding character. Atomic orbitals that have similar energies will have the strongest interactions, and result in bonding molecular orbitals with much lower energies than the component atomic orbitals. On the other hand, atomic orbitals with very unequal energies have a weaker interaction because the molecular orbitals are closer in energy to the atomic orbital energies, thus there is less energy benefit to putting electrons in the bonding molecular orbitals (Figure 4.1.4.2). When bonding or antibonding orbitals are close to the energies of the contributing atomic orbitals, those molecular orbitals may have some non-bonding character.

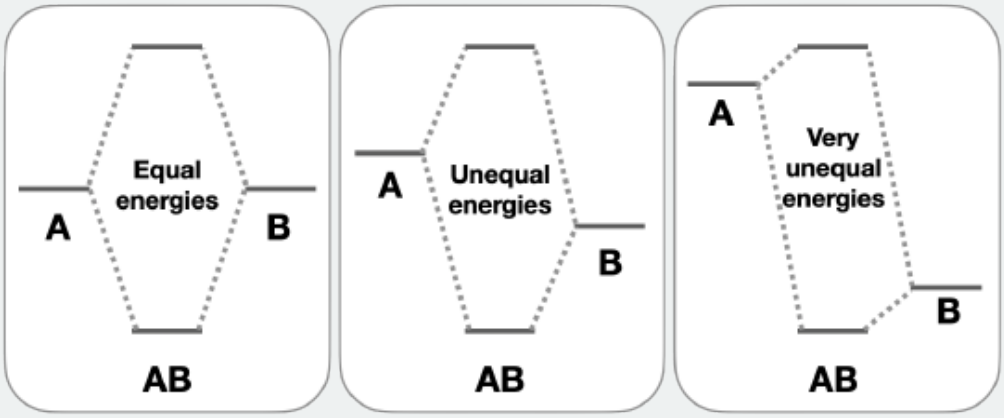


Figure 4.1.4.2. This figure illustrates how relative energies of atomic orbitals result in molecular orbitals that are more or less favorable. The greater the energy difference between atomic orbitals and the bonding molecular orbital, the more eneretically favorable it is for bonding to occur. (CC-BY-NC-SA, Kathryn Haas)

This page titled 4.1.4: Nonbonding Orbitals and Other Factors is shared under a CC BY-NC-SA 4.0 license and was authored, remixed, and/or curated by Kathryn Haas.

- 5.1.4: Nonbonding Orbitals and Other Factors by Kathryn Haas is licensed CC BY-SA 4.0.

4.2: HOMONUCLEAR DIATOMIC MOLECULES

In this section you will be introduced to the molecular orbital diagrams of several homonuclear diatomic molecules. Homonuclear diatomic molecules are molecules made of exactly two identical atoms, and they are relatively simple.

4.2.1: Molecular Orbitals

4.2.2: Orbital Mixing

4.2.3: Diatomic Molecules of the First and Second Periods

4.2.4: Photoelectron Spectroscopy

This page titled 4.2: Homonuclear Diatomic Molecules is shared under a CC BY-NC-SA 4.0 license and was authored, remixed, and/or curated by Kathryn Haas.

- 5.2: Homonuclear Diatomic Molecules by Kathryn Haas is licensed CC BY-SA 4.0.

4.2.1: Molecular Orbitals

There are several cases where our more elementary models of bonding (like Lewis Theory and Valence Bond Theory) fail to predict the actual molecular properties and reactivity. A classic example is the case of O_2 and its magnetic properties. At very cold temperatures, O_2 is attracted to a magnetic field, and thus it must be paramagnetic (unpaired electrons give rise to magnetism). Watch the video below!

YouTube Video

This interactive element is not available in this format. Visit the link or scan the QR code to access it online.

View this YouTube Video online

The magnetic properties of O_2 are easily rationalized by its **molecular orbital diagram**. A molecular orbital diagram is a diagram that shows the relative energies and identities of each molecular orbital in a molecule. Figure $4.2.1.1$ shows a simplified and generic molecular orbital diagram for a second-row homonuclear diatomic molecule. The diagram is simplified in that it assumes that interactions are limited to degenerate orbitals from two atoms (see next section).

There are some things you should note as you inspect Figure $4.2.1.1$ (and keep these in mind as you draw your own diagrams!). First, notice that there are the **same number of molecular orbitals as there are atomic orbitals**. Second, notice that **each orbital in the diagram is rigorously labeled** using labels (σ and π) that include the subscripts u and g. These labels and subscripts indicate the symmetry of the orbitals. The σ symbol indicates that the orbital is symmetric with respect to the internuclear axis, while the π label indicates that there is one node along that axis. The g and u stand for *gerade* and *ungerade*, the German words for *even* and *uneven*, respectively. The subscript g is given to orbitals that are *even*, or *symmetric*, with respect to an inversion center. The subscript u is given to orbitals that are *uneven*, or *antisymetric*, with respect to an inversion center. The pictures of calculated molecular orbitals are shown in Figure $4.2.1.1$ to illustrate the symmetry of each orbital.

Another important thing to notice is that the diagram in Figure $4.2.1.1$ lacks electrons (because it is generic for any second-row diatomic molecule). If this were a *complete* molecular orbital diagram it would **include the electrons for each atom and for the molecule**. Electrons in molecular orbitals are filled in the same way an atomic orbital diagram would be filled, where electrons occupy lower energy orbitals before higher energy orbitals, and electrons occupy empty degenerate orbitals before pairing. A complete molecular orbital diagram would show whether the molecule is diamagnetic or paramagnetic. It can also be used to calculate the bond order of the molecule (the number of bonds between atoms) using the formula below:

$$\text{Bond order } = \frac{1}{2}\left[\begin{pmatrix}\text{number of electrons}\\ \text{in bonding orbitals}\end{pmatrix} - \begin{pmatrix}\text{number of electrons}\\ \text{in antibonding orbitals}\end{pmatrix}\right]$$

In general, non-valence (core) electrons can be ignored because they contribute nothing to the bond order. In fact, many molecular orbital diagrams will ignore the core orbitals, as they are insignificant for bonding interactions and reactivity.

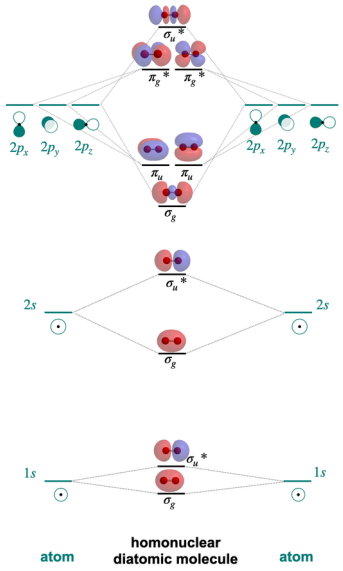


Figure 4.2.1.1: A generic molecular orbital diagram for a homonuclear diatomic molecule of second-row elements assuming no orbital mixing (interactions are formed by orbitals of the same energy from each atom). (CC-BY-NC-SA, Kathryn Haas)

Now, to see how this molecular orbital diagram can explain the magnetic behaviour of O_2, complete the example below.

Example 4.2.1.1

Let's change Figure 4.2.1.1 to make it specific for O_2. Re-draw the MO diagram (no need to draw the shapes of orbitals). Fill in the correct number of electrons for each oxygen atom on either side of the diagram. Then, fill in the total molecular electrons in the center. Calculate the bond order and determine whether it is diamagnetic or paramagnetic.

Solution

The diagram in Figure 4.2.1.1 includes core orbitals (the 1s) and valence electrons (2s, 2p). Therefore, we will consider all the electrons in an oxygen atom and a dioxygen molecule. An oxygen atom has eight total electrons. So we fill eight electrons into the atomic orbitals for the oxygen atom on the right, and eight electrons into the atomic orbitals for oxygen on the left. The total number of electrons for the molecule is sixteen, so fill in 16 electrons into the molecular orbitals, being sure to apply Hund's rule and the Aufbau principle. The result is a diagram that looks like the one drawn below in Figure 4.2.1.2.

The bond order is calculated using the molecular orbitals (we can ignore atomic orbitals). There are 10 electrons in binding orbitals and 6 electrons in antibonding orbitals). This gives a bond order of $\frac{1}{2}(10-6)=2$. This bond order is consistent with valence bond theory!

This diagram indicates that dioxygen is paramagnetic; it has two unpaired electrons in the π^* orbitals. This paramagnetic electron configuration explains why dioxygen is attacted to magnetic fields!

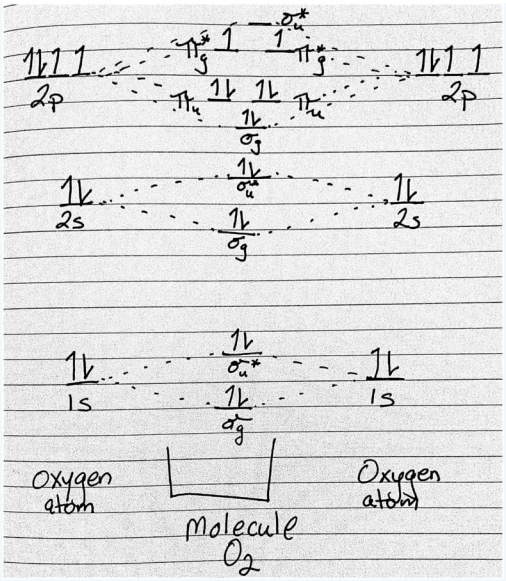


Figure 4.2.1.2: Hand-drawn molecular orbital diagram for dioxygen. (CC-BY-SA; Kathryn Haas)

Exercise 4.2.1.1

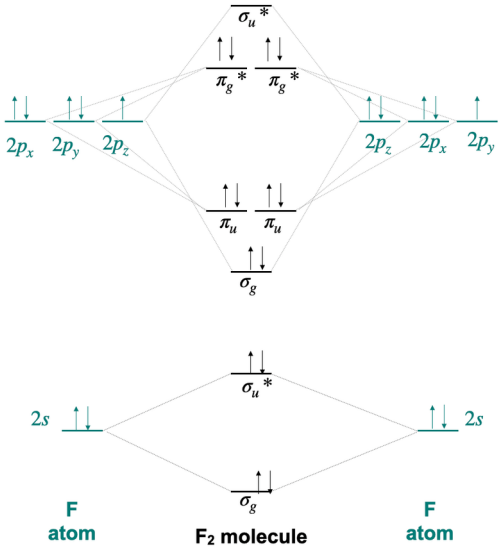
Draw the molecular orbital diagram for F_2; be sure to label your orbitals with the appropriate symmetry and count your orbitals to make sure that the total number of atomic orbitals and molecular orbitals is the same. As a shortcut, include only the valence orbitals and electrons. What is the bond order? Is the molecule diamagnetic or paramagnetic?

Answer available at the end of this section.

Answers

Exercise 4.2.1.1

The valence orbitals on an F atom are 2s and 2p. And, there are seven valence electrons in F. This gives fourteen total valence electrons. The MO diagram of the valence molecular orbitals can be constructed by combining the valence 2s and valence 2p orbitals from each F atom. The bond order is 1 and the molecule is diamagnetic.



This page titled 4.2.1: Molecular Orbitals is shared under a CC BY-NC-SA 4.0 license and was authored, remixed, and/or curated by Kathryn Haas.

- 5.2.1: Molecular Orbitals by Kathryn Haas is licensed CC BY-SA 4.0.

4.2.2: Orbital Mixing

In the previous section, we introduced a simplified molecular orbital (MO) diagram, assuming that interactions were limited to degenerate orbitals of compatible symmetry. A version of that *simplified* diagram for second-row homonuclear diatomics is shown on the left side of Figure $4.2.2.1$ (only valence orbitals shown).

In reality, orbitals of compatible symmetry can combine, or mix, even when they have different energies. When sets of orbitals mix, it has the effect of decreasing the energy of the lower-energy set and increasing the energy of the higher-energy set. There are two ways to explain mixing, described in the points below. The diagram on the right of side of Figure $4.2.2.1$ shows how energy levels are affected by orbital mixing.

- **Starting from the simplified MO diagram and mixing molecular orbitals of like symmetry**: If we start with the "no mixing" simplified diagram shown on the left, we can pick out the orbitals with like symmetry and consider what will happen if these molecular orbitals mix. For example, starting from the MO diagram on the left side of Figure $4.2.2.1$, we see that there are two σ_g orbitals that have identical symmetry (hence they have identical symmetry labels). Upon mixing, the lower-energy $\sigma_g(2s)$ will decrease in energy while the higher-energy $\sigma_g(2p)$ will increase in energy. Likewise, there are two σ_u^* orbitals that will mix, decreasing the energy of $\sigma_u^*(2s)$ while increasing the energy of $\sigma_u^*(2p)$.
- **Starting from and mixing atomic orbitals of compatible symmetry**: Starting from the atomic orbitals, we can select the orbitals that have compatible symmetry to make productive interactions, and combine them as a set to make molecular orbitals. From the two sets of atomic orbitals on the right panel in Figure $4.2.2.1$, there are two sets of four orbitals with compatable symmetry; one is the set of two $2s$ and two $2p_z$ orbitals. These four orbitals can combine to form molecular orbitals with σ symmetry. They combine to form one lowest-energy bonding σ_g, a highest-energy σ_u^*, and two orbitals with intermediate energy (σ_g, and σ_u^*). This treatment can be expressed as the linear combination of four atomic orbitals:

  $$\Psi = c_1\psi(2s_a) \pm c_2\psi(2s_b) \pm c_3\psi(2p_a) \pm c_4\psi(2p_b)$$

  where the coefficients $c_1 = c_2$ and $c_3 = c_4$ for homonuclear diatomic molecules.

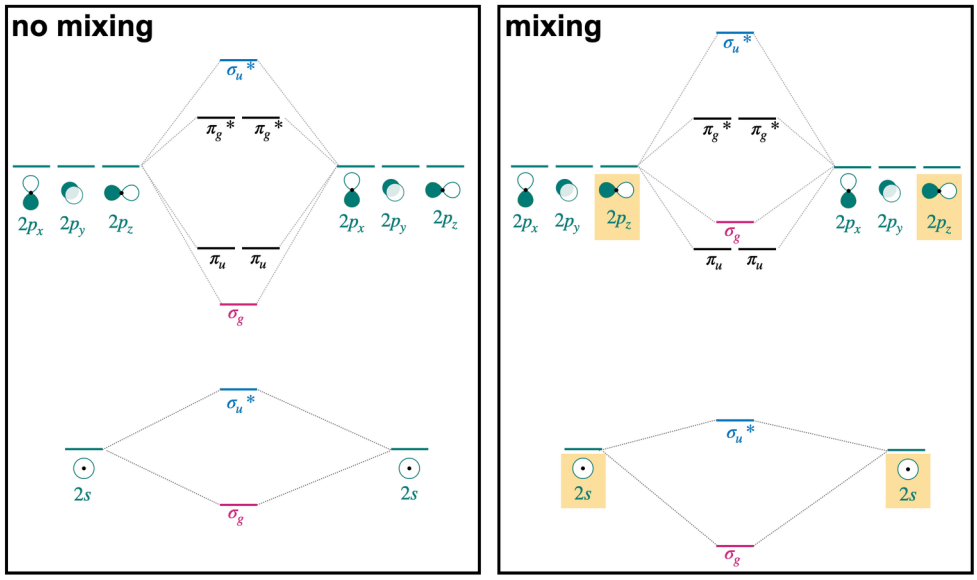


Figure $4.2.2.1$: Mixing of orbitals with like symmetry affects the energies of molecular orbitals. The simplified case where no mixing occurs is shown on the left. The effects of mixing are shown on the right. The σ_g orbitals of like symmetry are highlighted in fuschia and the σ_u^* orbitals of like symmetry are highlighted in blue. A group of atomic orbitals of similar symmetry are highlighted in yellow boxes; these atomic orbitals combine to give all σ molecular orbitals. (CC-BY-SA, Kathryn Haas)

In the case of homonuclear diatomic molecules of the second row, orbital mixing has important consequences for the energetic order of the $\sigma_g(2p)$ and $\pi_u(2p)$ orbitals. This will be discussed in the next section.

This page titled 4.2.2: Orbital Mixing is shared under a CC BY-NC-SA 4.0 license and was authored, remixed, and/or curated by Kathryn Haas.

- 5.2.2: Orbital Mixing by Kathryn Haas is licensed CC BY-SA 4.0.

4.2.3: Diatomic Molecules of the First and Second Periods

First Period Homonuclear Diatomic Molecules

In the first row of the periodic table, the valence atomic orbitals are $1s$. There are two possible homonuclear diatomic molecules of the first period:

Dihydrogen, H_2 $[\sigma_g^2(1s)]$: This is the simplest diatomic molecule. It has only two molecular orbitals (σ_g and σ_u^*), two electrons, a bond order of 1, and is diamagnetic. Its bond length is 74 pm. MO theory would lead us to expect bond order to decrease and bond length to increase if we either add or subtract one electron. The calculated bond length for the H_2^+ ion is approximately 105 pm.[1]

Dihelium, He_2 $[\sigma_g^2\sigma_u^{*2}(1s)]$: This molecule has a bond order of zero due to equal number of electrons in bonding and antibonding orbitals. Like other nobel gases, He exists in the atomic form and does not form bonds at ordinary temperatures and pressures.

Exercise 4.2.3.1

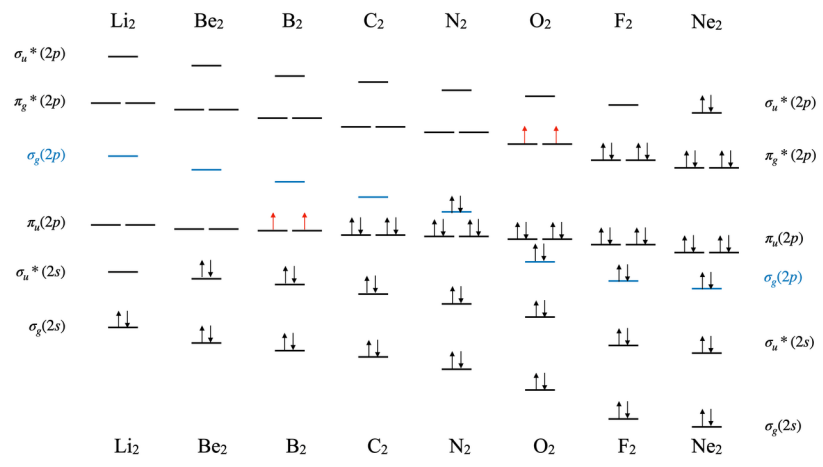
Draw the complete molecular orbital diagrams for H_2 and for He_2. Include sketches of the atomic and molecular orbitals.

Answer available at the end of this section.

Second Period Homonuclear Diatomic Molecules

The second period elements span from Li to Ne. The valence orbitals are 2s and 2p. In their molecular orbital diagrams, non-valence orbitals (1s in this case) are often disregarded in molecular orbital diagrams.

Orbital mixing has significant consequences for the magnetic and spectroscopic properties of second period homonuclear diatomic molecules because it affects the order of filling of the $\sigma_g(2p)$ and $\pi_u(2p)$ orbitals. Early in period 2 (up to and including nitrogen), the $\pi_u(2p)$ orbitals are lower in energy than the $\sigma_g(2p)$ (see Figure $4.2.3.1$). However, later in period 2, the $\sigma_g(2p)$ orbitals are pulled to a lower energy. This lowering in energy of $\sigma_g(2p)$ is not unique; all of the σ orbitals in the molecule are pulled to lower energy due to the increasing positive charge of the nucleus. The π orbitals in the molecule are also affected, but to a much lesser extent than σ orbitals. The reason has to do with the high penetration of s atomic orbitals compared to p atomic orbitals (recall our previous discussion on penetration and shielding, and its effect on periodic trends). The σ molecular orbitals have more s character and thus their energy is more influenced by increasing nuclear charge. As nuclear charge increases, the energy of the $\sigma_g(2p)$ orbital is lowered significantly more than the energy of the $\pi_u(2p)$ orbitals (Figure $4.2.3.1$).



	Li_2	Be_2	B_2	C_2	N_2	O_2	F_2	Ne_2
Unpaired e^-	0	0	2	0	0	2	0	0
Bond Order	1	0	1	2	3	2	1	0
Experimental* Bond Length (pm)	267.3	246.0	159.0	124.3	109.8	120.8	141.2	310.0

*Experimental bond lengths from "List of Experimental Diatomic Bond Lengths", NIST, https://cccbdb.nist.gov/diatomicexpbondx.asp

Figure 4.2.3.1: Molecular orbital energy-level diagrams for the diatomic molecules of the period 2 elements. Unlike earlier diagrams, *only the valence molecular orbital energy levels for the **molecules** are shown here (atomic orbitals not shown for simplicity).* For Li_2 through N_2, the $\sigma_g(2p)$ orbital is higher in energy than the $\pi_u(2p)$ orbitals. In contrast, from O_2 onward, the $\sigma_g(2p)$ orbital is *lower* in energy than the $\pi_u(2p)$ orbitals because the nuclear charge increases across the row. The experimental bond lengths correlate with the calculated bond order. (CC-BY-NC-SA, Kathryn Haas)

Dilithium, Li_2 $[\sigma_g^2(2s)]$**:** This molecule has a bond order of one and is observed experimentally in the gas phase to have one Li-Li bond.

Diberylium, Be_2 $[\sigma_g^2\sigma_u^{*2}(2s)]$**:** This molecule has a bond order of zero due to the equal number of electrons in bonding and antibonding orbitals. Although Be_2 does not exist under ordinary conditions, it can be produced in a laboratory and its bond length measured (Figure 4.2.3.2). Although the bond is very weak, its bond length is surprisingly ordinary for a covalent bond of the second period elements.[2]

Diboron, B_2 $[\sigma_g^2\sigma_u^{*2}(2s)\pi_u^1\pi_u^1(2p)]$**:** The case of diboron is one that is much better described by molecular orbital theory than by Lewis structures or valence bond theory. This molecule has a bond order of one. The molecular orbital description of diboron also predicts, accurately, that diboron is paramagnetic. The paramagnetism is a consequence of orbital mixing, resulting in the σ_g orbital's being at a higher energy than the two degenerate π_u^* orbitals.

Dicarbon, C_2 $[\sigma_g^2\sigma_u^{*2}(2s)\pi_u^2\pi_u^2(2p)]$**:** This molecule has a bond order of two. Molecular orbital theory predicts two bonds with π symmetry, and no σ bonding. C_2 is rare in nature because its allotrope, diamond, is much more stable.

Dinitrogen, N_2 $[\sigma_g^2\sigma_u^{*2}(2s)\pi_u^2\pi_u^2\sigma_g^2(2p)]$**:** This molecule is predicted to have a triple bond. This prediction is consistent with its short bond length and bond dissociation energy. The energies of the $\sigma_g(2p)$ and $\pi_u(2p)$ orbitals are very close, and their relative energy levels have been a subject of some debate (see next section for discussion).

Dioxygen, O_2 $[\sigma_g^2\sigma_u^{*2}(2s)\sigma_g^2\pi_u^2\pi_u^2\pi_g^{*1}\pi_g^{*1}(2p)]$**:** This is another case where valence bond theory fails to predict actual properties. Molecular orbital theory correctly predicts that dioxygen is paramagnetic, with a bond order of two. Here, the molecular orbital diagram returns to its "normal" order of orbitals where orbital mixing could be somewhat ignored, and where $\sigma_g(2p)$ is lower in energy than $\pi_u(2p)$.

Difluorine, F_2 $[\sigma_g^2\sigma_u^{*2}(2s)\sigma_g^2\pi_u^2\pi_u^2\pi_g^{*2}\pi_g^{*2}(2p)]$**:** This molecule has a bond order of one and like oxygen, the $\sigma_g(2p)$ is lower in energy than $\pi_u(2p)$.

Dineon, Ne_2 $[\sigma_g^2\sigma_u^{*2}(2s)\sigma_g^2\pi_u^2\pi_u^2\pi_g^{*2}\pi_g^{*2}\sigma_u^{*2}(2p)]$**:** Like other noble gases, Ne exists in the atomic form and does not form bonds at ordinary temperatures and pressures. Like Be_2, Ne_2 is an unstable species that has been created in extreme laboratory conditions and its bond length has been measured (Figure 4.2.3.2)

Exercise 4.2.3.2

Draw the complete molecular orbital diagram for O_2. Show calculation of its bond order and tell whether it is diamagnetic or paramagnetic.

Answer available at the end of this section.

Exercise 4.2.3.3: The Peroxide Ion

Use a qualitative molecular orbital energy-level diagram to predict the electron configuration, the bond order, and the number of unpaired electrons in the peroxide ion (O_2^{2-}).

Answer available at the end of this section.

Bond Lengths in Homonuclear Diatomic Molecules

The trends in experimental bond lengths are predicted by molecular orbital theory, specifically by the calculated bond order. The values of bond order and experimental bond lengths for the second period diatomic molecules are given in Figure 4.2.3.1, and shown in graphical format on the plot in Figure 4.2.3.2. From the plot, we can see that bond length correlates well with bond order, with a minimum bond length occurring where the bond order is greatest (N_2). The shortest bond distance is at N_2 due to its high bond order of 3. From N_2 to F_2 the bond distance increases despite the fact that atomic radius decreases.

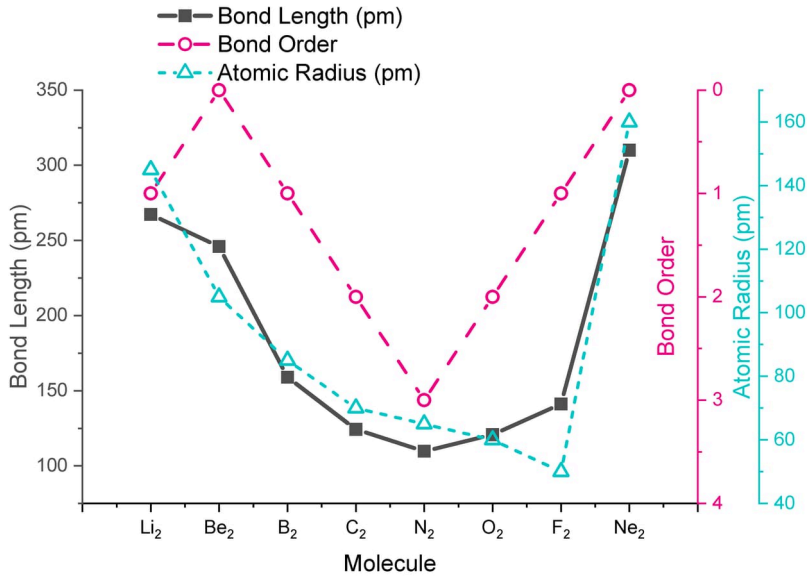


Figure 4.2.3.2: Overlayed plots of bond length (black squares), bond order (pink circles), and atomic radius (teal triangles) versus atomic number for second period homonuclear diatomic molecules. (CC-BY-NC-SA; Kathryn Haas)

References

1. NIST, Calculated Geometries available for H_2^+ (Hydrogen cation) 2Σg+ D∞h, available at https://cccbdb.nist.gov/diatomicexpbondx.asp
2. Merritt, J. M.; Bondybey, V. E.; Heaven, M. C., Beryllium Dimer-Caught in the Act of Bonding. *Science* **2009,** *324* (5934), 1548-1551.

Answers

Exercise 4.2.3.1

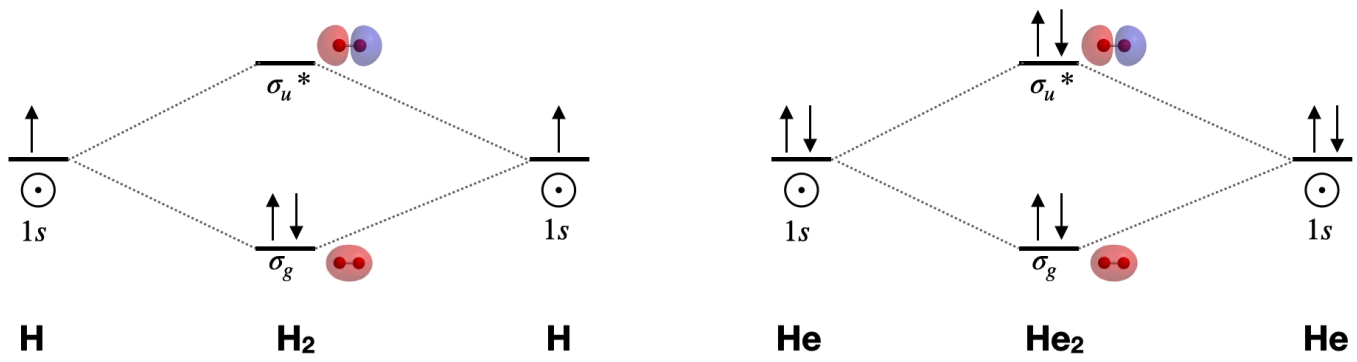


Figure for Exercise 4.2.3.1: Molecular orbital diagrams for dihydrogen and dihelium. Molecular orbital surfaces calculated using Spartan software. (CC-BY-NC-SA; Kathryn Haas)

A complete molecular orbital diagram includes all atomic orbitals and molecular orbitals, their symmetry labels, and electron filling.

Exercise 4.2.3.2

O_2 is paramagnetic with a bond order of 2. Its $\sigma_g(2p)$ molecular orbital is lower in energy that the set of $\pi_u(2p)$ orbitals.

$$\text{Bond order } = \frac{1}{2}\left[\left(\begin{array}{c}\text{8 electrons in}\\ \text{valence bonding orbitals}\end{array}\right) - \left(\begin{array}{c}\text{4 electrons in}\\ \text{valence antibonding orbitals}\end{array}\right)\right]$$

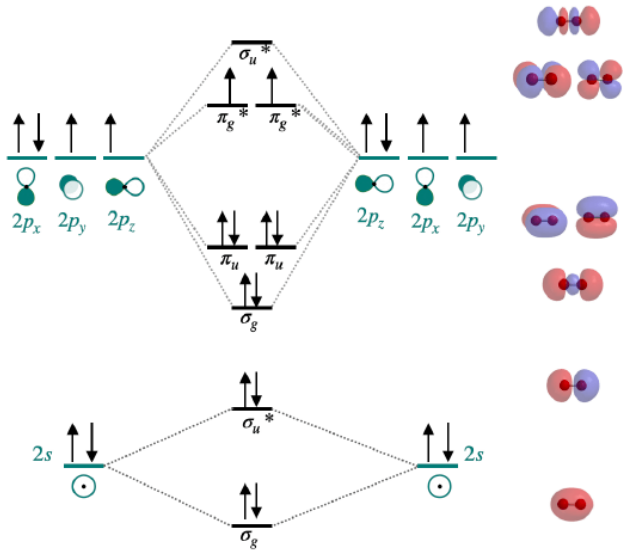


Figure for Exercise 4.2.3.2. Molecular orbital diagram of O_2. (CC-BY-NC-SA, Kathryn Haas)

Exercise 4.2.3.3**: The Peroxide Ion**

This diagram looks similar to that of O_2, except that there are two additional electrons.
$(\sigma_g(2s))^2 (\sigma_u^*(2s))^2 (\sigma_g(2p))^2 (\pi_u(2p))^4 (\pi_g(2p))^4$; bond order of 1; no unpaired electrons.

This page titled 4.2.3: Diatomic Molecules of the First and Second Periods is shared under a CC BY-NC-SA 4.0 license and was authored, remixed, and/or curated by Kathryn Haas.

- 5.2.3: Diatomic Molecules of the First and Second Periods by Kathryn Haas is licensed CC BY-SA 4.0.
- 5.P: Problems is licensed CC BY-SA 4.0.

4.2.4: Photoelectron Spectroscopy

A photoelectron spectrum can show the relative energies of occupied molecular orbitals by ionization. The *ionization energy* is a direct measure of the energy required to just remove the electron concerned from its initial level to the vacuum level (free electron). Photoelectron spectroscopy measures the relative energies of the ground and excited positive ion states that are obtained by removal of single electrons from the neutral molecule.

$$A + \text{photon} \rightarrow A^+ + e^-$$

The information obtained from photoelectron spectroscopy is typically discussed in terms of the electronic structure and bonding in the ground states of neutral molecules, with ionization of electrons occurring from bonding molecular orbitals, lone pairs, antibonding molecular orbitals, or atomic cores. These descriptions reflect the relationship of ionization energies to the molecular orbital model of electronic structure.

Ionization energies are directly related to the energies of molecular orbitals (by Koopmans' theorem).

Example: Photoelectron spectrum of dihydrogen

The molecular orbital description of dihydrogen involves two $1s$ atomic orbitals generating two molecular orbitals: a bonding σ_g and an antibonding σ_u^*. The two electrons occupy the σ_g bonding orbital, leaving the molecule with a bond order of one (Figure $4.2.4.1$). The PES spectrum of dihydrogen (Figure $4.2.4.1$) has a single band that corresponds to the ionization of one electron from the σ_g. The multiple peaks are due to electrons ejecting from a range of stimulated vibrational energy levels. When extensive vibrational structure is resolved in a PES molecular orbital, then the removal of an electron from that molecular orbital induces a significant change in the bonding (in this case an increase in the bond length due to decrease in bond order).

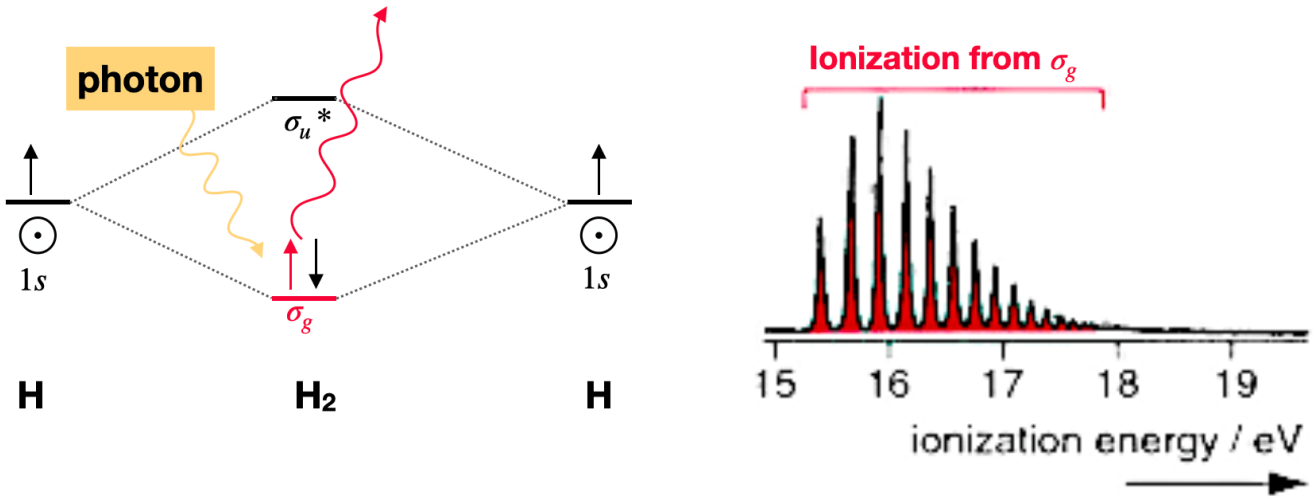


Figure $4.2.4.1$: The molecular orbital diagram and photoelectron spectrum of dihydrogen. (CC-BY-NC-SA; Libretexts)

Example: Photoelectron spectrum of dinitrogen

Diatomic nitrogen is more complex than hydrogen since multiple molecular orbitals are occupied. Five molecular orbitals are occupied; two of them are degenerate. Three bands in the photoelectron spectrum correspond to ionization of an electron in $\sigma_g(2p)$, $\pi_u(2p)$ and $\sigma_u^*(2s)$ molecular orbitals. Ionization of the fourth type of orbital, $\sigma_g(2s)$, does not appear in Figure $4.2.4.2$ because it is either off scale or because the incident light $h\nu$ used did not have sufficient energy to ionize electrons in that deeply stabilized molecular orbital. Note that extensive vibrational structure for the $\pi_u(2p)$ band indicates that the removal of an electron from this molecular orbital causes a significant change in the bonding.

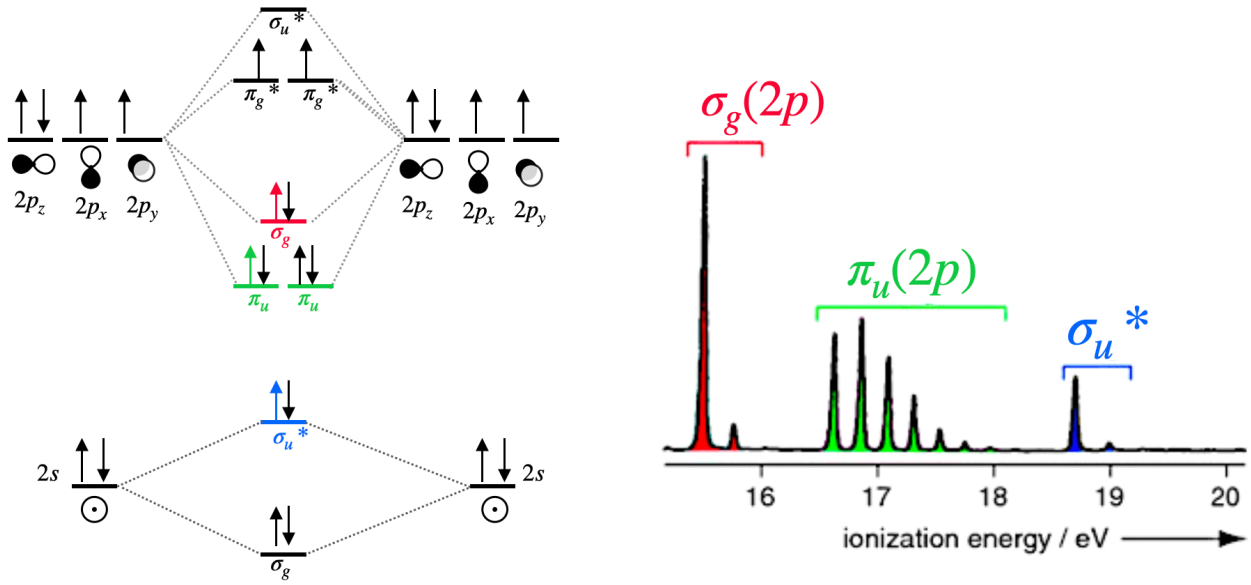


Figure 4.2.4.2: The molecular orbital diagram and photoelectron spectrum of dinitrogen. (CC-BY-NC-SA; Libretexts)

From the photoelectron spectrum of dinitrogen, we can see that the electrons in the $\sigma_g(2p)$ orbital can be ionized using less energy than required to ionize electrons in the $\pi_u(2p)$ orbital. This is evidence for $\sigma_g(2p)$ existing at a higher energy than the $\pi_u(2p)$ orbitals.

This page titled 4.2.4: Photoelectron Spectroscopy is shared under a CC BY-NC-SA 4.0 license and was authored, remixed, and/or curated by Kathryn Haas.

- 10.4: Photoelectron Spectroscopy by Roger Nix is licensed CC BY 4.0.

4.3: HETERONUCLEAR DIATOMIC MOLECULES

Diatomic molecules with two non-identical atoms are called **heteronuclear** diatomic molecules. When atoms are not identical, the molecule forms by combining atomic orbitals of unequal energies. *The result is a polar bond in which atomic orbitals contribute unevenly to each molecular orbital.*

The application of molecular orbital theory to heteronuclear diatomic molecules is similar to the case of homonuclear diatomics, except that the atomic orbitals from each atom have different energies and contribute unequally to molecular orbitals. Recall that atomic orbitals must have compatible symmetry and similar energy to combine into molecular orbitals. In the case where atomic orbitals of like symmetry have different energies, they combine less favorably than orbitals that are closer to one another in energy. As a general rule, orbitals that have energy differences of greater than 10-14 eV do not combine favorably. In the molecular orbital diagram, the closer a molecular orbital is to an atomic orbital, the more that atomic orbital contributes to the molecular orbital. This last point is helpful for back-of-the napkin estimations of what the molecular orbitals "look" like.

In this section, you should learn how to generate molecular orbital diagrams of heteronuclear diatomic molecules. To approach such a problem, we must start with a knowledge of the relative energies of electrons in different atomic orbitals. In other words, we need knowledge of the orbital potential energies (or orbital ionization energies).

4.3.1: Polar bonds

4.3.2: Ionic Compounds and Molecular Orbitals

Sources:

- Gray, Harry. *Electrons and Chemical Bonding*, Benjamin, 1964.
- Miessler, Gary L, and Donald A. Tarr. *Inorganic Chemistry*. Upper Saddle River, N.J: Pearson Education, 2014. Print.

This page titled 4.3: Heteronuclear Diatomic Molecules is shared under a CC BY-NC-SA 4.0 license and was authored, remixed, and/or curated by LibreTexts.

- 5.3: Heteronuclear Diatomic Molecules by Kathryn Haas is licensed CC BY-SA 4.0.

4.3.1: Polar bonds

Molecular orbital diagrams for heteronuclear diatomic molecules

The molecular orbital diagram of a heteronuclear diatomic molecule is approached in a way similar to that of a homonuclear diatomic molecule. The orbital diagrams may also look similar. A major difference is that the more electronegative atom will have orbitals at a lower energy level. Two examples of heteronuclear diatomic molecules will be explored below as illustrative examples.

Carbon monoxide MO diagram

Carbon monoxide is an example of a heteronuclear diatomic molecule where both atoms are second-row elements. The valence molecular orbitals in both atoms are the $2s$ and $2p$ orbitals. The molecular orbital diagram for carbon monoxide (Figure $4.3.1.1$) is constructed in a way similar to how you would construct dicarbon or dioxygen, except that the oxygen orbitals have a lower potential energy than analogous carbon orbitals. The labeling of molecular orbitals in this diagram follows a convention by which orbitals are given serial labels according to type of orbital (σ, π, etc.). The lowest energy orbitals of any type are assigned a value of 1 and higher energy orbitals of the same type are assigned by increasing intervals (..2, 3, 4...). The orbital labeling system described previously is inappropriate for heteronuclear diatomic molecules that cannot be assigned g and u subscripts.

A consequence of unequal atomic orbital energy levels is that orbital mixing is significant. Notice the order of the molecular orbitals labeled 1π and 3σ in Figure $4.3.1.1$. This is a similar order of π and σ orbitals to the one we saw in the case of the σ_g and π_u orbitals of N_2 and lighter diatomics of the second period. Because the oxygen $2p_z$ orbital is close in energy to both the carbon $2p_z$ and carbon $2s$, these three orbitals will have significant interaction (mixing). The result is an increase in the energy of the 3σ orbital and a decrease in energy of the $2\sigma^*$ orbital, resulting in the diagram shown in Figure $4.3.1.1$.

In the case of carbon monoxide (Figure $4.3.1.1$), atomic orbitals contribute unequally to each molecular orbital. For example, because the $2s$ orbital of oxygen is very close in energy to the 2σ moelcular orbital, it contributes to that molecular orbital more than the $2s$ orbital from carbon. Notice the shape of this 2σ orbital and how it is unevenly distributed over the two atoms; it is more heavily distributed on the oxygen because it is most like the oxygen $2s$. This is in line with the assumption that electron density is distributed more on oxygen because it is more electronegative than carbon. Likewise, the 1π orbitals are unevenly distributed, with more distribution close to the oxygen.

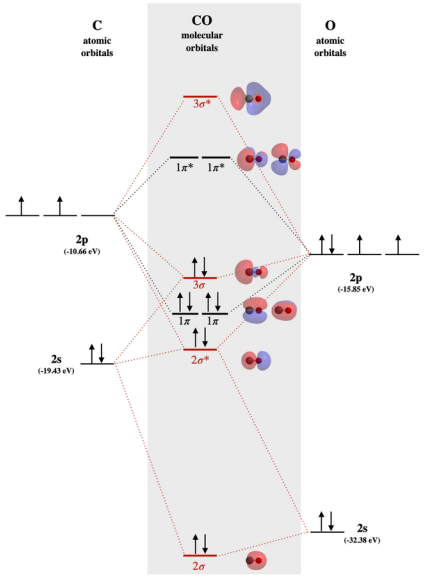
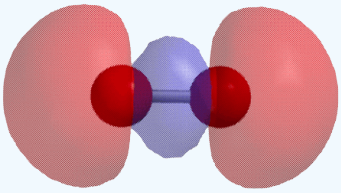


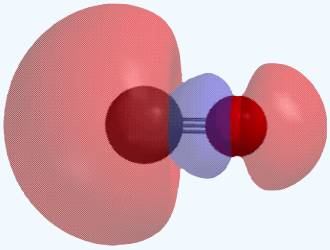
Figure $4.3.1.1$: Molecular orbital diagram of carbon monoxide. The labeling of molecular orbitals in this diagram follows a convention by which orbitals are given serial names according to the type of orbital (σ, π, etc.). The lowest energy orbitals of any type are assigned a value of 1 and higher energy orbitals of the same type are assigned by increasing intervals (..2, 3, 4...). The orbital labeling system described previously is inappropriate for heteronuclear diatomic molecules that cannot be assigned g and u subscripts. Molecular orbital surfaces were calculated using Spartan software. (Kathryn Haas, CC-BY-NC-SA)

Exercise 4.3.1.1

Examine the shape of the 3σ orbital of carbon monoxide in Figure 4.3.1.1. Describe what ways this shape is different from the shape of the σ_g orbitals from second period homonuclear diatomic molecules (see Fig. 5.2.1.1). Rationalize these differences. Both orbitals are re-created below for convenience.



σ_g of homonuclear diatomic



3σ of CO

Answer available at the end of this section.

Hydrogen fluoride MO diagram

Hydrogen fluoride is an example of a heteronuclear diatomic molecule in which the two atoms are from different periods. In this case, the valence orbital of H is $1s$ while those of F are $2s$ and $2p$. The molecular orbital diagram for HF is shown in Figure 4.3.1.2.

Three of these orbitals have compatible symmetry for mixing; these are the hydrogen $1s$, fluorine $2s$, and fluorine $2p$. However, the extent to which they will interact depends on their relative energies. Fluorine is more electronegative than H, and the fluorine atom has a higher first ionization energy than does hydrogen. From these trends, we can expect that the fluorine valence orbitals are lower in energy than that of hydrogen. From Table 5.3.1, we find that the 1s orbital of H (-13.6 eV) is higher in energy than both fluorine orbitals (-18.7 and -40.2 eV, respectively for $2p$ and $2s$). The energies of hydrogen $1s$ and fluorine $2p$ are a good match for combination; however, the fluorine $2s$ orbital is much too different to create a productive interaction. Therefore, we expect that the fluorine $2s$ will create a non-bonding molecular orbital, while the $1s$ and $2p_z$ orbitals combine to make σ bonding and σ^* antibonding molecular orbitals. The remaining $2p_x$ and $2p_y$ orbitals do not have compatible symmetry for bonding with hydrogen, and they will form non-bonding π molecular orbitals. The non-bonding orbitals will have similar energy and character as their component atomic orbitals.

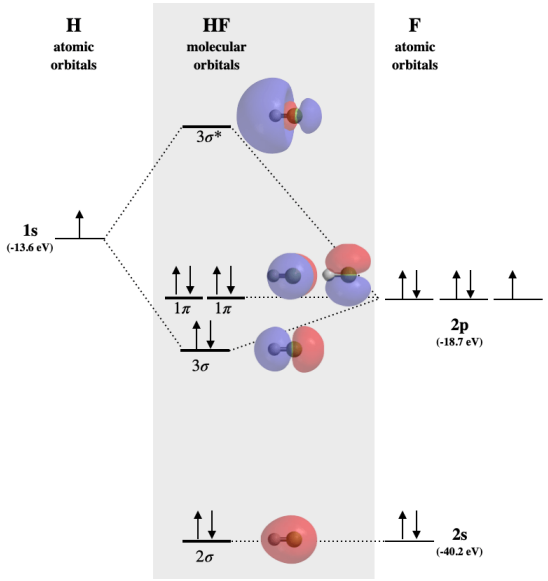


Figure 4.3.1.2: Molecular Orbital diagram of hydrogen fluoride. Molecular orbitals calculated using Spartan software. (Kathryn Haas, CC-BY-NC-SA)

Chemical reactions take place at the HOMO and LUMO orbitals

Knowledge of molecular orbital diagrams, and the shapes of molecular orbitals, can be used to accurately explain and predict chemical reactivity. Chemical reactions take place using the highest occupied molecular orbitals (HOMO) of a nucleophile or Lewis base, and the lowest unoccupied molecular orbital (LUMO) of an electrophile or Lewis acid.

> Lewis bases react using electrons in the HOMO, while Lewis acids react using the empty LUMO.

Example: Reactivity of CO with metal ions

CO is an excellent ligand for many metal ions. In fact, the strong affinity between CO and the heme iron (Fe) ions in hemoglobin can explain the mechanism of carbon monoxide poisoning. When CO binds in place of O_2 to hemoglobin, that hemoglobin can no longer carry O_2 to tissue cells. CO binding to hemoglobin is strong and practically irreversible. When CO binds to metal ions, it does so through the carbon atom. This is contrary to expectations based on the Lewis structure and the known bond polarity, where electron density is polarized toward oxygen. The distribution of the electron density of the HOMO of CO can explain this observation!

Exercise 4.3.1.2

Refer to the MO diagram for CO. Identify the HOMO and explain why CO bonds to metal ions through the carbon atom rather than through the oxygen atom.

Answer available at the end of this section.

Answers

Exercise 4.3.1.1

The 3σ orbital is like the σ_g in that it has three lobes and two nodes distributed along the internuclear bond. They are different in their distribution. The two external lobes of σ_g are evenly distributed because they are an equal combination of two p_z orbitals (one from each atom). The 3σ orbital is more heavily distributed toward the carbon atom, the less electronegative atom, than toward the oxygen. The unequal distribution of 3σ is apparent in the unequal sizes of its exterior lobes and the uneven shape of the interior lobe. The heavier distribution within the exterior lobe on carbon is caused by the mixing of the carbon $2s$ orbital with carbon and oxygen $2p_z$ orbitals. The uneven shape of the interior lobe, where it leans toward oxygen, is best explained by the fact that the 3σ orbital is closer in energy to the oxygen $2p_z$ than the carbon $2p_z$.

Exercise 4.3.1.2

In the interaction between CO and a metal ion, CO would act as a Lewis base; thus it will react using electrons in its HOMO. The MO diagram for CO is shown in

Figure 4.3.1.1: the HOMO is the 3σ orbital (also discussed in Exercise 4.3.1.1). The electron density of that MO is centered around the carbon atom, thus the carbon atom will be a better Lewis base than the O atom.

This page titled 4.3.1: Polar bonds is shared under a CC BY-NC-SA 4.0 license and was authored, remixed, and/or curated by Kathryn Haas.

- 5.3.2: Polar bonds by Kathryn Haas is licensed CC BY-SA 4.0.

4.3.2: Ionic Compounds and Molecular Orbitals

Ionic interactions lie at one extreme on a spectrum of bonding. On the opposite end of the spectrum are the non-polar covalent bonds (e.g., homonuclear diatomics). In these molecules, molecular orbitals are formed by equal-energy atomic orbitals, resulting in electron density evenly distributed over the molecule. In the middle of the spectrum are the cases of polar covalent bonds (e.g., heteronuclear diatomics), in which atomic orbitals of unequal energies contribute unequally to molecular orbitals, resulting in uneven distribution of electron density across the molecule. In the case of polar bonds, the electron density is shifted toward the more electronegative atom since that atom contributes more to the lowest energy bonding molecular orbitals. Molecular orbital diagrams can be drawn for ionic compounds as if they are extremely polar bonds in which electrons are not only shifted toward, but are transferred completely to the more electronegative atom.

Example: NaCl

In NaCl, the sodium $3s$ orbital (-5.2 eV) is significantly higher in energy than the chlorine valence orbitals. The chlorine $3s$ and $3p_z$ orbitals have compatible symmetry, yet only the $3p_z$ orbital (-13.8 eV) is close enough in energy to interact with the Na $3s$; still, the energy difference is large enough to make bonding weak. The Na $3s$ orbital combines with Cl $3p_z$ to form the molecular orbitals labeled 4σ and $4\sigma^*$ in Figure $4.3.2.1$. The 4σ orbital is weakly bonding, but is very close in energy to the Cl $3p_z$ orbital, and is mostly Cl-like in character. Notice that all σ orbitals look very much like either s or p orbitals centered on the Cl atom, while the $4\sigma^*$ orbital is centered almost entirely on Na. The lack of molecular orbitals that are distributed over both atoms at once is consistent with a lack of significant covalent bond character in NaCl. The bonding here is characterized by transfer of one electron from Na to Cl and is almost entirely electrostatic. Bonding that is mostly electrostatic in character is non-directional, unlike true covalent bonding.

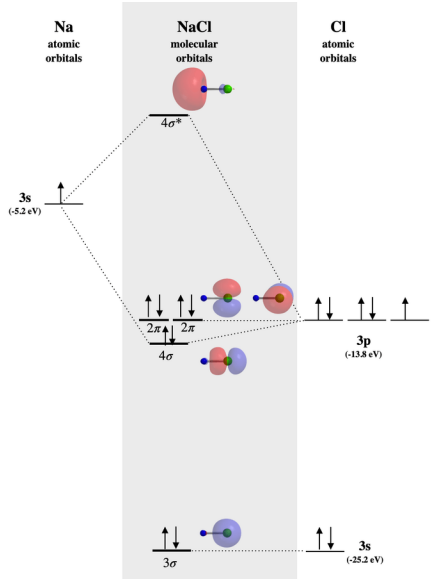


Figure $4.3.2.1$: The molecular orbital diagram for sodium chloride. Molecular orbital surfaces calculated using Spartan software indicate almost no covalent nature of bonding. (CC-BY-NC-SA, Kathryn Haas)

Exercise $4.3.2.1$

Draw the molecular orbital diagram for LiF. Make sure to label all molecular orbitals appropriately, and specify whether they are mostly bonding, non-bonding, or antibonding. Identify the HOMO and LUMO. Sketch the approximate shapes of all orbitals.

Answer available at the end of this section.

Answers

Exercise 4.3.2.1

We expect LiF to be an ionic compound because the energy difference in valence orbitals is at least 10-14 eV. (See Table 5.3.1) There are a variety of ways used to label molecular orbitals. In the figure below, we are using the convention of labeling each type of orbital with numbers starting from the lowest-energy orbitals. The 1σ orbital would be mostly F $1s$ in character and is not shown. The 2σ orbital is mostly non-bonding in nature, although it has a very small contribution from $2s$ of Li due to compatible symmetry. The 3σ orbital is slightly bonding but it is mostly F$2p$ in character. The two 1π orbitals are completely non-bonding. The $3\sigma^*$ orbital is antibonding.

- HOMO is 1π
- LUMO is $3\sigma^*$

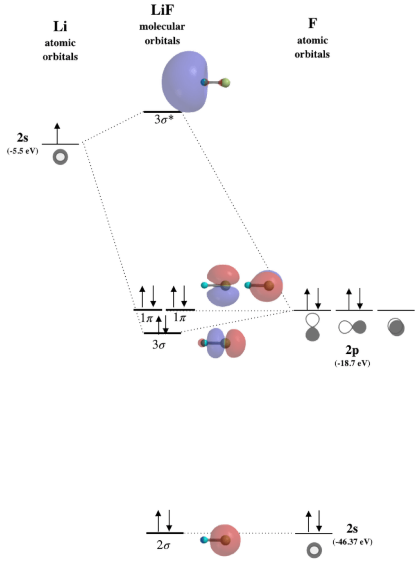


Figure for Exercise 4.3.2.1: Molecular orbital diagram for the ionic compund, LiF. (CC-BY-NC-SA, Kathryn Haas)

This page titled 4.3.2: Ionic Compounds and Molecular Orbitals is shared under a CC BY-NC-SA 4.0 license and was authored, remixed, and/or curated by Kathryn Haas.

- 5.3.3: Ionic Compounds and Molecular Orbitals by Kathryn Haas is licensed CC BY-SA 4.0.

4.P: Problems

Concept Review Questions

1. What are the assumptions (axioms) of molecular orbital (MO) theory?

2. Explain qualitatively why the vectorial addition of atomic orbitals creates molecular orbitals (which underlying physical phenomenon is described by the vectorial addition?).

3. Explain qualitatively why molecular orbital theory is suitable to describe covalent bonding.

4. What are the three criteria that determine the degree of covalent interaction in MO theory?

5. Which three rules determine the degree of orbital overlap in MO theory?

6. Explain why the combination of a large, diffuse orbital and a small orbital produces only weak covalent interaction.

7. Explain why sigma interactions between atomic orbitals typically produce larger orbital overlaps than pi interactions.

8. Explain why the combination of orbitals of the same energy leads to the largest degree of covalent interaction.

9. What can be said about energy and location of a bonding and an anti-bonding molecular orbital that are made from atomic orbitals of large energy difference?

10. MO theory – even though designed for covalent bonding – can also make statements about ionic bonding. Explain why.

11. Explain the principles of SALC.

Dr. Kai Landskron (Lehigh University). If you like this textbook, please consider to make a donation to support the author's research at Lehigh University: Click Here to Donate.

Homework Problems

Section 1

Exercise 1

What will most likely lead to the smallest covalent interaction?

a) Overlap of a small and a large orbital.

b) Overlap of two small orbitals.

c) Overlap of two large orbitals.

Answer available at the end of this section.

Exercise 2

What will most likely lead to the largest covalent interaction?

a) orbital overlap in sigma-fashion

b) orbital overlap in pi-fashion

c) orbital overlap in delta-fashion

Answer available at the end of this section.

Exercise 3

Qualitatively construct the MO diagrams composed of

a) two 2s atom orbitals A and B of equal energy.

b) two 2s atom orbitals where the orbital energy of atom A is significantly higher than that of B. If both the bonding and the antibonding MO are filled with electrons, where will bonding and antibonding electrons primarily be located? Briefly explain your decision.

Answer available at the end of this section.

Exercise 4

Decide by "inspection" which of the following combinations of orbitals have the "right" symmetries to form molecular orbitals.

a) The $2p_x$ orbital of the first N atom and the $2p_y$ orbital of the second N atom in the molecule N_2. The z axis is defined as the bond axis in N_2.

b) The F $2p_x$ and the H 1s orbital in the HF molecule. The z axis is defined as the bond axis.

c) The $2p_z$ orbital of F and the 1s orbital in the HF molecule. The z axis is defined as the bond axis.

Answer available at the end of this section.

Exercise 5

The CH_4 molecule belongs to the point group T_d. You can find the character table of the point group in the internet.

a) Calculate the reducible representation for the ligand group orbitals (LGOs).

b) Calculate the irreducible representations of the ligand group orbitals (LGOs).

c) Draw a qualitative molecular orbital diagram for CH_4.

Answer available at the end of this section.

Exercise 6

Which are the symmetry types of the central atom orbitals in the PCl_5 molecule?

Answer available at the end of this section.

Exercise 7

For the hypothetical $BrKr^+$ molecule: Toward which atom is the HOMO polarized? Explain briefly why.

Answer available at the end of this section.

Exercise 8

Reconstruct the MO diagram for water and NH_3 (repeat what we did in class without looking at your notes (only use the respective character tables).

Answer available at the end of this section.

Dr. Kai Landskron (Lehigh University). If you like this textbook, please consider to make a donation to support the author's research at Lehigh University: Click Here to Donate.

Exercise $4.P.1$

A Molecular Orbital Diagram for a diatomic molecule (two atoms) always has the same basic pattern.

- Draw a picture of the levels.
- Label each level with σ, σ*, π, π*

Answer available at the end of this section.

Exercise $4.P.2$

A Molecular Orbital Diagram for a diatomic molecule (two atoms) varies in the number of electrons. How do you populate the electrons?

Answer available at the end of this section.

Exercise $4.P.3$

Construct a qualitative molecular orbital diagram for chlorine, Cl_2. Compare the bond order to that seen in the Lewis structure (remember that an electron in an antibonding orbital cancels the stabilization due to bonding of an electron in a bonding orbital).

Answer available at the end of this section.

Exercise $4.P.4$

a. Construct a qualitative molecular orbital diagram for oxygen, O_2.
b. Compare the bond order to that seen in the Lewis structure.
c. How else does this MO picture of oxygen compare to the Lewis structure? What do the two structures tell you about electron pairing?
d. Compounds that have all of their electrons paired are referred to as diamagnetic. Those with unpaired electrons are referred to as paramagnetic. Paramagnetic materials are attracted by a magnetic field, but diamagnetic things are not. How would you expect molecular oxygen to behave?

Answer available at the end of this section.

Exercise 4.P.5

a. Construct a qualitative molecular orbital diagram for peroxide anion, O_2^{2-}.
b. Compare the bond order to that seen in the Lewis structure.
c. How else does this MO picture of oxygen compare to the Lewis structure? What do the two structures tell you about electron pairing?
d. Based on molecular orbital pictures, how easily do you think dioxygen could be reduced to peroxide (through the addition of two electrons)?

Answer available at the end of this section.

Exercise 4.P.6

Construct a qualitative molecular orbital diagram for diboron, B_2. Do you think boron-boron bonds could form easily, based on this picture?

Answer available at the end of this section.

Exercise 4.P.7

a. Construct a qualitative molecular orbital diagram for dicarbon, C_2.
b. Compare the bond order to that seen in the Lewis structure.
c. How else does this MO picture of oxygen compare to the Lewis structure? What do the two structures tell you about electron pairing?

Answer available at the end of this section.

Exercise 4.P.8

a. Construct a qualitative molecular orbital diagram for acetylide anion, C_2^{2-}.
b. Compare the bond order to that seen in the Lewis structure.
c. How else does this MO picture of oxygen compare to the Lewis structure? What do the two structures tell you about electron pairing?
d. Based on molecular orbital pictures, how easily do you think dicarbon could be reduced to acetylide (through the addition of two electrons)?

Answer available at the end of this section.

Exercise 4.P.9

Make drawings and notes to summarize the effect of populating antibonding orbitals.

Answer available at the end of this section.

Exercise 4.P.10

Researchers at Johns Hopkins recently reported the formation of Na_4Al_2 in a pulsed arc discharge (they put a lot of electric current through a sample of sodium and aluminum; Xinxing Zhang, Ivan A. Popov, Katie A. Lundell, Haopeng Wang, Chaonan Mu, Wei Wang, Hansgeorg Schnöckel, Alexander I. Boldyrev, Kit H. Bowen, *Angewandte Chemie International Edition*, **2018**, *57*(43), 14060-14064. Copyright 2018, John Wiley & Sons. Used with permission.).

a. The compound is ionic. Explain which atoms form the cations, based on periodic trends.
b. Therefore, what atoms form the anion?
c. The anion is one molecule. What is the charge on this molecule?
d. Show how to calculate the total valence electrons in this molecular anion.
e. Draw a Lewis structure for this molecular anion.
f. Construct a diatomic molecular orbital energy level diagram for this molecule. Label the energy levels (sigma, pi, etc.) and add in the correct number of electrons.
g. Show how to calculate the bond order in the molecule.

Answer available at the end of this section.

Exercise 4.P.1

Draw the molecular orbital diagram for (NO^-).

Answer available at the end of this section.

Exercise 4.P.1

Draw and compare the molecular orbital diagrams to the Lewis structure diagrams for O_2, O_2^-, and O_2^{2-}.

Answer available at the end of this section.

Exercise 4.P.1

Draw the molecular orbital diagram for hydroxide ion (OH^-).

Answer available at the end of this section.

Exercise 4.P.1

Draw the molecular orbital diagram for hydroxide fluoride (HF).

Answer available at the end of this section.

Exercise 4.P.1

Draw the molecular orbital diagram for borane (BN).

Answer available at the end of this section.

BH3

Exercise $4.P.1$

Draw the molecular orbital diagram for $(\mathrm{FeH_6})$.

Answer available at the end of this section.

Exercise $4.P.1$

Draw the molecular orbital diagram for boron trifluoride $(\mathrm{BF_3})$.

- What is the non-bonding orbital?
- What are the HOMO and LUMO orbitals?
- Why does e' have 2 lines of energy levels compared to a1', which has only a 1-line energy level?
- What is the bond order of $\mathrm{BH_3}$ in this MO diagram?

Answer available at the end of this section.

Answers

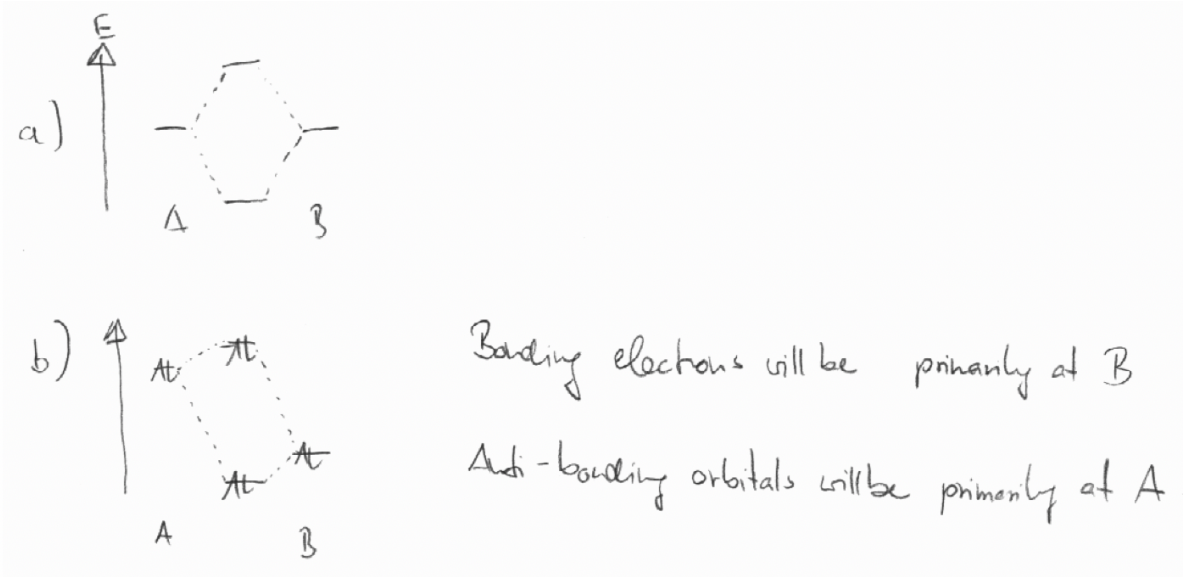
Exercise 1

a) Overlap of a small and a large orbital.

Exercise 2

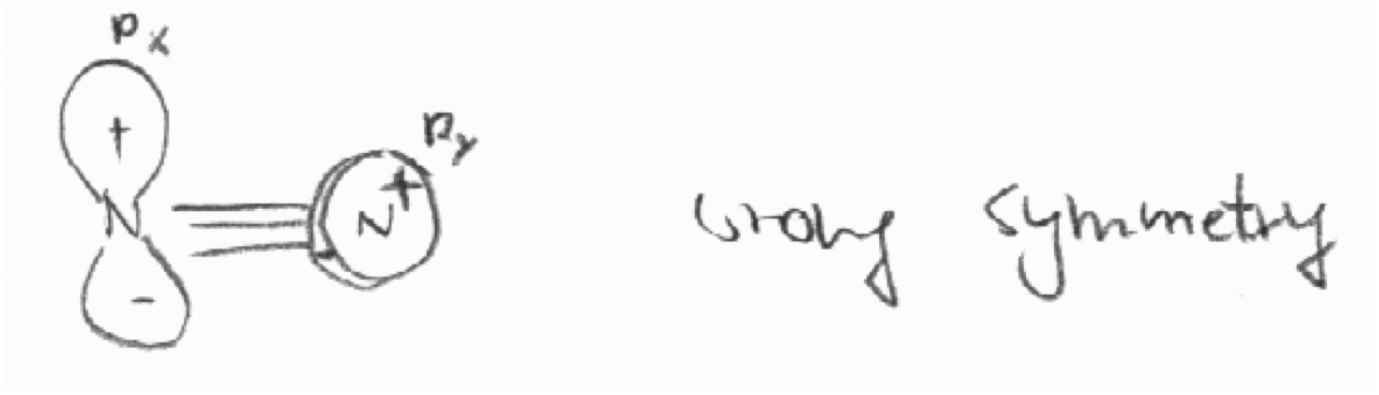
a) orbital overlap in sigma-fashion

Exercise 3

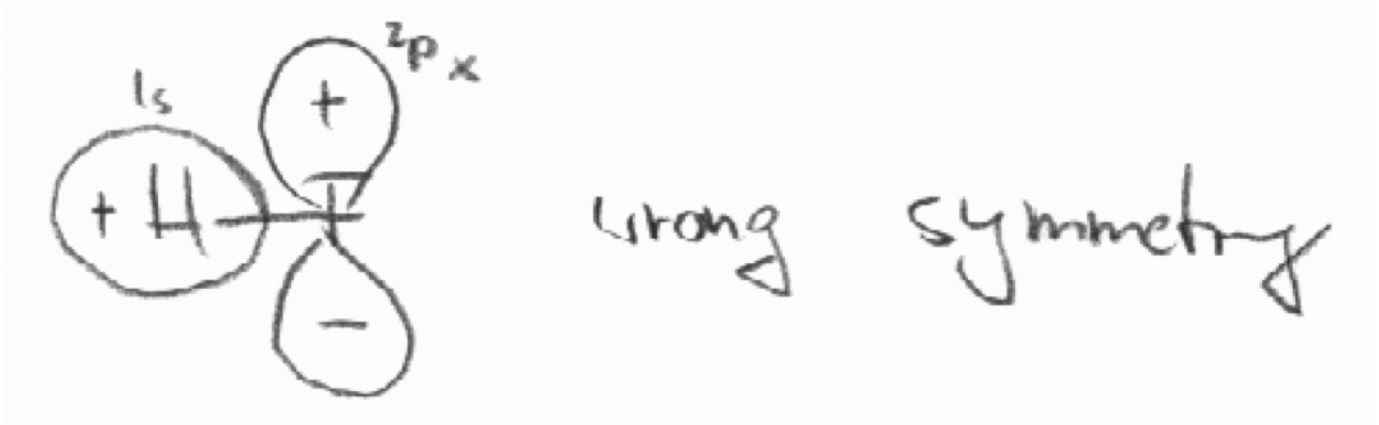


Exercise 4

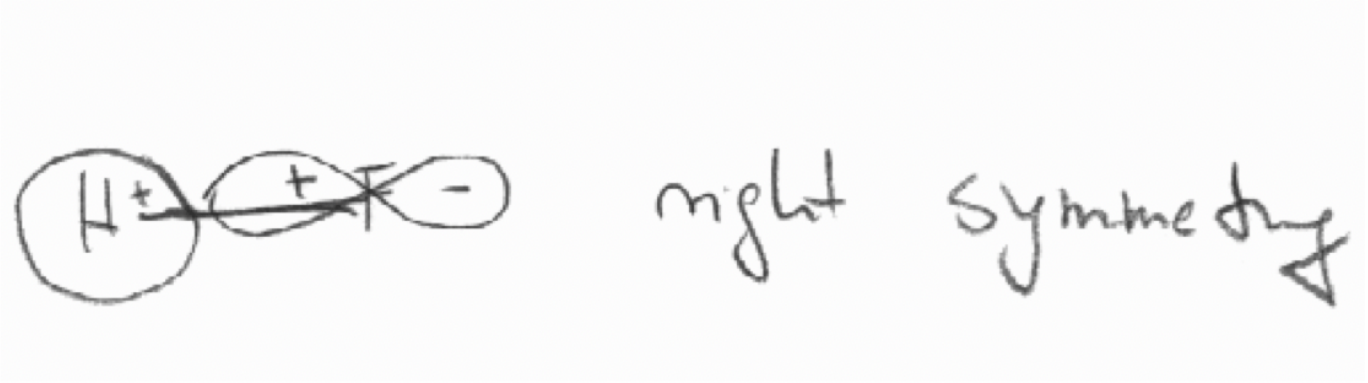
a)



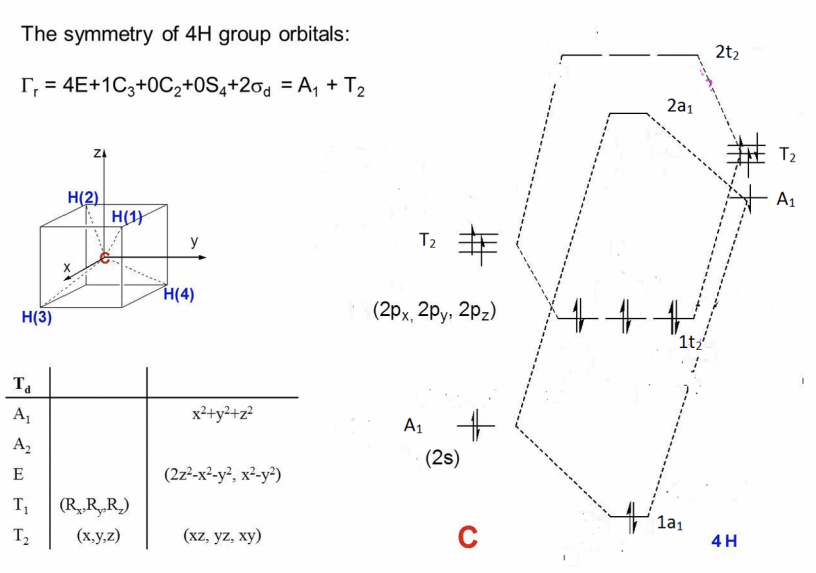
b)



c)



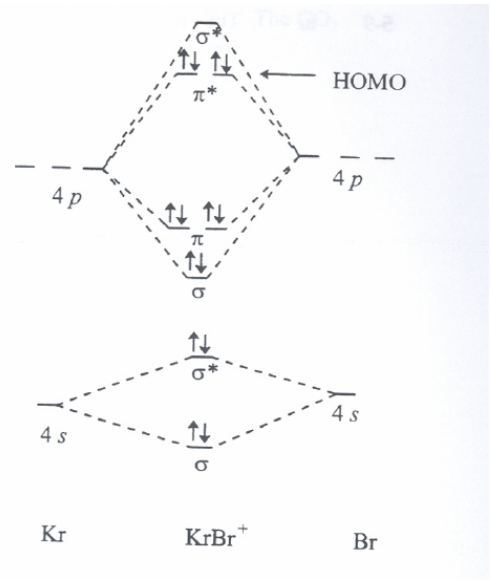
Exercise 5



Exercise 6

1. Determine point group of PCl_5. --> D_{3h}.
2. Decide what are the valence orbitals of the central atom: 3s, 3p
3. Look up the character table of D_{3h}, e.g., in the internet. You will find their symmetries to be: A_1' (3s), A_2'' ($3p_z$), E'($3p_x$, $3p_y$)

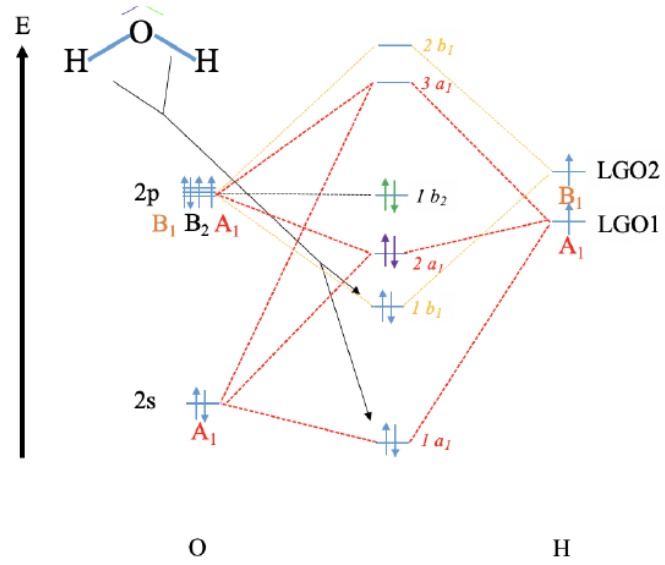
Exercise 7



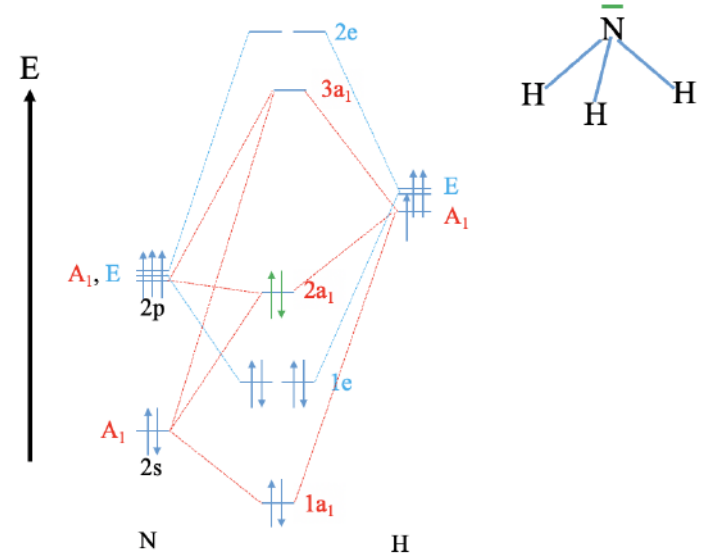
Orbital energies of Kr must be somewhat lower than the ones of Br because the electrons experience higher effective nuclear charge (Z_{eff} increases within a period). This means that the antibonding HOMO is polarized towards Br (HOMO energetically closer to 4p(Br) than 4p(Kr)).

Exercise 8

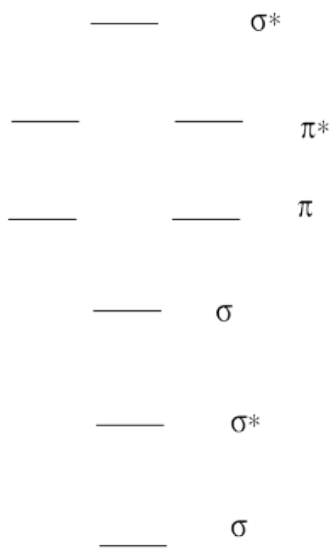
Water



NH_3



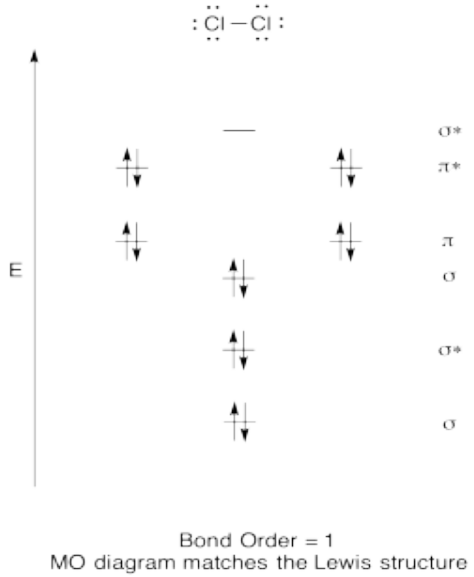
Exercise 4.*P*.1



Exercise $4.P.2$

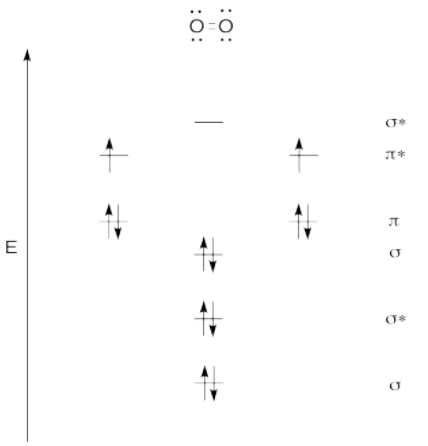
- Count the valence electrons on the molecule. That's the number of valence electrons on each atom, adjusted for any charge on the molecule. (eg C_2^{2-} has 10 valence electrons: 4 from each carbon -- that's 8 -- and two more for the 2- charge).
- Fill electrons into the lowest energy orbitals first.
- Pair electrons after all orbitals at the same energy level have one electron.

Exercise $4.P.3$



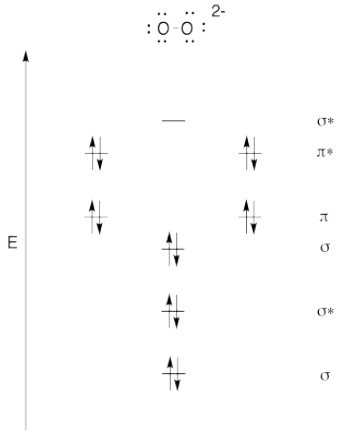
Bond Order = 1
MO diagram matches the Lewis structure

Exercise $4.P.4$



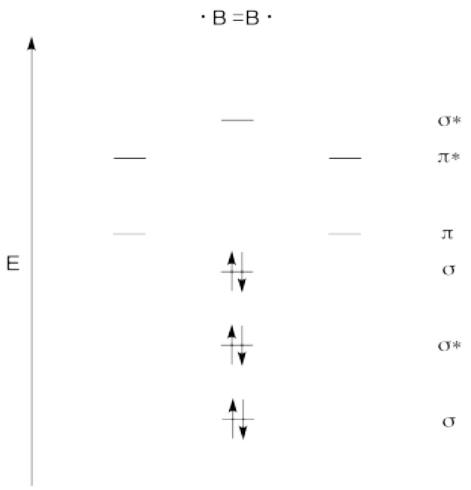
Bond Order = 2
MO diagram indicates two unpaired electrons and therefore does not match the Lewis structure. Based on the MO diagram oxygen would be paramagnetic and would be attracted to a magnetic field

Exercise $4.P.5$



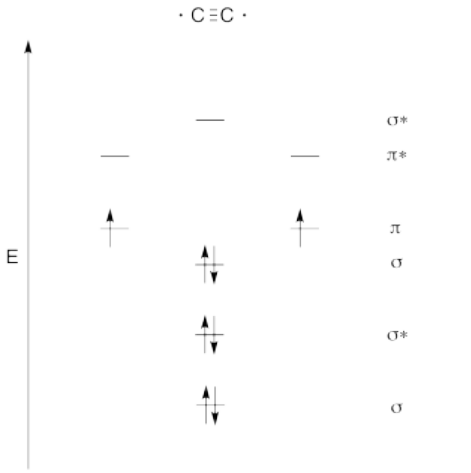
Bond Order = 1
MO diagram matches the Lewis structure. Both predict a Bond Order of 1 and 6 lone pairs of electrons. The addition of two electrons to O_2 to O_2^{2-} would be possible.

Exercise $4.P.6$



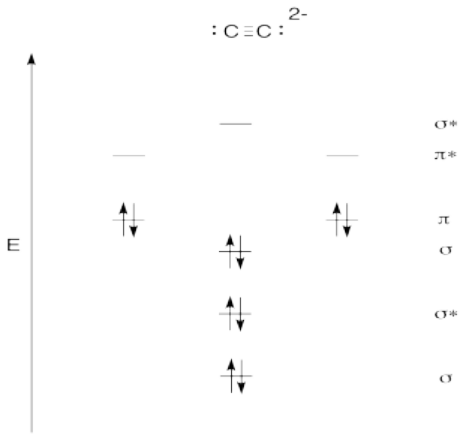
Bond Order = 1
Boron-Boron bonding should be possible

Exercise $4.P.7$



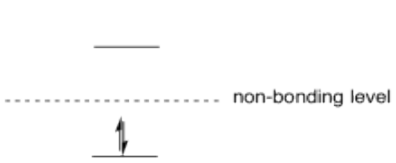
Bond Order = 2
MO diagram does not match the Lewis structure.
However, the MO diagram does concur about the
2 unpaired electrons.

Exercise $4.P.8$

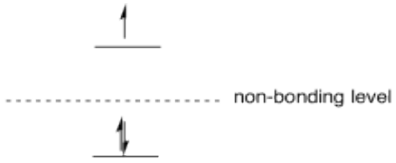


Bond Order = 3
MO diagram matches the Lewis structure. Both predict a Bond Order of 3 and 2 lone pairs of electrons. The addition of two electrons to C_2 to C_2^{2-} would be possible.

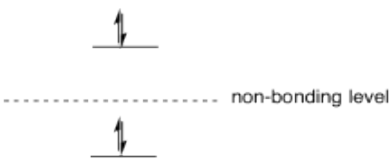
Exercise $4.P.9$



I'm stable!!!
And I have ONE FULL BOND!!!!



I'm kinda stable I guess...
Still got a half a bond...
Don't worry about me...



Not stable together.
No bonds here.

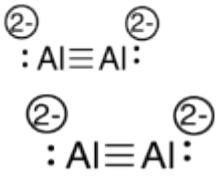
Exercise $4.P.10$

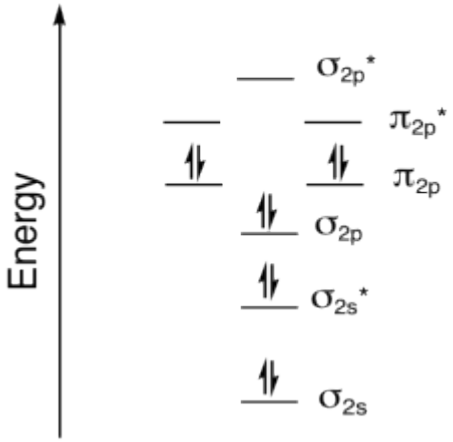
a) Na, because Na has a lower ionization potential (and a lower electronegativity) than Al.

b) Al

c) 4-, because there are four Na^+

d) total e^- = 2 x 3 e^- (per Al) + 4 e^- (for the negative charge) = 10 e-





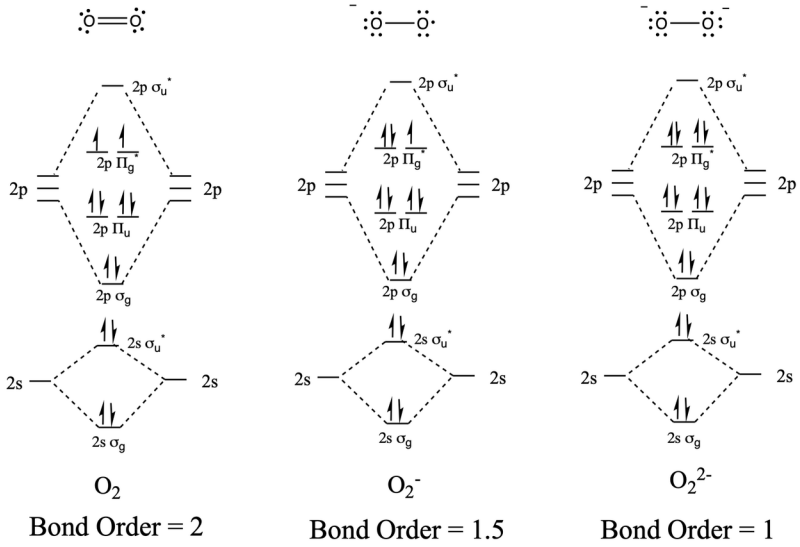
g) bond order $= \frac{(\#bonding\ e^- - \#antibonding\ 3^-)}{2} = \frac{8-2}{2} = 3$

Exercise $4.P.1$

Add texts here. Do not delete this text first.

Exercise $4.P.1$

The Lewis structures and MO diagrams are shown below. In general, the bond order derived from the MO diagram agrees with the Lewis structure for each species. In the case of the two ions, the number of unpaired electrons from MO theory and the Lewis structure also agrees. In the case of dioxygen, however, there is an inconsistency between the Lewis representation and the MO diagram. While the Lewis structure would lead us to believe that all electrons are paired, the MO diagram indicates paramagnetism, with two unpaired electrons. The MO diagram explains the magnetic behaviour of dioxygen.



Exercise $4.P.1$

Add texts here. Do not delete this text first.

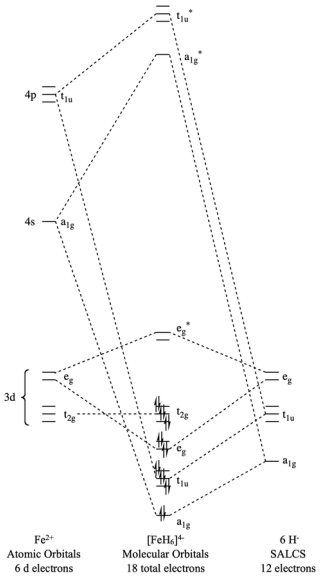
Exercise $4.P.1$

Add texts here. Do not delete this text first.

Exercise $4.P.1$

Add texts here. Do not delete this text first.

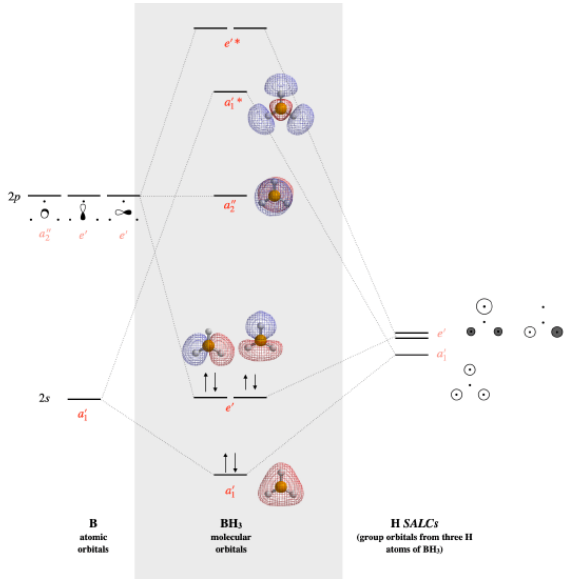
Exercise $4.P.1$



Exercise $4.P.1$

The calculated MO diagram is shown below.

- a_2'' is the lone non-bonding orbital.
- The HOMO is the a_2'' nonbonding orbital, the LUMO is a bonding e' set of two degenerate orbitals/
- e' is doubly degenerate
- The bond order is 3



This page titled 4.P: Problems is shared under a CC BY-NC-SA 4.0 license and was authored, remixed, and/or curated by LibreTexts.

- Concept Review Questions Chapter 3 by Kai Landskron is licensed CC BY 4.0.
- Homework Problems Chapter 3 by Kai Landskron is licensed CC BY 4.0.
- 13.6: Assembling the Complete Diagram and Electron Population by Chris Schaller is licensed CC BY-NC 3.0. Original source: https://employees.csbsju.edu/cschaller/structure.htm.

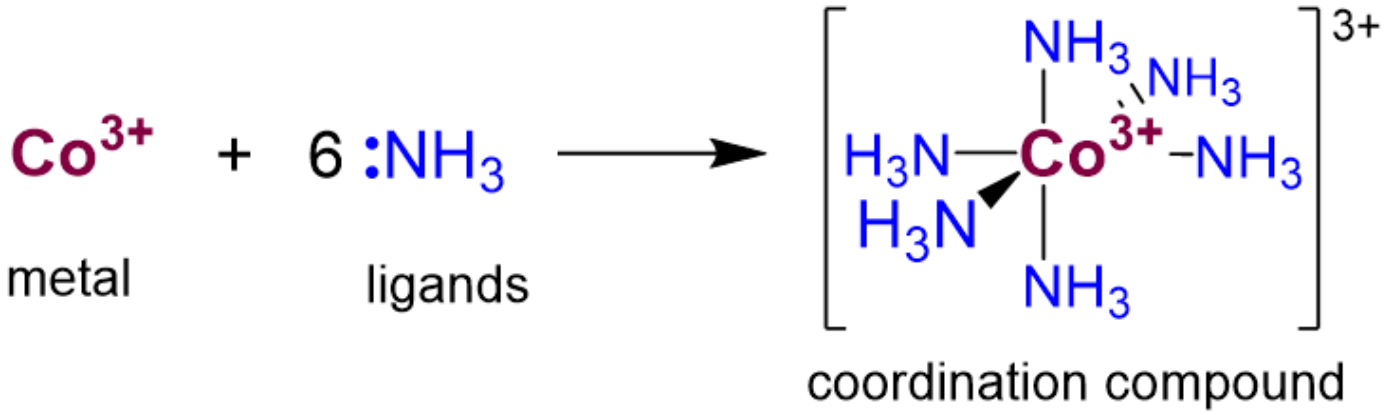
5: COORDINATION CHEMISTRY I - STRUCTURE AND ISOMERS

Coordination compounds are important to all areas of chemistry, engineering, the life and environmental sciences, and beyond. In the synthetic laboratory catalytic amounts of coordination compounds enable organic chemists to synthesize new compounds selectively and in high yield under mild condition. Applied industrially, coordination compound catalysts serve as vital catalysts that facilitate the conversion of raw petrochemical or bio-derived feedstocks into useful industrial and consumer products. Without them life as we know it would be impossible as many biochemical systems are coordination complexes. Examples include the hemoglobin which transports oxygen around our bodies and the myoglobin which stores it, the photosystems which harvest light and use light energy in photosynthesis, the constituents of the respiratory chain, and many of the enzymes involved in the expression and transmission of genetic information. In studying coordination chemistry you are about to take your first steps into a vast and exciting world.

What is a coordination compound?

Coordination compounds consist of one or more **metals** bound to one or more Lewis base **ligands**. For example, hexammineruthenium(3+) ion is a coordination complex in which six ammonia ligands coordinate a Co^{3+} ion, as shown in Scheme 5.I.

Scheme 5.I. Formation of hexammineruthenium(3+) ion from Co^{3+} and NH_3.



(5.1)

Such complexes are called coordination complexes because the ligand-metal bond may be thought of as a **coordinate covalent bond** in which both of the bonding electrons come from the ligand, which is then said to **coordinate** the metal. This coordinate covalent model is a very useful formalism for understanding the basic features of coordination chemistry, although it does not always accurately reflect the actual details of the bonding in every coordination complex. Nevertheless, even in those cases where the simple coordinate covalent bond model breaks down the coordinate covalent bond concept supplies the language sophisticated models employ to describe the more complex bonding involved.

Additional important terms

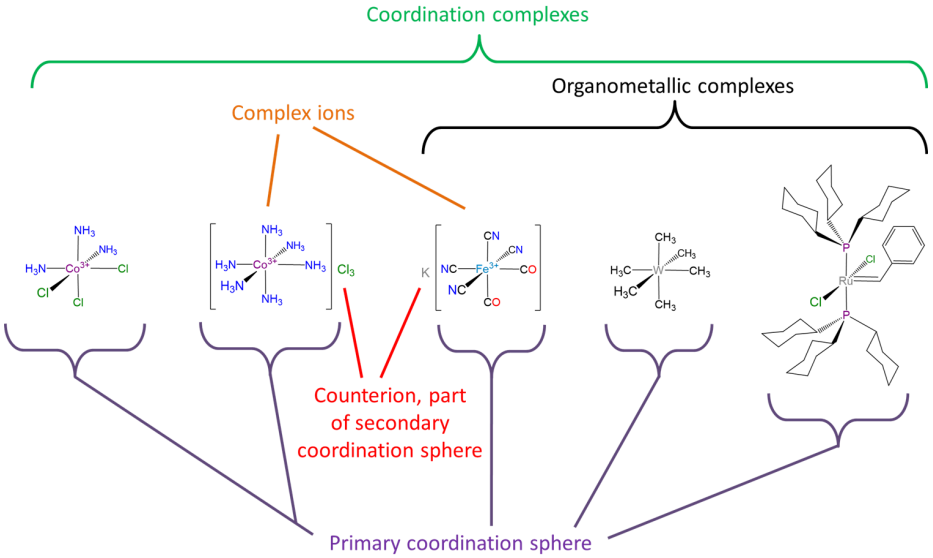
Some of the common widely terms that follow from the coordinate covalent model of bonding in coordination complexes include

- Coordination compounds are also called **coordination complexes**, **metal complexes**, or just **complexes**. The term **complex** refers to coordination compounds' composite nature, in that they may be thought of as comprised of multiple ligand and metal ion parts that can be restored by breaking the coordinate covalent bonds holding the complex together. This is in contrast to inorganic or organic molecules which are more commonly thought about as whole molecules held together by the sharing of electrons contributed by all the atoms.
- Coordination complexes that are ions are called **complex ions.**

- Ligands bound to the coordination complex are said to reside in the **primary** or **inner coordination sphere**. These bound ligands are not readily exchangeable, in contrast to nearby counterions and solvent molecules, which are said to reside in the **secondary** or **outer coordination sphere**.
- The portion of the complex contributing the electron pairs is said to be the **donor** and the portion which receives them the **acceptor**. In conventional coordination compounds the ligand is the donor and the metal the acceptor. In these cases it would be equally convenient to refer to the ligand donor as the Lewis base and the metal acceptor as the Lewis acid. However, in more complex bonding scenarios there may be multiple electron pair donation and acceptance interactions taking place between each pair of atoms and donor-acceptor language will be more convenient.
- The number of ligand sites donating lone pairs to the central atom is referred to as the **coordination number**. For most complexes this will just be equal to the number of ligand atoms bound to the metal. In simple complexes it is just equal to the number of ligands. For instance, the cobalt in Scheme 5.I has a coordination number of six.
- Although technically compounds with metal-carbon bonds are coordination complexes term coordination complex is sometimes used to refer to complexes which do not possess metal-carbon bonds in their primary coordination sphere. Complexes which possess metal-carbon bonds are called **organometallic compounds** instead. The use of the terms organometallic and coordination to distinguish organometallic compounds from other types of coordination compounds is often convenient since many organometallic ligands engage in more than simple σ donor acceptor coordinate covalent bond formation with the metal center. However, this is true of some wholly inorganic ligands too so it should always be kept in mind that organometallic compounds are just a type of coordination compound and that inorganic ligands can in principle be tuned in interact with a metal center in much the same way an organic ligand does.

A summary of some of the concepts and terms used to describe coordination compounds is given in Scheme 5.II.

Scheme 5.II. Some terms used to describe coordination compounds. This work by Stephen Contakes is licensed under a Creative Commons Attribution 4.0 International License.



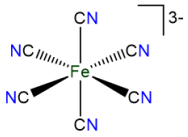
The formulae of coordination complexes

The way the formulae of coordination complexes are written reflects that it is often convenient to think of coordination compounds as a composite of metals and ligands. When writing the formulae of a complex

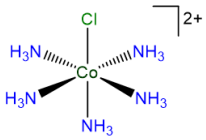
- the atoms of a ligand are not added to those of the rest of the compound. Instead, the ligand atoms are kept together, if necessary by enclosing the ligand formula in parentheses or giving an abbreviation for the ligand.
- For complex ions the metal and ligands are enclosed in square brackets. Sometimes this is also done for neutral coordination compounds as well. In either case the brackcets enclose those parts of the compound which comprise the primary coordination sphere; anything else is in the secondary coordination sphere outside.

A careful perusal of the examples in Scheme 5.III should make the important features of this system clear.

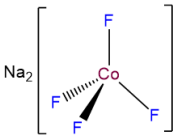
Scheme 5.III. Formulae of coordination compounds and complex ions.



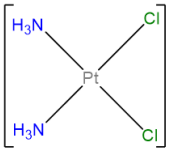
$[Fe(CN)_6]^{3-}$



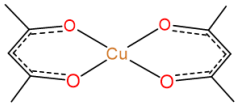
$[CoCl(NH)_5]^{2+}$



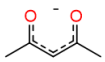
$Na_2[CoF_4]$



$PtCl_2(NH_3)_2$



$[Cu(acac)_2]$

acac = 

Contributors and Attributions

Stephen Contakes, Westmont College

Unless otherwise noted, all line drawings on this page are by Stephen Contakes and licensed under a Creative Commons Attribution 4.0 International License.

5.1: History

5.2: Nomenclature and Ligands

5.3: Isomerism

5.4: Coordination Numbers and Structures

5.5: Coordination Frameworks

5.6: Hard and Soft Acids and Bases

5.6.1: Quantitative Measures of Hardness, Softness, and Acid-Base Interactions from a Hard Soft Acid-Base Principle perspective involve orbital energies and or apportioning acid-base bonding in terms of electrostatic and covalent factors

5.6.2: Hard-Hard and Soft-Soft preferences may be explained and quantified in terms of electrostatic and covalent and electronic stabilization on the stability of Lewis acid-base adducts

This page titled 5: Coordination Chemistry I - Structure and Isomers is shared under a license and was authored, remixed, and/or curated by LibreTexts.

- 9: Coordination Chemistry I - Structure and Isomers by Stephen Contakes is licensed CC BY 4.0.

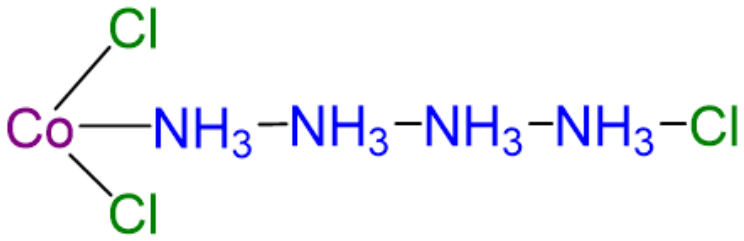
5.1: History

History of the Coordination Compounds

Coordination compounds have been known and used since antiquity; one of the oldest synthetic pigments is the blue pigment Egyptian blue, a copper complex of formula $CaCuSi_4O_{10}$ used by the Egyptians since the third Millenium B.C. (in ancient China the Ba analogue, Han blue, was discovered independently). The blue color of Egyptian blue is due to interlocked $Cu(Si_2O_7)_4$ units in which each copper is coordinated by four O atoms in a square planar arrangement. Later, in 1706, the Berlin painter Diesbach would discover another deep blue pigment, Prussian blue: $KFe_2(CN)_6$.

Despite their long use, the chemical nature of coordination compounds was unclear for a number of reasons. For example, many compounds called "double salts" were known, such as $AlF_3 \cdot 3\,KF$, $Fe(CN)_2 \cdot 4\,KCN$, and $ZnCl_2 \cdot 2\,CsCl$, which were combinations of simple salts in fixed and apparently arbitrary ratios. Why should $AlF_3 \cdot 3\,KF$ exist but not $AlF_3 \cdot 4\,KF$ or $AlF_3 \cdot 2\,KF$? And why should a 3:1 KF:AlF_3 mixture have different chemical and physical properties than either of its components? Similarly, adducts of metal salts with neutral molecules such as ammonia were also known—for example, $CoCl_3 \cdot 6\,NH_3$, which was first prepared sometime before 1798. Like the double salts, the compositions of these adducts exhibited fixed and apparently arbitrary ratios of the components. For example, $CoCl_3 \cdot 6\,NH_3$, $CoCl_3 \cdot 5\,NH_3$, $CoCl_3 \cdot 4\,NH_3$, and $CoCl_3 \cdot 3\,NH_3$ were all known and had very different properties, but despite all attempts, chemists could not prepare $CoCl_3 \cdot 2\,NH_3$ or $CoCl_3 \cdot NH_3$.

Although the chemical composition of such compounds was readily established by existing analytical methods, their chemical nature was puzzling and highly controversial. The major problem was that what we now call valence (i.e., the oxidation state) and coordination number were thought to be identical. As a result, highly implausible (to modern eyes at least) structures were proposed for such compounds. Of these the most influential was the Blomstrand-Jørgensen chain theory of bonding in coordination compounds, which predicted the "Chattanooga choo-choo" model for $CoCl_3{\cdot}4NH_3$ shown in Scheme 5.1.I.



Scheme 5.1.I. Blomstrand-Jørgensen chain theory model of bonding in $CoCl_3{\cdot}4NH_3$.

Nevertheless, this theory was not wholly illogical and, in fact, explained much of the analytical data on coordination compounds available to chemists of the time. This data included the electrical conductivity of aqueous solutions of these compounds, which was roughly proportional to the number of ions formed per mole, and the number of free chloride ions present, which could be determined by precipitating them gravimetrically as AgCl. In the case of $CoCl_3{\cdot}4NH_3$, two ions and one chloride were produced when the compound was dissolved in water, which Jørgensen was able to explain using the chain structure shown above by postulating that chlorides attached to NH_3 could dissociate while those attached to Co could not. The modern theory of coordination chemistry, which overthrew the chain theory, is based largely on the work of Alfred Werner (1866–1919; Nobel Prize in Chemistry in 1913). In a series of careful experiments carried out in the late 1880s and early 1890s, he examined the properties of several series of metal halide complexes with ammonia. For example, five different "adducts" of ammonia with $PtCl_4$ were known at the time: $PtCl_4{\cdot}nNH_3$ (n = 2–6). Some of Werner's original data on these compounds are shown in Table 5.1.1. Werner's data on $PtCl_4{\cdot}6NH_3$ in Table 5.1.1 showed that all the chloride ions were present as free chloride. In contrast, $PtCl_4{\cdot}2NH_3$, was a neutral molecule that did not give free chloride ions when dissolved in water.

Alfred Werner (1866–1919)

Werner, the son of a factory worker, was born in Alsace. He developed an interest in chemistry at an early age, and he did his first independent research experiments at age 18. While doing his military service in southern Germany, he attended a series of chemistry lectures, and he subsequently received his PhD at the University of Zurich in Switzerland, where he

was appointed professor of chemistry at age 29. He won the Nobel Prize in Chemistry in 1913 for his work on coordination compounds, which he performed as a graduate student and first presented at age 26. Apparently, Werner was so obsessed with solving the riddle of the structure of coordination compounds that his brain continued to work on the problem even while he was asleep. In 1891, when he was only 25, he woke up in the middle of the night and, in only a few hours, had laid the foundation for modern coordination chemistry.

Table 5.1.1*: Werner's Data on Complexes of Ammonia with* $PtCl_4$

Complex	Conductivity (ohm^{-1})	Number of Ions per Formula Unit	Number of Cl^- Ions Precipitated by Ag^+
$PtCl_4{\cdot}6NH_3$	523	5	4
$PtCl_4{\cdot}5NH_3$	404	4	3
$PtCl_4{\cdot}4NH_3$	299	3	2
$PtCl_4{\cdot}3NH_3$	97	2	1
$PtCl_4{\cdot}2NH_3$	0	0	0

These data led Werner to postulate that metal ions have two different kinds of valence: (1) a primary valence (oxidation state) that corresponds to the positive charge on the metal ion and (2) a secondary valence (coordination number) that is the total number of ligands bound to the metal ion. If Pt had a primary valence of 4 and a secondary valence of 6, Werner could explain the properties of the $PtCl_4{\cdot}NH_3$ adducts by the following reactions, where the metal complex is enclosed in square brackets:

$$[Pt(NH_3)_6]Cl_4 \rightarrow [Pt(NH_3)_6]^{4+}(aq) + 4Cl^-(aq) \tag{5.1.1}$$

$$[Pt(NH_3)_5Cl]Cl_3 \rightarrow [Pt(NH_3)_5Cl]^{3+}(aq) + 3Cl^-(aq) \tag{5.1.2}$$

$$[Pt(NH_3)_4Cl_2]Cl_2 \rightarrow [Pt(NH_3)_4Cl_2]^{2+}(aq) + 2Cl^-(aq) \tag{5.1.3}$$

$$[Pt(NH_3)_3Cl_3]Cl \rightarrow [Pt(NH_3)_3Cl_3]^{+}(aq) + Cl^-(aq) \tag{5.1.4}$$

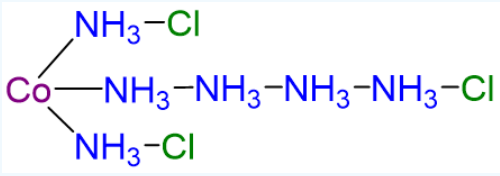
$$[Pt(NH_3)_2Cl_4] \rightarrow [Pt(NH_3)_2Cl_4]^{0}(aq) \tag{5.1.5}$$

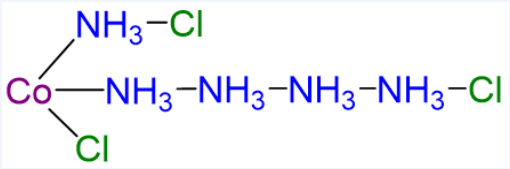
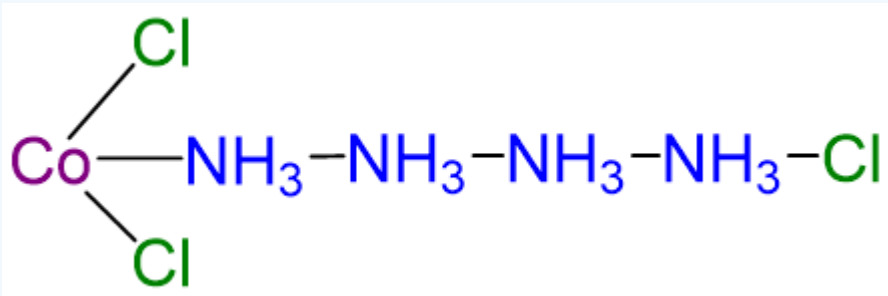
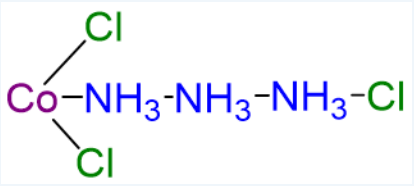
Further work showed that the two missing members of the series—$[Pt(NH_3)Cl_5]^-$ and $[PtCl_6]^{2-}$—could be prepared as their mono- and dipotassium salts, respectively. Similar studies established coordination numbers of 6 for Co^{3+} and Cr^{3+} and 4 for Pt^{2+} and Pd^{2+}.

Exercise 5.1.1. The $CoCl_3xNH_3$ series.

The series $CoCl_3{\cdot}xNH_3$ was particularly important in establishing the correctness of Werner's coordination theory over the rival chain theory. By ~1900 conductivity measurements suggested that the members of the series gave the number of ions shown in Table 5.1.1.

Table 5.1.1. *The CoCl3·xNH3 series according to coordination theory, chain theory, and experiment.*

Compound	Color	Werner formulation	Blomstrand-Jørgensen chain theory formulation	I s
$CoCl_3{\cdot}6NH_3$	yellow	$[Co(NH_3)_6]Cl_3$		4

Compound	Color	Werner formulation	Blomstrand-Jørgensen chain theory formulation	I s
$CoCl_3 \cdot 5NH_3$	violet	$[Co(NH_3)_5Cl]Cl_2$		3
$CoCl_3 \cdot 4NH_3$	green	$[Co(NH_3)_4Cl_2]Cl$		2
$CoCl_3 \cdot 3NH_3$	orange	$[Co(NH_3)_4Cl_3]$		(

What does this data suggest about the relative explanatory power of Werner's coordination theory and chain theory? Explain.

Answer available at the end of this section.

What ultimately convinced Jørgensen of the correctness of Werner's coordination model over his own chain theory was how Werner's explanation of the structure of cobalt coordination complexes using an octahedral coordination geometry explained the existence of isomers in Co complexes containing Cl and NH_3 ligands. In the case of $[Co(NH_3)_4Cl_2]Cl$ two isomers were known: one red and the other green. Because both compounds had the same chemical composition and the same number of groups of the same kind attached to the same metal, there had to be something different about the arrangement of the ligands around the metal ion. Werner's key insight was that the six ligands in $[Co(NH_3)_4Cl_2]Cl$ had to be arranged at the vertices of an octahedron because that was the only structure consistent with the existence of two, and only two, stereoisomers (Figure 5.1.1). His conclusion was also corroborated by the existence of two and only two stereoisomers of the next compound in the series: $Co(NH_3)_3Cl_3$.

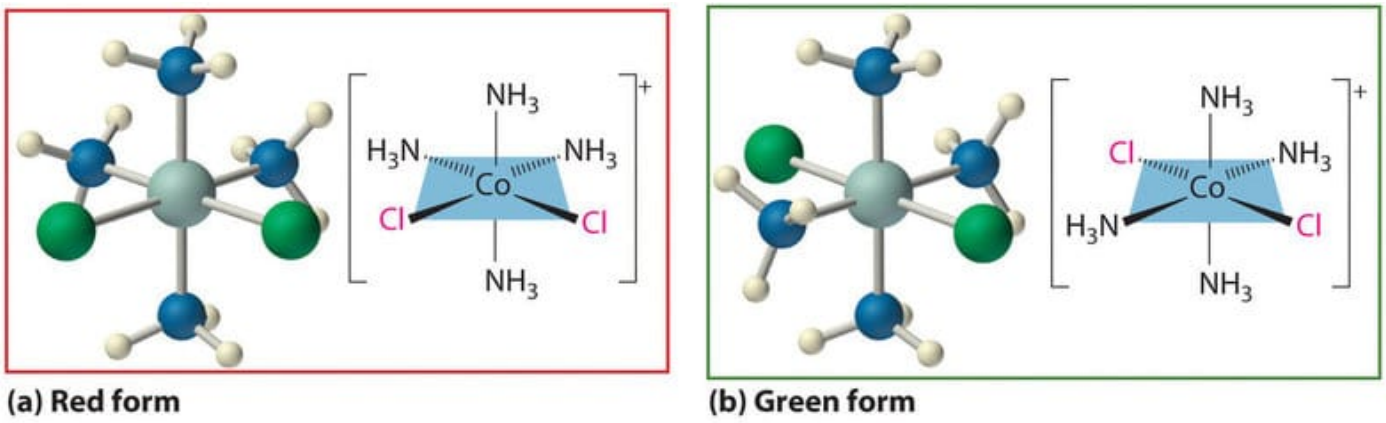


Figure 5.1.1. The $[Co(NH_3)_4Cl_2]^+$ ion can have two different arrangements of the ligands, which results in different colors: if the two Cl^- ligands are next to each other (*cis*), the complex is red (a), but if they are opposite each other (*trans*), the complex is green (b).

Example 5.1.1: Why did Werner propose an octahedral geometry for 6-coordinate complexes?

In Werner's time, many complexes of the general formula MA_4B_2 were known, but no more than two different compounds with the same composition had been prepared for any metal. To confirm Werner's reasoning that this suggests these complexes possess an octahedral geometry, calculate the maximum number of different structures possible for six-coordinate MA_4B_2 complexes with each of the three most symmetrical possible structures the ligands will form about the central metal - a hexagon, a trigonal prism, and an octahedron.

Assuming that the absence of evidence for additional compounds in this case serves as reasonable circumstantial evidence for their absence, what does the fact that no more than two forms of any MA_4B_2 complex were known suggest about the three-dimensional structures of these complexes?

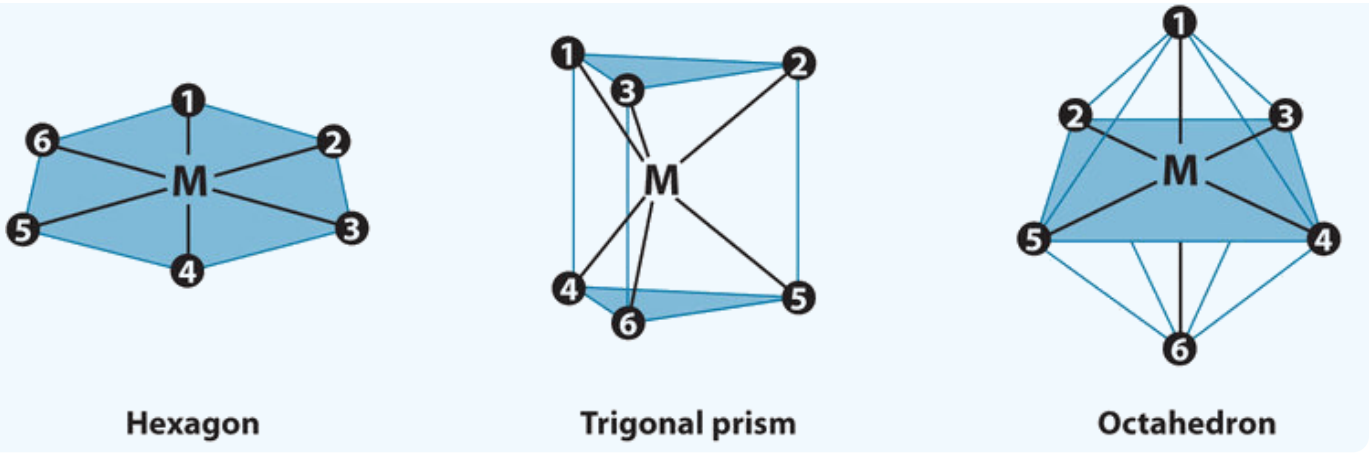
Solution

In this problem you are given

- the stochiometry of the complexes, MA_4B_2
- three possible coordination geometries - hexagonal, trigonal prismatic, and octahedral.

In order to calculate the number of isomers that could be present for each geometry it is best to follow a systematic approach. Since there are fewer B type ligands than A type ligands, the easiest way to do this for each geometry is to start by placing a B ligand at one vertex and then to determine how many different positions are available for the second B ligand.

The three regular six-coordinate structures are shown here, with each coordination position numbered so that we can keep track of the different arrangements of ligands. For each structure, all vertices are equivalent. We begin with a symmetrical MA_6 complex and simply replace two of the A ligands in each structure to give an MA_4B_2 complex:



For the hexagon, we place the first B ligand at position 1. There are now **three** possible places for the second B ligand:

- position 2 (or 6)
- position 3 (or 5)
- position 4

The (1, 2) and (1, 6) arrangements are chemically identical because the two B ligands are adjacent to each other. The (1, 3) and (1, 5) arrangements are also identical because in both cases the two B ligands are separated by an A ligand. Those of you who remember your ogranic chemistry might recognize that this situation is formally analogous to the *ortho*-, *meta*-, and *para*-isomerism in disubstituted benzenes.

Turning to the trigonal prism, we place the first B ligand at position 1. Again, there are three possible choices for the second B ligand:

- at position 2 or 3 on the same triangular face
- position 4 (on the other triangular face but adjacent to 1)
- position 5 or 6 (on the other triangular face but not adjacent to 1).

The (1, 2) and (1, 3) arrangements are chemically identical, as are the (1, 5) and (1, 6) arrangements.

In the octahedron, however, if we place the first B ligand at position 1, then we have only two choices for the second B ligand:

- position 2 (or 3 or 4 or 5)
- position 6.

In the latter, the two B ligands are at opposite vertices of the octahedron, with the metal lying directly between them. Although there are four possible arrangements for the former, they are chemically identical because in all cases the two B ligands are adjacent to each other.

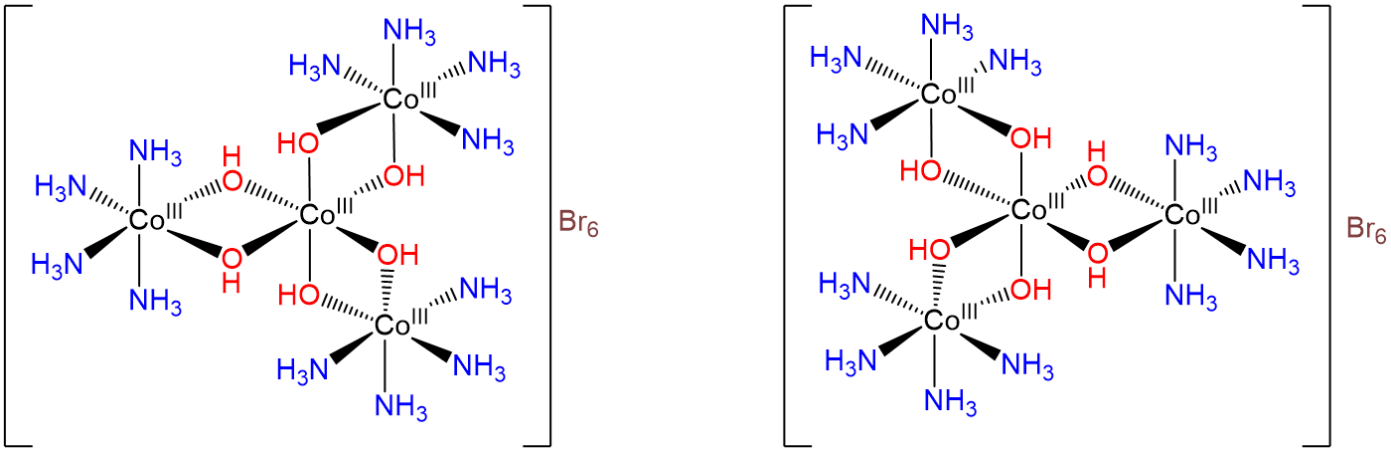
The number of possible MA_4B_2 arrangements for the three geometries is thus: hexagon, 3; trigonal prism, 3; and octahedron, 2. The fact that only two different forms were known for all MA_4B_2 complexes that had been prepared suggested that the correct structure was the octahedron but did not prove it. For some reason one of the three arrangements possible for the other two structures could have been less stable or harder to prepare and had simply not yet been synthesized. When combined with analogous results for other types of complexes (e.g., MA_3B_3), however, the data were best explained by an octahedral structure for six-coordinate metal complexes.

Exercise 5.1.1

Determine the maximum number of structures that are possible for a four-coordinate MA_2B_2 complex with either a square planar or a tetrahedral symmetrical structure.

Answer available at the end of this section.

Even Werner's explanation of isomerism in coordination complexes in terms of octahedral and other recognized coordination geometries did not convince all chemists until he was able to resolve a racemic mixture of *d*- and *l*-$[Co\{Co(NH3)_4(OH)_2\}_3]$ into its enantiomers, which are shown in Scheme 5.1.**II**. By doing so Werner demonstrated to chemists of his time (virtually none of whom knew group theory) that tetrahedral carbon atoms were not required for chirality; D_3 octahedral complexes were also chiral.



Scheme 5.1.II: d- and l-enantiomers of $[Co\{Co(NH3)_4(OH)_2\}_3]$, colloquially referred to as hexol. This work by Stephen Contakes is licensed under a Creative Commons Attribution 4.0 International License.

Answers

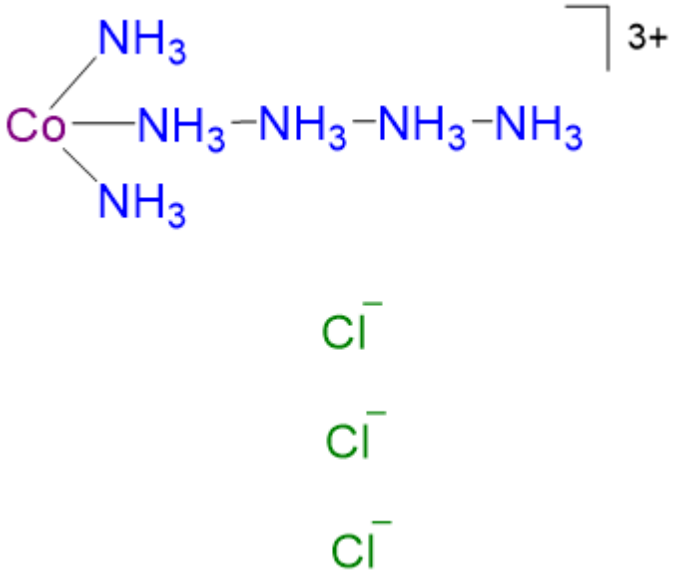
Exercise 5.1.1**. The $CoCl_3xNH_3$ series.**

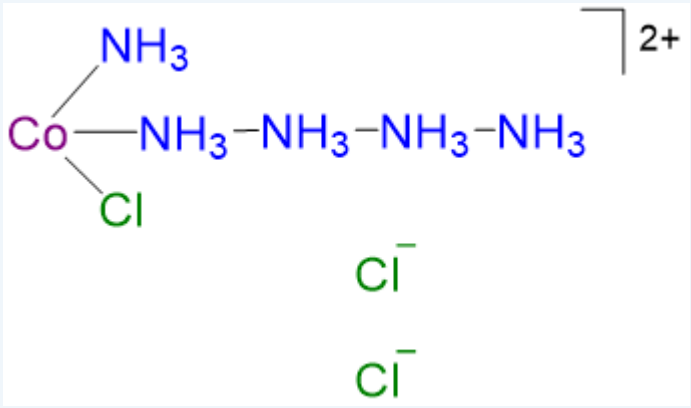
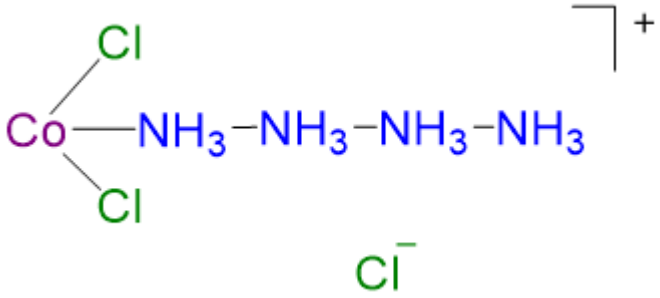
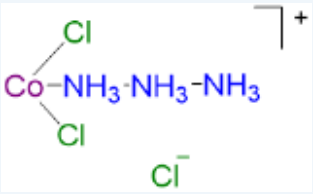
Remember that

- chain theory predicts that the number of ions is the number formed when the Cl atoms bound in a chain with NH_3 dissociate.
- coordination theory predicts the number of ions based on the number of complex ions and their counterions.

Based on this the predictions of coordination theory and chain theory can be compared with the experimental data, as is done in Table 5.1.2.

Table 5.1.2*: Comparison of ions predicted for the $CoCl_3{\cdot}xNH_3$ series by coordination theory and chain theory with the number obse experimentally.*

Compound	Color	Ions predicted by Werner's coordination theory	Number of ions predicted by coordination theory	Ions predicted by Blomstrand-Jørgensen chain theory	Numbe of ion predict by cha theory
$CoCl_3{\cdot}6NH_3$	yellow	$[Co(NH_3)_6]^{3+}$ Cl^- Cl^- Cl^-	4		4

Compound	Color	Ions predicted by Werner's coordination theory	Number of ions predicted by coordination theory	Ions predicted by Blomstrand-Jørgensen chain theory	Numbe of ion predict by cha theory
$CoCl_3 \cdot 5NH_3$	violet	$[Co(NH_3)_5Cl]^{2+}$ Cl^- Cl^-	3		3
$CoCl_3 \cdot 4NH_3$	green	$[Co(NH_3)_4Cl_2]^{+}$ Cl^-	2		2
$CoCl_3 \cdot 3NH_3$	orange	None	0		2

As can be seen by comparing the number of ions predicted by coordination and chain theory in Table 5.1.2, coordination theory successfully explains all the observed ion counts, while chain theory fails to explain the lack of ions observed for $CoCl_3 \cdot 3NH_3$.

Nevertheless, as is often the case when developing theoretical models using data from real experimental investigations, these observations did not convince Jørgensen, who could point to the experimental difficulty of determining the number of ions present from solution conductivity data.

Exercise 5.1.1

square planar, 2; tetrahedral, 1

This page titled 5.1: History is shared under a license and was authored, remixed, and/or curated by LibreTexts.

- 24.1: Werner's Theory of Coordination Compounds by Anonymous is licensed CC BY-NC-SA 4.0.

5.2: Nomenclature and Ligands

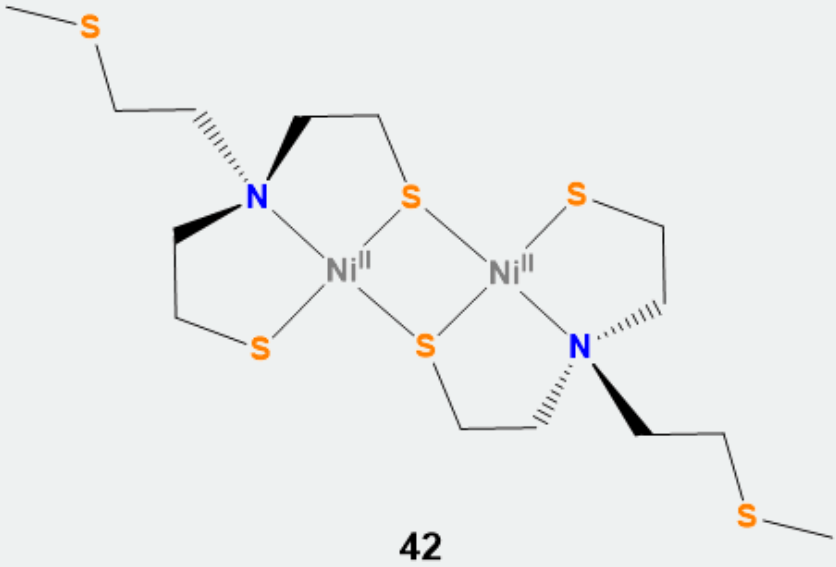
Systems of nomenclature and formulae are intended as tools, to be employed insofar as they are useful

There are well-established rules for both naming and writing the formulae of coordination compounds. The purpose of these rules is to facilitate clear and precise communication among chemists. As with all such rules, some are more burdensome than others to employ, and some serve more crucial roles in the communication process while others are more peripheral - and all are poorly used in the service of pedantic tyranny, especially when used against those who are otherwise doing good work. For this reason, you are urged to approach the rules in a spirit of generosity towards others in

- naming and writing formulas as reasonably accurately as you can so that ligands and metals are where readers expect them and thus can understand what you mean more easily.
- being gracious towards the many professional inorganic chemists who adhere loosely to some of the rules you are about to learn.
- recognizing that in cases when a structure is particularly complex and a picture may make be particularly useful, you should supply one (See the note below).

Note 5.2.1: Sometimes the most helpful name to give a compound is 42.

Even though the IUPAC nomenclature rules permit specification of even the most complex structures, it is often much easier and more effective to supply a numbered structure that can be referred to instead of the IUPAC name. Consider bis{[(μ-2-mercaptoethyl)(2-mercaptoethyl)-methylthioethylaminato (2-)]Nickel(II)}. Which is easier, to expect readers and hearers to work out the structure from that name or to just refer them to compound **42** in Scheme 5.2.I?



42

Scheme 5.2.I. Structure of bis{[(μ-2-mercaptoethyl)(2-mercaptoethyl)-methylthioethylaminato (2-)]Nickel(II)}. The authors of the synthesis of this compound in Inorganic syntheses1 may have had to figure out an IUPAC name for this compound but if you have this scheme in your paper and your instructor is OK with it you can just call it **42**

Coordination Complexes are named as the ligand derivatives of a metal

A variety of systems have been used for naming coordination compounds since the development of the discipline in the time of Alfred Werner. In this section the most common approaches as they are currently used by practicing chemists will be described. Those who need a more thorough and accurate acquaintance with the full IUPAC nomenclature rules are encouraged to consult

the IUPAC brief guide to inorganic nomenclature followed by complete guidelines, commonly known as the IUPAC red book. If those are still not enough a careful read of note 5.2.1 is suggested.

The systems for naming coordination compounds used at present are additive, meaning that they consider coordination compounds as comprising a central metal to which are added ligands. To specify the structure and bonding in this metal-ligand complex then involves:

1. when there are several different ways of attaching the metal and ligands, specifying the structural or stereoisomer
2. systematically listing the ligands in a way that, as necessary, conveys information about how they are linked to the metal and their stereochemistry
3. providing the identity of the metal and its oxidation state, or if the oxidation state is unclear, at least the overall charge on the complex
4. specifying any counterions present

Since the stereochemistry of coordination compounds forms the subject of the next section, in this section it will be addressed by simply giving the prefixes that designate stereochemistry as if they were self-evident. Do not worry about these for now. They will make sense after you have learned more about stereochemistry in the next section. At that time, you can go back over the examples in that section to solidify your understanding of how to name coordination compounds.

However, in order to name coordination compounds accurately you will need to learn how to think about and name ligands first.

Ligands

Ligands are classified based on whether they bind to the metal center through a single site on the ligand or whether they bind at multiple sites. Ligands that bind through only a single site are called **monodentate** from the Latin word for tooth; in contrast, those which bind through multiple sites are called **chelating** after the Greek $\chi\alpha\lambda\epsilon$ for "claw". These relationships are summarized in Figure 5.2.1.

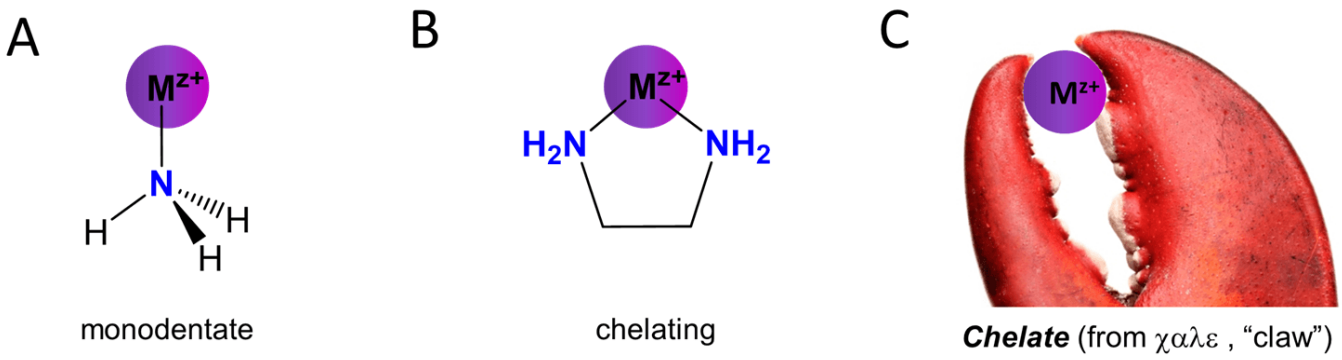
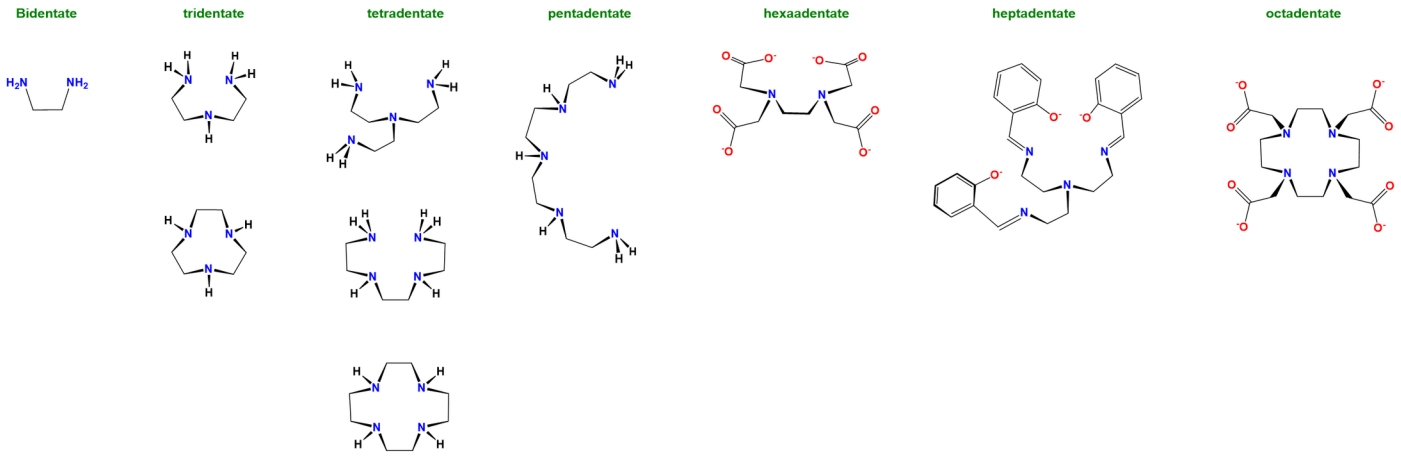


Figure 5.2.1. (A) Ammonia is a monodentate ligand while (B) ethylene diamine is a chelating ligand owing to its capacity to bind metals via its two amine functional groups. (C) Chelating ligands act like a lobster claw in attaching to the metal via multiple sites. The lobster claw image is adapted from https://www.clipart.email/download/1127636.html. Otherwise this work by Stephen Contakes is licensed under a Creative Commons Attribution 4.0 International License.

Following naturally from the classification of non-chelating ligands as monodentate, chelating ligands are further classified according to the number of sites which they can use to bind a metal center. This number of binding sites is called the denticity and ligands are referred to as monodentate (non- chelating), bidentate, tridentate, etc., based on the number of sites available. Ligands with two binding sites have a denticity of two and are said to be bidentate; those with three are tridentate, four tetradentate, and so on. To illustrate this classification system examples of chelating ligands classified according to denticity are given in Scheme 5.2.I.

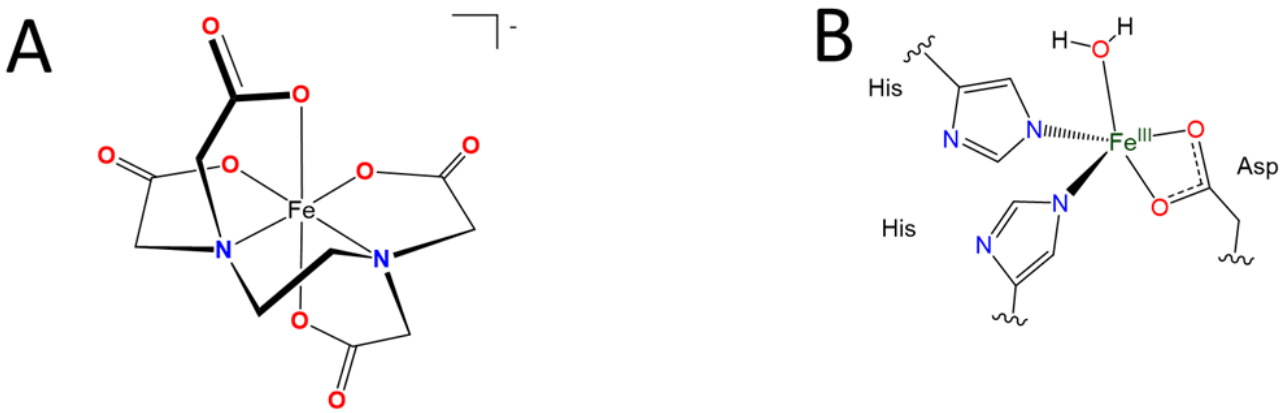
Scheme 5.2.I. A selection of chelating ligands classified according to denticity.



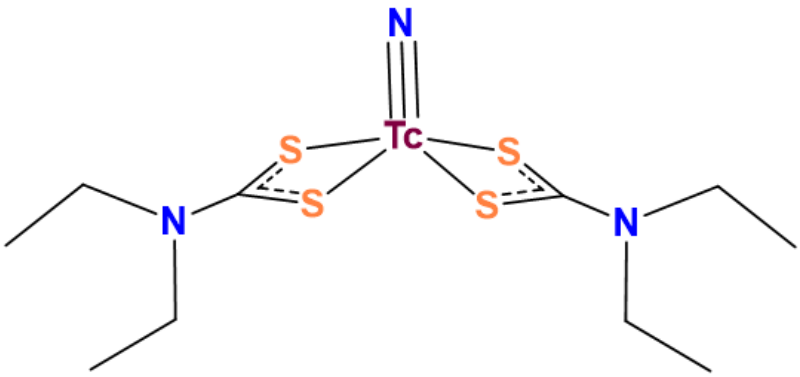
Scheme 5.2.IIA. Because only one oxygen per carboxylate *typically* binds, only one is counted when assigning a ligand's denticity. This work by Stephen Contakes is licensed under a Creative Commons Attribution 4.0 International License.

Although only one carboxylate oxygen *usually* binds to a metal, it is still possible to bind for both oxygens to bind to a single metal. As shown in Scheme 5.2.IIB, complexes in which both carboxylates bind to a metal are known, and in fact are common in the active sites of some enzymes. It is just that the binding of both oxygens gives a strained four-membered ring that is usually unstable.

Scheme 5.2.**II.** (A) Only one oxygen per carboxylate counts towards the denticity of EDTA since on binding the other oxygen generally points away from the metal center, as in the structure of $Fe(EDTA)^-$. (B) In some enzyme active sites both oxygens of a carboxylic acid (aspartate or Asp in this example) bind to a metal. The aspartate carboxylic acid group is bidentate while the EDTA carboxlic acid groups in A are monodentate. This work by Stephen Contakes is licensed under a Creative Commons Attribution 4.0 International License.



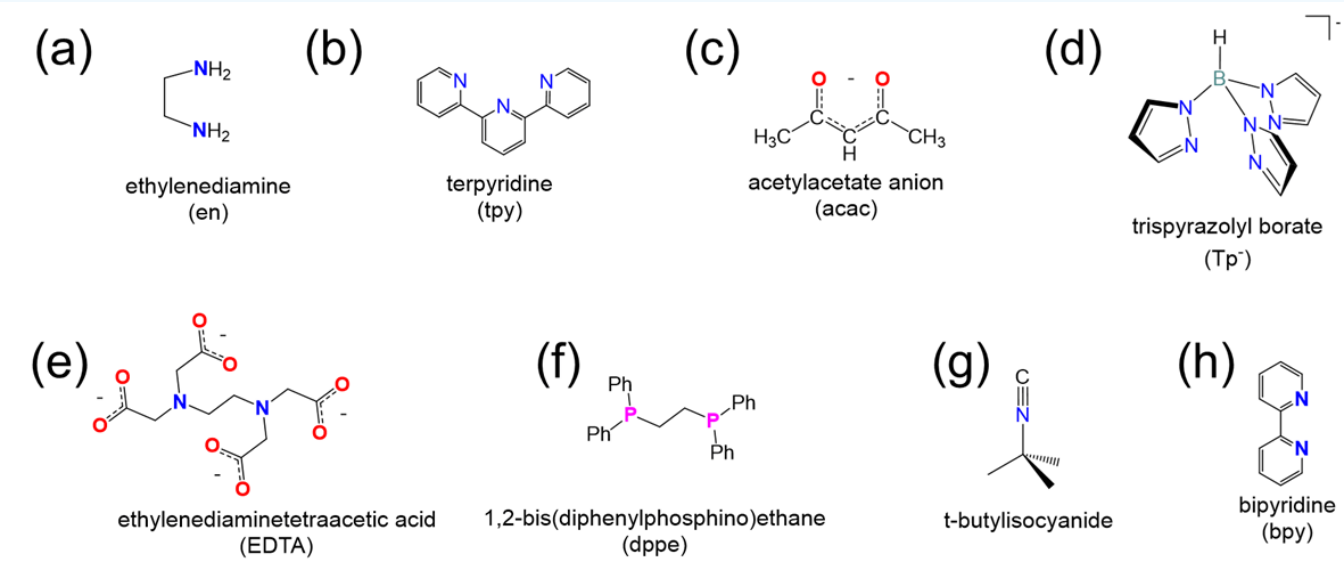
Scheme 5.2.**III.** As in this complex, dithiocarbamates commonly bind metals through both sulfur atoms. Consequently, dithiocarbamates are classified as bidentate. This work by Stephen Contakes is licensed under a Creative Commons Attribution 4.0 International License.



Because of these factors it is technically more correct to say that carboxylates *usually act as* monodentate ligands and dithiocarbamates bidentate ones than it is to say that carboxylates *are* monodentate ligands and dithiocarbamates bidentate ones. So in other words the ligand classifications presented here just represent common binding modes.

Exercise 5.2.1

Determine the denticity of each ligand in the list below and classify them as monodentate, tridentate, etc.



Answer available at the end of this section.

This experimentally-based classification of dithiocarbamates as bidentate and carboxylates as monodentate can be confusing to a beginner. Fortunately, such experimentally based classifications are embedded in the lists of common monodentate ligands as given in Table 5.2.1 and common chelating ligands in Table 5.2.2.

A perusal of the ligands in Table 5.2.1 reveals that several can bind to a metal in multiple ways. For example, thiocyanate, SCN^- can bind metals through its S or N atoms. Such ligands are called **ambidentate ligands**. In naming an ambidentate ligand, the atom through which it attaches to the metal is commonly specified after the ligand name using the italicized element symbol or, more formally, a κ followed by the italicized element symbol. An example is given in Scheme 5.2.I.[2]

Scheme 5.2.I. Two possible binding modes of nitrite acting as a ligand.[3]

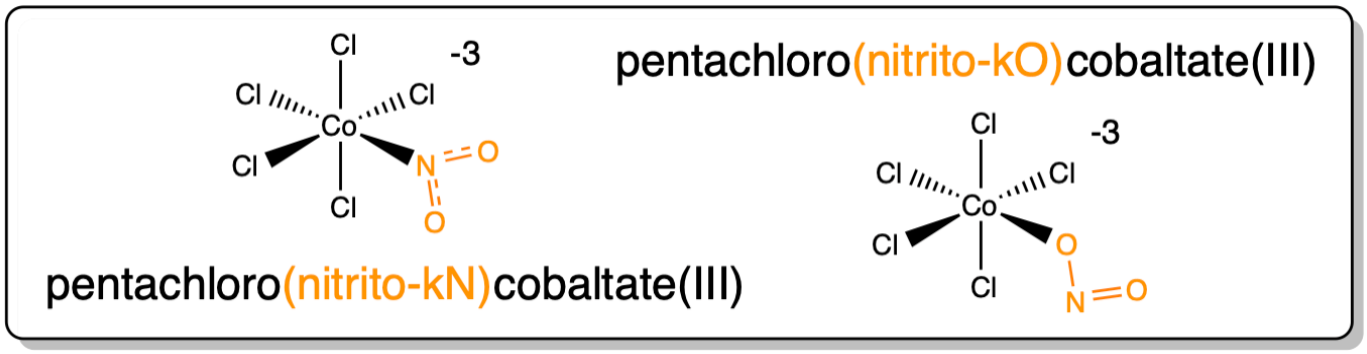
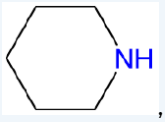
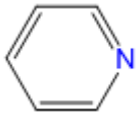
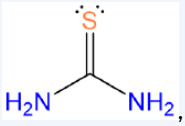


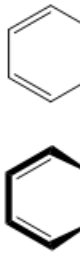
Table 5.2.1. *Common monodentate ligands. Most chemists still prefer common names over the IUPAC ones.*

Ligand	Common name	IUPAC name
H^- (H ligands are always considered anions for naming purposes)	hydrido	hydrido
F^-	fluoro	fluorido
Cl^-	chloro	chlorido
Br^-	bromo	bromido
I^-	iodo	iodido
CN^-, as M-CN	cyano	cyanido or cyanido-κC or cyanido-*C*
CN^-, as M-NC	isocyano	isocyanido or cyanido-κN or cyanido-*N*
CH_3NC	methylisocyanide	methylisocyanide
N_3^-	azido	azido
SCN^-, *e.g.* thiocyanate as M-SCN	thiocyanato	thiocyanato-κS or thiocyanato-S
NCS^-, *e.g.* thiocyanate as M-NCS	isothiocyanato	thiocyanato-κN or thiocyanato-*N*
$CH_3CO_2^-$	acetato	ethanoato
N^{3-}	nitrido	nitrido
NH^{2-}	imido	azanediido
NH_2^-	amido	azanido
NH_3	ammine	ammine
RNH_2, R_2NH, R_3N	alkylamine, dialkylamine, trialkalyamine (*e.g.* methylamine for CH_3NH_2)	alkylamine, dialkylamine, trialkalyamine (*e.g.* methylamine for CH_3NH_2)

Ligand	Common name	IUPAC name
 , piperidine, abbreviated pip	piperidine	piperidine
 , pyridine, abbreviated py	pyridine	pyridine
CH_3CN, acetonitrile, abbreviated MeCN	acetonitrile	acetonitrile
P^{3-}	phosphido	phosphido
PH_3	phosphine	phosphane
PR_3	trialkylphosphine (*e.g.* trimethylphosphine for Me_3P)	trialkylphosphane (*e.g.* trimethylphosphane for Me_3P)
PAr_3	triarylphosphine (*e.g.* triphenylphosphine for Ph_3P)	triarylphosphine (*e.g.* triphenylphosphane for Ph_3P)
 , dimethylsulfoxide or DMSO or dmso	dimethylsulfoxide (sometimes called dimethylsulfoxo but this usage is rare and violates the nomenclature rules for neutral ligands)	(methanesulfinyl)methane or dimethyl(oxido)sulfur
 , thiourea or tu	thiourea	thiourea
O^{2-}	oxo	oxido
OH^-	hydroxo	hydroxido
H_2O	aqua	aqua
S^{2-}	sulfo	sulfo
HS^-	hydrosulfido	hydrosulfido
RS^-	alkanethiolate (*e.g.* ethanthiolate for EtS^-)	thioalkanoate
H_2S	hydrogen sulfide	hydrogen sulfide
R_2S	alkylsulfanylalkane (*e.g.* ethylsulfanylethane for Et_2S)	dialkyl sulfide
O_2	dioxygen	dioxygen
O_2^-, superoxide	superoxido	dioxido(1-) or superoxido
O_2^{2-}, peroxide	peroxido	dioxido(2-) or peroxido
N_2	dinitrogen	dinitrogen

Ligand	Common name	IUPAC name
NO (are always considered neutral for naming purposes)	nitrosyl	nitrosyl
CO	carbonyl	carbonyl
CS	thiocarbonyl	thiocarbonyl
SO, as M-SO	sulfino	sulfur monoxide-κS or sulfur monoxide-*S*
NO_2, as M-NO_2	nitryl	nitrogen dioxide-κN or nitrogen dioxide-*N*
CO_3^{2-}	carbonato	carbonato
NO_2^-, as M-NO_2	nitro or nitrito-*N*	nitrito-κ*N* or nitrito-*N*
NO_2^-, as M-ONO	nitrito or nitrito-*O*	nitrito-κ*O* or nitrito-*O*
NO_3^-	nitrato	nitrato
SO_3^{2-}	sulfito	sulfito
SO_4^{2-}	sulfato	sulfato
$S_2O_3^{2-}$, as M-S-SO_2-O^-	thiosulfato-*S*	thiosulfato-κS or thiosulfato-*S*
$S_2O_3^{2-}$, as M-O-SO_2-S^-	thiosulfato-*O*	thiosulfato-κ*O* or thiosulfato-*O*

Table 5.2.2. *Common chelating ligands organized by denticity. Most chemists use the common names and abbreviations to describe*

Common Ligand name	IUPAC ligand name	abbreviation (if applicable)	structure or ionization s
bidentate ligands			
acetylacetonato	2,4-pentanediono	acac	
R-BINAP and *S*-BINAP	*R*- or *S*-2,2'-bis(diphenylphosphino)-1,1'-binapthyl	BINAP	

Common Ligand name	IUPAC ligand name	abbreviation (if applicable)	structure or ionization s
2,2'-bipyridine	2,2'-bipyridine	bpy or bipy	
cyclooctadiene	1,5-cyclooctadiene	COD	(binding to t
dialkyldithiocarbamato	dialkylcarbamodithiolato	$R_2NCS_2^-$ or dtc	
dimethylgloximato	butanedienedioxime	Hdmg or DMG	
diphenylphosphinoethane or 1,2-(diphenylphosphino)ethane	Ethane-1,2-diylbis(diphenylphosphane)	dppe	
ethylenediamine	Ethane-1,2-diamine	en	
ethylenedithiolato	Ethane-1,2-dithiolato	$C_2H_2S_2^{2-}$	

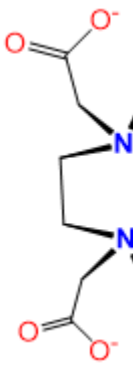
Common Ligand name	IUPAC ligand name	abbreviation (if applicable)	structure or ionization s
nacnac	*N*,*N*'-diphenyl-2,4-pentanediiminato	nacnac	
oxalato	oxalato	ox	
1,10-phenanthroline or *o*-phenanthroline	1,10-phenanthroline	phen or *o*-phen	
phenylpyridinato	2-phenylpyridinato-C^2,*N* or 2-phenylpyridinato-κC^2,*N*	ppy	
tridentate ligands			
triazacyclononane	1,4,7-triazacyclononane	tacn	
diethylenetriamine	1,4,7-triazaheptane	dien	

Common Ligand name	IUPAC ligand name	abbreviation (if applicable)	structure or ionization s
pyrazoylborato (scorpionate)	hydrotris(pyrazo-1-yl)borato	Tp	
terpyridine or 2,2';6',2"-terpyridine	$1^2,2^2:2^6,3^2$-terpyridine or 2,6-bis(2-pyridyl)pyridine, tripyridyl, 2,2′:6′,2″-terpyridine	tpy or terpy	
tetradentate ligands			
β, β', β"-triaminotriethylamine	β, β', β"-tris(2-aminoethyl)amine	tren	
triethylenetetramine	1,4,7,10-tetraazadecane	trien	
corroles	variable and generally not used	cor or Cor	

Common Ligand name	IUPAC ligand name	abbreviation (if applicable)	structure or ionization s
12-crown-4	1,4,7,10-tetraoxacyclododecane	12-crown-4	
tetramethylcyclam	1,4,8,11-tetramethyl-1,4,8,11-tetraazacyclotetradecane	TMC or cyclam	
cyclam	1,4,8,11-tetraazacyclotetradecane	cyclam	
cyclen	1,4,7,10-tetraazacyclododecane	cyclen	
tris(2-pyridylmethyl)amine	1-pyridin-2-yl-*N*,*N*-bis(pyridin-2-ylmethyl)methanamine	tpa or TPA	

Common Ligand name	IUPAC ligand name	abbreviation (if applicable)	structure or ionization s
phthalocyanines	variable and generally not used	variable, usually a modified Pc	
porphyrins	variable and generally not used	variable, usually a modified por, Por, or P (e.g. TPP = tetraphenylporphyrin)	
salen	2,2'-ethylenebis(nitrilomethylidene)diphenoxido	salen	
pentadentate ligands			
15-crown-5	1,4,7,10,13-Pentaoxacyclopentadecane	15-crown-5	

Common Ligand name	IUPAC ligand name	abbreviation (if applicable)	structure or ionization s
tetraethylenepentamine	1,4,7,10,13-pentaazatridecane	tepa or TEPA	
hexadentate ligands			
18-crown-6	1,4,7,10,13,16-hexaoxacyclooctadecane	18-crown-6	
2,1,1-cryptand	4,7,13,18-Tetraoxa-1,10-diazabicyclo[8.5.5]icosane	2,1,1-crypt or [2.1.1]-cryptand kryptofix 211 and variations thereof	
ethylenediaminetetraaceto	2,2′,2″,2‴-(Ethane-1,2-diyldinitrilo)tetraaceto	EDTA, edta, Y^{4-}	
heptadentate ligands			
2,2,1-cryptand	4,7,13,16,21-pentaoxa-1,10-diazabicyclo[8.8.5]icosane	2,2,1-crypt or [2.2.1]-cryptand kryptofix 221 and variations thereof	

Common Ligand name	IUPAC ligand name	abbreviation (if applicable)	structure or ionization s
octadentate ligands			
2,2,2-cryptand	4,7,13,16,21,24-Hexaoxa-1,10-diazabicyclo[8.8.8]hexacosan	2,2,2-crypt or [2.2.2]-cryptand kryptofix 222 and variations thereof	
pentetato acid or diethylenetriaminepentaacetato or DTPA	2-[bis[2-[bis(carboxylatomethyl)amino]ethyl]amino]acetato	DTPA	
DOTA or tetraxetan	1,4,7,10-Tetraazacyclododecane-1,4,7,10-tetraacetic acid	Dota, DOTA	

Rules for Naming Coordination Compounds

As explained above, the name of a coordination compound communicates

- as appropriate, information about isomerism
- systematically listing the ligands in a way that as necessary conveys information about their oxidation state and how they are linked to the metal
- the identity of the metal and its oxidation state
- any counterions present

Before going into these rules it is worth pointing out a few things.

1. It is easiest to learn these rules by starting with one or two of the rules, learning how to apply them, and then adding additional rules one at a time. To that end, instructors who wish to use a more programmed approach may find it convenient to first direct their students to this page which focuses on getting the names of the ligands and metal right, without worrying about isomerism or stereochemistry.

2. The rules also assume some familiarity with common coordination geometries and patterns of isomerism in metal complexes. Thus it might be easiest to learn about common coordination geometries first, followed by common patterns of isomerism in metal complexes before beginning this section. If you decide to dive right in to this section you might find it helpful to know that when applying nomenclature and formula rules most textbooks *assume*

- complexes in which the metal has a coordination number of six are octahedral
- complexes in which the metal has a coordination number of five are trigonal bipyramidal
- complexes in which Pt^{II} , Pd^{II} , or Rh^{I}, or Ir^{I} have a coordination number of four are square planar
- other complexes in which the metal has a coordination number of four are tetrahedral

Like all assumptions these don't always work in real life but they should be good enough to get you through your first inorganic chemistry course.

For the pedants among you, note that the complexes given as examples and in exercises on this page have been selected for pedagogical utility. Although many are well-known compounds, others are hypothetical.

Now on to the rules.

Rule 1: If ions are present, name the cation first, followed by the anion.

Examples:

$K_2[Pt^{II}Cl_4]$ potassium tetrachloroplatinate(2-)

$[Co^{III}(NH_3)_6](NO_3)_3$ hexaamminecobalt(3+) nitrate

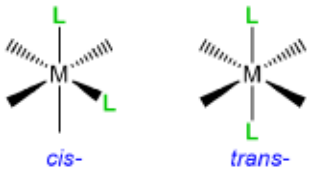
$[Co^{III}(NH_3)_6][Cr^{III}(C_2O_4)_3]$ hexaamminecobalt(3+) tris(oxalato)chromium(3-)

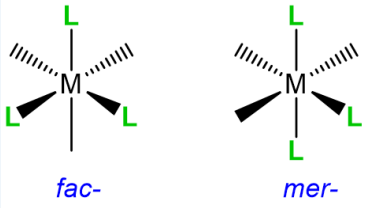
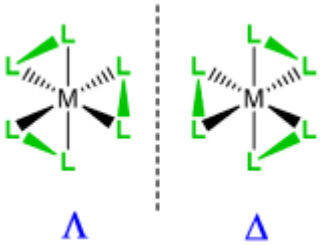
Rule 2: When multiple isomers are possible, designate the particular isomer in italics at the front of the name of each complex

If you have not yet learned about isomerism in coordination compounds skip this rule for now and return to it after you have.

When a complex might exist as one of two stereoisomers, prefixes are commonly used to designate which isomer is present. The most common cases are listed in Table 5.2.3.

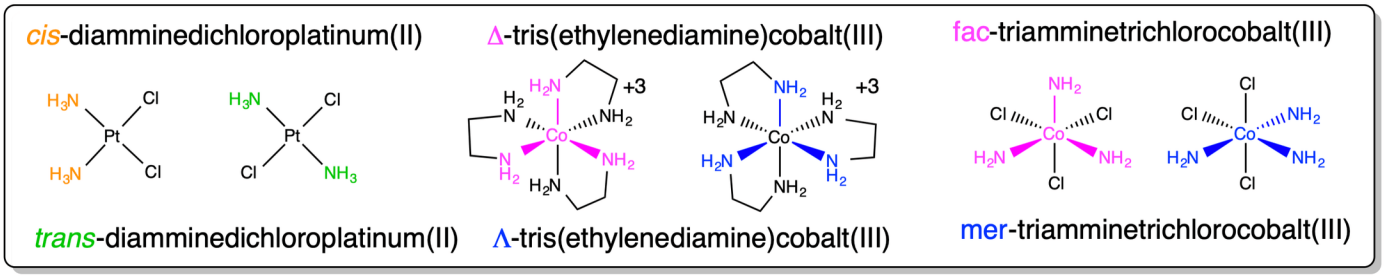
Table 5.2.3. *Prefixes used to specify isomerism about a metal center when naming and writing coordination compounds' formulae.*

Type of isomerism	Graphical reminder	Prefixes
Geometric, *cis-* , *trans-*		*cis-* or *trans-*

Type of isomerism	Graphical reminder	Prefixes
Geometric, *fac- /mer-*		*fac-* or *mer-*
Enantiomers, Λ-, Δ-		Λ- or Δ-

Examples of how isomerism about a metal center is designated are given in Scheme 5.2.II.

Scheme 5.2.II. Application of nomenclature rules for stereosimerism about a metal.[3]



There are a number of other cases where it might be advisable to specify the stereochemistry of a complex. These cases involve specifying

- the coordination geometry about a metal center (octahedral, trigonal prismatic, tetrahedral, square planar, etc.)
- the geometry cannot be unambigouously described by a single *cis/trans* or *fac/mer* relaionship of ligands

These cases may also be handled by using a designator to specify the coordination geometry and, as necessary, giving the position of ligated atoms in terms of designated numbered positions for that geometry. See the IUPAC red book for details as such cases fall outside the scope of what is normally advisable for an undergraduate course.

Rule 3: Specify the identity, number, and as appropriate, isomerism of the ligands present in alphabetical order by ligand name.

Before specifying the metal, the ligands are written as prefixes of the metal.

In specifying the ligands several rules are followed.

1. The ligands are written in alphabetical order by the ligand name only; symbols are not considered and prefixes do not count in determining alphabetical order.

   Example: In the name of the complex ion $[Co(NH_3)_5Cl]^{2+}$, pentamminechlorocobalt(II), the ammine ligand is named before the chloro ligand because the order is alphabetical by the ligand name by virtue of which ammine comes before chloro.

2. Prefixes are used to indicate the number of each ligand present. Specifically, *di-*, *tri-*, *tetra-* , *penta-*, *hexa-*, *etc.* prefixes are

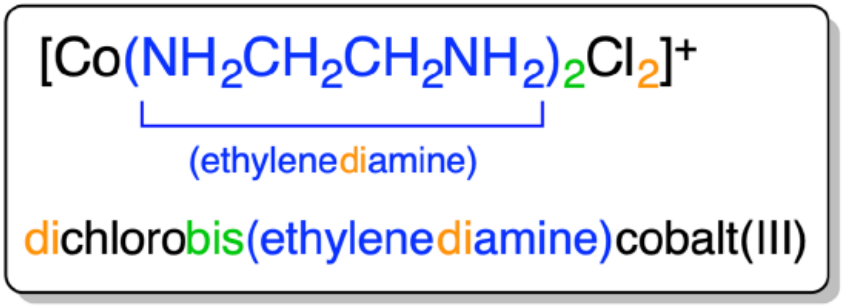
used to indicate multiple ligands of the same type EXCEPT when the ligand is polydentate or its name already has a *di-*, *tri-*, *tetra-* etc. In that case *bis-*,*tris-*, *tetrakis-*, etc. are used instead. These prefix rules are summarized in Table 5.2.3.

Table 5.2.3. *Prefixes used to specify the number of a given ligand present.*

Number of identical ligands	prefix used when the ligand name is simple	prefix used when the ligand is polydentate or its name already has a *di-*, *tri-*, *tetra-* etc.
2	di-	bis-
3	tri-	tris-
4	tetra-	tetrakis-
5	penta-	pentakis-
6	hexa-	hexakis-
7	hepta-	heptakis-
8	octa-	octakis-
9	nona-	nonakis-
10	deca-	decakis-

An example of the application of the prefix rule is given in Scheme 5.2.III.

Scheme 5.2.III. Example of the use of prefixes to specify the number of ligands of each type in a complex.[3]



3. Ligand names are based on their charge.

- Neutral and cationic ligand names are the same as the names of their neutral compounds with two caveats:

  i. names that involve spaces should either be put in parentheses or the spaces should be eliminated (preferred)

  Example: cis-dichlorobis(**dimethyl sulfoxide**)platinum(II) or *cis*-dichlorobis(**dimethylsulfoxide**)platinum(II)

  ii. A few ligands are given common names.

  - H_2O = aqua
  - NH_3 = ammine (notice that there are two n's)
  - CO = carbonyl
  - CS = thiocarbonyl
  - NO = nitrosyl

- For anionic ligands, the vowel at the end of their anion names is changed to an -"o"

  Examples: Cl^- = chloro, NH_2^- = amido, N_3^- = azido

  Caveat: some anionic ligands have common names that may also be used

Examples:

I^- = iodo or iodino

CN^- = cyano or cyanido

O^{2-} = oxo or oxido

The IUPAC and common names of many ligands are given in Tables 5.2.1. and 5.2.2.

4. When an ambidentate ligand is present, the atom through which it is bound to the metal is indicated by giving either its element symbol or a κ and its element symbol in italics after the ligand name.

   Example:

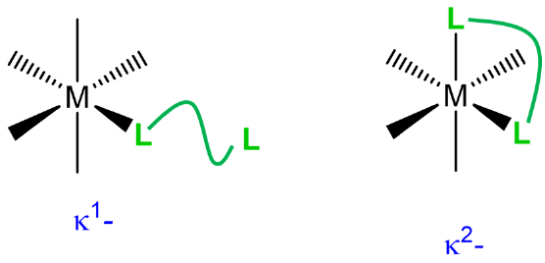
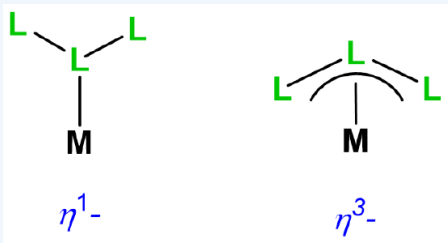
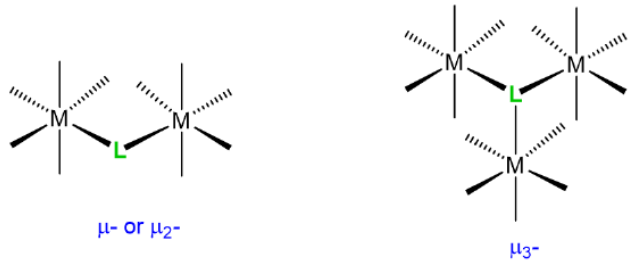
   M-SCN is thiocyanato-*S* or thiocyanato-κS

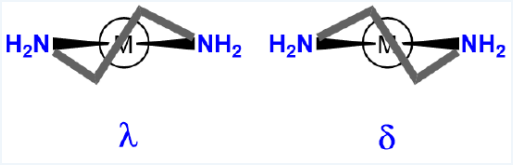
   M-NCS = thiocyanato-*N or* thiocyanato-κ*N*

   The use of κ and an element symbol to indicate how a ligand and metal are linked is called a **k-term**. More complex k-terms might also involve specifying the atoms by number, though their use is outside the scope of this text.

5. As appropriate, additional information about the way a ligand is bound to the metal center and/or its stereochemistry is specified using a prefix. The prefixes to provide linkage and stereochemistry for ligands are given in Table 5.2.4.

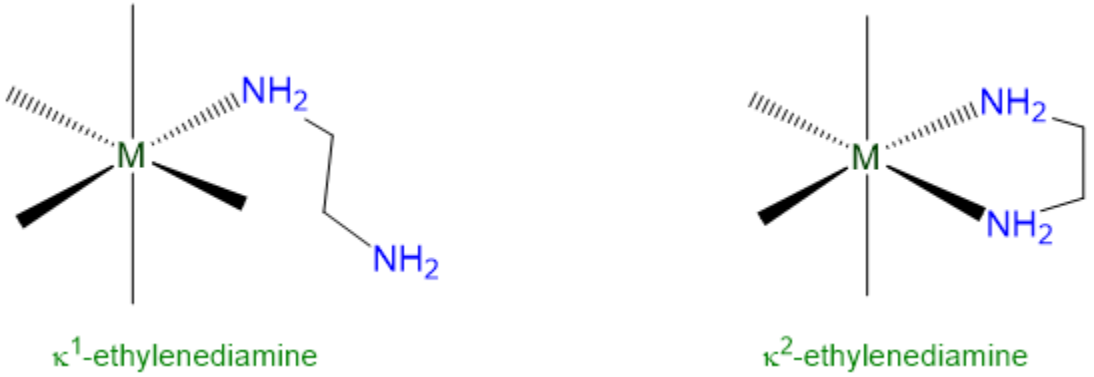
Table 5.2.4. *Prefixes used to specify ligands' isomerism when naming and writing coordination compounds' formulae. Some of these types of isomerism will be discussed in later pages.*

Type of isomerism	Graphical reminder	Prefixes
when a multidentate ligand binds through less than the full number of atoms		κ^n where n is the number of attached atoms; used when the attached atoms are not directly connected by a chemical bond. The metal-ligand bonding usually involves σ-type coordination.
hapticity		η^n where n is the number of attached atoms; used when the coordinated atoms are all connected by bonds. Usually the metal-ligand bonding involves π-type coordination. In speech, η^1=monohapto; η^2=dihapto; η^3 =trihapto, etc.
bridging ligands		μ_n where n is the number of atoms bridged. The number n is usually omitted when n =2.

Type of isomerism	Graphical reminder	Prefixes
chelating ligand ring twist		λ- or δ-

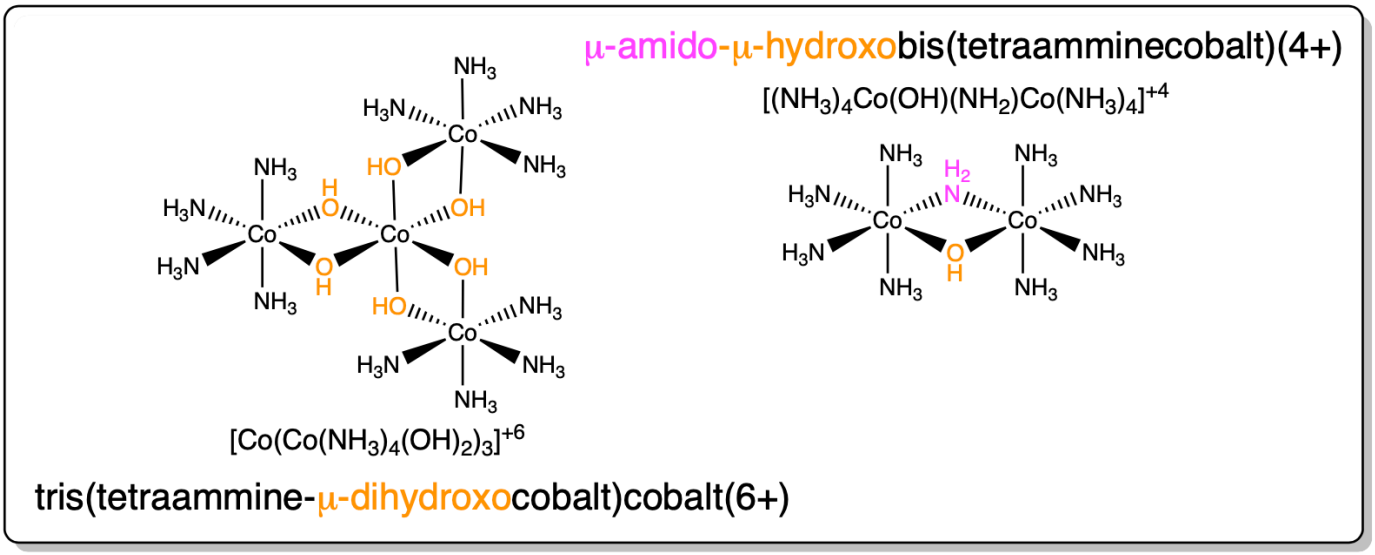
A example showing how the nomenclature rule is applied to a ligand that can have two coordination modes is given in Scheme 5.2.IV.

Scheme 5.2.IV**.** Use of the κ notation to specify the number of attached groups in a multidentate ligand.



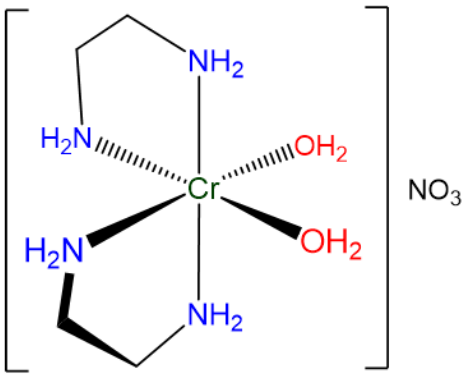
Scheme 5.2.V. The names of the complexes follow the rules described in 9.2.6: multinuclear coordination complexes.

Scheme 5.2.V**.** Use of the μ notation to specify bridging ligands in metal complexes.[3]



6. If desired, parentheses *may* be used to delineate a ligand name to make it easier to identify in the name of the complex. This can be particularly helpful when the entire name contains a lot of information to keep track of. An example is given in Scheme 5.2.VI.

   Scheme 5.2.VI**.** When naming the complex shown, *cis*-diaquabis(ethylenediamine)chromium(III) nitrate is easier to read than *cis*-diaquabisethylenediaminechromium(III) nitrate.



Rule 4: Specify the identity of the metal

- In neutral and cationic complexes the metal's name is used directly

  - *e.g.* as in hexammineruthenium(III) for $[Ru(NH_3)_6]^{3+}$

- In anionic complexes, *-ate* replaces *-ium*, *-en*, or *–ese* or adds to the metal name,

  e.g., as in hexachloromanganate(IV) for $MnCl_6^{2-}$

- In anionic complexes of some metals a Latin-derived name is used instead of the element's English name. These names are given in Table 5.2.5.

Table 5.2.5. *Latin terms for select metal Ions. Redrawn from this page describing the nomenclature of coordination complexes.*

Transition Metal	Latin
Copper	Cuprate
Gold	Aurate
Iron	Ferrate
Lead	Plumbate
Silver	Argentate
Tin	Stannate

An example of the application of the metal naming rules is given in Scheme \sf{{5{.}2{.}\eatSpaces{VII} \endSpaces}}\).

Scheme 5.2.V**II.** Example of the application of the metal specification rules to a cationic and an anionic platinum complex.[3]



Rule 5: Specify the oxidation state of the metal.

Two different systems are used to specify the oxidation state of the metal.

1. In the **Stock system** the metal's oxidation state is indicated in Roman numerals after the metal name.

Examples:

$[CoCl(NH_3)_5]Cl_2$ = pentamminechlorocobalt(III) chloride

$[PtBr_2(bpy)]$ = dibromobipyridineplatinium(II)

$K[Ag(SCN)_2]$ = potassium di-S-thiocyanatoargentate(I)

2. In the **Ewing-Bassett system** the charge on the complex is specified in Arabic numerals after the complex name. This provides a way of specifying a complex even when the oxidation state of the metal isn't known and, in cases where it is known, the value of the metal's oxidation state may be inferred from the complex ion's charge.

   $[CoCl(NH_3)_5]Cl_2$ = pentamminechlorocobalt(2+) chloride

   $[PtBr_2(bpy)]$ = dibromobipyridineplatinium(0)

   $K[Ag(SCN)_2]$ = potassium di-S-thiocyanatoargentate(1-)

Summary of rules for naming coordination complexes.

A graphical summary of the **rules for naming complexes** along with a few examples that you can use to review the nomenclature rules is given in Figure 5.2.1. This work by Stephen Contakes is licensed under a Creative Commons Attribution 4.0 International License.

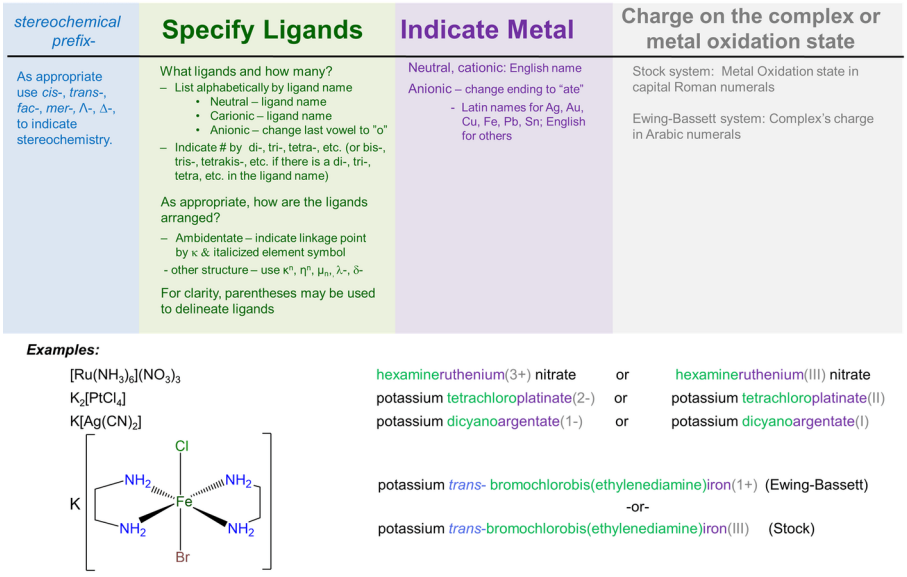


Figure 5.2.1. Summary of nomenclature rules for coordination complexes along with a few examples of their application.

When learning chemical nomenclature, practice makes perfect. The following examples and exercises are provided to give you this practice. Additional examples and exercises on the https://chem.libretexts.org/ site include a set of simple examples with explained solutions, a set of simple exercises with solutions, and a set of more challenging exercises without solutions.

Exercise 5.2.2. Assigning metal oxidation states in a complex

In order to name a complex in the Stock system it is necessary to assign a formal oxidation state to the metal. For this reason it is important to be able to assign the oxidation state of a metal in a complex. Fortunately, this is easy to do if you remember

1. The sum of all atoms' oxidation states will equal the overall charge on the complex

2. When determining the metal's oxidation state the ligands can be treated as having an oxidation state equal to their charge - *i.e.,* the charge they possess in the form in which they coordinate the metal, so if they need to lose a proton to bind, don't forget to account for that.

Given the above, assign the oxidation state of the metal in the following real and hypothetical complexes.

a. $K_3[Fe(CN)_6]$
b. $[CoCl(NH_3)_5](NO_3)_2$
c. $K_2[PtCl_4]$
d. [MnCl(por)]
e. $[Ru(bpy)_3]Cl_2$
f. $[PdCl_2(dppe)]$
g. $[Mn(en)_2(SCN)_2]$

Answer for K3[Fe(CN)6]3-. available at the end of this section.

Exercise 5.2.3: Simple Nomenclature Problems.

Name the following compounds in both the Stock and Ewing-Bassett systems:

a. $[Ru(NH_3)_6](NO_3)_3$
b. $K_2[PtCl_4]$
c. $K[Ag(CN)_2]$
d. $Cs[CuBrCl_2F]$
e. $[Cu(acac)_2]$

Answer available at the end of this section.

Exercise 5.2.4: More simple nomenclature problems.

Name the following compounds and ions in both the Stock and Ewing-Bassett systems.

a. $Cu(OH)_4^-$
b. $[AuXe_4]^{2+}$
c. $AuCl_4^-$
d. $Fe(CN)_6^{3-}$
e. $K_4[Fe(CN)_6]$
f. *trans*-$[Cu(en)_2(NO_2)_2]$ (the N is bound to Cu)
g. cis-$IrCl_2(CO)(PPh_3)$ (ignore stereochemistry)
h. $IrCl(PPh_3)_3$

Answer available at the end of this section.

Exercise 5.2.5: Even more simple nomenclature problems.

Name the following compounds and ions in both the Stock and Ewing-Bassett systems. Ignore prefixes for designating isomers if you haven't learned about those.

a. $Fe(acac)_3$
b. $K_2[CuBr_4]$
c. ReH_9

d. $[Ag(NH_3)_2]BF_4$
e. $[Ag(NH_3)_2][Ag(CN)_2]$
f. $[Ni(CN)_4]^{2-}$
g. $[Co(N_3)(NH_3)_5]SO_4$
h. $[CoBrCl(H_2O)(NH_3)]I$ (ignore stereochemistry)

Sample Answers available at the end of this section.

Exercise 5.2.6: Nomenclature problems, some of which involve consideration of isomerism.

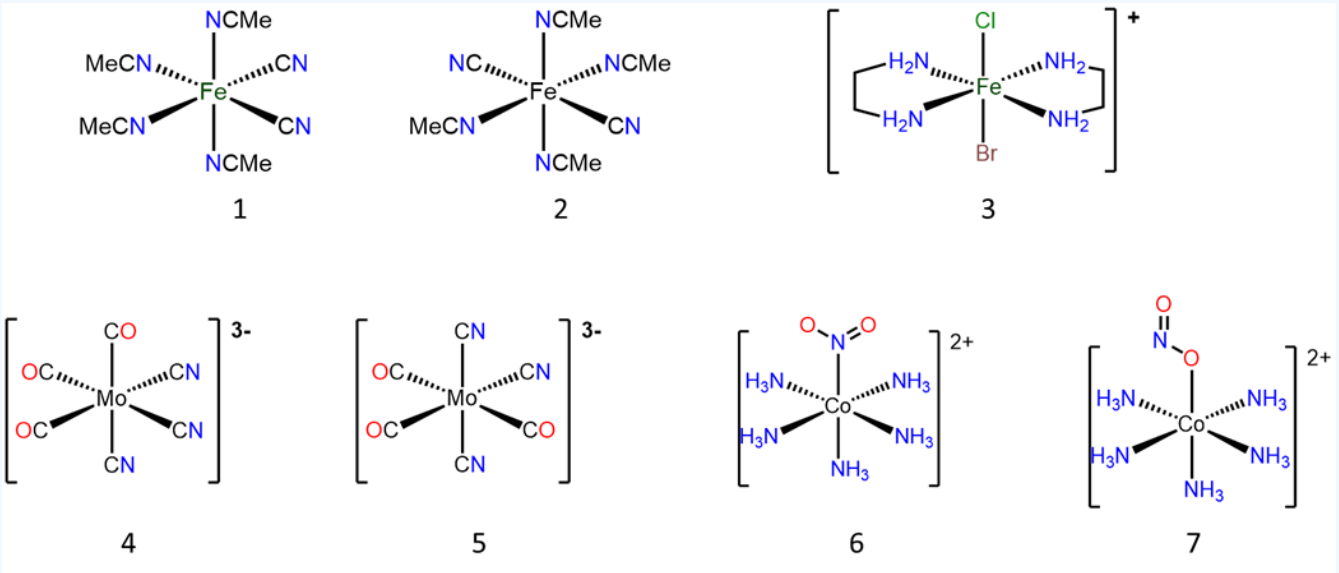
Name the following compounds and ions in both the Stock and Ewing-Bassett systems. Ignore prefixes for designating isomers if you haven't learned about those.

a. *trans*-$[Cu(dppe)_2(NO_2)_2]$ (the N is bound to Cu)
b. $[Pd(en)_2(SCN)_2]$, with the thiocyanates bound Pd-SCN
c. $[Mn(CO)_6]BPh_4$ (BPh_4 = tetraphenylborate)
d. $Rb[AgF_4]$
e. K_2ReH_9
f. K_3CrCl_6
g. $[Ru(H_2O)_6]Cl_2$
h. [*cis*-$Fe(CO)_4I_2$]
i. K_2[*trans*-$Fe(CN)_4(CO)_2$]
j. [*cis*-$MnCl(H_2O)_4(NH_3)](NO_3)$
k. K_3[*fac*-$RuCl_3(PMe_3)_3$]

Answer available at the end of this section.

Exercise 5.2.7

Name the compounds and ions below using both the Stock and Ewing-Bassett systems. Ignore prefixes for designating isomers if you haven't learned about those.



Answer available at the end of this section.

Exercise 5.2.8

Draw structural formulae for the following compounds and ions. You may assume that

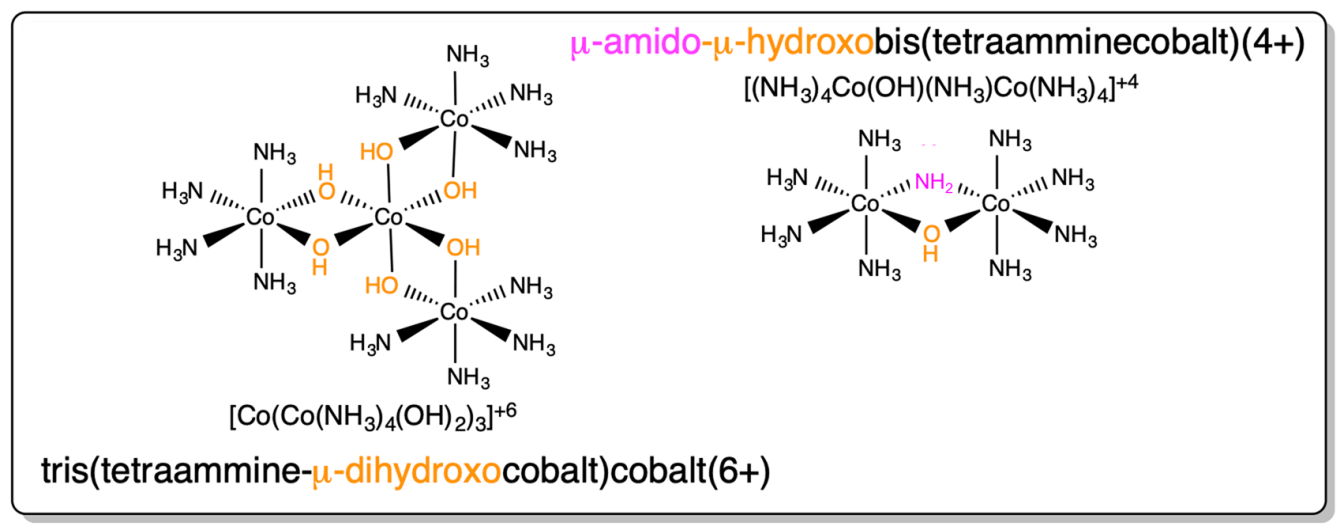
- complexes in which the metal has a coordination number of six are octahedral
- complexes in which the metal has a coordination number of five are trigonal bipyramidal
- complexes in which Pt^{II} , Pd^{II} , or Rh^{I}, or Ir^{I} have a coordination number of four are square planar
- other complexes in which the metal has a coordination number of four will be tetrahedral

a. (2,2'-bipyridine)tetracyanoruthenium(2-)
b. sodium tetrachloroaluminate (note that since Al is a main group metal with a generally fixed oxidation state no oxidation state is given)
c. pentaamminechlorocobalt(2+) sulfate
d. carbonylhydridotris(triphenylphosphine)rhodium(I) (the ligands in this complex occupy sterically preferred positions)
e. bromotrichlorocobaltate(III)
f. hexaaquacopper(2+) sulfate
g. sodium tris(oxalato)cobalt(III)
h. *fac*-(1,10-phenanthroline)tricarbonylchlororhenium(I)
i. *mer*-triaquatrichlorochromium(III)
j. *trans*-dichlorobis(ethylenediamine)platinum(IV)

Answers available at the end of this section.

Exercise 5.2.9.

The name of the structure named tris(tetraammine-μ-dihydroxocobalt)cobalt(6+) in Scheme 5.2.III (reproduced below) is incomplete. Give the complete name of the structure in both the Stock and Ewing-Basset systems.



Answer available at the end of this section.

Note: Rules for Writing the Formulae of Coordination Copounds

Rules for writing the formulae of coordination compounds

As organized predictable formulae can be easier to read and understand than haphazardly written ones, the rules for writing the formulae of coordination compounds have value. To support those who wish to employ them they are given in this section. The rules as given here are adapted from a summary by Robert Lancashire.

The rules for writing the formulae of coordination compounds follow the same convention used to specify their names.

1. If there are multiple ions present list the cations before anions.
2. Enclose all the constituents of each complex ion in square brackets.
3. For each complex ion,
   - Give the **central metal** atom first.
   - Then **ligands** next, listed in alphabetical order, ignoring prefixes according to the first letters in the ligand's symbol as written. This is true regardless of whether the symbol is an element symbol (like C, N, O, etc.) or a symbol for the ligand name (bpy, en, MeCN, etc.). Contrary to widely-circulated myths, the ligand's charge does not matter.[4]
   - The formulae or abbreviations (*e.g.* en) for all polyatomic ligands should be enclosed in ordinary parentheses.
   - As appropriate, use italicized atom symbols to indicate linkage isomerism and prefixes such as *cis*-, *trans*-, *fac*-, *mer*-, Λ-, Δ-, κ^n, η^n , μ_n, λ-, or δ- to indicate stereochemistry.
   - When a ligand is bound to a metal through a particular atom, preferably place that atom closest to the metal - *e.g.*, $[Fe(CN)_6]^{3-}$ not $[Fe(NC)_6]^{3-}$ (Note: this rule is used primarily for ambidentate ligands; although IUPAC recommends that aqua ligands be written as OH_2 when the O would be closest to its coordinated metal, they are still usually written as H_2O).

These rules are graphically summarized in Figure 5.2.2.

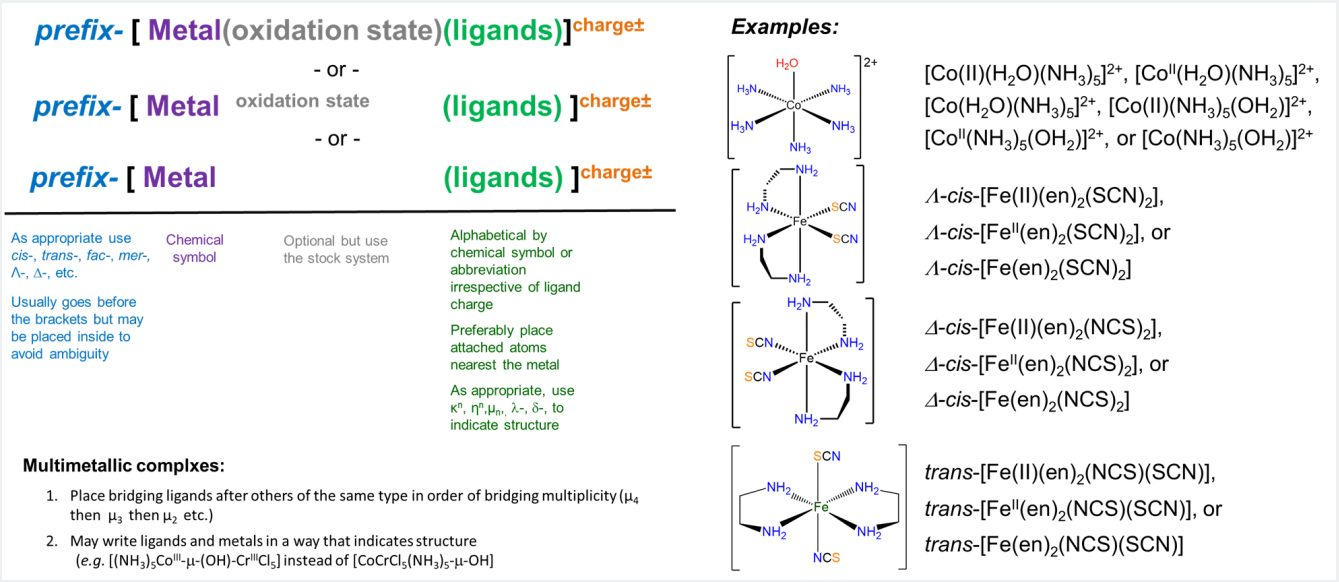
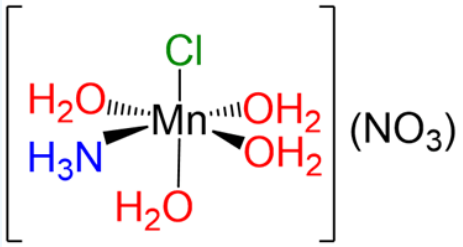


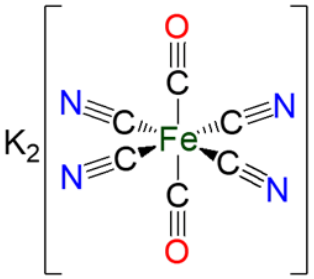
Figure 5.2.2. Summary of the rules for writing the formula of a coordination complexes along with a few examples of their application. This work by Stephen Contakes is licensed under a Creative Commons Attribution 4.0 International License.

Exercise 5.2.10

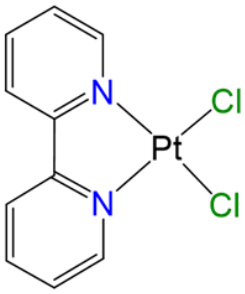
Give the formulae of the following complexes.



1



2



3

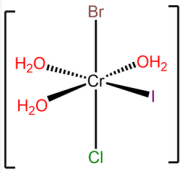
.

Answer available at the end of this section.

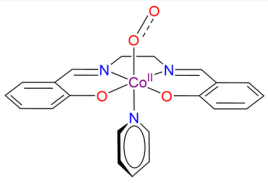
Exercise 5.2.11

Write formulae for each of the following compounds and ions. When multidentate ligands are present use suitable abbreviations.

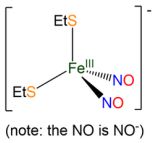
a. pentaamminechlorocobalt(2+) sulfate
b. Δ-diamminebis(oxalato)manganate(III)
c. *trans*-tetraacetonitriledicyanoiron(II)
d. tricarbonyldichlorobis(triphenylphosphine)molybdenum



e

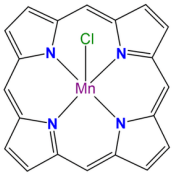


f

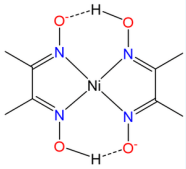


(note: the NO is NO⁻)

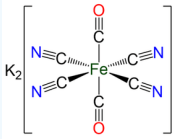
g



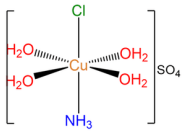
h



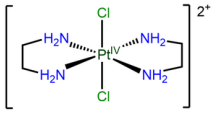
i



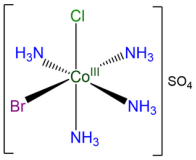
j



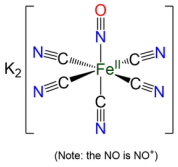
k



l



m



(Note: the NO is NO⁺)

n

Answers available at the end of this section.

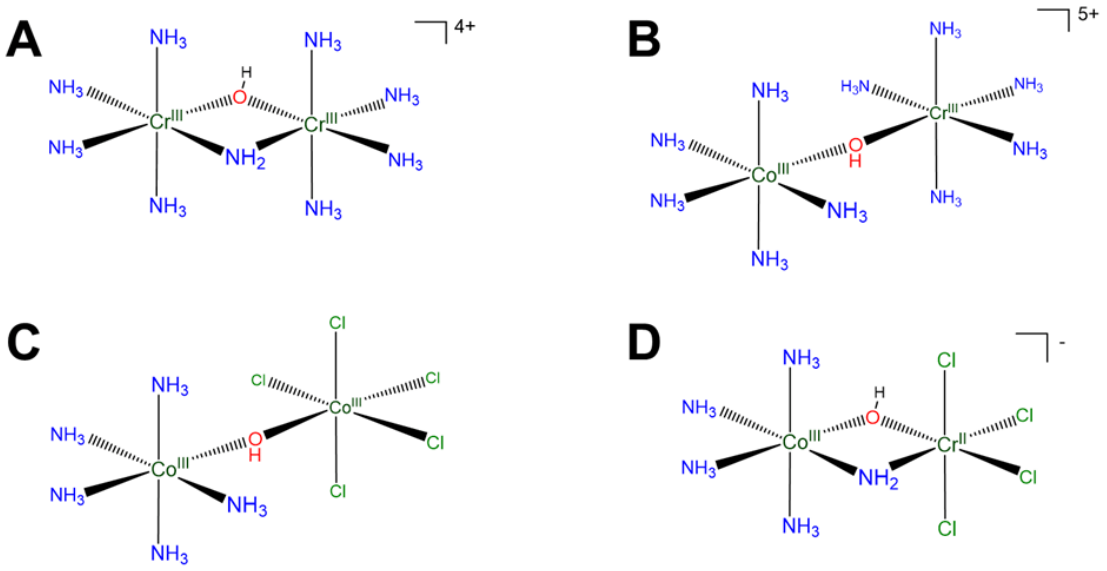
Multinuclear coordination complexes

Multinuclear coordination complexes contain multiple metals connected by one or more bridging ligands. The structures of bridging complexes can usually be inferred from their μ-tagged ligands in their names and formulae. For the benefit of instructors who wish to have their students name multinuclear complexes, the rules are presented below.

Multinuclear complexes are named differently depending on whether the groups on either side of the bridging ligands are

identical or different, as shown in Scheme 5.2.VIII.

Scheme 5.2.VIII. Multinuclear coordination complexes may be named differently depending on whether the groups on either side of the bridging ligands are the same or different. The groups are the same if the metal, ligands, and ligand arrangement are identical. This is true in A but in B the metals differ, in C the ligands differ, and in D both the metal and ligands differ.



Naming multinuclear complexes

Let's look at the rules for naming symmetric and asymmetric multinuclear complexes.

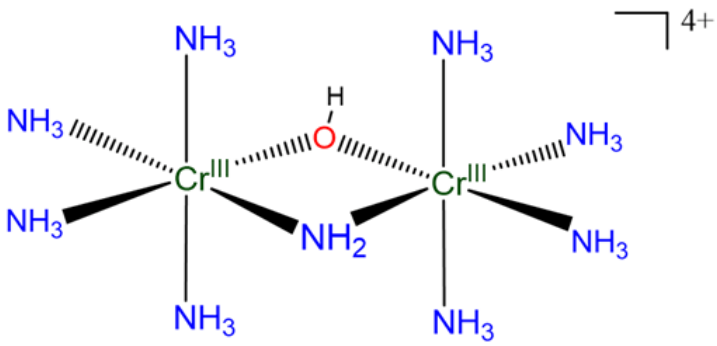
Application of the IUPAC system and variants thereof to symmetric complexes

The IUPAC naming system helpfully avoids the sort of ambiguities and *ad hoc* choices involved in most textbook-level nomenclature systems for multimetallic complexes. Unfortunately, it is correspondingly difficult for beginners to employ. Thus it will only be applied in depth to the case of symmetric complexes. Symmetric complexes are particularly easy to name in the IUPAC system and several of its variants that find common use. In these

1. The ligands are given in alphabetical order. When there are bridging and non-bridging ligands of the same type the bridging ligands are given first. When there are multiple bridging ligands of the same type but which use different bridging modes (*e.g.*, μ_4-, μ_3-, μ_2-), the bridging ligands are specified in decreasing order of bridging multiplicity, *e.g.*, μ_3 -sulfido-di-μ-sulfido.
2. The groups bridged are given afterwards using names that follow the ordinary rules. Generally this involves either
   a. naming all the ligands followed by all the metals, in both cases using prefixes to indicate the number of each, or
   b. naming each group of atoms individually as in the less formal naming system, using prefixes to indicate the number of ligands (this is an unofficial variant of the IUPAC system that some textbook authors seem to prefer).

These two rules are sufficient to describe simple symmetric bridging complexes.

Example: The compound in Scheme 5.2.VIIIA



may be named

[μ-amido-μ-hydroxo-octaamminedichromium(4+)] ion

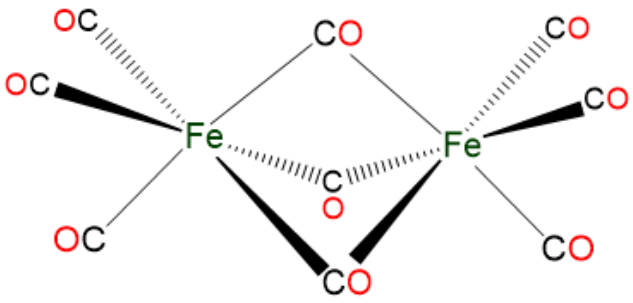
or

[μ-amido-μ-hydroxo-bis(tetraamminechromium(III))] ion

or

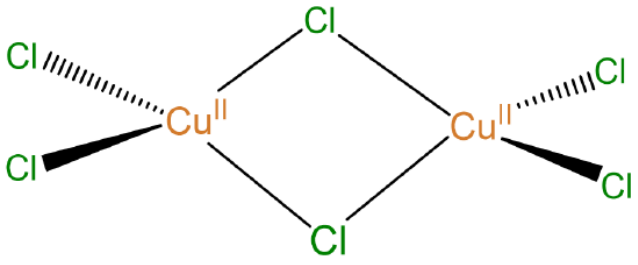
[μ-amido-μ-hydroxo-bis(tetraamminechromium)(4+)] ion

Example: The complex[5]



may be named [tri-μ-carbonyl-bis(tricarbonyliron)(0)], [tri-μ-carbonyl-bis(tricarbonyliron(0))], or [tri-μ-carbonyl-hexacarbonyldiiron)(0)]

Example: The complex



may be named di-μ-chlorido-tetrachloridodicopper(II), di-μ-chlorido-bis(dichlorocopper(II)), or di-μ-chlorido-bis(dichlorocopper)(0)

A note on the application of the IUPAC system and variants thereof to asymmetric complexes

For a symmetrical complex like the $[Cu_2Cl_4(\mu\text{-}Cl)_2]$ considered above it is enough to specify the existence of the two bridging and four terminal chloro ligands; there is no need to number the chloro ligands or to specify exactly which ones are involved in bridging or to clarify that the bridging involves κ^2 coordination of the chloro ligands. In cases where the two metal centers or the chloro ligands differ it is necessary to specify the exact ligands and metals involved and how they are connected.

For example, a more extensive IUPAC name for $[Cu_2Cl_4(\mu\text{-}Cl)_2]$ in which the chloro ligands are individually and more completely specified would read di-μ_2-chlorido-tetrachlorido-1κ^2Cl,2κ^2Cl-dicopper(II).

Even more extensive systems would involve numbering the metals and specifying how they are connected together too. The details of how this is done are typically beyond the level of most undergraduate and graduate courses in inorganic chemistry. Those who want to know the details should consult the red book. In many cases it is sufficient to reserve the use of formal IUPAC names for use in publications and to employ a convenient shorthand naming system for everyday use. An example of one type of system that is sometimes employed is given next.

Unofficial but commonly used methods applicable to complexes in which the groups bridged are identical or different.

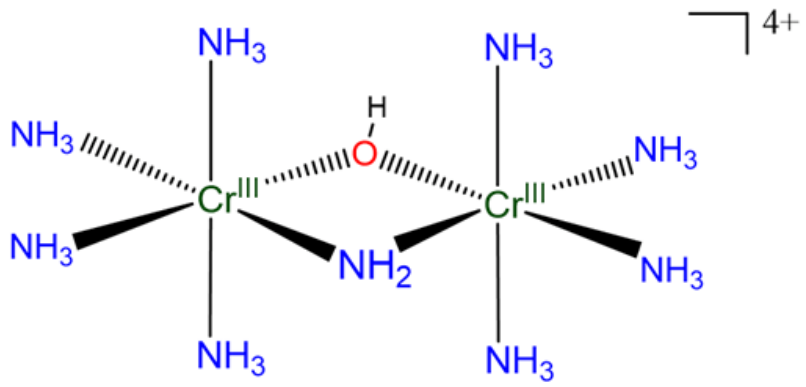
It can be quite complicated to use the IUPAC system to name asymmetric multinuclear coordination complexes. Fortunately it is rarely necessary and there are a variety of simpler somewhat *ad hoc* methods that work well for such cases. Since these methods are commonly used by textbooks and inorganic instructors it is likely worth your while to learn about their general features. In these methods

1. A multinuclear complex is named as a derivative of one of the metal centers and the other metal centers and their ligands are treated as ligands to the prioritized metal center.
2. Unfortunately, most of the time the choice of which metals are part of the ligands and which one is central is made haphazardly. In other words, there is no agreed upon system for assigning which metal center is the central metal and which should be regarded as part of the ligands around it. One way to be more systematic about the selection of the central and ligand-embedded metals is to assign the central metal as the metal of highest priority in the IUPAC priority rules. In the IUPAC priority rules, the central metal is the highest priority metal alphabetically by name; then if there is a tie the ligands on each tied metal center are ranked alphabetically and the tied metal center with the highest priority (or most highest priority) ligands wins.
3. The metal centers not chosen as the primary metal center and all ligands around them, including those bridging to the winning metal center, are then treated as a single ligand that coordinates the winning metal center.
4. When naming the ligands and the overall complex, again there is much that is haphazard. However, in the best systems each coordination sphere is named using the same rules as for mononuclear complexes - *i.e.,* the ligands are given in alphabetical order, etc.

    - This is true of any metal center-containing ligands.
    - When there is a bridging and non-bridging ligand of the same type, the bridging ligands are given first. When there are multiple bridging ligands of the same type but which use different bridging modes (*e.g.* μ_4-, μ_3-, μ_2-), the ligands are specified in decreasing order of bridging multiplicity, *e.g.* μ_3 -sulfido-di-μ-sulfido.

Let's apply these rules to the examples in Scheme 5.2.VIII.

Compound A:



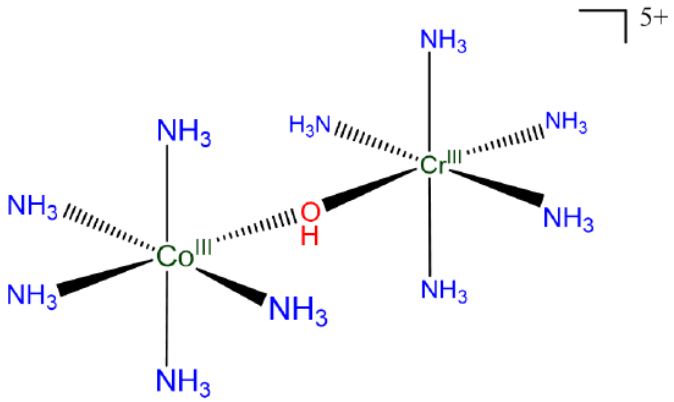
Using hydroxo for the OH^-, it may be named

[(μ-amido-tetraammine-μ-hydroxochromium(III))tetraamminechromium(III)] ion

or

[(μ-amido-tetraammine-μ-hydroxochromium)chromium(4+)] ion

Compound B:



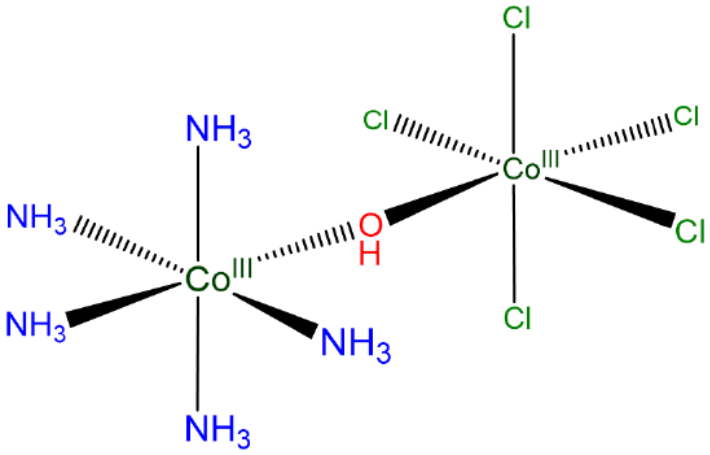
Using hydroxo for the OH^-, it may be named

[(pentaammine-μ-hydroxocobalt(III))tetraamminechromium(III)] ion

or

[(pentaammine-μ-hydroxocobalt)tetraamminechromium(5+)] ion

Compound C:



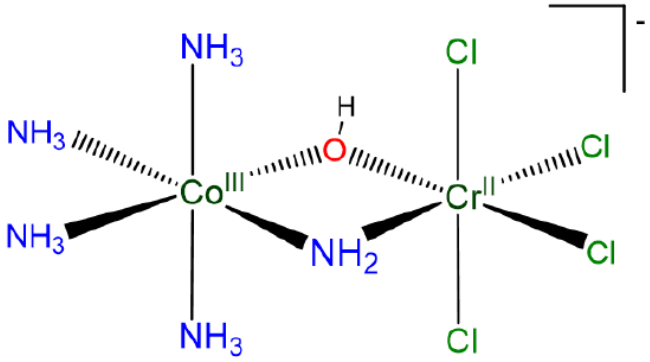
Using hydroxo for OH^-, it may be named

[pentaammine(pentachloro-μ-hydroxocobalt(III))cobalt(III)]

or

[pentaammine(pentachloro-μ-hydroxocobalt)cobalt](9)]

Compound D:



Using hydroxo for OH^- and chloro for Cl^-, it may be named

[pentaammine(pentachloro-μ-hydroxocobalt(III))chromate(III)] ion

or

[(tetrammine-μ-ammine-μ-hydroxocobalt)tetrachlorochromate](1-)] ion

As can be seen from the examples above this system gives serviceable names for multimetallic complexes but those names are not the IUPAC names and so should not be used to describe complexes outside of pedagogical and informal settings.

Writing and interpreting formulae for multinuclear complexes

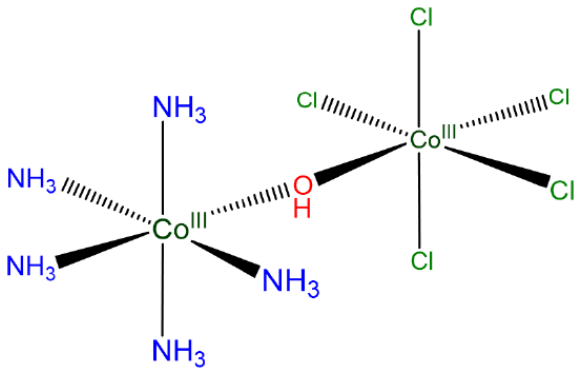
The rules for writing formulae for multinuclear complexes are the same as for mononuclear ones with two added details:

1. Write bridging ligands after nonbridging ligands of the same type. For example, Cu_2Cl_6 should be written as $[Cu_2Cl_4(\mu\text{-}Cl)_2]$
2. However, you may ignore that and other rules if you find it helpful to keep groups of metals and ligands together in a way that better conveys how the atoms are connected. Just as the structure of ethane may be more clearly conveyed as H_3CCH_3 instead of CH_3CH_3, the complex $[Cu_2Cl_4(\mu\text{-}Cl)_2]$ may be written as $[(Cl_2Cu)(\mu\text{-}Cl)_2(CuCl_2)]$.

Other Examples:

For dichromate write, $[Cr_2O_6(\mu\text{-}O)]^{2-}$ or $[O_5Cr\text{-}\mu\text{-}O\text{-}CrO_5]^{2-}$

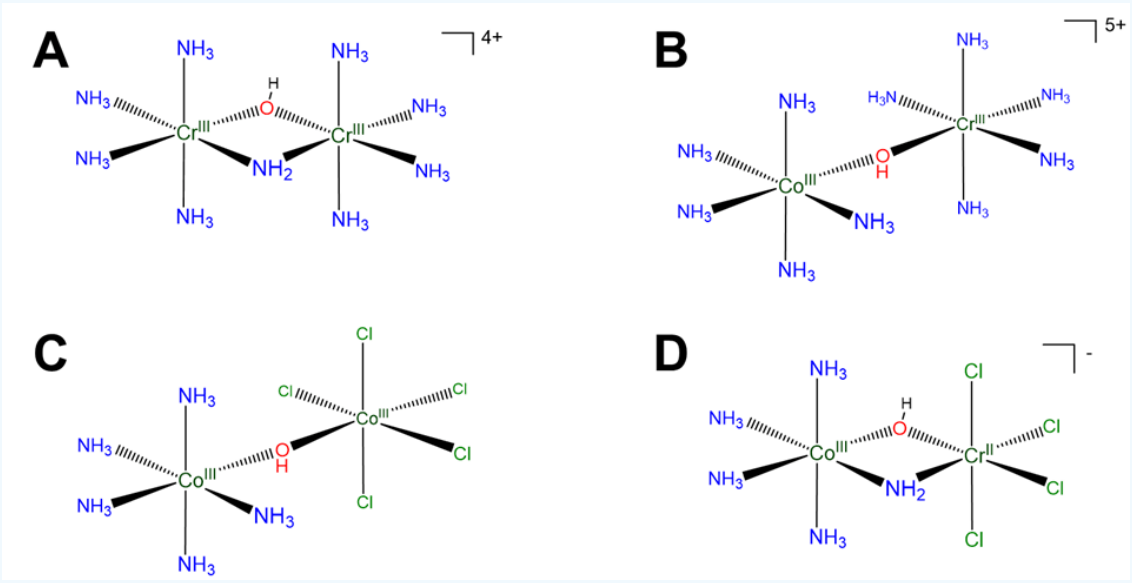
For compound C of Scheme 5.2.VIII.



write $[Co_2Cl_5(NH_3)_5(\mu\text{-}OH)]$ or, even better, $[(H_3N)_5Co(\mu\text{-}OH)CoCl_5]$.

Exercise 5.2.10

Write reasonable formulae for complexes A, B, and D in Scheme 5.2.VIII, which for convenience is reproduced below.



Sample answers for A available at the end of this section.

References

1. International Union of Pure and Applied Chemistry *Nomenclature of Inorganic Chemistry* Cambridge, UK, 2005.

2. The structure and name is taken from Choudhury, S. B.; Allan, C. B.; Maroney, M.; Wodward, A. D.; Lucas, C. R. *Inorg. Synth.* **1998**, *32*, 98-107.

3. Haas, K. Naming Transition Metal Complexes. https://chem.libretexts.org/Courses/Saint_Mary's_College%2C_Notre_Dame%2C_IN/CHEM_342%3A_Bio-inorganic_Chemistry/Readings/

4. There is a widely-circulated myth that anionic ligands should be named before neutral ones. This myth is false. According to the IUPAC red book (bolding mine):

> IR-2.15.3.4: Ordering ligands in formulae and names in formulae of coordination compounds,
>
> The formulae or abbreviations representing the ligands **are cited in alphabetical order as the general rule**. Bridging ligands are cited immediately after terminal ligands of the same kind, if any, and in increasing order of bridging multiplicity. (See also Sections IR-9.2.3 and IR-9.2.5.)
>
> IR-9.2.3.1 Sequence of symbols within the coordination formula
>
> (i) The central atom symbol(s) is (are) listed first.
>
> (ii) The **ligand symbols (line formulae, abbreviations or acronyms) are then listed in alphabetical order** (see Section IR-4.4.2.2).5 Thus, CH_3CN, MeCN and NCMe would be ordered under C, M and N respectively, and CO precedes Cl because single letter symbols precede two letter symbols. **The placement of the ligand in the list does not depend on the charge of the ligand.**
>
> (iii) More information is conveyed by formulae that show ligands with the donor atom nearest the central atom; this procedure is recommended wherever possible, even for coordinated water.

5. Technically organometallic complexes are named according to slightly different rules but the coordination compound naming system works here. Note that this complex was once thought to possess an Fe-Fe bond, in accordance with the predictions of the 18-electron rule. Consequently, older sources often give an [*Fe-Fe*] after the name to reflect the presence of that bond. However, as the complex is no longer thought to possess an Fe-Fe bond it is omitted here.

Contributors and Attributions

Stephen Contakes, Westmont College, to whom comments, corrections, and criticisms should be addressed.

with some examples taken from Naming Transition Metal Complexes by Kathryn Haas.

Consistent with the policy for original artwork made as part of this project, all unlabeled drawings of chemical structures are by Stephen Contakes and licensed under a Creative Commons Attribution 4.0 International License.

Answers

Exercise 5.2.1

(a) bidentate
(b) tridentate
(c) bidentate
(d) tridentate (only the lower N on each ring has a lone pair that can be used to bind the metal)
(e) hexadentate (remember that each carboxylate only counts as one point of attachment)
(f) bidentate
(g) monodentate (through the lone pair on the isocyanide C)
(h) bidentate

Exercise 5.2.2**. Assigning metal oxidation states in a complex**

This contains $[Fe(CN)_6]^{3-}$; so O.S.$_{Fe}$ + 6 x (-1) (for CN^-) = -3 (the complex's charge) so O.S.$_{Fe}$ = +3 or Fe^{3+}.

This contains $[CoCl(NH_3)_5]^{2+}$; so O.S.$_{Co}$ + 1 x (-1) (for Cl^-) + 0 x 5 (for NH_3) = +2 (the complex's charge) so O.S.$_{Co}$ = +3 or Co^{3+}.

This contains $2K^+$ and $[PtCl_4]^{2-}$; so O.S.$_{Pt}$ + 4 x (-1) (for Cl^-) = -2 (the complex's charge) so O.S.$_{Pt}$ = +2 or Pt^{2+}.

O.S.$_{Pt}$ + 1 x (-2) (for por; see table 9.2.2) + 1 x (-1) (for Cl^-) = +0 (the complex's charge) so O.S.$_{Mn}$ = +3 or Mn^{3+}.

The complex is $[Ru(bpy)3]^{2+}$ so O.S.$_{Ru}$ + 0 x 3 (for bpy) = +2 (the complex's charge) so O.S.$_{Ru}$ = +2 or Ru^{2+}.

O.S.$_{Pd}$ + 2 x (-1) (for Cl^-) + 0 x 3 (for dppe) = +0 (the complex's charge) so O.S.$_{Pd}$ = +2 or Pd^{2+}.

O.S.$_{Mn}$ + (2 x 0) (for en) + 2 x (-1) (for SCN^-) = +0 (the complex's charge) so O.S.$_{Mn}$ = +2 or Mn^{2+}.

Exercise 5.2.3: Simple Nomenclature Problems.

	Complex	Stock system name	Ewing-Bassett System name
a	$[Ru(NH_3)_6](NO_3)_3$	hexammineruthenium(III) nitrate	hexammineruthenium(3+) nitrate
b	$K_2[PtCl_4]$	potassium tetrachloroplatinate(II)	potassium tetrachloroplatinate(2-)
c	$K[Ag(CN)_2]$	potassium dicyanoargentate(I)	potassium dicyanoargentate(1-)
d	$Cs_2[CuBrCl_2F]$	cesium bromodichlorofluorocuprate(II)	cesium bromodichlorofluorocuprate(2-)
e	$[Cu(acac)_2]$	bis(acetylacetonato)copper(II)	bis(acetylacetonato)copper(0)

Exercise 5.2.4: More simple nomenclature problems.

	Compound	Stock System Name	Ewing-Bassett System Name
a	$Cu(OH)_4^-$	tetrahydroxidocuprate(III) or tetrahydroxidocuprate(III)	tetrahydroxidocuprate(1-) or tetrahydroxidocuprate(1-)
b	$[AuXe_4]^{2+}$	tetraxenongold(II)	tetraxenongold(2+)
c	$AuCl_4^-$	tetrachloroaurate(III)	tetrachloroaurate(1-)
d	$Fe(CN)_6^{3-}$	hexacyanoferrate(III) or hexacyanidoferrrate(III)	hexacyanoferrate(3-) or hexacyanidoferrate(3-)
e	$K_4[Fe(CN)_6]$	potassium hexacyanoferrate(II) or potassium hexacyanidoferrrate(II)	potassium hexacyanoferrate(4-) or potassium hexacyanidoferrrate(4-)
f	*trans*-$[Cu(en)_2(NO_2)_2]$ (the N is bound to Cu)	bis(ethylenediamine)bisnitrocopper(II) or bis(ethylenediamine)bis(nitrito-κN)copper(II)	bis(ethylenediamine)bisnitrocopper(0) or bis(ethylenediamine)bis(nitrito-κN)copper(0)
g	*cis*-$IrCl_2(CO)(PPh_3)$	*cis*-dichlorocarbonyltriphenylphosphineiridium(I) or *cis*-dichloro(carbonyl)(triphenylphosphine)iridium(I)	*cis*-dichlorocarbonyltriphenylphosphineiridium(0) or *cis*-dichloro(carbonyl)(triphenylphosphine)iridium(0)
h	$IrCl(PPh_3)_3$	chlorotris(triphenylphosphine)iridium(I)	chlorotris(triphenylphosphine)iridium(0)

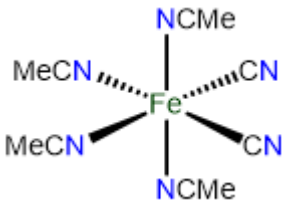
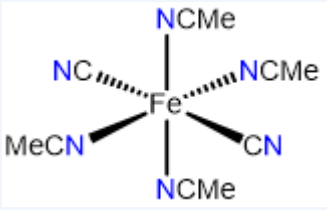
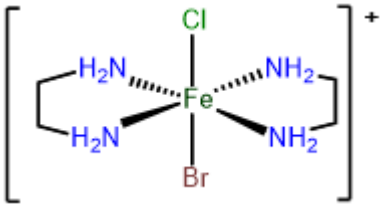
Exercise 5.2.5: Even more simple nomenclature problems.

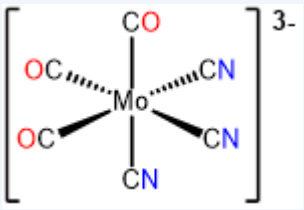
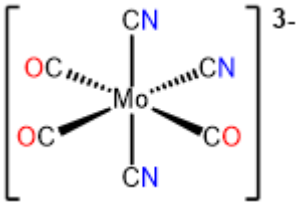
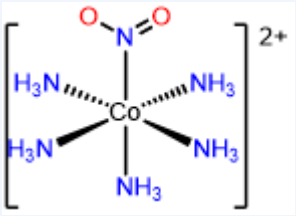
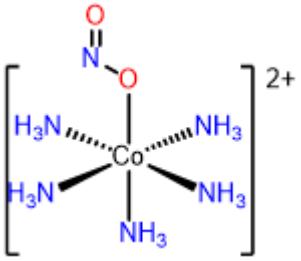
	Complex	Stock system name	Ewing-Bassett System name
a	$Fe(acac)_3$	tris(acetoacetato)iron(III)	tris(acetoacetato)iron(0)
b	$Na_2[CuBr_4]$	sodium tetrabromocuprate(II)	sodium tetrabromocuprate(2-)
c	$[Co(NH_3)_6][Co(ox)_3]$	hexamminecobalt(III) tris(oxalato)cobalt(III)	hexamminecobalt(3+) tris(oxalato)cobalt(3-)
d	$[Ag(NH_3)_2]BF_4$	diamminesilver(I) tetrafluoroborate	diamminesilver(1+) tetrafluoroborate
e	$[Ag(NH_3)_2][Ag(CN)_2]$	diamminesilver(I) dicyanoargentate(I) or diamminesilver(I) dicyanidoargentate(I)	diamminesilver(1+) dicyanoargentate(1-) or diamminesilver(1+) dicyanidoargentate(1-)
f	$[Ni(CN)_4]^{2-}$	tetracyanonickelate(II) or tetracyanonickelate(II) ion	tetracyanonickelate(2-) or tetracyanonickelate(2-) ion
g	$[Co(N_3)(NH_3)_5]SO_4$	pentammineazidocobalt(III) sulfate	pentammineazidocobalt(2+) sulfate
h	$[CoBrCl(H_2O)(NH_3)]I$ (ignore stereochemistry)	ammineaquabromochlorocobalt(III) iodide	ammineaquabromochlorocobalt(1+) iodide

Exercise 5.2.6: Nomenclature problems, some of which involve consideration of isomerism.

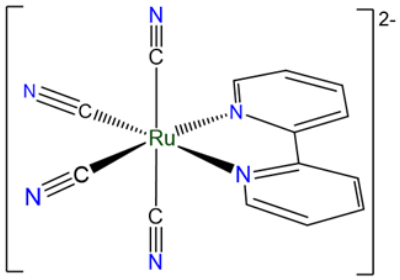
	Complex	Stock system name	Ewing-Bassett System name
a	*trans*-$[Cu(dppe)_2(NO_2)_2]$	*trans*-bis(diphenylphosphinoethane)bisnitrocopper(II) or *trans*-bis(diphenylphosphinoethane)bis(nitrito-κ *N*)copper(II)	*trans*-bis(diphenylphosphinoethane)bisı or *trans*-bis(diphenylphosphino)ethaneb *N*)copper(0)
b	$[Pd(en)_2(SCN)_2]$, with the thiocyanates bound Pd-SCN	bis(ethylenediamine)bisthiocyanatopalladium(II) or bis(ethylenediamine)bis(thiocyanato-S)palladium(II) or bis(ethylenediamine)bis(thiocyanato-κS)palladium(II)	bis(ethylenediamine)bisthiocyanatopalladium(0) or bis(ethylenediamine)bis(thiocyanato-S)palladi or bis(ethylenediamine)bis(thiocyanato-κS)pallad
c	$[Mn(CO)_6]BPh_4$	hexacarbonylmanganese(I) tetraphenylborate	hexacarbonylmanganese(1+) tetrapheny
d	$Rb[AgF_4]$	rubidium tetrafluoroargentate(III)	rubidium tetrafluoroargentate(1-)
e	K_2ReH_9	potassium nonahydridorhenium(VII)	potassium nonahydridorhenium(2-)
f	K_3CrCl_6 or $K_3[CrCl_6]$	potassium hexachlorochromium(III) or potassium hexachloridochromium(III)	potassium hexachlorochromium(3-) or potassium hexachloridochromium(3-)
g	$[Ru(H_2O)_6]Cl_2$	hexaaquaruthenium(II) chloride	hexaaquaruthenium(2+) chloride
h	[*cis*-$Fe(CO)_4I_2$]	*cis*-tetracarbonyldiiodoiron(II)	*cis*-tetracarbonyldiiodoiron(0)
i	K_2[*trans*-$Fe(CN)_4(CO)_2$]	potassium *trans*-dicarbonyltetracyanoferrate(II)	potassium *trans*-dicarbonyltetracyanofe
j	[*cis*-$MnCl(H_2O)_4(NH_3)](NO_3)$	*cis*-ammine tetraaquachloromanganese(0) nitrate	*cis*-ammine tetraaquachloromanganese
k	K[*fac*-$RuCl_3(PMe_3)_3$]	potassium *fac*-trichlorotris(triphenylphosphine)ruthenium(II)	potassium *fac*-trichlorotris(triphenylphosphine)ruth

Exercise 5.2.7

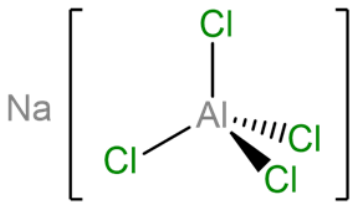
#	Structure	Stock system name	Ewing-Bassett system name
1		*cis*-tetraacetonitriledicyanoiron(II) or *cis*-tetraacetonitriledicyanidoiron(II)	*cis*-tetraacetonitriledicyanoiron(0) or *cis*-tetraacetonitriledicyanidoiron(0)
2		*trans*-tetraacetonitriledicyanoiron(II) or *trans*-tetraacetonitriledicyanidoiron(II)	*trans*-tetraacetonitriledicyanoiron(0) or *trans*-tetraacetonitriledicyanidoiron(0)
3		*trans*-bromochlorobis(ethylenediamine)iron(III) or *trans*-bromidochloridobis(ethylenediamine)iron(III)	*trans*-bromochlorobis(ethylenediamine)iron(1+) or *trans*-bromidochloridobis(ethylenediamine)iron(1+)

#	Structure	Stock system name	Ewing-Bassett system name
4		*fac*-tricarbonyltricyanomolybdate(0) or *fac*-tricarbonyltricyanidomolybdate(0)	*fac*-tricarbonyltricyanomolybdate(3-) or *fac*-tricarbonyltricyanidomolybdate(3-)
5		*mer*-tricarbonyltricyanomolybdate(0) or *mer*-tricarbonyltricyanidomolybdate(0)	*mer*-tricarbonyltricyanomolybdate(3-) or *mer*-tricarbonyltricyanidomolybdate(3-)
6		pentammineni trito-*N*-cobalt(III), pentammineni trito-κ*N*-cobalt(III), or pentammineni trocobalt(III)	pentammineni trito-*N*-cobalt(2+), pentammineni trito-κ*N*-cobalt(2+), or pentammineni trocobalt(2+)
7		pentammineni trito-*O*-cobalt(2+), pentammineni trito-κ*O*-cobalt(2+), or pentammineni tritocobalt(2+)	pentammineni trito-*O*-cobalt(2+), pentammineni trito-κ*O*-cobalt(2+), or pentammineni tritocobalt(2+)

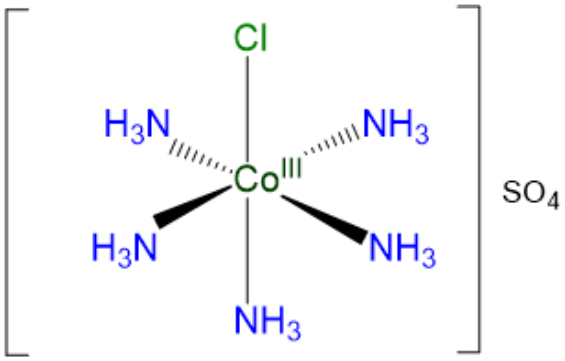
Exercise 5.2.8



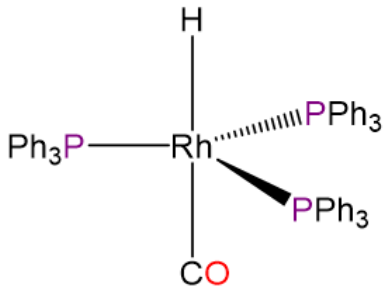
(2,2'-bipyridine)tetracyanoruthenium(2-)



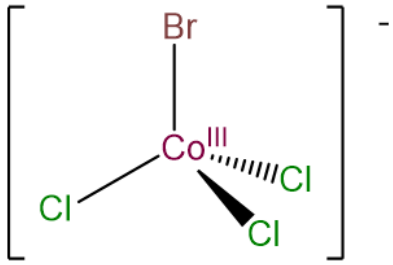
Sodium tetrachloroalumnate



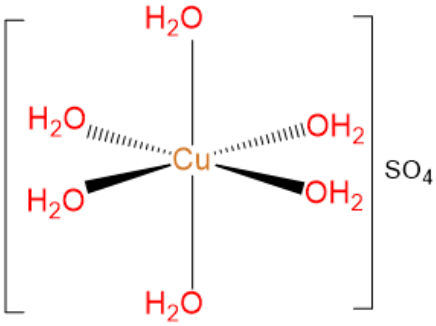
pentaamminechlorocobalt(2+) sulfate



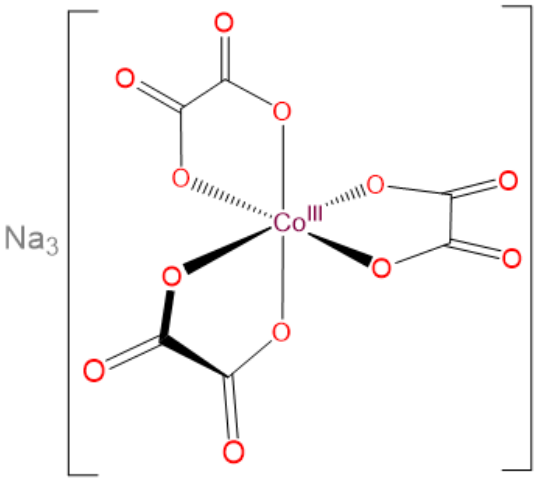
carbonylhydridotris(triphenylphosphine)rhodium(I)



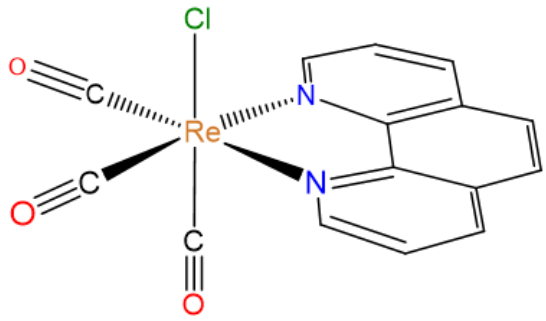
bromotrichlorocobaltate(III)



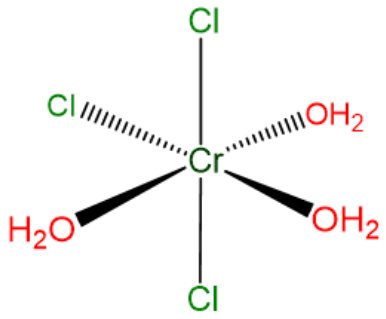
hexaaquacopper(2+) sulfate



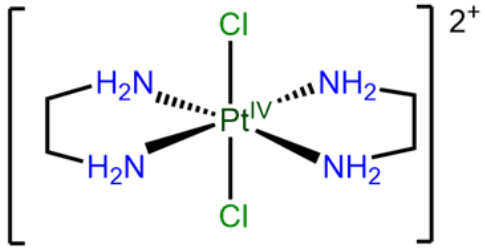
sodium tris(oxalato)cobalt(III)
Λ-enantiomer shown



fac-(1,10-phenanthroline)tricarbonylchlororhenium(I)



mer-triaquatrichlorochromium(III)

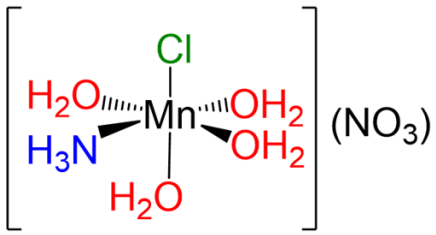


trans-dichlorobis(ethylenediamine)platinum(IV)

Exercise 5.2.9**.**

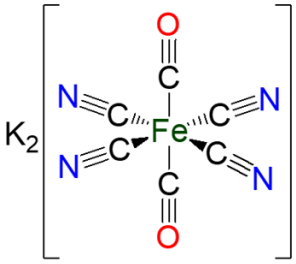
Δ-tris(tetraammine-μ-dihydroxocobalt)cobalt(6+) or Δ-tris(tetraammine-μ-dihydroxocobalt(III)cobalt(III)

Exercise 5.2.10



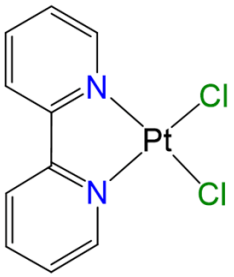
1

[*cis*-MnCl(H_2O)$_4$(NH_3)](NO_3)



2

K_2[*trans*-Fe(CN)$_4$(CO)$_2$]



3

[Pt(bpy)Cl_2]

Exercise 5.2.11

[CoCl(NH_3)$_5$](SO_4)

Δ-[Mn(NH_3)$_2$(ox)$_2$]$^-$

trans-[Fe(CN)$_2$($NCMe$)$_4$]

[$MoCl_2(CO)_3(PPh_3)$] or $MoCl_2(CO)_3(PPh_3)$

mer-[CrBrCl(H_2O)$_3$I]

[Co(O_2)py(salen)]

[Fe(NO)$_2$(SEt)$_2$]$^-$

[MnCl(por)]$^-$ or [MnCl(porphyrin)]$^-$

[Ni(DMG)$_2$] or [Ni($Hdmg$)$_2$]

potassium *trans*-[Fe(CN)$_2$(CO)$_4$]

trans-[CuCl(H_2O)$_4$(NH_3)]SO_4

trans-[$PtCl_2(en)_2$]$^{2+}$

cis-[CoBrCl(NH_3)$_4$]SO_4

K_2[Fe(CN)$_5$NO]

Exercise 5.2.10

[$Cr_2(NH_3)_8$-μ(NH_2)-μ(OH)]$^{4+}$ or [(H_3N)$_4$$Cr^{III}$-$\mu$($NH_2$)-$\mu$(OH)-$Cr^{II}$($NH_3$)$_4$] and variants thereof involving writing the H_3N as NH_3, μ as μ_2, etc.

[$CoCr(NH_3)_{10}$-μ(OH)]$^{5+}$ or, better, [(H_3N)$_5$$Co^{III}$-$\mu$(OH)-$Cr^{III}$($NH_3$)$_5$]$^{5+}$

This was already done as an example above, [$Co_2Cl_5(NH_3)_5$-μ(OH)] or, better, [(NH_3)$_5$$Co^{III}$-$\mu$(OH)-$Co^{III}Cl_5$] and variants thereof

[$CoCrCl_4(NH_3)_4$-μ(NH_2)-μ(OH)] or, better, [(H_3N)$_4$$Co^{III}$-$\mu$($NH_2$)-$\mu$(OH)-$Cr^{II}Cl_4$]

This page titled 5.2: Nomenclature and Ligands is shared under a license and was authored, remixed, and/or curated by LibreTexts.

- 9.3: Nomenclature and Ligands by Stephen M. Contakes has no license indicated.

5.3: Isomerism

Metal complexes present a rich, interesting, and diverse structural chemistry. Major points of variation in the structural chemistry of metal complexes include

1. **coordination number** and **coordination geometry**, which involve differences in how many ligands surround a central metal and their overall geometric arrangement. Examples of the latter include the tetrahedral and square planar geometries commonly observed for four-coordinate metal centers. Tetrahedral, square planar, and octahedral coordination serve as a backdrop to the discussion of isomerism on this page. Readers who are unfamiliar with these structures might consider reading the section on coordination geometries before this one.
2. **structural iosmerism** involves differences in how potential ligand atoms are bound to metals in a complex. Possibilities for structural isomerism include
   - linkage or ambidentate isomerism
   - hydrate/solvate isomerism
   - ionization isomerism
   - coordination isomerism.

   Of these, linkage isomerism should always be considered when working with ambidentate ligands. As classifications, the last three forms of structural isomerism are mainly of academic interest since they represent permutations of ordinary structure patterns for solvates, salts, and coordination complexes, respectively.

3. **stereochemistry**, which includes
   - which coordination geometry is adopted for a metal with a given set of ligands in a particular oxidation state. For instance, $[Ni^{II}Cl_4]^{2-}$ is tetrahedral while $[Pt^{II}Cl_4]^{2-}$ is square planar. Since this geometry is usually fixed by the metal and ligands it is typically not a source of stereoisomeric varierty.
   - metal-centric stereoisomerism involving possible variations in where ligands are located relative to one another around the metal. The possibilities depend on the coordination number, geometry, and number of different types of ligands. For instance, square planar complexes can exhibit *cis-/trans-* isomerism while tetrahedral ones cannot. Tetrahedral complexes with four different ligands exhibit *R* and *S* chirality but complexes of that type are relatively rare. The more common cases include *cis* and *trans* isomerism in square planar complexes and *cis* & *trans-*, *mer & fac-*, and Λ & Δ isomerism in octahedral ones, although some multidentate ligands present additional possibilities for stereochemical variation
   - Stereoisomerism centered on the ligands bound to a metal center. Possibilities include
     - stereoisomerism inherent to a ligand. This would include cases where the ligand itself is chiral or, as in the case of amines, exists as a rapidly interconverting mixture of isomers. Thus this sort of stereoisomerism is an extension of the isomerism encountered in ordinary organic and other main group compounds. The main new issues introduced by binding of such ligands to a metal center involve the creation of new possibilities for diastereoisomerism based on the stereochemistry of the metal center and the freezing out of stereocenter inversion on binding to a metal. The latter is particularly important for amines, which as free amines racemize rapidly by nitrogen inversion.
     - or conformational isomerism involving five-membered **chelate rings** created when a multidentate ligand binds to a metal. This isomerism is often called chelate ring twist since individual rings can exhibit one of two conformations depending on how they twist on binding.

A summary of these forms of isomerism is given in Figure 5.3.1.

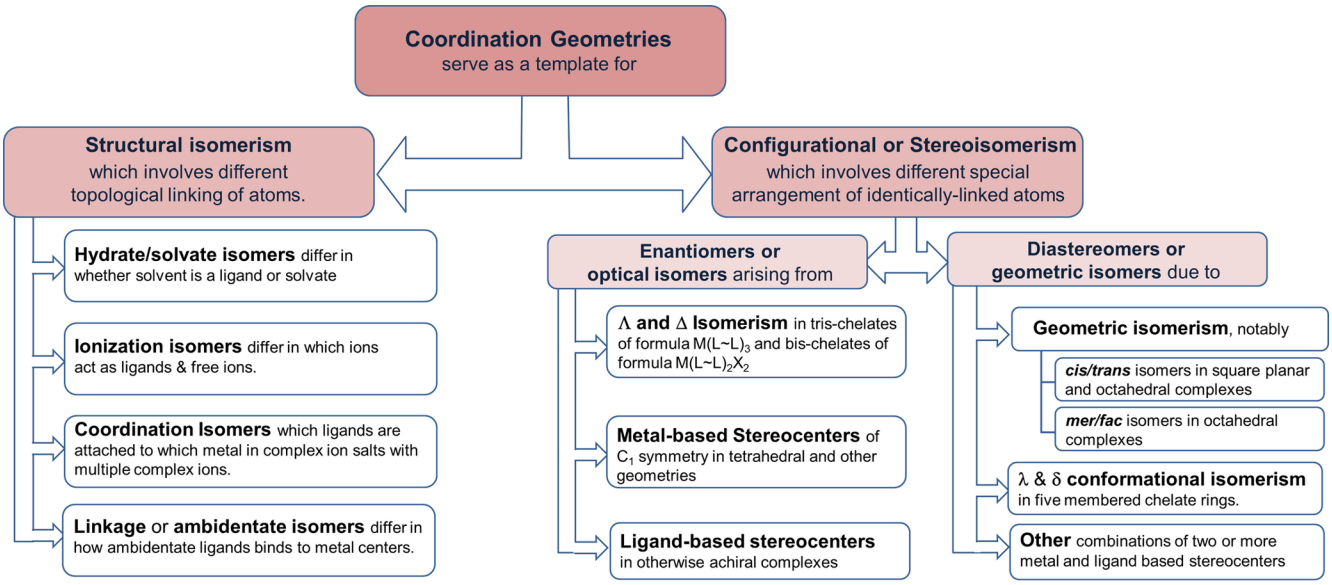


Figure 5.3.1. Relationship among the common types of isomerism in metal complexes. This work by Stephen Contakes is licensed under a Creative Commons Attribution 4.0 International License.

Structural isomers

Structural isomerism involves different topological linkages of atoms. Differences in atomic linkages distinctive to coordination chemistry involve the linkages between metals and ligands. The main variations are:

1. Hydrate/solvate isomerism

Solvate isomers differ in terms of whether a molecule acts as a ligand or whether it acts as a solvate by occupying a lattice site in the crystal. Among solvate isomers, the case in which water is the ligand or solvate is the best known. The resulting isomers are called **hydrate isomers** after the term for water acting as a solvate, hydrate. A well-known example that illustrates how solvate isomerism works is the series $[CrCl_x(H_2O)_{6-x}]Cl_{3-x}{\cdot}xH_2O$, for which x = 0-2. The structures of the complex ions involved in this series are shown in Figure 5.3.2.[1]

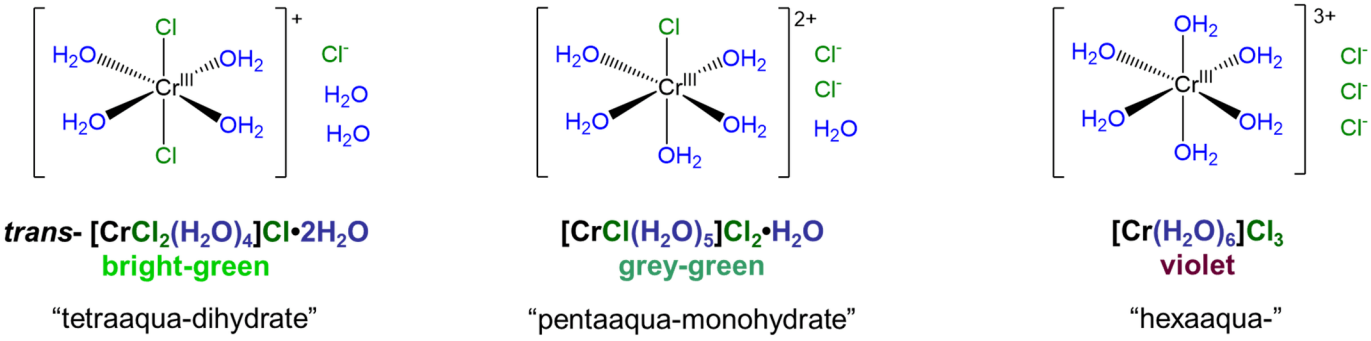


Figure 5.3.2. Complexes of the hydrate isomer series $[CrCl_x(H_2O)_{6-x}]Cl_{3-x}{\cdot}xH_2O$ (x = 0-2). This work by Stephen Contakes is licensed under a Creative Commons Attribution 4.0 International License.

As can be seen from the compounds in Figure 5.3.2, hydrate isomers differ both in terms of whether water acts as a ligand or hydrate *and* in terms of whether a potential counterion acts as a counterion or ligand. Thus, in *trans*-$[CrCl_2(H_2O)_4]Cl{\cdot}2H_2O$ two chlorides act as chloro ligands and four waters as aqua ligands while in $[CrCl(H_2O)_5]Cl_2{\cdot}H_2O$ five water molecules act as aqua ligands while only one chloride acts as a chloro ligand. In this way, solvate isomers simply represent cases in which two or more of the possible permutations for metal ligand binding among a set of solvent and counterion molecules are stable.

2. Ionization isomerism

In **ionization isomerism** there are two or more potential ions that can act as ligands. The ionization isomers differ in terms of which of these ions act as counterions and which act as ligands. Consider, for instance, the complexes shown in Figure 5.3.3. These complexes differ in terms of whether the chloride or sulfate acts as a ligand, with the other acting as a counterion.

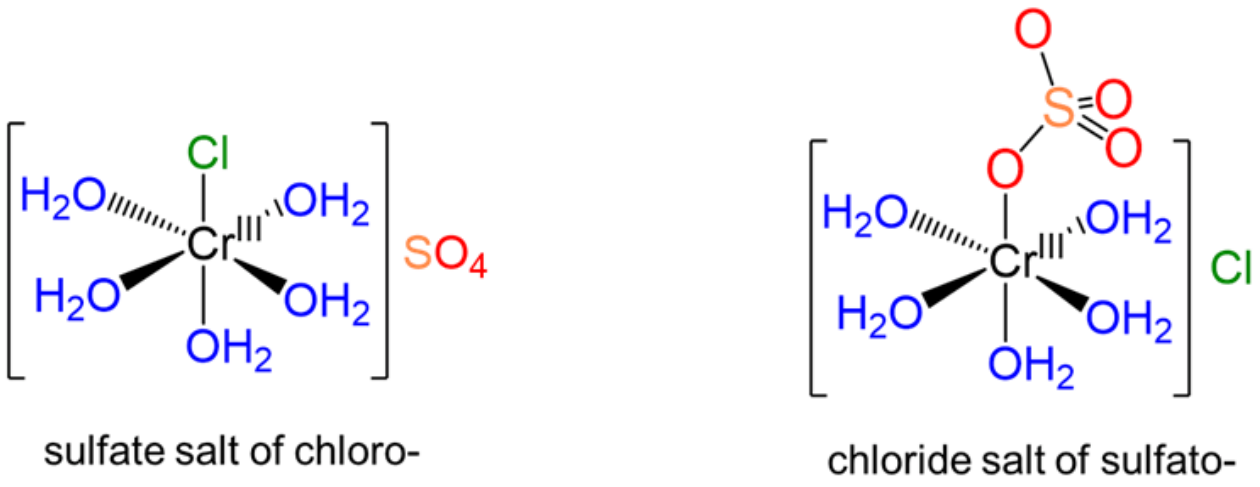


Figure 5.3.3. Ionization isomers comprising a pentaaquachromium(III) fragment and the anions chloride and sulfate. As with all ionization isomers, the isomers differ in terms of which anion acts as a ligand and which a counterion. This work by Stephen Contakes is licensed under a Creative Commons Attribution 4.0 International License.

3. Coordination isomerism

Coordination isomers exist in compounds containing two or more complexes, each of which possesses a different set of ligands that can in principle be swapped with a ligand of the other complex. An example involves $[Co^{III}(NH_3)_6][Cr^{III}(ox)_3]$, depicted in Figure 5.3.4A.[1] Coordination isomers of this complex involve swapping the ammine ligands around the Co^{3+} center for oxalato ligands surrounding the Cr^{3+} center. For instance, swapping all the ammine and oxalato ligands between the metal centers gives the coordination isomer $[Cr^{III}(NH_3)_6][Co^{III}(ox)_3]$ shown in Figure 5.3.4B.

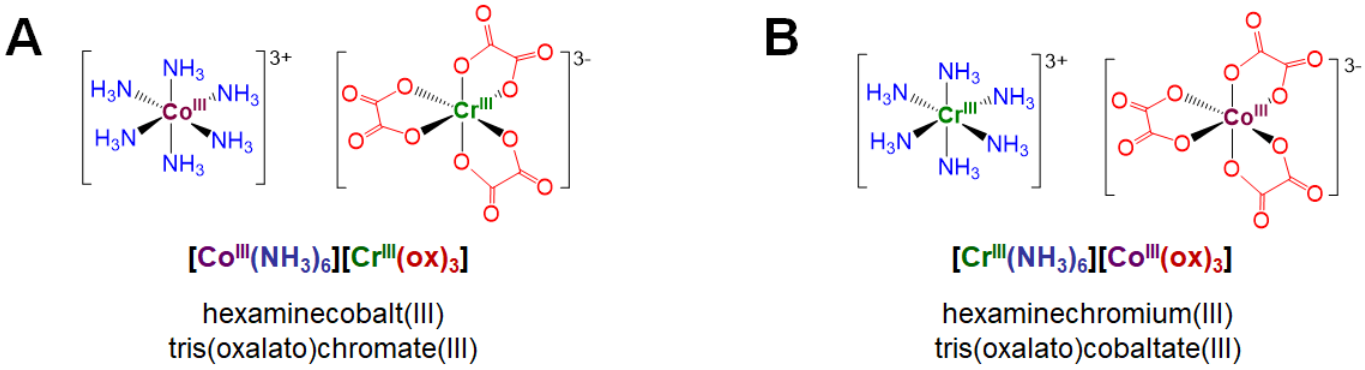
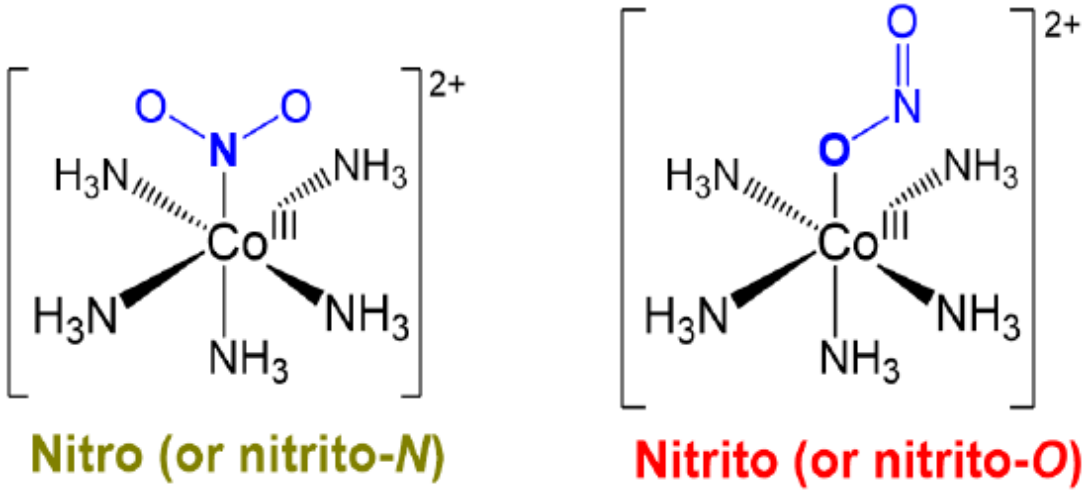


Figure 5.3.4. Two coordination isomers comprising a Co^{3+} ,Cr^{3+}, six NH_3. and three oxalato ligands. The isomers differ in terms of which ligand type is bound to which metal. This work by Stephen Contakes is licensed under a Creative Commons Attribution 4.0 International License.

As classifications, hydrate/solvate, ionization, and coordination isomerism represent permutations of ordinary structure patterns for solvates, salts, and coordination complexes, respectively. As a result these forms of isomerism are rarely used as independent conceptual frameworks when thinking and talking about the structure of coordination compounds. Not so the final type of structural isomerism, linkage isomerism. That is because linkage isomerism has to do with the special *capacity* of ambidentate ligands to bind metals in multiple ways.

4. Linkage or ambidentate isomerism

Linkage or ambidentate isomers differ in how one or more ambidentate ligands bind to metal centers in a complex. The classic example dating from the work of Jørgensen and Werner is given in Scheme 5.3.I.



Scheme 5.3.I. Linkage isomers of penaamminenitritocobalt(III) ion. This work by Stephen Contakes is licensed under a Creative Commons Attribution 4.0 International License.

Just as alkenes exist as *E* and *Z* isomers, compounds possessing ambidentate ligands exist as one among the possible linkage isomers. As such, when working with ambidentate ligands the particular linkage isomer formed should be determined experimentally and considered when interpreting the complex's chemical and physical behavior.

The main ambidentate ligands which give rise to linkage isomerism are

- cyanide, CN^-
- thiocyanate, SCN^-, and the O and Se analogues, OCN^- and $SeCN^-$
- nitrite, NO_2^-
- sulfite, SO_3^-
- nitrosyl, NO

Although ambidentate ligands can bind metals in multiple ways, most exhibit a preferred binding mode (*i.e.,* prefer to bind metal centers in one of the possible ways). For instance, cyanide almost always binds through its carbon atom and thiocyanate almost always binds through its nitrogen (μ-*N*). However, the other binding mode can sometimes be formed kinetically or by using conditions that particularly favor its formation. Thus thiocyanate forms M-SCN^- linkages in the presence of exceptionally soft metal centers or in hard polar solvents (in which Lewis acid groups can stablize the terminal nitrogen of a bound thiocyanate ligand).

Ambidentate ligands are of significant research interest because many don't just bind to metal centers in two ways; the linkage isomers sometimes have significantly different physical properties. In addition, the possibility of two binding modes introduces the possibility of exploiting linkage isomerism to take advantage of some of these ligands:

a. different structural chemistry in different coordination modes. In mononuclear complexes the coordination mode influences which side of the ligand faces away from the complex and might be susceptible to stabilization by interaction with solvent. Additionally, the orientation of the ligand relative to the metal center might differ between one coordination mode and another. For instance, as predicted from the minor contributor to its resonance structure, thiocyanate binds nonlinearly via its S atom and linearly via its N (Figure 5.3.5). Because of this the apparent steric bulk of the ligand around the metal center might differ between forms.

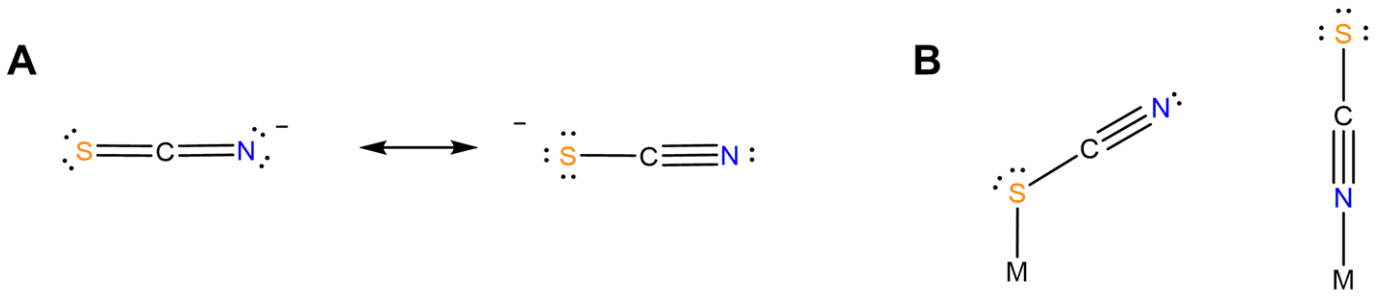


Figure 5.3.5. Thiocyanate generally prefers to bind metals nonlinearly but in some cases forms linear M-SCN bonds. This work by Stephen Contakes is licensed under a Creative Commons Attribution 4.0 International License.

b. bind two different metal centers at the same time, linking them together. Perhaps the best-known examples involve thiocyanate and cyanide. The latter forms linkages of the type M-C≡N-M'. In the dye Prussian blue these take the form Fe^{II}-C≡N-Fe^{III}. An example from the author's graduate research involved tetrahedral clusters containing four metal atoms linked by six cyano ligands, as shown in Figure 5.3.6.

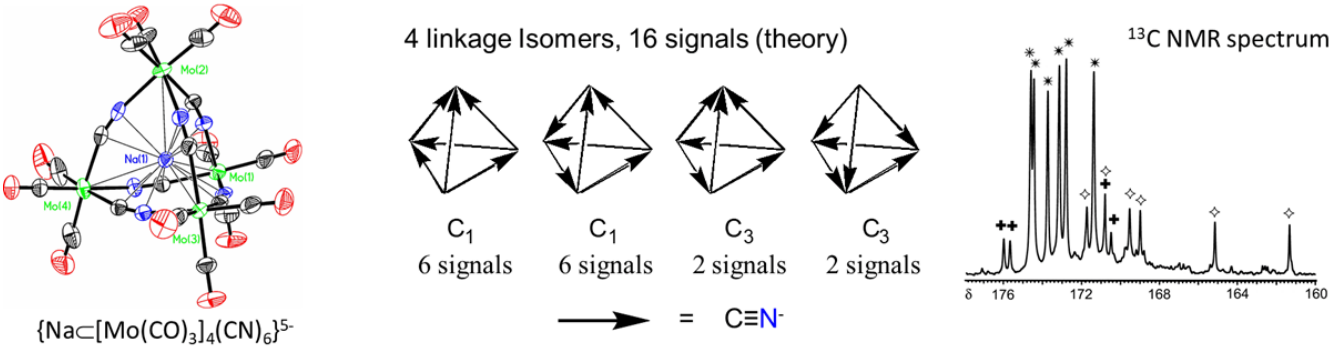


Figure 5.3.6. (A) Structure of $\{Na@[Mo(CO)_3]_4(CN)_6\}$ showing the linking of four Mo centers by six CN ligands. Thermal ellipsoids for the C atoms are shown in black; those of the N atoms in blue. (B) The complex exists as a mixture of four linkage isomers in which the bridging CN^- ligands are oriented in different ways, as may be seen from the presence of the expected sixteen signals in its ^{13}C NMR spectrum. Based on work reported in reference 2.

c. can be induced to change from one binding mode to another in response to a stimulus. The classic example involves the light-driven transformation of the thermodynamically more stable yellow nitro complex of pentamminecobalt(III), $[Co(NH_3)_5NO_2]^{2+}$ to the less stable red *O*-nitrito complex, $[Co(NH_3)_5ONO]^{2+}$. Less stable cyanometallate coordination networks like those in the red $K\{Fe^{II}[Cr^{III}(CN)_6]\}$ transform into the more stable green $K\{Fe^{II}[Cr^{III}(NC)_6]\}$ form on heating, as shown in Figure 5.3.7.[3]

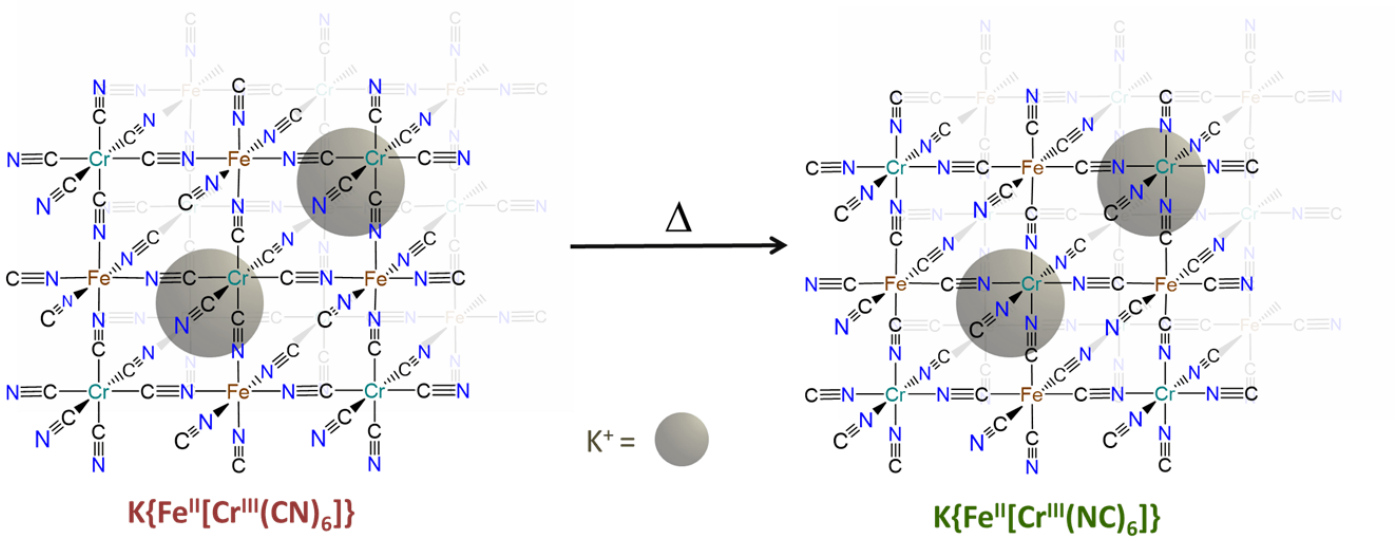


Figure 5.3.7. Thermally-induced transformation of one $K\{Fe^{II}[Cr^{III}(CN)_6]\}$ into its more stable green linkage isomer $K\{Fe^{II}[Cr^{III}(NC)_6]\}$ involves "flipping" the cyano ligands. This work by Stephen Contakes is licensed under a Creative Commons Attribution 4.0 International License.

Exercise 5.3.1: Bridging ambidentate ligands and the Hard-Soft Acid- Base Principle.

The hard-soft acid-base principle helps explain the preference of bridging ambidentate ligands for particular binding modes. How might the greater stability of the green $K\{Fe^{II}[Cr^{III}(NC)_6]\}$ over red $K\{Fe^{II}[Cr^{III}(CN)_6]\}$ be explained in terms of the hard and soft acid-base concept?

Answer available at the end of this section.

Stereoisomerism

Optical Isomerism/Chirality

Molecules of D_n, C_n, or C_1 symmetry with only proper rotation axes (including $E = C_1$) are chiral and exhibit optical isomerism. As described in Figure 5.3.1, the main sources of such optical isomerism in coordination chemistry are:

1. **Chirality inherent to an organic or main group ligand.**

   This type of isomerism is just an extension of the sort described in undergraduate organic texts and consequently does not merit separate discussion here, other than to note that some forms of optical isomerism which are of little importance in organic chemistry lead to optical activity in coordination compounds. In particular, the nitrogen inversion process which serves to rapidly racemize chiral amines is frozen out on formation of a metal-ligand bond. Because of this chiral amine, ligands bound to a metal form non-interconvertible *R* and *S* enantiomers, as shown in Figure 5.3.8.

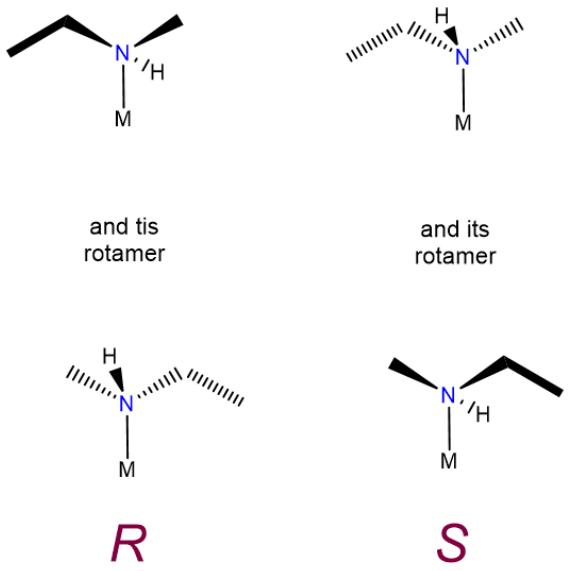


Figure 5.3.8. Two views of *R* and *S* enantiomers formed when the chiral amine ethylmethylamine binds a metal that are commonly used to represent chiral amines in complexes. This work by Stephen Contakes is licensed under a Creative Commons Attribution 4.0 International License.

2. Chirality arising from the symmetry of ligands about a metal center.

The two common situations through which such chirality arises involve:

i. Chirality at a tetrahedral metal center surrounded by four different ligand attachment points.

Such cases are often referred to as MABCD or Mabcd where M stands for the metal and a, b, c, and d the four different ligand attachment points. An example of such a complex is given in Figure 5.3.9A. The chirality of such complexes is analogous to the chirality arising from a tetrahedral carbon stereocenter. There are two caveats, though. First, it is not enough to have a four-coordinate complex; the metal must possess tetrahedral symmetry since, as shown in Figure 5.3.9B, square planar M complexes with four different ligands are identical to their mirror images. Second, such chirality is most easily realized using macrocyclic ligands like proteins. Metal ligand bonds involving sterically unhindered monodentate complexes like that in the example of Figure 5.3.9A are in general weaker and more flexible than analogous carbon-carbon bonds. Consequently, in such cases it is likely that the enantiomers would interconvert through a fluxional process, making their resolution difficult if not impossible.

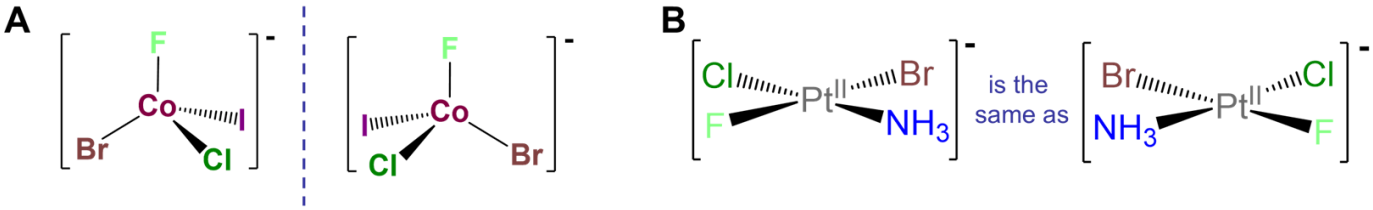


Figure 5.3.9. (A) In principle tetrahedral metal centers surrounded by four different ligands (Mabcd) exhibit chirality analogous to the chirality of tetrahedral carbon stereocenters; (B) in contrast, square planar Macbd complexes like $[PtBrClF(NH_3)]^-$ are not chiral since they are the same as their mirror images. (It is easiest to see this by either working out its point group (C_s) or by rotating the left $[PtBrClF(NH_3)]^-$ structure clockwise 180 degrees to give its mirror image. This work by Stephen Contakes is licensed under a Creative Commons Attribution 4.0 International License.

ii. Λ and Δ isomerism at octahedral metal centers surrounded by two or three chelating ligands.

Specifically,

a. Octahedral tris-chelates of formula $M(L\sim L)_3$ exhibit D_3 symmetry.

b. cis-octahedral bis-chelates of formula $M(L\sim L)_2XY$ exhibit C_2 or C_1 symmetry: C_2 if X = Y and C_1 if $X \neq Y$.

As shown in Figure 5.3.10A, octahedral tris-chelates like $[V(ox)_3]^{3-}$ are chiral and can exist as nonsuperimposable Λ and Δ enantiomers. The chirality of these tris-chelates is analogous to that of pinwheels. As shown in Figure 5.3.10B, when looking directly at the head of any individual pinwheel from above, the blades will be angled from back to front going around the pinwheel in either the clockwise or counterclockwise direction. As shown in Figure 5.3.10C, the case for which the blades are angled in the clockwise direction is analogous to the Λ enantiomer and the case when they are angled in the counterclockwise direction the Δ.

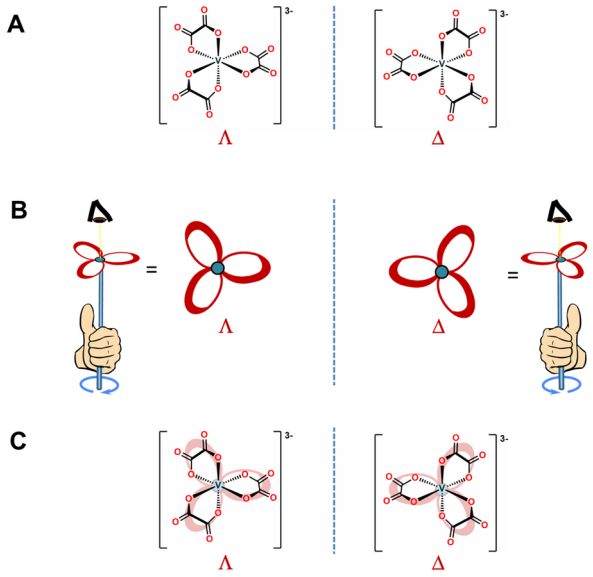


Figure 5.3.10. (A) Octahedral tris-chelates like $[V(ox)_3]^{3-}$ are chiral and can exist as Λ and Δ enantiomers. (B) The chirality in these systems is analogous to that of a pinwheel, with the Λ enantiomer exhibiting the symmetry of a left-handed pinwheel and the Δ enantiomer that of a right handed one. (C) The pinwheel-like nature of Λ and Δ enantiomers is easiest to see by overlaying the structures of $[V(ox)_3]^{3-}$ from A with the pinwheel structures of B. One way to recognize Λ and Δ enantiomers is to draw them in these projections. If a left hand is curled around the Λ enantiomer with the thumb facing up the curl of the fingers will flow from the back of each ligand towards the front. The same will be true if the right hand is curled around the Δ enantiomer. Credits: Although the image is largely an original drawing, the hand images used in part B are adapted from an image by SVGguru / CC BY-SA (https://creativecommons.org/licenses/by-sa/4.0). Otherwise this work by Stephen Contakes is licensed under a Creative Commons Attribution 4.0 International License.

The Λ and Δ chirality in octahedral bis-chelates is analogous to that in the tris-chelates except this time the third chelating ligand is replaced by an arbitrary pair of ligands. This lowers the symmetry of the complex to either C_2 or C_1, as shown for the C_2 complex $[CoCl_2(en)_2]^+$ in Figure 5.3.11A. In either case the result is that such complexes exist as Λ and Δ enantiomers analogous to those in the metal tris-chelates, as shown in Figure 5.3.11B.

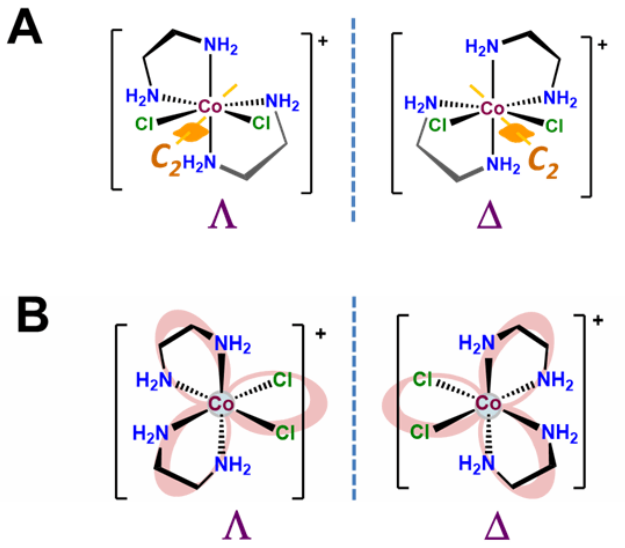


Figure 5.3.9C. This work by Stephen Contakes is licensed under a Creative Commons Attribution 4.0 International License.

Octahedral complexes containing ligands with denticities of four or more also exhibit Λ and Δ chirality; it is just that in such cases the bound ligand defines multiple rings within the complex that can be defined as existing in either Λ or Δ orientations relative to each other. The procedure for making these assignments is beyond the scope of most introductory inorganic courses but the result is that such complexes are designated as ΛΛ, ΔΔ, ΔΛ, ΔΔΔ, etc., depending on the number of relationships involving the rings defined by the bound ligand. Interested readers should consult reference 4 for more details.

Circular dichroism may be used to characterize optically active metal complexes.

At the present the most definitive way to determine the absolute configuration of an optically active coordination compound is to determine its 3D molecular structure using single crystal X-ray crystallography.[5] However, as that is not always possible or convenient, the optical activity of coordination complexes is also commonly studied using circular dichroism (CD) spectroscopy. CD spectroscopy is used because, unlike most chiral organics, optically active coordination complexes possess low-energy electronic transitions that occur in the far UV and visible range. This means that it is often convenient to use the ability of a complex to refract and absorb different circular polarizations of light to derive information about both the configuration of an optically active complex and its electronic structure. The focus of this section will be to explain how the determination of absolute configuration by circular dichroism and optical rotatory dispersion work, as well as the relationship of these techniques to the more ordinary sort of polarimetry used to measure optical rotation in organic systems. Only brief notes will be made about the instrumental and electronic structure applications of these techniques since the electronic spectra of metal complexes will be discussed in Chapter 11: Coordination Chemistry III - Electronic Spectra and the instrumental aspects of CD are well-treated elsewhere.

Both polarimetry and circular dichroism spectroscopy are grounded in the recognition that plane polarized light is equivalent to a superposition of left and right circularly polarized light, as shown in Figure 5.3.12.

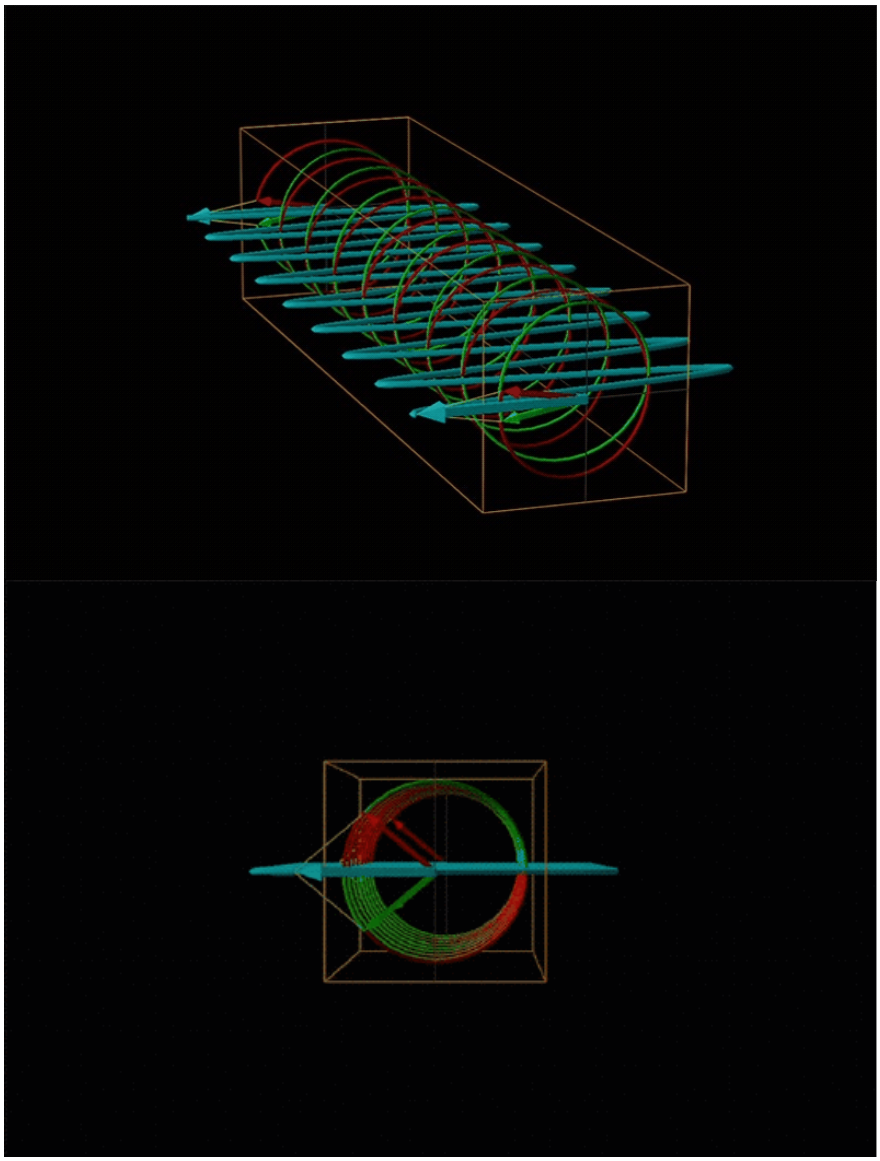


Figure 5.3.12. Angled and front view of plane polarized light (light blue) as the vector sum of left circularly polarized light (red) and right circularly polarized light (green). Created using EMANIM Version 1.2 (2011 July) by Andras Szilagyi (www.enzim.hu/~szia/emanim). This work by Stephen Contakes is licensed under a Creative Commons Attribution 4.0 International License.

When plane polarized light passes through a chiral medium, its left and right circularly polarized components move at different rates (*i.e.,* have different indices of refraction). This causes the plane of polarization to rotate in the direction of the faster component according to the relationship

$$\alpha = \frac{n_l - n_r}{\lambda}$$

where α is the angle of rotation, λ the light's wavelength, and n_l and n_r the refractive indices experienced by left and right circularly polarized light.

An example of such a rotation is shown in Figure 5.3.13.

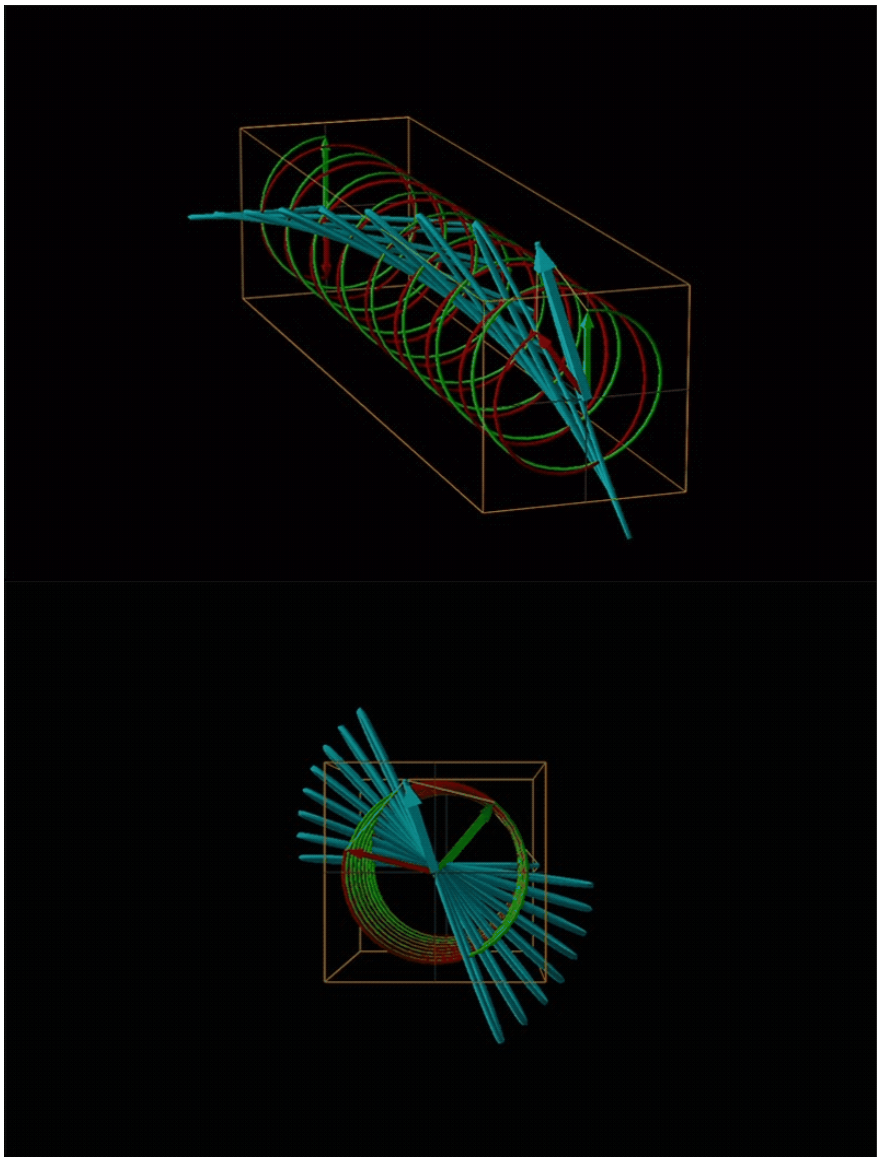


Figure 5.3.13. Angled and front view of plane polarized light (light blue) as it passes through a medium (represented by the orange box) in which left circularly polarized light (red) experiences a higher refractive index (and so moves slower) than right circularly polarized light (green). Created using EMANIM Version 1.2 (2011 July) by Andras Szilagyi (www.enzim.hu/~szia/emanim) with a refractive index of 1.05 for left circularly polarized light and 1.00 for right circularly polarized light. This work by Stephen Contakes is licensed under a Creative Commons Attribution 4.0 International License.

Chemists typically call this rotation of light by a chiral medium optical rotation. In organic chemistry it is common to measure the optical rotation at the sodium D wavelength of 589.29 nm, a much longer wavelength than most organics are able to absorb. Because of this the optical rotations commonly measured by organic chemists are largely independent of absorption and mainly serve as a characteristic physical property similar to melting points or are used to establish the purity of a mixture of enantiomers. The sort of spectroscopic data used to characterize chiral coordination compounds more commonly makes use of the relationship between absorption and optical rotation.

In coordination chemistry the wavelength-dependence of optical rotation is used to discern information about compounds' electronic spectra. This measurement of the wavelength dependence of optical rotation is called **optical rotatory dispersion (ORD)** and the resulting plots are called optical rotatory dispersion or ORD spectra or curves. Such ORD curves are useful for characterizing the chiral environment in a coordination complex because the ORD curves exhibit a characteristic shape. This characteristic shape is because according to the **Cotton Effect,** the optical rotation changes sign at the absorption maximum of a chromophore in the compound. For one configuration the rotation will go from negative to positive with increasing wavelength and is called a **positive cotton effect**; for the other configuration the rotation will go from positive to negative or exhibit a **negative cotton effect**. This behavior is summarized in the top two curves of Figure 5.3.14.

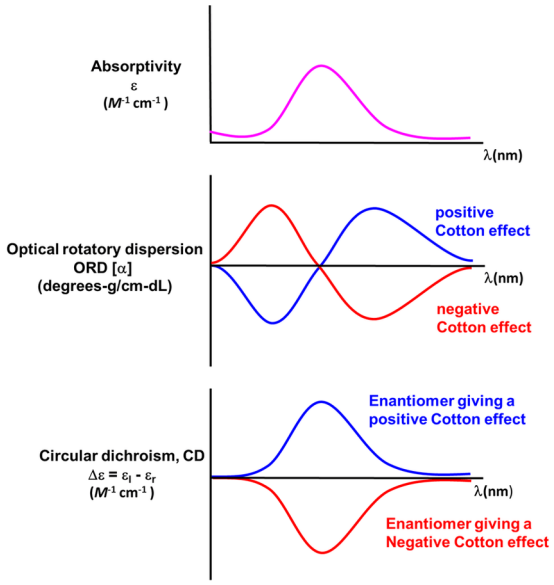


Figure 5.3.14. Idealized relationship between absorbance, ORD, and CD spectra for enantiomers exhibiting a positive and negative Cotton effect. This work by Stephen Contakes is licensed under a Creative Commons Attribution 4.0 International License.

A technique used even more often than ORD is **circular dichroism (CD)**, represented by the lowest spectrum in Figure 5.3.14 . Circular dichroism arises from the differential absorption of left and right circularly polarized light by a chiral compound. This gives elliptically polarized light as shown in Figure 5.3.15.

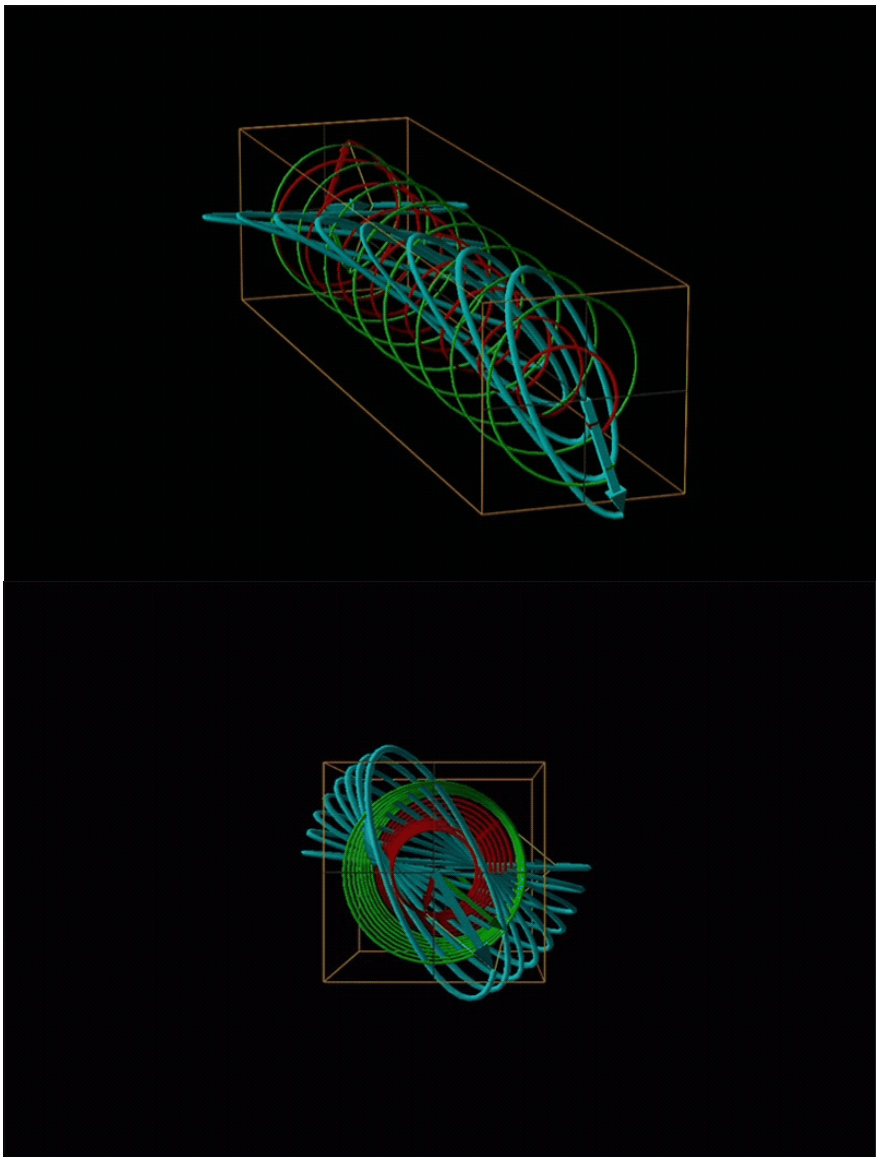


Figure 5.3.15. Angled and front view of plane polarized light (light blue) as it passes through a medium (represented by the orange box) in which left circularly polarized light (red) both experiences a higher refractive index and greater absorption than right circularly polarized light (green). Created using EMANIM Version 1.2 (2011 July) by Andras Szilagyi (www.enzim.hu/~szia/emanim) with a refractive index of 1.05 and an extinction coefficient of 0.05 for left circularly polarized light and a refractive index of 1.00 and extinction coefficient of 0 for right circularly polarized light. This work by Stephen Contakes is licensed under a Creative Commons Attribution 4.0 International License.

In circular dichroism (CD) spectroscopy a sample is irradiated with polarized light resulting in the transmission of elliptically polarized light due to differential refraction and absorption of the polarized light's left and right circularly polarized components. For achiral molecules the handedness doesn't affect absorbance, but for chiral molecules, which chiral ground and excited states the handedness of an EM wave affects can determine how readily that wave can distort the chiral ground state into the chiral excited one. For this reason chiral molecules absorb left and right circularly polarized light differently.

In CD spectroscopy the magnitudes of the left and right circularly polarized components of light that is transmitted by the sample are measured and used to determine how much light of each was absorbed (just as in regular absorbance spectroscopy). The difference in absorption between left and right circularly polarized light constitutes the primary signal in CD spectroscopy. More specifically, circular dichroism spectra (CD spectra) show the difference in extinction coefficients for left and right circularly polarized light, $\Delta\epsilon$, as a function of wavelength, where

$$\Delta\epsilon = \epsilon_l - \epsilon_r$$

where Missing open brace for subscript and Missing open brace for subscript are the extinction coefficients

observed with left and right circularly polarized light, respectively.

As with ORD spectra, the signs of the features in CD spectra like that of Δ–[Co(en)$_3$]Cl$_3$ given in Figure 5.3.16 are enantiomer-dependent. As illustrated in the lower spectrum in Figure 5.3.14 , the CD spectra of enantiomers mirror one another. Because of this difference in behavior it is possible in principle to determine the absolute configuration of a complex from its CD spectrum.

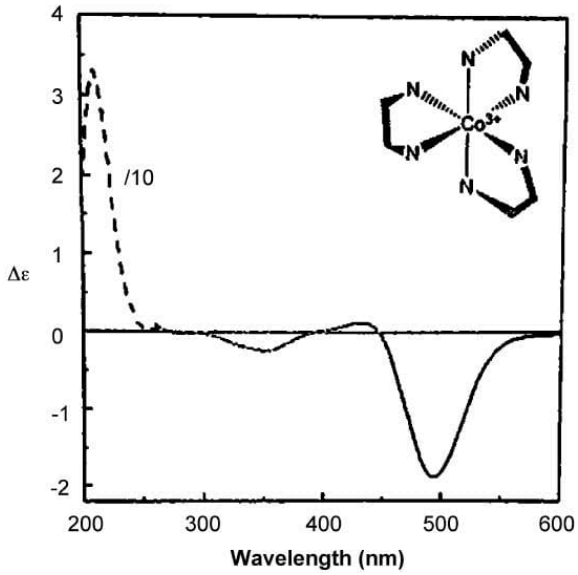


Figure 5.3.16. CD spectrum of Δ–[Co(en)$_3$]Cl$_3$. Taken from reference 6.

There are several ways that ORD and CD spectra can be useful for determining the absolute configuration of a chiral complex.

1. First, the sign of the Cotton effect and peaks in CD spectra exhibited by a given absolute configuration is often consistent across a series of compounds. Thus if a new member of the series is isolated, its configuration can be determined based on which enantiomer has the same Cotton effect. For instance, if both the Λ isomer of a metal diimine complex like [Ru(bpy)$_3$]$^{2+}$ exhibit a positive Cotton effect and a newly resolved metal diimine exhibits a negative Cotton effect it might reasonably be inferred that the newly-resolved complex is in the opposite or Δ configuration.
2. Second, for some systems the expected sign of the Cotton effect and CD peaks for each enantiomer may be predicted semi-empirically based on the spatial locations of substituents relative to the chromophore (the part of the molecule that changes electronic structure during the transition), although the details are beyond the scope of the present discussion.
3. Consideration of interactions between multiple chromophores in a compound can be used to infer absolute configuration. Again, the details are beyond the scope of the present discussion. Interested readers are referred to reference 7 for details.

Common patterns of Diastereomerism

Geometric isomerism

Geometric isomerism involves differences in the geometric placement of atoms in a compound. In coordination chemistry, geometric isomerism involves differences in the relative placement of a set of ligands about a metal center. There are two main types:

cis and *trans* isomerism

This type of isomerism has to do with how two ligands are oriented relative to one another in a square planar or octahedral complex. As shown in Figure 5.3.17, ligands that are next to one another with a L-M-L bond angle of 90° are said to be *cis*; those on opposite sides of the metal with a L-M-L bond angle of 180° are in the *trans* arrangement.

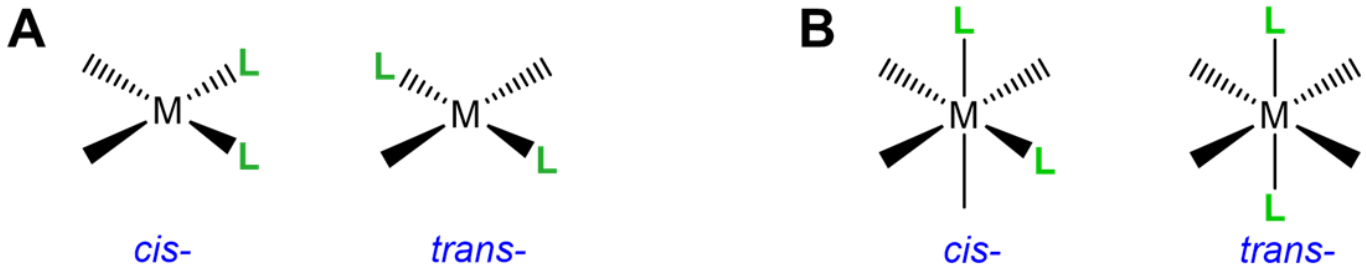


Figure 5.3.17. *cis* and *trans* arrangement of ligands around (A) square planar and (B) octahedral metal centers. Since both types of complexes feature 90° L-M-L bond angles, the arrangements are fundamentally the same in both cases. This work by Stephen Contakes is licensed under a Creative Commons Attribution 4.0 International License.

Simple *cis* and *trans* geometric isomers can be identified when there are two identical ligands (A) or chelating ligands with distinguishable attachment points (A~B) oriented about either a square planar or octahedral center. Examples are given in Figure 5.3.18. Notice from the example given in Figure 5.3.18C that multidentate ligands have the potential to constrain complexes to adopt a particular geometry.

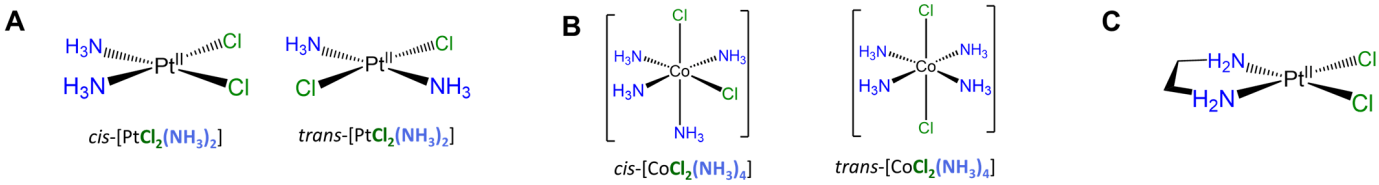


Figure 5.3.18. Examples of square planar and octahedral *cis* and *trans* isomers. (A) *cis* and *trans* isomers of $[PtCl_2(NH_3)_2]$; the former is medicinally important. Sold under the name cisplatin, the *cis* isomer is used as a chemotheraphy against various forms of cancer. (B) *cis* and *trans* isomers of $[CoCl_2(NH_3)_4]$, a compound of more academic interest. (C) $PtCl_2$(en) only exists as the *cis* isomer because the chelating en ligand can only bind in a *cis* arrangement. This work by Stephen Contakes is licensed under a Creative Commons Attribution 4.0 International License.

Slightly more involved examples involve perturbations of the simple cases above in which there are multiple distinguishable *cis* and/or *trans* relationships. Two square planar examples are given in Figure 5.3.19.

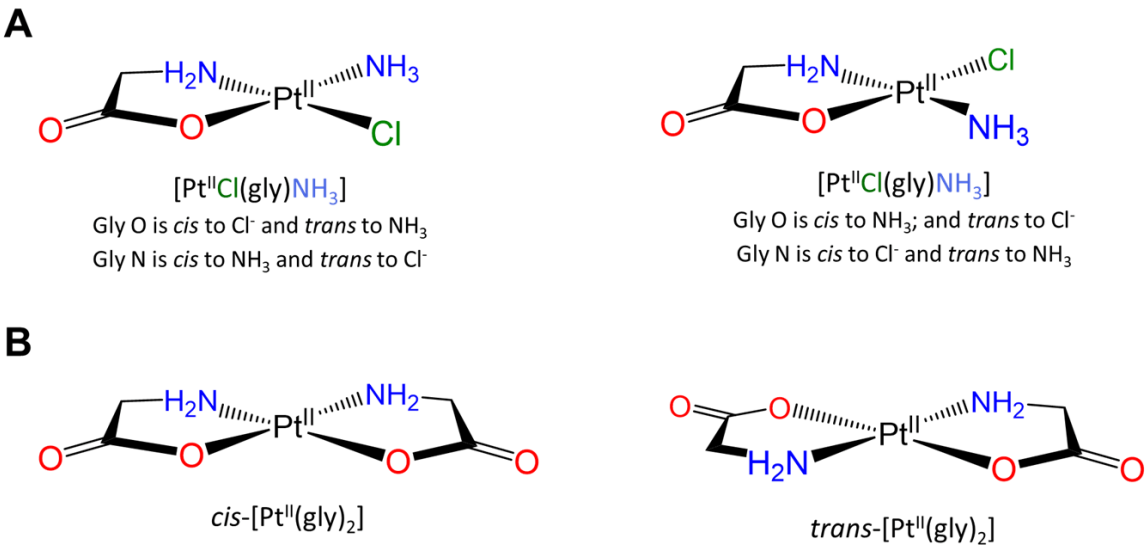


Figure 5.3.19. Examples of more complex square planar systems. (A) Geometric isomers of $[PtCl(gly)NH_3]$, a MA_2BC system for which A = gly^-, B = Cl^-, and C = NH_3. Swapping of the ammine and chloro ligands changes both the *cis* and *trans* relationships involving the Gly ligand. (B) Geometric isomers of $[Pt(gly)_2]$, an $M(A\sim B)_2$ system for which A = the κO glycine carboxy group and B its κN amine. The only possible geometric isomerism involves swapping the orientation of one glycine relative to the other. For this reason the two complexes shown can be designated as *cis* and *trans* isomers based on whether the κO and κN ends of the glycine are *cis* or *trans* to one another. This work by Stephen Contakes is licensed under a Creative Commons Attribution 4.0 International License.

More complex examples of *cis* and *trans* relationships between ligands in octahedral complexes are given in the exercises that conclude this page, which also demonstrates how a systematic approach may be used to identify isomers.

mer and *fac* isomerism

This type of isomerism has to do with how three ligands are oriented relative to one another in an octahedral complex. The arrangements are represented in Figure 5.3.20.

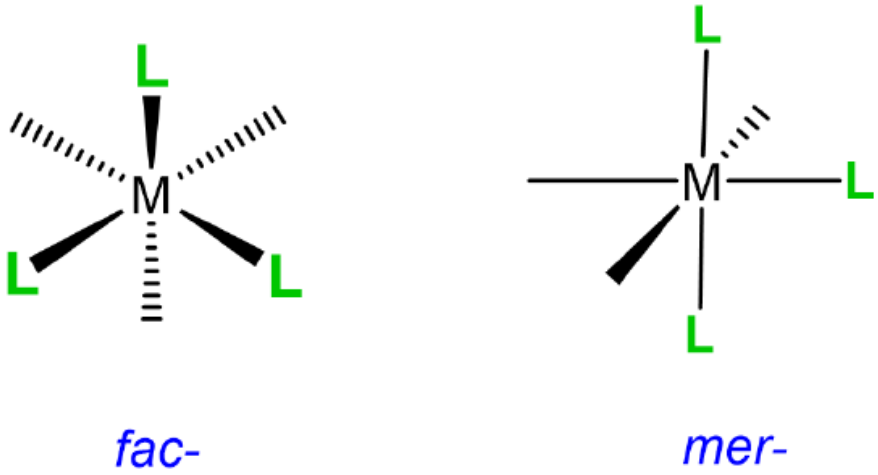


Figure 5.3.20. Simple representation of the *fac* and *mer* arrangements of ligands around an octahedral metal center. This work by Stephen Contakes is licensed under a Creative Commons Attribution 4.0 International License.

Since it can help to visualize the *mer* and *fac* geometry from multiple points of view, several representations are given in Figure 5.3.21. As shown in Figure 5.3.21, in ***fac*** or **facial arrangements**, the ligands occupy the same "face" of the octahedral coordination sphere, while in the ***mer*** or **meridional geometry** the ligands form a T shape in the same plane or its "meridian."[8]

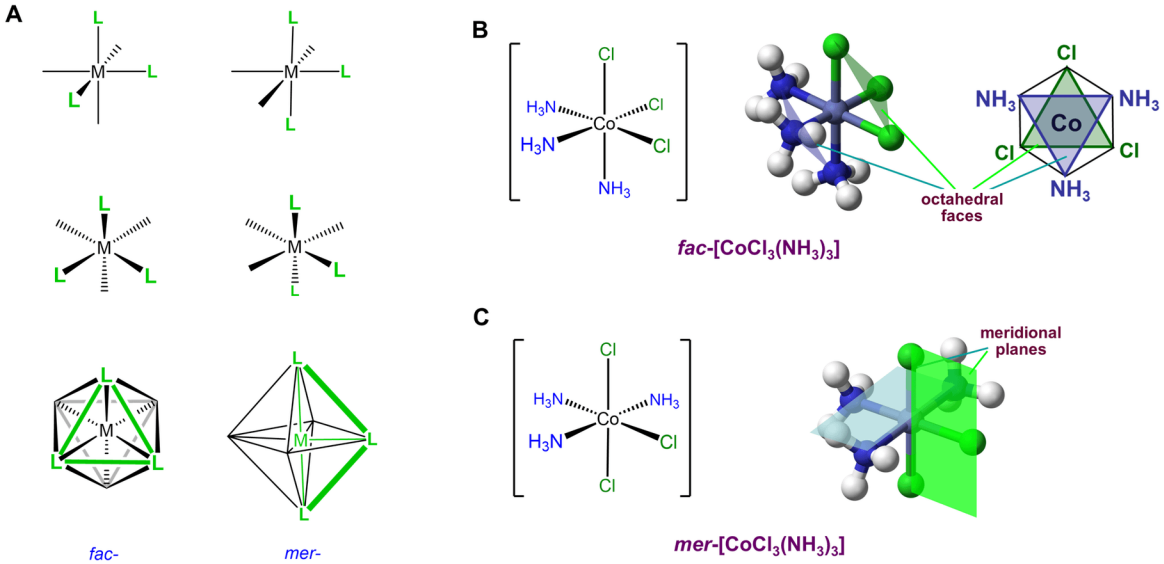
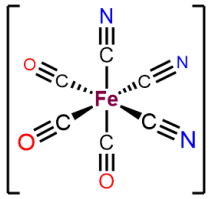


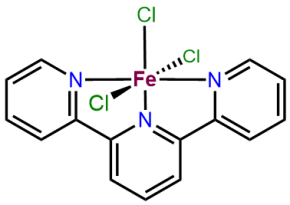
Figure 5.3.21. (A) Three projections of *fac* and *mer* arrangements of ligands around an octahedral metal center emphasizing that in the *fac* arrangement the ligands are oriented along a face of the octahedron while in the *mer* arrangement they are oriented in a plane. (B) Structure of *fac*-$[CoCl_3(NH_3)_3]$ showing the octahedral faces occupied by the chloro and amine ligands. (C) Structure of *mer*-$[CoCl_3(NH_3)_3]$ showing the planar arrangement of the chloro and ammine ligands. The ball and stick models are modified from images by Benjah-bmm27 - Own work, Public Domain, https://commons.wikimedia.org/w/inde...?curid=1874872 and curid=1874873. Otherwise this work by Stephen Contakes is licensed under a Creative Commons Attribution 4.0 International License.

Octahedral complexes with three identical ligands oriented about an octahedral center can only exist in *mer* and *fac*

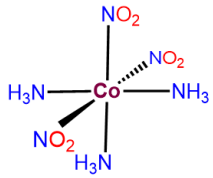
arrangements. Consequently, such complexes can be designated as *mer* and *fac* isomers. Examples are given in Figure 5.3.22.



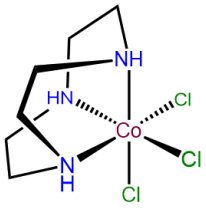
fac-$[Fe(CN)_3(CO)_3]^-$



mer-$[FeCl_3tpy]$



mer-$[Co(NH_3)(NO_2)_3]$



fac-$[FeCl_3(tacn)]$

Figure 5.3.22. Examples of *fac* and *mer* octahedral complexes. Note how some chelating ligands preferentially bind to the metal in a *fac* or *mer* arrangement and, in so doing, force the other ligands to also form a *mer* or *fac* arrangement. This work by Stephen Contakes is licensed under a Creative Commons Attribution 4.0 International License.

Diastereomerism arising from multiple ligand-associated chiral centers

Diastereomerism can also arise when two or more chiral ligands bind to a metal center. Such cases typically give rise to a complex mixture of isomers, as shown by the example in Figure 5.3.23. As may be seen from Figure 5.3.23, the differences between these isomers can arise from both changes in the stereochemical configuration of the ligand and the relationship of particular ligand centers relative to one another. For instance, the leftmost two structures in Figure 5.3.23 possess one *R* and *S* nitrogen center each but differ in whether the centers are oriented so that the *R* and *S* centers on the two ligands are *trans* or *cis* to one another.

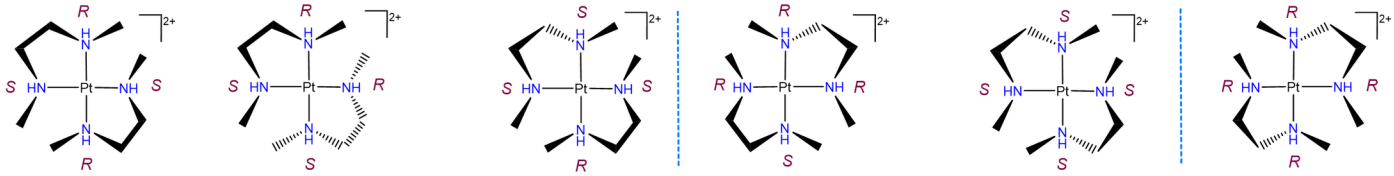


Figure 5.3.23. Diastereomers that can in principle be formed when two *N,N'*-dimethylethylenediamine ligands coordinate a Pt^{2+} center. This work by Stephen Contakes is licensed under a Creative Commons Attribution 4.0 International License.

Diastereomerism arising from λ and δ ring conformation isomerism.

Chelate rings are formed when a chelating ligand binds a metal

As may also be seen from the structures in Figure 5.3.23, when a multidentate ligand coordinates a metal, the ligand and metal center comprise one or more **chelate rings**. Examples of such chelate rings are shown in Figure 5.3.24.

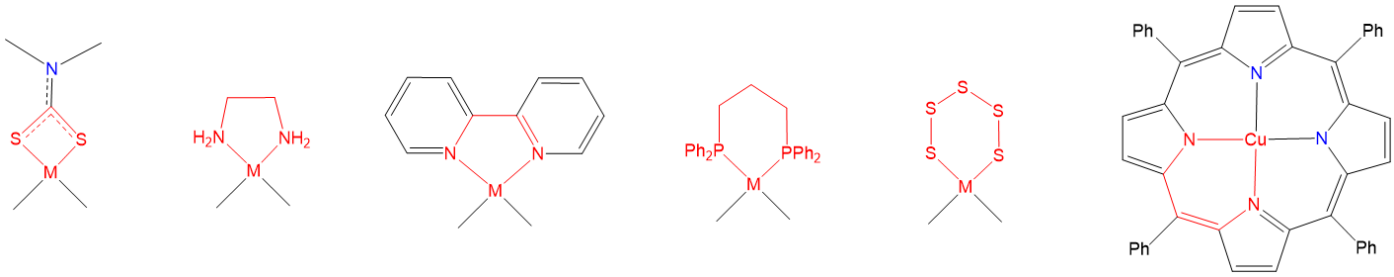


Figure 5.3.24. Four, five, and six-membered chelate rings (shown in red) formed by coordination of selected bidentate ligands to a metal center. This work by Stephen Contakes is licensed under a Creative Commons Attribution 4.0 International License.

As may be inferred from the examples in Figure 5.3.24, chelate rings may be of different sizes, although four, six, and especially five-membered rings are particularly common. Exactly which ring sizes will be more stable for a given system depends on the coordination geometry and, due to differences in M-L bond lengths, to a lesser degree on the metal. As a result, for octahedral and square planar complexes with 90° L-M-L bond angles between *cis* ligands, *five-membered rings tend to be especially stable* (Figure 5.3.25).

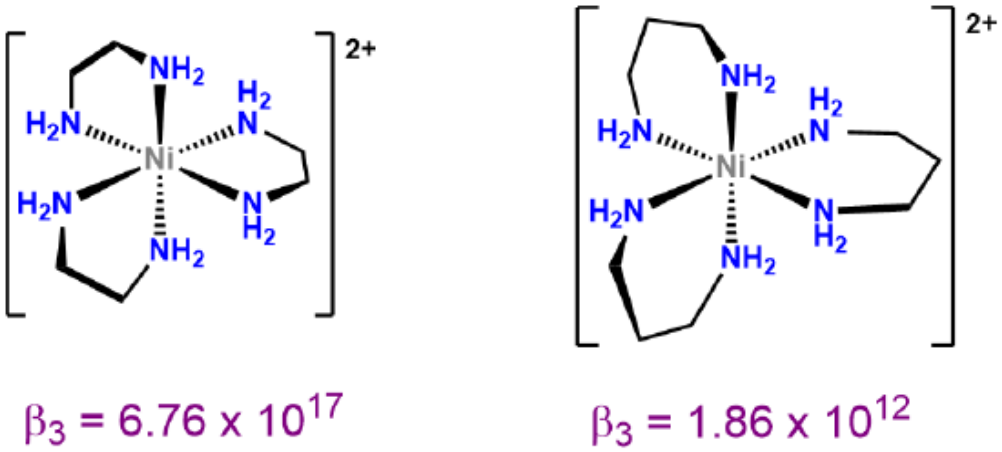


Figure 5.3.25. The greater stability of five-membered chelate rings involving Ni^{2+} and organic ligands is reflected in the higher overall formation constant (β_3) for the five-membered chelate rings contained in $[Ni(en)_3]^{2+}$ compared to that of $[Ni(et)_3]^{2+}$, which has six-membered rings. The data in this figure is taken from Stability of Metal Complexes and Chelation by Robert Lancashire. This work by Stephen Contakes is licensed under a Creative Commons Attribution 4.0 International License.

Not all metal chelates prefer to form five-membered rings. The steric requirements of chelate rings depend on both the preferred coordination geometry of the metal center and the stereochemistry of the ligand. Both of these effects are typically considered in terms of preferred L-M-L bond angles. From the perspective of the metal center, the preferred bond angle is determined by the coordination geometry. Octahedral and square planar metals prefer 90° L-M-L bond amgles, trigonal bipyramidal systems 90 and 120° L-M-L bond angles, and tetrahedral complexes 109.5° L-M-L angles. The larger preferred bond angles in tetrahedral and trigonal bipyramidal systems often require the formation of larger six or seven-membered chelate rings for maximum stability. The size of the chelate ring actually formed between a metal and ligand is determined by the ligand's structure. As the contributor of all the atoms in the chelate ring but one, the ligand directly determines the chelate ring size. More subtly, ligands naturally prefer to coordinate metals at a particular L-M-L angle, called the **bite angle**, as shown in Figure 5.3.26A. Ligands with bite angles corresponding to the ideal L-M-L angle for a metal's preferred geometry tend to form more stable complexes, although in turn ligand bite angles can cause metals with a weak coordination geometry preference to adopt the ligand's preferred geometry instead.[10] As may be seen from the values in Figure 5.3.26B, bite angles roughly increase with the size of the chelate ring formed but are also influenced by the types of structures used to connect the ligand's Lewis base sites. This facilitates the use of diphosphine ligands to tailor the structure and reactivity of phosphine-containing organometallic catalysts.

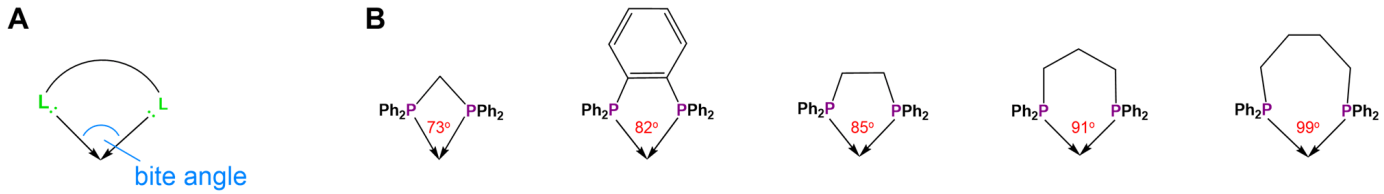


Figure 5.3.26. (A) Definition of the bite angle as the angle at which the ligand's preferred L-M-L angle when coordinating a metal center. (B) Bite angles of selected diphosphines.[9] The bite angles of many such diphosphines have been determined to facilitate the design of phosphine-containing organometallic catalysts. This work by Stephen Contakes is licensed under a Creative Commons Attribution 4.0 International License.

λ and δ isomerism involves differences in the conformation of nonplanar five-membered chelate rings

As shown in Figure 5.3.27, some chelate ring systems are planar while others are not.

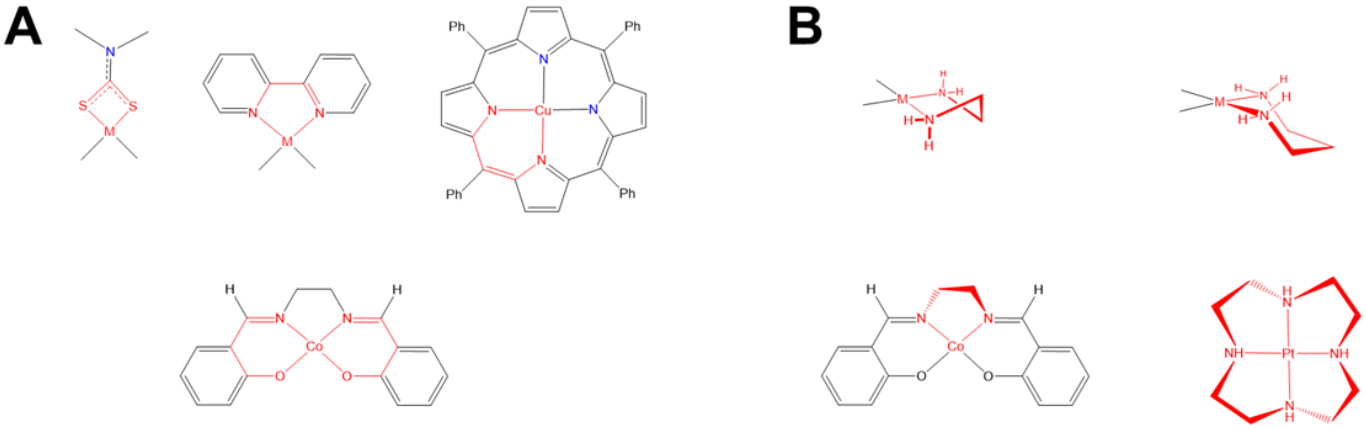


Figure 5.3.27. (A) Planar and (B) Nonplanar chelate rings shown highlighted in red. Notice how [Co(salen)] possesses a nonplanar chelate ring and two planar ones. This work by Stephen Contakes is licensed under a Creative Commons Attribution 4.0 International License.

Among the nonplanar chelate ring systems are ligands like en and dppe, which contain tetrahedral C, N, O, P, and S atoms. Because these atoms create kinks in the chelate ring they introduce additional opportunities for diastereomerism due to differences in the chelate ring conformation, called **ring twist**. Ring twist in nonplanar systems has been most extensively explored for five-membered chelates like those formed by dppe and by en and other chelating amines. Unlike the more rigid four-membered chelate rings, five-membered chelates tend to be conformationally flexible, but not so conformationally flexible that their conformers are rapidly interconverting at room temperature (at least not when the rings are substituted to introduce additional steric strain). This balance between flexibility and rigidity enables some five-membered chelate rings to exist as mixtures of distinguishable conformational isomers at room temperature.

To understand the two most stable conformers that five-membered chelates rings tend to form, it is helpful to think of five-membered chelate rings as involving two components (Figure 5.3.28):

- a planar L-M-L group, where L are the atoms directly attached to the metal, M, and
- the remaining two ring atoms, E, which form a rigid E-E bar across the back of the chelate ring.

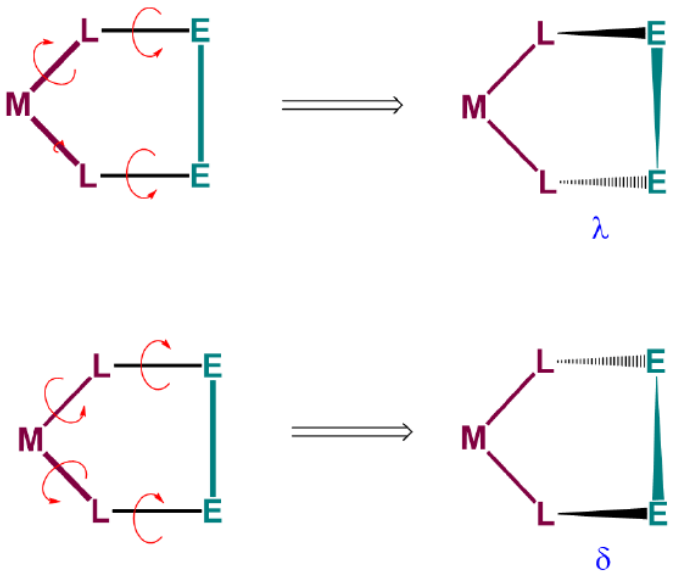


Figure 5.3.28. Five-membered chelate rings consist of a planar L-M-L group connected to a rigid E-E bar. Conformers arise as rotation about the M-L and L-E bonds causes twisting of the E-E bar relative to the L-M-L plane. This work by Stephen Contakes is licensed under a Creative Commons Attribution 4.0 International License.

As can be seen from Figure 5.3.28 , rotation about the M-L and L-E bonds causes twisting of the E-E bar relative to the L-M-L plane. The two most stable conformers produced by these motions are the λ or δ conformations as shown in Figures 5.3.29 and 5.3.29.

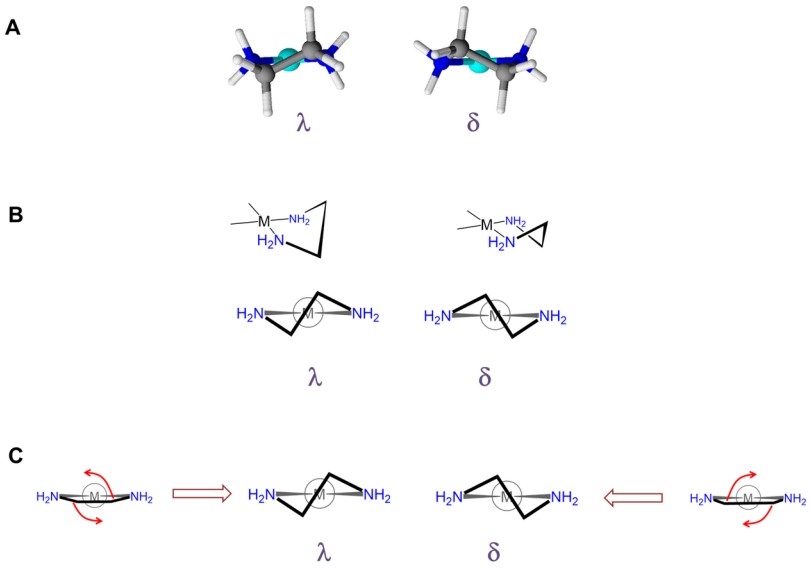


Figure 5.3.29. (A) λ and δ ring twist in a square planar metal ethylenediamine complex (B) along with several ways to represent it in line drawing form. (C) Of these, the projection looking down an axis bisecting the chelate ring makes it easiest to see that, starting with a planar chelate ring the λ conformer corresponds to a counterclockwise twist of the CH_2CH_2 bond relative to the N-M-N plane and the δ conformer a clockwise twist relative to the N-M-N plane. This work by Stephen Contakes is licensed under a Creative Commons Attribution 4.0 International License.

The relative stability of the λ and δ conformers will depend on the configuration of any stereocenters present and steric factors. As with organic ring systems, steric effects tend to favor conformers in which bulky groups are placed in the less sterically strained equatorial positions while the configuration of the stereocenters present can serve to restrict the allowable ring twist conformations, as illustrated in Figure 5.3.30. A detailed treatment of such systems is beyond the scope of this page. Interested readers are referred to reference 12 for more details.

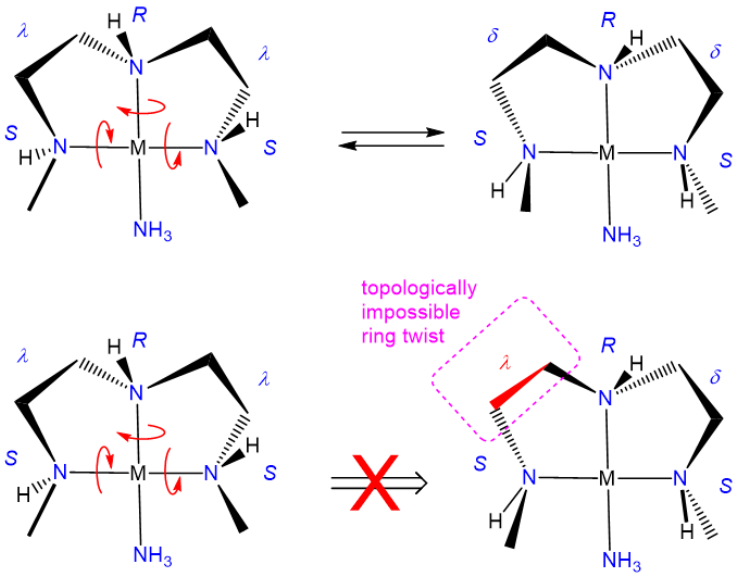


Figure 5.3.30. The configurations at nitrogen in the complex shown restrict the chelate ring conformations to either a $\lambda\lambda$ or $\delta\delta$ conformation because the rotations needed to enable a $\lambda\delta$ configuration are topologically impossible. This work by Stephen Contakes is licensed under a Creative Commons Attribution 4.0 International License.

In closing, it should be noted that it might seem to be making much of small effects in pointing out that one source of diastereomerism in metal complexes involves the freezing out of chelate ring conformations. However, that would be to mistake the impacts that ring conformations can have on the steric accessibility of a coordination site and shaping the course of processes that might occur there. As illustrated in Figure 5.3.31, a simple shift in the conformation of one ring in a square planar, pyramidal, or octahedral complex containing coplanar ethylene diamine ligands can exert a significant effect on the steric profile of the complex perpendicular to the MN_4 square plane. Because of effects like these, ring conformation isomerism plays a role in the design of stereoselective transition metal catalysts.

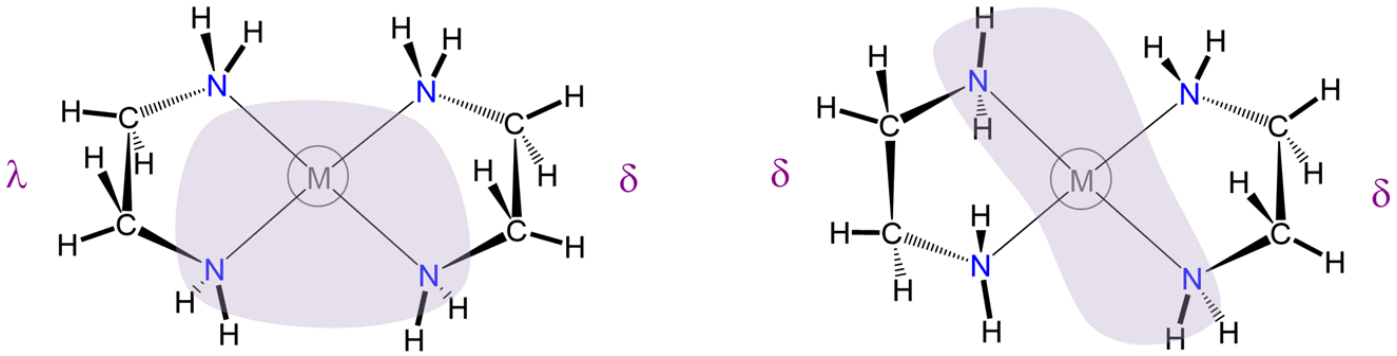


Figure 5.3.31. Schematic illustrating how the conformation of ethlyenediamine ligands bound to a metal center affects the steric accessibility of the metal (shown shaded in violet) to potential ligands attempting to bind from above the MN_4 plane. This work by Stephen Contakes is licensed under a Creative Commons Attribution 4.0 International License.

Exercises

Exercise 5.3.1. Identify the type of isomerism

What type of isomers are

a. $[CoCl(NH_3)_5](NO_3)$ and $[Co(NH_3)_5(N\text{-}NO_2)]Cl$?
b. $[Co(NH_3)_5\text{-}CN\text{-}Ru(NH_3)_5]^{4+}$ and $[Co(NH_3)_5\text{-}NC\text{-}Ru(NH_3)_5]^{4+}$
c. $[Cr(CN)_5\text{-}CN\text{-}Co(NH_3)_5]$ and $[Co(CN)_5\text{-}CN\text{-}Cr(NH_3)_5]$

d. *cis*-[Mn(en)$_2$(CN)$_2$] and *trans*-[Mn(en)$_2$(CN)$_2$]

Answer a. available at the end of this section.

Exercise 5.3.2. Assigning metal oxidation states in a complex

Many properties of transition metal complexes depend on the metal's oxidation state. For instance,

- octahedral complexes of Co^{II} lose and gain ligands rapidly
- octahedral complexes of Co^{III} lose and gain ligands very slowly
- four-coordinate complexes are generally tetrahedral
- EXCEPT four-coordinate complexes of metals like Pt^{II} , Pd^{II} , Rh^{I}, and Ir^{I}, among others, are square planar

For this reason it is important to be able to estimate the formal oxidation state of a metal in a complex. Fortunately, this is easy to do if you remember

1. The sum of all atoms' oxidation states will equal the overall charge on the complex
2. When determining the metal's oxidation state, the ligands can be treated as having an oxidation state equal to their charge - *i.e.,* the charge they possess in the form in which they coordinate the metal - so if they need to lose a proton to bind, don't forget to account for that.

Given the above, estimate the oxidation state of the metal in the following real and hypothetical complexes.

a. $Na_4[Fe(CN)_6]$
b. $[Cu(phen)_2]BF_4$
c. $[PtF_4(NH_3)_2]$
d. $[Ni(en)_2]SO_4$
e. $Co(acac)_3$
f. [MnCl(O)(salen)]

Answer available at the end of this section.

Exercise 5.3.3. Drawing isomers from descriptions

Draw structures that match the descriptions given, assuming that

- complexes in which the metal has a coordination number of six are octahedral
- complexes in which the metal has a coordination number of five are trigonal bipyramidal
- complexes in which Pt^{II} , Pd^{II} , or Rh^{I}, or Ir^{I} have a coordination number of four are square planar
- other complexes in which the metal has a coordination number of four will be tetrahedral

a. *mer*-triammineaqua-*trans*-dichlorocobalt(III) ion
b. Δ-diaminebis(oxalato)manganate(III)
c. $[CoCl_4]^{2-}$
d. *trans*-diamminebis(ethylenediamine)Nickel(2+) tetracyanopalladate(2-)
e. Λ-bis(ethylenediamine)cobalt(III)- μ-amido μ-hydroxo-Δ-bis(ethylenediamine)cobalt(III)

Answer a. mer-triammineaqua-trans-dichlorocobalt(III) ion. available at the end of this section.

Exercise 5.3.4. Stereoisomers of complexes containing only monodentate ligands.

Draw all the stereoisomers of the following real and hypothetical complexes. You may assume that

- complexes in which the metal has a coordination number of six are octahedral
- complexes in which the metal has a coordination number of five are trigonal bipyramidal
- complexes in which Pt^{II} , Pd^{II} , or Rh^{I}, or Ir^{I} have a coordination number of four are square planar
- other complexes in which the metal has a coordination number of four will be tetrahedral

a. $[IrCl(CO)(PPh_3)_2]$
b. $[CoCl_3(NH_3)_3]$
c. $[CoCl_2(H_2O)_2(NH_3)_2]^+$
d. $[CoBrCl(H_2O)_2(NH_3)_2]^+$
e. $[CoBrClI(NH_3)_3]$

Answer a. [IrCl(CO)(PPh3)2] available at the end of this section.

Exercise 5.3.5. Stereoisomers of complexes with bidentate ligands (ignoring ring twist).

Ignoring ring twist, draw all the stereoisomers of the following real and hypothetical octahedral complexes.

a. $[CoBr_2Cl_2(en)]^-$
b. $[CoBrCl(en)_2]^+$
c. $[CoBrCl(gly)_2]^-$
d. $[Co(en)_3]^{3+}$
e. $[Co(gly)_3]$

Answer a. [CoBr2Cl2(en)]- available at the end of this section.

Exercise 5.3.6. More stereoisomers: Now featuring linkage isomerism

Ignoring ring twist, draw all chemically reasonable stereoisomers for the following real and hypothetical complexes. You may assume that

- complexes in which the metal has a coordination number of six are octahedral
- complexes in which the metal has a coordination number of five are trigonal bipyramidal
- complexes in which Pt^{II} , Pd^{II} , or Rh^{I}, or Ir^{I} have a coordination number of four are square planar
- other complexes in which the metal has a coordination number of four will be tetrahedral

a. $[Pt(en)(SCN)_2]$
b. $[Pt(NH_3)_2(SCN)_2]$
c. $[Co(en)_2(SCN)_2]^+$

Answer a. [Pt(en)(SCN)2] available at the end of this section.

Exercise 5.3.7. Stereoisomer free for all.

Ignoring ring twist, draw all chemically reasonable stereoisomers for the following real and hypothetical complexes. You may assume that

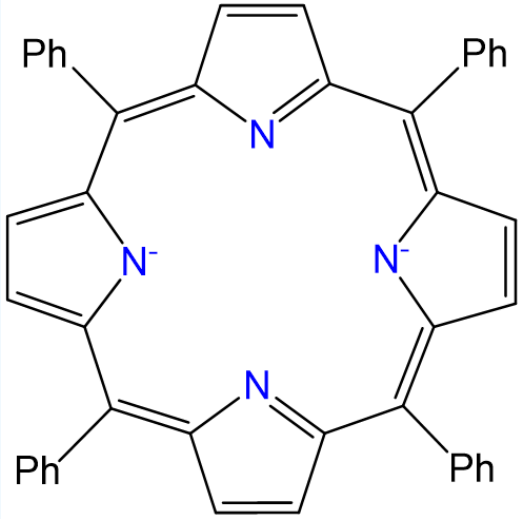
- complexes in which the metal has a coordination number of six are octahedral
- complexes in which the metal has a coordination number of five are trigonal bipyramidal
- complexes in which Pt^{II} , Pd^{II} , or Rh^{I}, or Ir^{I} have a coordination number of four are square planar
- other complexes in which the metal has a coordination number of four will be tetrahedral

a. $[Ru(bpy)(phen)(dppe)]^{2+}$
b. $[CoClF(PPh_3)(py)]^-$
c. $[Ni(en)_2(NO_2)_2]$
d. $[Fe(H_2O)_3(SCN)_3]$
e. $[PtClF(PPh_3)(py)]$
f. $[CoBr_2Cl(NH_3)_3]$

Answer a. [Ru(bpy)(phen)(dppe)]2+ available at the end of this section.

Exercise 5.3.8

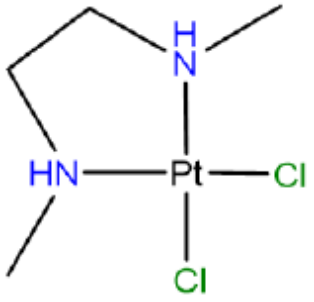
Complexes of formula $Ru(TPP)py_2$ have been prepared, in which TPP is tetraphenylporphyrin, which binds metals in the form given below. Draw all isomers of $Ru(TPP)py_2$.



Answer available at the end of this section.

Exercise 5.3.9

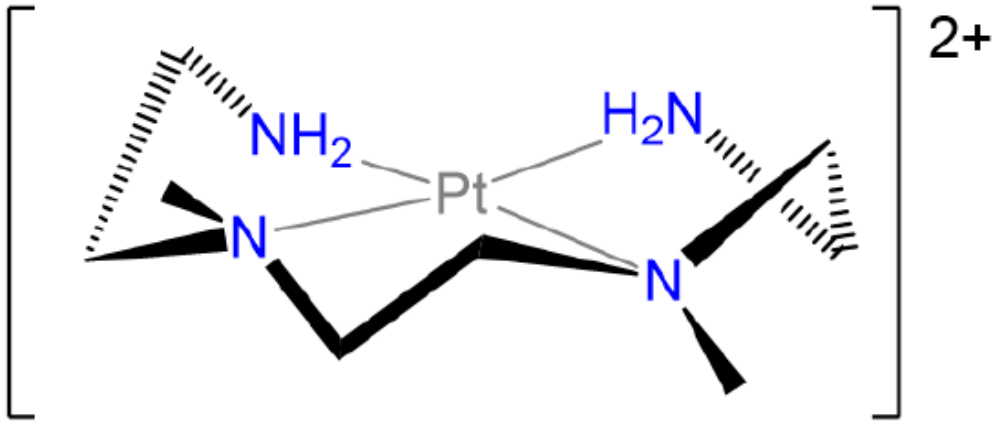
Draw the diastereomers formed due to the chirality of the amine nitrogen atoms in $[PtCl_2(N,N'$-dimethylethane-1,2-diamine)] which has the atomic connectivity represented below



Answer available at the end of this section.

Exercise 5.3.10

Label the conformations of all chelate rings in the structure below.



Answer available at the end of this section.

Answer available at the end of this section.

Appendix: The MABCDEF bookkeeping system for identifying isomers

The Mabcdef or MABCDEF system is one method for identifying the number of isomers in an octahedral complex, although since it is really just a bookkeeping and organizational system it can easily be extended to other geometries as well. The M in Mabcdef stands for metal and the other letters are used to stand in for ligands. The basic approach involves

- classifying the ligands as A, B, C, D, E, or F in order of multiplicity. Thus for

  $[Cr(NH_3)_6]^{3+}$ A = NH_3; there are no B, C, D,E, or F ligands; and the complex is classified as MA_6

  $[CoCl(NH_3)_5]^{2+}$ A = NH_3, B = Cl^-, and the complex is MA_5B

  $[CrCl_2(H_2O)_2(NH_3)_2]^+$ A = Cl^-, B = H_2O, C = NH_3, and the complex is $MA_2B_2C_2$

- in the classification above, multidentate ligands are typically classified before monodentate ones and are designated AA, AB, ABC, ABA, etc. based on the symmetry of the attachment points. Thus

  en has identical attachment amine points and is AA

  gly has a carboxy and amine attachment points and is AB

  trien is ABA

  $CoCl_2(en)_2^+$ is $M(AA)_2B_2$

  $CoCl_2(gly)_2^-$ is $M(AB)_2C_2$

  $CoCl_2(en)(gly)$ is $M(AA)(AB)C_2$

- Systematically list out the possible *trans* arrangements of ligands by
  1. assigning one pair of ligands to be *trans* to one another.
  2. Then systematically list out the other possible *trans* pairs by permuting the remaining trans arrangements. It can help to

organize the permutations in a table, such as that shown below for an MABCDEF complex where A and B are assigned *trans*. In looking at the table notice how the second set of trans permutations is systematically varied. This helps ensure that no possibility is skipped.

3. Go through the list of isomers and remove any duplicates you generated so far. For instance, notice in the table below that the last three stereoisomers are identical with the first three (*e.g.,* stereoisomer 4 is identical to stereoisomer 3, 5 with 2, and 6 with 1).

Stereoisomer 1	Stereoisomer 2	Stereoisomer 3	Stereoisomer 4 (same as isomer 3)	Stereoisomer 5 (same as isomer 2)	Stereoisomer 6 (same as isomer 1)
trans AB (fixed)	*trans* AB (fixed)	*trans* AB (fixed)	*trans* AB (fixed)	*trans* AB (fixed)	*trans* AB (fixed)
trans CD	*trans* CE	*trans* CF	*trans* DE	*trans* DF	*trans* EF
trans EF	*trans* DF	*trans* DE	*trans* CF	*trans* CE	*trans* CD

4. If the complex possesses multidentate ligands that demand that certain groups exist and *cis* pairs, then also remove any configurations which do not agree with the known binding capability of the ligand (*e.g.,* the two amine groups of ethylenediamine cannot be *trans* to one another, so if you have an en ligand, remove configurations like that from the list).
5. Next, swap or permute the original *trans* pair and repeat the process you just followed. In the case of Mabcdef this gives the following results:

Isomer	"fixed" trans pair	Additional trans pairs	
1	AB	CD	EF
2	AB	CE	DF
3	AB	CF	DE
4	AC	BD	EF
5	AC	BE	BF
6	AC	BF	DE
7	AD	BC	EF
8	AD	BE	CF
9	AD	BF	CE
10	AE	BC	DF
11	AE	BD	CF
12	AE	BF	CD
13	AF	BC	DE
14	AF	BD	CE
15	AF	BE	CD

- Since the procedure explained above only identifies isomers based on unique *trans* pairings, **it does not identify when a configuration is chiral and corresponds to a pair of enantiomers.** Any enantiomers can be identified by drawing out the complexes and either classifying their point groups or by drawing their mirror images and checking if they are superimposable. In the MABCDEF case - *i.e.,* where all the ligands are different - all of the isomers identified have C_1 symmetry so are chiral. This means there will be a pair of enantiomers for each, giving 15 x 2 = 30 different stereoisomers.

References

1. These examples are taken from http://wwwchem.uwimona.edu.jm/courses/inorgnom.html

2. Contakes S. M.; Rauchfuss, T.B. *Chem. Commun.* 2001, 553-554.

3. Shriver, D. F.; Shriver, S. A.; Anderson, S. E., *Inorg. Chem.* 1965, *4(5)*, 725-730.

4. Zelewsky, A. v., *Stereochemistry of Coordination Compounds* Wiley, 1996.

5. In the past it was difficult to determine absolute configurations from X-ray data alone, but recent advances have made it easier to do so.

6. Pavan M. V. Raja & Andrew R. Barron "Circular Dichroism Spectroscopy and its Application for Determination of Secondary Structure of Optically Active Species" in *Physical Methods in Chemistry and Nano Science* https://chem.libretexts.org/Bookshelves/Analytical_Chemistry/Book%3A_Physical_Methods_in_Chemistry_and_Nano_Science_(Barron)/07%3A_Molecular_and_Solid_State_Structure/7.07%3A_Circular_Dichroism_Spectroscopy_and_its_Application_for_Determination_of_Secondary_Structure_of_Optically_Active_S

7. Berova, N.; Bari, L. D.; Pescitelli, G., *Chemical Society Reviews* 2007, 36 (6), 914-931.

8. Of course, if one set of ligands occupies a meridional plane, then the other three ligands will be oriented in an equatorial one. The reason they may both be considered meridional is because if the complex were rotated, the equatorial plane would be meridional and vice versa. From that point of view both might be considered meridional planes - albeit not at the same time.

9. Bite angles are taken from Mansell, S. M., Catalytic applications of small bite-angle diphosphorus ligands with single-atom linkers. Dalton Transactions 2017, 46 (44), 15157-15174.

10. Hancock, R. D., The pyridyl group in ligand design for selective metal ion complexation and sensing. Chemical Society Reviews 2013, 42 (4), 1500-1524.

11. Sasi, D.; Ramkumar, V.; Murthy, N. N., Bite-Angle-Regulated Coordination Geometries: Tetrahedral and Trigonal Bipyramidal in Ni(II) with Biphenyl-Appended (2-Pyridyl)alkylamine N,N'-Bidentate Ligands. ACS Omega 2017, 2 (6), 2474-2481.

12. Ehnbom, A.; Ghosh, S. K.; Lewis, K. G.; Gladysz, J. A., Octahedral Werner complexes with substituted ethylenediamine ligands: a stereochemical primer for a historic series of compounds now emerging as a modern family of catalysts. Chemical Society Reviews 2016, 45 (24), 6799-6811.

Answers

Exercise 5.3.1: Bridging ambidentate ligands and the Hard-Soft Acid- Base Principle.

The greater stability of K{$Fe^{II}[Cr^{III}(NC)_6]$} over K{$Fe^{II}[Cr^{III}(CN)_6]$} reflects the greater stability of the Fe^{II}-CN-Cr^{III} linkages in the former over the Fe^{II}-NC-Cr^{III} linkages in the latter. This is consistent with the preference for hard-hard and soft-soft Lewis acid-base interactions of the Hard-Soft Acid-Base Principle.

The Fe^{II}-CN-Cr^{III} linkages are more stable because they possess bonds between

- the softer Lewis acid (Fe^{II}) and Lewis base (the C end of CN^-)
- the harder Lewis acid (Cr^{III}) and Lewis base (the N end of CN^-)

In contrast, the Fe^{II}-NC-Cr^{III} linkages in the less stable linkage isomer involve bonds between

- the softer base (the C end of CN^-) and harder acid (Cr^{III})
- the harder base (the N end of CN^-) and softer acid (Fe^{II})

Exercise 5.3.1. Identify the type of isomerism

Ionization isomers.

Linkage isomers.

Coordination isomers.

Geometric isomers, specifically *cis*/*trans* isomers.

Exercise 5.3.2. Assigning metal oxidation states in a complex

This contains $[Fe(CN)_6]^{4-}$; so $O.S._{Fe}$ + 6 x (-1) (for CN^-) = -4 (the complex's charge) so $O.S._{Fe}$ = +2 or Fe^{2+}.

Since tetrafluoroborate is a monoanion, the complex is $[Cu(phen)_2]^+$ so $O.S._{Cu}$ + 0 x 2 (for phen) = +1 (the complex's charge) so $O.S._{Cu}$ = +1 or Cu^+.

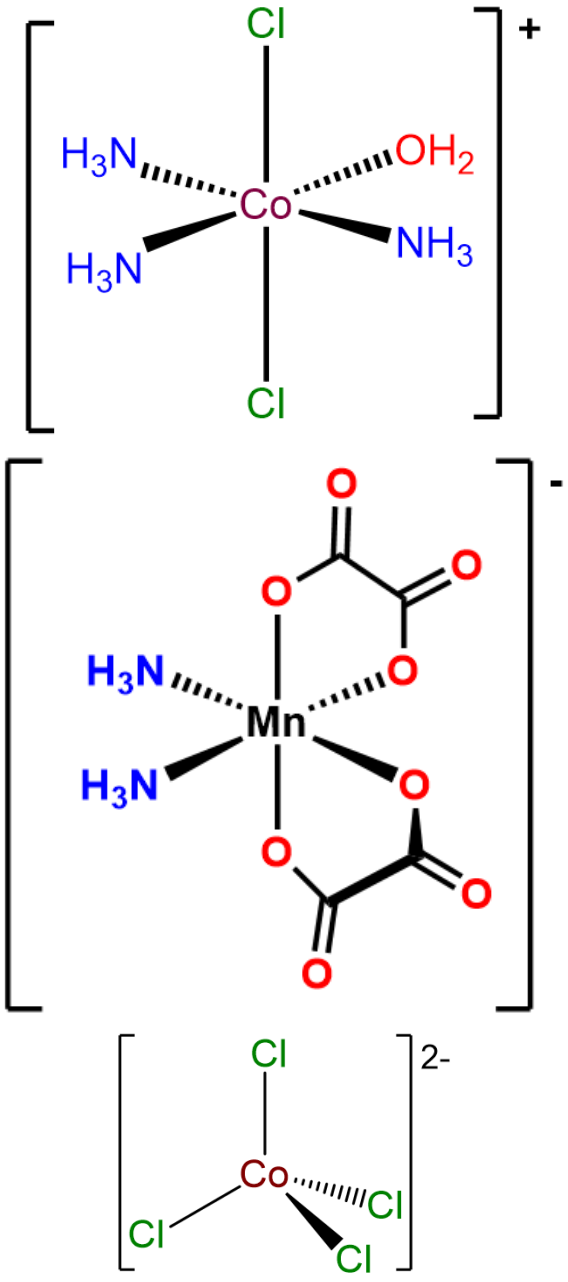
O.S.$_{Pt}$ + 4 x (-1) (for F^-) + 0 x 2 (for NH_3) = +0 (the complex's charge) so O.S.$_{Pt}$ = +4 or Pt^{4+}.

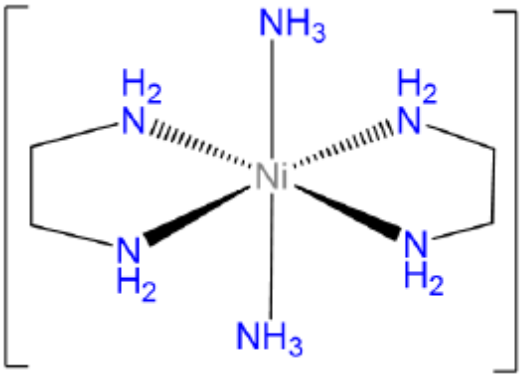
The complex is $[Ni(en)_2]^+$ so O.S.$_{Ni}$ + 0 x 2 (for en) = +2 (the complex's charge) so O.S.$_{Ni}$ = +2 or Ni^{2+}.

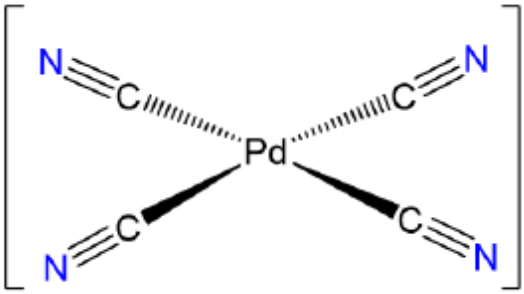
O.S.$_{Co}$ + 3 x (-1) (for acac; see table 9.2.2) = +0 (the complex's charge) so O.S.$_{Co}$ = +3 or Co^{3+}.

O.S.$_{Mn}$ + 1 x (-1) (for Cl^-) + 1 x (-2)(for oxo) + 1 x (-2) (for salen; see table 9.2.2) = +0 (the complex's charge) so O.S.$_{Mn}$ = +5 or Mn^{5+}.

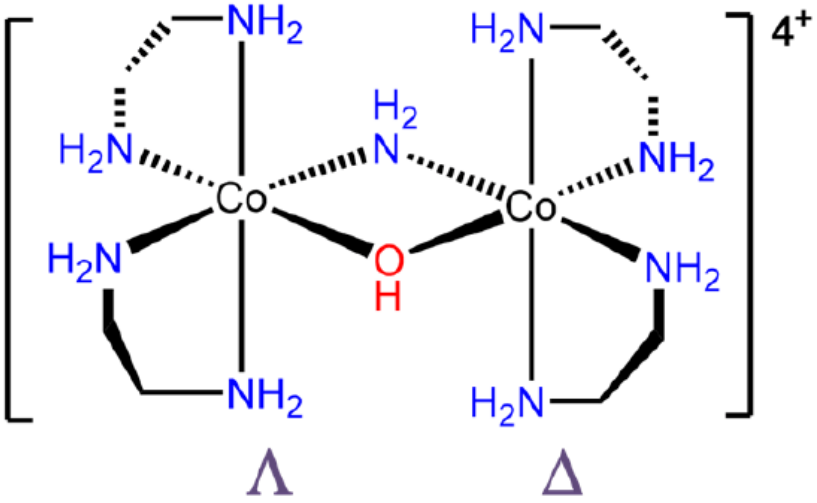
Exercise 5.3.3. Drawing isomers from descriptions





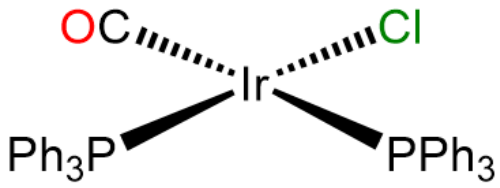


Note that since the Pd in $[Pd(CN)_4]^{2-}$ is Pd^{2+} it will be square planar.

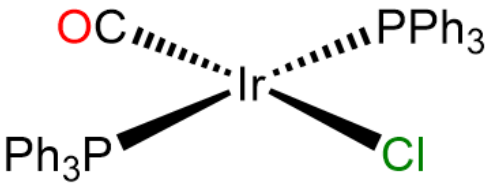


Exercise 5.3.4**. Stereoisomers of complexes containing only monodentate ligands.**

This is a 4-coordinate Ir^{I} complex and, as such will be square planar. Since two of the ligands are identical, it will have *cis* and *trans* isomers. The *trans* isomer is famous for its ability to form adducts and is called Vaska's complex.

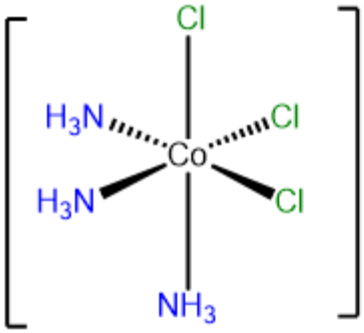


cis-

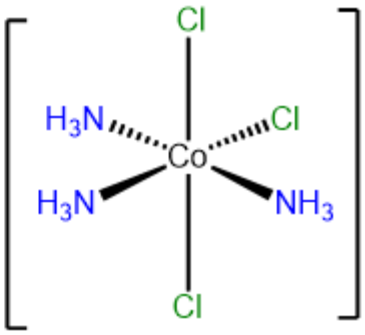


trans-

This complex contains three ammine and three chloro ligands and so will have *fac* and *mer* isomers.

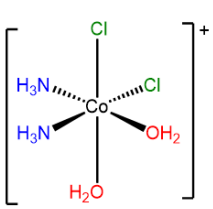


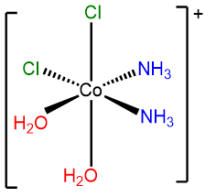
fac-



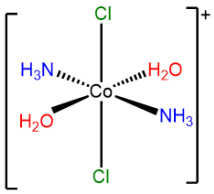
mer-

This is a case of an $MA_2B_2C_2$ system (A = Cl^-, B = H_2O, C = NH_3) involving multiple *cis* and *trans* relationships. The six stereoisomers are shown below.

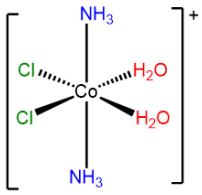




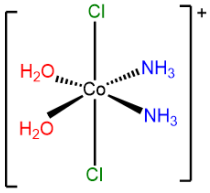
enantiomers of -*cis* NH_3, *cis*-Cl_2, *cis*-H_2O



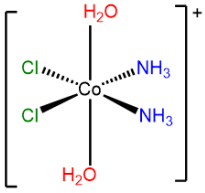
all trans



trans NH_3, *cis*-Cl_2, *cis*-H_2O



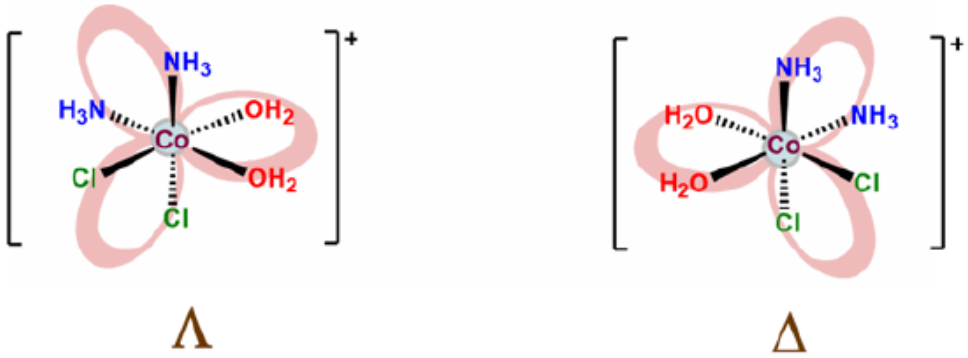
cis NH_3, *trans*-Cl_2, *cis*-H_2O



is NH_3, *cis*-Cl_2, *trans*-H_2O

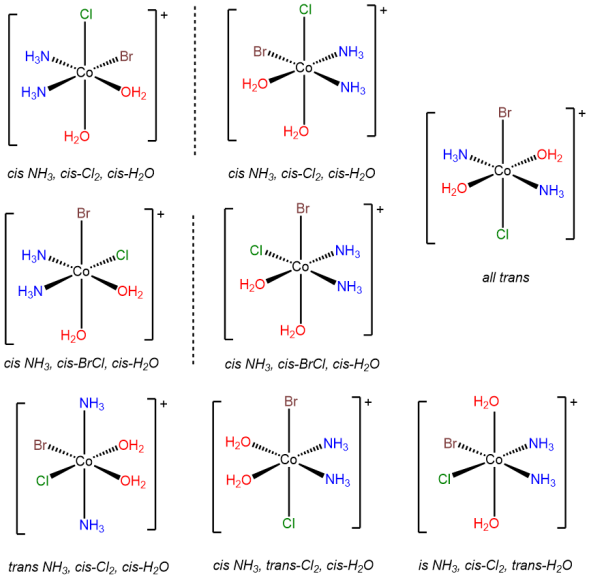
Since it may not be obvious how to arrive at a set of isomers like the ones above, it is worth considering how one might work through the possibilities for a system of ligands like this one. Several systems may be used to systematically identify isomers. Once approach is the Macbdef system described in Note 5.3.1 at the end of these exercises. The solutions presented here and in subsequent problems employ a variant of that approach.

- Start by fixing one set of ligands. In this case the chloro ligands were first fixed as *cis* to one another. Then the remaining ligands might be *cis* or *trans* to one another, although since the *chloro* ligands are already *cis*, the ammine and aqua ligands cannot both be *trans* at the same time. Thus for *cis* chloro ligands the possibilities for the others are:
  - *cis*-H_2O ,*cis*-NH_3,
  - *cis*--H_2O, *trans*-NH_3
  - *trans*-H_2O, *cis*-NH_3
- Swap the configuration of the ligand set you started with. In this case it means placing the chloro ligands *trans* to one another. From that configuration, the possibilities for the ammine and aqua ligands are
  - *cis*-H_2O ,*cis*-NH_3,
  - *trans*-H_2O, *trans*-NH_3
- Check for enantiomers and create mirror images of any chiral complexes you drew. The easiest way to do this is to assign point groups. However, it turns out that the octahedral all-*cis* case is D_3 and formally equivalent to the symmetry of a tris chelate, as shown below.

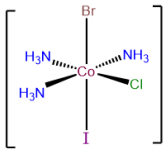


- finally, check to make sure you didn't include the same complex twice. Humans do make mistakes after all.

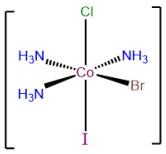
This problem is analogous to the one above except that this complex contains a bromo and chloro ligand in place of the two chloro ligands in $[CoCl_2(H_2O)_2(NH_3)_2]^+$. Consequently, when the bromo and chloro ligands are *cis* to one another, additional possibilities for isomers arise based on whether ammine or aqua ligands are *trans* to the chloro and bromo. The result is eight isomers.



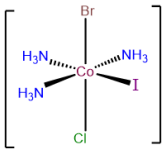
There are two possibilities for this complex - a *fac*-$(NH_3)_3$ and a *mer*-$(NH_3)_3$ arrangement. These may be taken as starting points for examining the possible permutations for the Cl^-, Br^-, and I^- ligands. The top row presents the three possibilities within the *mer*-$(NH_3)_3$ arrangement; each corresponds to a different ligand *trans* to an ammine ligand. The bottom row presents the two possible isomers with a *fac*-$(NH_3)_3$ arrangement. In each, the Cl^-, Br^-, and I^- ligands are *trans* to ammine ligands. However, the complexes possess C_1 symmetry and so are chiral and exist as enantiomers.



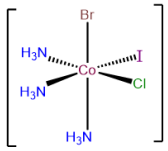
mer with Br *trans* to I

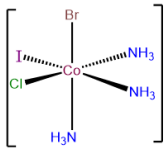


mer with Cl *trans* to I



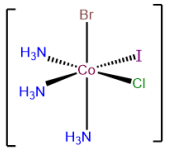
mer with Br *trans* to Cl



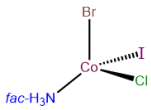


fac enantiomers

(C_1 symmetry or it you think of the *fac*-$(H_3N)_3$ as being "one uniform group" then the symmetry is equivalent to that of a chiral carbon)

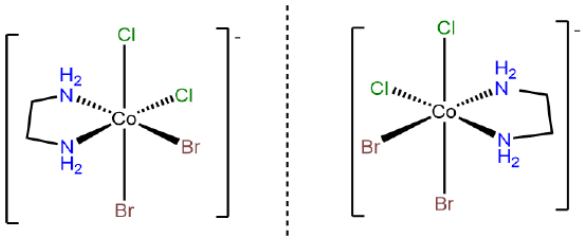


may be thought of as equivalent to

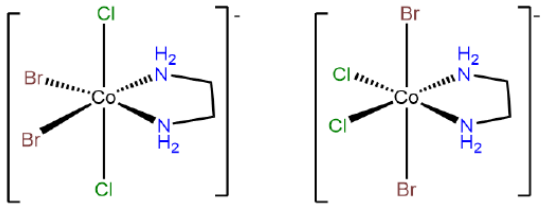


Exercise 5.3.5**. Stereoisomers of complexes with bidentate ligands (ignoring ring twist).**

This complex is analogous to $[CoCl_2(H_2O)_2(NH_3)_2]^+$ in possessing pairs of identical ligating groups. The main difference is that in $[CoBr_2Cl_2(en)]^-$ the two amine ligating group of the en ligand are restricted to a *cis* arrangement. Under the MABCDEF system explained in Note 5.3.1, $[CoCl_2(H_2O)_2(NH_3)_2]^+$ may be $MA_2B_2C_2$, but this complex, $[CoBr_2Cl_2(en)]^-$, is $M(AA)B_2C_2$. The isomers are:

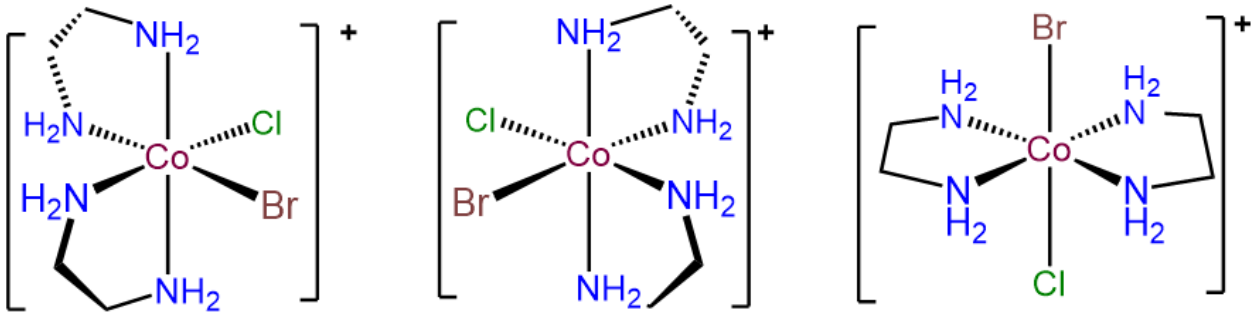


enantiomers of *cis*-Cl_2, *cis*-Br_2

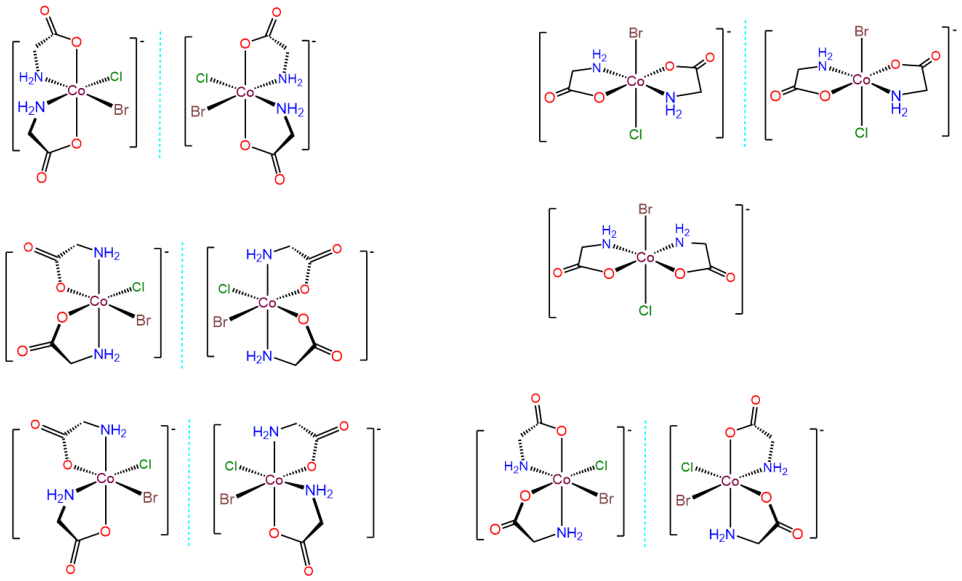


trans-Cl_2, *cis*-Br_2 *cis*-Cl_2, *trans*-Br_2

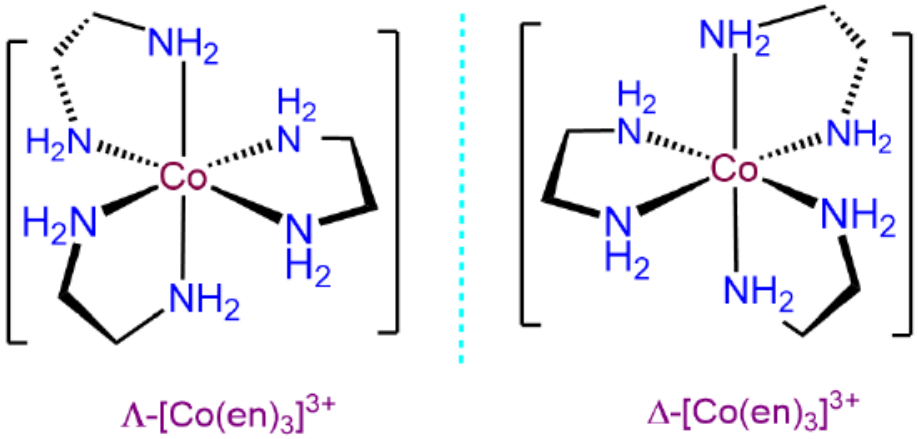
The key to problems like this is to focus on the unique ligands, in this case Br^- and Cl^-. These can exist in either a *cis* or *trans* arrangement. The *trans* form is achiral, but in the case where Br^- and Cl^- are *cis*, Λ and Δ enantiomers are possible. The result is three isomers.



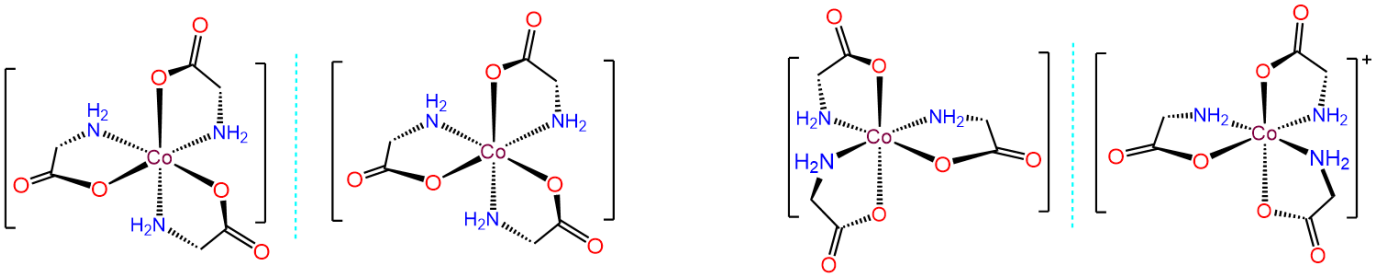
This case is analogous to the one above, but this time the bidentate ligand, gly, possesses distinguishable binding sites. Thus there are additional permutations involving how the gly ligands are bound relative to one another and/or whether the O or N end of the gly is bound *trans* to Br or Cl. The result is 11 different isomers, which are given below.



As a tris-chelate of symmetric bidentate ligands, ignoring ring twist, $[Co(en)_3]^{3+}$ will only exhibit Λ and Δ isomerism.



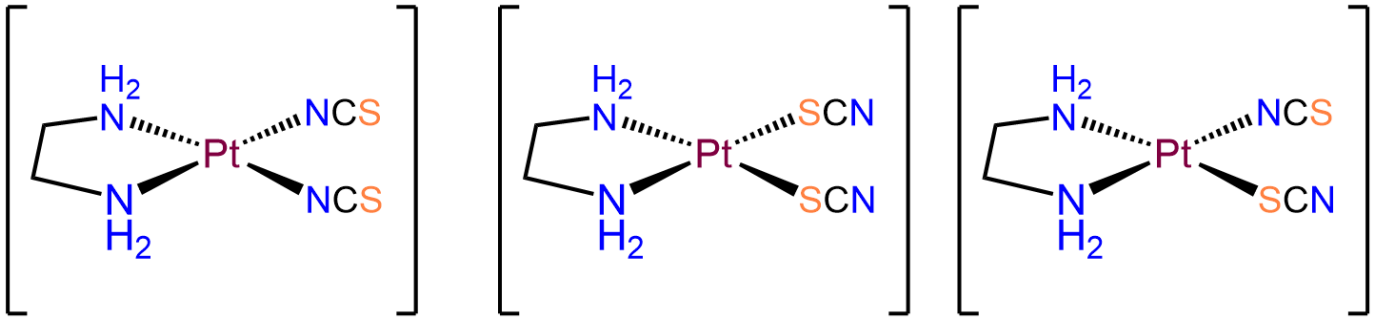
Since there are three gly ligands, each of which have carboxy and amine ends, the allowable arrangements involve whether the resulting three carboxy and three amine ends are oriented in a *mer* or *fac* arrangement. This gives two possibilities, each of which can exist as either the Λ or Δ enantiomer, for a total of four isomers, which are given below.



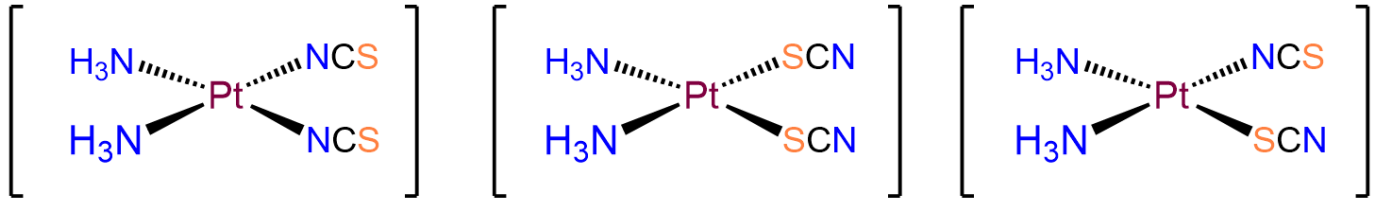
***fac* and Λ** ***fac* and Δ** ***mer* and Λ** ***mer* and Δ**

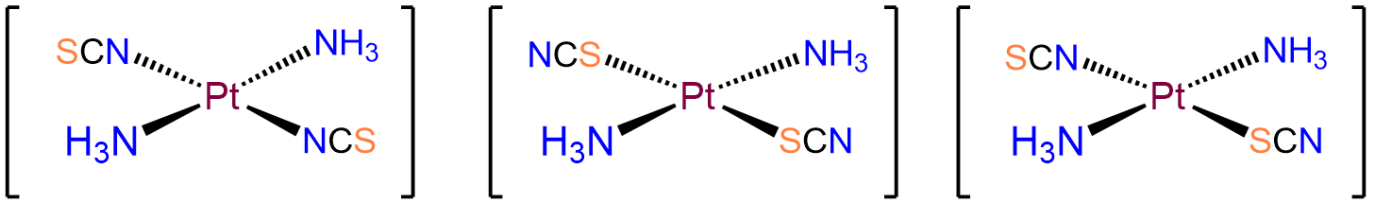
Exercise 5.3.6**. More stereoisomers: Now featuring linkage isomerism**

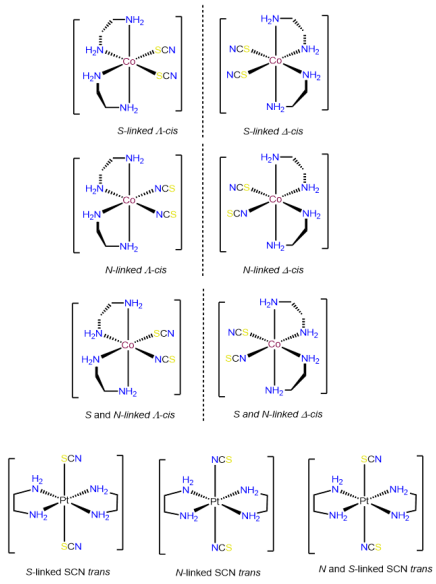
The Pt in this neutral complex must be Pt^{2+} to balance the negative charges of the two SCN^- ligands. Complexes of Pt^{2+} are square planar and four coordinate, consistent with the bidentate en and two thiocyanato ligands. Of the ligands, the en ligand must bind in a *cis* arrangement. Consequently, the two SCN^- ligands will be in a *cis* arrangement as well. The isomers will therefore only differ in whether the two SCN^- bind κN or κS. The possibilities are:



As with the preceding example, this will be a square planar Pt^{2+} complex. The main difference is that this time the coordinated nitrogens are not constrained to adopt a *cis* arrangement so there will be both *cis* and *trans* isomers.

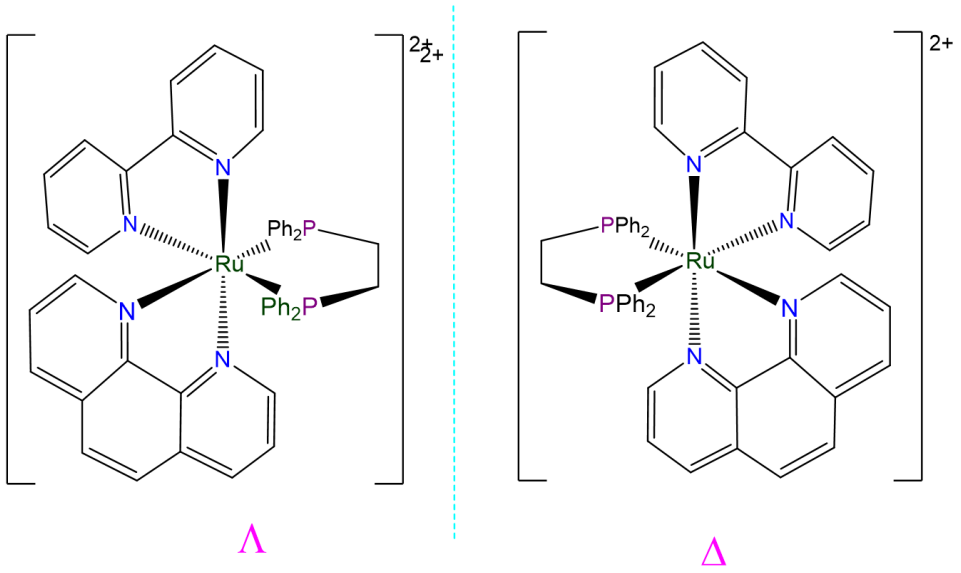




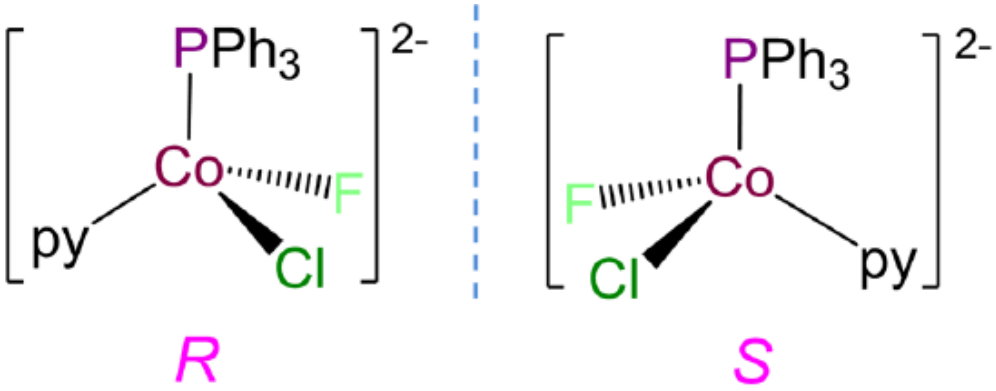


Exercise 5.3.7**. Stereoisomer free for all.**

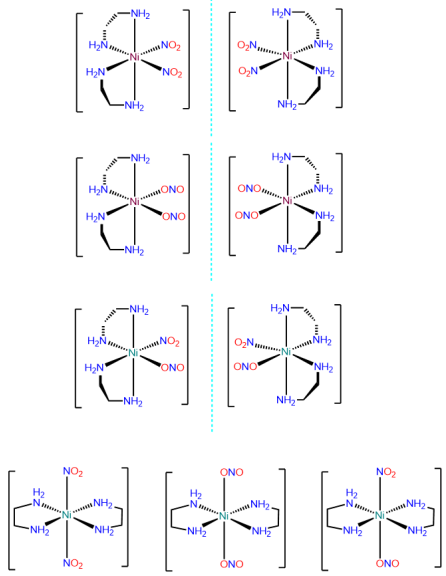
This complex is an octahedral tris-chelate containing symmetric ligands. As such it will exhibit Λ and Δ isomers:



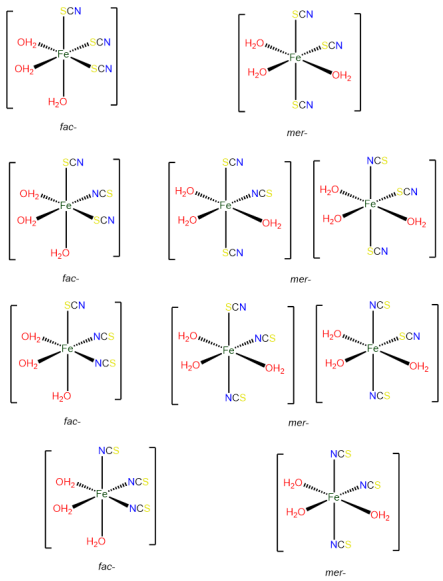
This complex has a coordination number of 4 and contains a Co^{2+} ion with a d^7 electron configuration, so a tetrahedral geometry is expected. Tetrahedral complexes like this one with four different ligands are chiral and can form *R* and S enantiomers.



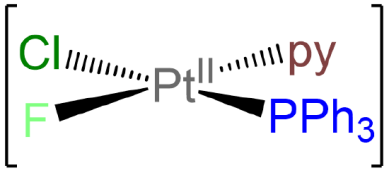
This is an octahedral bis-chelate and will exist in Λ and Δ configurations. Within each configuration the NO_2^- ligands can exist as *κN* and *κO*, leading to the following possibilities:



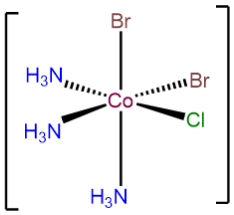
As an octahedral complex with three identical ligands it can exist in *mer* and *fac* configurations, with the ambidentate SCN ligand providing additional possibilities for isomerism.



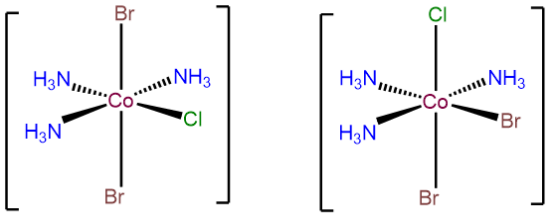
As a square planar complex with four nonidentical ligands, this complex exists as a single isomer.



As an octahedral complex with three identical ligands it will exhibit *mer* and *fac* isomerism. In addition, it will have two *mer* configurations that differ in terms of the cis and trans relationships between the bromo and chloro ligands.



fac

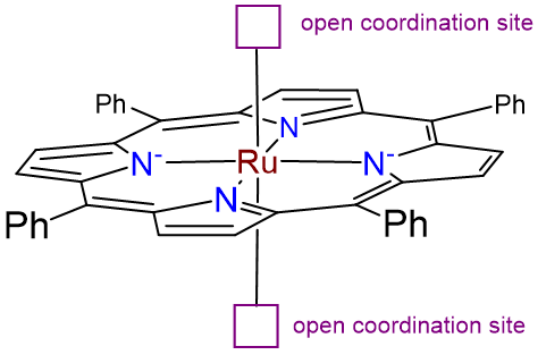


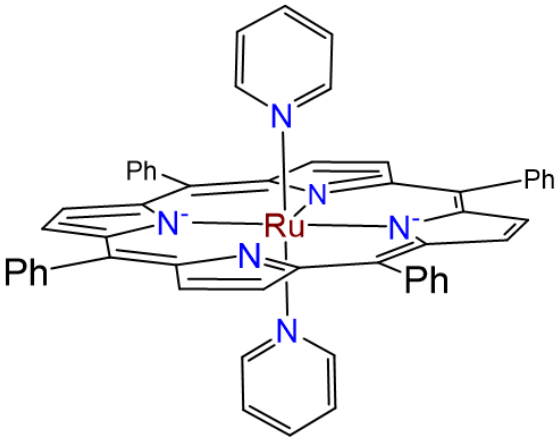
mer with Br *trans* to Br *mer* with Cl *trans* to Br

Exercise 5.3.8

There is only one isomer. While normally complexes containing two identical ligands (in this case py) can exhibit *cis* and *trans* isomerism, in this case the planar tetraphenylporphyrin ring ligates the Ru^{2+} ion in a square planar arrangement, as shown at left in the image below. This leaves only a pair of *trans* coordination sites for the chloro ligands to occupy, giving the isomer shown at right below.

When TPP ligates Ru^{2+} it leaves only *trans* open coordination sites so only the *trans* isomer can form.

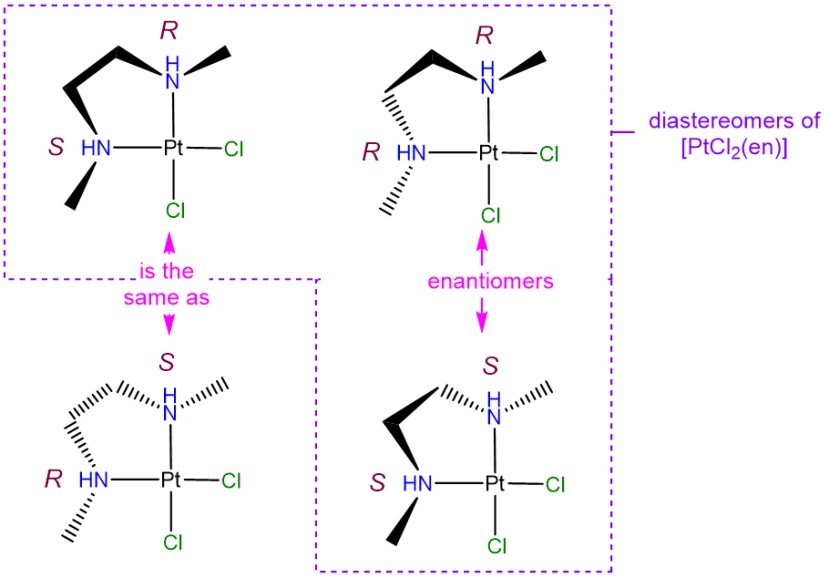




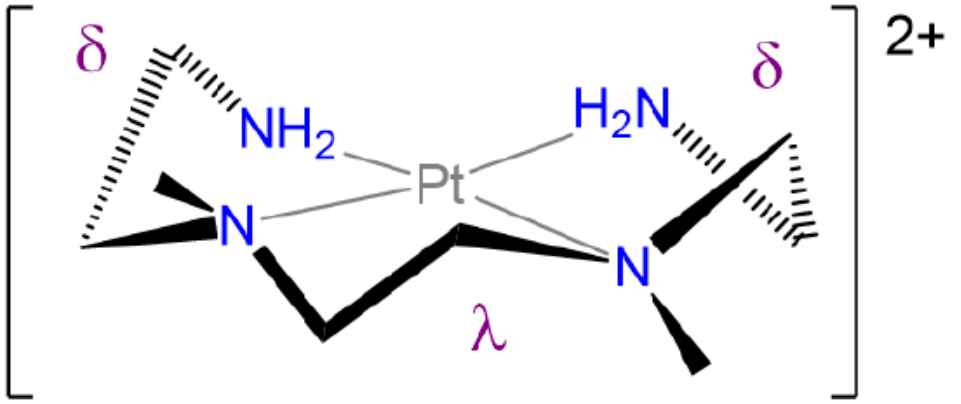
trans-[Ru(py)$_2$(TPP)]

Exercise 5.3.9

The diastereomers will differ in whether the N atoms adopt an *R* or S configuration at the nitrogen atoms. The possible permutations are (*R*,*R*), (S,S), (*R*,S), and (S,*R*). However, as may be seen from the image below, the (*R*,S) and (S,*R*) configurations are identical (the two projections shown can be interconverted through a C_2 rotation along an axis bisecting the Cl-Pt-Cl unit). As a result there are only three unique isomers. Of these, the (*R*,*R*) and (S,S) configurations are enantiomers (they are mirror images by reflection in the $PtCl_2N_2$ plane). Note that in solving problems like this one it can be helpful to keep track of possible isomers by assigning the stereochemistry at each chiral center as *R* or S using the Cahn-Ingold-Prelog-convention, though it is not strictly necessary to do so.



Exercise 5.3.10



Exercise 5.3.10

This page titled 5.3: Isomerism is shared under a license and was authored, remixed, and/or curated by LibreTexts.

- 9.4: Isomerism by Stephen M. Contakes is licensed CC BY 4.0.

5.4: Coordination Numbers and Structures

Why do coordination complexes form the structures they do?

As with all chemical structure, coordination complexes form the structures they do so as to best stabilize the metal center and ligands through the formation of metal-ligand bonds while avoiding destabilizing interactions like steric repulsions. The issue then is how many metal-ligand bonds should be formed and how those bonds should be arranged spatially to give the largest net stabilization possible. This question will eventually be considered in detail in connection with the nature of bonding in coordination compounds. For now, it will be helpful to think about it in terms of seven factors:

The stabilizing effect of metal-ligand bond formation.

The driving force for complex formation is the stabilization of electrons in covalent chemical bonds. In the vast majority of cases, this largely involves stabilization of the ligand lone pair as it experiences the effective nuclear charge of the metal, although a few instances involve stabilization of metal electrons by ligand nuclei (inverse ligand fields). Regardless, metal-ligand bond formation is stabilizing and classified by the way it preferences the addition of ligands to the complex.

Steric effects, specifically steric repulsions between ligands.

One reason coordination numbers do not increase indefinitely is that only so many ligands can fit around a metal. Exactly how many depends on

- *the size of the metal center*. This is one of the more important factors. Many metals tend to exhibit preferred coordination numbers, which depend on their oxidation state and size as shown in Figure 5.4.1. Larger inner transition metals like the Lanthanides and Actinides can accommodate 9-12 sterically undemanding ligands, while the smaller transition metals tend to accommodate up to six, although larger coordination numbers are more common for low valent metals and as size increases on moving from right to left across the transition metal block of the periodic table. Thus, the early transition metal molybdenum forms seven- and eight-coordinate $[Mo^{III}(CN)_7]^{4-}$ and $[Mo^{IV}(CN)_8]^{4-}$ with the sterically undemanding cyano ligand.
- *the size of the ligands*. As long as ligands are not excessively rigid and bulky, their size is less important than the size of the metal in determining the number of ligands that coordinate. Ligands' ability to donate electrons to the metal center also tends to influence coordination number more than ligand size. However, all other things being equal for a given metal and ligand donor ability, small ligands allow higher coordination numbers while fewer bulky ligands will fit around the metal center.
- *how the ligand bonds to the metal*. Again, all other things being equal, ligands that are more sterically demanding in the vicinity of the metal center tend to limit the ability of other ligands to bind more than those which bind through a small extended group. For example, a bulky isocyanide like t-BuCN will sterically crowd the metal less than a bulky phosphine like t-BuH_2P would. For this reason the effective size of a ligand is sometimes rated in terms of either a cone angle of space they are estimated to occupy around the metal (called the Tolman cone angle, it is commonly used to evaluate phosphines' steric bulk) or in terms of the percentage of the metal's coordination sphere the ligand occupies (called the percent buried volume, it is used to estimate the steric impact of *N*-heterocyclic carbenes).

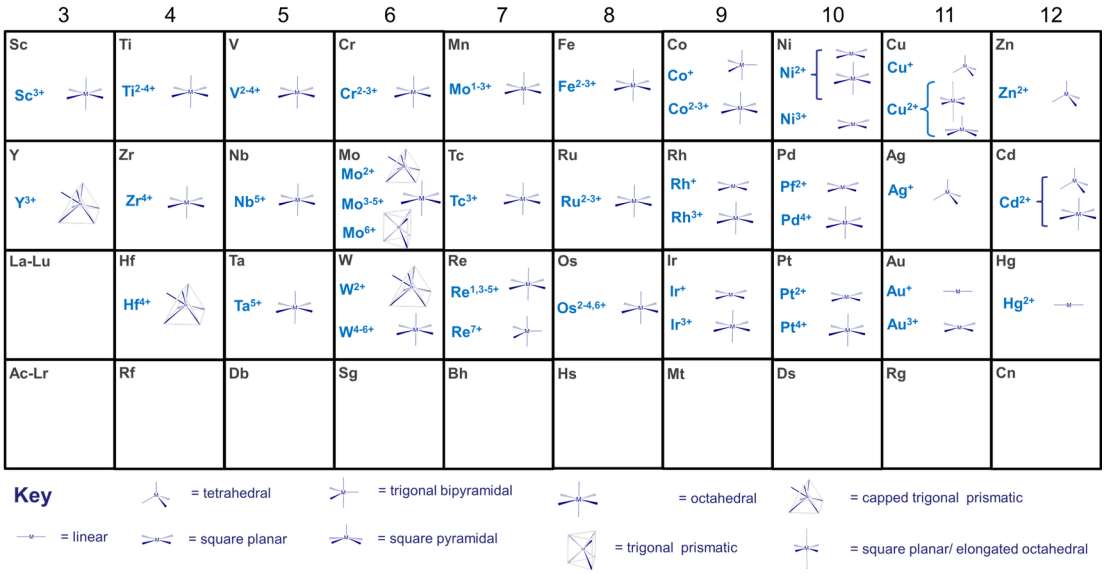


Figure 5.4.1. Preferred coordination geometries of the transition elements. Assignments are as reported in reference 1 except for Cu^{2+}, which is assigned above as square planar/elongated octahedral instead of the square planar assignment given in that work. This work by Stephen Contakes is licensed under a Creative Commons Attribution 4.0 International License.

Repulsion between M-L bonding electrons on different ligands.

For many complexes, steric effects are neither the only effects nor the most important. Among the additional factors that should be considered are the repulsions that occur between the electrons that different ligands donate to the metal-ligand bonding. These electron-electron repulsions affect the

a. **Coordination number.** When a ligand donates its electrons to a metal center to form a new metal-ligand bond, the electron density around the metal increases, raising the overall energy of the other M-L bonding electrons. This increased repulsion often limits the number of coordinated ligands. As more ligands are added, the electron-electron repulsions keep increasing until the lowering of energy of the ligand electrons in the new bond is insufficient to compensate for the raising of energy of the existing M-L bonding electrons. Based on this effect alone,
   - larger metals tend to achieve higher coordination numbers than smaller ones because the electron-electron repulsions are spread across a larger coordination sphere.
   - With a given metal, ligands that are more electron donating have a greater tendency to form complexes with lower coordination numbers with a given metal than similar neutral ones do. This is why anionic ligands (which tend to be better electron donors) tend to give lower coordination numbers than comparable neutral ligands (which tend to be weaker donors). Thus Co^{2+} forms $CoCl_4^{2-}$ with chloro ligands but $[Co(H_2O)_6]^{2+}$ with aqua ligands.

b. **Coordination geometry.** In the **Kepert model** for the shapes of coordination complexes, this intraligand repulsion determines the most stable coordination geometry by causing the ligands to move as far apart from one another on the metal's coordination sphere as possible.

Formally, according to the **Kepert model**

- any of the metal's valence electrons not involved in metal-ligand bonds occupy (n-1)*d* orbitals and function as core electrons. As core electrons they do not influence the molecular shape.
- electrons involved in bonding to a given ligand constitute an electron group that repels all other electron groups around the metal.
- all other things being equal, the complex will form the geometry that maximizes the intra-electron group repulsions.

Notice the similarities of these postulates to those of VSEPR theory. In predicting coordination geometries in terms of electron-electron repulsions, the Kepert model is just an extension of VSEPR theory to coordination compounds. The difference between VSEPR theory and the Kepert model is that in the Kepert model, only electrons involved in metal-ligand bonds count.

Coordination geometries predicted by the Kepert model for coordination numbers two through nine are given in Figure 5.4.2. As may be seen from the geometries listed in Figure 5.4.2, these are just equivalent to VSEPR geometries for cases in which the

number of electron groups is equal to the coordination number.

The difference between optimal and suboptimal coordination geometries is greater with few ligands, and becomes smaller as ligands become increasingly dispersed across the metal's coordination sphere. In complexes containing five, seven, eight, or higher coordinate metals, there are a number of geometries that are similar in energy to the preferred geometry. These geometries, which should be regarded as accessible, are also listed in Figure 5.4.2.

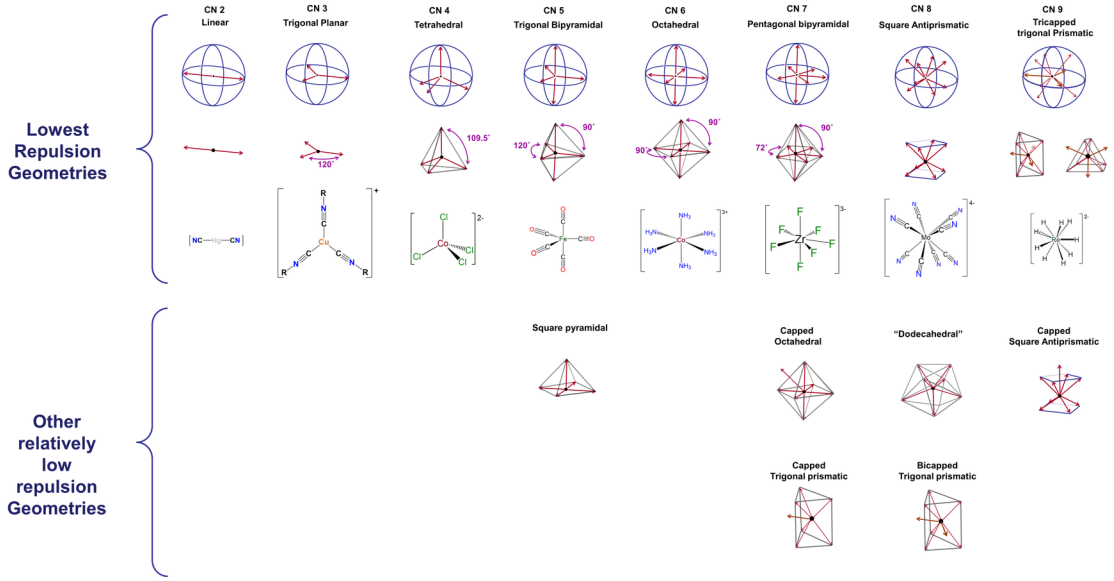


Figure 5.4.2. Coordination geometries predicted by the Kepert model for coordination numbers two through nine along with other coordination geometries similar in energy to the lowest repulsion geometry. This work by Stephen Contakes is licensed under a Creative Commons Attribution 4.0 International License.

d-electron effects

A few coordination geometries are noticeably absent from the Kepert-preferred and Kepert-accessible geometries in Figure 5.4.1. These include the trigonal prismatic geometries formed by compounds like $W(CH_3)_6$ and the very common square planar geometry illustrated by complexes like $[PtCl_4]^{2-}$ and $[IrClH(PPh_3)_2]$. One of the reasons the Kepert model fails to predict the existence of such structures is its neglect of directional interactions involving *d* electrons on the metal center. Metal *d* electrons exert a profound influence on almost all properties of transition metal complexes, including their structures. The way in which this occurs will be explored at length in the next chapter. For now, it is enough to note that both the ligand-donated electrons surrounding a metal center and the electrons occupying particular *d* orbitals on that metal are oriented in specific directions relative to one another. Because of this, the strength of the interactions between the ligand and metal *d* electrons depends on the number of *d* electrons present, how strongly metal-ligand binding affects their energy, and how the ligands are arranged about the metal center. The impact of these effects, here termed ligand field effects, differs from case to case and can include

- distortions of the complex's geometry. For instance, an ideal octahedral coordination geoemtry might be tetragonally distorted by flattening or elongating it.
- imparting a strong preference for non-Kepert coordination geometries. This is why, for example, 2nd and 3rd row complexes in which the metal has a d^8 electron configuration are almost always square planar.
- stabilizing non-Kepert geometries enough to permit complexes to adopt them in the presence of a rigid or semirigid ligand that prefers to coordinate the metal in that geometry.[3]

Because of these effects, square planar and trigonal prismatic geometries are also observed, and the list of coordination geometries given in Figure 5.4.2 may be extended to that shown in Figure 5.4.3.

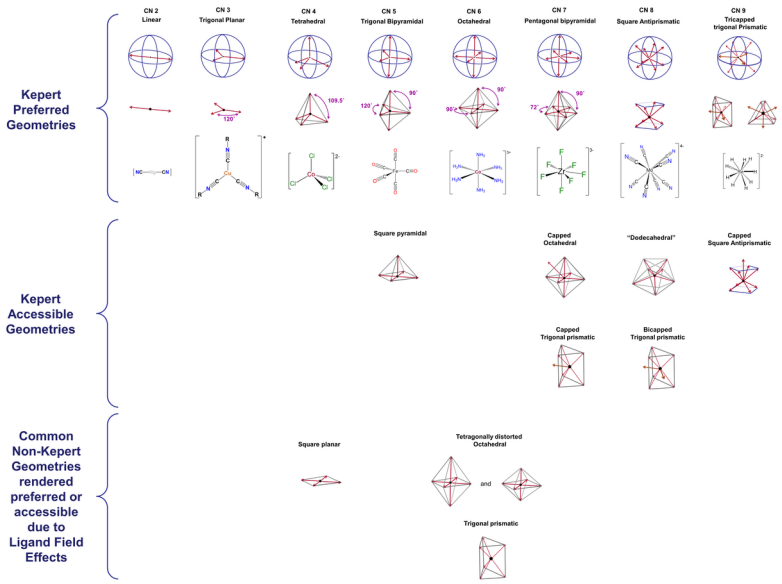


Figure 5.4.3. Coordination geometries accessible for 2-9 coordinate complexes even without constraint by rigid or semirigid ligands. This work by Stephen Contakes is licensed under a Creative Commons Attribution 4.0 International License.

Ligand constraints imposed by rigid or semirigid ligands

Rigid or semirigid ligands influence the coordination geometry of metal complexes in two main ways:

a. Bulky rigid ligands that crowd the metal center prevent other ligands from binding. Thus such ligands are useful for preparing low-coordinate complexes.
b. Rigid and semirigid ligands can impose their preferred coordination geometry on a metal center. This is because these ligands energetically prefer to adopt a particular conformation when they bind a metal center. In doing so they shift the coordination geometry energy landscape toward that preferred geometry. If the shift is large enough relative to the native preference due to ligand repulsion and ligand field effects, the complex will either adopt the ligand-preferred geometry or be distorted in the direction of the ligand-preferred geometry. Examples are given in Figure 5.4.4.

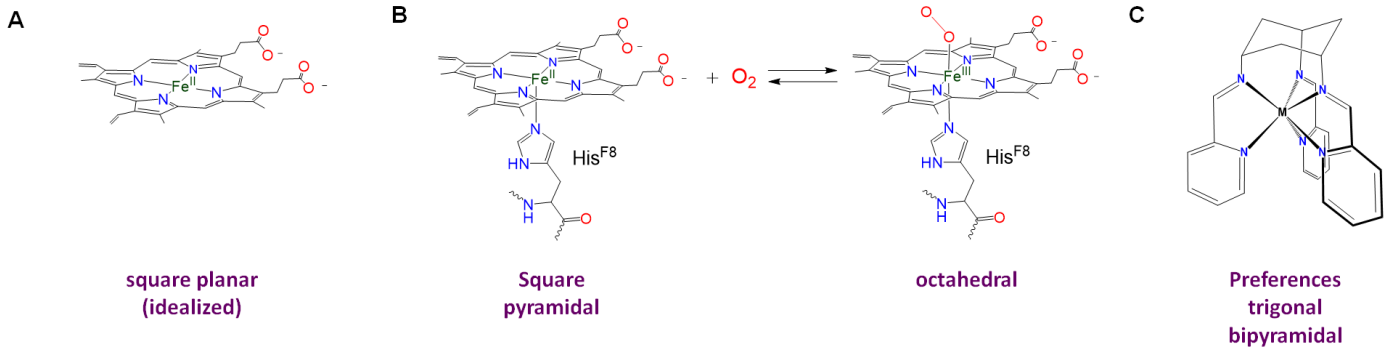


Figure 5.4.4. Examples of rigid/semirigid ligands that can impose their preferred coordination geometry on a metal center. Porphyrins, phyhalocyanines and related macrocycles tend to impose a slightly bent square planar coordination geometry, although (B) many such complexes, including the iron of myoglobin's heme cofactor, coordinate additional ligands to give square planar or octahedral complexes. (C) Synthetic multidentate ligands have been developed to preference trigonal prismatic coordination geometries, including the one shown here. It forms roughly trigonal prismatic complexes with Co^{II} and $Zn^{II,}$ albeit imperfect ones.[3] This work by Stephen Contakes is licensed under a Creative Commons Attribution 4.0 International License.

The influence of ligands on coordination geometry is important in living systems, in which proteins and nucleic acids can act as rigid or semirigid ligands. The ability of these ligands to distort the coordination geometries of metal atoms in ways that enable them to perform specific functions is so common that the resulting distorted geometries are termed entactic states. A particularly spectacular case of an entactic state involves the blue copper proteins azurin and plastocyanin, the structure of which is given in Figure 5.4.5.

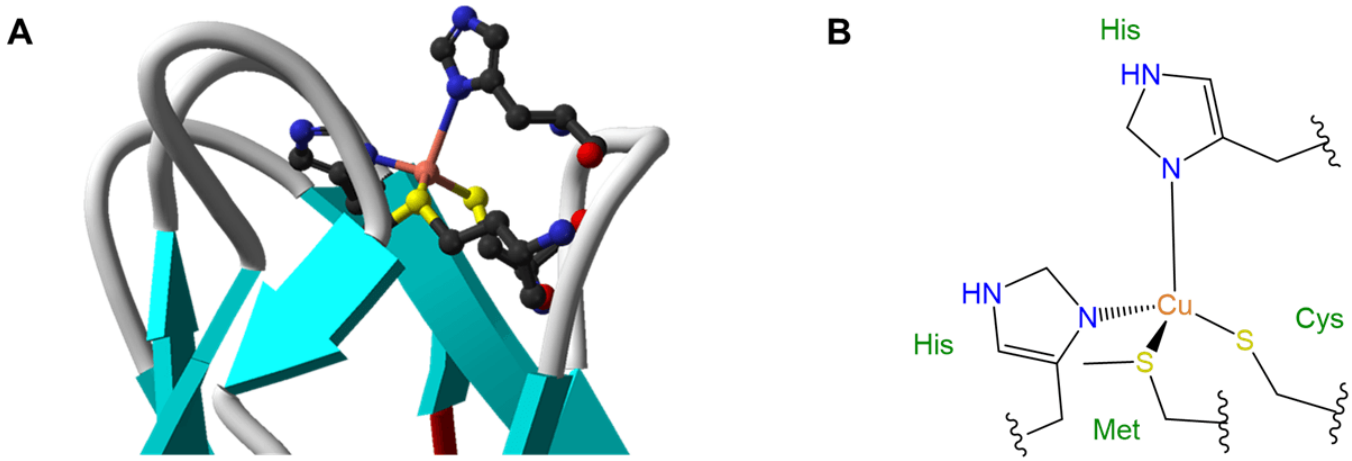


Figure 5.4.5. (A) Structure and (B) schematic of the plastocyanin active site showing the distorted tetrahedral coordination environment that the protein imposes on the copper center (tan), which is most evident from the long vertically oriented Cu-Histidine bond. The image in part A is cropped from an original image by Ben Mills - Own work, Public Domain, https://commons.wikimedia.org/w/inde...?curid=62020620. The image in part B is by Stephen Contakes and licensed under a Creative Commons Attribution 4.0 International License.

As may be seen from the structure in Figure 5.4.5, the copper in plastocyanin exibits a distorted tetrahedral coordination geometry. The protein is said to act like a medieval torture device called a rack in stretching the metal into its distorted geometry. This distortion makes it easier for the copper center to undergo facile redox reactions, enabling it to better function as an electron carrier.

Crystal packing effects, in which the energy-lowering packing of molecules and ions in a crystal drives the distortion of a complex's structure away from what it would adopt in the gas phase or solution

This effect is similar to that of ligand constraints except that in this case it arises not from the structure internal to a ligand but out of the forces involves in maximizing the stabilization energy of a crystal. With lower coordination number complexes, packing effects can shift the conformations of flexible ligands but only give rise to very small distortions of the overall coordination geometry. Packing effects can drive a shift in the overall coordination geometry of higher coordination number complexes, for which packing effects are significant relative to the small difference in energy between geometries. Thus while $[Mo(CN)_8]^{4-}$ has a square antiprismatic coordination geometry, in solution it exhibits a dodecahedral coordination geometry in the crystals of many of its salts.

Relativistic effects on orbital energies

The proximity of fast moving electrons to massive nuclei in the heavier transition elements results in relativistic expansion and contraction of orbitals. The net results are that

- heavier elements tend to be smaller than expected. This effect preferences lower coordination numbers.
- the relative energies of orbitals shift. Orbitals which become contracted are lowered in energy while those which are expanded increase in energy, as shown for the case of gold in Figure 5.4.6A.

The combination of smaller sizes and altered orbital energies affects coordination preferences. Relativistic effects contribute to the greater tendency of Au^{I} relative to other group 11 metals to form linear two-coordinate complexes. As shown in Figure 5.4.6B , the relative closeness in energy of the 6s and 5*d* orbitals of gold makes mixing of these orbitals more favorable, facilitating the ability of gold to form two-coordinate complexes with strong sigma bonds oriented 180/(^{\circ}\) from one another.

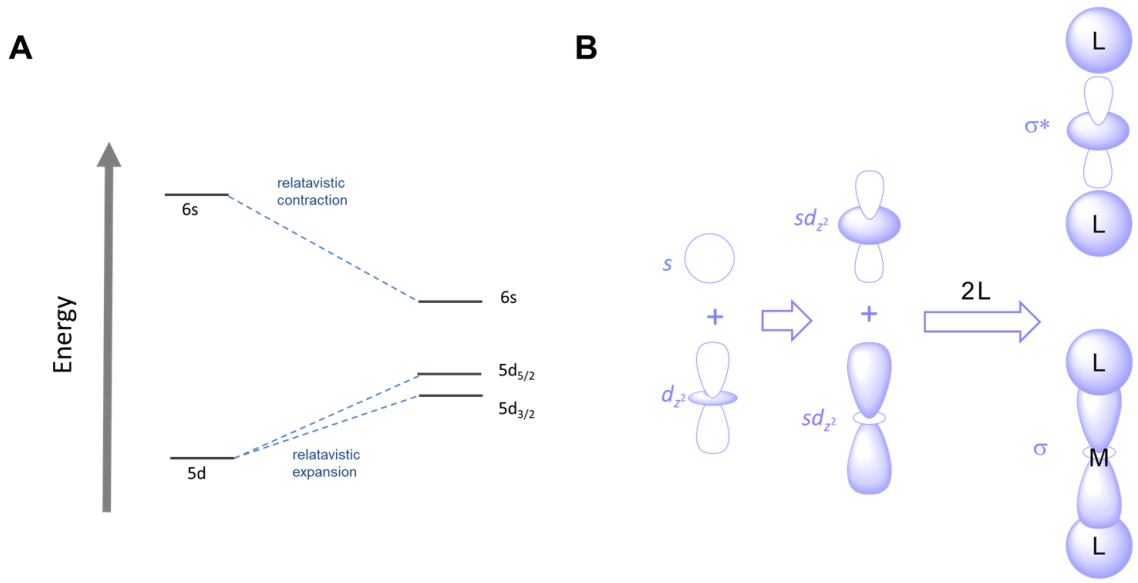


Figure 5.4.6. (A) Gold experiences relativistic expansion and contraction of its 5*d* and 6s orbitals, resulting in shifts to their relative energies. (B) This makes mixing of these orbitals more favorable, facilitating the ability of gold to form two-coordinate complexes with strong sigma bonds that involve considerable sd_{z^2} character. This work by Stephen Contakes is licensed under a Creative Commons Attribution 4.0 International License.

What structures do coordination complexes form?

Metal complexes with coordination numbers ranging from one to 16 are known, although values greater than seven are rare for the transition metals. In this section, examples of common coordination geometries will be presented in order of coordination number.

Coordination Number 1.

Condensed phase monocoordinate complexes are unknown for the transition metals, although the post-transition metals Tl and In form monocoordinate complexes with the bulky ligands triazapentadienyl and 2,6-tris(2,4,6-triisopropylphenyl)benzene as shown in Figure 5.4.7.

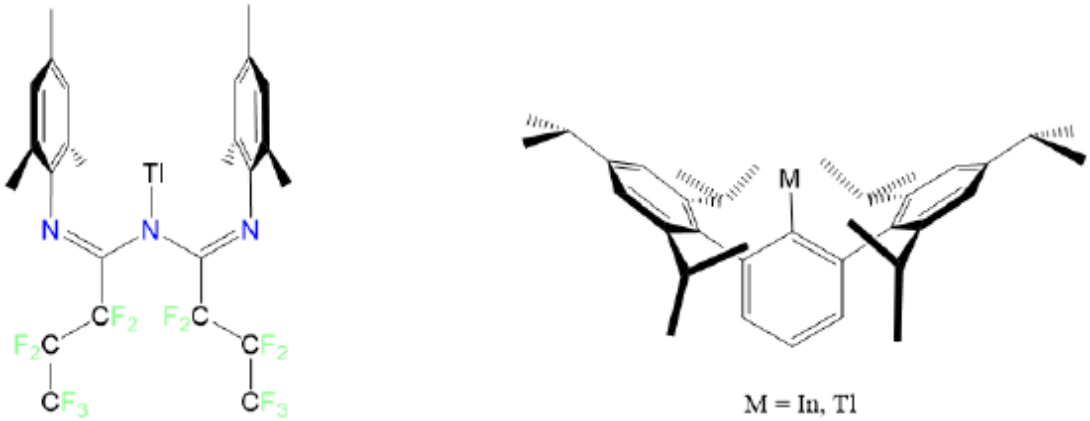
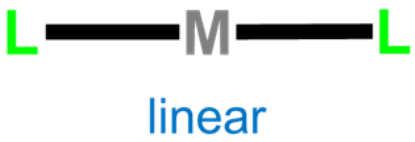


Figure 5.4.7. No monocoordinate transition metal complexes are known, but Tl^+ and In^+ form monocoordinate complexes with extremely bulky ligands. This work by Stephen Contakes is licensed under a Creative Commons Attribution 4.0 International License.

Coordination Number 2.

A coordination number of 2 is rare outside of ***d*^{10} complexes of the group 11 metals and mercury**, specifically, Cu^+, Ag^+, Au^+,

and Hg^{2+}. In accordance with the predictions of the Kepert model these give **linear complexes.**



Among these,

- Cu^{+} more commonly gives tetrahedral complexes but can be coaxed to give linear ones. The most prominent example is $[CuCl_2]^-$, which forms when CuCl is treated with concentrated HCl under anerobic conditions.
- Ag^{+} also commonly forms tetrahedral or trigonal planar complexes but can give linear ones. The most prominent example is $[Ag(NH_3)_2]^+$, which can be formed by treating silver slats with concentrated aqueous or liquid ammonia.
- Au^{+} almost always forms linear complexes, but many of these formally two-coordinate complexes associate as depicted in Figure 5.4.8. The ability of Au^{+} to form linear complexes with cyanide is even used to selectively extract metallic gold from low grade ores. The stability of $[Au(CN)_2]^-$ means that the dissolution of metallic gold in aqueous cyanide is thermodynamically favorable under aerobic conditions.

$$4\ Au + 8\ CN^- + O_2 + 2\ H_2O \longrightarrow 4\ [Au(CN)_2]^- + 4\ OH^-$$

- Hg^{2+}, like Au^{+}, benefits from relativistic effects and more commonly forms two-coordinate complexes with a linear geometry. Among these is $[Hg(CN)_2]$. However, its preference for linearity is not as rigid as for Au^{+}, and so complexes with a variety of coordination geometries are known.

And by means of honorary mention, the mercury(I) ion, Hg_2^{2+}, forms linear complexes of the type L-Hg-Hg-L, although since Hg_2^{2+} is often considered as a single unit, these aren't always considered to be two-coordinate complexes.



Figure 5.4.8. Many "linear" gold complexes associate side-on to form dimers, trimers, tetramers, and chains. Although in this chapter L is usually taken to represent a generic ligand, in this scheme L represents a neutral ligand that donates two electrons to the metal (py, PR_3, CO, etc.) and X an anionic one (*e.g.,* Cl^-, CN^-, etc.). Exactly which structure forms depends on the identity of L and X. Redrawn from reference 5. This work by Stephen Contakes is licensed under a Creative Commons Attribution 4.0 International License.

Two-coordinate complexes may also be formed through the use of bulky ligands that only allow for the binding of two to the metal center. The classic examples are given in Figure 5.4.9.

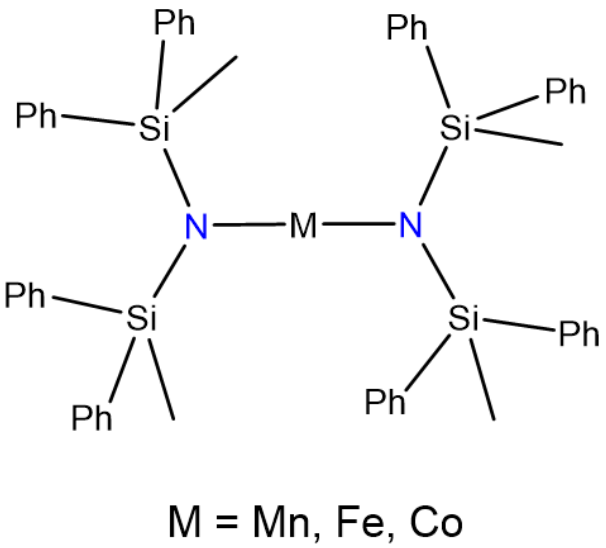


Figure 5.4.9. Two-coordinate complexes form between Mn^{2+}, Fe^{2+}, and Co^{2+} with $N(SiMePh_2)_2$.[6] This work by Stephen Contakes is licensed under a Creative Commons Attribution 4.0 International License.

Coordination Number 3

Three-coordinate complexes are similar to two-coordinate ones in that they are rare and, aside from the constraining influence of ligands, usually limited to d^{10} metal ions such as Cu^+ , Ag^+, Au^+, Hg^{2+}, and Pt(0). As expected from the Kepert model, in the absence of constraining ligands, three-coordinate complexes are trigonal planar.

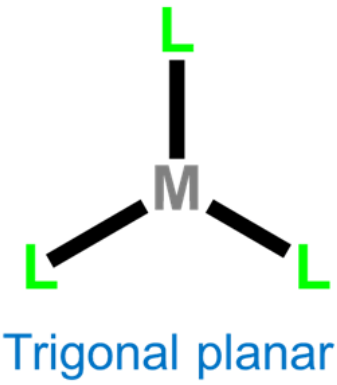
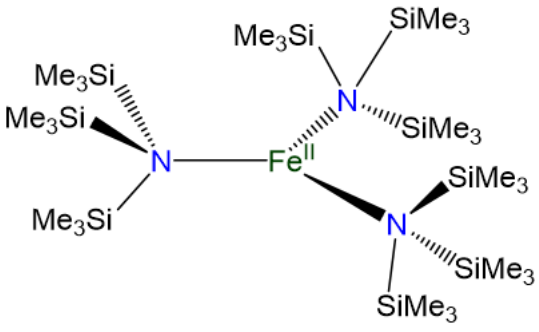


Figure 5.4.10.



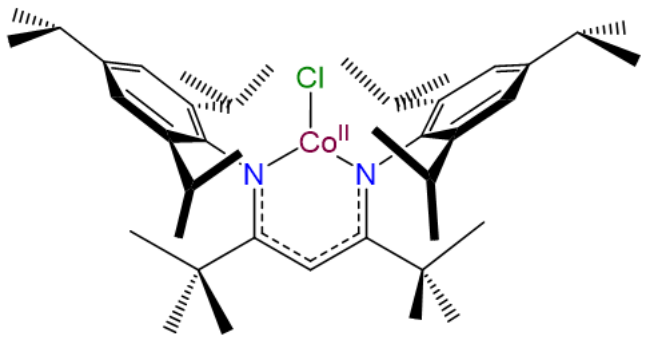
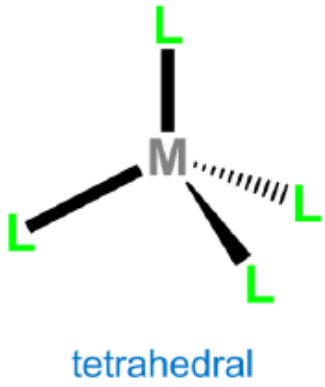


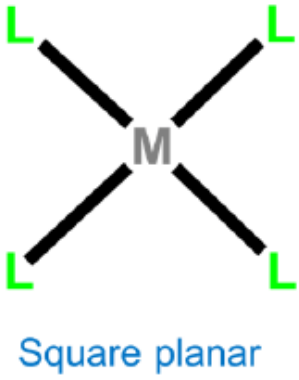
Figure 5.4.10. Three-coordinate complexes prepared using bulky and semirigid ligands. This work by Stephen Contakes is licensed under a Creative Commons Attribution 4.0 International License.

Coordination Number 4

The two common four-coordinate geometries are tetrahedral and square planar.



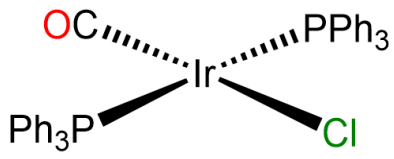
tetrahedral



Square planar

Tetrahedral complexes are commonly formed by metals possessing either a d^0 or d^{10} electron configuration. Monometallic examples of d^0 configurations include $TiCl_4$, VO_4^{3-}, WS_4^{2-}, MnO_4^-, CrO_4^{2-}, and OsO_4, while d^{10} examples are $[Ni(CO)_4]$, $[HgBr_4]^{2-}$, $[ZnCl_4]^{2-}$, and $[CdI_4]^{2-}$. For other electron configurations, tetrahedral complexes are known but much less common. Examples usually involve good donor ligands and include $[FeCl_4]^-$ (d^5), $[CoCl_4^{2-}]$ (d^6), and $[NiCl_4]^{2-}$ (d^7).

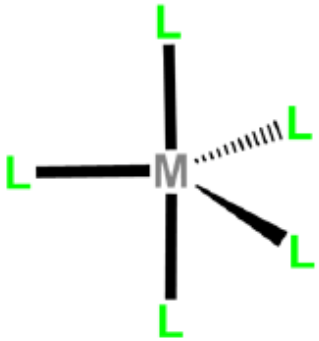
Second and third row transition metal centers with d^8 electron configurations like Rh^+, Ir^+, Pd^{2+}, Pt^{2+}, and Au^{3+} almost exclusively exhibit **square planar geometries**. Beyond this, square planar geometries are often formed by Ni^{2+} (d^8), Ni^{3+} (d^7), and Cu^{2+} (d^9). Examples of square planar complexes include $[Cu(acac)_2]$; $[PtCl_4]^{2-}$;Wilkinson's catalyst, $[RhCl(PPh_3)_3]$; and Vaska's complex, *trans*-$[Ir(CO)Cl(PPh_3)_2]$.



Vaska's Complex

Coordination Number 5

The two common coordination geometries for five-coordinate complexes are trigonal bipyramidal and square pyramidal.



Trigonal bipyramidal



Square pyamidal

Figure 5.4.11.

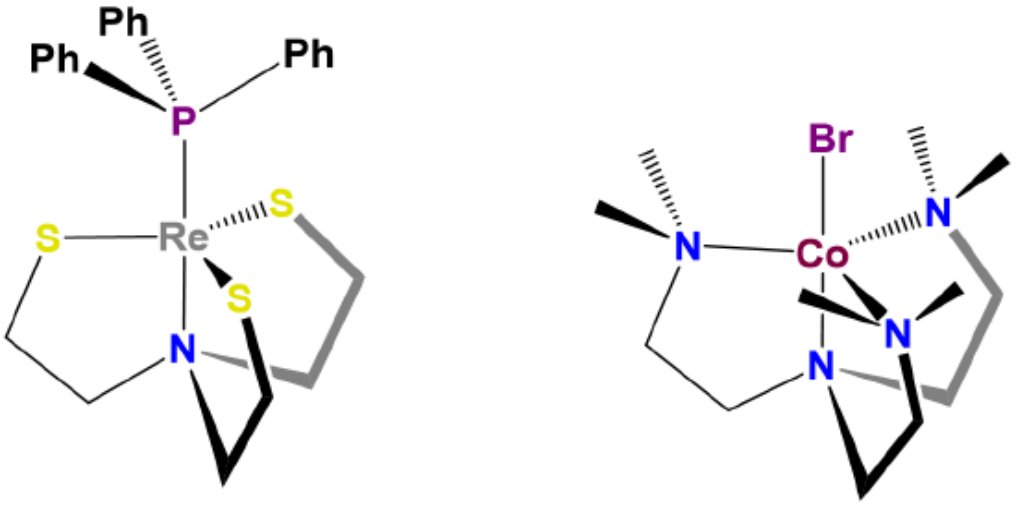


Figure 5.4.11. Some tripodal ligands preference the formation of trigonal bipyramidal complexes. This work by Stephen Contakes is licensed under a Creative Commons Attribution 4.0 International License.

Homoleptic $[Ni(CN)_5]^{3-}$ possesses a square pyramidal structure, although the geometry is more common for macrocyclic complexes like the iron protoporphyrin of deoxymyoglobin shown in figure 5.4.4 and for complexes containing oxo and nitrido ligands, examples of which are shown in Figure 5.4.12.

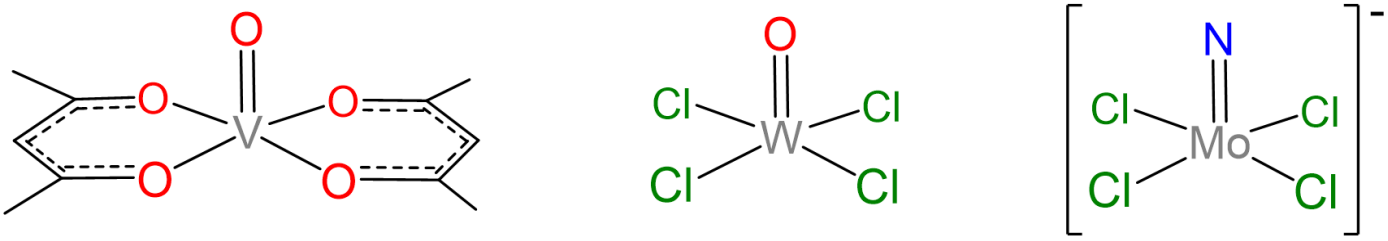


Figure 5.4.12. Some square pyramidal oxo and nitrido complexes. This work by Stephen Contakes is licensed under a Creative Commons Attribution 4.0 International License.

In the absence of rigid constraining ligands, the relatively low energy difference between the trigonal bipyramidal and square pyramidal coordination geometries provides a mechanism for interconversion of the axial and equatorial ligands in a trigonal planar complex. For example, pentacarbonyliron(0) exhibits fluxionality involving a square pyramidal intermediate via a Berry pseudorotation mechanism, as shown in Figure 5.4.13.

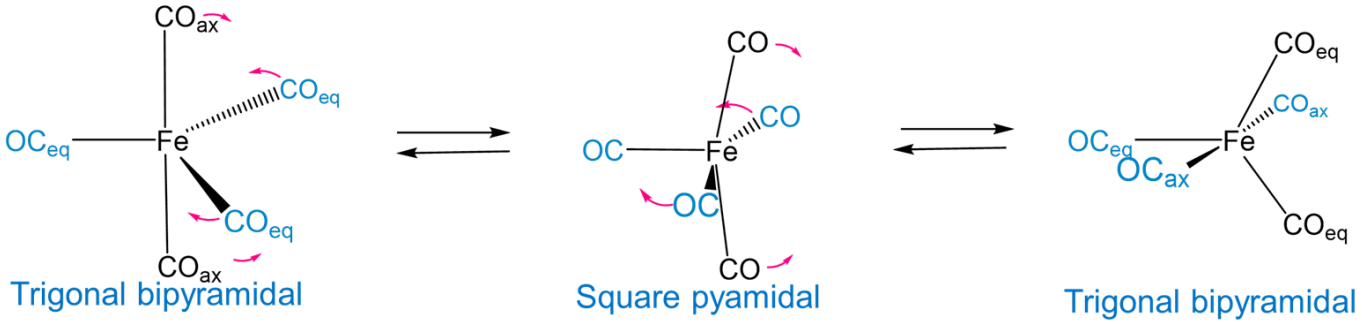


Figure 5.4.13. Fluxionality in pentacarbonyliron(0) involves exchange of axial and equatorial carbonyl ligands via Berry pseudorotation. Interconversion of the axial and equatorial carbonyl groups occurs faster than the NMR timescale at room temperature. As a result the ^{13}C NMR spectrum of $Fe(CO)_5$ exhibits a single signal rather than two separate signals for the axial and equatorial carbonyl carbons. This work by Stephen Contakes is licensed under a Creative Commons Attribution 4.0 International License.

Coordination Number 6

The two common coordination geometries for coordination number 8 are octahedral and trigonal prismatic.

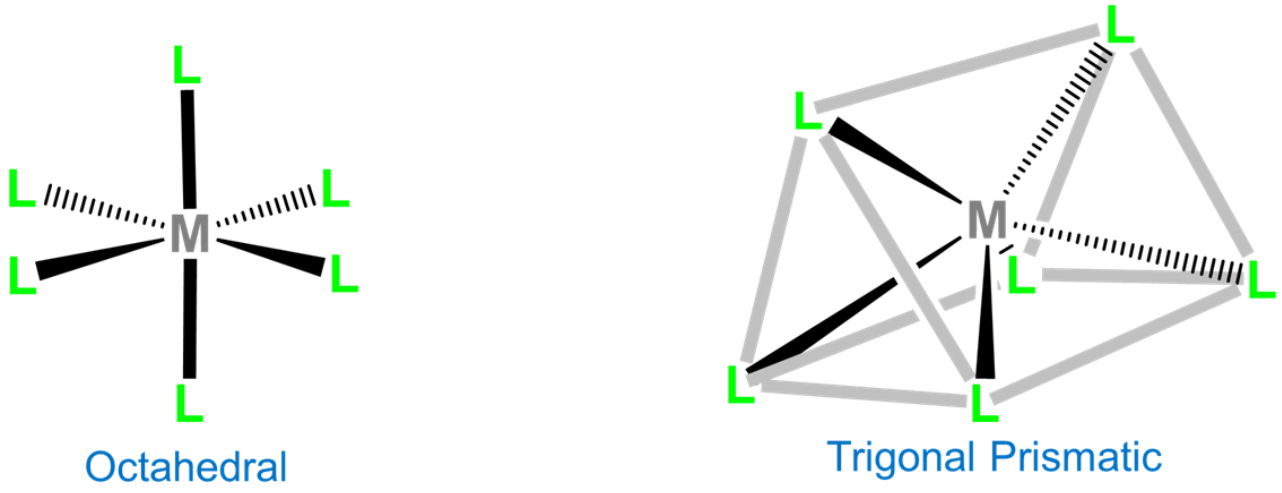


Figure 5.4.14.

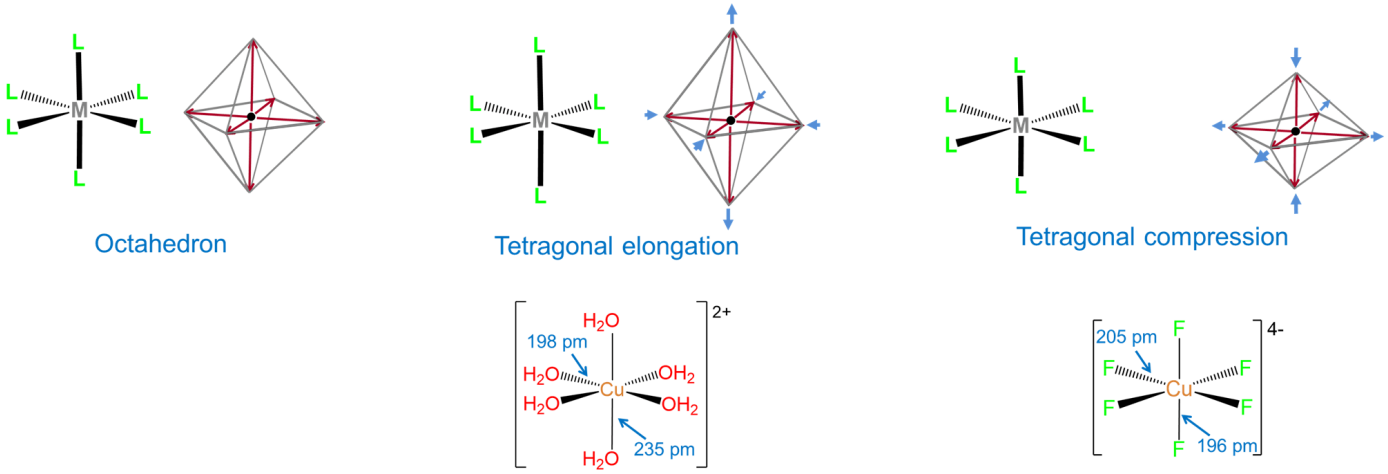


Figure 5.4.14. Tetragonal distortions commonly occur for d^4, d^7, and d^9 octahedral complexes. The most common type involves axial elongation in which the octahedron is stretched along a single *trans*-L-M-L axis, but axial compressions in which the octahedron is compressed along such an axis instead are sometimes observed. An example of an axial elongated complex is $[Cu(H_2O)_6]^{2+}$ in solution, while $[CuF_6]^{4-}$ is axially compressed when doped into a Ba_2ZrF_6 lattice (it is elongated when doped into a -----. Bond distances are taken from references 7 and 8. This work by Stephen Contakes is licensed under a Creative Commons Attribution 4.0 International License.

Trigonal prismatic coordination is related to octahedral coordination as shown in Figure 5.4.15. As may be seen in Figure 5.4.15 , an octahedral coordination sphere is just a trigonal antiprism in which all edge lengths are identical. Rotation of one triangular face relative to its opposite until the two are eclipsed gives a trigonal prismatic geometry. In fact, since continuation of this rotation gives another octahedral complex, the trigonal prismatic geometry is an intermediate in isomerization reactions involving octahedral complexes.

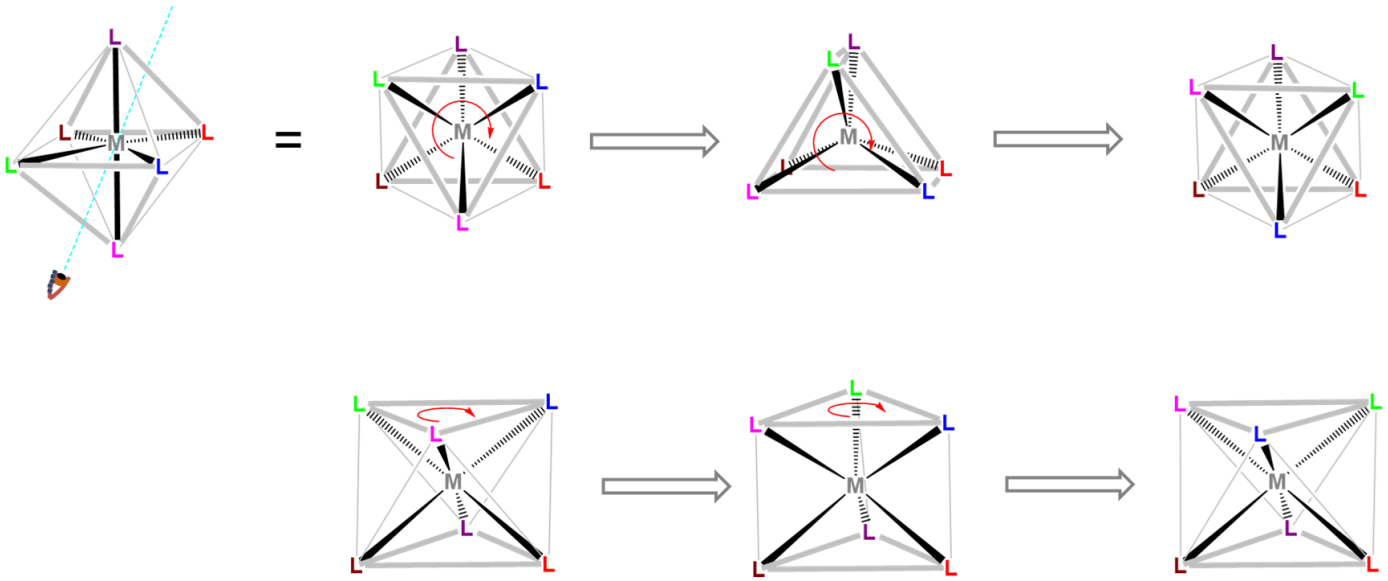


Figure 5.4.15. Since an octahedron is a trigonal antiprism, a trigonal prism may be produced by rotating or "twisting" one face of the octahedron relative to its opposite. Since continuation of the rotation gives an isomer of the original octahedron, when the energy landscape for twists like these is thermally or photochemically accessible, such twists provide one pathway for isomerization reactions involving octahedral complexes. In tris- and bis-chelates, such isomerizations are said to occur by Bailar and Ray-Dutt twists, which differ only in the relationship between the chelate rings and the faces twisted. Top: View looking down an axis bisecting a pair of opposing faces. Bottom: View perpendicular to that shown at top. This work by Stephen Contakes is licensed under a Creative Commons Attribution 4.0 International License.

In contrast to octahedral coordination geometries, trigonal prismatic coordination (and distorted versions thereof) are rare and occur mostly for d^0, d^1, and d^2 configurations. Examples of trigonal prismatic metal centers include the d^2 Mo^{4+} centers in MoS_2, d^1 $[Re(S_2C_2Ph_2)_3]^-$, and d^0 $[Ta(CH_3)_6]^-$, of which the latter two structures are given in Figure 5.4.16. Semirigid ligands like that shown in Figure 5.4.4C may be used to encourage the adoption of a trigonal prismatic geometry, although once the number of *d* electrons present exceeds two, the preference for octahedral coordination is too great for a trigonal prismatic geometry to occur.

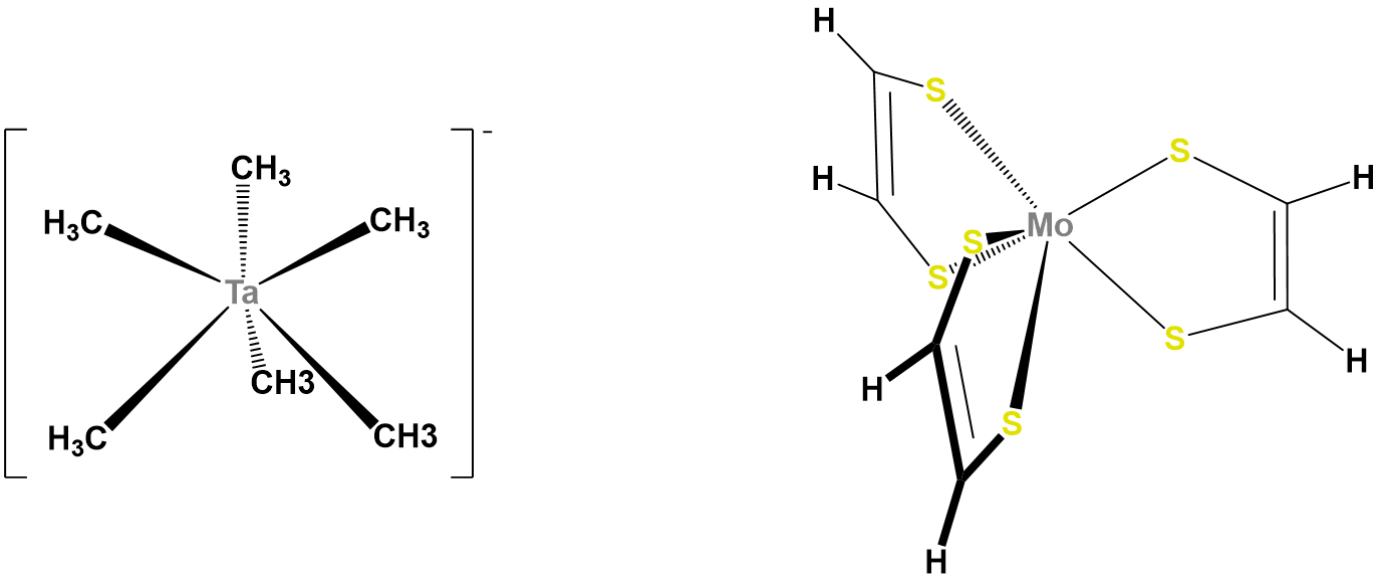
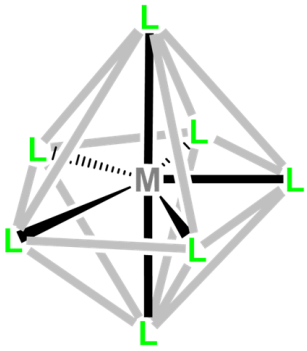


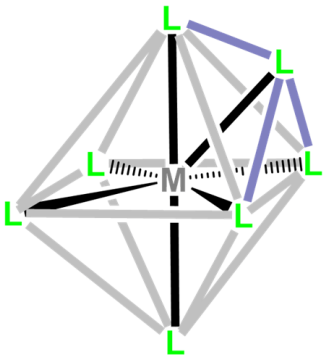
Figure 5.4.16. The complexes $[Ta(CH_3)_6]^-$ and $[Mo(S_2C_2H_2)_3]$ adopt a trigonal prismatic geometry. Trigonal prismatic coordination is common for d^0 and d^1 complexes with alkyl and dithiolene ligands. It is also typical for the dithiolene ligands to coordinate along the rectangular edges of the trigonal prism instead of the triangular ones. This work by Stephen Contakes is licensed under a Creative Commons Attribution 4.0 International License.

Coordination Number 7

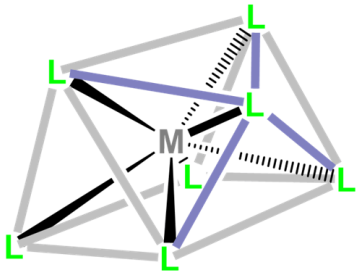
Seven-coordinate complexes are rare outside of the relatively large early transition metals, lanthanides, and actinides. The three common seven-coordinate geometries are pentagonal bipyramidal, monocapped octahedral, and monocapped trigonal prismatic. The latter two are often called capped octahedral and capped trigonal prismatic, with the mono- prefix being understood.



Pentagonal bipyramidal



Capped octahedral



Monocapped trigonal prismatic

Although intraligand repulsions are smaller in the pentagonal bipyramidal coordination geometry than the capped octahedral and capped trigonal prismatic geometries, the difference is small, and the three structures are often close in energy. As a result the structure observed is often dependent on ligand-based constraints, crystal packing, and solvent effects that preference one geometry over the others.

Heptacyano complexes are often pentagonal bipyramidal. Examples include $[Mo(CN)_7]^{3-}$, $[W(CN)_7]^{3-}$, and $[Os(CN)_7]^{3-}$. Seven-coordinate complexes containing oxo ligands commonly are pentagonal bipyramidal with the oxo ligand(s) in the less sterically hindered axial position. Examples include $[NbOF_6]^{3-}$ and, for the inner transition metals, $[UO_2F_5]^{3-}$. Ligands that have been used to promote formation of seven-coordinate species include 15-crown-5 and 2,2':6',2":6",2"'-quaterpyridine. Representative complexes are given in Figure 5.4.17.

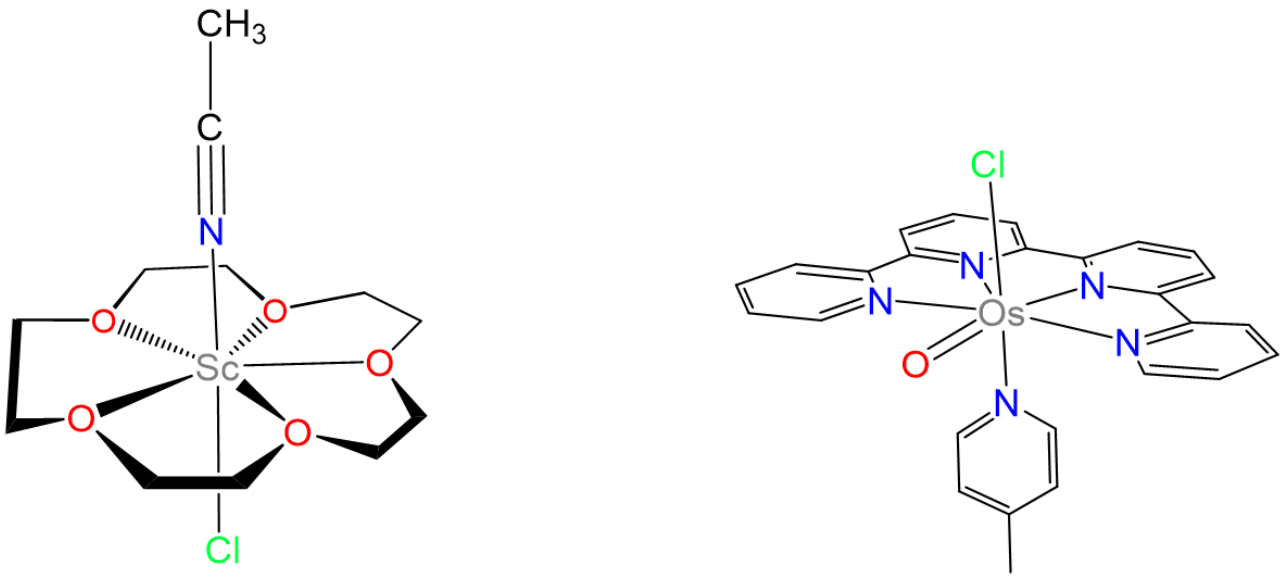


Figure 5.4.17. Seven-coordinate complexes containing ligands that encourage the formation of seven-coordinate geometries. Note that while in $[NbOF_6]^{3-}$ and $[UO_2F_5]^{3-}$ the oxo ligands occupy axial positions, the Osmium complex shown possesses an oxo ligand in an equatorial position. This is likely because the parent octahedral complex, in which the oxo ligand is not present, possesses an expanded outer N-Os-N angle of 121.655° that opens to 154.161° to accommodate the oxo group. Drawn based on the structures reported in references 9 and 10. This work by Stephen Contakes is licensed under a Creative Commons Attribution 4.0 International License.

Capped trigonal prismatic geometries are common for complexes of the early transition metals. Examples include $[NbF_7]^{2-}$,$[TaF_7]^{2-}$, and $[ZrF_7]^{3-}$ in $(NH_4)_3[ZrF_7]$.

Capped octahedral geometries are found in $[MoMe_7]^-$, $[WMe_7]^-$, and $[WBr_3(CO)_4]$, which contains three pairs of *trans*-Br and CO with the final CO capping the octahedron's $(CO)_3$ face, as shown in Figure 5.4.18.

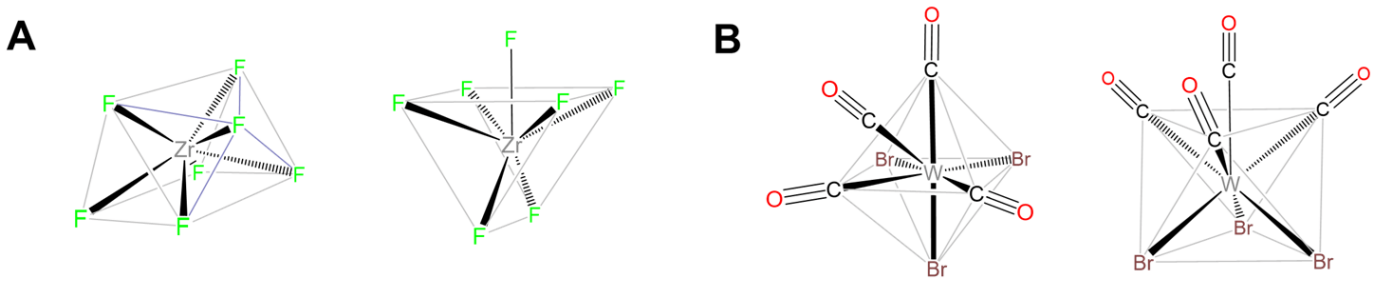


Figure 5.4.18. Examples of complexes that adopt monocapped triconal prismatic and monocapped octahedral geometries.(A) Two views of the structure of (A) capped trigonalprismatic $[ZrF_7]^{3-}$ and (B) capped octahedral $[WBr_3(CO)_4]$. This work by Stephen Contakes is licensed under a Creative Commons Attribution 4.0 International License.

In seven- and higher-coordinate complexes, ligand and crystal packing effects frequently give distorted coordination geometries. These geometries are intermediate between two or more of the idealized seven coordinate geometries, making it difficult to tell exactly which structure they are a distortion of (Figure 5.4.19).

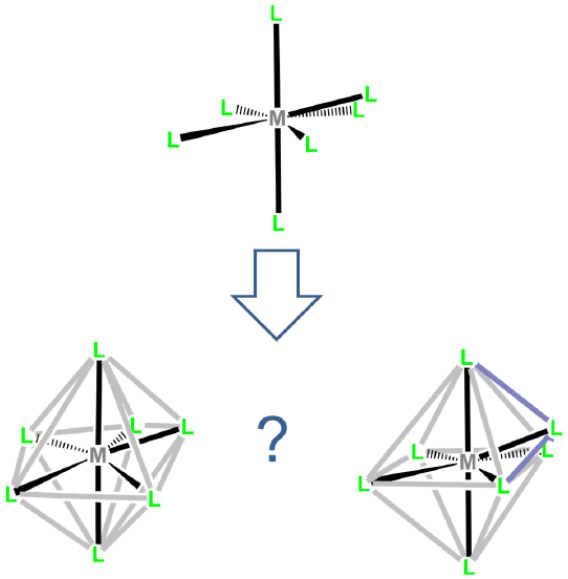


Figure 5.4.19. Many seven-coordinate structures are distorted and can be difficult to classify. For example, how should the geometry of this complex be described - as distorted trigonal bipyramidal or distorted monocapped octahedral? This work by Stephen Contakes is licensed under a Creative Commons Attribution 4.0 International License.

Coordination Number 8

Eight-coordinate complexes are rare and occurs in discrete molecules and ions only for the relatively large early transition metals, lanthanides, and actinides. The three common eight-coordinate geometries are square antiprismatic, dodecahedral, and bicapped trigonal prismatic. In contrast, the cubic coordination geometry is only found in ionic lattices like that of CsCl and in complexes of the inner transition metals such as $Na_3[UF_8]$.

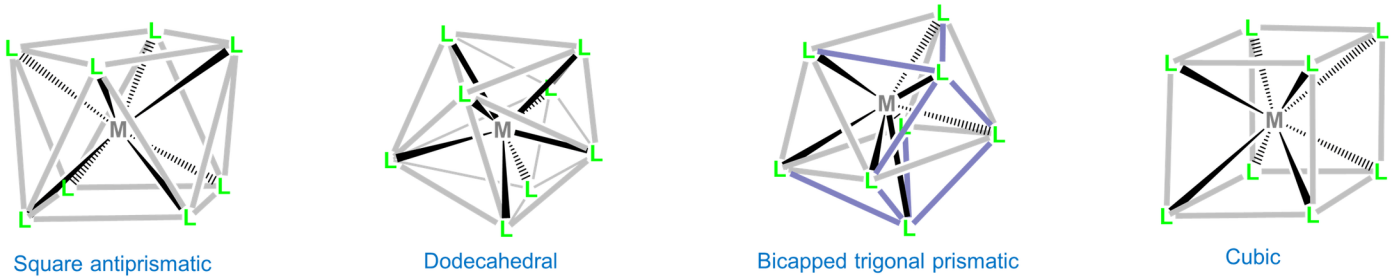


Figure 5.4.20. The square antiprism may be made by twisting one face of a cube relative to another, and the dodecahedron by folding opposing faces towards one another.

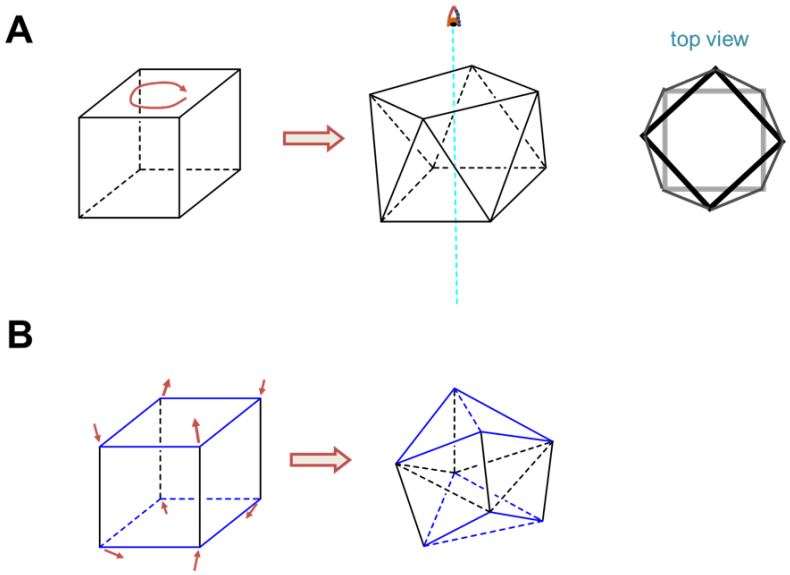


Figure 5.4.20. The (A) square antiprismatic and (B) dodecahedral coordination geometries are distorted cubic geometries. (A) The square antiprismatic coordination geometry is just a cubic coordination geometry in which one face has been rotated 45° relative to its opposite (and for which the distance between those faces need not be equal to the distance between adjacent atoms within a face) (B) The dodecahedral geometry may be thought of as a cube in which opposing faces are folded up and down relative to one another as shown. This work by Stephen Contakes is licensed under a Creative Commons Attribution 4.0 International License.

As with other high-coordinate structures, the energy difference between these eightfold coordination geometries is small enough that packing effects can significantly influence the observed structure. For example, octacyanomolybdates commonly adopt a square antiprismatic coordination geometry but depending on the counterions present can give dodecahedral or bicapped trigonal prismatic complexes. Examples are given in Figure 5.4.21.

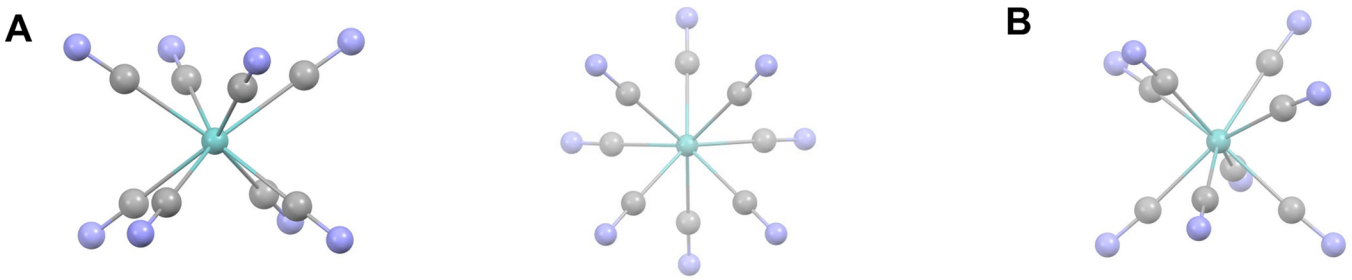


Figure 5.4.21: Structures reported for (A) square antiprismatic $[Mo(CN)_8]^{3-}$ as a solid 4,4'-Diazenediyldipyridinium salt and (B) dodecahedral $[Mo(CN)_8]^{4-}$ as a solid tetra-n-butylammonium salt.

Coordination Number 9

Again, nine-coordinate complexes typically require larger transition metals, lanthanides, and actinides. Coordination geometries

are typically either tricapped trigonal prismatic or idiosyncratically determined by the ligands. Simple examples include the aqua complexes $[Sc(H_2O)_9]^{3+}$, $[Y(H_2O)_9]^{3+}$, and $[La(H_2O)_9]^{3+}$, as well as $[TcH_9]^{2-}$ and $[ReH_9]^{2-}$.

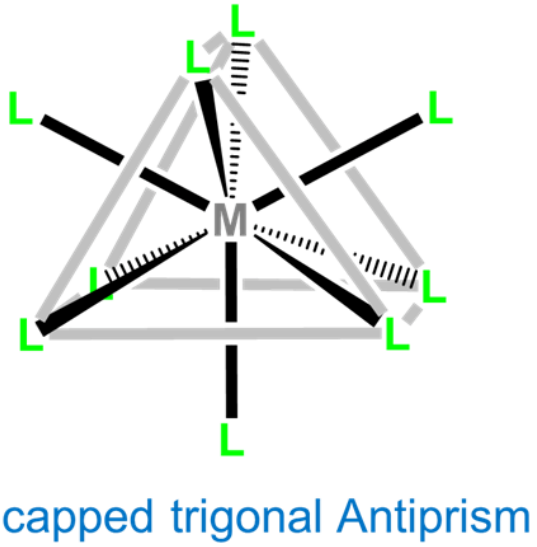


Figure 5.4.22.

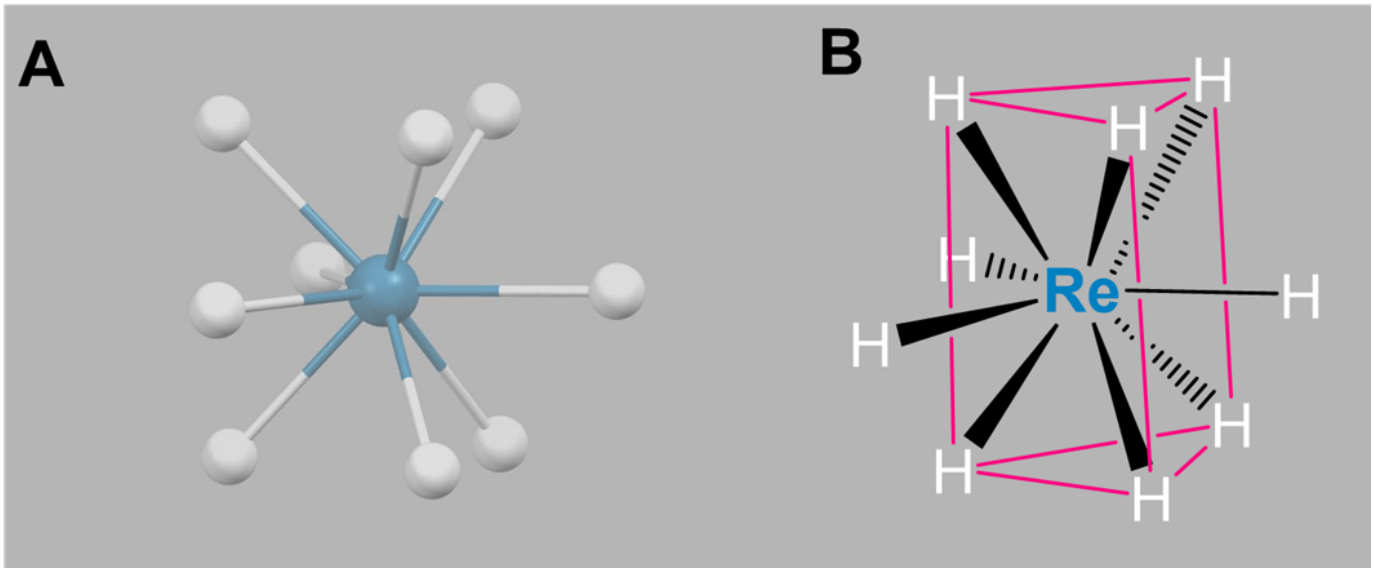


Figure 5.4.22. (A) Structure of $[ReH_9]^{2-}$ in $K_2[ReH_9]$ and (B) schematic showing how the structure maps onto a tricapped trigonal pyramidal coordination geometry. This work by Stephen Contakes is licensed under a Creative Commons Attribution 4.0 International License.

Coordination Numbers 10-16

Coordination numbers higher than nine are extremely rare for compounds that bind in κ fashion (form conventional metal-ligand bonds)[14] and usually involve some combination of large metals, sterically undemanding ligands, and special ligand structures that promote higher coordination. Noteworthy examples include

1. Twelve-coordinate $[Hf(BH_4)_4]$, which illustrates how small multidentate ligands promote higher coordination numbers. As shown in Figure 5.4.23, $[Hf(BH_4)_4]$ has a cubooctahedral structure in which BH_4^- acts as a tridentate ligand, with BH_3 units occupying triangular faces of the cubooctahedron to give a tetrahedron of BH_4^- ligands around the Hf.

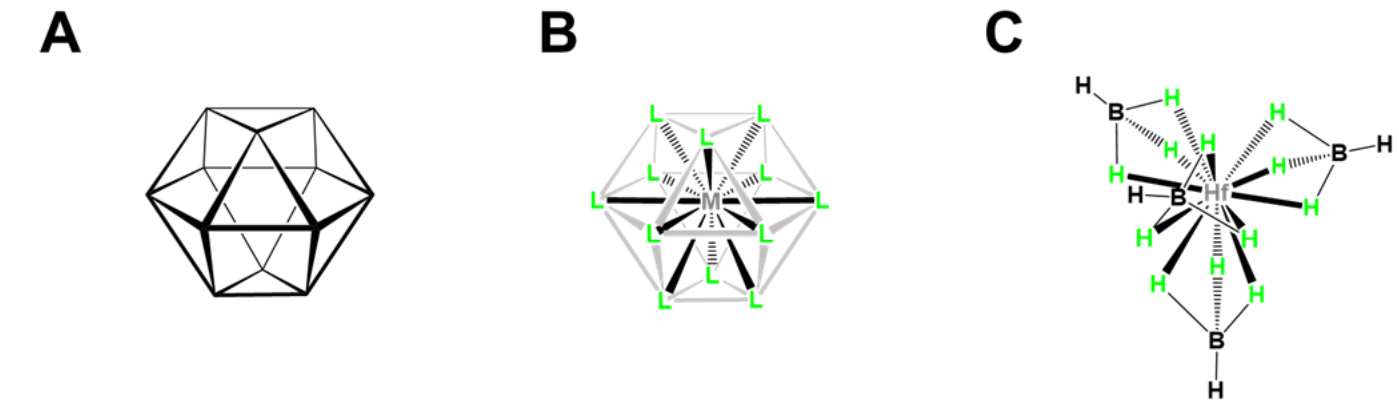


Figure 5.4.23. The anticubooctahedral coordination geometry is observed for $[Hf(BH_4)_4]$. (A) An anticubooctahedron consists of a hexagonal ring capped with antiparallel triangles above and below the ring. (B) Idealized anticubooctahedral complex. (C) Structure of $[Hf(BH_4)_4]$. This work by Stephen Contakes is licensed under a Creative Commons Attribution 4.0 International License.

2. Twelve-coordinate $[Ce(NO_3)_6]^{2-}$, in which the nitrate oxygens define an icosahedral coordination geometry as shown in Figure 5.4.24. The nitrates in the structure bind the Ce center in bidentate fashion in an octahedral array.

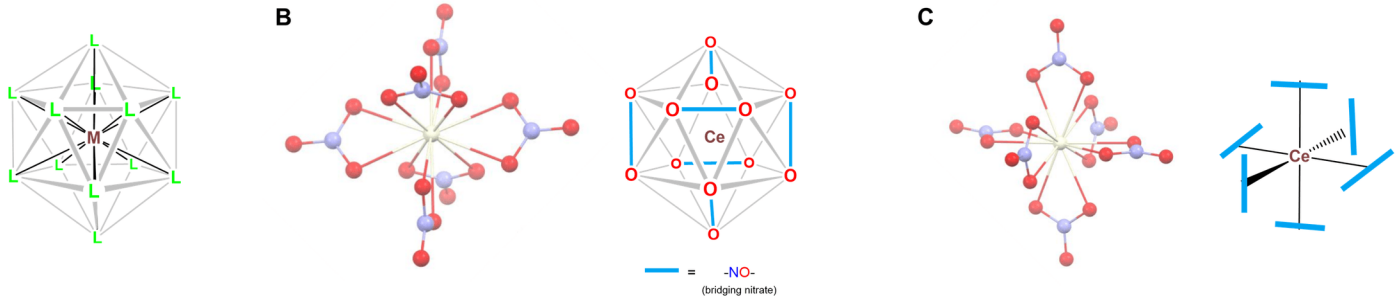


Figure 5.4.24. Coordination geometry of $[Ce(NO_3)_6]^{2-}$ in $[Mg(H_2O)_6][Ce(NO_3)_6]\cdot H_2O$. (A) Idealized icosahedral coordination. (B) View of the structure of $[Ce(NO_3)_6]^{2-}$ showing how it maps onto the icosahedral coordination geometry. (C) The structure may also be thought of as comprising an octahedral geometry in which each vertex of the octahedron is occupied by a κ^2-NO_3^-. The structure of $[Ce(NO_3)_6]^{2-}$ is rendered in Mercury from the cif data in reference 15. This work by Stephen Contakes is licensed under a Creative Commons Attribution 4.0 International License.

3. Fifteen-coordinate $[Th(H_3BNMe_2BH_3)_4]$, which also uses bridging H-B-H units that occupy little of the coordination sphere. In $[Th(H_3BNMe_2BH_3)_4]$, three of the four $H_3BNMe_2BH_3$ ligands bind in κ^4 fashion and one binds κ^3, giving the fifteen fold coordination.[16]

4. Sixteen-coordinate $[CoB_{16}]^-$, which possesses the highest coordination number yet observed. Its structure is given in Figure 5.4.25. The coordination geometry is an octahedral antiprism, and the complex should be considered to involve a Co center in the midst of a B_{16}^- "molecular drum" held together by cluster bonds.

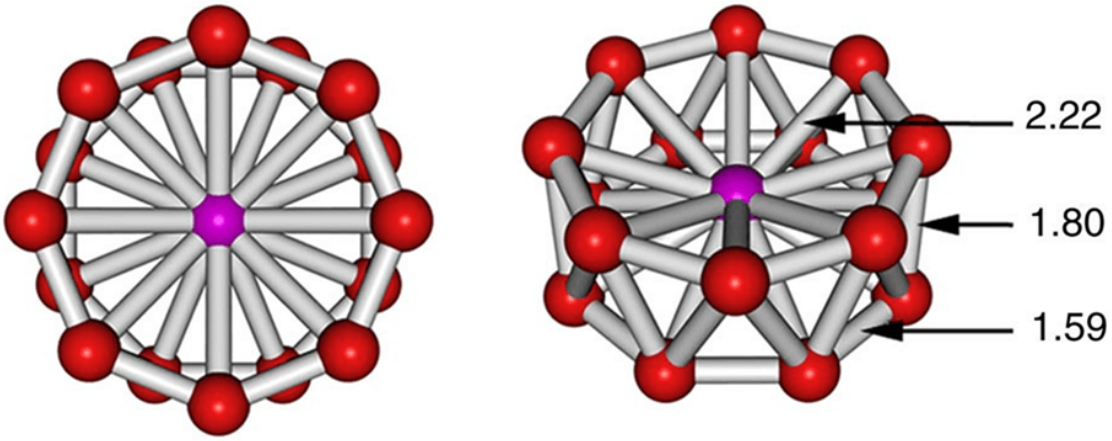


Figure 2A from Popov, I., Jian, T., Lopez, G. *et al*. Cobalt-centered boron molecular drums with the highest coordination number in the CoB_{16}^- cluster. *Nat Commun* **6,** 8654 (2015). https://doi.org/10.1038/ncomms9654, which is is licensed in that publication under a Creative Commons Attribution 4.0 International License.

References

1. Dudev, M.; Wang, J.; Dudev, T.; Lim, C., Factors Governing the Metal Coordination Number in Metal Complexes from Cambridge Structural Database Analyses. *The Journal of Physical Chemistry B* **2006**, *110(4)*, 1889-1895.
2. Kuppuraj, G.; Dudev, M.; Lim, C., Factors Governing Metal–Ligand Distances and Coordination Geometries of Metal Complexes. *The Journal of Physical Chemistry B* 2009, 113 (9), 2952-2960.
3. Cremades, E.; Echeverría, J.; Alvarez, S., The Trigonal Prism in Coordination Chemistry. *Chemistry – A European Journal* 2010, 16 (34), 10380-10396.
4. Xiong, X.-G.; Wang, Y.-L.; Xu, C.-Q.; Qiu, Y.-H.; Wang, L.-S.; Li, J., On the gold–ligand covalency in linear $[AuX_2]^-$ complexes. *Dalton Transactions* 2015, 44 (12), 5535-5546.
5. Concepción Gimeno, M. The Chemistry of Gold in Laguna, Antonio (ed.) *Modern Supramolecular Gold Chemistry: Gold-Metal Interactions and Applications*. Wiley, 2008.
6. Andersen, R. A.; Faegri, K.; Green, J. C.; Haaland, A.; Lappert, M. F.; Leung, W. P.; Rypdal, K., Synthesis of bis[bis(trimethylsilyl)amido]iron(II). Structure and bonding in M[N(SiMe3)2]2 (M = manganese, iron, cobalt): two-coordinate transition-metal amides. *Inorganic Chemistry* 1988, 27 (10), 1782-1786.
7. Persson, I., Hydrated metal ions in aqueous solution: How regular are their structures? Pure and Applied Chemistry 2010, *82(10)*, 1901.
8. Aramburu, J. A.; García-Fernández, P.; García-Lastra, J. M.; Moreno, M., Jahn–Teller and Non-Jahn–Teller Systems Involving CuF_6^{4-} Units: Role of the Internal Electric Field in Ba2ZnF6:Cu2+ and Other Insulating Systems. *The Journal of Physical Chemistry C* 2017, *121(9)*, 5215-5224.
9. Brown, M. D.; Levason, W.; Murray, D. C.; Popham, M. C.; Reid, G.; Webster, M., Primary and secondary coordination of crown ethers to scandium(iii). Synthesis, properties and structures of the reaction products of ScCl3(thf)3, ScCl3·6H2O and Sc(NO3)3·5H2O with crown ethers. Dalton Transactions 2003, (5), 857-865.
10. Liu, Y.; Ng, S.-M.; Lam, W. W. Y.; Yiu, S.-M.; Lau, T.-C., A Highly Reactive Seven-Coordinate Osmium(V) Oxo Complex: [OsV(O)(qpy)(pic)Cl]2+. Angewandte Chemie International Edition 2016, 55 (1), 288-291.
11. Popov, I., Jian, T., Lopez, G. *et al*. Cobalt-centred boron molecular drums with the highest coordination number in the CoB_{16}^- cluster. *Nat Commun* **6,** 8654 (2015). https://doi.org/10.1038/ncomms9654
12. The structures are rendered from cif data reported in the following publications: (A) square antiprismatic $[Mo(CN)_8]^{3-}$: Wen-Yan Liu, Hu Zhou, Ai-Hua Yuan, *Acta Crystallographica Section E: Structure Reports Online*, 2008, 64, m1151, (B) dodecahedral $[Mo(CN)_8]^{4-}$: B.J.Corden, J.A.Cunningham, R.Eisenberg, *Inorganic Chemistry*, 1970, 9, 356.
13. The structure of ReH_9^{2-} is rendered from the structure reported in Abrahams, S.C.; Ginsberg, A.P.; Knox, K. Transition metal-hydrogen compounds. II. The crystal and molecular structure of potassium rhenium hydride, K_2ReH_9 *Inorganic Chemistry*, **1964**, *3*, 558-567.
14. There are other complexes in which a metal may be said to interact with more than sixteen "ligand atoms", but these are not usually considered to possess a higher coordination number. For example, in some π complexes like η^5-Cp_4U, technically

there are 20 C atoms fastened to the U, but these complexes are better considered as 12-coordinate than twenty (since each cyclopentadienyl ring is isolobal with a *fac*-coordinated set of 3 L ligands), while the metal centers in endohedral fullerene species like La@C_{60} do not interact with all sixty carbon atoms at once, and so are better thought of as a metal trapped in a spacious sixty-carbon cage.

15. Zalkin, A.; Forrester, J.D.; Templeton, D.H. Crystal structure of cerium magnesium nitrate hydrate *Journal of Chemical Physics*, **1963**, *39*, 2881-2891.
16. Daly, S. R.; Piccoli, P. M. B.; Schultz, A. J.; Todorova, T. K.; Gagliardi, L.; Girolami, G. S., Synthesis and Properties of a Fifteen-Coordinate Complex: The Thorium Aminodiboranate [Th(H3BNMe2BH3)4]. Angewandte Chemie International Edition 2010, 49 (19), 3379-3381.
17. Popov, I., Jian, T., Lopez, G., Boldyrev, A. I.; Wang, L-S. Cobalt-centred boron molecular drums with the highest coordination number in the CoB_{16}^- cluster. *Nat Commun* **6,** 8654 (2015).

This page titled 5.4: Coordination Numbers and Structures is shared under a license and was authored, remixed, and/or curated by LibreTexts.

- 9.5: Coordination Numbers and Structures by Stephen M. Contakes is licensed CC BY 4.0.

5.5: Coordination Frameworks

Bridging ligands link metals in multicenter coordination complexes

Some ambidentate and multidentate ligands have the capacity to bridge two metal centers. For instance, the cyano ligands can bridge two metal centers by forming linear links of the type

$$\mathrm{M{-}CN{-}M'}$$

Linkages like these can be used to bridge multiple metal centers in a cluster or network solid, the latter of which is sometimes called a coordination framework. When the cyano ligand is combined with octahedral metal centers possessing 90° L-M-L bond angles, a cubic coordination network results. An example is the Prussian Blue coordination framework, which possesses the unit cell depicted in Figure 5.5.1A.

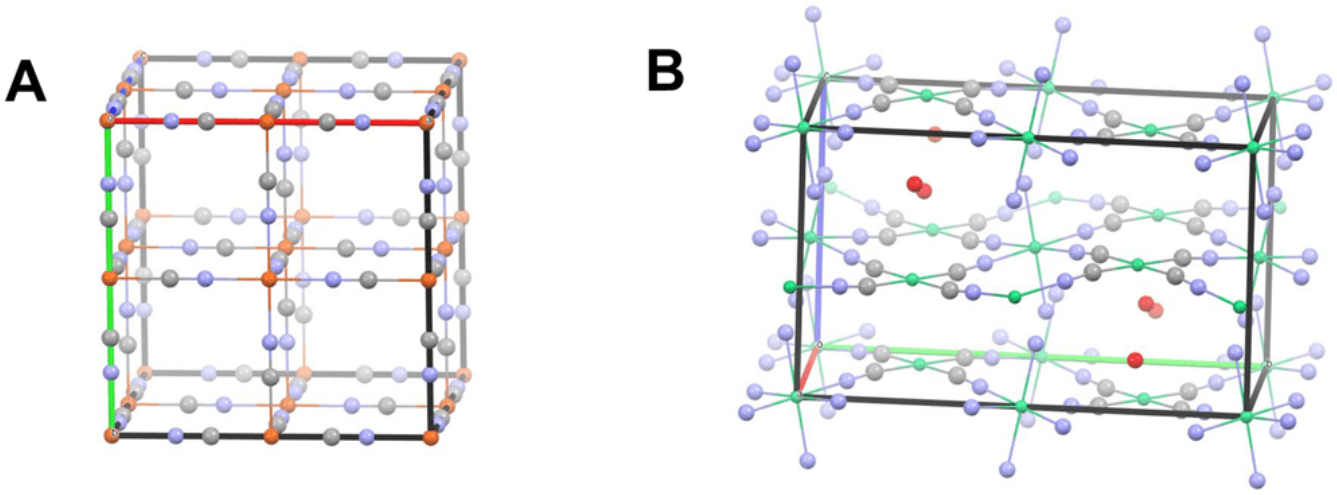


Figure 5.5.1. (A) Idealized unit cell of Prussian Blue showing the cubic coordination framework of interconnected $[Fe^{II}(CN)_6]^{4-}$ and Fe^{3+} units. Because the ratio of Fe^{3+} to $[Fe^{II}(CN)_6]^{4-}$ is 4:3, some of the $[Fe^{II}(CN)_6]^{4-}$ sites are occupied by aqua ligands. (B) Structure of a Hofmann-type clathrate consisting of layers of square planar $[Ni(CN)_4]^{2-}$ units linked by $Ni(NH_3)_2^{2+}$ units. In this structure water occupies the sites between the layers, but structures like these can adjust to accommodate a variety of organic molecules. Hydrogen atoms are omitted for clarity. Rendered from the structures reported in references 1. This work by Stephen Contakes is licensed under a Creative Commons Attribution 4.0 International License.

The cubic network shown in Figure 5.5.1A reflects the 3D structure of the octahedron, in which the M-L bonds point along the x, y, and z axes. If a square planar metal center is used, a 2D coordination network comprising interlinked squares is produced instead. An example is the Hofmann clathrate shown in Figure 5.5.1B, which depicts a Hofmann clathrate in which square planar $[Ni(CN)_4]^{2-}$ units are linked by *trans*-$Ni(NH_3)_2^{2+}$ units (which are octahedral but have a square plane of open coordination sites perpendicular to the NH_3-Ni-NH_3 axis).

The structures of coordination polyhedra and frameworks reflect ligand and metal coordination geometries

As illustrated by the Prussian Blue and Hofmann clathrate coordination networks shown in Figure 5.5.1, the structures formed when a bridging ligand links multiple metal centers depends on the geometry of the centers, the ligand, and the metal-ligand bonds formed. Because the directionality of metal-ligand bonding in many types of complexes is well-characterized and predictable, it is possible to design metal complexes and linkers that can serve as building blocks for clusters and networks. In particular

- metal complexes with combinations of labile (substitutable) ligands in particular topologies. These insure that the linking

ligand will be arranged around the metal center in those defined directions.
- Ligands that possess binding sites oriented in defined directions so that they link the metal centers together in particular topologies.

Examples of the sort of metal centers that can be used and examples of linking ligands are given in Figure 5.5.2.

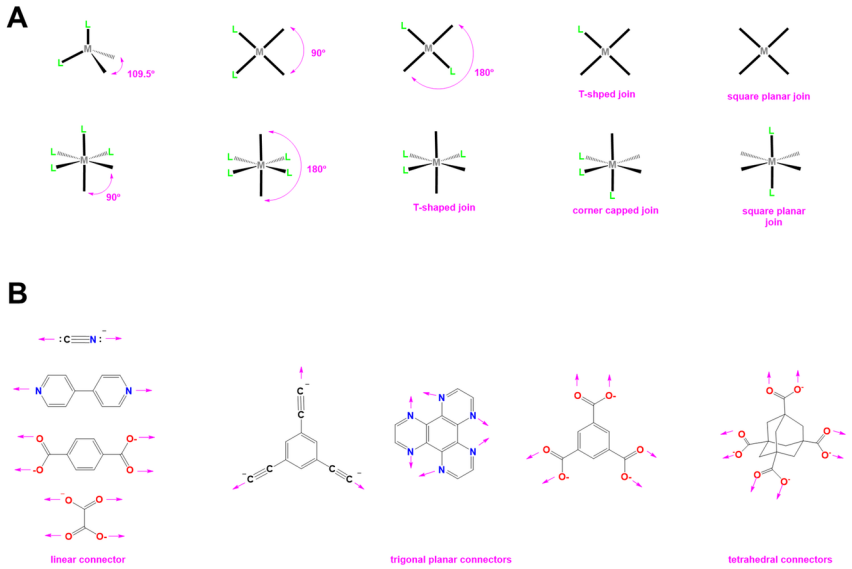


Figure 5.5.2. The directionality of M-L bonding permits the rational construction of structures using metal and ligand "building blocks". For example, (A) Tetrahedral, octahedral, and square planar metal centers alone can be used to connect sets of ligands at 90°, 109.5°, and 180° bond angles in a variety of arrangements while (B) the selection of organic linkers shown can be used as linear, trigonal planar, and tetrahedral linkers.

Examples of how the building blocks shown in Figure 5.5.2 might be used to prepare molecular polyhedra and coordination networks are depicted schematically as shown in Figure 5.5.3. Among the examples shown in Figure 5.5.3, those depicted on the right schematize the Hofmann clathrate (top) and Prussian Blue (bottom) coordination networks of Figure 5.5.1.

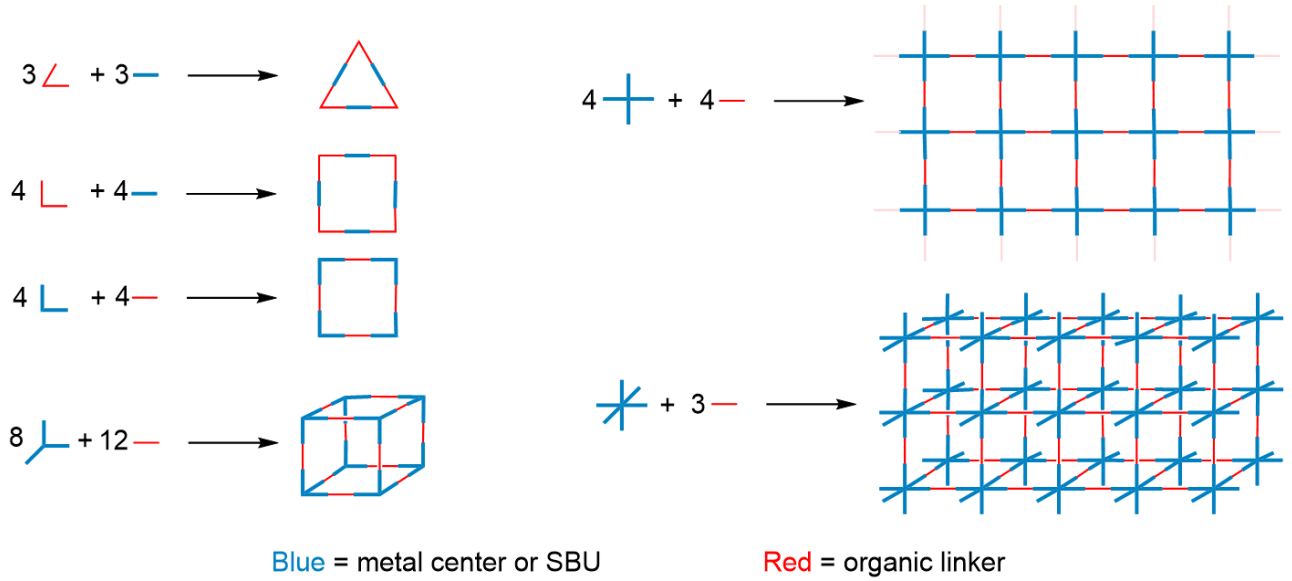


Figure 5.5.3. Examples illustrating how the combination of metal and organic linker units gives rise to polyhedral and network structures that reflect the geometry of the building blocks used.

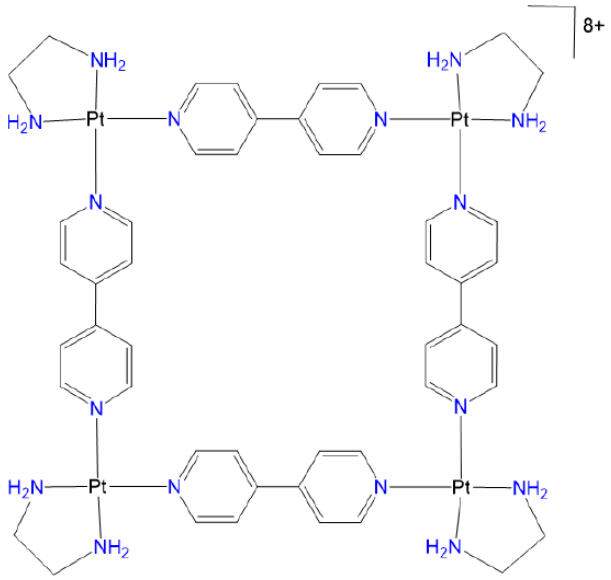


Figure 5.5.4. In its structure, the $Pt(en)^{2+}$ centers possess *cis*-90° coordination sites linked by the linear linker 4,4'-bipyridine.

A wider variety of structures are possible than those hinted at by the building blocks and structures shown in Figures 5.5.2 and 5.5.3. More may be obtained using the principles of molecular structure outlined in the sections on coordination geometry, ligands, and isomerism. In fact, one of the first coordination polyhedra prepared involved Jean-Marie Lehn's recognition that planar bidentate ligands in a tetrahedral bis-chelate are oriented perpendicular to one another, as shown in Figures 5.5.5A. This enabled him to prepare a molecular trigonal prism by combining a source of Cu^{2+} with the trigonal planar and linear-capable organic linkers that bind the Cu^{2+} in bidentate fashion, as shown in Figure 5.5.5B.

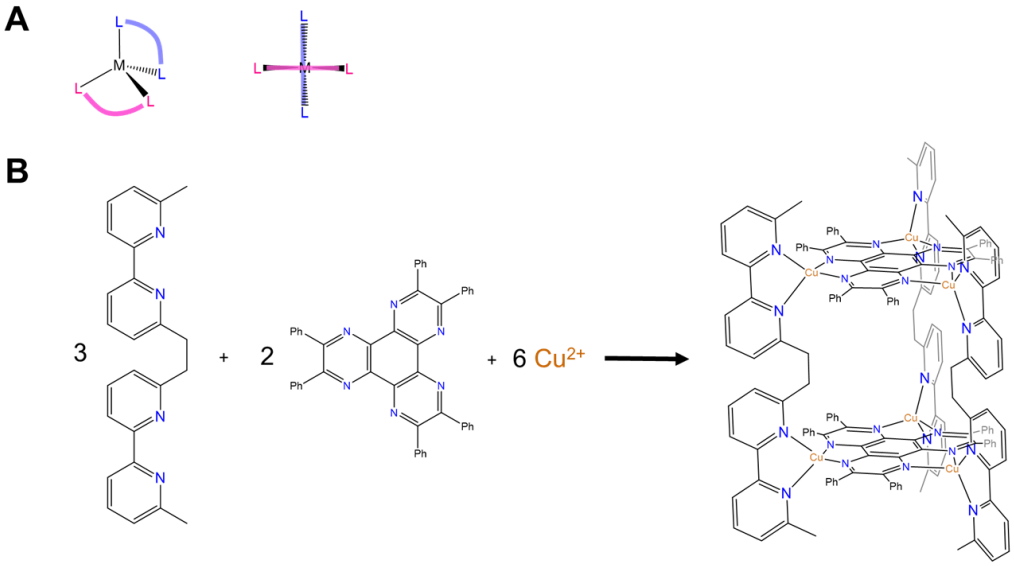


Figure 5.5.5. (A) When a tetrahedral metal center is coordinated by two planar bidentate ligands, the ligands are oriented at 90° to one another. (B) This permitted Jean Marie-Lehn and his cowokers to prepare a molecular trigonal prism consisting of six Cu^{2+} ions linked by the rigid and semirigid nitrogen-containing ligands on the prism's trigonal faces and rectangular edges as shown. Redrawn from structures given in reference 3.

Metal Organic Frameworks (MOFs) are porous coordination polymers in which metal "building units" are connected by rigid organic ligand "struts"

One class of coordination frameworks that has received much attention over the past 25 years is the metal organic frameworks (MOFs). These consist of metal centers linked by rigid organic ligands to give a porous structure similar to those of the aluminosilicate-based zeolites. The structure of one MOF, called MIL-53, is given in Figure 5.5.6A.

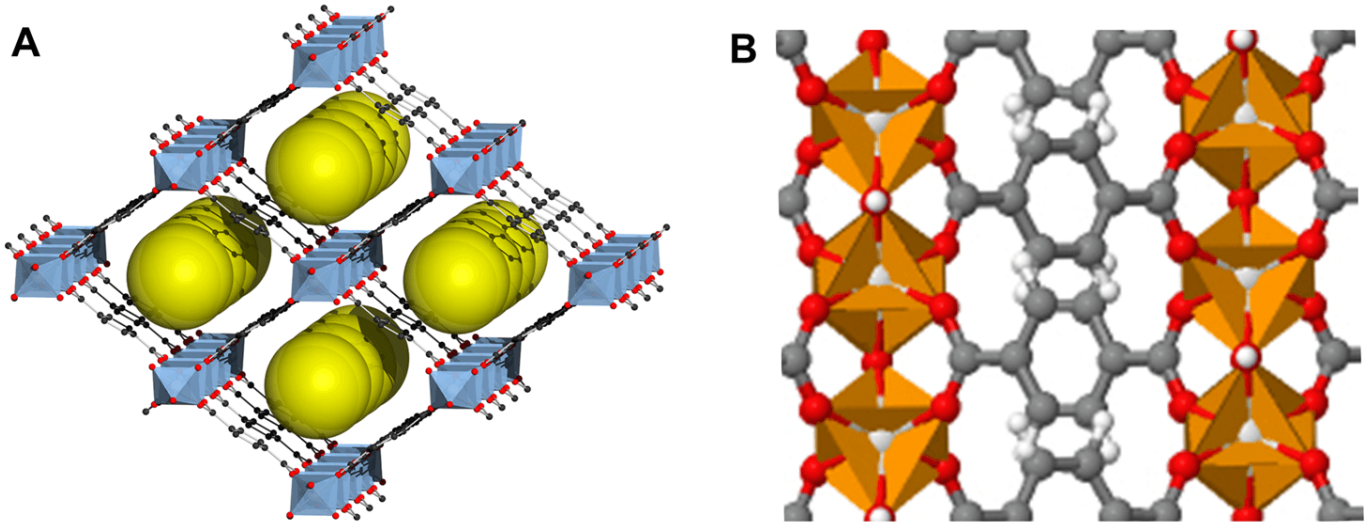


Figure 5.5.6. In metal organic frameworks containing carboxylate ligands, the two oxygens in each carboxylate usually bind to different metal centers. A simple example involves the structure of MIL-53, in which linear *p*-terephthalato (1,4'-benzenedicarboxylato or BDC) ligands bridge chains of linked MO_6 octahedra. (A) Structure of MIL-53 showing the open structure of the MOF, indicated by the yellow spheres. (B) Top-down image of an MIL-53 structure showing how the carboxylic acid oxygens in the BDC ligands coordinate two different metals. The image in part A is by Tony Boehle - Tony Boehle, Public Domain, https://commons.wikimedia.org/w/inde...curid=10328580 The image in part B is rendered from the jmol structure of MIL-53(Sc) at https://www.chemtube3d.com/mof-mil53sc-2/

As can be seen from the overall structure of MIL-53 depicted in Figure 5.5.6A, the structure possesses large rhombic prismatic voids, represented by the yellow spheres. These voids can in principle be occupied by small molecule substrates. Because of MOF's potential to bind and store substrates, there is considerable interest in developing MOFs that are useful for storing and separating particular gases.

A closer look at the structure of MIL-53 reveals that the carboxylate oxygens in the benzenedicarboxylato (BDU) linkers span two different metal centers rather than binding to only one. As explained in Figure 5.5.7, this binding mode enables the formation of rigid stable networks, although it requires the use of metal building blocks in which two or more metal centers are held in close proximity.

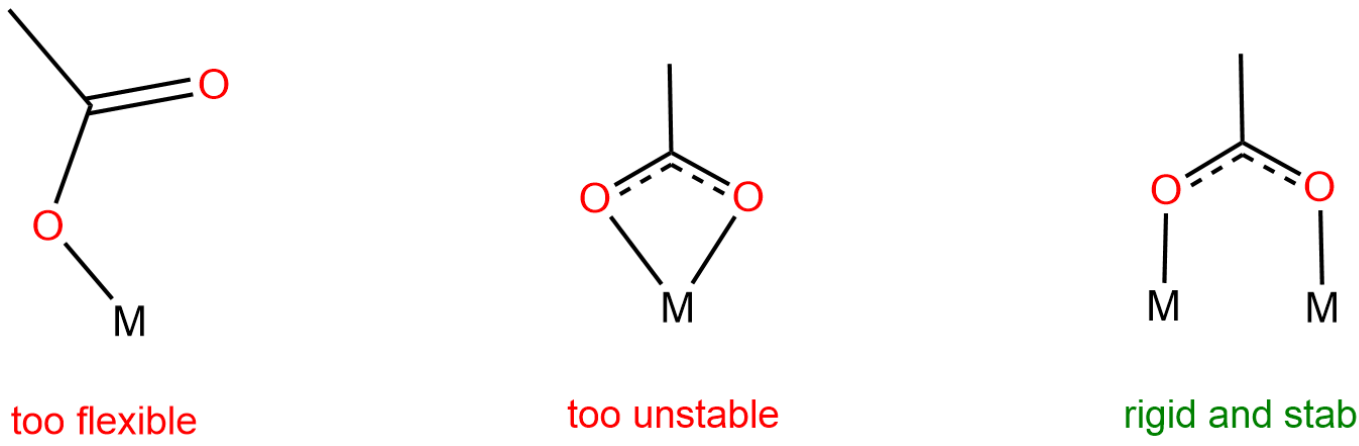


Figure 5.5.7. The carboxylate groups in the ligands of metal organic frameworks commonly bind κ^1 to two different metal centers rather than κ^1 or κ^2 to a single center because the single metal κ^1 binding mode is too flexible to give rigid networks while the small chelate rings and narrow bite angles of the κ^2 chelate rings make them less stable.

In MIL-53, the metal centers that the DBU ligands coordinate are chains of octahedral metal centers bridged by μ_2 hydroxo ligands. These chains form spontaneously as the network forms under the high temperature conditions of its synthesis. In other cases, metal secondary building units (SBUs) containing the necessary bridging dicarboxylate ligands are used. One common class of metal SBUs used is the paddlewheel carboxylates shown in Figure 5.5.8A. These consist of two metals spanned by a square plane of four carboxylates in a paddlewheel arrangment.

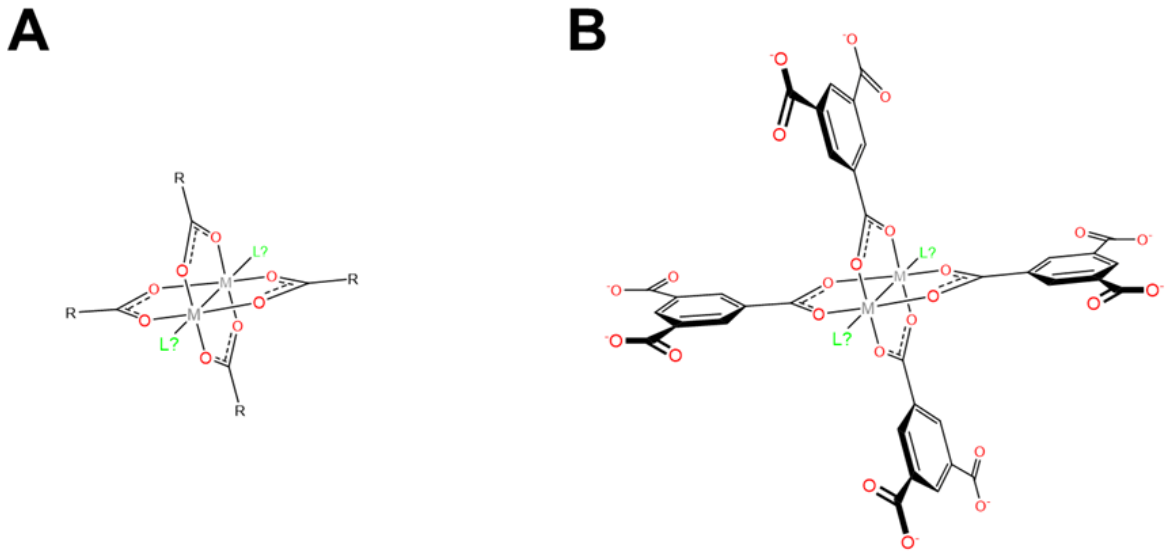


Figure 5.5.8. Metal organic frameworks do not use a metal center directly but instead employ a metal cluster as a secondary building unit (SBU). (A) Paddlewheel carboxylates are a common SBU. They consist of two metals surrounded by four carboxylato ligands in a square planar "paddlewheel" arrangement. (B) In complexes where the ligands contain additional carboxylates, they function as a planar center in a MOF. An example is the paddlewheel carboxylate present in the HKUST class of MOFs, in which each carboxylato ligand is capable of bridging to three dimetal units. Note that in the structures shown, the axial ligands shown in green may be present or absent depending on the specific metal carboxylate used and/or whether the ligand was removed during processing of the MOF.

The use of paddlewheel carboxylate metal SBUs and bridging organic carboxylate ligands enables the construction of coordination frameworks like that of HKUST-1 shown in Figure 5.5.9. The structure of these networks depends on the geometry of the linking ligand. For instance, in HKUST-1 the 1,3,5-benzenetricarboxylato bridging ligands each link three paddlewheel SBUs to give the cubic network shown in Figure 5.5.9. Other organic carboxylate ligands give different network topologies. In addition, the ability of some paddlewheel carboxylates to coordinate ligands perpendicular to the carboxylates, represented by the ligands marked L? in Figure 5.5.8, affords additional opportunities to use these networks to bind substrates that can coordinate those sites.

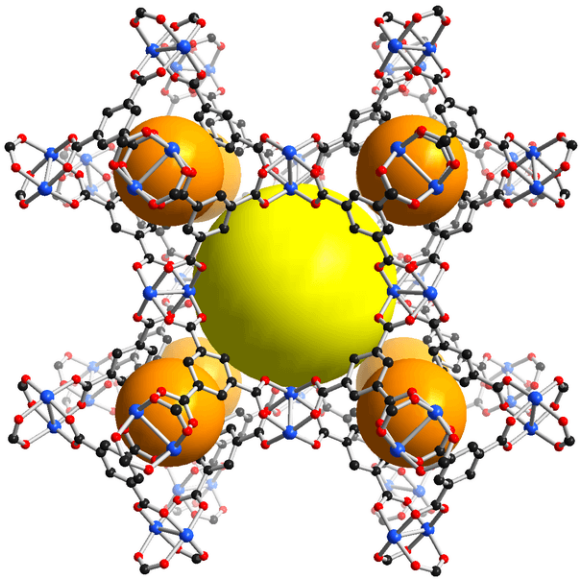


Figure 5.5.9. Desolvated HKUST-1 member of the HKUST class of MOFs showing open regions in the structure. The structure consists of paddlewheel carboxylates linked by trigonal planar tricarboxylate organic SBUs. The image is by Tony Boehle - Own work, CC BY-SA 3.0, https://commons.wikimedia.org/w/inde...curid=27424501

Another common metal SBU is the basic zinc acetate structure shown in Figure 5.5.10. As shown in Figure 5.5.10A, the structure is analogous to those of the basic beryllium acetates and involves an OZn_4 tetrahedron in which the tetrahedrally arranged Zn^{2+} are connected by carboxylate ligands spanning the tetrahedron's six edges. When these carboxylate ligands are replaced by rigid dicarboxylates (Figure 5.5.10B), the result is that the Zn_4O core is surrounded by an octahedral coordination sphere of carboxylate ligands (Figure 5.5.10C).

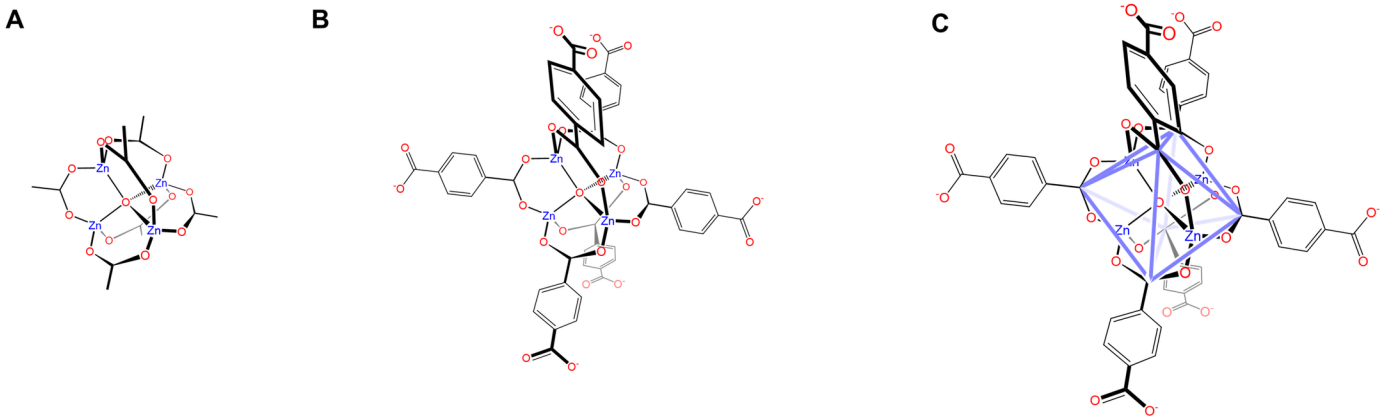


Figure 5.5.10. (A) Basic zinc acetate is a common SBU used as a pseudooctahedral center in MOFs. (B) Exchange of its acetate ligands with *p*-terephthalate (1,4-benzenedicarboxylate) linkers gives a complex in which the free dicarboxylates are oriented towards the vertices of an octahedron (C).

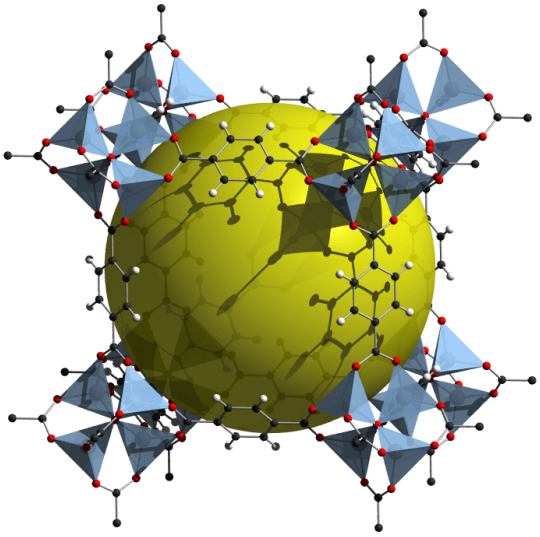


Figure 5.5.11. A cubic metal organic framework derived from the basic zinc acetate SBU. The structure is called MOF-5 and consists of Zn_4O^{6+} pseudooctahedra linked by linear *p*-terephthalate (1,4-benzenedicarboxylate) ligands. The large golden sphere inside the unit cell has a radius of 12 Angstroms (defined with the aromatic rings oriented as shown) and represents the space available for the framework to accommodate guest molecules. By Tony Boehle - Own work, Public Domain, https://commons.wikimedia.org/w/inde...curid=10319204.

The structure of MOF-5 also illustrates how the size of the pores in an MOF structure may be tailored by lengthening or shortening the organic linker. In particular, from Figure 5.5.11 it can be seen that the size of the MOF-5's cubic unit cell depends on the length of the organic portion of the carboxylate linker. In MOF-5 this linker consists of a single benzene unit and gives 9-Angstrom pores, while the use of two and three benzene rings increases the pore size to 13 and 16 Angstroms, respectively, as shown in 5.5.12.

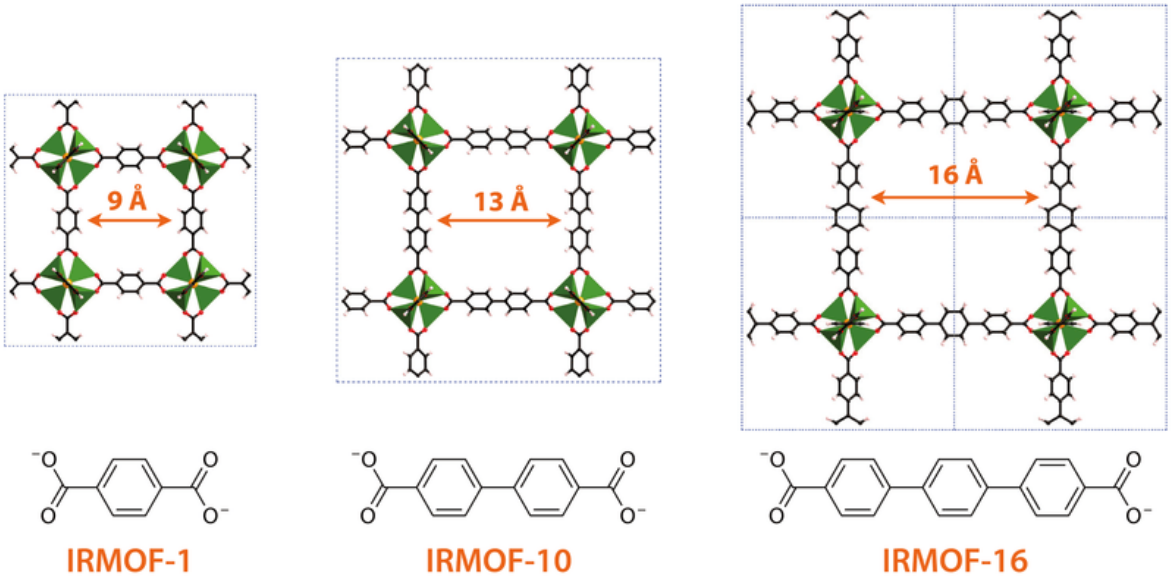


Figure 5.5.12. The spacing between metal centers in a coordination network may be tailored by the use of organic linkers of differing lengths. By François-Xavier Coudert - Own work, CC BY 4.0, https://commons.wikimedia.org/w/inde...curid=89656071

References

1. The structure of Prussian blue is rendered from that reported in Buser, H. J.; Schwarzenbach, D.; Petter, W.; Ludi, A., The crystal structure of Prussian Blue: $Fe_4[Fe(CN)_6]_3.xH_2O$. *Inorganic Chemistry* 1977, *16(11)*, 2704-2710; to simplify depiction of the coordination framework, water molecules were removed. The structure of the Hofmann-type clathrate is rendered from that reported in Rayner, J. H.; Powell, H. M., 688. Crystal structure of a hydrated nickel cyanide ammoniate. *Journal of the Chemical*

Society (Resumed) 1958, 3412-3418.

2. (a) Fujita, M.; Ogura, K., Transition-metal-directed assembly of well-defined organic architectures possessing large voids: From macrocycles to [2] catenanes. *Coordination Chemistry Reviews* 1996, *148*, 249-264. (b) Leininger, S.; Olenyuk, B.; Stang, P. J., Self-Assembly of Discrete Cyclic Nanostructures Mediated by Transition Metals. *Chemical Reviews* 2000, *100(3)*, 853-908.

3. Machado, V. G.; Baxter, P. N. W.; Lehn, J.-M., Self-assembly in self-organized inorganic systems: a view of programmed metallosupramolecular architectures. Journal of the Brazilian Chemical Society 2001, 12, 431-462.

4. Yaghi, O. M.; O'Keeffe, M.; Ockwig, N. W.; Chae, H. K.; Eddaoudi, M.; Kim, J., Reticular synthesis and the design of new materials. Nature 2003, 423 (6941), 705-714.

This page titled 5.5: Coordination Frameworks is shared under a license and was authored, remixed, and/or curated by LibreTexts.

- 9.6: Coordination Frameworks by Stephen M. Contakes is licensed CC BY 4.0.

5.6: HARD AND SOFT ACIDS AND BASES

Origin of the Hard-Soft Acid-Base Principle

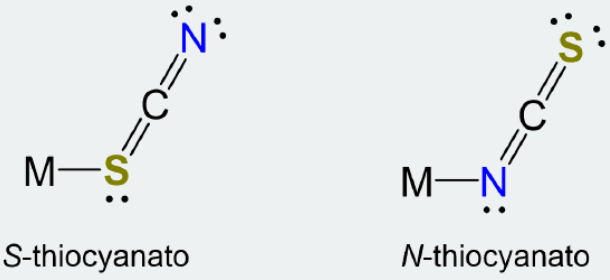
One of the strengths of the Lewis acid-base concept is the readiness with which it illuminates the role that covalent and electrostatic interactions in acid base behavior, specifically through its ability to explain chemical interactions in terms of frontier orbitals and the interactions between charged groups as electrons are donated from a base to an acid. However, simply acknowledging the presence of such interactions does little to illuminate the degree to which each mode of explanation best explains the bonding in a given system? To what extent is a given adduct better described as held together by covalent bonds as opposed to ionic ones - *e.g.* better described as a molecule rather than an ion pair? Moreover, does it even matter, given that the orbitals of quantum mechanics result from the combination of electrons' wavelike behavior with their electrostatic attraction to nuclei in either case?[1] These questions and more are addressed by one of the most important conceptual tools in contemporary inorganic chemistry, the Hard-Soft acid-base principle.

The **Hard-Soft acid-base principle (HSAB principle)** stems from the recognition that some Lewis acids and bases seem to have a natural affinity for one another.* Consider the following:

- Some metals are commonly found in nature as salts of chloride or as oxide ores while others are found in combination with sulfur. Geochemists even use the Goldschmidtt classification scheme to classify the halide and oxide formers as lithophiles and the sulfide formers as chalcophiles.
- In living systems small highly charged metals ions like Fe^{3+} are usually found bound to N and O atoms while larger metals with lower charges such as Zn^{2+} are often found attached to at least one S atom. Similarly, metals prefer to bind to one coordination site over the other when forming complexes with ambidentate ligands. The most well-known instances involve complexes of cyanate and thiocyanate, which can coordinate metals through either the N or chalcogen atom. For instance, Cu^{2+} and Zn^{2+} form *N*-thiocyanato complexes in species like $[Cu(NCS)_2(py)_2]$ and $[Zn(NCS)_4]^{2-}$ while their larger cogeners Au^{3+} and Hg^{2+} preferentially forms *S*-thiocyanato complexes, giving species like $[Hg(SCN)_4]^{2-}$.

Ambidentate ligands

Ambidentate ligands possess multiple coordination sites through which a metal may bind. For instance, thiocyanate may coordinate metals (M) at either the S or N to give *S*-thiocyanato or *N*-thiocyanato complexes.



S-thiocyanato *N*-thiocyanato

- The solubility trends for the alklai metal halides and silver halides are opposite, even though both involve salts of formula M^+X^- (salts can be thought of as involving Lewis acid-base adduct formation between the anions and cations). Specifically, although the silver halides are all relatively insoluble in water, the very modest solubility they possess follows the order:

$$X = F >> Cl > Br > I \text{ (for the solubility of AgX)}$$

In contrast, the much more ample solubility of the alkali metal halides** follows the opposite order. For example, the order for the lithium halides is

$$X = F << Cl < Br << I \text{ (for the solubility of LiX)}$$

Notes

1. Albeit suitably fudged through such niceties as the Aufbau principle and other approximations.

* Despite the fruitfulness of this observation, in general it is important to reduce the potential for observer bias by checking observations like these against compounds reported in the chemical literature and databases like the Inorganic Crystal Structure and Cambridge Crystallographic Databases.

** These are very soluble in water, to the point where some solutions are perhaps better described as solutions of water in the halide.

† This can be predicted based on the relative hardness of BF_3, BR_3, and BH_3 in the list of hard and soft acids. However, for those of you who may be confused as to why H is considered a better electron donor for the purposes of softening a Lewis acid center while alkyl groups are better electron donors for the purposes of stabilizing carbocations in organic chemistry, the dominant effect is the lower electronegativity of H relative to carbon (in CH_3). The effect of electron donation due to hyperconjugation isn't as great for thermodynamically stable bases like BX_3/BR_3.

5.6.1: Quantitative Measures of Hardness, Softness, and Acid-Base Interactions from a Hard Soft Acid-Base Principle perspective involve orbital energies and or apportioning acid-base bonding in terms of electrostatic and covalent factors

5.6.2: Hard-Hard and Soft-Soft preferences may be explained and quantified in terms of electrostatic and covalent and electronic stabilization on the stability of Lewis acid-base adducts

This page titled 5.6: Hard and Soft Acids and Bases is shared under a license and was authored, remixed, and/or curated by LibreTexts.

- 6.6: Hard and Soft Acids and Bases by Stephen M. Contakes is licensed CC BY 4.0.

5.6.1: Quantitative Measures of Hardness, Softness, and Acid-Base Interactions from a Hard Soft Acid-Base Principle perspective involve orbital energies and or apportioning acid-base bonding in terms of electrostatic and covalent factors

Pearson Absolute Hardness is a useful metric of hardness based on orbital energies

The recognition that hard acids and bases possess a large HOMO-LUMO gap suggests that the gap size itself might serve as a useful index of hardness. The basis for this idea may be found by considering Pearson's definition of absolute hardness, η.[1] **Pearson's absolute hardness, η**, is half the second derivative of a species' energy with respect to changes in total number of electrons, N_{e^-}.

$$\text{Pearson's absolute hardness} = \eta = \frac{1}{2}\frac{d^2E}{dN_{e^-}^2}$$

$$(in \;\; eV)$$

and, since acids' and bases' hardness and softness are inversely related, Pearson's absolute softness, σ, is just the inverse of hardness.

$$\text{Pearson's softness} = \frac{1}{\eta}$$

Of these, Pearson's absolute hardness is related to the **Mulliken definition of electronegativity** as the first derivative of a species' energy with respect to changes in total number of electrons.

$$\text{Mulliken electronegativity} = \chi = \frac{dE}{dN_{e^-}}$$

$$(in \;\; eV)$$

Operationally, both the Pearson hardness and Mulliken electronegativity are approximated in terms of the energies associated with unit changes in the number of electrons – *i.e.,* in terms of ionization energies and electronegativities. Specifically,

$$\text{Pearson's absolute hardness} = \eta \approx \frac{IE–EA}{2}$$

$$\text{Mulliken electronegativity} = \chi \approx \frac{IE + EA}{2}$$

where IE and EA are in eV.

The connection between Pearson's absolute hardness/softness and the HOMO-LUMO gap then follows from Koopman's theorem, in which the ionization energy (IE) is just the opposite of the HOMO energy.

$$IE = -E_{HOMO}$$

Similarly, the electron affinity (EA), defined as the opposite of the energy released on absorption of an electron, may be taken as an approximation of the LUMO energy.

$$E_{LUMO} \approx -EA$$

So Pearson's absolute hardness is just half the HOMO-LUMO gap (band gap) size in electron volts:

$$\text{Pearson's absolute hardness} = \eta \approx \frac{E_{LUMO} - E_{HOMO}}{2}$$

where all values are given in eV,

and the Mulliken electronegativity is just the average of the HOMO and LUMO energies (~Fermi energy):

$$Mulliken\ electronegativity, \chi \approx -\frac{E_{LUMO} + E_{HOMO}}{2}$$

$$where\ all\ values\ are\ given\ in\ eV$$

The relationships between the Pearson absolute hardness, Mulliken electronegativity, and HOMO and LUMO energies are depicted schematically for the group 1A monocations in Figure 5.6.1.1.

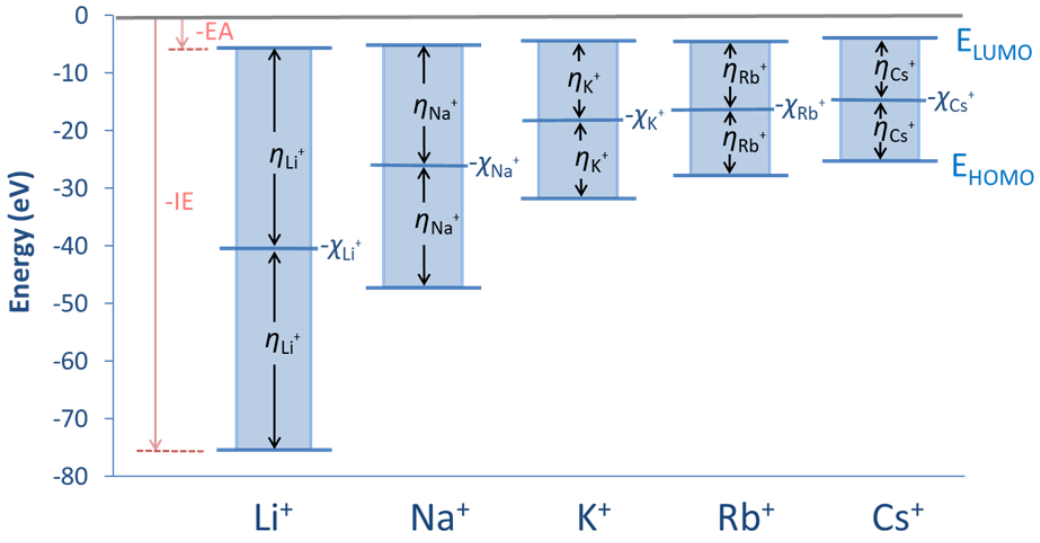


Figure 5.6.1.1. Relationships between Pearson absolute hardness, Mulliken electronegativity, and HOMO and LUMO energies for the group 1A monocations.

Values of the Pearson hardness and Mulliken electronegativity for several acids and bases are given in Table 5.6.1.1. The values in the table confirm the expected trends, showing an increase in hardness with size (down a group), with increasing charge, and as substituent electronegativity increases for a series of isolobal ions.

Table 5.6.1.1: Pearson Absolute Hardness and Related Parameters for Selected Acids and Bases.[2] *Taken from Pearson, R. G., Absolute electronegativity and hardness: application to inorganic chemistry. Inorganic Chemistry 1988, 27 (4), 734-740.*

Species	Ionization Energy, IE or I (eV)	Electron Affinity, EA or A (eV)	Mulliken Electronegativity, χ (eV)	Pearson Absolute Hardness, η (eV)
Selected Acids				
Group 1A monocations				
Li^+	75.64	5.39	40.52	35.12
Na^+	47.29	5.14	26.21	21.08
K^+	31.63	4.34	17.99	13.64
Rb^+	27.28	4.18	15.77	11.55
Cs^+	25.1	3.89	14.5	10.6

Species	Ionization Energy, IE or I (eV)	Electron Affinity, EA or A (eV)	Mulliken Electronegativity, χ (eV)	Pearson Absolute Hardness, η (eV)
Group 11 monocations				
Cu^+	20.29	7.73	14.01	6.28
Ag^+	21.49	7.58	14.53	6.96
Au^+	20.5	9.23	14.9	5.6
Isoelectronic Row 3 Metal Cations				
Na^+	47.29	5.14	26.21	21.08
Mg^{2+}	80.14	15.04	47.59	32.55
Al^{3+}	119.99	28.45	74.22	45.77
Changes with Transition Metal Ion Charge				
Fe^{2+}	30.65	16.18	23.42	7.24
Fe^{3+}	54.8	30.65	42.73	12.08
Co^{2+}	33.50	17.06	25.28	8.22
Co^{3+}	51.3	22.5	42.4	8.9
Boron trihalides				
BF_3	15.81	-3.5	6.2	9.7
BCl_3	11.60	0.33	5.97	5.64
BBr_3	10.51	0.82	5.67	4.85
CO_2	13.8	-3.8	5.0	8.8
CS_2	10.08	0.62	5.35	5.56
Selected Bases				
Group 17 monoanions (taken to be identical to the free atom values; for arguments as to why this is reasonable see Pearson, R. G., Inorg. Chem. 1988, 27 (4), 734-740.)				
F^-	17.42	3.40	10.41	7.01
Cl^-	13.01	3.62	8.31	4.70
Br^-	11.84	3.36	7.60	4.24
I^-	10.45	3.06	6.76	3.70
Group 15 hydrides				
NH_3	10.7	-5.6	2.6	8.2
PH_3	10.0	-1.9	4.1	6.0
Trimethylpnictides				
NMe_3	7.8	-4.8	1.5	6.3
PMe_3	8.6	-3.1	2.8	5.9
$AsMe_3$	8.7	-2.7	3.0	5.7
Group 16 hydrides				

Species	Ionization Energy, IE or I (eV)	Electron Affinity, EA or A (eV)	Mulliken Electronegativity, χ (eV)	Pearson Absolute Hardness, η (eV)
H_2O	12.6	-6.4	3.1	9.5
H_2S	10.5	-2.1	4.2	6.2
Phosphorous trihalides				
PF_3	12.3	-1.0	5.7	6.7
PCl_3	10.2	0.8	5.5	4.7
PBr_3	9.9	1.6	5.6	4.2

Drago-Wayland Acid-Base Parameters allow for estimation of the electrostatic and covalent contributions to the enthalpy of formation of a Lewis acid-base adduct.

Although Pearson hardness values are a useful metric of acids' and bases' hardness, they cannot easily be used to estimate the Lewis acid-base interaction energy. This is not the case for the EC model developed by Drago and Wayland.[3] In the **Drago and Wayland's EC Model,** the enthalpy of formation of an acid-base adduct, AB,

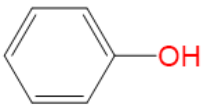
$$A + B \rightleftharpoons AB \qquad \Delta H_{AB\ adduct}$$

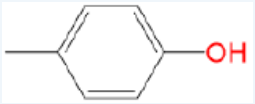
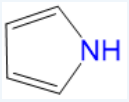
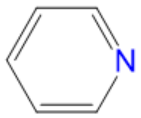
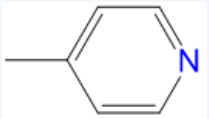
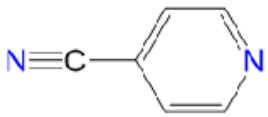
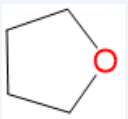
from the acid (A) and base (B) can be calculated as the sum of products of electrostatic (E) and covalent (C) factors that reflect the propensity of the acid and base to engage in strong electrostatic and covalent interactions with one another:

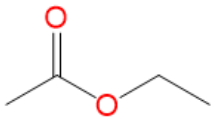
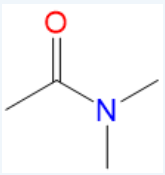
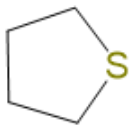
$$-\Delta H_{AB\ adduct} = E_A E_B + C_A C_B$$

where E_A and C_A are the electrostatic and covalent parameters for the acid and E_B and C_B the electrostatic and covalent parameters for the base given in units of kcal^{½} mol$^{-½}$. E and C parameters for selected acids and bases are given in Table 5.6.1.2 .

Table 5.6.1.2: E and C Parameters for selected Lewis acids and bases according to the ECW model.[4,5] Taken from Vogel, G. C.; Drago, R. S., The ECW Model. Journal of Chemical Education 1996, 73 (8), 701 and Drago, R. S. A modern approach to acid-base chemistry. Journal of Chemical Education 1974, 51 (5), 300 (for BF_3).

Species	E (kcal^{½} mol$^{-½}$)	C (kcal^{½} mol$^{-½}$)	W (kcal mol^{-1})	C/E
Acids				
I_2	0.5[†]	2[†]	0	4
ICl	2.92	1.66	0	0.57
H_2O	1.31	0.78	0	0.59
SO_2	0.51	1.56	0	3.1
$HCCl_3$ (chloroform)	1.56	0.44	0	0.28
$(CH_3)_3COH$	1.07	0.69	0	0.65
$(CF_3)_3COH$	3.06	1.88	-0.87	0.61
	2.27	1.07	0	0.47

Species	E (kcal^{½} mol$^{-½}$)	C (kcal^{½} mol$^{-½}$)	W (kcal mol^{-1})	C/E
	2.23	1.03	0	0.46
	2.30	1.11	0	0.48
	1.38	0.68	0	0.49
BF_3	1.62	9.88		6.10
$B(CH_3)_3$	2.90	3.60	0	1.2
$Al(CH_3)_3$	8.66	3.68	0	0.43
$Ga(C_2H_5)_3$	6.95	1.48	0	0.21
$In(CH_3)_3$	6.60	2.15	0	0.33
$Zn[N(Si(CH_3)_3)]_2$	2.75	2.32	0	0.84
$Cd[N(Si(CH_3)_3)]_2$	2.50	1.83	0	0.73
Bases				
NH_3	2.31	2.04		0.88
CH_3NH_2	2.16	3.13		1.4
$(CH_3)_2NH$	1.80	4.21		2.3
$(CH_3)_3N$	1.21	5.61		4.6
	1.78	3.54		2.0
	1.81	3.73		2.0
	1.53	2.94		1.9
CH_3CN	1.64	0.71		0.43
$ClCH_2CN$	1.67	0.33		0.20
$CH_3C(O)CH_3$	1.74	1.26		0.72
$(C_2H_5)_2O$	1.80	1.63		0.91
	1.64	2.18		1.3

Species	E (kcal^{½} mol$^{-½}$)	C (kcal^{½} mol$^{-½}$)	W (kcal mol^{-1})	C/E
 (EtOAc)	1.63	0.95		0.58
	2.35†	1.31		0.56
$(CH_3)_2S$	0.25	3.75		15
$(CH_3CH_2)_2S$	0.24	3.92†		15
	0.26	4.07		16
$(CH_3)_2Se$	0.05	4.24		83
$(CH_3)_2SO$	2.4	1.47		0.61
$(CH_3)_3P$	0.25	5.81		24
$(CH_3O)_3P$	0.13	4.83		37
$(C_6H_5)_3PO$	2.59	1.67		0.64
$(C_6H_5)_3PS$	0.35	3.65		10
C_6H_6	0.70	0.45		0.64

† These values were fixed to parameterize the rest of the E and C parameters.

Trends in the relative values of C and E for the acids and bases in Table 5.6.1.2 are very roughly consistent with the trends in hardness and softness outlined earlier. However, the parameters suggest that some trends in hardness reflect changes in species' ability to engage in ionic interactions while others reflect changes in species' ability to engage in strong covalent interactions. For example, C_B for the dimethylchalcogenides increases steadily from 1.5 to 4.25 kcal^{½} mol$^{-½}$ on going from Me_2O to Me_2Se while E_B decreases from 1.68 to 0.05 kcal^{½} mol$^{-½}$, suggesting that electrostatic and covalent factors are both involved in a decrease in base hardness down group 16. However, in the case of phosphines and amines it appears that electrostatic factors are primarily responsible for the decrease in hardness down group 15. On going from Me_3N to Me_3P, C_B only increases slightly from 5.61 to 5.81 kcal^{½} mol$^{-½}$ while E_B decreases from 1.21 to 0.25 kcal^{½} mol$^{-½}$ - *i.e.*, to 20% of the Me_3N value.

However, some species tend to have very high values for both E and C, reflecting their ability to engage in strong electrostatic and covalent interactions, while others have small values for both, reflecting their relative stability as free species in solution.

As can be seen by comparing the acids and bases listed in the absolute hardness table (Table 5.6.1.1) and the EC parameters table (Table 5.6.1.2). The EC model has primarily been applied to organic and main group organometallic acids and bases. However, a variety of extensions have been proposed that enable its wider applicability.

The simple EC model only includes electrostatic and covalent considerations and thus ignores steric, lattice energy, and other contributions to the interaction energy. Thus it is only useful for analyzing the interaction energies of sterically unhindered adducts in which solvation energy and other contributions to the overall interaction energy are insignificant. However, additional refinements of the model attempt to extend its usefulness by accomodating various factors, such as

- *Steric strain.* Specifically, Hancock and Martell[6] introduced a D parameter to account for any additional steric strain introduced upon adduct formation,* giving

$$-\Delta H_{AB\ adduct} = E_A E_B + C_A C_B - D_A D_B$$

- *Charge transfer upon adduct formation.* As discussed in section 6.4.2, the formation of a Lewis acid-base complex results in a net transfer of electron density from the electron donor (base) to the acceptor (acid). Drago and Wong[7] extended the EC model to include that charge transfer by adding what they called receptance factors that account for the acid's ability to receive electron density (R_A) and transference factors that account for the base's ability to donate electron density (T_B), giving

$$-\Delta H_{AB\ adduct} = E_A E_B + C_A C_B + R_A T_B$$

  This extension of the EC model is called the **electrostatic-covalent-transfer or ECT model**. Notably, it has been applied successfully to adducts involving ions, for which the R_AT_B term can account for as much as 31% of the interaction energy.

- *Any constant energy term, such as the energy needed to cleave a dimer in order to make the Lewis acid (e.g., $Al_2Cl_6 \rightarrow 2AlCl_3$).* Drago and Vogel[4] extended the EC model to accommodate these constant energy terms, which they designated W. The resulting model is called the **ECW model,** for which

$$-\Delta H_{AB\ adduct} = E_A E_B + C_A C_B + W$$

where

$$W = W_A + W_B$$

A simple application of EC and extended EC models is that they allow the enthalpy of adduct formation to be calculated. These enthalpy calculations based on the EC model are consistent with the superior interaction energy of hard-hard and soft-soft interactions compared to hard-soft ones. Consider, for example, the transfer of I_2 between BF_3 and $InMe_3$, H_3N-BF_3, and H_3N-$InMe_3$.

$$H_3N - BF_3 + InMe_3 \rightleftharpoons BF_3 + H_3N - InMe_3$$

Since H_3N is a hard base and BF_3 and $InMe_3$ are harder and softer acids, respectively, the equilibrium is expected to favor the reactant, H_3N-BF_3. Assuming the equilbrium is enthalpically driven, this qualitative analysis is consistent with the expected endothermic enthalpy of the reaction, as may be seen from the calculated enthalpies of adduct formation for both H_3N-BF_3 and H_3N-$InMe_3$.

For H_3N-BF_3:

$$-\Delta H_{H_3N-BF_3} = E_{BF_3}E_{NH_3} + C_{BF_3}C_{NH_3}$$

$$-\Delta H_{H_3N-BF_3} = (1.62)(2.31) + (9.88)(2.04)$$

$$-\Delta H_{H_3N-BF_3} = 3.74\ kcal/mol + 20.1\ kcal/mol = 23.8\ kcal/mol$$

$$\Delta H_{H_3N-BF_3} = -23.8\ kcal/mol$$

For H_3N-$InMe_3$:

$$-\Delta H_{H_3N-InMe_3} = E_{InMe_3}E_{NH_3} + C_{InMe_3}C_{NH_3}$$

$$-\Delta H_{H_3N-InMe_3} = (6.6)(2.31) + (2.15)(2.04)$$

$$-\Delta H_{H_3N-InMe_3} = 15.25\ kcal/mol + 4.39\ kcal/mol = 19.63\ kcal/mol$$

$$\Delta H_{H_3N-InMe_3} = -19.63\ kcal/mol$$

So H_3N-BF_3 is enthalpically favored by -4.2 kcal/mol [=-23.8 kcal/mol - (-19.63 kcal/mol) according to Hess' Law].

In addition to their utility for estimating enthalpies of Lewis acid-base complex formation, EC and related models serve as a

useful tool for estimating the relative importance of ionic, covalent, and steric factors in complex formation. Specifically,

- The relative contributions of ionic and covalent factors can be calculated directly, as from the E and C terms. This can provide insight into why some complexes are more stable than others. Such calculations reveal that the hard-hard adduct H_3N-BF_3 is favored over the hard-soft adduct H_3N-$InMe_3$ because of the strong covalent interaction holding together H_3N-BF_3. The covalent term accounts for 84% of the energy of the H_3N-BF_3 interaction and is largely lost upon formation of H_3N-$InMe_3$, for which it contributes only 22% of the interaction energy. When the electrostatic term is accounted for, it can be seen that the formation of H_3N-$InMe_3$ from H_3N-BF_3 is disfavored, since it would result in a loss of 15.7 kcal/mol of covalent stabilization that would be incompletely compensated for by a gain of 11.5 kcal/mol of electrostatic stabilization.
- The role of other contributions to the bonding in a Lewis acid-base complex may be estimated from the discrepancy between the experimental and EC model calculated stabilization energies. This is because the EC parameters assume sigma bonding and so any deviation between the calculated and experimental enthalpies of complex formation can be attributed to non-sigma contributions.
  - This is done explicitly in extensions of the EC model. For instance, in the case of the Hancock and Martell, ECT, and ECW extensions of the EC model, the contributions of the steric, charge transfer, and constant energy factors (like dimer dissociation) are directly computed in the model.
  - Comparisons of the difference between the energies calculated using ordinary EC parameters and the observed enthalpies has also been used as an estimate of the
    - steric strain energy in strained adducts, which exhibit a less exothermic heat of adduct formation than expected
    - π-backbonding energy in adducts which are capable of such interactions and exhibit a more exothermic heat of formation than expected.[8-10]
  - For examples see (a) Drago, R. S., The interpretation of reactivity in chemical and biological systems with the E and C model. Coordination Chemistry Reviews 1980, 33 (3), 251-277; (b) Drago, R. S.; Bilgrien, C. J., Inductive transfer and coordination of ligands in metal—metal bonded systems. Polyhedron 1988, 7 (16), 1453-1468; (c) Drago, R. S., The question of a synergistic metal-metal interaction leading to .pi.-back-bond stabilization in dirhodium tetrabutyrate adducts. Inorganic Chemistry 1982, 21 (4), 1697-1698.
- The role of electrostatic, covalent, and other contributions to the spectroscopic behavior of Lewis acid-base complexes can be assessed similarly using specialized versions of the ECW or ECT model that allow for calculation of changes in spectroscopic parameters upon adduct formation - *e.g.,* OH stretching frequencies. Details are beyond the scope of this text but may be found in the original literature,[11] for example, Drago, R. S.; Vogel, G. C. *JACS* 1992, 114 (24), 9527-9532; Vogel, G. C.; Drago, R. S., *J. Chem. Educ.* 1996, 73 (8), 701; Drago, R. S.; Wong, N. M., *J. Chem. Educ.* 1996, 73 (2), 123.).

Pearson Softness Parameters have been proposed as a means of calculating the equilibrium constant for formation of a Lewis acid-base adduct, although they are more commonly used to estimate metal toxicity

Pearson also proposed a softness parameter that can be used to estimate the thermodynamics of Lewis acid-base complex formation, this time in the form of the equilibrium constant for

$$A + B \overset{K}{\rightleftharpoons} AB$$

for which Pearson proposed

$$logK = S_A S_B + \sigma_A \sigma_B$$

where S_A and S_B are acid and base parameters related to the strength of the acid-base interaction and σ_A and σ_B are acid and base parameters related to softness. This approach hasn't found as wide an acceptance in studies of chemical reactivity as the Drago-Wayland and absolute hardness parameters. However, because the toxicity of metal ions sometimes depends on their propensity to bind soft Lewis bases in living systems, the softness parameters which Pearson and Mawby subsequently proposed based on the relative energies of metal fluorine and metal iodine bonds[12] have been widely used as a tool for predicting metal ion toxicity.[13]

References

1. Pearson, R. G., Absolute electronegativity and absolute hardness of Lewis acids and bases. *Journal of the American Chemical Society* 1985, 107 (24), 6801-6806.

2. Pearson, R. G., Absolute electronegativity and hardness: application to inorganic chemistry. *Inorganic Chemistry* 1988, 27 (4), 734-740.

3. Drago, R. S.; Wayland, B. B., A Double-Scale Equation for Correlating Enthalpies of Lewis Acid-Base Interactions. *Journal of the American Chemical Society* 1965, 87 (16), 3571-3577.

4. Vogel, G. C.; Drago, R. S., The ECW Model. *Journal of Chemical Education* 1996, 73 (8), 701.

5. Drago, R. S. A modern approach to acid-base chemistry. *Journal of Chemical Education* 1974, 51 (5), 300

6. Hancock, R. D.; Martell, A. E., Hard and Soft Acid-Base Behavior in Aqueous Solution: Steric Effects Make Some Metal Ions Hard: A Quantitative Scale of Hardness-Softness for Acids and Bases. *Journal of Chemical Education* 1996, 73 (7), 654.

7. Drago, R. S.; Wong, N. M., The Role of Electron-Density Transfer and Electronegativity in Understanding Chemical Reactivity and Bonding. *Journal of Chemical Education* 1996, 73 (2), 123.

8. Drago, R. S., The interpretation of reactivity in chemical and biological systems with the E and C model. Coordination Chemistry Reviews 1980, 33 (3), 251-277.

9. Drago, R. S.; Bilgrien, C. J., Inductive transfer and coordination of ligands in metal—metal bonded systems. Polyhedron 1988, 7 (16), 1453-1468.

10. Drago, R. S., The question of a synergistic metal-metal interaction leading to .pi.-back-bond stabilization in dirhodium tetrabutyrate adducts. Inorganic Chemistry 1982, 21 (4), 1697-1698.

11. Drago, R. S.; Vogel, G. C., Interpretation of spectroscopic changes upon adduct formation and their use to determine electrostatic and covalent (E and C) parameters. *Journal of the American Chemical Society* 1992, 114 (24), 9527-9532.

12. Pearson, R. G.; Mawby, R. J. The Nature of Metal-Halogen Bonds in Gutmann, V. *Halogen Chemistry, vol. 3.* Academic Press: London, 1967, pp. 55-84.

13. Kinraide, T. B. Improved Scales for Metal Ion Softness and Toxicity *Environmental Toxicology and Chemistry* 2009, 28 (3), 525-533.

Notes

* More precisely, the D parameters account for the difference in steric strain in the adduct relative to a water adduct of the Lewis acid.

This page titled 5.6.1: Quantitative Measures of Hardness, Softness, and Acid-Base Interactions from a Hard Soft Acid-Base Principle perspective involve orbital energies and or apportioning acid-base bonding in terms of electrostatic and covalent factors is shared under a license and was authored, remixed, and/or curated by LibreTexts.

- 6.6.1: Quantitative Measures of Hardness, Softness, and Acid-Base Interactions from a Hard Soft Acid-Base Principle Perspective Involve Orbital Energies and/or Apportioning Acid-Base Bonding in Terms of Electrostatic and Covalent Factors by Stephen M. Contakes is licensed CC BY 4.0.

5.6.2: Hard-Hard and Soft-Soft preferences may be explained and quantified in terms of electrostatic and covalent and electronic stabilization on the stability of Lewis acid-base adducts

The Hard Soft Acid Base Principle is a Conceptual Tool for Thinking About Patterns of Lewis Acid-Base Reactivity

The explanation of the trends in metal distribution, halide salt solubility, and preferred metal coordination patterns is rooted in Arland, Chatt, and Davies' observation that *Lewis acids and bases could be classified into two groups based on their propensity to form stable compounds with one another* (*e.g.* acids in a class tend to form more stable adducts with bases in the same class than they did with bases in the other).[1] Arland, Chatt, and Davies somewhat boringly termed these groups class a and class b but today they are known by Ralph Pearson's name for them. Pearson called the class a acids and bases hard and class b acids and bases soft. These terms reflect how "soft" these substance's electron clouds are towards distortion or, in other words, their polarizability (Figure 5.6.2.1). Pearson terms acids and bases which are relatively polarizable **soft** and those which are difficult to polarize **hard.**

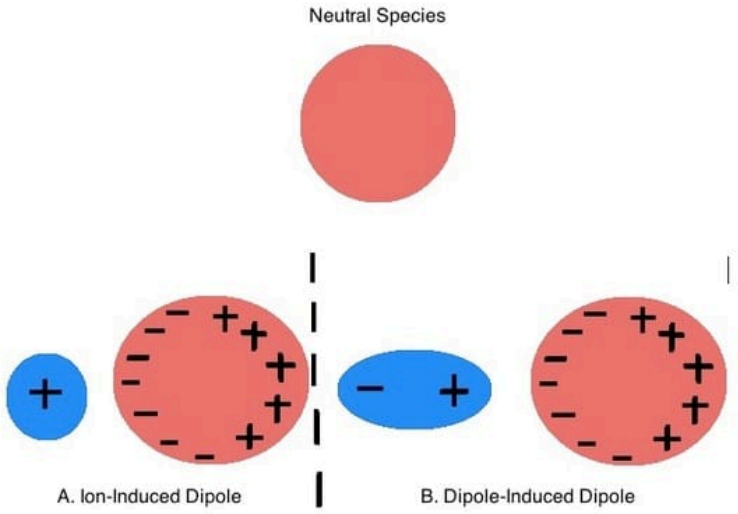


Figure 5.6.2.1: Polarizability refers to the ease with which a substance's electron cloud may be distorted under the action of an electric field. A fragment's polarizability determines the degree to which its electron cloud is distorted by A.) an Ion and B.) a polar molecule to induce a dipole moment. The figure is taken from (and the caption expanded from) Cox, Kelly and Dana Reusser "Polarizability"

Recognizing Hard and Soft Acids and Bases

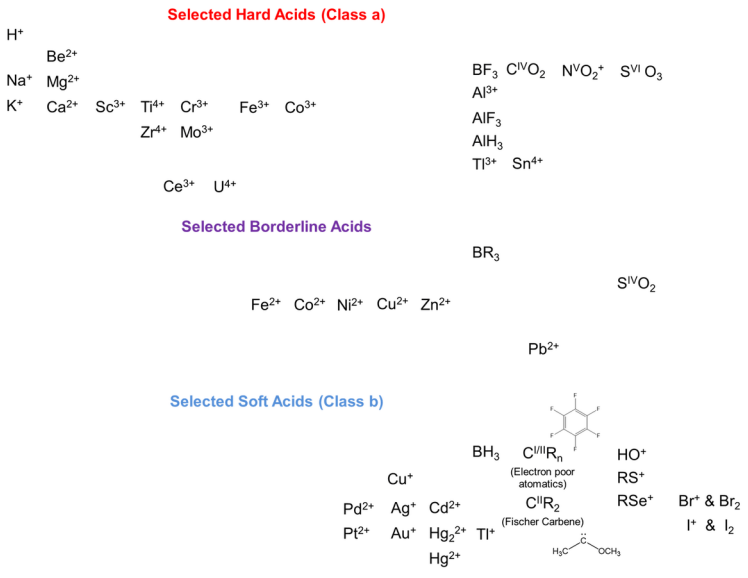
Hard acids and bases come in two varieties:

1. hard acid and base sites that possess few valence electrons and for which polarization therefore involves distorting core electrons, which are difficult to distort because they are close to the nucleus and experience a high nuclear charge. The most common examples of such substances are Lewis acid hard acids towards the left of the periodic table.
2. hard acid and base sites with a high charge density (highly charged relative to size) and/or which are electron deficient. In these cases polarization involves distorting electrons that already experience strong unshielded electrostatic interactions.

Soft acids and bases also come in two varieties

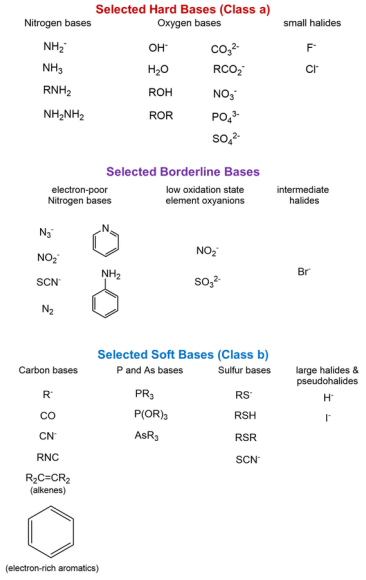
1. soft acids and bases which posses many valence electrons and so are more readily polarized. In consequence, all other things being equal, soft acids and bases are more likely to be found towards the middle or right of the periodic table.
2. soft acids and bases with little charge density and/or which are relatively electron rich.

Note that the hard-soft classification should not be thought of as if all hard acids and bases are equally hard and all soft acids and bases equally soft. There is a graduation in hardness and softness and a number of intermediate acids and bases which do not fit neatly in either category. With this caveat in mind, representative **hard, soft, and borderline acids** are given below. Notice how they illustrate the trends just outlined.



As expected, hard acids tend to be found towards the left side of the periodic table and involve higher oxidation states and/or electron donating substituents while soft acids are more common to the right of the periodic table and involve lower oxidation states and/or electron donating substituents.

Illustrative hard, soft, and borderline bases are given below. Again, notice how these substances illustrate the general trends.



Qualitative Estimation of the Relative Hardness and Softness of Lewis Acids and Bases

As can be seen from the examples above, **hard acids are relatively electron-poor and hard bases electron-rich** since they have comparatively

- small frontier orbitals, reflective of their relatively small atom/ion/fragment sizes
- high (for acids) or low (for bases) oxidation states on the base atom, reflected in a large positive formal charge (for acids) or negative formal charge (for bases)
- low polarizability, due to loss or gain of substantial numbers of electrons, or the localization of
  - positive charge on an electropositive element or an atom bearing electron-withdrawing substituents
  - negative charge on an electronegative element or an atom bearing electron-donating substituents

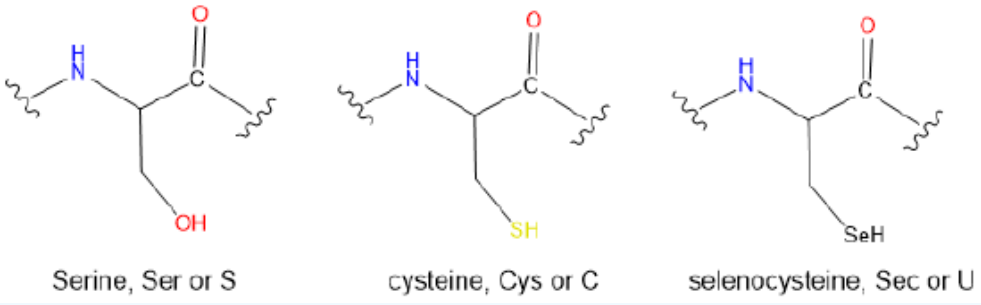
In contrast to hard acids and bases, **soft acids are relatively electron-rich and soft bases larger and more electron poor** since they have comparatively

- large frontier orbitals, reflective of their relatively large atom/ion/fragment sizes
- low oxidation states, often resulting in small or nonexistent atomic charges
- high polarizability, as might be expected of species in which electron-electron repulsions are lower and electrons are spread over a large volume. Sometimes this is indicated by
  - positive charge on an electronegative element or an atom bearing electron-donating substituents
  - negative charge on an electropositive element or an atom bearing electron-withdrawing substituents

Exercise 5.6.2.1

Rank the acids or bases in each set in increasing order of expected hardness.

a. Cr^{2+} and Cr^{3+}
b. H^+, Cs^+, and Tl^+
c. SCN^- (acting as a base at N) and SCN^- (acting as a base at S)
d. AlF_3, AlH_3, $AlMe_3$
e. The side chains of the following proteinogenic amino acids



Answer available at the end of this section.

The Hard-Soft Acid-Base Principle (HSAB Principle)

The **Hard-Soft acid-base principle (HSAB Principle) explains patterns in Lewis acid-base reactivity in terms of a *like reacts with like preference***. Both thermodynamically and kinetically, hard acids prefer hard bases and soft acids soft bases. Specifically,

- Thermodynamically, hard acids form stronger acid-base complexes with hard bases while soft acids form stronger complexes with soft bases.

- Kinetically, hard acids/electrophiles react more quickly with hard bases/nucleophiles while soft acids/electrophiles react more quickly with soft bases/neucleophiles.

Applications of the HSAB principle include

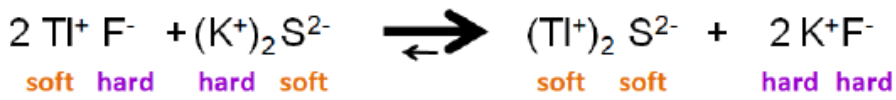
1. Predicting the equilibrium or speed of *Lewis acid-base metathesis and displacement reactions*. In a Lewis acid-base **metathesis reaction** the acids and bases swap partners

$$\mathrm{A_1 : B_1 + A_2 : B_2 \overset{k_1,\, K_{eq}}{\rightleftharpoons} A_1 : B_2 + A_2 : B_1}$$

For example, the equilibrium position of the metathesis reaction between TlF and $\mathrm{K_2S}$ favors the products:

$$\mathrm{2\,TlF + H_2S \rightleftharpoons Tl_2S + 2\,KF}$$

consistent with the HSAB's hard-hard and soft-soft preference.



The HSAB principle also allows for prediction of the position of displacement reactions, in which a Lewis acid or base forms an adduct using a base or acid from an existing Lewis acid-base complex. In these reactions, the displacement of acid or base from the reactant complex may be thought of as a sort of metathesis reaction, one in which in the unbound acid or base switches places with one in the complex. For example, the reaction between HI and methylmercury cation

$$\mathrm{HI + HgSCH_3^+ \rightleftharpoons CH_3SHgI + H^+}$$

involves displacement of an iodide from HI to give $\mathrm{CH_3HgI}$. The position of the equilibrium favors $\mathrm{CH_3HgI}$ since both $\mathrm{CH_3Hg^+}$ and $\mathrm{I^-}$ are soft, while $\mathrm{H^+}$ is a hard acid.



Exercise 5.6.2.2

Predict the position of equilibrium for the following reaction.

$$\mathrm{Fe_2O_3 + 3\,Ag_2S \rightleftharpoons Fe_2S_3 + 3\,Ag_2O}$$

Answer available at the end of this section.

Exercise 5.6.2.3

Predict whether K for the following equilibria will be <<1, ~1, or >>1.

a. $\mathrm{2\,HF + (CH_3Hg)_2S \rightleftharpoons 2\,CH_3HgF + H_2S}$
b. $\mathrm{Ag(NH_3)_2^+ + 2\,PH_3 \rightleftharpoons Ag(PH_3)_2^+ + 2\,NH_3}$
c. $\mathrm{Ag(PH_3)_2^+ + 2\,H_3B{-}SH_2 \rightleftharpoons 2\,H_3B{-}PH_3 + Ag(SH_2)_2^+}$
d. $\mathrm{H_3B{-}NH_3 + F_3B{-}SH_2 \rightleftharpoons H_3B{-}SH_2 + F_3B{-}NH_3}$

Answer available at the end of this section.

2. Predicting the relative strengths of a given set of *Lewis acids or bases towards a particular substrate*. Consider, for example, the relative strengths of a BH_3, BMe_3, and BF_3 towards group 15 hydrides like NH_3, PH_3, and AsH_3. Of the boranes listed, the hardest acid BF_3 is the strongest acid towards the hard base NH_3 while BH_3 is the strongest towards AsH_3.[†]

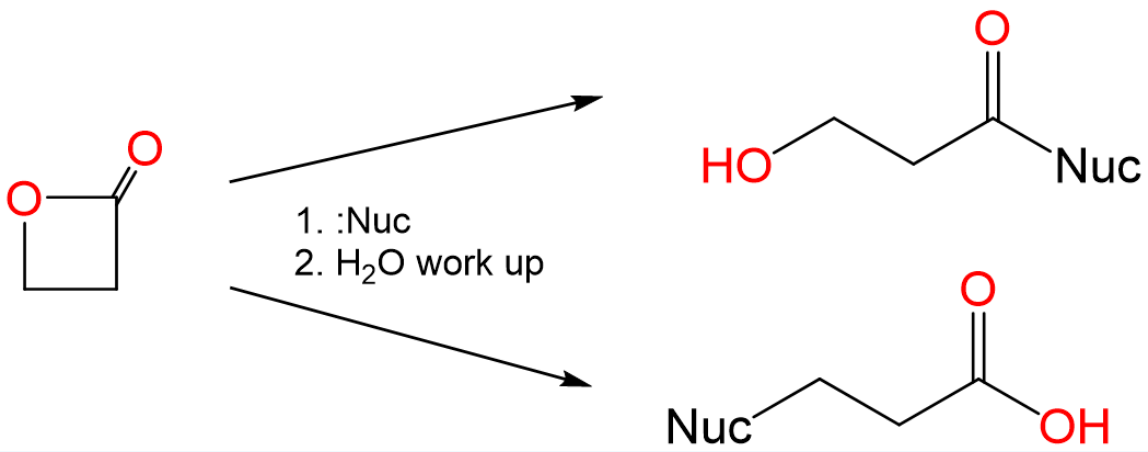
Exercise 5.6.2.4

Which acid will form the most stable complex with CO: BH_3, BF_3, or BMe_3?

Answer available at the end of this section.

Exercise 5.6.2.5

When lactones react with nucleophiles, they can undergo ring opening reactions to give either an alcohol or a carboxylic acid, as shown for propiolactone below:



In the reaction above, sterically unhindered alkoxides give one product and sterically unhindered thioalkoxides the other. Explain why this is the case and predict the products of the reaction between propiolactone and the sodium salts of ethoxide and thioethoxide.

Answer available at the end of this section.

The theoretical interpretation of the hard-soft acid-base principle is that hard-hard preferences reflect superior electrostatic stabilization while soft-soft preferences reflect superior covalent stabilization.

The hard-hard and soft-soft preferences in Lewis acid-base interactions reflect that

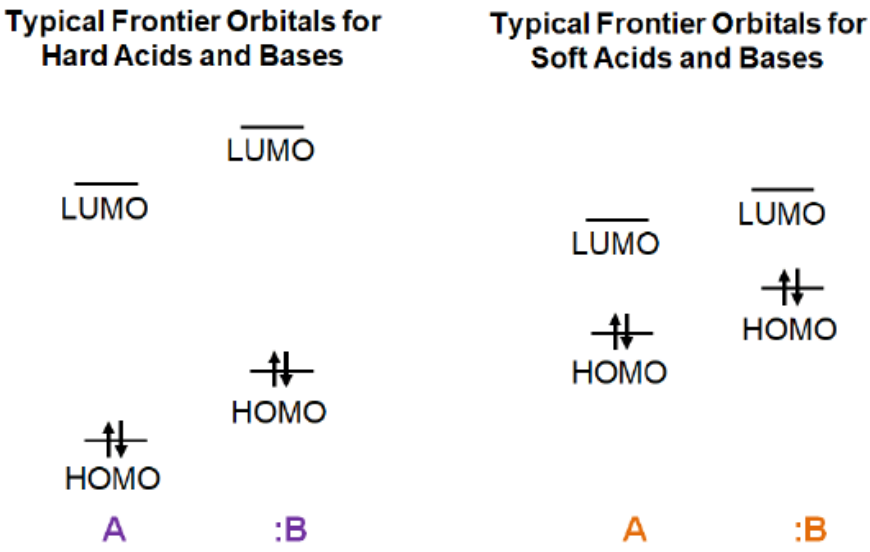
- The lone pair of a hard base is strongly stabilized electrostatically by a hard acid.
- The lone pair of a soft base is strongly stabilized by forming a covalent bond with a soft acid.
- The lone pair of a hard or soft base is comparatively weakly stabilized by an acid opposite to it in hardness or softness since the overall electrostatic and covalent stabilization of the adduct is comparatively weak.

To see why this is the case it is helpful to divide the contributions to the interaction energy between an acid and a base as follows:

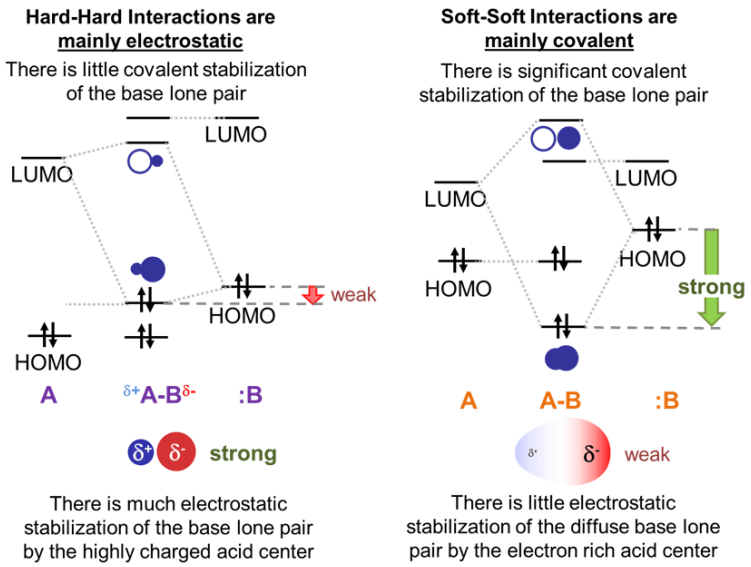
Interaction Energy = Electrostatic attractions and repulsions of partial atomic charges (Ionic term) + Interactions between filled orbitals on one fragment and unfilled orbitals on the other (Covalent term) + Electrostatic repulsions between filled orbitals on the two fragments (Steric term)

Of the three contributions to the interaction energy, only the ionic and covalent terms directly relate to the hardness of the interacting acid and base. One approach to thinking about how hardness influences the ionic and covalent contributions is to consider the frontier orbitals involved in the acid-base interaction. This is sometimes done through the use of the Salem-Klopman equation,[1,*] although in the treatment which follows a more qualitative approach will be employed.

Both hard acids and bases will have comparatively low energy HOMO levels and high energy LUMO levels, with a correspondingly high HOMO-LUMO gap. In contrast, soft acids and bases will have comparatively high-energy HOMO levels and low-energy LUMO levels, giving a comparatively smaller HOMO-LUMO gap.



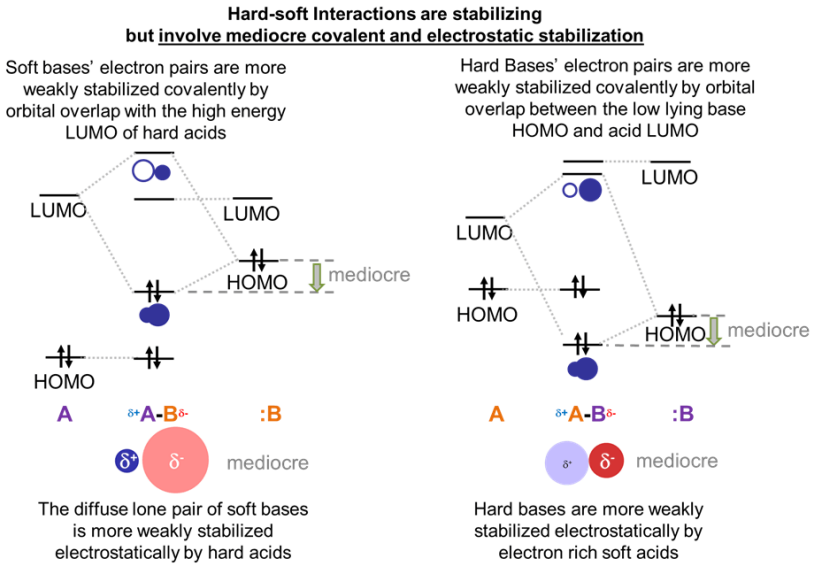
Given this, consider the frontier orbital interactions involved in the formation of an acid-base complex for the possible cases, as illustrated schematically below.



The large gap in energy between hard bases' highly stabilized HOMO lone pairs and the high energy LUMO of hard acids ensures that in **hard acid-hard base adducts the dominant stabilizing interaction will involve electrostatic attraction between the base lone pair and the electropositive Lewis acid center**. Fortunately, since the electron clouds in hard bases are relatively dense and electron rich while hard Lewis acids are highly charged and small, these electrostatic interactions are strong.

In contrast, in **soft acid-soft base adducts, the dominant stabilizing interaction will be covalent.** This is because the small gap in energy between a soft base HOMO and soft acid LUMO enables the formation of a well-stabilized bonding orbital with significant electron density between the acid and base.

The orbitals' interactions between hard acids and soft bases and soft acids and hard bases are intermediate between the hard acid-hard base and soft acid-soft base cases.



This means that the adducts are stable relative to free acid and base – just not as well stabilized as in the hard acid and hard base case. In the case of hard acids and soft bases the hard acids are less able to stabilize the soft bases' relatively diffuse electron pair electrostatically and there isn't as much covalent stabilization as in adducts of soft acids and bases due to the hard acid's high energy.

References

1. Ahrland, S.; Chatt, J.; Davies, N. R., The relative affinities of ligand atoms for acceptor molecules and ions. Quarterly Reviews, Chemical Society 1958, 12 (3), 265-276.

2. Pearson, R. G., Hard and Soft Acids and Bases. Journal of the American Chemical Society 1963, 85 (22), 3533-3539.

3. Fleming, I., Molecular orbitals and organic chemical reactions. Reference ed.; Wiley: Hoboken, N.J., 2010.

Notes

* Despite the fruitfulness of this observation, in general it is important to reduce the potential for observer bias by checking observations like these against compounds reported in the chemical literature and databases like the Inorganic Crystal Structure and Cambridge Crystallographic Databases.

** These are very soluble in water, to the point where some solutions are perhaps better described as solutions of water in the halide.

† This can be predicted based on the relative hardness of BF_3, BR_3, and BH_3 in the list of hard and soft acids. However, for those of you who may be confused as to why H is considered a better electron donor for the purposes of softening a Lewis acid center while alkyl groups are better electron donors for the purposes of stabilizing carbocations in organic chemistry, the dominant effect is the lower electronegativity of H relative to carbon (in CH_3). The effect of electron donation due to hyperconjugation isn't as great for thermodynamically stable bases like BX_3/BR_3.

†† For more on the Salem-Klopman equation see Fleming, I., Molecular orbitals and organic chemical reactions. Reference ed.; Wiley: Hoboken, N.J., 2010; pp. 138-143.

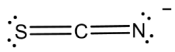
Answers

Exercise 5.6.2.1

(a) $Cr^{2+} < Cr^{3+}$ All other things being equal, hardness increases with oxidation state.

(b) $Tl^+ < Cs^+ < H^+$ The order reflects Cs^+ and Tl^+'s larger size relative to H^+ (which doesn't possess any electrons that can be polarized anyway) and that Tl^+ still possesses two valence electrons while Cs^+ possesses none.

(c) SCN^- (acting as a base at S) < SCN^- (acting as a base at N). The order reflects the greater electronegativity of N than S and N's possession of a more negative formal charge of -1.



Formal charge 0 0 -1

(d) $AlH_3 < AlMe_3 < AlF_3$. The hardness increases as the substituents on the Lewis acid Al center become less electron donating and more electron withdrawing (and, incidentally, harder bases) as their electronegativity increases in the order $H^- < CH_3^- < F^-$. Note that the order of electron donating ability for H^- and CH_3^- is the opposite observed for carbocations, for which hyperconjugation plays a larger role.

(e) Sec < Cys < Ser. The hardness increases as the electronegativity of the Lewis base chalcogen increases on going from a selenol to a thiol to an alcohol.

Exercise 5.6.2.2

The equilibrium will favor the reactants (K<1) since the hard-hard and soft-soft interactions in the reactants are more stable than the hard-soft interactions in the products.



hard hard soft soft hard soft soft hard

Exercise 5.6.2.3

a. K< < 1 since the reactant adducts are hard-hard and soft-soft while the products involve hard-soft interactions.

b. K>>1 since the reactant complex, diamine silver(I), is a complex of a hard base, NH_3, with the soft acid, Ag^+, while the product is a complex of the same soft acid with the soft base phosphine.

c. K~1 since all the adducts amongst the reactants and products involve soft acids and bases.

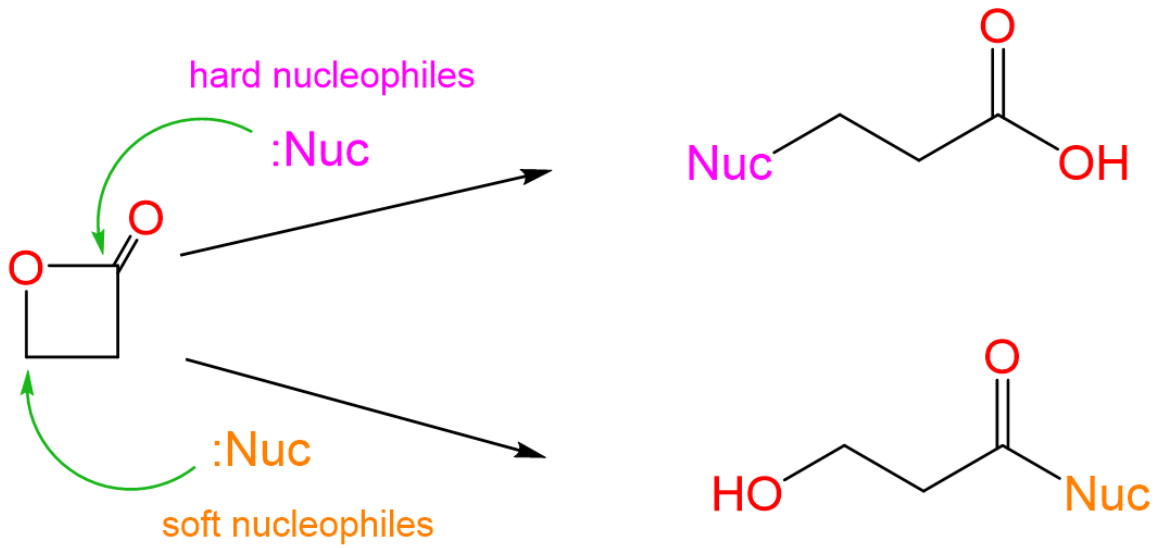
d. K>>1 since BH_3 is a softer acid than BF_3, so it will form a stronger complex with the softer base H_2S while the harder BF_3 forms a stronger complex with the harder base NH_3.

Exercise 5.6.2.4

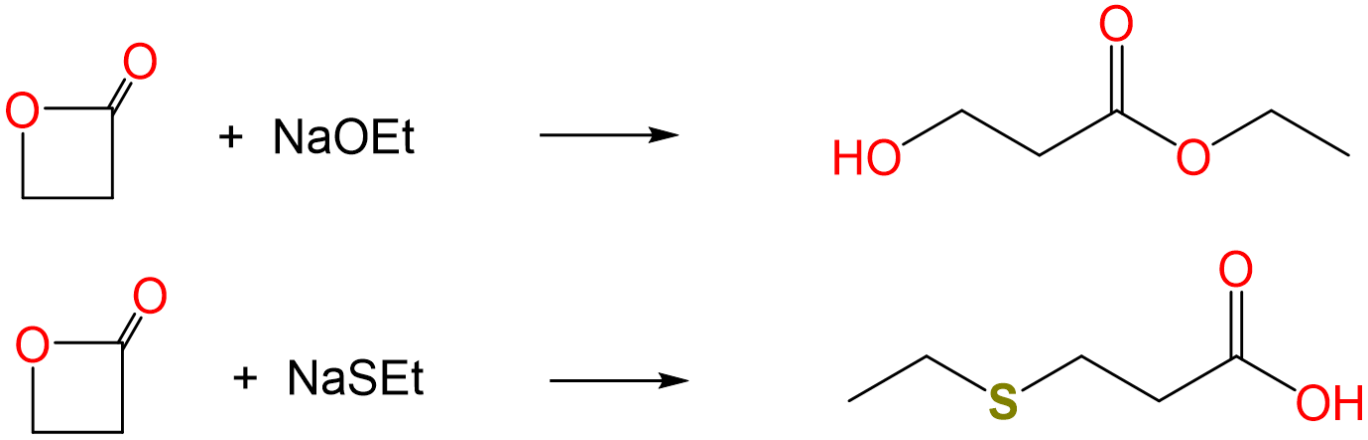
BH_3. Since CO forms complexes primarily through its carbon lone pair, it is a soft base and so will form the strongest complex with the softest Lewis acid.

Exercise 5.6.2.5

The two reaction products correspond to nucleophilic attack at the lactones' two electrophilic carbon centers. Specifically, the acid is produced by attack at the softer C^{I} center of the CH_2 directly attached to the ester oxygen and the alcohol by nucleophilic attack at the harder C^{III} center of the ester carbonyl.



Consequently, it is reasonable to expect that the harder base ethoxide will nucleophilically attack the harder carbonyl carbon while the softer thioethoxide will attack the softer methylene carbon.



This page titled 5.6.2: Hard-Hard and Soft-Soft preferences may be explained and quantified in terms of electrostatic and covalent and electronic stabilization on the stability of Lewis acid-base adducts is shared under a license and was authored, remixed, and/or curated by LibreTexts.

- 6.6.2: Hard-Hard and Soft-Soft preferences may be explained and quantified in terms of electrostatic and covalent and electronic stabilization on the stability of Lewis acid-base adducts by Stephen M. Contakes is licensed CC BY 4.0.

6: SYMMETRY AND GROUP THEORY

6.1: Symmetry Elements and Operations

6.2: Successive Operations

6.3: Significance of Recognizing Symmetry Elements

6.4: Point Groups

6.4.1: Groups of Low and High Symmetry

6.4.2: Other Groups

6.5: Character Tables - An Introduction

6.6: Character Tables

6.7: Properties and Representations of Groups

6.7.1: Matrices

6.7.2: Representations of Point Groups

6.8: Examples and Applications of Symmetry

6.8.1: Chirality

6.8.2: Molecular Vibrations

6.8A: Vibrational Spectroscopy

6.8C: Vibrational Spectroscopy of Linear and Bent triatomic Molecules

6.9: Larger (Polyatomic) Molecules

6.9.1: CO_2 (Revisted with Projection Operators)

6.9.2: BF_3

6.9.3: Bifluoride anion

6.9.4: Carbon Dioxide

6.9.5: H_2O

6.9.6: NH_3

6.10: MO Theory Applied to Polyatomic Molecules BH_3, NH_3, and CH_4

6.10A: BH_3

6.10B: NH_3

6.10C: CH_4

6.10D: A Comparison of MO and VB Bonding Models

6.P: Problems (under construction)

This page titled 6: Symmetry and Group Theory is shared under a license and was authored, remixed, and/or curated by LibreTexts.

- 4: Symmetry and Group Theory by Kathryn Haas has no license indicated.

6.1: Symmetry Elements and Operations

Click here to see a lecture on this topic.

Introduction

The symmetry of a molecule consists of **symmetry operations** and **symmetry elements**. A symmetry operation is an operation that is performed to a molecule which leaves it indistinguishable and superimposable on the original position. Symmetry operations are performed with respect to symmetry elements (points, lines, or planes).

An example of a symmetry operation is a 180° rotation of a water molecule in which the resulting position of the molecule is indistinguishable from the original position (see Figure 6.1.1). In this example, the symmetry operation is the rotation and the symmetry element is the axis of rotation.

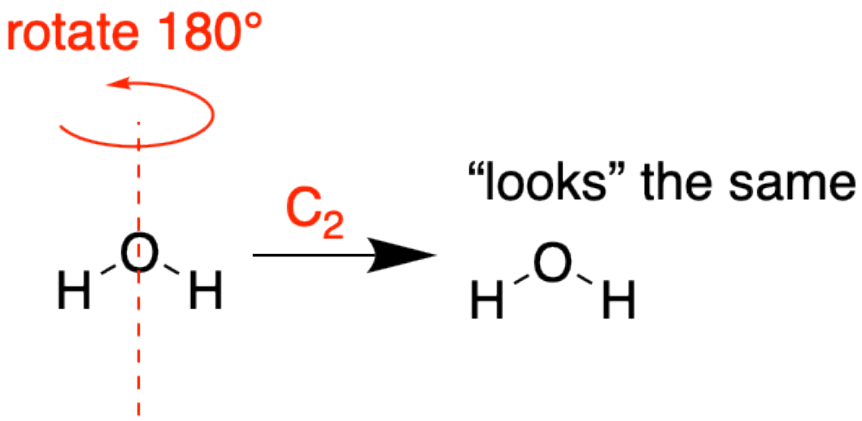


Figure 6.1.1: An example of a symmetry operation is a 180° rotation where the resulting position is indistinguishable from the original. A 180° rotation is called a C_2 operation; the axis of rotation is the symmetry element. (Kathryn Haas; CC-NC-BY-SA)

There are five types of symmetry operations including **identity**, **reflection**, **inversion**, **proper rotation**, and **improper rotation**. The improper rotation is the sum of a rotation followed by a reflection. The symmetry elements that correspond to the five types of symmetry operations are listed in Table 6.1.1.

Table 6.1.1: Table of elements and operations

Element	Operation	Symbol
Identity	identity	E
Proper axis	rotation by $(360/n)^o$	C_n
Symmetry plane	reflection in the plane	σ
Inversion center	inversion of a point at (x,y,z) to (-x,-y,-z)	*i*
Improper axis	rotation by $(360/n)^o$, followed by reflection in the plane perpendicular to the rotation axis	S_n

Symmetry Operations and Elements

Identity (E)

All molecules have the identity element. The identity operation is doing nothing to the molecule (it doesn't rotate, reflect, or invert...it just is).

Proper Rotation and Proper Axis (C_n)

A "proper" rotation is just a simple rotation operation about an axis. The symbol for any proper rotation or proper axis is $C_{(360/n)}$, where n is the degree of rotation. Thus, a 180° rotation is a C_2 rotation around a C_2 axis, and a 120° rotation is a C_3 rotation about a C_3 axis.

> **PRINCIPAL AXIS**: The principal axis of a molecule is the highest order proper rotation axis. For example, if a molecule had C_2 and C_4 axes, the C_4 is the principal axis.

Reflection and Symmetry Planes (σ)

Symmetry planes are mirror planes within the molecule. A reflection operation occurs with respect to a plane of symmetry. There are three classes of symmetry elements:

1. σ_h (horizontal): horizontal planes are perpendicular to principal axis
2. σ_v (vertical): vertical planes are parallel to the principal axis
3. σ_d (dihedral): dihedral planes are parallel to the principal axis and bisecting two C_2' axes

Inversion and Inversion Center (i)

The inversion operation requires a point of symmetry (a center of symmetry within a molecule). In other words, a point at the center of the molecule that can transform (x,y,z) into (-x,-y,-z) coordinate. Structures of tetrahedrons, triangles, and pentagons lack an inversion center.

Improper rotation (S_n)

Improper rotation is a combination of a rotation with respect to an axis of rotation (C_n), followed by a reflection through a plane perpendicular to that C_n axis. In short, an S_n operation is equivalent to C_n followed by σ_h.

References

1. Introduction to Molecular Symmetry by J. S Ogden
2. Inorganic Chemistry by Catherine Housecroft And Alan G. Sharpe.

This page titled 6.1: Symmetry Elements and Operations is shared under a license and was authored, remixed, and/or curated by LibreTexts.

- 4.1: Symmetry Elements and Operations by Kathryn Haas is licensed CC BY-NC-SA 4.0.

6.2: Successive Operations

Sometimes, new symmetry operations form by carrying out two or more simpler operations successively to result in an indistinguishable configuration. For example, the improper rotation axis that was introduced in the last section results from rotation about an axis of rotation (C_n) followed by reflection about a plane perpendicular to that axis (σ_h).

$$S_n = C_n \times \sigma_h$$

Note also that C_n in this case need not be a symmetry element for the molecule. For example, staggered ethane has an S_6 symmetry element although it does not have a C_6. Another example of a symmetry element that results from a combination of two different elements is the inversion center (i), which results from a C_2 rotation followed by a reflection about a plane perpendicular to that axis (σ_h).

$$i = C_2 \times \sigma_h$$

Note that an inversion center is a special case of an improper rotation axis because it results when, in the first equation, $n = 2$. That is,

$$i = S_2$$

In fact, any symmetry operation can be carried out multiple time in a row. For example, when BH_3 is rotated twice by 120°, the two-step operation can be symboled by C_3^2. When the C_3 operation is performed a third time, the molecule returns to its original configuration; i.e,

$$C_3^3 = E$$

In general,

$$C_n^n = E$$

This page titled 6.2: Successive Operations is shared under a license and was authored, remixed, and/or curated by LibreTexts.

- 3.3: Successive Operations is licensed CC BY-NC-SA 4.0.

6.3: Significance of Recognizing Symmetry Elements

In the forgoing sections of this chapter, the necessary tools to assign a point group to a molecule and to be able to read a character table were introduced. A good question at this point is: What is the importance of these tools in inorganic chemistry?

In fact, there are many applications in the study of inorganic chemistry where these symmetry tools become handy. In general, these applications belong to one of the following categories:

- Understanding the spectroscopic properties of moelcules (introduced in section 3.7);
- Determining the chirality of molecular species (introduced in section 3.8);
- Constructing molecular and hybrid orbitals (Chapter 5).

This page titled 6.3: Significance of Recognizing Symmetry Elements is shared under a license and was authored, remixed, and/or curated by LibreTexts.

- 3.6: Significance of Recognizing Symmetry Elements is licensed CC BY-NC-SA 4.0.

6.4: POINT GROUPS

Click here to see a lecture on this topic.

Introduction

A **Point Group** describes all the symmetry operations that can be performed on a molecule that result in a conformation indistinguishable from the original. Point groups are used in Group Theory, the mathematical analysis of groups, to determine properties such as a molecule's molecular orbitals.

Assigning Point Groups

While a point group contains all of the symmetry operations that can be performed on a given molecule, it is not necessary to identify all of these operations to determine the molecule's overall point group. Instead, a molecule's point group can be determined by following a set of steps which analyze the presence (or absence) of particular symmetry elements.

Steps for assigning a molecule's point group:

1. Determine if the molecule is of high or low symmetry.
2. If not, find the highest order rotation axis, C_n.
3. Determine whether the molecule has any C_2 axes perpendicular to the principal C_n axis. If so, then there are n such C_2 axes, and the molecule is in the D set of point groups. If not, it is in either the C or S set of point groups.
4. Determine whether the molecule has a horizontal mirror plane (σ_h) perpendicular to the principal C_n axis. If so, the molecule is either in the C_{nh} or D_{nh} set of point groups.
5. Determine whether the molecule has a vertical mirror plane (σ_v) containing the principal C_n axis. If so, the molecule is either in the C_{nv} or D_{nd} set of point groups. If not, and if the molecule has n perpendicular C_2 axes, then it is part of the D_n set of point groups.
6. Determine whether there is an improper rotation axis, S_{2n}, collinear with the principal C_n axis. If so, the molecule is in the S_{2n} point group. If not, the molecule is in the C_n point group.

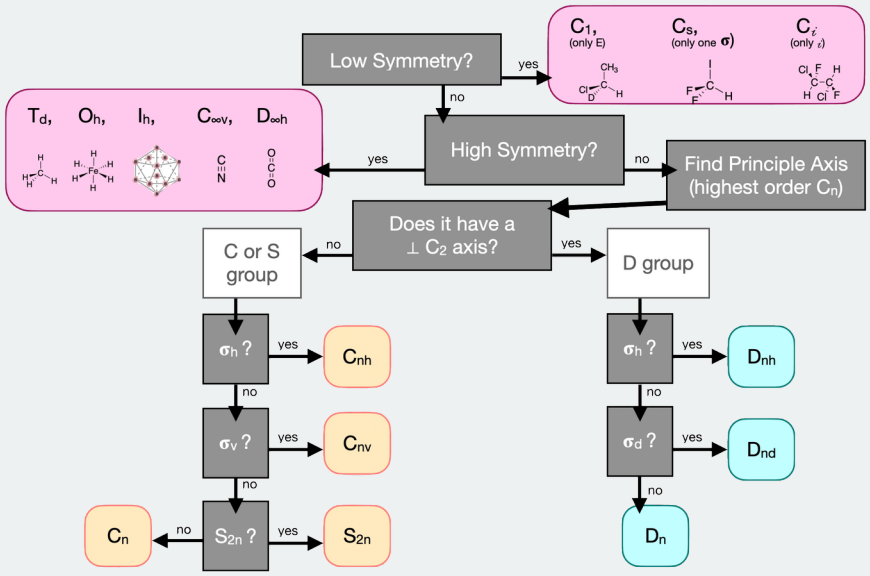


Figure 6.4.1: Decision tree for determining a molecule's point group (CC-BY-NC-SA; Kathryn Haas)

Example 6.4.1

Find the point group of benzene (C_6H_6).

Answer available at the end of this section.

See Also

Symmetry Gallery

Answers

Example 6.4.1

Solution

1. Benzene is neither high nor low symmetry
2. Highest order rotation axis: C_6
3. There are 6 C_2 axes perpendicular to the principal axis
4. There is a horizontal mirror plane (σ_h)

Benzene is in the D_{6h} point group.

6.4.1: Groups of Low and High Symmetry

6.4.2: Other Groups

This page titled 6.4: Point Groups is shared under a license and was authored, remixed, and/or curated by LibreTexts.

- 4.2: Point Groups by Kathryn Haas has no license indicated.

6.4.1: Groups of Low and High Symmetry

Click here to see a lecture on this topic.

Low Symmetry Point Groups

Low symmetry point groups include the C_1, C_s, and C_i groups

Group	Description	Example
C_1	only the identity operation (E)	CHFClBr
C_s	only the identity operation (E) and one mirror plane	C_2H_2ClBr
C_i	only the identity operation (E) and a center of inversion (i)	$C_2H_2Cl_2Br$

High Symmetry Point Groups

High symmetry point groups include the T_d, O_h, I_h, $C_{\infty v}$, and $D_{\infty h}$ groups. The table below describes their characteristic symmetry operations. The full set of symmetry operations included in the point group is described in the corresponding character table.

Group	Description	Example
$C_{\infty v}$	linear molecule with an infinite number of rotation axes and vertical mirror planes (σ_v)	HBr
$D_{\infty h}$	linear molecule with an infinite number of rotation axes, vertical mirror planes (σ_v), perpendicular C_2 axes, a horizontal mirror plane (σ_h), and an inversion center (i)	CO_2
T_d	typically have tetrahedral geometry, with 4 C_4 axes, 3 C_2 axes, 3 S_4 axes, and 6 dihedral mirror planes (σ_d)	CH_4
O_h	typically have octahedral geometry, with 3 C_4 axes, 4 C_3 axes, and an inversion center (i) as characteristic symmetry operations	SF_6
I_h	typically have an icosahedral structure, with 6 C_5 axes as characteristic symmetry operations	$B_{12}H_{12}^{2-}$

See Also

Symmetry Gallery

This page titled 6.4.1: Groups of Low and High Symmetry is shared under a license and was authored, remixed, and/or curated by LibreTexts.

- 4.2.1: Groups of Low and High Symmetry by Kathryn Haas has no license indicated.
- 1.2: Molecular Point Groups by Wikipedia is licensed CC BY-SA 4.0. Original source: https://en.wikibooks.org/wiki/Advanced_Inorganic_Chemistry.

6.4.2: Other Groups

Click here to see a lecture on this topic.

D Groups

The D set of point groups is classified as D_{nh}, D_{nd}, or D_n, where n refers to the principal axis of rotation. Overall, the D groups are characterized by the presence of n C_2 axes perpendicular to the principal C_n axis. Further classification of a molecule in the D groups depends on the presence of horizontal or vertical/dihedral mirror planes.

Group	Description	Example
D_{nh}	n perpendicular C_2 axes, and a horizontal mirror plane (σ_h)	benzene, C_6H_6 is D_{6h}
D_{nd}	n perpendicular C_2 axes, and a vertical mirror plane (σ_v)	propadiene, C_3H_4 is D_{2d}
D_n	n perpendicular C_2 axes, no mirror planes	$[Co(en)_3]^{3+}$ is D_3

C Groups

The C set of point groups is classified as C_{nh}, C_{nv}, or C_n, where n refers to the principal axis of rotation. The C set of groups is characterized by the absence of n C_2 axes perpendicular to the principal C_n axis. Further classification of a molecule in the C groups depends on the presence of horizontal or vertical/dihedral mirror planes.

Group	Description	Example
C_{nh}	horizontal mirror plane (σ_h) perpendicular to the principal C_n axis	boric acid, H_3BO_3, is C_{3h}
C_{nv}	vertical mirror plane (σ_v) containing the principal C_n axis	ammonia, NH_3, is C_{3v}
C_n	no mirror planes	$P(C_6H_5)_3$ is C_3

S Groups

The S set of point groups is classified as S_{2n}, where n refers to the principal axis of rotation. The S set of groups is characterized by the absence of n C_2 axes perpendicular to the principal C_n axis, as well as the absence of horizontal and vertical/dihedral mirror planes. However, there is an improper rotation (or a rotation-reflection) axis collinear with the principal C_n axis.

Group	Description	Example
S_{2n}	improper rotation (or a rotation-reflection) axis collinear with the principal C_n axis	12-crown-4 is S_4

See Also

Symmetry Gallery

This page titled 6.4.2: Other Groups is shared under a license and was authored, remixed, and/or curated by LibreTexts.

- 4.2.2: Other Groups by Kathryn Haas has no license indicated.
- 1.2: Molecular Point Groups by Wikipedia is licensed CC BY-SA 4.0. Original source: https://en.wikibooks.org/wiki/Advanced_Inorganic_Chemistry.

6.5: Character Tables - An Introduction

Although the method of assigning a point group to a molecule depends on some knowledge of the symmetry elements the molecule has, it does not require the consideration of all elements. For example, the molecule CO_2 can be assigned the point group $D_{\infty h}$ using the scheme in section 3.4 by merely knowing that the molecule is linear and that it has the a center io inversion i. The point group assignment in this case did not require knowing that the molecule also has σ_h, for example. This type of knowledge is gained by examining character tables.

Definition

A character table is a table that contains the symmetry information of the molecule. This information can be used to analyze the molecule's behavior in many application, among which is spectroscopy. Each point group has its own character table. The following table is the character table of the point group C_{2v}:

Table 1: *The character table of the point group C_{2v}.*

C_{2v}	E	C_2 (z)	σ_v(xz)	σ_v(yz)	h = 4	
A_1	1	1	1	1	z	x^2, y^2, z^2
A_2	1	1	-1	-1	R_z	xy
B_1	1	-1	1	-1	x, R_y	xz
B_2	1	-1	-1	1	y, R_x	yz

Understanding Character Tables

Symbols under the first column of the character tables

A (Mulliken Symbol)	(singly degenerate or one dimensional) symmetric with respect to rotation of the principle axis
B (Mulliken Symbol)	(singly degenerate or one dimensional) anti-symmetric with respect to rotation of the principle axis
E (Mulliken Symbol)	(doubly degenerate or two dimensional)
T (Mulliken Symbol)	(thirdly degenerate or three dimensional)
Subscript 1	symmetric with respect to the $C_n$principle axis, if no perpendicular axis, then it is with respect to σ_v
Subscript 2	anti-symmetric with respect to the $C_n$principle axis, if no perpendicular axis, then it is with respect to σ_v
Subscript g	symmetric with respect to the inverse
subscript u	anti-symmetric with respect to the inverse
prime	symmetric with respect to σ_h (reflection in horizontal plane)
double prime	anti-symmetric with respect to σ_h (opposite reflection in horizontal plane)

Symbols in the first row of the character tables

E	describes the degeneracy of the row (A and B= 1) (E=2) (T=3)

C_n	2pi/n= number of turns in one circle on the main axis without changing the look of a molecule (rotation of the molecule)
C_n'	2π/n= number of turns in one circle perpendicular to the main axis, without changing the structure of the molecule
C_n''	2π/n= number of turns in one circle perpendicular to the C_n' and the main axis, without changing the structure
σ'	reflection of the molecule perpendicular to the other sigma
σ_v (vertical)	reflection of the molecule vertically compared to the horizontal highest fold axis.
σ_h or σ_d (horizontal)	reflection of the molecule horizontally compared to the horizontal highest fold axis.
i	Inversion of the molecule from the center
S_n	rotation of 2π/n and then reflected in a plane perpendicular to rotation axis.
#C_n	the # stands for the number of irreducible representation for the C_n
#σ	the # stands for the number irreducible representations for the sigmas.
the number in superscript	in the same rotation there is another rotation, for instance O_h has $3C_2=C_4^2$
other useful definitions	
(R_x,R_y)	the (,) means they are the same and can be counted once.
x^2+y^2, z^2	without (,) means they are different and can be counted twice.

This page titled 6.5: Character Tables - An Introduction is shared under a license and was authored, remixed, and/or curated by LibreTexts.

- 3.5: Character Tables - An Introduction is licensed CC BY-NC-SA 4.0.

6.6: Character Tables

Introduction to Character Tables, using C_{2v} as example

A character table is the complete set of irreducible representations of a symmetry group. In the previous section, we derived three of the four irreducible representations for the C_{2v} point group. These three irreducible representations are labeled A_1, B_1, and B_2. The fourth irreducible representation, A_2, can be derived using the properties (or "rules") for irreducible representations listed below.

Properties of Characters of Irreducible Representations in Point Groups

1. There is always a totally symmetric representation in which all the characters are 1.
   e.g. In C_{2v}, A_1 is totally symmetric.
2. The order of the group (h) is the total number of symmetry operations in the group.
   e.g. In C_{2v}, $h = 4$
3. Similar operations are listed as classes (R) and appear as columns in the table.
   e.g. In C_{2v}, there are four classes of operations, E, C_2, $\sigma_{v(xz)}$, and $\sigma'_{v(yz)}$
4. The number of irreducible representations (rows) must equal the number of classes (columns). This results in all character tables being square.
   e.g. In C_{2v}, there are four classes and four irreducible representations.
5. The sum of squares of all characters under E is equal to the order of the group: $h = \sum [\chi_i]^2$
   e.g. In C_{2v}, $h = 1^2 + 1^2 + 1^2 + 1^2 = 4$
6. For any irreducible representation (i), the sum of squares of its characters multiplied by the number of operations in the class is the order of the group: $h = \sum [\chi_i(R)]^2$
   e.g. For A_2 in C_{2v}, $h = (1 \times 1)^2 + (1 \times 1)^2 + (-1 \times 1)^2 + (-1 \times 1)^2 = 4$
7. Irreducible representations are orthogonal. For any two representations (i and j): $\sum[\chi_i * (R)\chi_j(R)] = 0$
   e.g. For B_1 and B_2 of C_{2v}, $[1 \times 1] + [-1 \times -1] + [1 \times -1] + [-1 \times 1] = 0$

The complete character table for C_{2v} is given below.

C_{2v}	E	C_2	σ_v	σ'_v	$h = 4$	
A_1	1	1	1	1	z	x^2, y^2, z^2
A_2	1	1	-1	-1	R_z	xy
B_1	1	-1	1	-1	x, R_y	xz
B_2	1	-1	-1	1	y, R_x	yz

The various sections of the table are as follows:

i. The first element in the table gives the name of the point group, usually in Schoenflies (C_{2v}) notation.
ii. Along the first row are the symmetry operations of the group, E, C_2, σ_v and σ_v ″, followed by the order of the group, h.
iii. In the first column are the irreducible representations of the group, represented by Mulliken Labels. In C_{2v} the irreducible representations are A_1, A_2, B_1 and B_2. The Mulliken labels indicate the symmetry of each representation (explained further below).
iv. The characters (χ) of the irreducible representations under each symmetry operation are given in the bulk of the table.
v. The final column(s) of the table lists a number of functions that transform as the various irreducible representations of the group. These are the Cartesian axes (x, y, z), the Cartesian products $(z^2, x^2 + y^2, xy, xz, yz)$, and the rotations (R_x, R_y, R_z) (explained further below).

Another example: C_{3v}

Th C_{3v} point group has three classes of operations: E, C_3, and $\sigma_{v(xz)}$. The derivation of transformation matrices for E and $\sigma_{v(xz)}$ is similar to the case for C_{2v}. However, the C_{3v} operation does not give simple 1 or -1 characters. If we carry out a rotation about z by

an angle θ, our x and y axes are transformed onto new axes x' and y'. The new axes can each be written as a linear combination of our original x and y axes. The derivation of the rotation matrices will not be covered in this text, but is described elsewhere:

$$\begin{aligned} x' &= x\cos\theta + y\sin\theta \\ y' &= -x\sin\theta + y\cos\theta \end{aligned}$$

For a C_3 rotation counterclockwise through 120° (or $\frac{2\pi}{3}$):

$$\begin{aligned} x' &= x\cos(2\pi/3) + y\sin(2\pi/3) &&= -\tfrac{1}{2}x - \tfrac{\sqrt{3}}{2}y \\ y' &= -x\sin(2\pi/3) + y\cos(2\pi/3) &&= \tfrac{\sqrt{3}}{2}x - \tfrac{1}{2}y \end{aligned}$$

The transformation matrices for symmetry operations of C_{3v} are as follows:

$$E = \begin{pmatrix} 1 & 0 & 0 \\ 0 & 1 & 0 \\ 0 & 0 & 1 \end{pmatrix} \; C_3 = \begin{pmatrix} -\frac{1}{2} & -\frac{\sqrt{3}}{2} & 0 \\ \frac{\sqrt{3}}{2} & -\frac{1}{2} & 0 \\ 0 & 0 & 1 \end{pmatrix} \; \sigma'_{v(xz)} = \begin{pmatrix} 1 & 0 & 0 \\ 0 & -1 & 0 \\ 0 & 0 & 1 \end{pmatrix}$$

The C_3 transformation matrix contains off-diagonal entries, and therefore it cannot be block diagonalized as 1x1 matrices. However, the first two lines can be diagonalized as a 2x2 and the last line as a 1x1 matrix (Figure 6.6.1):

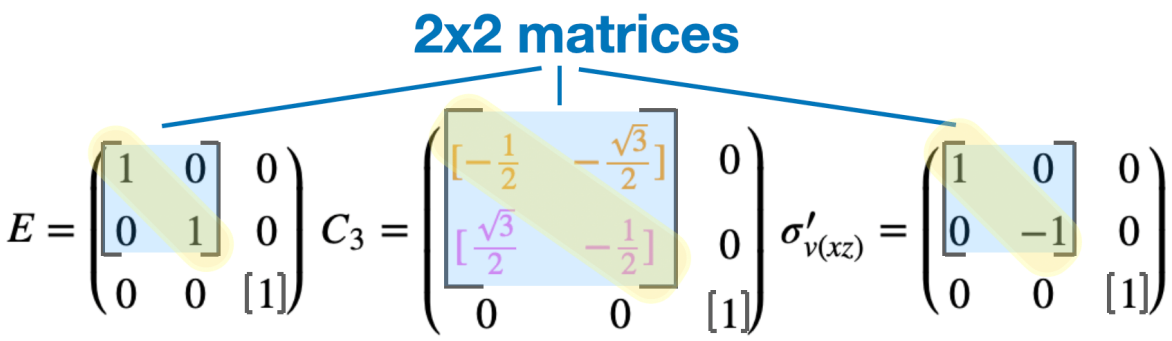


Figure 6.6.1: The C_3 transformation matrix contains off-diagonal entries, and therefore it cannot be block diagonalized as 1x1 matrices. However, the first two lines can be diagonalized as a 2x2 and the last line as a 1x1 matrix. (CC-BY-NC-SA; Kathryn Haas)

The character from a 2x2 matrix is the sum of the trace of that matrix. So, for the C_3 operation, the 2x2 matrix gives the character -1 (from $-\frac{1}{2} + -\frac{1}{2}$).

The character table for C_{3v} is shown below.

C_{3v}	E	$2C_3$	$3\sigma_v$	$h = 6$
A_1	1	1	1	$z, z^2, x^2 + y^2$
A_2	1	1	−1	R_z
E	2	−1	0	$(x, y), (xy, x^2 + y^2), (xz, yz), (R_x, R_y)$

Additional features of character tables

Additional Features of Character Tables

1. Symmetry operations of the same class are grouped into the same column (class) in the character table and not listed separately.
   e.g. In the C_{3v} point group, there are four operations: E, C_3, C_3^2, and σ_v. The C_3 and C_3^2 operations are listed together in the character table as $2C_3$.
2. IF there are multiple C_2 axes (in a D group), the C_2 axes that are perpendicular to the principle axis are labeled with primes (e.g. C_2' and C_2''); when there are multiple types of perpendicular C_2 axes, one prime (C_2') means that it passes through more atoms, while a double prime (C_2'') means it goes between atoms.

3. Mirror planes that are perpendicular to the principle axis are "horizontal" mirror planes and are designated with an h subscript (σ_h). Mirror planes that are in-plane with the principle axis are "vertical" mirror planes, σ_v. When there are two types of vertical mirror planes, those that run through more atoms are σ_v while those that run between atoms are "dihedral", σ_d.
4. Matching the symmetry operations listed in the character table to the symmetry operations of a molecule can confirm its point group.
5. Irreducible representations are each assigned a Mulliken label, listed in the left-hand column, that indicates the symmetry of that representation as follows:

Mulliken Labels	**meaning**
A	singly degenerate (1x1), symmetric to principle axis
B	singly degenerate (1x1), antisymmetric to principle axis
E	doubly degenerate (2x2)
T	triply degenerate (3x3)
Subscripts and superscripts	**meaning**
1	symmetric to $\sigma_v$or perpendicular to C_2
2	anti-symmetric to $\sigma_v$or perpendicular to C_2
g	symmetric to inversion center
u	anti-symmetric to inversion center
$'$	symmetric to σ_h
$''$	anti-symmetric to σ_h

6. The right-hand columns of the character table list a number of functions that transform as the various irreducible representations of the group. These are the Cartesian axes (x, y, z), the Cartesian products $(z^2, x^2 + y^2, xy, xz, yz)$, and the rotations (R_x, R_y, R_z). These expressions indicate the properties of orbitals within the symmetry group. The s-orbital, which is totally symmetric, corresponds to the irreducible representation that possesses symmetry of x^2, y^2 and z^2 combined. The p-orbitals each possess the symmetry of the corresponding axis (e.g. p_x corresponds to the x axis). Each of the d-orbitals possess the symmetry of the corresponding binary product (e.g. d_{xy} corresponds to the binary product, xy, in the character table).

The functions listed in the final column of the table are important in many chemical applications of group theory, particularly in spectroscopy. For example, by looking at the transformation properties of x, y and z (sometimes given in character tables as T_x, T_y, T_z) we can discover the symmetry of translations along the x, y, and z axes. Similarly, R_x, R_y and R_z represent rotations about the three Cartesian axes. The transformation properties of x, y, and z can be used to determine whether or not a molecule is IR-active or whether or not it can absorb a photon of x-, y-, or z-polarized light and undergo a spectroscopic transition. The Cartesian products play a similar role in determining selection rules for Raman transitions, which involve two photons.

A visual summary of the sections and their significance is given in Figure 6.6.2. Character tables for common point groups are given in the References section of LibreTexts Bookshelves.

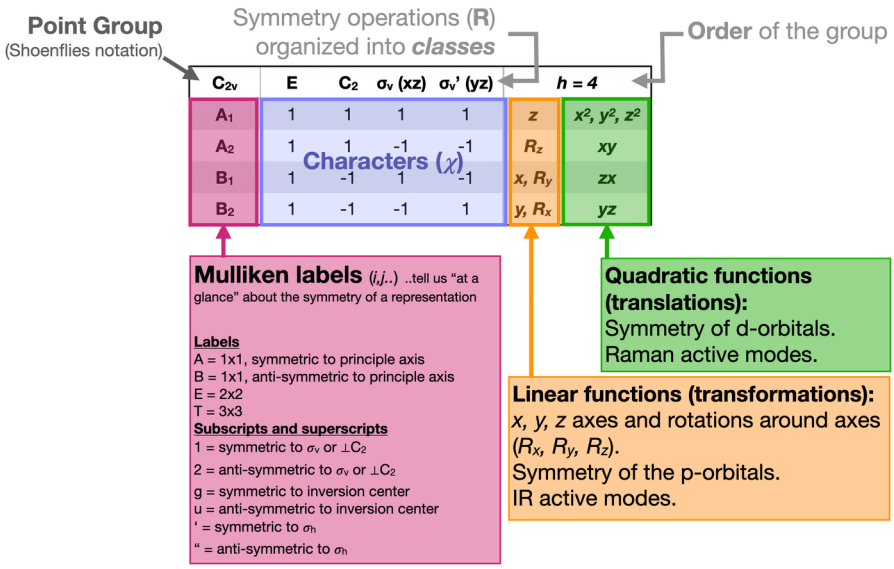


Figure 6.6.2: Visual summary of the sections of a character table and their meaning. (CC-BY-NC-SA; Kathryn Haas)

Contributors and Attributions

- Curated or created by Kathryn Haas
- Claire Vallance (University of Oxford)

  adapted from Character Tables (click here)

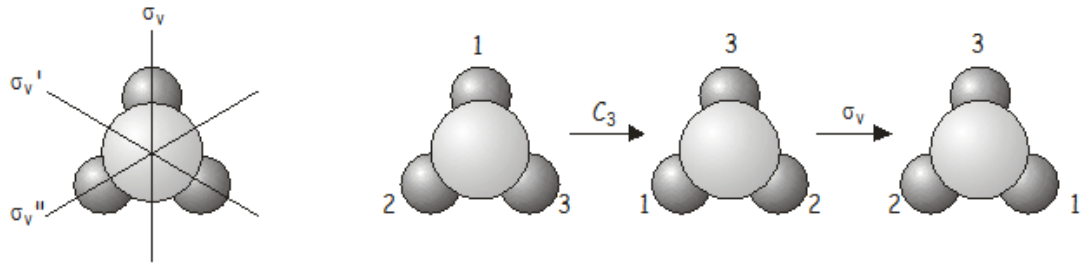
This page titled 6.6: Character Tables is shared under a license and was authored, remixed, and/or curated by Kathryn Haas.

- 4.3.3: Character Tables by Kathryn Haas is licensed CC BY-NC-SA 4.0.

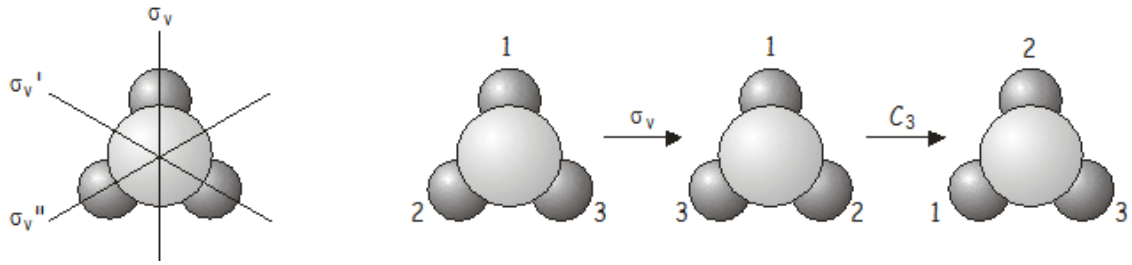
6.7: PROPERTIES AND REPRESENTATIONS OF GROUPS

Group Multiplication

Now we will investigate what happens when we apply two symmetry operations in sequence. As an example, consider the NH_3 molecule, which belongs to the C_{3v} point group. Consider what happens if we apply a C_3rotation (120˚ counter-clockwise) followed by a σ_v reflection (reflection over the σ_v axis). We write this combined operation $\sigma_v C_3$ (when written, symmetry operations operate on the thing directly to their right, just as operators do in quantum mechanics – we therefore have to work backwards from right to left from the notation to get the correct order in which the operators are applied). As we shall soon see, the order in which the operations are applied is important.



The combined operation $\sigma_v C_3$ is equivalent to σ_v'' (note the double prime on σ_v''!), which is also a symmetry operation of the C_{3v} point group. Now let's see what happens if we apply the operators in the reverse order, i.e., $C_3\sigma_v$ is (σ_v followed by C_3).



Again, the combined operation $C_3\sigma_v$ is equivalent to another operation of the point group, this time σ_v' (note the single prime on σ_v'!).

There are two important points that are illustrated by this example:

1. The order in which two operations are applied is important. For two symmetry operations A and B, AB is not necessarily the same as BA, i.e. symmetry operations do not in general ***commute***. In some groups the symmetry elements do commute; such groups are said to be ***Abelian***.
2. If two operations from the same point group are applied in sequence, the result will be equivalent to another operation from the point group. Symmetry operations that are related to each other by other symmetry operations of the group are said to belong to the same ***class***. In NH_3, the three mirror planes σ_v, σ_v' and σ_v'' belong to the same class (related to each other through a C_3 rotation), as do the rotations C_3^+ and C_3^- (anticlockwise and clockwise rotations about the principal axis, related to each other by a vertical mirror plane).

Four Properties of Mathematical Groups

Now that we have explored some of the properties of symmetry operations and elements and their behavior within point groups, we are ready to introduce the formal mathematical definition of a group. The definitions below will be put into the context of *molecular* symmetry.

A mathematical group is defined as a set of elements (A_1, A_2, A_3...) together with a rule for forming combinations A_i,A_j... For our purposes, A_1, A_2, A_3, etc. are symmetry elements and A_i, A_j, etc. are symmetry operations described in a previous section. The elements of the group and the rule for combining them must satisfy the following four criteria.

1. The group must include the **identity** E, which commutes with other members of the group. In other terms, $EA_i = A_i$ for all the elements of the group. Application of the identity operation before or after another operation, A_i, results in the same outcome as A_i alone.
2. The elements must satisfy the group property that the combination of any pair of elements is also an element of the group. For example, in the C_{3v} point group, a C_3 rotation followed by a σ_v gives another operation that is already part of the group: a σ_v ″.
3. Each symmetry operation A_i must have an inverse A_i^{-1}, which is also an element of the group, such that
$$A_i A_i^{-1} = A_i^{-1} A_i = E$$
The inverse g_i^{-1} effectively 'undoes' the effect of the symmetry operation g_i. For example, in the C_{3v} point group, the inverse of C_3^+ is C_3^-.
4. The rule of combination must be associative
$$(A_i A_j)(A_k) = A_i(A_j A_k)$$
Or $A(BC) = (AB)C$. In other words, the order of operations should not matter.

Group theory is an important area in mathematics, and luckily for chemists the mathematicians have already done most of the work for us. Along with the formal definition of a group comes a comprehensive mathematical framework that allows us to carry out a rigorous treatment of symmetry in molecular systems and learn about its consequences.

Many problems involving operators or operations (such as those found in quantum mechanics or group theory) may be reformulated in terms of matrices. Any of you who have come across transformation matrices before will know that symmetry operations such as rotations and reflections may be represented by matrices. It turns out that the set of matrices representing the symmetry operations in a group obey all the conditions laid out above in the mathematical definition of a group, and using matrix representations of symmetry operations simplifies carrying out calculations in group theory. Before we learn how to use matrices in group theory, it will probably be helpful to review some basic definitions and properties of matrices.

*This page was adapted from here (click).

Contributors and Attributions

- Claire Vallance (University of Oxford)
- Curated or created by Kathryn Haas

6.7.1: Matrices

6.7.2: Representations of Point Groups

This page titled 6.7: Properties and Representations of Groups is shared under a license and was authored, remixed, and/or curated by LibreTexts.

- 4.3: Properties and Representations of Groups by Kathryn Haas is licensed CC BY-NC-SA 4.0.

6.7.1: Matrices

The symmetry of molecules is essential for understanding the structures and properties of organic and inorganic compounds. The properties of chemical compounds are often easily explained by consideration of symmetry. For example, the symmetry of a molecule determines whether the molecule has a permanent dipole moment or not. The theories that describe optical activity, infrared and ultraviolet spectroscopy, and crystal structure involve the application of symmetry considerations. Matrix algebra is the most important mathematical tool in the description of symmetry.

The properties of symmetry groups are organized in character tables (discussed later in this chapter). Character tables are constructed based on matrices. This page is a brief description of matrices and matrix multiplication.

What is a matrix?

An $m \times n$ matrix $\mathbf{A}$ is a rectangular array of numbers with m rows and n columns. The numbers m and n are the dimensions of $\mathbf{A}$. The numbers in the matrix are called its entries. The entry in row i and column j is called a_{ij}.

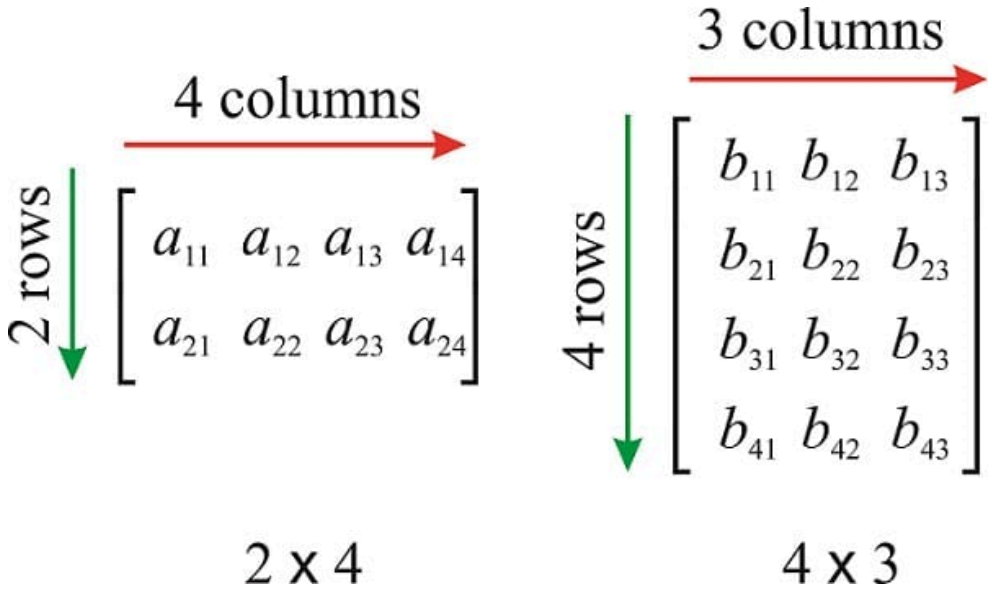


Figure 6.7.1.1: Matrices of different dimensions

Some types of matrices have special names:

- A square matrix:

$$\begin{pmatrix} 3 & -2 & 4 \\ 5 & 3i & 3 \\ -i & 1/2 & 9 \end{pmatrix}$$

  with $m = n$
- A rectangular matrix:

$$\begin{pmatrix} 3 & -2 & 4 \\ 5 & 3i & 3 \end{pmatrix}$$

  with $m \neq n$
- A column vector:

$$\begin{pmatrix} 3 \\ 5 \\ -i \end{pmatrix}$$

with $n = 1$

- A row vector:

$$\begin{pmatrix} 3 & -2 & 4 \end{pmatrix}$$

with $m = 1$

- The identity matrix:

$$\begin{pmatrix} 1 & 0 & 0 \\ 0 & 1 & 0 \\ 0 & 0 & 1 \end{pmatrix}$$

with $a_{ij} = \delta_{i,j}$, where $\delta_{i,j}$ is a function defined as $\delta_{i,j} = 1$ if $i = j$ and $\delta_{i,j} = 0$ if $i \neq j$.

- A diagonal matrix:

$$\begin{pmatrix} a & 0 & 0 \\ 0 & b & 0 \\ 0 & 0 & c \end{pmatrix}$$

with $a_{ij} = c_i \delta_{i,j}$.

- An upper triangular matrix:

$$\begin{pmatrix} a & b & c \\ 0 & d & e \\ 0 & 0 & f \end{pmatrix}$$

All the entries below the main diagonal are zero.

- A lower triangular matrix:

$$\begin{pmatrix} a & 0 & 0 \\ b & c & 0 \\ d & e & f \end{pmatrix}$$

All the entries above the main diagonal are zero.

- A triangular matrix is one that is either lower triangular or upper triangular.

The Trace of a Matrix

The trace of an $n \times n$ square matrix $\mathbf{A}$ is the sum of the diagonal elements, and formally defined as $Tr(\mathbf{A}) = \sum_{i=1}^{n} a_{ii}$.

For example,

$$\mathbf{A} = \begin{pmatrix} 3 & -2 & 4 \\ 5 & 3i & 3 \\ -i & 1/2 & 9 \end{pmatrix} ; Tr(\mathbf{A}) = 12 + 3i$$

Singular and Nonsingular Matrices

A square matrix with nonzero determinant is called *nonsingular*. A matrix whose determinant is zero is called *singular*. (Note that you cannot calculate the determinant of a non-square matrix).

For a 2x2 matrix,

$$\mathbf{B} = \begin{pmatrix} a & b \\ c & d \end{pmatrix} ; det(\mathbf{B}) = ad - cb$$

For a 3x3 matrix,

$$\mathbf{C} = \begin{pmatrix} a & b & c \\ d & e & f \\ g & h & i \end{pmatrix}$$

$$det(\mathbf{C}) = a \begin{pmatrix} e & f \\ h & i \end{pmatrix} - b \begin{pmatrix} d & f \\ g & i \end{pmatrix} + c \begin{pmatrix} d & e \\ g & h \end{pmatrix}$$

$$det(\mathbf{C}) = aei - ahf - bdi + bgf + cdh - cge$$

The Matrix Transpose

The matrix transpose, most commonly written $\mathbf{A}^T$, is the matrix obtained by exchanging $\mathbf{A}$'s rows and columns. It is obtained by replacing all elements a_{ij} with a_{ji}. For example:

$$\mathbf{A} = \begin{pmatrix} 3 & -2 & 4 \\ 5 & 3i & 3 \end{pmatrix} \rightarrow \mathbf{A}^T = \begin{pmatrix} 3 & 5 \\ -2 & 3i \\ 4 & 3 \end{pmatrix}$$

Matrix Multiplication

To multiply two matrices, the number of vertical columns in the first matrix must be the same as the number of rows in the second matrix. If $\mathbf{A}$ has dimensions $m \times n$ and $\mathbf{B}$ has dimensions $n \times p$, then the product $\mathbf{AB}$ is defined, and has dimensions $m \times p$.

$$c_{ij} = \sum a_{ij} \times b_{ij}$$

The entry $a_{ij} \times b_{ij}$ is obtained by multiplying row i of $\mathbf{A}$ by column j of $\mathbf{B}$, which is done by multiplying corresponding entries together and then adding the results:

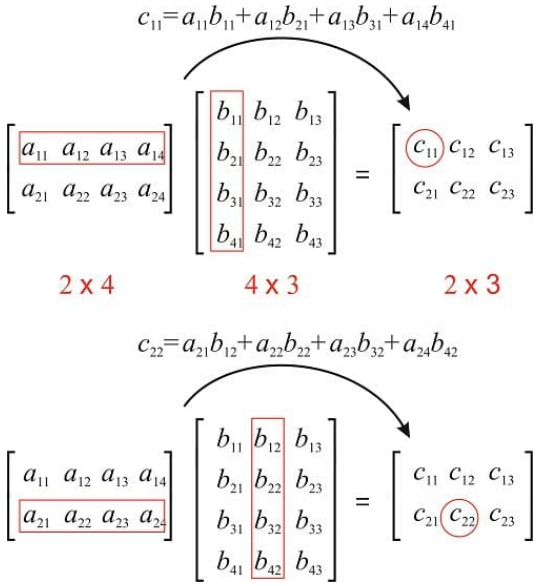


Figure 6.7.1.1: Matrix multiplication

Example 6.7.1.1

Calculate the product

$$\begin{pmatrix} 1 & -2 & 4 \\ 5 & 0 & 3 \\ 0 & 1/2 & 9 \end{pmatrix} \begin{pmatrix} 1 & 0 \\ 5 & 3 \\ -1 & 0 \end{pmatrix}$$

Solution

We need to multiply a 3×3 matrix by a 3×2 matrix, so we expect a 3×2 matrix as a result.

$$\begin{pmatrix}1 & -2 & 4\\ 5 & 0 & 3\\ 0 & 1/2 & 9\end{pmatrix}\begin{pmatrix}1 & 0\\ 5 & 3\\ -1 & 0\end{pmatrix}=\begin{pmatrix}a & b\\ c & d\\ e & f\end{pmatrix}$$

To calculate a, which is entry (1,1), we use row 1 of the matrix on the left and column 1 of the matrix on the right:

$$\begin{pmatrix}1 & -2 & 4\\ 5 & 0 & 3\\ 0 & 1/2 & 9\end{pmatrix}\begin{pmatrix}1 & 0\\ 5 & 3\\ -1 & 0\end{pmatrix}=\begin{pmatrix}a & b\\ c & d\\ e & f\end{pmatrix}\rightarrow a=1\times 1+(-2)\times 5+4\times(-1)=-13$$

To calculate b, which is entry (1,2), we use row 1 of the matrix on the left and column 2 of the matrix on the right:

$$\begin{pmatrix}1 & -2 & 4\\ 5 & 0 & 3\\ 0 & 1/2 & 9\end{pmatrix}\begin{pmatrix}1 & 0\\ 5 & 3\\ -1 & 0\end{pmatrix}=\begin{pmatrix}a & b\\ c & d\\ e & f\end{pmatrix}\rightarrow b=1\times 0+(-2)\times 3+4\times 0=-6$$

To calculate c, which is entry (2,1), we use row 2 of the matrix on the left and column 1 of the matrix on the right:

$$\begin{pmatrix}1 & -2 & 4\\ 5 & 0 & 3\\ 0 & 1/2 & 9\end{pmatrix}\begin{pmatrix}1 & 0\\ 5 & 3\\ -1 & 0\end{pmatrix}=\begin{pmatrix}a & b\\ c & d\\ e & f\end{pmatrix}\rightarrow c=5\times 1+0\times 5+3\times(-1)=2$$

To calculate d, which is entry (2,2), we use row 2 of the matrix on the left and column 2 of the matrix on the right:

$$\begin{pmatrix}1 & -2 & 4\\ 5 & 0 & 3\\ 0 & 1/2 & 9\end{pmatrix}\begin{pmatrix}1 & 0\\ 5 & 3\\ -1 & 0\end{pmatrix}=\begin{pmatrix}a & b\\ c & d\\ e & f\end{pmatrix}\rightarrow d=5\times 0+0\times 3+3\times 0=0$$

To calculate e, which is entry (3,1), we use row 3 of the matrix on the left and column 1 of the matrix on the right:

$$\begin{pmatrix}1 & -2 & 4\\ 5 & 0 & 3\\ 0 & 1/2 & 9\end{pmatrix}\begin{pmatrix}1 & 0\\ 5 & 3\\ -1 & 0\end{pmatrix}=\begin{pmatrix}a & b\\ c & d\\ e & f\end{pmatrix}\rightarrow e=0\times 1+1/2\times 5+9\times(-1)=-13/2$$

To calculate f, which is entry (3,2), we use row 3 of the matrix on the left and column 2 of the matrix on the right:

$$\begin{pmatrix}1 & -2 & 4\\ 5 & 0 & 3\\ 0 & 1/2 & 9\end{pmatrix}\begin{pmatrix}1 & 0\\ 5 & 3\\ -1 & 0\end{pmatrix}=\begin{pmatrix}a & b\\ c & d\\ e & f\end{pmatrix}\rightarrow f=0\times 0+1/2\times 3+9\times 0=3/2$$

The result is:

$$\begin{pmatrix}1 & -2 & 4\\ 5 & 0 & 3\\ 0 & 1/2 & 9\end{pmatrix}\begin{pmatrix}1 & 0\\ 5 & 3\\ -1 & 0\end{pmatrix}=\begin{pmatrix}-13 & -6\\ 2 & 0\\ -13/2 & 3/2\end{pmatrix}$$

Example 6.7.1.2

Calculate

$$\begin{pmatrix}1 & -2 & 4\\ 5 & 0 & 3\end{pmatrix}\begin{pmatrix}1\\ 5\\ -1\end{pmatrix}$$

Solution

We are asked to multiply a 2×3 matrix by a 3×1 matrix (a column vector). The result will be a 2×1 matrix (a vector).

$$\begin{pmatrix} 1 & -2 & 4 \\ 5 & 0 & 3 \end{pmatrix} \begin{pmatrix} 1 \\ 5 \\ -1 \end{pmatrix} = \begin{pmatrix} a \\ b \end{pmatrix}$$

$$a = 1 \times 1 + (-2) \times 5 + 4 \times (-1) = -13$$

$$b = 5 \times 1 + 0 \times 5 + 3 \times (-1) = 2$$

The solution is:

$$\begin{pmatrix} 1 & -2 & 4 \\ 5 & 0 & 3 \end{pmatrix} \begin{pmatrix} 1 \\ 5 \\ -1 \end{pmatrix} = \begin{pmatrix} -13 \\ 2 \end{pmatrix}$$

Need help? The link below contains solved examples: Multiplying matrices of different shapes (three examples): http://tinyurl.com/kn8ysqq

External links:

- Multiplying matrices, example 1: http://patrickjmt.com/matrices-multiplying-a-matrix-by-another-matrix/
- Multiplying matrices, example 2: http://patrickjmt.com/multiplying-matrices-example-2/
- Multiplying matrices, example 3: http://patrickjmt.com/multiplying-matrices-example-3/

The Commutator

Matrix multiplication is not, in general, commutative. For example, we can perform

$$\begin{pmatrix} 1 & -2 & 4 \\ 5 & 0 & 3 \end{pmatrix} \begin{pmatrix} 1 \\ 5 \\ -1 \end{pmatrix} = \begin{pmatrix} -13 \\ 2 \end{pmatrix}$$

but cannot perform

$$\begin{pmatrix} 1 \\ 5 \\ -1 \end{pmatrix} \begin{pmatrix} 1 & -2 & 4 \\ 5 & 0 & 3 \end{pmatrix}$$

Even with square matrices, that can be multiplied both ways, multiplication is not commutative. In this case, it is useful to define the **commutator**, defined as:

$$[\mathbf{A}, \mathbf{B}] = \mathbf{AB} - \mathbf{BA}$$

Example 6.7.1.3

Given $\mathbf{A} = \begin{pmatrix} 3 & 1 \\ 2 & 0 \end{pmatrix}$ and $\mathbf{B} = \begin{pmatrix} 1 & 0 \\ -1 & 2 \end{pmatrix}$

Calculate the commutator $[\mathbf{A}, \mathbf{B}]$

Solution

$$[\mathbf{A}, \mathbf{B}] = \mathbf{AB} - \mathbf{BA}$$

$$\mathbf{AB} = \begin{pmatrix} 3 & 1 \\ 2 & 0 \end{pmatrix} \begin{pmatrix} 1 & 0 \\ -1 & 2 \end{pmatrix} = \begin{pmatrix} 3 \times 1 + 1 \times (-1) & 3 \times 0 + 1 \times 2 \\ 2 \times 1 + 0 \times (-1) & 2 \times 0 + 0 \times 2 \end{pmatrix} = \begin{pmatrix} 2 & 2 \\ 2 & 0 \end{pmatrix}$$

$$\mathbf{BA} = \begin{pmatrix} 1 & 0 \\ -1 & 2 \end{pmatrix} \begin{pmatrix} 3 & 1 \\ 2 & 0 \end{pmatrix} = \begin{pmatrix} 1\times 3 + 0 \times 2 & 1 \times 1 + 0 \times 0 \\ -1 \times 3 + 2 \times 2 & -1 \times 1 + 2 \times 0 \end{pmatrix} = \begin{pmatrix} 3 & 1 \\ 1 & -1 \end{pmatrix}$$

$$[\mathbf{A}, \mathbf{B}] = \mathbf{AB} - \mathbf{BA} = \begin{pmatrix} 2 & 2 \\ 2 & 0 \end{pmatrix} - \begin{pmatrix} 3 & 1 \\ 1 & -1 \end{pmatrix} = \begin{pmatrix} -1 & 1 \\ 1 & 1 \end{pmatrix}$$

$$[\mathbf{A}, \mathbf{B}] = \begin{pmatrix} -1 & 1 \\ 1 & 1 \end{pmatrix}$$

Multiplication of a vector by a scalar

The multiplication of a vector $\vec{v}_1$ by a scalar n produces another vector of the same dimensions that lies in the same direction as $\vec{v}_1$;

$$n \begin{pmatrix} x \\ y \end{pmatrix} = \begin{pmatrix} nx \\ ny \end{pmatrix}$$

The scalar can stretch or compress the length of the vector, but cannot rotate it (figure [fig:vector_by_scalar]).

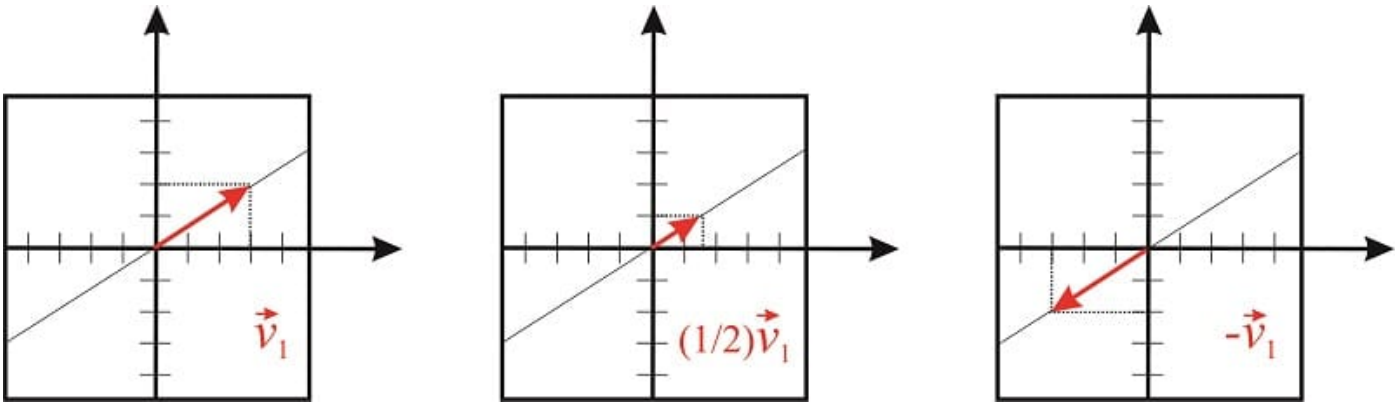


Figure 6.7.1.2: Multiplication of a vector by a scalar

Multiplication of a square matrix by a vector

The multiplication of a vector $\vec{v}_1$ by a square matrix produces another vector of the same dimensions of $\vec{v}_1$. For example, we can multiply a 2×2 matrix and a 2-dimensional vector:

$$\begin{pmatrix} a & b \\ c & d \end{pmatrix} \begin{pmatrix} x \\ y \end{pmatrix} = \begin{pmatrix} ax + by \\ cx + dy \end{pmatrix}$$

For example, consider the matrix

$$\mathbf{A} = \begin{pmatrix} -2 & 0 \\ 0 & 1 \end{pmatrix}$$

The product

$$\begin{pmatrix} -2 & 0 \\ 0 & 1 \end{pmatrix} \begin{pmatrix} x \\ y \end{pmatrix}$$

is

$$\begin{pmatrix} -2x \\ y \end{pmatrix}$$

We see that 2×2 matrices act as operators that transform one 2-dimensional vector into another 2-dimensional vector. This

particular matrix keeps the value of y constant and multiplies the value of x by -2 (Figure $6.7.1.3$).

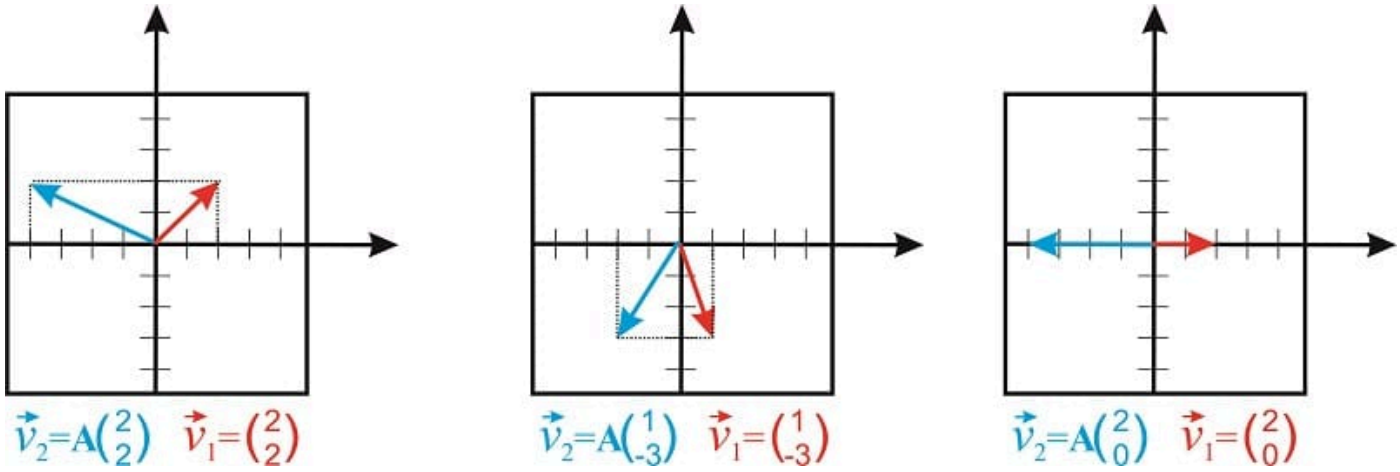


Figure $6.7.1.3$: Multiplication of a vector by a square matrix

Notice that matrices are useful ways of representing operators that change the orientation and size of a vector. An important class of operators that are of particular interest to chemists are the so-called symmetry operators.

Attribution

This page was adapted from Matrices (click here), contributed by Marcia Levitus, Associate Professor (Biodesign Institute) at Arizona State University.

Curated or created by Kathryn Haas

This page titled 6.7.1: Matrices is shared under a license and was authored, remixed, and/or curated by LibreTexts.

- 4.3.1: Matrices by Kathryn Haas is licensed CC BY-NC-SA 4.0.

6.7.2: Representations of Point Groups

Symmetry Operations: Matrix Representations

A **symmetry operation**, such as a rotation around a symmetry axis or a reflection through a plane, is an operation that, when performed on an object, results in a new orientation of the object that is indistinguishable from the original. For example, if we rotate a square in the plane by $\pi/2$ or π, the new orientation of the square is superimposable on the original one (Figure $6.7.2.1$).

If rotation by an angle θ of a molecule (or object) about some axis results in an orientation of the molecule (or object) that is superimposable on the original, the axis is called a rotation axis. The molecule (or object) is said to have an n-fold rotational axis, where n is $2\pi/\theta$. The axis is denoted as C_n. The square of Figure $6.7.2.1$ has a C_4 axis perpendicular to the plane because a 90° rotation leaves the figure indistinguishable from the initial orientation. This axis is also a C_2 axis because a 180° degree rotation leaves the square indistinguishable from the original square. In addition, the figure has several other C_2 axis that lie on the same plane as the square:

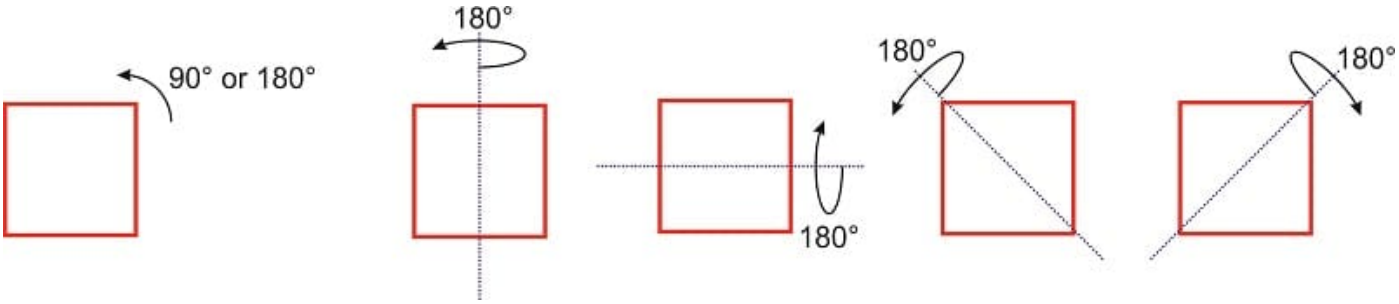


Figure $6.7.2.1$: Symmetry operations performed on a square

A symmetry operation moves all the points of the object from one initial position to a final position, and that means that symmetry operators are 3×3 square matrices (or 2×2 in two dimensions). Each symmetry operation can be expressed as a **transformation matrix** where the vector (x', y', z') represents the new coordinates of the point (x, y, z) after the symmetry operation.

$$[\text{New Coordinates}(x', y', z')] = [\text{Transformation Matrix}] \times [\text{Old Coordinates}(x, y, z)]$$

We will use the example of water, which is in the C_{2v} point group, to illustrate how transformation matrices can be used to represent the symmetry of a group.

Figure $6.7.2.2$ shows the three symmetry elements of the molecule of water (H_2O). This molecule has only one rotation axis, which is 2-fold, and therefore we call it a "C_2 axis." It also has two mirror planes, one that contains the two hydrogen atoms (σ_{yz}), and another one perpendicular to it (σ_{xz}). Both planes contain the C_2 axis.

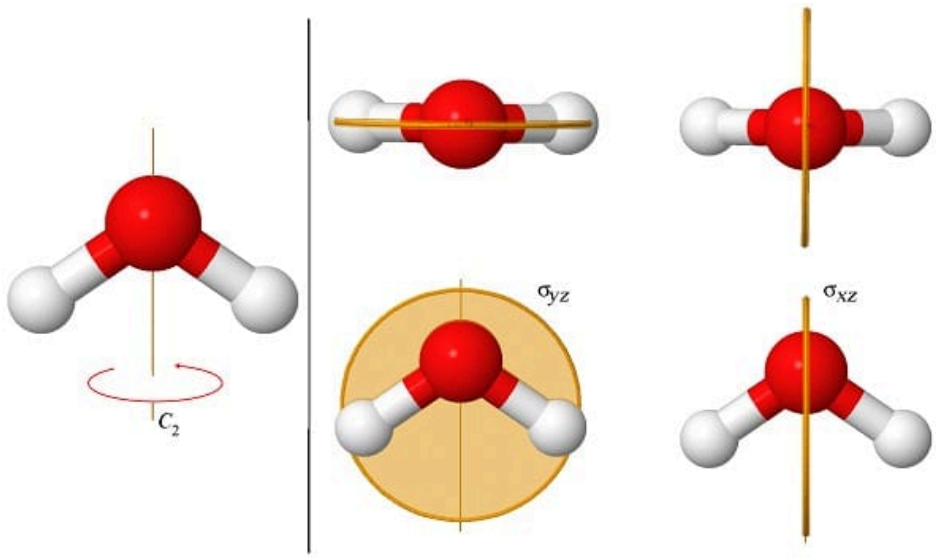


Figure 6.7.2.2: The symmetry elements of the molecule of water

Transformation Matrix of C_2 rotation

A 2-fold rotation around the z −axis changes the location of a point (x, y, z) to $(-x, -y, z)$ (see Figure 6.7.2.3). By convention, rotations are always taken in the counterclockwise direction.

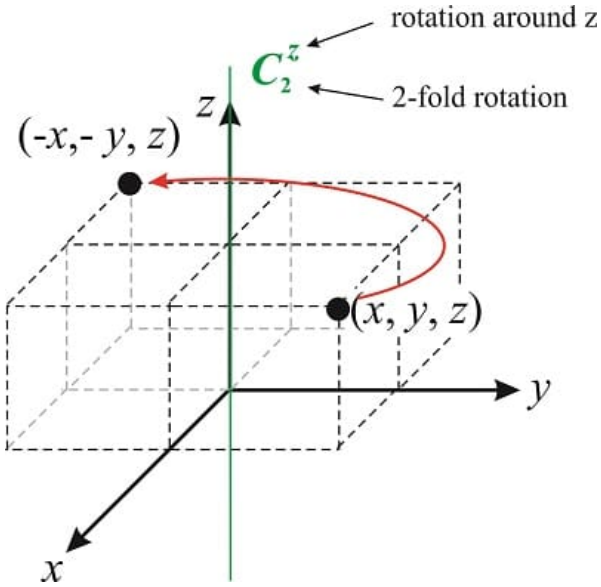


Figure 6.7.2.3: A 2-fold rotation around the z-axis

What is the matrix that represents the C_2 rotation? The matrix transforms the vector (x, y, z) into $(-x, -y, z)$, so

$$C_2(x, y, z) = (-x, -y, z)$$

$$\begin{pmatrix} a_{11} & a_{12} & a_{13} \\ a_{21} & a_{22} & a_{23} \\ a_{31} & a_{32} & a_{33} \end{pmatrix} \begin{pmatrix} x \\ y \\ z \end{pmatrix} = \begin{pmatrix} -x \\ -y \\ z \end{pmatrix}$$

We know the matrix is a 3×3 square matrix because it needs to multiply a 3-dimensional vector. In addition, we write the vector as a vertical column to satisfy the requirements of matrix multiplication.

$$\begin{pmatrix} a_{11} & a_{12} & a_{13} \\ a_{21} & a_{22} & a_{23} \\ a_{31} & a_{32} & a_{33} \end{pmatrix} \begin{pmatrix} x \\ y \\ z \end{pmatrix}$$

$$a_{11}x + a_{12}y + a_{13}z = -x$$

$$a_{21}x + a_{22}y + a_{23}z = -y$$

$$a_{31}x + a_{32}y + a_{33}z = z$$

and we conclude that $a_{11} = -1$, $a_{12} = a_{13} = 0$, $a_{22} = -1$, $a_{21} = a_{23} = 0$ and $a_{33} = 1$, $a_{31} = a_{32} = 0$. The transformation matrix of the C_2 operation of the C_{2v} point group is:

$$C_2 = \begin{pmatrix} -1 & 0 & 0 \\ 0 & -1 & 0 \\ 0 & 0 & 1 \end{pmatrix}$$

Transformation Matrix of σ_{xz} reflection

Rotations are not the only symmetry operations we can perform on a molecule. Figure 6.7.2.4 illustrates the reflection of a point through the xz plane. This operation transforms the vector (x, y, z) into the vector $(x, -y, z)$. Symmetry operators involving reflections through a plane are usually denoted with the letter σ, so the operator that reflects a point through the xz plane is $\hat{\sigma}_{xz}$:

$$\sigma_{xz}(x, y, z) = (x, -y, z)$$

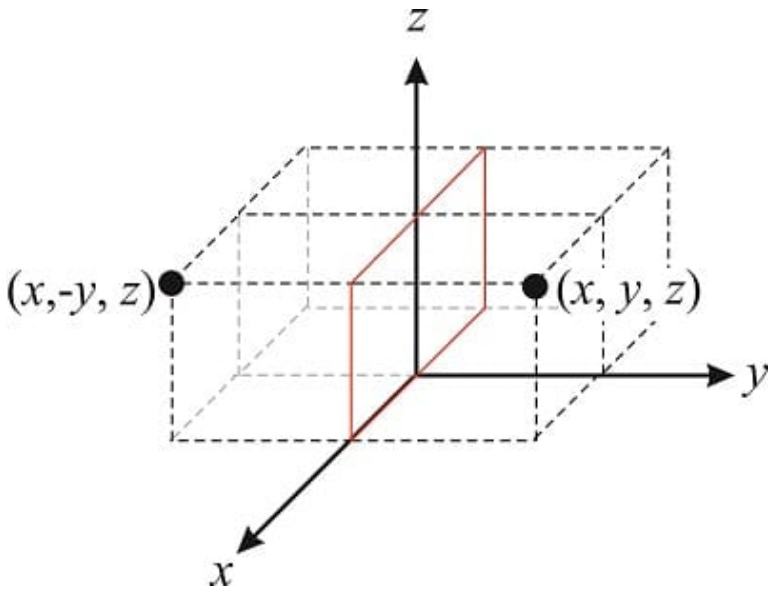


Figure 6.7.2.3: A reflection through the xz plane

Following the same logic we used for the rotation matrix, we can write the σ_{xz} transformation matrix as:

$$\sigma_{x,z} = \begin{pmatrix} 1 & 0 & 0 \\ 0 & -1 & 0 \\ 0 & 0 & 1 \end{pmatrix}$$

This is true because

$$\begin{pmatrix} 1 & 0 & 0 \\ 0 & -1 & 0 \\ 0 & 0 & 1 \end{pmatrix} \begin{pmatrix} x \\ y \\ z \end{pmatrix} = \begin{pmatrix} x \\ -y \\ z \end{pmatrix}$$

Exercise 6.7.2.1

Find the transformation matrix of the identity (E) and the $\sigma_{y,z}$ operations under the C_{2v} point group.

Answer available at the end of this section.

Characters

For a square matrix, the ***character*** is the trace of the matrix. For the C_2 operation, with the transformation matrix

$$\begin{pmatrix} -1 & 0 & 0 \\ 0 & -1 & 0 \\ 0 & 0 & 1 \end{pmatrix},$$

the trace is $(-1) + (-1) + 1 = -1$.

The set of characters for a point group is called a **reducible representation (Γ)**. The reducible representation for the C_{2v} point group is:

C_{2v}	E	C_2	σ_v	σ'_v
Γ	3	-1	1	1

Exercise 6.7.2.1

Prove that the characters in the reducible representation for C_{2v} are correct:

C_{2v}	E	C_2	σ_v	σ'_v
Γ	3	-1	1	1

Answer available at the end of this section.

Reducible and Irreducible Representations

Let us now go back and look in more detail at the transformation matrices of the C_{2v} point group that we derived above. If we look at the matrices carefully we see that they all take the same block diagonal form (a square matrix is said to be **block diagonal** if all the elements are zero except for a set of submatrices lying along the diagonal).

$$E = \begin{pmatrix} [1] & 0 & 0 \\ 0 & [1] & 0 \\ 0 & 0 & [1] \end{pmatrix}, C_2 = \begin{pmatrix} [-1] & 0 & 0 \\ 0 & [-1] & 0 \\ 0 & 0 & [1] \end{pmatrix}, \sigma'_{v(xz)} = \begin{pmatrix} [1] & 0 & 0 \\ 0 & [-1] & 0 \\ 0 & 0 & [1] \end{pmatrix}, \sigma_{v(yz)''} = \begin{pmatrix} [-1] & 0 & 0 \\ 0 & [1] & 0 \\ 0 & 0 & [1] \end{pmatrix}$$

All the non-zero elements become 1x1 matrices that each represent individual x, y, z coordinates. In other words, the element a_{11} represents x, a_{22} represents y, and a_{33} represents z. The matrix elements for x from each transformation matrix combine to form an irreducible representation of the C_{2v} point group. Likewise, the matrix elements for y combine to form a second irreducible representation, and the same is true for z elements. These irreducible representations are shown below:

C_{2v}	E	C_2	σ_v	σ'_v	Coordinate Used
	1	-1	1	-1	x
	1	-1	-1	1	y
	1	1	1	1	z
Γ	3	-1	1	1	

The irreducible representations add to form the reducible representation, Γ. This Γ, which is the set of 3x3 matrices, can be reduced to the set of 1x1 matrices of the irreducible representations. The irreducible representations cannot be reduced further,

hence their name.

Sources & Attribution

- Parts of this page was adapted from Matrices (click here) (Symmetry Operators), contributed by Marcia Levitus, Associate Professor (Biodesign Institute) at Arizona State University.
- Parts of this page were adapted from Reductions of Representations, contributed by

  Claire Vallance (University of Oxford)

- Curated or created by Kathryn Haas

Answers

Exercise 6.7.2.1

The transformation matrix for E is $\begin{pmatrix} 1 & 0 & 0 \\ 0 & 1 & 0 \\ 0 & 0 & 1 \end{pmatrix}$.

The transformation matrix for $\sigma_{v(yz)''}$ is $\begin{pmatrix} -1 & 0 & 0 \\ 0 & 1 & 0 \\ 0 & 0 & 1 \end{pmatrix}$.

Exercise 6.7.2.1

For the E operation, with the transformation matrix $\begin{pmatrix} 1 & 0 & 0 \\ 0 & 1 & 0 \\ 0 & 0 & 1 \end{pmatrix}$, the trace is $1+1+1=3$.

For the C_2^z operation, with the transformation matrix $\begin{pmatrix} -1 & 0 & 0 \\ 0 & -1 & 0 \\ 0 & 0 & 1 \end{pmatrix}$, the trace is $(-1)+(-1)+1=-1$.

For the $\sigma_{v(xz)'}$ operation, with the transformation matrix $\begin{pmatrix} 1 & 0 & 0 \\ 0 & -1 & 0 \\ 0 & 0 & 1 \end{pmatrix}$, the trace is $1+(-1)+1=1$.

For the $\sigma_{v(yz)''}$ operation, with the transformation matrix $\begin{pmatrix} -1 & 0 & 0 \\ 0 & 1 & 0 \\ 0 & 0 & 1 \end{pmatrix}$, the trace is $-1+1+1=1$.

This gives the reducible representation

C_{2v}	E	C_2	σ_v	σ_v'
Γ	3	−1	1	1

This page titled 6.7.2: Representations of Point Groups is shared under a license and was authored, remixed, and/or curated by LibreTexts.

- 4.3.2: Representations of Point Groups by Kathryn Haas is licensed CC BY-NC-SA 4.0.

6.8: EXAMPLES AND APPLICATIONS OF SYMMETRY

The purpose of learning group theory is that molecular symmetry can be applied to understand the properties of molecules. This chapter introduces two applications of symmetry: chirality and molecular vibrations (in the context of analyzing IR and Raman spectra). An additional application of symmetry, to understand molecular bonding, deserves its own chapter and will be explored in Chapter 5.

6.8.1: Chirality

6.8.2: Molecular Vibrations

6.8A: Vibrational Spectroscopy

6.8C: Vibrational Spectroscopy of Linear and Bent triatomic Molecules

This page titled 6.8: Examples and Applications of Symmetry is shared under a license and was authored, remixed, and/or curated by LibreTexts.

- 4.4: Examples and Applications of Symmetry by Kathryn Haas has no license indicated.

6.8.1: Chirality

Introduction

Around the year 1847, the French scientist Louis Pasteur provided an explanation for the optical activity of tartaric acid salts. When he carried out a particular reaction, Pasteur observed that two types of crystals precipitated. Patiently and carefully using tweezers, Pasteur was able to separate the two types of crystals. Pasteur noticed that the types rotated plane-polarized light by the same amount but in different directions. These two compounds are called enantiomers.

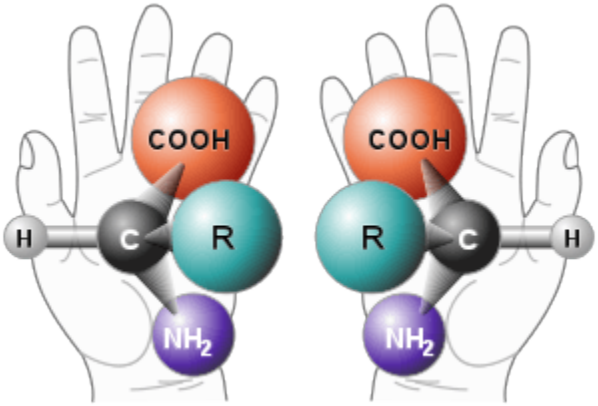


Figure 6.8.1.1: Two enantiomers of an amino acid (with side chain R).

What is chirality?

A molecule is **chiral** (or **dissymetric**) if it is non-superimposable on its mirror image. The two mirror images of a chiral molecule are called enantiomers. Enantiomers have the same physical properties (e.g., melting point, etc.). They differ in their ability to rotate plane polarized light and in their reactivity with other chiral molecules. Due to their ability to rotate plane polarized light, they are referred to as being *optically active*.

Using Symmetry to Determine Chirality

There are some general rules of thumb that help determine whether a molecule is chiral or achiral. The point group of the molecule, and the symmetry operations within that point group, can give clues as to whether the molecule is chiral.

Symmetry operations of chiral molecules

A chiral molecule cannot possess a plane of symmetry (σ), a center of inversion (i), or an improper rotation (S_n). Due to the fact that all groups that lack both σ and i also lack S_n, **a molecule that belongs to any group that lacks S_n is chiral**.

An example of an inorganic coordination complex is tris(ethylenediamine)cobalt(III) (Figure 6.8.1.1). Figure 6.8.1.1 shows the two enantiomers of tris(ethylenediamine)cobalt(III): the Δ and Λ isomers.

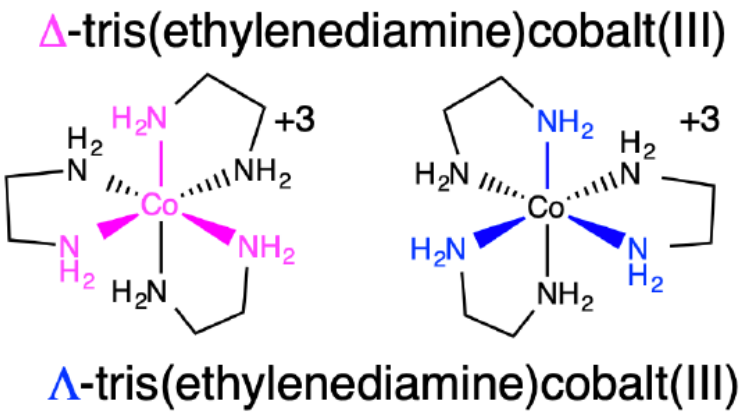


Figure 6.8.1.2: Two chiral enantiomers of tris(ethylenediamine)coalt(III).

You can visualize the Λ and Δ isomers by imagining that the ligands around the metal centers are blades of a fan. To push the air toward you, you would need to rotate the Δ isomer clockwise, and the Λ isomer counter-clockwise.

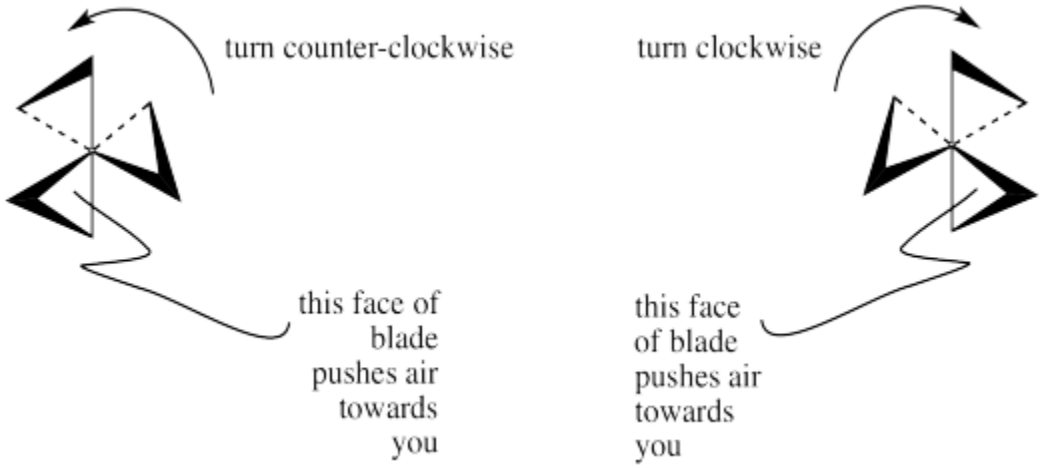


Figure 6.8.1.3: Another way of thinking about the chirality of the two chiral enantiomers of tris(ethylenediamine)coalt(III) shown in Figure 6.8.1.2. This figure was taken from Structure and Reactivity in Organic, Biological, and Inorganic Chemistry.

Exercise 6.8.1.1

Which point groups are possible for chiral molecules?

Answer available at the end of this section.

Answers

Exercise 6.8.1.1

As a result of the previous discussion, there are a few classes of point groups that lack an improper axis. Those classes are C_1, C_n, and D_n.

This page titled 6.8.1: Chirality is shared under a CC BY-NC 4.0 license and was authored, remixed, and/or curated by LibreTexts.

- 4.4.1: Chirality by Kathryn Haas is licensed CC BY-NC 4.0.

6.8.2: Molecular Vibrations

Symmetry and group theory can be applied to understand molecular vibrations. This is particularly useful in the context of predicting the number of peaks expected in the infrared (IR) and Raman spectra of a given compound.

We will use water as a case study to illustrate how group theory is used to predict the number of peaks in IR and Raman spectra.

How many IR and Raman peaks would we expect for H_2O?

To answer this question with group theory, a pre-requisite is that you **assign the molecule's point group and assign an axis system** to the entire molecule. By convention, the z axis is collinear with the principle axis, the x axis is in-plane with the molecule or the most number of atoms. It is a good idea to stick with this convention (see Figure 6.8.2.1).

What is the point group for H_2O? (click to see answer)

H_2O has the following operations: E, C_2, σ_v, σ_v'. The point group is C_{2v}.

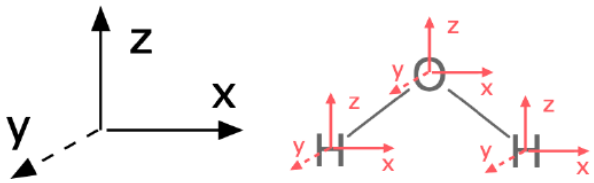


Figure 6.8.2.1: The first step to finding normal modes is to assign a consistent axis system to the entire molecule and to each atom. (CC-BY-SA; Kathryn Haas)

Now that we know the molecule's point group, we can use group theory to determine the symmetry of all motions in the molecule, or the symmetry of each of its degrees of freedom. Then we will subtract rotational and translational degrees of freedom to find the vibrational degrees of freedom. The number of degrees of freedom depends on the number of atoms (N) in a molecule. Each atom in the molecule can move in three dimensions (x, y, z), and so the number of degrees of freedom is three dimensions times N number of atoms, or $3N$. The total degrees of freedom include a number of vibrations, three translations (in x, y, and z), and either two or three rotations. Linear molecules have two rotational degrees of freedom, while non-linear molecules have three. The vibrational modes are represented by the following expressions:

$$\begin{aligned} \text{Linear Molecule Degrees of Freedom} &= 3N-5 \\ \text{Non-Linear Molecule Degrees of Freedom} &= 3N-6 \end{aligned}$$

Our goal is to find the symmetry of all degrees of freedom, and then determine which are vibrations that are IR- and Raman-active.

STEP 1: Find the reducible representation for all normal modes Γ_{modes}.

The first major step is to **find a reducible representation (Γ)** for the movement of all atoms in the molecule (including rotational, translational, and vibrational degrees of freedom). We'll refer to this as Γ_{modes}. To find normal modes using group theory, **assign an axis system** to each individual atom to represent the three dimensions in which each atom can move. Each axis on each atom should be consistent with the conventional axis system you previously assigned to the entire molecule (see Figure 6.8.2.1).

Γ_{modes} is the sum of the characters (trace) of the transformation matrix for the entire molecule (in the case of water, there are 9 degrees of freedom and this is now a 9x9 matrix). Let's walk through this step-by-step. The transformation matrix of E and C_2 are shown below:

$$E = \begin{pmatrix} 1 & 0 & 0 & 0 & 0 & 0 & 0 & 0 & 0 \\ 0 & 1 & 0 & 0 & 0 & 0 & 0 & 0 & 0 \\ 0 & 0 & 1 & 0 & 0 & 0 & 0 & 0 & 0 \\ 0 & 0 & 0 & 1 & 0 & 0 & 0 & 0 & 0 \\ 0 & 0 & 0 & 0 & 1 & 0 & 0 & 0 & 0 \\ 0 & 0 & 0 & 0 & 0 & 1 & 0 & 0 & 0 \\ 0 & 0 & 0 & 0 & 0 & 0 & 1 & 0 & 0 \\ 0 & 0 & 0 & 0 & 0 & 0 & 0 & 1 & 0 \\ 0 & 0 & 0 & 0 & 0 & 0 & 0 & 0 & 1 \end{pmatrix} \begin{pmatrix} x_{oxygen} \\ y_{oxygen} \\ z_{oxygen} \\ x_{hydrogen-a} \\ y_{hydrogen-a} \\ z_{hydrogen-a} \\ x_{hydrogen-b} \\ y_{hydrogen-b} \\ z_{hydrogen-b} \end{pmatrix} = \begin{pmatrix} x'_{oxygen} \\ y'_{oxygen} \\ z'_{oxygen} \\ x'_{hydrogen-a} \\ y'_{hydrogen-a} \\ z'_{hydrogen-a} \\ x'_{hydrogen-b} \\ y'_{hydrogen-b} \\ z'_{hydrogen-b} \end{pmatrix}, \chi = 9$$

$$C_2 = \begin{pmatrix} -1 & 0 & 0 & 0 & 0 & 0 & 0 & 0 & 0 \\ 0 & -1 & 0 & 0 & 0 & 0 & 0 & 0 & 0 \\ 0 & 0 & 1 & 0 & 0 & 0 & 0 & 0 & 0 \\ 0 & 0 & 0 & 0 & 0 & 0 & -1 & 0 & 0 \\ 0 & 0 & 0 & 0 & 0 & 0 & 0 & -1 & 0 \\ 0 & 0 & 0 & 0 & 0 & 0 & 0 & 0 & 1 \\ 0 & 0 & 0 & -1 & 0 & 0 & 0 & 0 & 0 \\ 0 & 0 & 0 & 0 & -1 & 0 & 0 & 0 & 0 \\ 0 & 0 & 0 & 0 & 0 & 1 & 0 & 0 & 0 \end{pmatrix} \begin{pmatrix} x_{oxygen} \\ y_{oxygen} \\ z_{oxygen} \\ x_{hydrogen-a} \\ y_{hydrogen-a} \\ z_{hydrogen-a} \\ x_{hydrogen-b} \\ y_{hydrogen-b} \\ z_{hydrogen-b} \end{pmatrix} = \begin{pmatrix} x'_{oxygen} \\ y'_{oxygen} \\ z'_{oxygen} \\ x'_{hydrogen-a} \\ y'_{hydrogen-a} \\ z'_{hydrogen-a} \\ x'_{hydrogen-b} \\ y'_{hydrogen-b} \\ z'_{hydrogen-b} \end{pmatrix}, \chi = 1$$

It is unnecessary to find the transformation matrix for each operation since it is only the TRACE that gives us the character, and any off-diagonal entries do not contribute to Γ_{modes}. The values that contribute to the trace can be found simply by performing each operation in the point group and assigning a value to each individual atom to represent how it is changed by that operation. If the atom moves away from itself, that atom gets a character of zero (this is because any non-zero characters of the transformation matrix are off of the diagonal). If the atom remains in place, each of its three dimensions is assigned a value of $\cos\theta$. For the example of H_2O under the C_{2v} point group, the axes that remain unchanged ($\theta = 0°$) are assigned a value of $\cos(0°) = 1$, while those that are moved into the negative of themselves (rotated or reflected to $\theta = 180°$) are assigned $\cos(180°) = -1$. The character for Γ is the sum of the values for each transformation.

Let's walk through the steps to assign characters of Γ_{modes} for H_2O to illustrate how this works:

For the operation E, performed on H_2O, all three atoms remain in place. The three axes x, y, z on each atom remain unchanged. Thus, each of the three axes on each of three atom (nine axes) is assigned the value $\cos(0°) = 1$, resulting in a sum of $\chi = 9$ for the Γ_{modes}.

For the operation C_2, the two hydrogen atoms are moved away from their original position, and so the hydrogens are assigned a value of zero. The oxygen remains in place; the z-axis on oxygen is unchanged ($\cos(0°) = 1$), while the x and y axes are inverted ($\cos(180°)$). The sum of these characters gives $\chi = -1$ in the Γ_{modes}.

Now you try! Find the characters of $\sigma_{v(xz)}$ and $\sigma_{v(yz)}$ under the C_{2v} point group. Compare what you find to the Γ_{modes} for all normal modes given below.

C_{2v}	E	C_2	σ_v	σ'_v
Γ_{modes}	9	−1	3	1

(6.8.2.1)

STEP 2: Break Γ_{modes} into its component irreducible representations

Now that we've found the Γ_{modes} (6.8.2.1), we need to break it down into the individual irreducible representations ($i, j, k...$) for the point group. We can do this systematically using the following formula:

$$\#\text{ of } i = \frac{1}{h}\sum(\#\text{ of operations in class}) \times (\chi_\Gamma) \times (\chi_i) \tag{6.8.2.2}$$

In other words, the number of irreducible representations of type i is equal to the sum of the number of operations in the class $\times$ the character of the Γ_{modes} $\times$ the character of i, and that sum is divided by the order of the group (h).

Using equation 6.8.2.2, we find that for all normal modes of H_2O:

$$\Gamma_{modes} = 3A_1 + 1A_2 + 3B_1 + 2B_2. \tag{6.8.2.3}$$

Notice there are 9 irreducible representations in Equation 6.8.2.3. These irreducible representations represent the symmetries of all 9 motions of the molecule: vibrations, rotations, and translations.

Exercise 6.8.2.1: Derive the irreducible representation in equation 6.8.2.3.

Derive the nine irreducible representations of Γ_{modes} for H_2O, expression 6.8.2.3.

Hint available at the end of this section.

Answer available at the end of this section.

STEP 3: Subtract rotations and translations to find vibrational modes.

Because we are interested in molecular vibrations, we need to subtract the rotations and translations from the total degrees of freedom.

$$\text{Vibrations} = \Gamma_{modes} - \text{Rotations} - \text{Translations}$$

In the example of H_2O, the total degrees of freedom are given above in equation 6.8.2.3, and therefore the vibrational degrees of freedom can be found by:

$$H_2O \text{ vibrations} = (3A_1 + 1A_2 + 3B_1 + 2B_2) - \text{Rotations} - \text{Translations} \tag{6.8.2.4}$$

But which of the irreducible representations are ones that represent rotations and translations? The symmetry of rotational and translational degree modes can be found by inspecting the right-hand columns of any character table. Rotational modes correspond to irreducible representations that include R_x, R_y, and R_z in the table, while each of the three translational modes has the same symmetry as the x, y and z axes. For a non-linear molecule, subtract three rotational irreducible representations and three translational irreducible representations from the total Γ_{modes}.

In the specific case of water, we refer to the C_{2v} character table:

C_{2v}	E	C_2	σ_v	σ_v'	$h = 4$	
A_1	1	1	1	1	z	x^2, y^2, z^2
A_2	1	1	−1	−1	R_z	xy
B_1	1	−1	1	−1	x, R_y	xz
B_2	1	−1	−1	1	y, R_x	yz

In C_{2v}, translations correspond to B_1, B_2, and A_1 (respectively for x, yz), and rotations correspond to B_2, B_1, and A_1 (respectively for R_x, R_y, R_z). Subtracting these six irreducible representations from Γ_{modes} will leave us with the irreducible representations for vibrations.

$$\begin{aligned} H_2O \text{ vibrations} &= \Gamma_{modes} - \text{Rotations} - \text{Translations} \\ &= (3A_1 + 1A_2 + 3B_1 + 2B_2) - (A_1 + B_1 + B_2) - (A_2 + B_1 + B_2) \\ &= 2A_1 + 1B_1 \end{aligned}$$

The three vibrational modes for H_2O are $2A_1 + 1B_1$. Note that we have the correct number of vibrational modes based on the expectation of $3N - 6$ vibrations for a non-linear molecule.

STEP 4: Determine which of the vibrational modes are IR-active and Raman-active.

The next step is to determine which of the vibrational modes is IR-active and Raman-active. To do this, we apply the IR and

Raman Selection Rules below:

IR and Raman Selection Rules

Infrared selection rules:

If a vibration results in the change in the molecular dipole moment, it is IR-active. In the character table, we can recognize the vibrational modes that are IR-active by those with symmetry of the x, y, and z axes.

In C_{2v}, any vibrations with A_1, B_1 or B_2 symmetry would be IR-active.

Raman selection rules:

If a vibration results in a change in the molecular polarizability, it will be Raman-active. In the character table, we can recognize the vibrational modes that are Raman-active by those with symmetry of any of the binary products (xy, xz, yz, x^2, y^2, and z^2) or a linear combination of binary products (e.g. $x^2 - y^2$).

In C_{2v}, any vibrations with A_1, A_2, B_1 or B_2 symmetry would be Raman-active.

In our H_2O example, we found that of the three vibrational modes, two have A_1 and one has B_1 symmetry. Both A_1 and B_1 are IR-active, and both are also Raman-active. ***There are three possible IR peaks and three possible Raman peaks expected for water***.*

*It is important to note that this prediction tells only what is possible, but not what we might actually see in the IR and Raman spectra. For example, if two IR peaks overlap, we might actually notice only one peak in the spectrum. Or, if one or more peaks is off-scale, we wouldn't see it in actual data. Group theory tells us what is *possible and allows us to make predictions or interpretations of spectra.*

Summary of Analysis for Water

Each molecular motion for water, or any molecule, can be assigned a symmetry under the molecule's point group. For water, we found that there are a total of 9 molecular motions; $3A_1 + A_2 + 3B_1 + 2B_2$. Six of these motions are not the translations and rotations. The remaining motions are vibrations; two with A_1 symmetry and one with B_1 symmetry.

We can tell what these vibrations would look like based on their symmetries. The two A_1 vibrations must be completely symmetric, while the B_1 vibration is antisymmetric with respect to the principal C_2 axis.

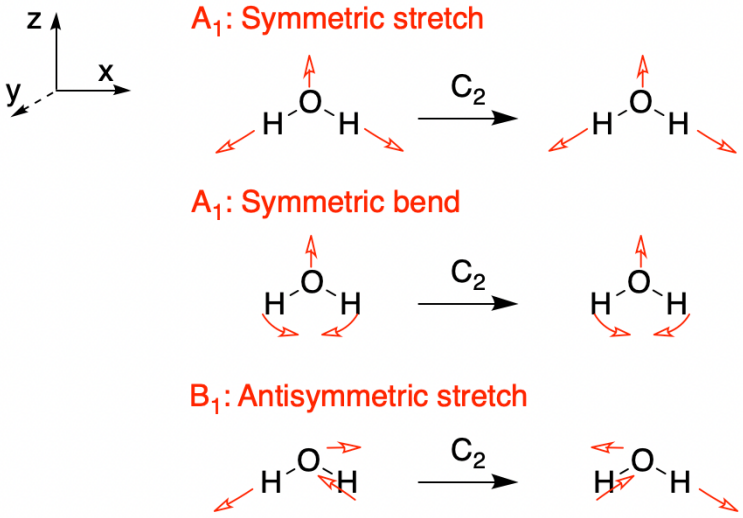


Figure 6.8.2.2: Illustration of the vibrational motions of water. The antisymmetric stretch has B_1 symmetry, while the symmetric stretch and symmetric bend both have A_1 symmetry. (Click here to see animation) (CC-BY-NC-SA; Kathryn Haas)

Table 6.8.2.1: Summary of the Symmetry of Molecular Motions for Water

All Motions (step 2 above)	Translations (x,y,z)	Rotations (R_x, R_y, R_z)	Remaining Vibrations	Description of Vibration
$3A_1$	$1A_1$		$2A_1$	One is a symmetric stretch. The other is a symmetric bend. Both are *IR-active* and *Raman-active*
A_2		$1A_2$		
$3B_1$	$1B_1$	$1B_1$	$1B_1$	Antisymmetric stretch that is *IR-active* and *Raman-active*.
$2B_2$	$1B_2$	$1B_2$		

Exercise 6.8.2.2

Find the symmetries of all motions of the square planar complex, tetrachloroplatinate (II). Determine which are rotations, translations, and vibrations. Determine which vibrations are IR and Raman active.

Answer available at the end of this section.

Selected Vibrational Modes

The interpretation of CO stretching vibrations in an IR spectrum is particularly useful. Symmetry and group theory can be applied to predict the number of CO stretching bands that appear in a vibrational spectrum for a given metal coordination complex. A classic example of this application is in distinguishing isomers of metal-carbonyl complexes. For example, the *cis*- and *trans*-isomers of square planar metal dicarbonyl complexes ($ML_2(CO)_2$) have a different number of IR stretches that can be predicted and interpreted using symmetry and group theory. Another example is the case of *mer*- and *fac*- isomers of octahedral metal tricarbonyl complexes ($ML_3(CO)_3$). Structures of the two types of metal carbonyl configurations and their isomers are shown in Figure 6.8.2.1. The isomers in each case can be distinguished using vibrational spectroscopy.

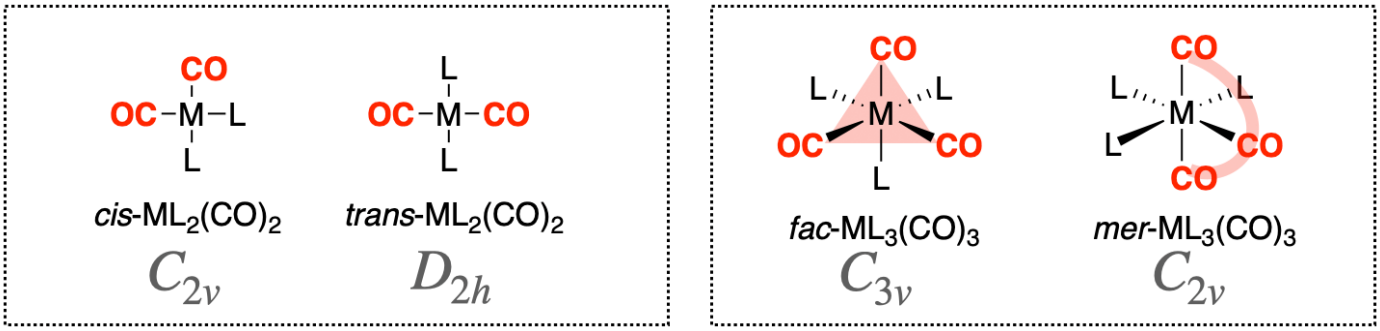


Figure 6.8.2.3: Cis- and *trans*- isomers of square planar metal dicarbonyl complexes ($ML_2(CO)_2$) are shown in the left box. *Mer*- and *fac*-isomers of octahedral metal tricarbonyl complexes ($ML_3(CO)_3$) are shown in the right box. The point group for each of the general structures is also shown. (CC-BY-NC-SA; Kathryn Haas)

EXAMPLE 1: Distinguishing *cis*- and *trans*- isomers of square planar metal dicarbonyl complexes

General structures of the *cis*- and *trans*- isomers of square planar metal dicarbonyl complexes ($ML_2(CO)_2$) are shown in the left box in Figure 6.8.2.1. We can use symmetry and group theory to predict how many carbonyl stretches we should expect for each isomer following the steps below.

Step 1: Assign the point group and Cartesian coordinates for each isomer.

The *cis*-isomer has C_{2v} symmetry and the *trans*-isomer has D_{2h} symmetry. We assign the Cartesian coordinates so that z is colinear with the principle axis in each case. For the D_2h isomer, there are several orientations of the z axis possible. The axes shown in Figure $6.8.2.2$ will be used here.

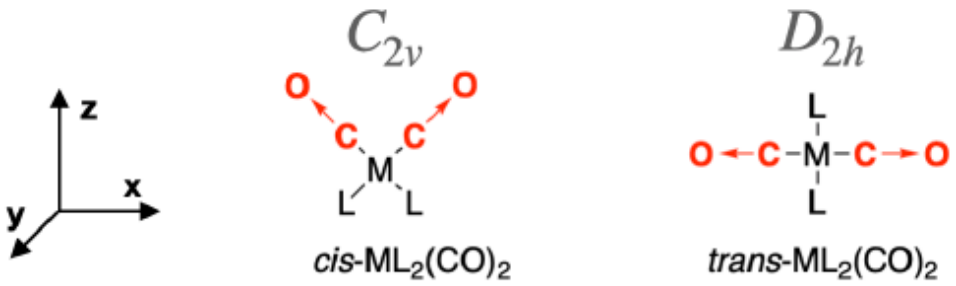


Figure $6.8.2.4$: Cis- and *trans*- isomers of square planar metal dicarbonyl complexes ($ML_2(CO)_2$) are shown and oriented with respect to the Cartesian coordinates shown at the left so that the highest-order rotation axis is colinear with z and the molecule is co-planar with the xz plane. The vector along each C—O bond is shown using a red arrow (→). These vectors represent the direction of C—O stretching motions. (CC-BY-NC-SA; Kathryn Haas)

Step 2: Produce a reducible representation (Γ) for CO stretches in each isomer

First, assign a vector along each C—O bond in the molecule to represent the direction of C—O stretching motions, as shown in Figure $6.8.2.2$ (red arrows →). These vectors are used to produce a reducible representation (Γ) for the C—O stretching motions in each molecule. Using the symmetry operations under the appropriate character table, assign a value of 1 to each vector that remains in place during the operation, and a value of 0 if the vector moves out of place. There will be no occasion where a vector remains in place but is inverted, so a value of -1 will not occur.

cis- $ML_2(CO)_2$:

For *cis*- $ML_2(CO)_2$, the point group is C_{2v} and so we use the operations under the C_{2v} character table to create the Γ_{cis-CO}.

[redacted]

trans- $ML_2(CO)_2$:

For trans- $ML_2(CO)_2$, the point group is D_{2h} and so we use the operations under the D_{2h} character table to create the $\Gamma_{trans-CO}$.

[redacted]

Step 3: Break each Γ into its component irreducible representations

Each Γ can be reduced using inspection or by the systematic method described previously.

In the case of the *cis*- $ML_2(CO)_2$, the CO stretching vibrations are represented by A_1 and B_1 irreducible representations:

[redacted]

$(6.8.2.5)$

In the case of *trans*- $ML_2(CO)_2$, the CO stretching vibrations are represented by A_1 and B_{3u} irreducible representations:



These irreducible representations correspond to the symmetries of only the selected C—O vibrations. Since these motions are isolated to the C—O group, they do not include any rotations or translations of the entire molecule, and so we do not need to find and subtract rotationals or translations (unlike the previous cases where all motions were considered).

Step 4: Determine which vibrational modes are IR-active and/or Raman-active

Apply the infrared selection rules described previously to determine which of the CO vibrational motions are IR-active and Raman-active. The two isomers of $ML_2(CO)_2$ are described below.

In the case of the *cis*- $ML_2(CO)_2$, the CO stretching vibrations are represented by A_1 and B_1 irreducible representations. The characters of both representations and their functions are shown above, in 6.8.2.5 (and can be found in the C_{2v} character table). Under C_{2v}, both the A_1 and B_1 CO vibrational modes are IR-active and Raman-active. Therefore, two bands in the IR spectrum and two bands in the Raman spectrum are possible.

In the case of the trans- $ML_2(CO)_2$, the CO stretching vibrations are represented by A_g and B_{3u} irreducible representations. The characters of both representations and their functions are shown above, in 6.8.2.5 (and can be found in the D_{2h} character table). Under D_{2h}, the A_g vibrational mode is is Raman-active only, while the B_{3u} vibrational mode is IR-active only. Therefore, only one IR band and one Raman band are possible for this isomer.

Summary

It is possible to distinguish between the two isomers of square planar $ML_2(CO)_2$ using either IR or Raman vibrational spectroscopy. The *cis*- $ML_2(CO)_2$ can produce two CO stretches in an IR or Raman spectrum, while the *trans*- $ML_2(CO)_2$ isomer can produce only one band in either type of vibrational spectrum. If a sample of $ML_2(CO)_2$ produced two CO stretching bands, we could rule out the possibility of a pure sample of *trans*-$ML_2(CO)_2$.

Exercise 6.8.2.3

Repeat the steps outlined above to determine how many CO vibrations are possible for *mer*-$ML_3(CO)_3$ and *fac*-$ML_3(CO)_3$ isomers (see Figure 6.8.2.1) in both IR and Raman spectra. Could either of these vibrational spectroscopies be used to distinguish the two isomers?

Answer available at the end of this section.

Answers

Exercise 6.8.2.1: Derive the irreducible representation in equation 6.8.2.3.

To find the number of each kind of irreducible representation that combine to form the Γ_{modes}, we need the characters of Γ_{modes} that we found above (6.8.2.1), the C_{2v} character table (below), and equation 6.8.2.2.

C_{2v}	$1E$	$1C_2$	$1\sigma_v$	$1\sigma_v'$	$h=4$	
A_1	1	1	1	1	z	x^2, y^2, z^2
A_2	1	1	−1	−1	R_z	xy
B_1	1	−1	1	−1	x, R_y	xz
B_2	1	−1	−1	1	y, R_x	yz

In the C_{2v} point group, each class has only one operation, so the number of operations in each class (from equation 6.8.2.2) is 1 for each class. This has been explicitly added to the character table above for emphasis.

Exercise 6.8.2.1: Derive the irreducible representation in equation 6.8.2.3.

The number of $A_1 = \frac{1}{4}[(1\times 9\times 1)+(1\times(-1)\times 1)+(1\times 3\times 1)+(1\times 1\times 1)] = 3A_1$

The number of $A_2 = \frac{1}{4}[(1\times 9\times 1)+(1\times(-1)\times 1)+((-1)\times 3\times 1)+((-1)\times 1\times 1)] = 1A_2$

The number of $B_1 = \frac{1}{4}[(1\times 9\times 1)+((-1)\times(-1)\times 1)+(1\times 3\times 1)+((-1)\times 1\times 1)] = 3B_1$

The number of $B_2 = \frac{1}{4}[(1\times 9\times 1)+((-1)\times(-1)\times 1)+((-1)\times 3\times 1)+(1\times 1\times 1)] = 2B_2$

Exercise 6.8.2.2

The point group of $[PtCl_4]^{2-}$ is D_{4h} (refer to its character table). There are five atoms and 15 vectors (x, y, z for each atom $\times$ 5 atoms).

STEP 1: The first major step is to **find a reducible representation (Γ)** for the movement of all atoms in the molecule.

$$\begin{array}{cccccccccc} C_{2v} & E & 2C_4 & C_2 & 2C_2' & 2C_2'' & i & 2S_4 & \sigma_h & 2\sigma_v & 2\sigma_d \\ \Gamma_{modes} & 15 & 1 & -1 & -3 & -1 & -3 & -1 & 5 & 3 & 1 \end{array} \tag{6.8.2.6}$$

.

STEP 2: Break Γ_{modes} into its component irreducible representations.

Following the process described earlier, we come to $A_{1g} + A_{2g} + B_{1g} + B_{2g} + E_g + 2A_{2u} + B_{2u} + 3E_u$. This accounts for all modes of movement, including rotations and translations.

STEP 3: Subtract rotations and translations to find vibrational modes.

The translations are $A_{2u} + E_u$ and the rotations are $A_{2g} + E_g$.
The remaining normal modes are: $A_{1g} + B_{1g} + B_{2g} + A_{2u} + B_{2u} + 2E_u$

STEP 4: Determine which of the vibrational modes are IR-active and Raman-active:

$A_{2u} + E_u$ are IR-active. Since A_{2u} is singly degenerate and E_u is doubly degenerate, we expect three possible IR bands.
$A_{1g} + B_{1g} + B_{2g}$ are Raman-Active. Each of these is singly degenerate, so we expect three possible Raman bands.

Exercise 6.8.2.3

Step 1: Assign the point group and Cartesian coordinates for each isomer.
The *fac*-isomer is C_{3v}. The *mer*-isomer is C_{2v}.

Step 2: Produce a reducible representation for CO stretches in each isomer.

Step 3: Break each into its component irreducible representations.

Step 4: Determine which vibrational modes are IR-active and/or Raman-active.

***For fac*-$ML_3(CO)_3$**, the point group is C_{3v} and so we use the operations under the C_{3v} character table to create the Γ_{fac-CO}. Then break it into its irreducible representations and determine which are IR and Raman active:



This reduces to $A_1 + E$. Both of these are IR active, and since one is singly degenerate while the other is doubly degenerate, we expect three possible IR bands from this isomer. Both vibrational modes are also Raman active, and again we would expect three possible bands in the Raman spectrum.

For mer-$ML_3(CO)_3$, the point group is C_{2v} and so we use the operations under the C_{2v} character table to create the Γ_{mer-CO}. Then break it into its irreducible representations and determine which are IR and Raman active:



This reduces to $2A_1 + B_1$; both A_1 and B_1 are IR and Raman active. So this isomer would have three possible IR bands and three possible Raman Bands.

These two isomers have the same number of possible bands in both IR and Raman spectroscopy. It would not be straightforward to distinguish them from each other based on the number of possible bands in the vibrational spectrum.

This page titled 6.8.2: Molecular Vibrations is shared under a license and was authored, remixed, and/or curated by Kathryn Haas.

- 4.4.2: Molecular Vibrations by Kathryn Haas is licensed CC BY-NC 4.0.

6.8A: Vibrational Spectroscopy

All molecules are constantly vibrating, and can absorb energy from an incoming photon to increase their vibrations. The two types of vibrational spectroscopy are infrared spectroscopy and Raman spectroscopy. Vibrational spectroscopy is the science of measuring exactly which wavelengths of light are absorbed by a molecule. This technique could be used identify an unknown molecule by comparing its absorption to that of other molecules. Or vibrational spectroscopy could be used to gain further understanding of the physical properties of a known molecule.

Introduction

Molecular vibration can be modeled by balls attached by springs. Displacing an atom from its most stable position requires energy proportional to the displacement. IR spectroscopy can be used to characterize a molecule is the energy of its vibrations falls in the infrared range. Alternatively, higher energy light can be absorbed, the re-emitted at a different wavelength and/or in a different direction; this leads to Raman spectroscopy. So a molecule can absorb radiation to change bond lengths or positions with respect to the other atoms in the molecule.[3]

From the number, frequency, and intensity of these absorptions or emissions we can gain insight into the composition of the sample being measured. The number of different absorptions is indicative of the number of different atoms and shape of the molecule. The frequency or wavelength absorbed is indicative of the energy of the bonds and vibrations. And the intensity of the absorptions is related to the concentration of the analyte.[1]

Vibrational Modes

The different possible vibrations are called vibrational modes. Vibrational modes are determined by all the different ways the atoms in the molecule can move with respect to eachother, called the vibrational degrees of freedom. Vibrational degrees of freedom differ from the total degrees of freedom in that translation (movement through space) and rotation do not contribute to the vibrational degrees of freedom.[4]

To find the number of vibrational modes one must first know the point group of the molecule. From there, the point group's character table will list all of the possible symmetry operations for the molecule. Each symmetry operation will leave some atoms in the molecule in place and/or move other atoms in the molecule. Count up the number of atoms that do not move for each symmetry operation, and multiply that number by the symmetry operation's contribution. This gives the total representation of atomic motion. From there, the vibrational modes can be found by reducing the total representation, according to the equation:

$$n = 1/h * \Sigma XR * XI * N$$

where n is the number of modes with that symmetry, h is the total number of symmetry operations, X_I is the number of irreducible representations (the value calculated above), X_R is the number of reducible representations (the entry in the character table), and N is the number of identical symmetry operations. Finally, subtracting the rotational modes and translational modes from the reduced representation gives the number of vibrational modes.[6]

Symmetrical stretching.gifAsymmetrical stretching.gifScissoring.gif

Three of the vibrational modes for the C_{2V} point group. Used with permission from http://en.Wikipedia.org/wiki/Infrared_spectroscopy

Infrared Spectroscopy

A vibrational mode will be observed in an infrared spectrum if it leads to a change in the molecular dipole moment. Compared to Raman spectroscopy, the infrared photon is completely absorbed and its energy is transfered to the vibration of the molecule, not re-emitted.[4]

Different bonds have different energies associated with them, and require different amounts of energy to stretch or bend. In general, the stronger the bond, the more energy required to deform it. So very weak bonds will only be deformed by low energy radiation, and strong bonds will only be deformed by high energy radiation. This leads to characteristic frequencies where only certain vibrations are absorbed. For example, C-H bonds are typically the only bonds observed in the range from 2960-2850 cm^{-1}. So if an absorption is present at that frequency, it can be assumed that it is due to a C-H bond.[1]

Raman Spectroscopy

alt

A vibrational mode will be observed in Raman spectroscopy if it
leads to a change in the polarizability of the electron cloud of a molecule.[4]

If a photon has energy that is significantly higher than the energy of the vibrational states, it may either be deflected without any change in energy, or it may interact with the molecule and either take energy from it or give energy to it.[2]

When the photon is absorbed and re-emitted in a different direction, it is called Rayleigh scattering, and this is strongly dependent on the wavelength of the incoming light. When there is a change in the energy of the photon, it is called Stokes scattering or anti-Stokes scattering, depending on whether energy is absorbed or lost by the molecule. This change in the behavior of the incoming photons can be measured, and will provide information about the concentration and chemical properties of the analyte.[3]

Diagram used with permission from http://en.Wikipedia.org/wiki/Raman_spectroscopy

References

1. Jones, Llewellyn. *Inorganic Vibrational Spectroscopy*. 1. Los Alamos, New Mexico: Marcel Dekker, 1971. Print.
2. Steele, Derek. *Theory of Vibrational Spectroscopy*. Philadelphia: W. B. Saunders Company, 1971. Print.
3. Skoog, Douglas, James Holler, and Stanley Crouch.*Principles of Instrumental Analysis*. 6th. Belmont, California: Brooks/Cole, 2007. Print.
4. Housecroft, Catherine, and Alan Sharpe. *Inorganic Chemistry*. 3rd. New York: Pearson Prentice Hall, 2008. Print.
5. Ogden, J. S. *Introduction to Molecular Symmetry*. New York: Oxford University Press, Print.

Outside Links

- http://www2.ess.ucla.edu/~schauble/m...vibrations.htm
- http://www.webqc.org/symmetry.php
- www.ch.embnet.org/MD_tutorial/
- http://en.Wikipedia.org/wiki/Molecular_vibration
- http://en.Wikipedia.org/wiki/Raman_spectroscopy

Problems

1. Why is it that the symmetric stretch of carbon dioxide (CO_2) is IR inactive, while the symmetric stretch of carbonyl sulfide (COS) is IR active?

A: Because the symmetric stretch of CO_2 does not lead to a change in the dipole moment of the molecule, but the symmetric stretch of COS does.

2. How many vibrational modes are IR and Raman active for C_{20}?

A: 17 IR active modes, 29 Raman Active modes.

3. Are there any differences between the vibrational spectrums of H_2O, H_2S, and H_2Se?

A: Although they have the same number of atoms, the same point group, and the same number of vibrational modes, the

frequencies at which the vibrational modes occur will be different.

This page titled 6.8A: Vibrational Spectroscopy is shared under a license and was authored, remixed, and/or curated by LibreTexts.

- 3.7A: Vibrational Spectroscopy is licensed CC BY-NC-SA 4.0.

6.8C: Vibrational Spectroscopy of Linear and Bent triatomic Molecules

Vibrational spectroscopy, AKA Infrared (IR) Spectroscopy, is a highly useful and beneficial tool for determining structures and functional groups contained in compounds. Although used for many different structure types of polyatomic molecules, this particular Module is dedicated to triatomic molecules with bent and linear spacial molecular geometry.

Introduction

Triatomic molecules are molecules that contain three atoms. The atoms in triatomic molecules can all be the same, as in I_3^-, all be different, as in HCN, or can be a mix like CO_2. Examples include H_2O, which is a bent and has a bond angle of 109°, and a linear triatomic molecule such as CO_2. All bent tri-atomic molecules belong to the point group C_{2v}, while all the liner tri-atomic molecules with an inversion center belong to the $D_{infinity\text{-}h}$ point group; Those without an inversion center belong to the point group $C_{infinity\text{-}v}$. This gives these two structures very different infrared spectrum even though they have the same number of atoms.

Linear molecules

Using VESPR theory there are several ways to achieve a linear structure. Tri-atomic molecules where the central atom is using ALL of its electrons in the bonds with the surrounding molecules, or in other words the central atom does not have any lone pairs surrounding it, will give rise to a linear molecule. Examples include CO_2 and BeH_3. This electronic configuration gives the central atom a sp hybridization. Triatomic molecules where the central atom does not use all of its electron pairs in the bonds between the other two atoms will, under certain circumstances, also give rise to a linear species. When the central atom is surrounded by three, or four lone pairs in addition to the two elements already attached will also give rise to a linear molecule. Examples include KrF_2.

Bent Molecules

There are also several ways to give rise to bent molecules using VESPR theory. A tri-atomic molecule with one, or two lone pair on the central atom will also give rise to bent species. One lone pair examples include SO_2, and two lone pair examples include H_2O

References

1. Volhardt and Schore. " Organic Chemistry: Structure and Function." 5th edition
2. Bruice, Paula, and Yukanis. "organic chemistry." 5th edition.

Contributors and Attributions

- David Phinney (UC Davis)

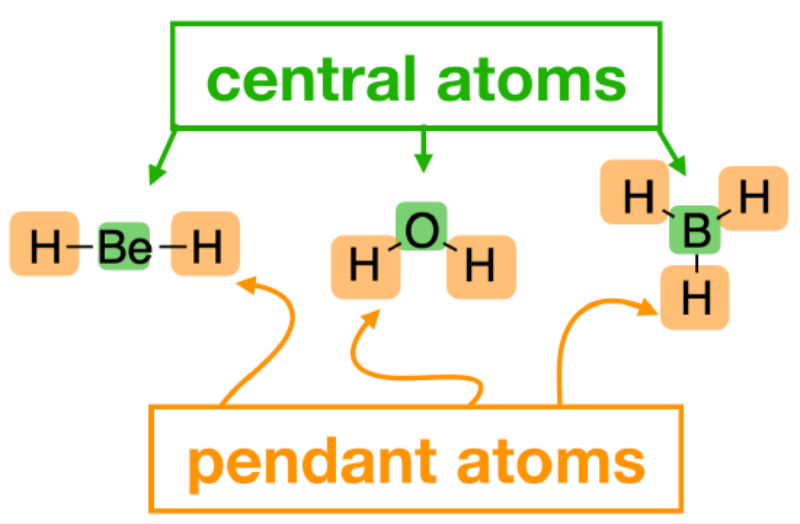
This page titled 6.8C: Vibrational Spectroscopy of Linear and Bent triatomic Molecules is shared under a license and was authored, remixed, and/or curated by LibreTexts.

- 3.7C: Vibrational Spectroscopy of Linear and Bent triatomic Molecules is licensed CC BY-NC-SA 4.0.

6.9: LARGER (POLYATOMIC) MOLECULES

We can extend the method we used for diatomic molecules to draw the molecular orbitals of more complicated, polyatomic molecules (molecules with more than two atoms). To combine several different atoms in a molecular orbital diagram, we will group orbitals from different atoms into sets that match the symmetry of a central atom. These **group orbitals** are also referred to as **symmetry adapted linear combinations (SALCs)**. We'll use a stepwise approach to do this as summarized below.

Symmetry adapted linear combinations (SALCs)



We need SALCs (aka group orbitals) to draw molecular orbital (MO) diagrams of *polyatomic* molecules. SALCs are groups of orbitals on **pendant atoms**. These groups of orbitals much match the symmetry of valence orbitals on the **central atom** in order to create a productive interaction. When we combine SALCs with the atomic orbitals on the central atom, we can generate an MO diagram that gives us information about the molecule's bonding and electronic states.

Below is a set of steps you can follow to find SALCs and draw an MO Diagram. Each step will be illustrated in detail through the examples in the subsections that follow this page.

1. Find the **point group** of the molecule and assign Cartesian coordinates so that z is the principal axis.
   Sometimes we can simplify things by looking only at the point group of the relevant orbitals. Only simplify when instructed to do so.*
2. Identify and count the pendant atoms' valence orbitals.
   Is there more than 1 type for each atom (ex. just s, or s and p?) We expect 1 SALC for each ligand orbital.
3. Generate a **reducible representation (Γ)** for the group of pendant atom orbitals using the appropriate character table.
   You have to do this for each set of orbital types. If you only have s orbitals for each ligand, you only need to generate 1 reducible representation. If you have p orbitals, you would generate additional Γ's for p_x, p_y, and p_z.
4. Break the Γ into its component **irreducible representations** from the character table. Note the symmetry of each irreducible representation, its associated orbitals, and their degeneracy.
5. If you are asked to sketch the shapes of SALCs, determine what they "look like" using one of the following strategies.
   (a) Shortcut: if the reducible representations are listed with s, p, or d orbitals in the character table, just draw them (... and skip steps b-c)
   (b) Systematic (Projection Operator) method: Draw an expanded character table and draw your molecule with each ligand identified by letters or numbers (*a,b,c...* or *i,j,k...* or *1,2,3...*) Determine where each pendant atom/orbital ends up under each of the operations of your expanded table. Project the values for each irreducible representation onto the chart you created and then add up the values. Positive and negative values are opposite signed orbitals.
6. Draw the MO diagram by combining SALCs with AO's of like symmetry. When drawing SALC energy levels, remember that the more nodal planes in your SALC orbital drawing, the higher the energy for that SALC orbital.

> * When we are focused on orbitals, as in the case for finding group orbitals and drawing molecular orbital diagrams, the symmetry of the orbitals is what we are interested in. In the case of high-symmetry point groups, like $D_{\infty h}$ and $C_{\infty v}$, even though the molecule may have a C_∞ axis, the orbitals do not necessarily retain this symmetry element. For example, the p_x orbital would not have a C_∞ axis, but rather a C_2 axis. It is sufficient and useful to substitute D_{2h} for $D_{\infty h}$ and C_{2v} for $C_{\infty v}$ to simplify the problem.

6.9.1: CO_2 (Revisted with Projection Operators)

6.9.2: BF_3

6.9.3: Bifluoride anion

6.9.4: Carbon Dioxide

6.9.5: H_2O

6.9.6: NH_3

This page titled 6.9: Larger (Polyatomic) Molecules is shared under a CC BY-NC-SA 4.0 license and was authored, remixed, and/or curated by LibreTexts.

- 5.4: Larger (Polyatomic) Molecules is licensed CC BY-SA 4.0.

6.9.1: CO_2 (Revisted with Projection Operators)

The process for finding SALCs and constructing the molecular orbital diagram for carbon dioxide was described in a previous section (Section 5.4.2). However, we also just presented an alternative strategy, the projection operator method, to finding the shapes of SALCs in Section 5.4.4. Let's revisit carbon dioxide and demonstrate how you can use the projection operator method to find SALCs for carbon dioxide.

Just as before, we can simplify the problem by approximating the $D_{\infty h}$point group using D_{2h}. The first four steps for constructing the MO diagram would be the same as described in Section 5.4.2. and we will pick up from that point (with Step 5) to find what the SALCs look like using the projection operator method.

The projection operator method applied to $\mathrm{CO_2}$

Step 5.1: Label the pendent atoms.

We can label the pendant atoms as O_a and O_b, as in Figure $6.9.1.1$.

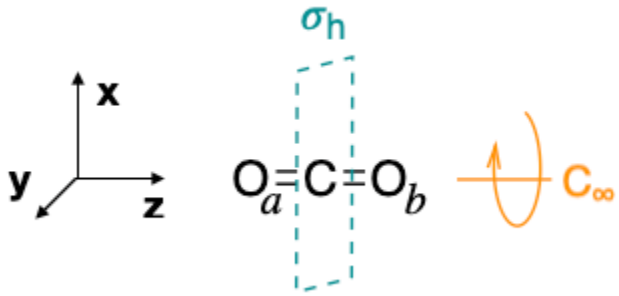


Figure $6.9.1.1$: The structure of carbon dioxide with pendant oxygen atoms distinguished with labels a and b. Note that we will approximate the C_∞ axis as a C_2 axis to simplify the process of finding the SALCs. (CC-BY-SA; Kathryn Haas)

Step 5.2: Create an expanded character table with one pendant atom's projected position for each operation

The D_{2h} character table needs no expansion because each operation is in its own class. We will arbitrarily choose to determine the new position of O_a after each operation.

[redacted]

Step 5.3: Find the contribution of each pendant atom to each SALC

Create a linear combination of the projections for each or the SALCs. The irreducible representations were found in step 4 in Section 5.4.2. Eight irreducible representations were found to be: $2A_g + 2B_{1u} + B_{2g} + B_{3u} + B_{3g} + B_{2u}$. For each of the irreducible representations, multiply the projection by the respective character of the operation.

$$\text{Contribution of each atom to the SALC } = \sum(\text{Projection of } H_a \times \chi)$$

The linear combination for all irreducible representations of D_{2h} are shown below.

Table $6.9.1.1$: The symmetry adapted linear combination (SALC) for each irreducible representations of C_3v are shown.



(6.9.1.1)

Notice that there are only two irreducible representations that produce SALCs, the A_g and the B_{1u}. Since we found two of each ($2A_g + 2B_{1u}$) when we found the irreducible representations, we know that there will be two SALCs of A_g symmetry and two of B_{1u} symmetry; that is four total SALCs from the pendant oxygens. This is the same as what we found in Section 5.4.2 using a different method.

Step 5.4: Sketch the SALCs

The SALCs with A_g symmetry: Quantitatively, we can apply the normalizing factor, N, for these SALCs. Each atom contributes equally to the SALCs, thus the normalizing factor for the A_g SALC is $N = \left(\frac{1}{\sqrt{1^2+1^2}}\right) = \frac{1}{\sqrt{2}}$. This tells us that each oxygen contributes $\frac{1}{\sqrt{2}}$ to each of the normalized A_g group orbitals:

$$A_g \text{ group orbital } = \frac{1}{\sqrt{2}}\left[\psi_{O_a} + \psi_{O_b}\right]$$

The linear combination $4\mathrm{O}_a + 4\mathrm{O}_b$ indicates that wavefunctions from each oxygen atom contribute equally to each of the two SALCs, with the same sign of the wavefunction for each. Because we know that A_g is totally symmetric (all 1's in the characters), we can assume that the SALC's will look like a symmetric arrangement of oxygen orbitals. But which orbitals contribute? We could peek at the character table to get a hint. But we'll treat this problem systematically.

The SALCs with B_{1u} symmetry: The linear combination $4\mathrm{O}_a - 4\mathrm{O}_b$ indicates that each oxygen atom contributes equally, but that they have opposite wavefunctions. Application of the normalizing factor would give us:

$$B_{1u} \text{ group orbital } = \frac{1}{\sqrt{2}}\left[\psi_{O_a} + \psi_{O_b}\right]$$

But how do we know what the SALCs look like? Again, the character table can give us some hints, but we'll use a systematic process, below.

What do the SALCs look like? One way to systematically derive the SALC shapes is to perform the projection (Step 5.3) on specific groups of orbitals on the oxygen atom. For example, if we replicate Table 6.9.1.1 using just the group of oxygen 2s orbitals and the A_g and B_{1u} representations, we get the following:



(6.9.1

This tells us that one of the A_g SALCs looks like two oxygen 1s orbitals with equal signs and contributions. It also tells us that one of the B_{1u} SALCs looks like two s orbitals with opposite signs and equal magnitudes. These two SALCs are shown in Figure 6.9.1.2 .

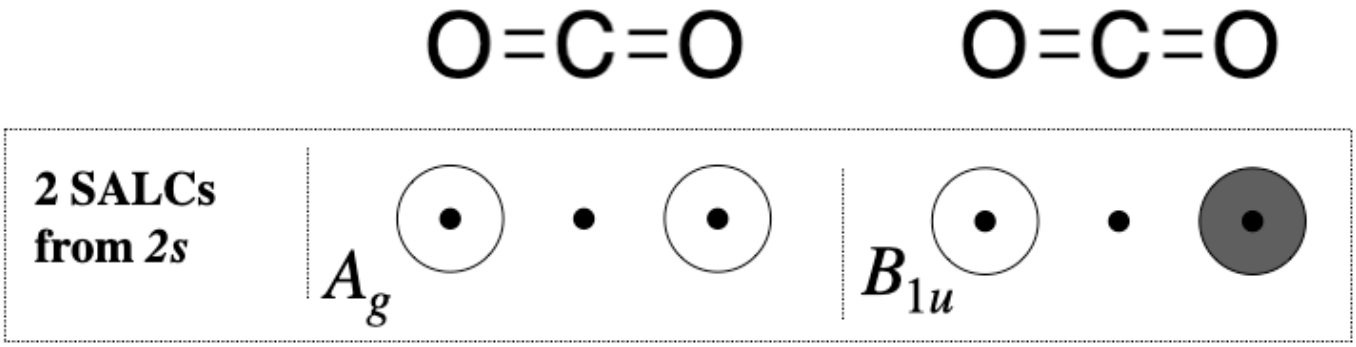


Figure $6.9.1.2$: SALCs derived from two oxygen $2s$ orbitals from carbon dioxide. Compare to Section 5.4.2. (CC-BY-SA; Kathryn Haas)

If we do the same for the $2p_z$ orbitals, we need to pay attention to the orientation of the p orbital lobes. If the orbital is moved into the opposite orientation, it would get a negative sign in the projection (see below).



This tells us that one of the A_g SALCs is derived from two $2p_z$ orbitals of opposite sign but equal magnitude. In other words, the two p orbitals are pointing in opposite directions, but the lobes that are facing one another are of the same sign (see Figure $6.9.1.3$, left). This also tells us that one of the B_{1u} orbitals is derived from two p_z orbitals of equal magnitude and equal sign (pointing in the same directions, with lobes facing one another of opposite sign!) (see Figure $6.9.1.3$, right).

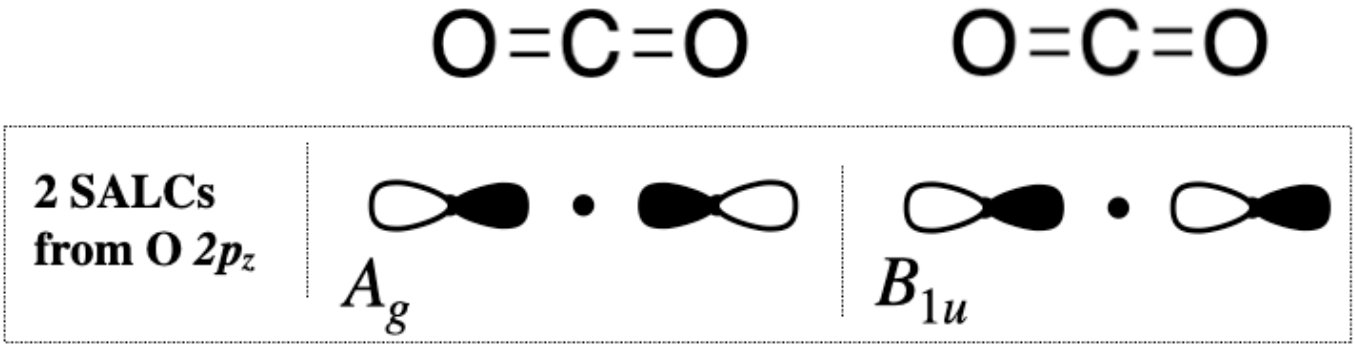


Figure $6.9.1.3$: SALCs derived from two oxygen $2p_z$ orbitals from carbon dioxide. Compare to Section 5.4.2. (CC-BY-SA; Kathryn Haas)

Now we have reached the same SALCs that we found previously in Section 5.4.2, but by an alternate method.

This page titled 6.9.1: CO_2 (Revisted with Projection Operators) is shared under a CC BY-NC-SA 4.0 license and was authored, remixed, and/or curated by LibreTexts.

- 5.4.4: NH_3 by Kathryn Haas is licensed CC BY-SA 4.0.

6.9.2: BF_3

The case of boron trifluoride (BF_3) is an example of a molecule with one more layer of complexity than the other examples we have seen in previous sections in this chapter. (BF_3) is more complex than previous examples because it is the first case in which there are multiple types of valence orbitals on the pendant atoms. (BF_3) possesses s and p orbitals on *both* the central atom and all of the pendant atoms. We can follow the same steps that we have previously to derive other molecular orbital diagrams; however, there is one important difference: we will treat each type of pendant orbital as an individual set of SALCs.

Step 1. Find the point group of the molecule and assign Cartesian coordinates so that z is the principal axis.

The BH_3 molecule is trigonal planar, and its point group is D_{3h}. The z axis is colinear with the principle axis, the C_3 axis.

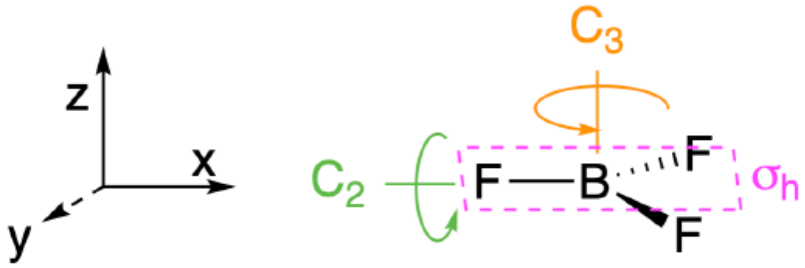


Figure 6.9.2.1: The molecule is in the D_{3h} point group. (CC-BY-NC-SA; Kathryn Haas)

Step 2. Identify and count the pendant atoms' valence orbitals.

Each of the three pendant fluorine atoms has four valence orbitals: one $2s$ and three $2p$ orbitals. Thus, we can expect a total of twelve SALCs from the three atoms. However, we will treat each type of orbital from the F atoms as its own set; each will have its own set of coordinates, with the y axis along the M-L bond. Thus we expect the following:

- One set of $2s$ SALCs: there is one 2s orbital on each of three atoms. This set will have three SALCs.
- One set of $2p_x$ SALCs: there is one $2p_x$ orbital on each of three atoms. Each of these individual orbitals is perpendicular to the M-L bond and coplanar with the molecule. This set will have three SALCs.
- One set of $2p_y$ SALCs: there is one $2p_y$ orbital on each of three atoms. Each of these individual orbitals is colinear with the M-L bond. This set will have three SALCs.
- One set of $2p_z$ SALCs: there is one $2p_z$ orbital on each of three atoms. Each of these individual orbitals is perpendicular to the M-L bond and parallel with the principal axis of the molecule. This set will have three SALCs.

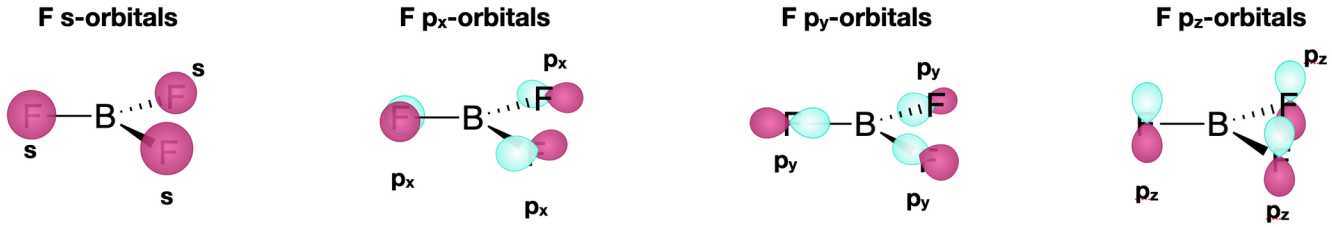


Figure 6.9.2.2: Individual sets of pendant fluorine atomic orbitals will create separate sets of SALCs. (CC-BY-SA; Kathryn Haas)

Step 3. Generate the Γ's for each set of SALCs

Use the D_{3h} character table to generate one reducible representation (Γ) for each of the four sets of pendant atomic orbitals shown in Figure $6.9.2.2$; in this case we need four Γ because there are four types of valence orbital (the s, p_x, p_y, p_z).

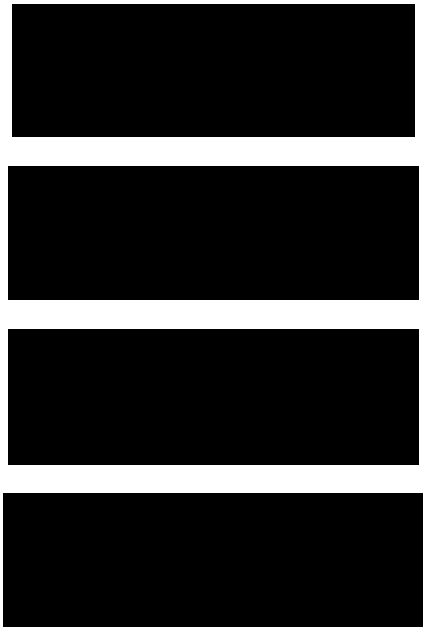
- For the set of s orbitals: perform the operation for each class in the character table. Each s orbital is assigned a value depending on whether it moves or not: assign a value of 1 if it remains in place during the operation, or 0 (zero) if it moves out of its original place.
- for each set of p orbitals: Now there are phases (signs of the wavefunction), so a negative value is possible. Assign a value of 1 to each p orbital if it remains in place and in phase during the operation; assign a -1 if the atom's position remains, while the phase of the orbital is inverted (the positive lobe moves to the position of the negative lobe and vice versa); assign a 0 if it moves out of its original position.

The Γ for each type is given below:



Step 4. Break Γ's into irreducible representations for individual SALCs

Reduce each Γ into its component irreducible representations. Using either of the processes described previously, we find that each of the Γ reduces to two irreducible representations under the D_{3h} point group; in each case one is singly degenerate (A) and the other doubly degenerate (E). This equates to three SALCs for each Γ (orbital type) and a total of twelve SALCs. This should give us confidence! We were in fact expecting 12 SALCs because we found that there were twelve pendant atomic orbitals to start with.



Step 5: Sketch the SALCs

We'll skip this step for now to make this problem simpler.

Step 6: Draw the MO diagram by combining SALCs with AO's of like symmetry.

We now know the symmetries of different pendant orbital SALCs - and it is helpful if we also know their relative energies, and the energies of the valence orbitals on the central boron atom. We can make predictions based on periodic trends, or we can use a table of ionization energies as a guide. The symmetries of the boron $2s$ and $2p$ orbitals can be found from the D_{3h} character table.

This page titled 6.9.2: BF_3 is shared under a CC BY-NC-SA 4.0 license and was authored, remixed, and/or curated by LibreTexts.

- 5.4.4: NH_3 by Kathryn Haas is licensed CC BY-SA 4.0.

6.9.3: Bifluoride anion

Finding SALCs and drawing the MO diagram for [F-H-F]$^-$

The linear anion [F-H-F]$^-$ is a good place to start as an example to illustrate the process of generating pendant atom SALCs and then constructing a molecular orbital diagram for a polyatomic molecule. We will proceed using the steps outlined on the previous page for generating SALCs and a molecular orbital diagram.

Step 1. Find the point group of the molecule and assign Cartesian coordinates so that z is the principal axis.

We begin by assigning the appropriate point group for this molecule: $D_{\infty h}$ (Figure $6.9.3.1$). As mentioned in the previous page, it is useful to substitute D_{2h} for $D_{\infty h}$ when generating SALCs and molecular orbital diagrams. The z axis is assigned to be colinear with the principal axis, and in this case is the same as the C_∞ axis (Figure $6.9.3.1$).

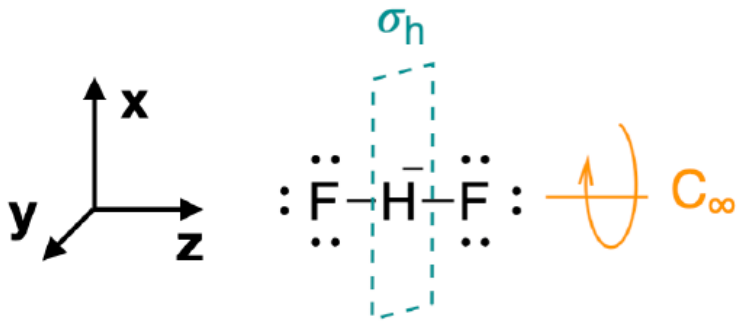


Figure $6.9.3.1$: The [FHF]$^-$ anion belongs to the $D\infty_h$ point group. (CC-BY-NC-SA; Kathryn Haas)

Step 2. Identify and count the pendant atoms' valence orbitals.

The next step is to identify the valence orbitals on the pendant F atoms that will form SALCs. In most cases, you should consider all of the valence orbitals. In this case, each of the fluorine atoms has four valence orbitals ($2s$, $2p_x$, $2p_y$, and $2p_z$). From these eight fluorine valence orbitals, we should expect eight group orbitals (SALCs).

3. - 5. Generate SALCS (shortcut)

To draw these SALCs for this molecule is rather simple, and we don't need to follow all the steps of finding the Γ's and reducing them. Rather, you can proceed as if you are creating bonding and antibonding molecular orbitals between the two F atoms, except that the F orbitals are separated by the H atom. Approximate sketches of the eight SALCs from F valence orbitals are shown in Figure $6.9.3.2$.

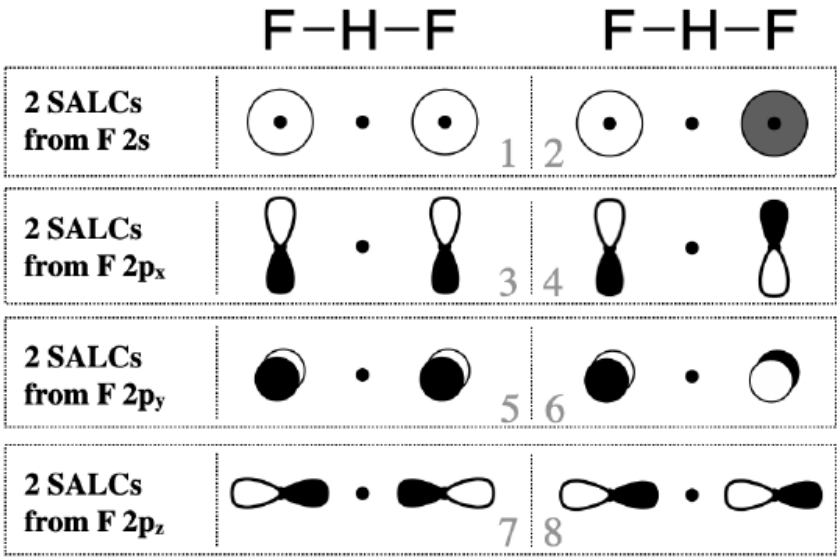


Figure 6.9.3.2: Eight SALCs from the valence orbitals of two fluorine atoms. (CC-BY-NC-SA; Kathryn Haas)

6. Draw the MO diagram by combining SALCs with AO's of like symmetry.

SALCs can productively interact with the central atom only when symmetry is compatible. Just some of the groups of orbitals in Figure 6.9.3.2 possess appropriate symmetry to combine with the hydrogen atom valence orbital (the H $1s$). In this simple case, you can decide whether orbitals have compatible symmetry by visually inspecting the shapes of the group orbitals. The F $2p_y$ and $2p_x$ orbitals do not have appropriate symmetry to bond to the H $1s$ orbital because the nodes of these orbitals run through the center of the H $1s$ orbital, thus we can eliminate all SALCs composed from F $2p_x$ and $2p_y$ (*these are SALCs numbered 3-6 in Figure* 6.9.3.2). On the other hand, the F $2s$ and $2p_z$ orbitals individually do have appropriate shape and direction in space for productive interaction with an H $1s$ orbital. However only SALCs where the *entire group* has appropriate symmetry will combine with H $1s$ to produce bonding or antibonding molecular orbitals. Only the SALCs labeled with numbers 1 and 7 can combine with an s orbital in the center of the group. The ways in which these SALCs are able to combine with H $1s$ are illustrated in Figure 6.9.3.3.

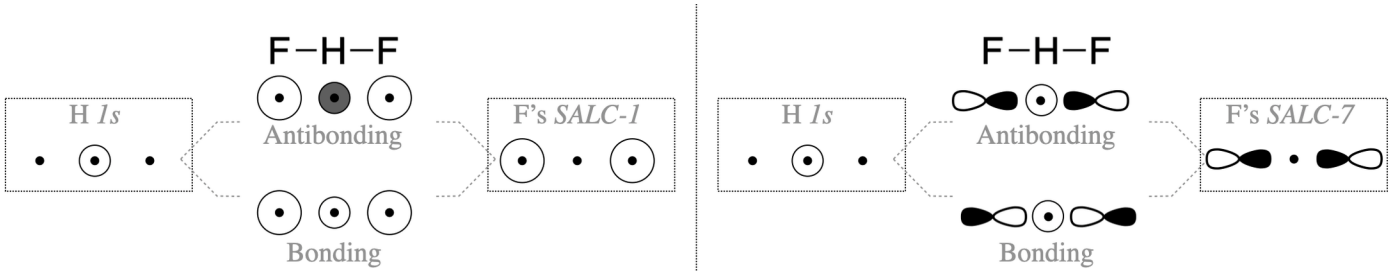


Figure 6.9.3.3: Combinations of a central H $1s$ orbital with the group orbitals, SALC-1 and SALC-7 from Figure 6.9.3.2, to create bonding and antibonding interactions. (CC-BY-NC-SA; Kathryn Haas)

Before we assume that both SALC-1 and SALC-7 will combine with the H $1s$ orbital, we must consider the energies of all atomic orbitals. The F $2p_z$ orbital has a potential energy of -18.7 eV (see Table 5.3.1). This is a good match for the H $1s$ orbital (-13.6 eV). However, the F $2s$ orbital has a much lower energy of -46.37 eV and would have weak interaction with the H $1s$.

The molecular orbital diagram for [F-H-F]$^-$ is shown in Figure 6.9.3.4. Notice that all atomic orbitals, group orbitals (SALCs), and molecular orbitals in Figure 6.9.3.4 are assigned a symmetry label that corresponds to each element's symmetry under the D_{2h} point group. The molecular orbital labels correspond to **lower-case Mulliken Labels** of individual reducible representations from the D_{2h} character table. Upper-case symbols are used to indicate symmetry and irreducible representations, while lower-case symbols are used to indicate the identity of an orbital with that symmetry. The labeling methods described for simple diatomic linear molecules (σ, π) are not sufficient to indicate the more complex symmetries of the molecular orbitals in polyatomic molecules. The use of lower-case Mulliken symbols is the most rigorous way to label the orbitals. Refer to your instructor for how you should label orbitals for any graded work.

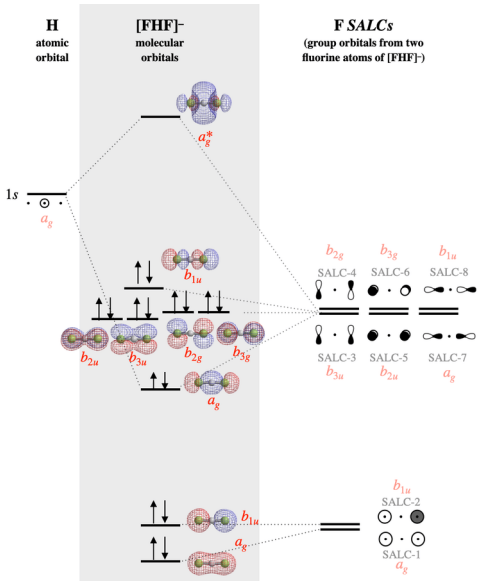
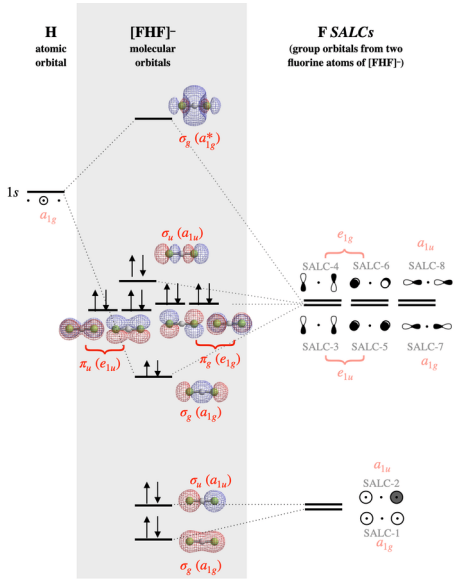


Figure 6.9.3.4:The molecular orbital diagram for [F-H-F]$^{-}$. The molecular orbital surfaces and relative energy levels were calculated using Spartan software. SALCs are labeled according to numbers assigned in Figure 6.9.3.2. The symmetry of each SALC and orbital under the D_{2h} **point group** is shown in red font. (CC-BY-NC-SA; Kathryn Haas)

Click here for a version of Figure 6.9.3.4 using $D_{\infty h}$ labeling:

For high-symmetry groups, a shortcut is to use a lower-symmetry group that maintains the critical symmetry elements. In the case of the $D_{\infty h}$ point group, it is often sufficient to use the approximation of the D_{2h} point group and character table. This is the same MO diagram as shown above, but using the symmetry labels appropriate for the D_{2h} approximation.



Alternate Figure 6.9.3.4: The molecular orbital diagram for [F-H-F]$^{-}$. The molecular orbital surfaces and relative energy levels were calculated using Spartan software. SALCs are labeled according to numbers assigned in Figure 6.9.3.2. The symmetry of each SALC and orbital under the D_{2h} **point group** is shown in red font. (CC-BY-NC-SA; Kathryn Haas)

Constructing the MO diagram

After identifying the atomic orbitals and constructing SALCs, place the atomic orbitals of H on one side of the diagram and all SALCs from F on the other side. Molecular orbitals are in the center.

The lowest-energy fluorine SALCs will be those composed of the lowest-energy atomic orbitals of fluorine; these would be SALC-1 (a_{1g}) and SALC-2 (a_{1u}) that are constructed from fluorine s atomic orbitals. Of these two orbitals, the one with zero nodes would be slightly lower in energy than the one with one node. When these two orbitals form molecular orbitals, the completely symmetric SALC-1 will be mostly non-bonding with slight bonding character from minor combination with the hydrogen $1s$ orbital. SALC-2, however is symmetrically incompatible with hydrogen $1s$ and will be a truly non-bonding orbital distributed over both F atoms.

The six SALCs constructed of fluorine p orbitals will have higher energy since the fluorine p atomic orbitals are higher in energy than the s orbitals (SALC-3 through SALC-8). Again, we expect SALCs with more nodes (SALC-4, -6, -8) to have slightly higher energy than those with fewer nodes (SALC-3, -5, -7). SALC-7 will form a bonding and antibonding interaction with the hydrogen $1s$ orbital. All other SALCS are truly non-bonding, but are non-degenerate non-bonding orbitals.

In bifluoride, there is an important distinction between the Lewis structure and molecular orbital description of lone pairs. In Lewis theory, the lone pairs are localized to individual fluorine atoms, while in the molecular orbital description each lone pair is distributed over both fluorine atoms at once (see surface depiction of each molecular orbital in Figure $6.9.3.4$).

This page titled 6.9.3: Bifluoride anion is shared under a CC BY-NC-SA 4.0 license and was authored, remixed, and/or curated by LibreTexts.

- 5.4.1: Bifluoride anion is licensed CC BY-SA 4.0.

6.9.4: Carbon Dioxide

Construct SALCs and the molecular orbital diagram for CO_2

Carbon dioxide is another linear molecule. This example is slightly more complex than the previous example of the bifluoride anion. While bifluoride had only one valence orbital to consider in its central H atom (the $1s$ orbital), carbon dioxide has a larger central atom, and thus more valence orbitals that will interact with SALCs.

Preliminary Steps

Step 1. Find the point group of the molecule and assign Cartesian coordinates so that z is the principal axis.

The CO_2 molecule is linear and its point group is $D_{\infty h}$. The z axis is collinear with the C_∞ axis. We will use the D_{2h} point group as a substitute since the orbital symmetries are retained in the D_{2h} point group.

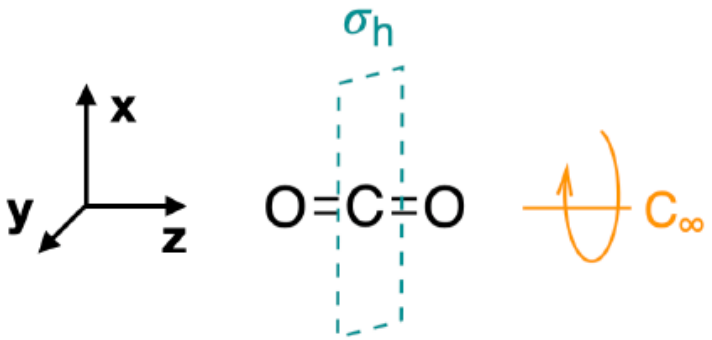


Figure $6.9.4.1$: CO_2 belongs to the $D_{\infty h}$ point group. (CC_BY-NC-SA; Kathryn Haas)

Step 2. Identify and count the pendant atoms' valence orbitals.

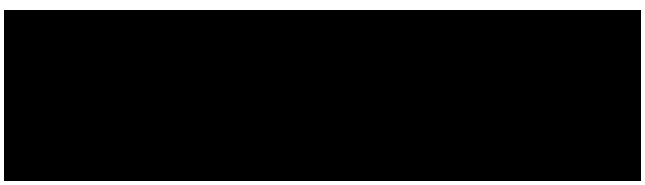
Each of the two pendant oxygen atoms has four valence orbitals; $2s$, $2p_x$, $2p_y$, and $2p_z$. Thus, we can expect a total of eight SALCs.

Generate SALCs

The SALCs for CO_2 are identical in shape and symmetry to those described in the previous example for the bifluoride anion. But instead of cutting to the shortcut, we will systematically derive the SALCs here to demonstrate the process.

Step 3. Generate the Γ's

Use the D_{2h} character table to generate four reducible representations ($\Gamma's$); one for each of the four types of pendant atom orbitals ($s,\ p_x,\ p_y,\ p_z$). For each s orbital, assign a value of 1 if it remains in place during the operation or zero if it moves out of its original place. For each p orbital, assign 1 if there is no change, -1 if it remains in place but is inverted, and 0 if it moves out of its original position. The four Γ's are given below:



Step 4. Break Γ's into irreducible representations for individual SALCs

Reduce each Γ into its component irreducible representations. There are two strategies that can be used to do this. The quick and easy way is to do it "by inspection", but this only works well for simple cases. The other is by using the systematic approach for breaking a Γ into reducible representations described previously in section 4.4.2 using the following formula:

$$\text{number of } i = \frac{1}{h}\sum(\text{number of operations in class}) \times (\chi_\Gamma) \times (\chi_i) \tag{6.9.4.1}$$

In other words, the number of irreducible representations of type i is equal to the sum of the number of operations in the class $\times$ the character of the Γ_{modes} $\times$ the character of i, and that sum is divided by the order of the group (h).

Using either approach results in the following eight irreducible representations ($2A_g + 2B_{1u} + B_{2g} + B_{3u} + B_{3g} + B_{2u}$):



Step 5. Sketch the SALCs

From the systematic process above, you have found the symmetries (the irreducible representations) of all eight SALCs under the D_{2h} point group. To sketch the SALC that corresponds to each irreducible representation, again we use the D_{2h} character table, and specifically the functions listed on the right side columns of the table.

Two A_g SALCs (one from s and one from p_z): The A_g SALCs are each singly degenerate and symmetric with respect to both the principal axis (z) and the inversion center (i) (based on its Mulliken Label). We can look at the functions in the D_{2h} character table that correspond to A_g and see that it is completely symmetric under the group (because the combination of x^2, y^2, z^2 shows that it is totally symmetric). This would be the same symmetry as an s orbital on the central atom. From this information, we know that these SALCs must have symmetry compatible with an s orbital on the central atom, and we can draw the two A_g SALCs shown in Figure 6.9.4.2.

Two B_{1u} SALCs (one from s and one from p_z): The Mulliken Label tells us that the B_{1u} SALCs are each antisymmetric with respect to both the principal axis and the inversion center. The function, z, appearing with B_{1u} in the character table tells us that these SALCs have the same symmetry as the z axis, or a p_z orbital on the central atom. From this information, we know that these two SALCs should be compatible with a p_z orbital on the central atom, and we can draw the two B_{1u} SALCs shown in Figure 6.9.4.2 .

All other SALCs shown below are derived using a strategy similar to the one in the two cases described above.

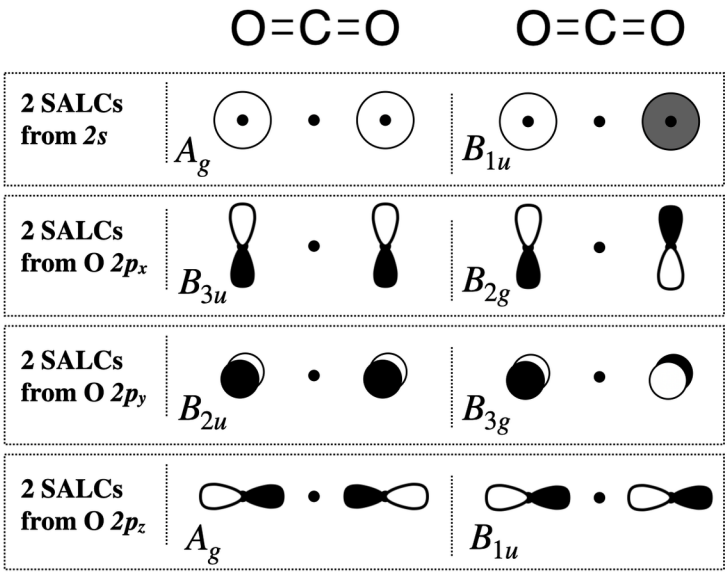


Figure 6.9.4.2: SALCs from the valence orbitals of oxygen atoms in CO_2. (CC-BY-NC-SA; Kathryn Haas)

Draw the MO diagram for CO_2

Step 6. Combine SALCs with AO's of like symmetry.

First we identify the valence orbitals on carbon: there are four including $2s$, $2p_x$, $2p_y$, and $2p_z$. Now we identify the symmetry of each using the D_{2h} character table. The symmetry of a central s orbital corresponds to the combination of functions x^2, y^2, and z^2 in the character table; this is A_g. The p_z orbital corresponds to the symmetry of the linear function z in the character table; this is B_{1u}. And so on... The symmetries of the C valence orbitals are listed below.

$$2s = A_g$$
$$2p_x = B_{3u}$$
$$2p_y = B_{2u}$$
$$2p_z = B_{1u}$$

Now that we have identified the symmetries of the eight oxygen SALCs and the four valence orbitals on carbon, we know which atomic orbitals and SALCs may combine based on compatible symmetries. We also need to know the relative orbital energy levels so that we can predict the relative strength of orbital interactions. The orbital ionization energies are listed in Section 5.3.

With knowledge of both orbital symmetries and energies, we can construct the molecular orbital diagram. The carbon atom goes on one side of the diagram while the oxygen SALCs are drawn on the opposite side. Molecular orbitals are drawn in the center column of the diagram:

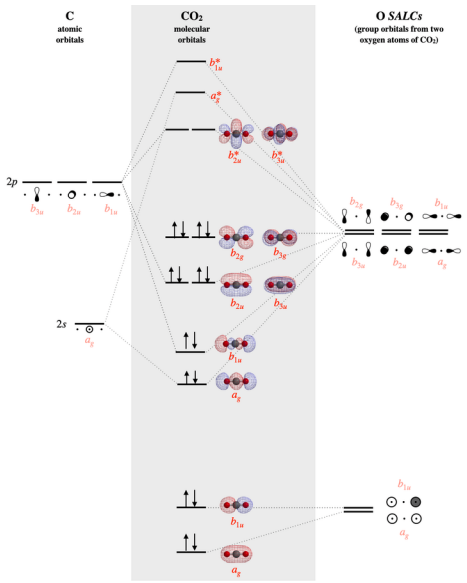


Figure 6.9.4.3: Molecular orbital diagram for carbon dioxide. (CC-BY-NC-SA; Kathryn Haas)

The SALCs on the right side of the diagram above are constructed from groups of either the $2s$ atomic orbitals of oxygen, or the $2p$ atomic orbitals of oxygen. Each SALC will combine with the atomic orbitals of carbon that have compatible symmetry; but the strength of the interaction depends on their relative energies. The individual valence atomic orbitals of oxygen have energies of $-32.36eV$ ($2s$) and $-15.87eV$ ($2p$), while the valence orbitals of carbon have energies of $-19.47eV$ ($2s$) and $-10.66eV$ ($2p$). The $2s$ orbitals of the oxygen are far lower in energy ($-32.36eV$) than all other valence orbitals, and so we should expect that molecular orbitals that are constructed from these oxygen $2s$ will be mostly non-bonding. These mostly non-bonding orbitals are the a_{1g} and b_{1g} orbitals shown at the bottom of Figure 6.9.4.3. The a_g orbital is lower in energy than the b_{1u} due to slight mixing with other orbitals of a_g symmetry.

The bonding orbitals of CO_2 include two $sigma$ molecular orbitals of a_g and b_{1u} symmetry and two π molecular orbitals of b_{2u} and b_{3u} symmetry. Each of these bonding molecular orbitals possesses a higher-energy antibonding partner. The b_{2g} and b_{3g} SALCs that are formed from oxygen $2p_x$ and $2p_y$ orbitals have no compatible match with carbon valence orbitals; thus they form two b_{2g} and b_{3g} molecular orbitals, which are truly non-bonding and mostly oxygen in character. Still, notice that each orbital is spread across both oxygen atoms at once, and again we see that each non-bonding electron pair in the HOMO is very different in molecular orbital theory compared to Lewis theory. Each non-bonding pair is distributed over both oxygen atoms at once in molecular orbital theory, while in Lewis theory each lone pair is isolated to one atom or to localized bonds attached to that atom.

This page titled 6.9.4: Carbon Dioxide is shared under a CC BY-NC-SA 4.0 license and was authored, remixed, and/or curated by Kathryn Haas.

- 5.4.2: Carbon Dioxide by Kathryn Haas is licensed CC BY-SA 4.0.

6.9.5: H_2O

Construct SALCs and the molecular orbital diagram for H_2O.

This is the first example so far that is not a linear molecule. Water is a bent molecule, and so it is important to remember that interactions of pendant ligands are dependent on their positions in space. You should consider the positions of the three atoms in water to be essentially fixed in relation to each other. The process for constructing the molecular orbital diagram *for a non-linear molecule*, like water, is similar to the process for linear molecules. We will walk through the steps below to construct the molecular orbital diagram of water.

Preliminary Steps

Step 1. Find the point group of the molecule and assign Cartesian coordinates so that z is the principal axis.

The H_2O molecule is bent and its point group is C_{2v}. The z axis is collinear with the principal axis, the C_2 axis. There is no need to simplify this problem, as we had done for previous examples. The C_{2v} point group is simple enough.

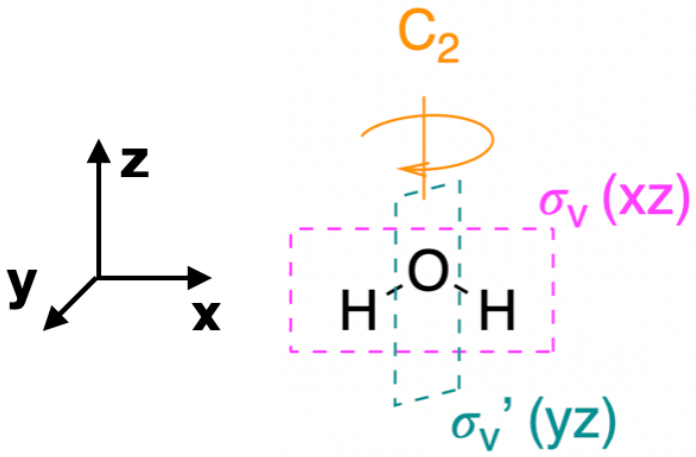


Figure $6.9.5.1$: The water molecular is in the C_{2v} point group. (CC-BY-NC-SA; Kathryn Haas)

Step 2. Identify and count the pendant atoms' valence orbitals.

Each of the two pendant hydrogen atoms has one valence orbital, the $1s$. Thus, we can expect a total of two SALCs from these two atoms.

Generate SALCs

The SALCs for H_2O are quite simple, yet we will systematically derive the SALCs here to demonstrate the process.

Step 3. Generate the Γ's

Use the C_{2v} character table to generate one reducible representation (Γ); in this case we need only one Γ because there is only one type of valence orbital (the $1s$). For each s orbital, assign a value of 1 if it remains in place during the operation or zero if it moves out of its original place. The Γ is given below:

[redacted]

Step 4. Break Γ's into irreducible representations for individual SALCs

Reduce each Γ into its component irreducible representations. Using either of the processes described previously, we find that the Γ reduces to the two irreducible representations A_1 and B_1 under the C_{2v} point group.

[redacted]

Step 5. Sketch the SALCs

From the systematic process above, you have found the symmetries (the irreducible representations) of both SALCs under the C_{2v} point group. To sketch the SALC that corresponds to each irreducible representation, again we use the C_{2v} character table, and specifically the functions listed on the right side columns of the table.

One A_1 SALC: The A_1 SALC is singly degenerate and symmetric with respect to both the principle axis (z) and the inversion center (i) (based on its Mulliken Label). We can look at the functions in the C_{2v} character table that correspond to A_1 and see that it is completely symmetric under the group (because the combination of x^2, y^2, z^2 shows that it is totally symmetric). This would be the same symmetry as an s orbital on the central oxygen atom. From this information, we know that this SALC must have symmetry compatible with an s orbital on the central atom. We can also see from the character table that the z axis, and thus a p_z orbital on oxygen, also possesses A_1 symmetry. This tells us that in addition to being compatible with the oxygen s orbital, it should also be compatible with the oxygen p_z orbital. From this information we can draw the A_1 SALC shown in Figure 6.9.5.2 . *If it is not obvious how the A_1 sketch in Fig. 6.9.5.2 is compatible with the s and p_z orbitals of oxygen, inspect the drawings corresponding to molecular orbitals $2a_1$ and $3a_1$ in Fig. 6.9.5.3.*

One B_1 SALC: The Mulliken Label tells us that the B_1 SALC is singly degenerate and antisymmetric with respect to both the principal axis and the inversion center. The function, x, appearing with B_1 in the character table tells us that this SALC has the same symmetry as the x axis, or a p_x orbital on the central oxygen atom. From this information, we know that this SALC should be compatible with a p_x orbital on the central atom, and we can draw the B_1 SALCs shown in Figure 6.9.5.2. *If it is not obvious how the B_1 sketch in Fig. 6.9.5.2 is compatible with the p_x orbital of oxygen, inspect the drawing corresponding to molecular orbital $1b_1$ in Fig. 6.9.5.3.*

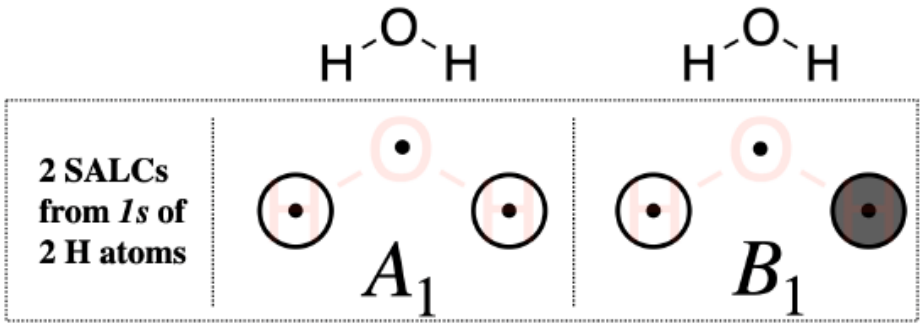


Figure 6.9.5.2: Sketch of the A_1 and B_1 hydrogen SALCs of water. (CC-BY-NC-SA; Kathryn Haas)

Not convinced about the sketches of these SALCs? You can convince yourself by putting them to the test. Try the exercise below.

Exercise 6.9.5.1

Perform all operations of the C_{2v} point group on the two sketches of H SALCs shown in Figure 6.9.5.2, and convince yourself that each sketch does possess the A_1 and B_1 symmetries assigned to them, respectively, under the C_{2v} point group.

Answer available at the end of this section.

Draw the MO diagram for H_2O

Step 6. Combine SALCs with AO's of like symmetry.

First we must identify the valence orbitals on the central oxygen: there are four including $2s$, $2p_x$, $2p_y$, and $2p_z$. Now we identify the symmetry of each using the C_{2v} character table. The symmetry of a central $2s$ orbital corresponds to the combination of functions x^2, y^2, and z^2 in the character table; this is A_1. The p_z orbital also corresponds to A_1. And so on... The symmetries of oxygen valence orbitals are listed below.

$$2s = A_1$$
$$2p_x = B_1$$
$$2p_y = B_2$$
$$2p_z = A_1$$

Now that we have identified the symmetries of the two hydrogen SALCs and the four valence orbitals on oxygen, we know which atomic orbitals and SALCs may combine based on compatible symmetries. We also need to know the relative orbital energy levels so that we can predict the relative strength of orbital interactions. The orbital ionization energies are listed in Section 5.3.1.

With knowledge of both orbital symmetries and energies, we can construct the molecular orbital diagram. The valence orbitals of oxygen go on one side of the diagram while the hydrogen group orbitals are drawn on the opposite side. Molecular orbitals are drawn in the center column of the diagram, as shown in Figure 6.9.5.3:

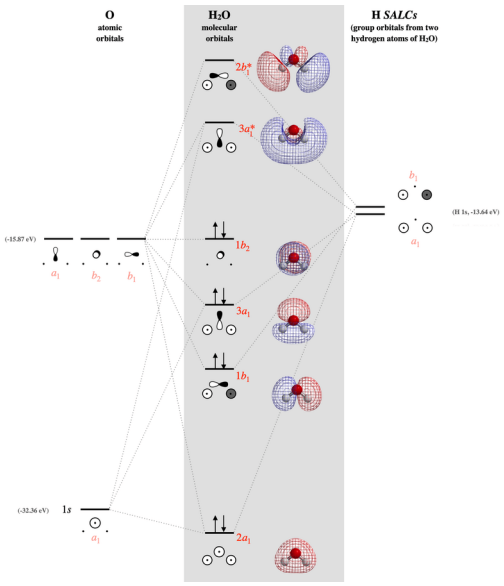


Figure 6.9.5.3: The molecular orbital diagram of water. Molecular orbital surfaces calculated using Spartan software. The surface of the $3a_1^*$ orbital has been trimmed. (CC-BY-NC-SA; Kathryn Haas)

Example 6.9.5.1

In the previous examples shown for the molecular orbital diagrams of the bifluoride anion and carbon dioxide, we discussed differences in the understanding of those molecules from molecular orbital theory compared to Lewis structures. Water contains two lone pairs in its Lewis structure. Compare the predictions about water's lone pairs of electrons and its reactivity based on (1) the combination of elementary models (Lewis, Valence Bond, and Hybridized Orbital theories) and (2) Molecular Orbital theory. Specifically address and explain how the elementary models differ from molecular orbital theory in the following respects:

a. Where are the lone pairs in water?

b. Are the two lone pairs equivalent or are they different?
c. Where are sites on the molecule that will undergo reaction with electrophiles and nucleophiles?

Solution

1) Elementary models: The Lewis structure predicts that two lone pairs are (a) localized on the oxygen atom of water and that (b) both lone pairs are equivalent. The Lewis structure, combined with Valence Bond Theory, would predict that lone pairs occupy two equivalent hybridized sp^3 atomic orbitals on oxygen. (c) Lewis theory would predict that the oxygen lone pairs are nucleophiles; thus an electrophile would react with the oxygen atom lone pairs. The polarized O-H bond leaves the H atoms as the most electrophilic locations on the water molecule; thus nucleophiles would react at the H atoms of water.

2) Molecular orbital theory: The molecular orbitals predict that (a) the two lone pairs of water are not equivalent, and that (b) each is distributed over the entire molecule. One lone pair is in the truly non-bonding $1b_2$ orbital (Figure $6.9.5.3$), which is also the HOMO. There is not another truly non-bonding orbital in the molecule, but the lowest-energy $2a_1$ orbital could be considered mostly non-bonding due to the large energy difference between it and other valence orbitals. (c) Although the $2a_1$ orbital can be considered mostly non-bonding, we cannot expect the electrons in $2a_1$ to react readily, as they are in the lowest-energy molecular orbital. Molecular orbital theory predicts that reactions occur at the HOMO and LUMO orbitals. The HOMO reacts with electrophiles, and in this case, the HOMO is distributed over the top and bottom faces of the molecule, and is centered on the oxygen atom. The LUMO would react with nucleophiles. The LUMO is the orbital labeled $3a_1^*$ in Figure $6.9.5.3$, and has a major lobe that is distributed more heavily over the H atoms, and from this we should predict H atoms to be the preferred site of reaction for nucleophiles.

Expressing molecular orbitals in terms of Ψ

The general expression for a molecular orbital, or the linear combination of atomic orbitals (LCAO), was given previously as $\Psi = c_a\psi_a + c_b\psi_b$. In this expression, the wavefunction of two atoms (ψ_a and ψ_b) is combined to form the wavefunction of the molecular orbital. The coefficients c_a and c_b quantify the contribution of each atomic ψ to the molecular Ψ.

$$\Psi = c_a\psi_a + c_b\psi_b$$

In the case of polyatomic orbitals, each LCAO is constructed of atomic orbitals from a central atom and group orbitals (SALCs) from the pendent atoms. In the case of water, the expression above could be modified to give the expression below.

$$\Psi = c_{oxygen}\left(\psi_{oxygen}\right) + c_{SALCs}\left(N(\psi_{H_a} \pm \psi_{H_b})\right)$$

N represents the normalizing requirement that was mentioned previously in reference to the requirements for electron wavefunctions and probability functions. The normalizing requirement simply stated is the requirement that the probability of finding the electron in any orbital, including group orbitals, is 1. In general, the value of N for a group orbital is...

$$N = \frac{1}{\sum c_i^2}$$

...where c_i is the coefficient of each unique atomic orbital that contributes to the group. For the hydrogen SALCs of water, there are two atomic orbitals that contribute to equally to each SALC, and so the coefficient on each of the two orbitals is 1. This gives $N = \left(\frac{1}{\sqrt{1^2+1^2}}\right) = \frac{1}{\sqrt{2}}$ for the H SALCs of water.

There are only two hydrogen SALCs: the one in which the hydrogen wavefunctions are added ($N(\psi_{H_a} + \psi_{H_b})$) has A_1 symmetry, and the one in which the hydrogen wavefunctions are subtracted ($N(\psi_{H_a} - \psi_{H_b})$) has B_1 symmetry.

The molecular orbitals from Figure $6.9.5.3$ are expressed below in terms of their LCAO of individual wavefunctions. Yet, note that these expressions are simplifications that ignore orbital mixing. For example, as expressed below, they ignore contributions of oxygen $2s$ to the higher energy moelcular orbitals with A_1 symmetry (the $3a_1$ and $3a_1^*$ in Figure $6.9.5.3$).



Answers

Exercise 6.9.5.1

Add texts here. Do not delete this text first.

This page titled 6.9.5: H_2O is shared under a CC BY-NC-SA 4.0 license and was authored, remixed, and/or curated by LibreTexts.

- 5.4.3: H_2O is licensed CC BY-SA 4.0.

6.9.6: NH_3

Construct SALCs and the molecular orbital diagram for $\mathrm{NH_3}$

This is the first example so far that has more than two pendant atoms and the first example in which the molecule has atoms that lie in three dimensions (i.e., it is not flat). Ammonia is a trigonal pyramidal molecule, with three pendant hydrogen atoms. The three-dimensional shape and the odd number of pendant atoms makes this example more complicated than the previous cases of water, carbon dioxide, and bifluoride. In this case, sketching the shapes (step 5) of pendant atom SALCs is less straightforward; rather, an alternative method, the **projection operator method**, is preferred for generating pictorial representations of the SALCs.

As in previous examples, it is important to remember that interactions of pendant ligands are dependent on their positions in three-dimensional space. You should consider the positions of the four atoms in ammonia to be essentially fixed in relation to each other. We will walk through the steps used to construct the molecular orbital diagram of ammonia. The first few steps are the same as you've seen before:

Step 1. Find the point group of the molecule and assign Cartesian coordinates so that z is the principal axis.

The NH_3 molecule is trigonal pyramidal and its point group is C_{3v}. The z axis is collinear with the principal axis, the C_3 axis.

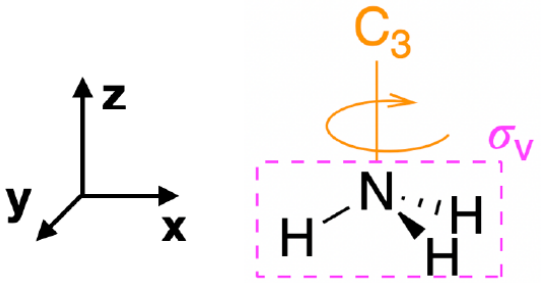


Figure 6.9.6.1: The ammonia molecule is in the C_{3v} point group. (CC-BY-NC-SA; Kathryn Haas)

Step 2. Identify and count the pendant atoms' valence orbitals.

Each of the three pendant hydrogen atoms has one valence orbital; the $1s$. Thus, we can expect a total of three SALCs from these three atoms.

Step 3. Generate the Γ's

Use the C_{3v} character table to generate one reducible representation (Γ); in this case we need only one Γ because there is only one type of valence orbital (the $1s$). For each s orbital, assign a value of 1 if it remains in place during the operation or zero if it moves out of its original place. The Γ is given below:

[redacted]

Step 4. Break Γ's into irreducible representations for individual SALCs

Reduce each Γ into its component irreducible representations. Using either of the processes described previously, we find that the Γ reduces to the two irreducible representations A_1 and E under the C_{3v} point group.

[redacted]

Notice that we only found TWO irreducible representations. But, in fact we have THREE different SALCs. The E irreducible representation is doubly degenerate, which in this context means that it corresponds to two degenerate SALCs. Thus, we have already found the symmetries of the three SALCs for ammonia: Two of the SALCs are degenerate with E symmetry under the C_{3v} point group, while the third SALC has A_1 symmetry.

Step 5. Sketch the SALCs using the PROJECTION OPERATOR METHOD

From the first four steps (described above), you have found the symmetries (the irreducible representations) of all three SALCs under the C_{3v} point group. To sketch the SALC that corresponds to each irreducible representation, again we use the C_{3v} character table. But now we will introduce the **projection operator method** to derive the surface representation of each SALC.

Step 5.1: Label the pendent atoms

In the projection operator method, first **label each of the pendant atoms so that we can distinguish identical atoms from one another**; for example, identify the three hydrogen atoms on ammonia as H_a, H_b, and H_c (Figure 6.9.6.2).

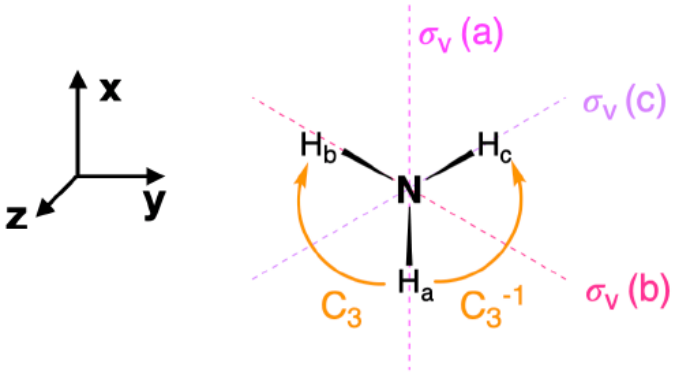


Figure 6.9.6.2: The three H's in NH_3 are chemically identical, but we can distinguish them using labels for the purpose of applying the projection operator method. In this figure, we have placed the z axis along the principal C_3 axis and placed the x axis colinear with one H. Each of the three H atoms has been labeled as H_a, H_b, or H_c. The σ_v that is coplanar with each H is labeled similarly (a, b, c) to keep account of each individual plane of symmetry. (CC-BY-NC-SA; Kathryn Haas)

Step 5.2: Create an expanded character table with one pendant atom's projected position after each operation

We will **perform each operation of the C_{3v} point group on this labeled molecule** and follow where one of the atoms is projected after the operation is complete. We will arbitrarily choose H_a. For example, upon performing the identity operation, E, the H_a atom is projected onto itself. On the other hand, H_a is projected onto H_b upon a clockwise C_3 rotation (as drawn in Figure 6.9.6.2). We take into account the result of each operation using an expanded character table (refer to the table below, 6.9.6.1). In the expanded character table, each operation within each class is written separately (i.e., $2C_3$ is accounted for separately as C_3 and C_3^{-1}).

Table 6.9.6.1: The expanded character table, and the projection of H_a by each operation is shown below.

[redacted] (6.9.6.1)

Step 5.3: Find the contribution of each pendant atom to each SALC

Next, **create a linear combination of the projections for each of the SALCs** (the irreducible representations found in step 4). For each of the irreducible representations, multiply the projection by the respective character of the operation.

$$\text{Contribution of each atom to the SALC } = \sum(\text{Projection of } H_a \times \chi)$$

The linear combination for all irreducible representations of C_3v is shown below.

Table 6.9.6.2: The symmetry adapted linear combination (SALC) for each irreducible representation of C_3v is shown.



(6.9.6.2)

Notice that there are only two irreducible representations that produce SALCs, and these are the same that were found in Step 4, above. This illustrates the fact that only the irreducible representations found through the reduction of the Γ will produce SALCs. We can ignore any irreducible representations that were not found in Step 4. Or, you can check your work in Step 4 by applying the projection operator to any irreducible representations not found in Step 4, and finding that they produce a sum of zero.

Step 5.4: Sketch the SALCs

The meaning of the linear combinations found in Table 6.9.6.2 is as follows:

- **Sketch the SALC with A_1 symmetry:** The linear combination $2H_a + 2H_b + 2H_c$ indicates all contributions to this SALC are of the same sign (of the wavefunction). Qualitatively, this means there is no node in this SALC. We can take this SALC almost literally to assume that all three H 1s wavefunctions contribute equally to the SALC. We can also use the fact that the A_1 representation possesses the full symmetry of the C_3v point group, is compatible with an s orbital on N, and thus is a totally symmetric SALC.

  Quantitatively, we can apply the normalizing factor, N, for this SALC. The linear combination for the A_1 SALC in Table 6.9.6.2 shows us that the coefficient for each orbital is 1. Thus, the normalizing factor for the A_1 SALC is $N = \left(\frac{1}{\sqrt{1^2+1^2+1^2}}\right) = \frac{1}{\sqrt{3}}$. This tells us that H_a, H_b, and H_c each contribute $\frac{1}{\sqrt{3}}$ to the normalized A_1 group orbital:

  $$A_1 \text{ group orbital } = \frac{1}{\sqrt{3}}\left[\psi_{H_a} + \psi_{H_b} + \psi_{H_c}\right]$$

  This is shown visually in Figure 6.9.6.3.
- **Sketch two SALCs with E symmetry:** The linear combination $2H_a - H_b - H_c$ indicates that there are contributions with both positive and negative sign to the wavefunction for each of the E group orbitals. Qualitatively, this tells us that there is a node within each of these two SALCs, and that the total contribution of the positive portion of the wavefunction is equal to the contribution of the negative portion.
  - **Finding the first E SALC:**
    For one of the SALCs, we can take the linear combination from Table 6.9.6.2 almost literally: The contribution from H_a is equal and opposite to the sum of the contributions from $H_b + H_c$. This would result in a SALC as shown in Figure 6.9.6.3 (E, left), that would have symmetry of the x axis and that would be compatible with the p_x orbital on N. The node exists in the yz plane and there is an equal contribution of positive and negative parts of the total wavefunction.

    We can also apply the normalizing factor, N, to find this SALC. The linear combination for the E SALC in Table 6.9.6.2 shows us that the coefficients for orbital contributions are 2, -1, and -1. Thus, the normalizing factor for the first E SALC is $N = \left(\frac{1}{\sqrt{2^2+(-1)^2+(-1)^2}}\right) = \frac{1}{\sqrt{6}}$. This normalized E group orbital is:

    $$\text{First } E \text{ group orbital } = \frac{1}{\sqrt{6}}\left[2\psi_{H_a} - \psi_{H_b} - \psi_{H_c}\right]$$

    This is shown visually in Figure 6.9.6.3 (E, left).
  - **Finding the second E SALC:**

The second SALC is less obvious at first glance. We must use clues from the character table to help us determine what it should "look like". Since the E representation transforms as the group, (x, y), we know that one of the SALCs will have the symmetry of the x axis and p_x orbital on the central nitrogen atom, while the other should possess the symmetry of the y axis and be compatible with the p_y orbital on nitrogen. This alone could lead you to the sketch of the second SALC with E symmetry shown in Figure $6.9.6.3$ (E, right). This second E SALC must have a node in the xz plane, and because H_a lies in this node, H_a cannot contribute to this group orbital. Retaining the fact that the positive and negative contributions of the linear combination must be equal, we can arrive at a SALC that has equal but opposite contributions of H_b and H_c, and no contribution by H_c (Figure $6.9.6.3$, right).

We can also apply the normalizing factor, N, to find this SALC. But we must apply the fact that H_a cannot contribute to the SALC with "y" symmetry. We remove the contribution of H_a, leaving us with coefficients of 0 for H_a and 1 for H_b and H_c. Thus, the normalizing factor for the second E SALC is $N = \left(\frac{1}{\sqrt{0^2+1^2+1^2}}\right) = \frac{1}{\sqrt{2}}$. To this, we must add positive and negative coefficients so that the entire wavefunction of this SALC is normalized. The result for this normalized E group orbital is:

$$\text{Second } E \text{ group orbital } = \frac{1}{\sqrt{2}}\left[\psi_{H_b} - \psi_{H_c}\right]$$

This is shown visually in Figure $6.9.6.3$.

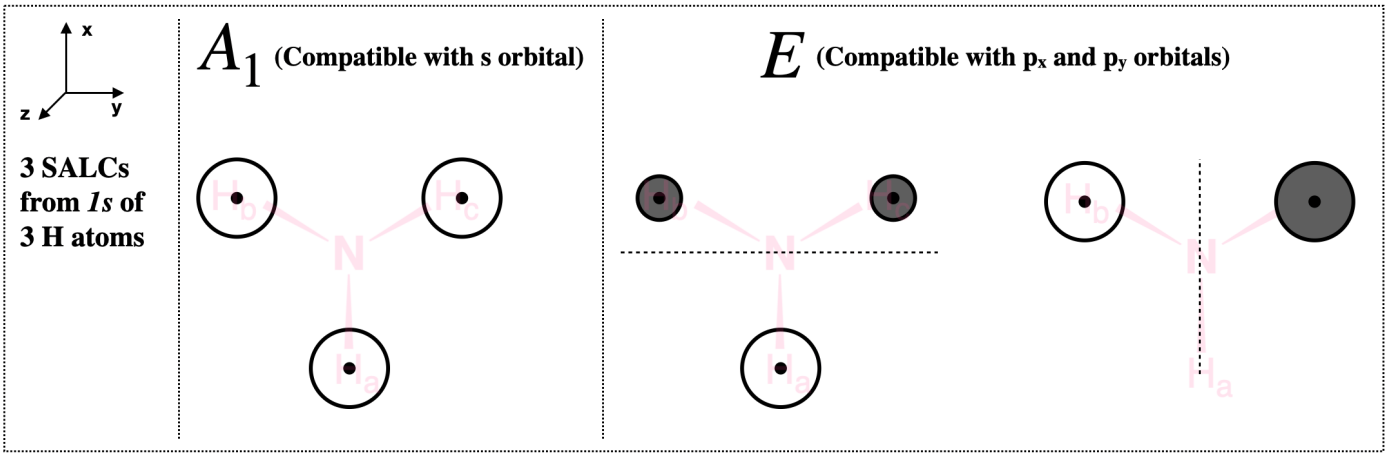


Figure $6.9.6.3$: Sketches of H SALCs of ammonia from the perspective of the C_3 axiz (z axis). The A_1 SALC is shown at the left, while two degenerate SALCs with E symmetry are shown on the right. Nodes for E group orbitals are shown as dashed lines. (CC-BY-NC-SA; Kathryn Haas)

Step 6. Combine SALCs with AO's of like symmetry to draw the MO diagram for NH_3

First we must identify the valence orbitals on the central nitrogen: there are four including $2s$, $2p_x$, $2p_y$, and $2p_z$. Now we identify the symmetry of each using the C_{3v} character table. The symmetry of a central $2s$ orbital corresponds to the combination of functions x^2, y^2, and z^2 in the character table; this is A_1. The p_z orbital also corresponds to A_1. And so on... The symmetries of nitrogen valence orbitals are listed below.

$$2s = A_1$$
$$(2p_x,\ 2p_y) = E$$
$$2p_z = A_1$$

The next step is to get a sense of the relative energies of valence atomic orbitals for nitrogen and hydrogen, and then construct the molecular orbital diagram. The nitrogen $2s$ orbital is about 12 eV lower in energy than a H $1s$. This difference is an acceptable energy-match for the H orbitals to interact, but would not usually result in a strong interaction. On the other hand, the nitrogen 2p orbitals have an energy very close to the hydrogen 1s, different by only 0.5 eV. Knowledge of the relative energies of the atomic orbitals tells us that, when constructing a diagram, we can place the H SALCs at an energy similar to that of the N $2p$ orbitals, while the N $2s$ is much lower (Figure $6.9.6.4$).

The $2s$ and $2p_z$ orbitals have A_1 symmetry and can combine with the A_1 SALC. These orbitals will give three molecular orbitals.

The $2s$ orbital will not have strong interactions with the other orbitals of A_1 symmetry due to the large energy difference. The $2p_z$ orbital will not have good overlap with the wavefunctions for the three hydrogen orbitals due to their positions in space: The $2p_z$ orbital has half of its angular distribution pointed away from the hydrogen orbitals, and half pointed toward the center of a triangle formed by the three hydrogen atoms. The nitrogen $2s$ and $2p_z$ will combine with the hydrogen SALC of A_1 symmetry to give three molecular orbitals; one low-energy bonding orbital, one mid-energy non-bonding orbital, and one high-energy antibonding orbital. The mid-level non-bonding a_1 molecular orbital is close in energy to, and resembles, the nitrogen $2p_z$ orbital. The lowest energy a_1 molecular orbital will be lower in energy, but be similar to the nitrogen $2s$.

The remaining two $2p$ orbitals are degenerate and possess E symmetry under the C_{3v} point group. Although these orbitals are a good energy match, again, their orientation and positions in space do not allow for good orbital overlap, and their bonding and antibonding interactions are relatively weak compared to what we might otherwise expect from such a good energy match. The e atomic orbitals of nitrogen will combine with the e SALCs to give a set of two degenerate bonding molecular orbitals and a set of two degenerate antibonding orbitals (four total molecular orbitals of e symmetry). The MO diagram for NH_3 is shown in Figure $6.9.6.4$, with calculated electron density surfaces of each MO shown.

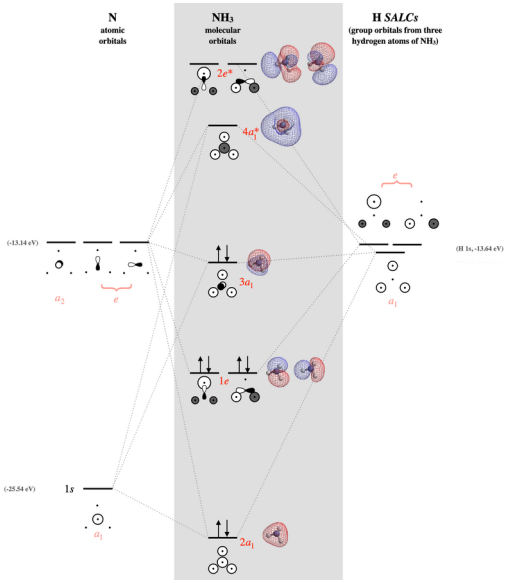


Figure $6.9.6.4$: The molecular orbital diagram of ammonia. Molecular orbitals surfaces calculated using Spartan software. (CC-BY-NC-SA; Kathryn Haas)

This page titled 6.9.6: NH_3 is shared under a CC BY-NC-SA 4.0 license and was authored, remixed, and/or curated by LibreTexts.

- 5.4.4: NH_3 by Kathryn Haas is licensed CC BY-SA 4.0.

6.10: MO THEORY APPLIED TO POLYATOMIC MOLECULES BH_3, NH_3, AND CH_4

- Topic hierarchy

6.10A: BH_3

6.10B: NH_3

6.10C: CH_4

6.10D: A Comparison of MO and VB Bonding Models

This page titled 6.10: MO Theory Applied to Polyatomic Molecules \(BH_3\), \(NH_3\), and \(CH_4\) is shared under a license and was authored, remixed, and/or curated by LibreTexts.

- 5.5: MO Theory Applied to Polyatomic Molecules \(BH_3\), \(NH_3\), and \(CH_4\) is licensed CC BY-NC-SA 4.0.

6.10A: BH_3

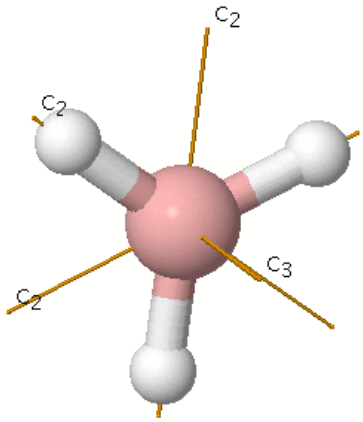


Figure 1: Molecule structure of BH_3 (Used with permission from Dean.H Johnston)

Symmetry Labels

E"	2	-1	0	-2	1	0	(R_x,R_y)	(xz,yz)

FIGURE2: Character table for the the point group D3h

B atom in BH3:

+s-orbital: with the shape of the sphere, its function is $x^2+y^2+z^2$. Therefore, 2s orbital has a_1' symmetry

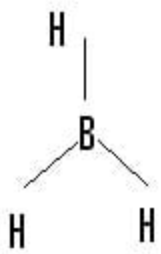
+p-orbital: has 3 orbitals , p_x, p_y, p_z. Therefore, $2p_z$ orbital has $a_2"$ symmetry

$2p_x$ and $2p_y$ orbital are degenerate and have e' symmetry

3 Hydrogen atoms in BH3: (Ligand group orbitals)

a. Symmetry labels of LGOs:

-With the symmetry operations of BH3 above, we can determine how many LGO unmoved by creating the following table:



D_{3h}	E	$2C_3$	$3C_2$	σ_h	$2S_3$	$3\sigma_v$
LGO	3	0	1	3	0	1

-Next, with these values we can apply the following formula to identify the symmetry labels of the Ligan group orbitals

a= 1/h ∑[(N).Xr(R).Xi(R)]

h: the total number of coeficients of symmetry operation

N: the coeficient of the each symmetry operation

Xr(R): the character of the reducible representation corresponding to the R (values that just found in the LGO row

Xi(R): the character of the irreducible representation corresponding to the R (from the character table)

Calculation:

A1'= 1/12 [(1)(3)(1)+(2)(0)(1)+(3)(1)(1)+(1)(3)(1)+(2)(0)(1)+(3)(1)(1)] = 1 A1'

A2'= 1/12 [(1)(3)(1)+(2)(0)(1)+(3)(1)(-1)+(1)(3)(1)+(2)(0)(1)+(3)(1)(-1)]= 0 A2'

E'= 1/12 [(1)(3)(2)+(2)(0)(-1)+(3)(1)(0)+(1)(3)(2)+(2)(0)(-1)+(3)(1)(0)]= 1E'

A1"= 1/12 [(1)(3)(1)+(2)(0)(1)+(3)(1)(1)+(1)(3)(-1)+(2)(0)(-1)+(3)(1)(-1)]= 0 A1"

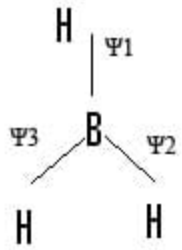
A2"= 1/12 [(1)(3)(1)+(2)(0)(1)+(3)(1)(-1)+(1)(3)(-1)+(2)(0)(-1)+(3)(1)(1)] = 0 A2"

E"= 1/12 [(1)(3)(2)+(2)(0)(-1)+(3)(1)(0)+(1)(3)(-2)+(2)(0)(1)+(3)(1)(0)] = 0 E "

Thus, LGO's symmetry labels are a1' + e'

b. How to determine the shapes of the LGOS?

-LGO's symmetry labels are a1' + e'. There are 3 LGOs that can be made out of these symmetry labels,one LGO is from a1' and two LGOs are from e' due to doubly degenerate. In order to determine the shape of each LGO, we would use the wavefunctions.



-Three hydrogens in BH3 are assigned with Ψ1, Ψ2, Ψ3. Now lets look at how each Ψ is affected by the symmetry operations of the D3h and their results are completed in the following table:

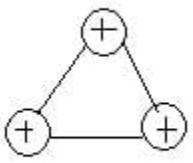
D_{3h}	E	C_3	C^2_3	C_2	C_2'	C_2''	σ_h	S_3	S^2_3	σ_v	σ_v'	σ_v''
Ψ1	Ψ1	Ψ2	Ψ3	Ψ1	Ψ3	Ψ2	Ψ1	Ψ2	Ψ3	Ψ1	Ψ3	Ψ2
a1'	1	1	1	1	1	1	1	1	1	1	1	1
LGO1	Ψ1	Ψ2	Ψ3	Ψ1	Ψ3	Ψ2	Ψ1	Ψ2	Ψ3	Ψ1	Ψ3	Ψ2

Ψ (a1') = 4Ψ1+4Ψ2+4Ψ3

= 4(Ψ1+Ψ2+Ψ3)

Ψ(a1')= 1/√3 (Ψ1+Ψ2+Ψ3)

-The shape of the LGO1 is



D_{3h}	E	C_3	C^2_3	C_2	C_2'	C_2''	σ_h	S_3	S^2_3	σ_v	σ_v'	σ_v''
Ψ1	Ψ1	Ψ2	Ψ3	Ψ1	Ψ3	Ψ2	Ψ1	Ψ2	Ψ3	Ψ1	Ψ3	Ψ2
e'	2	-1	-1	0	0	0	2	-1	-1	0	0	0

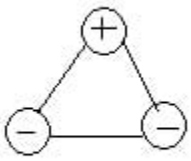
LGO1	2Ψ1	-Ψ2	-Ψ3	0	0	0	2Ψ1	-Ψ2	-Ψ3	0	0	0

Ψ(e') = 4 (Ψ1)-2 (Ψ2)-2 (Ψ3)

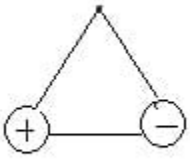
= 2[2(Ψ1)-Ψ2-Ψ3]

Ψ(e') = 1/ √6 (2 Ψ1-Ψ2-Ψ3)

-The shape of the LGO2 is



-Noticed that in the LGO2, we have 1 nodal plane which is the horizonal line between the positive charge and negative charge. Therefore, the LGO3 (doubly degenerate with e') would also 1 nodal plane and its wavefunction would be Ψ(e') = 1/√2 (Ψ2-Ψ3). The shape of the LGO3 is



MO diagram

-As we can see in this diagram, the energy level of 3 LGOs are higher than the 2s orbital and below the 2 p orbital dued to the electronegativy of both Boron and Hydrogen. Hydrogen has higher electronegativity than boron, therefore hydrogen would have lower energy level in the MO diagram.

-In addition, B has 3 electrons in the valence electrons and 3 hydrogens have total 3 electrons. Therefore, the total number of electrons filled in orbitals are 6. With all of the informations above about symmetry labels of B atom and the 3 LGOs, we now construct the MO diagram of BH3. Noticed that, the bonding formation only happens to atoms that have the same symmetry labels. 2s orbital and LGO(1) would contribute 1 electron to give 2 spin pairs electrons at the a_1' energy level. $2p_x$ and $2p_y$ orbitals would bond to the LGO(2) and LGO(3), which give 2 spin pairs electrons at the e' energy level.

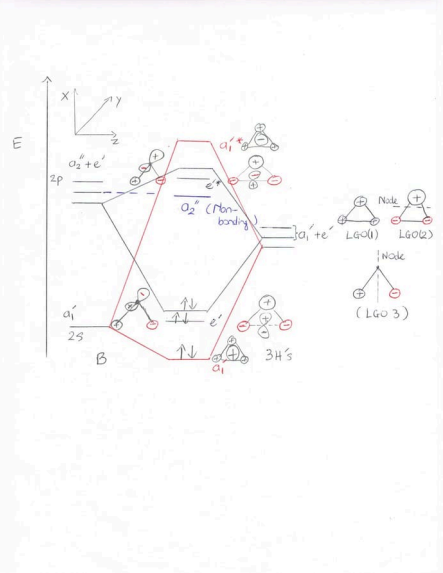


FIGURE 3: MO diagram for the formation of BH3

-there is a detailed explaination that performed in this video

YouTube Video

This interactive element is not available in this format. Visit the link or scan the QR code to access it online.

View this YouTube Video online

References

1. Pople, John A.. *Approximate Molecular Orbital Theory (Advanced Chemistry)*. New York: Mcgraw-Hill (Tx), 1970. Print., Phy Sci Engr Library QD461. P66
2. Noebe, Guillermo (EDT)/, Ronald D. (EDT)/ Abel, and Phillip B. (EDT) Bozzolo. *Applied Computational Materials Modeling*. Berlin and Heidelberg: Springer Verlag, 2007. Print. Phy Sci Engr Library TA 404.23.A66
3. Housecroft, Catherine, and Alan G. Sharpe. *Housecroft Inorganic Chemistry 3e (3rd Edition)*. 3 ed. Alexandria, VA: Prentice Hall, 2008. 128

Outside Links

- symmetry.otterbein.edu/gallery/index.html
- http://www.youtube.com/watch?v=82u4v...ext=1&index=25

Problems

1. What are the non-bonding orbital in this BH_3? '
2. In the above MO diagram, why does e' have 2 lines energy levels compared to a1' has only 1 line energy level?
3. What is the bond order of BH3 in this MO diagram?
4. Assume that we have d orbitals in this BH_3, what are symmetry labels that d-orbitals have based on the character table?
5. Explain why a1' has the lowest energy level in the MO diagram.

Answers

1. a2"
2. because e' is doubly degenerate molecule orbital.
3. B.O = 3
4. a1' + e' + e"

5. a1' has no node, so it is stable and has lowest energy compare to e'.

This page titled 6.10A: \(BH_3\) is shared under a license and was authored, remixed, and/or curated by LibreTexts.

- 5.5A: \(BH_3\) is licensed CC BY-NC-SA 4.0.

6.10B: NH_3

C_{3v}	E	$2C_3$	$3\sigma_v$	Linear Rotations	Quadratic
A_1	1	1	1	z	x^2+y^2,z^2
A_2	1	1	-1	R_z	
E	2	-1	0	$(x,y)(R_x, R_y)$	$(x^2-y^2, xy)(xz,yz)$

Contributors and Attributions

- Name #1 here (if anonymous, you can avoid this) with university affiliation
- Name #2 here with university affiliation

Tags below. If no tags exist, then add two new ones: "Vet1" and the level of the module content (e.g. "Fundamental"). See FAQ for more details.

This page titled 6.10B: \(NH_3\) is shared under a license and was authored, remixed, and/or curated by LibreTexts.

- 5.5B: \(NH_3\) is licensed CC BY-NC-SA 4.0.

6.10C: CH_4

This module seeks to explain the bonding of the 4 Hydrogen atoms to the 1 Carbon atom in the molecule CH4 (methane),using the molecular orbital theory. Molecular orbital theory describes orbitals that are formed with the interaction of the atomic orbitals of given atoms. These orbitals are spread out over the entire molecule and electrons fill these orbitals in accordance with the aufbau principle.

1. Introduction
2. The Symmetry of CH4
3. Character Table for Td Point group
4. Molecular Orbital Diagram for CH4
5. References
6. Outside Links
7. Problems
8. Contributors and Attributions

Introduction

Various concepts explain the molecular orbital theory in the bonding in methane, including character tables, symmetry, LGOs (ligand group orbital approach), and a qualitative MO diagram.

The Symmetry of CH_4

- CH_4 belongs to the T_d point group and contains: $8C_3$ axes, $3C_2$ axes, $6S_4$ axes, and a dihedral plane of symmetry. Using the character table for the T_d point group,

Character Table for T_d Point group

T_d	E	$8C_3$	$3C_2$	$6S_4$	$6sigma_d$
A_1	1	1	1	1	1
A_2	1	1	1	-1	-1
E	2	-1	2	0	0
T_1	3	0	-1	1	-1
T_2	3	0	-1	-1	1

Molecular Orbital Diagram for CH4

Rename to desired sub-topic. You can delete the header for this section and place your own related to the topic. Remember to hyperlink your module to other modules via the link button on the editor toolbar.

References

1. Housecroft, C; Sharpe, A. (2008). Bonding in Polyatomic Molecules. In: Pearson Education Limited *Inorganic Chemistry*. Edinburgh Gate: Pearson Education Limited. pgs. 33, 130-131.

Outside Links

- This is not meant for references used for constructing the module, but as secondary and unvetted information available at other site
- Link to outside sources. Wikipedia entries should probably be referenced here.

Problems

What are ligand group orbitals, and how are they used in MO theory in polyatomic molecules?

How many Vibrational modes and IR/Ramen stretches are there in CH_4?

What are the major differences between VB theory and MO theory applied to polyatomic molecules?

Contributors and Attributions

- Name #1 here (if anonymous, you can avoid this) with university affiliation

This page titled 6.10C: \(CH_4\) is shared under a license and was authored, remixed, and/or curated by LibreTexts.

- 5.5C: \(CH_4\) is licensed CC BY-NC-SA 4.0.

6.10D: A Comparison of MO and VB Bonding Models

This page titled 6.10D: A Comparison of MO and VB Bonding Models is shared under a license and was authored, remixed, and/or curated by LibreTexts.

6.P: Problems (under construction)

Problems

1. Chlorophyll *a* is a green pigment that is found in plants. Its molecular formula is $C_{55}H_{77}O_5N_4Mg$. How many degrees of freedom does this molecule possess? How many vibrational degrees of freedom does it have?
2. CCl_4 was commonly used as an organic solvent until its severe carcinogenic properties were discovered. How many vibrational modes does CCl_4 have? Are they IR and/or Raman active?
3. The same vibrational modes in H_2O are IR and Raman active. WF_6^- has IR active modes that are not Raman active and vice versa. Explain why this is the case.
4. How many IR peaks do you expect from SO_3? Estimate where these peaks are positioned in an IR spectrum.
5. Calculate the symmetries of the normal coordinates of planar BF_3.

Answers to Problems

1. Chlorophyll *a* has 426 degrees of freedom and 420 vibrational modes.
2. The point group is T_d, $T_{vib} = a_1 + e + 2t_2$; a_1 and e are Raman active, t_2 is both IR and Raman active.
3. For molecules that possess a center of inversion i, modes cannot be simultaneously IR and Raman active.
4. Point group is D_{3h}; one would expect three IR active peaks. Asymmetric stretch highest (1391 cm^{-1}), two bending modes (both around 500 cm^{-1}). The symmetric stretch is IR inactive.
5. $T_{3N} = A_1' + A_2' + 3E' + 2\ A_2'' + E''$ and $T_{vib} = A_1' + 2E' + A_2''$

Contributors and Attributions

- Kristin Kowolik, University of California, Davis

Problems

1. The water molecule H_2O was used as an example; it was mentioned that when water was rotated 180 degrees around an axis bisecting the oxygen, the molecule was superimposable on the original water molecule. How about CO_2? Will it be like the water molecule since CO_2 also has 2 atoms of oxygen?

Of course not, because every molecule has a different molecular shape. To recognize the symmetry of any molecule, the structure and the molecular shape of that molecule should be defined. The water molecule is bent but CO_2 is not, and if CO_2 is rotated 360 degrees around the axis bisecting the C atom, then it can be superimposed on the original molecule. We then see the symmetry for the CO_2.

2. Why should all of the five symmetry elements be done on a molecule in order to find the point group the molecule belongs to? Why is performing only one or two of the symmetry elements not enough for recognizing the point group?

One or two of the symmetry elements will not be able to tell us everything about the molecule's symmetry, since those one or two properties do not tell us everything about the molecule. Also, while different molecules may have one or two symmetrical properties in common, the five properties will not be the same for all molecules.

3. What does the symbol C_n stand for and what does n represent? Why is it important to identify n?

C is the axis of rotation and n is the order of the axis.

4. How are the character tables helpful?

The character table tells us about all the operational elements performed on the molecule and indicates whether we have forgotten to perform any of the symmetry elements. The tables serve as a checklist because all the operational elements should be done on the molecule in order to find the point group of the molecule.

5. Why is important to find symmetry in molecules?

Symmetry tells us about bonding for that molecule.

This page titled 6.P: Problems (under construction) is shared under a license and was authored, remixed, and/or curated by LibreTexts.

- 4.P: Problems (under construction) by Kathryn Haas has no license indicated.

7: LIGAND FIELD THEORY (LFT) AND CRYSTAL FIELD THEORY (CFT) OF OCTAHEDRAL COMPLEXES



CHEM 431: *Inorganic Chemistry*
Fall 2020: Dr. Kathryn Haas

Home • **Readings** • **Course Info & Tools**

This unit introduces two different models that, most of the time, can be used to reach similar conclusions. Each of these models has its advantages and disadvantages. I'd like you to know both theories and to be able to pull pieces of each model when appropriate.

1. **Crystal Field Theory (CFT)** is one of the simplest models for explaining the structures and properties of transition metal complexes. The theory is based on simple electrostatics of the metal-ligand interaction, and some of the assumptions behind the theory are inaccurate. It was developed to explain spectroscopic (colors) and magnetic properties of coordination complexes, and *does not describe bonding*. Although it is primitive, does not describe bonding, and is based on naive ideas, it is still useful. Because the model makes effective use of molecular symmetry, it can be surprisingly accurate in describing the magnetism, colors, structure, and relative stability of metal complexes. The major advantage of CFT is that it is simple.
2. **Ligand Field Theory (LFT)** is more advanced in that it is rooted in molecular orbital theory. It is more complex, but it is also more correct. LFT will not only get you to the correct answer more often, but it is also based on accurate ideas (as far as we know).

We will start by examining how each theory treats the most common type of metal complex geometry: the **octahedral geometry**.

7.1: Introduction to Crystal Field Theory (Octahdral complexes)

7.2: Introduction to Ligand Field Theory (Octahedral complexes)

7.3: Ligand Field Stabilisation Energy (LFSE)

7.4: The Effect of the Metal Ion on d-Orbital Splitting

7.5: The Effect of Ligands and the Spectrochemical Series

Additional resources: The Organometallic reader, Ligand Field Theory & Froteir MO Theory.

This page titled 7: Ligand Field Theory (LFT) and Crystal Field Theory (CFT) of Octahedral Complexes is shared under a license and was authored, remixed, and/or curated by LibreTexts.

7.1: Introduction to Crystal Field Theory (Octahdral complexes)



One of the most striking characteristics of transition-metal complexes is the wide range of colors they exhibit. In this section, we describe crystal field theory (CFT), a bonding model that describes the electronic structure of transition metal complexes, with an explicit focus on the five valence d-orbitals. This model can be used to explain many important properties of transition-metal complexes, including their colors and magnetism. The central (naive) assumption of CFT is that metal-ligand interactions are purely electrostatic, and that *the electrons in metal d-orbitals are repelled by the ligands' electrons*. Even though this assumption is clearly not valid, this theory enables chemists to explain many of the properties of transition-metal complexes with a reasonable degree of accuracy. The Learning Objective of this Module is to understand how crystal field theory explains the electronic structures and colors of metal complexes.

d-Orbital Splittings

CFT focuses on the interaction of the five valence ($(n-1)d$) orbitals with a "field" of negative charge (electrons) from ligands arranged around a transition-metal ion. We will focus on the application of CFT to *octahedral complexes*, which are by far the most common and the easiest to visualize. Other common structures, such as square planar complexes, can be treated as a distortion of the octahedral model.

CFT, was developed to explain the interesting spectroscopic properties (eg various colors) of transition metal complexes. It was developed, quite literally, on the back of a napkin as two faculty members discussed how they might explain the observations of their UV-vis spectra. It was never meant to describe bonding. In fact, at the time of its development, bonding in metals was not considered covalent. Only later, with development of Ligand Field Theory and Molecular Orbital Theory, was the nature of bonding in transition metals described.

We begin by considering how the energies of the d orbitals of a transition-metal ion are affected by an octahedral arrangement of six negative charges. Recall that the five d orbitals are initially degenerate (have the same energy). If we add ligands and distribute their electrons' negative charges uniformly over the surface of a sphere, the d orbitals remain degenerate, but their energy will be higher due to repulsive electrostatic interactions between the spherical shell of negative charge and electrons in the d orbitals (part (a) in Figure $7.1.1$). Placing the six negative charges at the vertices of an octahedron does not change the average energy of the d orbitals, but it does remove their degeneracy: the five d orbitals split into two groups whose energies depend on their orientations. As shown in part (b) in Figure $7.1.1$, the d_{z^2} and $d_{x^2-y^2}$ orbitals point directly at the six negative charges located on the x, y, and z axes. Consequently, the energy of an electron in these two orbitals (collectively labeled the e_g orbitals) will be greater than it will be for a spherical distribution of negative charge because of increased electrostatic repulsions. In contrast, the other three d orbitals (d_{xy}, d_{xz}, and d_{yz} collectively called the t_{2g} orbitals) are all oriented at a 45° angle to the coordinate axes, so they point between the six negative charges. The energy of an electron in any of these three orbitals is lower than the energy for a spherical distribution of negative charge.

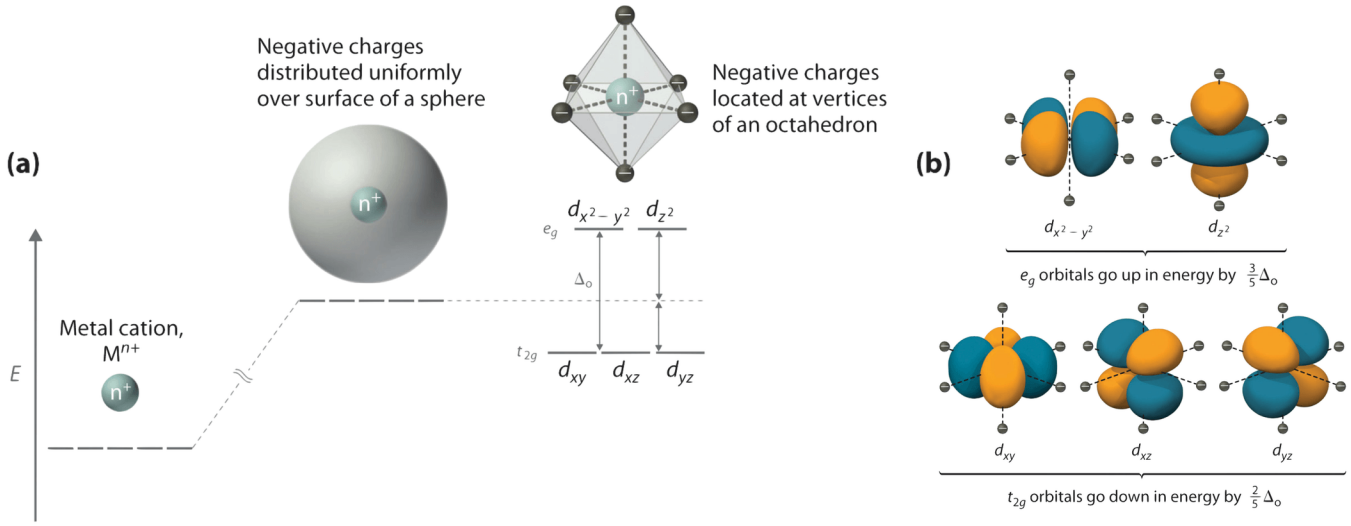


Figure 7.1.1: An Octahedral Arrangement of Six Negative Charges around a Metal Ion Causes the Five d Orbitals to Split into Two Sets with Different Energies. (a) According to CFT, the uniform distribution of negative charge from a *ligand field* over a spherical surface surrounding a metal ion causes the energy of all five d orbitals to *increase* due to electrostatic repulsion; *the five d orbitals remain degenerate in this spherical field*. If the ligands are arranged in a octahedral geometry, each of the d orbitals interacts differently with the ligands' negative charge, causeing the d orbitals to split into two groups with different energies: the $d_{x^2-y^2}$ and d_{z^2} orbitals increase in energy as a set with e_g symmetry, while the, d_{xy}, d_{xz}, and d_{yz} orbitals decrease in energy as a set with t_{2g} symmetry. (b) The two e_g orbitals (top) point directly at the six negatively charged ligands, which increases their energy compared with a spherical distribution of negative charge. In contrast, the three t_{2g} orbitals (bottom) point between the negatively charged ligands, which decreases their energy compared with a spherical distribution of charge.

The difference in energy between the two sets of d orbitals is called the crystal field splitting energy (Δ_o, where the *subscript o stands for octahedral*. As we shall see, the *magnitude of the splitting depends on the charge on the metal ion, the position of the metal in the periodic table, and the nature of the ligands*. (Crystal field splitting energy also applies to other geometries. For example, in tetrahedral complexes a *t* subscript indicates *tetrahedral*: Δ_t.) It is important to note that the splitting of the d orbitals in a crystal field does not change the total energy of the five d orbitals: the two e_g orbitals are increased in energy by $0.6\Delta_o$, and thus contribute a total energy of $2 \times 0.6\Delta_o = 1.2\Delta_o$. The three t_{2g} orbitals *decrease* in energy by $-0.4\Delta_o$, and thus contribute a total energy of $3 \times -0.4\Delta_o = -1.2\Delta_o$. The total change in energy is $2(0.6\Delta_o) + 3(-0.4\Delta_o) = 0$.

> Crystal field splitting does not change the total energy of the d orbitals.

But, the crystal field slplitting can change the energy of the electrons. For example, in a d^1 metal in an octahedral field, the lone electron would occupy one of the lower-energy orbitals. This electrn would be stabilized (due to a decrease in energy) by $1\text{electron} \times -0.4\Delta_o = -0.4\Delta_o$. The energy difference between the the hypothetical electron configuration of the degenerate orbitals, and that of the electrons in the ligand field is called the Crystal Field Stabilization Energy (CFSE). This is very similar to the concepts of Ligand Field Stabilization Energy (LFSE), which will be discussed later in this unit.

Electronic Structures of Octahedral Metal Complexes

We can use the d-orbital energy-level diagram in Figure 7.1.1: to predict electronic structures and some of the properties of transition-metal complexes. We start with the Ti^{3+} ion, which contains a single d electron, and proceed across the first row of the transition metals by adding a single electron at a time. We place additional electrons in the lowest-energy orbital available, while keeping their spins parallel as required by Hund's rule. As shown in Figure 7.1.2, for d^1–d^3 systems—such as $[Ti(H_2O)_6]^{3+}$, $[V(H_2O)_6]^{3+}$, and $[Cr(H_2O)_6]^{3+}$, respectively—the electrons successively occupy the three degenerate t_{2g} orbitals with their spins parallel, giving one, two, and three unpaired electrons, respectively. We can summarize this for the complex $[Cr(H_2O)_6]^{3+}$, for example, by saying that the chromium ion has a d^3 electron configuration or, more succinctly, Cr^{3+} is a d^3 ion.

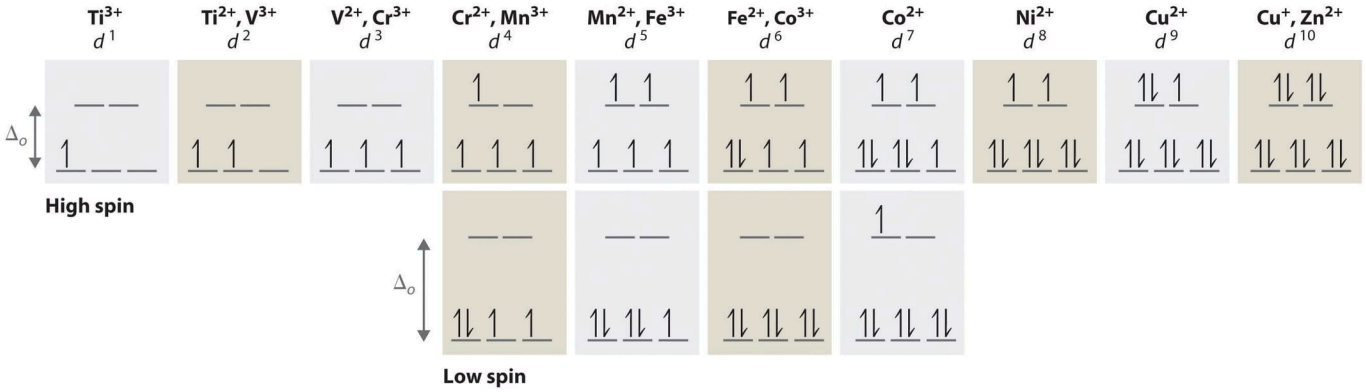


Figure 7.1.2: The Possible Electron Configurations for Octahedral d^n Transition-Metal Complexes (n = 1–10). Two different configurations are possible for octahedral complexes of metals with d^4, d^5, d^6, and d^7 configurations; the magnitude of Δ_o determines which configuration is observed.

When we reach the d^4 configuration, there are two possible choices for the fourth electron: it can occupy one of the empty e_g orbitals, or it can pair in one of the singly occupied t_{2g} orbitals. The e_g orbitals are at a higher energy level, and so there is an energy cost associated with an electron occupying an e_g rather than a lower-energy t_{2g}; that energy cost is equal to Δ_o. But there is another cost associated with pairing electrons in the lower-energy t_{2g} orbitals. Pairing two electrons in the same orbital causes electron-electron repulsion; this energy cost is called the spin-pairing energy (P). The more favorable electron configuration will be the one that minimizes the lenergy of the entire system. If (\Delta_o\) is less than P, then the lowest-energy arrangement has the fourth electron e_g orbitals. Conversely, if (\Delta_o\) is greater than P, then the lowest-energy arrangement has the fourth electron in one of the occupied t_{2g} orbitals.

When there are two possible electron configurations (eg the cases of $d^4 - d^7$), the arrangement that results in more unpaired electrons is called a **high-spin configuration**. A complex that has a high-spin configuration (eg $[Cr(H_2O)_6]^{2+}$ ion) is called a high-spin complex. The arrangement that results in less unpaired electrons is called a **low-spin configuration**, and a complex with this electron configuration (eg $[Mn(CN)_6]^{3-}$ ion) is called a low-spin complex. Similarly, metal ions with the d^4, d^5, d^6,, or d^7 electron configurations have either high spin or low spin electron configurations, depending on the magnitude of Δ_o. Complexes that have large Δ_o are also called "strong field" while those that have small Δ_o are also called "weak field".

In contrast, only one arrangement of d electrons is possible for metal ions with d^8–d^{10} electron configurations. For example, the $[Ni(H_2O)_6]^{2+}$ ion is d^8 with two unpaired electrons, the $[Cu(H_2O)_6]^{2+}$ ion is d^9 with one unpaired electron, and the $[Zn(H_2O)_6]^{2+}$ ion is d^{10} with no unpaired electrons. It is incorrect to refer to these complexes or their electron configurations as high-spin or low-spin. However, we can refer to them in terms of the magnitude of Δ_o and the relative "strength" on the ligand field.

> If Δ_o is less than the spin-pairing energy, a high-spin configuration results. Conversely, if Δ_o is greater, a low-spin configuration forms.

This page titled 7.1: Introduction to Crystal Field Theory (Octahdral complexes) is shared under a license and was authored, remixed, and/or curated by LibreTexts.

7.2: Introduction to Ligand Field Theory (Octahedral complexes)



Concepts from molecular orbital (MO) theory are useful in understanding the reactivity of coordination compounds. One of the basic ways of applying MO concepts to coordination chemistry is in Ligand Field Theory (LFT). LFT is essentially a version of MO theory that focuses on how the d-orbitals of a metal ion interact with ligand orbitals to create bonding, antibonding, and non-bonding interactions. These interactions result in orbitals that are close in energy to the original d-orbitals of the metal. Due to their similarity to the metal d-orbitals, they are usually referred to as the metal d-orbitals even though they are actually molecular orbitals. The interactions of ligand orbitals with metal d-orbitals results in different splitting of the metal d-orbitals into sets of bonding, antibonding and non-bonding orbitals. In the octahedral case, the splitting of d-orbitals is the same in LFT as we saw previously in CFT. The main difference between the two theories is the explanation of how this splitting is derived. LFT also describes bonding, while CFT can't.

The symmetry of the central metal orbital and that of the ligand group orbitals (aka SALCs, symmetry adapted linear combinations of atomic orbitals) determines the relative eenergies (eg the splitting) of the d-oritals of the metal complex. The symmetry of the SALCs depends on the coordination geometry of the ligands and the specific type of orbitals involved (eg s vs p). For example, ligand s orbitals in a tetrahedral coordination sphere will have a different symmetries and different abilities to interact with the metal d-orbitals than orbitals in an octahedral coordination sphere because they will interact with the different d orbitals in different ways.

> Ligand Field Theory looks at the effect of donor atoms on the energy of d orbitals in the metal complex.
>
> The effect depends on the coordination geometry of the ligands.

A simple octahedral case

Let's start with an example of six ligand s-orbitals in an octahedral coordination structure. Assume the six ligands all lie along the x, y and z axes and that they interact with the metal using *just* their s orbitals (see Figure $7.2.1$).

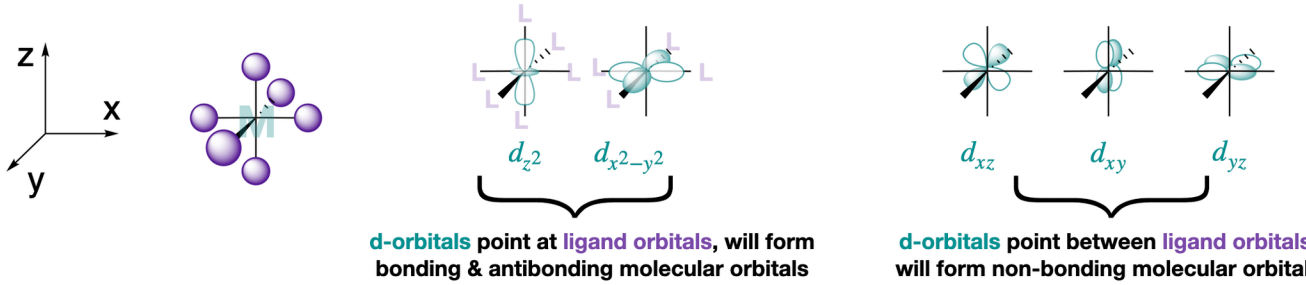


Figure 7.2.1: An octahedral arrangement of ligand s-orbitals (purple) around a central metal (teal). Two of the metal d-orbitals ($d_{x^2-y^2}$ and d_{z^2}) are compatible to bond with ligand s-orbitals, while the other three (d_{xy}, d_{xz}, d_{yz} cannot form productive interactions with ligand s-orbitals (CC-BY-NC-SA; Kathryn Haas).

Because the ligand s orbitals lie on the axes, there are two d orbitals that will form productive interactions with these ligands: the $d_{x^2-y^2}$ which has lobes that point directly along the x and y axes, and the d_{z^2}, which has lobes that point along the z axis and along the xy plane. The ligand s orbitals have two SALCs with appropriate symmetry to interact with these two metal d-orbitals. However, the remaining three orbitals, the d_{xy}, d_{xz}, and d_{yz}, cannot form productive interactions with ligand s-orbitals.

Exercise 7.2.1

Sketch the two ligand SALCs that would interact with the d-orbitals, as shown in Figure 7.2.1. What is the symmetry of these SALCs under the octahedral point group?

Answer available at the end of this section.

The metal $d_{x^2-y^2}$ and d_{z^2} will combine with the e_g SALCs (see exercise above) to form new bonding and antibonding molecular orbitals. A simplified drawing of this interaction, which forms bonding and antibonding molecular orbitals is shown below in Figure 7.2.2. There are also for other ligand SALCs that will interact with s and p orbitals, but for the moment we're not going to worry about them.

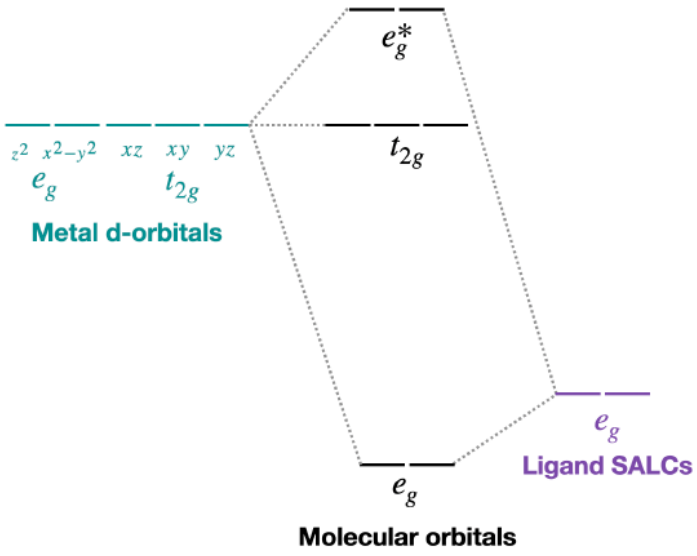


Figure 7.2.2: Diagram of metal d orbitals (left) and ligand e_g SALCs (right) along with their relative energies. The orbitals in the middle represent the molecular orbitals: there is a set of bonding e_g, a set of antibonding e_g^*, and set of non-bonding t_{2g} orbitals. The metal d-orbitals are considered to be "split" into the t_{2g} and e_g^* molecular orbitals, while the bonding e_g have mostly ligand character (this is all based on relative energies of molecular orbitals compared to metal and ligand atomic orbtials. Energy increases from bottom to top. (CC-BY-NC-SA; Kathryn Haas)

Now, remember that metals usually have d electrons that are much higher in energy than those on typical donor atoms (like oxygen, sulfur, nitrogen or phosphorus). That means the antibonding combinations will be much closer in energy to the original d orbitals, because both are relatively high in energy. The bonding combination will be much closer in energy to the original ligand orbitals, because these ones are all relatively low in energy.

That energetic similarity generally translates into a similarity in shape and location as well. In other words, the antibonding combination between a d orbital and a ligand orbital is a lot like the original d orbital. The bonding combination is more like the original ligand orbital than the original d orbital. Because of those similarities, inorganic chemists often refer to those antibonding orbitals as if they were still the original d orbitals.

Exercise 7.2.1

Use the diagram in Figure 7.2.2. Fill in the diagram for a d^3 metal complex. Identify the froteir orbtials (the HOMO and the LUMO).

Answer available at the end of this section.

Summary for simple octahedral case

- Assume the six ligands all lie along the x, y and z axes.
- The $d_{x^2-y^2}$ and the d_{z^2} orbitals point at the ligands along the axes.
- These two orbitals "become" antibonding orbitals and are thus "raised" relatively high in energy.
- These orbitals are called the "**e_g**" set of orbitals due to their symmetry under the octahedral point group.

On the other hand, the other three d orbitals, the d_{xy}, d_{xz} and d_{yz}, all lie *between* the donor ligands, rather than hitting them head-on. These orbitals will interact less strongly with the donor electrons.

- The d_{xy}, d_{xz} and d_{yz} orbitals all lie between the bond axes.
- These three orbitals will be changed in energy only a little.
- These orbitals are more like non-bonding orbitals.
- These orbitals are sometimes called the "**t_{2g}**" set of orbitals.

Remember, only the energy of the *electrons* affects the overall energy of the system. The unoccupied d orbitals are raised in energy, but the occupied orbitals go down in energy (or else stay the same).

Apart from the stabilization of the complex, there is another consequence of this picture. What we are left with is two distinct sets of d energy levels, one lower than the other. That will have an effect on the electron configuration at the metal atom in the complex. In other words, there will be cases where electrons could be paired or unpaired, depending on how these orbitals are occupied.

Take the case of the biologically important iron(II) ion. It has a d^6 valence electron configuration. In less formal parlance of inorganic chemistry, "iron(II) is d^6." In an iron(II) ion all alone in space, all the d orbitals would have the same energy level. We would put one electron in each orbital, and have one left. The left over electron would need to pair up in one of the d orbitals (Notice that, in the chemistry of transition metal *ions*, the valence s and p orbitals are always assumed to be unoccupied).

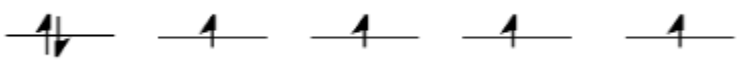


Figure 7.2.5:

Things are very different in an octahedral complex, like $K_4[Fe(CN)_6]$. In that case, the d orbitals are no longer at the same energy level. There are two possible configurations to consider.

In one case, one electron would go into each of the lower energy d orbitals. A choice would be made for the fourth electron. Does it go into the higher energy d orbital, or does it pair up with one of the lower energy d electrons? The choice depends on how

much higher in energy the upper d orbitals are, compared to how much energy it costs to put two electrons in the same d orbital.

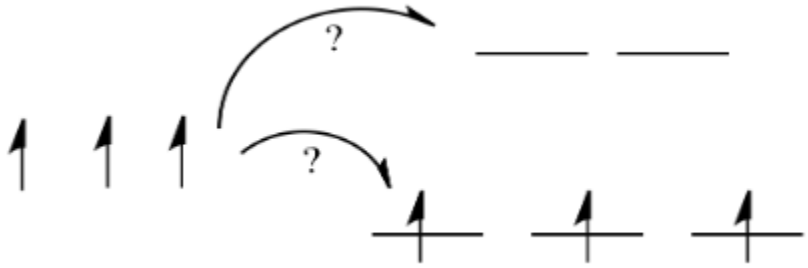


Figure 7.2.6:

If the "d orbital splitting energy" is pretty low, so that the two sets of d orbitals are still pretty similar in energy, the next electron can go into a higher orbital. Pairing would not be required until the final electron. Overall, that would leave four unpaired electrons, just like in the case of a lone metal ion in space. This is called the "high-spin" case, because electrons can easily go into the higher orbital.

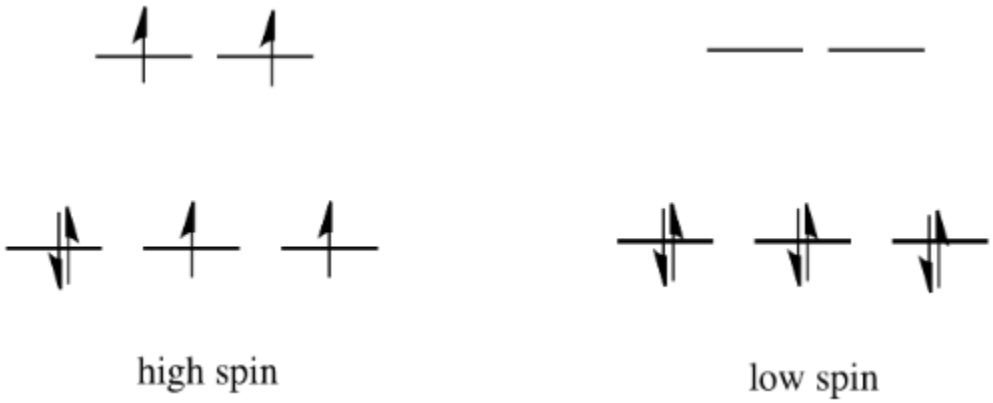


Figure 7.2.7:

If the d orbital splitting energy is too high, the next electron must pair up in a lower orbital. All three remaining electrons pair up, and so there are no unpaired electrons in the complex. This is called the "low-spin" case, because electrons more easily pair up in the orbital.

So the overall rule is that if the energy to pair up the electrons is greater than the energy needed to get to the next level, the electron will go ahead and occupy the next level.

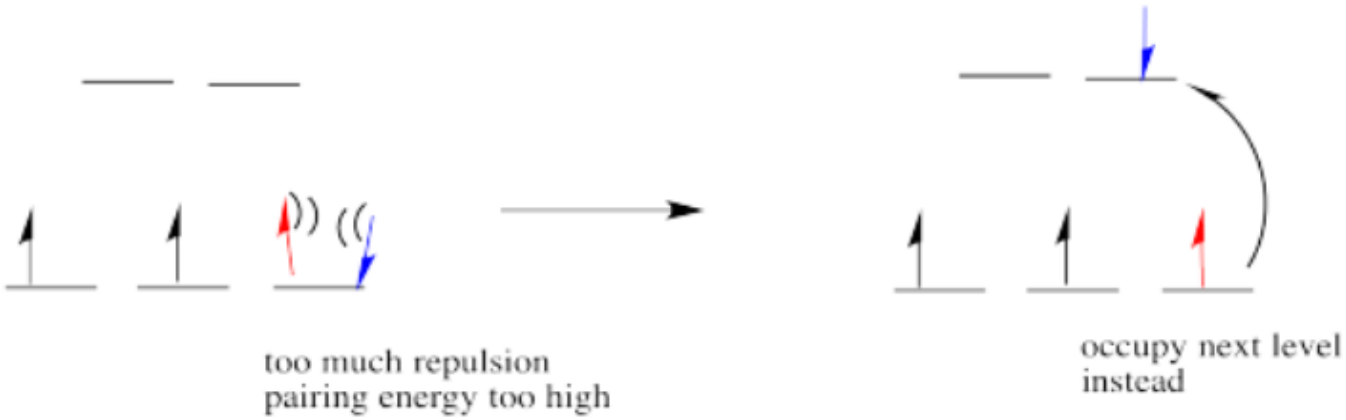


Figure 7.2.8:

However, if the energy it takes to get to the next level is more than it would cost to pair up, the electrons will just pair up instead.

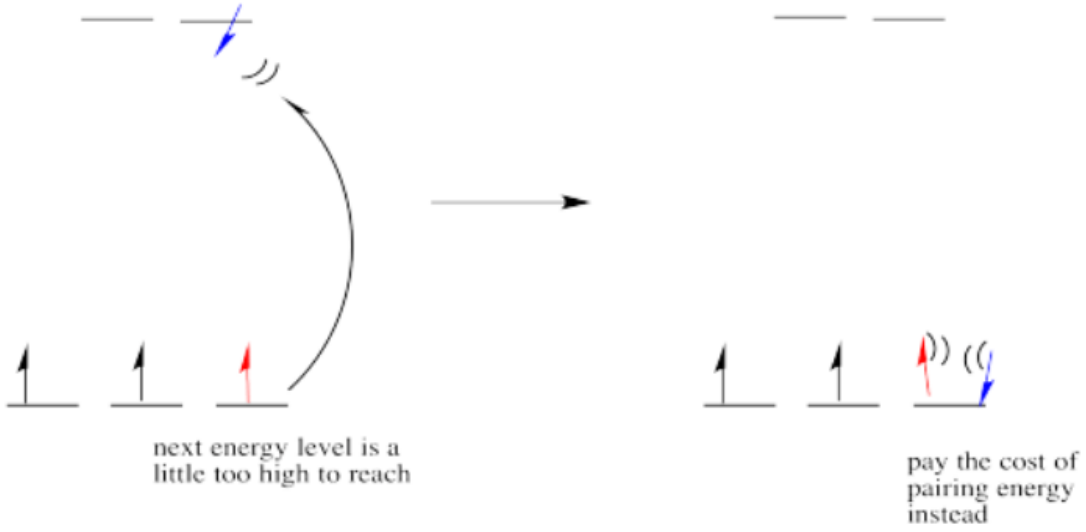


Figure 7.2.9:

> The electron configuration can be "high spin" or "low-spin", depending on how large the energy splitting is between the two sets of d orbitals.

The difference between the high-spin case and the low-spin case is significant because unpaired electrons affect the magnetic properties of a material. The low-spin case would be diamagnetic, resulting in no interaction with a magnetic field. However, the high-spin case would be paramagnetic, and would be attracted to a magnetic field.

It turns out $K_4[Fe(CN)_6]$ is diamagnetic. Thus, it is pretty clear that it is a low-spin complex. The energy difference between the two d orbital levels is relatively large in this case.

In addition to influencing magnetic properties, whether a complex is high- or low-spin also influences reactivity. Compounds with high-energy d electrons are generally more labile, meaning they let go of ligands more easily.

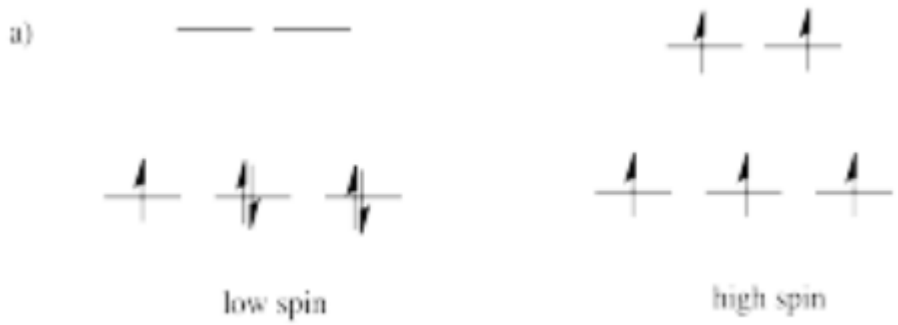
- electron configuration influences magnetic properties
- electron configuration influences lability (how easily ligands are released)

Exercise

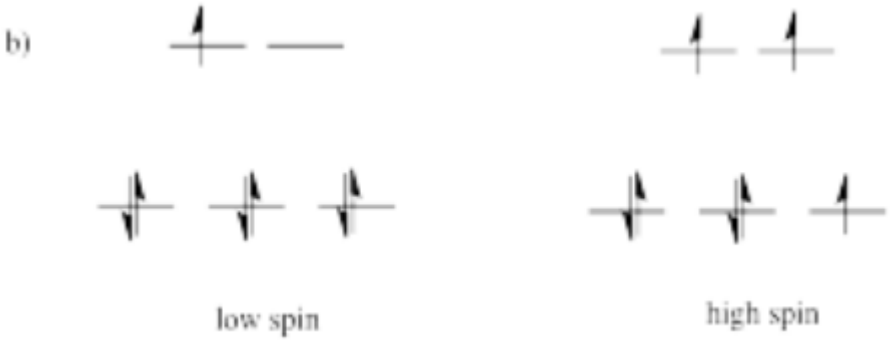
Draw both high spin and low spin d-orbital splitting diagrams for the following ions in an octahedral environment and determine the number of unpaired electrons in each case.

a) Mn^{2+} b) Co^{2+} c) Ni^{2+} d) Cu^{+} e) Fe^{3+} f) Cr^{2+} g) Zn^{2+}

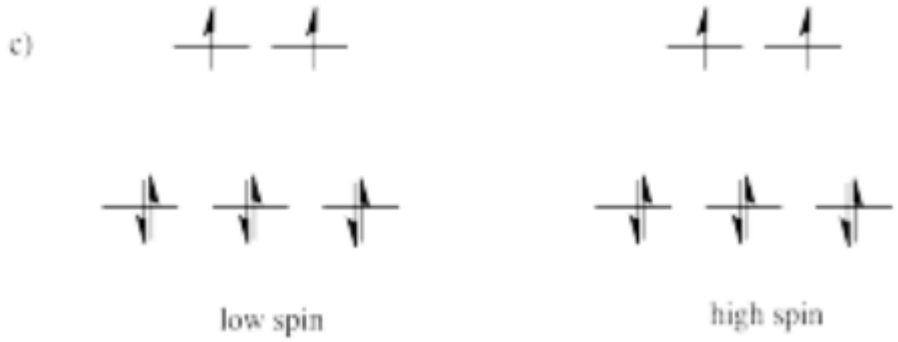
Answer a)



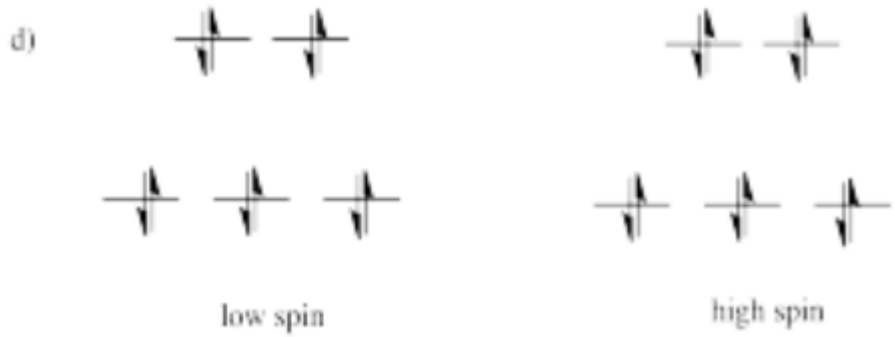
Answer b)



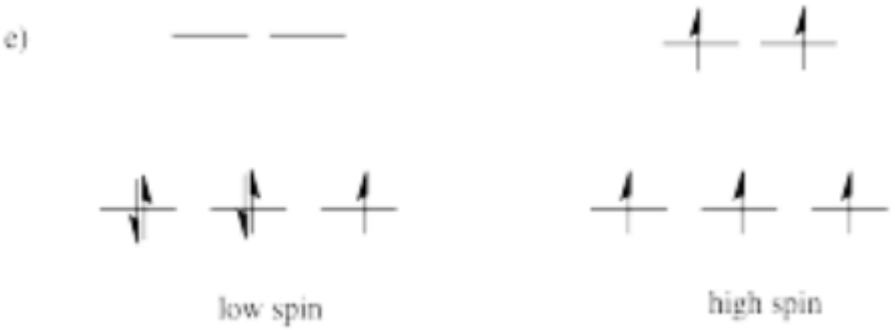
Answer c)



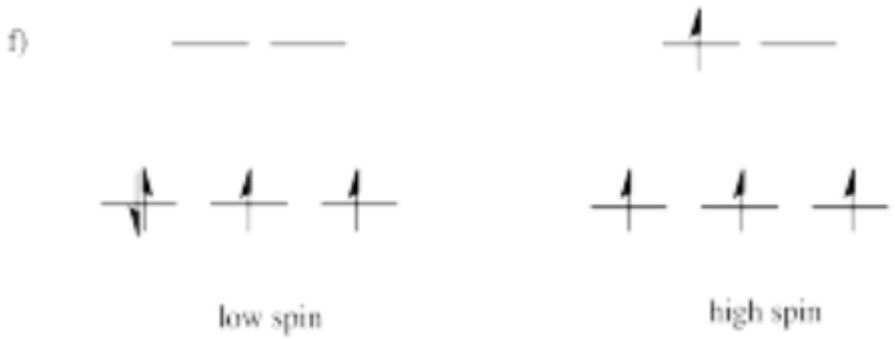
Answer d)



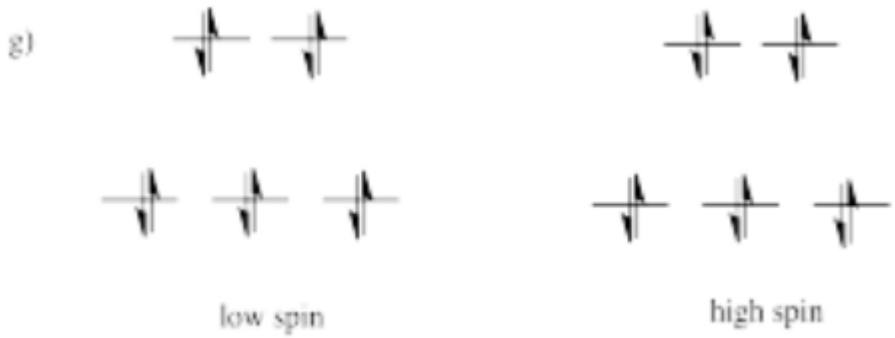
Answer e)



Answer f)

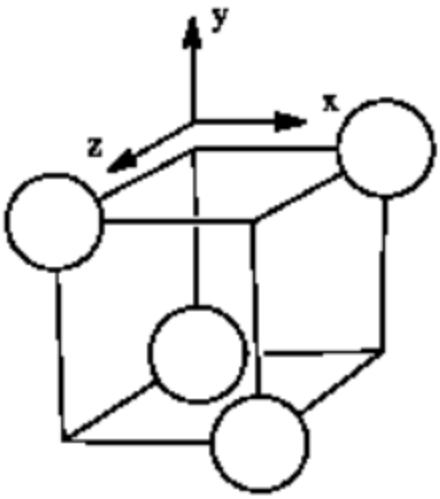


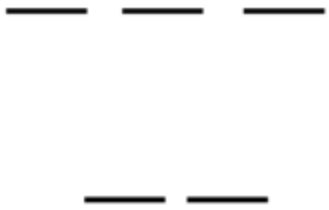
Answer g)



Exercise

The d orbital splitting diagram for a tetrahedral coordination environment is shown below. Given this diagram, and the axes in the accompanying picture, identify which d orbitals are found at which level. In the picture, the metal atom is at the center of the cube, and the circle represent the ligands.



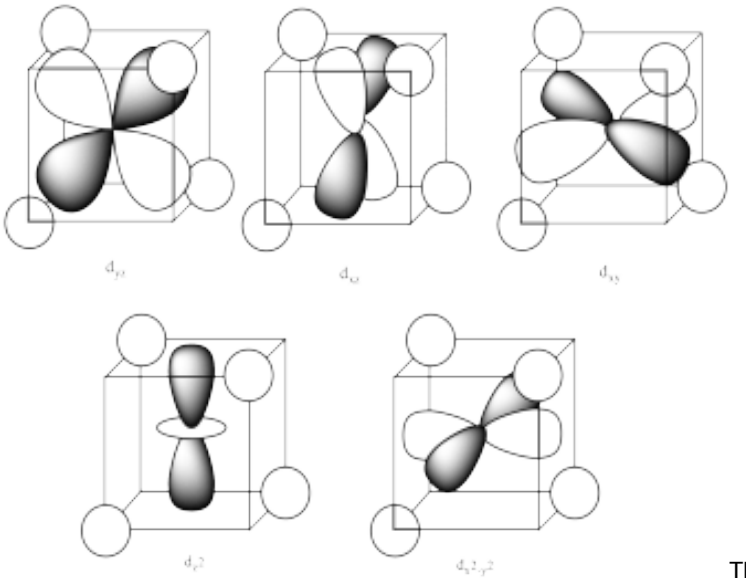


d orbital energy levels

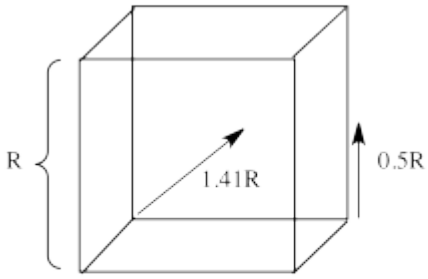
Figure :

Answer

The three orbitals shown above interact a little more strongly with the ligands. The three orbitals shown below interact a little more weakly.



The reason for the difference in the interaction has to do with how close the nearest lobe of a d orbital comes to a ligand. There are really two possible positions: the face of a cube or the edge of a cube. If the ligands are at alternating corners of the cube, then the orbitals pointing at the edges are a little closer than those pointing at the faces of the cube.



$$\sqrt{R^2 + R^2} = 0.5\sqrt{2R^2} = 0.705R$$

Exercise

Typically, the d orbital splitting energy in the tetrahedral case is only about 4/9 as large as the splitting energy in the analogous octahedral case. Explain why it is smaller for the tetrahedral case.

Answer

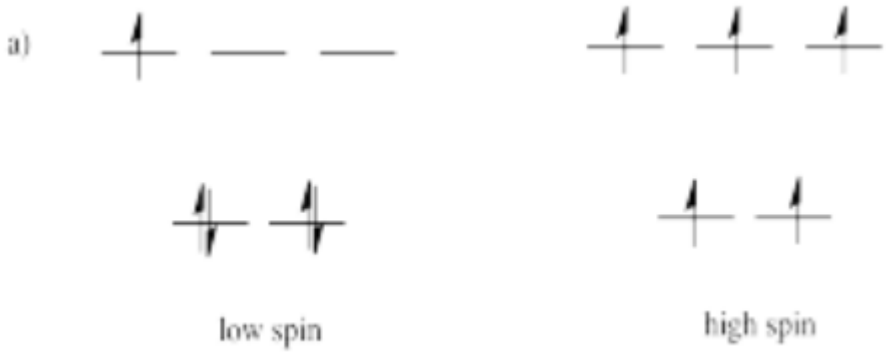
The ligands do not overlap with the d orbitals as well in tetrahedral complexes as they do in octahedral complexes. Thus, there is a weaker bonding interaction in the tetrahedral case. That means the antibonding orbital involving the d electrons is not raised as high in energy, so the splitting between the two d levels is smaller.

Exercise

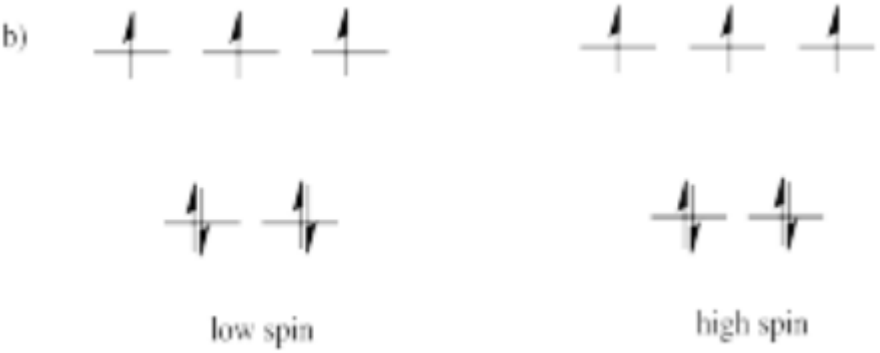
Suppose each of the ions in Exercise (CC8.1) were in tetrahedral, rather than octahedral, coordination environments. Draw the d

orbital diagrams for the high spin and the low spin case for each ion.

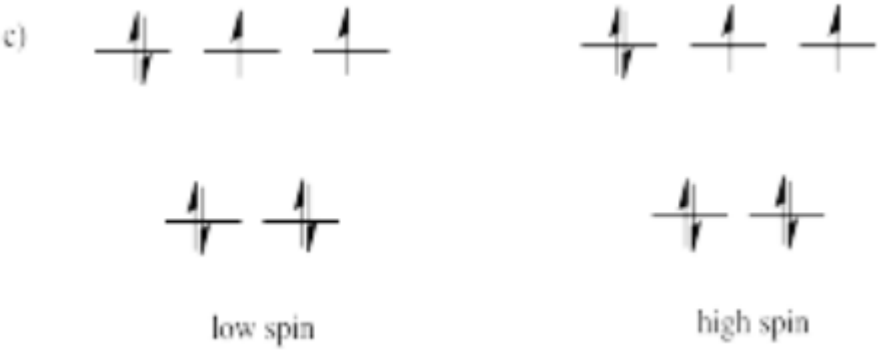
Answer a)



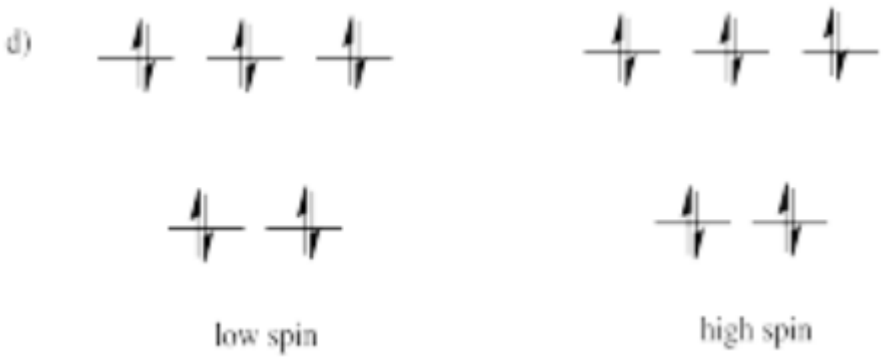
Answer b)



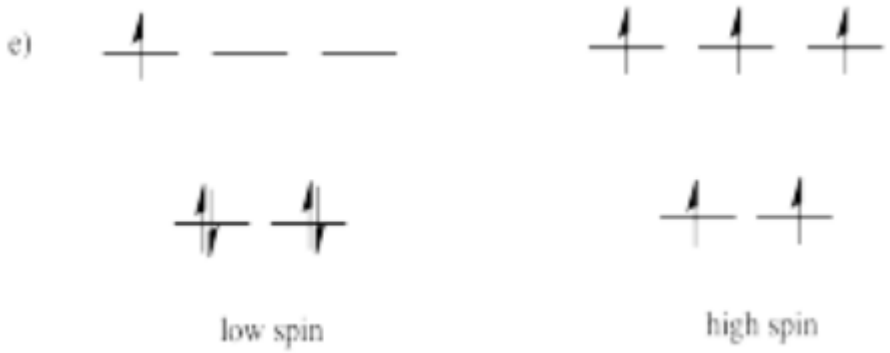
Answer c)



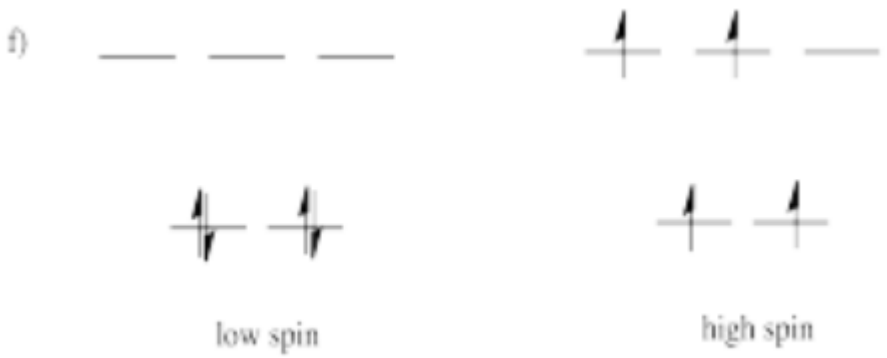
Answer d)



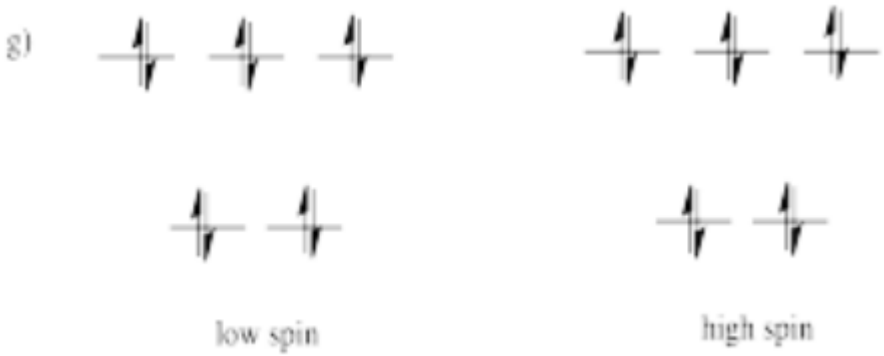
Answer e)



Answer f)



Answer g)



Exercise

Usually, tetrahedral ions are high spin rather than low spin. Explain why.

Answer

> Because the d orbital splitting is much smaller in the tetrahedral case, it is likely that the energy required to pair two electrons in the same orbital will be greater than the energy required to promote an electron to the next energy level. In most cases, the complex will be high spin.

Exercise

The d orbital splitting diagram for a square planar environment is shown below. Given this diagram, and the axes in the accompanying picture, identify which d orbitals are found at which level.

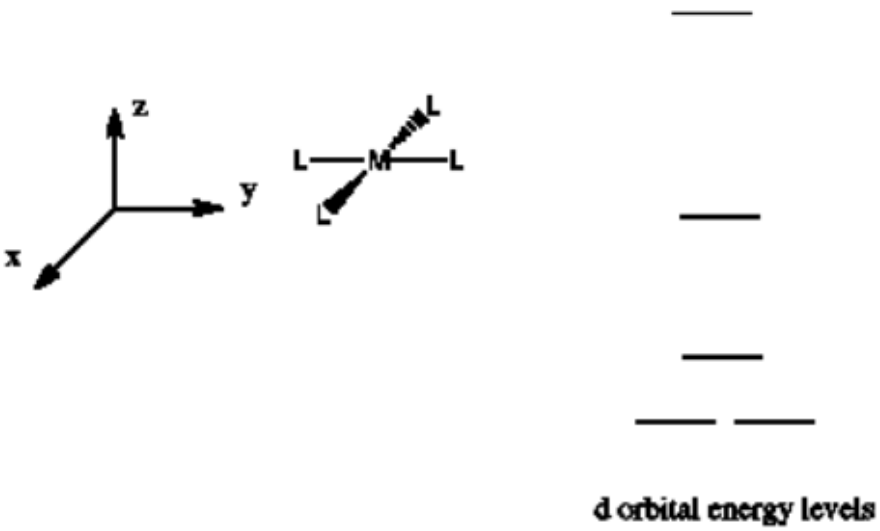
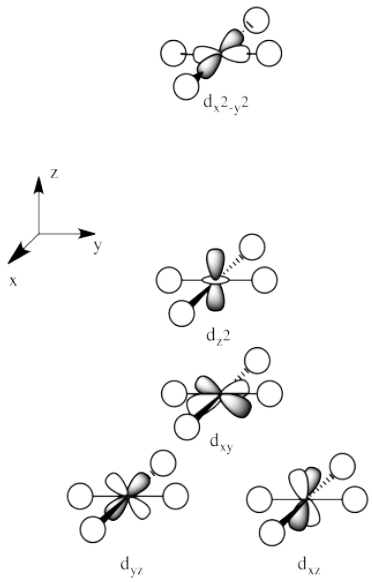


Figure :

Answer

The orbitals are shown in order of energy.



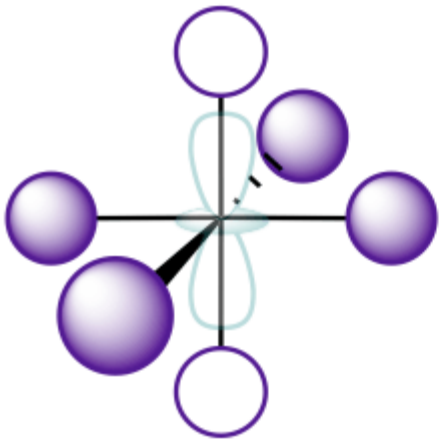
Attribution

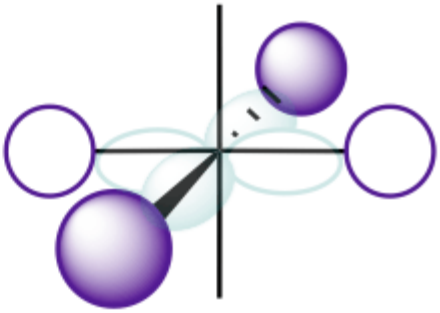
Chris P Schaller, Ph.D., (College of Saint Benedict / Saint John's University)

Answers

Exercise 7.2.1

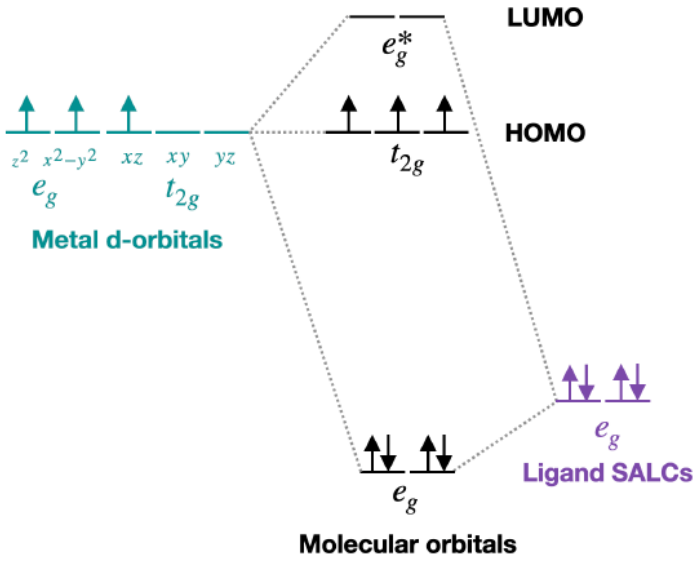
The sketches are shown below, where the purple lobes show the group orbital and the teal transparent orbital in the center is the d-orbital with compatible symmetry. These sketches were drawn simply by matching the symmetry of the central metal orbital. A full explanation for how to systematically generate such sketches is described in a previous chapter. The octahedral character table tells us that the (d_{x^2-y^2}\) and d_{z^2} orbitals transform together with e_g symmetry. Thus, the two SALCs sketched below would also transform with e_g symmetry.





Exercise 7.2.1

When filling in electrons to this diagram we assume that each ligand bonds to the metal by donating two electrons; two SALCs results in four ligand electrons to add to the system. The metal has three d orbitals according to the description. The molecular orbitals should then be filled starting with the lowest energy orbitals. The HOMO-LUMO gap is between the t_{2g} non-bonding and e_g^* antibonding orbitals:



This page titled 7.2: Introduction to Ligand Field Theory (Octahedral complexes) is shared under a license and was authored, remixed, and/or curated by LibreTexts.

7.3: Ligand Field Stabilisation Energy (LFSE)

Saint Mary's College: CHEM 342
Bioinorganic Chemistry
Spring 2020: Dr. Kathryn Haas

Agenda • **Readings** • **Worksheets** • **Essays** • **WiSEWIKI**

There is a variation on how to think about d orbital splitting diagrams that can be useful in deciding how the d electrons are configured in transition metal complexes. We can use the relative energy levels of the d orbitals in a given complex to calculate whether the overall energy would be higher or lower in a high-spin vs. a low-spin case, for example. The calculation provides us with a value that is called the ligand field stabilisation energy (LFSE). Although we have been thinking of bonding in transition metal complexes in terms of molecular orbital ideas, ligand field stabilisation energy actually has its roots in a separate approach called crystal field theory.

Origin Story: LFSE originally comes from CFT

Crystal field theory (CFT) was independently developed around 1930 by German physicist Hans Bethe and American physicist John Hasbrouck van Vleck; the two later became professors of physics at Cornell and Harvard, respectively. CFT actually pre-dates the molecular orbital approach that we have been using so far, but it reaches similar conclusions about transition metal electron configurations.

Both scientists were interested in the magnetic properties of metals and metal salts. They knew these properties were related to unpaired electrons. Compounds with unpaired electrons (paramagnetic) are attracted by magnetic fields, whereas compounds having only paired electrons (diamagnetic) are not. They were interested in the factors that influenced the d electron configuration of transition metal salts, because how the d electrons filled could result in different numbers of unpaired electrons. Those differences influenced how strongly the compounds interacted with magnetic fields.

Crystal field theory does not consider any bonding interactions in transition metal compounds. It focuses only on the repulsion between the electrons on an anion and the electrons on a metal cation. Of course, all of these electrons have negative charges. As an anion approaches a metal, the physicists reasoned, both sets of electrons would experience repulsive forces that would increase their energy level.

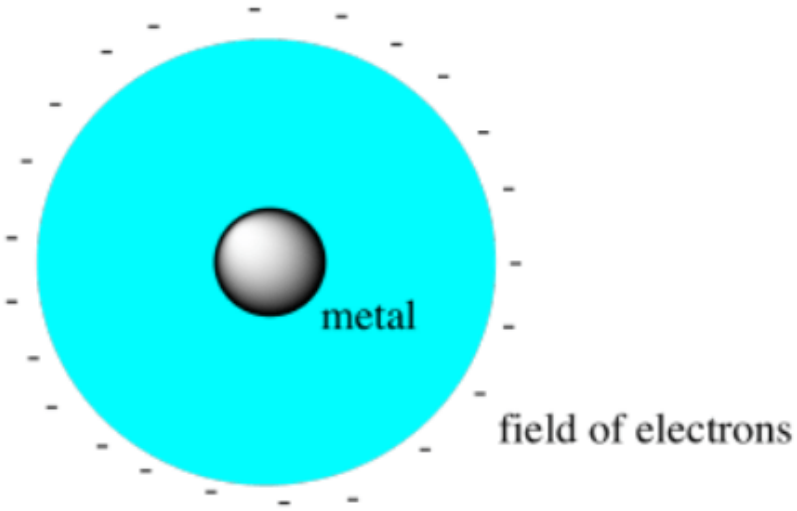


Figure 7.3.1:

If the metal were surrounded by a spherical field of electrons (physicists like to assume things are spherical because it makes the math easier), then all of the electrons on the metal would be raised equally high in energy by these repulsive forces.



Figure 7.3.2:

But in a metal salt, electrons are not approaching the metal from all directions. The geometry comes in because of the fact that the cations and anions pack together in specific arrays. For example, if a metal cation is sitting in an octahedral hole, electrons would only approach from six directions: at each end of the x, y, and z axes.

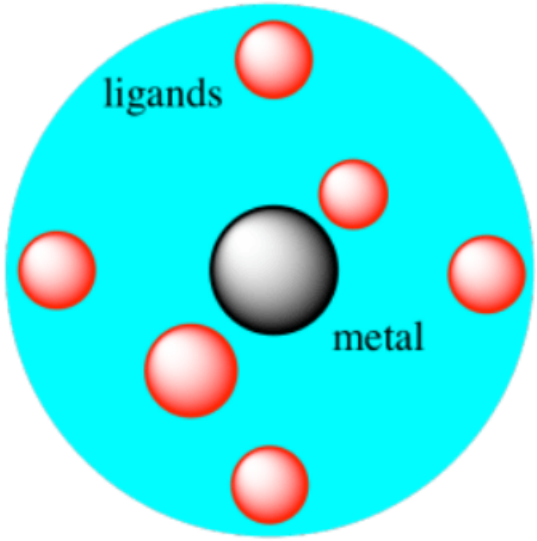


Figure 7.3.3:

In that case, only the electrons in d orbitals that were aligned along the x, y and z axes would be raised significantly by repulsion with the approaching electrons on the anions. The electrons in the off-axis orbitals would be lower in energy than they would have been in a perfectly spherical field.

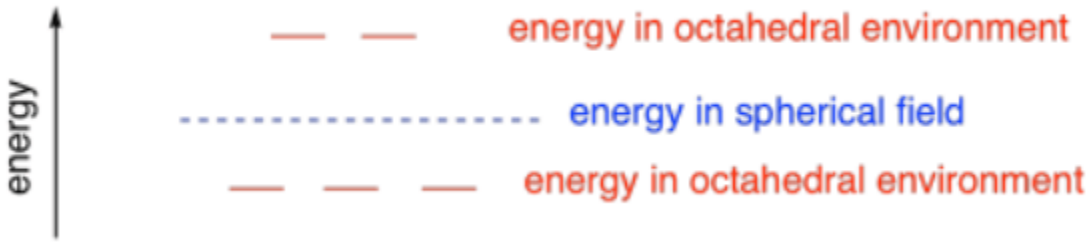


Figure 7.3.4:

Scientists later adapted this idea to octahedral coordination complexes, in which the metal sits amidst six ligands rather than getting packed among six anions.

That result leads to a picture that is pretty similar to what we get from molecular orbital theory, at least as far as the d orbitals are concerned. In fact, the true mathematical approach to molecular orbital theory does take these electron-electron repulsions into account, but it also factors in attractions between the electrons of the ligands and the nucleus of the metal (and vice versa). The biggest difference is that molecular orbital theory includes what happens to the kinetic energy of the ligand lone pairs as they become shared with the metal (it goes down; that's a big part of why the bonds form).

The calculation of LFSE

You don't really have to appreciate where this approach came from to be able to see how it is commonly used. If we take the five d orbitals after they have been placed in an octahedral environment, we see that they are at two different energy levels. The average energy level is not, as it might first appear, halfway between these levels. That's because there are three lower energy level orbitals and two higher energy level orbitals. The average is two-fifths of the way up from the bottom three, or three-fifths of the way down from the top two.

That average energy level of the five d orbitals is called the "**barycenter**"; it is assigned a relative energy of zero. The difference between the top level and the bottom level is the field splitting; for an octahedral complex, this field splitting is given the symbol Δ_o; here, Δ stands for the energy difference and *o* stands for octahedral.



Figure 7.3.5:

If the barycenter is at an energy level of zero, then the lower orbitals are below zero. How far? They are two-fifths of the total Δ_o below the barycenter. Any electrons in those orbitals are **$-0.4\Delta_o$** below 0 in energy. Electrons in the upper orbitals are **$+0.6\Delta_o$** above zero in energy.

Example d^4:

Suppose there are four electrons. The first three electrons sit in each of the three lower orbitals, the ones we sometimes label the t_{2g} orbitals. The fourth will either go into the upper level, which we sometimes call the e_g level, or else pair up with another electron at the lower level.

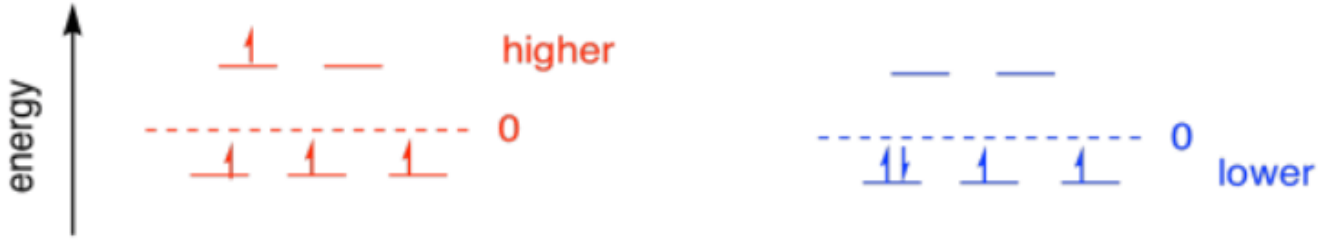


Figure 7.3.6:

We can now calculate the energy difference between these two possible cases. We can calculate what is called the ligand field stabilisation energy, LFSE (sometimes called crystal field stabilisation energy, or CFSE). It's just the sum of the energies of each of the electrons.

$$LFSE = [(0.6 \times number\ of\ e_g\ electrons) - (0.4 \times number\ of\ t_{2g}\ electrons)]\Delta_o \tag{7.3.1}$$

or if that's too much jargon, $LFSE = [(0.6 \times\ \#upper\ e^-) - (0.4 \times\ \#lower\ e^-)]\Delta_o$

For the d^4 high-spin case:

$$LFSE = [(0.6 \times 1) - (0.4 \times 3)]\Delta_o = [0.6 - 1.2]\Delta_o = -0.6\Delta_o \tag{7.3.2}$$

For the \(d^4 low-spin case:

$$LFSE = [(0.6 \times 0) - (0.4 \times 4)]\Delta_o = -1.6\Delta_o \tag{7.3.3}$$

So far, it certainly seems like the low-spin case is at lower energy and thus more stable. Remember, though, that low-spin configuration requires that we place two electrons together into the same orbital.

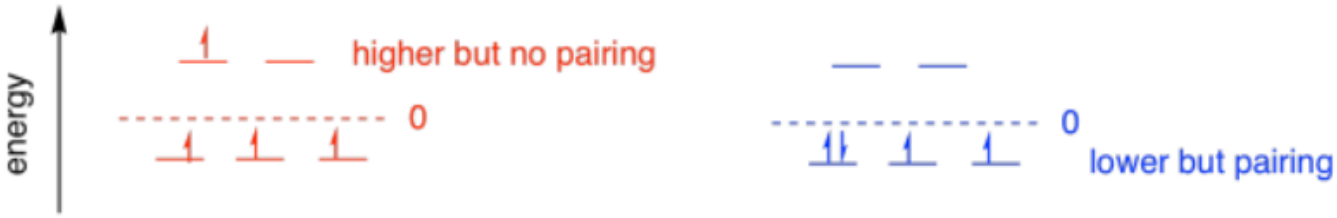


Figure 7.3.7:

Pairing electrons in the same orbital is going to cost some energy. But how much?



Figure 7.3.8:

This repulsion between a pair of electrons in one orbital is called the pairing energy (PE). For each pair of electrons that occupy the same orbital, that energy must be added to take that repulsion into account. As a result, a calculation of the overall stabilization energy (SE) includes both the LFSE and the PE.

$$SE = LFSE + PE \tag{7.3.4}$$

If there were two sets of paired electrons, we would add 2PE; if there were three sets of paired electrons, we would add 3PE, and so on.

Overall, deciding quantitatively whether a complex will be high spin or low spin is the most useful application of an LFSE calculation. However, you do have to know the values of the parameters (the field splitting and the pairing energy) for a definitive decision.

Exercise 7.3.1

Use SE calculations to determine stabilisation in both high spin and low spin cases. Just leave your answer expressed in terms of Δ_o and PE.

a. Fe^{+2}

b. Co^{+2}

c. Co^{+3}

d. Mn^{+2}

e. Ti^{+3}

Answer a) available at the end of this section.

SE depends on the Magnitude of Δ_o and total PE

Right now, let's think about Δ_o. How much energy is it? How big is the gap between the d orbitals? And how do we know? Well, we can easily measure this gap using a simple spectrophotometer. A spectrophotometer measures how much light is absorbed by a sample. Furthermore, it measures what specific colors of light are absorbed by the sample. As it happens, the absorption

of ultraviolet and visible light by a material is associated with electrons in that material becoming promoted to a higher energy level. Shine a light on a transition metal complex, and an electron may jump the gap.

So all we have to do is shine different colors of monochromatic light on the complex and see whether it absorbs one of the colors.

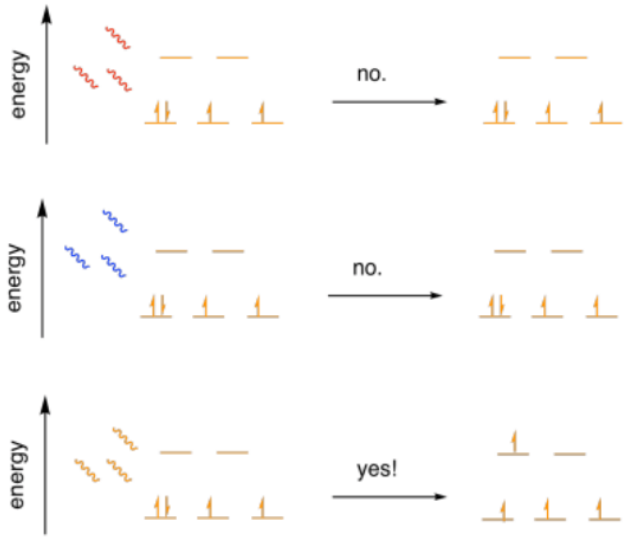


Figure 7.3.9:

This experiment is quite reproducible. A specific compound will always absorb the same colors of light. That's why specific materials have specific colors; the color we see represents the light that is *not* absorbed by the material.

Different colors of light have different amounts of energy. Blue light has higher energy than orange light, which has higher energy than red light. Max Planck and Albert Einstein worked out that the energy of a photon (a "particle" or "packet" of light) is directly proportional to the frequency at which the photon oscillates or vibrates. Blue light has a higher frequency than red light, so it has higher energy.

Planck and Einstein expressed this idea with an equation,

$$E = h\nu$$

in which the Greek letter ν, pronounced "noo," stands for the frequency (some people just use *f* for frequency) and *h* stands for a sort of conversion factor called Planck's constant.

Blue light has too much energy to promote an electron to the next energy level in this case. It would send the electron way past the next level, and quantum mechanics does not allow that sort of thing. Red light does not have enough energy for the electron to get there. Orange light, in this case, is just right. It has exactly the right amount of energy to jump the gap.

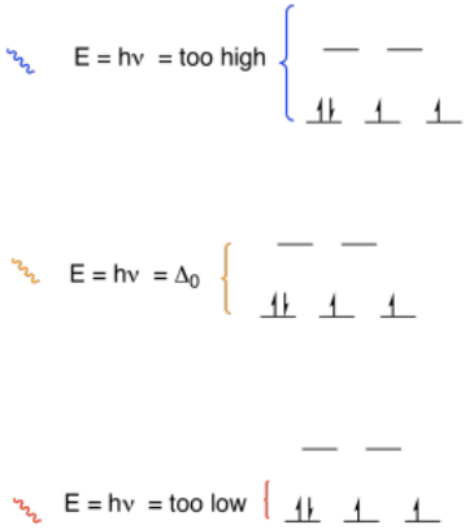


Figure 7.3.10:

So, if we know the frequency of orange light, we know how much energy there is in an orange photon, and we know how big the field splitting is between the d orbitals.

Historically, it turns out that people have most often described visible light in terms of wavelength rather than frequencies. The wavelength is just the distance from one "peak" to the next as the wave of the photon rolls along. The higher the frequency, the closer these peaks are together, and the shorter the wavelength. Blue light has a shorter wavelength, around 400 nm, than red light, around 700 nm. A nanometer (nm) is 10^{-9} meters (m); a meter is around a yard.

Orange light has a wavelength of around 600 nm, or 600 x 10^{-9} m, or 6 x 10^{-7} m. For reasons we won't get into, spectroscopists in the past (people who measure the interaction of light and matter) sometimes preferred to work in centimeters, cm; there are 100 cm in 1 m, so orange light has a wavelength of 6 x 10^{-5} cm. Now, because they knew there was an inverse relationship between wavelength and energy (the longer the wavelength, the lower the energy; the shorter the wavelength, the higher the energy), they simply took the reciprocal of the wavelength in centimeters to get a number in cm^{-1}, which they called wavenumbers. They used this as a unit of energy. An orange photon has an energy of 1/0.00006 cm = 16,000 cm^{-1}.

So the gap, the field splitting, Δ_o in this complex is 16,000 cm^{-1}.

Let's go back to our comparison between the high-spin and low-spin case. For high spin:

$$LFSE = [(0.6 \times 1) - (0.4 \times 3)]\Delta_o = [0.6 - 1.2]\Delta_o = -0.6\Delta_o = -0.6 \times 16000cm^{-1} = -9600cm^{-1} \tag{7.3.5}$$

For the low-spin case:

$$LFSE = [(0.6 \times 0) - (0.4 \times 4)]\Delta_o = -1.6\Delta_o = -1.6 \times 16000cm^{-1} = -25600cm^{-1} \tag{7.3.6}$$

These LFSE calculations show that the low-spin case is lower in energy, by 14,000 cm^{-1}. However, we still need to include the pairing energy. Like the field splitting, the pairing energy varies from one complex to another. 20,000 cm^{-1} is a ballpark estimate of a typical pairing energy.

If we use this average value for PE in the example we were discussing above for the high-spin case:

$$SE = LFSE + PE = -9600 + 0cm^{-1} = -9600cm^{-1} \tag{7.3.7}$$

For the low-spin case:

$$SE = LFSE + PE = -25600 + 20000cm^{-1} = -5600cm^{-1} \tag{7.3.8}$$

Taking the pairing energy into account in this case suggests that the high-spin case is favored. It cost less energy to jump the gap and put an electron in a high-lying e_g orbital than it did to pair electrons in a low-lying t_{2g} orbital.

Reminder: Factors that influence Δ_o

Let's take a look at some real examples of field splitting values to get an idea of how large they are, and what factors they depend on.

The metal influences Δ_o

For example, we can look at the charge on the metal ion:

Table of Field Splitting Values, Δ_o, in Hexaquo Complexes of Differing Charges[a]						
Metal Complex	$[Mn(OH_2)_6]^{2+}$	$[Mn(OH_2)_6]^{3+}$	$[Fe(OH_2)_6]^{2+}$	$[Fe(OH_2)_6]^{3+}$	$[Co(OH_2)_6]^{2+}$	$[Co(OH_2)_6]^{3+}$
Δ_o (cm^{-1})	7,800	21,100	10,400	13,800	9,300	18,300
a) Holleman, A. F.; Wiberg, E.; Wiberg, N. Inorganic Chemistry, 34th Ed. Academic Press: Berlin, 2001.						

In this case, it looks like increased charge on the metal ion results in an increased field splitting. The same thing happens in all three examples: manganese, iron, and cobalt. As the metal ion becomes more charged, attraction of the d electrons toward the nucleus increases. The lower-lying t_{2g} level is more strongly attracted to the nucleus because it is a little closer; consequently, it drops a little further than the e_g level, and the gap gets bigger.

Charge on the metal ion is one of two key factors that influences the size of the field splitting. The other factor is the period or row in the periodic table.

Table of Field Splitting Values, Δ_o, in Hexammine Complexes of Group 9[a,b]			
Metal Complex	$[Co(NH_3)_6]^{3+}$	$[Rh(NH_3)_6]^{3+}$	$[Ir(NH_3)_6]^{3+}$
Δ_o (cm^{-1})	21,500	33,100	41,100
a) Holleman, A. F.; Wiberg, E.; Wiberg, N. Inorganic Chemistry, 34th Ed. Academic Press: Berlin, 2001. b) Miessler, G. L.; Tarr, D. A. Inorganic Chemistry, 4th Ed. Pearson, 2010.			

Moving from one row to the next in group 9 of the periodic table, we see that the field splitting increases by about 10,000 cm^{-1} each row.

In general:

- Δ_o increases with charge on the metal
- Δ_o increases with the period in the periodic table

The ligand identity influences Δ_o

The metal ion is not the only factor that affects the field splitting. The ligands also play an important role, as seen in the table below.

Table of Field Splitting Values, Δ_o, in Assorted Complexes[a]							
Metal Complex	$[CrCl_6]^{3-}$	$[CrF_6]^{3-}$	$[Fe(OH_2)_6]^{2+}$	$[Fe(CN)_6]^{4-}$	$[Co(OH_2)_6]^{3+}$	$[Co(NH_3)_6]^{3+}$	$[Co(CN)_6]^{3-}$
Δ_o (cm^{-1})	13,300	15,300	10,400	33,200	18,300	23,000	33,700

a) Holleman, A. F.; Wiberg, E.; Wiberg, N. Inorganic Chemistry, 34th Ed. Academic Press: Berlin, 2001.	

If we sort these ligands into three broad categories, we can form a trend for these effects. It may be easiest to start with the three entries on the right, involving cobalt. The oxygen donor in water has two lone pairs, whereas the nitrogen donor in ammonia has only one. The extra lone pair allows water to act as a π (pi) donor; the lone pair can donate to an orbital on the metal to form a pi bond. In this case, it looks like the π donor (water) results in a smaller Δ_o than the normal σ (sigma) donor (ammonia).

The cyanide ligand has a donor atom that is also participating in a π bond within the ligand; there is a triple bond between the C and N of the cyanide. That means there is also an associated antibonding orbital, π*. That antibonding orbital raises the possibility of back-bonding from the metal. The metal can donate into the π* orbital to make a pi bond. Cyanide is a π-acceptor. Its field splitting is much larger than the sigma donor.

Those conclusions can be confirmed by looking at the entries for iron in the middle of the table. Cyanide is a π-acceptor whereas water is a π-donor. The field splitting in the aquo complex should be much smaller than the field splitting in the cyano complex, and it is.

The two entries for chromium on the left both show halides, which are π-donors. They illustrate a factor that can be used to predict field strength between two ligands from the same group, such as two π-donors or two π-acceptors. In general, the more basic the ligand, the greater the field splitting. Fluoride ion is more basic than chloride ion (because chloride is a more stable anion than fluoride) so it results in a slightly greater value of Δ_o.

The Pairing Energy

In order to thoroughly estimate the stabilisation energy, we also need reliable values for the pairing energy. Pairing energies can be calculated for free metal ions; correction factors can be applied to arrive at a corresponding value in a complex. In general, the values in coordination complexes are somewhat lower than the values in free metal ions. In the table below, we have made a general estimate that the value in the complex is about 20% lower than in the free metal ion.

Table of Pairing Energies, PE, in Free Ions, with Estimated PE in Complexes						
Metal Ion	Mn^{2+}	Mn^{3+}	Fe^{2+}	Fe^{3+}	Co^{3+}	Ru^{3+}
PE, free ion (cm^{-1})	28,000	25,500	17,700	30,100	21,100	~15,000[b]
PE, complex (est., cm^{-1})	20,400	22,900	14,200	24,100	16,900	~12,000[b]
a) Holleman, A. F.; Wiberg, E.; Wiberg, N. Inorganic Chemistry, 34th Ed. Academic Press: Berlin, 2001. b) Estimate.						

If we compare the pairing energies (PE) of the 2+ ions to those of the 3+ ions, we see that PE is always lower in the more highly charged ion. That's the opposite of the trend in Δ_o. Pairing energy is largely dependent on the size of the ion. The smaller the ion, the smaller the orbital, and the more repulsion between two electrons in the same orbital. Because a Mn^{3+} ion is smaller than a Mn^{2+} ion (Coulomb's Law says there is greater attraction for the electrons in the former case, so the ion shrinks), a pair of electrons on Mn^{3+} is closer together than a pair of electrons on Mn^{2+}.

In general, pairing energies also get smaller upon moving down a column in the periodic table. Second row transition metals are larger than first-row transition metals, so the pairing energy is smaller in the second row than in the first. Third row transition metals are about the same size as first row metals, so their pairing energies are similar to those of the second row. That's because of a phenomenon called "the lanthanide contraction": third row transition metals contain an extra set of protons in their nuclei because of the f block elements before them; consequently they are a little smaller than might be expected.

Exercise 7.3.2

Compare pairing energies to field splitting values to determine whether the following complexes would be high-spin or low spin.

a) $Mn(OH_2)_6^{2+}$ b) $Fe(CN)_6^{4-}$ c) $Co(NH_3)_6^{3+}$

Answer a) available at the end of this section.

Attribution

Chris P Schaller, Ph.D., (College of Saint Benedict / Saint John's University)

Curated or created by Kathryn Haas

Answers

Exercise 7.3.1

Fe^{+2}

d^6 low spin
SE = [-0.4(6)+ 0.6(0)] Δo + 3PE
= [-2.4] Δo + 3PE

d^6 high spin
SE = [-0.4(4)+ 0.6(2)] Δo + 1PE
= [-.4] Δo + 1PE

Co^{+2}

d^7 low spin
SE = [-0.4(6)+ 0.6(1)] Δo + 3PE
= [-1.8] Δo + 3PE

d^7 high spin
SE = [-0.4(5)+ 0.6(2)] Δo + 2PE
= [-.8] Δo + 2PE

Co^{+3}

d^6 so this looks the same as Fe^{+2}

Mn^{+2}

d^5 low spin
SE = [-0.4(5)+ 0.6(0)] Δo + 2PE
= [-2.0] Δo + 2PE

d^5 high spin
SE = [-0.4(3)+ 0.6(2)] Δo + 0PE
= [0] Δo

Ti^{+3}

d^1 so there is no possibility of low spin or high spin

Exercise 7.3.2

Δ_o < PE, so high-spin.

Δ_o > PE, so low-spin.

Δ_o > PE, so low-spin.

This page titled 7.3: Ligand Field Stabilisation Energy (LFSE) is shared under a license and was authored, remixed, and/or curated by LibreTexts.

7.4: The Effect of the Metal Ion on d-Orbital Splitting



The Magnitude of Δ_o

For octahedral complexes, the magnitude of Δ_o dictates whether a complex with four, five, six, or seven d electrons is high spin or low spin, which affects its magnetic properties, structure, and reactivity. Large values of Δ_o (i.e., $\Delta_o > P$) yield a low-spin complex, whereas small values of Δ_o (i.e., $\Delta_o < P$) produce a high-spin complex. As we noted, the magnitude of Δ_o depends on three factors: the charge on the metal ion, the principal quantum number of the metal (and thus its location in the periodic table), and the nature of the ligand. Values of Δ_o for some representative transition-metal complexes are given in Table 7.4.1.

Table 7.4.1***:*** *Crystal Field Splitting Energies for Some Octahedral (Δ_o)* and Tetrahedral (Δ_t) Transition-Metal Complexes*

Octahedral Complexes	Δ_o (cm^{-1})	Octahedral Complexes	Δ_o (cm^{-1})	Tetrahedral Complexes	Δ_t (cm^{-1})
$[Ti(H_2O)_6]^{3+}$	20,300	$[Fe(CN)_6]^{4-}$	32,800	VCl_4	9010
$[V(H_2O)_6]^{2+}$	12,600	$[Fe(CN)_6]^{3-}$	35,000	$[CoCl_4]^{2-}$	3300
$[V(H_2O)_6]^{3+}$	18,900	$[CoF_6]^{3-}$	13,000	$[CoBr_4]^{2-}$	2900
$[CrCl_6]^{3-}$	13,000	$[Co(H_2O)_6]^{2+}$	9300	$[CoI_4]^{2-}$	2700
$[Cr(H_2O)_6]^{2+}$	13,900	$[Co(H_2O)_6]^{3+}$	27,000		
$[Cr(H_2O)_6]^{3+}$	17,400	$[Co(NH_3)_6]^{3+}$	22,900		
$[Cr(NH_3)_6]^{3+}$	21,500	$[Co(CN)_6]^{3-}$	34,800		
$[Cr(CN)_6]^{3-}$	26,600	$[Ni(H_2O)_6]^{2+}$	8500		
$Cr(CO)_6$	34,150	$[Ni(NH_3)_6]^{2+}$	10,800		
$[MnCl_6]^{4-}$	7500	$[RhCl_6]^{3-}$	20,400		
$[Mn(H_2O)_6]^{2+}$	8500	$[Rh(H_2O)_6]^{3+}$	27,000		
$[MnCl_6]^{3-}$	20,000	$[Rh(NH_3)_6]^{3+}$	34,000		
$[Mn(H_2O)_6]^{3+}$	21,000	$[Rh(CN)_6]^{3-}$	45,500		

***Energies obtained by spectroscopic measurements are often given in units of wave numbers (cm^{-1}); the wave number is the reciprocal of the wavelength of the corresponding electromagnetic radiation expressed in centimeters: 1 cm^{-1} = 11.96 J/mol.**

Octahedral Complexes	Δ_o (cm^{-1})	Octahedral Complexes	Δ_o (cm^{-1})	Tetrahedral Complexes	Δ_t (cm^{-1})
$[Fe(H_2O)_6]^{2+}$	10,400	$[IrCl_6]^{3-}$	25,000		
$[Fe(H_2O)_6]^{3+}$	14,300	$[Ir(NH_3)_6]^{3+}$	41,000		

***Energies obtained by spectroscopic measurements are often given in units of wave numbers (cm^{-1}); the wave number is the reciprocal of the wavelength of the corresponding electromagnetic radiation expressed in centimeters: 1 cm^{-1} = 11.96 J/mol.**

Source of data: Duward F. Shriver, Peter W. Atkins, and Cooper H. Langford, Inorganic Chemistry, 2nd ed. (New York: W. H. Freeman and Company, 1994).

Charge on the Metal Ion

Increasing the charge on a metal ion has two effects: the radius of the metal ion decreases, and negatively charged ligands are more strongly attracted to the metal. Both factors decrease the metal–ligand distance, which in turn causes the negatively charged ligands to interact more strongly with the d orbitals. Consequently, the magnitude of Δ_o increases as the charge on the metal ion increases. Typically, Δ_o for a tripositive ion is about 50% greater than for the dipositive ion of the same metal; for example, for $[V(H_2O)_6]^{2+}$, Δ_o = 11,800 cm^{-1}; for $[V(H_2O)_6]^{3+}$, Δ_o = 17,850 cm^{-1}.

Principal Quantum Number of the Metal

For a series of complexes of metals from the same group in the periodic table with the same charge and the same ligands, the magnitude of Δ_o increases with increasing principal quantum number: Δ_o (3d) < Δ_o (4d) < Δ_o (5d). The data for hexaammine complexes of the trivalent Group 9 metals illustrate this point:

$$[Co(NH_3)_6]^{3+}\ \Delta_o = 22{,}900\ cm^{-1}$$
$$[Rh(NH_3)_6]^{3+}\ \Delta_o = 34{,}100\ cm^{-1}$$
$$[Ir(NH_3)_6]^{3+}\ \Delta_o = 40{,}000\ cm^{-1}$$

The increase in Δ_o with increasing principal quantum number is due to the larger radius of valence orbitals down a column. In addition, repulsive ligand–ligand interactions are most important for smaller metal ions. Relatively speaking, this results in shorter M–L distances and stronger d orbital–ligand interactions.

Reasons for Low-spin vs. High-spin: The Effect of the Metal Ion

There are a few factors that determine the magnitude of the d orbital splitting and dictate whether or not an electron can occupy the higher energy set of orbitals instead of pairing up. These factors are based partly on ligand field strength, which is explored on the next page. They also depend on the charge on the metal ion and whether the metal is in the first, second, or third row of the transition metals.

The higher the charge on the metal, the greater the splitting between the d orbital energy levels. For example, Fe(II) is usually high spin. It has a smaller splitting between the lower and higher d orbital levels, so electrons can more easily go to the higher level rather than pair up un the lower level.

On the other hand, Fe(III) is usually low spin. It has a larger splitting between the d levels. In that case, it costs less energy for electrons to pair up in the lower level than to go up to the higher level.

- High-spin versus low-spin cases involve a trade-off between the d orbital splitting energy and the pairing energy.
- 2nd and 3rd row transition metals are usually low spin
- 1st row transition metals are often high spin
- However, 1st row transition metals and be low spin if they are very positive (usually 3+ or greater)

There is a lot going on in metal ions, but we'll take a simplified view of things. Thinking only about electrostatics, we can try to

imagine what happens to those electrons when the charge on the metal ion changes.

First we need to know about Coulomb's law. Coulomb's law states that the force of attraction between the electron and the nucleus depends on only two factors: the amount of positive charge in the nucleus, and the distance between the nucleus and the electron.

The greater the charge on the nucleus, the greater the attraction between the electron and the nucleus.

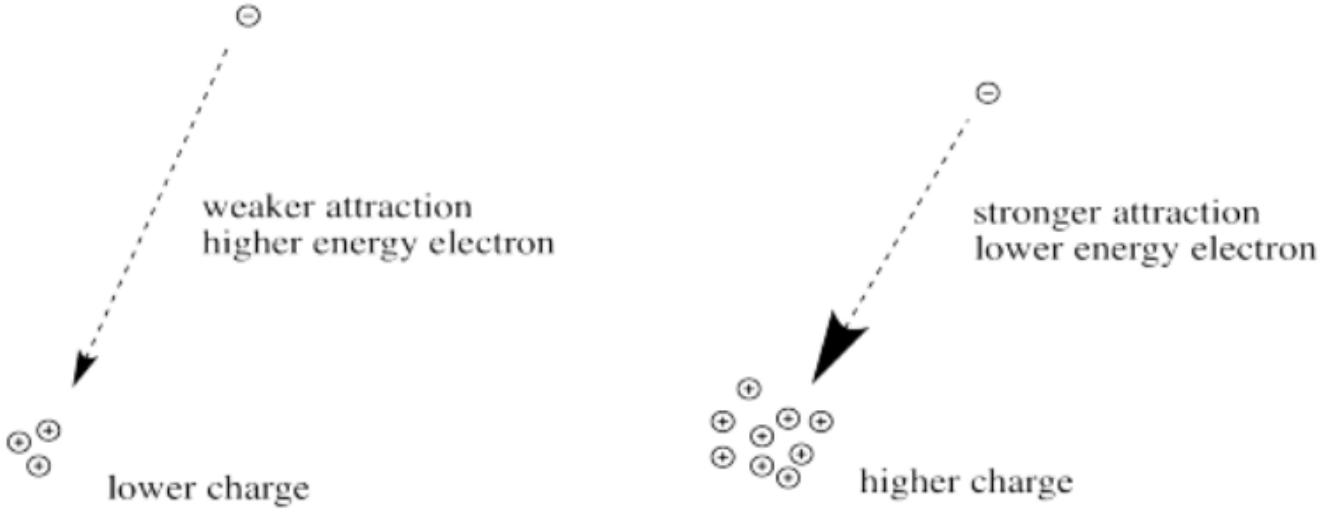


Figure 7.4.10:

The farther an electron is from the nucleus, the weaker the attraction between the electron and the nucleus.

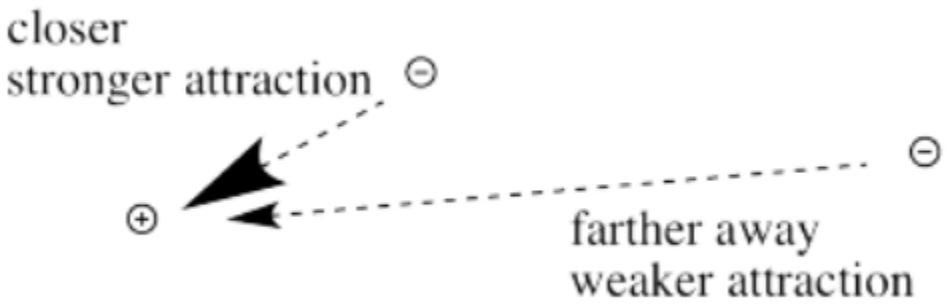


Figure 7.4.11:

Coulomb's law can be used to evaluate the potential energy of the electron. It is one of the factors that determines how high or low those electronic energy levels are that we see in energy level diagrams for atoms, ions and molecules. The energy of the electron varies in a roughly similar way: the greater the charge on the nucleus, the lower the energy of the electron. Also, the closer the electron is to the nucleus, the lower its energy.

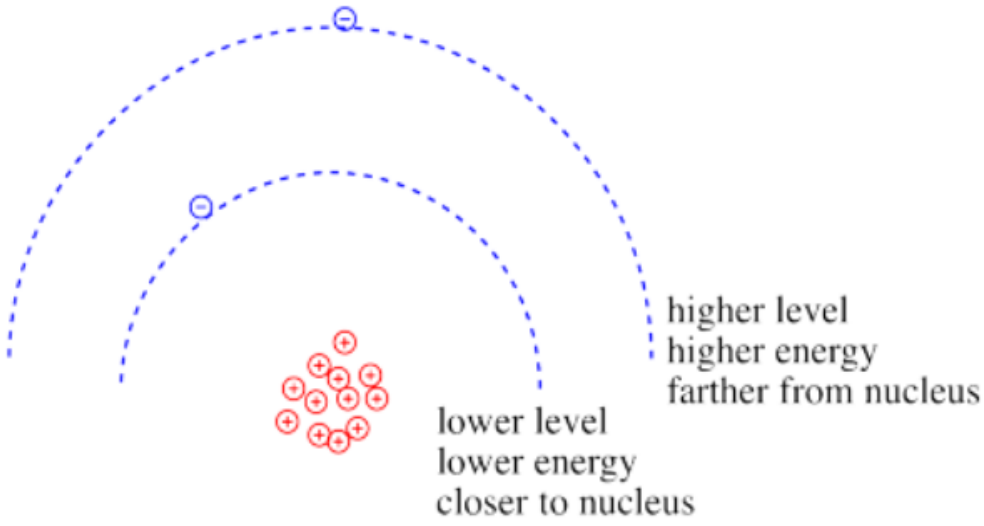


Figure 7.4.12:

Roughly speaking, electrons at higher energy are farther from the nucleus. Electrons at lower energy are closer to the nucleus.

What happens if the charge increases? Maybe a lot more protons are added to the nucleus. Maybe some electrons are lost, so that to the remaining electrons it just *feels like* the charge of the nucleus has increased. Then the electrons should be more attracted to the nucleus. They get a little closer. Their potential energy drops.

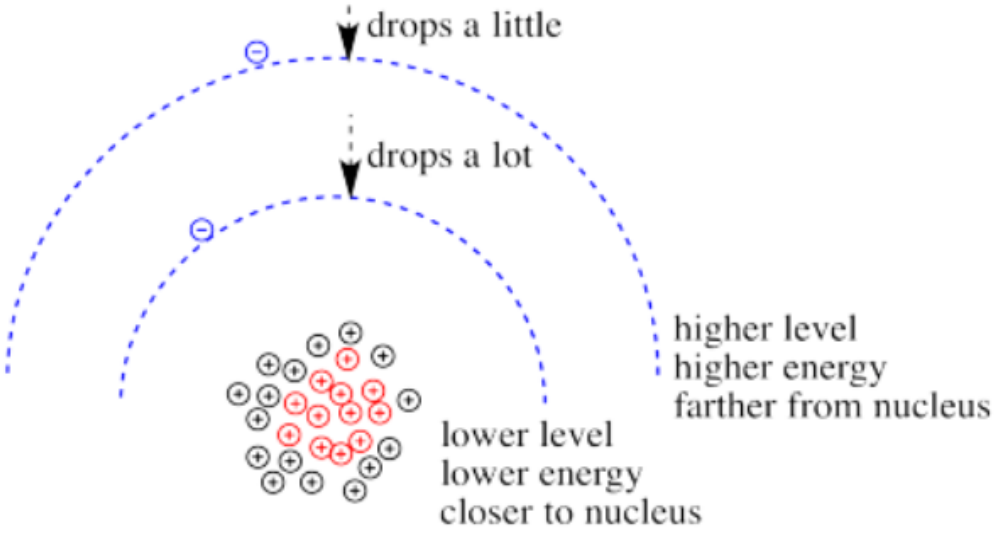


Figure 7.4.13:

Of course, if one electron is closer to the nucleus already, it feels that increase in positive charge more strongly than an electron that is farther away. Consequently it drops further in energy than an electron that is further away.

If we translate that idea into a picture of the d orbital energy levels in an octahedral geometry, it looks like this:

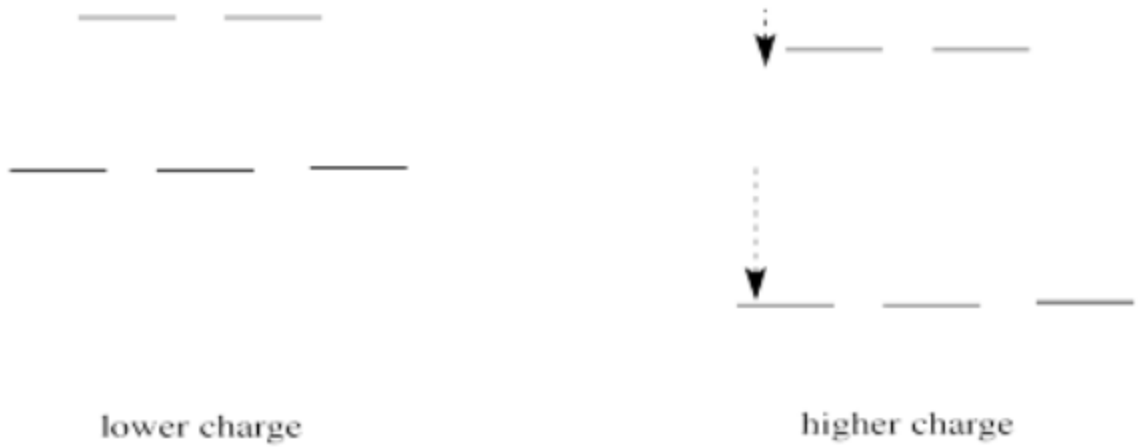


Figure 7.4.14:

When the charge on the metal ion is increased, both the higher and the lower levels drop in energy. However, the lower level drops more. Thus, the gap between the levels gets wider.

Metals in the second and third row of the periodic table almost never form high-spin complexes. The d orbital energy splitting in these cases is larger than for first row metals. From a very simple point of view, these metals have many more protons in their nuclei than the first row transition metals, dropping that lower set of d electrons lower with respect to the higher set.

That isn't the whole picture for the second and third row transition metals, however. Remember, we are simplifying, and there are factors we won't go into. However, it is important to know that metal-ligand bond strengths are much greater in the second and third row than in the first. We'll look at the whole interaction diagram for an octahedral complex now, including contributions form metal s and p orbitals.

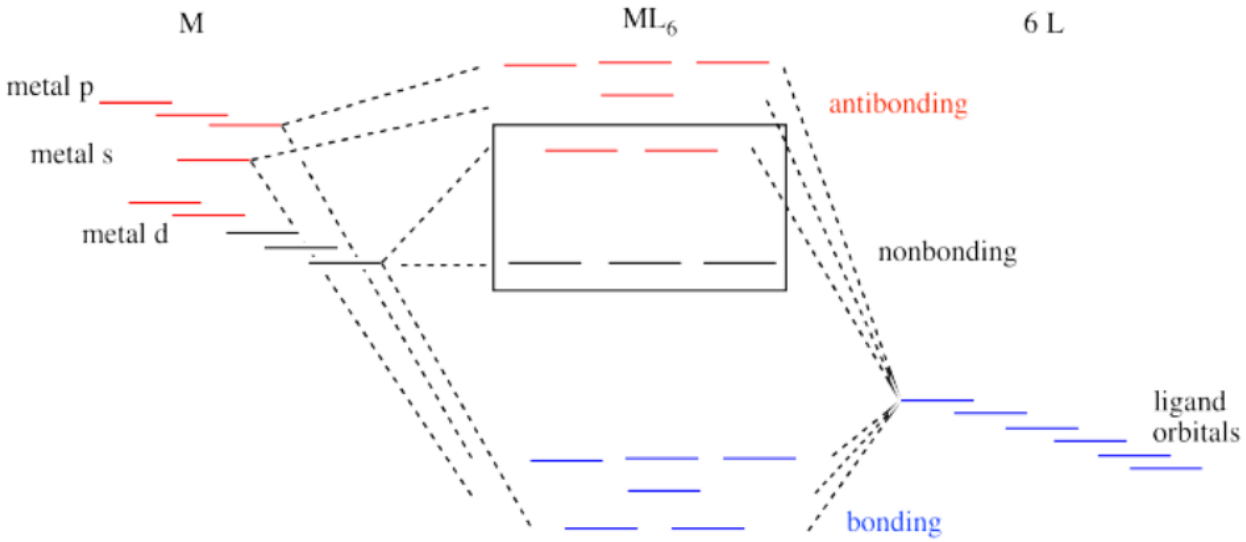


Figure 7.4.15:

Like all ligand-metal interaction diagrams, the energy levels of the ligands by themselves are shown on one side. The metal's electronic energy levels are shown on the other side. The result of their interaction, a metal-ligand complex, is shown in the middle. The d orbital splitting diagram is shown in a box.

Suppose the diagram above is for a first row transition metal. The diagram for a second or third row metal is similar, but with stronger bonds.

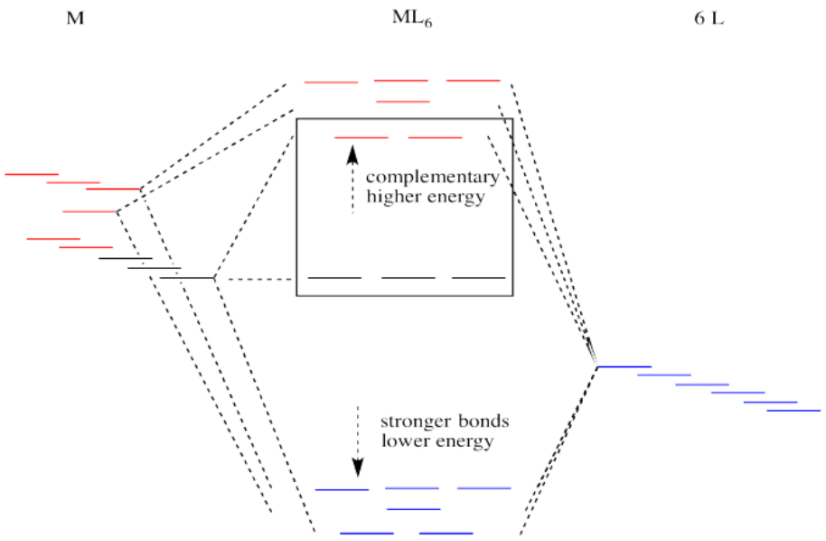


Figure 7.4.16:

If the bonding interaction is stronger between the metal and ligand, then so is the antibonding interaction. The antibonding levels are bumped higher in energy as the bonding levels sink lower. Generally that's OK, because when the electrons are filled in, they will be found preferentially at the lower levels, not the higher ones. There will be a net lowering of electronic energy.

Why do second and third row transition metals form such strong bonds? Bond strengths are very complicated. In general, there is greater covalency between these metals and their ligands because of increased spatial and energetic overlap. Rather than go into those factors, we'll just think about all those extra protons in the nucleus that are attracting the ligand electrons more strongly.

There is one more important distinction that makes second and third row transition metals low spin. In addition, the pairing energy is lower in these metals because the orbitals are larger. There is more room for two electrons in one orbital, with less repulsion. As a result, electrons are much more likely to pair up than to occupy the next energy level.

- 2nd and 3rd row transition metals have stronger bonds, leading to a larger gap between d orbital levels
- 2nd and 3rd row transition metals have more diffuse orbitals, leading to a lower pairing energy

It is significant that most important transition metal ions in biology are from the first row of the transition block and are pretty labile. That fact plays an important role in the ease of formation and deconstruction of transition-metal containing proteins. In terms of formation, if the metal is more easily released by its previous ligands (either water or some compound that delivers the metal to the site of protein construction), it can form the necessary protein more quickly. However, even if a metal-containing enzyme plays a useful role, it should not be too stable, because we need to be able to regulate the level of protein concentration for optimum activity, or disassemble protein if it becomes damaged. Thus, it is important that the metal ion can be removed easily.

Metal ion properties that effect Δ_o

- **Position on the periodic table (period or shell number)**
  The splitting of the d-orbitals in any ligand field *increases as shell number increases going down the periodic table*. In general, with octahedral ligand fields, the $3d$ metal ions can be either weak-field or strong-field depending on other factors. With octahedral complexes, the $4d$ and larger metal ions are generally strong-field.
- **Oxidation state (charge of the metal ion)**
  As the *metal oxidation state increases, the strength of the field also increases*. The charge on a $3d$ metal ion can contribute to whether it is weak-field or strong-field (and thus high-spin or low-spin for $d^4 - d^7$ metal ions). In octahedral $3d$ metals, the +3 metal ions favor stronger-field (and sometimes low spin) complexes. The +2 metal ions in this series favor weaker-field (and usually high spin); but we cannot make a good prediction about this without knowing about the identity of the ligands.

Exercise

Predict whether each compound will be high or low spin.

a. $[Fe(py)_6]^{2+}$

b. $[Fe(H_2O)_6]^{2+}$

c. $[FeBr_6]^{3-}$

d. $[Co(NH_3)_6]^{3+}$

e. $[Cu(NH_3)_6]^{2+}$

f. $[Rh(CO)_6]^{3+}$

g. $[Cr(CO)_6]^{3+}$

h. $[PtCl_6]^{2-}$

Answer a)

$[Fe(py)_6]^{2+}$ 3d metal, M^{+2}, pi acceptor ligand → low spin

Answer b)

$[Fe(H_2O)_6]^{2+}$ 3d metal, M^{+2}, pi donor ligand → high spin

Answer c)

$[FeBr_6]^{3-}$ 3d metal, M^{+3}, pi donor ligand → high spin

Answer d)

$[Co(NH_3)_6]^{3+}$ 3d metal, M^{+3}, sigma donor ligand → low spin

Answer e)

$[Cu(NH_3)_6]^{2+}$ 3d metal, M^{+2}, sigma donor ligand → low spin

Answer f)

$[Rh(CO)_6]^{3+}$ 4d metal, M^{+3} → low spin

Answer g)

$[Cr(CO)_6]^{3+}$ 3d metal, M^{+3}, pi acceptor ligand → low spin

Answer h)

$[PtCl_6]^{2-}$ 5d metal, M^{+4} → low spin

This page titled 7.4: The Effect of the Metal Ion on d-Orbital Splitting is shared under a license and was authored, remixed, and/or curated by LibreTexts.

7.5: The Effect of Ligands and the Spectrochemical Series

Saint Mary's College: CHEM 342
Bioinorganic Chemistry
Spring 2020: Dr. Kathryn Haas

The Nature of the Ligands

Experimentally, it is found that the Δ_o observed for a series of complexes of the same metal ion depends strongly on the nature of the ligands. For a series of chemically similar ligands, the magnitude of Δ_o decreases as the size of the donor atom increases. For example, Δ_o values for halide complexes generally decrease in the order $F^- > Cl^- > Br^- > I–$ because smaller, more localized charges, such as we see for F^-, interact more strongly with the d orbitals of the metal ion. In addition, a small neutral ligand with a highly localized lone pair, such as NH_3, results in significantly larger Δ_o values than might be expected. Because the lone pair points directly at the metal ion, the electron density along the M–L axis is greater than for a spherical anion such as F^-. The experimentally observed order of the crystal field splitting energies produced by different ligands is called the spectrochemical series, shown here in order of decreasing Δ_o:

$$\underset{\text{strong-field ligands}}{CO \approx CN^- > NO_2^-} > en > NH_3 > \underset{\text{intermediate-field ligands}}{SCN^- > H_2O} > oxalate^{2-} > OH^- > F > acetate^- > \underset{\text{weak-field ligands}}{Cl^- > Br^- > I^-}$$

The values of Δ_o listed in Table $7.5.1$ illustrate the effects of the charge on the metal ion, the principal quantum number of the metal, and the nature of the ligand.

> The largest Δ_os are found in complexes of metal ions from the third row of the transition metals with charges of at least +3 and ligands with localized lone pairs of electrons.

Another factor that plays a key role in whether a transition metal complex is high- or low-spin is the nature of the ligands. The d orbital energy splitting is influenced by how strongly the ligand interacts with the metal. Ligands that interact weakly only produce little change in the d orbital energy levels, whereas ligands that interact strongly produce a larger change in d orbital energy levels. The spectrochemical series is a list of ligands based on the strength of their interaction with metal ions. Ligands are often listed from weaker to stronger ligands, something like this:

$$I^- < Br^- < S^{2-} < SCN^- < Cl^- < NO_3^- < N_3^- < F^- < OH^- < C_2O_4^{2-} < H_2O < NCS^- < CH_3CN < py < NH_3$$

$$< en < bipy < phen < NO_2^- < PPh_3 < CN^- < CO$$

in which py = pyridine; en = ethylenediamine; bipy = 2,2'-bipyridine; phen = 1,10-phenanthroline; SCN means the ligand is bound via sulfur and NCS via nitrogen. The list can vary from one metal ion to another, since some ligands bind preferentially to certain metals (as seen in hard and soft acid and base chemistry).

Exercise

What empirical trends can you see within the spectrochemical series? Are there any factors that make something a stronger field ligand?

Answer

The weaker donors include halides and oxygen donors. Nitrogen atom donors are mostly a little stronger than that. The strongest donors include carbon donors, especially with pi bonds.

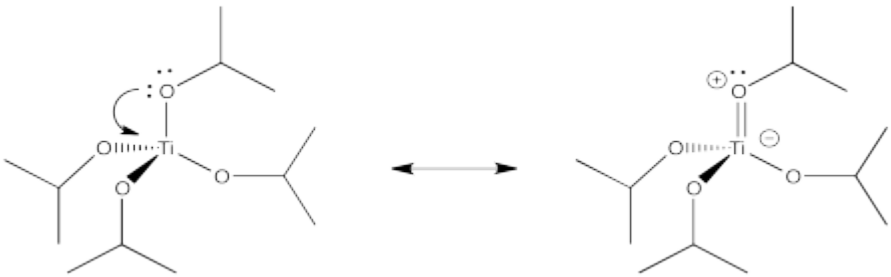
The d orbitals that rise in energy in the presence of a ligand can be thought of as forming an antibonding molecular orbital combination with an orbital on the ligand. In addition, there would also be a bonding combination for this interaction. That bonding orbital would be more like the initial ligand orbital. This premise is based on the idea that a ligand orbital is initially lower in energy than the metal orbital, so a bonding combination between these two orbitals is more like the initial ligand orbital, both in energy and location. The d orbital is initially higher in energy than the ligand orbital, so an antibonding combination between these two orbitals is more like the initial d orbital, both in energy and location.

- When orbitals on two different kinds of atoms combine, the antibonding orbital is considered to be more like the orbital that was initially at higher energy.
- In this case, it is still close to a d orbital in energy, location, and shape.
- When orbitals on two different kinds of atoms combine, the bonding orbital is considered to be more like the orbital that was initially at lower energy.

Exercise

Suppose a ligand has more than one lone pair on the donor atom. The donor atom could share an extra pair of electrons with the metal, to form a double bond. This type of interaction is called pi-donation, because a bond is formed (not to be confused with sigma donation from a bond, as in alkene binding). Show an example using titanium isopropoxide .

Answer

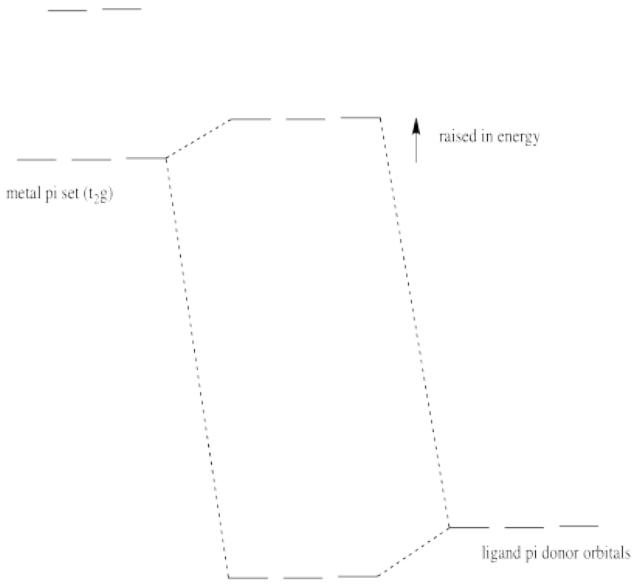


Exercise

In an octahedral environment, three of the d orbitals were not affected by sigma donation from the ligands. Show what happens to the energy level of these d orbitals in the presence of a donor.

Answer

Pi donation raises the electrons (the d electrons of proper symmetry for pi overlap with the ligands in an octahedral geometry).



Exercise

Some ligands can accept a pair of electrons from the metal. An example is a carbonyl complex, which has a C=O antibonding orbital that can interact with a d orbital.

a. Show the antibonding orbital on the carbonyl (CO) ligand.
b. Show how a metal d orbital can interact with this orbital.

Exercise

In the previous problem, a lower-energy atomic orbital on the metal interacts with a higher-energy antibonding orbital on the ligand. Show what happens to the energies of these two orbitals when they interact with each other.

Some of the trends we see in the spectrochemical series arise from pi-donating and pi-accepting effects in the ligand. Ligands that have additional lone pairs (other than the one that sigma donates) are π donors. π donors raise the otherwise non-bonding t_{2g} orbitals, because the lone pair on the ligand forms a π bond with the metal. The t_{2g} orbitals and the ligand lone pair orbitals form two new orbitals. The antibonding orbital is closer in energy to the high-energy d orbitals. The bonding orbital is closer in energy to the low-energy ligand orbital.

- π donation raises the t_{2g} set of d orbitals in energy.
- As a result, the d orbital splitting gets smaller.
- Also as a result, a complex with π donation is a little less stable than a complex without π donation.

This type of interaction can be seen in the following pictures (a tetrahedral case).

On the other hand, ligands in which the donor atom is already π bonding to another atom can accept π donation from the metal. This happens by donating an electron pair from a metal t_{2g} orbital into a $\pi*$ orbital on the ligand. In this case, because the $\pi*$ is an antibonding orbital, it is higher in energy than the metal d orbital (or the t_{2g} orbital). The resulting bonding orbital is more like the lower energy metal orbital, whereas the resulting antibonding orbital is more like the higher energy $\pi*$ orbital on the ligand.

- π accepting ligands lower the t_{2g} set of d orbitals in energy.
- As a result, the d orbital splitting gets larger.
- Also as a result, a complex with a π accepting ligand is a little more stable than a complex without a π accepting ligand.

This type of interaction can be seen in the following case (a tetrahedral complex).

The spectrochemical series gets its name because of a shift in a band of the UV-Vis spectrum when two similar complexes are compared that have two different ligands. The effect of the ligand on the d orbital splitting has an effect on the wavelength of light associated with a d orbital (filled) to d orbital (empty) electronic transition. This transition is actually not associated with

a major absorption. However, because it often occurs in the region of visible light, it is associated with colored transition metal complexes.

Exercise

Explain what happens to the wavelength of light absorbed for the d-d transition when a chloride ligand on a metal complex is replaced with a hydroxide ligand.

Answer

Because chloride is a weaker ligand than hydroxide, the d orbital splitting gets smaller. A d-d transition would involve less energy, so it would move to longer wavelength (red shift).

Exercise

Predict whether each compound will be square planar or tetrahedral.

a. $[Zn(NH_3)_4]^{2+}$

b. $[NiCl_4]^{2+}$

c. $[Ni(CN)_4]^{2-}$

d. $[Ir(CO)(OH)(PCy_3)_2]^{2+}$; Cy = cyclohexyl

e. $[Ag(dppb)_2]^{+}$; dppb = 1,4-bis(diphenylphosphino)butane

f. $PtCl_2(NH_3)_2$

g. $PdCl_2(NH_3)_2$

h. $[CoCl_4]^{2-}$

i. $Rh(PPh_3)_3Cl$

Answer a)

$[Zn(NH_3)4]^{2+}$ 3d metal, d^{10}, sigma donor ligand → tetrahedral

Answer b)

$[NiCl_4]^{2+}$ 3d metal, d^8, pi donor ligand → tetrahedral

Answer c)

$[Ni(CN)_4]^{2-}$ 3d metal, d^8, pi acceptor ligand → square planar

Answer d)

$[Ir(CO)(OH)(PCy_3)_2]^{2+}$ 5d metal, d^8 → square planar

Answer e)

$[Ag(dppb)_2]^{1+}$ 4d metal, d^{10}, sigma donor ligand → tetrahedral

Answer f)

$[PtCl_2(NH_3)_2]$ 5d metal, d^8 → square planar

Answer g)

$[PdCl_2(NH_3)_2]$ 4d metal, d^8, M^{+2}, sigma donor ligand → square planar

Answer h)

$[CoCl_4]^{2-}$ 3d metal, d^7, sigma donor ligand → tetrahedral

Answer i)

$[Rh(PPh_3)_3Cl]$ 5d metal, d^8 → square planar

Contributors

- Chris P Schaller, Ph.D., (College of Saint Benedict / Saint John's University)

This page titled 7.5: The Effect of Ligands and the Spectrochemical Series is shared under a license and was authored, remixed, and/or curated by LibreTexts.

8: LFT FOR OTHER GEOMETRIES / SPECTROSCOPIC PROPERTIES

Saint Mary's College: CHEM 342
Bioinorganic Chemistry
Spring 2020: Dr. Kathryn Haas

Agenda • **Readings** • **Worksheets** • **Essays** • **WiSEWIKI**

8.1: The d-orbital splitting patterns for non-octahedral complexes

8.1.1: Tetrahedral and Octahedral Geometries

8.1.2: The Jahn-Teller Effect

8.1.3: Summary of the three most common geometries

8.2: Absorption Spectra and Magnetic Properties

8.2.1: Colors of Coordination Compounds (Electronic Absorption Spectra)

8.2.2: Predicting UV-visible Absorption

This page titled 8: LFT for Other Geometries / Spectroscopic Properties is shared under a license and was authored, remixed, and/or curated by LibreTexts.

8.1: THE D-ORBITAL SPLITTING PATTERNS FOR NON-OCTAHEDRAL COMPLEXES

8.1.1: Tetrahedral and Octahedral Geometries

8.1.2: The Jahn-Teller Effect

8.1.3: Summary of the three most common geometries

This page titled 8.1: The d-orbital splitting patterns for non-octahedral complexes is shared under a license and was authored, remixed, and/or curated by LibreTexts.

8.1.1: Tetrahedral and Octahedral Geometries

Saint Mary's College: CHEM 342
Bioinorganic Chemistry
Spring 2020: Dr. Kathryn Haas

Until this point, we have focused on one of the most common cases for metal complexes, the 6-coordinate octahedral ligand field geometry. Now, we will examine other geometries, with a focus on 4-coordinate ligand fields. Almost everything you have already learned about octahedrons can be applied to 4-coordinate metal complexes (effects of metal and ligands on Δ); the main difference is the splitting pattern of d-orbitals is different in each 4-coordinate complex than it was in the octahedral cases. Also, the magnitudes of splitting are different in important ways.

Since CFT is simpler than LFT, let's use CFT to describe and derive these "new-to-you" splitting patterns. Now is a good time to go back and recall how CFT was used to derive the splitting of d-orbitals in an octahedral field so that you can use that as a launching pad for deriving the tetrahedron (harder) and square planar geometries:

Exercise 8.1.1.1

The d orbital splitting diagram for a tetrahedral coordination environment is shown below. Given this diagram, and the axes in the accompanying picture, identify which d orbitals are found at which level. In the picture, the metal atom is at the center of the cube, and the circle represent the ligands.

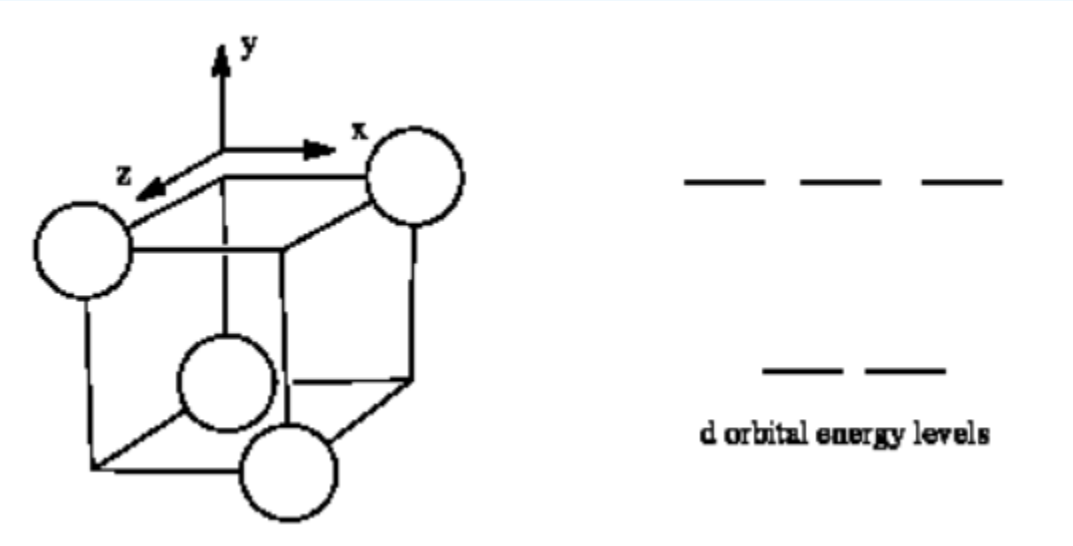


Figure 8.1.1.1:

Answer available at the end of this section.

Exercise 8.1.1.2

Typically, the d orbital splitting energy in the tetrahedral case is only about 4/9 as large as the splitting energy in the analogous octahedral case. Explain why it is smaller for the tetrahedral case.

Answer available at the end of this section.

Exercise 8.1.1.3

Suppose each of the ions below were in tetrahedral coordination environments. Draw the d orbital diagrams for the high-spin and the low-spin case for each ion. Which one (high-spin or low-spin) is more likely?

a) Mn^{2+} b) Co^{2+} c) Ni^{2+} d) Cu^{+} e) Fe^{3+} f) Cr^{2+} g) Zn^{2+}

Answer a) available at the end of this section.

Exercise 8.1.1.4

Usually, tetrahedral ions are high spin rather than low spin. Explain why.

Answer available at the end of this section.

Exercise 8.1.1.5

The d orbital splitting diagram for a square planar environment is shown below. Given this diagram, and the axes in the accompanying picture, identify which d orbitals are found at which level.

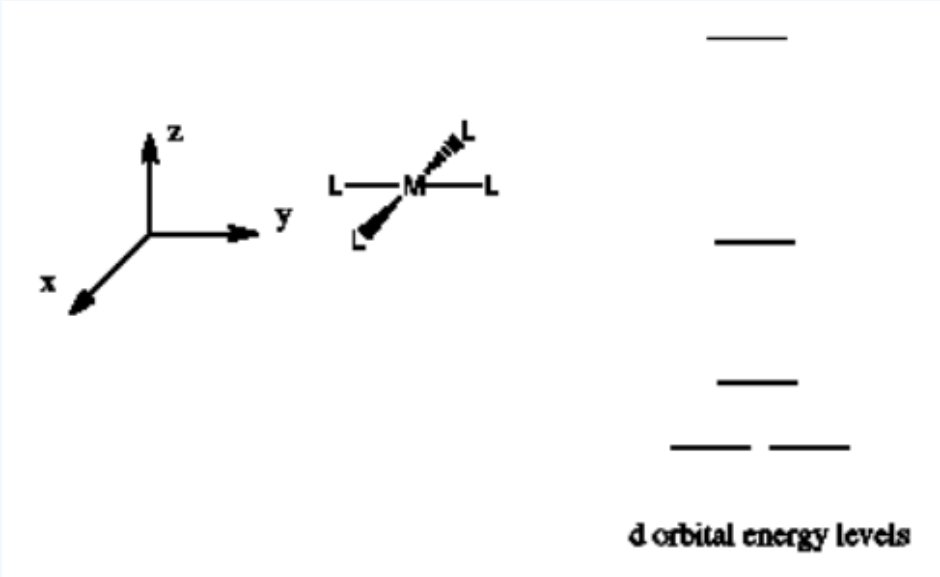


Figure 8.1.1.18:

Answer available at the end of this section.

Exercise 8.1.1.6

Predict whether each compound will be square planar or tetrahedral.

a. $[Zn(NH_3)_4]^{2+}$

b. $[NiCl_4]^{2+}$

c. $[Ni(CN)_4]^{2-}$

d. $[Ir(CO)(OH)(PCy_3)_2]^{2+}$; Cy = cyclohexyl

e. $[Ag(dppb)_2]^{+}$; dppb = 1,4-bis(diphenylphosphino)butane

f. $PtCl_2(NH_3)_2$

g. $PdCl_2(NH_3)_2$

h. $[CoCl_4]^{2-}$

i. $Rh(PPh_3)_3Cl$

Answer a) available at the end of this section.

LFSE and SE for Other Geometries

Just like in the case of octahedral metal complexes, we can apply CFT (or LFT) to calculate LFSE and SE of 4-coordinate (or any-coordinate) metal complexes. Once again, in terms of the d orbital splitting diagram, the results are similar to what we see from molecular orbital theory. For tetrahedral geometry, which is the most common geometry when the coordination number is four, we get a set of two high-lying orbitals and three lower ones.

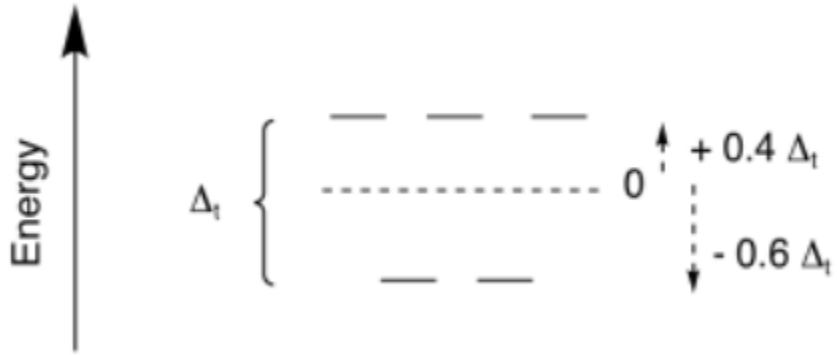


Figure 8.1.1.11:

The overall splitting is expressed as Δ_t; the t stands for tetrahedral. However, sometimes it is useful to compare different geometries. In crystal field theory, it can be shown that the amount of splitting in a tetrahedral field is much smaller than in an octahedral field. In general, $\Delta_t = 4/9\ \Delta_o$.



Figure 8.1.1.12:

Which geometries are most likely?

We wouldn't usually use crystal field theory to decide whether a metal is more likely to adopt a tetrahedral or an octahedral geometry. In most cases, the outcome is more strongly dependent on factors other than the d orbital energies. For example, maybe a complex would be too crowded with six ligands, so it only binds four; it becomes tetrahedral rather than octahedral. Or maybe a metal does not have enough electrons in its valence shell, so it binds a couple more ligands; it becomes octahedral rather than tetrahedral.

However, this comparison between Δ_o and Δ_t does help to explain why tetrahedral complexes are much more likely than octahedral complexes to adopt high-spin configurations. The splitting is smaller in tetrahedral geometry, so pairing energy is more likely to become the deciding factor there than it is in octahedral cases.

Exercise 8.1.1.1

Tetrahedral complexes are pretty common for high-spin d^6 metals, even though the 18-electron rule suggests octahedral complexes should form. In contrast, low-spin d^6 complexes do not usually form tetrahedral complexes. Use calculations of stabilisation energies to explain why.

Answer available at the end of this section.

Crystal field theory has also been used to determine the splitting between the orbitals in a square planar geometry. That is a much more complicated case, because there are four different levels. Once again, the energy levels are often expressed in terms of Δ_o.

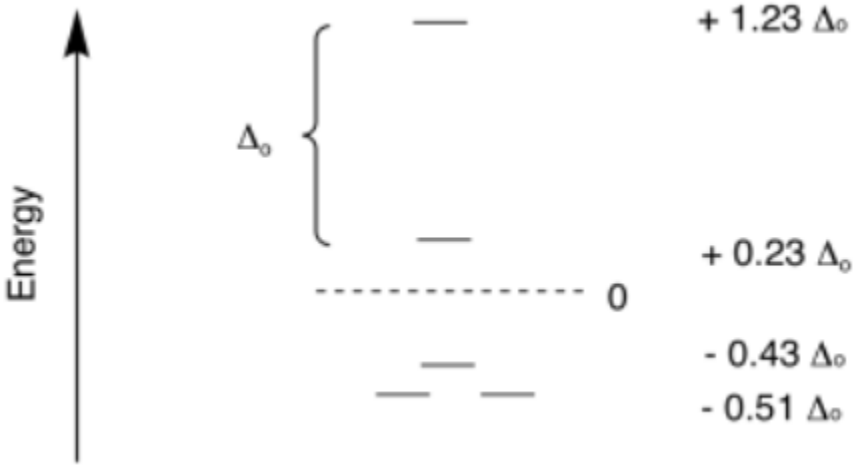


Figure 8.1.1.13:

We could use a calculation of stabilisation energy to predict whether a particular complex is likely to adopt a tetrahedral or a

square planar geometry. Both geometries are possible, so it would be useful to be able to predict which geometry occurs in which case. However, just as in the case of comparing octahedral and tetrahedral gemoetries, there is another factor that is often more important.

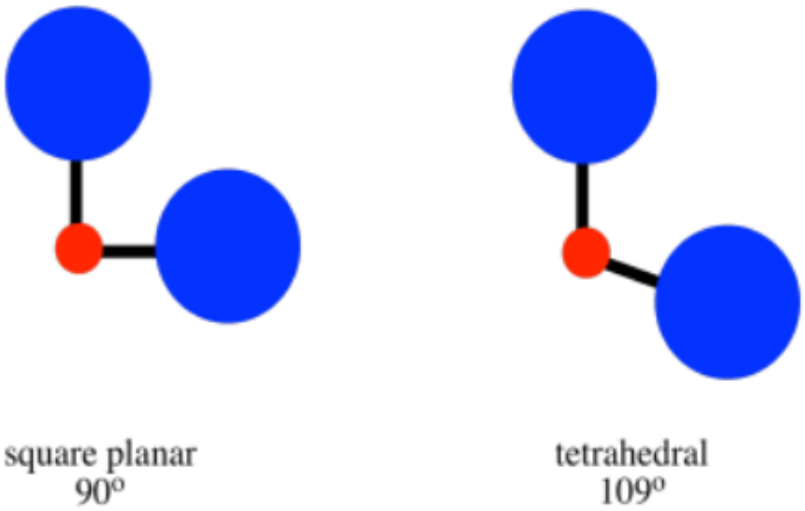


Figure 8.1.1.14:

That factor is steric crowding. In a tetrahedron, all the ligands are 109° from each other. In a square planar geometry, the ligands are only 90° away from each other. Tetrahedral geometry is always less crowded than square planar, so that factor always provides a bias toward tetrahedral geometry. As a result, we might expect square planar geometry to occur only when sterics is heavily outweighed by ligand field stabilisation energy.

Exercise 8.1.1.2

The most common examples of square planar complexes have metals that are d^8. Use calculations of the stabilisation energy to explain why if the complex is:

(a) low-spin

(b) high-spin

Answer a) available at the end of this section.

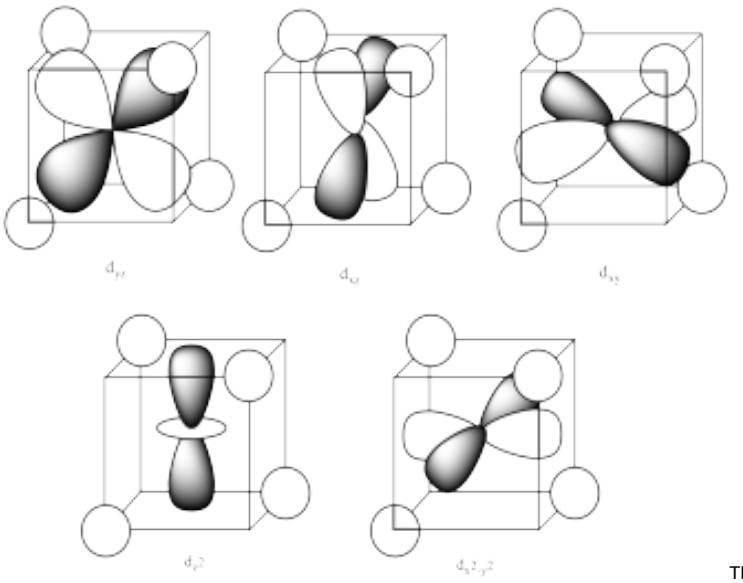
Attribution

Chris P Schaller, Ph.D., (College of Saint Benedict / Saint John's University)

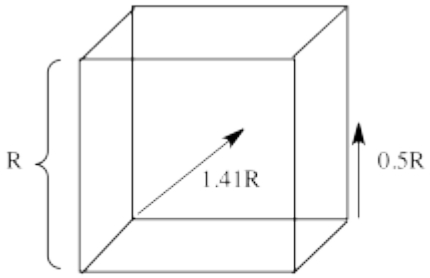
Answers

Exercise 8.1.1.1

The three upper orbitals (dy, dx, dz) interact a little more strongly with the ligands. The two lower orbitals (dz^2 and dx^2-y^2) interact a little more weakly.



The reason for the difference in the interaction has to do with how close the nearest lobe of a d orbital comes to a ligand. There are really two possible positions: the face of a cube or the edge of a cube. If the ligands are at alternating corners of the cube, then the orbitals pointing at the edges are a little closer than those pointing at the faces of the cube.



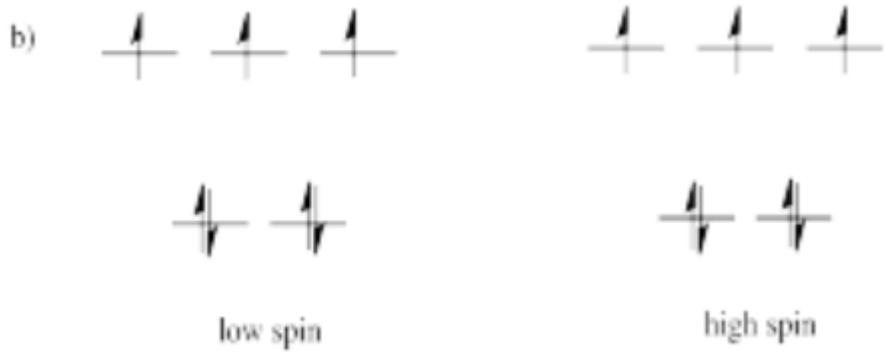
$$\sqrt{R^2 + R^2} = 0.5\sqrt{2R^2} = 0.705R$$

Exercise 8.1.1.2

The ligands do not overlap with the d orbitals as well in tetrahedral complexes as they do in octahedral complexes. Thus, there is a weaker bonding interaction in the tetrahedral case. That means the antibonding orbital involving the d electrons is not raised as high in energy, so the splitting between the two d levels is smaller.

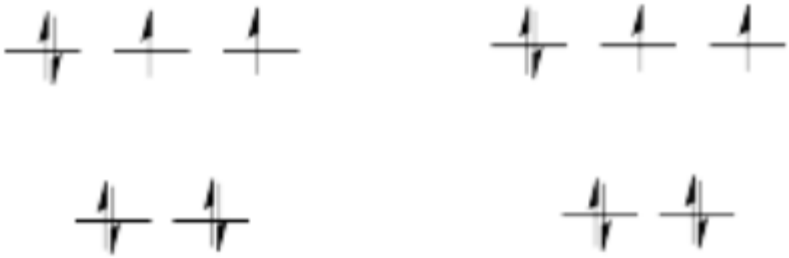
Exercise 8.1.1.3

High spin is more likely for tetrahedral coordination geometry due to weak interactions between ligand orbitals and metal d-orbitals.



High spin is more likely for tetrahedral coordination geometry due to weak interactions between ligand orbitals and metal d-orbitals.

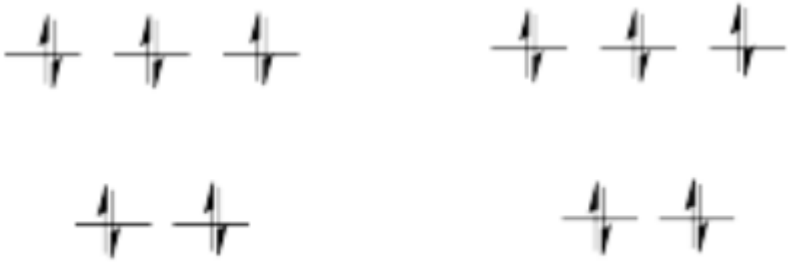
c)



low spin high spin

High spin is more likely for tetrahedral coordination geometry due to weak interactions between ligand orbitals and metal d-orbitals.

d)



low spin high spin

High spin is more likely for tetrahedral coordination geometry due to weak interactions between ligand orbitals and metal d-orbitals.

e)



low spin high spin

High spin is more likely for tetrahedral coordination geometry due to weak interactions between ligand orbitals and metal d-orbitals.

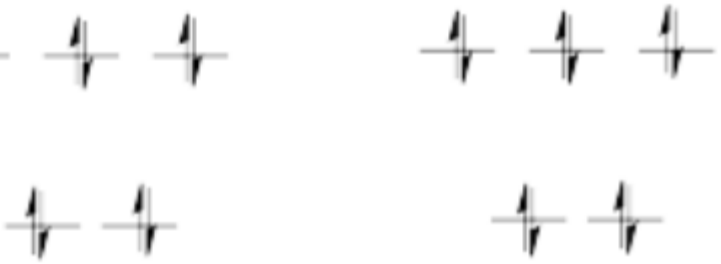
f)



low spin high spin

High spin is more likely for tetrahedral coordination geometry due to weak interactions between ligand orbitals and metal d-orbitals.

g)



low spin high spin

High spin is more likely for tetrahedral coordination geometry due to weak interactions between ligand orbitals and metal d-orbitals.

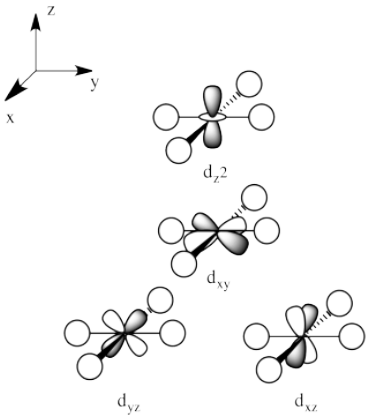
Exercise 8.1.1.4

Because the d orbital splitting is much smaller in the tetrahedral case, it is likely that the energy required to pair two electrons in the same orbital will be greater than the energy required to promote an electron to the next energy level. In most cases, the complex will be high spin.

Exercise 8.1.1.5

The orbitals are shown in order of energy.





Exercise 8.1.1.6

$[Zn(NH_3)4]^{2+}$ 3d metal, d^{10}, sigma donor ligand → tetrahedral

$[NiCl_4]^{2+}$ 3d metal, d^8, pi donor ligand → tetrahedral

$[Ni(CN)_4]^{2-}$ 3d metal, d^8, pi acceptor ligand → square planar

$[Ir(CO)(OH)(PCy_3)_2]^{2+}$ 5d metal, d^8 → square planar

$[Ag(dppb)_2]^{1+}$ 4d metal, d^{10}, sigma donor ligand → tetrahedral

$[PtCl_2(NH_3)_2]$ 5d metal, d^8 → square planar

$[PdCl_2(NH_3)_2]$ 4d metal, d^8, M^{+2}, sigma donor ligand → square planar

$[CoCl_4]^{2-}$ 3d metal, d^7, sigma donor ligand → tetrahedral

$[Rh(PPh_3)_3Cl]$ 5d metal, d^8 → square planar

Exercise 8.1.1.1

high-spin d^6



octahedral

SE = [2(0.6) -4(0.4)]Δ_o + PE

SE = -0.4Δ_o + PE

tetrahedral

SE = [3(0.4) - 3(0.6](4/9)Δ_o + PE

SE = -0.6Δ_o + PE

ΔSE = SE_{oh} - SE_{td} = -0.4Δ_o + PE -(-0.6Δ_o + PE) = +0.2Δ_o

This is a slight preference for tetrahedral.

low-spin d^6



octahedral

SE = [0(0.6) -6(0.4)]Δ_o + 3PE

SE = -2.4Δ_o + 3PE

tetrahedral

SE = [2(0.4) - 4(0.6](4/9)Δ_o + 2PE

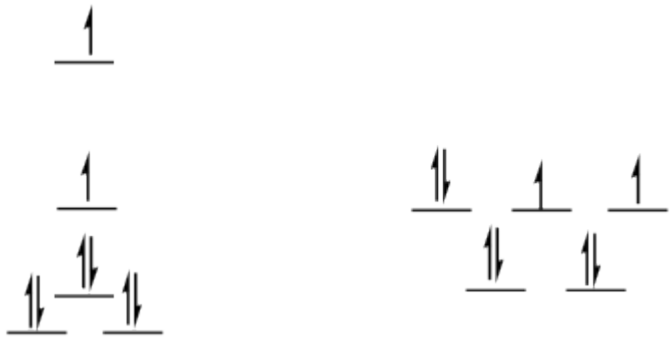
SE = -1.6Δ_o + PE

ΔSE = SE_{oh} - SE_{td} = -2.4Δ_o + 3PE -(-1.6Δ_o + 2PE) = -0.8Δ_o + PE

This is a preference for octahedral, although it would be offset by the pairing energy.

Exercise 8.1.1.2

high-spin d^8



square planar

SE = [1.23 + 0.23 - 2(0.43) -4(0.51)]Δ_o + 3PE

SE = -1.44Δ_o + 3PE

tetrahedral

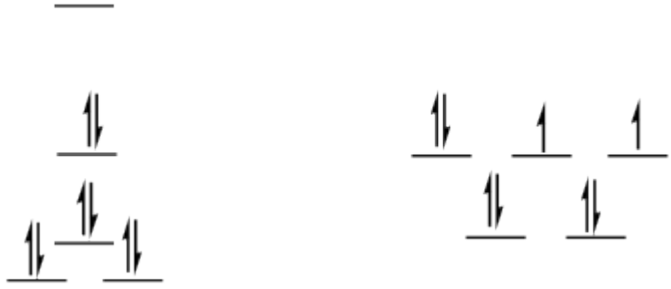
SE = [4(0.4) - 4(0.6](4/9)Δ_o + 3PE

SE = -0.36Δ_o + 3PE

ΔSE = SE_{sq} - SE_{td} = -1.44Δ_o + 3PE -(-0.36Δ_o + 3PE) = -1.08Δ_o

This is an appreciable preference for square planar.

low-spin d^8



square planar

SE = [0 + 2(0.23) - 2(0.43) -4(0.51)]Δ_o + 4PE

SE = -2.44Δ_o + 4PE

tetrahedral = same as before (ls = hs for d^8 tetrahedral)

$\Delta SE = SE_{sq} - SE_{td} = -2.44\Delta_o + 3PE - (-0.36\Delta_o + 3PE) = -2.08\Delta_o + PE$

This is an even more appreciable preference for square planar, although it is offset by pairing energy. Pairing energy would have to be twice as big as Δ_o in order to completely offset the LFSE.

This page titled 8.1.1: Tetrahedral and Octahedral Geometries is shared under a license and was authored, remixed, and/or curated by LibreTexts.

8.1.2: The Jahn-Teller Effect

The Jahn-Teller effect is a geometric distortion of a non-linear molecular system that reduces its symmetry and energy. This distortion is typically observed among octahedral complexes where the two axial bonds can be shorter or longer than those of the equatorial bonds. This effect can also be observed in tetrahedral compounds. This effect is dependent on the electronic state of the system.

Introduction

In 1937, Hermann Jahn and Edward Teller postulated a theorem stating that "stability and degeneracy are not possible simultaneously unless the molecule is a linear one," in regards to its electronic state.[1] This leads to a break in degeneracy which stabilizes the molecule and by consequence, reduces its symmetry. Since 1937, the theorem has been revised which Housecroft and Sharpe have eloquently phrased as "any non-linear molecular system in a degenerate electronic state will be unstable and will undergo distortion to form a system of lower symmetry and lower energy, thereby removing the degeneracy."[2] This is most commonly observed with transition metal octahedral complexes, however, it can be observed in tetrahedral compounds as well.

For a given octahedral complex, the five d atomic orbitals are split into two degenerate sets when constructing a molecular orbital diagram. These are represented by the sets' symmetry labels: t_{2g} (d_{xz}, d_{yz}, d_{xy}) and e_g (d_{z^2} and $d_{x^2-y^2}$). When a molecule possesses a degenerate electronic ground state, it will distort to remove the degeneracy and form a lower energy (and by consequence, lower symmetry) system. The octahedral complex will either elongate or compress the z ligand bonds as shown in Figure $8.1.2.1$ below:

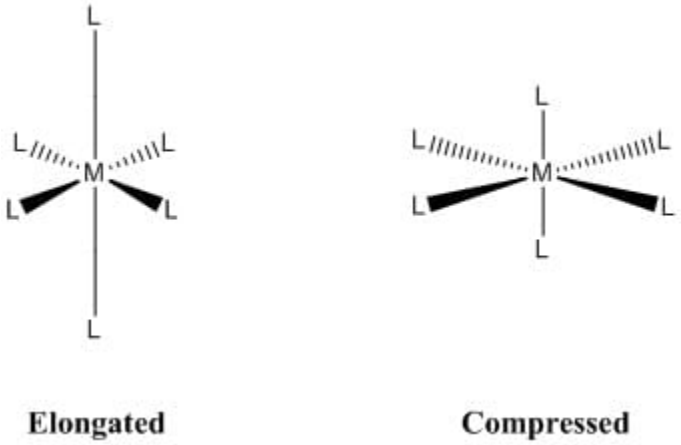


Figure $8.1.2.1$: Jahn-Teller distortions for an octahedral complex.

When an octahedral complex exhibits elongation, the axial bonds are longer than the equatorial bonds. For a compression, it is the reverse; the equatorial bonds are longer than the axial bonds. Elongation and compression effects are dictated by the amount of overlap between the metal and ligand orbitals. Thus, this distortion varies greatly depending on the type of metal and ligands. In general, the stronger the metal-ligand orbital interactions are, the greater the chance for a Jahn-Teller effect to be observed.

Elongation

Elongation Jahn-Teller distortions occur when the degeneracy is broken by the stabilization (lowering in energy) of the d orbitals with a *z* component, while the orbitals without a *z* component are destabilized (higher in energy) as shown in Figure $8.1.2.2$ below:

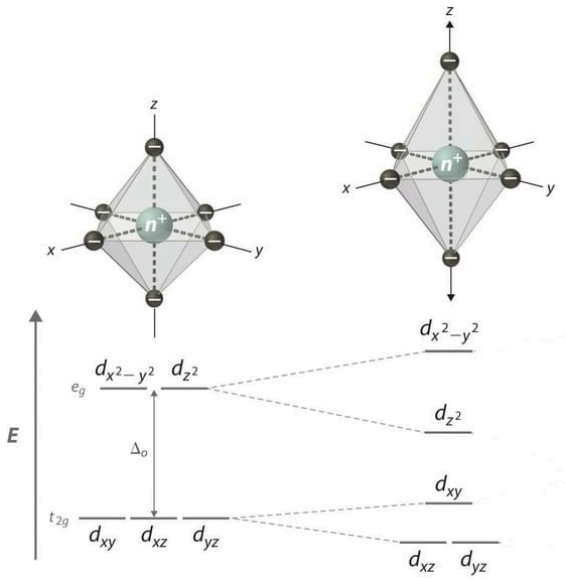


Figure 8.1.2.2: Illustration of tetragonal distortion (elongation) for an octahedral complex.

This is due to the d_{xy} and $d_{x^2-y^2}$ orbitals having greater overlap with the ligand orbitals, resulting in the orbitals being higher in energy. Since the $d_{x^2-y^2}$ orbital is antibonding, it is expected to increase in energy due to elongation. The d_{xy} orbital is still nonbonding, but is destabilized due to the interactions. Jahn-Teller elongations are well-documented for copper(II) octahedral compounds. A classic example is that of copper(II) fluoride as shown in Figure 8.1.2.3.

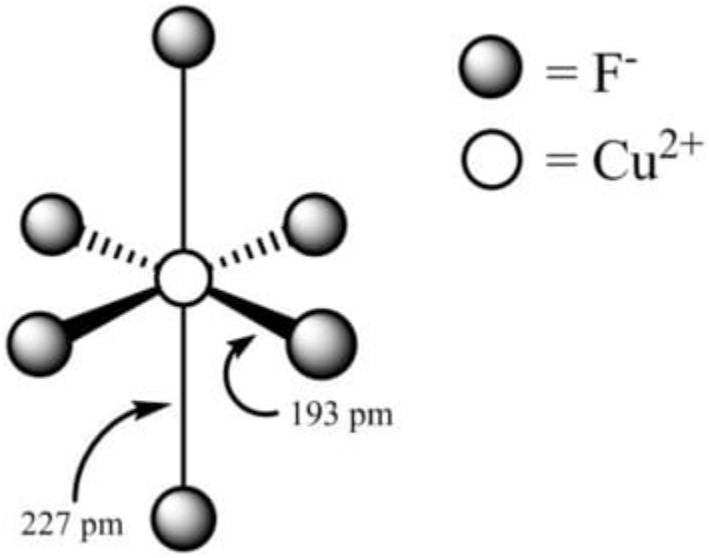


Figure 8.1.2.3: Structure of octahedral copper(II) fluoride.[3]

Notice that the two axial bonds are both elongated and the four shorter equatorial bonds are the same length as each other. According the theorem, the orbital degeneracy is eliminated by distortion, making the molecule more stable based on the model presented in Figure 8.1.2.2.

Compression

Compression Jahn-Teller distortions occur when the degeneracy is broken by the stabilization (lowering in energy) of the d orbitals *without* a *z* component, while the orbitals with a *z* component are destabilized (higher in energy) as shown in Figure 8.1.2.4 below:

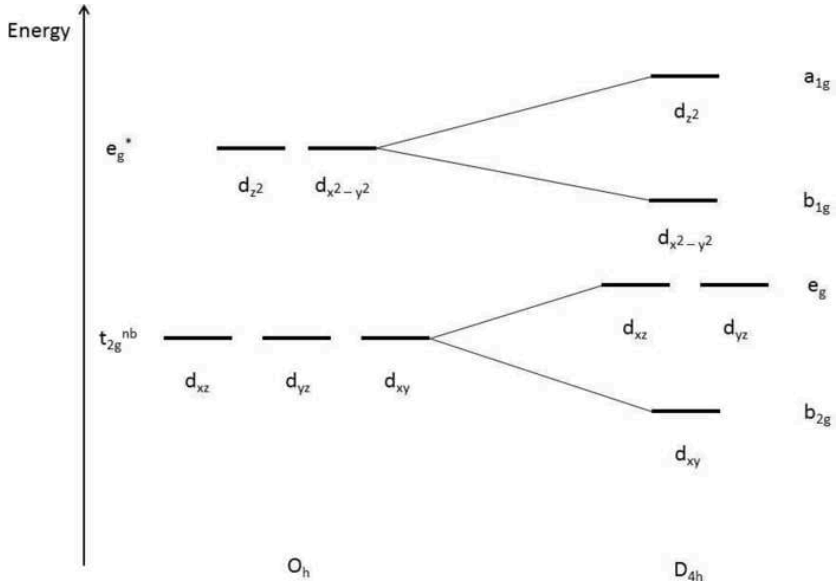


Figure 8.1.2.4: Illustration of tetragonal distortion (compression) for an octahedral complex.

This is due to the *z*-component d orbitals having greater overlap with the ligand orbitals, resulting in the orbitals being higher in energy. Since the d_{z^2} orbital is antibonding, it is expected to increase in energy due to compression. The d_{xz} and d_{yz} orbitals are still nonbonding, but are destabilized due to the interactions.

Electronic Configurations

For Jahn-Teller effects to occur in transition metals there must be degeneracy in either the t_{2g} or e_g orbitals. The electronic states of octahedral complexes depend on the number of d-electrons and the splitting energy, Δ. When Δ is large and is greater than the energy required to pair electrons, electrons pair in t_{2g} before occupying e_g. On the other hand, when $Delta$ small and is less than the pairing energy, electrons will occupy e_g before pairing in t_{2g}. The Δ of an octahedral complex is dictated by the chemical environment (ligand identity), and the identity and charge of the metal ion. If there electron configurations for any d-electron count is different depending on Δ, the configuration with more paired electrons is called low spin while the one with more unpaired electrons is called high spin.

The electron configurations diagrams for d1 through d10 with large and small δ are illustrated in the figures below. Notice that the electron configurations for d^1, d^2, d^3, d^8, d^9, and d^{10} are the same no matter what the magnitude of Δ. Low spin and high spin configurations exist only for the electron counts d^4, d^5, d^6, and d^7.

Large Δ

Figure 8.1.2.5 (below) shows the various electronic configurations for octahedral complexes with large Δ, including the low-spin configurations of d^4, d^5, d^6, and d^7:

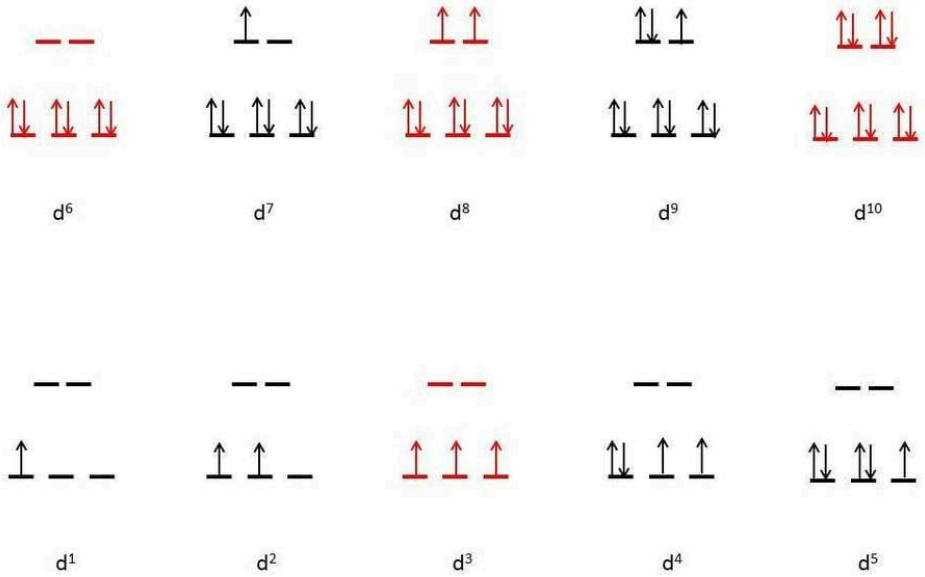


Figure 8.1.2.5: Electron configuration diagram of octahedral complexes (red indicates no degeneracies possible, thus no Jahn-Teller effects).

The figure illustrates the electron configurations in the case of large Δ. The electron configurations highlighted in red (d^3, low spin d^6, d^8, and d^{10}) **do not** exhibit Jahn-Teller distortions. On the other hand d^1, d^2, low spin d^4, low spin d^5, low spin d^7, and d^9, would be expected to exhibit Jhan-Teller distortion. These electronic configurations correspond to a variety of transition metals. Some common examples include Cr^{3+}, Co^{3+}, and Ni^{2+}.

Small Δ

Figure 8.1.2.6 (below) shows the various electronic configurations for octahedral complexes with small Δ, including the high-spin configurations of d^4, d^5, d^6, and d^7::

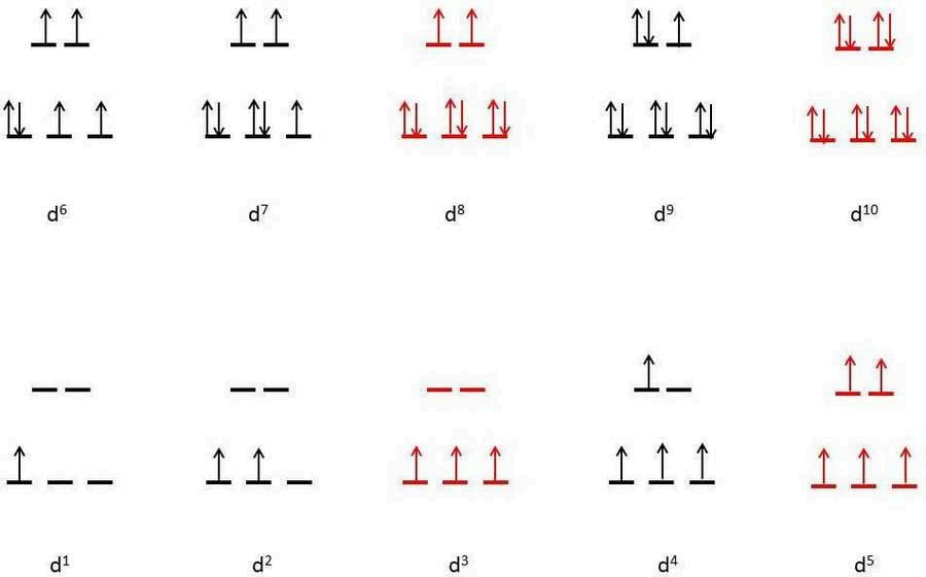


Figure 8.1.2.6: High spin octahedral coordination diagram (red indicates no degeneracies possible, thus no Jahn-Teller effects).

The figure illustrates the electron configurations in the case of small Δ. The electron configurations highlighted in red (d^3, high spin d^5, d^8, and d^{10}) **do not** exhibit Jahn-Teller distortions. In general, degenerate electronic states occupying the e_g orbital set tend to show stronger Jahn-Teller effects. This is primarily caused by the occupation of these high energy orbitals. Since the system is more stable with a lower energy configuration, the degeneracy of the e_g set is broken, the symmetry is reduced, and

occupations at lower energy orbitals occur.

Spectroscopic Observation

Jahn-Teller distortions can be observed using a variety of spectroscopic techniques. In UV-VIS absorption spectroscopy, distortion causes splitting of bands in the spectrum due to a reduction in symmetry (O_h to D_{4h}). Consider a hypothetical molecule with octahedral symmetry showing a single absorption band. If the molecule were to undergo Jahn-Teller distortion, the number of bands would increase as shown in Figure 8.1.2.7 below:

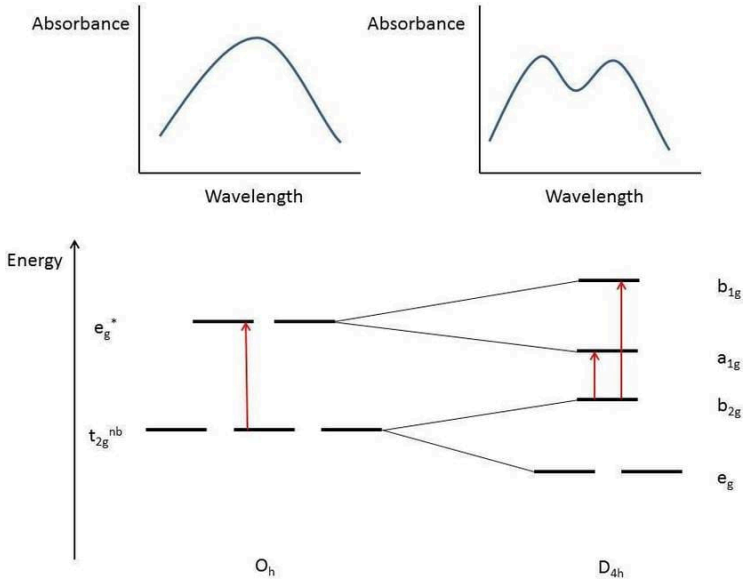


Figure 8.1.2.7: Hypothetical absorption spectra of an octahedral molecule (left) and the same molecule with Jahn-Teller elongation (right). The red arrows indicate electronic transitions.

A similar phenomenon can be seen with IR and Raman vibrational spectroscopy. The number of vibrational modes for a molecule can be calculated using the 3n - 6 rule (or 3n - 5 for linear geometry) rule. If a molecule exhibits an O_h symmetry point group, it will have fewer bands than that of a Jahn-Teller distorted molecule with D_{4h} symmetry. Thus, one could observe Jahn-Teller effects through either IR or Raman techniques. This effect can also be observed in EPR experiments as long as there is at least one unpaired electron.

Table 8.1.2.1: Examples of Jahn-Teller distorted complexes

$CuBr_2$	4 Br at 240 pm 2 Br at 318 pm
$CuCl_2$	4 Cl at 230 pm 2 Cl at 295 pm
$CuCl_2.2H_2O$	2 O at 193 pm 2 Cl at 228 pm 2 Cl at 295 pm
$CsCuCl_3$	4 Cl at 230 pm 2 Cl at 265 pm
CuF_2	4 F at 193 pm 2 F at 227 pm
$CuSO_4.4NH_3.H_2O$	4 N at 205 pm 1 O at 259 pm 1 O at 337 pm
K_2CuF_4	4 F at 191 pm 2 F at 237 pm
$KCuAlF_6$	2 F at 188 pm 4 F at 220 pm
CrF_2	4 F at 200 pm 2 F at 243 pm
$KCrF_3$	4 F at 214 pm 2 F at 200 pm
MnF_3	2 F at 209 pm 2 F at 191 pm 2 F at 179 pm

The Jahn-Teller Theorem predicts that distortions should occur for *any degenerate state*, including degeneracy of the t_{2g} level,

however distortions in bond lengths are much more distinctive when the degenerate electrons are in the e_g level.

References

1. Jahn, H. A.; Teller, E. *Proc. R. Soc. London A*, **1937**, *161*, 220-235. DOI: 10.1098/rspa.1937.0142
2. Housecroft, C.; Sharpe, A. G. *Inorganic Chemistry*. Prentice Hall, 3rd Ed., 2008, p. 644. ISBN: 978-0-13-175553-6
3. Billy, C.; Haendler, H. A. *J. Am. Chem. Soc.*, **1957**, *79*, 1049–1051. DOI: 10.1021/ja01562a011

References

- Janes, R.; Moore, E. A. *Metal-ligand bonding*. The Open University, 2004, p. 23. ISBN 0-85404-979-7
- P.T.Miller, P.G.Lenhert and M.D.Joesten, *Inorg. Chem.*, 11, 2221, 1972.
- J.S.Wood, C.P.Keijzers and R.O.Day, *Acta Crystallogr., Sect.C (Cr. Str. Comm.)*, 40, 404, 1984.
- M.D.Joesten, M.S.Hussain and P.G.Lenhert, *Inorg. Chem.*, 9, 151, 1970.

Practice Questions

1. Why do d^3 complexes not show Jahn-Teller distortions?
2. Does the spin system (high spin v. low spin) of a molecule play a role in Jahn-Teller effects?
3. What spectroscopic method would one utilize in order to observe Jahn-Teller distortions in a diamagnetic molecule?
4. What spectroscopic method(s) would one utilize in order to observe Jahn-Teller distortions in a paramagnetic molecule?
5. Why are Jahn-Teller effects most prevalent in inorganic (transition metal) compounds?

Answers

1. Complexes with d^3 electron configurations do not show Jahn-Teller distortions because there is no ground state degeneracy.
2. Yes. Examining the d^5 electron configuration, one finds that the high spin scenario contains all singly occupied d orbitals (no degeneracy). However, the low spin d^5 electron configuration shows degeneracy, which then leads to possible Jahn-Teller effects.
3. UV-VIS absorption spectroscopy is one of the most common techniques for observing these effects. In general, it is independent of magnetism (diamagnetic v. paramagnetic). Thus, one would see the effect in the spectrum of UV-VIS absorption analysis. Note that EPR requires at least one unpaired electron, and therefore not EPR active.
4. Inorganic, specifically transition metal, complexes are most prevalent in showing Jahn-Teller distortions due to the availability of d orbitals. The most common geometry that the Jahn-Teller effect is observed is in octahedral complexes (see **Figures 2, 4, 5** and **6** above) due to the splitting of d orbitals into two degenerate sets. Due to stabilization, the degeneracies are removed, making a lower symmetry and lower energy molecule.
5. In addition to UV-VIS absorption, one can also employ EPR spectroscopy if a molecule possesses and unpaired electron.

Contributors and Attributions

- Kamran Ghiassi (UC Davis)
- Prof. Robert J. Lancashire (The Department of Chemistry, University of the West Indies)

This page titled 8.1.2: The Jahn-Teller Effect is shared under a license and was authored, remixed, and/or curated by LibreTexts.

- Jahn-Teller Distortions is licensed CC BY-NC-SA 4.0.

8.1.3: Summary of the three most common geometries

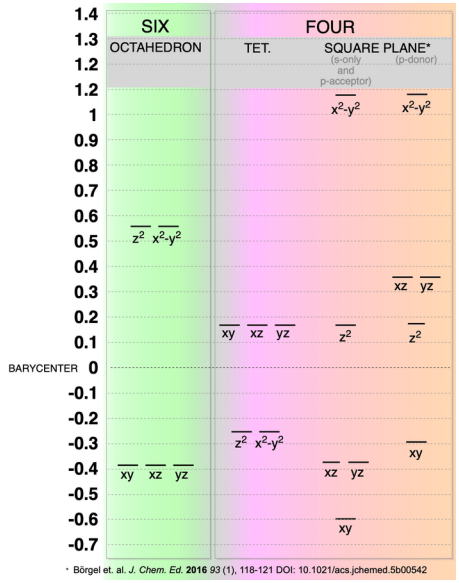
Saint Mary's College: CHEM 342
Bioinorganic Chemistry
Spring 2020: Dr. Kathryn Haas

A brief summary of the factors for predicting geometry

The three most important factors for determining metal complex geometry in biological metal binding sites:

1. Stabilization Energy (including LFSE)
2. Steric interactions between ligands
3. Protein folding or constraints caused by limitations in bond angle (geometric constraints)

Splitting of d-orbitals in the three most-common geometries:



OCTAHEDRAL (most common)

- Is the preferred geometry for most metals because 6 ligands contribute to stabilizing electrophilic metal center.
- Will always have more negative (stable) LFSE than analogous tetrahedral case.
- Is more sterically crowded

Tetrahedral (2nd most common)

- Small Δ means less negative LFSE (less stable in terms of LFSE)
- Always high spin

- Best case in terms of steric crowding around the metal center

Square Plane (d^8 and d^9)

- The bigger the Δ, the more likely it will be square planar due to huge LFSE benefit.
  - Pt and Pd are almost always square planar while Ni is often tetrahedral.
  - In the case of Ni, strong filed ligands favor square plane.
- d^9 metals prefer square plane (or something similar) as a result of Jahn-Teller distortion of octahedral geometry.
- Highest-energy orbital is usually empty in d^8.

Attribution

Curated or created by Kathryn Haas

This page titled 8.1.3: Summary of the three most common geometries is shared under a license and was authored, remixed, and/or curated by LibreTexts.

8.2: ABSORPTION SPECTRA AND MAGNETIC PROPERTIES



CHEM 431: *Inorganic Chemistry*
Fall 2020: Dr. Kathryn Haas

8.2.1: Colors of Coordination Compounds (Electronic Absorption Spectra)
8.2.2: Predicting UV-visible Absorption

This page titled 8.2: Absorption Spectra and Magnetic Properties is shared under a license and was authored, remixed, and/or curated by LibreTexts.

8.2.1: Colors of Coordination Compounds (Electronic Absorption Spectra)

The d-orbital splitting in coordination complexes results in a gap (Δ) that happens to be just the right magnitude to absorb visible light. Because metal complexes can absorb visible light, the display an array of colors. Not only is the color attractive to the eye, it is an indication of the chemical and physical properties of the metal complex. The color (like the magnitude of Δ) depends on the identity of the metal ion, the coordination geometry, and the ligand identity. Chemists don't just "look" at color, though - we measure it using a UV-visible spectrometer.

An example of such a measurement is shown below in Figure $8.2.1.1$ for a Cu(II) complex. The sample appears a pinky-purple color to the eye, and when it is measured using a UV-visible spectrometer, it is shown to absorb visible light at 525 nm. The absorption spectrum can tell us a lot about which ligands are bound to the Cu(II) ion and what the coordination geometry is. This example might be familiar to you if you've had Advanced Lab with Dr. Haas!

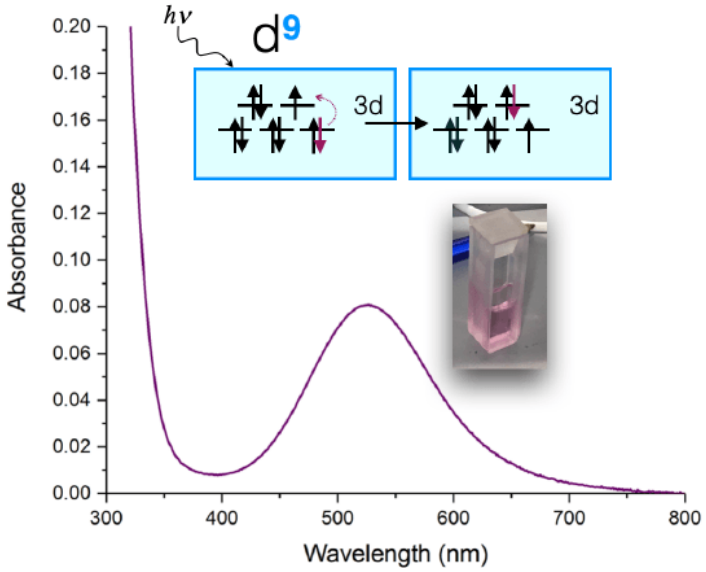


Figure $8.2.1.1$: A UV-visible spectrum of a Cu(II)-peptide complex. A photo of the sample shows its pinky-purple color. The splitting diagram for its approximation as an octahdral complex is shown, where an electronic transition from t_{2g} to e_g is shown. (CC-BY-NC-SA; Kathryn Haas)

In some ways this is a "simple" spectrum because it has only one visible-light d-d transition at 525 nm. Let's assume that the coordination geometry is *approximately* octahedral (although it is actually a Jhan-Teller distorted octahedron, and more like a square plane). If we assume it's octahedral, then the d-orbital splitting diagram might lead us to expect one transition: an electron from the t_{2g} is excited to e_g. We might expect then, that the energy absorbed is equal to the energy of the Δ_o. However, the actual energy of the transition is also effected by electron-electron repulsion energies, and so it is not quite so simple.

If we would want to determine Δ_o from the spectrum shown in Figure $8.2.1.1$, we need to use Tanabe-Sugano diagrams, which

account for electronelectron repulsions, to extract the value of Δ_o. An objective in the next Unit is to learn use Tanabe-Sugano diagrams to extract Δ values and assign the specific electronic transitions that result in UV-vis spectra. But first, let's remind ourselves of where color comes from and learn the basics of how this applies to transition metal complexes.

The Electromagnetic Spectrum

The electromagnetic spectrum (EM) spectrum is made up of photons of different wavelengths. Photons, unique in displaying the properties of both waves and particles, create visible light and colors in a small portion of the EM spectrum. This visible light portion has wavelengths in approximately the 400-700 nanometer range (a nanometer, "nm," is 10^{-9} meters). Each specific wavelength corresponds to a different color (Figure 8.2.1.2), and when all the wavelengths are present, it appears as white light.

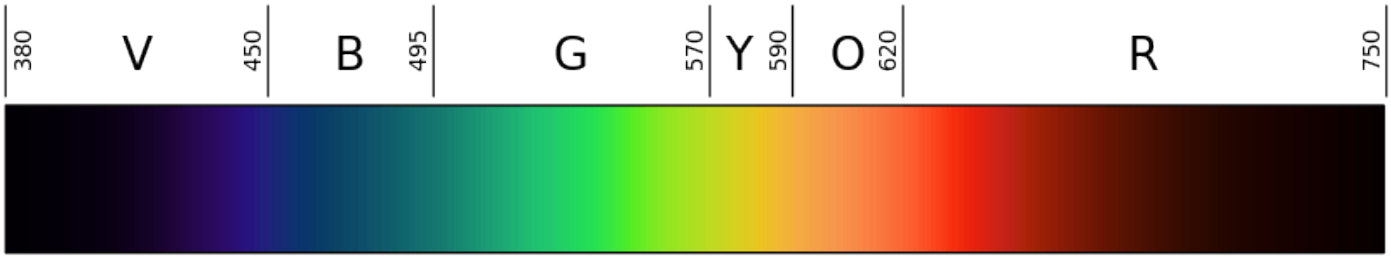


Figure 8.2.1.2: A linear representation of the visible light spectrum. (Public Domain; Gringer via Wikipedia)

The wavelength (λ) and frequency (ν) of a wave are inversely proportional: as one increases, the other decreases; this is a consequence of all light traveling at the same speed.

$$\lambda = \nu^{-1} \tag{8.2.1.1}$$

Because of this relationship, blue light has a shorter wavelength, higher frequency, more energy than red light. In general, photons to the right of the EM spectrum have increasingly higher energy than photons to the left.

Perceiving Color

Color is perceived in two ways, through additive mixing, where different colors are made by combining different colors of light, and through subtractive mixing, where different wavelengths of light are taken out so that the light is no longer pure white. For colors of coordination complexes, subtractive mixing is considered. As shown in Figure 8.2.1.3, the idea behind subtractive mixing is that white light (which is made from all the colors mixed together) interacts with an object. The object absorbs some of the light, and then reflects or transmits (or both, depending on the object) the rest of the light, which contacts the eye. The object is perceived as whichever color is not absorbed. In Figure 8.2.1.2, white light (simplified as blue, green, yellow, orange, and red squiggly arrows) is shone through a solution. The solution absorbs the yellow wavelengths; other wavelengths are transmitted and the appears a pinky-purple color.



Figure 8.2.1.3: Subtractive mixing. (CC-BY-NC-SA; Kathryn Haas)

This phenomenon takes place whenever an object displays visible color. If none of the light is absorbed, and all is reflected back off, the object appears white; if all of the light is absorbed, and there is none left to reflect or transmit through, the object appears black.

Colors of metal complexes (d-d transitions)

In the case of an octahedral metal complex, as certain wavelengths of visible light are absorbed, subtractive color mixing occurs

and the coordination complex solution appears colored. If there is no electronic transition (eg a d^{10} complex), the solutions appear colorless; in reality, they still have a measured energy and absorb certain wavelengths of light, but these wavelengths are not in the visible portion of the EM spectrum and no color is perceived by the eye.

In general, a larger Δ_o indicates that higher energy photons are absorbed, and the solution appears further to the left on the EM spectrum shown in Figure 8.2.1.1. This relationship is described in the equation

$$\Delta_o \approx hc/\lambda \tag{8.2.1.2}$$

where h and c are constants, and λ is the wavelength of light absorbed. The "≈ symbol is used to indicate that this relationship is only approximate. As mentioned earlier, changes in electron-electron repulsion energies must also be accounted for.

Determining color

Using a color wheel can be useful for determining what color a solution will appear based on what wavelengths it absorbs (Figure 8.2.1.4). If a complex absorbs a particular color, it will have the appearance of whatever color is directly opposite it on the wheel. For example, if a complex is known to absorb photons in the orange range, it can be concluded that the solution will look blue. This concept can be used in reverse to determine Δ for a complex from the color of its solution.

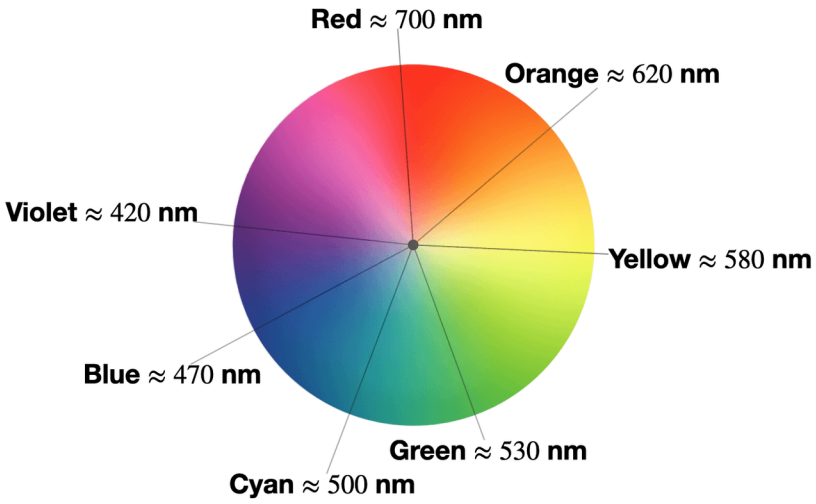


Figure 8.2.1.4: Color wheel with approximate wavelengths of colors. (CC-BY-NC-SA; Kathryn Haas)

Relating the Colors of Coordination Complexes to the Spectrochemical Series

A description of the spectrochemical series is available in a previous section. Weaker-field ligands contribute to smaller Δ values, and thus *absorbance* of lower-energy light with longer λ (ie a "red shift"). Stronger-field ligands do the opposite; they contribute to a larger magnitude of Δ and *absorbance* of higher-energy light with shorter λ (ie a "blue shift").

Example 8.2.1.1

If a solution with a dissolved octahedral complex appears yellow to the eye, approximately what wavelength/color of light does it absorb? If the "borderline" between high and low spin complexes is roughly around 588 nm, is this complex expected to be low spin or high spin?

Solution

A solution that looks yellow absorbs light that is violet, which is roughly 410 nm from the color wheel. This is higher-energy than 588 nm, and so this complex must have a rather large Δ; at least large enough to expect low spin.

Example 8.2.1.2

An octahedral metal complex absorbs light with wavelength 535 nm. What is the crystal field splitting Δ_o for the complex? Approximately what color is it to the eye?

Solution

To solve this question, we need to use the equation $\Delta_o \approx \frac{hc}{\lambda}$

with

- h is Planck's constant and is $6.625 \times 10^{-34} J \cdot s$ and
- c is the speed of light and is $2.998 \times 10^{8}\ m/s$.

It is also important to remember that 1 nm is equal to 1×10^{-9} meters. With all this information, the final equation looks like this:

$$\Delta_o \approx \frac{(6.625 \times 10^{-34}\, J \cdot s)(2.998 \times 10^{8}\, m/s)}{(535nm)\left(\frac{1\, m}{1 \times 10^{9}\, nm}\right)} = 3.712\, J/molecule$$

It is not necessary to use any equations to solve the second part of the problem. Light that is 535 nm is green, and because green light is absorbed, the complex appears redish (light red is pink) (refer to Figures 8.2.1.2 and 8.2.1.4 for this information).

Note: the fact that the complex is octahedral makes no impact when solving this problem. Although the splitting is different for complexes of different structures, the mechanics of solving the problem are identical.

Example 8.2.1.3

There are two solutions, one orange and one blue. Both solutions are known to be made up of a cobalt complex; however, one has chloride ligands, while the other has ammonia ligands. Which solution is expected to be orange?

Solution

In order to solve this problem, it is necessary to know the relative field-strengths of the ligands involved. NH_3 is a stronger-field ligand than Cl^-, which means that the complex involving NH_3 has a greater Δ_o. Because of the larger Δ, the electrons absorb higher-energy light, and the solution will have the appearance of a lower energy (more red) color. Since orange light is less energetic than blue light, the orange solution is the cobalt complex with NH_3 ligands.

References

1. Cox, P. A. Instant Notes Inorganic Chemistry. Second ed. Grand Rapids: Garland, Incorporated, 2004.
2. Nassau, Kurt. The Physics and Chemistry of Color : The Fifteen Causes of Color. Second ed. New York: Wiley-Interscience, 2001.
3. Petrucci, Ralph H., William S. Harwood, and Geoff E. Herring. General Chemistry : Principles and Modern Applications. Ninth ed. Upper Saddle River: Prentice Hall PTR, 2006.
4. Petrucci, Ralph H., Carey Bissonnette, F. Geoffrey Herring, Jeffrey D. Madura. General Chemistry: Principles and Modern Applications. Tenth Ed. Upper Saddle River: Pearson Education, Inc. 2011.

Problems

1. What color will a complex be that absorbs light that is 600 nm be?
2. What color will a complex an octahedral complex appear if it has a Δ_o of $3.75 \times 10^{-19}\ J$?
3. Would you expect a green coordination complex to be high spin or low spin? What about a yellow complex?
4. There are two solutions, one which is yellow and another which is violet. The solutions are $[Co(H_2O)_6]^{3+}$and $[Co(CN^-)_6]^{3-}$. What are the colors of each solution?

Answers

1. Blue. The color absorbed is orange.
2. It is red. Using $\Delta=hc/\lambda$, $h=6.626*10^{-34}J*s$, $c=2.998*10^{8}m/s$, wavelength would equal 530 nm. So green is absorbed, and the complementary color of green is red, so red is the color of the complex.
3. We were told in a previous exercise that the "line" between high and low spin is approximately 580 nm.
   Green Complex: The complementary color of green is red, which has $\lambda \approx 420$ nm. The green solution has a rather small Δ and we could expect it to be high-spin.
   Yellow complex: The complementary color of yellow is violet, absorbed is green, which has $\lambda \approx 700$ nm. The yellow complex has a rather large Δ_o and thus we could expect a low-spin complex.
4. $[Co(H_2O)_6]^{3+}$ is violet and $[Co(CN^-)_6]^{3-}$ is yellow. Looking at the spectrochemical series, H_2O is a weak-field ligand, so it absorbs colors of long wavelengths—in this case, the longer wavelength is yellow, so the color reflected is violet. CN^- is a strong-field ligand, so it absorbs colors of shorter wavelengths-in this case, the shorter wavelength is violet, so the color reflected is yellow.

Contributors and Attributions

- Deyu Wang (UCD)
- Curated or created by Kathryn Haas

This page titled 8.2.1: Colors of Coordination Compounds (Electronic Absorption Spectra) is shared under a license and was authored, remixed, and/or curated by LibreTexts.

8.2.2: Predicting UV-visible Absorption



CHEM 431: *Inorganic Chemistry*
Fall 2020: Dr. Kathryn Haas

A note from Dr. Haas: The Inorganic Spectroscopy Tutorial from the University of Alberta is an excellent resource for brushing up on Inorganic Spectroscopies. Conveniently, it has a tutorial on UV-visible spectroscopy for Inorganic complexes. Please review this tutorial before reading the page below.

Types of transitions related to the metal ion:

1. **d-d transitions**: d-d transitions are electronic transitions that occur between the molecular orbitals (MOs) that are mostly metal in character; specifically the orbitals that we think of as the d-orbitals of a transition metal complex. These transitions are useful in determining the energy of splitting and can be used to indicate coordination chemistry (geometry and ligand sets). In octahedral complexes, d-d transitions occur between the t_{2g} and e_g orbitals (across Δ). These transitions cannot occur in metal complexes where the d-orbital is completely empty (d^0) or completely full (d^{10}). In other words, a d-d transition is only possible in $d^1 - d^9$ metal ions. In a UV-visible absorption spectrum, d-d transitions appear as relatively weak absorption with extinction coefficients (ε) less than 1,000.
2. **Charge transfer (CT) transitions**: Charge transfer transitions occur between MOs that are mostly metal in character and those that are mostly ligand in character. These transitions depend on the type of ligand: they occur only when the metal is bound to ligands that are π-donors or π-acceptors. And there are two types of CT transitions. If the metal is bound to a π-donor ligand, electrons from lower-energy MO's that are mostly ligand in character can become excited to MO's that are mostly metal in character. These are **ligand to metal charge transfers (LMCT) transitions** (Figure $8.2.2.1$, left diagram). If the the metal is bound to ligands that are π-acceptors, electrons from the MO's that are mostly metal in character can become excited to higher-energy orbitals that are mostly ligand in character. These are **metal to ligand charge transfer (MLCT)** transitions (Figure $8.2.2.1$, right diagram). In a UV-visible absorption spectrum, CT transitions appear as relatively intense absorptions with extinction coefficients (ε) much greater than 1,000.

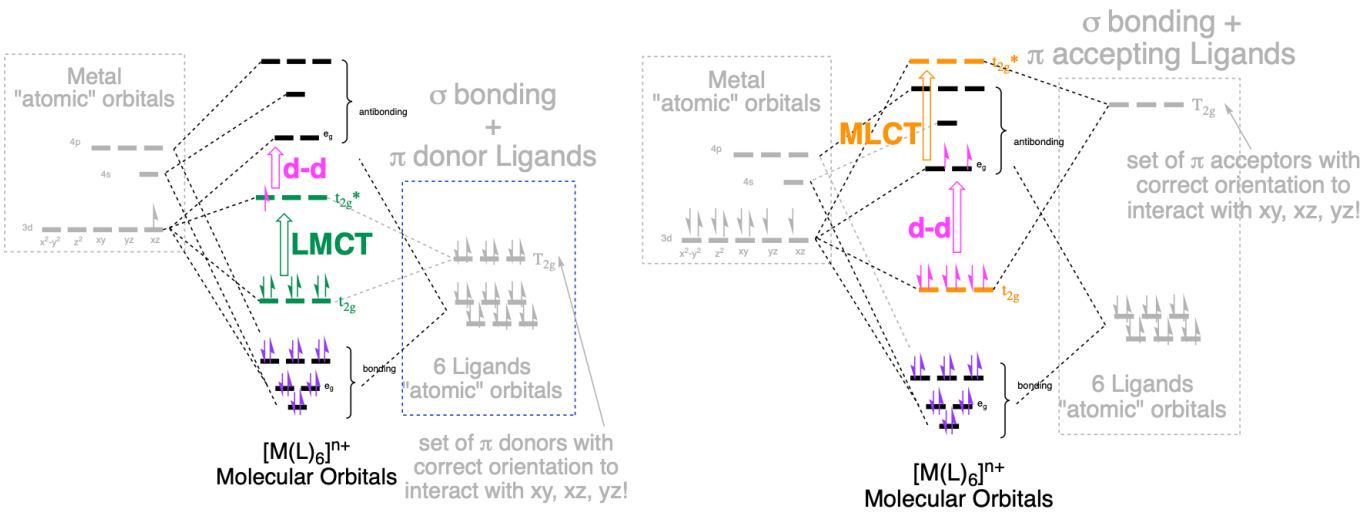


Figure 8.2.2.1: Abbreviated and annotated MO diagrams for example cases of metal ions in octahdral geometry with sets of π -donor and π-acceptor lignads. In both example MO diagrams, d-d transitions are shown (pink, open arrow from t_{2g} to e_g). **Left:** LMCT transitions are possible with π-donor ligands when electrons are excited from MOs that are mostly ligand in character to MOs that are mostly metal in character. An example of LMCT is shown (green, open arrow from t_{2g} to $t*_{2g}$). **Right:** MLCT transitions are possible with π-acceptor ligands when electrons from MOs that are mostly metal in character are excited to orbitals that are mostly ligand in character (the π^* orbitals from ligands). An example MLCT is shown ((orange, open arrow from e_g to $t*_{2g}$).

Attribution

Curated or created by Kathryn Haas

This page titled 8.2.2: Predicting UV-visible Absorption is shared under a license and was authored, remixed, and/or curated by Kathryn Haas.

9: SPECTROSCOPIC AND MAGNETIC PROPERTIES

9.1: Quantum Numbers of Multielectron Atoms

9.2: Electronic Spectra of Coordination Compounds

9.3: Tanabe-Sugano Diagrams

9.4: Magnetic Properties of Coordination Compounds

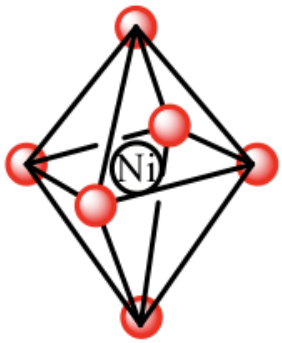
9.5: Magnetic Properties of Materials

This page titled 9: Spectroscopic and Magnetic Properties is shared under a license and was authored, remixed, and/or curated by LibreTexts.

9.1: Quantum Numbers of Multielectron Atoms

Electronic Spectra

Let us take a closer look at optical absorption spectra, also called electronic spectra of coordination compounds. We have previously argued that ligand field theory can predict and explain the electronic spectra. However, only in relatively few cases ligand field theory is sufficient to explain the spectra.



$[Ni(OH_2)_6]^{2+} = d^8$ ion

Figure 9.1.1 hexaaqua nickel (2+) complex

For example the hexaaqua nickel (2+) complex is an octahedral d^8-complex. According to ligand field theory the metal d-orbitals in an octahedral field are the t_{2g} and the e_g–orbitals. Six electrons are in the t_{2g} orbitals, and two electrons are in the e_g orbitals. Ligand field theory would predict that there is one electron transition possible, namely the promotion of an electron from a t_{2g} into an e_g orbital. This process would be triggered by the absorption of light whereby the wavelength of the light would depend on the Δ_o between the t_{2g} and the e_g orbitals. Overall, this should lead to a single absorption band in the absorption spectrum of the complex. We can check this prediction by experimentally recording the absorption spectrum of the complex.

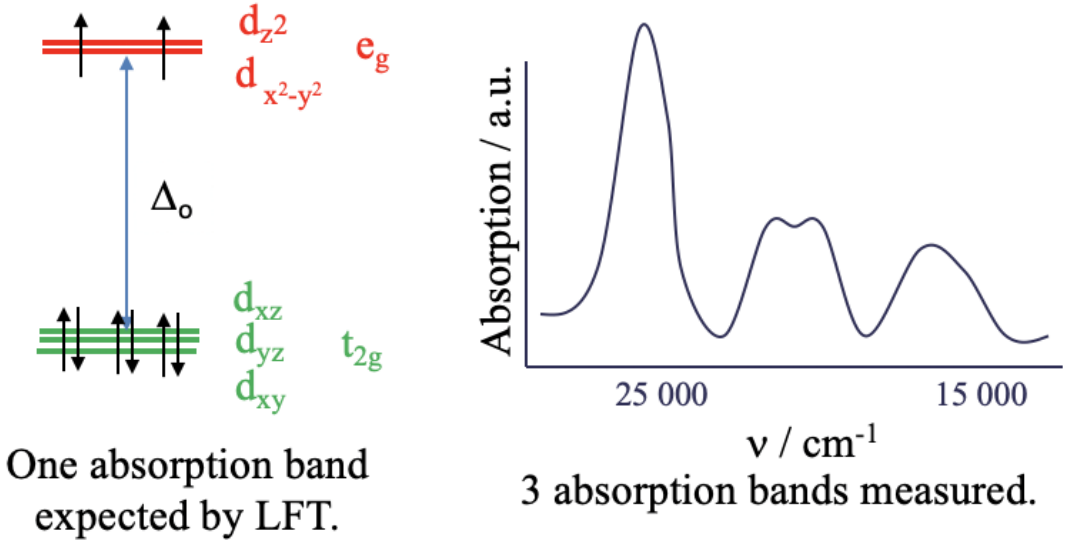


Figure 9.1.2 Absorption spectrum of the hexaaqua nickel (2+) complex expected by LFT vs actual

What we find is that the absorption spectrum is far more complex than expected. Instead of just a single absorption band there

are multiple. Obviously, ligand field theory is unable to explain this spectrum. The question is why? The answer is: LFT assumes that there are no electron-electron interactions. However, in reality there is repulsion between electron in d-orbitals and this has an effect on their energy.

Effect of Electron-Electron Interactions

Let us look closer at this. To simplify the problem let us consider a d^2 ion in an octahedral ligand field first.

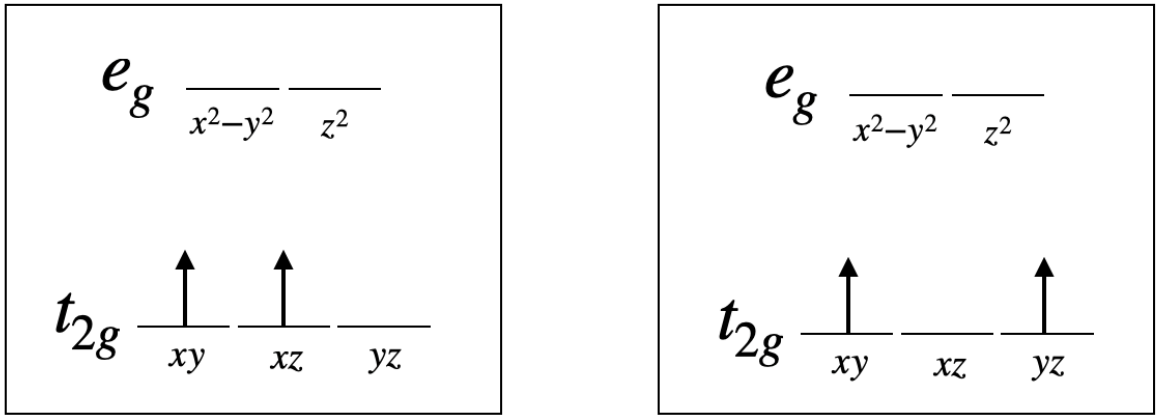


Figure 9.1.3 Two microstates with different energies for d^2 ion in an octahedral ligand field (CC-BY; Kathryn Haas)

According to ligand field theory, the two electrons would be in the t_{2g} orbitals when in the ground state. For instance, they could be in the xy, and the xz orbitals. This is called a microstate. It is called a microstate of a state because there are other combinations of orbitals possible. For example, the ground state would also be realized if the two electrons were in the xz and the yz orbitals. This combination would be another microstate associated with the ground state electron configuration. Upon excitation using light the electron in the d_{xy} orbital could be promoted into an e_g orbital, which could be either the d_{z^2} or the $d_{x^2-y^2}$. Those two possibilities reflect to different microstates associated with the excited state. Let us assume the electron goes into the d_{z^2} orbitals. In this microstate one electron would be in the d_{xz} orbital and the other one in the d_{z^2} orbital. Now there us another possibility how to excite an electron. We could assume that not the d_{xy} electron is promoted into the d_{z^2} orbital, but the d_{xz} electron gets promoted. In this case, we would realize a microstate in which one electron in the d_{xy} orbital and the other one in the d_{z^2} orbital.



Figure 9.1.4 Orbital shapes of the two different microstates

Now let us compare the two cases. Ligand field theory would argue that both excited microstates have the same energy. However,

in fact they do not. Why? That is because the electrons in the two excited microstates interact differently. This becomes plausible when considering the orbital shapes. The d_{xz} orbital has electron density on the z-axis, while the d_{xy} orbital has not. Therefore, electrons in these orbitals would be expected to interact differently with an electron in a d_{z^2} orbital which has most of its electron density on the z-axis. As a result the two excited microstates do not have the same energy. This means that in order to promote the electron into the two different microstates we need different amounts of energies. Thus, the complex would absorb light with more than just one wavelength. This is in contrast to what ligand field theory predicts. What will we need to do in order to predict correctly how many absorption bands we get? The answer is, we must find all possible microstates for the d^2 electron configuration and group those together which have the same energy. A group of microstates with the same energy is called a term. The number of electron transitions can then be predicted from the number of terms.

Russell Saunders Coupling of Electrons in Free Ions

Our task is now to find all the terms for the octahedral complex with d^2 electron configuration. To simplify matters let us first look at a free d^2 ion. This is an ion which is not coordinated by any ligand.

$$m_l = \text{angular momentum of a single electron } (m_l = -l.....l)$$

$$M_L = \Sigma\, m_l$$

$$M_L = \text{total orbital angular momentum (of all electrons)}$$

$$\text{maximum } M_L \text{ value} = L$$

$$L = \text{total angular orbital quantum number}$$

$$\#\text{ of microstates in the term due to angular momentum} = 2L+1$$

Figure 9.1.5 Necessary terms to calculate the number of microstates due to angular momentum

The energy of microstates depends on the magnetic quantum number m_l of the orbitals. This is because the magnetic quantum number of the electrons determines how the electrons interact. This is also called the Russell-Saunders coupling of electrons. Thus, a term is defined by the quantum number m_l of the orbitals. In fact, a term is defined by the microstate with the highest quantum number M_L. Whereby M_L is nothing but the sum of the quantum numbers m_l of the individual electrons. The maximum M_L value is also called the total orbital angular momentum quantum number L. The L value also tells you how many microstates belong to a term due to these magnetic interactions. The number of microstates is 2L+1. This is because M_L can vary between –L and +L. So for instance if L=2, M_L can adopt the values -2, -1, 0, +1, and +2, and that is 2L+1=5 microstates.

The quantum number L alone does not define the term yet. In addition, we must also consider the interaction of the spins of the electrons.

m_s = angular momentum of a single electron

$M_S = \Sigma\, m_s$

maximum M_s value = S

S = total spin angular momentum quantum number

of microstates in the term due to spin = 2S+1

Figure 9.1.6 Necessary terms to calculate the number of microstates due to spin

The spin quantum number m_s of a single electron can be either +1/2 or -1/2. When the spins of electrons interact, their spin quantum numbers add up, defining the total spin Ms. The microstate with the maximum M_s value defines the total spin quantum number S. The number of microstates due to the spin-spin interactions that belong to the term is 2S+1. This is also called the spin multiplicity.

of overall microstates in the term = (2L+1) 2S+1

Figure 9.1.7 Equation for the calculation of overall microstates

Overall the term has (2L+1)(2S+1) microstates. The total orbital angular quantum number L and the total orbital spin quantum number S define the term symbol.

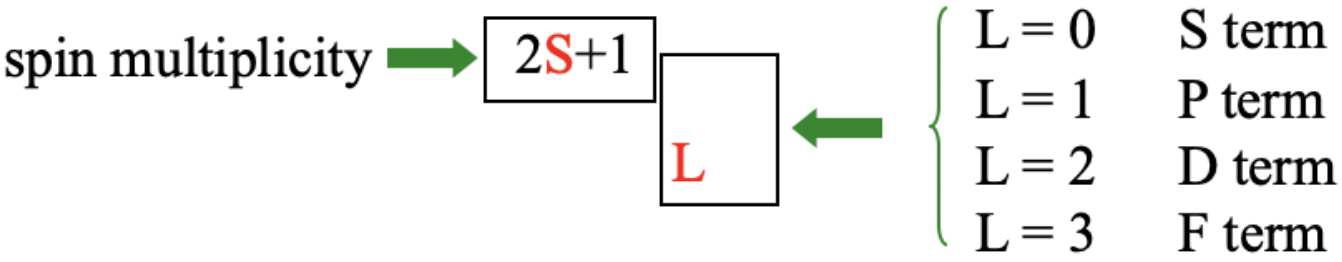


Figure 9.1.8 Determining spin multiplicity

When L=0 we have an S term, when L=1, we have a P term, when L=2, we call it a D term, and when L=3 we call it an F term. These symbols are chosen in analogy to the symbols s, p, d, and f for orbitals. The spin multiplicity 2S+1 is then written as a superscript in front of the letter defined by L. This gives the overall term symbol for a term. We call a term with a spin multiplicity of 1 a singlet term, when 2S+1=2, we call the term a doublet term. A term with a spin multiplicity of three is called a triplet term, one with a spin-multiplicity of 4 a quartet term, and so forth.

Microstates for a free d^2 ion

What are the possible microstates and the overall number of microstates for a free ion with d^2-electron configuration? We can express this in a so-called microstate table.

M_s \ M_L	-4	-3	-2	-1	0	+1	+2	+3	+4
-1	Not possible (Pauli principle)	$-2^{-}\,-1^{-}$	$-2^{-}\,0^{-}$	$-2^{-}\,1^{-}$ $-1^{-}\,0^{-}$	$-2^{-}\,2^{-}$ $-1^{-}\,1^{-}$	$-1^{-}\,2^{-}$ $0^{-}\,1^{-}$	$0^{-}\,2^{-}$	$1^{-}2^{-}$	Not possible (Pauli principle)
0	$-2^{-}\,-2^{+}$	$-2^{-}\,-1^{+}$ $-2^{+}\,-1^{-}$	$-2^{-}\,0^{+}$ $-2^{+}\,0^{-}$ $-1^{-}\,-1^{+}$	$-2^{-}\,1^{+}$ $-2^{+}\,1^{-}$ $-1^{-}\,0^{+}$ $-1^{+}\,0^{-}$	$-2^{-}\,2^{+}$ $-2^{+}\,2^{-}$ $-1^{-}\,1^{+}$ $-1^{+}\,1^{-}$ $0^{-}\,0^{+}$	$-1^{-}\,2^{+}$ $-1^{+}\,2^{-}$ $0^{-}\,1^{+}$ $0^{+}\,1^{-}$	$0^{-}\,2^{+}$ $0^{+}\,2^{-}$ $1^{-}\,1^{+}$	$1^{-}2^{+}$ $1^{+}2^{-}$	$2^{-}\,2^{+}$
+1	Not possible (Pauli principle)	$-2^{+}\,-1^{+}$	$-2^{+}\,0^{+}$	$-2^{+}\,1^{+}$ $-1^{+}\,0^{+}$	$-2^{+}\,2^{+}$ $-1^{+}\,1^{+}$	$-1^{+}\,2^{+}$ $0^{+}\,1^{+}$	$0^{+}\,2^{+}$	$1^{+}2^{+}$	Not possible (Pauli principle)

Figure 9.1.9 d^2 electron configuration microstate table

You can see the microstate table for the d^2 electron configuration depicted above. Each column represents a possible value M_L. For the d^2 configuration, M_L can adopt value from -4 to +4, hence there there are 9 columns. Each row represents possible M_S value. For the d^2 electron configuration, M_S can vary between +1 and -1. +1 means both electrons have the spin +1/2, 0 means one electron has the spin +1/2 and the other one has the spin -1/2. The M_S value of -1/2 is adopted when both electrons have the spin -1/2. Now we can combine each M_S value with each M_L value which defines a particular field in the table. You can see that some field are empty due to the Pauli principle. For example, the field for M_L=-4 and M_S=-1 is not filled because in this case both electrons would have the same quantum numbers, namely m_l=-2, and m_s =-1/2. We can further see that for some fields only one combination of electrons is possible, while for others there are multiple. For example, for the field with M_L=4 and M_S=0 there is only one combination of electron possible. You can see symbol "2-2+" in this field. This means that the first electron has an m_l value of 2 and and a spin of -1/2 and the second electron also has an m_l value of 2 and an m_s value of +1/2. The most populated field is the field for M_L=0 and M_S=0. There are overall five microstates with that combination of M_L and M_S values. If we count the number of microstates in the table then we arrive at the number 45. This consistent with what we could expect according to the formula #microstates = (2L+1)(2S+1). In our example L=4 and S = 1, and thus the number of microstates is ((2x4)+1)((2x1)+1)=45. In general for a d^n electron configuration with n d-electrons the number of microstates is (10!)/((10-n)!n!).

One useful property of a microstate table is that we can derive the terms and term symbols for a particular electron configuration from it. For simplification sake, we indicate a possible microstate in the table just by an "x". Then we draw the largest possible rectangular box into the microstable that contains only fields with at least one possible electron combination.

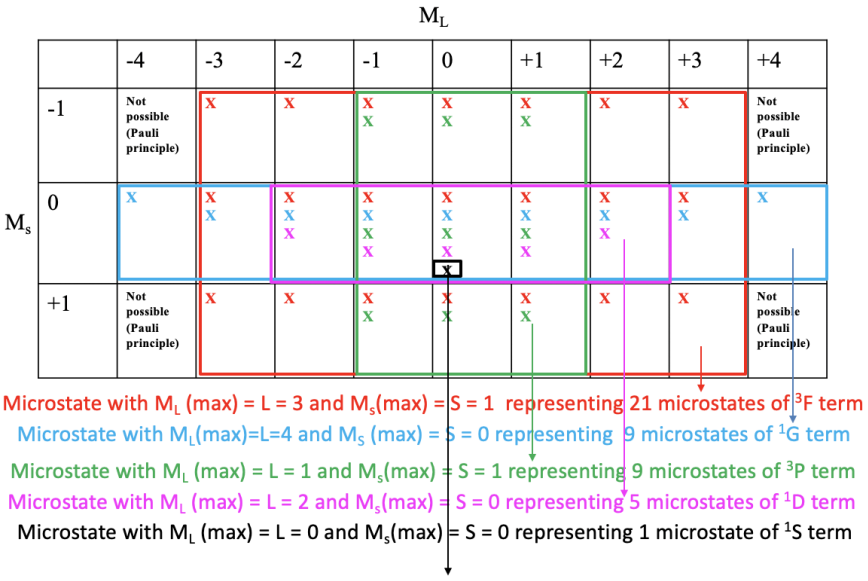


Figure 9.1.10 Deriving the terms and term symbols for a particular electron configuration from the microstate table

You can see that the largest possible box is the red box drawn. This box contains the microstates that belong to the first term of the electron configuration d^2. The number of microstates is equal to the number of fields within the red box. That makes 7x3=21 microstates. What is the term symbol for this term? In order to answer this question we need to find the microstate in the red box that has the highest M_L and the highest M_S value. You can see that it is the one with M_L=3 and M_S = 2. Thus, L=3 and S=1. This defines the term as a ^{3}F term as 2S+1 = 3, and L=3 corresponds to the term symbol F. This term is a triplet term. Note that a triplet term also includes microstates with paired spins. Overall 7 of the 21 microstates have Ms=0.

Next, we look what is the next largest rectangular box we can draw which contain microstates we did not consider yet. We can see that the blue box contains 9 fields equaling 9 microstates. The microstate within this box that has the highest M_L and M_S values is the one with M_L=4 and M_S=0. This defines a ^{1}G term. This is a singlet term. Note that a singlet term ONLY has microstates with paired spins (Ms=0).

There is another rectangular box which also contains 9 microstates. It is the green one. The microstate with the highest M_L and M_S values is the one with M_L=1 and M_S=1. Thus, L =1, and 2S+1=3 which defines a ^{3}P term. Note that despite this being a triplet term the term also contains three microstates with paired spins.

The next largest box is the purple one containing five fields and five microstates. What the there term with the highest M_L and M_S values? It is the one with M_L=2 and M_S=0. This means that L=2 and S=0 which defined a ^{1}D term. This is a singlet term. A singlet term contains only microstates with paired spins. There is one microstate left we did not consider thus far. It is one with M_L=0 and M_S = 0. These are highest M_L and M_S values because there is no other microstate. Thus, this term contains only one microstate and the term symbol is ^{1}S. Now we have found all terms and term symbols.

The Energy of Terms

What is the relative energy of the terms. First we need to consider Hund's rule which states that the higher the spin multiplicity the lower the energy of a term.

Rule 1: The higher spin multiplicity the lowest energy (Hund's rule).

Figure 9.1.11 Hund's Rule

We therefore first need to rank the terms with regards to the spin multiplicity. Secondly, we need to consider the value of the total orbitals angular momentum quantum number L. The higher the value the lower the energy for the term. This means that the energy of terms decreases from S, to P, to D, to F.

Rule 2: When the spin-multiplicity is the same then the energy increases with increasing L value.

Figure 9.1.12 Rule to consider the value of total orbitals angular momentum quantum number L

Note that this is contrary to orbital energies which increase from s, to p, to d, to f. Therefore, what would be the expected energy sequence for the terms associated with a d^2 free ion? It should be: $^3F<^3P<^1D<^1S$. However, the actual energy sequence is $^3F<^1D<^3P<^1G<^1S$. This, means that unexpected the ^1D is energetically lower than the ^3P term. Here we see that Hund's rule is a called a rule and not a law because there are exceptions. In most, but not all cases a triplet term has a lower energy than a singlet term, but there are exceptions.

Free-Ion Terms of Other D Electron Configurations

What are the term of the other d-electron configurations.

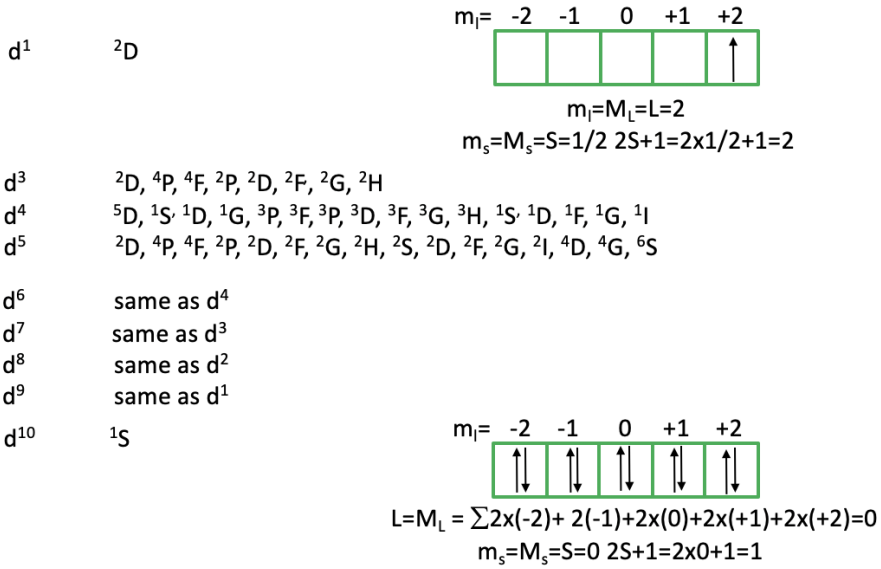


Figure 9.1.13 Terms for the other d-electron configurations

You can see above that there is only a single ^2D term for a d^1 ion. How can we explain this term? Because there is no other electron, there are no electron-electron interactions, and thus every possible microstate has the same energy. This explains why there is only one term. Why is it ^2D? Well, the term symbol is determined by the microstate with the highest M_L value and the highest M_S value. This is achieved when we fill the electron spin-up into the d-orbital with $m_l=2$. Because there is only one electron, $m_l=M_L=L=2$. This makes the term a D term. It is a doublet term because M_S is maximized when the electron is spin-up or $m_S=+1/2$. Thus, $m_S=M_S=S=1/2$. $2S+1=2x1/2+1=2$, thus we have a doublet state. How many microstates are associated with this term? $(2L+1)(2S+1)=5x2=10$. What does that mean? This means that we can fill the one electron that we have either spin-up or spin down in any of the five d-orbitals. All the 10 microstates are energetically equal.

When do go from d^2 to d^3 to d^4 to d^5 you can see that the number of the terms increases dramatically. This is because with increasing electron numbers the number of possible permutations increases, and thus the number of possible microstates. As a consequence, there are more terms. From d^6 to d^{10} the number of terms decreases again. The terms for d^6 are the same as the terms for d^4, the d^7-terms are identical to those for d^3, the d^8-terms are the same as the d^2 and the d^9-terms are the same as terms for the electron configuration d^1. Why is that? This is because unoccupied slots in orbitals permute the same way as occupied ones do. For instance, in the d^3 electro configuration has three occupied slots and seven unoccupied ones, while the d^7 electron configuration has seven occupied slots and three unoccupied ones. The d^{10} electron configuration has also only one term with the term symbol ^1S? Can we explain this? In the d^{10} electron configuration, there is no way to permute the electrons, hence there is only one microstate possible. In this microstate L=0. Why is that? When we sum up the individual m_l-values of the ten electrons then that sum is $2x(-2)+2(-1)+2x(0)+2x(+1)+2x(+2)=0$. The spin multiplicity of the microstate is 0 because all electrons are paired. Hence, we have a singlet ^1S term.

Spin-Orbit Coupling

We have still not considered all electron-electron interactions. In addition to the interaction between the angular magnetic momenta, and the magnetic interactions between the spins, there are also magnetic interactions between the angular momenta and the spins. This is called the spin-orbit coupling. It is expressed by an additional quantum number J. J can run from L+S to L-S.

$$J = L+S \ldots\ldots\ldots L\text{-}S$$

Figure 9.1.14 Equation for J

The quantum number J is added as a subscript behind letter describing the term. So a full term symbol is described as $^{2S+1}L_J$. Spin-orbit coupling may lead to additional terms depending on L and S.

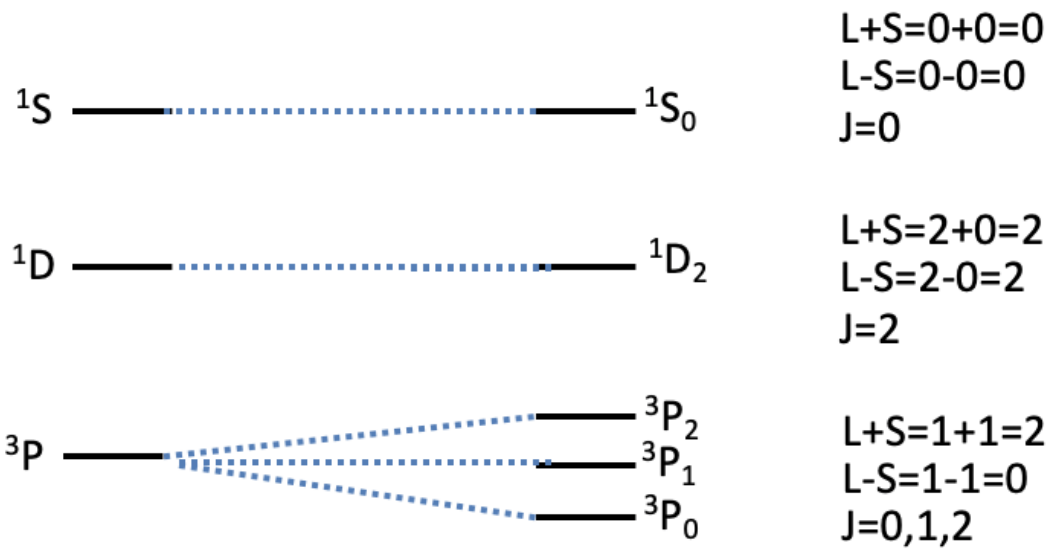


Figure 9.1.15 Examples of spin-orbital coupling

For instance, for a ^3P term, S=1, and L=1. Thus J can adopt values between L+S=1+1=2 and L-S=1-1=0. Thus, overall J can adopt the values, 0, 1, 2. This means a ^3P term splits into three terms due to the spin-orbit coupling. Their term symbols are $^3P_0$, $^3P_1$, and $^3P_2$. Their energy increases with increasing quantum number J. ^1S and ^1D terms on the other hand to do not split into additional terms. For a ^1S term L+S=0+0=0, and L-S=0-0=0. The full term symbol is $^1S_0$. For the ^1D term, L+S=2+0=2 and L-S=2-0=2, thus the full term symbol is $^1D_2$. Overall, the energy differences between terms due to J are very small, in the order of a tens of wavenumbers, and orders of magnitudes smaller than energy differences due to LS-coupling, which is typically in the order of tens of thousands of wavenumbers. Thus, we usually ignore the effect of J when interpreting electronic spectra.

Contributors and Attributions

- Dr. Kai Landskron (Lehigh University). If you like this textbook, please consider to make a donation to support the author's research at Lehigh University: Click Here to Donate.

This page titled 9.1: Quantum Numbers of Multielectron Atoms is shared under a CC BY 4.0 license and was authored, remixed, and/or curated by Kai Landskron.

9.2: Electronic Spectra of Coordination Compounds

Term Splitting of Terms in an Octahedral Field

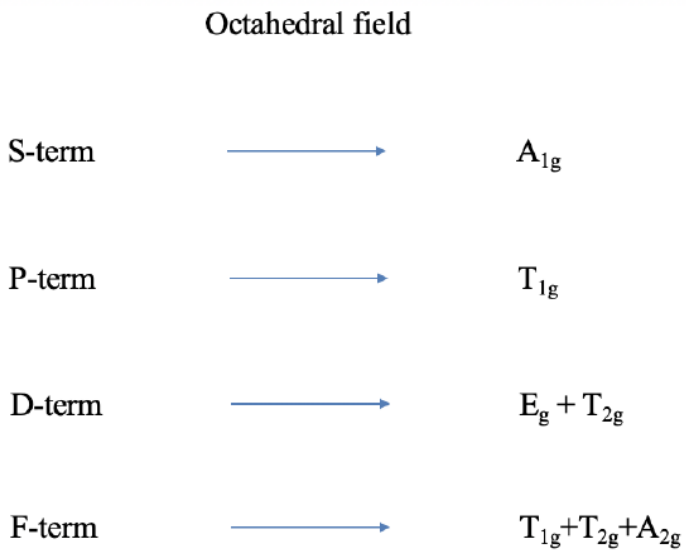


Figure 9.2.1: Octahedral field term splitting

Thus far we have only considered free ion terms, that means terms without the presence of a ligand field. Let us next think about the influence of an octahedral field on a term. Terms are wavefunctions, just like orbitals, and therefore they behave like orbitals in a ligand field. D-orbitals split into t_{2g} and e_g orbitals in an octahedral ligand field. A D-term behaves similarly. It splits into T_{2g} and E_g terms. P-orbitals are triple-degenerate having T_{1g} symmetry in the point group O_h and do not split in energy. P-terms have the same symmetry and also do not split. We can call a P-term in an octahedral ligand field a T_{1g} term. Following analogous arguments, S terms become A_{1g} terms. F terms do split in energy like f-orbitals and become T_{1g}, T_{2g}, and A_{2g} terms. Overall, the presence of the octahedral field increases the number of terms from four to seven (Fig. 9.2.1). It is easy to see that the ligand field leads to many states, and many potential electron transitions. Thus, we would expect quite complicated spectra. For other ligand fields, the terms also behave analogously to orbitals. For, instance in a tetrahedral field D-terms split into E and T_2 terms, and so forth.

Term Splitting for octahedral d^2 metal complexes

Now let us think about how the term energies of our free d^2-ion changes when placed in an octahedral ligand field, depending on the ligand field strength. We can express this by a correlation diagram (Fig. 8.2.2). In a correlation diagram, we plot the energies of the terms relative to the field strength.

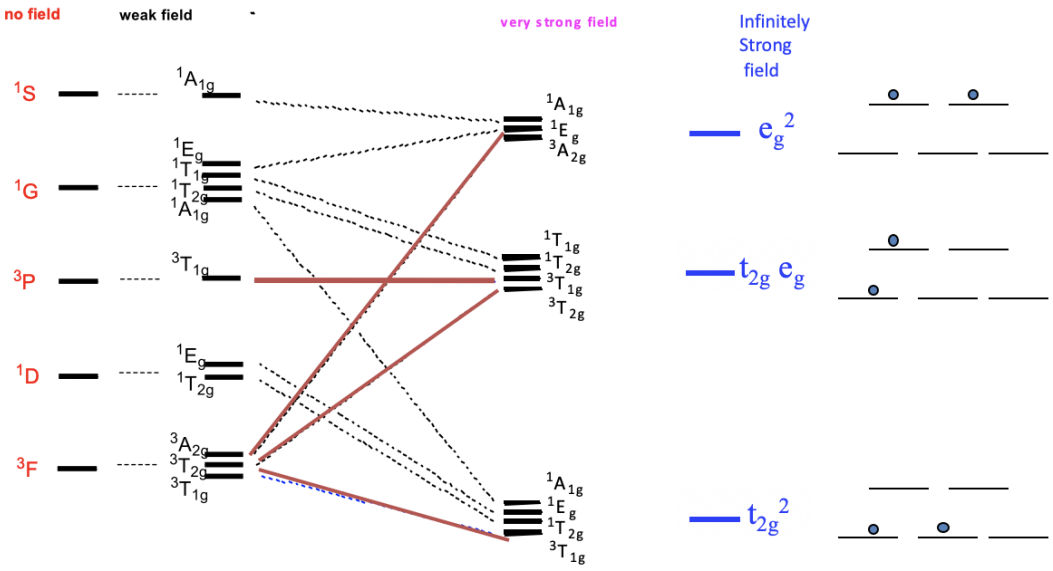


Figure 8.2.2 Correlation diagram

On the left side we plot the terms without any field according to their energies. In the case of a d^2 ion, the energies are $^3F<^1D<^3P<^1G<^1S$. Next, we plot the relative energies in a weak octahedral ligand field, and label the terms according to their symmetry. We can see that the D, F, and G terms split in energy, while the S and P terms do not. Because of the weak field, energy differences are very small. Now let us increase the ligand field strength continuously, until we have reached a very strong ligand field. We see that some of the terms move up in energy, while other terms move down as the ligand field increases. For example, two of the three terms resulting from the F-terms increase in energy while one decreases. It is also possible that a term does not change its energy. For example, the $^3T_{1g}$ term from the ^3P term does not change its energy. In very strong ligand field there are three groups of terms that have similar energy. In the hypothetical case of an infinitely strong ligand field, the terms that belong to a particular group become identical in energy. In this case, there are only three states for the electrons possible. The field is considered so strong so that the energy associated with electron-electron interactions become negligible compared to the energy of the field. The electrons behave as though there were no electron-electron interactions. Therefore, we can call the lowest energy state the t_{2g}^2 state. It is equivalent to the state of the two electrons being in the t_{2g} orbitals. The second state is called the $t_{2g}e_g$ state. It is equivalent to the state of one electron being in the t_{2g} and one electron being in the e_g orbitals. The third state is called the e_g^2 state, which is equivalent to the state with both electrons in the e_g^2-orbitals.

Selection Rules

In most cases, the ligand field strength is in between the very weak and very strong case, and thus, we could expect very complicated spectra. Fortunately, nature does not make things quite as complicated, because not all possible electron transitions are quantum-mechanically allowed. The allowed transitions are defined by two rules: The spin selection rule and the Laporte rule.

The **spin selection rule** states that transitions with $\Delta S = 0$ are allowed.

The spin selection rule states that only transitions are allowed in which the total spin quantum number S does not change. When S does not change also the spin multiplicity does not change. Thus, electron transitions are only allowed for transitions that do not involve a change in spin multiplicity. For example, it would be allowed to excite an electron from a triplet term to another triplet term, but not from a triplet term to a doublet or singlet term.

The **Laporte rule** states that the transitions with the change of parity, g → u or u → g are allowed.

The Laporte rule state that transitions are only allowed when there is a change of parity. This means a transition from a gerade (g) to an ungerade (u)-term and vice versa is possible, but not a transition from a g-term to another g-term, or the transition from a u-term to another u-term. For example, the transition from a T_{2g} to a T_{1u} term would be allowed, but not the transition from a T_{2g} to a T_{1g} term.

Tanabe-Sugano diagram of a d^2 octahedral complex

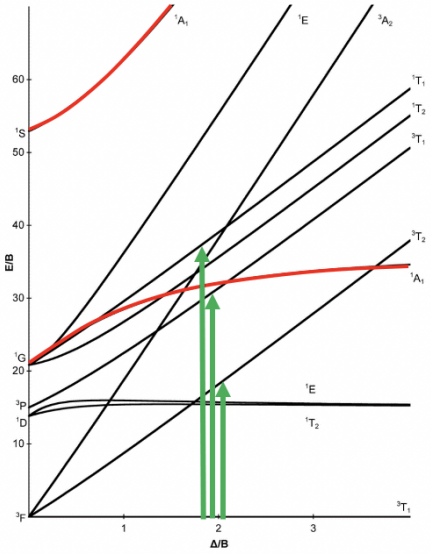


Figure 8.2.3 Tanabe-Sugano diagram of a d^2 octahedral complex (Attribution: Chem507f091 / Public domain https://commons.wikimedia.org/wiki/F...o_diagrams.png)

A particular correlation diagram is the Tanabe-Sugano diagram (Fig. 8.2.3). It is illustrated here for an octahedral d^2 complex. The difference to the previously discussed correlation diagram is that the energy of the ground state is plotted horizontally, and the energy of all other terms are plotted relative to that. In the case of the d^2 electron configuration, the $^3T_{1g}$ term is the ground term and is plotted as a horizontal line. We can see that the ligand field strength on the x-axis is given in units of B, and the energy of the terms is also given in units of B. B is a so-called Racah parameter, that is a quantum-mechanical energy unit for the electromagnetic interactions between the electrons. It is chosen because it provides “handy” numbers.

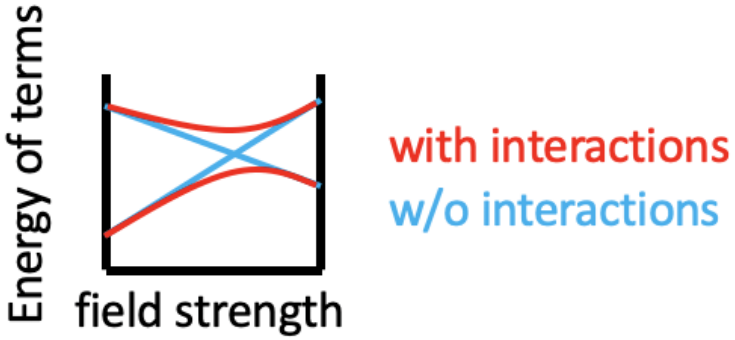


Figure 8.2.4 Origin of line-bending in Tanabe-Sugano diagrams.

You can see that some lines in the diagram are bent, and some are straight. Bending of lines occurs when two terms interact

with each other because they are close in energy and have the same symmetry. This is again an analogy to orbitals. Like orbitals interact when they have the same symmetry type and similar energy, also terms interact when they have the same symmetry and the similar energy. Without taking their interactions into account, their energies can cross when the energy of term A declines and the energy of term B increases with increasing field strength (Fig. 8.2.4). The closer the terms come to the point where they cross, the stronger their interactions, because their energies become more and more similar. The interactions lead to the fact that the terms "bend away" from each other, leading to bent curves. This means that curves for two terms of the same symmetry type will bend away in a Tanabe-Sugano diagram and never cross. For example the terms for the two $^1A_{1g}$ terms bend away from each other and do not cross.

Next, let us think about which electron transitions would be allowed under the consideration of the spin selection and the Laporte rule. We notice that in the symmetry types the “g” for gerade has been omitted (Fig. 8.2.3). This is a common simplification made in the literature. We have to remind us that all the terms in the diagram are “g” terms. What does this mean for the allowance of electron transitions? It means that no electron transition would be allowed, and that would imply that the complex could not absorb light. The Laporte selection rule however does not hold strictly. It only says that the probability of the electron-transition is reduced, however, not forbidden. This means that an absorption band that disobeys the Laporte rule will have lower intensity compared to one that follows the Laporte rule, but it can still be observed. The spin-selection rule, however, holds strictly, and transitions between terms of different spin multiplicity are strictly forbidden, meaning that they have near zero probability to occur. Overall, we can therefore excite an electron from the $^3T_1$ ground state to other triplet terms, namely the $^3T_2$ term, and the $^3A_2$ term (Fig. 8.2.3).

Tanabe-Sugano diagram of d^3 octahedral complexes

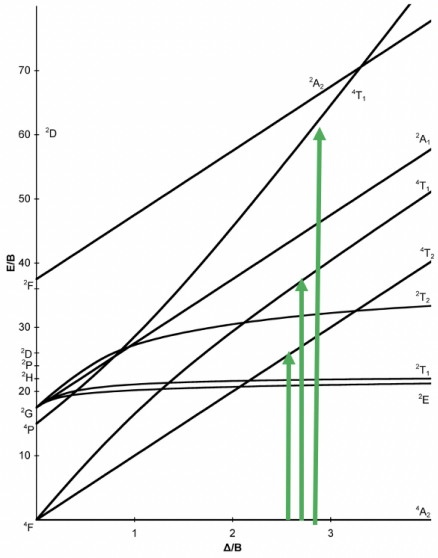


Figure 8.2.7 Tanabe-Sugano diagram of d^3 octahedral complexes (Attribution: Chem507f091 / Public domain https://commons.wikimedia.org/wiki/F...no_diagram.png)

Now, let us have a look at the Tanabe-Sugano diagram of a d^3 ion in an octahedral ligand field (Fig. 8.2.7). What is the ground term? We can see the term designation on the horizontal line reads “$^4A_2$”, therefore this term is the ground term. How many electron transitions from the ground state should we expect? To answer this question we need to count the number of other quartet terms. There is the $^4T_2$, the $^4T_1$, and another $^4T_1$. Thus, there are overall three electron transitions possible. Can we understand why the ground state is a quartet term?

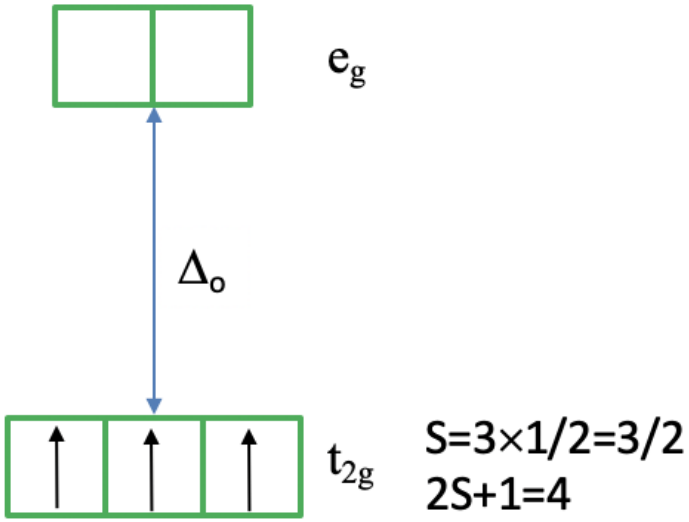


Figure 8.2.8 d-orbitals in an octahedral ligand field for the electron configuration d^3

It helps to consider how we would fill the electrons into the d-orbitals for the electron configuration d^3. All three electrons would be filled spin-up in the t_{2g} orbital following Hund's rule (Fig. 8.2.8). Because each electron has the spin +1/2 the total spin of all three electrons is 3x1/2=3/2. Thus, the spin multiplicity is ((3x3/2)+1)=4. Note that the microstate we have drawn is actually only one of the (2L+1)(2S+1) microstates. S=3x1/2=3/2, but what is L? You can see one the left side of the diagram that the $^4A_2$ term originated from a ^4F term. This means L=3, and (2L+1)((2S+1)=7x4=28. This means that there are actually 27 other microstates that have the same energy as the microstate that we drew. Why did we draw this microstate in favor of the others? This is because this microstate is the state with the maximum M_L (=L) and M_S (=S) values determining the term symbol.

Tanabe-Sugano diagram of d^4 octahedral complexes

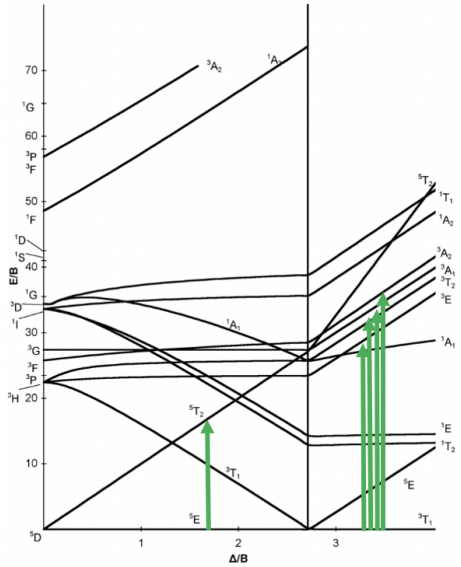


Figure 8.2.9 Tanabe-Sugano diagram of the d^4 octahedral complex (Attribution: Chem507f091 / Public domain https://commons.wikimedia.org/wiki/F...no_diagram.png)

Now let us look at the Tanabe-Sugano diagram of a d^4 octahedral complex. You can see that this diagram is separated into two parts separated by a vertical line. The line indicates the ligand field strength at which the complex changes from a high spin complex. At lower ligand field strengths, the ground term is a ^5E term. At higher field strength the ground term is a ^3T term.

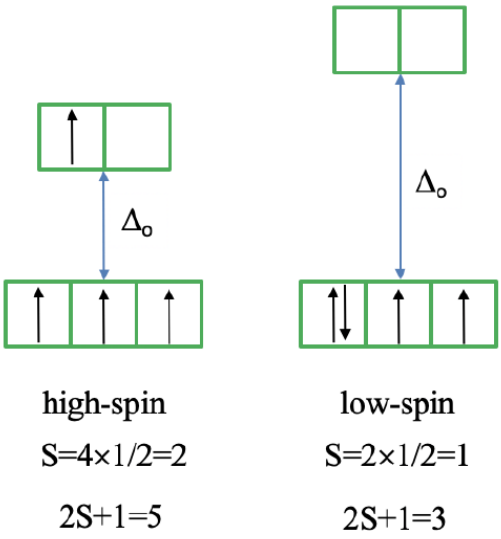


Figure 8.2.10 d-orbitals in the octahedral ligand field for the electron configuration d^4

We can rationalize this again by drawing the orbital box representation of the d-orbitals in the octahedral ligand field. In the high spin state, there are four unpaired electrons, thus S=4x1/2=2, and 2S+1=5. In the low spin state, there are two unpaired electrons, and thus S=2x1/2=1, and 2S+1=3. This explains the quintet and the triplet nature of the high and low spin ground terms. Note again, that the two microstates represented by the orbital box diagrams (Fig. 8.2.10) are not the only microstates that have the respective energy. They are only the "representative" microstates because the have the maximum M_L and M_S values.

How many electron transitions are possible from the ground term? For a high spin complex there is only one because the is only one other quintet term, namely the $^5T_2$ term. For the low spin complex, there are five transitions because there are five other triplet terms.

Tananbe-Sugano diagram of d^5 octahedral complexes

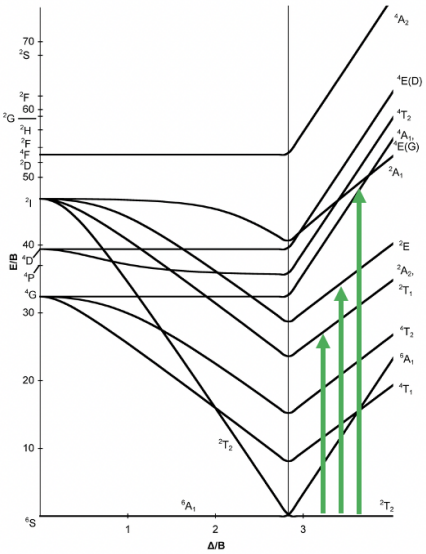


Figure 8.2.11 Tanabe-Sugano diagram of the d^5 octahedral complex (Attribution: Chem507f091 / Public domain https://commons.wikimedia.org/wiki/F...no_diagram.png)

Also the Tanabe-Sugano diagram of a d^5 octahedral complex is divided into two parts separated by a vertical line (Fig. 8.2.11). The left part reflects the high spin and the right part the low spin complex.

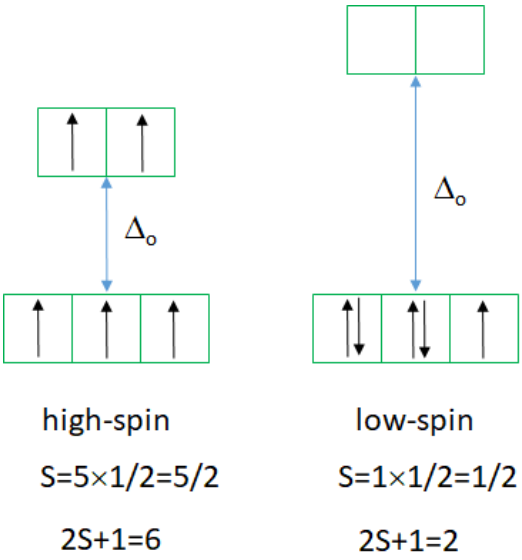


Figure 8.2.12 d-orbitals in the octahedral ligand field for the electron configuration d^5

The high spin ground state is a sextet term, and the low spin ground state is a doublet term. We can understand the sextet and doublet nature of the terms when considering that the associated electron box diagram have five and one unpaired electrons respectively. S=5x1/2=5/2 and 2S+1=6 for the high spin term, and S=1x1/2=1/2 and 2S+1=2 for the low spin term. What are the possible electron transitions from the ground state? For the high-spin complex there is no other sextet term, meaning that there is no electron transition possible. Hence, high-spin octahedral d^5-complexes are colorless. An example is the hexaaqua manganese (2+) complex. A solution of this complex is near colorless, only very slightly pinkish. The slight color is because also spin-forbidden transitions can occur, albeit at a very low probability. For a d^5-low spin complex there are three additional doublet states, and thus there are three electron transitions possible.

Tanabe-Sugano diagram of d^6 octahedral complexes

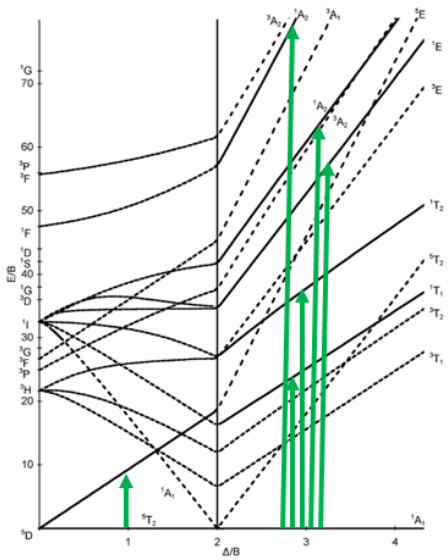


Figure 8.2.13 Tanabe-Sugano diagram of the d^6 octahedral complex (Chem507f091 / Public domain https://commons.wikimedia.org/wiki/F...no_diagram.png)

The next diagram is the one for the d^6 electron configuration (Fig. 8.2.13). Again, the diagram is separated into parts for high and low spin complexes. You can see dotted lines in the diagram. They indicate the terms that have a different spin multiplicity than the ground term. This way we can more easily see how many electron transitions are allowed.

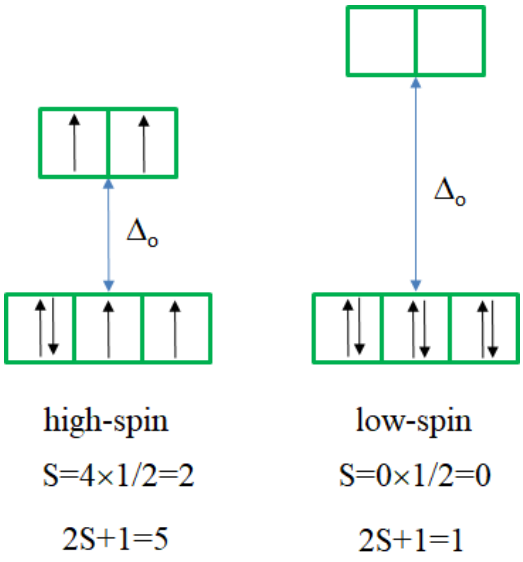


Figure 8.2.14 d-orbitals in the octahedral ligand field for the electron configuration d^6

The ground term for the high-spin complex is the quintet $^5T_2$ term. It is a quintet term because four electrons in the d-orbitals are unpaired, and two are paired. The value for S is thus 4x1/2=2, and the spin multiplicity is 2S+1=5. The ground term for the low spin complex is a $^1A_1$ term. It is a singlet term because all electrons are paired, and thus S=0, and 2S+1=1. How many electron transitions are there for the high-spin complex? There is only one because the ^5E term is the only other quintet term. There are five transitions possible for the low-spin case because there are five additional singlet terms.

Tanabe-Sugano diagram of d^7 octahedral complexes

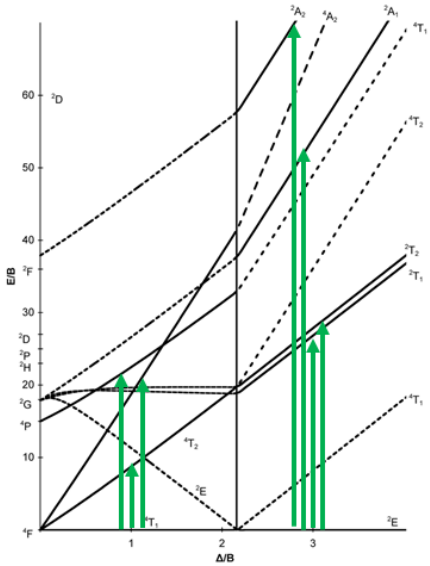


Figure 8.2.15 Tanabe-Sugano diagram of the d^7 octahedral complex (Attribution: Chem507f091 / Public domain https://commons.wikimedia.org/wiki/F...no_diagram.png)

Next, let us look at the Tanabe-Sugano diagram of a d^7 octahedral complex (Fig. 8.2.15). In this case, the high spin complex has a $^4T_1$ ground term, and the low spin complex has a ^2E ground term.

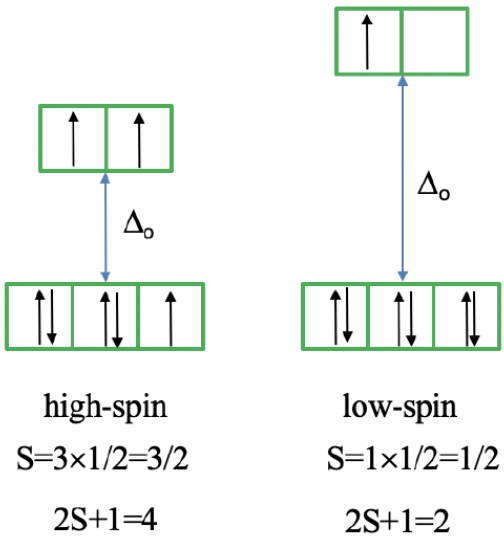


Figure 8.2.16 d-orbitals in the octahedral ligand field for the electron configuration d^7

The microstate that "represents" the high spin ground term has three unpaired electrons, hence the spin quantum number S=3/2 and the spin multiplicity is 2S+1=4. The microstate that represents the low spin ground term has one unpaired electron, an S value of ½, and a spin multiplicity of 2. There are three other quartet terms, and four other doublet terms, hence there are three electrons transitions for the high-spin complex, and four for the low spin complex.

Tanabe-Sugano diagram of d^8 octahedral complexes

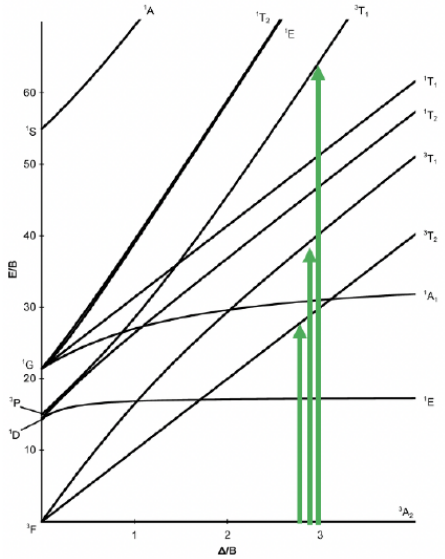


Figure 8.2.17 Tanabe-Sugano diagram of the d^8 octahedral complex (Attribution: Chem507f091 / Public domain https://commons.wikimedia.org/wiki/F...no_diagram.png)

Now let us look at an octahedral complex with d^8 electron configuration. For this electron configuration, there are no high and low spin complexes possible, therefore, the Tanabe-Sugano diagram is no longer divided into two parts (Fig. 8.2.17).

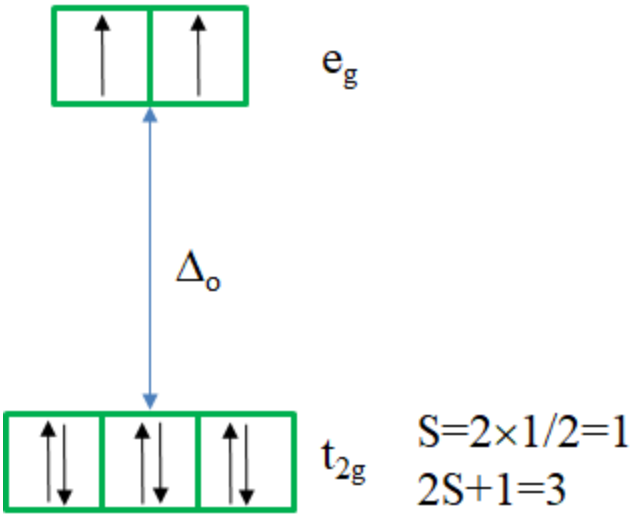


Figure 8.2.18 d-orbitals in the octahedral ligand field for the electron configuration d^8

There is a single ground term of the type $^3A_2$. It is a triplet state because the microstate representing the term has two unpaired electrons in the e_g orbitals (Fig. 8.2.18). Thus, S=2x1/2=1, and the spin multiplicity is 2S+1=2. How many electron transitions would you expect? There are three other triplet states, namely the $^3T_2$ and two $^3T_1$ terms. Therefore, there are three electron transitions possible.

We could also ask: Are there Tanabe-Sugano diagrams for d^1, d^9, and d^{10}? For, d^1 there are no electron-electron interactions, thus the simple orbital picture is sufficient. The ^2D term splits into T_{2g} and E_g terms, and there is only one electron transition possible. The d^9 electron configuration is the “hole-analog” of the d^1 electron configuration. It has also just one ^2D term which splits into a T_{2g} and an E_g term in the octahedral ligand field. Therefore, also in this case there is only one electron transition from the T_{2g} into the E_g term possible. In the case of d^{10} all microstates are filled with orbitals, and there is only the ^1S term which does not split in an octahedral ligand field. Therefore, there are no electron transitions in this case.

Finally, it should be mentioned that it is also possible to construct Tanabe-Sugano diagrams for other shapes such as the tetrahedral shape, but we will not discuss these further here.

Charge Transfer Transitions

Zn^{2+}		d^{10} ion	white
$[Cu(MeCN)_4]^+$	Cu(I)	d^{10} ion	colourless
$[Cu(phen)_2]^+$	Cu(I)	d^{10} ion	dark orange
TiF_4		d^0 ion	white
$TiCl_4$		d^0 ion	white
$TiBr_4$		d^0 ion	orange
TiI_4		d^0 ion	dark brown
$[MnO_4]^-$	Mn(VII)	d^0 ion	extremely purple
$[Cr_2O_7]^-$	Cr(VI)	d^0 ion	bright orange

Figure 8.2.19 Some examples of complexes with d^0 and d^{10} electron configurations, and their color. Attribution: E.R. Schofield.

We are still not done with our electronic spectra. Thus, far we have only considered transitions of d-electrons between d-orbitals, and their terms. They are called d-d transitions. However, there are also so-called charge transfer transitions possible, that are not d-d transitions. We can easily see that there must be other transitions but d-d transitions when we look at the color of d^{10} and d^0 ions. For those, the are no d-d transitions possible. Therefore, they all should be colorless. However, that is not always true. Some of these ions are indeed colorless, but some are not (Fig. 8.2.19). For example, Zn^{2+}, a d^{10} ion is colorless in complexes, but not Cu(I) which is also d^{10}. While tetrakis(acetonitrile)copper (+) is colorless, bis(phenanthrene) copper(+) is dark orange. Similar is true for d^0 ions. While TiF_4 and $TiCl_4$ are colorless, $TiBr_4$ is orange, and TiI_4 is brown. Some d^0 species are even extremely colorful, for example permanganate with Mn^{7+} which is extremely purple, and dichromate with Cr(VI) which is bright orange.

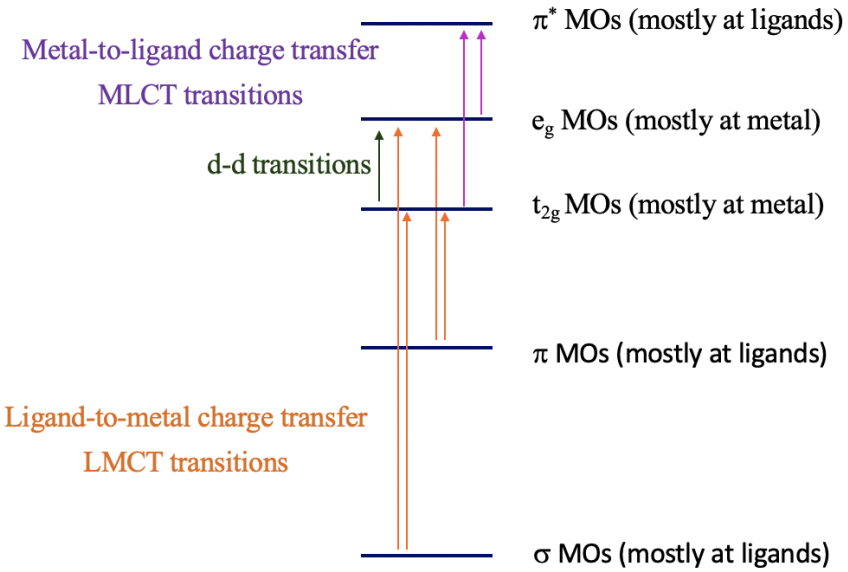


Figure 8.2.20 Charge-transfer transitions. Attribution: E.R. Schofield.

The explanation of these phenomena are charge-transfer transitions (Fig. 8.2.20). There are two types of charge-transfer transitions, the ligand-to-metal (LMCT) and the metal-to-ligand (MLCT) charge transfer transitions. For the ligand-to-metal transitions, electrons from bonding σ and π-orbitals get excited into metal d-orbitals in the ligand field, for example the t_{2g} and the e_g orbitals in an octahedral complex. If the energy difference between the σ/π-orbitals and the d-orbitals is small enough,

then this electron-transition is associated with the absorption of visible light. The transition is called a ligand-to-metal transition because the ligand σ/π-orbitals are mostly located at the ligands, while the metal-d-orbitals in a ligand field are mostly located at the metal. Vice versa, the metal-to-ligand transition involves the transition of an electron from metal d-orbitals in a ligand field to ligand π*-orbitals. This essentially moves electron density from the metal to the ligand, hence the name ligand-to-metal-charge transfer transition. If the energy-difference between the ligand π* and the metal orbitals is small enough, then the absorption occurs in the visible range. Charge-transfer transitions are usually both spin- and Laporte allowed, hence if they occur the color is often very intense. How can we distinguish between d-d and charge transfer transitions? Charge transfer transitions often change in energy as the solvent polarity is varied (solvatochromic) as there is a change in polarity of the complex associated with the charge transfer transition. This can be used to distinguish between d-d transitions and charge-transfer bands.

LMCT Transitions

Can we predict when the energy windows between the bonding molecular orbitals and the metal d-orbitals are small enough so that LMCT transitions in the visible can take place? Generally, it would be desirable if the energy of the metal orbitals was as low as possible and the energy of the bonding ligand orbitals are as high as possible. The energy of metal d-orbitals decreases with increasing positive charge at the metal because the effective nuclear charge on the metal increases. This means that very high metal oxidation states favor an LMCT transition. The d-orbitals should have few or no electrons, so that electrons can be promoted into the orbitals, and orbital energy decreases because electron-electron repulsion is minimized. Examples are Mn(VII), Cr(VI), and Ti(IV). The energy of MOs from bonding ligand orbitals increases when the ligand orbitals have high energy this is typically the case for π-donor ligand with negative charge (Fig. 8.2.21).

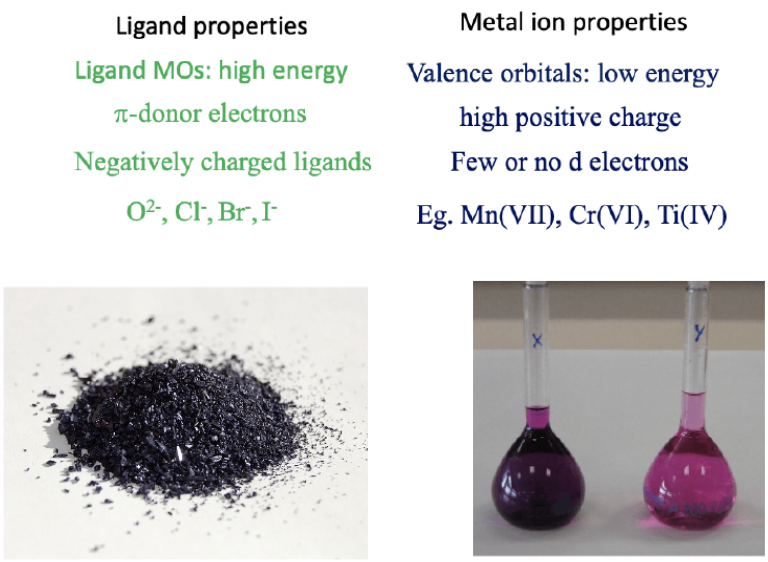


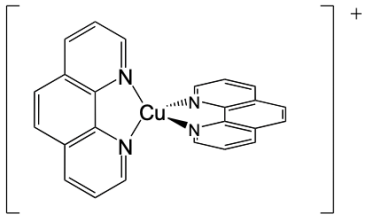
Figure 8.2.21 The properties of the metal ion and ligands suitable for LMCT transitions. MnO_4^- is deep purple due to LMCT transitions (Attribution: Benjah-bmm27 / Public domain https://commons.wikimedia.org/wiki/F...ate-sample.jpg) and (Attribution: Pradana Aumars / CC0 https://commons.wikimedia.org/wiki/F...entrations.jpg), respectively.

Examples of ligands are oxo- and halo ligands. This explains for example the LMCT transitions in permanganate. The Mn is in the very high oxidation state +7, and the ligands are are oxo-ligands wich are π-donors with a 2- negative charge. The transitions are both Laporte and spin-allowed leading to very high intensity of light absorption, and thus color (Fig. 8.2.21).

MLCT Transitions

What are favorable metal ion and ligand properties for a metal-to-ligand transition, then? In this case we would like to keep the energy of the metal orbitals as high as possible so that the energy difference between a metal d-orbital and a π*-orbital is minimized. This is accomplished when the positive charge at the metal ion is small, and there are many d-electrons that can repel each other, thereby increasing orbital energies, for examples Cu(I), Fig. 8.2.22.

Metal ion properties	Ligand properties
low metal ion charge	π-acceptor ligand with low-lying π* orbitals
many electrons	
Cu(I), d^{10} ion	1,10-phenanthroline, CN^-, CO, SCN^-



$[Cu(phen)_2]^+$, dark orange

Figure 8.2.22 bis(phenanthroline) copper(+). Attribution: E.R. Schofield.

The ligand should be a π-acceptor with low-lying π*-orbitals, for example phenanthroline, CN^-, SCN^-, and CO. For instance, the bis(phenanthroline) copper(+) is dark-orange and has a MLCT absorption band at 458 nm. Also, the MLCT transfer is both spin and Laporte-allowed.

It should be mentioned that some complexes allow for both metal-to-ligand and ligand to metal transitions. For example, in the $Cr(CO)_6$ complex the σ-orbitals are high enough and the π*-orbitals are low enough in energy to allow for light absorption in the visible range. Finally, also intraligand bands are possible when the ligand is a chromophore.

Dr. Kai Landskron (Lehigh University). If you like this textbook, please consider to make a donation to support the author's research at Lehigh University: Click Here to Donate.

This page titled 9.2: Electronic Spectra of Coordination Compounds is shared under a license and was authored, remixed, and/or curated by Kai Landskron.

- 8.2: Term splitting in ligand fields, selection rules, Tanabe-Sugano diagrams. Metal to ligand, and ligand to metal transitions by Kai Landskron is licensed CC BY 4.0.

9.3: Tanabe-Sugano Diagrams

ATTENTION! All the diagrams in this section have the X-axis incorrectly labeled! It is actually $\frac{10\Delta}{B}$.

Tanabe-Sugano diagrams are used in coordination chemistry to predict electromagnetic absorptions of metal coordination compounds of tetrahedral and octahedral complexes. The analysis derived from the diagrams can also be compared to experimental spectroscopic data. Armed with spectroscopic data, an approximation to the crystal field splitting energy (10Dq), generated by ligands attached to a metal center, can be found.

Crystal Field Splitting Energy

Within Crystal Field Theory, the interaction of the metal and ligand arise from the positive charge of the metal and negative charge on the ligands. The theory is developed by looking at the five degenerate d-orbitals and how the energies are changed on being surrounded by the negative point charges of the ligands. As the ligands are moved closer to the metal the repulsion between the electrons of the metal and ligands break the degeneracy of the d-orbitals. In the case of an octahedral complex 6 ligands surround a metal center with a single pair on each axis. This raises the energies of $d_{x^2-y^2}$, d_{z^2} relative to those of d_{xy} d_{xz} d_{yz}. This energy split is called Δ_{oct}. The tetrahedral energy split is about $4/9\Delta_{oct}$.[1]

Racah Parameters

Racah parameters were generated as a means to describe the effects of electron-electron repulsion within the metal complexes. The Racah parameters are *A*, *B* and *C*. In the case of Tanabe-Sugano diagrams each electron configuration split has an energy that can be related by the *B* value. *A* is ignored because it is roughly the same for any metal center and *C* generally approximated as being 1/4*B*. What *B* represents is an approximation of the bond strength between the ligand and metal.[1] Comparisons between tabulated free ion *B* and *B* of a coordination complex is called the nephelauxetic ratio (the effect of reducing electron-electron repulsion via ligands). This effect is what gives rise to the spectrochemical series of ligands described later.

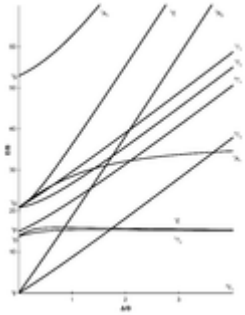
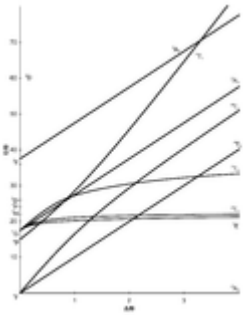
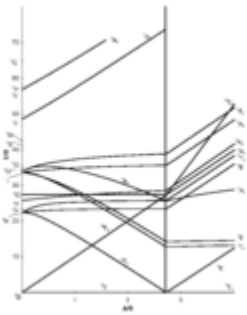
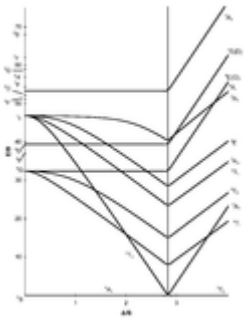
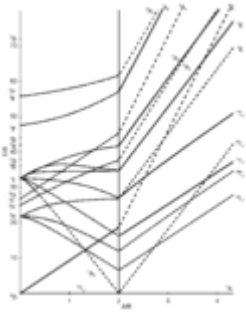
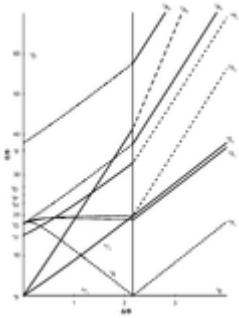
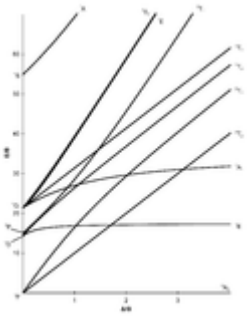
$$\beta = \frac{\beta_{complex}}{\beta_{freeion}} \tag{1}$$

Parameters

The x-axis in a Tanabe-Sugano diagram is in terms of the crystal field splitting parameter, 10Dq, or Δ_{oct}, scaled by the *B* Racah Parameter. The y-axis is in terms of energy of a electronic transition, E, scaled by *B*. Each line represents the energy of an electronic state while varying the strength of octahedral ligand field. And while only a few electronic states are spin allowed the spin forbidden electron transitions are included since spin forbidden transitions can appear in spectrum. Each term symbol is created from the splitting of term symbols from spherical to octahedral symmetry. With the relative energy ordering of the states are determined via Hund's rules.

Diagrams for d^4, d^5, d^6, and d^7 metal ions have a discontinuity in energies as the ligand field is varied. The discontinuity, shown with the vertical line, represents complexes changing from high-spin to low-spin complexes. At the line, the spin pairing energy is equal to the crystal field splitting energy. To the left of the line metal complexes are high-spin as the spin pairing energy is greater than that of the ligand field splitting. To the right of the line metal complexes are low-spin as the spin pairing energy is less than that of the ligand field splitting energy.

Diagrams

			
d^2 Tanabe-Sugano diagram	d^3 Tanabe-Sugano diagram	d^4 Tanabe-Sugano diagram	d^5 Tanabe-Sugano diagram
			Note: Each of the images is a thumbnail clicking on one will expand the image.
d^6 Tanabe-Sugano diagram	d^7 Tanabe-Sugano diagram	d^8 Tanabe-Sugano diagram	

How to use the Diagrams

1. Before looking at the diagrams the d-configuration of the metal ion must be determined.
2. Choose the appropriate Tanabe-Sugano diagram matching the d-configuration (http://chemistry.bd.psu.edu/jircitano/TSdiagram.pdf has full page diagrams necessary for measurements).
3. Take a spectrum of the complex and identify λ_{max} for spin-allowed (strong intensity) and spin forbidden (weak intensity) transitions.
4. Convert λ_{max} to wavenumbers and generate energy ratios relative to the lowest allowed transition. (i.e. $E_2/E_1$and E_3/E_1)
5. Using a ruler, slide it across the printed diagram until the E/*B* ratios between lines is equivalent to the ratios found in step 4.
6. Solve for *B* using the E/*B* values (y-axis, step 4) and Δ_{oct}/B (x-axis, step 5) to yield the ligand field splitting energy 10Dq.

Example 9.3.1: Chromium Splitting

A Cr^{3+} metal complex has strong transitions and λ_{max} at

- 431.03 nm,
- 781.25 nm, and
- 1,250 nm.

Determine the Δ_{oct} for this complex.

Solution

1. Cr has 6 electrons. Cr^{3+} has three electrons so its has a d-configuration of d^3
2. Locate the d^3 Tanabe-Sugano diagram
3. Convert to wavenumbers:

$$\frac{10^7(nm/cm)}{1250\ nm} = 8,000\ cm^{-1}$$

$$\frac{10^7(nm/cm)}{781.25\ nm} = 13,600\ cm^{-1}$$

$$\frac{10^7(nm/cm)}{431.03\ nm} = 23,200\ cm^{-1}$$

4. Allowed transitions are $^4T_{1g} \leftarrow {}^4A_{2g}$, $^4T_{1g} \leftarrow {}^4A_{2g}$ and $^4T_{2g} \leftarrow {}^4A_{2g}$.

Transition	Energy cm^{-1}	Ratios to lowest
$^4T_{1g} \leftarrow {}^4A_{2g}$	23,200	2.9
$^4T_{1g} \leftarrow {}^4A_{2g}$	13,600	1.7
$^4T_{2g} \leftarrow {}^4A_{2g}$	8,000	1

5. Sliding the ruler perpendicular to the x-axis of the d^3 diagram yields the following values:

Δ_{oct}/B	10	20	30	40
Height E(ν_3)/B	29	45	64	84
Height E(ν_2)/B	17	30	40	51
Height E(ν_1)/B	10	20	30	40
Ratio E(ν_3)/E(ν_1)	2.9	2.25	2.13	2.1
Ratio E(ν_2)/E(ν_1)	1.7	1.5	1.33	1.275

6. Based on the two tables above it should be assessed that the Δ_{oct}/B value is 10. B is found by finding the dividing E by the height.

Energy cm^{-1}	Height	B
23,200	29	800
13,600	17	800
8,000	10	800

7. Next multiply Δ_{oct}/B by B to yield the Δ_{oct} energy.

$$10 \times 800 = 8000\ cm^{-1} = \Delta_{oct}$$

Each problem is of varying complexity as several steps may be needed to find the correct Δ_{oct}/B values that yield the proper energy ratios.

Nephelauxetic Effect

Imagine you had an abundance of $V(H_2O)_6^{3+}$ (d^2) which has two absorptions. If you had no other available metal centers, but an abundance of ligands, the complex's absorption spectrum (therefore its color) could be changed via application of the spectrochemical series:

$$I^- < Br^- < S^{2-} < SCN^- < Cl^- < NO_3^- < N_3^- < F^- < OH^- < C_2O_4^{2-} \approx H_2O < NCS^- < CH_3CN < py\ (pyridine) < NH_3 < en\ (ethylenediamine) < bipy\ (2,2'\text{-}bipyridine) < phen\ (1,10\text{-}phenanthroline) < NO_2^- < PPh_3 < CN^- \approx CO$$

If you wanted higher energy absorptions (shift toward purple colors) you use ligands to the right of H_2O and if you wanted redder colors attach ligands to the left of H_2O. Here you could measure the nephelauxetic ratio of the ligands to compare how each ligand modifies the *B* Racah parameter. The series of complexes would also serve as a very good demonstration for a classroom. The reason behind modifying metal ligands has implications for commercial products. Unique colors in ceramics and glass products can be traced back to many metal compounds.

References

1. H.A.O. Hill, P. Day. Physical Methods in Advanced Inorganic Chemistry. John Wiley & Sons, Inc. 1968.
2. Tanabe, Yukito; Sugano, Satoru (1954). "On the absorption spectra of complex ions I". Journal of the Physical Society of Japan 9 (5): 753–766.
3. Tanabe, Yukito; Sugano, Satoru (1954). "On the absorption spectra of complex ions II". Journal of the Physical Society of Japan 9 (5): 766–779
4. Tanabe, Yukito; Sugano, Satoru (1956). "On the absorption spectra of complex ions III". Journal of the Physical Society of Japan 11 (8): 864–877.

Problems

1. For a d^7 metal ion determine the energy ratios for allowed transitions at Δ_{oct}/B of 20.
2. For a d^6metal ion of Δ_{oct}/B = 30 and B=530 cm^{-1} what would the energies of the 5 allowed transitions be? How many are in the UV-Vis range? How many are in the IR range?
3. Write out the allowed transitions for a d^5 metal ion in a E/*B*> 28 ligand field.
4. A d^4 complex exhibits absorptions at 5500 cm^{-1} (strong) and 31350 cm^{-1} (weak). What are the transitions that are being exhibited in the complex? What is the corresponding Δ_{oct} for the complex?
5. A spectrum of d^7 metal complex seemingly exhibits only two intense transitions. What is the Δ_{oct}/B that this situation occurs? Please use reference to specific transitions and energy splitting.

Answers

1. Δ_{oct}/B of 20 yields E/*B* values of 38, 32, 18. Ratios then are 2.11 and 1.78
2. Δ_{oct}/B = 30 yields E/*B* heights of 27, 40, 57, 65, 85. Energies are then 14310, 21200, 30210, 34450 and 45050 cm^{-1}. All are in the UV-Vis range. *note you need to infer the E/*B* value for the last transition as the diagram does not extend that far up.
3. $^2A_{2g}$<-$^2T_{2g}$, $^2T_{1g}$<-$^2T_{2g}$, ^2E_g<-$^2T_{2g}$, and $^2A_{1g}$<-$^2T_{2g}$.
4. 31,350/5,500 gives a ratio of 5.7/1. The only Δ_{oct}/B value that matches is at 10. *B* value is then 550 cm^{-1}. Δ_{oct}equals 5500 cm^{-1}.
5. Three transitions are generated at low Δ_{oct}/B. However, at about a value of Δ_{oct}/B = 13 the transitions $^4A_{2g}$<-$^4T_{1g}$, and $^4T_{1g}$<-$^4T_{1g}$ have the same energies which results in the appearance of only two absorptions.

Contributors and Attributions

- Evan Sarina, UC Davis

This page titled 9.3: Tanabe-Sugano Diagrams is shared under a license and was authored, remixed, and/or curated by LibreTexts.

- Tanabe-Sugano Diagrams is licensed CC BY-NC-SA 4.0.

9.4: Magnetic Properties of Coordination Compounds

Saint Mary's College: CHEM 342
Bioinorganic Chemistry
Spring 2020: Dr. Kathryn Haas

Agenda • **Readings** • **Worksheets** • **Essays** • **WiSEWIKI**

Experimental evidence of magnetic measurements supports the theory of high- and low-spin complexes. Remember that molecules such as O_2 that contain unpaired electrons ar e paramagnetic. Paramagnetic substances are attracted to magnetic fields. (see video)

YouTube Video

This interactive element is not available in this format. Visit the link or scan the QR code to access it online.

View this YouTube Video online

Many transition metal complexes have unpaired electrons and hence are paramagnetic. Molecules such as N_2 and ions such as Na^+ and $[Fe(CN)_6]^{4-}$ that contain no unpaired electrons are **diamagnetic** . Diamagnetic substances have a slight tendency to be **repelled** by magnetic fields.

When an electron in an atom or ion is unpaired, the magnetic moment due to its spin makes the entire atom or ion **paramagnetic**. The size of the magnetic moment of a system containing unpaired electrons is directly related to the number of such electrons: the greater the number of unpaired electrons, the larger the magnetic moment. Magnetic susceptibility measures the force experienced by a substance in a magnetic field. When we compare the weight of a sample to the weight measured in a magnetic field (Figure $9.4.1$), paramagnetic samples that are attracted to the magnet will appear heavier because of the force exerted by the magnetic field. We can calculate the number of unpaired electrons based on the increase in weight.

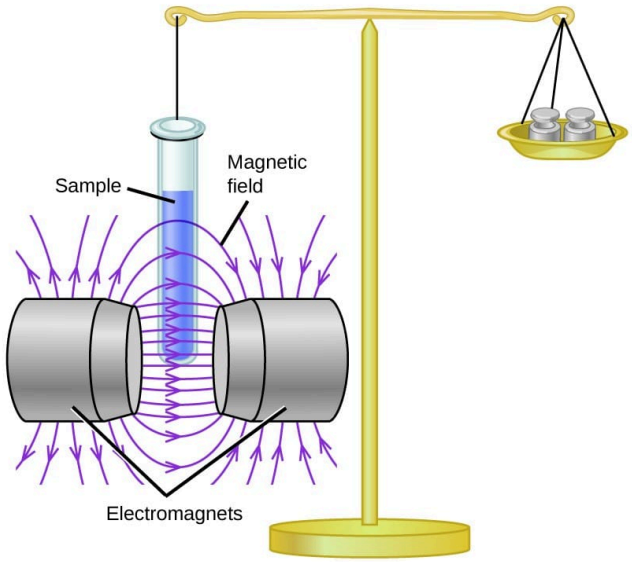


Figure 9.4.1: A Gouy balance compares the mass of a sample in the presence of a magnetic field with the mass with the electromagnet turned off to determine the number of unpaired electrons in a sample. (CC BY-SA 3.0; OpenStax).

From this experiment, the measured magnetic moment of low-spin d^6 $[Fe(CN)_6]^{4-}$ ion confirms that iron is diamagnetic, whereas the high-spin d^6 $[Fe(H_2O)_6]^{2+}$ complex has four unpaired electrons with a magnetic moment that confirms this arrangement. Therefore, the observed magnetic moment is used to determine the number of unpaired electrons present.

Magnetic Properties of Coordination Compounds

An interesting characteristic of transition metals is their ability to form magnets. Metal complexes that have unpaired electrons are magnetic. Since the last electrons reside in the d orbitals, this magnetism must result from unpaired d electrons. Considering only monometallic complexes, unpaired electrons arise because the complex has an odd number of electrons or because electron pairing is destabilized. For example, the Ti(III) ion has one d electron and must be (weakly) paramagnetic, regardless of the geometry or the nature of the ligands. However, the Ti(II) ion with two d-electrons, sometimes forms complexes with two unpaired electrons and sometimes forms complexes with no unpaired electrons.

As an example, Fe^{3+} has five d electrons prefers octahedral geometry. The complex $[FeF_6]^{3-}$ is high-spin d^5 and is attracted strongly to magnetic fields; however, $[Fe(CN)_6]^{3-}$ is low-spin d^5 and only has one unpaired electron, making it a weaker magnet. This trend can be explained based on the properties of the ligands.

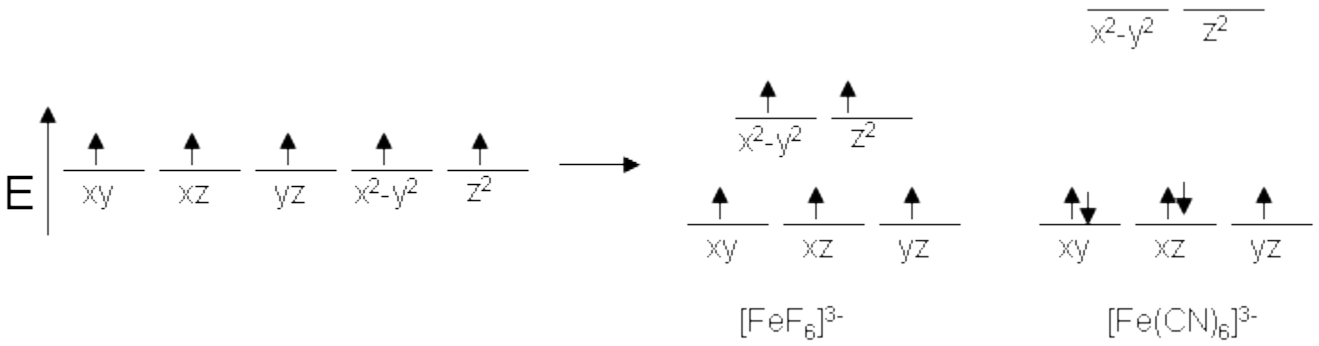


Figure 9.4.2: Crystal field theory splitting diagram. Example of influence of ligand electronic properties on d orbital splitting. This shows the comparison of low-spin versus high-spin electrons.

Example 9.4.1:

Which one of the following coordination compounds would you expect to be paramagnetic?

a. $[Zn(NH_3)_4]Cl_2$
b. $K[FeCl_4]$
c. $[Cd(H_2O)_6]SO_4$

Solution

Let's consider each compound individually. Since each compound has only one complex ion, we only need to consider how the d electrons are distributed in the ligand field of that ion. We can ignore the other parts (the counter ions) of the compound.

a. The zinc ion in $[Zn(NH_3)_4]Cl_2$ has a +2 oxidation state and is a d^{10}. This is a diamagnetic compound.
b. The iron ion in $K[FeCl_4]$ has a +3 oxidation state and is d^5. It only has four electrons and is more likely to be in a tetrahedral geometry than square planar. For tetrahedral geometries, we expect high spin; further, it has weak-field ligands. This compound will be paramagnetic (with five unpaired electrons).
c. The cadmium ion in $[Cd(H_2O)_6]SO_4$ has a +2 oxidation state, and is d^{10}. This is a diamagnetic compound.

Exercise 9.4.1

Predict the number of unpaired electrons for each of the following complex ions, and tell whether it will be attracted or repelled by a magnetic field.

a. $[Fe(CN)_6]^{4-}$
b. $[Ru(NH_3)_6]^{3+}$
c. $[Cr(NH_3)_6]^{2+}$

Answer available at the end of this section.

In bi- and polymetallic complexes, in which the individual centers have an odd number of electrons or electrons are high-spin, the situation is more complicated. If there is interaction between the two (or more) metal centers, the electrons may couple, resulting in a weak magnet, or they may enhance each other. When there is no interaction, the two (or more) individual metal centers behave as if they are in two separate molecules.

Answers

Exercise 9.4.1

a. Fe^{2+}: a $3d^6$ ion bound to strong field ligands; thus we expect low spin and 0 unpaired electrons. This diamagnetic compound will be repelled by a magnetic field.
b. Ru^{3+}: a $4d^5$ ion; thus we expect low spin with 1 unpaired electron. This paramagnetic compound will be weakly attracted to a magnetic field.
c. Cr^{2+}: a $3d^4$ ion bound to weak field ligands; thus we expect high spin and 4 unpaired electrons. This paramagnetic complex will be strongly attracted to a magnetic field.

This page titled 9.4: Magnetic Properties of Coordination Compounds is shared under a license and was authored, remixed, and/or curated by LibreTexts.

- 8.1.3: Magnetic Properties of Coordination Compounds by Kathryn Haas is licensed CC BY-NC-SA 4.0.

9.5: Magnetic Properties of Materials

Ferromagnetism is the basic mechanism by which certain materials (such as iron) form permanent magnets. This means the compound shows permanent magnetic properties rather than exhibiting them only in the presence of a magnetic field (Figure 9.5.1). In a ferromagnetic element, electrons of atoms are grouped into domains in which each domain has the same charge. In the presence of a magnetic field, these domains line up so that charges are parallel throughout the entire compound. Whether a compound can be ferromagnetic or not depends on its number of unpaired electrons and on its atomic size.

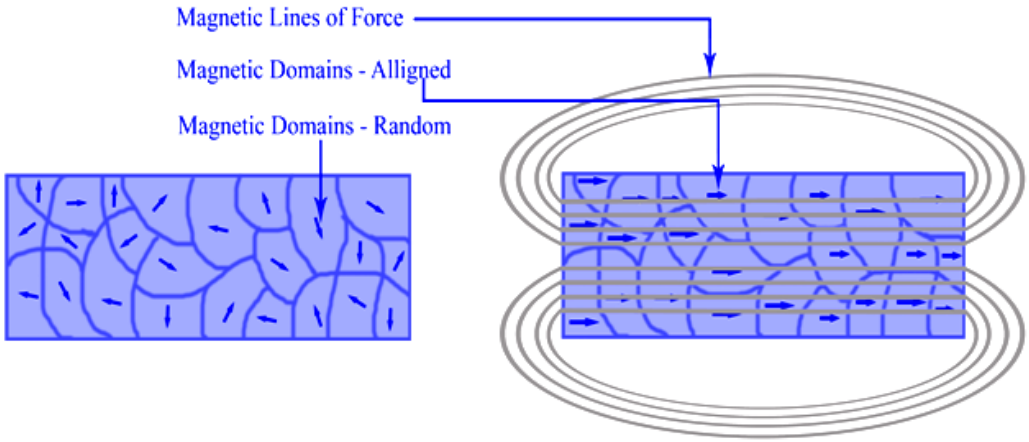


Figure 9.5.1: Ferromagnetism (a) nonmagnatized material and (2) Magnetized material with corresponding magnetic fields shown.

Ferromagnetism, the permanent magnetism associated with nickel, cobalt, and iron, is a common occurrence in everyday life. Examples of the knowledge and application of ferromagnetism include Aristotle's discussion in 625 BC, the use of the compass in 1187, and the modern-day refrigerator. Einstein declared that electricity and magnetism are inextricably linked in his theory of special relativity.

The magnetic moment of a system measures the strength and the direction of its magnetism. The term itself usually refers to the magnetic dipole moment. Anything that is magnetic, like a bar magnet or a loop of electric current, has a magnetic moment. A magnetic moment is a vector quantity, with a magnitude and a direction. An electron has an electron magnetic dipole moment, generated by the electron's intrinsic spin property, making it an electric charge in motion. There are many different magnetic forms: including paramagnetism, and diamagnetism, ferromagnetism, and anti-ferromagnetism. Only the first two are introduced below.

Paramagnetism

Paramagnetism refers to the magnetic state of an atom with one or more unpaired electrons. The unpaired electrons are attracted by a magnetic field due to the electrons' magnetic dipole moments. Hund's Rule states that electrons must occupy every orbital singly before any orbital is doubly occupied. This may leave the atom with many unpaired electrons. Because unpaired electrons can spin in either direction, they display magnetic moments in any direction. This capability allows paramagnetic atoms to be attracted to magnetic fields. Diatomic oxygen, O_2 is a good example of paramagnetism (described via molecular orbital theory). The following video shows liquid oxygen attracted into a magnetic field created by a strong magnet:

YouTube Video

This interactive element is not available in this format. Visit the link or scan the QR code to access it online.

View this YouTube Video online

A chemical demonstration of the paramagnetism of oxygen, as shown by the attraction of liquid oxygen to a magnet. Carleton University, Ottawa, Canada.

As shown in the video, molecular oxygen (O_2 is paramagnetic and is attracted to the magnet. Incontrast, Molecular nitrogen, N_2 , however, has no unpaired electrons and it is diamagnetic (this concept is discussed below); it is therefore unaffected by the magnet.

There are some exceptions to the paramagnetism rule; these concern some transition metals, in which the unpaired electron is not in a d-orbital. Examples of these metals include Sc^{3+}, Ti^{4+}, Zn^{2+}, and Cu^{+}. These metals are the not defined as paramagnetic: they are considered diamagnetic because all d-electrons are paired. Paramagnetic compounds sometimes display bulk magnetic properties due to the clustering of the metal atoms. This phenomenon is known as ferromagnetism, but this property is not discussed here.

Diamagnetism

Diamagnetic substances are characterized by paired electrons—except in the previously-discussed case of transition metals, there are no unpaired electrons. According to the Pauli Exclusion Principle which states that no two identical electrons may take up the same quantum state at the same time, the electron spins are oriented in opposite directions. This causes the magnetic fields of the electrons to cancel out; thus there is no net magnetic moment, and the atom cannot be attracted into a magnetic field. In fact, diamagnetic substances are weakly ***repelled*** by a magnetic field. In fact, diamagnetic substances are weakly ***repelled*** by a magnetic field as demonstrated with the pyrolytic carbon sheet in Figure $9.5.6$.

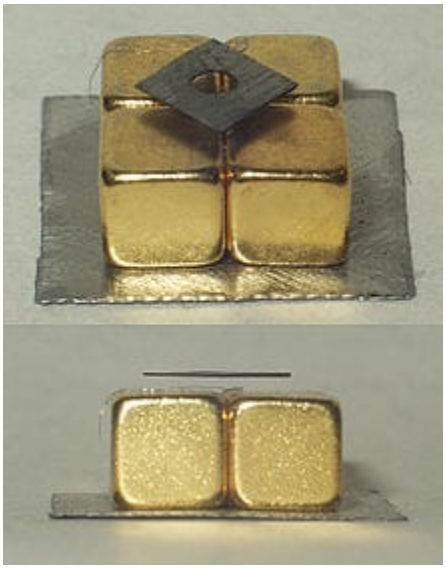


Figure $9.5.6$: Levitating pyrolytic carbon: A small (~6 mm) piece of pyrolytic graphite levitating over a permanent neodymium magnet array (5 mm cubes on a piece of steel). Note that the poles of the magnets are aligned vertically and alternate (two with

north facing up, and two with south facing up, diagonally). from Wikipedia.

How to Tell if a Substance is Paramagnetic or Diamagnetic

The magnetic form of a substance can be determined by examining its electron configuration: if it shows unpaired electrons, then the substance is paramagnetic; if all electrons are paired, the substance is diamagnetic. This process can be broken into four steps:

1. Find the electron configuration
2. Draw the valence orbitals
3. Look for unpaired electrons
4. Determine whether the substance is paramagnetic (one or more unpaired electrons) or diamagnetic (all electrons paired)

Example 9.5.4: Chlorine atoms

Are chlorine atoms paramagnetic or diamagnetic?

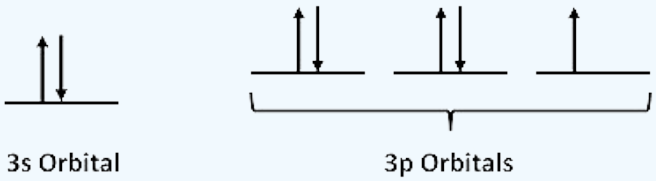
Solution

Step 1: Find the electron configuration

For Cl atoms, the electron configuration is $3s^2 3p^5$

Step 2: Draw the valence orbitals

Ignore the core electrons and focus on the valence electrons only.



Step 3: Look for unpaired electrons

There is one unpaired electron.

Step 4: Determine whether the substance is paramagnetic or diamagnetic

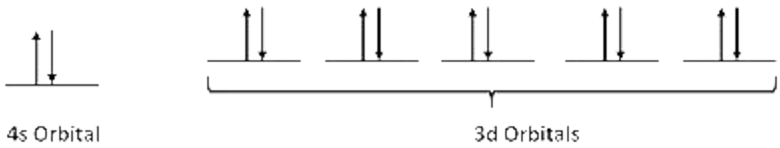
Since there is an unpaired electron, Cl atoms are paramagnetic (but is quite weak).

Example 2: Zinc Atoms

Step 1: Find the electron configuration

For Zn atoms, the electron configuration is $4s^2 3d^{10}$

Step 2: Draw the valence orbitals



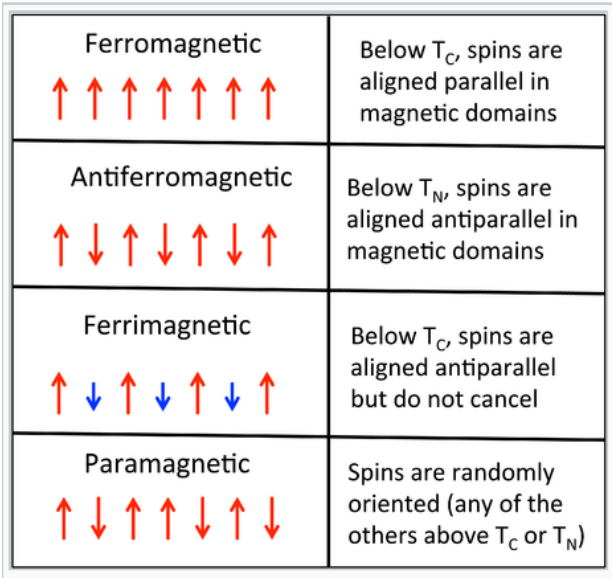
Step 3: Look for unpaired electrons

There are no unpaired electrons.

Step 4: Determine whether the substance is paramagnetic or diamagnetic

Because there are no unpaired electrons, Zn atoms are diamagnetic.

The magnetism of metals and other materials are determined by the orbital and spin motions of the unpaired electrons and the way in which unpaired electrons align with each other. All magnetic substances are **paramagnetic** at sufficiently high temperature, where the thermal energy (kT) exceeds the interaction energy between spins on neighboring atoms. Below a certain critical temperature, spins can adopt different kinds of ordered arrangements.



A pictorial description of the ordering of spins in ferromagnetism, antiferromagnetism, ferrimagnetism, and paramagnetism

Let's begin by considering an individual atom in the bcc structure of iron metal. Fe is in group VIIIb of the periodic table, so it has eight valence electrons. The atom is promoted to the $4s^1 3d^7$ state in order to make bonds. A localized picture of the d-electrons for an individual iron atom might look like this:



Since each unpaired electron has a spin moment of 1/2, the total spin angular momentum, **S**, for this atom is:

$S = 3\frac{1}{2} = \frac{3}{2}$ (in units of h/2π)

We can think of each Fe atom in the solid as a little bar magnet with a spin-only moment **S** of 3/2. The spin moments of neigboring atoms can align in parallel (↑ ↑), antiparallel (↑ ↓), or random fashion. In bcc Fe, the tendency is to align parallel because of the positive sign of the exchange interaction. This results in **ferromagnetic** ordering, in which all the spins within a magnetic domain (typically hundreds of unit cells in width) have the same orientation, as shown in the figure at the right. Conversely, a negative exchange interaction between neighboring atoms in bcc Cr results in **antiferromagnetic** ordering. A third arrangement, **ferrimagnetic** ordering, results from an antiparallel alignment of spins on neighboring atoms when the magnetic moments of the neighbors are unequal. In this case, the spin moments do not cancel and there is a net magnetization. The ordering mechanism is like that of an antiferromagnetic solid, but the magnetic properties resemble those of a ferromagnet. Ferrimagnetic ordering is most common in metal oxides, as we will learn in Chapter 7.

Magnetization and susceptibility

The **magnetic susceptibility**, **χ**, of a solid depends on the ordering of spins. Paramagnetic, ferromagnetic, antiferromagnetic, and ferrimagnetic solids all have $\chi > 0$, but the magnitude of their susceptibility varies with the kind of ordering and with temperature. We will see these kinds of magnetic ordering primarily among the **3d** and **4f** elements and their alloys and compounds. For example, Fe, Co, Ni, $Nd_2Fe_{14}B$, $SmCo_5$, and YCo_5 are all ferromagnets, Cr and MnO are antiferromagnets, and Fe_3O_4 and $CoFe_2O_4$ are ferrimagnets. Diamagnetic compounds have a weak *negative* susceptibility ($\chi < 0$).

Definitions

- H = applied magnetic field (units: Henry (H))
- B = induced magnetic field in a material (units: Tesla (T))
- M = magnetization, which represents the magnetic moments within a material in the presence of an external field H.

Magnetic susceptibility $\chi = M/H$

Usually, χ is given in *molar* units in the *cgs system*:

χ_M = molar susceptibility (units: cm^3/mol)

Typical values of χ_M:

Compound	Type of Magnetism	χ at 300K (cm^3/mol)
SiO_2	Diamagnetic	-3×10^{-4}
Pt metal	Pauli paramagnetic	$+2 \times 10^{-4}$
$Gd_2(SO_4)_3 \cdot 8H_2O$	Paramagnetic	$+5 \times 10^{-2}$
Ni-Fe alloy	Ferromagnetic	$+10^4 - 10^6$

To correlate χ with the number of unpaired electrons in a compound, we first correct for the small diamagnetic contribution of the core electrons:

$$\chi^{corr} = \chi^{obs} - \chi^{diamagnetic\ cores} \tag{9.5.1}$$

Susceptibility of paramagnets

For a paramagnetic substance,

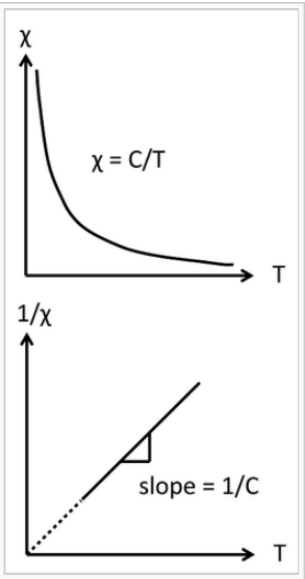
$$\chi_M^{corr} = \frac{C}{T} \tag{9.5.2}$$

The inverse relationship between the magnetic susceptibility and T, the absolute temperature, is called **Curie's Law**, and the proportionality constant C is the **Curie constant**:

$$C = \frac{N_A}{3k_B}\mu_{eff}^2 \tag{9.5.3}$$

Note that C is not a "constant" in the usual sense, because it depends on μ_{eff}, the **effective magnetic moment** of the molecule or ion, which in turn depends on its number of unpaired electrons:

$$\mu_{eff} = \sqrt{n(n+2)}\mu_B \tag{9.5.4}$$



Curie law behavior of a paramagnet. A plot of 1/χ vs. absolute temperature is a straight line, with a slope of 1/C and an intercept of zero.

Here μ_B is the Bohr magneton, a physical constant defined as $\mu_B = eh/4\pi m_e = 9.274 \times 10^{-21}$ erg/gauss (in cgs units).

In cgs units, we can combine physical constants,

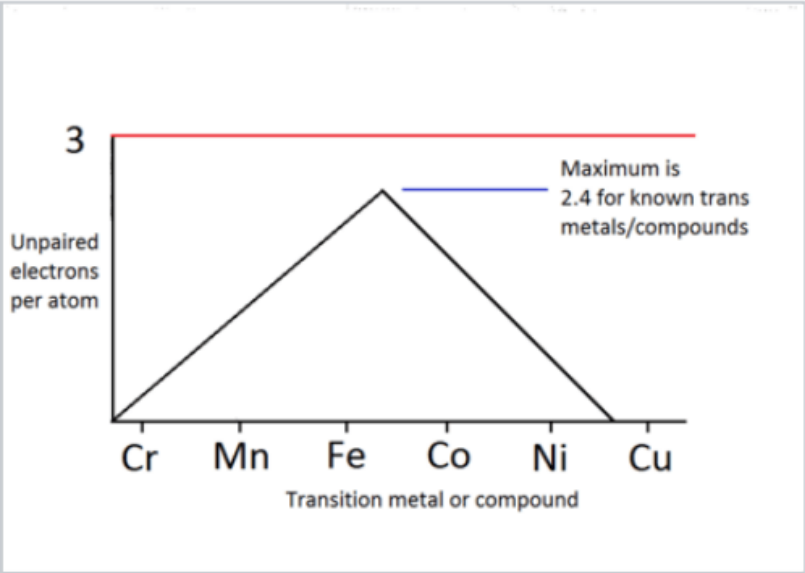
$$\frac{N_A}{3k_B}\mu_B^2 = .125 \tag{9.5.5}$$

Combining these equations, we obtain

$$\chi_M^{corr} = \frac{.125}{T}\left(\frac{\mu_{eff}}{\mu_B}\right)^2 \tag{9.5.6}$$

These equations relate the molar susceptibility, a bulk quantity that can be measured with a magnetometer, to μ_{eff}, a quantity that can be calculated from the number of unpaired electrons, n. Two important points to note about this formula are:

- The magnetic susceptibility is inversely proportional to the absolute temperature, with a proportionality constant C (Curie's Law)
- So far we are talking only about paramagnetic substances, where there is no interaction between neighboring atoms.



Number of unpaired electrons per atom, determined from Curie constants of transition metals and their 1:1 alloys.

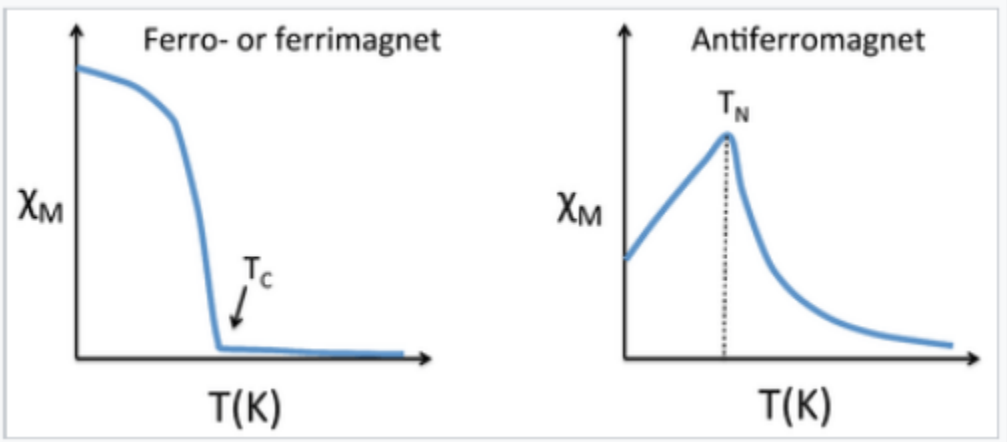
Returning to the isolated Fe atom with its three unpaired electrons, we can measure the Curie constant for iron metal (above the temperature of its transition to a paramagnetic solid) and compare it to the calculation of μ_{eff}. Since n = 3, we calculate:

$$\mu_{eff} = \sqrt{(3)(5)}\mu_B = 3.87\mu_B \tag{9.5.7}$$

The plot at the right shows the number of unpaired electrons per atom, calculated from measured Curie constants, for the magnetic elements and 1:1 alloys in the 3d series. The plot peaks at a value of 2.4 spins per atom, slightly lower than we calculated for an isolated iron atom. This reflects that fact that there is some pairing of d-electrons, i.e., that they do contribute somewhat to bonding in this part of the periodic table.

Susceptibility of ferro-, ferri-, and antiferromagnets

Below a certain critical temperature, the spins of a solid paramagnetic substance order and the susceptibility deviates from simple Curie-law behavior. Because the ordering depends on the short-range exchange interaction, this critical temperature varies widely. Metals and alloys in the 3d series tend to have high critical temperatures because the atoms are directly bonded to each other and the interaction is strong. For example, Fe and Co have critical temperatures (also called the Curie temperature, T_c, for ferromagnetic substances) of 1043 and 1400 K, respectively. The Curie temperature is determined by the strength of the magnetic exchange interaction and by the number of unpaired electrons per atom. The number of unpaired electrons peaks between Fe and Co as the d-band is filled, and the exchange interaction is stronger for Co than for Fe. In contrast to ferromagnetic metals and alloys, paramagnetic salts of transition metal ions typically have critical temperatures below 1K because the magnetic ions are not directly bonded to each other and thus their spins are very weakly coupled in the solid state. For example, in gadolinium sulfate, the paramagnetic Gd^{3+} ions are isolated from each other by SO_4^{2-} ions.

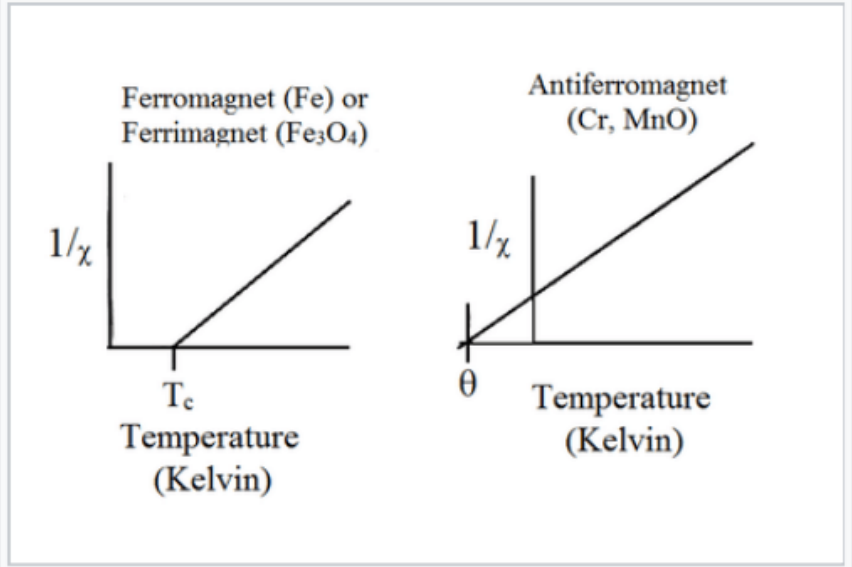


Magnetic susceptibility vs temperature (Kelvin) for ferrimagnetic, ferromagnetic, and antiferromagnetic materials

Above the critical temperature T_C, **ferromagnetic** compounds become paramagnetic and obey the **Curie-Weiss law:**

$$\chi = \frac{C}{T - T_c} \tag{9.5.8}$$

This is similar to the Curie law, except that the plot of 1/χ vs. T is shifted to a positive intercept T_C on the temperature axis. This reflects the fact that ferromagnetic materials (in their paramagnetic state) have a greater tendency for their spins to align in a magnetic field than an ordinary paramagnet in which the spins do not interact with each other. Ferrimagnets follow the same kind of ordering behavior. Typical plots of χ vs. T and 1/χ vs. T for ferro-/ferrimagnets are shown above and below.



Plots of 1/χ vs. T for ferromagnets, ferrimagnets, and antiferromagnets.

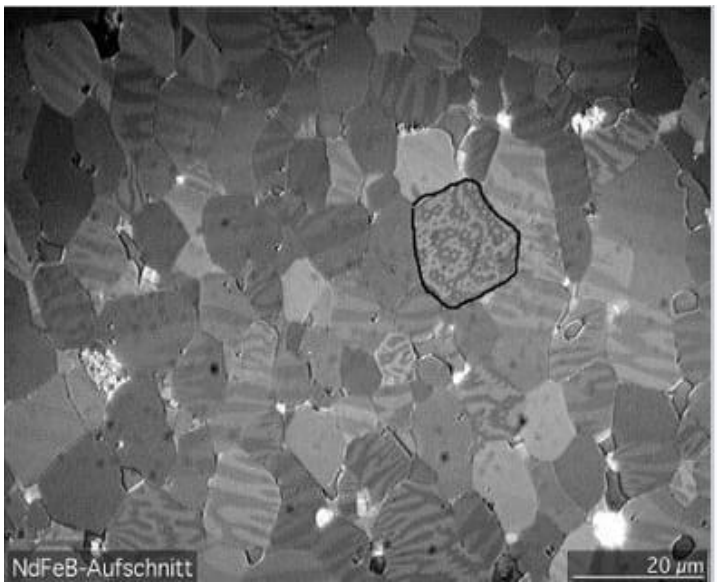
Antiferromagnetic solids are also paramagnetic above a critical temperature, which is called the Néel temperature, T_N. For antiferromagnets, χ reaches a maximum at T_N and is smaller at higher temperature (where the paramagnetic spins are further disordered by thermal energy) and at lower temperature (where the spins pair up). Typically, antiferromagnets retain some positive susceptibility even at very low temperature because of canting of their paired spins. However the maximum value of χ is much

lower for an antiferromagnet than it is for a ferro- or ferrimagnet. The Curie-Weiss law is also modified for an antiferromagnet, reflecting the tendency of spins (in the paramagnetic state above T_N) to resist parallel ordering. A plot of $1/\chi$ vs. T intercepts the temperature axis at a negative temperature, $-\theta$, and the Curie-Weiss law becomes:

$$\chi = \frac{C}{T + \theta} \tag{9.5.9}$$

Ordering of spins below T_C

Below T_C, the spins align spontaneously in ferro- and ferrimagnets. Complex magnetization behavior is observed that depends on the history of the sample. For example, if a ferromagnetic material is cooled in the absence of an applied magnetic field, it forms a mosaic structure of magnetic domains that each have internally aligned spins. However, neighboring domains tend to align the opposite way in order to minimize the total energy of the system. This is illustrated in the figure at the left for a Nd-Fe-B magnet. The sample consists of 5-10 μm wide crystal grains that can be easily distinguished by the sharp boundaries in the image. Within each grain are a series of lighter and darker stripes (imaged by using the optical Kerr effect) that are ferromagnetic domains with opposite orientations. Averaged over the whole sample, these domains have random orientation so the net magnetization is zero.



Microcrystalline grains within a piece of $Nd_2Fe_{14}B$ (the alloy used in neodymium magnets) with magnetic domains made visible with a Kerr microscope. The domains are the light and dark stripes visible within each grain.

When a sample like this one is magnetized (i.e., exposed to a strong magnetic field), the domain walls move and the favorably aligned domains grow at the expense of those with the opposite orientation. This transformation can be seen in real time in the Kerr microscope. The domain walls are typically hundreds of atoms wide, so movement of a domain wall involves a cooperative tilting of spin orientation (analogous to "the wave" in a sports stadium) and is a relatively low energy process.

The movement of domain walls in a grain of silicon steel is driven in this movie by increasing the external magnetic field in the "downward" direction, and is imaged using a Kerr microscope. White areas are domains with their magnetization directed up, dark areas - which eventually comprise the entire grain - are domains with their magnetization directed down.

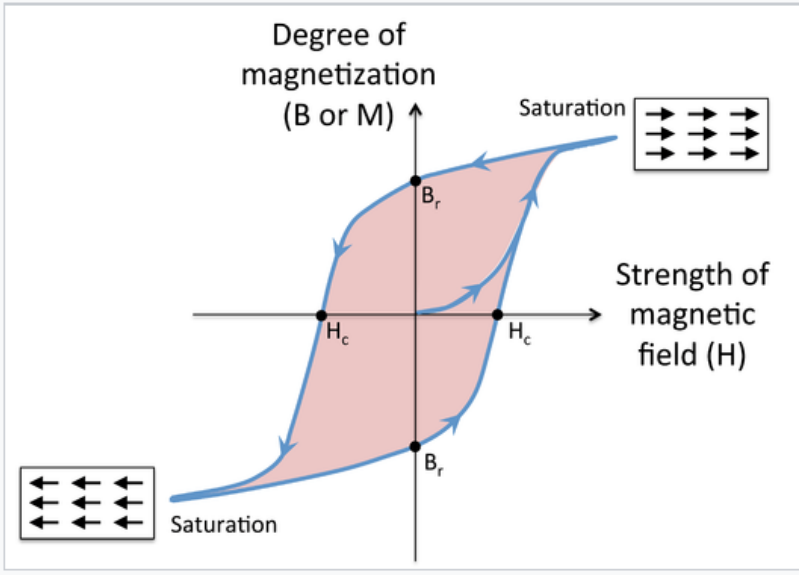
The process of magnetization moves the solid away from its lowest energy state (random domain orientation), so magnetization involves input of energy. When the external magnetic field is removed, the domain walls relax somewhat, but the solid (especially

in the case of a "hard" magnet) can retain much of its magnetization. If you have ever magnetized a nail or a paper clip by using a permanent magnet, what you were doing was moving the walls of the magnetic domains inside the ferromagnet. The object thereafter retains the "memory" of its magnetization. However, annealing a permanent magnet destroys the magnetization by returning the system to its lowest energy state in which all the magnetic domains cancel each other.



Rotation of orientation and increase in size of magnetic domains in response to an externally applied magnetic field.

Magnetic hysteresis. Cycling a ferro- or ferrimagnetic material in a magnetic field results in hysteresis in the magnetization of the material, as shown in the figure at the left. At the beginning, the magnetization is zero, but it begins to rise rapidly as the magnetic field is applied. At high field, the magnetic domains are aligned and the magnetization is said to be saturated. When the field is removed, a certain **remanent magnetization** (indicated as the point $\mathbf{B_r}$ on the graph) is retained, i.e., the material is magnetized. Applying a field in the opposite direction begins to orient the magnetic domains in the other direction, and at a field $\mathbf{H_c}$ (the **coercive field**), the magnetization of the sample is reduced to zero. Eventually the material reaches saturation in the opposite direction, and when the field is removed again, it has remanent magnetization Br, but in the opposite direction. As the field continues to reverse, the magnet follows the hysteresis loop as indicated by the arrows. The area of colored region inside the loop is proportional to the magnetic work done in each cycle. When the field cycles rapidly (for example, in the core of a transformer, or in read-write cycles of a magnetic disk) this work is turned into heat.



Magnetization of a ferro- or ferrimagnet vs. applied magnetic field H. Starting at the origin, the upward curve is the initial magnetization curve. The downward curve after saturation, along with the lower return curve, form the main loop. The intercepts Hc and Br are the coercivity and remanent magnetization.

Contributors and Attributions

- Neele Holzenkaempfer, Jesse Gipe
- Chris P Schaller, Ph.D., (College of Saint Benedict / Saint John's University)
- Paul Flowers (University of North Carolina - Pembroke), Klaus Theopold (University of Delaware) and Richard Langley (Stephen F. Austin State University) with contributing authors. Textbook content produced by OpenStax College is licensed under a Creative Commons Attribution License 4.0 license. Download for free at http://cnx.org/contents/85abf193-2bd...a7ac8df6@9.110).
- Jim Clark (Chemguide.co.uk)
- Dr. Richard Spinney (The Ohio State University)

This page titled 9.5: Magnetic Properties of Materials is shared under a license and was authored, remixed, and/or curated by LibreTexts.

- 24.6: Magnetic Properties of Coordination Compounds and Crystal Field Theory is licensed CC BY-NC-SA 4.0.
- 23.5: Color and Magnetism is licensed CC BY-NC-SA 3.0.
- 6.8: Ferro-, Ferri- and Antiferromagnetism by Chemistry 310 is licensed CC BY-SA 4.0. Original source: https://en.wikibooks.org/wiki/Introduction_to_Inorganic_Chemistry.

10: THERMODYNAMICS, TRENDS IN METAL COMPLEX STABILITY



CHEM 431: *Inorganic Chemistry*
Fall 2020: Dr. Kathryn Haas

10.1: Introduction to Substitution Reactions
10.2: Metal-Ligand Association Constants
10.3: Trends in M-L stability (Thermodynamics)

This page titled 10: Thermodynamics, Trends in Metal Complex Stability is shared under a license and was authored, remixed, and/or curated by LibreTexts.

10.1: Introduction to Substitution Reactions

Chemical Reactivity and Reactions of Complexes

In this chapter we will discuss the chemical reactivity and reactions of coordination compounds. First, let us briefly review what are the basic parameters that define if a reaction can be observed or not. The first parameter is the Gibbs free energy of reaction ΔG. The Gibbs free energy defines the thermodynamic driving force for the reaction. The more negative ΔG is, the greater the thermodynamic driving force. The Gibbs free energy of reaction is a measure for the difference in the stability of the reactants and products. The less stable the reactants, and the more stable the products, the more negative ΔG. The second parameter is the kinetics of a reaction. The kinetics is a measure of the speed at which a reaction occurs. The kinetics is independent from the thermodynamics. This means that even if there is a strong thermodynamic driving force for the reaction, the rate of the reaction may be extremely slow, and practically no reaction is observed. For example, graphite is thermodynamically more stable than diamond at ambient pressure and temperature, but the kinetics of the conversion at room temperature is so slow, so that practically no reaction is observed. The rate of the reaction is determined by the the activation energy that needs to be overcome to make the reaction happen. The lower the activation energy, the faster the reaction. In coordination chemistry the activation energy and the reaction rates are associated with the inertness and the lability of complexes. The more inert and the less labile a complex is the higher the activation barrier and the more slowly it reacts. The lability is the opposite of the inertness and is defined by the half-life time of a dative bond. The greater the half-life time, the more inert, and the less labile the complex.

Inert and Labile Complexes

The greater the half-life time of a dative bond, the more inert, and the less labile the complex. Where do we actually draw the borderline between a labile and an inert complex? A commonly accepted definition is that complexes with metal-ligand bond half life times of <30 s at standard conditions are considered labile complexes with a low activation energy. Those complexes undergo fast substitution reactions, and the chemical equilibrium is reached fast (Fig. 9.1.1).

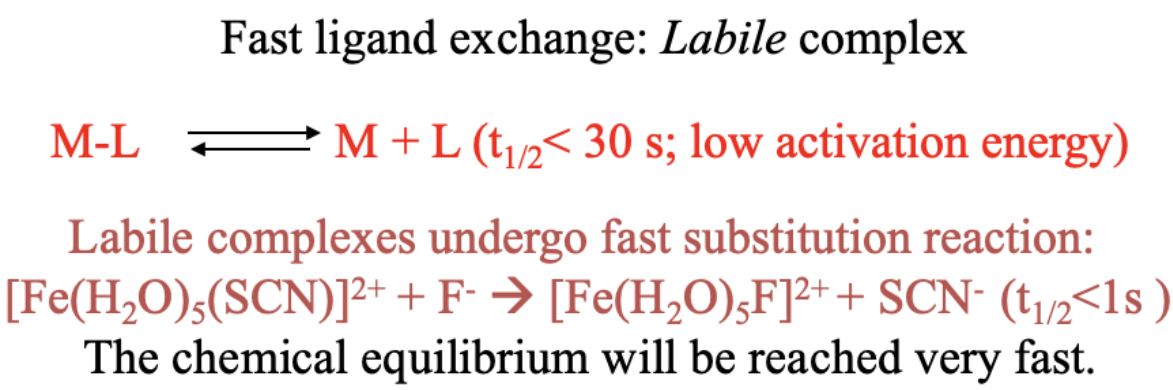


Figure 9.1.1 Properties of labile complexes

An example is the substitution of a thiocyanato ligand in a pentaaquathiocyanato iron (2+) complex by a fluoro ligand. This substitution reaction is fast because the half-life time of the metal-ligand bond is smaller than a second.

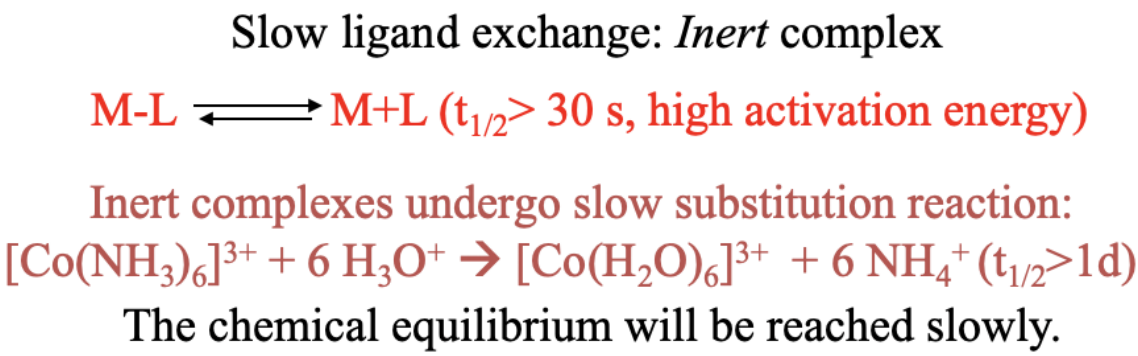


Figure 9.1.2 Properties of inert complexes

If the half-life time is greater than 30s, then the complex is considered inert. For example, the hydrolysis of hexaammine cobalt (3+) is slow because the half-life time of the Co-N bond is larger than a day. The chemical equilibrium is reached only slowly (Fig. 9.1.2).

Can we predict which complexes are labile, and which ones are inert? Many factors determine this, but there are some trends we can keep in mind. For transition metals, octahedral d^3, low spin d^4-d^6, and square planar d^8 complexes tend to be inert. A second trend is that the lability decreases with the period within a group. For instance, we would expect that in group 10 the lability decreases from Ni to Pd to Pt. This is because covalency of the bonds tends to increase with increasing period due to the softer nature of higher period metals. A third trend is that higher positive charges at the metal ion lead to a decrease in liability. Metal ions with higher oxidation numbers also tend to make more covalent bonds because the high positive charge at the metal is stabilized by covalent interactions (Fig. 9.1.3).

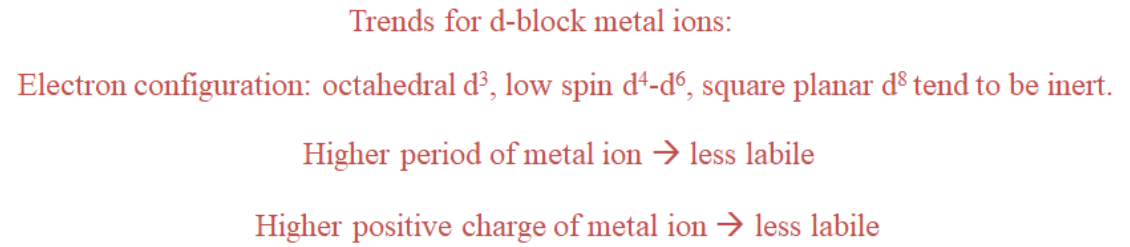


Figure 9.1.3 Trends for d-block metal ions

We can also compare the d-block metals with the other blocks. S-block metal complexes tend to have the greatest lability, followed by the f-block, followed by the d-block. P-block metal complexes can widely vary in lability (Fig. 9.1.4).

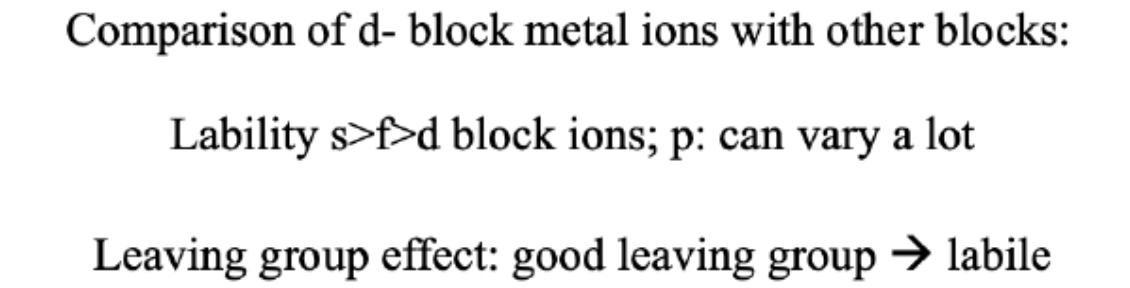


Figure 9.1.4 Trends for the blocks and leaving groups

Also the nature of the ligand influences the lability. Generally, when the ligand is a good leaving group, then the bond tends to be labile. A ligand is usually a good leaving group when it is stable in the uncoordinated form. For instance, a chloro ligand is a good leaving group because chloride anions are quite stable in their non-coordinated form. An alkyl ligand on the other hand would not be considered as a good leaving group because the an alkylide anion is not a very stable species in the free form.

Stability of Complexes

Now let us have a closer look at the stability of complexes. The more negative the Gibbs free energy of formation, the greater the equilibrium constant of formation K. The larger the equilibrium constant K of formation, the more stable the complex. This can be expressed by the van't Hoff equation $\Delta G = -RT\ln K$.

$$M + L \rightarrow M\text{-}L \quad \Delta G<0$$

$$K = \frac{[ML]}{[M]\,[L]}$$

Figure 9.1.5 Equilibrium constant for a reaction that forms a single metal-ligand bond. Reaction proceeds to the right if $\Delta G<0$.

For the formation of a single dative bond M-L the constant of formation is given by K=[ML]/[M][L] (Fig. 9.1.5). The greater K, the farther the equilibrium is on the side of the product. K is usually reported as logK because K can vary over 35 orders of magnitude.

Rationalizing the Different Stability of Complexes

How can we rationalize the different stabilities of coordination bonds, and coordination compounds? Here, the HSAB concept is very useful. Hard-hard and soft-soft interactions are typically strong and lead to high constants of formation and stable complexes. Hard-soft interactions lead to small constants of formation and less stable complexes.

	hardest			softest
	NH_3	F^-	Cl^-	Br^-
Ag^+	3.30	-0.17	3.08	4.30
soft				

Figure 9.1.6 Formation constants log K for Ag^+ complexes

Let us understand this better by the example of the interaction of Ag^+ with different ligands (Fig. 9.1.6). You can see in the table the logK values for the different ligands. Br^- has the largest one, followed by NH_3 and Cl^-. F^- has the smallest one. Can we explain this with the HSAB concept? Ag^+ is a soft cation, thus it would be expected to make the strongest interactions with the softest ligand. Bromide is the softest of the four, and hence HSAB correctly predicts the stability. F^- is the hardest ligand and would be expected to make the weakest complex. This is in accordance with the small logK value for F^-. NH_3 and Cl^- have similar intermediate hardness, which is consistent with the similar, intermediate logK values.

Stabilities of Multi-ligand Complexes

Example ML_4

1.	$M + L \rightarrow ML$	$K_1 = [ML] / [M] [L]$
2.	$ML + L \rightarrow ML_2$	$K_2 = [ML_2] / [ML] [L]$
3.	$ML_2 + L \rightarrow ML_3$	$K_3 = [ML_3] / [ML_2] [L]$
4.	$ML_3 + L \rightarrow ML_4$	$K_4 = [ML_4] / [ML_3] [L]$

$$K_1 > K_2 > K_3 > K_4$$

Figure 9.1.7 Equilibria associated with a complex of the composition ML_4

How does the stability of a complex change as more ligands are added? Let us take a look at the constants of formation to answer the question. The addition of an additional ligand is associated with an additional chemical equilibrium which relates to an additional constant of formation. The number of equilibrium constants is equal to the number of ligands. For instance, when we have a complex ML_4 with four ligands, then for the addition of the first ligand we get a constant K_1= [ML] / [M] [L] , for the second ligand we get a constant K_2=[ML_2] / [ML] [L] , for the third ligand there is a constant K_3=[ML_3] / [ML_2] [L], and for the fourth ligand there is a constant K_4=[ML_4] / [ML_3] [L]. When we analyze the K-values, we notice that they decline from K_1 to K_4. For a general complex ML_n we find that the constants decline from K_1 to K_n. How can this be explained? The explanation is that the more ligands are getting added, the less many free ligands are available that could be further added. Thus, the probability that further ligands are added decreases, and this results in a smaller equilibrium constant. So it is a statistical effect that explains the phenomenon.

The stepwise and overall stability constants K are related as follows:

ML_4: $K = K_1.K_2.K_3.K_4$

ML_n: $K = K_1.K_2.....K_n$

Figure 9.1.8 Overall stability constants for a general complex ML_n

Then what is the overall stability constant K of the complex associated with the equation M + 4 L → ML_4 and more general M + nL → ML_n? It is the product of the constants associated with each step. For the complex ML_4 it is $K=K_1K_2K_3K_4$. For the general complex ML_n it is $K=K_1K_2.....K_n$ (Fig. 9.1.8).

There are exceptions from the rule that the stability constants of complexes associated with the addition of one ligand decreases with the number of ligands. If there is an exception, then this is because the ligand addition causes a major change in the electronic structure of the complex. Here are a couple of examples.

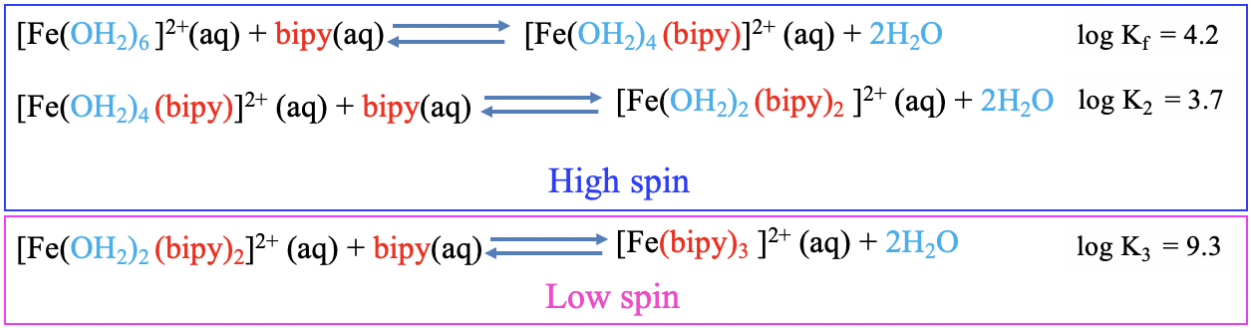


Figure 9.1.9 Example 1 for exceptions to the rule for stability constants

In the first example (Fig. 9.1.9) the aqua ligands of a hexaaqua iron (2+) complex are substituted by bipyridyl ligands. The bipyridyl ligand is a bidentate ligand, and so one bipydridyl ligand substitutes two aqua ligands. In the first substitution, the two aqua ligands get replaced by one bipyridyl ligand to form a tetraaqua(bipyridyl) iron (2+) complex. This step is associated with a $\log K_1$ value of 4.2.

In the second substitution step, two aqua ligands of the tetraaqua(bipyridyl) iron (2+) complex get replaced by another bipyridyl ligand to form a diaqua bis(bipyridyl) iron(2+) complex. As expected this step is associated with a smaller $\log K_2$ value of 3.7.

In the third step, the last two aqua ligands get substituted by another bipyridyl ligand forming a tris(bipyridyl) iron(2+) complex. What is the $\log K_3$ value? It is 9.3! This is much larger than $\log K_1$ and $\log K_2$, so this result is unexpected. A major change in electronic structure must have occurred. What is it? In this case it is a change from a high-spin to a low spin complex. The bipyridyl ligands are strong π-acceptors that increase Δ_o. Substitution of the first four aqua ligands increases Δ_O but the increase is not large enough yet so that it induces a switch from a high-spin to a low-spin complex. Only the third bipyridyl ligand does that. As a consequence, the formation constant $\log K_3$ is unusually large.

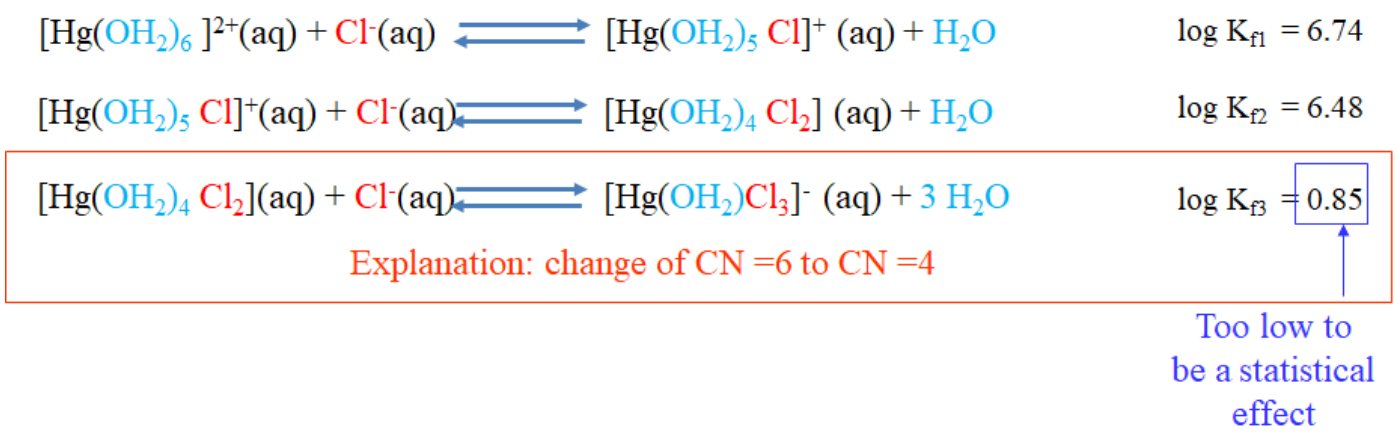


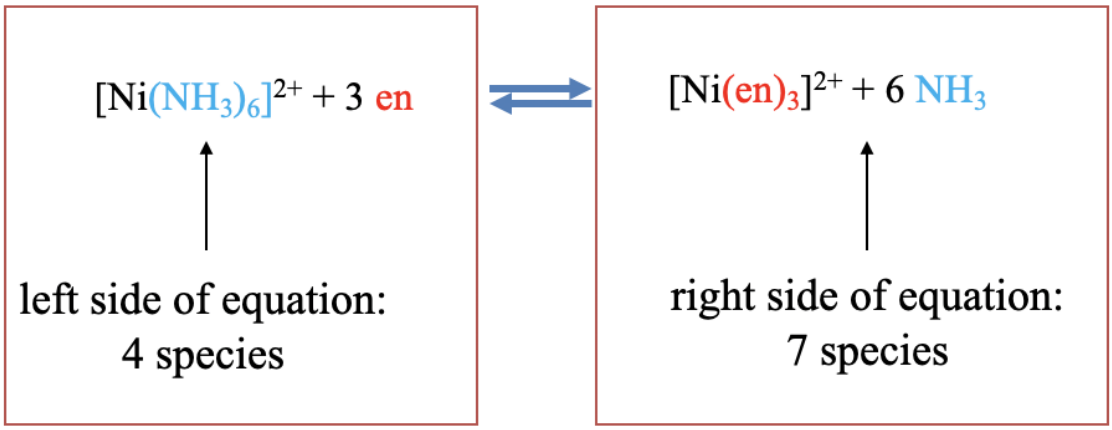
Figure 9.1.10 Example 2 for exceptions to the rule for stability constants

In the second example (Fig. 9.1.10) we subsequently substitute aqua ligands by chloroligands in a hexaaqua mercury(2+) complex. The first substitution leads to a pentaaquachloro mercury(+) complex. This reaction is associated with a $\log K_1$ value of 6.74. The second substitution leads to a tetraaquadichloro mercury(0) complex, and this reaction is associated with a smaller $\log K_2$ value of 6.48. The third substitution reaction leads to an aquatrichloro mercury(1-) complex. The $\log K_3$ value for this reaction is 0.85. We see that this value is smaller than $\log K_2$, and this is what we expected, but the difference between $\log K_3$ and $\log K_2$ is much larger than that between $\log K_1$ and $\log K_2$. The increased difference is too large to be just caused by a statistical effect, but must be induced by a change in electronic structure. In this case it is a change in coordination number. As the third chloro ligand is added, the complex does not lose only one but three aqua ligands. This reduces the coordination number from six to four.

Stability of Chelate Complexes

The Thermodynamic Chelate Effect

Chelating complexes tend to be more stable than complexes with monodentate ligands. This is called the “thermodynamic chelate effect”. The effect deserves an explanation. The explanation is the increase of entropy that occurs when two or more monodentate ligands are replaced by a chelating ligand. The entropy increases because the overall number of particles increases as the substitution takes place.



$$\Delta S° = +88 \text{ J K}^{-1} \text{ mol}^{-1}$$

Figure 9.1.11 Example of the thermodynamic chelate effect

For example, the substitution of six ammine ligands in the hexaammine nickel (2+) complex by three ethylenediamine chelating ligands increases the number of molecules from four to seven, and hence the entropy increases, in this case by 88 J K^{-1} and mol^{-1} (Fig. 9.1.11)

The Kinetic Chelate Effect

In addition to the thermodynamic chelate effect, there is the kinetic chelate effect. Chelate complexes are frequently more inert than complexes with monodentate ligands. Chelate complexes are more inert for two reasons (Fig. 9.1.12).

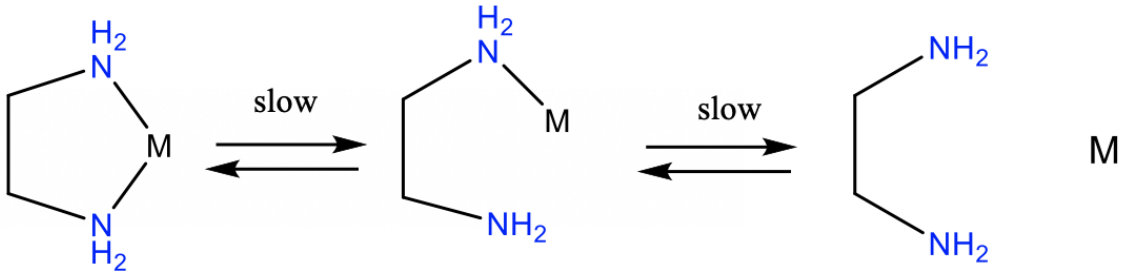
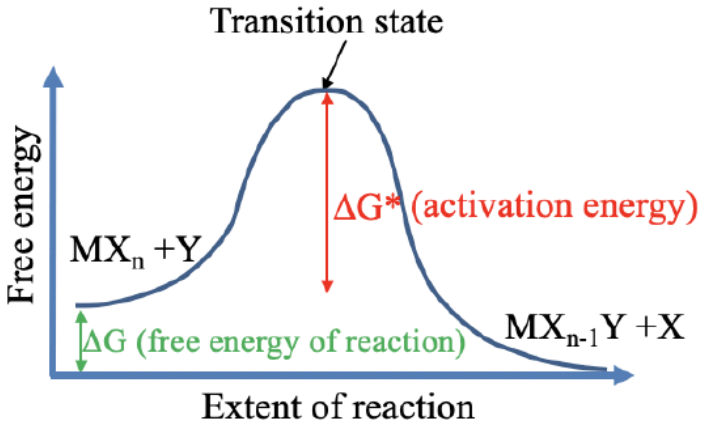


Figure 9.1.12 Illustration of the kinetic chelate effect

Firstly, the whole ligands needs to rotate and bend in order to cleave the first metal-ligand bond. This requires time and slows the kinetics of the bond cleavage. The second reason is that the detached donor atom cannot leave the proximity of the complex because the ligand is still attached via the other donor atom. This increases the probability of the re-formation of the metal-ligand bond which decreases the probability of both bonds being cleaved.

Mechanism of Ligand Substitution Reactions

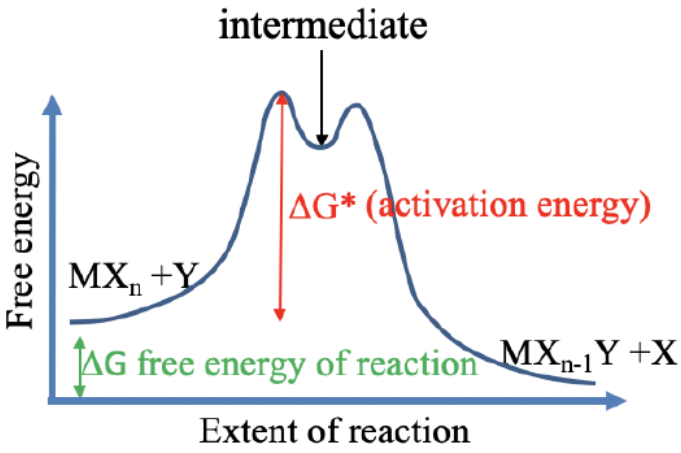
Now let us talk about the mechanism of ligand substitution reactions. We know two basic mechanisms according to which a ligand substitution can occur. One is called the intimate mechanism, and the other one is called the stoichiometric mechanism.



Intimate mechanism

Figure 9.1.13 Intimate mechanism

The intimate mechanism goes through a single transition state as the reaction proceeds.



Stoichiometric mechanism

Figure 9.1.14 Stoichiometric mechanism

The stoichiometric mechanism goes through an intermediate. The intermediate is a shallow local minimum on the reaction coordinate. The transition state is the maximum on the reaction coordinate. For both mechanisms the principle of microscopic reversibility holds. This means that the reverse reaction follows the same free energy path as the forward reaction. For both mechanisms the free Gibbs energy of reaction is given by the difference between the free energy of the products and the free energy of the reactants. The reaction can only spontaneously occur if the free energy of the products is smaller than the free energy of the reactants. The activation energy is the free energy difference between the transition state and the reactants.

Classifications of Mechanisms

There are two forms of the stoichiometric mechanism: The dissociate mechanism D and the associative mechanism A. In the dissociative mechanism (Fig. 9.1.15), an old ligand X is lost first, and the intermediate has a lower coordination number. In the associative mechanism (Fig. 9.1.16), the new ligand Y is added first and the intermediate has a higher coordination number. The intermediates must be detectable, thus must be present in relatively high concentration to measurable with an analytical technique. This requires are relatively deep local thermodynamic minimum for the intermediate. In practice, many local minima are too shallow to allow for the clear detection of the intermediate. We call such a mechanism an Interchange mechanism. There are two forms of interchange mechanisms: I_a and I_d. I_a stands for associative interchange mechanism and I_D stands for dissociative interchange mechanism. Overall we can have a continuous range of mechanisms that range from A to I_a to intimate to I_d to D.

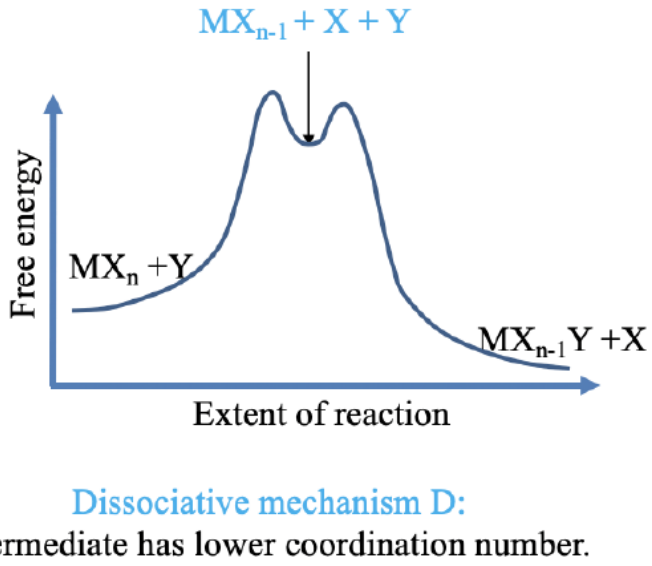


Figure 9.1.15 Dissociative mechanism

For a dissociative and the I_d mechanism the dissociation is the rate limiting step. This is because the activation energy is associated with the dissociative step. We need to go strongly uphill to achieve dissociation, and go into the local thermodynamic minimum. From, there we only need to go slightly uphill to add the new ligand.

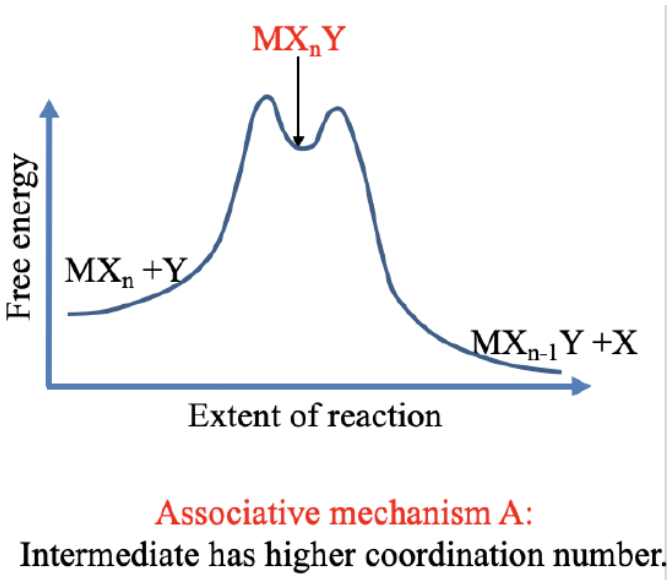


Figure 9.1.16 Associative mechanism

For the associative and the I_a mechanism (Fig. 9.1.16), the associative step is the rate limiting step because the activation energy is associated with the associative step. In this case we first need to go energetically strongly uphill to achieve association and reach the local thermodynamic minimum. We only need to go slightly uphill from the local thermodynamic minimum to lose the old ligand.

How to Distinguish Between D/I_d and A/A_d

We can use the relationships between the rate determining step and the mechanism to experimentally distinguish between associative A/I_a and dissociative D/I_d mechanisms. If the reaction rate strongly depends on the new ligand, then we likely have an associative or I_a mechanism. This is because the associative step is the rate determining step. If the reaction rate does not strongly depend on the new ligand, then the mechanism is likely dissociative D or I_d. This is because in the dissociate mechanism, the addition of the new ligand is not the rate-determining step.

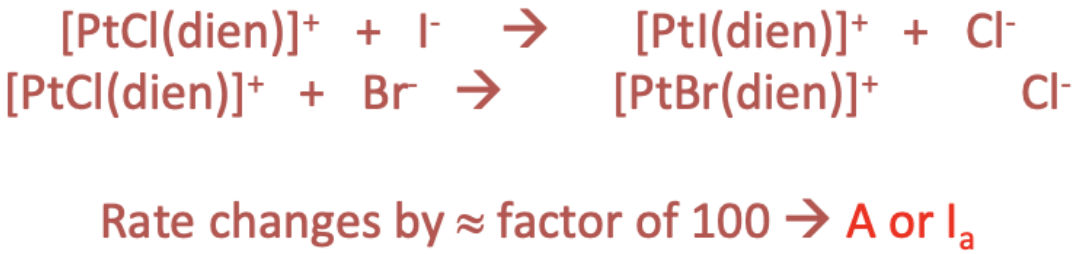


Figure 9.1.17 Distinguishing between D/I_d and A/A_d

For example, we can substitute a chloro ligand in a $[PtCl(dien)]^+$ complex by iodo and bromo ligands, respectively (Fig. 9.1.17). What we measure is that the reaction rates are by a factor of 100 different. This means that the reaction rates does depend on the new ligand and this indicates an associative or I_a mechanism.

Steric arguments can help to predict if a mechanism is associative or dissociative. Lower coordination numbers and little steric crowding tends to favor A and I_a mechanisms, while higher coordination numbers and greater steric crowding tend to favor the dissociative mechanism.

Dr. Kai Landskron (Lehigh University). If you like this textbook, please consider to make a donation to support the author's research at Lehigh University: Click Here to Donate.

This page titled 10.1: Introduction to Substitution Reactions is shared under a license and was authored, remixed, and/or curated by Kai Landskron.

- 9.1: Substitution Reactions and their Mechanisms by Kai Landskron is licensed CC BY 4.0.

10.2: Metal-Ligand Association Constants



Introduction

The thermodynamic stability of a coordination complex is defined according the the equilibrium constant of its formation reaction. And since its formation is a many-step process, there are many reactions to consider. The **absolute formation** of a metal complex is defined by an equilibrium reaction that is independent of solution conditions and is expressed as if all ligands associate to the metal ion at once (this is practically impossible when there are multiple ligands). This *absolute formation* also accounts for all H^+ ions that may be released from the ligand when it binds to the metal ion. The *absolute formation* of a Cu complex is defined below.

$$m\mathrm{Cu} + l\mathrm{L} + h\mathrm{H} \rightarrow \mathrm{Cu}_m\mathrm{L}_l\mathrm{H}_h \tag{10.2.1}$$

$$\beta_{lmh} = \frac{[\mathrm{Cu}_m\mathrm{L}_l\mathrm{H}_h]}{[\mathrm{Cu}]^m[\mathrm{L}]^l[\mathrm{H}]^h} \tag{10.2.2}$$

Notice that, according to the equation above, H^+ ions are involved in this reaction, thus the reaction is pH-dependent. Most metal-ligand formations are dependent on pH because by its nature, a ligand is a Lewis Bases that can react with H^+. If we are interested in the thermodynamics in the context of aqueous solution, the β value is not very useful; what we would actually want is a pH-dependent **conditional** affinity constant, (K_{cond}), that can be calculated from the β and the pK_a values of the ligands. Alternatively, an **apparent** binding constant (K_{app}, also called K_{eff} for **effective** affinity constant) can be measured directly as the equilibrium constant under the specified solution conditions of *pH and buffer components*. An in-depth explanation of the relationship between β, K_{cond}, and K_{app} is given below.

Ligand Protonation Constants

General treatment of ligand protonation constants for a ligand with four dissociable protons is shown below:

Stepwise Ligand Protonation Constants

$$\begin{aligned}
\mathrm{L}^{(\mathrm{n})} + \mathrm{H}^+ &\overset{\beta_1=K_{a1}}{\rightleftharpoons} \mathrm{LH}^{(\mathrm{n}+1)} && K_{a1} = \frac{[\mathrm{LH}]}{[\mathrm{L}][\mathrm{H}]} = \beta_1 \\
\mathrm{LH}^{(\mathrm{n}+1)} + \mathrm{H}^+ &\overset{K_{a2}}{\rightleftharpoons} \mathrm{LH}_2^{(\mathrm{n}+2)} && K_{a2} = \frac{[\mathrm{LH}_2]}{[\mathrm{LH}][\mathrm{H}]} \\
\mathrm{LH}_2^{(\mathrm{n}+2)} + \mathrm{H}^+ &\overset{K_{a3}}{\rightleftharpoons} \mathrm{LH}_3^{(\mathrm{n}+3)} && K_{a3} = \frac{[\mathrm{LH}_3]}{[\mathrm{LH}_2][\mathrm{H}]} \\
\mathrm{LH}_3{}^{(\mathrm{n}+3)} + \mathrm{H}^+ &\overset{K_{a4}}{\rightleftharpoons} \mathrm{LH}_4^{(\mathrm{n}+4)} && K_{a4} = \frac{[\mathrm{LH}_4]}{[\mathrm{LH}_3][\mathrm{H}]}
\end{aligned} \tag{10.2.3}$$

Absolute Ligand Protonation Constants

$$\begin{aligned}
&\mathrm{L^{(n)} + H^+ \overset{\beta_1 = K_{a1}}{\rightleftharpoons} LH^{(n+1)}} && \beta_1 = \frac{[\mathrm{LH}]}{[\mathrm{L}][\mathrm{H}]} = K_{a1} \\
&\mathrm{L^{(n)} + 2H^+ \overset{\beta_2}{\rightleftharpoons} LH_2^{(n+2)}} && \beta_2 = \frac{[\mathrm{LH_2}]}{[\mathrm{L}][\mathrm{H}]^2} = K_{a1}K_{a2} \\
&\mathrm{L^{(n)} + 2H^+ \overset{\beta_3}{\rightleftharpoons} LH_3^{(n+3)}} && \beta_3 = \frac{[\mathrm{LH_3}]}{[\mathrm{L}][\mathrm{H}]^3} = K_{a1}K_{a2}K_{a3} \\
&\mathrm{L^{(n)} + 2H^+ \overset{\beta_4}{\rightleftharpoons} LH_4^{(n+4)}} && \beta_4 = \frac{[\mathrm{LH_4}]}{[\mathrm{L}][\mathrm{H}]^4} = K_{a1}K_{a2}K_{a3}K_{a4}
\end{aligned} \tag{10.2.4}$$

For the purpose of defining protonation constants in terms of absolute values and stepwise values, it is useful to start with a specific example. Here we will use glycine. Many of us are familiar with protonation constants as pKa values, or stepwise protonation constants. For glycine, the stepwise protonation events can be defined as dissociation events or association events. The stepwise association equilibria for glycine are below. The dissociation equilibrium would be written in the apposite direction and their equilibria constants would be defined as the inverse of the association constant expression.

$$\mathrm{Gly^{2-} + H^+ \overset{\beta_1 = K_1}{\rightleftharpoons} GlyH^{1-}} \qquad \beta_1 = K_1 = \frac{[\mathrm{GlyH^{-1}}]}{[\mathrm{Gly^{-2}}][\mathrm{H^+}]} \tag{10.2.5}$$

$$\mathrm{GlyH^{1-} + H^+ \overset{K_2}{\rightleftharpoons} GlyH_2} \qquad K_2 = \frac{[\mathrm{GlyH_2}]}{[\mathrm{GlyH^{-1}}][\mathrm{H^+}]} \tag{10.2.6}$$

Take the log of K_1 or K_2 to find pK_1 or pK_2.

Many people are less familiar with the protonation constants that are defined as absolute association constants, or β values. For the first protonation event of glycine (equ. 10.2.5), the β_1 is defined by the same equilibrium constant expression as the more familiar K_1. However, for the second protonation event, the β value is defined as two protons associating with the unprotonated ligand (equ. 10.2.7 below).

$$\mathrm{Gly^{2-} + 2H^+ \overset{\beta_2 = K_1K_2}{\rightleftharpoons} GlyH_2} \quad \beta_2 = \frac{[\mathrm{GlyH_2}]}{\left[\mathrm{Gly^{-2}}\right]\left[\mathrm{H^+}\right]^2} = K_1K_2 \tag{10.2.7}$$

By multiplying the expression for K1 and K2 (Equations 10.2.5 & 10.2.7), we arrive at the equilibrium constant express ion for β_2 . Notice that β values are absolute and are defined by association of protons to ligand in a single step. On the other hand, K values are stepwise protonation events.

Metal-Ligand Association Constants

The metal-ligand association constant, β, is defined as the pH-independent absolute association constant and is often denoted β_{lm} according to Equation 10.2.8 below. M is metal, L is ligand, and l and m denote the complex $\mathrm{M}_m\mathrm{L}_l$. When $m = 1$ the second subscript is omitted. Sometimes $\mathrm{H^+}$ ion is incorporated into this expression, as seen with Equation 10.2.2. If $\mathrm{H^+}$ ion is incorporated, then the resulting β_{lmh} is pH-dependent because it depends on the hydrogen ion concentration [H]. For the purposes here, $\mathrm{H^+}$ ion is left out of the equation and we use β_{lm} as defined here.

$$m\mathrm{M} + l\mathrm{L} \overset{\beta_{lm}}{\rightleftharpoons} \mathrm{M}_m\mathrm{L}_l \quad \beta_{lm} = \frac{[\mathrm{M}_m\mathrm{L}_l]}{[M]^m[L]^l} \tag{10.2.8}$$

The association of metal and ligand can involve exchange of protons, which can effect the affinity of ligand for metal depending on the pH of solution. The conditional β value is denoted β', or K. The β' is the pH-dependent constant, and is also referred to as the *conditional* constant or *effective* association constant. The absolute β value can be converted into a pH-dependant conditional value as follows:

$$\beta'_{lm} = \frac{\beta_{lm}}{(\alpha_M)^{\mathrm{m}}\,(\alpha_L)^{\mathrm{n}}} \tag{10.2.9}$$

$$\alpha_M = \frac{([\mathrm{M}] + [\mathrm{MOH}] + [\mathrm{M(OH)_2}] + ...)}{[M]} \tag{10.2.10}$$

$$\alpha_L = \frac{([\mathrm{L}] + [\mathrm{LH}] + [\mathrm{LH_2}] + ...)}{[L]} \tag{10.2.11}$$

The expressions for α_M and α_L correspond to the fractions of metal and ligand in solution that do not exist as complexed species with OH or L, respectively. These expressions can be reduced to the following equations.

$$\alpha_M = 1 + 10^{(\mathrm{pH}-\mathrm{pK_{a1}})} + 10^{(2\mathrm{pH}-\mathrm{pK_{a1}}-\mathrm{pK_{a2}})} + ... \tag{10.2.12}$$

$$\alpha_L = 1 + 10^{(\mathrm{pK_{a1}}-\mathrm{pH})} + 10^{(\mathrm{pK_{a1}}+\mathrm{pK_{a2}}-2\mathrm{pH})} + ... \tag{10.2.13}$$

Proof for Simplification of α_M (Conversion of Equation 10.2.10 to Equation 10.2.12)

Equation 10.2.10 can be expressed as the following:

$$\alpha_M = \frac{[M]}{[M]} + \frac{[MOH]}{[M]} + \frac{[M(OH)_2]}{[M]} + ... \tag{10.2.14}$$

The expression for metal hydroxide formation is

$$M + OH \rightleftharpoons \mathrm{MOH} \quad \mathrm{K_1} = \frac{[\mathrm{MOH}]}{[\mathrm{M}][\mathrm{OH}]} \tag{10.2.15}$$

This expression can put in terms of [H] by multiplying by the equilibrium constant expression for the dissociation of water:

$$\mathrm{K_w} = [OH][H] \tag{10.2.16}$$

$$\mathrm{K_1} = K_1 K_W = \frac{[\mathrm{MOH}]}{[\mathrm{M}][\mathrm{OH}]} \times [OH][H] = \frac{[MOH][H]}{[M]} \tag{10.2.17}$$

Rearrange the expression and put [H] in terms of pH and K_1 in terms of pK_1.

$$\frac{[\mathrm{MOH}]}{[\mathrm{M}]} = \frac{\mathrm{K_1}}{[\mathrm{H}]} = \frac{10^{-\mathrm{pK_1}}}{10^{-\mathrm{pH}}} = 10^{\mathrm{pH}-\mathrm{pK_1}} \tag{10.2.18}$$

Treat the second hydrolysis component similarly:

$$M + 2(OH) \rightleftharpoons \quad M(OH)_2 \tag{10.2.19}$$

$$\beta_2 = \frac{[M(OH)_2]}{[M][OH]^2} = \beta_2 \left(K_W\right)^2 = \frac{[M(OH)_2]\,[H]^2}{[M]} \tag{10.2.20}$$

$$\frac{[M(OH)_2]}{[M]} = \frac{\beta_2}{[H]^2} = \frac{K_1 K_2}{[H]^2} = \frac{10^{-pK_1-pK_2}}{10^{-2pH}} = 10^{2pH-pK_1-pK_2} \tag{10.2.21}$$

Substitute (10.2.18) and (10.2.21) into (10.2.14) to get Equation 10.2.12.

Proof for Simplification of a_L (Conversion of Equation 10.2.11 to Equation 10.2.13):

Equation 10.2.11 can be expressed as the following:

$$\alpha_M = \frac{[M]}{[M]} + \frac{[MOH]}{[M]} + \frac{[M(OH)_2]}{[M]} + ... \tag{10.2.22}$$

The stepwise equilibria for protonation of L are shown in (10.2.3). For the first protonation, The Expression for K_{a1} in (10.2.3) can be rearranged to Equation 10.2.23 and put in terms of pH and pKa1 instead of [H] and Ka1:

$$\frac{[HL]}{L} = \frac{[\mathrm{H}]}{[\mathrm{K_{a1}}]} = \frac{10^{-\mathrm{pH}}}{10^{-\mathrm{pK_{a1}}}} = 10^{\mathrm{pK_{a1}}-\mathrm{pH}} \tag{10.2.23}$$

Treat the term for the second protonation similarly using the expression of β_2 from the asbolute protonation equilibria shown in 10.2.4. The expression for β_2 can be rearranged and put in terms of pH and pKa's (recall that $\beta_2 = K_{a1}K_{a2}$) .

$$\frac{[H_2L]}{[\mathrm{L}]} = \frac{[\mathrm{H}]^2}{[\beta_2]} = \frac{[\mathrm{H}]^2}{[\mathrm{K_{a1}K_{a2}}]} = \frac{10^{-2\mathrm{pH}}}{10^{-\mathrm{pK_{a1}}-\mathrm{pK_{a2}}}} = 10^{\mathrm{pK_{a1}}+\mathrm{pK_{a2}}-2\mathrm{pH}} \tag{10.2.24}$$

Substitute (10.2.23) and (10.2.24) into (10.2.22) to get Equation 10.2.13.

Please note that for the equations above, the pK_{a1} value is the highest pK_a value for any given ligand. We define pK_a as an ASSOCIATION constant. In many sources, the K_a or pK_a values given are actually ACID DISSOCIATION constants defined by the *dissociation* rather than *association* of ligand and proton. It is very important to use the association constant value for the least acidic proton for pK_{a1} to get the correct values using the α_M and α_L equations above.

Other components in solution, such as buffer or competing ligand can affect the measured stability constant. The apparent stability constant (K_{app}) is defined as the constant measured in the presence of other species (salt, buffer components) that may interfere with determination of the pure pH-dependent conditional association constant.

Curated or created by Kathryn Haas

This page titled 10.2: Metal-Ligand Association Constants is shared under a CC BY-NC-SA 4.0 license and was authored, remixed, and/or curated by Kathryn Haas.

10.3: Trends in M-L stability (Thermodynamics)

In the context of inorganic chemistry, the sub-field of thermodynamics focuses on how stable or unstable a metal-ligand complex is. This is directly related to the equilibrium constant associated with forming the metal-ligand complex.

What factors give rise to stability?

This page will summarize trends in metal-ligand complex stability *in the absence of the chelate effect*.

Electrostatics (charge density):

When comparing metal complexes with identical ligand sets, the stability correlates with charge density of the metal ion. The more highly-charged the metal ion is, and the higher its charge density, the more attracted it will be to the ligands, and the more stable the resulting complex becomes.

Exercise

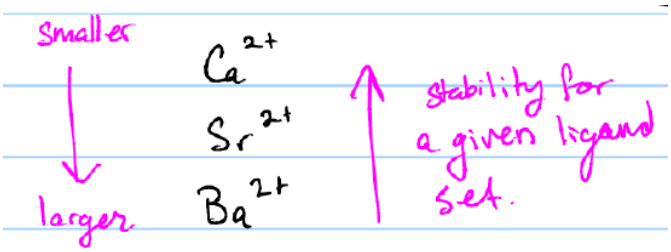
Arrange the following sets of ions according to charge density and expected stability of their hexaaquo complexes.

a)

b)

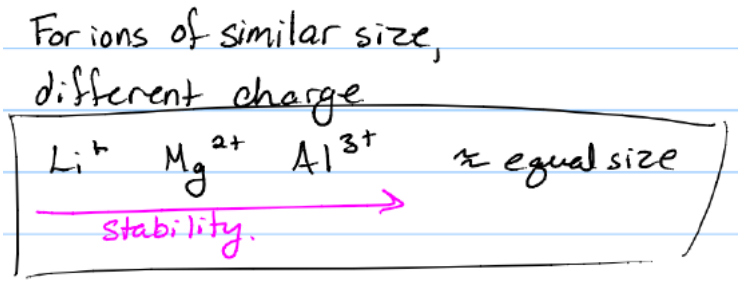
Answer a)

This is a series of ions with the same charge and in the same column of the periodic table.



Answer b)

This is a series of ions that are spread across the periodic table. They have similar size but different charges.



Hard-Soft Acid-Base Character

The hard-soft character of the ligand donor atoms and the metal ion contributes to stability.

Ligand Field Stabilization Energy

The Irving-Williams series is an observed trend in the stabilities of the divalent (+2) transition metal ions; the trend holds for any set of ligands. For the reaction of the metal hexaaquo complex with any ligand:

$$[M(OH_2)_6]^{2+} + L \rightleftharpoons [M(OH_2)_5L]^{2+} + H_2O \tag{10.3.1}$$

The observed trend in the equilibrium constant for formation of the M-L complex, K_f, (the Irving-Williams series) is:

$$Mg^{2+} < Mn^{2+} < Fe^{2+} < Co^{2+} < Ni^{2+} < Cu^{2+} > Zn^{2+} \tag{10.3.2}$$

This trend can be expanded to include divalent alkali metals:

$$Ba^{2+} < Sr^{2+} < Ca^{2+} < Mg^{2+} < Mn^{2+} < Fe^{2+} < Co^{2+} < Ni^{2+} < Cu^{2+} > Zn^{2+} \tag{10.3.3}$$

This trend also holds for substitution by additional ligands as well as for chelating ligands.

Notice that the metal ions listed above are all M^{2+} alkali metals or 3d-transition metals. As written above, from left to right in this series, size decreases while charge remains the same. This means that there should be an increase in charge density across this series, and thus a steady increase in affinity. However, electrostatics alone cannot explain the observed relative stabilities within the Irving-Williams series; the metals $Fe^{2+}, Co^{2+}, Ni^{2+}$, and Cu^{2+} have significant increases in their K_f values compared to the values that would be expected based on electrostatics alone. This increase in K_f is proportional to the LFSE value for each ion's d-electron count. The K_f values for Cu^{2+} are an anomaly, and are unusually high due to additional stability by LFSE due to Jhan-Teller distortion.

The Irving-Williams series can only be explained using a combination of electrostatics and LFSE.

Attribution

Curated or created by Kathryn Haas

This page titled 10.3: Trends in M-L stability (Thermodynamics) is shared under a license and was authored, remixed, and/or curated by LibreTexts.

11: KINETICS, TRENDS IN KINETIC LABILITY



CHEM 431: *Inorganic Chemistry*
Fall 2020: Dr. Kathryn Haas

11.1: Trends in Kinetic Lability
11.2: The Kinetic Chelate Effect
11.3: The Eigen-Wilkins Mechanism
11.4: Mechanisms of Substitution
11.5: The trans-effect
11.6: Redox Mechanisms
11.6.1: Outer Sphere Electron Transfer
11.6.2: Inner Sphere Electron Transfer

This page titled 11: Kinetics, Trends in Kinetic Lability is shared under a license and was authored, remixed, and/or curated by LibreTexts.

11.1: Trends in Kinetic Lability



Introduction

Kinetics is a branch of chemistry that is concerned with the rates of chemical reactions. In this section, we will discuss the rates of metal-ligand (M-L) substitution reactions.

Let's start with some examples. In the table below are three examples of ligand substitution reactions of hexaaquo metal complexes to form hexaammine complexes. These reactions are nearly identical with the exception of the metal ion. The products are thermodynamically favored in all cases.

Reaction	Rate constant (k)	Labile or Inert
$[Ni(OH_2)]^{2+} + 6NH_3 \rightleftharpoons [Ni(NH_3)_6]^{2+}$	$k = 10^4 s^{-1}$ (1 ns)	Labile (happens in < 1 min)
$[Cr(OH_2)]^{3+} + 6NH_3 \rightleftharpoons [Cr(NH_3)_6]^{3+}$	$k = 10^{-3} s^{-1}$ (6 days)	Inert (slow, takes hours)
$[Cu(OH_2)]^{2+} + 6NH_3 \rightleftharpoons [Cu(NH_3)_6]^{2+}$	$k = 10^8 s^{-1}$	Very Labile (happens in seconds)

DefinitionS

- **Labile** - Metal complexes that undergo "kinetically fast" substitution reactions are **labile**. These reactions usually happen in less than one minute.
- **Inert** - Metal complexes that undergo "kinetically slow" substitution reactions are **inert** or **non-labile**. These reactions usually take hours.
- **Intermediate** - Metal complexes that undergo "kinetically intermediate" substitution reactions are **intermediate**.

A common pitfall is to confuse the meaning of kinetic terms, like *labile* and *inert,* with thermodynamic terms, like *stable* and *unstable*. It is important to distinguish between kinetics and thermodynamics. For example, the complex $[Fe(H_2O)Cl]^{2+}$ has a large formation constant and is thermodynamically stable; yet it is also labile. On the other hand, the complex $[Co(NH_3)_6]^{3+}$ is unstable in acidic aqueous solution and decomposes spontaneously to $[Co(H_2O)_6]^{3+}$; yet it decomposes slowly because it is inert. It is good practice to distinguish between meanings by using terms such as "kinetically labile" or "kinetically inert" and "thermodynamically stable" and "thermodynamically unstable".

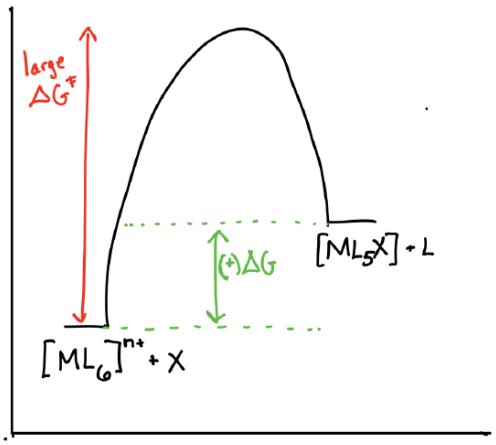
Exercise

Draw the reaction coordinate diagrams for a reaction of the form in the following scenarios:

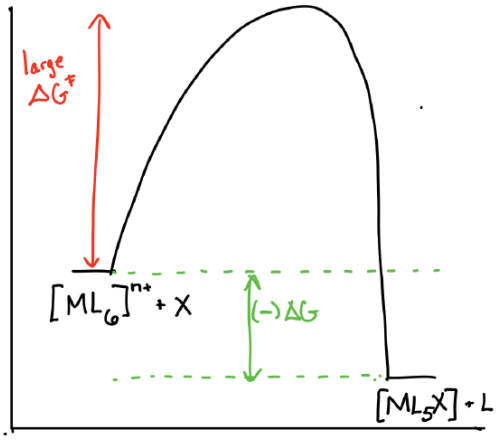
a. is theromdynamically stable and kinetically inert.

b. is theromdynamically unstable and kinetically inert.
c. is theromdynamically stable and kinetically labile.
d. is theromdynamically unstable and kinetically labile.

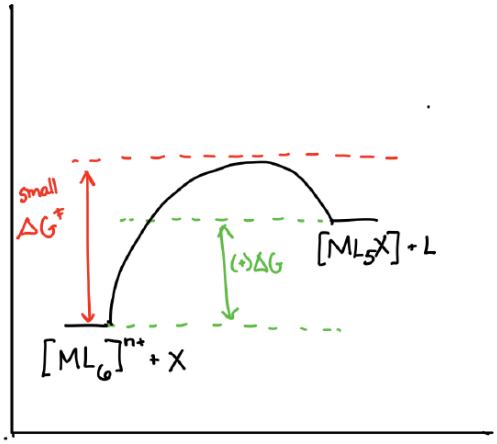
Answer a)



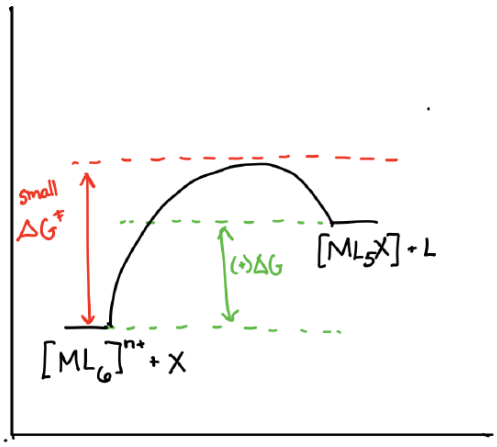
Answer b)



Answer c)



Answer d)



Factors that affect rates of substitution reactions:

Some of the factors that affect rates of ligand substitution reactions are those that also affect thermodynamic stability. It is important to remember that kinetic and thermodynamic factors are related, yet separate. The same factors that make a complex stable can also make it more inert. However, it is incorrect to assume that stability is always correlated with reaction rates.

Why are kinetic factors related to thermodynamic stability? For a complex to react or exchange one ligand for another, it must change its geometry to form an intermediate or transition state. For example, inert octahedral complexes often have stable electron configurations. When the reactant electron configuration is particularly stable, it can result in a higher activation energy associated with moving away from the stable configuration.

Factors to consider:

1. Electron configuration and LFSE: Electron configurations that place electrons in higher-energy orbitals (particularly antibonding orbitals) result in more labile complexes. As long as there are not electrons in higher-energy orbitals, the lability correlates roughly with LFSE. The more negative the LFSE, the more inert.
2. Size and charge of the metal ion: In general, higher charge denisity on the metal ion leads to stronger electrostatic attraction between metal and ligand; higher charge density generally correlates with slower rates of ligand substitution.

Taube's observations of metal complex substitution rates

Henry Taube (Nobel Prize, 1983) tried to understand lability by comparing the factors that govern bond strengths in ionic complexes to observations about the rates of reaction of coordination complexes. He saw some things that were unsurprising. He also drew some new conclusions based on ligand field theory.

Exercise

In which compound from each pair would you expect the strongest ionic bonds? Why?

a) LiF vs KBr
b) $CaCl_2$ vs. KCl

Answer a

The ions in LiF are both smaller than in KBr, so the force of attraction between the ions in LiF is greater because of the smaller separation between the charges.

Answer b

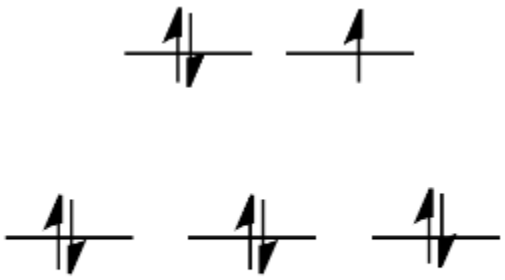
Calcium has a 2+ charge in $CaCl_2$, whereas potassium has only a + charge, so the chloride ions are more strongly attracted to the calcium than to the potassium.

Taube observed that **many M^{+1} ions (M = metal) are more labile than many M^{+3} ions**, in general. That isn't too surprising, since metal ions function as electrophiles or Lewis acids and ligands function as nucleophiles or Lewis bases in forming coordination complexes. In other words, *metals with higher charges ought to be stronger Lewis acids, and so they should bind ligands more tightly*. However, there were exceptions to that general rule. For example, Taube also observed that Mo_5^+ compounds are more labile than Mo_3^+ compounds. So, there must be more going on here than *just* the effects of electrostatic attraction.

Another factor that governs ionic bond strengths is the *size of the ion*. Typically, **ions with smaller atomic radii form stronger bonds** than ions with larger radii. Taube observed that Al^{3+}, V^{3+}, Fe^{3+} and Ga^{3+} ions are all about the same size. All these ions exchange ligands at about the same rate. That isn't surprising, because they have the same charge and the same radius. However, Cr^{3+} is also about the same size as those ions and it also has the same charge, but it is much less labile. Once again, there are exceptions to our regular expectations based on simple electrostatic considerations. Furthermore, 4d and 5d transition metals (Y→Cd, and Ac→Hg) are much more inert than 3d transition metals (Sc→Zn). This is unexpected when we consider size; the 4d and 5d metals are much larger than the 3d metals. This unexpected behavior tells us that electrostatics alone cannot predict lability.

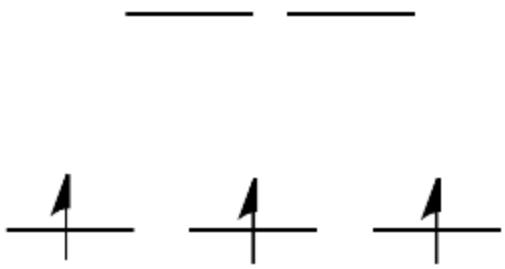
Taube came up with a hypothesis that could explain the seeming contradictory oservations described above: *kinetic lability must be affected by d-electron configuration*. This idea forms the basis of Taube's rules about lability.

For example, metals like Ni^{2+} and Cu^{2+} are very labile. The d orbital splitting diagrams for those compounds would have d electrons in the e_g set. Remember, the e_g set arises from interaction with the ligand donor orbitals; this set corresponds to a σ antibonding level.



Cu^{2+}

By comparison, V^{2+} is rather inert. The d orbital splitting diagram in this case has electrons in the t_{2g} set, but none in the e_g set.



V^{2+}

So, having electrons in the higher energy, antibonding e_g level weakens the bond to the ligand, so the ligand can be replaced more easily. In the absence of those higher energy electrons, the bond to the ligand is stronger, and the ligand isn't replaced as easily.

On the other hand, metals like Ca^{2+}, Sc^{3+} and Ti^{4+} are pretty labile. The d orbital splitting diagrams in those cases are pretty simple: there are no d-electrons at all in these ions.

That means having no electrons in these mostly non-bonding levels leaves the complex susceptible to ligand replacement. But it's hard to see why population of an orbital that is mostly non-bonding would have an effect on ligand bond strength.

Instead, this factor probably has something to do with the part of ligand substitution that we have ignored so far. Not only does one ligand need to leave, but a second one needs to bond in its place. So, having an empty orbital for the ligand to donate electrons into (or, put another way, not having electrons in the way that may complicate donation from the ligand) makes that part of the reaction easier.

Exercise

Consider all possible electron configurations for octahedral complexes (to , high spin and low spin cases): predict whether each case would be inert, intermediate, or labile.

Answer

Slow Reactions (Inert)	Intermediate	Fast Reactions (Labile)
d^3, low spin d^4, d^5, and d^6		d^1, d^2, high spin d^4, d^5 and d^6
Strong field d^8 (square planar)	weak-field d^8 (usually Td)	d^7, d^9, d^{10}

Exercise

Put the metal ions in order of decreasing reaction rate (from labile to inert):

a)

b)

Answer (a)

Most Labile to most inert:

These are metal ions with similar size and varying charge. They are in order of increasing charge and increasing

density from left to right.

Answer (b)

Most labile to most inert:

These metal ions have the same charge, and vary in size. They are in order of decreasing charge and increasing charge density from left to right.

Exercise

Some metals, like Mn^{2+}, can be either labile or inert, depending on whether they are high spin or low spin. Explain why using d orbital splitting diagrams.

Answer

Add texts here. Do not delete this text first.

Exercise

Predict whether the following metals, in octahedral complexes, are labile or not.

a) Co^{3+} (high spin)

b) Co^{3+} (low spin)

c) Fe^{2+} (low spin)

d) Fe^{2+} (high spin)

e) Zn^{2+}

Answer
Answer a

labile (electrons in higher energy d orbital set)

Answer b

not labile (all electrons in lower energy d orbitals)

Answer c

not labile (all electrons in lower energy d orbitals)

Answer d

labile (electrons in higher energy d orbital set)

Answer e

labile (electrons in higher energy d orbital set)

Overall Generalizations for Kinetics:

1. s-block metals are very labile, except for those with very high charge density (eg. $Mg^{2+}\ is\ inert$)
2. d^{10} metals are labile (eg: Zn^{2+}, Cu^{+}, Hg^{2+})

3. Other ions with a full shell are labile (eg: Ln^{3+} of f-block)
4. 3d M^{2+}, *when high spin,* are generally labile (eg. $Cu^{2+} is\ very\ labile$)
5. 4d and 5d are usually inert due to higher LFSE (low spin, high LFSE)
6. M^{2+} is more labile than the same metal as M^{3+}
7. d^3 and low spin d^6 are inert (eg. $Cr^{3+}, Co^{3+},$ low spin Fe^{2+})

Attribution

Chris P Schaller, Ph.D., (College of Saint Benedict / Saint John's University)

Curated or created by Kathryn Haas

This page titled 11.1: Trends in Kinetic Lability is shared under a license and was authored, remixed, and/or curated by LibreTexts.

11.2: The Kinetic Chelate Effect



We discussed the increased thermodynamic stability of chelating ligands in a previous section on the chelate effect. This thermodynamic benefit is related to a change in the rate of binding and dissociation events.

Recall that there is a relationship between the equilibrium constant and rate constants of any chemical reaction. The relationship is demonstrated below for a general reaction.

$$aA + bB \rightleftharpoons cC + dD \tag{11.2.1}$$

$$\text{forward rate} = k_f[A]^a[B]^b \tag{11.2.2}$$

$$\text{reverse rate} = k_r[C]^c[D]^d \tag{11.2.3}$$

At equilibrium, the rate of the forward reactions is equal to the rate of the reverse reaction. Therefore:

$$\text{forward rate} = \text{reverse rate} \tag{11.2.4}$$

$$k_f[A]^a[B]^b = k_r[C]^c[D]^d \tag{11.2.5}$$

Rearrangement of the equation above gives:

$$\frac{k_f}{k_r} = \frac{[C]^c[D]^d}{[A]^a[B]^b} = K_{eq} \tag{11.2.6}$$

Because chelating ligands have larger values of K_{eq} than analogous monodentate ligands, there must also be a change in the relative rates of the forward (binding) and reverse (dissociation) reactions. In fact, there is a kinetic benefit that makes a metal bound to a polydentate ligand more inert than the analogous complex with monodentate ligands: this is called the ***kinetic chelate effect***.

The kinetic chelate effect is a result of a slower first dissociation step and faster re-association step relative to that of a monodentate ligand. The complete dissociation of a bidentate ligand, for example, would require two dissociation steps (see first reaction in figure below). It is the first dissociation step that is slower in a bidentate ligand ($k_1 < k_1'$ in the figure below). This first dissociation step is slower in part because the chelate would have to rotate to move the free ligand away from the open coordinate site on the metal ion. For the same reason, the reverse of this step (association) is faster than the association of a monodentate ligand ($k_{-1} > k_{-1}'$).

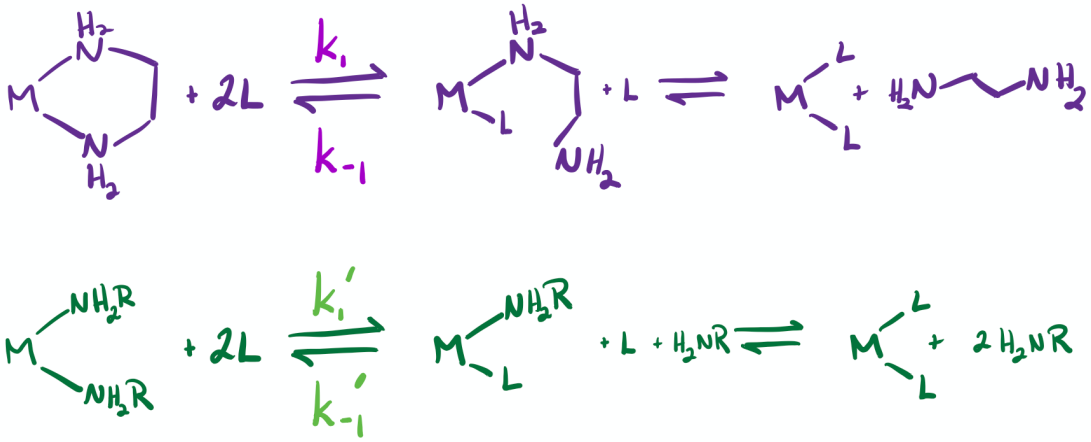


Figure 11.2.1: Step-wise dissociation of a bidentate ligand and analogous monodentate ligands. (CC-BY-NC-SA; Kathryn Haas)

Sources:

(1) Carter, M. J.; Beattie, J. K. Kinetic Chelate Effect. Chelation of Ethylenediamine on Platinum(II). Inorg. Chem.1970, 9 (5), 1233–1238. https://doi.org/10.1021/ic50087a044.

Attribution:

Curated or created by Kathryn Haas

This page titled 11.2: The Kinetic Chelate Effect is shared under a license and was authored, remixed, and/or curated by LibreTexts.

11.3: The Eigen-Wilkins Mechanism

UNDER CONSTRUCTION

Introduction

Most octahedral complexes react through either an associative or dissociative interchange mechanism (I_a or I_d). Although the rate laws should be different for these two cases, it is difficult to distinguish between them. The difficulty lies in the seemingly conflicting observations from experiments performed under limiting conditions of the incoming ligand. For example, in the case of the reaction of hexaaquochromium(III) ($[Cr(H_2O)_6]$) with ammonia (NH_3), the rate laws determined at high and low concentrations of the incoming ligand give different apparent rate laws. Under most conditions, the rate law appears to indicate a dissociative mechanism (ie rate is independent of the $[NH_3]$). But, at very high $[NH_3]$, the rate law appears to indicate an associative mechanism (ie the rate depends on $[NH_3]$).

This information might seem contradictory. However, it can be explained by the formation of a transient ion pair, usually called an encounter complex, in a step prerequisite to the rate-determining step(s). The Eigen-Wilkins Mechanism is based on this idea.

The Eigen-Wilkins mechanism

The Eigen-Wilkins *mechanism* is also a rate law, and it governs the reactions of octahedral metal complexes. This mechanism does not define the rate-limiting step; rather, it defines the existence of a pre-equilibrium step (ie an initial step that is not rate-determining) that results in formation of an encounter complex. The encounter complex is a short-lived ion pair of the metal complex and the incoming ligand; it is an intermediate formed through Coulomb interactions. For the conversion of a generic metal complex, where X is the leaving group and Y is the entering group, the overall reaction, pre-equilibrium step, and formation of products from the encounter complex are shown below:

	CHEMICAL EQUATION	EQUILIBRIUM EXPRESSION
Overall Reaction:	$ML_5X + Y \rightleftharpoons ML_5Y + X$	$K = \frac{[ML_5Y][X]}{[ML_5X][Y]}$
Pre-Equilibrium Step:	$ML_5X + Y \underset{k_{-1}}{\overset{k_1}{\rightleftharpoons}} (ML_5X \cdot Y)$	$K_E = \frac{[(ML_5X \cdot Y)]}{[ML_5X][Y]}$
Formation of Products:	$(ML_5X \cdot Y) \xrightarrow{k_2} ML_5Y + X$	$K_2 = \frac{[ML_5Y][X]}{[(ML_5X \cdot Y)]}$

(11.3.1)

Let's derive the rate law for the overall reaction. First let's lay out an important assumtion. The Eigen-Wilkins mechanism assumes that formation of the encounter complex is a pre-equilibrium step. In other words, it is a fast step. Once it forms, it also can quickly fall apart to re-form the reactant complex. Therefore, the rate law for formation of the encounter complexdepends on both the formation and the decomposition of the encounter complex. The rate of formation of the encounter complex can be written as follows:

$$\text{rate} = k_1\ [ML_5X][Y] - k_{-1}[(ML_5X, Y)] \tag{11.3.2}$$

The rate of formation of the product from the encounter complex (the second step) is the rate-determining step. We assume that the foward $\text{rate} = k_2\ [(ML_5X \cdot Y)]$

This page titled 11.3: The Eigen-Wilkins Mechanism is shared under a license and was authored, remixed, and/or curated by LibreTexts.

11.4: Mechanisms of Substitution

Mechanisms of Ligand Substitution Reactions

Now let us talk about the mechanism of ligand substitution reactions. A mechanism is the sequence of elementary steps by which a reaction proceeds. There are two aspects that describe the mechanism of a substitution reaction. One is called the **stoichiometric mechanism**, and the other one is called the **intimate mechanism**. The *stoichiometric* part of the mechanism is defined by the identity of the intermediate, or lack thereof. The *intimate* part of the mechanism is defined by the rate limiting step, and how the rate is dependent on the identity of the incoming ligand.

Stoichiometric Mechanisms

The *stoichiometric* part of the mechanism is defined by the identity of the intermediate, or lack thereof.

Associative (A) Mechanism

Associative (A) mechanisms involve a first step where the incoming ligand bonds to the metal ion, creating **an intermediate with a higher coordination number**. The leaving group leaves in a second step to form the product. The generic reaction below illustrates the steps of an associative mechanism. Note that the intermediate, $\mathrm{ML}_n\mathrm{XY}$, has a higher coordination number than that of the reactant, $\mathrm{ML}_n\mathrm{X}$.

$$\begin{aligned} \text{Overall Reaction:} \quad & \mathrm{ML}_n\mathrm{X} + \mathrm{Y} \rightleftharpoons \mathrm{ML}_n\mathrm{Y} + \mathrm{X} \\ \text{Step 1 (Association):} \quad & \mathrm{ML}_n\mathrm{X} + \mathrm{Y} \rightleftharpoons \mathrm{ML}_n\mathrm{XY} \\ \text{Step 2 (Dissociation):} \quad & \mathrm{ML}_n\mathrm{XY} \rightleftharpoons \mathrm{ML}_n\mathrm{Y} + \mathrm{X} \end{aligned} \tag{11.4.1}$$

Associative mechanisms are typical of square planar, d^8 complexes. The important features that distinguish this mechanism from others is that the **intermediate is long-lived** enough that it is detectable, and that the intermediate has a **higher coordination number** than the reactant complex.

Dissociative (D) Mechanism

Dissociative (D) mechanisms involve a first step where a bond between the metal ion and the leaving group breaks, creating **an intermediate with a lower coordination number.** The entering group enters in a second step to form the product. The generic reaction below illustrates the steps of a dissociative mechanism. Note that the intermediate, ML_n, has a lower coordination number than that of the reactant, $\mathrm{ML}_n\mathrm{X}$.

$$\begin{aligned} \text{Overall Reaction:} \quad & \mathrm{ML}_n\mathrm{X} + \mathrm{Y} \rightleftharpoons \mathrm{ML}_n\mathrm{Y} + \mathrm{X} \\ \text{Step 1 (Dissociation):} \quad & \mathrm{ML}_n\mathrm{X} \rightleftharpoons \mathrm{ML}_n + \mathrm{X} \\ \text{Step 2 (Association):} \quad & \mathrm{ML}_n + \mathrm{Y} \rightleftharpoons \mathrm{ML}_n\mathrm{Y} \end{aligned} \tag{11.4.2}$$

The important features that distinguish this mechanism from others is that the **intermediate is long-lived** enough that it is detectable, and that the intermediate has a **lower coordination number** than the reactant complex.

Interchange (I) Mechanism

Interchange (I) Mechanisms take place in one concerted step where the entering group enters as the leaving group leaves. Bond formation and bond breaking occur simultaneously. In the case of an interchange mechanism, no intermediate is detectable. This means that either there is no intermediate, or that the intermediate is too high-energy and short-lived to be detected. The generic reaction below illustrates the single step of an interchange mechanism. Note that the species, $[\mathrm{Y}\cdots\mathrm{ML}_n\cdots\mathrm{X}]^{\ddagger}$, can be defined as either a transition state or a very short-lived intermediate. The distinction between these two possibilities is difficult; *when the intermediate is undetectable it is not considered a true intermediate*.

$$\begin{aligned} &\text{Overall Reaction:} && \mathrm{ML}_n\mathrm{X} + \mathrm{Y} \rightleftharpoons \mathrm{ML}_n\mathrm{Y} + \mathrm{X} \\ &\text{Step 1 (Concerted):} && \mathrm{ML}_n\mathrm{X} + \mathrm{Y} \rightleftharpoons [\mathrm{Y}\cdots\mathrm{ML}_n\cdots\mathrm{X}]^{\ddagger} + \rightleftharpoons \mathrm{ML}_n\mathrm{Y} + \mathrm{X} \end{aligned} \tag{11.4.3}$$

The interchange mechanism is common for many six-coordinate (octahedral) metal complexes. The hallmark feature that distinguishes the interchange mechanism from other possible mechanisms is the **absence of a detectable intermediate**. If an intermediate is detected, the mechanism is considered associative (A). Another piece of evidence that can indicate an interchange mechanism is stereochemical changes from reactant to product. If specific sterochemistry (ie cis or trans relationships) is changed, it may be taken as evidence that an intermediate exists long enough to allow rearrangement to occur.

Distinguishing A, D, and I Mechanisms

Figure 11.4.1 shows examples of possible reaction profiles for each of the stoichiometric mechanisms described above. The profile of A and D mechanisms can be similar; they each require an intermediate, and the primary difference between A and D is the sequence of steps. An I mechanism lacks a true intermediate. These three cases can be difficult to distinguish experimentally, and especially if characterization of an intermediate is difficult. Notice that the reaction coordinate diagram for A and D pathways, shown in Figure 11.4.1, are similar. The only necessary difference between them is in the identity of the intermediate species.

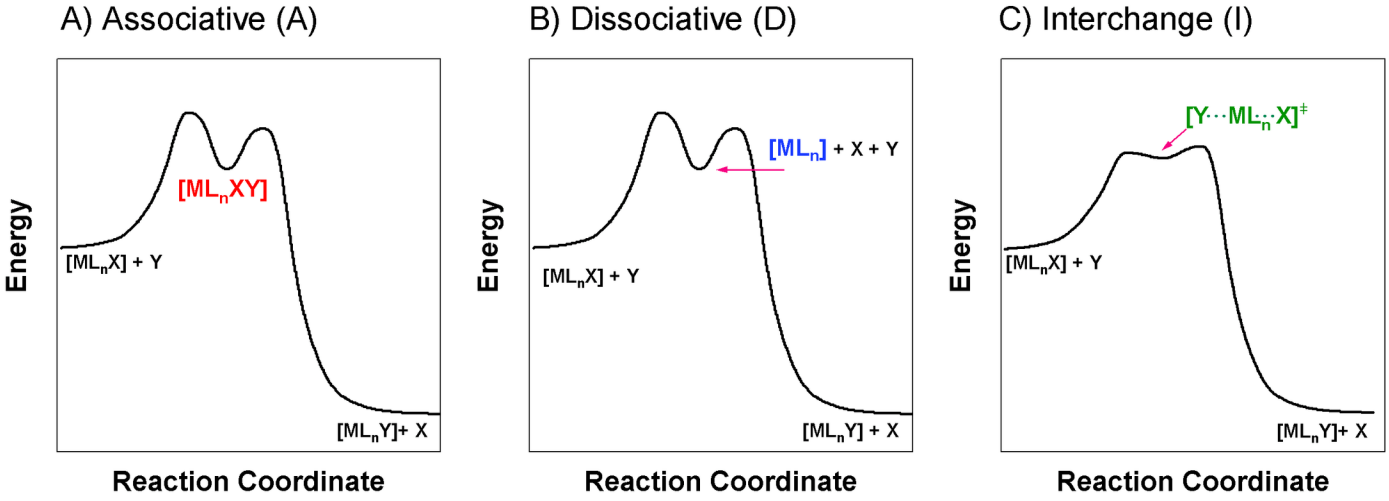


Figure 11.4.1: Example reaction coordinate diagrams for generic reactions that proceed through associative, dissociative, or interchange mechanisms. (Panel A) A reaction proceeds through an Associative pathway if it forms an intermediate with higher coordination number than its reactant complex. Here, an exergonic reaction is shown, where intermediate Extra close brace or missing open brace has a higher coordination number than reactant Extra close brace or missing open brace. (Panel B) A reaction proceeds through a Dissociative pathway if it forms an intermediate of lower coordination number than its reactant. Here, an exergonic reaction is shown where intermediate, Extra close brace or missing open brace, has lower coordination number than the reactant complex, Extra close brace or missing open brace. (Panel C) A reaction proceeds through an Interchange pathway if there is no true intermediate and the reaction proceeds in one step where bonds are broken and formed simultaneously. Shown here is an exergonic reaction where there is a high-energy species that is too unstable to be isolated; thus it is not a true intermediate and is considered equivalent to a transition state. (CC-BY-NC-SA; Kathryn Haas).

Intimate Mechanisms

The intimate mechanism is defined by characteristics of the rate-limiting step. The reaction is classified as associatively-activated (using a subscript, a) if the rate changes by more than 10-fold as the entering group is varied. The reaction is classified as dissociatively-activated (using a subscript, d) if the rate changes by less than 10-fold as the entering group is varied.

Associatively-Activated Mechanisms

The rate-limiting step of an associatively activated pathway is formation of a bond between the entering group and the central metal ion. These reactions also require formation of an encounter complex in a pre-equilibrium step prior to bond forming or bond breaking steps discussed here (see Eigen-Wilkins Mechanism).

Associatively-activated A and I (A_a and I_a)

In the case of an associatively-activated associative pathway ($\mathrm{A_a}$) or an associatively-activated interchange pathway ($\mathrm{I_a}$), the rate-limiting step is the association of the entering group (Y) with the reactant, $\mathrm{ML}_n\mathrm{X}$. In the case of the A_a pathway, it is the first step (bolded) below.

$$\begin{array}{c} \mathrm{A}_a \text{ Mechanism} \\ \textbf{Step 1 (Association):} \quad \mathrm{ML_nX + Y} \overset{\mathrm{k_1}}{\underset{\blacksquare}{\rightleftharpoons}} \mathrm{ML_nXY} \quad \Longleftarrow \textbf{RATE LIMITING ASSOCIATION} \\ \text{Step 2 (Dissociation):} \quad \mathrm{ML}_n\mathrm{XY} \overset{\mathrm{k_2}}{\underset{\blacksquare}{\rightleftharpoons}} \mathrm{ML}_n\mathrm{Y + X} \end{array} \tag{11.4.4}$$

In the case of A_a, the first step shown above is slower than the second step ($k_1 < k_2$). In this case, an intermediate may not be detected because its steady state concentration is close to zero (ie it reacts as soon as it forms). Thus, distinguishing between A_a and I_a mechanisms is often impossible.

Associatively-activated D (D_a)

In the case of an associatively-activated dissociative reaction ($\mathrm{D_a}$), the rate limiting step is the association of the entering group (Y) with the intermediate ML_n; the second step (bolded) in the mechanism shown below:

$$\begin{array}{c} \mathrm{D}_a \text{ Mechanism} \\ \text{Step 1 (Dissociation):} \quad \mathrm{ML}_n\mathrm{X} \overset{\mathrm{k_1}}{\underset{\blacksquare}{\rightleftharpoons}} \mathrm{ML}_n + \mathrm{X} \\ \textbf{Step 2 (Association):} \quad \mathrm{ML_nX + Y} \overset{\mathrm{k_2}}{\underset{\blacksquare}{\rightleftharpoons}} \mathrm{ML_nY} \quad \Longleftarrow \textbf{RATE LIMITING ASSOCIATION} \end{array} \tag{11.4.5}$$

In this case, the intermediate concentration should be measurable since the second step is slower than the first ($k_1 > k_2$).

Exercise 11.4.1

Draw the reaction coordinate diagrams (aka reaction profiles) of reactions that proceed through A_a, I_a, and D_a pathways. Use these diagrams to explain why it is impossible to distinguish between A_a and I_a.

Hint available at the end of this section.

Answer available at the end of this section.

Dissociatively-Activated Mechanisms

When the rate-determining step is the breaking of a bond between the central metal ion and the leaving group, it is considered a dissociatively-activated (subscript d) mechanism. The rates of these reactions are largely independent of the identity of the incoming ligand.

Dissociatively-activated A (A_d)

In the case of a dissociatively-activated associative pathway ($\mathrm{A_d}$), the rate-limiting step is the dissociation of the leaving group (X) from the intermediate, $\mathrm{ML}_n\mathrm{XY}$; the second step (bolded) below.

$$\begin{array}{c} \mathrm{A}_d \text{ Mechanism} \\ \text{Step 1 (Association):} \quad \mathrm{ML}_n\mathrm{X + Y} \overset{\mathrm{k_1}}{\underset{\blacksquare}{\rightleftharpoons}} \mathrm{ML}_n\mathrm{XY} \\ \textbf{Step 2 (Dissociation):} \quad \mathrm{ML_nXY} \overset{\mathrm{k_2}}{\underset{\blacksquare}{\rightleftharpoons}} \mathrm{ML_nY + X} \quad \Longleftarrow \textbf{RATE LIMITING DISSOCIATION} \end{array} \tag{11.4.6}$$

In this case, the intermediate concentration should be measurable since the second step is slower than the first ($k_1 > k_2$.

Dissociatively-activated D and I (D_a and I_a)

In the case of a dissociatively-activated dissociative reaction ($\mathrm{D_d}$), or a dissociatively-activated interchange pathway ($\mathrm{I_d}$), the rate limiting step is the dissociation of the leaving group (X) from the reactant, $\mathrm{ML}_n\mathrm{X}$. For D_d the rate limiting step is the first step (bolded) in the mechanism shown below:

$$\begin{array}{l} \mathrm{D}_d \text{ Mechanism} \\ \textbf{Step 1 (Dissociation):} \quad \mathrm{ML_nX} \overset{\mathrm{k_1}}{\rightleftharpoons} \mathrm{ML_n + X} \quad \Longleftarrow \textbf{RATE LIMITING DISSOCIATION} \\ \text{Step 2 (Association):} \quad \mathrm{ML}_n\mathrm{X + Y} \overset{\mathrm{k_2}}{\rightleftharpoons} \mathrm{ML}_n\mathrm{Y} \end{array} \tag{11.4.7}$$

In the case of D_d, the first step shown above is slower than the second step ($k_1 < k_2$ and an intermediate may not be detected because its steady state concentration is close to zero (ie it reacts as soon as it forms). Thus, distinguishing between D_d and I_d mechanisms is often impossible.

Exercise 11.4.2

You should complete Excercise 11.4.1 before attempting this excercise.
Draw the reaction coordinate diagrams (aka reaction profiles) of reactions that proceed through A_d, I_d, and D_d pathways.

Answer available at the end of this section.

Curated or created by Kathryn Haas

Answers

Exercise 11.4.1

Notice that the reaction coordinate diagrams for A and D pathways, shown in Figure 11.4.1, are similar. The only necessary difference between them is the identity of the intermediate. These diagrams can be modified to represent associatively-activated pathways by altering the relative energy of the transition state for the associative step; the energy barrier for the associative step must be greater than that of the dissociative step. In other words, the difference between A_a, D_a is in the relative energies of the first and second transition states. In the case of I_a, the diagram could be similar to the I profile shown in Figure 11.4.1, with the exception that the energy barrier for making the M-Y bond is greater than the energy barrier for breaking the M-X bond.

Exercise 11.4.1

The three reaction coordinate diagrams shown in the figure below represent A_a, I_a, and D_a mechanisms respectively. If your diagram does not match this perfectly, that may be OK. The important features are:

- A_a: This reaction profile should show an intermediate with higher coordination number than the reactant. The intermediate should be relatively stable. The energy barrier for formation of this intermediate is the associative step, and therefore it should also be the rate-limiting step for an A_a mechanism; in other words, the first step should have the highest energy barrier.
- I_a: This reaction profile should lack a stable intermediate. The energy barrier for creating of the M-Y bond must be rater-limiting. The diagram shown below is an acceptable solution, but a diagram like shown in Panel C of Figure 11.4.1 is also correct. It is not clear from the diagram alone whether bond breaking or bond making are rate-limiting; this nuance would lie primarily in the identity of the transition state, and whether the M-Y bond is stronger or weaker than the M-X bond in the transition state.
- D_a: This reaction profile should show an intermediate with lower coordination number than the reactant. The intermediate should be relatively stable. The energy barrier for association of the entering group with the intermediate (the second step) must be rate-limiting in a D_a mechanism. In other words, the second step should have the highest energy barrier.

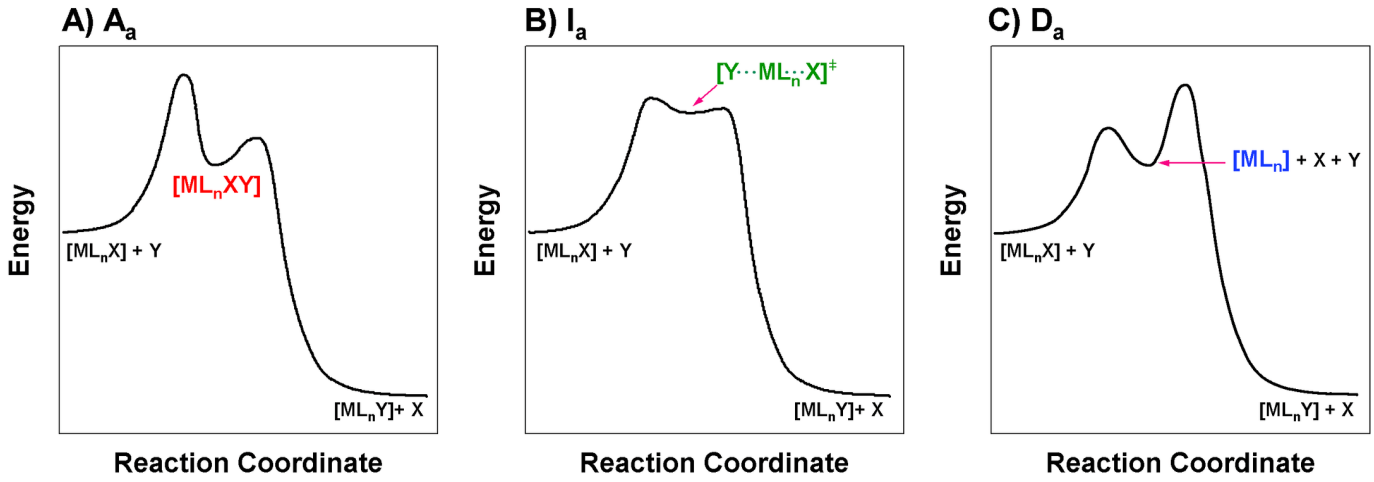


Figure for Excercise 11.4.1: Reaction coordinate diagrams for associatively-activated mechanisms. (A) Associatively-activated associative, A_a. (B) Associatively-activated interchange, I_a. (C) Associatively-activated dissociative, D_a. (CC-BY-NC-SA; Kathryn Haas)

The A_a and I_a mechanisms have different reaction profiles while still the rate-limiting step is the initial association of the incoming ligand to the metal center. These two types of mechanisms are difficult to distinguish because in the case of A_a, there is a relatively small energy barrier for reaction of the intermediate to form product; thus this intermediate is not long-lived and would be difficult to detect. Experimental distinction between A_a and I_a lies in the detection and characterization of this intermediate, and since it may be elusive in A_a, it is difficult to unambiguously determine whether an associatively-activated mechanism is A_a or I_a.

Exercise 11.4.2

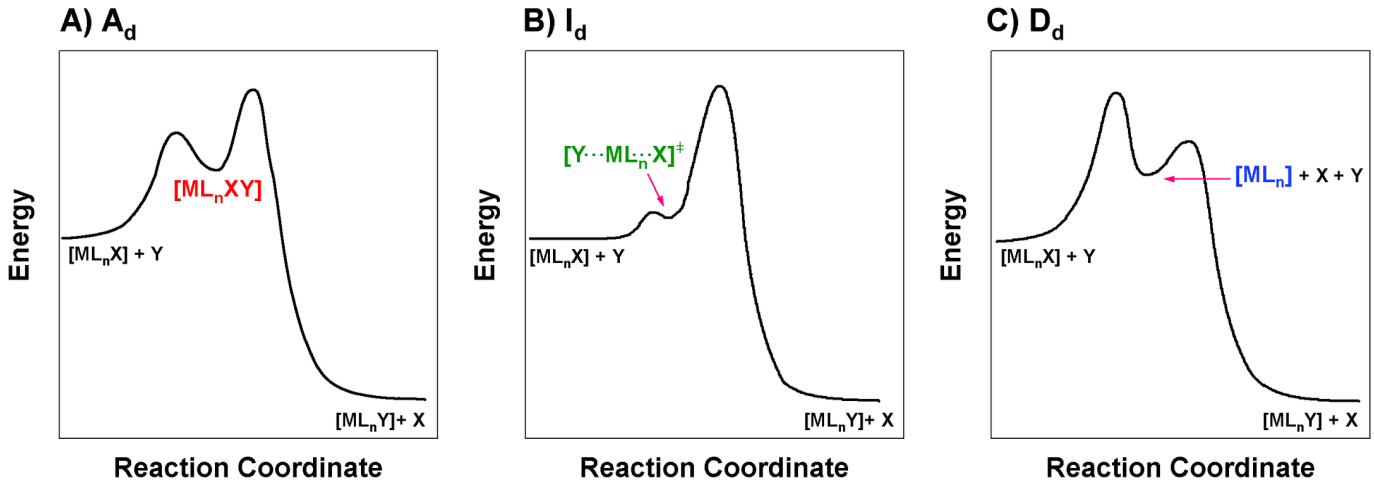
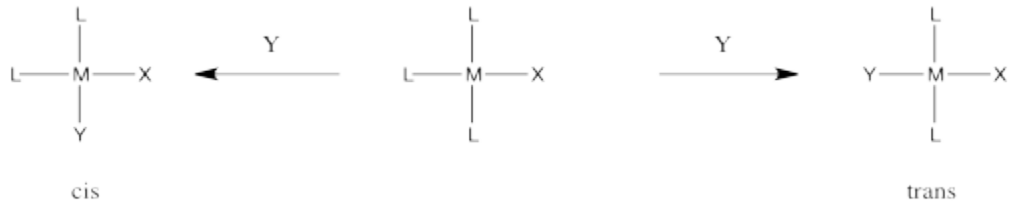


Figure for Excercise 11.4.2: Reaction coordinate diagrams for dissociatively-activated mechanisms. (A) Dissociatively-activated associative, A_d. (B) Dissociatively-activated interchange, I_d. (C) Dissociatively-activated dissociative, D_d. (CC-BY-NC-SA; Kathryn Haas)

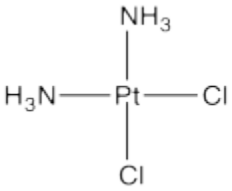
This page titled 11.4: Mechanisms of Substitution is shared under a license and was authored, remixed, and/or curated by Kathryn Haas.

11.5: The trans-effect

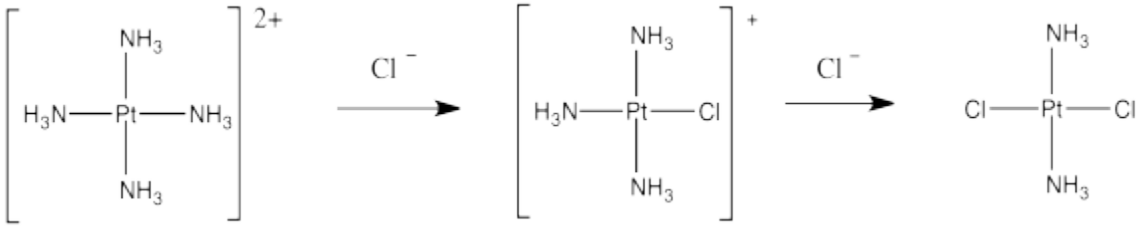
Occasionally in ligand substitution there is a situation in which there are two identical ligands that could be replaced, but two different products would result depending on which ligand left. This situation often happens in square planar complexes, for example. Replacement of one ligand would lead to a *cis* product. Replacement of the other one would lead to a *trans* product.



An important example of this issue is in the synthesis of cis-platin, an antitumour medication frequently used to treat ovarian and testicular cancer.

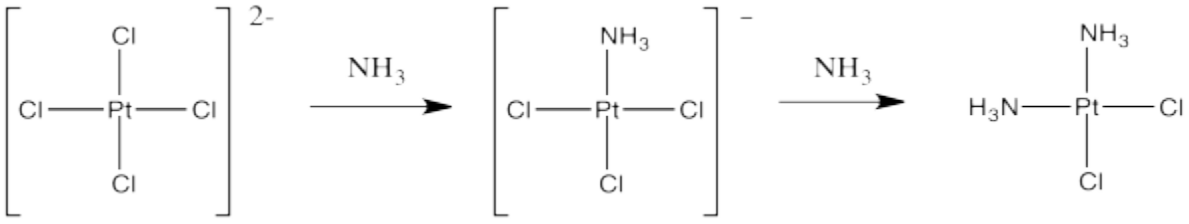


Cis-platin could be made from treatment of tetraammineplatinum(II) with chloride salts. The chloride ion could replace two of the ammonia ligands.



But that doesn't work. That synthesis results in the formation of *trans*-platin, a compound that has all of the nasty side effects of the *cis* isomer but with none of the therapeautic benefit.

If instead you were to start with tetrachloroplatinate salts and treat them with ammonia, you could replace two of the chloride ligands. That works really well, and it provides *cis*-platin, not *trans*-platin.



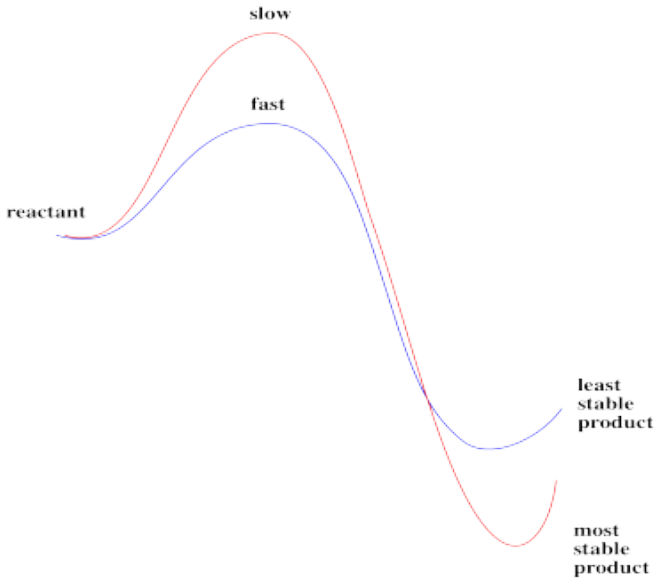
Exercise 11.5.1

What do you think is the mechanism of substitution of the two reactions above? Why?

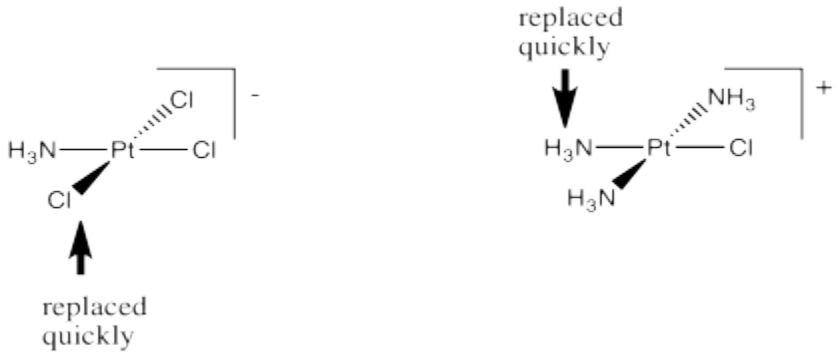
Answer available at the end of this section.

This reaction, if run under these conditions, is clearly not always under thermodynamic control. Two different products result, depending on how the reaction is done. One of those isomers is probably more stable than the other; if thermodynamics were in charge, it would form the same thing both times.

Instead, there may be an element of kinetic control for at least one of the pathways. A given product might be made, not because it is more stable, but simply because it forms more quickly than the other one.



Take another look at those two reactions. One of the things that they have in common is that the ligand that gets replaced is *trans* to a chloride. It is not *trans* to an ammonia. Maybe the other ligands in the complex can influence how quickly one ligand can leave.



Specifically, the "*trans* effect" is the role of *trans*-ligands in influencing substitution rates in square planar complexes.

The following kinetic data were obtained for substitutions on square planar platinum complexes, in the reaction:

$$trans-(PEt_3)_2PtLCl + py \rightarrow trans-(PEt_3)_2PtLpy^+ + Cl^-$$

L	k_{obs} (s^{-1})	T, °C
PMe_3	0.20	0
H^-	0.047	0
PEt_3	0.041	0
CH_3^-	6.0 x 10^{-4}	25

$C_6H_5^-$	1.2×10^{-4}	25
Cl^-	3.5×10^{-6}	25

Ref: Cooper Langford & Harry Gray, *Ligand Substitution Processes*, W.A. Benjamin, NY, 1965, p. 25.

Exercise 11.5.2

Draw structures for each of the complexes listed in the table.

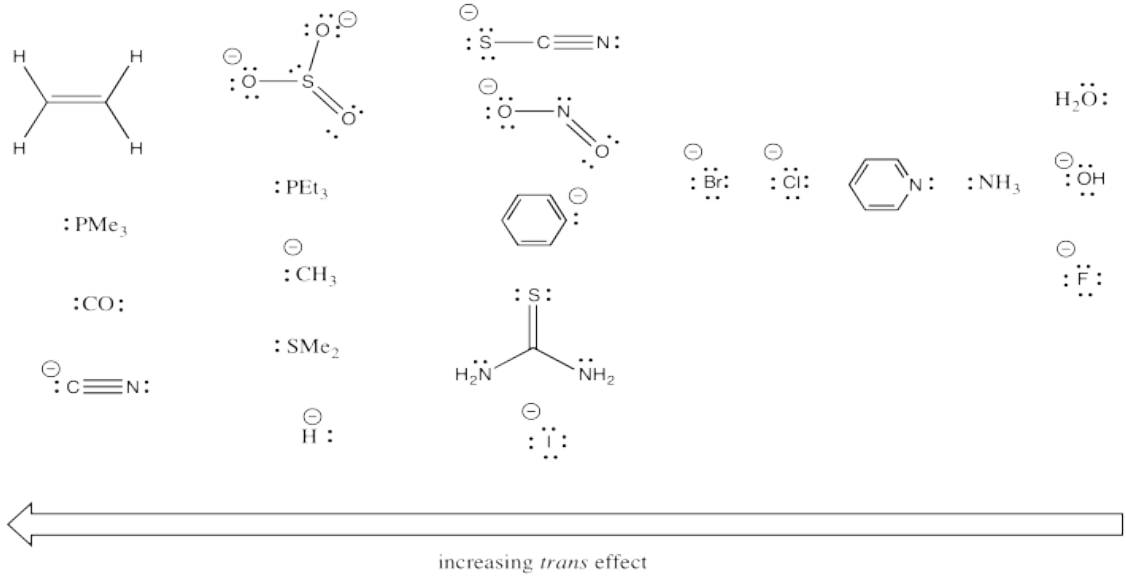
Answer available at the end of this section.

Exercise 11.5.3

Provide a mechanism with arrows for the reaction studied in the table.

Answer available at the end of this section.

Clearly that *trans* ligand has a dramatic effect on how quickly the chloride can be substituted in the above study. Additional studies like this one have led to some general trends. Below, the ligands on the left have strong *trans*-effects. Ligands *trans* to them are substituted very quickly. The ligands on the right have very modest *trans* effects. Ligands *trans* to them are substituted only slowly.



Exercise 11.5.4

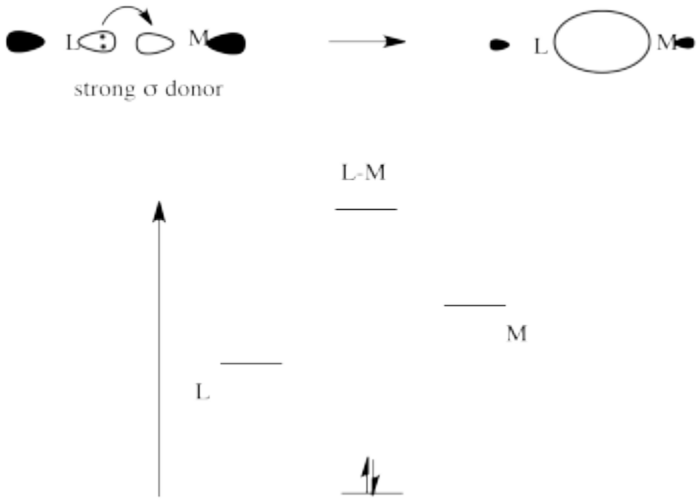
Look for empirical trends in the series of ligands above. Without trying to explain exactly why, find chemically relevant factors that may be responsible for these reactivity trends.

Answer available at the end of this section.

In general, explanations of the trans effect have focused on two separate types of ligands. These are strong sigma donors and strong pi acceptors.

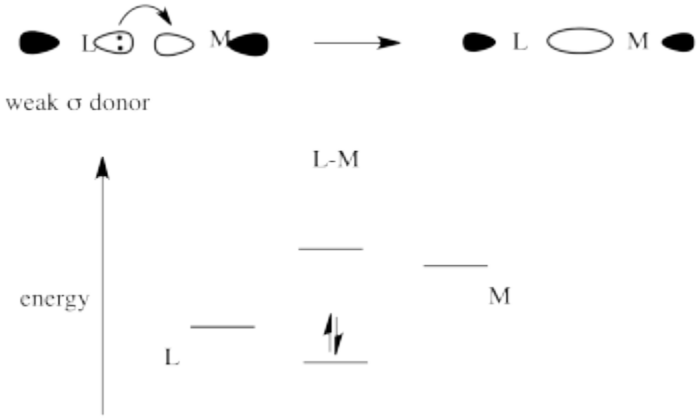
Strong sigma donors donate electrons very effectively to the metal via a sigma bond. Because the ligand trans to this donor would

be bonding via donation to the same metal p orbital, there is a competition. The metal p orbital bonds more favorably with the strong sigma donor, and the ligand trans to it is left with a weaker bond.

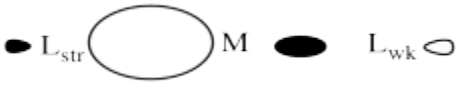


The strong sigma donor gets good overlap with the metal orbital and the resulting interaction goes down low in energy.

The weak sigma donor gets poorer overlap with the metal orbital and only weak stabilization of the donor electrons.



Place these two choices together, and the metal orbital will engage in a strong bonding interaction with the strong σ-donor. Doing so lowers the electronic energy significantly. It won't interact very much with the weak σ-donor, because doing that won't result in as much lowering of electronic energy. The result is a strong bond on one side of the metal and a weak bond on the other. That weak bond will break easily and that ligand will be replaced easily.

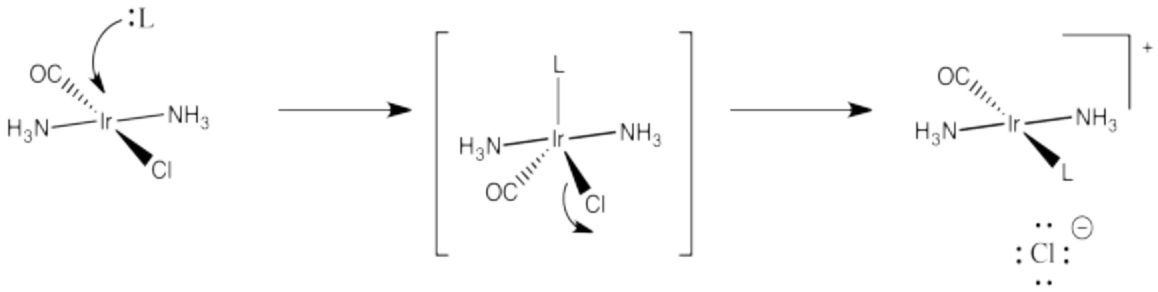


Exercise 11.5.5

Which of the ligands in the *trans* effect series are probably strong σ-donors? Why?

Answer available at the end of this section.

Strong pi acceptors exert their trans effect in a different way. They are thought to stabilize a particular geometry of the five-coordinate intermediate in substitution of square planar complexes. We haven't worried too much about the geometry of that intermediate, but it is probably trigonal bipyramidal. It would have three ligands in an equatorial plane and two more directly opposite each other, in the axial positions.



Essentially, the incoming ligand pushes two of the ligands down from the square plane to form this trigonal bipyramid. When it comes time for a ligand to leave, it is probably going to be one of these ligands that is already on the move. They are already on a trajectory out of the square plane, anyway.

A strong pi acceptor like CO exerts its *trans* effect by making sure it, along with the ligand opposite it, gets into that equatorial plane. It does that by a stabilizing delocalization that happens when the π-acceptor is in the electron-rich equatorial plane. In that position, it can draw electron density via π-donation from two different donors. If it were in an axial position, it could still delocalize electrons this way, but it would draw most effectively from just one donor rather than two.



favoured

So which of those two ligands is going to keep moving and leave the complex? It certainly won't be the one that is exerting a stabilizing, delocalizing effect on the complex via its strong bonding interactions. It will be the unlucky *trans* ligand that got dragged along with it.

Exercise 11.5.6

Which of the ligands in the *trans*-effect series are probably strong π-acceptors? Show why.

Exercise 11.5.7

Draw an orbital picture showing the -delocalization described in the trigonal bipyramidal intermediate. Label the orbitals, assuming the z axis is along the axis of the trigonal bipyramid (i.e. the equatorial plane is the xy plane).

Answer available at the end of this section.

Exercise 11.5.8

Substitution of trans ligands in μ-oxo-bis(μ-acetato)diruthenium complexes: Synthesis and kinetic studies. Hussain, Bhatt, Kumar, Thorat, Padhiyar and Shukla, *Inorganica Chemica Acta*, **2009**, *362*, 1101-1108.

Given the structure $[Ru_2O(L)_6(acetate)_2](PF_6)_2$, in which L is a neutral donor,

a) Draw the structure of the counterion, PF_6^-.

b) Provide an account of the valence electron count in the ruthenium coordination complex.

Valence electrons on metal	
Total charge on ligands	
Charge on the metal	
Revised count on metal	
Electrons donated by ligands	
Total electrons on metal in complex	

Data shows that the ligands L are *trans* to the bridging oxo ligand are labile.

c) Use orbital cartoons and words to provide an explanation for this effect.

When water is added to an acetone solution of $[Ru_2O(pyridine)_4(L)_2(acetate)_2](PF_6)_2$, then $[Ru_2O(pyridine)_4(H_2O)_2(acetate)_2](PF_6)_2$ is formed.

d) Draw the product of this reaction.

When pyridine is added to $[Ru_2O(pyridine)_4(H_2O)_2(acetate)_2](PF_6)_2$, then $[Ru_2O(pyridine)_6(acetate)_2](PF_6)_2$ is formed. The following rate constants were observed for this reaction.

[pyridine] mol L^{-1}	k_{obs} s^{-1} (x 10^{-3})
0.005	1.75
0.012	2.53
0.025	9.7
0.049	16.7
0.100	35.2

e) Use the data from this table to determine the order in pyridine. Provide an explanation for your conclusion.

f) Draw a mechanism for the reaction, consistent with the data.

g) Write a rate law for the reaction.

h) The authors studies the same reaction with different ligands instead of pyridine. They observed an increase in rate constants with increasing basicity of the incoming ligands. Provide an explanation for this observation.

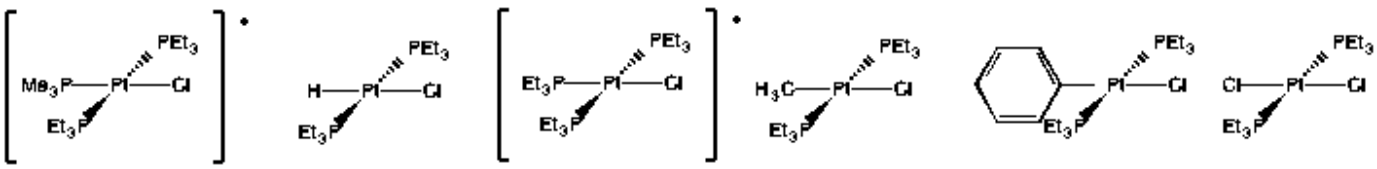
Answer a available at the end of this section.

Answers

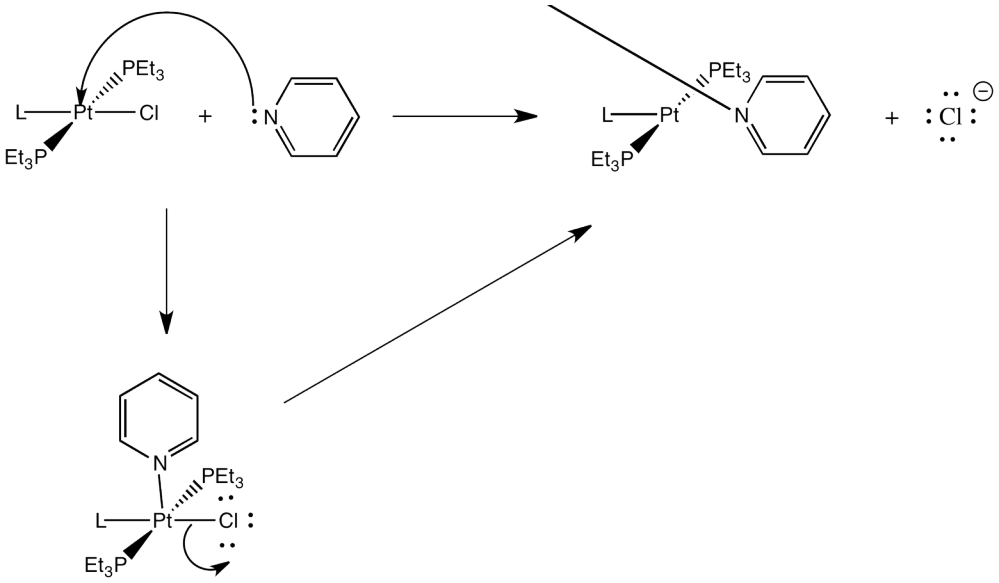
Exercise 11.5.1

This is probably an associative mechanism because of the square planar geometry.

Exercise 11.5.2



Exercise 11.5.3



Exercise 11.5.4

There is an electronegativity trend: the less electronegative, the greater the *trans* effect (see the halogens, as well as the series O,N,C and also the orders within several pairings: S,P; O,S and N,P).

Alternatively, some of the above could be described by a polarizability trend: more polarizable atom, greater *trans* effect (for example, the halogens).

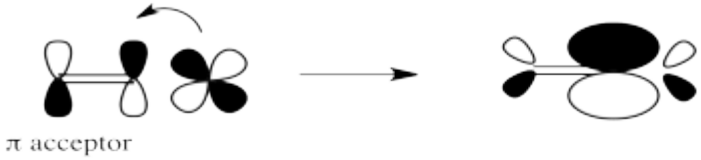
Most of the ligands containing π-bonds have strong *trans* influence (but not all).

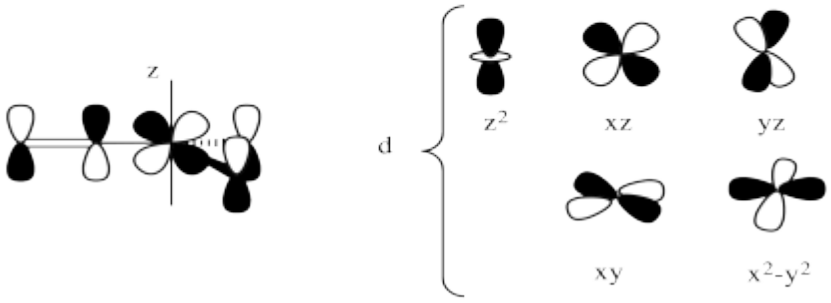
Most of the π-donors have a weaker *trans* influence. However, these ligand cover a very broad range in this series.

Exercise 11.5.5

The strongest σ-donors are typically those with more polarizable donor atoms (such as S, P, I) as well as those with less electronegative donor ions such as C^- and H^-.

Exercise 11.5.7





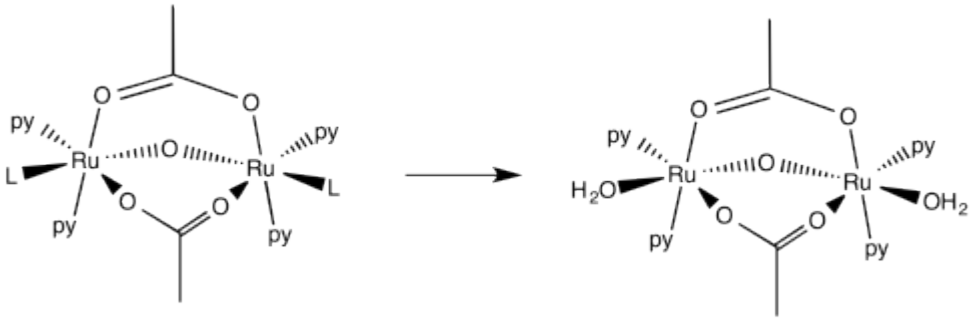
Exercise 11.5.8



5 valence electrons - 6 bonds - 0 nonbonding = -1

Valence electrons on metal	8
Total charge on ligands	-4 (-2 per Ru)
Charge on the metal	+2
Revised count on metal	6
Electrons donated by ligands	12
Total electrons on metal in complex	18

The oxo is a strong sigma donor and hogs the orbital with the metal thus leaving very little room for orbital bonding trans to the sigma donor.



First order. Although there is some amount of error in the data, doubling the pyridine concentration generally results in a doubling of the rate.
The mechanism you draw would have to involve a first associative step; because the complex is already 18 electrons, associative interchange is likely.

$$Rate = k[ML_n][py]$$

Basic ligands have stronger attraction to the metal thus accelerating the reaction.

This page titled 11.5: The trans-effect is shared under a license and was authored, remixed, and/or curated by LibreTexts.

- 3.7: The Trans Effect by Chris Schaller is licensed CC BY-NC 3.0. Original source: https://employees.csbsju.edu/cschaller/ROBI2.htm.

11.6: REDOX MECHANISMS

Henry Taube created a solution of $ceCr^{3}+_{aq}$, which is blue in color. He added I_2 and observed a color change to the hallmark green color of Cr(III). The green color was a result of oxidation to form $[\mathrm{Cr}(\mathrm{H}_2\mathrm{O})_5\mathrm{I}]^{2+}$. Taube figured that for this transformation to occur, that a Cr-I bond must form prior to Cr(II) being oxidized by I_2. Subsequently, he performed another experiment using $[(NH_3)_5CoCl]^{2+}$ as an oxidant and found that Cr^{2+}(aq) was converted into $[Cr(H_2O)_6]^{3+}$ via a green $[(H_2O)_5CrCl]_{2+}$. This reaction established the inner-sphere electron transfer mechanism in which a Co-Cl-Cr bridge forms between Co^{3+} and Cr^{2+} and led to the Nobel Prize in a later year.

Redox reactions

The oxidation number of the central metal in a transition-metal compound can vary. Namely, the oxidation state of a compound is changeable by **red**uction/**ox**idation (redox) reactions in which electrons are transfered to one species to another. As a consequence of this, the bond distance and the bond angle between the metal and coordinating elements, or between metals, change, and at times the whole structure of a complex can be distorted remarkably or the compound may even decompose.

The reactions of a metal compound with various reducing or oxidizing agents are also very important from the viewpoint of synthetic chemistry. Especially, reduction reactions are used in the preparation of organometallic compounds, such as metal carbonyls or cluster compounds.

Meanwhile, the study of electron transfer between complexes, especially the redox reactions of transition metal complexes, has developed. Taube won the Nobel Prize (1983) for the study of electron transfer reactions in transition metal complexes, classifying such reactions into two mechanisms. The mechanism of electron transfer in which a bridging ligand is shared between two metals is called the **inner-sphere mechanism**, and the one involving a direct transfer of electrons between two metals without a bridging ligand is called the **outer-sphere mechanism**.

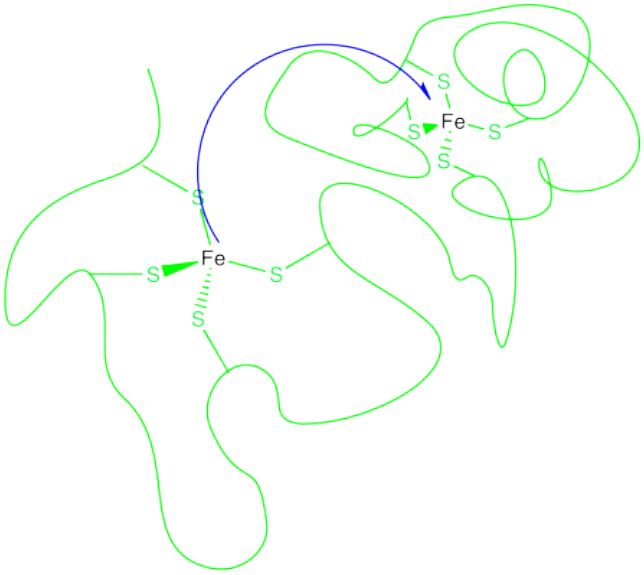
11.6.1: Outer Sphere Electron Transfer

11.6.2: Inner Sphere Electron Transfer

This page titled 11.6: Redox Mechanisms is shared under a license and was authored, remixed, and/or curated by LibreTexts.

11.6.1: Outer Sphere Electron Transfer

How does an electron get from one metal to another? This might be a more difficult task than it seems. In biochemistry, an electron may need to be transfered a considerable distance. Often, when the transfer occurs between two metals, the metal ions may be constrained in particular binding sites within a protein, or even in two different proteins.



That means the electron must travel through space to reach its destination. Its ability to do so is generally limited to just a few Angstroms (remember, an Angstrom is roughly the distance of a bond). Still, it can react with something a few bond lengths away. Most things need to actually bump into a partner before they can react with it.

This long distance hop is called an outer sphere electron transfer. The two metals react without ever contacting each other, without getting into each others' coordination spheres. Of course, there are limitations to the distance involved, and the further away the metals, the less likely the reaction. But an outer sphere electron transfer seems a little magical.

Barrier to Reaction: A Qualitative Picture of Marcus Theory

So, what holds the electron back? What is the barrier to the reaction? Rudy Marcus at Caltech has developed a mathematical approach to understanding the kinetics of electron transfer, in work he did beginning in the late 1950's. We will take a very qualitative look at some of the ideas in what is referred to as "Marcus Theory". An electron is small and very fast. All those big, heavy atoms involved in the picture are lumbering and slow. The barrier to the reaction has little to do with the electron's ability to whiz around, although even that is limited by distance. Instead, it has everything to do with all of those things that are barely moving compared to the electron.

Imagine an iron(II) ion is passing an electron to an iron(III) ion. After the electron transfer, they have switched identities; the first has become an iron(III) and the second has become an iron(II) ion.

Nothing could be simpler. The trouble is, there are big differences between an iron(II) ion and an iron(III) ion. For example, in a coordination complex, they have very different bond distances. Why is that a problem? Because when the electron hops, the two iron atoms find themselves in sub-optimal coordination environments.

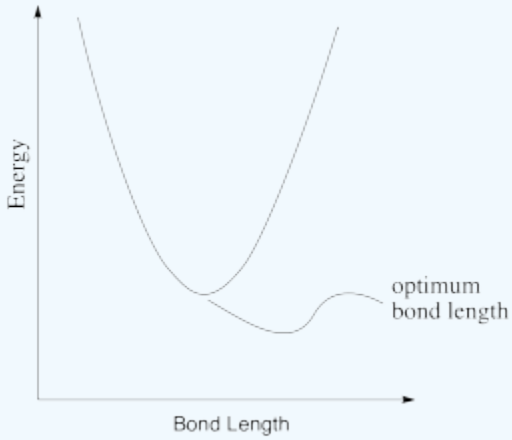
Exercise 11.6.1.1

Suppose an electron is transferred from an Fe(II) to a Cu(II) ion. Describe how the bond lengths might change in each case, and why. Don't worry about what the specific ligands are.

Answer available at the end of this section.

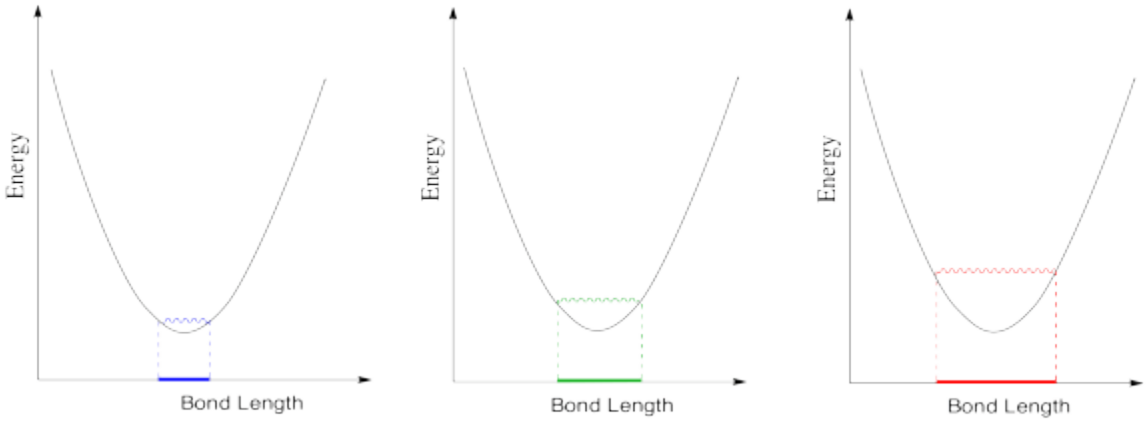
Exercise 11.6.1.2

In reality, a bond length is not static. If there is a little energy around, the bond can lengthen and shorten a little bit, or vibrate. A typical graph of molecular energy vs. bond length is shown below.



a. Why do you think energy increases when the bond gets shorter than optimal?
b. Why do you think energy increases when the bond gets longer than optimal?
c. In the following drawings, energy is being added as we go from left to right. Describe what is happening to the bond length as available energy increases.

Answer a available at the end of this section.



Exercise 11.6.1.3

The optimum C-O bond length in a carbon dioxide molecule is 1.116 Å. Draw a graph of what happens to internal energy when this bond length varies between 1.10 Å and 1.20 Å. Don't worry about quantitative labels on the energy axis.

Answer available at the end of this section.

Exercise 11.6.1.4

The optimum O-C-O bond angle in a carbon dioxide molecule is 180 °. Draw a graph of what happens to internal energy when this bond angle varies between 170 ° and 190 °. Don't worry about quantitative labels on the energy axis.

Answer available at the end of this section.

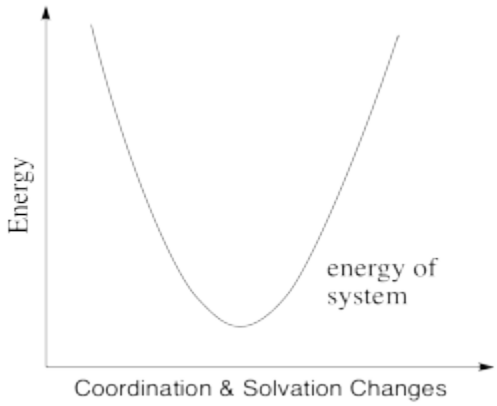
The barrier to electron transfer has to do with reorganizations of all those big atoms before the electron makes the jump. In terms of the coordination sphere, those reorganizations involve bond vibrations, and bond vibrations cost energy. Outside the coordination sphere, solvent molecules have to reorganize, too. Remember, ion stability is highly influenced by the surrounding medium.

Exercise 11.6.1.5

Draw a Fe(II) ion and a Cu(II) ion with three water molecules located somewhere in between them. Don't worry about the ligands on the iron or copper. Show how the water molecules might change position or orientation if an electron is transferred from iron to copper.

Answer available at the end of this section.

Thus, the energetic changes needed before electron transfer can occur involve a variety of changes, including bond lengths of several ligands, bond angles, solvent molecules, and so on. The whole system, involving both metals, has some optimum set of positions of minimum energy. Any deviations from those positions requires added energy. In the following energy diagram, the x axis no longer defines one particular parameter. Now it lumps all changes in the system onto one axis. This picture is a little more abstract than when we are just looking at one bond length or one bond angle, but the concept is similar: there is an optimum set of positions for the atoms in this system, and it would require an input of energy in order to move any of them move away from their optimum position.

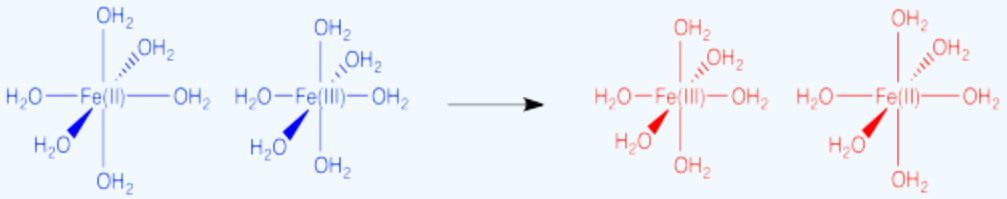


It is thought that these kinds of reorganizations -- involving solvent molecules, bond lengths, coordination geometry and so on -- actually occur prior to electron transfer. They happen via random motions of the molecules involved. However, once they have happened, there is nothing to hold the electron back. Its motion is so rapid that it can immediately find itself on the other atom before anything has a chance to move again.

Consequently, the barrier to electron transfer is just the amount of energy needed for all of those heavy atoms to get to some set of coordinates that would be accessible in the first state, before the electron is transferred, but that would also be accessible in the second state, after the electron is transfered.

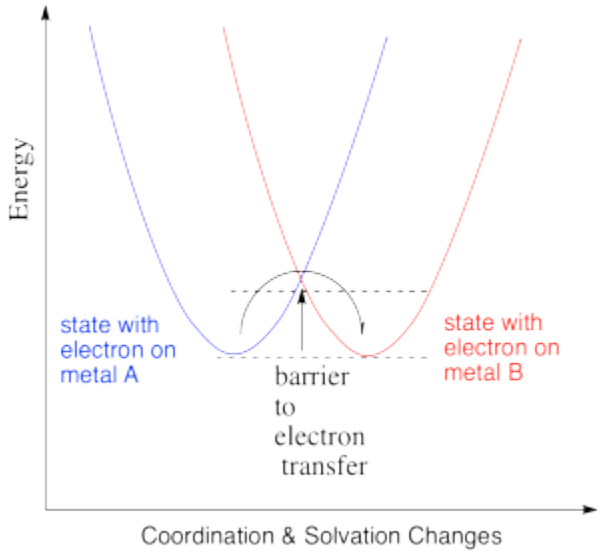
Exercise 11.6.1.6

Describe some of the changes that contribute to the barrier to electron transfer in the following case.

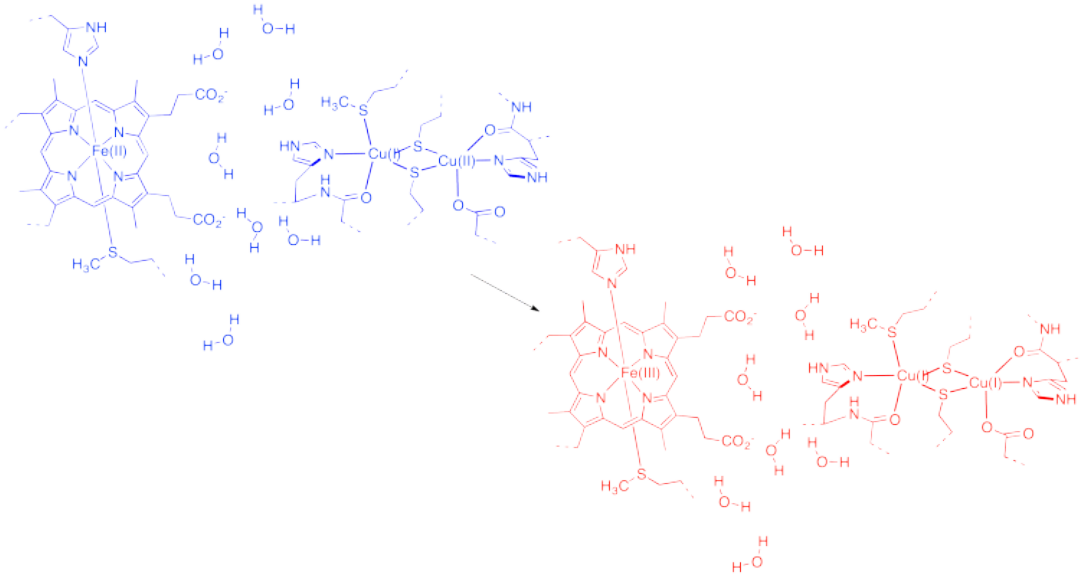


Answer available at the end of this section.

In the drawing below, an electron is transferred from one metal to another metal of the same kind, so the two are just switching oxidation states. For example, it could be an iron(II) and an iron(III), as pictured in the problem above. In the blue state, one iron has the extra electron, and in the red state it is the other iron that has the extra electron. The energy of the two states are the same, and the reduction potential involved in this transfer is zero. However, there would be some atomic reorganizations needed to get the coordination and solvation environments adjusted to the electron transfer. The ligand atoms and solvent molecules have shifted in the change from one state to another, and so our energy surfaces have shifted along the x axis to reflect that reorganization.



That example isn't very interesting, because we don't form anything new on the product side. Instead, let's picture an electron transfer from one metal to a very different one. For example, maybe the electron is transferred from cytochrome c to the "copper A" center in cytochrome c oxidase, an important protein involved in respiratory electron transfer.



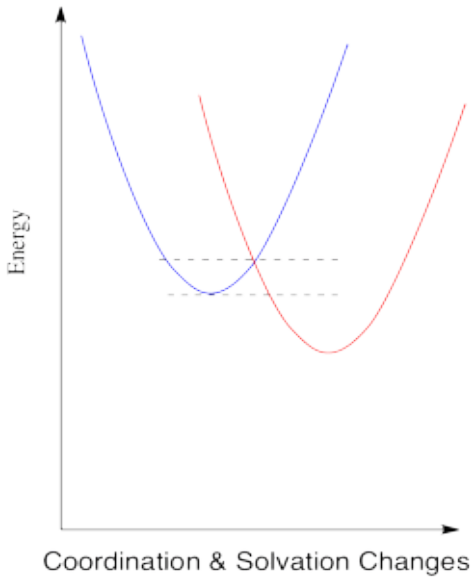
Exercise 11.6.1.7

In the drawing above, some water molecules are included between the two metal centres.

a. Explain what happens to the water molecules in order to allow electron transfer to occur, and why.
b. Suppose there were a different solvent, other than water, between the complexes. How might that affect the barrier to the reaction?

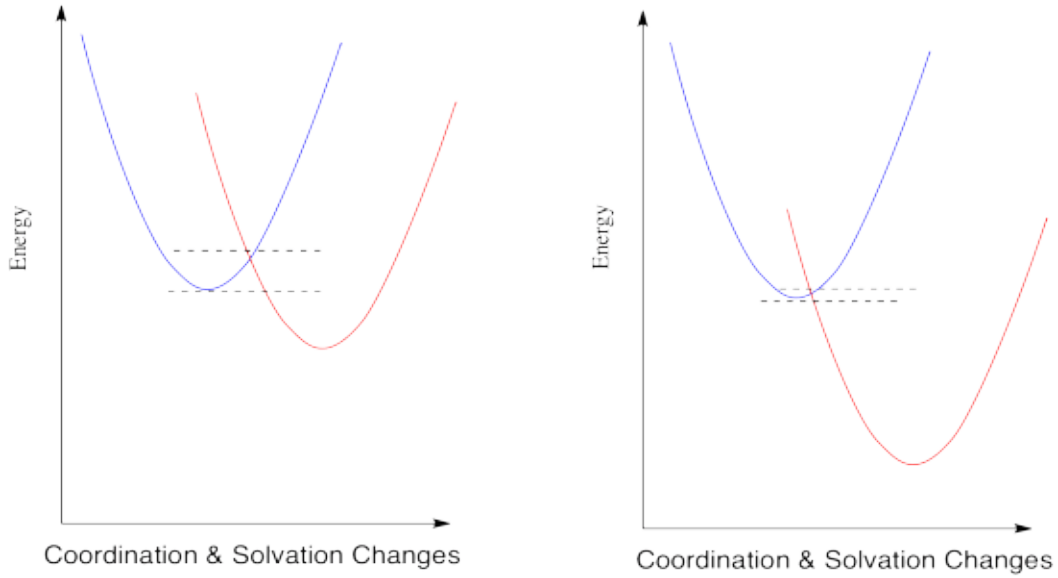
Answer a available at the end of this section.

The energy diagram for the case involving two different metals is very similar, except that now there is a difference in energy between the two states. The reduction potential is no longer zero. We'll assume the reduction potential is positive, and so the free energy change is negative. Energy goes down upon electron transfer.



Compare this picture to the one for the degenerate case, when the electron is just transferred to a new metal of the same type. A positive reduction potential (or a negative free energy change) has the effect of sliding the energy surface for the red state downwards. As a result, the intersection point between the two surfaces also slides downwards. Since that is the point at which the electron can slide from one state to the other, the barrier to the reaction decreases.

What would happen if the reduction potential were even more positive? Let's see in the picture below.



The trend continues. According to this interpretation of the kinetics of electron transfer, the more exothermic the reaction, the lower its barrier will be. It isn't always the case that kinetics tracks along with thermodynamics, but this might be one of them.

But is all of this really true? We should take a look at some experimental data and see whether it truly works this way.

Oxidant	E°	k ($M^{-1}s^{-1}$) (margin of error shown in parentheses)
$Co(diene)(NH_3)_2^{3+}$	0.12	3.0(4)
$Co(diene)H_2O)NCS^{2+}$	0.38	11(1)
$Co(diene)(H_2O)_2^{3+}$	0.53	800(100)
Co(EDTA)	0.60	6000(1000)

As the reduction potential becomes more positive, free energy gets more negative, and the rate of the reaction dramatically increases. So far, Marcus theory seems to get things right.

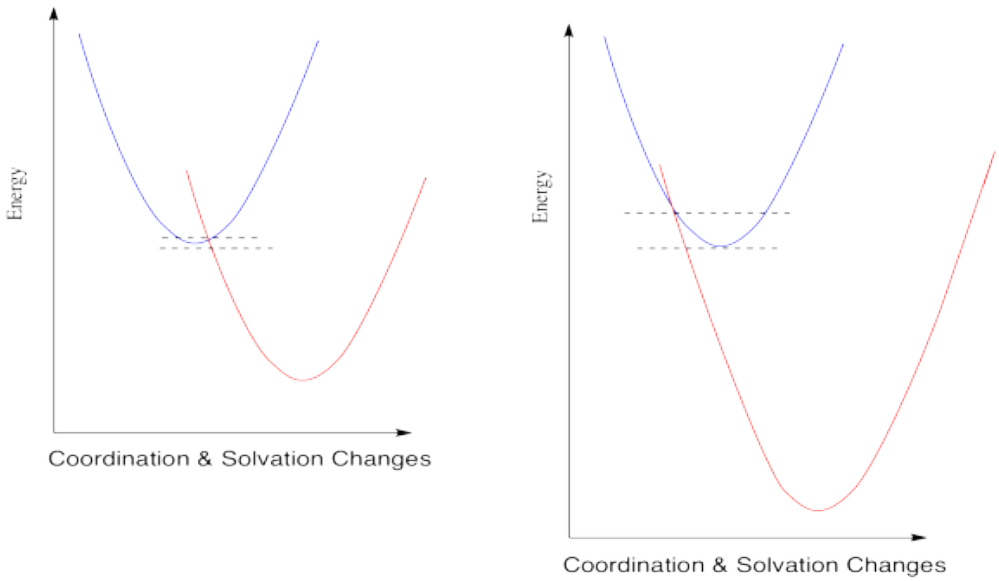
Exercise 11.6.1.8

a. Plot the data in the above table.
b. How would you describe the relationship? Is it linear? Is it exponential? Is it direct? Is it inverse?
c. Plot rate constant versus free energy change. How does this graph compare to the first one?

Answer a available at the end of this section.

Marcus Inverted Region

When you look a little closer at Marcus theory, though, things get a little strange. Suppose we make one more change and see what happens when the reduction potential becomes *even more* positive.

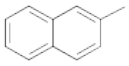
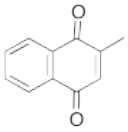
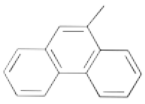
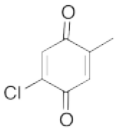
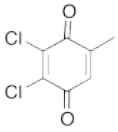


So, if Marcus is correct, at some point as the reduction potential continues to get more positive, reactions start to slow down again. They don't just reach a maximum rate and hold steady at that plateau; the barrier gets higher and higher and the reactions get slower and slower. If you feel a little skeptical about that, you're in good company.

Marcus always maintained that this phenomenon was a valid aspect of the theory, and not just some aberration that should be ignored. The fact that nobody had ever actually observed such a trend didn't bother him. The reason we didn't see this kind of thing, he said, was that we just hadn't developed technology that was good enough to measure these kind of rates accurately.

But technology did catch up. Just take a look at the following data (from Miller, *J. Am.Chem. Soc.* **1984**, *3047*).



Acceptor	ΔG	k	Acceptor	ΔG	k
	-0.05	2×10^6		-1.9	6×10^8
	-0.2	2×10^7		-2.2	1×10^8
	-0.5	1×10^9		-2.4	6×10^7

Don't worry that there are no metals involved anymore. An electron transfer is an electron transfer. Here, an electron is sent from the aromatic substructure on the right to the substructure on the left. By varying the part on the left, we can adjust the reduction potential (or the free energy change, as reported here.

Exercise 11.6.1.9

a. Plot the data in the above table.

b. How would you describe the relationship?

Answer a available at the end of this section.

As the reaction becomes more exergonic, the rate increases, but then it hits a maximum and decreases again. Data like this means that the "Marcus Inverted Region" is a real phenomenon. Are you convinced? So were other people. In 1992, Marcus was awarded the Nobel Prize in Chemistry for this work.

Exercise 11.6.1.10

Take a look at the donor/acceptor molecule used in Williams' study, above. a) Why do you suppose the free energy change is pretty small for the first three compounds in the table? b) Why does the free energy change continue to get bigger over the last three compounds in the table?

Answer available at the end of this section.

Exercise 11.6.1.11

The rates of electron transfer between cobalt complexes of the bidentate bipyridyl ligand, $Co(bipy)_3^{n+}$, are strongly dependent upon oxidation state in the redox pair. Electron transfer between Co(I)/Co(II) occurs with a rate constant of about 10^9 $M^{-1}s^{-1}$, whereas the reaction between Co(II)/Co(III) species proceeds with k = 18 $M^{-1}s^{-1}$.

a. What geometry is adopted by these complexes?
b. Are these species high spin or low spin?
c. Draw d orbital splitting diagrams for each complex.
d. Explain why electron transfer is so much more facile for the Co(I)/Co(II) pair than for the Co(II)/Co(III) pair.

Answer a available at the end of this section.

Answers

Exercise 11.6.1.1

The bonds to iron would contract because the increased charge on the iron would attract the ligand donor electrons more strongly. The bonds to copper would lengthen because of the lower charge on the copper.

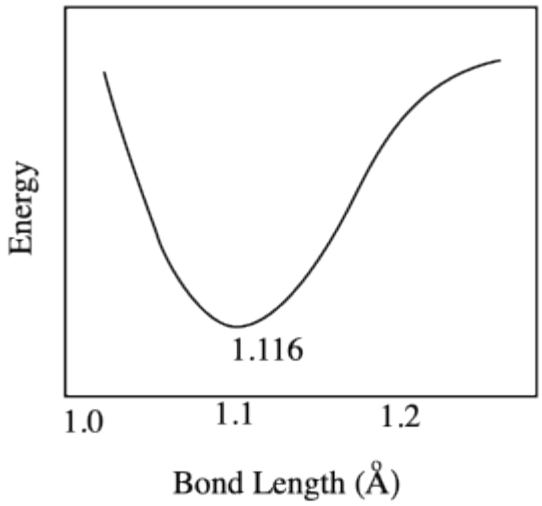
Exercise 11.6.1.2

a) Most likely there are repulsive forces between ligands if the bonds get too short.

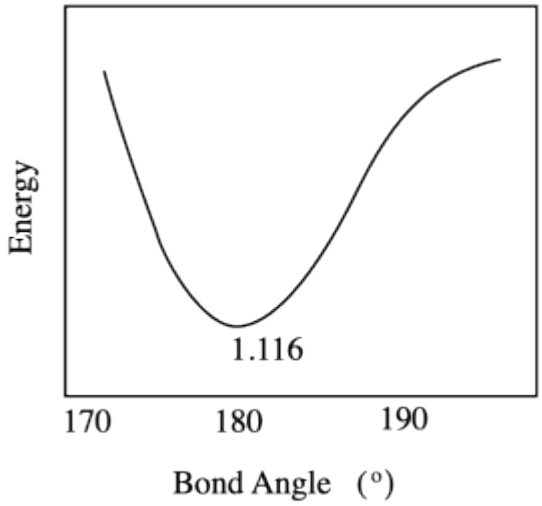
b) Insufficient overlap between metal and ligand orbitals would weaken the bond and raise the energy.

c) The range of possible bond lengths gets broader as energy is increased. The bond has more latitude, with both longer and shorter bonds allowed at higher energy.

Exercise 11.6.1.3

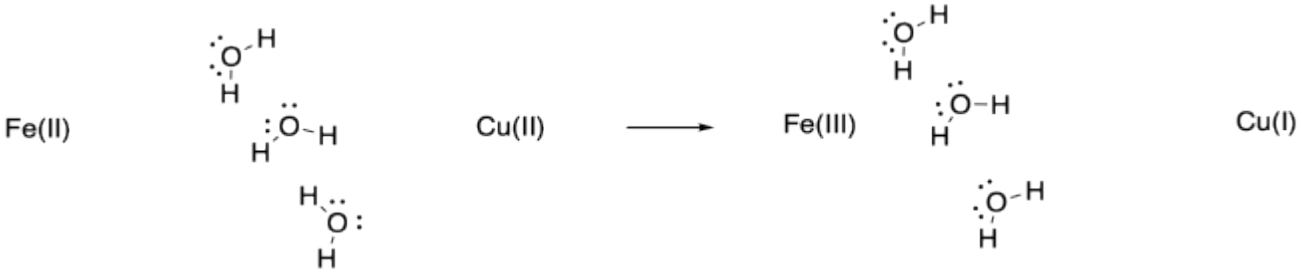


Exercise 11.6.1.4



Exercise 11.6.1.5

The water molecules may pivot toward the more highly charged Fe(III), or they may shift closer to it because of the attraction between the ion and the dipole of the water molecule.



Keep in mind that such adjustments would happen in non-polar solvents, too, although they would involve weaker IMFs such as ion - induced dipole interactions.

Exercise 11.6.1.6

The reactants and products are very similar in this case. However, the Fe(III) complex has shorter bonds than the Fe(II) complex because of greater electrostatic interaction between the metal ion and the ligands. These changes in bond length needed in order to get ready to change from Fe(III) to Fe(II) (or the reverse) pose a major barrier to the reaction.

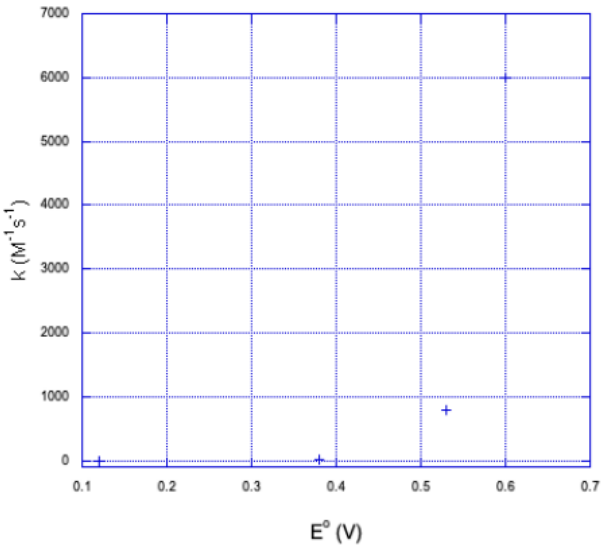
Exercise 11.6.1.7

a) The drawing is an oversimplification, but in general the water molecules are shown reorienting after the electron transfer because of ion-dipole interactions. In this case, the waters are shown orienting to present their negative ends to the more positive iron atom after the electron transfer. In reality, in a protein there are lots of other charges (including charges on the ligand) that may take part in additional ion-dipole interactions.

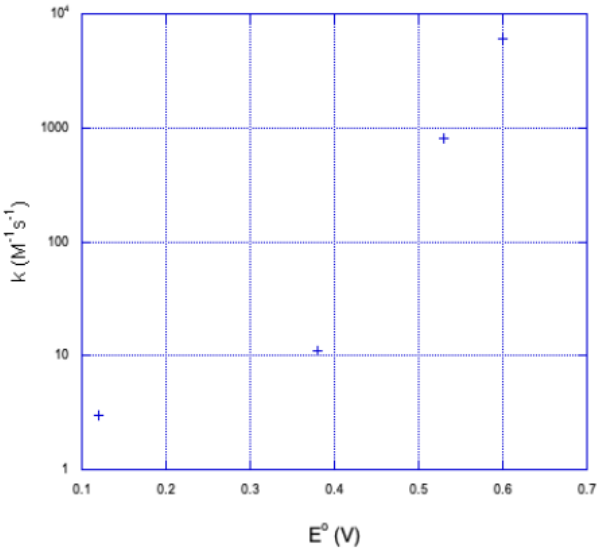
b) Because electron transfer is so fast, atomic and molecular reorganisations are actually thought to happen before the electron transfer. The water molecules would happen to shift into a position that would provide the greatest possible stabilisation for the ions and then the electron would be transferred. A less polar solvent than water would be less able to stabilize ions and the electron would be slower to transfer as a result. In addition, a less polar solvent than water would be a poor medium to transmit an electron, which is charged and therefore stabilized by interactions with polar solvents.

Exercise 11.6.1.8

a) Here is a plot of the data.

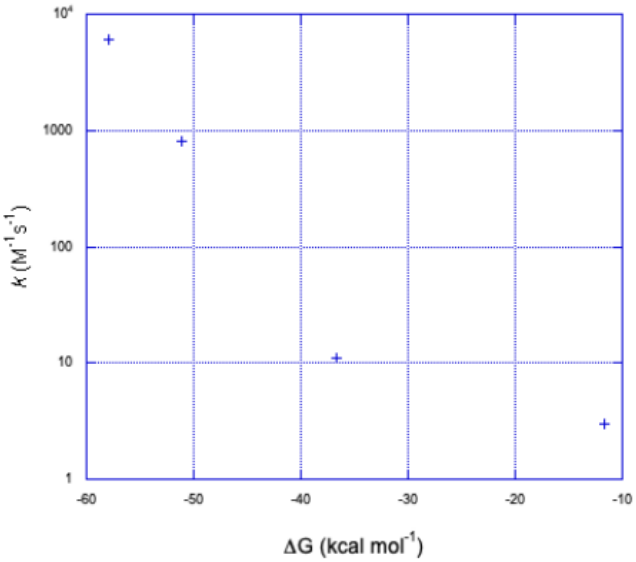


b) It doesn't look linear. If we plot the y axis on a log scale, things become a little more linear.



It looks closer to a logarithmic relationship than a linear one.

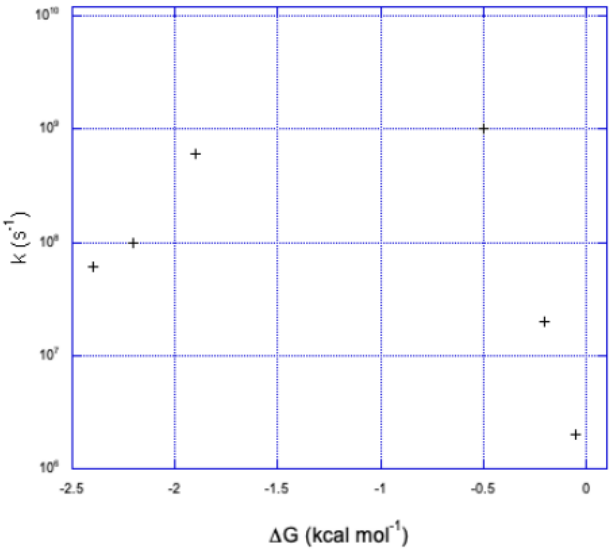
c) Assuming one electron transfer:



The graph takes the same form but in the opposite direction along the x axis.

Exercise 11.6.1.9

a)



b) We can see two sides of an inverted curve. The reaction gets much faster as the free energy becomes more negative, but at some point the rate begins to decrease again.

Exercise 11.6.1.10

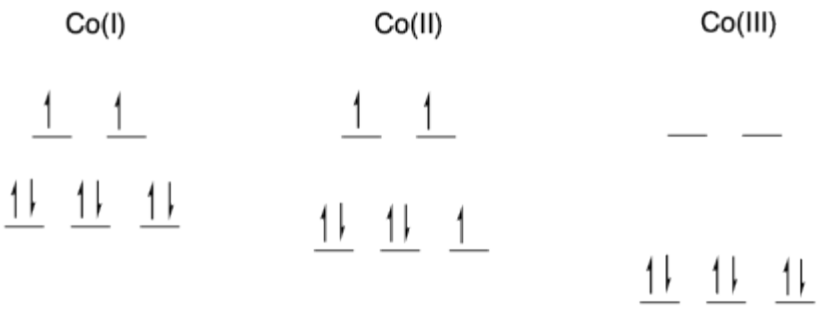
The acceptor compound becomes an anion when it accepts an electron. The first three compounds do not appear to be strongly electrophilic; they can accept electrons simply because of resonance stability of the resulting anion. The last three have electron withdrawing groups (chlorines and oxygens) that would stabilize the anion even further.

Exercise 11.6.1.11

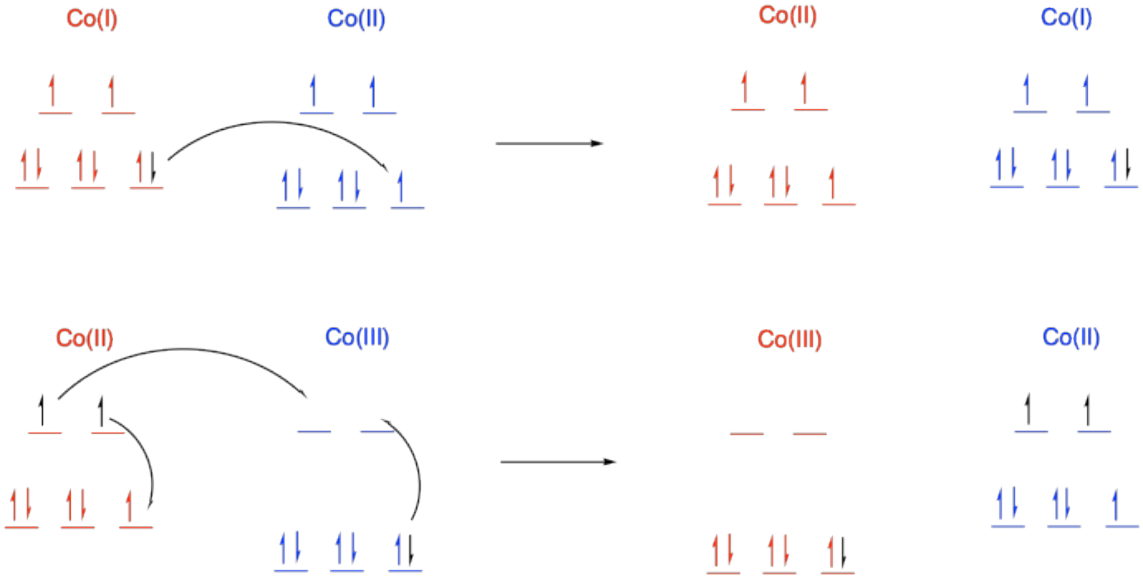
a) octahedral; bpy is a bidentate ligand.

b) Co is first row; Co(I) and Co(II) have relatively low charge. Usually we would expect them to be high spin. Co(III) is at a cut-off point in the first row; it is just electronegative enough that it is usually low spin.

c)



d) In a transfer from Co(II) to Co(III), there is additional reorganization needed because the metal changes between high and low spin. Not only does one electron have to move from one metal to another metal, but additional electrons have to shuffle from one orbital to another on the same metal to accommodate the change. These reorganizations have a barrier, slowing the reaction.



This page titled 11.6.1: Outer Sphere Electron Transfer is shared under a CC BY-NC 4.0 license and was authored, remixed, and/or curated by Chris Schaller.

- 1.9: Outer Sphere Electron Transfer by Chris Schaller is licensed CC BY-NC 3.0. Original source: https://employees.csbsju.edu/cschaller/ROBI3.htm.

11.6.2: Inner Sphere Electron Transfer

In some cases, electron transfers occur much more quickly in the presence of certain ligands. For example, compare the rate constants for the following two electron transfer reactions, involving almost exactly the same complexes:

$$Co(NH_3)_6{}^{3+} + Cr^{2+} \longrightarrow Co^{2+} + Cr^{3+} + 6\,NH_3 \;\; k = 10^{-4} M^{-1} s^{-1}$$

$$Co(NH_3)_5Cl^{2+} + Cr^{2+} \longrightarrow Co^{2+} + CrCl^{2+} + 6\,NH_3 \;\; k = 6 \times 10^{5} M^{-1} s^{-1}$$

(Note: aqua ligands are omitted for simplicity. Ions, unless noted otherwise, are aqua complexes.)

Notice two things: first, when there is a chloride ligand involved, the reaction is much faster. Second, after the reaction, the chloride ligand has been transferred to the chromium ion. Possibly, those two events are part of the same phenomenon.

Similar rate enhancements have been reported for reactions in which other halide ligands are involved in the coordination sphere of one of the metals.

In the 1960's, Henry Taube of Stanford University proposed that halides (and other ligands) may promote electron transfer via bridging effects. What he meant was that the chloride ion could use one of its additional lone pairs to bind to the chromium ion. It would then be bound to both metals at the same time, forming a bridge between them. Perhaps the chloride could act as a conduit for electron transfer. The chloride might then remain attached to the chromium, to which it had already formed a bond, leaving the cobalt behind.

Electron transfers that occur via ligands shared by the two metals undergoing oxidation and reduction are termed "inner sphere" electron transfers. Taube was awarded the Nobel Prize in chemistry in 1983; the award was based on his work on the mechanism of electron transfer reactions.

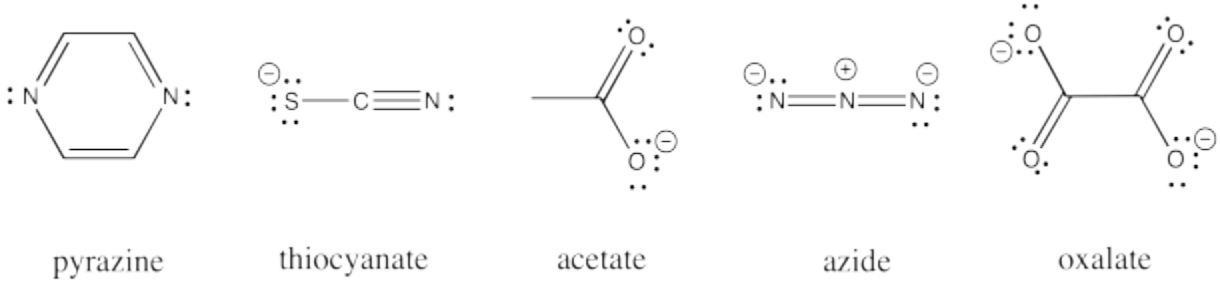
Exercise 11.6.2.1

Take another look at the two electron transfer reactions involving the cobalt and chromium ion, above.

a. What geometry is adopted by these complexes?
b. Are these species high spin or low spin?
c. Draw d orbital splitting diagrams for each complex.
d. Explain why electron transfer is accompanied by loss of the ammonia ligands from the cobalt complex.
e. The chloride is lost from the cobalt complex after electron transfer. Why does it remain on the chromium?

Answer a available at the end of this section.

Other ligands can be involved in inner sphere electron transfers. These ligands include carboxylates, oxalate, azide, thiocyanate, and pyrazine ligands. All of these ligands have additional lone pairs with which to bind a second metal ion.



pyrazine thiocyanate acetate azide oxalate

Exercise 11.6.2.2

Draw an example of each of the ligands listed above bridging between a cobalt(III) and chromium(II) aqua complex.

Answer available at the end of this section.

Exercise 11.6.2.3

Explain, with structures and d orbital splitting diagrams, how the products are formed in the following reaction, in aqueous solution.

$$\mathrm{Fe(OH_2)_6}^{2+} + \mathrm{(SCN)Co(NH_3)_5}^{2+} \longrightarrow \mathrm{(NCS)Fe(OH_2)_5}^{2+} + \mathrm{Co(OH_2)_6}^{2+} + 5\,\mathrm{NH_3}$$

Answer available at the end of this section.

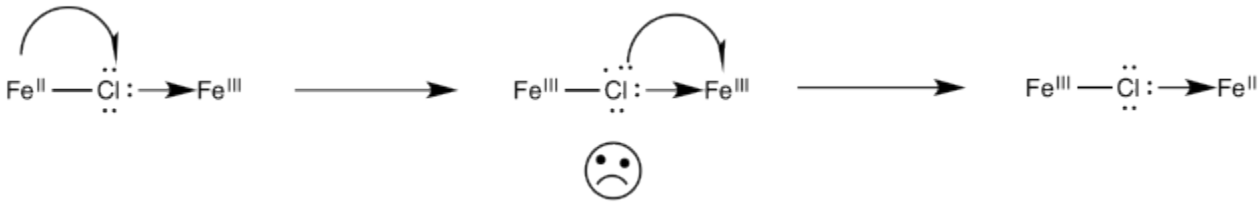
How does the electron travel over the bridge?

Once the bridge is in place, the electron transfer may take place via either of two mechanisms. Suppose the bridging ligand is a chloride. The first step might actually involve an electron transfer from chlorine to the metal; that is, the chloride could donate one electron from one of its idle lone pairs. This electron could subsequently be replaced by an electron transfer from metal to chlorine.



Sometimes, we talk about the place where an electron *used to be*, describing it as a "hole". In this mechanism, the electron donated from the bridging chloride ligand leaves behind a hole. The hole is then filled with an electron donated from the other metal.

Alternatively, an electron might first be transferred from metal to chlorine, which subsequently passes an electron along to the other metal. In the case of chlorine, this idea may be unsatisfactory, because chlorine already has a full octet. Nevertheless, some of the other bridging ligands may have low-lying unoccupied molecular orbitals that could be populated by this extra electron, temporarily.



Exercise 11.6.2.4

For the iron / cobalt electron transfer in problem Exercise 11.6.2.3 (RO9.3.), show

a. an electron transfer mechanism via a hole migration along the bridge
b. an electron transfer mechanism via an electron migration along the bridge

Answer a available at the end of this section.

Exercise 11.6.2.5

One of the many contributions to the barrier for electron transfer between metal ions is internal electronic reorganization.

a) Draw d orbital splitting diagrams for each of the following metal ions in an octahedral environment.

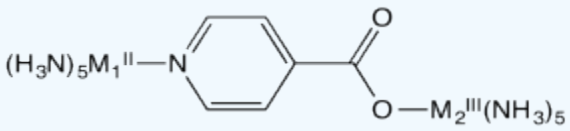
Ru(II) or Os(II)

Ru(III) or Os(III)

Co(II)

Co(III)

Flash photolysis is a method in which an electron can be moved instantly "uphill" from one metal to another (e.g. from M_2^{II} to M_1^{III}, below); the electron transfer rate can then be measured as the electron "drops" back from M_1^{II} to M_2^{III}.



b) Explain the relative rates of electron transfer reaction in this system, as measured by flash photolysis in the table below.

M_1^{II}	M_2^{III}	k_{obs} s^{-1}
Os	Ru	> 5 x 10^9
Os	Co	1.9 x 10^5

c) Does the reaction above probably occur via an inner sphere or by an outer sphere pathway? Why?

Answer a available at the end of this section.

Exercise 11.6.2.6

Outer sphere electron transfer rates depend on the free energy change of the reaction (ΔG°) and the distance between oxidant and reductant (d) according to the relation

Rate constant = $k = Ae^{(-\Delta G)}e^{-d}$

a) What happens to the rate of the reaction as distance increases between reactants?

One potential problem in measuring rates of intramolecular electron transfer (i.e. *within* a molecule) is competition from intermolecular electron transfer (*between* molecules).

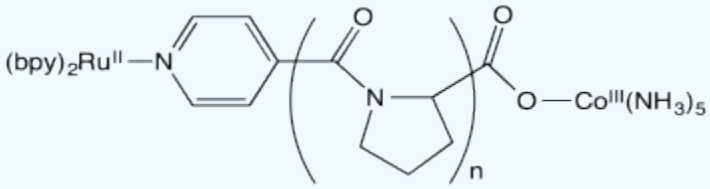
b) What would you do in the flash photolysis experiment above to discourage intermolecular electron transfer?

c) How could you confirm whether you were successful in discouraging intermolecular reaction?

Answer a available at the end of this section.

Exercise 11.6.2.7

Stephan Isied and coworkers at Rutgers measured the following electron transfer rates between metal centers separated by a peptide. (*Chem Rev* **1992**, *92*, 381-394)



a. The proline repeating unit is crucial in ensuring a steady increase in distance between metal centers with increased repeat units, n. Why?
b. An inner sphere pathway in this case is expected to be somewhat slow because of the lack of conjugation in the polyproline bridge. Explain why.
c. Plot the data below, with log*k* on the y axis (range from 4-9) and d on the x axis (12-24 Angstroms).

n	d (Å)	k_{obs} (s^{-1})
1	12.2	5×10^8
2	14.8	1.6×10^7
3	18.1	2.3×10^5
4	21.3	5.1×10^4
5	24.1	1.8×10^4

d) A linear relationship is in agreement with Marcus theory; log*k* = - c x d. Is your plot linear?

Isied offers a number of possible explanations for the data, all of which involve two competing reaction pathways.

e) Suggest one explanation for the data.

Answer a

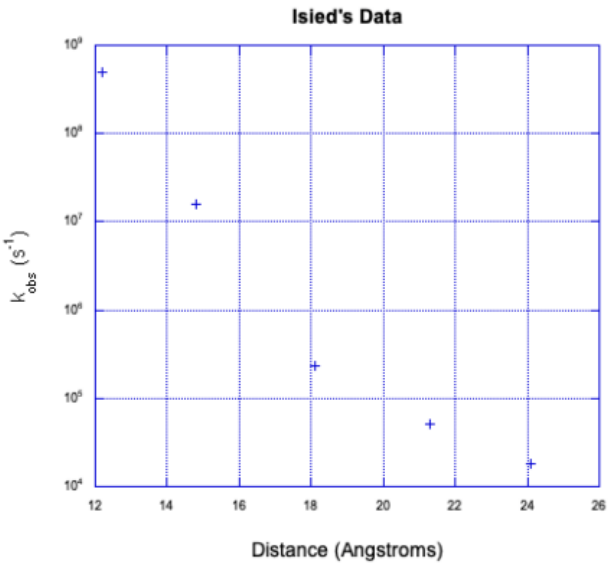
a) Rings are frequently used to introduce conformational rigidity (or decrease conformational flexibility), limiting the range of potential shapes a molecule could adopt. If the molecule can't wiggle around as much, then the distance between the ends of the molecule should be more constant.

Answer b

b) Although the ligand is bridging, it would be difficult to picture either an electron or hole mechanism of inner sphere electron transfer. There are few pi bonds or lone pairs to use as places to put electrons or temporarily remove electrons from, shuttling the electrons from place to place along the ligand. A conjugated system would be much more likely to carry out inner sphere electron transfer.

Answer c

c)



Answer d

d) The data is not linear.

Answer e

e) The data appear to show two lines that cross. That's a classic symptom of two competing mechanisms. The faster mechanism, to the left, is probably an intramolecular electron transfer. The slower mechanism, to the right, may be an intermolecular electron transfer.

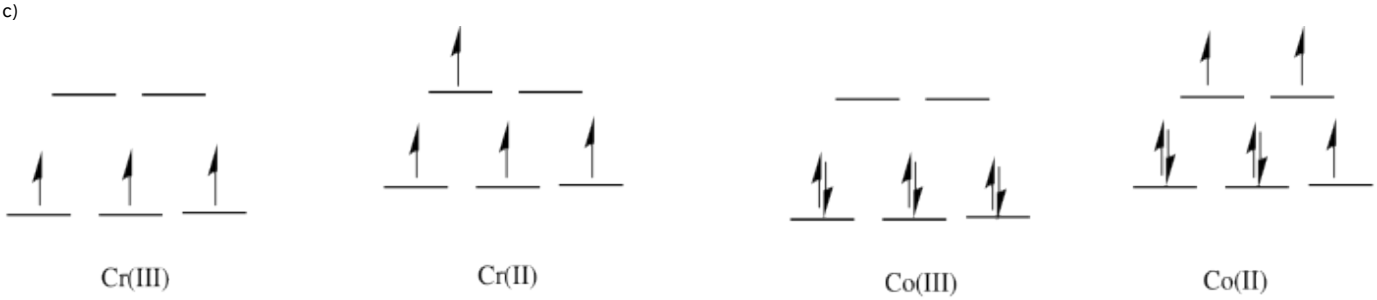
Answers

Exercise 11.6.2.1

a) octahedral

b) In the first row, 2^+ complexes are almost always high spin. However, 3^+ complexes are sometimes low spin.

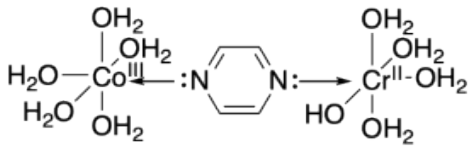
c)

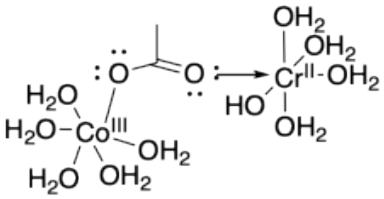


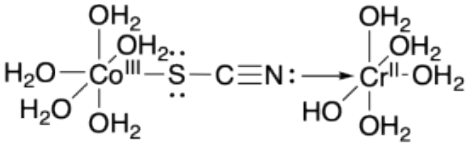
d) The Co(II) complex is high spin and labile. The ligands are easily replaced by water.

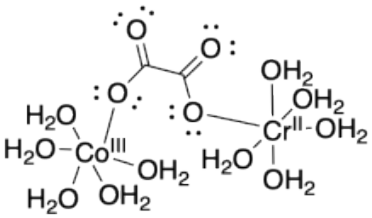
e) The Cr(III) complex is only d^3; it is inert.

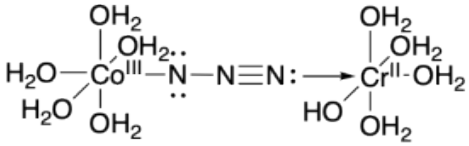
Exercise 11.6.2.2



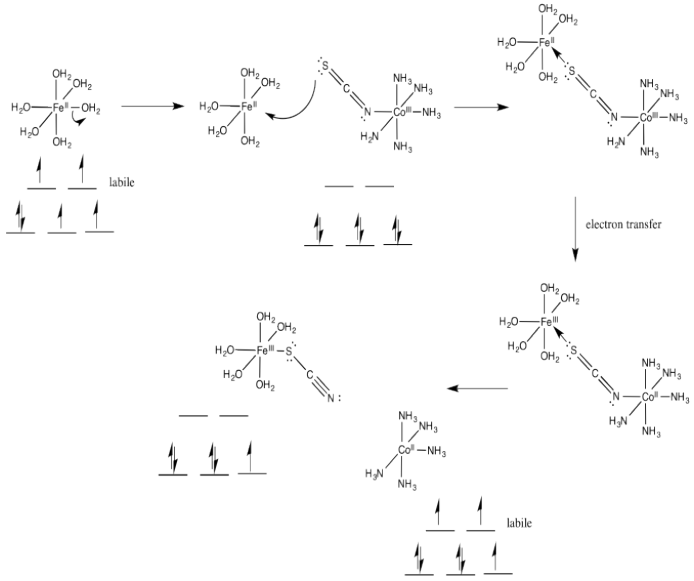




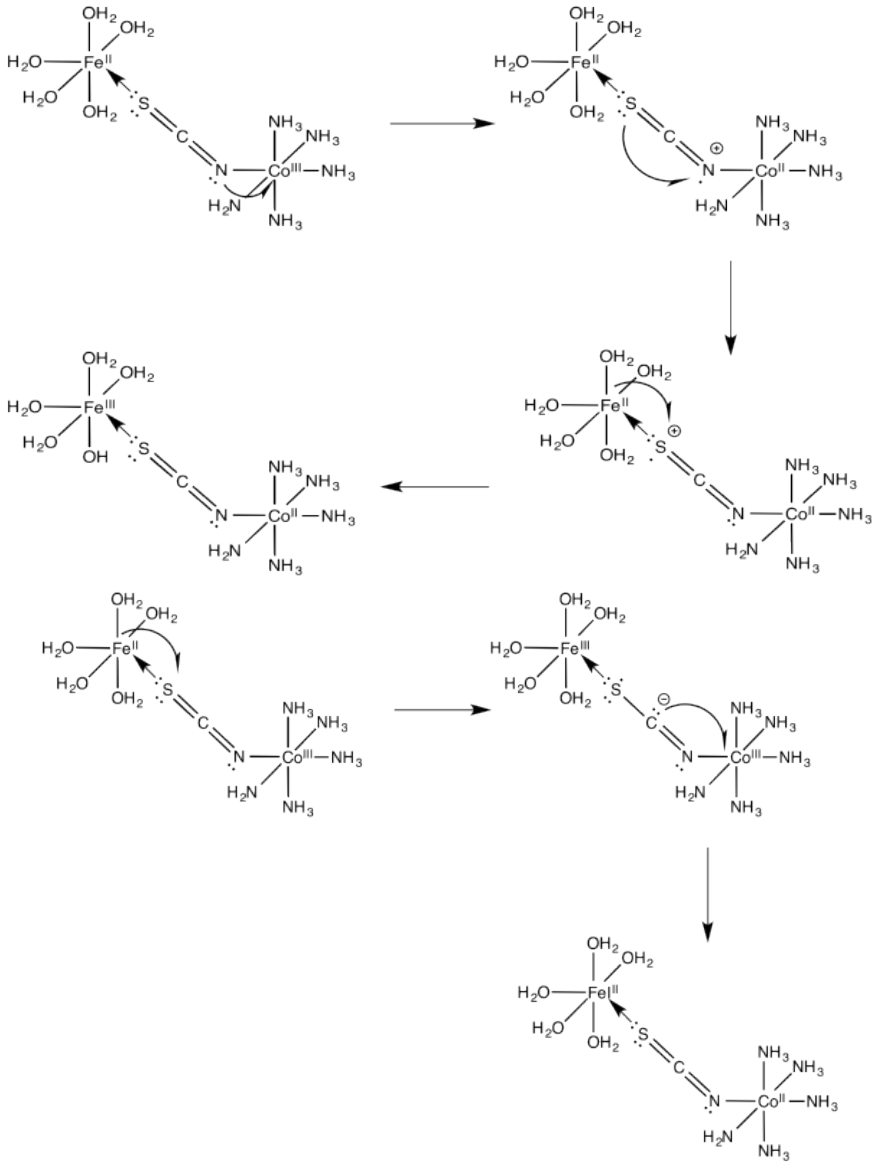




Exercise 11.6.2.3

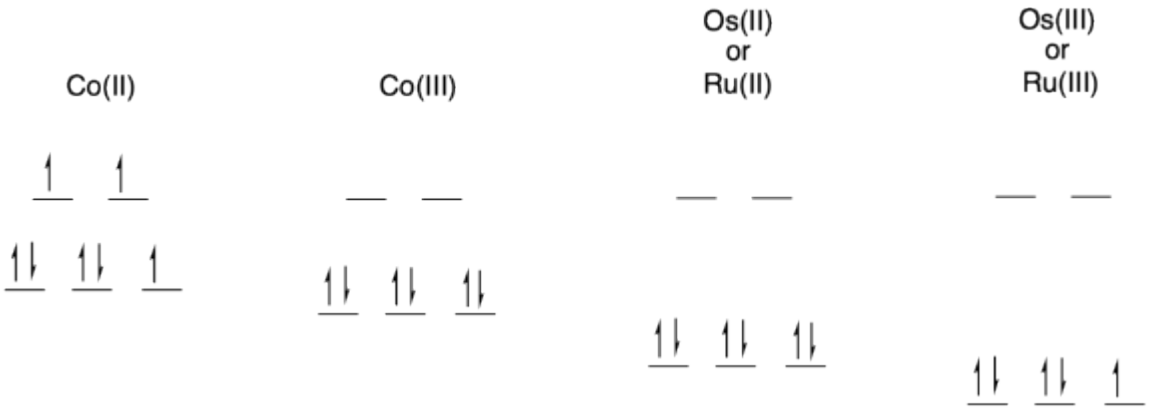


Exercise 11.6.2.4



Exercise 11.6.2.5

a)



b) The electron transfer between Os(II) and Ru(III) will not involve any electron reorganization because both are low spin to begin with. However, the electron transfer between Os(II) and Co(III) will result in cobalt changing from low spin to high spin. The need to move electrons between different d orbitals on the cobalt will add to the barrier, slowing down the reaction.

c) The pathway is probably inner sphere because of the bridging ligand. Furthermore, the conjugation in the bridging ligand would help in conducting an electron from one end of the ligand to the other, either through an electron mechanism or a hole mechanism.

Exercise 11.6.2.6

a) The rate decreases exponentially as distance increases.

b) You might keep the concentration low in order to increase the distance between molecules, reducing the likely hood of an outer-sphere electron transfer.

c) If you ran the experiment at a series of dilutions, intramolecular electron transfer would be unaffected but outer sphere electron transfer would not. If the rates were the same across a number of different concentrations, the reaction would probably be intramolecular.

This page titled 11.6.2: Inner Sphere Electron Transfer is shared under a CC BY-NC 4.0 license and was authored, remixed, and/or curated by Chris Schaller.

- 1.10: Inner Sphere Electron Transfer by Chris Schaller is licensed CC BY-NC 3.0. Original source: https://employees.csbsju.edu/cschaller/ROBI3.htm.

12: STRUCTURES AND ENERGETICS OF METALLIC AND IONIC SOLIDS

12.1: Alloys and Intermetallic Compounds

12.1A: Substitutional Alloys

12.1B: Interstitial Alloys

12.1C: Intermetallic Compounds

12.2: Bonding in Metals and Semicondoctors

12.2A: Electrical Conductivity and Resistivity

12.2B: Band Theory of Metals and Insulators

12.2C: The Fermi Level

12.2D: Band Theory of Semiconductors

12.3: Ionic Lattices

12.3A: Structure - Rock Salt (NaCl)

12.3B: Structure - Caesium Chloride (CsCl)

12.3C: Structure - Fluorite (CaF_2)

12.3D: Structure - Antifluorite

12.3E: Structure - Zinc Blende (ZnS)

12.3F: Structure - β-Cristobalite (SiO_2)

12.3H: Structure - Rutile (TiO_2)

12.3I: Structure - Layers (CdI_2 and $CdCl_2$)

12.3J: Structure - Perovskite ($CaTiO_3$)

12.4: Lattice Energy - The Born-Haber Cycle

12.5: Defects in Solid State Lattices

12.5.E: Defects in Solid State Lattices (Exercises)

12.5A: Schottky Defect

12.5B: Frenkel Defect

12.5C: Experimental Observations of Schottky and Frenkel Defects

12.5D: Non-Stoichiometric Compounds

12.5E: Color Centers (F-Centers)

12.5F: Thermodynamic Effects of Crystal Defects

12.6: Introduction

12.7: Packing of Spheres

12.7A: Cubic and Hexagonal Closed Packing

12.7B: The Unit Cell of HPC and CCP

1.1: The Unit Cell

12.7C: Interstitial Holes in HCP and CCP

12.7D: Non-closed Packing- Simple Cubic and Body Centered Cubic

12.8: The Packing of Spheres Model Applied to the Structures of Elements

12.8A: Group 18 Elements in the Solid State

12.8B: H_2 and F_2 Solids

12.8C: Solid Metallic Elements

12.9: Polymorphism in Metals

12.9A: Polymorphism - Phase Changes in the Solid State

12.9B: Phase Diagrams

12.10: Metallic Radii

12.11: Melting Points and Standard Enthalpies of Atomization of Metals

12.12: Size of Ions

12.12A: Ionic Radii

12.12B: Periodic Trends in Ionic Radii

12.13: Crystal Structure of Semiconductors

This page titled 12: Structures and Energetics of Metallic and Ionic solids is shared under a license and was authored, remixed, and/or curated by LibreTexts.

- 6: Structures and Energetics of Metallic and Ionic solids is licensed CC BY-NC-SA 4.0.

12.1: ALLOYS AND INTERMETALLIC COMPOUNDS

Alloys are mixtures of metals or a mixture of a metal and another element. An alloy may be a *solid solution* of metal elements (a homogeneous mixture) or a mixture of metallic phases (a heterogeneous mixture of two or more solutions).



- Topic hierarchy

12.1A: Substitutional Alloys

12.1B: Interstitial Alloys

12.1C: Intermetallic Compounds

This page titled 12.1: Alloys and Intermetallic Compounds is shared under a license and was authored, remixed, and/or curated by LibreTexts.

- 6.7: Alloys and Intermetallic Compounds is licensed CC BY-NC-SA 4.0.

12.1A: Substitutional Alloys

When a molten metal is mixed with another substance, there are two mechanisms that can cause an alloy to form: (1) *atom exchange* or (2) *interstitial mechanism*. The relative size of each element in the mix plays a primary role in determining which mechanism will occur.

When the atoms are relatively similar in size, the atom exchange method usually happens, where some of the atoms composing the metallic crystals are substituted with atoms of the other constituent. This is called a *substitutional alloy*. Examples of substitutional alloys include bronze and brass, in which some of the copper atoms are substituted with either tin or zinc atoms.

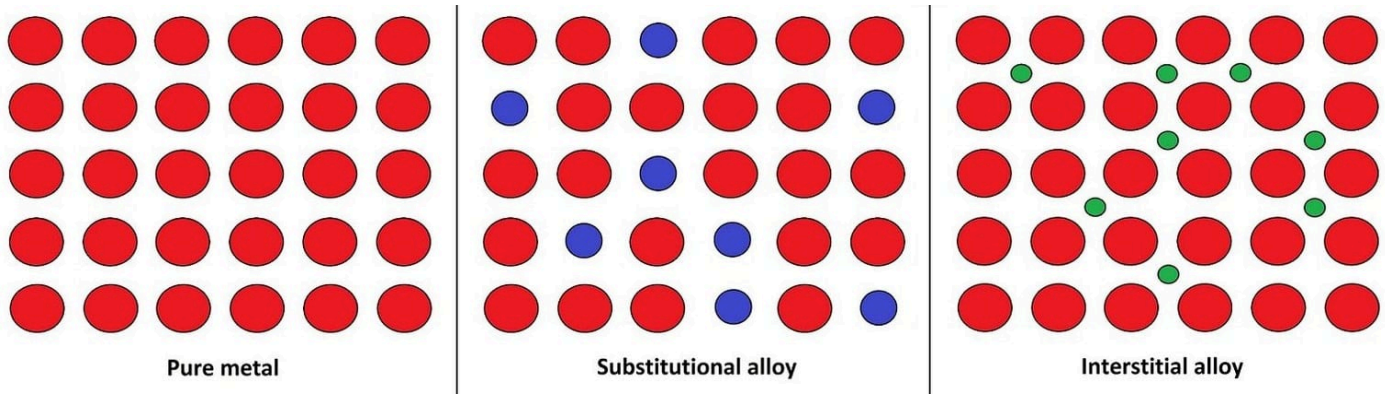


Figure 12.1A.1: Different atomic mechanisms of alloy formation, showing pure metal, substitutional, and interstitial structures. (CCO; Hbf878 via Wikipedia)

Why Substitutional Alloys Occur: Bonding

The bonding between two metals is best described as a combination of metallic electron "sharing" and covalent bonding, one can't occur without the other and the proportion of one to the other changes depending on the constituents involved. Metals share there electrons throughout there structure, this flow of electrons is the reason behind many of the characteristics associated with metals, including their ability to act as conductors. The different amount and strength of covalent bonds can change depending on the different specific metals involved and how they are mixed. The covalent bonding is what is responsible for the crystal structure as well as the melting point and various other physical properties.

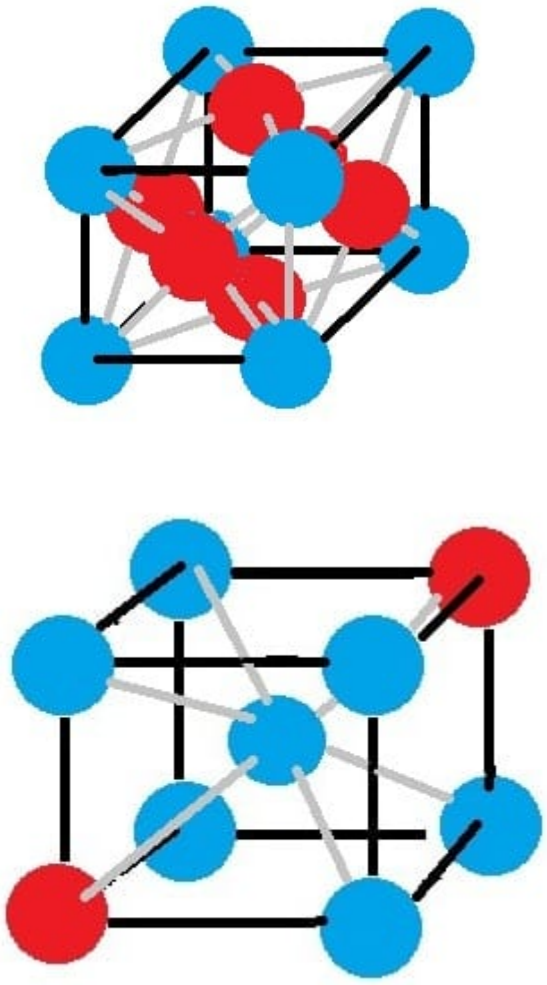


Figure 12.1A.2: Examples of Substitutional Metal Alloys. Depending on the specific type of substitutional alloy they can have multiple crystal structures. Two of the possible structures include Face Center Cubic (left), and Cubic Center Cubic (right). The structure of the metal alloy is not limited to these two structures, but combined they represent a large portion of the common alloys.

As the similarities between the electron structure of the metals involved in the alloy increase, the metallic characteristics of the alloy decrease. Pure metals are useful but their applications are often limited to each individual metal's properties. Alloys allow metal mixtures that have increased resistance to oxidation, increased strength, conductivity, and melting point; Essentially any property can be manipulated by adjusting alloy concentrations. An example could be Brass Door fixtures, they are strong and resist corrosion better then pure zinc or copper, the two major metals that constitute a brass alloy. The combination also has a low melting point allowing it to be easily cast into many different shapes and sizes.(1) There are many other aspects of substitutional alloys that could be explored in depth, but the basic concept is the idea that each individual metal in an alloy give the final product its chemical and physical properties.

Substitutional alloys played an important role in the development of human society and culture as we know it today. The Bronze age itself is named after the Substitutional alloy consisting of tin in a metallic solution of copper. Ancient bronzes are very impure, or even mislabeled, containing large amounts of zinc and arsenic as well as lots of impurities. These many substitutional alloys allowed for stronger tools and weapons, they allowed for increased productivity in the workshop as well as on the battlefield. The need for raw materials like tin and copper for the production of bronze also spurred an increase in trade, since their ores are rarely found together. The current chemical understanding of substitutional alloys would not be so in depth if it weren't for the usefulness of the alloys to humans.

Summary

An alloy is a mixture of metals that has bulk metallic properties different from those of its constituent elements. Alloys can be formed by substituting one metal atom for another of similar size in the lattice (substitutional alloys), by inserting smaller atoms into holes in the metal lattice (interstitial alloys), or by a combination of both. Although the elemental composition of most alloys can vary over wide ranges, certain metals combine in only fixed proportions to form intermetallic compo

References

1. Smallman, R. E., Ngan, A. H. W., & Smallman, R. E. (2007). *Physical metallurgy and advanced materials*. Amsterdam: Butterworth Heinemann.
2. Wang, F. E.. (2005). *Bonding theory for metals and alloys*. Amsterdam: Elsevier.
3. Dickinson, O. T. P. K. (1994). *The Aegean Bronze age*. Cambridge world archeology. Cambridge: Cambridge University Press.

Problems

1. Are substitutional metal alloys naturally occurring on earths surface?
2. What are two characteristics of a metal required for a substitutional alloy to form?
3. Can Oxygen or Nitrogen be a part of the crystal structure of a substitutional alloy?

Solutions

1. No, the oxidizing nature of the earths atmosphere, as well as the need for specific and concentrated metals keeps these from being found naturally occurring.
2. Similar radii and similar electronegativity.
3. Only metallic elements can form the necessary metallic bonds that allow alloys to form.

This page titled 12.1A: Substitutional Alloys is shared under a license and was authored, remixed, and/or curated by LibreTexts.

- 6.7A: Substitutional Alloys is licensed CC BY-NC-SA 4.0.

12.1B: Interstitial Alloys

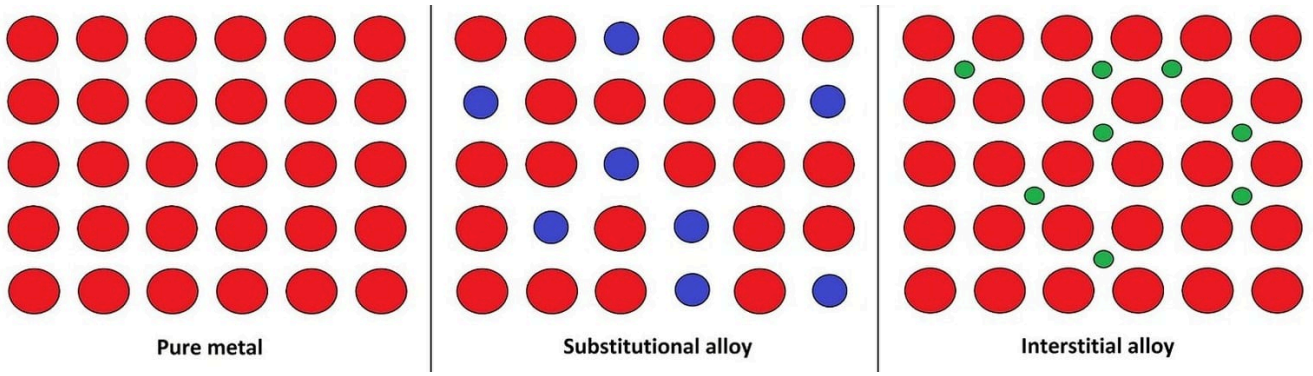


Figure 6.7B.1: *Different atomic mechanisms of alloy formation, showing pure metal, substitutional, and interstitial structures. from Wikipedia.*

With the interstitial mechanism, one atom is usually much smaller than the other, so cannot successfully replace an atom in the crystals of the base metal. The smaller atoms become trapped in the spaces between the atoms in the crystal matrix, called the *interstices*. This is referred to as an *interstitial alloy*. Steel is an example of an interstitial alloy, because the very small carbon atoms fit into interstices of the iron matrix. Stainless steel is an example of a combination of interstitial and substitutional alloys, because the carbon atoms fit into the interstices, but some of the iron atoms are replaced with nickel and chromium atoms.

This page titled 12.1B: Interstitial Alloys is shared under a license and was authored, remixed, and/or curated by LibreTexts.

- 6.7B: Interstitial Alloys is licensed CC BY-NC-SA 4.0.

12.1C: Intermetallic Compounds

Intermetallic compounds are solid phases containing two or more metallic elements, with optionally one or more non-metallic elements, whose crystal structure differs from that of the other constituents. Under this definition the following are included

- The definition of a metal is taken to include:
  - the so-called post-transition metals, i.e. aluminium, gallium, indium, thallium, tin and lead
  - some, if not all, of the metalloids, e.g. silicon, germanium, arsenic, antimony and tellurium.

Contributors and Attributions

- Wikipedia

This page titled 12.1C: Intermetallic Compounds is shared under a license and was authored, remixed, and/or curated by LibreTexts.

- 6.7C: Intermetallic Compounds is licensed CC BY-NC-SA 4.0.

12.2: BONDING IN METALS AND SEMICONDOCTORS

12.2A: Electrical Conductivity and Resistivity
12.2B: Band Theory of Metals and Insulators
12.2C: The Fermi Level
12.2D: Band Theory of Semiconductors

This page titled 12.2: Bonding in Metals and Semicondoctors is shared under a license and was authored, remixed, and/or curated by LibreTexts.

- 6.8: Bonding in Metals and Semicondoctors is licensed CC BY-NC-SA 4.0.

12.2A: Electrical Conductivity and Resistivity

Electrical resistivity and conductivity is an important property for materials. Different materials have different conductivity and resistivity. Electrical conductivity is based on electrical transport properties. These can be measured with multiple techniques by using a variety of instruments. If electricity easily flows through a material, that material has high conductivity. Some materials that have high conductivity include copper and aluminum. Electrical conductivity is the measure of how easily electricity flows through a material.

Conductivity vs Resistivity

Conductivity and resistivity are inversely proportional to each other. When conductivity is low, resistivity is high. When resistivity is low, conductivity is high. The equation is as follows:

$$\rho = \frac{1}{\sigma} \tag{12.2A.1}$$

where

- Resistivity is represented by ρ and is measured in **Ohm-meters** (Ωm),
- Conductivity is represented by σ and is measured in **Siemens** $(1/\Omega m)$.

Since conductivity is the measure of how easily electricity flows, electrical resistivity measures how much a material resists the flow of electricity.

Electrical Transport Properties

Simply put, electricity is the movement of electrons through a material. As electrons move through a material, it comes into contact with atoms in the material. Collisions slow the electrons down. Each collision increases the resistivity of the material. The easier the electrons continue through a material, the fewer collisions that take place and the higher the conductivity.

When temperature increases, the conductivity of metals usually decreases, while the conductivity of semiconductors increases. This of course assumes that the material is homogenous, which is not always the case. You can calculate resistivity using the following equation

$$\frac{E}{J} = \rho \tag{12.2A.2}$$

As you already read, ρ is the symbol for resistivity. E is the electric field and has units of Volts per meter (V/m). J is the current density and has units of amps per meter squared (A/m2). The electric field is calculated by dividing the Voltage by the length, l, that voltage is applied.

$$E = \frac{V}{l} \tag{12.2A.3}$$

The current density is calculated by the equation below

$$J = \frac{I}{A} \tag{12.2A.4}$$

I is the current and is divided by the cross sectional area, A, over which the current flows.

Resistivity vs Resistance

Resistivity and resistance are two different things. Resistivity does not depend on size or shape. Resistance, however, does. You can calculate resistance with the equation below.

$$R = \frac{V}{I} \tag{12.2A.5}$$

R refers to resistance and is measured in Ω. V is the voltage and is measured in volts. I measures the current and its unit is amps (A).

References

1. Electrical Conductivity and Resistivity, Heaney, Michael, Electrical Measurement, Signal Processing, and Displays. Jul 2003
2. Levy, Peter M., and Shufeng Zhang. "Electrical Conductivity of Magnetic Multilayered Structures." *Physical Review Letters* 65.13 (1990): 1643-646. Print.

Problems

1. What is the current density of a material with a resistivity of 12.Ωm and an electric field of 64.V/m?
2. If the voltage of 6V is passed through a substance with a radius of 2m and a length of 3m, what is the electric field?
3. What is the electric field of a material when the current is equal to 25A, the resistance is measured to be 78Ω, the current density equals 24A/m2, and the length the current flows is 100m?
4. A material has a voltage of 150V and width of 24m. The material also has a current of 62A and travels a distance of 5m. What is the conductivity?
5. A metal originally has an electron colliding with every fifth atom and increases from a temperature of 6K to 100K. A semiconductor originally has an electron colliding with every fifth atom and increases from a temperature of 6K to 100K. What material will have a greater resistivity? Why?

Answers to Problems:

1. E/J = ρ ---> J=E/ρ = 64V/m /12Ωm = 5.33A/m^2

2. E=V/l = 6V/3m = 2V/m

3. E=V/l

V=IR ---> E=IR/l = 25A x 78Ω/100m = 19.5V/m

4. E/J = ρ

E=V/l

J=I/A ---> ρ=(V/l)/(I/A) = (150V/5m)/(62A/(24m x 5m) = 58Ωm

ρ = 1/σ ---> 1/ρ = σ = 1/58Ωm

5. The material that has the greatest resistivity is the metal because as temperature increases metals are more likely to increase in resistivity and semiconductors usually decrease in resistivity as temperature increase.

Contributors and Attributions

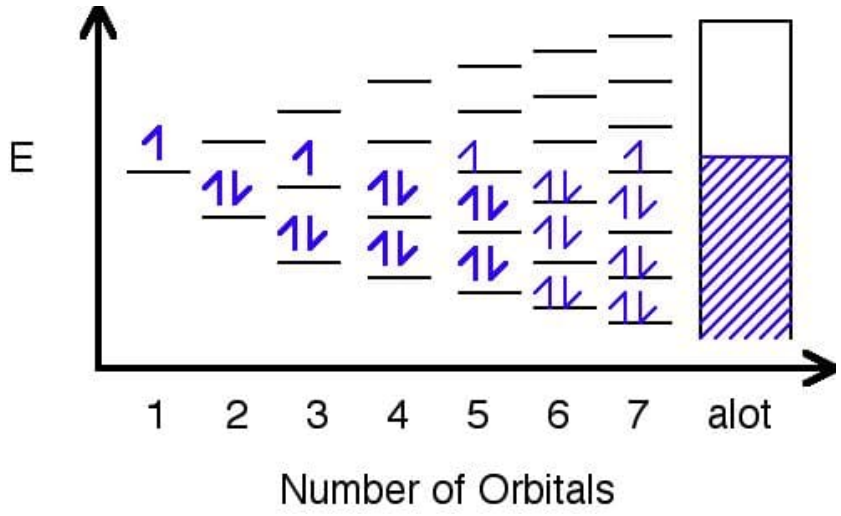
- Michael Ford (UCD) and Alexandra Christman (UCD)

This page titled 12.2A: Electrical Conductivity and Resistivity is shared under a license and was authored, remixed, and/or curated by LibreTexts.

- 6.8A: Electrical Conductivity and Resistivity is licensed CC BY-NC-SA 4.0.

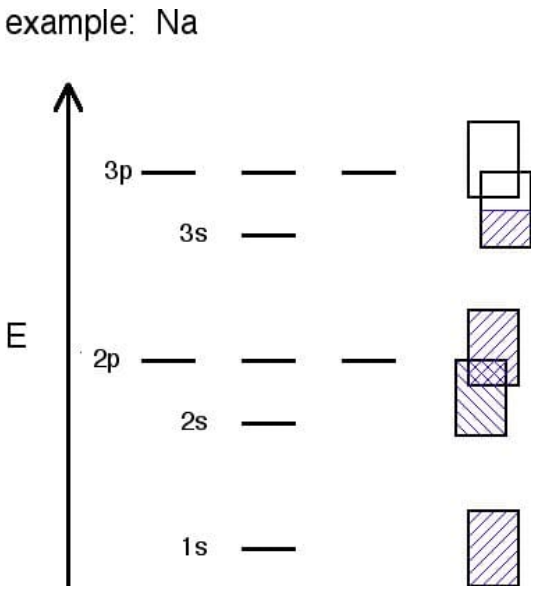
12.2B: Band Theory of Metals and Insulators

Band Theory was developed with some help from the knowledge gained during the quantum revolution in science. In 1928, Felix Bloch had the idea to take the quantum theory and apply it to solids. In 1927, Walter Heitler and Fritz London discovered bands- very closely spaced orbitals with not much difference in energy.



In this image, orbitals are represented by the black horizontal lines, and they are being filled with an increasing number of electrons as their amount increases. Eventually, as more orbitals are added, the space in between them decreases to hardly anything, and as a result, a band is formed where the orbitals have been filled.

Different metals will produce different combinations of filled and half filled bands.



Sodium's bands are shown with the rectangles. Filled bands are colored in blue. As you can see, bands may overlap each other (the bands are shown askew to be able to tell the difference between different bands). The lowest unoccupied band is called the conduction band, and the highest occupied band is called the valence band.

Bands will follow a trend as you go across a period:

- In Na, the 3s band is 1/2 full.
- In Mg, the 3s band is full.
- In Al, the 3s band is full and the 3p ban is 1/2 full... and so on.

The probability of finding an electron in the conduction band is shown by the equation:

$$P = \frac{1}{e^{\Delta E/RT} + 1} \tag{12.2B.1}$$

The ΔE in the equation stands for the change in energy or energy gap. T stands for the temperature, and R is a bonding constant. That equation and this table below show how the bigger the difference in energy is, or gap, between the valence band and the conduction band, the less likely electrons are to be found in the conduction band. This is because they cannot be excited enough to make the jump up to the conduction band.

ELEMENT	ΔE(kJ/mol) of energy gap	# of electrons/cm^3 in conduction band	insulator, or conductor?
C (diamond)	524 (big band gap)	10^{-27}	insulator
Si	117 (smaller band gap, but not a full conductor)	10^{9}	semiconductor
Ge	66 (smaller band gap, but still not a full conductor)	10^{13}	semiconductor

Conductors, Insulators and Semiconductors

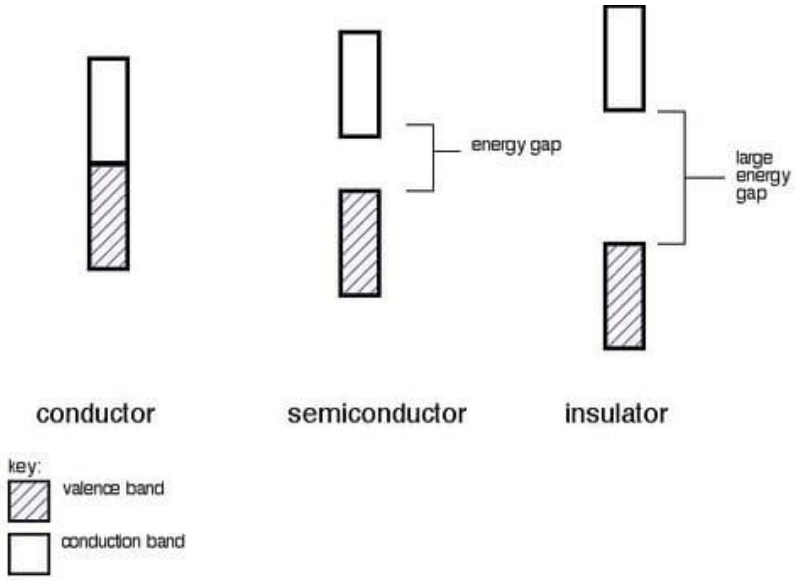


Diagram comparing conductor, semiconductor, and insulator energy bands. Conductor has overlapping bands; semiconductor has small gap; insulator has large gap. Key: valence and conduction bands.

A. Conductors

Metals are conductors. There is no band gap between their valence and conduction bands, since they overlap. There is a continuous availability of electrons in these closely spaced orbitals.

B. Insulators

In insulators, the band gap between the valence band the the conduction band is so large that electrons cannot make the

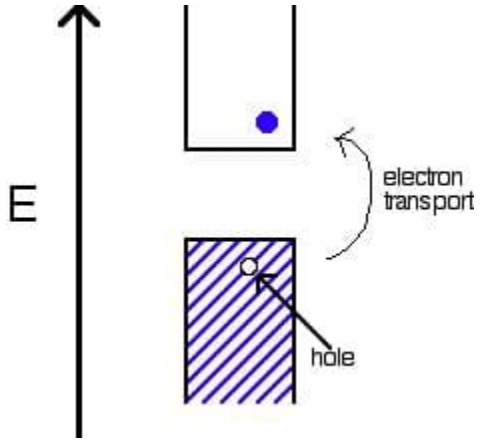
energy jump from the valence band to the conduction band.

C. Semiconductors

Semiconductors have a small energy gap between the valence band and the conduction band. Electrons can make the jump up to the conduction band, but not with the same ease as they do in conductors. There are two different kinds of semiconductors: **intrinsic** and **extrinsic**.

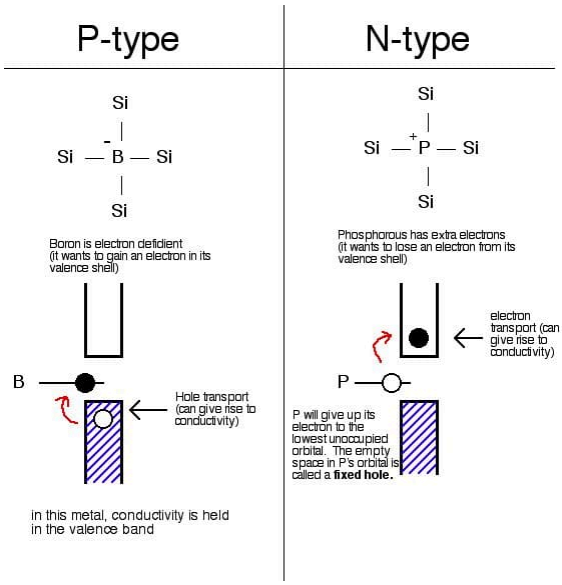
i. Intrinsic Semiconductors

An intrinsic semiconductor is a semiconductor in its pure state. For every electron that jumps into the conduction band, the missing electron will generate a hole that can move freely in the valence band. The number of holes will equal the number of electrons that have jumped.



ii. Extrinsic Semiconductors

In extrinsic semiconductors, the band gap is controlled by purposefully adding small impurities to the material. This process is called **doping**. Doping, or adding impurities to the lattice can change the electrical conductivity of the lattice and therefore vary the efficiency of the semiconductor. In extrinsic semiconductors, the number of holes will not equal the number of electrons jumped. There are two different kinds of extrinsic semiconductors, p-type (positive charge doped) and n-type (negative charge doped).



Exercise 12.2B.1

How do you distinguish between a valence band and a conduction band?

Answer available at the end of this section.

Exercise 12.2B.2

Is the energy gap between an insulator smaller or larger than the energy gap between a semiconductor?

Answer available at the end of this section.

Exercise 12.2B.3

What two methods bring conductivity to semiconductors?

Answer available at the end of this section.

Exercise 12.2B.4

You are more likely to find electrons in a conduction band if the energy gap is smaller/larger?

Answer available at the end of this section.

References

1. Petrucci, Harwood, Herring, Madura. GENERAL CHEMISTRY Principles and Modern Applications 9th Edition. Macmillan Publishing Co: New Jersey. 1989.
2. Moore, John T. Chemistry Made Simple. Random House Inc: New York. 2004.

Answers

Exercise $12.2B.1$

The valence band is the highest band with electrons in it, and the conduction band is the highest band with no electrons in it.

Exercise $12.2B.2$

Larger

Exercise $12.2B.3$

Electron transport and hole transport

Exercise $12.2B.4$

Smaller

This page titled 12.2B: Band Theory of Metals and Insulators is shared under a license and was authored, remixed, and/or curated by LibreTexts.

- Band Structure by Jim Clark, Sierra Blair is licensed CC BY-NC 4.0.

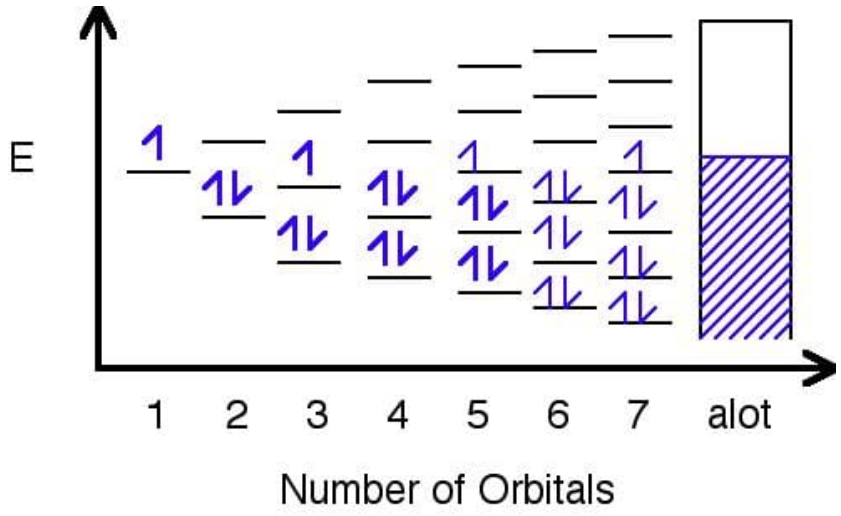
12.2C: The Fermi Level

This page titled 12.2C: The Fermi Level is shared under a license and was authored, remixed, and/or curated by LibreTexts.

- 6.8C: The Fermi Level is licensed CC BY-NC-SA 4.0.

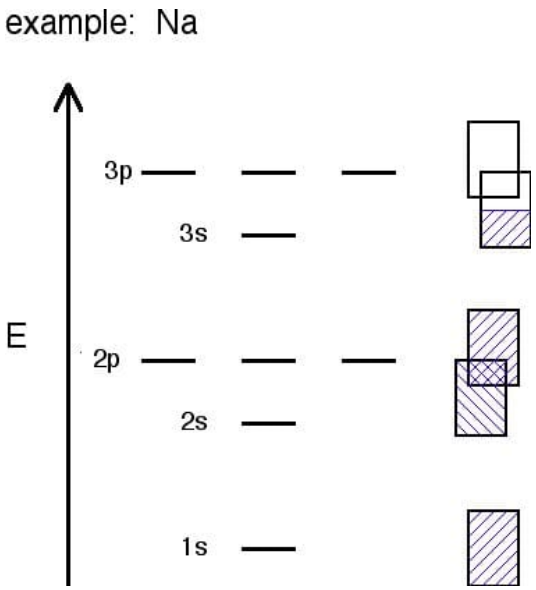
12.2D: Band Theory of Semiconductors

Band Theory was developed with some help from the knowledge gained during the quantum revolution in science. In 1928, Felix Bloch had the idea to take the quantum theory and apply it to solids. In 1927, Walter Heitler and Fritz London discovered bands- very closely spaced orbitals with not much difference in energy.



In this image, orbitals are represented by the black horizontal lines, and they are being filled with an increasing number of electrons as their amount increases. Eventually, as more orbitals are added, the space in between them decreases to hardly anything, and as a result, a band is formed where the orbitals have been filled.

Different metals will produce different combinations of filled and half filled bands.



Sodium's bands are shown with the rectangles. Filled bands are colored in blue. As you can see, bands may overlap each other (the bands are shown askew to be able to tell the difference between different bands). The lowest unoccupied band is called the conduction band, and the highest occupied band is called the valence band.

Bands will follow a trend as you go across a period:

- In Na, the 3s band is 1/2 full.
- In Mg, the 3s band is full.
- In Al, the 3s band is full and the 3p ban is 1/2 full... and so on.

The probability of finding an electron in the conduction band is shown by the equation:

$$P = \frac{1}{e^{\Delta E/RT} + 1} \tag{12.2D.1}$$

The ΔE in the equation stands for the change in energy or energy gap. T stands for the temperature, and R is a bonding constant. That equation and this table below show how the bigger the difference in energy is, or gap, between the valence band and the conduction band, the less likely electrons are to be found in the conduction band. This is because they cannot be excited enough to make the jump up to the conduction band.

ELEMENT	ΔE(kJ/mol) of energy gap	# of electrons/cm^3 in conduction band	insulator, or conductor?
C (diamond)	524 (big band gap)	10^{-27}	insulator
Si	117 (smaller band gap, but not a full conductor)	10^{9}	semiconductor
Ge	66 (smaller band gap, but still not a full conductor)	10^{13}	semiconductor

Conductors, Insulators and Semiconductors

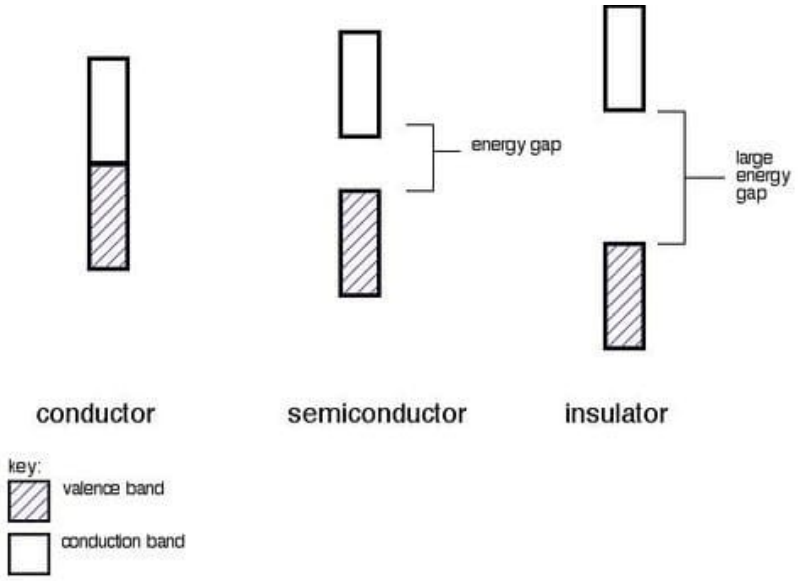


Diagram comparing conductor, semiconductor, and insulator energy bands. Conductor has overlapping bands; semiconductor has small gap; insulator has large gap. Key: valence and conduction bands.

A. Conductors

Metals are conductors. There is no band gap between their valence and conduction bands, since they overlap. There is a continuous availability of electrons in these closely spaced orbitals.

B. Insulators

In insulators, the band gap between the valence band the the conduction band is so large that electrons cannot make the

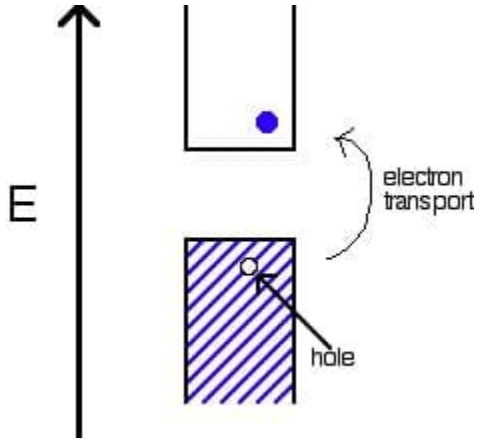
energy jump from the valence band to the conduction band.

C. Semiconductors

Semiconductors have a small energy gap between the valence band and the conduction band. Electrons can make the jump up to the conduction band, but not with the same ease as they do in conductors. There are two different kinds of semiconductors: **intrinsic** and **extrinsic**.

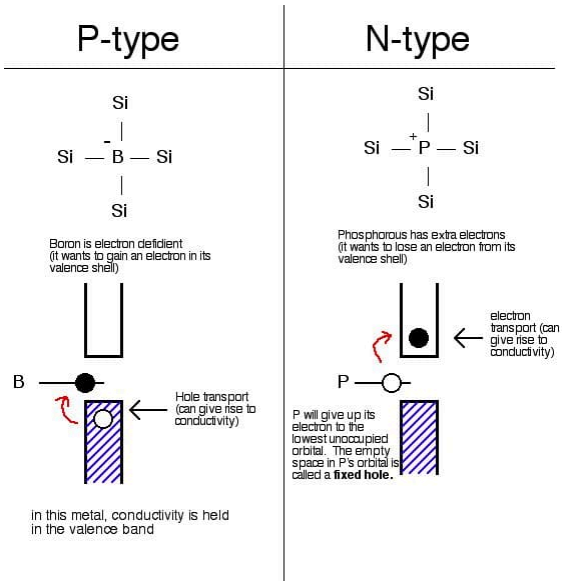
i. Intrinsic Semiconductors

An intrinsic semiconductor is a semiconductor in its pure state. For every electron that jumps into the conduction band, the missing electron will generate a hole that can move freely in the valence band. The number of holes will equal the number of electrons that have jumped.



ii. Extrinsic Semiconductors

In extrinsic semiconductors, the band gap is controlled by purposefully adding small impurities to the material. This process is called **doping**. Doping, or adding impurities to the lattice can change the electrical conductivity of the lattice and therefore vary the efficiency of the semiconductor. In extrinsic semiconductors, the number of holes will not equal the number of electrons jumped. There are two different kinds of extrinsic semiconductors, p-type (positive charge doped) and n-type (negative charge doped).



Exercise 12.2D.1

How do you distinguish between a valence band and a conduction band?

Answer available at the end of this section.

Exercise 12.2D.2

Is the energy gap between an insulator smaller or larger than the energy gap between a semiconductor?

Answer available at the end of this section.

Exercise 12.2D.3

What two methods bring conductivity to semiconductors?

Answer available at the end of this section.

Exercise 12.2D.4

You are more likely to find electrons in a conduction band if the energy gap is smaller/larger?

Answer available at the end of this section.

References

1. Petrucci, Harwood, Herring, Madura. GENERAL CHEMISTRY Principles and Modern Applications 9th Edition. Macmillan Publishing Co: New Jersey. 1989.
2. Moore, John T. Chemistry Made Simple. Random House Inc: New York. 2004.

Answers

Exercise $12.2D.1$

The valence band is the highest band with electrons in it, and the conduction band is the highest band with no electrons in it.

Exercise $12.2D.2$

Larger

Exercise $12.2D.3$

Electron transport and hole transport

Exercise $12.2D.4$

Smaller

This page titled 12.2D: Band Theory of Semiconductors is shared under a license and was authored, remixed, and/or curated by LibreTexts.

- Band Structure by Jim Clark, Sierra Blair is licensed CC BY-NC 4.0.

12.3: IONIC LATTICES



-  Topic hierarchy 

12.3A: Structure - Rock Salt (NaCl)

12.3B: Structure - Caesium Chloride (CsCl)

12.3C: Structure - Fluorite (CaF_2)

12.3D: Structure - Antifluorite

12.3E: Structure - Zinc Blende (ZnS)

12.3F: Structure - β-Cristobalite (SiO_2)

12.3H: Structure - Rutile (TiO_2)

12.3I: Structure - Layers (CdI_2 and $CdCl_2$)

12.3J: Structure - Perovskite ($CaTiO_3$)

This page titled 12.3: Ionic Lattices is shared under a license and was authored, remixed, and/or curated by LibreTexts.

- 6.11: Ionic Lattices is licensed CC BY-NC-SA 4.0.

12.3A: Structure - Rock Salt (NaCl)

Rock salt also known as NaCl is an ionic compound. It occurs naturally as white cubic crystals. The structure of NaCl is formed by repeating the unit cell. It has an organized structure and has a 1:1 ratio of Na:Cl.

Introduction

Rock salt (NaCl) is an ionic compound that occurs naturally as white crystals. It is extracted from the mineral form halite or evaporation of seawater. The structure of NaCl is formed by repeating the face centered cubic unit cell. It has 1:1 stoichiometry ratio of Na:Cl with a molar mass of 58.4 g/mol. Compounds with the sodium chloride structure include alikali halides and metal oxides and transition-metal compounds. An important role to many important applications is structure and dynamics of water. Some applications include crystallization of proteins and conformational behavior of peptides and nucleic acids.

Structure

Figure $12.3A.1$ shows how the Na^+ and Cl^- ions occupy the space. The smaller ions are the Na^+ with has an atomic radius of 102 pm, and the larger ions are the Cl^- with an atomic radium of 181 pm. Since NaCl are one to one ratio as a compound, the coordination numbers of Na and Cl are equal. The larger green ions represent Cl^- and the smaller purple ions represent Na^+. However, the structure of this molecule allows their positions to be switched since the coordination numbers are equivalent.

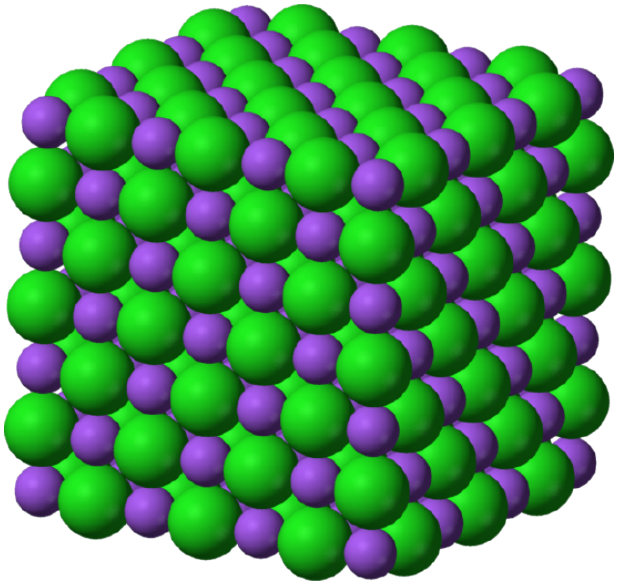


Figure $12.3A.1$: The crystal structure of sodium chloride, NaCl, a typical ionic compound. The smaller purple spheres represent sodium cations, $\mathrm{Na^+}$, and the larger green spheres represent chloride anions, $\mathrm{Cl^-}$. (Public Domain; Benjah-bmm27 via Wikipedia)

A Unit Cell

The unit cell of NaCl consists of $\mathrm{Na^+}$ ions and $\mathrm{Cl^-}$ ions. There are four types of site: unique central position, face site, edge sites and corner site, which are used to determine the number of Na^+ ions and Cl^- ions in the unit cell of NaCl. When counting the number of ions, a corner site would be shared by 7 other unit cells. Therefore, 1 corner would be 1/8 of an ion. A similar occurrence happens with the face site and the edge sites. For a face site, it is shared by 1 other unit cell and for an edge site, the ion is shared by 3 other unit cells. NaCl is a face centered cubic unit cell which has four cations and four anions. This can be shown by counting the number of ions and multiplying them in relation to their position.

- $\mathrm{Na^+}$:

$$1_{center} + 12_{edge} \times \frac{1}{4} = 4 \,\text{sodium ions total per cell}$$

- Cl^-:

$$4_{face} \times \frac{1}{2} + 8_{corner} \times \frac{1}{8} = 4 \,\text{chloride ions total per cell}$$

Each ion in this lattice has six of the other kind of ion as its nearest neighbors, and twelve of the same kind of ions as its second nearest neighbors. There are many ionic compounds that assume this structure including all other halides of Na, Li, K and Rb. CsF, AgF, AgCl, BaO, CoO, and SrS are also among many that will form similar structures to NaCl.

Outside Links

- Video about structure of NaCl: http://www.youtube.com/watch?v=csfOBynrF8E
- Unit Cell. http://www.case.edu/artsci/chem/chim...ids/xtal1.html

References

1. Gao, H.X., L.-M. Peng, and J.M Zuo. "Lattice dynamics and Debye-Waller factors of some compounds with the sodium chloride structure." *Acta Crystallographica: Section A (Wiley-Blackwell)* 55.6 (1999): 1014. *Academic Search Complete*. EBSCO. Web.
2. Housecroft, Catherine E., and Alan G. Sharpe. *Inorganic Chemistry*. 3rd ed. Harlow: Pearson Education, 2008. Print.
3. Jun Soo, Kim, and Yethiraj Arun. "A Diffusive Anomaly of Water in Aqueous Sodium Chloride Solutions at Low Temperatures." *Journal of Physical Chemistry B* 112.6 (2008): 1729-1735. *Academic Search Complete*. EBSCO. Web.

Contributors and Attributions

- Michael Ford

This page titled 12.3A: Structure - Rock Salt (NaCl) is shared under a license and was authored, remixed, and/or curated by LibreTexts.

- 6.11A: Structure - Rock Salt (NaCl) is licensed CC BY-NC-SA 4.0.

12.3B: Structure - Caesium Chloride (CsCl)

This page is going to discuss the structure of the molecule cesium chloride (CsCl), which is a white hydroscopic solid with a mass of 168.36 g/mol. Cesium Chloride is a type of unit cell that is commonly mistaken as Body-Centered Cubic. This misconception is easy to make, since there is a center atom in the unit cell, but CsCl is really a **non-closed packed structure** type.

Introduction

CsCl has a boiling point of 1303 degrees Celsius, a melting point of 646 degrees Celsius, and is very soluble in water. For the most part this molecule is stable, but is not compatible with strong oxidizing agents and strong acids. Although it is not hazardous, one should not prolong their exposure to CsCl. CsCl is an ionic compound that can be prepared by the reaction:

$$\mathrm{Cs_2CO_3 + 2\,HCl \longrightarrow 2\,CsCl + H_2O + CO_2} \tag{12.3B.1}$$

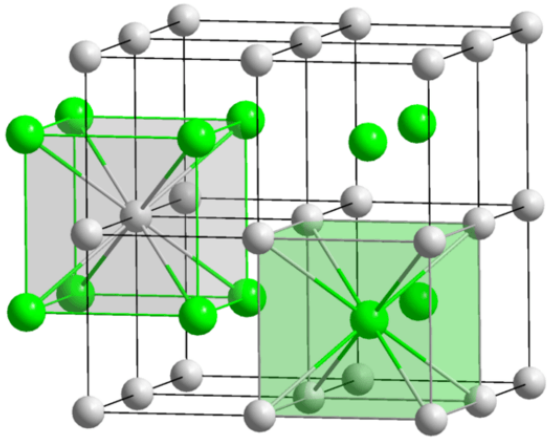


Figure $12.3B.1$: CsCl Coordination Cubes. (Public Domain; Solid State via Wikipedia)

CsCl crystallize in a primitive cubic lattice which means the cubic unit cell has nodes only at its corners. The structure of CsCl can be seen as two interpenetrating cubes, one of Cs^+ and one of Cl^-. The ions are not touching one another. Touching would cause repulsion between the anion and cation. Some may mistake the structure type of CsCl with NaCl, but really the two are different. CsCl is more stable than NaCl, for it produces a more stable crystal and more energy is released.

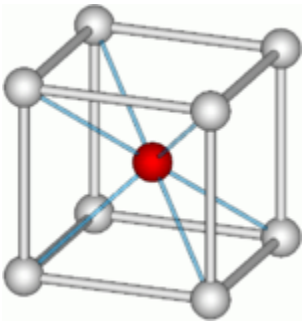


Figure $12.3B.2$: Unit Cell of CsCl (en.Wikipedia.org/wiki/Caesium_chloride

Anions and cations have similar sizes. Each Cs^+ is surrounded by 8 Cl^- at the corners of its cube and each Cl^- is also surrounded by 8 Cs^+ at the corners of its cube. The cations are located at the center of the anions cube and the anions are located at the

center of the cations cube. There is one atom in CsCl. To determine this, the following equation is given:

8 Corners of a given atom x 1/8 of the given atom's unit cell = 1 atom

Applications

Cesium chloride is used in centrifugation, a process that uses the centrifugal force to separate mixtures based on their molecular density. It is also used in the preparation of electrically conducting glasses. Radioactive CsCl is used in some types of radiation therapy for cancer patients, although it is blamed for some deaths.

References

1. Carter, C. Barry., and M. Grant. Norton. "Binary Compounds." *Ceramic Materials Science and Engineering*. New York, NY: Springer, 2007. pg87-88
2. Quéré, Yves. "Stable Structure of Halides." *Physics of Materials*. Amsterdam: Gordon and Breach Science, 1998.

Contributors and Attributions

- Ana Popovich

This page titled 12.3B: Structure - Caesium Chloride (CsCl) is shared under a license and was authored, remixed, and/or curated by LibreTexts.

- 6.11B: Structure - Caesium Chloride (CsCl) is licensed CC BY-NC-SA 4.0.

12.3C: Structure - Fluorite (CaF_2)

Calcium Fluoride is a solid and forms a cube like structure that is centralized around the calcium molecules. The crystal lattice structure that Calcium Fluoride is also known as the fluorite structure (Figure $12.3C.1$) where the Ca^{2+} ions are eight-coordinate, being centered in a cube of eight F^- ions. Each F^- is coordinated to four Ca^{2+} in the shape of a tetrahedron.

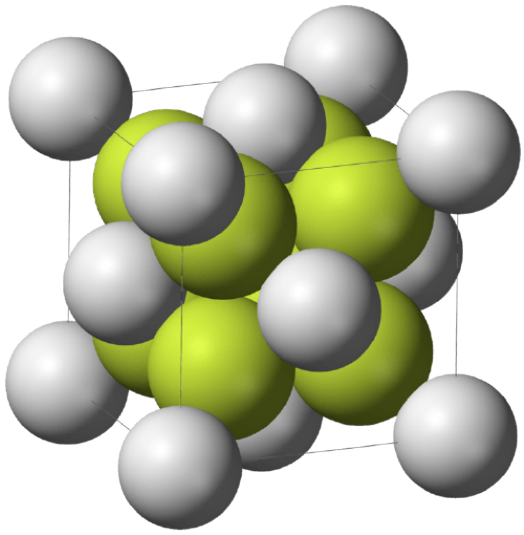


Figure $12.3C.1$: Fluorite unit cell. (Public Domain; Benjah-bmm27 via Wikipedia)

Calcium Fluoride is Quasilinear

When Calcium Fluoride is in a single molecule it forms a Quasilinear structure. Quasilinear means the molecule resonates between a linear shape and a bent shape.Calcium Fluoride is a polyatomic molecule that contains one calcium molecule and two fluoride molecules. Calcium Fluoride is a quasilinear molecule the bonds are created from the single electrons of calcium and the single electron from fluoride. $\mathrm{CaF_2}$ has its electrons contained with in the 3d orbitals and are able to move between d_{yz} and d_z^2 squared. The molecule in linear when they are in the d_z^2 orbitals the molecule is also the most stable in this shape. When the electrons are in the d_{yz} orbitals the molecule becomes bent. The molecule resonates between these two shapes making it quasilinear. Figures two and three show how the d-orbitals cause the molecule to bend.

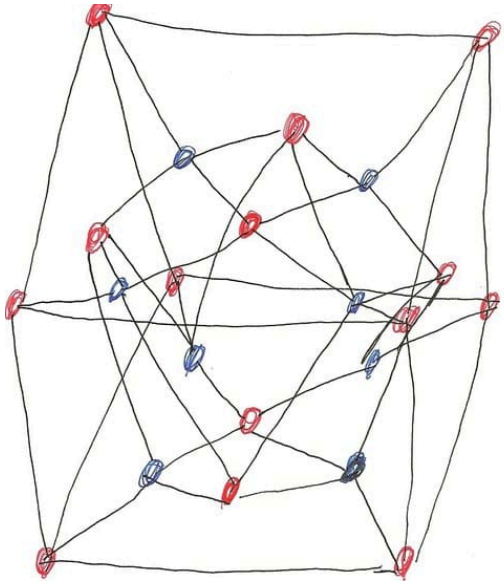


Fig # 1

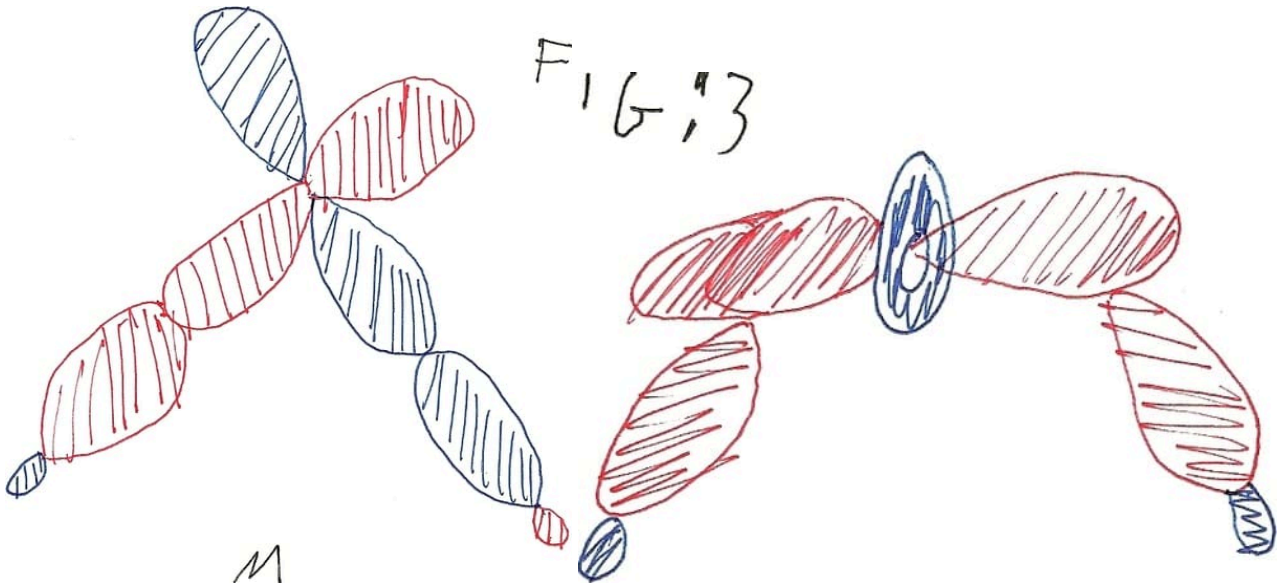


Fig # 2 Fig # 3

References

1. Maushake, Peter. Calcium fluoride Chrystals. Wiley-VCH Verlag GmbH & CO. http://www.wiley-vch.de/berlin/journals/op/08-02/OP0802_S46-S47.pdf (October 07, 2010)
2. Fergus, Jeffery W. The Application of Solid Fluoride Electrolytes in Chemical Sensors. Sensors and Actuators B: Chemical. Web Journal, 22. no 2. www.sciencedirect.com/science...f&searchtype=a (Oct 7, 2010)
3. Housecroft, Catherine. Inorganic Chemistry. Pearson Prentice Hall 2008.

This page titled 12.3C: Structure - Fluorite (CaF_2) is shared under a license and was authored, remixed, and/or curated by LibreTexts.

- 6.11C: Structure - Fluorite (CaF_2) is licensed CC BY-NC-SA 4.0.

12.3D: Structure - Antifluorite

Antifluorite is a mineral with a crystal structure identical with that of fluorite but with the positions of the cations and anions reversed (Figure $12.3D.1$).

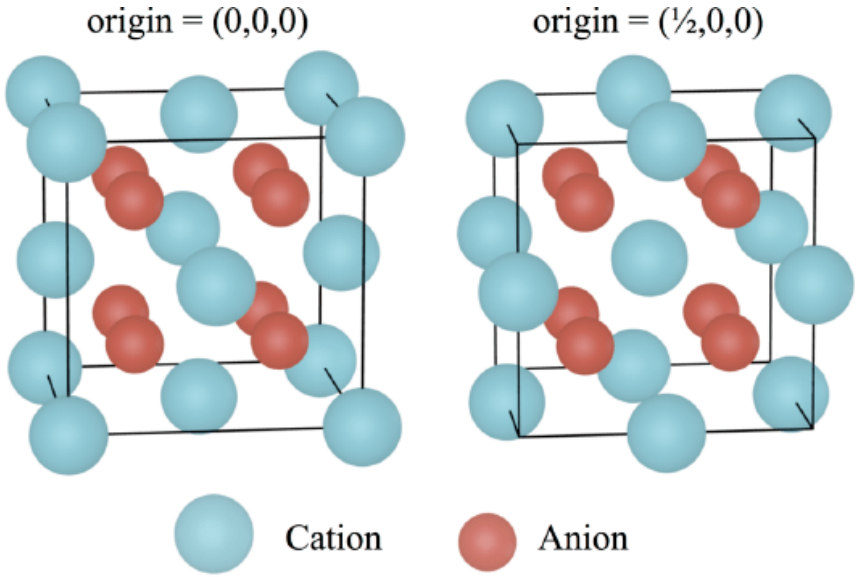


Figure $12.3D.1$: Unit cell of the fluorite structure, from two equivalent perspectives. In the antifluorite structure, the blue positions are taken by the anion, the red positions by the cation. (CC BY-SA 4.0; Paburr via source)

The same crystal structure is found in numerous ionic compounds with formula AB2, such as ceria (CeO2), zirconia (cubic ZrO2), uranium dioxide (UO2). In the corresponding anti-structure, called the antifluorite structure, anions and cations are swapped, such as beryllium carbide (Be2C) or lithium oxide (Li2O), potassium sulfate (K2SO4).

Contributors and Attributions

- en.Wikipedia.org/wiki/Anti-structure

This page titled 12.3D: Structure - Antifluorite is shared under a license and was authored, remixed, and/or curated by LibreTexts.

- 6.11D: Structure - Antifluorite is licensed CC BY-NC-SA 4.0.

12.3E: Structure - Zinc Blende (ZnS)

ZnS has a unique structure type compared to other molecules, having different types of unique structures. ZnS can have a zinc blende structure which is a "diamond-type network" and at a different temperature, ZnS can become the wurtzite structure type which has a hexagonal type symmetry. Structure-wise, the zinc blende structure is more thermodynamically favored, however, because of the wurtzite structures slow construction, both forms of ZnS can be found.

Summary: Zinc blend is a compound that comes in two forms: sphalerite and wurtzite. These are characterized by a 1:1 stoichiometric ratio of Zinc to Sulfur. It maintains a tetrahedral arrangement in both forms.

Introduction

Zinc sulfide (ZnS) is a unique compound that forms two types of crystalline structures. These two polymorphs are wurtzite and zincblende (also known as sphalerite). Wurtzite has a hexagonal structure, while zincblende is cubic. It is characterized by single bonds between each atom and maintenance of a 1:1 zinc to sulfur ratio.

sphalerite:

Site	Zn	S
Central	4	0
Face	0	6(1/2) = 3
Corner	0	8(1/8) = 1
Total	4	4

Since the number of atoms in a single unit cell of Zn and S is the same, it is consistent with the formula ZnS.

The ionic radius for Zn^{2+} is 74pm and for S^{2-} is 190pm. Therefore the ratio between cationic and anionic radii in zinc blend is 0.39 (74pm/190 pm) .This suggests a tetrahedral ion arrangement and four nearest neighbors from standard crystal structure prediction tables. Therefore, four sulfur atoms surround each zinc atom and four zinc atoms surround each sulfur atom.[2] The coordination number, the number of of electron pairs donated to a metal by its ligands, for both zinc an sulfur is four.[1,2] The difference between wurtzite and zincblende lies in the different arrangements of layers of ions.[2]

Zincblende (Sphalerite)

Zincblende is characterized as a **cubic closet packing** (ccp), also known as face-centered cubic, structure.[1,4] This crystal lattice structure is shown in Figures 1 & 2 below.

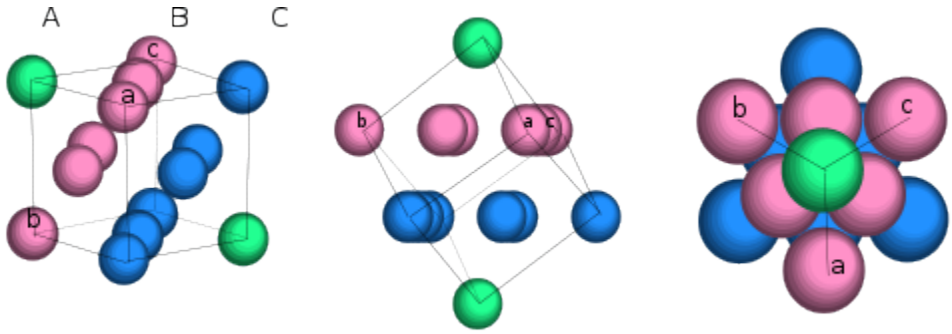


Fig. 1. A break down of cubic closest packing. (Author: Maghémite Date: May 5, 2008. Licensed under the Creative Commons Attribution-Share Alike 3.0 Unported, 2.5 Generic, 2.0 Generic and 1.0 Generic license.)

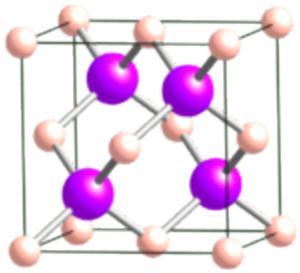


Fig. 2. A representation of ccp structure. (from Public Domain)

Notice how only half of the tetrahedral sites are occupied.

Thermal stability

Density tends to decrease as temperature increases. In this case, since ccp structures are more dense than hcp structures, so a conversion from sphalerite to wurtzite occurs naturally over time at a rate similar to that of diamond to graphite. The sphalerite structure is favored at 298k by 13kJ/mol, but at 1296K the transition to wurtzite occurs.[3]

Wurtzite

Wurtzite has a hexagonal closest packing structure (hcp), which is characterized by 12 ions in the corners of each unit that create a hexagonal prism (seen in Fig. 3).[2] As discussed previously, zincblende slowly transforms to wurtzite due to thermodynamic stability.

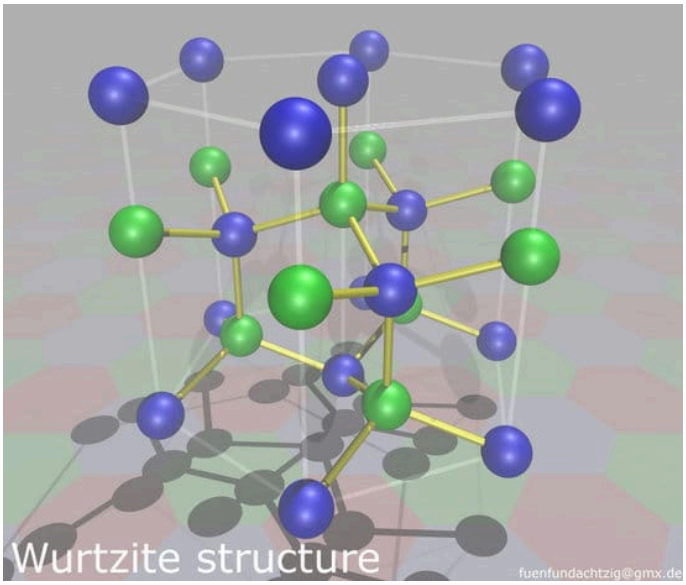


Fig 3. HCP structure of wurtzite. (Creator: Alexander Mann Date: 01/14/2006 Licensed under the Creative Commons Attribution-Share Alike 2.0 Germany license)

Calculating density of a crystal structure

Density = Mass of unit cell / volume of unit cell.

where:

Mass of unit cell = Number of atoms in a unit cell x the mass of each atom

volume of unit cell = $a^3 \times 10^{-30}$

Contributors and Attributions

- Emma Mele, UC Davis Animal Biology

This page titled 12.3E: Structure - Zinc Blende (ZnS) is shared under a license and was authored, remixed, and/or curated by LibreTexts.

- 6.11E: Structure - Zinc Blende (ZnS) is licensed CC BY-NC-SA 4.0.

12.3F: Structure - β-Cristobalite (SiO_2)

Silicon dioxide, SiO_2, also known as silica is a linear molecule that is formed by one silicon atom and two oxygen atoms with two sets of doubles bonds and 4 single bonds. Because of its main component: glass, silicon dioxide is a very common and important molecule in the construction industry. One of the forms of silicon dioxide is quartz, which is found in sand.

The Structure of Silica

SiO_2 is a 3 dimensional structure and comes from the tetrahedral structure, SiO_4. Each of the Silicon atoms are connected to each other with an oxygen atom, which creates a "diamond type network". All forms of SiO_2 possess a 3 dimensional shape and has a diamond structure. The bonding angle of Si-O-Si, which is the building block of the SiO_2 molecule, is 144 degrees. These are called polymorph and in order to be stable, 3 of these polymorph are suppose to exist. This stable unit creates a a temperature for each of the different forms of SiO_2. Forms that have (alpha) are at low temperature, while forms with (beta) are at high temperature. The structure of the different forms of SiO_2 is important because it gives each of the different forms of SiO_2 different characteristics and functions. Commercially, SiO_2 is very important in steel, electronic, and semiconductor industries because of its structure, SiO_2 is able to undergo rapid temperature changes and still maintain its shape and structure.

Different Forms of Silica and Their Uses

There are many different forms of SiO_2, which mainly derived quartz glass. One form that is derived from quartz is beta-cristobalite, which is found in high temperature. Some other forms are beta-quartz, alpha-quartz, beta-tridymite, alpha-tridymite, alpha=cristobalite, and many more. The alpha and beta stands for the temperature range. Alpha molecules have low temperature while beta molecules have high temperature.

References

1. Ed. Papier, Eugene. 2000. Absorption on Silica Surfaces. Marcek Dekker. New York.
2. Pacific Rim Conference on Ceramic and Glass Technology. 2006. Advances in Glass and Optical Materials II. American Ceramic Society. Westerville, Ohio.
3. Housecroft, Catherine E., and Alan G. Sharpe. 2008. Inorganic Chemistry. 3rd ed. Harlow: Pearson Education.

This page titled 12.3F: Structure - β-Cristobalite (SiO_2) is shared under a license and was authored, remixed, and/or curated by LibreTexts.

- 6.11F: Structure - β-Cristobalite (SiO_2) is licensed CC BY-NC-SA 4.0.

12.3H: Structure - Rutile (TiO_2)

This page titled 12.3H: Structure - Rutile (TiO_2) is shared under a license and was authored, remixed, and/or curated by LibreTexts.

12.3I: Structure - Layers (CdI_2 and $CdCl_2$)

The following headers are meant as a guide to the sections that you need in your module. Here, before the table of contents, give a two-four sentence overview of the Module. Be straight to the point. No examples and no figures in this section. Keep the following text for automatic table of contents based on the headings below (seen in edit mode only).

1. Introduction
2. Heading #1
3. Heading #2
4. References
5. Outside Links
6. Problems
7. Contributors and Attributions

Introduction

Please use only heading 2 and lower, heading 1 is ugly and is avoided. In this section, give a short introduction to your topic to put it in context. The module should be easy to read; please reduce excess space, crop figures to remove white spaces, full justify all text, with the exception of equations, which should use the equation command for construction (see FAQ).

Heading #1

Rename to desired sub-topic. This is where you put the core text of your module. Add any number of headings necessary for your topic. Try to reduce unnecessary discussion and get to the point in a terse, yet informative, manner possible.

Heading #2

Rename to desired sub-topic. You can delete the header for this section and place your own related to the topic. Remember to hyperlink your module to other modules via the link button on the editor toolbar.

References

1. This is meant for references used for constructing the module. They must be primary and accessible to readers at a library.
2. You need at least two different sources here. Websites are not allowed. DOI links to J. Chem. Ed. are ideal Do not reference class notes. Also, do not reference textbooks for maximal credit. Using the insert citation button to automatically handle references is highly suggested (bottom right button on editor toolbar).

Outside Links

- This is not meant for references used for constructing the module, but as secondary and unvetted information available at other site
- Link to outside sources. Wikipedia entries should probably be referenced here.

Problems

Be careful not to copy from existing textbooks. Originality is rewarded. Make up some practice problems for the future readers. Five original with varying difficulty questions (and answers) are ideal.

Contributors and Attributions

- Name #1 here (if anonymous, you can avoid this) with university affiliation
- Name #2 here with university affiliation

Tags below. If no tags exist, then add two new ones: "Vet1" and the level of the module content (e.g. "Fundamental"). See FAQ for more details.

This page titled 12.3I: Structure - Layers (\(CdI_2\) and \(CdCl_2\)) is shared under a license and was authored, remixed, and/or curated by LibreTexts.

- 6.11I: Structure - Layers (\(CdI_2\) and \(CdCl_2\)) is licensed CC BY-NC-SA 4.0.

12.3J: Structure - Perovskite ($CaTiO_3$)

Figure 2: A distroted perovskite SmNiO3 with orthorhombic symmetry.

Figure 2: Superconducting Sr_2RuO_4 (wikis.lib.ncsu.edu/index.php/Perovskite)

Some other unique properties that sets perovskites apart and makes them ideal for technological applications include: it is the only crystal structure that is ferroelectric (spontaneous alignment of the electric dipoles caused by interactions between them) not because of an external magnetic field but due to its crystal structure, its ferro-, pyro-, and piezo-electric properties, and structural properties such as durability and chemical flexibility.

Contributors and Attributions

- Matthew Ibbotson: Undergraduate in Chemical Engineering, Senior

This page titled 12.3J: Structure - Perovskite (\(CaTiO_3\)) is shared under a license and was authored, remixed, and/or curated by LibreTexts.

- 6.11J: Structure - Perovskite (\(CaTiO_3\)) is licensed CC BY-NC-SA 4.0.

12.4: Lattice Energy - The Born-Haber Cycle

Ionic solids tend to be very stable compounds. The enthalpies of formation of the ionic molecules cannot alone account for this stability. These compounds have an additional stability due to the lattice energy of the solid structure. However, lattice energy cannot be directly measured. The Born-Haber cycle allows us to understand and determine the lattice energies of ionic solids.

Introduction

This module will introduce the idea of lattice energy, as well as one process that allows us to calculate it: the Born-Haber Cycle. In order to use the Born-Haber Cycle, there are several concepts that we must understand first.

Lattice Energy

Lattice Energy is a type of potential energy that may be defined in two ways. In one definition, the lattice energy is the energy required to break apart an ionic solid and convert its component atoms into gaseous ions. This definition causes the value for the lattice energy to always be positive, since this will always be an endothermic reaction. The other definition says that lattice energy is the reverse process, meaning it is the energy released when gaseous ions bind to form an ionic solid. As implied in the definition, this process will always be exothermic, and thus the value for lattice energy will be negative. Its values are usually expressed with the units kJ/mol.

Lattice Energy is used to explain the stability of ionic solids. Some might expect such an ordered structure to be less stable because the entropy of the system would be low. However, the crystalline structure allows each ion to interact with multiple oppositely charge ions, which causes a highly favorable change in the enthalpy of the system. A lot of energy is released as the oppositely charged ions interact. It is this that causes ionic solids to have such high melting and boiling points. Some require such high temperatures that they decompose before they can reach a melting and/or boiling point.

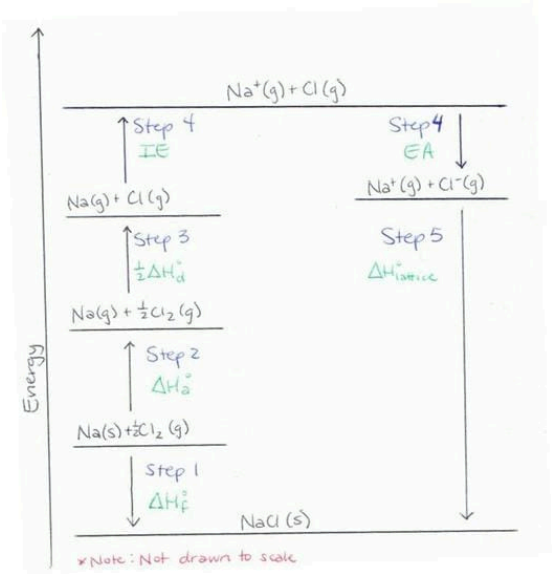
Born-Haber Cycle

There are several important concept to understand before the Born-Haber Cycle can be applied to determine the lattice energy of an ionic solid; ionization energy, electron affinity, dissociation energy, sublimation energy, heat of formation, and Hess's Law.

- **Ionization Energy** is the energy required to remove an electron from a neutral atom or an ion. This process always requires an input of energy, and thus will always have a positive value. In general, ionization energy increases across the periodic table from left to right, and decreases from top to bottom. There are some excepts, usually due to the stability of half-filled and completely filled orbitals.
- **Electron Affinity** is the energy released when an electron is added to a neutral atom or an ion. Usually, energy released would have a negative value, but due to the definition of electron affinity, it is written as a positive value in most tables. Therefore, when used in calculating the lattice energy, we must remember to subtract the electron affinity, not add it. In general, electron affinity increases from left to right across the periodic table and decreases from top to bottom.
- **Dissociation energy** is the energy required to break apart a compound. The dissociation of a compound is always an endothermic process, meaning it will always require an input of energy. Therefore, the change in energy is always positive. The magnitude of the dissociation energy depends on the electronegativity of the atoms involved.
- Sublimation energy is the energy required to cause a change of phase from solid to gas, bypassing the liquid phase. This is an input of energy, and thus has a positive value. It may also be referred to as the energy of atomization.
- **The heat of formation** is the change in energy when forming a compound from its elements. This may be positive or negative, depending on the atoms involved and how they interact.
- **Hess's Law** states that the overall change in energy of a process can be determined by breaking the process down into steps, then adding the changes in energy of each step. The Born-Haber Cycle is essentially Hess's Law applied to an ionic solid.

Using the Born-Haber Cycle

The values used in the Born-Haber Cycle are all predetermined changes in enthalpy for the processes described in the section above. Hess' Law allows us to add or subtract these values, which allows us to determine the lattice energy.



Step 1

Determine the energy of the metal and nonmetal in their elemental forms. (Elements in their natural state have an energy level of zero.) Subtract from this the heat of formation of the ionic solid that would be formed from combining these elements in the appropriate ration. This is the energy of the ionic solid, and will be used at the end of the process to determine the lattice energy.

Step 2

The Born-Haber Cycle requires that the elements involved in the reaction are in their gaseous forms. Add the changes in enthalpy to turn one of the elements into its gaseous state, and then do the same for the other element.

Step 3

Metals exist in nature as single atoms and thus no dissociation energy needs to be added for this element. However, many nonmetals will exist as polyatomic species. For example, Cl exists as Cl_2 in its elemental state. The energy required to change Cl_2 into 2Cl atoms must be added to the value obtained in Step 2.

Step 4

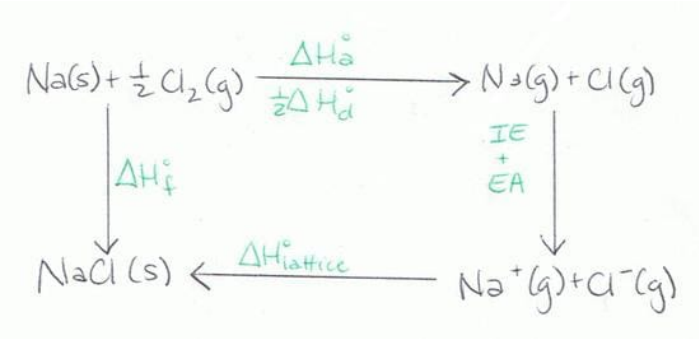
Both the metal and nonmetal now need to be changed into their ionic forms, as they would exist in the ionic solid. To do this, the ionization energy of the metal will be added to the value from Step 3. Next, the electron affinity of the nonmetal will be subtracted from the previous value. It is subtracted because it is a release of energy associated with the addition of an electron.

*This is a common error due to confusion caused by the definition of electron affinity, so be careful when doing this calculation.

Step 5

Now the metal and nonmetal will be combined to form the ionic solid. This will cause a release of energy, which is called the lattice energy. The value for the lattice energy is the difference between the value from Step 1 and the value from Step 4.

The diagram below is another representation of the Born-Haber Cycle.



Equation

The Born-Haber Cycle can be reduced to a single equation:

Heat of formation= Heat of atomization+ Dissociation energy+ (sum of Ionization energies)+ (sum of Electron affinities)+ Lattice energy

*Note: In this general equation, the electron affinity is added. However, when plugging in a value, determine whether energy is released (exothermic reaction) or absorbed (endothermic reaction) for each electron affinity. If energy is released, put a negative sign in front of the value; if energy is absorbed, the value should be positive.

Rearrangement to solve for lattice energy gives the equation:

Lattice energy= Heat of formation- Heat of atomization- Dissociation energy- (sum of Ionization energies)- (sum of Electron Affinities)

References

1. Cheetham, A.K. and P. Day. Solid State Chemistry. Oxford: Clarendon Press, 1992.
2. Jenkins, H. Donald B. "Thermodynamics of the Relationship between Lattice Energy and Lattice Enthalpy." Journal of Chemical Education. Vol. 82, P. 950-952. Coventry, West Midlands, UK: University of Warwick, 2005.
3. Ladd, Mark. Crystal Structures: Lattices and Solids in Stereoview. Chichester: Horwood, 1999.
4. Ladd, Mark. Chemical Bonding in Solids and Fluids. Chichester: Horwood, 1994.
5. Suzuki, Takashi. Free energy and Self-interacting Particles. Boston: Birkhauser, 2005.

Problems

1. Define lattice energy, ionization energy, and electron affinity.
2. What is Hess' Law?
3. Find the lattice energy of KF(s).
   Note: Values can be found in standard tables.
4. Find the lattice energy of $MgCl_2$(s).
5. Which one of the following has the greatest lattice energy?
   a. A) MgO
   b. B) NaC
   c. C) LiCl
   d. D) $MgCl_2$
6. Which one of the following has the greatest Lattice Energy?
   a. NaCl
   b. $CaCl_2$

c. $AlCl_3$
d. KCl

Solutions

1. Lattice energy: The difference in energy between the expected experimental value for the energy of the ionic solid and the actual value observed. More specifically, this is the energy gap between the energy of the separate gaseous ions and the energy of the ionic solid.
   Ionization energy: The energy change associated with the removal of an electron from a neutral atom or ion.
   Electron affinity: The release of energy associated with the addition of an electron to a neutral atom or ion.
2. Hess' Law states that the overall energy of a reaction may be determined by breaking down the process into several steps, then adding together the changes in energy of each step.
3. Lattice Energy= [-436.68-89-(0.5*158)-418.8-(-328)] kJ/mol= **-695.48 kJ/mol**
4. Lattice Energy= [-641.8-146-243-(737.7+1450.6)-(2*-349)] kJ/mol= **-2521.1 kJ/mol**
5. MgO. It has ions with the largest charge.
6. $AlCl_3$. According to the periodic trends, as the radius of the ion increases, lattice energy decreases.

References

1. Ralph, William, F.Geoffrey, and Jeffry. General Chemistry. Ninth ed. New Jersey:Pearson Education, Inc. 2007. p500;513-515.
2. Combs, Leon. "Lattice Energy". Dr. Leon L. Combs. 1999. erkki.kennesaw.edu/genchem8/ge00002.htm
3. Picture of NaCl diagram intro.chem.okstate.edu/1314f0...BornHaber2.GIF
4. Housecroft, Catherine E. and Alan G. Sharpe. Inorganic Chemistry. 3rd ed. England: Pearson Education Limited, 2008.174-175.

This page titled 12.4: Lattice Energy - The Born-Haber Cycle is shared under a license and was authored, remixed, and/or curated by LibreTexts.

- Lattice Energy: The Born-Haber cycle is licensed CC BY-NC-SA 4.0.

12.5: DEFECTS IN SOLID STATE LATTICES

- Topic hierarchy

12.5.E: Defects in Solid State Lattices (Exercises)

12.5A: Schottky Defect

12.5B: Frenkel Defect

12.5C: Experimental Observations of Schottky and Frenkel Defects

12.5D: Non-Stoichiometric Compounds

12.5E: Color Centers (F-Centers)

12.5F: Thermodynamic Effects of Crystal Defects

Template:HideTOC

This page titled 12.5: Defects in Solid State Lattices is shared under a license and was authored, remixed, and/or curated by LibreTexts.

- 6.17: Defects in Solid State Lattices is licensed CC BY-NC-SA 4.0.

12.5.E: Defects in Solid State Lattices (Exercises)

Crystal Defects and Solids

Problems

All diagrams must be hand drawn, no photocopies or computer images will be accepted.

1. Nonstoichiometric compounds
2. Stoichiometric titanium (II) oxide and magnesium oxides have densities of 4.93 and 3.58 g cm^{-3} respectively. X-ray diffraction studies have shown that both have the NaCl structure, with unit cell edges of 416.2 and 421.2 pm respectively. Assume that the presence of vacancies does not affect the cell edge lengths. Estimate the percentage of vacancies in these solids.
3. Explain the Pilling-Bedworth principle regarding the protective behaviour of oxide films of metal (Swaddle: p103-104). From the following densities (d), evaluate the molar volumes (V^o = molar mass/d) of the metals and of the oxides. Suggest which oxides forms protective layers?

```
Metal  d(metal)   Oxide   d(oxide)   Vo(metal)  Vo(oxide)  Protective?
-----  --------   -----   --------   ---------  ---------  ----------
  Be      1.85      BeO     3.01
  Ca      1.54      CaO    3.25-3.38
  Al      2.70     Al2O3    3.97
  Fe      7.86      FeO     5.7
                   Fe2O3    5.24
                   Fe3O4    5.18
  Ti      4.50     TiO2     4.26
------------------
FeO, wuestite; Fe2O3, hematite; Fe3O4, magnetite;
TiO2, rutile.
```

   What advantages and disadvantages do Al and Ti have in their application as material for tableware? This is an open ended question, and give a common-sense type discussion.
4. y = 1.6 nm after 1 day
   y = 3.5 nm after 1 year Estimate *c* and *k*. What are the thickness of the oxide layer at *t* = 5, 10, and 20 years?

   What effect does moisture have on the oxidation of iron?

Contributors and Attributions

- Chung (Peter) Chieh (Professor Emeritus, Chemistry @ University of Waterloo)

This page titled 12.5.E: Defects in Solid State Lattices (Exercises) is shared under a license and was authored, remixed, and/or curated by LibreTexts.

- 6.17.E: Defects in Solid State Lattices (Exercises) is licensed CC BY-NC-SA 4.0.

12.5A: Schottky Defect

Lattice structures are not perfect; in fact most of the time they experience defects. Lattice structures (or crystals) are prone to defects especially when their temperature is greater than 0 K [1]. One of these defects is known as the Schottky defect, which occurs when oppositely charged ions vacant their sites [1].

Introduction

Like the human body, lattice structures (most commonly known as crystals) are far from perfection. Our body works hard to keep things proportional but occasionally our right foot is bigger than our left; similarly, crystals may try to arrange it's ions under a strict layout, but occasionally an ion slips to another spot or simply goes missing. Realistically speaking, it should be expected that crystals will depart itself from order (not surprising considering defects occurs at temperature greater than 0 K). There are many ways a crystal can depart itself from order (thus experiences defects); these defects can be grouped in different categories such as Point Defects, Line Defects, Planar Defects, or Volume or Bulk Defects [2]. We will focus on Point Defects, specifically the defect that occurs in ionic crystal structures (i.e. NaCl) called the Schottky Defect.

Point Defects

Lattice structures (or crystals) undergoing point defects experience one of two types:

1. atoms or ions leaving their spot (thus creating vacancies).
2. atoms or ions slipping into the little gaps in between other atoms or ions; those little gaps are known as interstitials--since atoms or ions in the crystals are occupying interstitials, they inherently become (create) interstitials.

By the simplest definition, the Schottky defect is defined by type one, while type two defects are known as the Frenkel defect. The Schottky defect is often visually demonstrated using the following layout of anions and cations:

+	-	+	-	+	-	+	-	+	-	+
-	+	-	+	-	+	-	+	(vacant)	+	-
+	-	+	-	+	-	+	-	+	-	+
-	+	-	(vacant)	-	+	-	+	-	+	-
+	-	+	-	+	-	+	-	+	-	+
-	+	-	+	-	+	-	+	-	+	-

Figure $12.5A.1$*: The positive symbols represents cations (i.e. Na^+) and the negative symbol represents anions (i.e. Cl^-).*

In addition, this layout is applicable only for ionic crystal compounds of the formula MX--layout for ionic crystals with formula MX_2 and M_2X_3 will be discussed later--where M is metal and X is nonmetal. Notice the figure has exactly one cation and one anion vacating their sites; that is what defines a (one) Schottky Defect for a crystal of MX formula--for every cation that vacant its site, the same number of anion will follow suit; essentially the vacant sites come in pairs. This also means the crystal will neither be too positive or too negative because the crystal will always be in equilibrium in respect to the number of anions and cations.

It is possible to approximate the number of Schottky defects (n_s) in a MX ionic crystal compound by using the equation:

$$N = \exp^{-\frac{\Delta H}{2RT}} \tag{12.5A.1}$$

where

- ΔH is the enthalpy of defect formation,
- R is the gas constant,

- T is the absolute temperature (in K), and

N can be calculated by:

$$N = \frac{\text{density of the ionic crystal compound} \times N_A}{\text{molar mass of the ionic crystal compound}} \tag{12.5A.2}$$

From Equation 12.5A.1, it is also possible to calculate the fraction of vacant sites by using the equation:

$$\frac{n_s}{N} = \exp^{-\frac{\Delta H}{2RT}} \tag{12.5A.3}$$

Schottky defects for MX_2 and M_2X_3

As mentioned earlier, a Schottky defect will always result a crystal structure in equilibrium--where no crystal is going to be too positive or too negative; thus in the case of:

- MX_2: one Schottky defect equals one cation and two anion vacancy.
- M_2X_3: one Schottky defect equals two cation and three anion vacancy.

References

1. Housecroft, Catherine. Inorganic Chemistry. Pearson Prentice Hall 2008.
2. Sólyom, J.(Jenö). Fundamentals of the Physics of Solids. Translated by Attila Piróth. New York : Springer, c2007.
3. Tilley, Richard. Understanding Solids. John Wiley & Sons, LTD. 2004.

Problems

1. How does an ionic crystal structure maintain electrical neutrality despite undergoing a Schottky defect?
2. How is a Schottky defect defined for a compound with a MX formula? MX_2? M_2X_3?
3. Given that the enthalpy of defect formation for LiCl is 3.39 x 10^{-19} J and the density of LiCl is 2.068 g/cm^{-3}. Calculate the number of Schottky defect at 873 K.
4. Using the number of Schottky defect solved for question 3, determine the fraction of vacant site for LiCl.
5. If a anion and a cation vacant its site and occupies a space between other anions and cations, is it still a Schottky defect?

Answers

1. For a MX compound: one anion and one cation vacant their sites, so the overall charge will remain balanced. This is the same for MX_2 and M_2X_3 because appropriate numbers of anions and cations vacant their site thus leaving the overall charge neutral.
2. MX compound: one Schottky defect is when one anion and one cation leave their sites. MX_2 compound: one Schottky defect is when one anion and two cations leave their sites. M_2X_3 is when two anions and three cations leave their sites.

This page titled 12.5A: Schottky Defect is shared under a license and was authored, remixed, and/or curated by LibreTexts.

- Schottky Defects is licensed CC BY-NC-SA 4.0.

12.5B: Frenkel Defect

The **Frenkel defect** (also known as the Frenkel pair/disorder) is a defect in the lattice crystal where an atom or ion occupies a normally vacant site other than its own. As a result the atom or ion leaves its own lattice site vacant.

The Frenkel Defect in a Molecule

The Frenkel Defect explains a defect in the molecule where an atom or ion (normally the cation) leaves its own lattice site vacant and instead occupies a normally vacant site (Figure $12.5B.1$). The cation leaves its own lattice site open and places itself between the area of all the other cations and anions. This defect is only possible if the cations are smaller in size when compared to the anions.

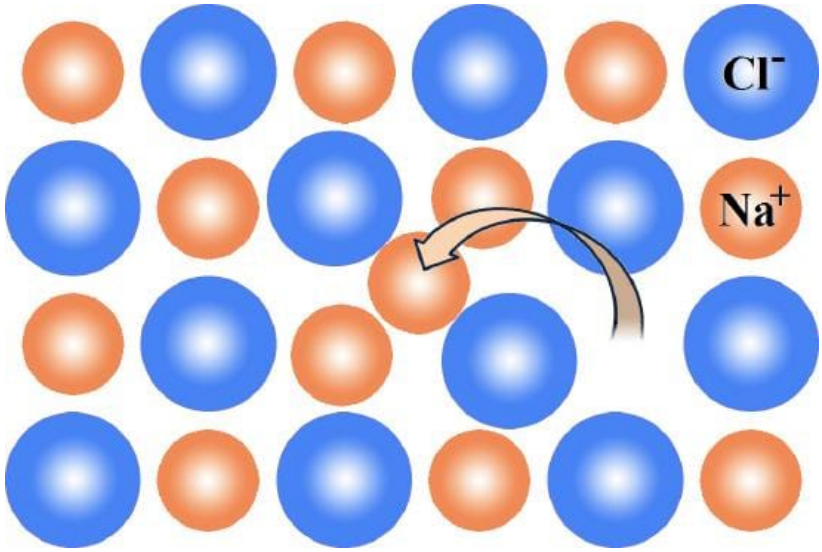


Figure $12.5B.1$: The Frenkel defect within the NaCl structure. (CC BY-SA 3.0; VladVD via Wikipedia)

The number of Frenkel Defects can be calculated using the equation:

$$\sqrt{NN^*}\, e^{\frac{\Delta H}{2RT}}$$

where N is the number of normally occupied positions, N^* is the number of available positions for the moving ion, the ΔH of formation is the enthalpy formation of one Frenkel defect, and R is the gas constant. Frenkel defects are intrinsic defects because the existence causes the Gibbs energy of a crystal to decrease, which means it is favorable to occur.

Solids Found with a Frenkel Defect

The crystal lattices are relatively open and the coordination number is low.

References

1. Housecroft, Catherine E., and Alan G. Sharpe. *Inorganic Chemistry*. 3rd ed. Harlow: Pearson Education, 2008. Print.
2. Tilley, Richard. *Understanding Solids*. John Wiley & Sons, LTD. 2004.

Problems

1. What requirements are needed in order for the Frenkel defect to occur in an atom?
2. What are the differences between the Schottky defect and the Frenkel defect?

Answers

1. A low coordination number as well as having the crystal lattices open for the molecule.
2. The Frenkel defect causes an cation to leave its own lattice and go to another, while Sckhotty defect depicts that an equal number of cations and anions must be absent to maintain charge neutraility.

Contributors and Attributions

- Stanley Hsia, UC Davis

This page titled 12.5B: Frenkel Defect is shared under a license and was authored, remixed, and/or curated by LibreTexts.

- Frenkel Defect is licensed CC BY-NC-SA 4.0.

12.5C: Experimental Observations of Schottky and Frenkel Defects

This page titled 12.5C: Experimental Observations of Schottky and Frenkel Defects is shared under a license and was authored, remixed, and/or curated by LibreTexts.

12.5D: Non-Stoichiometric Compounds

This page titled 12.5D: Non-Stoichiometric Compounds is shared under a license and was authored, remixed, and/or curated by LibreTexts.

12.5E: Color Centers (F-Centers)

This page titled 12.5E: Color Centers (F-Centers) is shared under a license and was authored, remixed, and/or curated by LibreTexts.

12.5F: Thermodynamic Effects of Crystal Defects

This page titled 12.5F: Thermodynamic Effects of Crystal Defects is shared under a license and was authored, remixed, and/or curated by LibreTexts.

12.6: Introduction

Crystalline solids

- The atoms, molecules or ions pack together in an ordered arrangement
- Such solids typically have flat surfaces, with unique angles between faces and unique
- 3-dimensional shape
- Examples of crystalline solids include diamonds, and quartz crystals

Amorphous solids

- No ordered structure to the particles of the solid
- No well defined faces, angles or shapes
- Often are mixtures of molecules which do not stack together well, or large flexible molecules
- Examples would include glass and rubber

This page titled 12.6: Introduction is shared under a license and was authored, remixed, and/or curated by LibreTexts.

- 6.1: Introduction is licensed CC BY-NC-SA 4.0.

12.7: PACKING OF SPHERES

- Topic hierarchy

12.7A: Cubic and Hexagonal Closed Packing

12.7B: The Unit Cell of HPC and CCP

1.1: The Unit Cell

12.7C: Interstitial Holes in HCP and CCP

12.7D: Non-closed Packing- Simple Cubic and Body Centered Cubic

This page titled 12.7: Packing of Spheres is shared under a license and was authored, remixed, and/or curated by LibreTexts.

- 6.2: Packing of Spheres is licensed CC BY-NC-SA 4.0.

12.7A: Cubic and Hexagonal Closed Packing

This page titled 12.7A: Cubic and Hexagonal Closed Packing is shared under a license and was authored, remixed, and/or curated by LibreTexts.

12.7B: THE UNIT CELL OF HPC AND CCP

Close message

Learn more

Welcome to your new guide!

Click on "New" to build out your guide.

1.1: The Unit Cell

This page titled 12.7B: The Unit Cell of HPC and CCP is shared under a license and was authored, remixed, and/or curated by LibreTexts.

- 6.2B: The Unit Cell of HPC and CCP is licensed CC BY-NC-SA 4.0.

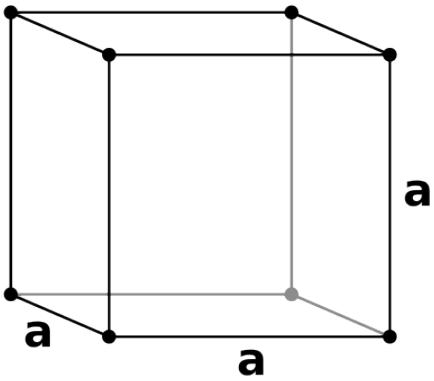
1.1: The Unit Cell

The Unit Cell refers to a part of a simple crystal lattice, a repetitive unit of solid, brick-like structures with opposite faces, and equivalent edge points. In 1850, Auguste Bravais proved that crystals could be split into fourteen unit cells. Although there are several types of unit cells found in cubic lattices, we will be discussing the basic ones: Simple Cubic, Body-centered Cubic, and Face-centered Cubic. If any atom recrystalizes, it will eventually become the original lattice. Crystallization refers the purification processes of molecular or structures;.

Introduction

The Unit Cell contains seven crystal systems and fourteen crystal lattices. These unit cells are given types and titles of symmetries, but we will be focusing on cubic unit cells. One of the most commonly known unit cells is rock salt NaCl (Sodium Chloride), an octahedral geometric unit cell. The whole lattice can be reproduced when the unit cell is duplicated in a three dimensional structure. These unit cells are imperative for quite a few metals and ionic solids crystallize into these cubic structures. Calculating with unit cells is a simple task because edge-lengths of the cell are equal along with all 90^0 angles.

Simple Cubic Unit Cells



Simple Cubic unit cells indicate when lattice points are only at the corners. They are the simplest (hence the title) repetitive unit cell. The lattice points at the corners make it easier for metals, ions, or molecules to be found within the crystalline structure. This phenomena is rare due to the low packing of density, but the closed packed directions give the cube shape.

Since the edges of each unit cell are equidistant, each unit cell is identical. In order to be labeled as a "Simple Cubic" unit cell, each eight cornered same particle must at each of the eight corners. This unit cell only contains one atom. Its packing efficiency is about 52%.

To packing efficiency, we multiply eight corners by one-eighth (for only one-eighth of the atom is part of each unit cell), giving us one atom.

8 Corners of a given atom x 1/8 of the given atom's unit cell = 1 atom

To calculate edge length in terms of *r* the equation is as follows:

2r

An example of a Simple Cubic unit cell is Polonium.

Body-centered Cubic Unit Cells

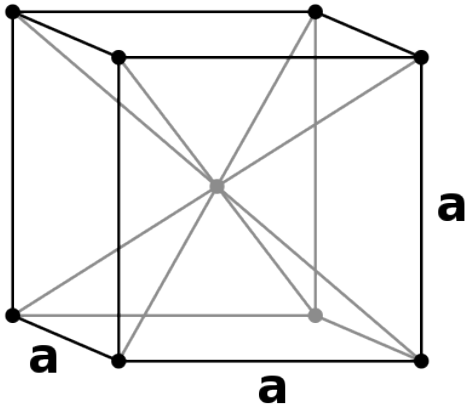
Body-centered Cubic (BCC) unit cells indicate where the lattice points appear not only at the corners but in the center of the unit cell as well. The atoms touch one another along the cube's diagonal crossing, but the atoms don't touch the edge of the cube. All atoms are identical. This type of unit cell is more common than that of the Simple Cubic unit cell due to tightly packed atoms. Its packing efficiency is about 68% compared to the Simple Cubic unit cell's 52%.

This unit cells contains two atoms.

To determine this, we multiply the previous eight corners by one-eighth and *add* one for the additional lattice point in the center.

(8 Corners of a given atom x 1/8 of the given atom's unit cell) + 1 additional lattice point = 2 atoms)

To calculate edge length in terms of *r* the equation is as follows:



$$\frac{4r}{\sqrt{3}} \tag{1.1.1}$$

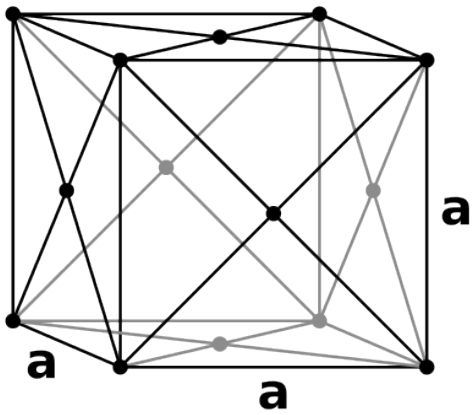
Some examples of BCCs are Iron, Chromium, and Potassium.

It is a common mistake for CsCl to be considered bcc, but it is not. Instead, it is non-closed packed.

Face-centered Cubic Unit Cells

Face-centered Cubic (FCC) unit cells indicate where the lattice points are at both corners and on each face of the cell.

This is a more common type of unit cell since the atoms are more tightly packed than that of a Simple Cubic unit cell. Like the BCC, the atoms don't touch the edge of the cube, but rather the atoms touch diagonal to each face. Its packing efficiency is the highest with a percentage of 74%. Atoms touch one another along the face diagonals. All atoms are identical.



This unit cell contains four atoms.

To determine this, we take the equation from the aforementioned Simple Cubic unit cell and *add* to the parenthesized six faces of the unit cell multiplied by one-half (due to the lattice points on each face of the cubic cell).

(8 corners of a given atom x 1/8 of the given atom's unit cell) + (6 faces x 1/2 contribution) = 4 atoms)

To calculate edge length in terms of *r* the equation is as follows:

$$2\sqrt{2}r \tag{1.1.2}$$

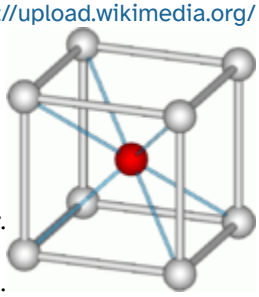
References

1. Brown, Theodore L. *Chemistry: the Central Science*. 10th ed. Upper Saddle River, NJ: Pearson Prentice Hall, 2006. Print. (Pgs 466-467)
2. Housecroft, Catherine E., and Alan G. Sharpe. *Inorganic Chemistry*. 3rd ed. Harlow: Pearson Education, 2008. Print. (Pgs 149-151)
3. Tro, Nivaldo J. *Chemistry: a Molecular Approach*. 1st ed. Upper Saddle River, NJ: Pearson/Prentice Hall, 2008. Print. (Pgs 498-500)

Outside Links

- Simple Cubic Unit Cell image adapted from the Wikimedia Commons file "Image: http://en.Wikipedia.org/wiki/File:La...mple_cubic.svg"

- Body-centered Cubic Unit Cell image adapted from the Wikimedia Commons file "http://en.Wikipedia.org/wiki/File:La...ered_cubic.svg"
- Face-centered Cubic Unit Cell image adapted from the Wikimedia Commons file "Image: http://en.Wikipedia.org/wiki/File:La...ered_cubic.svg"
- Image from Problem 3 adapted from the Wikimedia Commons file "Image: http://upload.wikimedia.org/wikipedi...Cl_crystal.png"



Problems

1. What is the edge length of the atom Polonium if its radius is 167 pm?
2. What type of unit cell is Caesium Chloride as seen in the picture. Briefly explain your answer. Diagram---------->
3. Give two other examples (none of which is shown above) of a Face-Centered Cubic Structure metal. Briefly explain your reasonings.
4. Silver crystallizes with a FCC; the raidus of the atom is 160 pm. What is the density of the solid silver in grams per cubic centimeters?

Answers

1. Polonium is a Simple Cubic unit cell, so the equation for the edge length is *2r*. Therefore, 2(167pm) = 334pm
2. Caesium Chloride is a non-closed packed unit cell. It is common for one to mistake this as a body-centered cubic, but it is not. The reason for this is because the ions do not touch one another. Also, in order to be considered BCC, all the atoms must be the same. Since the middle atome is different than the corner atoms, this is not a BCC.
3. Two examples of a FCC cubic structure metals are Lead and Aluminum. Each contains four atoms, six of which run diagonally on each face.
4. We approach this problem by first finding the mass of the unit cell. Mass of Silver is 107.87 g/mol, thus we divide by Avagadro's number 6.022 x $10^{-22.}$

We end up with 1.79 x 10^{-22} g/atom. Next we find the mass of the unit cell by multiplying the number of atoms in the unit cell by the mass of each atom (1.79 x 10^{-22} g/atom)(4) = 7.167 x 10^{-22} grams.

Next we find the edge length by:

$$2\sqrt{2} * 160pm \tag{1.1.3}$$

Which equals 4.525 x 10^{-10} meters.

Now we find the volume which equals the edge length to the third power. We convert meters into centimeters by dividing the edge length by 1 cm/10^{-2}m to the third power. (4.525 x 10^{-10} m x 1cm/10^{-2}m = 9.265 x 10^{-23} cubic centimeters.)

Finally, we find the density by mass divided by volume. So, 7.167 x 10^{-22} grams/9.265 x 10^{-23} cubic centimeters = 7.74 g/cm^3

Contributors and Attributions

- Sonika Sidher--UC Davis

This page titled 1.1: The Unit Cell is shared under a license and was authored, remixed, and/or curated by LibreTexts.

- 1.1: The Unit Cell is licensed CC BY-NC-SA 4.0.

12.7C: Interstitial Holes in HCP and CCP

This page titled 12.7C: Interstitial Holes in HCP and CCP is shared under a license and was authored, remixed, and/or curated by LibreTexts.

12.7D: Non-closed Packing- Simple Cubic and Body Centered Cubic

This page titled 12.7D: Non-closed Packing- Simple Cubic and Body Centered Cubic is shared under a license and was authored, remixed, and/or curated by LibreTexts.

12.8: THE PACKING OF SPHERES MODEL APPLIED TO THE STRUCTURES OF ELEMENTS

- Topic hierarchy

12.8A: Group 18 Elements in the Solid State

12.8B: H_2 and F_2 Solids

12.8C: Solid Metallic Elements

This page titled 12.8: The Packing of Spheres Model Applied to the Structures of Elements is shared under a license and was authored, remixed, and/or curated by LibreTexts.

- 6.3: The Packing of Spheres Model Applied to the Structures of Elements is licensed CC BY-NC-SA 4.0.

12.8A: Group 18 Elements in the Solid State

This page titled 12.8A: Group 18 Elements in the Solid State is shared under a license and was authored, remixed, and/or curated by LibreTexts.

12.8B: H_2 and F_2 Solids

Hydrogen and Fluorine, as well as Chlorine, Bromine and Iodine, exist as diatomic molecules. Both diatomic Hydrogen and diatomic Florine exist as gasses at room temperature and exhibit extremely low melting and boiling points. If the temperature of the system is lowered below the respective melting points of Hydrogen or Fluorine, molecular motion is reduced and a crystalline lattice is formed, creating a solid.

Solid State Hydrogen and Fluorine

Elemental Hydrogen and Elemental Fluorine, H_2 and F_2 respectively, exist as gases at room temperature. Though the melting point of H_2 is 20.4 K (-252.75 °C), a temperature of 14.0 K (-259.15 °C) is required for the solidification of H_2.[3,4] As the solid structure is formed, the diatomic Hydrogen molecules adopt a hexagonal close packing (hcp) structure.[4] Fluorine exhibits similar behaviour. The melting point of Fluorine is 53.54K (-219.61 °C), at which point the diatomic Fluorine adopts a cubic close packed crystalline arrangement (ccp), instead of a hexagonal close packed arrangement.[3,4]

Ability to use the sphere model of Crystalline structure for H_2 and F_2 solids

When solid, both dihydrogen and difluorine are small enough to allow for rotation within the solid structure (the radius of Fluorine is about equivalent to that of Hydrogen). This rotation occurs about a central axis midway between the two distal atoms of the molecule, creating two equal radii from the middle of the H-H or F-F bond to the outer boundary of each H or F atom. This rotation occurs 360° in the x, y and z directions of the central axis, as well as all manner of combinations of these three variables. The rotation of the molecule in all directions creates what can be though of as a spherical shell, the boundary of which is created by the distal atoms.[4]

Some common uses for solid hydrogen include gamma-ray ablation cages for elemental analysis, and a solid state cage in which to look at hydrogen bonding within molecules. [1,2]

References

1. Palaszewski, B. (2002) "Solid Hydrogen Experiments for Atomic Propellants: Particle Formation Energy and Imaging Analysis" Retrieved from gltrs.grc.nasa.gov/reports/20...002-211915.pdf
2. Wang, X., Andrews, L. *J. Phys. Chem. A*, 2004, 108 (7), pp 1103–1106 **DOI:** 10.1021/jp037382q
3. Merck Index. 14th ed. Merck: Whitehouse Station, NJ, 2007; 4896
4. Sharpe, Housecroft "Inorganic Chemistry" 3 ed.

Outside Links

- This is not meant for references used for constructing the module, but as secondary and unvetted information available at other site
- Link to outside sources. Wikipedia entries should probably be referenced here.

Problems

1. Why can F_2 and H_2 be considered similar molecules and thus exhibit similar behaviour in rotation?

2. What is the different between a cubic close packing structure and hexagonal close packing?

3. Why do difluorine and dihydrogen exhibit different packing structures.

Contributors and Attributions

- Name #1 here (if anonymous, you can avoid this) with university affiliation

This page titled 12.8B: H_2 and F_2 Solids is shared under a license and was authored, remixed, and/or curated by LibreTexts.

- 6.3B: H_2 and F_2 Solids is licensed CC BY-NC-SA 4.0.

12.8C: Solid Metallic Elements

A metal (from Greek μέταλλον métallon, "mine, quarry, metal") is a material (an element, compound, or alloy) that is typically hard, opaque, shiny, and has good electrical and thermal conductivity. Metals are generally *malleable* - that is, they can be hammered or pressed permanently out of shape without breaking or cracking - as well as *fusible* (able to be fused or melted) and *ductile* (able to be drawn out into a thin wire). About 91 of the 118 elements in the periodic table are metals (some elements appear in both metallic and non-metallic forms).

Atoms of metals readily lose their outer shell electrons, resulting in a free flowing cloud of electrons within their otherwise solid arrangement. This provides the ability of metallic substances to easily transmit heat and electricity. While this flow of electrons occurs, the solid characteristic of the metal is produced by electrostatic interactions between each atom and the electron cloud. This type of bond is called a metallic bond.

Cubic and hexagonal close packing.

Crystalline solids consist of repeating patterns of its components in three dimensions (a crystal lattice) and can be represented by drawing the structure of the smallest identical units that, when stacked together, form the crystal. This basic repeating unit is called a *unit cell*.

Many metals adopt close packed structures i.e. cubic close packed (face centred cubic) and hexagonal close packed structures. A simple model for both of these is to assume that the metal atoms are spherical and are packed together in the most efficient way (close packing or closest packing). For closest packing, every atom has 12 equidistant nearest neighbours, and therefore a coordination number of 12. If the close packed structures are considered as being built of layers of spheres then the difference between hexagonal close packing and cubic close packed is how each layer is positioned relative to others. It can be envisaged that for a regular buildup of layers:

- hexagonal close packing has alternate layers positioned directly above/below each other, A,B,A,B,...
- cubic close packed (face centered cubic) has every third layer directly above/below each other, A,B,C,A,B,C,...

Body centred cubic

This is not a close packed structure. Here each metal atom is at the centre of a cube with 8 nearest neighbors, however the 6 atoms at the centres of the adjacent cubes are only approximately 15% further away so the coordination number can therefore be considered to be 14 when these are included. Note that if the body centered cubic unit cell is compressed along one 4 fold axis the structure becomes cubic close packed (face centred cubic).

lattice types

cubic close packing (ccp) packing efficiency =74% CN=12	

hexagonal close packing (hcp) packing efficiency =74% CN=12	

body-centred cubic packing (bcc) packing efficiency =68% CN=8

Trends in melting point

Melting points are chosen as a simple measure of the stability or strength of the metallic lattice. Some simple trends can be noted. The transition metals have generally higher melting points than the others. In the alkali metals (Group 1) and alkaline earth metals (Group 2) the melting point decreases as atomic number increases, but in transition metal groups with incomplete d-orbital subshells, the heavier elements have higher melting points. For a given period, the melting points reach a maximum at around Group 6 and then fall with increasing atomic number.

Mercury, caesium and gallium have melting points below 30 °C whereas all the other metals have sufficiently high melting points to be solids at "room temperature". The structures of the metals can be summarised by the table below which shows that most metals crystallise in roughly equal amounts of bcc, hcp and ccp lattices.

Crystal structure of metallic elements in the periodic table

1	2	3	4	5	6	7	8	9	10	11	12	13	14	15	16	17
H																
453.69 Li bcc	1560 Be hcp					MP (K) At. Symbol Lattice type						B	C	N	O	F
370.87 Na bcc	923 Mg hcp											933.47 Al ccp	Si	P	S	Cl
336.53 K bcc	1115 Ca ccp	1814 Sc hcp	1941 Ti hcp	2183 V bcc	2180 Cr bcc	1519 Mn	1811 Fe bcc	1768 Co hcp	1728 Ni ccp	1357.8 Cu ccp	692.68 Zn hcp	302.91 Ga	Ge	As	Se	Br
312.46 Rb bcc	1050 Sr ccp	1799 Y hcp	2128 Zr hcp	2750 Nb bcc	2896 Mo bcc	2430 Tc hcp	2607 Ru hcp	2237 Rh ccp	1828 Pd ccp	1235 Ag ccp	594 Cd	430 In	505 Sn	904 Sb	Te	I
301.59 Cs bcc	1000 Ba bcc		2506 Hf hcp	3290 Ta bcc	3695 W bcc	3459 Re hcp	3306 Os hcp	2719 Ir ccp	2041.4 Pt ccp	1337.33 Au ccp	234.32 Hg	577 Tl hcp	600.61 Pb ccp	544.7 Bi	527 Po	At

Group 1: Alkali metals

The alkali metals have their outermost electron in an s-orbital and this electronic configuration results in their characteristic properties. The alkali metals provide the best example of group trends in properties in the periodic table, with elements exhibiting well-characterized homologous behaviour.

The alkali metals have very similar properties: they are all shiny, soft, highly reactive metals at standard temperature and pressure and readily lose their outermost electron to form cations with charge +1. They can all be cut easily with a knife due to their softness, exposing a shiny surface that tarnishes rapidly in air due to oxidation by atmospheric moisture and oxygen. Because of their high reactivity, they must be stored under oil to prevent reaction with air, and are found naturally only in salts and never as the free element. In the modern IUPAC nomenclature, the alkali metals comprise the group 1 elements, excluding hydrogen (H), which is only nominally considered a group 1 element.

Group 2: Alkali Earth Metals

extended structures of Li, Mg, Ca

Lithium -bcc	

Magnesium -hcp ☐Spacefill ☐UnitCell ☐All Layers ☐ A ☐B ☐ A ☐ B ☐ A layers	

Calcium -ccp
☐Spacefill ☐UnitCell ☐All Layers
☐ A ☐B ☐C
☐ A ☐ B ☐C layers

Note that Housecroft and Sharpe has Ca and Sr both listed as hexagonal and not cubic (face) close packed lattices. Calcium and Strontium exist in several allotropic forms and the lowest temperature forms (for Ca < 450 °C) are ccp. At high temperatures phase transitions occur to give hexagonal.

Return to the course outline or move on to Lecture 5: Structure of the elements Boron, Carbon and Phosphorus, Sulfur.

References

Much of the information in these course notes has been sourced from Wikipedia under the Creative Commons License.
'Inorganic Chemistry' - C. Housecroft and A.G. Sharpe, Prentice Hall, 4th Ed., 2012, ISBN13: 978-0273742753, pps 24-27, 43-50, 172-176, 552-558, 299-301, 207-212
'Basic Inorganic Chemistry' - F.A. Cotton, G. Wilkinson and P.L. Gaus, John Wiley and Sons, Inc. 3rd Ed., 1994.
'Introduction to Modern Inorganic Chemistry' - K.M. Mackay, R.A. Mackay and W. Henderson, International Textbook Company, 5th Ed., 1996.

This page titled 12.8C: Solid Metallic Elements is shared under a license and was authored, remixed, and/or curated by LibreTexts.

- 6.3C: Solid Metallic Elements is licensed CC BY-NC-SA 4.0.

12.9: POLYMORPHISM IN METALS

Polymorphism is the ability of a solid material to exist in more than one form or crystal structure.



-  Topic hierarchy 

12.9A: Polymorphism - Phase Changes in the Solid State

12.9B: Phase Diagrams

This page titled 12.9: Polymorphism in Metals is shared under a license and was authored, remixed, and/or curated by LibreTexts.

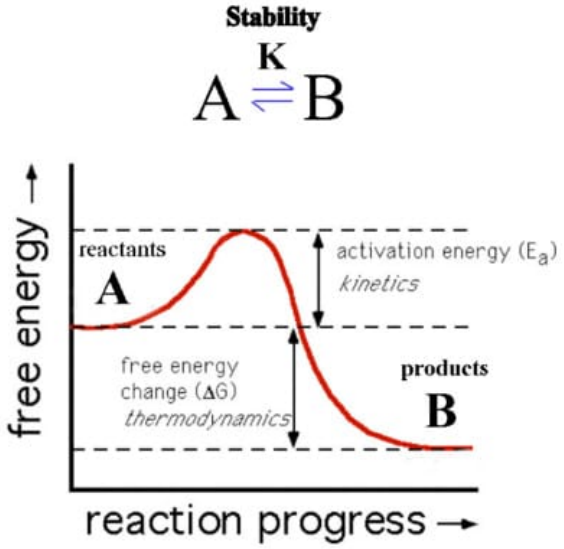
- 6.4: Polymorphism in Metals is licensed CC BY-NC-SA 4.0.

12.9A: Polymorphism - Phase Changes in the Solid State

Polymorphism is when a solid material can exist in more than one form or crystal structure. Polymorphism is very similar to Allotropy, but they should not be confused, polymorphism describes molecules, while Allotropy is used to describe atoms. Polymorphism has many uses whether it was in pharmaceutical, explosives or even food. This process was discovered by Eilhard Mitscherlich in 1821.

Kinetic vs. Thermodynamic Stability

When discussing the concept of Stability it is necessary to distinguish between thermodynamic and kinetic stability.



Here B is at lower energy than A so that ΔG is negative. The reaction should therefore proceed spontaneously and B is the more thermodynamically stable species.

The reaction as shown though has a barrier to the progress of the reaction called the Activation Barrier (Ea) and so the reaction may proceed very slowly. The thermodynamics describes only the starting and ending position of the reaction and not the intermediate or transition state. If the kinetics is slow, A is described as being **inert** while if it proceeds quickly then A is described as being **labile**.

The conditions that distinguish them are:
if the reaction takes longer than 1 minute under the conditions of concentration 0.1 M, temperature 25°C, then it is INERT,
if under the same conditions the reaction time < 1 minute, then it is LABILE.

In the lecture on isomerism, we depend on the samples being kinetically stable i.e. inert.

In the lecture on Chelation and Stability we concentrate on thermodynamic stability and look at the changes in free energy, enthalpy and entropy during the reaction. When we consider thermodynamic stability we need to be familiar with 2 formulae:

$\Delta G^{\ominus} = - RT \ln(K)$ or alternatively $\Delta G^{\ominus} = - 2.303RT \log_{10}(K)$ ---(1)
$\Delta G^{\ominus} = \Delta H^{\ominus} - T\Delta S^{\ominus}$ ---(2)

The first relates the free energy to the stability constant and the second shows the breakdown into the component enthalpy and entropy terms.

This page titled 12.9A: Polymorphism - Phase Changes in the Solid State is shared under a license and was authored, remixed, and/or curated by LibreTexts.

- 6.4A: Polymorphism - Phase Changes in the Solid State is licensed CC BY-NC-SA 4.0.

12.9B: Phase Diagrams

This page titled 12.9B: Phase Diagrams is shared under a license and was authored, remixed, and/or curated by LibreTexts.

12.10: Metallic Radii

Atomic radius is the radius of an atom which measures the distant from its nucleus to the electron. And metallic radii are the radii of the metallic atoms. It is the size of a metallic atom. However the actually measurement of the radius is very vague because electrons don't stay at one point, they orbits around.

This page titled 12.10: Metallic Radii is shared under a license and was authored, remixed, and/or curated by LibreTexts.

- 6.5: Metallic Radii is licensed CC BY-NC-SA 4.0.

12.11: Melting Points and Standard Enthalpies of Atomization of Metals

This page titled 12.11: Melting Points and Standard Enthalpies of Atomization of Metals is shared under a license and was authored, remixed, and/or curated by LibreTexts.

12.12: SIZE OF IONS

- Topic hierarchy

12.12A: Ionic Radii

12.12B: Periodic Trends in Ionic Radii

This page titled 12.12: Size of Ions is shared under a license and was authored, remixed, and/or curated by LibreTexts.

- 6.10: Size of Ions is licensed CC BY-NC-SA 4.0.

12.12A: Ionic Radii

In a crystal lattice, the ionic radius is a measure of the size of the atom's ion.[6] When formed, ionic atoms change in size with respect to their orginal atom. Cation radii will decrease and the anion radii will increase in size compared to their neutral atoms. Questions such as: "What methodology is used by chemists to measure ionic radii?" and "Are there any non-experimental ways to estimate the size of ionic radii?" will be answered in this module. Accordingly, there are many ways to determine ionic radii.

1. Introduction
2. Hard-Sphere model
3. Periodic Trends
4. References
5. Outside Links
6. Problems
7. Answers

Introduction

In the past, after an atom is ionized, X-ray diffraction is used to measure how much the radius of the atom increased or decreased. However, scientists wanted to use another technique, due to the fact, that X-ray diffraction is difficult to distinguish a boundary between two ions. As a result, the *hard sphere model* can be used.

Hard-Sphere model

The Hard-Sphere model are impenetrable spheres that do not overlap in space.[5] The Hard-Sphere model has been tested by well-known scientists; Lande', Pauling and Goldsmidt. The ion radii measured under crystal state of ionic compound which cations and anions are stacking in pattern as shown below.

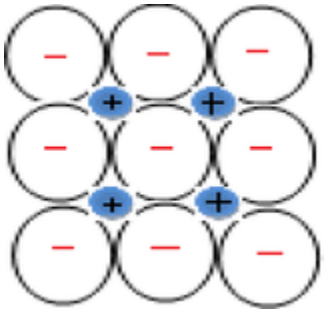


Figure 1: Schematic of the hard-sphere model

The Hard-Sphere model can be applied to metallic and ionic compounds such as NaCl, which is shown below.

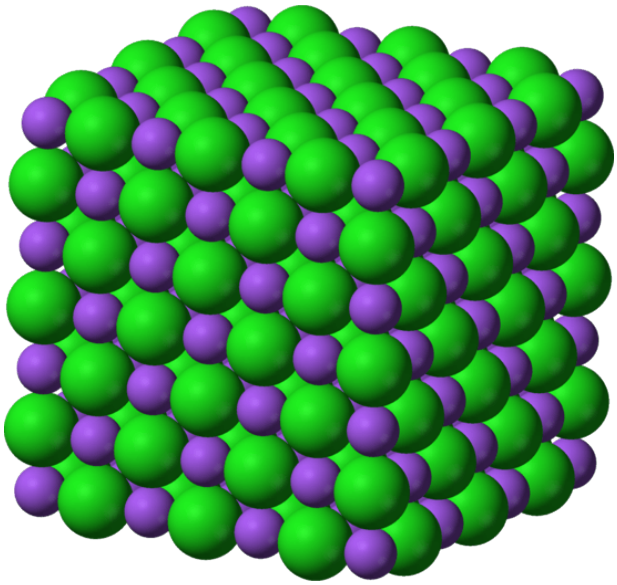


Figure 2: 3-D hard sphere model of Sodium Chloride, taken with permission from en.Wikipedia.org/wiki/File:So...e-3D-ionic.png

In general, scientists uses formula of Internuclear distance to test out the radii of ion then compared with the ion radii had done on X-ray diffraction:

$$\text{Internuclear distance (d)} = r_{cation} + r_{anion}\ ^{2}$$

*To calculate ion radii, Lande used ionic compound under solid state (ex: NaCl). This will minize the distribution of electrons.

1. Find the radii of anion (r^-) atom.
2. Find internuclear distance (d) between anion and cation.
3. Use Internuclear distance formula to find the r^+.

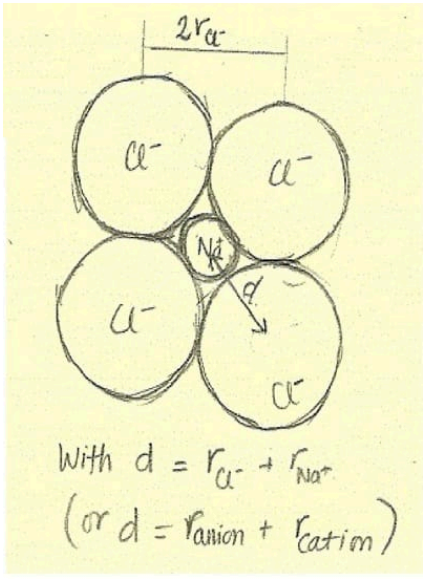


Figure 3: The Hard sphere model can roughly determine the ion radii.

Periodic Trends

As described earlier, cations are smaller in size compared to their neutral atoms while anions are larger in size.Cations are smaller than its neutral atoms because the positive nuclear charge, which holds the electrons in closer, exceeds the negative charge

when a metal atom loses an electron. On the contrary, anions are larger because the electrons are not held as tightly, repulsions of electrons increase, and the electrons spread out more due to nonmetal atoms gaining an electron. Refer to the outside link to learn more about the periodic trends for ionic radii (http://abulafia.mt.ic.ac.uk/shannon/ptable.php).

References

1. Kotz, Treichel, Weaver,2006, *Chemistry and Chemical Reactivity*, Thomson Brooks/Cole, Mason, OH, p.358-364
2. Housecroft C., and Shappe A., 2008, *Inorganic Chemistry 3rd edition,* Pearson Education Limited, England, p.162-164
3. Barrera, M, and FZuloagat. "*Determination of the ionic radii by means of the Kohn-Sham potential: Identification of the chemical potential*." International journal of quantum chemistry 106.9 (2006):2044-2053.
4. "*Ionic radii for Group 1 and Group 2 halide, hydride, fluoride, oxide, sulfide, selenide and telluride crystals*." Dalton transactions 39.33 (2010):7786-.
5. http://en.Wikipedia.org/wiki/Hard_spheres
6. http://en.Wikipedia.org/wiki/Ionic_radius

Outside Links

- http://abulafia.mt.ic.ac.uk/shannon/ptable.php

Problems

1. What is the most general formula that used to determine the ion radii for hard sphere model?

2. Find radius for Cacium ion in Calcium Chloride ($CaCl_{2)}$. List out all the steps (numbers are not necessary)

3. Determine which is larger:

a) K^+ or Cs^+?

b) La^{3+} or Lu^{3+}?

c) Ca^{2+} or Zn^{2+}?

Answers

1. Internuclear distance (d) = $r_{cation} + r_{anion}$

2. Find the radii of anion (r^-*) atom; Find internuclear distance (d) between anion and cation; Use Internuclear distance formula to find the* r^+.

3. a.) Cs^+ b.) La^{3+} c.) Ca^{2+}

This page titled 12.12A: Ionic Radii is shared under a license and was authored, remixed, and/or curated by LibreTexts.

- 6.10A: Ionic Radii is licensed CC BY-NC-SA 4.0.

12.12B: Periodic Trends in Ionic Radii

This page titled 12.12B: Periodic Trends in Ionic Radii is shared under a license and was authored, remixed, and/or curated by LibreTexts.

12.13: Crystal Structure of Semiconductors

- Topic hierarchy

This page titled 12.13: Crystal Structure of Semiconductors is shared under a license and was authored, remixed, and/or curated by LibreTexts.

- 6.12: Crystal Structure of Semiconductors is licensed CC BY-NC-SA 4.0.

13: INTRODUCTION TO ORGANOMETALLIC COMPLEXES

13.1: What is Organometallic Chemistry?
13.2: Historical Background
13.3: The 18 Electron Rule
13.4: Reactions Involving Gain or Loss of Ligands
13.5: Organometallic Catalysts

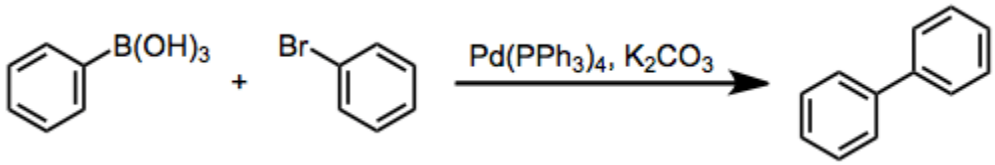
This page titled 13: Introduction to Organometallic Complexes is shared under a license and was authored, remixed, and/or curated by LibreTexts.

13.1: What is Organometallic Chemistry?

Let's begin with a few simple questions: what is organometallic chemistry? What, after studying organometallic chemistry, will we know about the world that we didn't know before? Why is the subject worth studying? And what kinds of problems is the subject meant to address? The purpose of this post is to give the best answers I currently know of to these questions. The goal of this otherwise content-free post is twofold: (1) to help motivate us as we move forward (that is, to constantly remind us that there is a point to all this!); and (2) to illustrate the kinds of problems we'll be able to address using concepts from the field. You might be surprised by the spine-chilling power you feel after learning about the behavior of organometallic compounds and reactions!

Put most bluntly, organometallic (OM) chemistry is the study of compounds containing, and reactions involving, metal-carbon bonds. The metal-carbon bond may be transient or temporary, but if one exists during a reaction or in a compound of interest, we're squarely in the domain of organometallic chemistry. Despite the denotational importance of the M-C bond, bonds between metals and the other common elements of organic chemistry also appear in OM chemistry: metal-nitrogen, metal-oxygen, metal-halogen, and even metal-hydrogen bonds all play a role. Metals cover a vast swath of the periodic table and include the alkali metals (group 1), alkali earth metals (group 2), transition metals (groups 3-12), the main group metals (groups 13-15, "under the stairs"), and the lanthanides and actinides. We will focus most prominently on the behavior of the transition metals, so called because they cover the transition between the electropositive group 2 elements and the more electron-rich main group elements.

Why is the subject worth studying? Well, for me, it mostly comes down to synthetic flexibility. There's a reason the "organo" comes first in "organometallic chemistry"—our goal is usually the creation of new bonds in organic compounds. The metals tend to just be along for the ride (although their influence, obviously, is essential). And the fact is that you can do things with organometallic chemistry that you cannot do using straight-up organic chemistry. Case in point:



The venerable Suzuki reaction...unthinkable without palladium!

The establishment of the bond between the phenyl rings through a means other than dumb luck seems unthinkable to the organic chemist, but it's natural for the palladium-equipped metal-organicker. Bromobenzene looks like a potential electrophile at the bromine-bearing carbon, and if you're familiar with hydroboration you might see phenylboronic acid as a potential nucleophile at the boron-bearing carbon. Catalytic palladium makes it all happen! Organometallic chemistry is full of these mind-bending transformations, and can expand the synthetic toolbox of the organic chemist considerably.

To throw another motive into the mix for the non-specialist (or the synthesis-spurning chemist), organometallic chemistry is full of intriguing stories of scientific inquiry and discovery. Exploring how researchers take a new organometallic reaction from "ooh pretty" to strong predictive power is instructive for anyone interested in "how science works," in a practical sense. We'll examine a number of classical experiments in organometallic chemistry, both for their value to the field and their contributions to the general nature of scientific inquiry.

What kinds of problems should we be able to address as we move forward? Here's a bulleted list of the most commonly encountered types of problems in an organometallic chemistry course:

- Describe the structure of an organometallic complex...
- Predict the product of the given reaction conditions...
- Draw a reasonable mechanism based on evidence...
- Devise a synthetic route to synthesize a target organometallic compound...
- Explain the observation(s)...
- Predict the results of a series of experiments...

The first four are pretty standard organic-esque problems, but it's the last two, more general classes that really make organometallic chemistry compelling. Just imagine putting yourself in the shoes of the pioneers and making the same predictions

they did!

There you have it, a short introduction to organometallic chemistry and why it's worth studying. Of course, we'll use the remainder of space in the blog to fully describe what organometallic chemistry really is...but it's helpful to keep these motives in mind as you study. Keep a thirst for predictive power, and it's hard to go wrong with organometallic chemistry!

This page titled 13.1: What is Organometallic Chemistry? is shared under a license and was authored, remixed, and/or curated by Michael Evans.

- 1.2: What is Organometallic Chemistry? by Michael Evans is licensed CC BY-NC-SA 4.0.

13.2: Historical Background

10.1: Historical Background

This page titled 13.2: Historical Background is shared under a license and was authored, remixed, and/or curated by Kai Landskron.

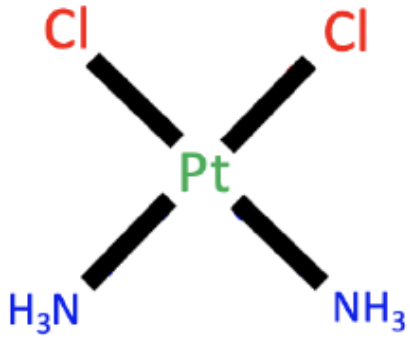
13.3: The 18 Electron Rule

Electron Counting In Transition Metal Complexes

In this chapter we will learn how to count valence electrons in coordination compounds. Electron counting is important because the number of electrons in a complex can tell us a lot about the stability and reactivity in a coordination compound. In addition, it allows us to predict and understand structures to a certain extent. Electron counting sounds trivial, but it is not as trivial as it seems, actually there are even two different methods for electron counting. Each method leads to the same result. Which method you prefer is “personal taste”, but each method is about equally common in the literature, so you need to know both of them.

The Neutral Atom Method

The first method is called the “neutral atom method”. As the name suggests, we will break up the complex into neutral fragments, and count the electrons that contribute to the bonding in each of the fragments. The neutral atom method is carried out according to the following three steps. First, we count the number of the valence electron of the metal. We consider the metal as neutral atom. The number valence electrons is the same as the group number of the transition metal in the periodic table. For transition metals the group number varies from 3 to 12. In the second step, we account for the ionic charge of the complex, if the complex is not neutral. This will reduce the number of electrons for a complex cation, and increase the number of valence electrons for a complex anion. In the third step, we need to determine how many electrons are contributed by each ligand. This is the most complicated step. To determine the number of electrons must cleave each metal-ligand bond so that a ligand fragment results that is neutral. We then count the number of electrons at the ligand that contributed to the bond. The number of electrons contributed by each ligand is then summed up. This is sum is then added to the number of electrons determined by the previous steps. This is gives the overall number of valence electrons.



	Number of e’s
Pt	10
charge	0
2 Cl	2 · 1 = 2
2 N	2 · 2 = 4
Total	= 16

Figure 6.1.1 Example of neutral atom method

Let us apply these rules by an example, the cis-platinum complex. We first need to count the number of electrons of the metal. The metal is platinum which is located in group 10 of the periodic table. Therefore, a neutral platinum atom has ten valence electrons.

Next, we look at the charge of the complex. In this case, there is no charge, and therefore no electrons are added or subtracted.

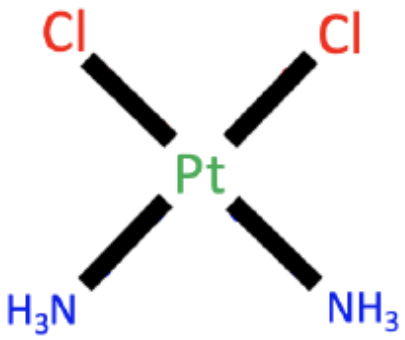
Lastly, we count the electrons of the ligands. There are two types of ligands, the chloro-ligands and the ammine ligands. Now, our task is to cleave the Pt-ligand bond so that neutral ligand fragments result. We can see that for the chloro-ligands we must cleave the Pt-Cl bond, homoleptically, meaning in the middle, assigning one electron to the Pt and one electron to Cl, because doing so creates a neutral chlorine atom. The fact that we cleaved the bond homoleptically, means that the chloro ligand contributed one electron. Because we have two chloro ligands, there are overall two electrons.

Now, let us think about how many electrons the ammine ligands contribute. In this case we need to cleave the metal-ligand bond heteroleptically to produce a neutral ligand fragment. Both bonding electrons are assigned to the ligand. This produces a neutral NH3 molecule. This means that each ammine ligand contributes two electrons. Overall, that makes four electrons, because we have two ammine ligands.

Finally, we need to sum up the electrons from all three steps. That is ten electrons from Pt, zero electrons due to charge, two electrons from the chloro ligands, and four electrons from the ammine ligands equaling 16 valence electrons total. This is the final result.

"Oxidation State" Method

The oxidation state method is also comprised of three steps. The first step is the same as in the neutral atom method. We determine the number of electrons of the neutral metal which the same as its group number in the periodic table. The next step is different though. It requires the determination of the oxidation state of the metal. How can we determine it? First, we cleave the metal-ligand bonds heteroleptically so that all bonding electrons are assigned to the ligands. Then we determine what is the charge of the ligands? Ligands can either be neutral of negatively charged. We determine the overall number of charges at the ligands. The difference between that number and the charge of the complex is the oxidation state of the metal. We either add or subtract electrons depending on the oxidation state of the metal. If the oxidation state is positive we subtract electrons, if it is negative, which is rare, then we add electrons. The third step counts the number of the electrons contributed by the ligands. Because we cleaved all bonds homoleptically, all bonding electrons are considered to be contributed by the ligands, and we count them accordingly. Finally, we sum up the electrons of all three steps which gives the total number of electrons.



	Number of electrons
Pd	10
Oxid. state	-(+2)
2 Cl^-	$+2 \cdot 2 = 4$
2 N	$+2 \cdot 2 = 4$
Total	**= 16**

Figure 6.1.2 Example of oxidation state method

Let us apply the method to the previous example cis-platinum. Applying the first step gives us 10 valence electrons for the platinum.

Next, we need to determine the oxidation state of Pt. To do so, we must now cleave all metal-ligands heteroleptically, so that all bonding electrons are assigned to the ligand. By the way, this is equivalent to saying that we treat all the bonds as dative bonds with all electrons coming from the ligands as the donors. When we do this for the chloro ligands we see that this created chloride anions with a 1- charge. Cleaving the Pt-N bonds heteroleptically leads to neutral NH_3 molecules. Therefore the overall number of charges at the ligands is 2x(-1)+2x0=-2. The charge at the complex is zero, therefore the oxidation state of Pt is 0-(-2)=+2. We must therefore subtract two electrons from the 10 electrons of the platinum.

Now we must determine the number electrons coming from the ligands. Because all bonds are considered as dative bonds, the chloro ligands contribute two electrons each, and the ammine ligands contribute two electrons each. That makes overall four electrons.

In sum, 10 electrons from the neutral Pt atom minus two electrons due to the +2 oxidation state of Pt plus 2x2=4 electrons from Cl plus 2x2=4 electrons from NH_3 gives 16 electrons total. We can see that we have arrived at the same results as in the case of the oxidation state method.

We can discuss the advantages and disadvantages of both methods, also. They neutral atom method has the advantage that we do not have to think about charges at ligands and oxidation states. However, we have to think about how to cleave bonds to create neutral fragments. We may need ot cleave bonds in an way that is not reflecting the donor-acceptor nature of a coordination compound. The oxidation method does account for the donor-acceptor nature of a coordination compound because the bonds are considered dative bonds, and the electrons are assigned to the ligands and metal accordingly. We not not need to think how to cleave bonds, because we cleave the bonds always heteroleptically. However, it requires us to think about charges at the ligands to determine oxidation states which is an additional, non-trivial step.

Counting Electrons: Ligand Contributions

The most difficult step in electron counting is mostly the determination of the number of electrons a ligand provides. Therefore, let us practice this by a few example.

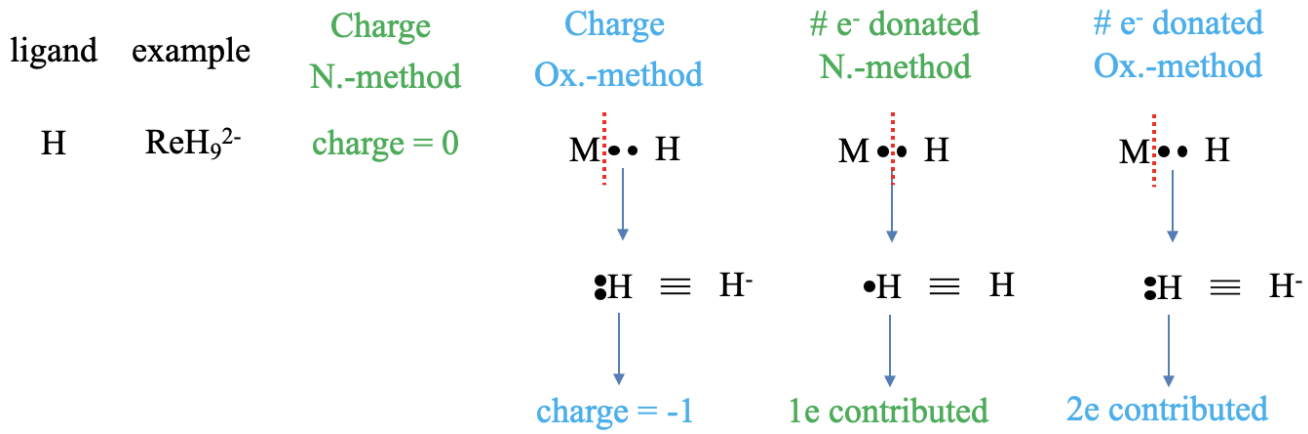


Figure 6.1.3 Example of counting electrons with a hydrido ligand

Let us first look at an hydrido ligand which for example occurs in the nonohydridorhentate(2-) complex. What is the charge of the ligand in the two methods? In the neutral atom method the charge is always zero, this is a no-brainer. In the case of the oxidation statement method, we need to treat the bond as a dative bond, and that means that we must cleave the bond heteroleptically, so that both bonding electrons can be assigned to the ligand. An H atom with two electrons is a hydride anion with a -1 charge. Next, let us think about the number of electrons donated. In the neutral atom method we need to produce neutral ligand fragments. To do so we must cleave the M-H bond homoleptically, because this will create a neutral hydrogen atom. How many electron will it contribute. It will contribute one electron, because we cleaved the bond homoleptically assigning only one of the two bonding electrons to H. In the oxidation state method, the hydrido ligand contributes two electrons because the bond was considered dative and therefore cleaved heteroleptically. Both bonding electrons were assigned to the ligand, therefore the ligand contributes two electrons.

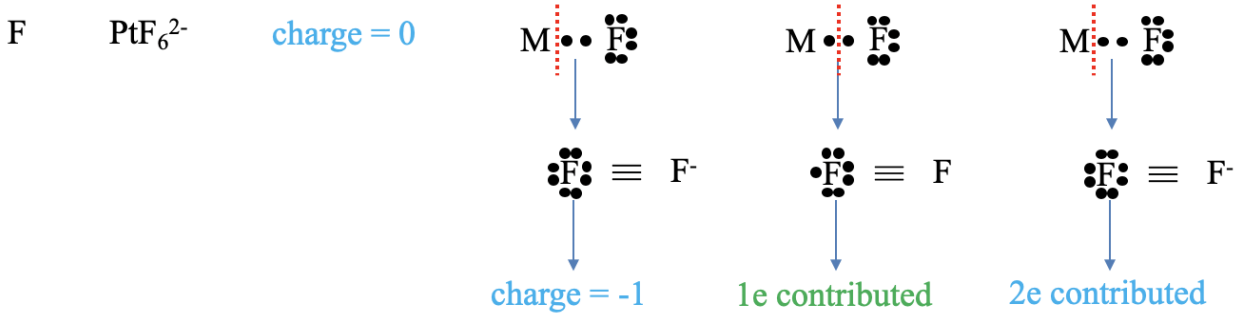


Figure 6.1.4 Example of counting electrons with a halogenide ligand

Next, let us consider a halogenide ligand. What is the charge at the ligand. For the neutral atom method, the answer is trivial, the charge is always zero. In the oxidation state method both bonding electrons in the M-L bond get assigned to the ligand. This gives the ligand a -1 charge. What is the number of electrons contributed? In the neutral atom method we need to think again how to cleave the M-L bond to create a neutral ligand fragment. We need to see that we must cleave the bond homoleptically to produce that fragment. Cleaving the bond homolopetically means that that ligand has contributed one electron. In the oxidation state method, we cleave the bond always heteroleptically so that all bonding electrons are assigned to the ligand. Thus, the ligand contributes two electrons.

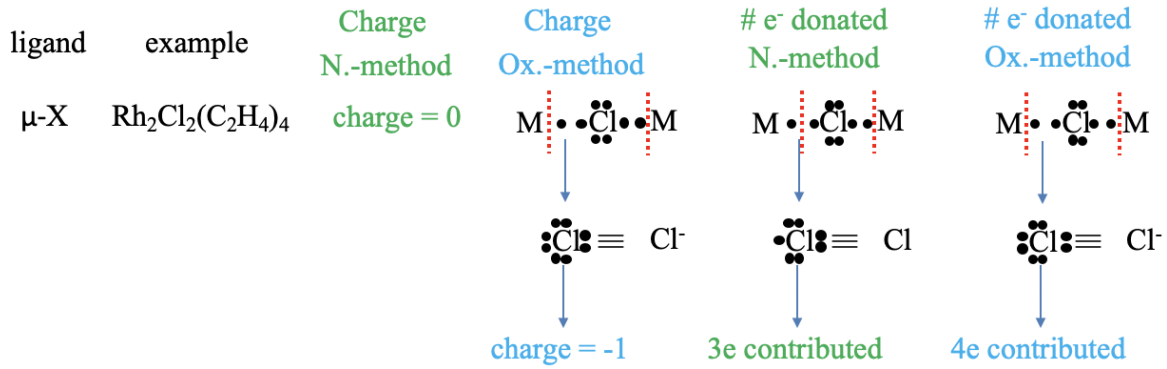


Figure 6.1.5 Example of counting electrons with a bridging halogenide ligand

A halogenide anion as a ligand cannot only be terminal, but bridging. An example is the μ-dichloro bis(tetraethylene rhodium(I)) complex in which two chloro-ligands bridge two rhodium atoms. What is the charge in the neutral atom method. Of course, it is zero. What is the charge in the oxidation state method? We can see that if we consider both metal-ligand bonds dative bonds, and cleave the bonds heteroleptically, that the Cl atom is surrounded by eight unshared electrons, which give it a -1 charge. How, many electrons are contributed in the neutral atom method? To answer this question, we need to decide if we have to cleave the bonds homo- or heteroleptically to produce a neutral Cl atom. Can you see it? The answer is: We must cleave one bond homoleptically, and the other one heteroleptically. How many electrons are then contributed by the chloro ligan? It is the two electrons from the heteroleptically cleaved bond, and one electron from the homoleptically cleaved bond. So overall it is three electrons. What about the oxidation state method? In this case both bonds very cleaved heteroleptically, and this means that overall four electrons have been contributed.

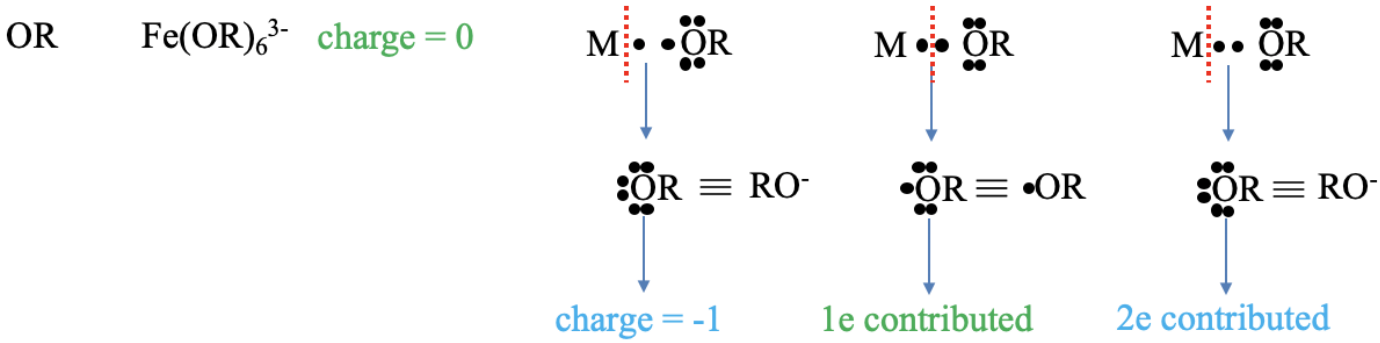


Figure 6.1.6 Example of counting electrons with an OR ligand

What are the charges and electrons contributed by an alkoxy ligand? An example for a complex with such as ligand is pentaphenoxy ferrate (3-). The charge according to the neutral atom method is zero. In the oxidation state method we cleave the bonds heteroleptically, and our ligand becomes an alkoxide anion. This anion has a 1- charge. How many electrons does the ligand contribute? To get a neutral fragment we must cleave the bond homoleptically. This actually produces an alkoxy radical. This radical contributes its radical electron, thus there is one contributed electron. In the oxidation state method we treated the bond as a dative bond and cleaved the bond heteroleptically. Therefore two electrons are contributed according to the oxidation state method.

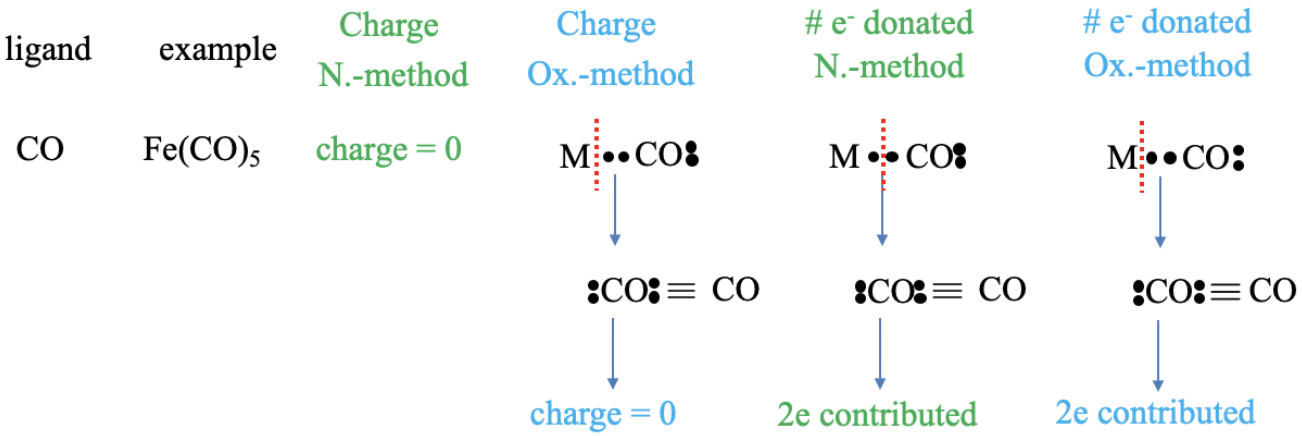


Figure 6.1.7 Example of counting electrons with a carbonyl ligand

Next, let us apply electron counting to the carbonyl ligand. For example four carbon monoxide molecules form an iron pentacarbonyl complex with iron. The charge at the ligand in the neutral atom method is zero. In the oxidation state method, we assign both bonding electrons to the ligand, and that produces a neutral carbon monoxide molecule. Note that the carbon atom is formally negatively charged, because it is surrounded by 5 electrons, but the oxygen atom is positively charged because it is surrounded by five electrons. So overall, the molecule is neutral. What is the number of electrons contributed in the neutral atom method? To produce a neutral ligand we must cleave the bond heteroleptically. This produces a neutral carbon monoxide molecule. Because we cleaved the bond heteroleptically, the ligand contributes two electrons. In the oxidation state method we always cleave the bonds heteroleptically, and thus two electrons come from the ligand.

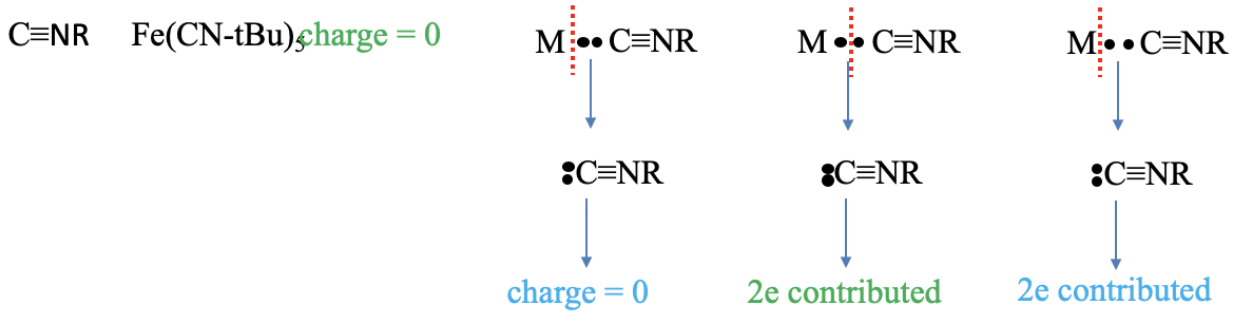


Figure 6.1.8 Example of counting electrons with

The last ligand we discuss here is the isonitrile ligand. An example is the pentakis-(tert-butyl isonitrile) iron molecule. The charge of the ligand is zero in the neutral atom method, but what is it in the oxidation state method? Let us see what happens as we assign both bonding electrons to the ligand. We we see that the carbon is now surrounded by five electrons. Three are in the carbon-nitrogen triple bond and they other two come from the electron lone pair at the carbon atom. This means that the carbon atom has a -1 charge. Now, let us look at the N atom. We see that it is surrounded by four electrons, three coming from the C-N triple bond, and one from the C-R bond. That means that the N atom has a +1 charge. Overall, the molecule is neutral and does not carry a charge. What about the number of electrons contributed? We can see that we must cleave the bond heteroleptically to produce a neutral isoitrile, there are two electrons are contributed in the neutral atom method. The oxidation state method must cleave the bond heteroleptically, therefore, the number of electrons is also two.

18 Electron Rule

Electron counting is important in the context of an important rule in coordination chemistry: The 18 electron rule. The 18 electron rule states that for d-block elements *normally* complexes with 18 electrons in the shell ($ns^2(n-1)d^{10}np^6$ configuration) are most stable. If this number is not reached, the species is **coordinatively unsaturated** and tend to add more ligands. It also tends to be reduced because adding electrons brings the complex to or at least closer to 18 electrons. Coordinatively unsaturated complexes therefore tend to have a higher reactivity.

Definition: Coordinatively Unsaturated

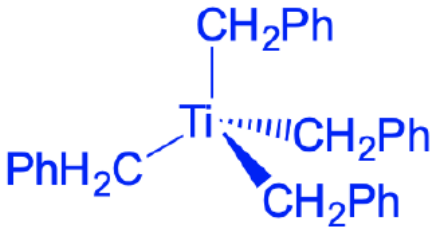
A species is coordinatively unsaturated when the 18 electrons are not reached in the ($ns^2(n-1)d^{10}np^6$ configuration) shell. They tend to add more ligands, and to be reduced. They are associated with higher reactivity.

If a species has more than 18 electrons it is coordinatively oversaturated and tends to lose ligands. It is usually easily oxidized. Both loss of ligands and oxidation reduces to the number of electrons to or at least closer to 18.

Definition: Coordinatively Oversaturated

A species is coordinatively oversaturated when it has more than 18 electrons in the shell ($ns^2(n-1)d^{10}np^6$ configuration) shell. They tend to lose ligands and are easily oxidized.

The 18 electron rule has many exceptions, and therefore needs to be applied with caution. In particular group 3, 4, and 10 complexes deviate often from the 18 electron rule.



Contribution metal:	4e
Oxidation state: +4	-4e
Electrons contributed by ligands:	4x2e=8e
Sum:	**8e**

Figure 6.1.9 Example of counting electrons in the tetrahedral tetrabenzyltitanium(0) complex

For illustration purposes, let count the number of electrons of the tetrahedral tetrabenzyltitanium(0) complex by the oxidation state method. We could also use the neutral atom method, which would give the same results. This complex is a group 4 complex because titanium is in group 4. How many electrons will the titanium contribute? Because number of electrons is always the same as the group number, it will contribute four electrons. Next, what is oxidation state of Ti? To determine it we must determine the charge at the ligands. To do that we cleave the bonds heteroleptically. This will give benzylate anions with -1 charge. There are four of these ions, and therefore there will be four negative charges overall. The complex is charge-neutral, and thus the oxidation state is +4 because -4+4=0. Therefore, we need to subtract four electrons. Because we cleaved the bond heteroleptically, each ligand contributed two electrons, giving overall eight electrons coming from the four ligands. This means that we have overall eight electrons, or an 8-electron complex. This is far, far away from 18 electrons. Nonetheless, the complex is quite stable, does not have a tendency to get reduced, or to add ligands. How can we explain this. The answer is that in order to achieve 18 electrons it would need to add five additional ligands if each ligand is considered a 2-electron donor. This would increase the coordination number to 9 which is too high to produce a stable complex. In order to reduce the complex to an 18 electron complex, 10 electrons would need to be added. This would produce a complex with a -10 charge which is way to high to be stable. The arguments are generalizable for group 3 and group 4 complexes. Because these elements only have a few d electrons, the ligands would contribute a lot of electrons to produce an 18 electrons complex. This would require just too many ligands to add. The coordination numbers would get too high. If electrons are added instead to ligands, the negative charge at the complex would be to high to be stable based on electron-electron repulsion arguments.



Contribution metal:	10e
Charge:	0e
Electrons contributed by Cl ligands:	2x1e=2e
Electrons contributed by NH_3 ligands:	2x2e=4e
Sum:	**16e**

Figure 6.1.10 Example of counting electrons in the dichlorodiammine palladium complex

These arguments cannot be applied for group 10 elements, because these elements have many d electrons. The explanation in this case is that these elements like to make square planar complexes when in the common oxidation state +2. Square planar complexes prefer 16 instead of electrons. You can see that the square planar dichlorodiammine palladium complex shown is square planar and has sixteen electrons. There are 10 electrons coming from Pd. If we use the neutral atom method, no electrons need to be added or subtracted due to the charge at complex. The complex is charge-neutral. To assess how many electrons come from the ligands we need to cleave the bonds so that neutral ligands are produced. The Pd-Cl bonds need to be cleave homoleptically, the Pd-N bonds need to be cleave heteroleptically. Therefore, the two chloro ligands are 1e donors, and the two ammine ligands are 2e donors. This gives 10+4+2=16 electrons

This page titled 13.3: The 18 Electron Rule is shared under a license and was authored, remixed, and/or curated by Kai Landskron.

13.4: Reactions Involving Gain or Loss of Ligands

Chapter 12.1: Reactions Involving Gain or Loss of Ligands

This page titled 13.4: Reactions Involving Gain or Loss of Ligands is shared under a license and was authored, remixed, and/or curated by LibreTexts.

13.5: Organometallic Catalysts

Chapter 12.2: Organometallic Catalysts

This page titled 13.5: Organometallic Catalysts is shared under a license and was authored, remixed, and/or curated by LibreTexts.

14: EXPERIMENTAL TECHNIQUES

14.1: Introduction

14.2: Separation and Purification Techniques

14.2A: Gas Chromatography (GC)

14.2B: Liquid Chromatography (LC)

14.2C: High-Performance Liquid Chromatography (HPLC)

14.2D: Recrystallization

14.3: Elemental Analysis

14.3A: CHN Analysis by Combustion

14.3B: Atomic Absorption Spectroscopy (AAS)

14.4: Computational Analysis - Thermogravimetry (TG)

14.5: Mass Spectrometry

14.5A: Electron Ionization (EI)

14.5B: Fast Atom Bombardment (FAB)

14.5C: Matrix-Assisted Laser Desorption Ionization Time-of-Flight (MALDI-TOF)

14.5D: Electrospray Ionization (ESI)

14.6: Infrared and Raman Spectroscopies

14.6A: Energies and Wavenumbers of Molecular Vibrations

14.6B: The Fourier Transform Infrared (FT-IR) Spectrometer and Sample Preparation

14.6C: Diagnostic Absorptions

14.6D: Deuterium/Hydrogen Exchange

14.6E: Raman Spectroscopy

14.7: Electronic Spectroscopy

14.7A: UV-VIS Absorption Spectroscopy

14.7B: Types of Absorption

14.7C: Absorbance and the Beer-Lambert Law

14.7D: Emission Spectroscopy

14.8: Nuclear Magnetic Resonance (NMR) Spectroscopy

14.8A: NMR Active Nuclei and Isotope Abundance

14.8B: Which Nuclei are Suitable for NMR Spectroscopic Studies

14.8C: Resonance Frequencies and Chemical Shifts

14.8D: Chemical Shift Ranges

14.8E: Solvents for Solution Studies

14.8F: Integration of Signals and Signal Broadening

14.8G: Homonuclear spin-spin coupling - $^{1}H - ^{1}H$

14.8H: Heteronuclear spin-spin coupling - $^{13}C - ^{1}H$

14.8I: Case Studies

14.8J: Stereochemically Non-Rigid Species
14.8K: Exchange Processes in Solution

14.9: Electron Paramagnetic Resonance (EPR) Spectroscopy
14.9A: What is EPR Spectroscopy?
14.9B: The Zeeman Electronic Effect
14.9C: EPR Spectra

14.10: Mossbauer Spectroscopy
14.10A: The Technique of Mossbauer Spectroscopy
14.10B: What Can Isomer Shift Data Tell Us?

14.11: Structure Determination - Diffraction Methods
14.11A: X-Ray Diffraction (XRD)
14.11B: Single Crystal X-Ray Diffraction
14.11C: Powder X-Ray Diffraction
14.11D: Single Crystal Neutron Diffraction
14.11E: Electron Diffraction
14.11F: Low-Energy Electron Diffraction (LEED)
14.11G: Structural Databases

14.12: Photoelectron Spectroscopy (PES, UPS, XPS, ESCA)

14.13: Computational Methods
14.13A: Hartree-Fock Theory
14.13B: Density Functional Theory
14.13C: Hückel MO Theory
14.13D: Molecular Mechanisms (MM)

14.14: Magnetism
14.14.1: example magnetic moment data and their interpretation
14.14.2: Magnetic Moments
14.14.3: Magnetic Moments 1
14.14.4: Magnetic Susceptibility Measurements
14.14.5: Magnetism

This page titled 14: Experimental Techniques is shared under a license and was authored, remixed, and/or curated by LibreTexts.

- 4: Experimental Techniques is licensed CC BY-NC-SA 4.0.

14.1: Introduction

This page titled 14.1: Introduction is shared under a license and was authored, remixed, and/or curated by LibreTexts.

14.2: SEPARATION AND PURIFICATION TECHNIQUES



- Topic hierarchy

14.2A: Gas Chromatography (GC)

14.2B: Liquid Chromatography (LC)

14.2C: High-Performance Liquid Chromatography (HPLC)

14.2D: Recrystallization

This page titled 14.2: Separation and Purification Techniques is shared under a license and was authored, remixed, and/or curated by LibreTexts.

- 4.2: Separation and Purification Techniques is licensed CC BY-NC-SA 4.0.

14.2A: Gas Chromatography (GC)

This page titled 14.2A: Gas Chromatography (GC) is shared under a license and was authored, remixed, and/or curated by LibreTexts.

14.2B: Liquid Chromatography (LC)

This page titled 14.2B: Liquid Chromatography (LC) is shared under a license and was authored, remixed, and/or curated by LibreTexts.

14.2C: High-Performance Liquid Chromatography (HPLC)

This page titled 14.2C: High-Performance Liquid Chromatography (HPLC) is shared under a license and was authored, remixed, and/or curated by LibreTexts.

14.2D: Recrystallization

Recrystallization

This page titled 14.2D: Recrystallization is shared under a license and was authored, remixed, and/or curated by LibreTexts.

14.3: ELEMENTAL ANALYSIS



- Topic hierarchy

14.3A: CHN Analysis by Combustion

14.3B: Atomic Absorption Spectroscopy (AAS)

This page titled 14.3: Elemental Analysis is shared under a license and was authored, remixed, and/or curated by LibreTexts.

- 4.3: Elemental Analysis is licensed CC BY-NC-SA 4.0.

14.3A: CHN Analysis by Combustion

This page titled 14.3A: CHN Analysis by Combustion is shared under a license and was authored, remixed, and/or curated by LibreTexts.

14.3B: Atomic Absorption Spectroscopy (AAS)

Guystav Kirchoff and Robert Bunsen first used atomic absorption spectroscopy—along with atomic emission—in 1859 and 1860 as a means for identify atoms in flames and hot gases. Although atomic emission continued to develop as an analytical technique, progress in atomic absorption languished for almost a century. Modern atomic absorption spectroscopy has its beginnings in 1955 as a result of the independent work of A. C. Walsh and C. T. J. Alkemade.[13] Commercial instruments were in place by the early 1960s, and the importance of atomic absorption as an analytical technique was soon evident.

10.4.1 Instrumentation

Atomic absorption spectrophotometers use the same single-beam or double-beam optics described earlier for molecular absorption spectrophotometers (see Figure 10.26 and Figure 10.27). There is, however, an important additional need in atomic absorption spectroscopy—we must covert the analyte into free atoms. In most cases our analyte is in solution form. If our sample is a solid, then we must bring it into solution before the analysis. When analyzing a lake sediment for Cu, Zn, and Fe, for example, we bring the analytes into solution as Cu^{2+}, Zn^{2+}, and Fe^{3+} by extracting them with a suitable reagent. For this reason, only the introduction of solution samples is considered in this text.

What reagent we choose to use depends on our research goals. If we need to know the total amount of metal in the sediment, then we might use a microwave digestion using a mixture of concentrated acids, such as HNO_3, HCl, and HF. This destroys the sediment's matrix and brings everything into solution. On the other hand, if our interest is biologically available metals, we might extract the sample under milder conditions, such as a dilute solution of HCl or CH_3COOH at room temperature.

Atomization

The process of converting an analyte to a free gaseous atom is called **atomization**. Converting an aqueous analyte into a free atom requires that we strip away the solvent, volatilize the analytes, and, if necessary, dissociate the analyte into free atoms. Desolvating an aqueous solution of $CuCl_2$, for example, leaves us with solid particulates of $CuCl_2$. Converting the particulate $CuCl_2$ to gas phases atoms of Cu and Cl requires thermal energy.

$$\mathrm{CuCl_{2(aq)} \rightarrow CuCl_{2(s)} \rightarrow Cu_{(g)} + 2\,Cl_{(g)}} \tag{14.3B.1}$$

There are two common atomization methods: flame atomization and electrothermal atomization, although a few elements are atomized using other methods.

Flame Atomizer

Figure 10.42 shows a typical flame atomization assembly with close-up views of several key components. In the unit shown here, the aqueous sample is drawn into the assembly by passing a high-pressure stream of compressed air past the end of a capillary tube immersed in the sample. When the sample exits the nebulizer it strikes a glass impact bead, converting it into a fine aerosol mist within the spray chamber. The aerosol mist is swept through the spray chamber by the combustion gases—compressed air and acetylene in this case—to the burner head where the flame's thermal energy desolvates the aerosol mist to a dry aerosol of small, solid particles. The flame's thermal energy then volatilizes the particles, producing a vapor consisting of molecular species, ionic species, and free atoms.

Compressed air is one of the two gases whose combustion produces the flame.

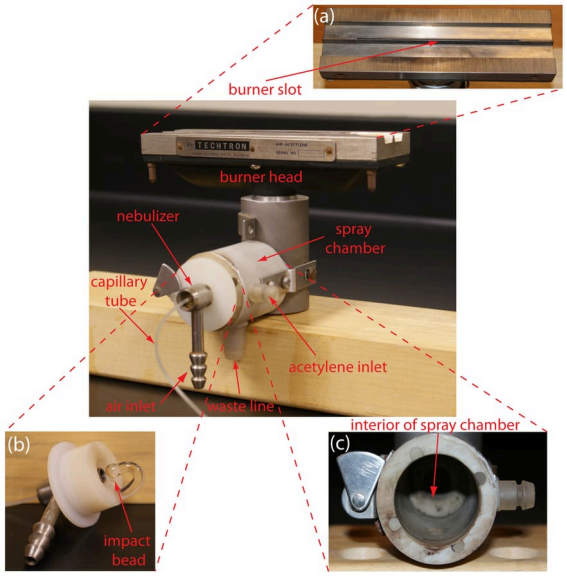


Figure 10.42 *Flame atomization assembly with expanded views of (a) the burner head showing the burner slot where the flame is located; (b) the nebulizer's impact bead; and (c) the interior of the spray chamber. Although the unit shown here is from an older instrument, the basic components of a modern flame AA spectrometer are the same.*

Burner. The slot burner in Figure 10.42a provides a long optical pathlength and a stable flame. Because absorbance increases linearly with the path length, a long path length provides greater sensitivity. A stable flame minimizes uncertainty due to fluctuations in the flame.

The burner is mounted on an adjustable stage that allows the entire assembly to move horizontally and vertically. Horizontal adjustments ensure that the flame is aligned with the instrument's optical path. Vertical adjustments adjust the height within the flame from which absorbance is monitored. This is important because two competing processes affect the concentration of free atoms in the flame. The more time the analyte spends in the flame the greater the atomization efficiency; thus, the production of free atoms increases with height. On the other hand, a longer residence time allows more opportunity for the free atoms to combine with oxygen to form a molecular oxide. For an easily oxidized metal, such as Cr, the concentration of free atoms is greatest just above the burner head. For metals, such as Ag, which are difficult to oxidize, the concentration of free atoms increases steadily with height (Figure 10.43). Other atoms show concentration profiles that maximize at a characteristic height.

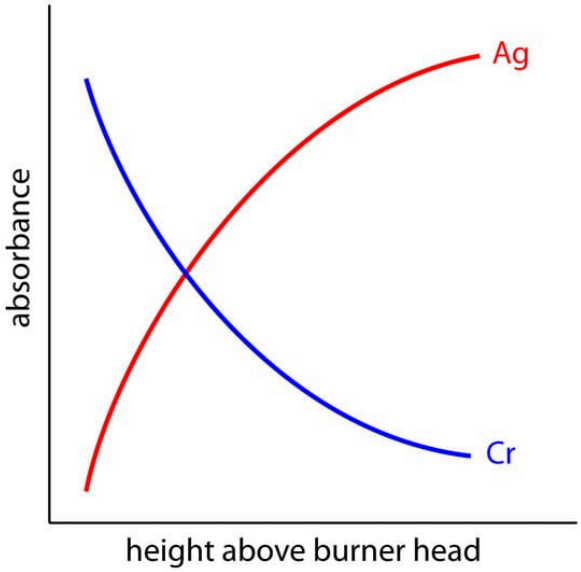


Figure 10.43 *Absorbance versus height profiles for Ag and Cr in flame atomic absorption spectroscopy.*

Flame. The flame's temperature, which affects the efficiency of atomization, depends on the fuel–oxidant mixture, several examples of which are listed in Table 10.9. Of these, the air–acetylene and the nitrous oxide–acetylene flames are the most popular. Normally the fuel and oxidant are mixed in an approximately stoichiometric ratio; however, a fuel-rich mixture may be necessary for easily oxidized analytes.

Table 10.9 *Fuels and Oxidants Used for Flame Combustion*

fuel	oxidant	temperature range (°C)
natural gas	air	1700–1900
hydrogen	air	2000–2100
acetylene	air	2100–2400
acetylene	nitrous oxide	2600–2800
acetylene	oxygen	3050–3150

Figure 10.44 shows a cross-section through the flame, looking down the source radiation's optical path. The primary combustion zone is usually rich in gas combustion products that emit radiation, limiting is usefulness for atomic absorption. The interzonal region generally is rich in free atoms and provides the best location for measuring atomic absorption. The hottest part of the flame is typically 2–3 cm above the primary combustion zone. As atoms approach the flame's secondary combustion zone, the decrease in temperature allows for formation of stable molecular species.

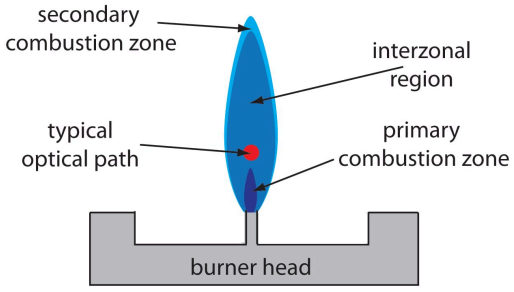


Figure 10.44 *Profile of typical flame using a slot burner. The relative size of each zone depends on many factors, including the choice of fuel and oxidant, and their relative proportions.*

Sample Introduction. The most common means for introducing samples into a flame atomizer is a continuous aspiration in which the sample flows through the burner while we monitor the absorbance. Continuous aspiration is sample intensive, typically requiring from 2–5 mL of sample.

Flame microsampling allows us to introduce a discrete sample of fixed volume, and is useful when we have a limited amount of sample or when the sample's matrix is incompatible with the flame atomizer. For example, continuously aspirating a sample that has a high concentration of dissolved solids—sea water, for example, comes to mind—may build-up a solid deposit on the burner head that obstructs the flame and that lowers the absorbance. Flame microsampling is accomplished using a micropipet to place 50–250 µL of sample in a Teflon funnel connected to the nebulizer, or by dipping the nebulizer tubing into the sample for a short time. Dip sampling is usually accomplished with an automatic sampler. The signal for flame microsampling is a transitory peak whose height or area is proportional to the amount of analyte that is injected.

Advantages and Disadvantages of Flame Atomization. The principal advantage of flame atomization is the reproducibility with which the sample is introduced into the spectrophotometer. A significant disadvantage to flame atomizers is that the efficiency of atomization may be quite poor. There are two reasons for poor atomization efficiency. First, the majority of the aerosol droplets produced during nebulization are too large to be carried to the flame by the combustion gases. Consequently, as much as 95% of the sample never reaches the flame. A second reason for poor atomization efficiency is that the large volume of combustion gases significantly dilutes the sample. Together, these contributions to the efficiency of atomization reduce sensitivity because the analyte's concentration in the flame may be a factor of 2.5×10^{-6} less than that in solution.[14] This is the reason for the waste line shown at the bottom of the spray chamber in Figure 10.42.

Electrothermal Atomizers

A significant improvement in sensitivity is achieved by using the resistive heating of a graphite tube in place of a flame. A typical electrothermal atomizer, also known as a **graphite furnace**, consists of a cylindrical graphite tube approximately 1–3 cm in length and 3–8 mm in diameter. As shown in Figure 10.45, the graphite tube is housed in an sealed assembly that has optically transparent windows at each end. A continuous stream of an inert gas is passed through the furnace, protecting the graphite tube from oxidation and removing the gaseous products produced during atomization. A power supply is used to pass a current through the graphite tube, resulting in resistive heating.

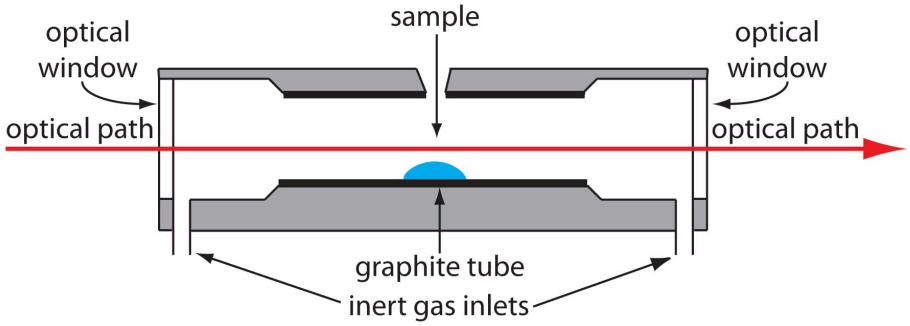


Figure 10.45*: Diagram showing a cross-section of an electrothermal analyzer.*

Samples of between 5–50 µL are injected into the graphite tube through a small hole at the top of the tube. Atomization is achieved in three stages. In the first stage the sample is dried to a solid residue using a current that raises the temperature of the graphite tube to about 110°C. In the second stage, which is called ashing, the temperature is increased to between 350–1200°C. At these temperatures any organic material in the sample is converted to CO_2 and H_2O, and volatile inorganic materials are vaporized. These gases are removed by the inert gas flow. In the final stage the sample is atomized by rapidly increasing the temperature to between 2000–3000°C. The result is a transient absorbance peak whose height or area is proportional to the absolute amount of analyte injected into the graphite tube. Together, the three stages take approximately 45–90 s, with most of this time used for drying and ashing the sample.

Electrothermal atomization provides a significant improvement in sensitivity by trapping the gaseous analyte in the small volume within the graphite tube. The analyte's concentration in the resulting vapor phase may be as much as 1000× greater than in a flame atomization.[15] This improvement in sensitivity—and the resulting improvement in detection limits—is offset by a significant decrease in precision. Atomization efficiency is strongly influenced by the sample's contact with the graphite tube, which is difficult to control reproducibly.

Miscellaneous Atomization Methods

A few elements may be atomized by a chemical reaction that produces a volatile product. Elements such as As, Se, Sb, Bi, Ge, Sn, Te, and Pb, for example, form volatile hydrides when reacted with $NaBH_4$ in acid. An inert gas carries the volatile hydrides to either a flame or to a heated quartz observation tube situated in the optical path. Mercury is determined by the cold-vapor method in which it is reduced to elemental mercury with $SnCl_2$. The volatile Hg is carried by an inert gas to an unheated observation tube situated in the instrument's optical path.

10.4.2 Quantitative Applications

Atomic absorption is widely used for the analysis of trace metals in a variety of sample matrices. Using Zn as an example, atomic absorption methods have been developed for its determination in samples as diverse as water and wastewater, air, blood, urine, muscle tissue, hair, milk, breakfast cereals, shampoos, alloys, industrial plating baths, gasoline, oil, sediments, and rocks.

Developing a quantitative atomic absorption method requires several considerations, including choosing a method of atomization, selecting the wavelength and slit width, preparing the sample for analysis, minimizing spectral and chemical interferences, and selecting a method of standardization. Each of these topics is considered in this section.

Developing a Quantitative Method

Flame or Electrothermal Atomization? The most important factor in choosing a method of atomization is the analyte's concentration. Because of its greater sensitivity, it takes less analyte to achieve a given absorbance when using electrothermal atomization. Table 10.10, which compares the amount of analyte needed to achieve an absorbance of 0.20 when using flame atomization and electrothermal atomization, is useful when selecting an atomization method. For example, flame atomization is the method of choice if our samples contain 1–10 mg Zn^{2+}/L, but electrothermal atomization is the best choice for samples containing 1–10 µg Zn^{2+}/L.

Table 10.10: *Concentration of Analyte Yielding an Absorbance of 0.20*

	Concentration (mg/L)[a]	
element	**flame atomization**	**electrothermal atomization**
Ag	1.5	0.0035
Al	40	0.015
As	40[b]	0.050
Ca	0.8	0.003
Cd	0.6	0.001
Co	2.5	0.021
Cr	2.5	0.0075
Cu	1.5	0.012
Fe	2.5	0.006

	Concentration (mg/L)[a]	
Hg	70[b]	0.52
Mg	0.15	0.00075
Mn	1	0.003
Na	0.3	0.00023
Ni	2	0.024
Pb	5	0.080
Pt	70	0.29
Sn	50[b]	0.023
Zn	0.3	0.00071

[a] Source: Varian Cookbook, SpectraAA Software Version 4.00 Pro.

[b] As: 10 mg/L by hydride vaporization; Hg: 11.5 mg/L by cold-vapor; and Sn:18 mg/L by hydride vaporization

Selecting the Wavelength and Slit Width. The source for atomic absorption is a hollow cathode lamp consisting of a cathode and anode enclosed within a glass tube filled with a low pressure of Ne or Ar (Figure 10.46). Applying a potential across the electrodes ionizes the filler gas. The positively charged gas ions collide with the negatively charged cathode, sputtering atoms from the cathode's surface. Some of the sputtered atoms are in the excited state and emit radiation characteristic of the metal(s) from which the cathode was manufactured. By fashioning the cathode from the metallic analyte, a hollow cathode lamp provides emission lines that correspond to the analyte's absorption spectrum.

Because atomic absorption lines are narrow, we need to use a line source instead of a continuum source (compare, for example, Figure 10.18 with Figure 10.20). The effective bandwidth when using a continuum source is roughly 1000× larger than an atomic absorption line; thus, $P_T \approx P_0$, $\%T \approx 100$, and $A \approx 0$. Because a hollow cathode lamp is a line source, P_T and P_0 have different values giving a $\%T < 100$ and $A > 0$.

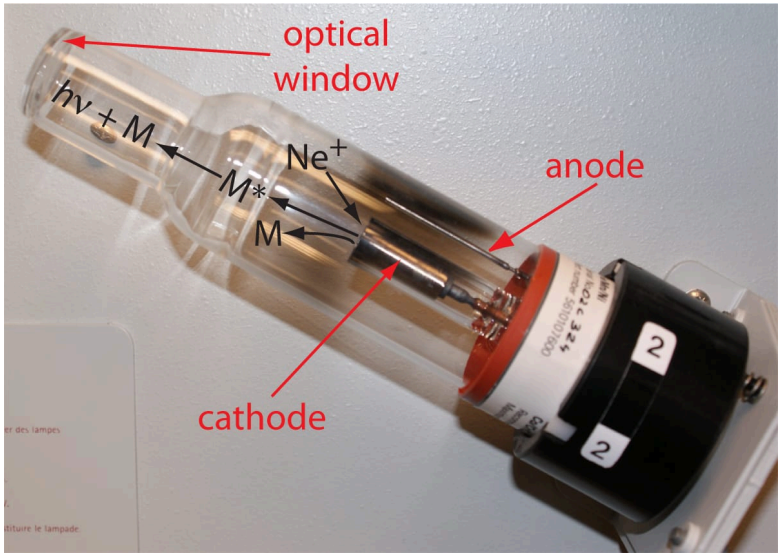


Figure 10.46: *Photo of a typical multielemental hollow cathode lamp. The cathode in this lamp is fashioned from an alloy containing Co, Cr, Cu, Fe, Mn, and Ni, and is surrounded by a glass shield to isolate it from the anode. The lamp is filled with Ne gas. Also shown is the process leading to atomic emission. See the text for an explanation.*

Each element in a hollow cathode lamp provides several atomic emission lines that we can use for atomic absorption. Usually the wavelength that provides the best sensitivity is the one we choose to use, although a less sensitive wavelength may be more appropriate for a larger concentration of analyte. For the Cr hollow cathode lamp in Table 10.11, for example, the best sensitivity is obtained using a wavelength of 357.9 nm.

Another consideration is the intensity of the emission line. If several emission lines meet our need for sensitivity, we may wish to use the emission line with the largest relative P_0 because there is less uncertainty in measuring P_0 and P_T. When analyzing samples containing ≈10 mg Cr/L, for example, the first three wavelengths in Table 10.11 provide an appropriate sensitivity. The wavelengths of 425.5 nm and 429.0 nm, however, have a greater P_0 and will provide less uncertainty in the measured absorbance.

Table 10.11 *Atomic Emission Lines for a Cr Hollow Cathode Lamp*

wavelength (nm)	slit width (nm)	mg Cr/L giving A = 0.20	P_0 (relative)
357.9	0.2	2.5	40
425.4	0.2	12	85
429.0	0.5	20	100
520.5	0.2	1500	15
520.8	0.2	500	20

The emission spectrum from a hollow cathode lamp includes, besides emission lines for the analyte, additional emission lines for impurities present in the metallic cathode and from the filler gas. These additional lines are a source of stray radiation that leads to an instrumental deviation from Beer's law. The monochromator's slit width is set as wide as possible, improving the throughput

of radiation, while, at the same time, being narrow enough to eliminate the stray radiation.

Preparing the Sample. Flame and electrothermal atomization require that the sample be in solution. Solid samples are brought into solution by dissolving in an appropriate solvent. If the sample is not soluble it may be digested, either on a hot-plate or by microwave, using HNO_3, H_2SO_4, or $HClO_4$. Alternatively, we can extract the analyte using a Soxhlet extractor. Liquid samples may be analyzed directly or extracted if the matrix is incompatible with the method of atomization. A serum sample, for instance, is difficult to aspirate when using flame atomization and may produce an unacceptably high background absorbance when using electrothermal atomization. A liquid–liquid extraction using an organic solvent and a chelating agent is frequently used to concentrate analytes. Dilute solutions of Cd^{2+}, Co^{2+}, Cu^{2+}, Fe^{3+}, Pb^{2+}, Ni^{2+}, and Zn^{2+}, for example, can be concentrated by extracting with a solution of ammonium pyrrolidine dithiocarbamate in methyl isobutyl ketone.See Chapter 7 to review different methods for preparing samples for analysis.

Minimizing Spectral Interference. A spectral interference occurs when an analyte's absorption line overlaps with an interferent's absorption line or band. Because they are so narrow, the overlap of two atomic absorption lines is seldom a problem. On the other hand, a molecule's broad absorption band or the scattering of source radiation is a potentially serious spectral interference.

An important consideration when using a flame as an atomization source is its effect on the measured absorbance. Among the products of combustion are molecular species that exhibit broad absorption bands and particulates that scatter radiation from the source. If we fail to compensate for these spectral interference, then the intensity of transmitted radiation decreases. The result is an apparent increase in the sample's absorbance. Fortunately, absorption and scattering of radiation by the flame are corrected by analyzing a blank.

Spectral interferences also occur when components of the sample's matrix other than the analyte react to form molecular species, such as oxides and hydroxides. The resulting absorption and scattering constitutes the sample's background and may present a significant problem, particularly at wavelengths below 300 nm where the scattering of radiation becomes more important. If we know the composition of the sample's matrix, then we can prepare our samples using an identical matrix. In this case the background absorption is the same for both the samples and standards. Alternatively, if the background is due to a known matrix component, then we can add that component in excess to all samples and standards so that the contribution of the naturally occurring interferent is insignificant. Finally, many interferences due to the sample's matrix can be eliminated by increasing the atomization temperature. For example, by switching to a higher temperature flame it may be possible to prevent the formation of interfering oxides and hydroxides.

If the identity of the matrix interference is unknown, or if it is not possible to adjust the flame or furnace conditions to eliminate the interference, then we must find another method to compensate for the background interference. Several methods have been developed to compensate for matrix interferences, and most atomic absorption spectrophotometers include one or more of these methods.

One of the most common methods for **background correction** is to use a continuum source, such as a D_2 lamp. Because a D_2 lamp is a continuum source, absorbance of its radiation by the analyte's narrow absorption line is negligible. Only the background, therefore, absorbs radiation from the D_2 lamp. Both the analyte and the background, on the other hand, absorb the hollow cathode's radiation. Subtracting the absorbance for the D_2 lamp from that for the hollow cathode lamp gives a corrected absorbance that compensates for the background interference. Although this method of background correction may be quite effective, it does assume that the background absorbance is constant over the range of wavelengths passed by the monochromator. If this is not true, subtracting the two absorbances may underestimate or overestimate the background.

> Other methods of background correction have been developed, including Zeeman effect background correction and Smith–Hieftje background correction, both of which are included in some commercially available atomic absorption spectrophotometers. Consult the chapter's additional resources for additional information.

Minimizing Chemical Interferences. The quantitative analysis of some elements is complicated by chemical interferences occurring during atomization. The two most common chemical interferences are the formation of nonvolatile compounds containing the analyte and ionization of the analyte.

One example of the formation of nonvolatile compounds is the effect of PO_4^{3-} or Al^{3+} on the flame atomic absorption analysis of Ca^{2+}. In one study, for example, adding 100 ppm Al^{3+} to a solution of 5 ppm Ca^{2+} decreased the calcium ion's absorbance

from 0.50 to 0.14, while adding 500 ppm PO_4^{3-} to a similar solution of Ca^{2+} decreased the absorbance from 0.50 to 0.38. These interferences were attributed to the formation of nonvolatile particles of $Ca_3(PO_4)_2$ and an Al–Ca–O oxide.[16]

When using flame atomization, we can minimize the formation of nonvolatile compounds by increasing the flame's temperature, either by changing the fuel-to-oxidant ratio or by switching to a different combination of fuel and oxidant. Another approach is to add a releasing agent or a protecting agent to the samples. A **releasing agent** is a species that reacts with the interferent, releasing the analyte during atomization. Adding Sr^{2+} or La^{3+} to solutions of Ca^{2+}, for example, minimizes the effect of PO_4^{3-} and Al^{3+} by reacting in place of the analyte. Thus, adding 2000 ppm $SrCl_2$ to the Ca^{2+}/PO_4^{3-} and Ca^{2+}/Al^{3+} mixtures described in the previous paragraph increased the absorbance to 0.48. A **protecting agent** reacts with the analyte to form a stable volatile complex. Adding 1% w/w EDTA to the Ca^{2+}/PO_4^{3-} solution described in the previous paragraph increased the absorbance to 0.52.

Ionization interferences occur when thermal energy from the flame or the electrothermal atomizer is sufficient to ionize the analyte

$$\mathrm{M}_{(g)} \overset{\Delta}{\rightleftharpoons} \mathrm{M}^{+}_{(g)} + e^{-} \tag{10.24}$$

where M is the analyte. Because the absorption spectra for M and M^+ are different, the position of the equilibrium in reaction 10.24 affects absorbance at wavelengths where M absorbs. To limit ionization we add a high concentration of an **ionization suppressor**, which is simply a species that ionizes more easily than the analyte. If the concentration of the ionization suppressor is sufficient, then the increased concentration of electrons in the flame pushes reaction 10.24 to the left, preventing the analyte's ionization. Potassium and cesium are frequently used as an ionization suppressor because of their low ionization energy.

Standardizing the Method. Because Beer's law also applies to atomic absorption, we might expect atomic absorption calibration curves to be linear. In practice, however, most atomic absorption calibration curves are nonlinear, or linear for only a limited range of concentrations. Nonlinearity in atomic absorption is a consequence of instrumental limitations, including stray radiation from the hollow cathode lamp and the variation in molar absorptivity across the absorption line. Accurate quantitative work, therefore, often requires a suitable means for computing the calibration curve from a set of standards.

Most instruments include several different algorithms for computing the calibration curve. The instrument in my lab, for example, includes five algorithms. Three of the algorithms fit absorbance data using linear, quadratic, or cubic polynomial functions of the analyte's concentration. It also includes two algorithms that fit the concentrations of the standards to quadratic functions of the absorbance.

When possible, a quantitative analysis is best conducted using external standards. Unfortunately, matrix interferences are a frequent problem, particularly when using electrothermal atomization. For this reason the method of standard additions is often used. One limitation to this method of standardization, however, is the requirement that there be a linear relationship between absorbance and concentration.

The best way to appreciate the theoretical and practical details discussed in this section is to carefully examine a typical analytical method. Although each method is unique, the following description of the determination of Cu and Zn in biological tissues provides an instructive example of a typical procedure. The description here is based on Bhattacharya, S. K.; Goodwin, T. G.; Crawford, A. J. *Anal. Lett.* **1984**, *17*, 1567–1593, and Crawford, A. J.; Bhattacharya, S. K. Varian Instruments at Work, Number AA–46, April 1985.

Representative Method 10.2: Determination of Cu and Zn in Tissue Samples

Description of Method

Copper and zinc are isolated from tissue samples by digesting the sample with HNO_3 after first removing any fatty tissue. The concentration of copper and zinc in the supernatant are determined by atomic absorption using an air-acetylene flame.

Procedure

Tissue samples are obtained by a muscle needle biopsy and dried for 24–30 h at 105°C to remove all traces of moisture. The fatty tissue in the dried samples is removed by extracting overnight with anhydrous ether. After removing the ether, the sample is dried to obtain the fat-free dry tissue weight (FFDT). The sample is digested at 68°C for 20–24 h using 3 mL of 0.75 M HNO_3. After centrifuging at 2500 rpm for 10 minutes, the supernatant is transferred to a 5-mL volumetric flask. The digestion is repeated two more times, for 2–4 hours each, using 0.9-mL aliquots of 0.75 M HNO_3. These supernatants are added to the 5-mL volumetric flask, which is diluted to volume with 0.75 M HNO_3. The concentrations of Cu and Zn in the diluted supernatant are determined by flame atomic absorption spectroscopy using an air-acetylene flame and external standards. Copper is analyzed at a wavelength of 324.8 nm with a slit width of 0.5 nm, and zinc is analyzed at 213.9 nm with a slit width of 1.0 nm. Background correction using a D_2 lamp is necessary for zinc. Results are reported as mg of Cu or Zn per gram of FFDT.

Questions

1. Describe the appropriate matrix for the external standards and for the blank?

The matrix for the standards and the blank should match the matrix of the samples; thus, an appropriate matrix is 0.75 M HNO_3. Any interferences from other components of the sample matrix are minimized by background correction.

2. Why is a background correction necessary for the analysis of Zn, but not for the analysis of Cu?

Background correction compensates for background absorption and scattering due to interferents in the sample. Such interferences are most severe when using a wavelength less than 300 nm. This is the case for Zn, but not for Cu.

3. A Cu hollow cathode lamp has several emission lines. Explain why this method uses the line at 324.8 nm.

wavelength (nm)	slit width (nm)	mg Cu/L for A = 0.20	P_0 (relative)
217.9	0.2	15	3
218.2	0.2	15	3
222.6	0.2	60	5
244.2	0.2	400	15
249.2	0.5	200	24
324.8	0.5	1.5	100
327.4	0.5	3	87

With 1.5 mg Cu/L giving an absorbance of 0.20, the emission line at 324.8 nm has the best sensitivity. In addition, it is the most intense emission line, which decreases the uncertainty in the measured absorbance.

Example 10.10

To evaluate the method described in Representative Method 10.2, a series of external standard is prepared and analyzed, providing the results shown here.[17]

µg Cu/mL	absorbance	µg Cu/mL	absorbance
0.000	0.000	0.500	0.033
0.100	0.006	0.600	0.039
0.200	0.013	0.700	0.046
0.300	0.020	1.000	0.066
0.400	0.026		

A bovine liver standard reference material was used to evaluate the method's accuracy. After drying and extracting the sample, a 11.23-mg FFDT tissue sample gives an absorbance of 0.023. Report the amount of copper in the sample as µg Cu/g FFDT.

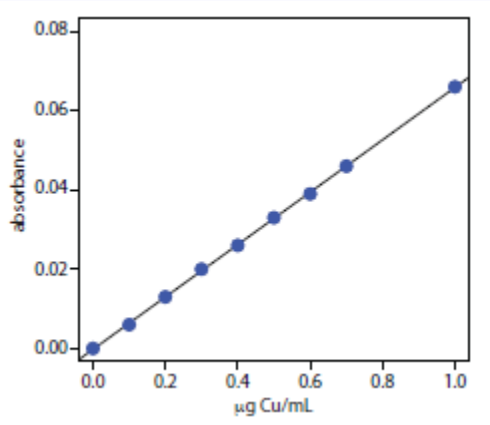
Solution

Linear regression of absorbance versus the concentration of Cu in the standards gives a calibration curve with the following equation.

$$A = -0.0002 + 0.0661 \times \frac{\text{g Cu}}{\text{mL}} \tag{14.3B.2}$$

Substituting the sample's absorbance into the calibration equation gives the concentration of copper as 0.351 µg/mL. The concentration of copper in the tissue sample, therefore, is

$$\frac{\dfrac{0.351\ \text{g Cu}}{\text{mL}} \times 5.000\ \text{mL}}{0.01123\ \text{g sample}} = 156\ \text{g Cu/g FFDT} \tag{14.3B.3}$$



10.4.3 - Evaluation of Atomic Absorption Spectroscopy

Scale of Operation

Atomic absorption spectroscopy is ideally suited for the analysis of trace and ultratrace analytes, particularly when using electrothermal atomization. For minor and major analyte, sample can be diluted before the analysis. Most analyses use a macro or a meso sample. The small volume requirement for electrothermal atomization or flame microsampling, however, makes practical the analysis micro and ultramicro samples.

> See Figure 3.5 to review the meaning of macro and meso for describing samples, and the meaning of major, minor, and ultratrace for describing analytes.

Accuracy

If spectral and chemical interferences are minimized, an accuracy of 0.5–5% is routinely attainable. When the calibration curve is nonlinear, accuracy may be improved by using a pair of standards whose absorbances closely bracket the sample's absorbance and assuming that the change in absorbance is linear over this limited concentration range. Determinate errors for electrothermal atomization are often greater than that obtained with flame atomization due to more serious matrix interferences.

Precision

For absorbance values greater than 0.1–0.2, the relative standard deviation for atomic absorption is 0.3–1% for flame atomization and 1–5% for electrothermal atomization. The principle limitation is the variation in the concentration of free analyte atoms resulting from variations in the rate of aspiration, nebulization, and atomization when using a flame atomizer, and the consistency of injecting samples when using electrothermal atomization.

Sensitivity

The sensitivity of a flame atomic absorption analysis is influenced strongly by the flame's composition and by the position in the flame from which we monitor the absorbance. Normally the sensitivity of an analysis is optimized by aspirating a standard solution of the analyte and adjusting operating conditions, such as the fuel-to-oxidant ratio, the nebulizer flow rate, and the height of the burner, to give the greatest absorbance. With electrothermal atomization, sensitivity is influenced by the drying and ashing stages that precede atomization. The temperature and time used for each stage must be optimized for each type of sample.

> See Chapter 14 for several strategies for optimizing experiments.

Sensitivity is also influenced by the sample's matrix. We have already noted, for example, that sensitivity can be decreased by chemical interferences. An increase in sensitivity may be realized by adding a low molecular weight alcohol, ester, or ketone to the solution, or by using an organic solvent.

Selectivity

Due to the narrow width of absorption lines, atomic absorption provides excellent selectivity. Atomic absorption can be used for the analysis of over 60 elements at concentrations at or below the level of μg/L.

Time, Cost, and Equipment

The analysis time when using flame atomization is short, with sample throughputs of 250–350 determinations per hour when using a fully automated system. Electrothermal atomization requires substantially more time per analysis, with maximum sample throughputs of 20–30 determinations per hour. The cost of a new instrument ranges from between $10,000–$50,000 for flame atomization, and from $18,000–$70,000 for electrothermal atomization. The more expensive instruments in each price range

include double-beam optics, automatic samplers, and can be programmed for multielemental analysis by allowing the wavelength and hollow cathode lamp to be changed automatically.

Contributors

David Harvey (DePauw University)

This page titled 14.3B: Atomic Absorption Spectroscopy (AAS) is shared under a license and was authored, remixed, and/or curated by LibreTexts.

14.4: Computational Analysis - Thermogravimetry (TG)

- Topic hierarchy

This page titled 14.4: Computational Analysis - Thermogravimetry (TG) is shared under a license and was authored, remixed, and/or curated by LibreTexts.

- 4.4: Computational Analysis - Thermogravimetry (TG) is licensed CC BY-NC-SA 4.0.

14.5: MASS SPECTROMETRY



- Topic hierarchy

14.5A: Electron Ionization (EI)

14.5B: Fast Atom Bombardment (FAB)

14.5C: Matrix-Assisted Laser Desorption Ionization Time-of-Flight (MALDI-TOF)

14.5D: Electrospray Ionization (ESI)

This page titled 14.5: Mass Spectrometry is shared under a license and was authored, remixed, and/or curated by LibreTexts.

- 4.5: Mass Spectrometry is licensed CC BY-NC-SA 4.0.

14.5A: Electron Ionization (EI)

This page titled 14.5A: Electron Ionization (EI) is shared under a license and was authored, remixed, and/or curated by LibreTexts.

14.5B: Fast Atom Bombardment (FAB)

This page titled 14.5B: Fast Atom Bombardment (FAB) is shared under a license and was authored, remixed, and/or curated by LibreTexts.

14.5C: Matrix-Assisted Laser Desorption Ionization Time-of-Flight (MALDI-TOF)

This page titled 14.5C: Matrix-Assisted Laser Desorption Ionization Time-of-Flight (MALDI-TOF) is shared under a license and was authored, remixed, and/or curated by LibreTexts.

14.5D: Electrospray Ionization (ESI)

This page titled 14.5D: Electrospray Ionization (ESI) is shared under a license and was authored, remixed, and/or curated by LibreTexts.

14.6: INFRARED AND RAMAN SPECTROSCOPIES



- Topic hierarchy

14.6A: Energies and Wavenumbers of Molecular Vibrations

14.6B: The Fourier Transform Infrared (FT-IR) Spectrometer and Sample Preparation

14.6C: Diagnostic Absorptions

14.6D: Deuterium/Hydrogen Exchange

14.6E: Raman Spectroscopy

This page titled 14.6: Infrared and Raman Spectroscopies is shared under a license and was authored, remixed, and/or curated by LibreTexts.

- 4.6: Infrared and Raman Spectroscopies is licensed CC BY-NC-SA 4.0.

14.6A: Energies and Wavenumbers of Molecular Vibrations

This page titled 14.6A: Energies and Wavenumbers of Molecular Vibrations is shared under a license and was authored, remixed, and/or curated by LibreTexts.

14.6B: The Fourier Transform Infrared (FT-IR) Spectrometer and Sample Preparation

This page titled 14.6B: The Fourier Transform Infrared (FT-IR) Spectrometer and Sample Preparation is shared under a license and was authored, remixed, and/or curated by LibreTexts.

14.6C: Diagnostic Absorptions

This page titled 14.6C: Diagnostic Absorptions is shared under a license and was authored, remixed, and/or curated by LibreTexts.

14.6D: Deuterium/Hydrogen Exchange

This page titled 14.6D: Deuterium/Hydrogen Exchange is shared under a license and was authored, remixed, and/or curated by LibreTexts.

14.6E: Raman Spectroscopy

This page titled 14.6E: Raman Spectroscopy is shared under a license and was authored, remixed, and/or curated by LibreTexts.

14.7: ELECTRONIC SPECTROSCOPY



- Topic hierarchy

14.7A: UV-VIS Absorption Spectroscopy

14.7B: Types of Absorption

14.7C: Absorbance and the Beer-Lambert Law

14.7D: Emission Spectroscopy

This page titled 14.7: Electronic Spectroscopy is shared under a license and was authored, remixed, and/or curated by LibreTexts.

- 4.7: Electronic Spectroscopy is licensed CC BY-NC-SA 4.0.

14.7A: UV-VIS Absorption Spectroscopy

This page titled 14.7A: UV-VIS Absorption Spectroscopy is shared under a license and was authored, remixed, and/or curated by LibreTexts.

14.7B: Types of Absorption

This page titled 14.7B: Types of Absorption is shared under a license and was authored, remixed, and/or curated by LibreTexts.

14.7C: Absorbance and the Beer-Lambert Law

This page titled 14.7C: Absorbance and the Beer-Lambert Law is shared under a license and was authored, remixed, and/or curated by LibreTexts.

14.7D: Emission Spectroscopy

This page titled 14.7D: Emission Spectroscopy is shared under a license and was authored, remixed, and/or curated by LibreTexts.

14.8: NUCLEAR MAGNETIC RESONANCE (NMR) SPECTROSCOPY

- Topic hierarchy

14.8A: NMR Active Nuclei and Isotope Abundance

14.8B: Which Nuclei are Suitable for NMR Spectroscopic Studies

14.8C: Resonance Frequencies and Chemical Shifts

14.8D: Chemical Shift Ranges

14.8E: Solvents for Solution Studies

14.8F: Integration of Signals and Signal Broadening

14.8G: Homonuclear spin-spin coupling - $^{1}H - ^{1}H$

14.8H: Heteronuclear spin-spin coupling - $^{13}C - ^{1}H$

14.8I: Case Studies

14.8J: Stereochemically Non-Rigid Species

14.8K: Exchange Processes in Solution

This page titled 14.8: Nuclear Magnetic Resonance (NMR) Spectroscopy is shared under a license and was authored, remixed, and/or curated by LibreTexts.

- 4.8: Nuclear Magnetic Resonance (NMR) Spectroscopy is licensed CC BY-NC-SA 4.0.

14.8A: NMR Active Nuclei and Isotope Abundance

This page titled 14.8A: NMR Active Nuclei and Isotope Abundance is shared under a license and was authored, remixed, and/or curated by LibreTexts.

14.8B: Which Nuclei are Suitable for NMR Spectroscopic Studies

This page titled 14.8B: Which Nuclei are Suitable for NMR Spectroscopic Studies is shared under a license and was authored, remixed, and/or curated by LibreTexts.

14.8C: Resonance Frequencies and Chemical Shifts

This page titled 14.8C: Resonance Frequencies and Chemical Shifts is shared under a license and was authored, remixed, and/or curated by LibreTexts.

14.8D: Chemical Shift Ranges

This page titled 14.8D: Chemical Shift Ranges is shared under a license and was authored, remixed, and/or curated by LibreTexts.

14.8E: Solvents for Solution Studies

This page titled 14.8E: Solvents for Solution Studies is shared under a license and was authored, remixed, and/or curated by LibreTexts.

14.8F: Integration of Signals and Signal Broadening

This page titled 14.8F: Integration of Signals and Signal Broadening is shared under a license and was authored, remixed, and/or curated by LibreTexts.

14.8G: Homonuclear spin-spin coupling - ^1H $-^1H$

This page titled 14.8G: Homonuclear spin-spin coupling - \(^1H-^1H\) is shared under a license and was authored, remixed, and/or curated by LibreTexts.

14.8H: Heteronuclear spin-spin coupling - ^{13}C $-^{1}$ H

This page titled 14.8H: Heteronuclear spin-spin coupling - \(^{13}C-^1H\) is shared under a license and was authored, remixed, and/or curated by LibreTexts.

14.8I: Case Studies

This page titled 14.8I: Case Studies is shared under a license and was authored, remixed, and/or curated by LibreTexts.

14.8J: Stereochemically Non-Rigid Species

This page titled 14.8J: Stereochemically Non-Rigid Species is shared under a license and was authored, remixed, and/or curated by LibreTexts.

14.8K: Exchange Processes in Solution

This page titled 14.8K: Exchange Processes in Solution is shared under a license and was authored, remixed, and/or curated by LibreTexts.

14.9: ELECTRON PARAMAGNETIC RESONANCE (EPR) SPECTROSCOPY

- Topic hierarchy

14.9A: What is EPR Spectroscopy?

14.9B: The Zeeman Electronic Effect

14.9C: EPR Spectra

This page titled 14.9: Electron Paramagnetic Resonance (EPR) Spectroscopy is shared under a license and was authored, remixed, and/or curated by LibreTexts.

- 4.9: Electron Paramagnetic Resonance (EPR) Spectroscopy is licensed CC BY-NC-SA 4.0.

14.9A: What is EPR Spectroscopy?

This page titled 14.9A: What is EPR Spectroscopy? is shared under a license and was authored, remixed, and/or curated by LibreTexts.

14.9B: The Zeeman Electronic Effect

Magnetism results from the circular motion of charged particles. This property is demonstrated on a macroscopic scale by making an electromagnet from a coil of wire and a battery. Electrons moving through the coil produce a magnetic field (Figure $14.9B.1$), which can be thought of as originating from a magnetic dipole or a bar magnet.

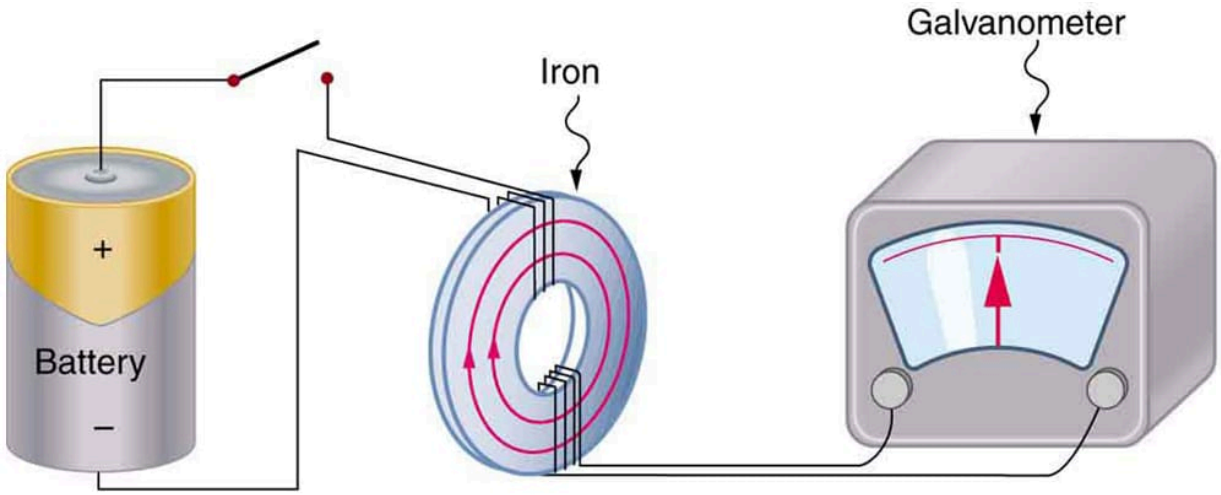


Figure $14.9B.1$: Faraday's apparatus for demonstrating that a magnetic field can produce a current. A change in the field produced by the top coil induces an emf and, hence, a current in the bottom coil. When the switch is opened and closed, the galvanometer registers currents in opposite directions. No current flows through the galvanometer when the switch remains closed or open. (CC BY 3.0; OpenStax).

Magnetism results from the circular motion of charged particles.

Electrons in atoms also are moving charges with angular momentum so they too produce a magnetic dipole, which is why some materials are magnetic. A magnetic dipole interacts with an applied magnetic field, and the energy of this interaction is given by the scalar product of the magnetic dipole moment, and the magnetic field, $\vec{B}$.

$$E_B = -\vec{\mu}_m \cdot \vec{B} \tag{14.9B.1}$$

Magnets are acted on by forces and torques when placed within an external applied magnetic field (Figure $14.9B.2$). In a uniform external field, a magnet experiences no net force, but a net torque. The torque tries to align the magnetic moment ($\vec{\mu}_m$ of the magnet with the external field $\vec{B}$. The magnetic moment of a magnet points from its south pole to its north pole.

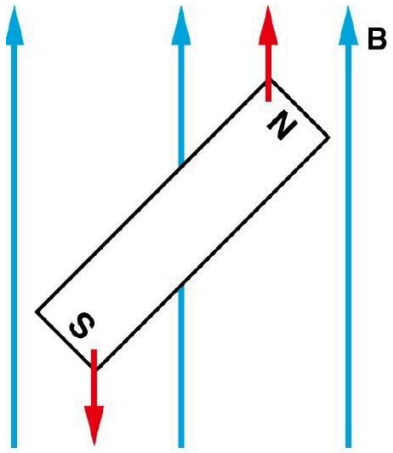


Figure $14.9B.2$: A magnet will feel a force to realign in an external field, i.e., go from a higher energy to a lower energy. The energy of this system is determined by Equation $14.9B.1$ and classical can vary since the angle between $\vec{\mu}_m$ and $\vec{B}$ can vary continuously from 0 (low energy) to 180° (high energy).

In a non-uniform magnetic field a current loop, and therefore a magnet, experiences a net force, which tries to pull an aligned dipole into regions where the magnitude of the magnetic field is larger and push an anti-aligned dipole into regions where magnitude the magnetic field is smaller.

Quantum Effects

As expected, the quantum picture is different. Pieter Zeeman was one of the first to observe the splittings of spectral lines in a magnetic field caused by this interaction. Consequently, such splittings are known as the **Zeeman effect**. Let's now use our current knowledge to predict what the Zeeman effect for the 2p to 1s transition in hydrogen would look like, and then compare this prediction with a more complete theory. To understand the Zeeman effect, which uses a magnetic field to remove the degeneracy of different angular momentum states, we need to examine how an electron in a hydrogen atom interacts with an external magnetic field, $\vec{B}$. Since magnetism results from the circular motion of charged particles, we should look for a relationship between the angular momentum $\vec{L}$ and the magnetic dipole moment $\vec{\mu}_m$.

The relationship between the magnetic dipole moment $\vec{\mu}_m$ (also referred to simply as the magnetic moment) and the angular momentum $\vec{L}$ of a particle with mass m and charge q is given by

$$\vec{\mu}_m = \frac{q}{2m}\vec{L} \tag{14.9B.2}$$

For an electron, this equation becomes

$$\vec{\mu}_m = -\frac{e}{2m_e}\vec{L} \tag{14.9B.3}$$

where the specific charge and mass of the electron have been substituted for q and m. The magnetic moment for the electron is a vector pointing in the direction opposite to $\vec{L}$, both of which classically are perpendicular to the plane of the rotational motion.

Exercise $14.9B.1$

Will an electron in the ground state of hydrogen have a magnetic moment? Why or why not?

The relationship between the angular momentum of a particle and its magnetic moment is commonly expressed as a ratio, called the gyromagnetic ratio, γ. Gyro is Greek for turn so gyromagnetic simply relates turning (angular momentum) to magnetism. Now you also know why the Greek sandwiches made with meat cut from a spit turning over a fire are called gyros.

$$\gamma = \frac{\mu_m}{L} = \frac{q}{2m} \tag{14.9B.4}$$

In the specific case of an electron,

$$\gamma_e = -\frac{e}{2m_e} \tag{14.9B.5}$$

Exercise $14.9B.2$

Calculate the magnitude of the gyromagnetic ratio for an electron.

To determine the energy of a hydrogen atom in a magnetic field we need to include the operator form of the hydrogen atom Hamiltonian. The Hamiltonian always consists of all the energy terms that are relevant to the problem at hand.

$$\hat{H} = \hat{H}^0 + \hat{H}_m \tag{14.9B.6}$$

where $\hat{H}^0$ is the Hamiltonian operator in the absence of the field and $\hat{H}_m$ is written using the operator forms of Equations 14.9B.1 and 14.9B.3),

$$\hat{H}_m = -\hat{\mu}\cdot\vec{B} = \frac{e}{2m_e}\hat{L}\cdot B \tag{14.9B.7}$$

The scalar product

$$\hat{L} \cdot \vec{B} = \hat{L}_x B_x + \hat{L}_y B_y + \hat{L}_z B_z \tag{14.9B.8}$$

simplifies if the z-axis is defined as the direction of the external field because then B_x and B_y are automatically 0, and Equation 14.9B.6 becomes

$$\hat{H} = \hat{H}^0 + \frac{eB_z}{2m_e}\hat{L}_z \tag{14.9B.9}$$

where B_z is the magnitude of the magnetic field, which is along the z-axis.

We now can ask, "What is the effect of a magnetic field on the energy of the hydrogen atom orbitals?" To answer this question, we will not solve the Schrödinger equation again; we simply calculate the expectation value of the energy, $\langle E \rangle$, using the existing hydrogen atom wavefunctions and the new Hamiltonian operator.

$$\langle E \rangle = \left\langle \hat{H}^0 \right\rangle + \frac{eB_z}{2m_e}\left\langle \hat{L}_z \right\rangle \tag{14.9B.10}$$

where

$$\left\langle \hat{H}^0 \right\rangle = \int \psi^*_{n,l,m_l} \hat{H}^0 \psi_{n,l,m_l} d\tau = E_n \tag{14.9B.11}$$

and

$$\left\langle \hat{L}_z \right\rangle = \int \psi^*_{n,l,m_l} \hat{L}_z \psi_{n,l,m_l} d\tau = m_l \hbar \tag{14.9B.12}$$

Exercise 14.9B.3

Show that the expectation value $\left\langle \hat{L}_z \right\rangle = m_l \hbar$.

The expectation value approach provides an exact result in this case because the hydrogen atom wavefunctions are eigenfunctions of both $\hat{H}^0$ and $\hat{L}_z$. If the wavefunctions were not eigenfunctions of the operator associated with the magnetic field, then this approach would provide a first-order estimate of the energy. First and higher order estimates of the energy are part of a general approach to developing approximate solutions to the Schrödinger equation. This approach, called perturbation theory, is discussed in the next chapter.

The expectation value calculated for the total energy in this case is the sum of the energy in the absence of the field, E_n, plus the Zeeman energy, $\frac{e\hbar B_z m_l}{2m_e}$

$$\langle E \rangle = E_n + \frac{e\hbar B_z m_l}{2m_e} \tag{14.9B.13}$$

$$= E_n + \mu_B B_z m_l \tag{14.9B.14}$$

The factor

$$\frac{e\hbar}{2m_e} = -\gamma_e \hbar = \mu_B \tag{14.9B.15}$$

defines the constant μ_B, called the **Bohr magneton**, which is taken to be the fundamental magnetic moment. It has units of 9.2732×10^{-21} erg/Gauss or 9.2732×10^{-24} Joule/Tesla. This factor will help you to relate magnetic fields, measured in Gauss or Tesla, to energies, measured in ergs or Joules, for any particle with a charge and mass the same as an electron.

Equation 14.9B.14 shows that the m_l quantum number degeneracy of the hydrogen atom is removed by the magnetic field. For example, the three states ψ_{211}, ψ_{21-1}, and ψ_{210}, which are degenerate in zero field, have different energies in a magnetic field, as shown in Figure 14.9B.3.

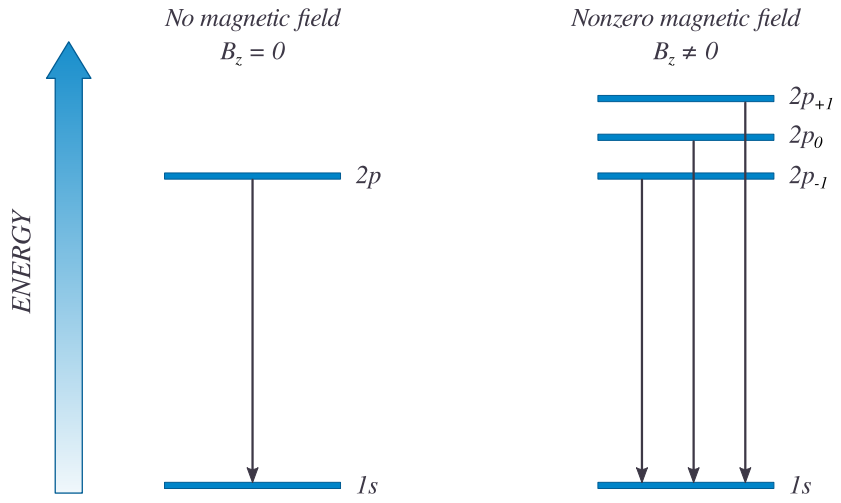


Figure $14.9B.3$: The Zeeman effect. Emission when an electron switches from a 2p orbital to a 1s orbital occurs at only one energy in the absence of a magnetic field, but can occur at three different energies in the presence of a magnetic field.

The $m_l = 0$ state, for which the component of angular momentum and hence also the magnetic moment in the external field direction is zero, experiences no interaction with the magnetic field. The $m_l = +1$ state, for which the angular momentum in the z-direction is +ħ and the magnetic moment is in the opposite direction, against the field, experiences a raising of energy in the presence of a field. Maintaining the magnetic dipole against the external field direction is like holding a small bar magnet with its poles aligned exactly opposite to the poles of a large magnet (Figure $14.9B.5$). It is a higher energy situation than when the magnetic moments are aligned with each other.

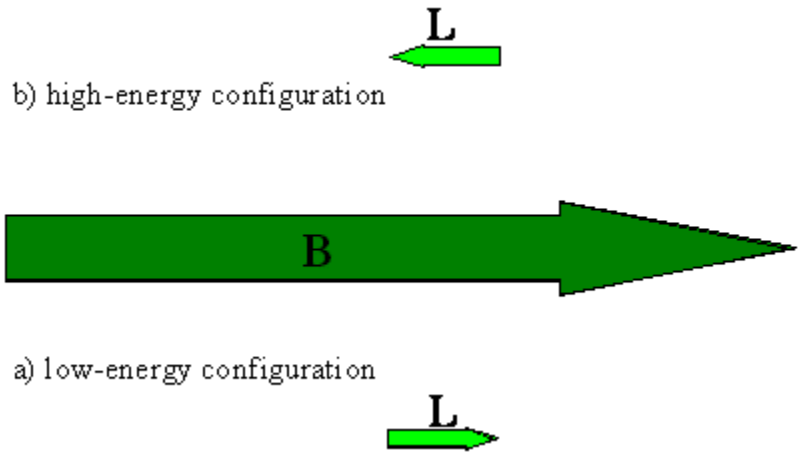


Figure $14.9B.4$: The effect of an external magnetic field (B) on the energy of a magnetic dipole (L) oriented a) with and b) against the applied magnetic field.

Exercise $14.9B.4$

Carry out the steps going from Equation 14.9B.10 to Equation 14.9B.14.

Exercise $14.9B.5$

Consider the effect of changing the magnetic field on the magnitude of the Zeeman splitting. Sketch a diagram where the magnetic field strength is on the x-axis and the energy of the three 2p orbitals is on the y-axis to show the trend in splitting magnitudes with increasing magnetic field. Be quantitative, calculate and plot the exact numerical values using a software package of your choice.

Exercise $14.9B.6$

Based on your calculations in Exercise $14.9B.2$ sketch a luminescence spectrum for the hydrogen atom in the n = 2 level in a magnetic field of 1 Tesla. Provide the numerical value for each of the transition energies. Use cm^{-1} or electron volts for the energy units.

This page titled 14.9B: The Zeeman Electronic Effect is shared under a license and was authored, remixed, and/or curated by LibreTexts.

- 8.4: Magnetic Properties and the Zeeman Effect by David M. Hanson, Erica Harvey, Robert Sweeney, Theresa Julia Zielinski is licensed CC BY-NC-SA 4.0. Original source: https://web.archive.org/web/20200619182410/http://www.chemeddl.org.

14.9C: EPR Spectra

This page titled 14.9C: EPR Spectra is shared under a license and was authored, remixed, and/or curated by LibreTexts.

14.10: MOSSBAUER SPECTROSCOPY



- Topic hierarchy

14.10A: The Technique of Mossbauer Spectroscopy

14.10B: What Can Isomer Shift Data Tell Us?

This page titled 14.10: Mossbauer Spectroscopy is shared under a license and was authored, remixed, and/or curated by LibreTexts.

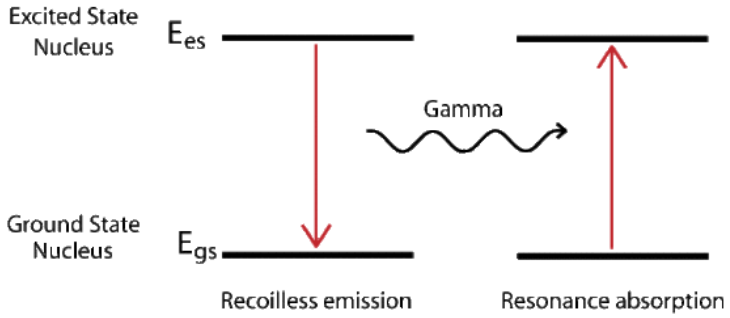
- 4.10: Mossbauer Spectroscopy is licensed CC BY-NC-SA 4.0.

14.10A: The Technique of Mossbauer Spectroscopy

Mössbauer spectroscopy is a versatile technique used to study nuclear structure with the absorption and re-emission of gamma rays, part of the electromagnetic spectrum. The technique uses a combination of the Mössbauer effect and Doppler shifts to probe the hyperfine transitions between the excited and ground states of the nucleus. Mössbauer spectroscopy requires the use of solids or crystals which have a probability to absorb the photon in a recoilless manner, many isotopes exhibit Mössbauer characteristics but the most commonly studied isotope is ^{57}Fe.

Introduction

Rudolf L. Mössbauer became a physics student at Technical University in Munich at the age of 20. After passing his intermediate exams Mössbauer began working on his thesis and doctorate work in 1955, while working as an assistant lecturer at Institute for Mathematics. In 1958 at the age of 28 Mössbauer graduated, and also showed experimental evidence for recoilless resonant absorption in the nucleus, later to be called the Mössbauer Effect. In 1961 Mössbauer was awarded the Nobel Prize in physics and, under the urging of Richard Feynman, accepted the position of Professor of Physics at the California Institute of Technology.



Mössbauer Effect

The recoil energy associated with absorption or emission of a photon can be described by the conservation of momentum. In it we find that the recoil energy depends inversely on the mass of the system. For a gas the mass of the single nucleus is small compared to a solid. The solid or crystal absorbs the energy as phonons, quantized vibration states of the solid, but there is a probability that no phonons are created and the whole lattice acts as the mass, resulting in a recoilless emission of the gamma ray. The new radiation is at the proper energy to excite the next ground state nucleus. The probability of recoilless events increases with decreasing transition energy.

$$P_R = P_\gamma$$

$$P_\gamma^2 = P_\gamma^2$$

$$2ME_R = \frac{E_\gamma^2}{c^2}$$

$$E_R = \frac{E_\gamma^2}{2Mc^2}$$

Doppler Effect

The Doppler shift describes the change in frequency due to a moving source and a moving observer. f is the frequency measured at the observer, v is the velocity of the wave so for our case this is the speed of light c, v_r is the velocity of the observer, v_s is the velocity of the source which is positive when heading away from the observer, and f_0 is the initial frequency.

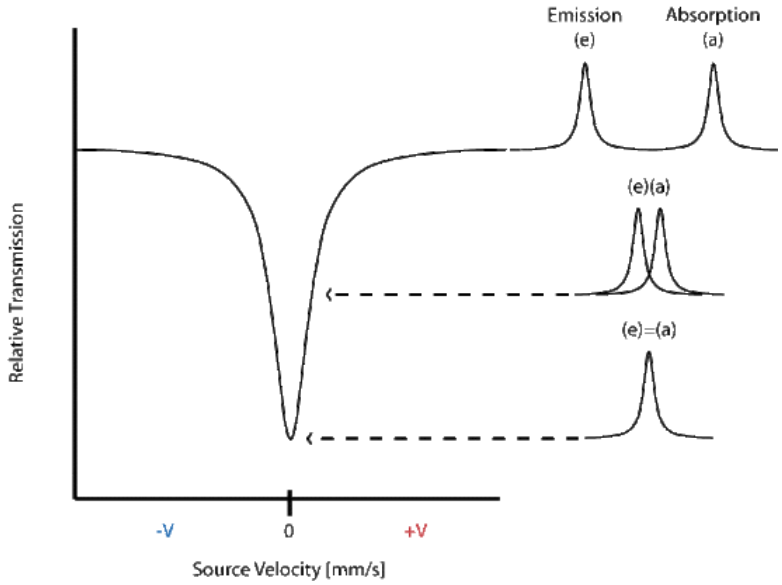
$$f = \left(\frac{v + v_r}{v + v_s}\right) f_0$$

$$f = \left(\frac{c}{c + v_s}\right) f_0$$

In the case where the source is moving toward a stationary observer the perceived frequency is higher. For the opposite situation where the source travels away from the observer frequencies recorded at the observer will be of lower compared to the initial wave. The energy of a photon is related to the product of Planck's constant and the frequency of the electromagnetic radiation. Thus for increasing frequencies the corresponding energy also increase, and the same is true in the reverse case where frequencies decrease and therefore energy decreases.

$$E = \frac{hc}{\lambda} = hv$$

The energy differences between hyperfine states are minimal (fractions of an eV) and the energy variation is achieved by the moving the source toward and away from the sample in an oscillating manner, commonly at a velocity of a few mm/s. The transmittance is then plotted against the velocity of the source and a peak is seen at the energy corresponding to the resonance energy.



In the above spectrum the emission and absorption are both estimated by the Lorentzian distribution.

Mössbauer Isotopes

By far the most common isotopes studied using Mössbauer spectroscopy is ^{57}Fe, but many other isotopes have also displayed a Mössbauer spectrum. Two criteria for functionality are

1. The excited state is of very low energy, resulting in a small change in energy between ground and excited state. This is because gamma rays at higher energy are not absorbed in a recoil free manner, meaning resonance only occurs for gamma rays of low energy.
2. The resolution of Mössbauer spectroscopy depends upon the lifetime of the excited state. The longer the excited state lasts the better the image.

Both conditions are met by ^{57}Fe and it is thus used extensively in Mössbauer spectroscopy. In the figure to the right the red colored boxes of the periodic table of elements indicate all elements that have isotopes visible using the Mössbauer technique.

Hyperfine Interactions

Mössbauer spectroscopy allows the researcher to probe structural elements of the nucleus in several ways, termed isomer shift, quadrupole interactions, and magnetic splitting. These are each explained by the following sections as individual graphs, but in practice Mössbauer spectrum are likely to contain a combination of all effects.

Isomer Shift

An isomeric shift occurs when non identical atoms play the role of source and absorber, thus the radius of the source, R_s, is different that of the absorber, R_a, and the same holds that the electron density of each species is different. The Coulombic interactions affects the ground and excited state differently leading to a energy difference that is not the same for the two species. This is best illustrated with the equation:

H																	He
Li	Be											B	C	N	O	F	Ne
Na	Mg											Al	Si	P	S	Cl	Ar
K	Ca	Sc	Ti	V	Cr	Mn	Fe	Co	Ni	Cu	Zn	Ga	Ge	As	Se	Br	Kr
Rb	Sr	Y	Zr	Nb	Mo	Tc	Ru	Rh	Pd	Ag	Cd	In	Sn	Sb	Te	I	Xe
Cs	Ba	La	Hf	Ta	W	Re	Os	Ir	Pt	Au	Hg	Ti	Pb	Bi	Po	At	Rn
Fr	Ra	Ac	Rf	Db	Sq	Bh	Hs	Mt	Ds								

Ce	Pr	Nd	Pm	Sm	Eu	Gd	Tb	Dy	Ho	Er	Tm	Yb	Lu
Th	Pa	U	Np	Pu	Am	Cm	Bk	Cf	Es	Fm	Md	No	Lr

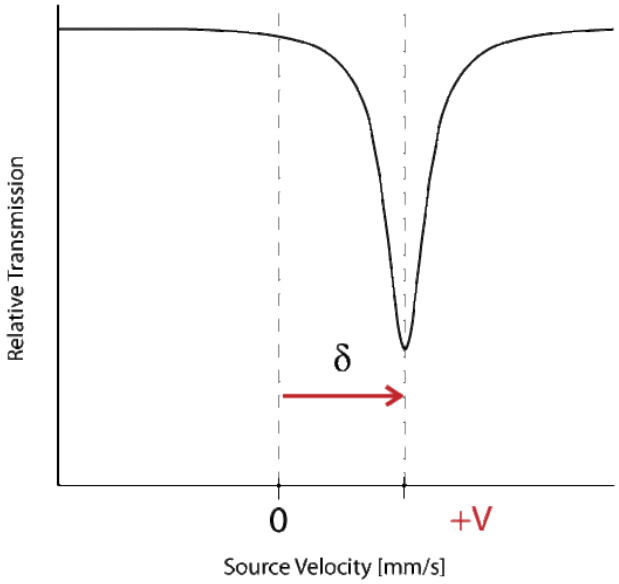
$$R_A \neq R_S$$

$$\rho_S \neq \rho_S$$

$$E_A \neq E_S$$

$$\delta = E_A - E_S = \frac{2}{3} nZe^2(\rho_A - \rho_S)(R_{es}^2 - R_{gs}^2)$$

Where delta represents the change in energy necessary to excite the absorber, which is seen as a shift from the Doppler speed 0 to V_1. The isomer shift depends directly on the s-electrons and can be influenced by the shielding p, d, f electrons. From the measured delta shift there is information about the valance state of the absorbing atom



The energy level diagram for δ shift shows the change in source velocity due to different sources used. The shift may be either positive or negative.

Quadrupole Interaction

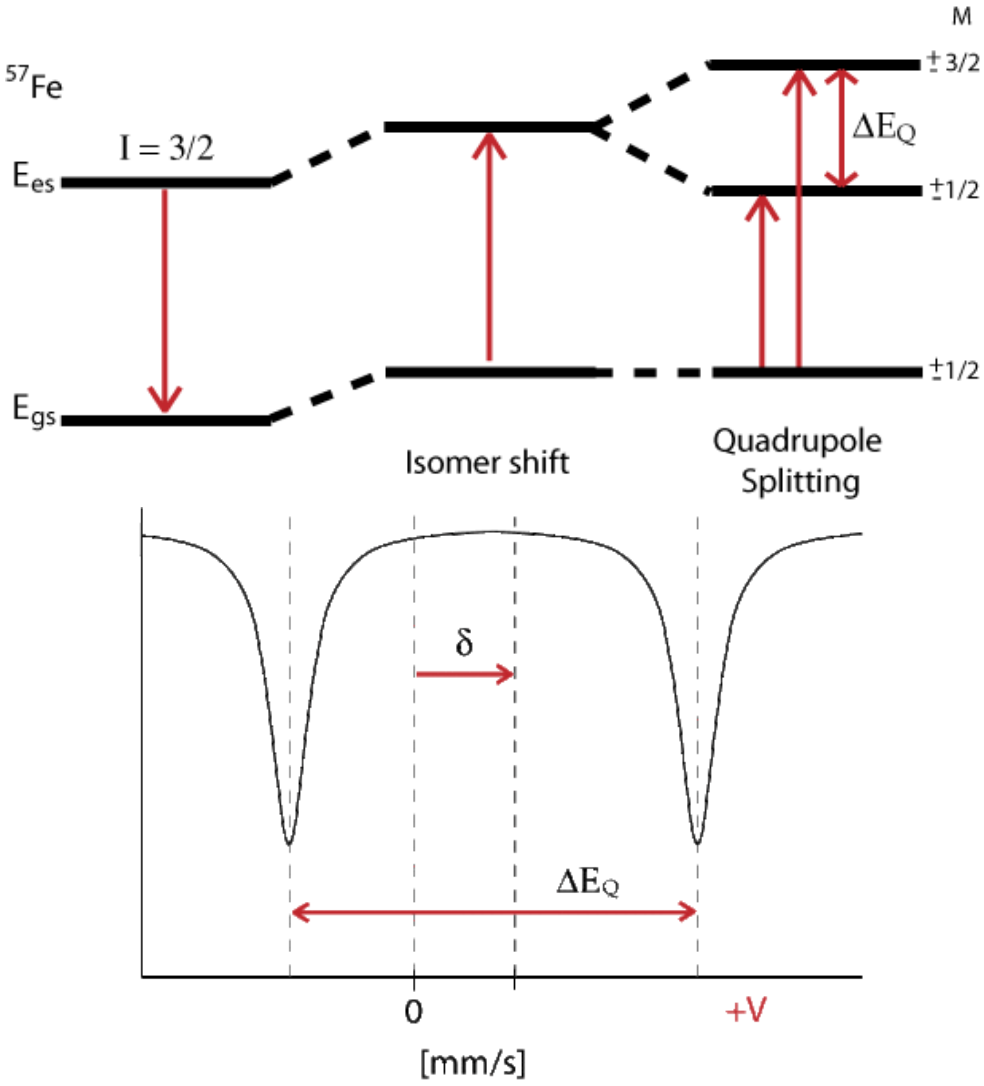
The Hamiltonian for quadrupole interaction using ^{57}Fe nuclear excited state is given by

$$H_Q = \frac{eQV_{ZZ}}{12}[3I_Z^2 - I(I+1) + \eta(I_X^2 - I_y^2)]$$

where the nuclear excited states are split into two degenerate doublets in the absence of magnetic interactions. For the asymmetry parameter $\eta = 0$ doublets are labeled with magnetic quantum numbers $m_{es} = \pm 3/2$ and $m_{es} = \pm 1/2$, where the $m_{es} = \pm 3/2$ doublet has the higher energy. The energy difference between the doublets is thus

$$\Delta EQ = \frac{eQV_{zz}}{2}\sqrt{1 + \frac{\eta^2}{3}}$$

The energy diagram and corresponding spectrum can be seen as

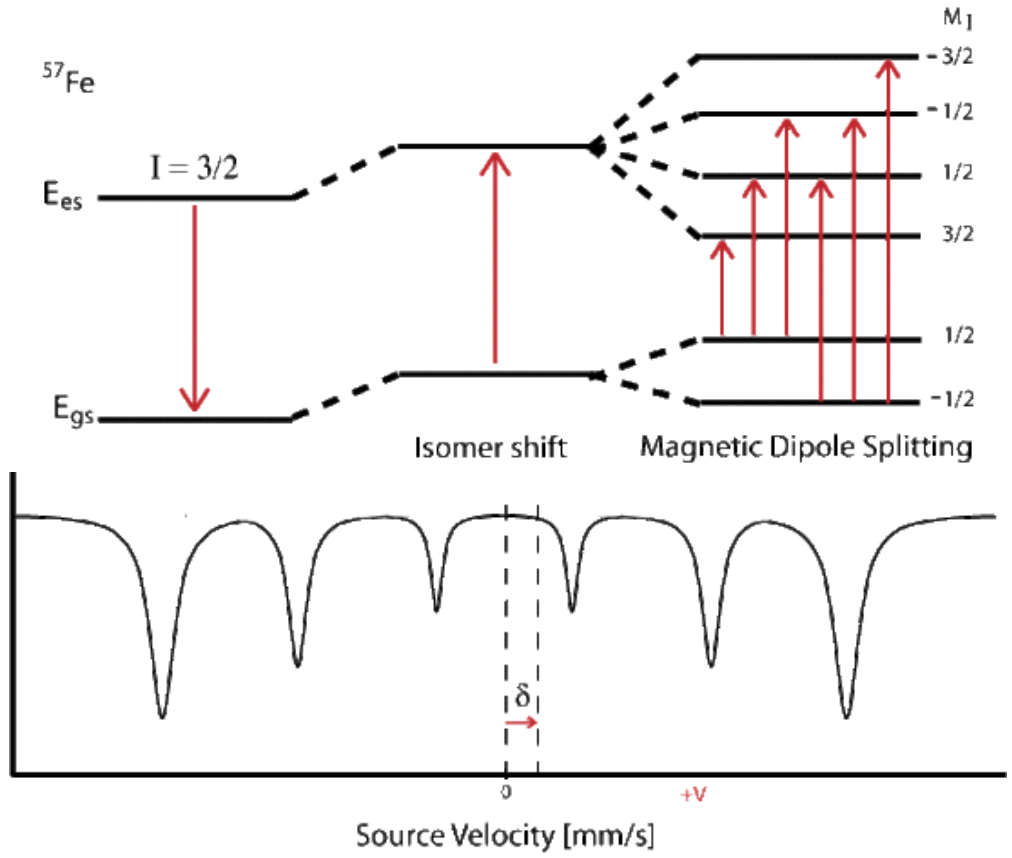


Magnetic Splitting

Magnetic splitting of seen in Mössbauer spectroscopy can be seen because the nuclear spin moment undergoes dipolar interactions with the magnetic field

$$E(m_I) = -g_n \beta_n B_{eff} m_I \tag{14}$$

where g_n is the nuclear g-factor and β_n is the nuclear magneton. In the absence of quadrupole interactions the Hamiltonian splits into equally spaced energy levels of



The allowed gamma stimulated transitions of nuclear excitation follows the magnetic dipole transition selection rule:

$$\Delta I = 1$$

and

$$\Delta m_I = 0, \pm 1$$

where m_I is the magnetic quantum number and the direction of β defines the nuclear quantization axis. If we assume g and A are *isotropic* (direction independent) where $g_x = g_y = g_z$ and B is actually a combination of the applied and internal magnetic fields:

$$H = g\beta S \cdot B + AS \cdot I - g_n \beta_n B \cdot I$$

The electronic Zeeman term is far larger then the nuclear Zeeman term, meaning the electronic term dominates the equation so S is approximated by $\langle S \rangle$ and

$$\langle S_z \rangle = m_s = \pm \frac{1}{2}$$

and

$$\langle S_x \rangle = \langle S_y \rangle \approx 0$$

$$H_n = A\langle S \rangle \cdot I - g_n \beta_n B \cdot I$$

Pulling out a $-g_n \beta_n$ followed by I leaves

$$H_n = -g_n \beta_n \left(-\frac{A\langle S \rangle}{g_n \beta_n} + B \right) I$$

Substituting the internal magnetic field with

$$B_{int} = -\frac{A\langle S\rangle}{g_n\beta_n}$$

results in a combined magnetic field term involving both the applied magnetic field and the internal magnetic field

$$H_n = -g_n\beta_n(B_{int} + B)\cdot I$$

which is simplified by using the effective magnetic field B_{eff}

$$H_n = -g_n\beta_n B_{eff}\cdot I$$

References

1. Gütlich, P. , Link, R. , & Trautwein, A. (1978). *Mössbauer spectroscopy and transition metal chemistry*. Inorganic chemistry concepts, v. 3. Berlin: Springer-Verlag.
2. G J Long and F Grandjean (1993) *Mössbauer Spectroscopy Applied to Magnetism and Materials*. New York. , Science Vol. 1,, eds.
3. Lawrence Que, J. , Ed. (2000). *Physical Methods in Bioinorganic Chemistry*. Sausalito, CA, University Science Books.
4. Filatov, M. (2007). "On the calculation of Mössbauer isomer shift. " The Journal of Chemical Physics 127(8): 8.
5. Introduction to mossbauer spectroscopy. 2013]. Available from http://www. rsc. org/Membership/Networking/InterestGroups/MossbauerSpect/part2. asp.
6. Bubek, Moritz, and Dennis Rettinger. 2004. Mossbauer-effekt.
7. Haskins, J. R. 1965. Advanced mossbauer-effect experiments. American Journal of Physics: 646.
8. Kistner, O. C. , and A. W. Sunyar. 1960. Evidence for quadrupole interaction of Fe57m, and influence of chemical binding on nuclear gamma-ray energy. Physical Review Letters 4 (8): 412.
9. Preston, R. S. , S. S. Hanna, and J. Heberle. 1962. Mössbauer effect in metallic iron. Physical Review 128 (5): 2207.

Problems

1. The magnetic splitting of $m_I = 0$ intensity of transition is related to $sin^2(\theta)$ of the angle between the incoming gamma ray and the effective magnetic field. When is the intensity of transition at max?
2. Why is it important for the sample to be in solid or crystalline state?
3. What case will result in a delta shift of 0. 00 mm/s?
4. Why is the Doppler effect important to Mössbauer spectroscopy?
5. Why are both the emission and absorption distributions the same? (both estimated with Lorentzian functions)

This page titled 14.10A: The Technique of Mossbauer Spectroscopy is shared under a license and was authored, remixed, and/or curated by LibreTexts.

- Mössbauer Spectroscopy by Kevin MacDow is licensed CC BY 4.0.

14.10B: What Can Isomer Shift Data Tell Us?

Among the drawbacks of the technique are the limited number of gamma ray sources and the requirement that samples be solid in order to eliminate the recoil of the nucleus. Mössbauer spectroscopy is unique in its sensitivity to subtle changes in the chemical environment of the nucleus including oxidation state changes, the effect of different ligands on a particular atom, and the magnetic environment of the sample.

As an analytical tool Mössbauer spectroscopy has been especially useful in the field of geology for identifying the composition of iron-containing specimens including meteors and moon rocks. In situ data collection of Mössbauer spectra has also been carried out on iron rich rocks on Mars.[10]

In another application, Mössbauer spectroscopy is used to characterize phase transformations in iron catalysts, e.g., those used for Fischer–Tropsch synthesis. While initially consisting of hematite (Fe_2O_3), these catalysts transform into a mixture of magnetite (Fe_3O_4) and several iron carbides. The formation of carbides appears to improve catalytic activity, however it can also lead to the mechanical break-up and attrition of the catalyst particles, which can cause difficulties in the final separation of catalyst from reaction products.[11]

Mössbauer spectroscopy has also been used to determine the relative concentration change in the oxidation state of antimony (Sb) during the selective oxidation of olefins. During calcination all the Sb ions in an antimony-containing tin dioxide catalyst transform into the +5 oxidation state. Following the catalytic reaction, almost all Sb ions revert from the +5 to the +3 oxidation state. A significant change in the chemical environment surrounding the antimony nucleus occurs during the oxidation state change which can easily be monitored as an isomer shift in the Mössbauer spectrum.[12]

This technique has also been used to observe the second-order transverse Doppler effect predicted by the theory of relativity, because of very high energy resolution.[13]

Contributors and Attributions

- Wikipedia

This page titled 14.10B: What Can Isomer Shift Data Tell Us? is shared under a license and was authored, remixed, and/or curated by LibreTexts.

- 4.10B: What Can Isomer Shift Data Tell Us? is licensed CC BY-NC-SA 4.0.

14.11: STRUCTURE DETERMINATION - DIFFRACTION METHODS

- Topic hierarchy

14.11A: X-Ray Diffraction (XRD)

14.11B: Single Crystal X-Ray Diffraction

14.11C: Powder X-Ray Diffraction

14.11D: Single Crystal Neutron Diffraction

14.11E: Electron Diffraction

14.11F: Low-Energy Electron Diffraction (LEED)

14.11G: Structural Databases

This page titled 14.11: Structure Determination - Diffraction Methods is shared under a license and was authored, remixed, and/or curated by LibreTexts.

- 4.11: Structure Determination - Diffraction Methods is licensed CC BY-NC-SA 4.0.

14.11A: X-Ray Diffraction (XRD)

This page titled 14.11A: X-Ray Diffraction (XRD) is shared under a license and was authored, remixed, and/or curated by LibreTexts.

14.11B: Single Crystal X-Ray Diffraction

This page titled 14.11B: Single Crystal X-Ray Diffraction is shared under a license and was authored, remixed, and/or curated by LibreTexts.

14.11C: Powder X-Ray Diffraction

This page titled 14.11C: Powder X-Ray Diffraction is shared under a license and was authored, remixed, and/or curated by LibreTexts.

14.11D: Single Crystal Neutron Diffraction

This page titled 14.11D: Single Crystal Neutron Diffraction is shared under a license and was authored, remixed, and/or curated by LibreTexts.

14.11E: Electron Diffraction

This page titled 14.11E: Electron Diffraction is shared under a license and was authored, remixed, and/or curated by LibreTexts.

14.11F: Low-Energy Electron Diffraction (LEED)

This page titled 14.11F: Low-Energy Electron Diffraction (LEED) is shared under a license and was authored, remixed, and/or curated by LibreTexts.

14.11G: Structural Databases

This page titled 14.11G: Structural Databases is shared under a license and was authored, remixed, and/or curated by LibreTexts.

14.12: Photoelectron Spectroscopy (PES, UPS, XPS, ESCA)

Learning Objectives

- Demonstrate how photoelectron spectroscopy can be used to resolve the absolute energies of molecular orbitals.

Photoelectron spectroscopy (PES) utilizes photo-ionization and analysis of the kinetic energy distribution of the emitted photoelectrons to study the composition and electronic state of the surface region of a sample.

- **X-ray Photoelectron Spectroscopy** (XPS) uses soft x-rays (with a photon energy of 200-2000 eV) to examine electrons in *core*-levels.
- **Ultraviolet Photoelectron Spectroscopy** (UPS) using vacuum UV radiation (with a photon energy of 10-45 eV) to examine electrons in *valence* levels.

Both photoelectron spectroscopies are based upon a single photon in/electron out process. The energy of a photon of all types of electromagnetic radiation is given by the Planck–Einstein relation:

$$E = h\nu \tag{14.12.1}$$

where h is Planck constant and ν is the frequency (Hz) of the radiation. UPS is a powerful technique to exam molecular electron structure since we are interested in the molecular orbitals from polyatomic molecules (especially the valence orbitals) and is the topic of this page.

Photoelectron spectroscopy uses monochromatic sources of radiation (i.e. photons of fixed energy). In UPS the photon interacts with valence levels of the molecule or solid, leading to ionization by removal of one of these valence electrons. The kinetic energy distribution of the emitted photoelectrons (i.e. the number of emitted photoelectrons as a function of their kinetic energy) can be measured using any appropriate electron energy analyzer and a photoelectron spectrum can thus be recorded.

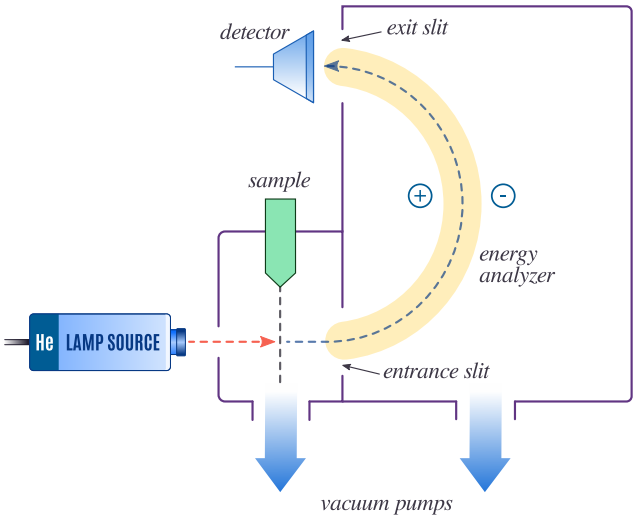


Figure 10.4.1: Diagram of a basic, typical PES instrument used in UPS, where the radiation source is an UV light source. When the sample is irradiated, the released photoelectrons pass through the lens system which slows them down before they enter the energy analyzer. The analyzer shown is a spherical deflection analyzer which the photoelectrons pass through before they are collected at the collector slit. (CC BY 4.0; Ümit Kaya via LibreTexts)

The process of photoionization can be considered in several ways. One way is to look at the overall process for a species A:

$$A + \text{photon} \rightarrow A^{+} + e^{-} \tag{14.12.2}$$

Conservation of energy then requires that (after using Equation 14.12.1):

$$E(A) + h\nu = E(A^+) + E(e^-) \tag{14.12.3}$$

Since the free electron's energy is present solely as kinetic energy (KE) (i.e., there is no internal energy in a free electron)

$$E(e^-) = KE$$

Equation 14.12.3 can then be rearranged to give the following expression for the KE of the photoelectron:

$$KE = h\nu - \left[E(A^+) - E(A)\right] \tag{14.12.4}$$

The final term in brackets represents the difference in energy between the ionized and neutral species and is generally called the **vertical ionization energy** (IE) of the ejected electron; this then leads to the following commonly quoted equations:

$$KE = h\nu - IE \tag{14.12.5}$$

or

$$IE = h\nu - KE \tag{14.12.6}$$

The vertical ionization energy is a direct measure of the energy required to just remove the electron concerned from its initial level to the vacuum level (i.e., a free electron). Photoelectron spectroscopy measures the relative energies of the ground and excited positive ion states that are obtained by removal of single electrons from the neutral molecule.

Note

Equation 14.12.5 may look familiar to you as it the same equation Einstein used to describe the photoelectric effect except the vertical ionization energy (IE) is substituted for workfunction Φ. Both vertical ionization energy and workfunctions are metrics for the binding energy of an electron in the sample.

At a fundamental level, ionization energies are well-defined thermodynamic quantities related to the heats of protonation, oxidation/reduction chemistry, and ionic and covalent bond energies. Ionization energies are closely related to the concepts of electronegativity, electron-richness, and the general reactivity of molecules. The energies and other characteristic features of the ionization bands observed in photoelectron spectroscopy provide some of the molecular orbitals detailed and specific quantitative information regarding the electronic structure and bonding in molecules.

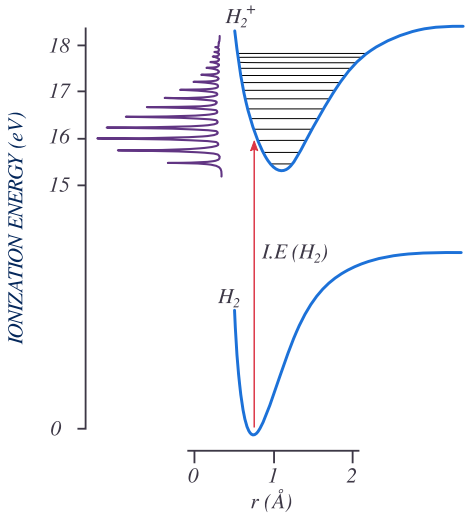


Figure 10.4.2: Vertical ionization process for molecular hydrogen. (CC BY 4.0; Ümit Kaya via LibreTexts)

Ionization is explicitly defined in terms of transitions between the ground state of a molecule and ion states as shown in Equation 14.12.6 and as illustrated in the Figure 10.4.2. Nonetheless, the information obtained from photoelectron spectroscopy is typically discussed in terms of the electronic structure and bonding in the ground states of neutral molecules, with ionization of electrons occurring from bonding molecular orbitals, lone pairs, antibonding molecular orbitals, or atomic cores. These descriptions reflect the relationship of ionization energies to the molecular orbital model of electronic structure.

Ionization energies are directly related to the energies of molecular orbitals by Koopmans' theorem, which states that the negative of the eigenvalue of an occupied orbital from a Hartree-Fock calculation is equal to the *vertical ionization energy* to the ion state formed by removal of an electron from that orbital (Figure 10.4.3), provided the distributions of the remaining electrons do not change (i.e., frozen).

$$I_j = -\epsilon_j \tag{14.12.7}$$

There are many limitations to Koopmans' theorem, but in a first order approximation each ionization of a molecule can be considered as removal of an electron from an individual orbital. The ionization energies can then be considered as measures of orbital stabilities, and shifts can be interpreted in terms of orbital stabilizations or destabilizations due to electron distributions and bonding. Koopmans' theorem is implicated whenever an orbital picture is involved, but is not necessary when the focus is on the total electronic states of the positive ions.

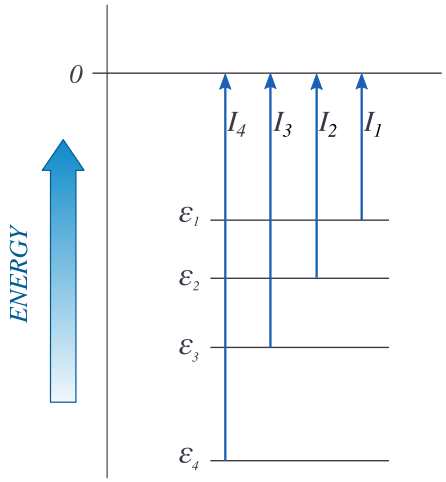


Figure 10.4.3: Within Koopmans' Theorem, the energies of the orbitals ϵ have an attractively simple physical interpretation: they give the amount of energy necessary to remove (ionize) the electron out of the molecular orbital, which corresponds to the negative of the experimentally observable ionization potential (I). (CC BY 4.0; Ümit Kaya via LibreTexts)

Koopmans' Theorem

Koopmans' theorem argues that the negative of the eigenvalue of an occupied orbital from a Hartree-Fock calculation is equal to the vertical ionization energy to the ion state formed by removal of an electron from that orbital.

Several different ionization energies can be defined, depending on the degree of vibrational excitation of the cations. In general, the following two types of ionization energies are considered (Figure 10.4.4):

- Adiabatic ionization energy corresponds to the ionization energy associated with this transition

  $$M(X, v''= 0) + h\nu \rightarrow M^+(x, v' = 0) + e^-$$

  Adiabatic ionization energy that is, the minimum energy required to eject an electron from a molecule in its ground vibrational state and transform it into a cation in the lowest vibrational level of an electronic state x of the cation.
- Vertical ionization energy corresponds to the ionization energy associated with this transition

  $$M(X, v''= 0) + h\nu \rightarrow M^+(x, v' = n) + e^-$$

where, the value n of the vibrational quantum number v' corresponds to the vibrational level whose wavefunction gives the largest overlap with the v" = 0 wavefunction. This is the most probable transition and usually corresponds to the vertical transition where the internuclear separations of the ionic state are similar to those of the ground state.

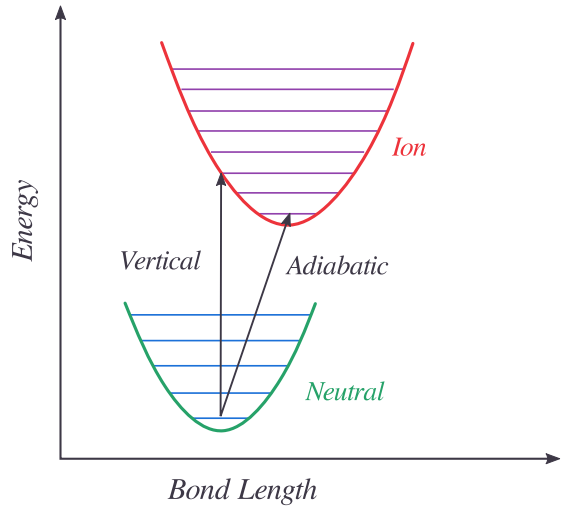


Figure 10.4.4: Difference between vertical and adiabatic ionization energies for a simple harmonic oscillator system. (CC BY 4.0; Ümit Kaya via LibreTexts)

The geometry of an ion may be different from the neutral molecule. The measured ionzation energy in a PES experiment can refer to the vertical ionization energy, in which case the ion is in the same geometry as the neutral, or to the adiabatic ionzaiton energy, in which case the ion is in its lowest energy, relaxed geometry (mostly the former though). This is illustrated in the Figure 10.4.4. For a diatomic the only geometry change possible is the bond length. The figure shows an ion with a slightly longer bond length than the neutral. The harmonic potential energy surfaces are shown in green (neutral) and red (ion) with vibrational energy levels. The vertical ionzation energy is **always greater** than the adiabatic ionzation energy.

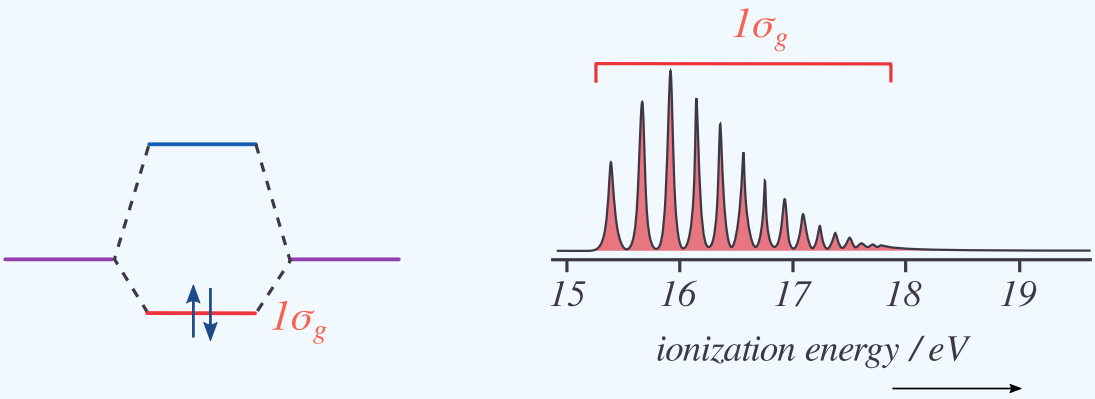
Differing Ionization Energies

You have been exposed to three metrics of ionization energies already, which are similar, but with distinct differences:

- The *ionization energy* (also called *adiabatic ionization energy*) is the lowest energy required to effect the removal of an electron from a molecule or atom, and corresponds to the transition from the lowest electronic, vibrational and rotational level of the isolated molecule to the lowest electronic, vibrational and rotational level of the isolated ion.
- The *binding energy* (also called *vertical ionization energy*) is the energy change corresponding to an ionization reaction leading to formation of the ion in a configuration which is the same as that of the equilibrium geometry of the ground state neutral molecule.
- The *workfunction* is the minimum energy needed to remove an electron from a (bulk) solid to a point in the vacuum.

Example 10.4.1: Molecular Hydrogen

As you remember, the molecular orbital description of molecular hydrogen involves two $|1s\rangle$ atomic orbitals generating a bonding $1\sigma_g$ and antibonding $2\sigma_u^*$ molecular orbitals. The two electrons that are responsible for the H_2 bond are occupied in the $1\sigma_g$.

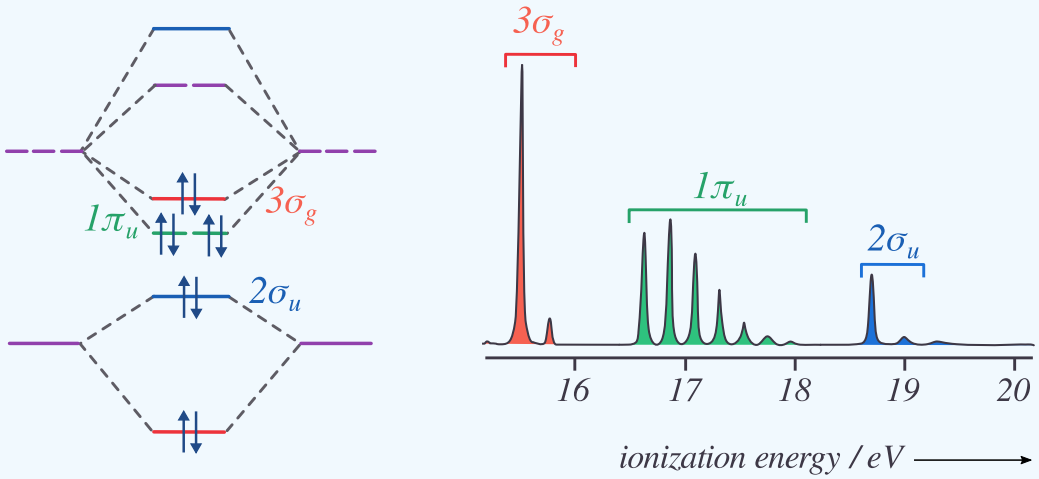


MO diagram and PES spectrum of H_2. (CC BY 4.0; Ümit Kaya via LibreTexts)

The PES spectrum has a single band that corresponds to the ionization of a $1\sigma_g$ electron. The multiple peaks are due to electrons ejecting from a range of stimulated vibrational energy levels. When extensive vibrational structure is resolved in a PES molecular orbital, then the removal of an electron from that molecular orbital induces a significant change in the bonding (in this case an increase in the bond length since the bond order has been reduced).

Example 10.4.2: Molecular Nitrogen

Diatomic nitrogen is more complex than hydrogen since multiple molecular orbitals are occupied. Four molecular orbitals are occupied (the two $1\pi_u$ orbitals are both occupied). The UV photoelectron spectrum of N_2, has three bands corresponding to $3\sigma_g$, $1\pi_u$ and $2\sigma_u$ occupied molecular orbitals. Both $3\sigma_g$ and $2\sigma_u$ are weakly bonding and antibonding. The $1\sigma_g$ orbital is not resolved in this spectrum since the incident light $h\nu$ used did not have sufficient energy to ionize electrons in that deeply stabilized molecular orbital.



MO diagram and PES spectrum of N_2. (CC BY 4.0; Ümit Kaya via LibreTexts)

Note that extensive vibrational structure for the $1\pi_u$ band indicates that the removal of an electron from this molecular orbital causes a significant change in the bonding.

Hydrogen Chloride

The molecular energy level diagram for HCl is reproduced in Figure 10.4.5

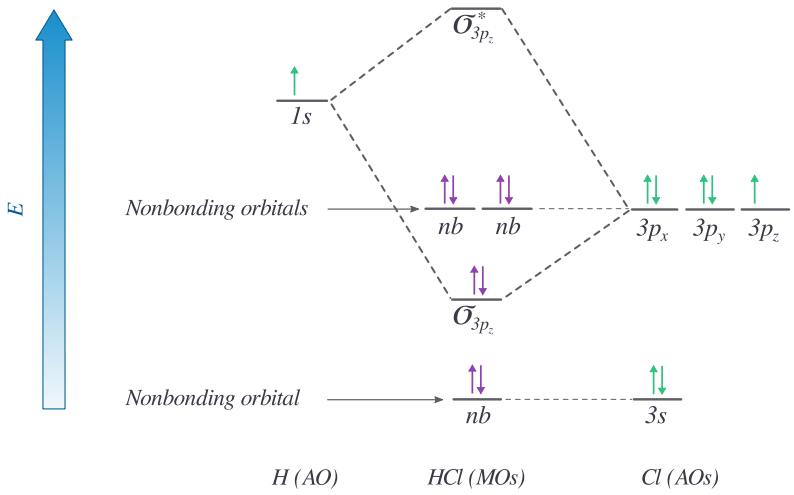


Figure 10.4.5: Molecular Orbital Energy-Level Diagram for HCl. The hydrogen 1s atomic orbital interacts molecular orbitals strongly with the $3p_z$ orbital on chlorine, producing a bonding/antibonding pair of molecular orbitals. The other electrons on Cl are best viewed as nonbonding. As a result, only the bonding σ orbital is occupied by electrons, giving a bond order of 1. (CC BY 4.0; Ümit Kaya via LibreTexts)

Important aspects of molecular orbital diagram in Figure 10.4.5:

- The H 1s energy lies well above the Cl 2*s* and 2*p* atomic orbitals;
- The valence electron configuration can be written $3\sigma^2 1\pi^4$;
- The H 1s orbital contributes only to the σ molecular orbitals, as does one of the Cl 2*p* orbitals (hence the lines in Figure 10.4.5 connecting these atomic orbitals and the 3σ and 4σ molecular orbitals);
- The remaining Cl 2*p* orbitals (ie those perpendicular to the bond axis) are unaffected by bonding, and these form the 1π molecular orbitals;
- The 1π orbitals are nonbonding - they are not affected energetically by the interaction between the atoms, and are hence neither bonding nor antibonding;
- The 3σ orbital is weakly bonding, and largely Cl 2*p*;
- The 3σ* orbital is antibonding, and primarily of H 1s character;

Figure 10.4.6 shows the analogous MO diagram and photoelectron spectrum for HCl. The spectrum has two bands corresponding to non-bonding 1*p* (or 1π) molecular orbitals (with negligible vibrational structure) and the 3s bonding molecular orbital (vibrational structure).

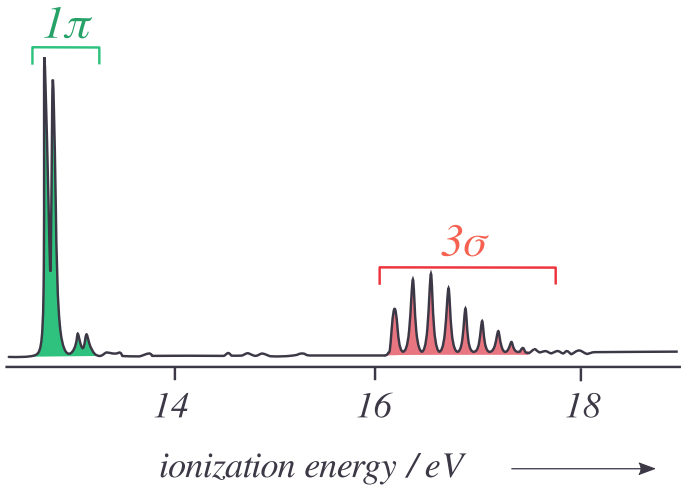


Figure 10.4.6: Photoelectron spectrum HCl. (CC BY 4.0; Ümit Kaya via LibreTexts)

The higher energy (more stabilized) core molecular orbitals are not observed since the incident photon energy $h\nu$ is below their ionization energies.

Water

In the simplified valence bond theory perspective of the water molecule, the oxygen atom form four sp^3 hybrid orbitals. Two of these are occupied by the two lone pairs on the oxygen atom, while the other two are used for bonding. Within the molecular orbital picture, the electronic configuration of the $\mathrm{H_2O^+}$ molecule is $(1a_1)^2(2a_1)^2(1b_2)^2(3a_1)^2(1b_1)^2$ where the symbols a_1, b_2 and b_1 are orbital labels based on molecular symmetry that will be discussed later (Figure 10.4.7). Within Koopmans' theorem:

- The energy of the $1b_1$ HOMO corresponds to the ionization energy to form the $\mathrm{H_2O^+}$ ion in its ground state $(1a_1)^2(2a_1)^2(1b_2)^2(3a_1)^2(1b_1)^1$.
- The energy of the second-highest molecular orbitals $3a_1$ refers to the ion in the excited state $(1a_1)^2(2a_1)^2(1b_2)^2(3a_1)^1(1b_1)^2$.

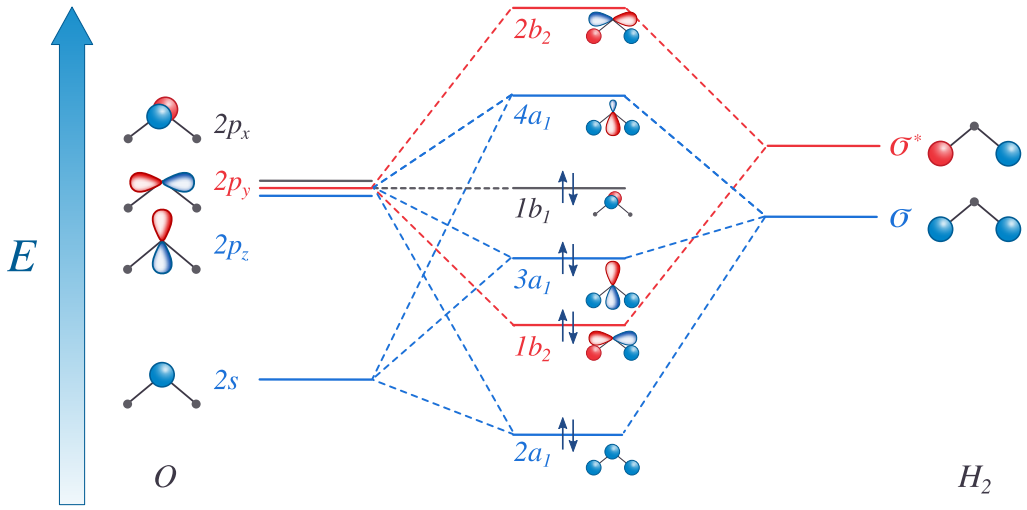


Figure 10.4.7: MO diagram for water. (CC BY 4.0; Ümit Kaya via LibreTexts)

The Hartree–Fock orbital energies (with sign changed) of these orbitals are tabulated below and compared to the experimental ionization energies.

Molecular orbital	Hartree–Fock orbital Energies (eV)	Experimental Ionization Energies (eV)
$2a_1$	36.7	32.2
$1b_2$	19.5	18.5
$3a_1$	15.9	14.7
$1b_1$	13.8	12.6

As explained above, the deviations between orbital energy and ionization energy is small and due to the effects of orbital relaxation as well as differences in electron correlation energy between the molecular and the various ionized states.

The molecular orbital perspective has the lone pair in different orbitals (one in a non-bonding orbital ($1b_1$ and one in the bonding orbitals). We tern to the photoelectron spectroscopy to help identify which theory is more accurate (i.e., describes reality better). The photoelectron spectrum of water in Figure 10.4.6 can be interpreted as having three major peaks with some fine structure arises from vibrational energy changes. The light source used in this experiment is not sufficiently energetic to ionize electrons from the lowest lying molecular orbitals.

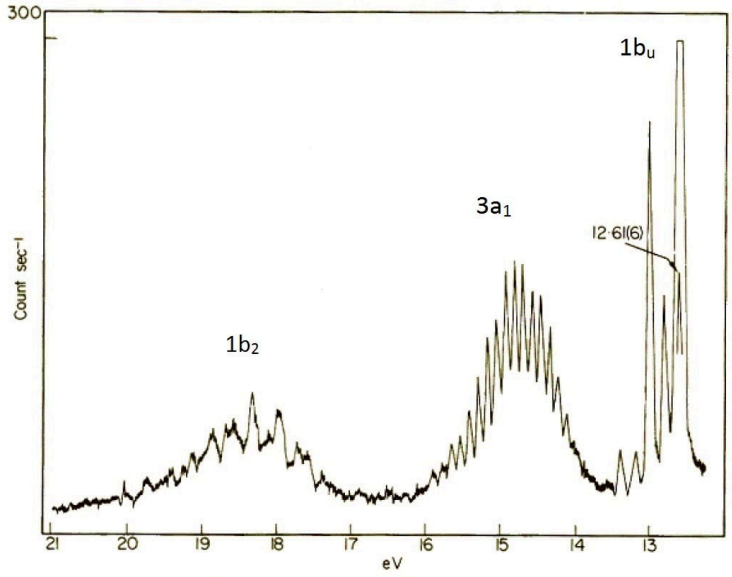


Figure 10.4.8: Photoelectron spectrum of water. Note the energy axes is flipped compared to other spectra on this page. This spectrum does not go to high enough energy to show the deep $2a_1$ molecular orbital.

If water was formed two identical O-H bonds and two lone pairs on the oxygen atom line valence bond theory predicts, then the PES in Figure 10.4.8 would have two (degenerate) peaks, one for the two bonds and one for the two lone pairs. The photoelectron spectrum clearly shows three peaks in the positions expected for the molecular orbitals in Figure 10.4.8.

If the molecular orbitals in Figure 10.4.7 represent the real electronic structure, how do we view the bonding? These molecular orbitals are delocalized and bare little relationship to the familiar 2-center bonds used in valence bond theory. For example, the $2a_1$ $1b_1$ and $3a_1$ molecular orbitals all have contributions from all three atoms, they are really 3-centered molecular orbitals. The bonds however can be thought of as representing a build up of the total electron density which loosely put is a total of all the orbital contributions. Despite this, we keep the ideas of hybridization and 2-center bonds because they are useful NOT because they represent reality

Summary

A photoelecton spectrum can show the relative energies of occupied molecular orbitals by ionization. (i.e. ejection of an electron). A photoelectron spectrum can also be used to determine energy spacing between vibrational levels of a given electronic state. Each orbital energy band has a structure showing ionization to different vibrational levels.

This page titled 14.12: Photoelectron Spectroscopy (PES, UPS, XPS, ESCA) is shared under a license and was authored, remixed, and/or curated by LibreTexts.

- 10.4: Photoelectron Spectroscopy by Roger Nix is licensed CC BY 4.0.

14.13: COMPUTATIONAL METHODS



-  Topic hierarchy 

14.13A: Hartree-Fock Theory

14.13B: Density Functional Theory

14.13C: Hückel MO Theory

14.13D: Molecular Mechanisms (MM)

This page titled 14.13: Computational Methods is shared under a license and was authored, remixed, and/or curated by LibreTexts.

- 4.13: Computational Methods is licensed CC BY-NC-SA 4.0.

14.13A: Hartree-Fock Theory

In a modern *ab initio* electronic structure calculation on a closed shell molecule, the electronic Hamiltonian is used with a single determinant wavefunction. This wavefunction, ψ, is constructed from molecular orbitals, ψ that are written as linear combinations of contracted Gaussian basis functions, φ

$$\varphi_j = \sum_k c_{jk}\psi_k \tag{14.13A.1}$$

The contracted Gaussian functions are composed from primitive Gaussian functions to match Slater-type orbitals (STOs). The exponential parameters in the STOs are optimized by calculations on small molecules using the nonlinear variational method and then those values are used with other molecules. The problem is to calculate the electronic energy from

$$E = \frac{\int \psi^* \hat{H} \psi d\tau}{\int \psi^* \psi d\tau} \tag{14.13A.2}$$

and find the optimum coefficients c_{jk} for each molecular orbital in Equation 14.13A.1 by using the Self Consistent Field Method and the Linear Variational Method to minimize the energy as was described in the previous chapter for the case of atoms.

To obtain the total energy of the molecule, we need to add the internuclear repulsion to the electronic energy calculated by this procedure. The total energy of the molecule can be calculated for different geometries (i.e. bond lengths and angles) to find the minimum energy configuration. Also, the total energies of possible transition states can be calculated to find the lowest energy pathway to products in chemical reactions.

$$V_{rs} = \sum_{r=1}^{N-1} \sum_{s=r+1}^{N} \frac{Z_r Z_s}{r_{rs}} \tag{14.13A.3}$$

Exercise 14.13A.1

For a molecule with three nuclei, show that the sums in Equation 14.13A.3 correctly include all the pairwise potential energy terms without including any twice.

As we improve the basis set used in calculations by adding more and better functions, we expect to get better and better energies. The variational principle says an approximate energy is an upper bound to the exact energy, so the lowest energy that we calculate is the most accurate. At some point, the improvements in the energy will be very slight. This limiting energy is the lowest that can be obtained with a single determinant wavefunction. This limit is called the *Hartree-Fock limit*, the energy is the *Hartree-Fock energy*, the molecular orbitals producing this limit are called *Hartree-Fock orbitals*, and the determinant is the *Hartree-Fock wavefunction*.

Exercise 14.13A.2

Write a one-sentence definition of the Hartree-Fock wavefunction that captures all the essential features of this function.

Restricted vs. Unrestricted Hartree-Fock

You may encounter the terms *restricted* and *unrestricted* Hartree-Fock. The above discussion pertains to a restricted HF calculation. In a restricted HF calculation, electrons with α spin are restricted or constrained to occupy the same spatial orbitals as electrons with β spin. This constraint is removed in an unrestricted calculation. For example, the spin orbital for electron 1 could be $\psi_A(r_1)\alpha(1)$, and the spin orbital for electron 2 in a molecule could be $\psi_B(r_2)\beta(2)$, where both the spatial molecular orbital and the spin function differ for the two electrons. Such spin orbitals are called *unrestricted*. If both

electrons are constrained to have the same spatial orbital, e.g. $\psi_A(r_1)\alpha(1)$ and $\psi_A(r_2)\beta(2)$, then the spin orbital is said to be *restricted*. While unrestricted spin orbitals can provide a better description of the electrons, twice as many spatial orbitals are needed, so the demands of the calculation are much higher. Using unrestricted orbitals is particular beneficial when a molecule contains an odd number of electrons because there are more electrons in one spin state than in the other.

Carbon Dioxide

Now consider the results of a self-consistent field calculation for carbon monoxide, CO. It is well known that carbon monoxide is a poison that acts by binding to the iron in hemoglobin and preventing oxygen from binding. As a result, oxygen is not transported by the blood to cells. Which end of carbon monoxide, carbon or oxygen, do you think binds to iron by donating electrons? We all know that oxygen is more electron-rich than carbon (8 vs 6 electrons) and more electronegative. A reasonable answer to this question therefore is *oxygen*, but experimentally it is carbon that binds to iron.

A quantum mechanical calculation done by Winifred M. Huo, published in J. Chem. Phys. 43, 624 (1965), provides an explanation for this counter-intuitive result. The basis set used in the calculation consisted of 10 functions: the 1s, 2s, $2p_x$, $2p_y$, and $2p_z$ atomic orbitals of C and O. Ten molecular orbitals (mo's) were defined as linear combinations of the ten atomic orbitals, which are written as

$$\psi_k = \sum_{j=1}^{10} C_{kj}\varphi_j \tag{14.13A.4}$$

where k identifies the mo and j identifies the atomic orbital basis function. The ground state wavefunction ψ is written as the Slater Determinant of the five lowest energy molecular orbitals ψ_k. Equation 14.13A.5 gives the energy of the ground state,

$$E = \frac{\left\langle \psi | \hat{H} | \psi \right\rangle}{\langle \psi | \psi \rangle} \tag{14.13A.5}$$

where the denominator accounts for the normalization requirement. The coefficients C_{kj} in the linear combination are determined by the variational method to minimize the energy. The solution of this problem gives the following equations for the molecular orbitals. Only the largest terms have been retained here. These functions are listed and discussed in order of increasing energy.

- $1s \approx 0.941 s_o$. The 1 says this is the first σ orbital. The σ says it is symmetric with respect to reflection in the plane of the molecule. The large coefficient, 0.94, means this is essentially the 1s atomic orbital of oxygen. The oxygen 1s orbital should have a lower energy than that of carbon because the positive charge on the oxygen nucleus is greater.
- $2s \approx 0.921 s_c$. This orbital is essentially the 1s atomic orbital of carbon. Both the 1σ and 2σ are "nonbonding" orbitals since they are localized on a particular atom and do not directly determine the charge density between atoms.
- $3s \approx (0.722 s_o + 0.182 p_{zo}) + (0.282 s_c + 0.162 p_{zc})$. This orbital is a "bonding" molecular orbital because the electrons are delocalized over C and O in a way that enhances the charge density between the atoms. The 3 means this is the third σ orbital. This orbital also illustrates the concept of hybridization. One can say the 2s and 2p orbitals on each atom are hybridized and the molecular orbital is formed from these hybrids although the calculation just obtains the linear combination of the four orbitals directly without the *à priori* introduction of hybridization. In other words, hybridization just falls out of the calculation. The hybridization in this bonding LCAO increases the amplitude of the function in the region of space between the two atoms and decreases it in the region of space outside of the bonding region of the atoms.
- $4s \approx (0.372 s_c + 0.12 p_{zc}) + (0.542 p_{zo} - 0.432 s_0)$. This molecular orbital also can be thought of as being a hybrid formed from atomic orbitals. The hybridization of oxygen atomic orbitals, because of the negative coefficient with $2s_O$, decreases the electron density between the nuclei and enhances electron density on the side of oxygen facing away from the carbon atom. If we follow how this function varies along the internuclear axis, we see that near carbon the function is positive whereas near oxygen it is negative or possibly small and positive. This change means there must be a node between the two nuclei or at the oxygen nucleus. Because of the node, the electron density between the two nuclei is low so the electrons in this orbital do not serve to shield the two positive nuclei from each other. This orbital therefore is called an "antibonding" mo and the electrons assigned to it are called antibonding electrons. This orbital is the antibonding partner to the 3σ orbital.
- $1\pi \approx 0.322 p_{xc} + 0.442 p_{xo} \mathrm{and} 2\pi \approx 0.322 p_{yc} + 0.442 p_{yo}$. These two orbitals are degenerate and correspond to bonding orbitals made up from the p_x and p_y atomic orbitals from each atom. These orbitals are degenerate because the x and y directions are equivalent in this molecule. π tells us that these orbitals are antisymmetric with respect to reflection in a plane containing the nuclei.
- $5\sigma \approx 0.382_{sC} - 0.382_{pC} - 0.292 p_{zO}$. This orbital is the sp hybrid of the carbon atomic orbitals. The negative coefficient for $2p_C$

puts the largest amplitude on the side of carbon away from oxygen. There is no node between the atoms. We conclude this is a nonbonding orbital with the nonbonding electrons on carbon. This is not a “bonding” orbital because the electron density between the nuclei is lowered by hybridization. It also is not an antibonding orbital because there is no node between the nuclei. When carbon monoxide binds to Fe in hemoglobin, the bond is made between the C and the Fe. This bond involves the donation of the 5σ nonbonding electrons on C to empty d orbitals on Fe. Thus mo theory allows us to understand why the C end of the molecule is involved in this electron donation when we might naively expect O to be more electron-rich and capable of donating electrons to iron.

Exercise 14.13A.3

Summarize how Quantum Mechanics is used to describe bonding and the electronic structure of molecules.

Exercise 14.13A.4

Construct an energy level diagram for CO that shows both the atomic orbitals and the molecular orbitals. Show which atomic orbitals contribute to each molecular orbital by drawing lines to connect the mo’s to the ao’s. Label the molecular orbitals in a way that reveals their symmetry. Use this energy level diagram to explain why it is the carbon end of the molecule that binds to hemoglobin rather than the oxygen end.

This page titled 14.13A: Hartree-Fock Theory is shared under a license and was authored, remixed, and/or curated by LibreTexts.

- 10.8: The Self-Consistent Field and the Hartree-Fock Limit by David M. Hanson, Erica Harvey, Robert Sweeney, Theresa Julia Zielinski is licensed CC BY-NC-SA 4.0. Original source: https://web.archive.org/web/20200619182410/http://www.chemeddl.org.

14.13B: Density Functional Theory

This page titled 14.13B: Density Functional Theory is shared under a license and was authored, remixed, and/or curated by LibreTexts.

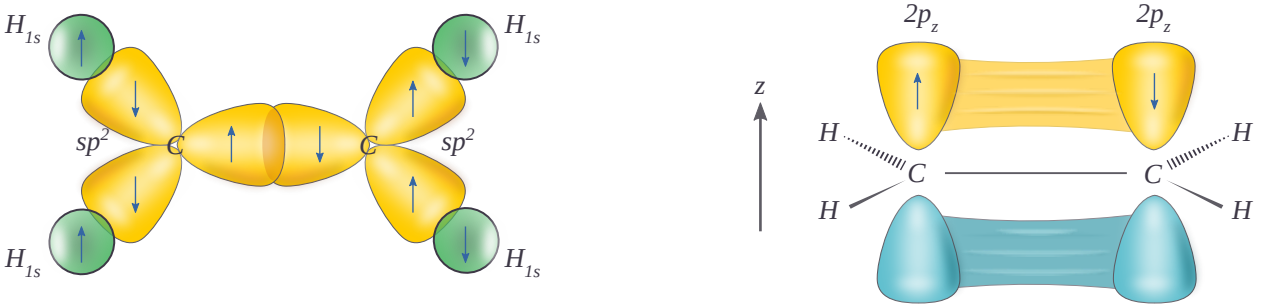
14.13C: Hückel MO Theory

Learning Objectives

- Demonstrate how Hückel's theory approximates the full molecular orbital picture of molecules by treating the σ-bonding and π-bonding networks independently.

Molecular orbital theory has been very successfully applied to large conjugated systems, especially those containing chains of carbon atoms with alternating single and double bonds. An approximation introduced by Hückel in 1931 considers only the delocalized *p* electrons moving in a framework of π-bonds. This is, in fact, a more sophisticated version of a free-electron model.

The simplest hydrocarbon to consider that exhibits π bonding is ethylene (ethene), which is made up of four hydrogen atoms and two carbon atoms. Experimentally, we know that the $\mathrm{H-C-H}$ and $\mathrm{H-C-C}$ angles in ethylene are approximately 120°. This angle suggests that the carbon atoms are sp^2 hybridized, which means that a singly occupied sp^2 orbital on one carbon overlaps with a singly occupied s orbital on each H and a singly occupied sp^2 lobe on the other C. Thus each carbon forms a set of three σ bonds: two C–H (sp^2 + s) and one C–C (sp^2 + sp^2) (part a of Figure 10.5.1).



(a) C_2H_4 σ - bonded framework *(b) C_2H_4 π bonding*

Figure 10.5.1 : (a) The σ-bonded framework is formed by the overlap of two sets of singly occupied carbon sp^2 hybrid orbitals and four singly occupied hydrogen 1s orbitals to form electron-pair bonds. This uses 10 of the 12 valence electrons to form a total of five σ bonds (four C–H bonds and one C–C bond). (b) One singly occupied unhybridized $2p_z$ orbital remains on each carbon atom to form a carbon–carbon π bond. (Note: by convention, in planar molecules the axis perpendicular to the molecular plane is the *z*-axis.) (CC BY-NC; Ümit Kaya via LibreTexts)

The Hückel approximation is used to determine the energies and shapes of the π molecular orbitals in conjugated systems. Within the Hückel approximation, the covalent bonding in these hydrocarbones can be separated into two independent "frameworks": the σ-bonding framework and the the σ-bonding framework. The wavefunctions used to describe the bonding orbitals in each framework results from different combinations of atomic orbitals. The method limits itself to addressing conjugated hydrocarbons and specifically only π electron molecular orbitals are included because these determine the general properties of these molecules; the sigma electrons are ignored. This is referred to as *sigma-pi separability* and is justified by the orthogonality of σ and π orbitals in planar molecules. For this reason, the Hückel method is limited to planar systems. Hückel approximation assumes that the electrons in the π bonds “feel” an electrostatic potential due to the entire σ-bonding framework in the molecule (i.e. it focuses only on the formation of π bonds, given that the σ bonding framework has already been formed).

Conjugated Systems

A conjugated system has a region of overlapping p-orbitals, bridging the interjacent single bonds, that allow a *delocalization* of π electrons across all the adjacent aligned p-orbitals. These π electrons do not belong to a single bond or atom, but rather to a group of atoms.

Ethylene

Before considering the Hückel treatment for ethylene (C_2H_4), it is beneficial to review the general bonding picture of the molecule. Bonding in ethylene involves the sp^2 hybridization of the $2s$, $2p_x$, and $2p_y$ atomic orbitals on each carbon atom; leaving the $2p_z$ orbitals untouched (Figure 10.5.2).

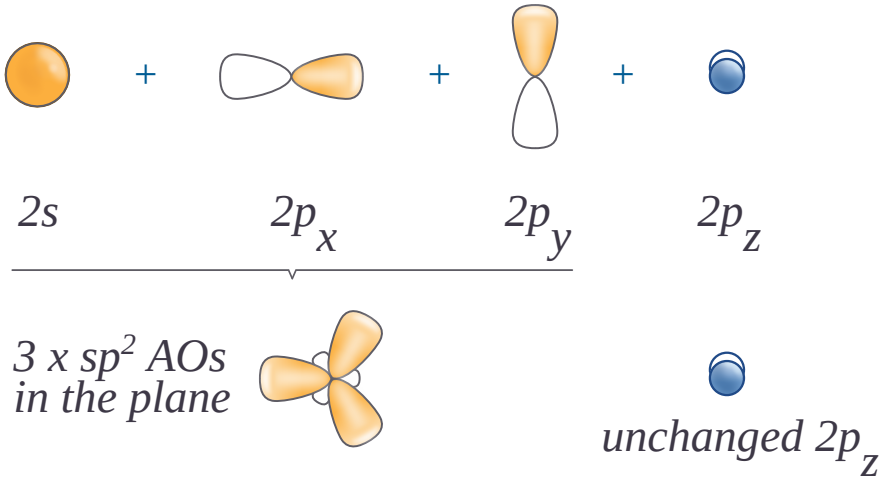


Figure 10.5.2 : Hybridizing of the carbon atomic orbitals to give sp^2 hybrid orbitals for bonding to hydrogen atoms in ethylene. (CC BY-NC; Ümit Kaya via LibreTexts)

The use of hybrid orbitals in the molecular orbital approach describe here is merely a convenience and not invoking valence bond theory (directly). An identical description can be extracted using exclusively atomic orbitals on carbon, but the interpretation of the resulting wavefunctions is less intuitive. For example, the ith molecular orbital can be described via hybrid orbitals

$$|\psi_1\rangle = c_1|sp_1^2\rangle + c_2|1s_a\rangle$$

or via atomic orbitals.

$$|\psi_1\rangle = a_1|2s\rangle + a_1|2p_x\rangle + a_1|2p_y\rangle + a_4|1s_a\rangle$$

where $\{a_i\}$ and $\{c_i\}$ are coefficients of the expansion. Either describe will work and both are identical approaches since

$$|sp_1^2\rangle = b_1|2s\rangle + b_1|2p_x\rangle + b_1|2p_y\rangle$$

where $\{c_i\}$ are coefficients describing the hybridized orbital.

The bonding occurs via the mixing of the electrons in the sp^2 hybrid orbitals on carbon and the electrons in the $1s$ atomic orbitals of the four hydrogen atoms (Figure 10.5.1 ; left) resulting in the σ-bonding framework. The π-bonding framework results from the unhybridized $2p_z$ orbitals (Figure 10.5.2 ; right). The independence of these two frameworks is demonstrated in the resulting molecular orbital diagram in Figure 10.5.3 ; Hückel theory is concerned only with describing the molecular orbitals and energies of the π bonding framework.

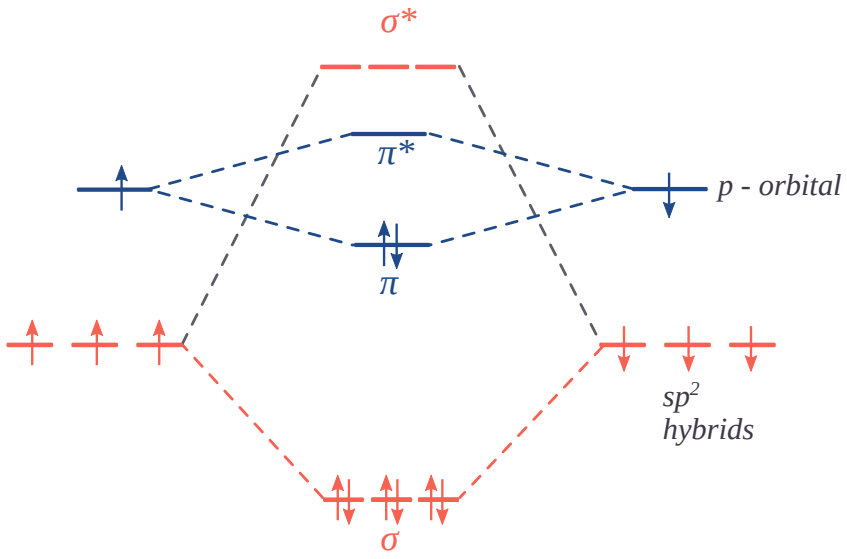


Figure 10.5.3 : Molecular orbitals demonstrating the sigma-pi separability of the π-bonding framework (blue) and the σ-bonding frameworks (red) of ethylene. (CC BY-NC; Ümit Kaya via LibreTexts)

Hückel treatment is concerned only with describing the molecular orbitals and energies of the π bonding framework.

Since Hückel theory is a special consideration of molecular orbital theory, the molecular orbitals $|\psi_i\rangle$ can be described as a linear combination of the $2p_z$ atomic orbitals ϕ at carbon with their corresponding $\{c_i\}$ coefficients:

$$|\psi_i\rangle = c_1|\phi_1\rangle + c_2|\phi_2\rangle \tag{14.13C.1}$$

This equation is substituted in the Schrödinger equation:

$$\hat{H}|\psi_i\rangle = E_i|\psi_i\rangle$$

with $\hat{H}$ the Hamiltonian and E_i the energy corresponding to the molecular orbital to give:

$$\hat{H}c_1|\phi_1\rangle + \hat{H}c_2|\phi_2\rangle = Ec_1|\phi_1\rangle + Ec_2|\phi_2\rangle \tag{14.13C.2}$$

If Equation 14.13C.2 is multiplied by $\langle\phi_1|$ (and integrated), then

$$c_1(H_{11} - ES_{11}) + c_2(H_{12} - ES_{12}) = 0 \tag{14.13C.3}$$

where H_{ij} are the Hamiltonian matrix elements (see note below)

$$H_{ij} = \langle\phi_i|\hat{H}|\phi_j\rangle = \int \phi_i H \phi_j \mathrm{d}v$$

and S_{ij} are the overlap integrals.

$$S_{ij} = \langle\phi_i|\phi_j\rangle = \int \phi_i \phi_j \mathrm{d}v$$

If Equation 14.13C.2 is multiplied by $\langle\phi_2|$ (and integrated), then

$$c_1(H_{21} - ES_{21}) + c_2(H_{22} - ES_{22}) = 0 \tag{14.13C.4}$$

Both Equations 14.13C.3 and 14.13C.4 can better represented in matrix notation,

$$\begin{bmatrix} c_1(H_{11} - ES_{11}) + c_2(H_{12} - ES_{12}) \\ c_1(H_{21} - ES_{21}) + c_2(H_{22} - ES_{22}) \end{bmatrix} = 0$$

or more simply as a product of matrices.

$$\begin{bmatrix} H_{11} - ES_{11} & H_{12} - ES_{12} \\ H_{21} - ES_{21} & H_{22} - ES_{22} \end{bmatrix} \times \begin{bmatrix} c_1 \\ c_2 \end{bmatrix} = 0 \tag{14.13C.5}$$

All diagonal Hamiltonian integrals H_{ii} are called **Coulomb integrals** and those of type H_{ij} are called **resonance integrals**. Both integrals are negative and the resonance integrals determines the strength of the bonding interactions. The equations described by Equation 14.13C.5 are called the ***secular equations*** and will also have the trivial solution of

$$c_1 = c_2 = 0$$

Within linear algebra, the secular equations in Equation 14.13C.5 will also have a non-trivial solution, if and only if, the secular determinant is zero

$$\begin{vmatrix} H_{11} - ES_{11} & H_{12} - ES_{12} \\ H_{21} - ES_{21} & H_{22} - ES_{22} \end{vmatrix} = 0 \tag{14.13C.6}$$

or in shorthand notation

$$\det(H - ES) = 0$$

Everything in Equation 14.13C.6 is a known number except E. Since the secular determinant for ethylene is a 2×2 matrix, finding E, requires solving a quadratic equation (after expanding the determinant)

$$(H_{11} - ES_{11})(H_{22} - ES_{22}) - (H_{21} - ES_{21})(H_{12} - ES_{12}) = 0$$

There will be two values of E which satisfy this equation and they are the molecular orbital energies. For ethylene, one will be the bonding energy and the other the antibonding energy for the π-orbitals formed by the combination of the two carbon $2p_z$ orbitals (Equation 14.13C.1). However, if more than two $|\phi\rangle$ atomic orbitals were used, e.g., in a bigger molecule, then more energies would be estimated by solving the secular determinant.

Solving the secular determinant is simplified within Hückel method via the following four assumptions:

1. All overlap integrals S_{ij} are set equal to zero. This is quite reasonable since the $\pi -$ orbitals are directed perpendicular to the direction of their bonds (Figure 10.5.1). This assumption is often call neglect of differential overlap (NDO).
2. All resonance integrals H_{ij} between non-neighboring atoms are set equal to zero.
3. All resonance integrals H_{ij} between neighboring atoms are equal and set to β.
4. All coulomb integrals H_{ii} are set equal to α.

These assumptions are mathematically expressed as

$$H_{11} = H_{22} = \alpha$$

$$H_{12} = H_{21} = \beta$$

Assumptions 1 means that the overlap integral between the two atomic orbitals is 0

$$S_{11} = S_{22} = 1$$

$$S_{12} = S_{21} = 0$$

Matrix Representation of the Hamiltonian

The Coulomb integrals

$$H_{ii} = \langle \phi_i | H | \phi_i \rangle$$

and resonance integrals.

$$H_{ij} = \langle \phi_i | H | \phi_j \rangle \;\; (i \neq i)$$

are often described within the matrix representation of the Hamiltonian (specifically within the $|\phi\rangle$ basis):

$$\hat{H} = \begin{bmatrix} H_{11} & H_{12} \\ H_{21} & H_{22} \end{bmatrix}$$

or within the Hückel assumptions

$$\hat{H} = \begin{bmatrix} \alpha & \beta \\ \beta & \alpha \end{bmatrix}$$

The Hückel assumptions reduces Equation 14.13C.5 in two homogeneous equations:

$$\begin{bmatrix} \alpha - E & \beta \\ \beta & \alpha - E \end{bmatrix} \times \begin{bmatrix} c_1 \\ c_2 \end{bmatrix} = 0 \tag{14.13C.7}$$

if Equation 14.13C.7 is divided by β:

$$\begin{bmatrix} \dfrac{\alpha - E}{\beta} & 1 \\ 1 & \dfrac{\alpha - E}{\beta} \end{bmatrix} \times \begin{bmatrix} c_1 \\ c_2 \end{bmatrix} = 0$$

and then a new variable x is defined

$$x = \frac{\alpha - E}{\beta} \tag{14.13C.8}$$

then Equation 14.13C.7 simplifies to

$$\begin{bmatrix} x & 1 \\ 1 & x \end{bmatrix} \times \begin{bmatrix} c_1 \\ c_2 \end{bmatrix} = 0 \tag{14.13C.9}$$

The trivial solution gives both wavefunction coefficients equal to zero and the other (non-trivial) solution is determined by solving the secular determinant

$$\begin{vmatrix} x & 1 \\ 1 & x \end{vmatrix} = 0$$

which when expanded is $x^2 - 1 = 0$ so $x = \pm 1$.

Knowing that $E = \alpha - x\beta$ from Equation 14.13C.8, the energy levels can be found to be

$$E = \alpha - \pm 1 \times \beta$$

or

$$E = \alpha \mp \beta$$

Since β is negative, the two energies are ordered (Figure 10.5.4)

- For π_1: $E_1 = \alpha + \beta$
- For π_2: $E_2 = \alpha - \beta$

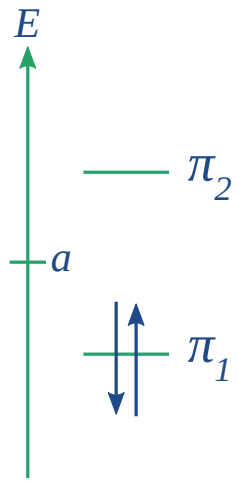


Figure 10.5.4 : π energies of ethylene with occupation. (CC BY-NC; Ümit Kaya via LibreTexts)

To extract the coefficients attributed to these energies, the corresponding x values can be substituted back into the Secular Equations (Equation 14.13C.9). For the lower energy state ($x = -1$)

$$\begin{bmatrix} -1 & 1 \\ 1 & -1 \end{bmatrix} \times \begin{bmatrix} c_1 \\ c_2 \end{bmatrix} = 0$$

This gives $c_1 = c_2$ and the molecular orbitals attributed to this energy is then (based off of Equation 14.13C.1):

$$|\psi_1\rangle = N_1(\phi_1\rangle + |\phi_2\rangle) \tag{14.13C.10}$$

where N_1 is the normalization constant for this molecular orbital; this is the **bonding** molecular orbital.

For the higher energy molecular orbital ($x = -1$) and then

$$\begin{bmatrix} 1 & 1 \\ 1 & 1 \end{bmatrix} \times \begin{bmatrix} c_1 \\ c_2 \end{bmatrix} = 0$$

This gives $c_1 = -c_2$ and the molecular orbitals attributed to this energy is then (based off of Equation 14.13C.1):

$$\psi_2\rangle = N_2(\phi_1\rangle - |\phi_2\rangle) \tag{14.13C.11}$$

where N_2 is the normalization constant for this molecular orbital; this is the **anti-bonding** molecular orbital.

The normalization constants for both molecular orbitals can obtained via the standard normalization approach (i.e., $\langle\psi_i|\psi_i\rangle = 1$) to obtain

$$N_1 = N_2 = \frac{1}{\sqrt{2}}$$

These molecular orbitals form the π-bonding framework and since each carbon contributes one electron to this framework, only the lowest molecular orbital ($|\psi_1\rangle$) is occupied (Figure 10.5.5) in the ground state. The corresponding electron configuration is then π_1^2.

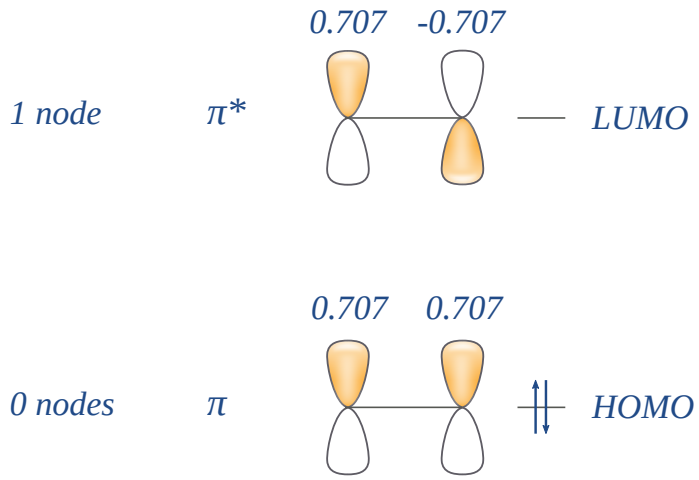


Figure 10.5.5 : Schemetic representation of the π molecular orbitals framework for ethylene . Notice that the antibonding molecular orbital has one more node than the bonding molecular orbital as expected since it is higher in energy. (CC BY-NC; Ümit Kaya via LibreTexts)

HOMO and LUMO are acronyms for highest occupied molecular orbital and lowest unoccupied molecular orbital, respectively and are often referred to as frontier orbitals. The energy difference between the HOMO and LUMO is termed the HOMO–LUMO gap.

The 3-D calculated π molecular orbitals are shown in Figure 10.5.6 .

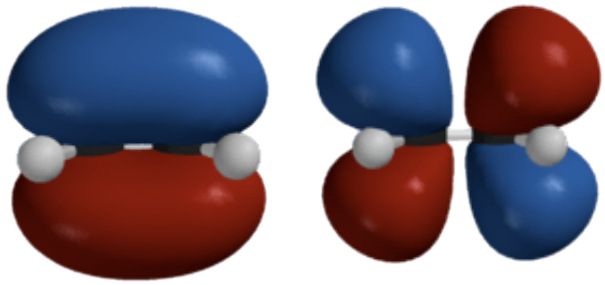


Figure 10.5.6 : Calculated π molecular orbitals for ethylene . (left) the bonding orbital (|\psi_1 \rangle\) and (right) the antibonding $(|\psi_2\rangle$ orbital.

Limitations of Hückel Theory

Hückel theory was developed in the 1930's when computers were unavailable and a simple mathematical approaches were very important for understanding experiment. Although the assumptions in Hückel theory are drastic they enabled the early calculations of molecular orbitals to be performed with mechanical calculators or by hand. Hückel Theory can be extended to address other types of atoms in conjugated molecules (e.g., nitrogen and oxygen). Moreover, it can be extended to also treat σ orbitals and this "Extended Hückel Theory" is still used today. Despite the utility of Hückel Theory, it is highly qualitative and we should remember the limitations of Hückel Theory:

- Hückel Theory is very approximate
- Hückel Theory cannot calculate energies accurately (electron-electron repulsion is not calculated)
- Hückel Theory typically overestimates predicted dipole moments

Hückel Theory is best used to provide simplified models for understanding chemistry and for a detailed understanding modern *ab initio* molecular methods discussed in Chapter 11 are needed.

This page titled 14.13C: Hückel MO Theory is shared under a license and was authored, remixed, and/or curated by LibreTexts.

- 10.5: The pi-Electron Approximation of Conjugation (Hückel Theory) by Seymour Blinder is licensed CC BY-NC-SA 4.0.

14.13D: Molecular Mechanisms (MM)

This page titled 14.13D: Molecular Mechanisms (MM) is shared under a license and was authored, remixed, and/or curated by LibreTexts.

14.14: MAGNETISM

- Topic hierarchy

14.14.1: example magnetic moment data and their interpretation

14.14.2: Magnetic Moments

14.14.3: Magnetic Moments 1

14.14.4: Magnetic Susceptibility Measurements

14.14.5: Magnetism

This page titled 14.14: Magnetism is shared under a license and was authored, remixed, and/or curated by LibreTexts.

- 4.14: Magnetism is licensed CC BY-NC-SA 4.0.

14.14.1: example magnetic moment data and their interpretation

Summary of applicable formulae

1) Spin-Only magnetic moment
$\mu_{s.o.} = \sqrt{\{4S(S+1)\}}$ B.M.

2) For A and E ground terms
$\mu_{eff} = \mu_{s.o.} (1-\alpha \lambda / \Delta)$ B.M.
Do not expect Temperature dependence.

3) For T ground terms with orbital angular momentum contribution
$\mu_{S+L} = \sqrt{\{4S(S+1) + L(L+1)\}}$ B.M.
T terms generally show marked Temperature dependence.

The examples that follow are arranged showing the experimentally observed values, the theoretical "spin-only" value and possible variations expected.

A number of the examples involve "alums" where the central Transition Metal ion can be considered to be octahedrally coordinated by water molecules.

---

d^1

VCl_4
V(IV) tetrahedral

01	80K	300K	μs.o. /B.M.
02	1.6	1.6	1.73

^2E ground term - hence don't expect Temperature dependence and small variation from spin-only value can be accounted for by equation 2) above. For less than a half-filled d shell, the sign of λ is positive so the effect on μ should be that $\mu_{eff} < \mu_{s.o.}$

VCl_6^{2-}
V(IV) octahedral

01	80K	300K	μs.o. /B.M.
02	1.4	1.8	1.73

$^2T_{2g}$ ground term - hence do expect Temperature dependence and large variation from spin-only value may be observed at low temperatures.
Since there is a direct orbital angular momentum contribution we should calculate μ_{S+L} from equation 3) above.
For a full S+L contribution this would give $\mu_{S+L} = 3$ B.M. which is clearly much higher than the 1.8 B.M. found at 300K. So, $\mu_{s.o.} < \mu_{obs} < \mu_{S+L}$
showing that the magnetic moment is partially quenched.

d^2

V^{3+} in $(NH_4)V(SO_4)_2.12H_2O$ (an alum)
V(III) octahedral

01	80K	300K	μs.o. /B.M.
02	2.7	2.7	2.83

$^3T_{1g}$ ground term - hence do expect Temperature dependence and large variation from spin-only value may be observed at low temperatures.
Since there is a direct orbital angular momentum contribution we should calculate μ_{S+L} from equation 3) above.
For a full S+L contribution this would give $\mu_{S+L} = \sqrt{(20)} = 4.47$ B.M. which is clearly much higher than the 2.7 B.M. found at 300K.
So, $\mu_{obs} < \mu_{s.o.} < \mu_{S+L}$
showing that the magnetic moment is significantly quenched.
In this case, there is no observed Temperature variation between 80 and 300K and it may require much lower temperatures to see the effect?

d^3

Cr^{3+} in $KCr(SO_4)_2.12H_2O$ (an alum)
Cr(III) octahedral

01	80K	300K	μs.o. /B.M.
02	3.8	3.8	3.87

$^4A_{2g}$ ground term - hence don't expect Temperature dependence and small variation from spin-only value can be accounted for by equation 2) above. For less than a half-filled d shell the sign of λ is positive so the effect on μ should be that $\mu_{eff} < \mu_{s.o.}$

d^4

$CrSO_4.6H_2O$
Cr(II) octahedral

01	80K	300K	μs.o. /B.M.
02	4.8	4.8	4.9

^5E_g ground term - hence don't expect Temperature dependence and small variation from spin-only value can be accounted for by equation 2) above. For less than a half-filled d shell the sign of λ is positive so the effect on μ should be that $\mu_{eff} < \mu_{s.o.}$

$K_3Mn(CN)_6$
Mn(III) low-spin octahedral

01	80K	300K	μs.o. /B.M.
02	3.1	3.2	2.83

$^3T_{1g}$ ground term - hence do expect Temperature dependence and large variation from spin-only value may be observed at low temperatures.
Since there is a direct orbital angular momentum contribution we should calculate μ_{S+L} from equation 3) above.
For a full S+L contribution this would give $\mu_{S+L} = \sqrt{(20)} = 4.47$ B.M. which is clearly much higher than the 3.2 B.M. found at 300K.

So, $\mu_{s.o.} < \mu_{obs} < \mu_{S+L}$
showing that the magnetic moment is partially quenched.
In this case, there is a small Temperature variation observed between 80 and 300K.

d^5

$K_2Mn(SO_4)_2.6H_2O$ (an alum)
Mn(II) high-spin octahedral

01	80K	300K	μs.o. /B.M.
02	5.9	5.9	5.92

$^6A_{1g}$ ground term - hence do not expect Temperature dependence and L=0 so no orbital contribution possible.
Expect $\mu_{eff} = \mu_{s.o.}$

$K_3Fe(CN)_6$
Fe(III) low-spin octahedral

01	80K	300K	μs.o. /B.M.
02	2.2	2.4	1.73

$^2T_{2g}$ ground term - hence do expect Temperature dependence and large variation from spin-only value may be observed at low temperatures.
Since there is a direct orbital angular momentum contribution we should calculate μ_{S+L} from equation 3) above.
For a full S+L contribution this would give $\mu_{S+L} = \sqrt{(9)} = 3$ B.M. which is clearly much higher than the 2.4 B.M. found at 300K.
So, $\mu_{s.o.} < \mu_{obs} < \mu_{S+L}$
showing that the magnetic moment is partially quenched.

d^6

Fe^{2+} in $(NH_4)_2Fe(SO_4)_2.6H_2O$ (an alum)
Fe(II) high-spin octahedral

01	80K	300K	μs.o. /B.M.
02	5.4	5.5	4.9

$^5T_{2g}$ ground term - hence do expect Temperature dependence and large variation from spin-only value may be observed at low temperatures.
Since there is a direct orbital angular momentum contribution we should calculate μ_{S+L} from equation 3) above.
For a full S+L contribution this would give $\mu_{S+L} = \sqrt{(30)} = 5.48$ B.M. which is close to the 5.5 B.M. found at 300K.
So, $\mu_{s.o.} < \mu_{obs} \sim \mu_{S+L}$
showing that the magnetic moment is not showing much quenching.

d^7

Cs_2CoCl_4
Co(II) tetrahedral

01	80K	300K	μs.o. /B.M.

02	4.5	4.6	3.87

$^4A_2$ ground term - hence don't expect Temperature dependence and small variation from spin-only value can be accounted for by equation 2) above. For more than a half-filled d shell the sign of λ is negative so the effect on μ should be that $\mu_{eff} > \mu_{s.o.}$
The observed values are somewhat bigger than expected for the small (0.2 B.M.) variation due to equation 2) so other factors must be affecting the magnetic moment. These effects will not be covered in this course!

Co^{2+} in $(NH_4)_2Co(SO_4)_2.6H_2O$ (an alum)
Co(II) high-spin octahedral

01	80K	300K	μs.o. /B.M.
02	4.6	5.1	3.88

$^4T_{1g}$ ground term - hence do expect Temperature dependence and large variation from spin-only value may be observed at low temperatures.
Since there is a direct orbital angular momentum contribution we should calculate μ_{S+L} from equation 3) above.
For a full S+L contribution this would give $\mu_{S+L} = \sqrt{(27)} = 5.2$ B.M. which is close to the 5.1 B.M. found at 300K.
So, $\mu_{s.o.} < \mu_{obs} \sim \mu_{S+L}$
showing that the magnetic moment is not showing much quenching.

d^8

Ni^{2+} in $(NH_4)_2Ni(SO_4)_2.6H_2O$ (an alum)
Ni(II) octahedral

01	80K	300K	μs.o. /B.M.
02	3.3	3.3	2.83

$^3A_{2g}$ ground term - hence don't expect Temperature dependence and small variation from spin-only value can be accounted for by equation 2) above. For more than a half-filled d shell the sign of λ is negative so the effect on μ should be that $\mu_{eff} > \mu_{s.o.}$
The observed values are somewhat bigger than expected for the small (0.2 B.M.) variation due to equation 2) so other factors must be affecting the magnetic moment. These effects will not be covered in this course!

$(Et_4N)_2NiCl_4$
Ni(II) tetrahedral

01	80K	300K	μs.o. /B.M.
02	3.2	3.8	2.83

$^3T_2$ ground term - hence do expect Temperature dependence and large variation from spin-only value may be observed at low temperatures.
Since there is a direct orbital angular momentum contribution we should calculate μ_{S+L} from equation 3) above.
For a full S+L contribution this would give $\mu_{S+L} = \sqrt{(20)} = 4.47$ B.M. which is higher than the 3.8 B.M. found at 300K.
So, $\mu_{s.o.} < \mu_{obs} < \mu_{S+L}$
showing that the magnetic moment is partially quenched.

d^9

Cu^{2+} in $(NH_4)_2Cu(SO_4)_2.6H_2O$ (an alum)
Cu(II) octahedral

```
        80K         300K              μs.o. /B.M.
        1.9         1.9                    1.73
```

^2E_g ground term - hence don't expect Temperature dependence and small variation from spin-only value can be accounted for by equation 2) above. For more than a half-filled d shell the sign of λ is negative so the effect on μ should be that $\mu_{eff} > \mu_{s.o.}$

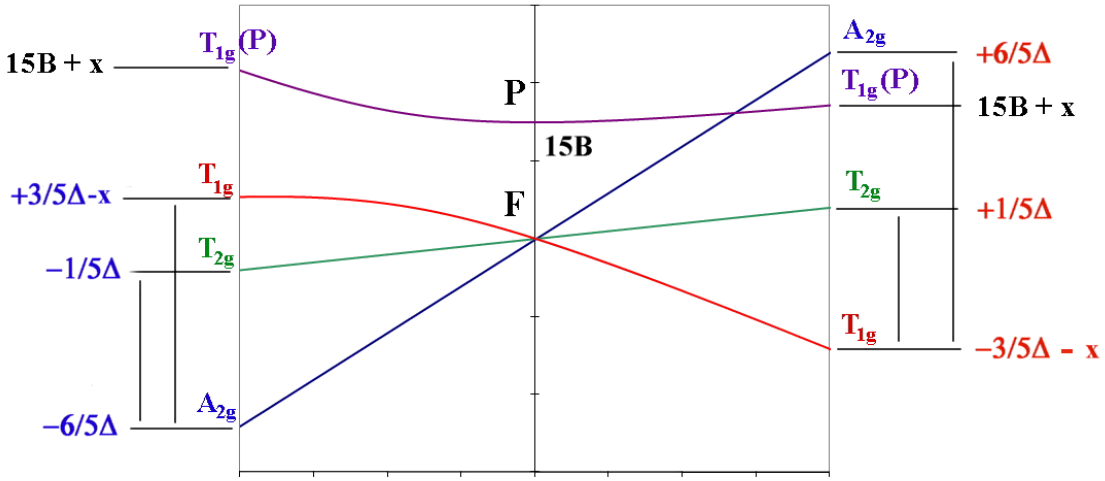
Contributors and Attributions

- Prof. Robert J. Lancashire (The Department of Chemistry, University of the West Indies)

This page titled 14.14.1: example magnetic moment data and their interpretation is shared under a license and was authored, remixed, and/or curated by LibreTexts.

- 4.14.1: example magnetic moment data and their interpretation is licensed CC BY-NC-SA 4.0.

14.14.2: Magnetic Moments



oct d^3,d^8 tet d^2,d^7 ←----------→ oct d^2,d^7 tet d^3,d^8

Three peaks are predicted in their electronic spectra, namely:

- $^4T_2 \leftarrow {}^4A_2$ ν1
- $^4T_1(F) \leftarrow {}^4A_2$ ν2
- $^4T_1(P) \leftarrow {}^4A_2$ ν3 ** the band observed in the visible region

The energy of the third transitions is approximately ν_3 = 6/5 Δ + 15B (where B is the Racah parameter and ignoring configuration interactions). For Co(II) tetrahedral complexes B has generally been found to be about 750 cm^{-1}. Hence Δ for the three complexes above can be calculated to be roughly, Δ = (ν_3 - 15x750) x 5/6, or:

$Copyr_2Cl_2$ (16260-15x750) x 5/6 = 4175 cm^{-1}
$Copyr_2Br_2$ (15870-15x750) x 5/6 = 3850 cm^{-1}
$Copyr_2I_2$ (14925-15x750) x 5/6 = 3063 cm^{-1}

For three unpaired electrons the spin only magnetic moment is predicted to be 3.87 BM. Using a value for the free ion spin orbit coupling constant (λ) of -172 cm^{-1} then a better approximation of the magnetic moment can be obtained by using the third formula above. This would give a value of:

- $Copyr_2Cl_2$ 3.87*(1+ 688/4175) = 4.49 B.M. found 4.42 BM
- $Copyr_2Br_2$ 3.87*(1+ 688/3850) = 4.57 B.M. found 4.50 BM
- $Copyr_2I_2$ 3.87*(1+ 688/3063) = 4.76 B.M. found 4.48 BM

In the case of the series;

$$CoI_4^{2-},\ CoBr_4^{2-},\ CoCl_4^{2-},\ Co(NCS)_4^{2-}$$

the magnetic moments have been recorded as

4.77, 4.65, 4.59, 4.40 BM

showing even more clearly the inverse effect of the spectrochemical series on the magnetic moment.

This page titled 14.14.2: Magnetic Moments is shared under a license and was authored, remixed, and/or curated by LibreTexts.

- 4.14.2: Magnetic Moments is licensed CC BY-NC-SA 4.0.

14.14.3: Magnetic Moments 1

Magnetic Moments

Lecture 4. CHEM1902 Coordination Chemistry

Magnetic moments are often used in conjunction with electronic spectra to gain information about the oxidation number and stereochemistry of the central metal ion in coordination complexes.

A common laboratory procedure for the determination of the magnetic moment for a complex is the Gouy method which involves weighing a sample of the complex in the presence and absence of a magnetic field and observing the difference in weight. A template is provided for the calculations involved.

For first row transition metal ions in the free ion state, i.e. isolated ions in a vacuum, all 5 of the 3d orbitals are degenerate.

A simple crystal field theory approach to the bonding in these ions assumes that when they form octahedral complexes, the energy of the d orbitals are no longer degenerate but are split such that two orbitals, the d_{x2-y2} and the d_{z2} (e_g subset) are at higher energy than the d_{xy}, d_{xz}, d_{yz} orbitals (the t_{2g} subset).

For octahedral ions with between 4 and 7 d electrons, this gives rise to 2 possible arrangements called either high spin/ weak field or low spin/strong field respectively. The energy gap is dependent on the position of the coordinated ligands in the SPECTROCHEMICAL SERIES.

See an interactive JAVA applet for examples.

Note: For CHEM1902, we assume that all Co(III), d^6 complexes are octahedral and LOW spin, i.e. t_{2g}^6.

In tetrahedral complexes, the energy levels of the orbitals are again split, such that the energy of two orbitals, the d_{x2-y2} and the d_{z2} (e subset) are now at lower energy (more favoured) than the remaining three d_{xy}, d_{xz}, d_{yz} (the t2 subset) which are destabilised.

Tetrahedral complexes are ALL high spin since the difference between the 2 subsets of energies of the orbitals is much smaller than is found in octahedral complexes.

The usual relationship quoted between them is: $\Delta_{tet} \approx 4/9\ \Delta_{oct}$.

Square planar complexes are less commmon than tetrahedral and **for CHEM1902 we will assume that the only ions forming square planar complexes are d^8 e.g. Ni(II), Pd(II), Pt(II), etc.** *d^8 can therefore be either square planar or tetrahedral.* As with octahedral complexes, the energy gap between the dxy and dx^2-y^2 is Δoct and these d^8 systems are all considered strong field / low spin complexes hence they are all diamagnetic, μ=0 Bohr Magneton (B.M.).

The formula used to calculate the spin-only magnetic moment can be written in two forms; the first based on the number of **unpaired** electrons, n, and the second based on the **total** electron spin quantum number, S. Since for each unpaired electron, n=1 and S=1/2 then the two formulae are clearly related and the answer obtained must be identical.

Return to Coordination Chemistry Course Outline.

Dr Bird logoReturn to Chemistry, UWI-Mona, Home Page

Copyright © 1995-2015 by Robert John Lancashire, all rights reserved.

Prof. Robert J. Lancashire,
The Department of Chemistry, University of the West Indies,

Mona Campus, Kingston 7, Jamaica.

Created Dec 1995. Links checked and/or last modified 23rd March 2015.
URL http://wwwchem.uwimona.edu.jm/spectra/MagMom.html

This page titled 14.14.3: Magnetic Moments 1 is shared under a license and was authored, remixed, and/or curated by LibreTexts.

- 4.14.3: Magnetic Moments 1 is licensed CC BY-NC-SA 4.0.

14.14.4: Magnetic Susceptibility Measurements

The Gouy Method

Perhaps the simplest technique for measuring the magnetic susceptibility of metal complexes is the Gouy Method.

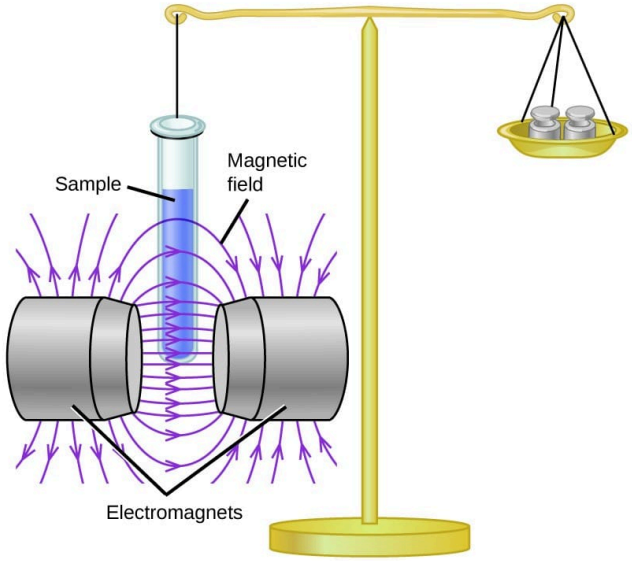


Figure 14.14.4.1: A Gouy balance compares the mass of a sample in the presence of a magnetic field with the mass with the electromagnet turned off to determine the number of unpaired electrons in a sample. (CC BY-SA 3.0; OpenStax).

From a classical description of magnetism, Lenz's Law (around 1834) can be written as

$$\frac{B}{H} = 1 + 4\pi\frac{I}{H} \tag{14.14.4.1}$$

or

$$\frac{B}{H} = 1 + 4\pi\kappa \tag{14.14.4.2}$$

where

- B/H is called the **magnetic permeability** of the material and
- κ is the magnetic susceptibility per unit volume (I/H).

The determination of a **magnetic susceptibility** depends on the measurement of B/H. Experimentally, the Gouy method involves measuring the force on the sample by a magnetic field and is dependent on the tendency of a sample to concentrate a magnetic field within itself.

At any given point, dx, of the sample, the force is given by:

$$dF = \mu\backslash\mathrm{circH}\ \kappa\ dV\left(\frac{dH}{dx}\right) \tag{14.14.4.3}$$

where

- μ° is the permeability of a vacuum (=1 when using c.g.s. units)
- H is the magnitude of the magnetic field at point, dx,
- dV is the volume of the sample at point dx,

- κ is the magnetic susceptibility per unit volume.

The sample is uniformly packed into a glass tube (Gouy tube) each end of which is at a constant field strength. This is attained by using a tube that is packed to a certain height (say 10 cm) and the tube is suspended between the poles of a magnet such that the bottom of the sample is in the center of the field (a region where a uniform field strength can be readily obtained) whilst the top of the sample is out of the field, i.e. $H = 0$. By integrating the above equation, the total force on the sample can be given as:

$$F = \frac{1}{2}\mu^{\circ} A\kappa(H^2 - H^{\circ 2}) \tag{14.14.4.4}$$

and since $H^o = 0$ at the top of the sample then

$$F = \frac{1}{2}\mu^{\circ} A\kappa H^2 \tag{14.14.4.5}$$

where A is the cross sectional area of the sample.

The force is measured by the apparent change in mass when the magnetic field is switched on, or

$$F = g\ \delta w = \frac{1}{2}\mu^{\circ} A\kappa H^2 \tag{14.14.4.6}$$

where δw is the apparent change in mass, and g is the acceleration due to gravity.

An allowance needs to be made for the tube, since it will have its own magnetic properties as a result of the air within the tube (which is displaced from the tube when the sample is introduced) and also from the materials used in its construction. Equation 14.14.4.6 becomes:

$$g\delta w' = 1/2A\mu^{o}(\kappa - \kappa')H^2$$

where

- $\delta w' = \delta w + \delta$
- δ is a constant allowing for the magnetic properties of the empty tube
- κ' is the volume susceptibility of the displaced air.

This leads to:

$$\kappa = \frac{2g\delta w'}{\mu^{\circ} AH^2} + \kappa'$$

Converting from volume susceptibility to gram susceptibility (χ_g) leads to:

$$\chi_g = \frac{\kappa}{\rho} = \frac{\kappa\ V}{W}$$

where ρ is the density of the sample so that

$$\chi_g = \frac{\beta\delta w'}{W} + \frac{\kappa' V}{W}$$

or

$$\chi_g = \frac{\alpha + \beta\delta w'}{W}$$

where

- α is a constant allowing for the air displaced by the sample,
- β is a constant that is dependent on the field strength, = $\frac{2gV}{\mu^{\circ} AH^2}$
- W is the weight of the sample used.

Written more simply then:

$$\chi_g\ (cal) = \frac{\beta\delta w'}{W\ (cal)} + \cancelto{\approx 0}{\frac{\alpha}{W\ (cal)}}$$

the last expression is usually negligible.

β is then obtained and from this

$$\chi_g\ (sample) = \frac{\beta\delta w'}{W\ (sample)} + \cancelto{\approx 0}{\frac{\alpha}{W\ (sample)}}$$

the χ_g sample can be obtained, again the factor for the susceptibility of air is usually negligible.

To accurately determine the gram magnetic susceptibility of a sample, it is necessary to predetermine the value of the constants α, β and δ. Since these constants are dependent on the amount of sample placed in the tube, the tube itself and the magnetic field strength, it should be emphasized that each experimenter **must** determine these constants for their particular configuration. That is, results obtained with one tube are **not transferable** to other Gouy tubes.

The field strength is determined by the current supplied to the electromagnet. In order to ensure a constant magnetic field strength from one measurement to the next, always set the current to the same value. Note that the magnet may display hysteresis effects so that if you do go beyond the 5 Amp value it may take some time to reestablish itself, after you have decreased the power.

Determination of the Constants

Select a tube and piece of nichrome wire to make an assembly which will allow the tube to be suspended from the analytical balance so that the bottom of the tube is aligned halfway between the polefaces of the magnet and the top of the sample is above the magnet and hence subject to essentially zero field, H=0.



1: Determining δ

Adjust the zero setting on the balance, then suspend the empty tube from the balance and weigh it (W1). Set the field to the required strength and reweigh the tube (W2). The force on the tube, δ, therefore is:

$$\delta = W2 - W1 \tag{14.14.4.7}$$

this will normally be negative since the tubes are generally diamagnetic and pushed out of the field, ie. weigh less.

2: Determining α

Fill the tube to the required height with water and weigh it (check the zero first), this will give W3. Assuming the density of water at this temperature is 1.00 g cm^{-3} this gives the volume of water (and also that of the sample).

vol. =(W3-W1)/1.00 where the weight changes should be expressed in g.

$$\alpha = \kappa'.V \tag{14.14.4.8}$$

α= 0.029 x (W3-W1) in 10^{-6} c.g.s. units,

where 0.029 is the volume susceptibility of air /cm^3. For strongly paramagnetic samples this correction is generally insignificant.

3: Determining β

The determination of β requires the use of a compound whose magnetic properties have been well established. Common calibrants include $HgCo(SCN)_4$ and $[Ni(en)_3]S_2O_3$. Since the magnetic properties are often temperature dependent, the susceptibility of the calibrant must be calculated for the temperature at which the sample is measured.

Record the temperature, T1. Fill the tube to the required height with the calibrant (in this case either $HgCo(SCN)_4$ or $[Nien_3]S_2O_3$ and weigh it with the field off (W4) and with the field on (W5).

For $HgCo(SCN)_4$ the following relationship can be used:

χ_g = 4985 / (T+10) in 10^{-6} c.g.s units at temperature T, while the corresponding relationship for $[Ni(en)_3]S_2O_3$ is:

$$\chi_g = 3172 / T \text{ in } 10^{-6} \text{ c.g.s units at temperature T}$$

Using this χ_g then

$$\beta = \frac{\chi_g W - \alpha}{\delta w'}$$

where $\delta w' = (W5 - W4) - \delta$ in mg and $W = (W4 - W1)$ in g

Determination of the Magnetic Susceptibility of your sample

Once α and β are known, then $\chi_{m'}$ can be determined for the sample in question. Fill the tube to the required height with your sample and weigh it with the field off (W6) and with the field on (W7). From this calculate:

$$\chi_g = \frac{\alpha + \beta\delta w'}{W}$$

where δw' = (W7 - W6) - δ in mg and W = (W6 - W1) in g

To convert from χ_g to χ_m the molar mass must be accurately known, since:

$$\chi_m = \chi_g x R.M.M.$$

The final correction is for the diamagnetism of the sample

$$\chi'_m = \chi_m + \chi_m(dia)$$

where $\chi_m(dia)$ is the susceptibility arising from the diamagnetic properties of the electron pairs (and therefore not a property of the unpaired electrons) and must be allowed for. The values for $\chi_m(dia)$ have been well documented (Pascal's constants) for different atoms and ions and a selection of them are tabulated.

To summarize, the overall procedure is:

```
Weigh the empty tube              - magnet off/on   W1/W2
Weigh the tube with water         - magnet off      W3
Weigh the tube with calibrant     - magnet off/on   W4/W5
Weigh the tube with your sample   - magnet off/on   W6/W7
Record the temperature(s) of calibrant/sample       T1/T2 in K
Calculate the Molar Mass of your sample             M.M.
Estimate the total diamagnetic correction for your sample D.C.
```

Calculate the magnetic moment using:

&delta = (W2 - W1) in mg

$\alpha = 0.029 \times (W3 - W1)$ in 10^{-6} c.g.s. units

$\beta = [(\chi_m\{Calibrant\}) (W4 - W1) - \alpha] / [(W5 - W4) - \delta]$ at temperature T1

χ_m {Sample} = $[\alpha + \beta \{(W7 - W6) - \delta\}]/(W6 - W1)$ at temperature T2

$\chi'_m = (\chi_m \times R.M.M.) + \chi_m$ dia

also $\chi'_m = \mu \circ \mu_b^2 N/3k. \mu eff^2/T$

where μ_b is the Bohr Magneton, N is Avogadro's number and k is the Boltzmann constant. Hence,

$\mu_{eff} = \sqrt{} (3k/\mu \circ \mu_b^2 N). \sqrt{} (\chi'_m T2)$ B.M.

or $\mu_{eff} = 2.828 \sqrt{} (\chi'_m T2 \times 10^{-6})$ at temperature T2

where the 10^{-6} that has been ignored in these expressions is finally included.

(Determination of the magnetic moment using the Gouy method has been simplified by the use of an on-line template or spreadsheet.)

This page titled 14.14.4: Magnetic Susceptibility Measurements is shared under a license and was authored, remixed, and/or curated by Robert J. Lancashire.

- 4.14.4: Magnetic Susceptibility Measurements by Robert J. Lancashire is licensed CC BY-NC-SA 4.0. Original source: http://wwwchem.uwimona.edu.jm/lab_manuals/gouytheory.html.

14.14.5: Magnetism

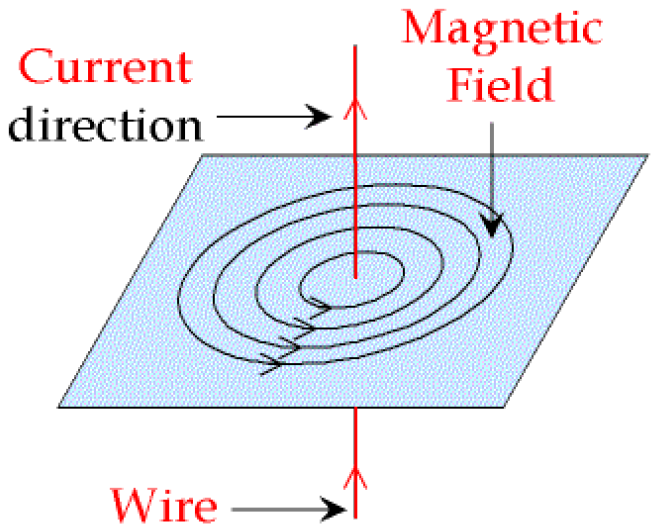


***Figure 1**: The "Right Hand Rule" for an induced magnetic field*

In an atom, the magnetic field is due to the coupled spin and orbital magnetic moments associated with the motion of electrons. The spin magnetic moment is due to the precession of the electrons about their own axes where as the orbital magnetic moment is due to the motion of electrons around the nucleus. The resultant combination of the spin and orbital magnetic moments of the constituent atoms of a material gives rise to the observed magnetic properties.

Historically, magnetism has been recognized for thousands of years. An account, that is probably apochryphal, tells of a shepherd called Magnes in Crete who around 900 B.C discovered the naturally occurring magnet lodestone (a form of the the spinel magnetite, Fe_3O_4) in a region later named Magnesia. Supposedly while he was walking over a deposit, the lodestone pulled the nails out of his sandals and the metal tip from his staff.

Contributors and Attributions

- Prof. Robert J. Lancashire (The Department of Chemistry, University of the West Indies)

This page titled 14.14.5: Magnetism is shared under a license and was authored, remixed, and/or curated by LibreTexts.

- 4.14.5: Magnetism is licensed CC BY-NC-SA 4.0.

Tanabe Sugano Diagrams

02: Tanabe Sugano Diagrams

This page titled Tanabe Sugano Diagrams is shared under a license and was authored, remixed, and/or curated by LibreTexts.

INDEX

A

antifluorite
12.3D: Structure - Antifluorite

Aufbau principle
2.2.3: Aufbau Principle

B

bent
3.2: Valence Shell Electron-Pair Repulsion

block diagonal
6.7.2: Representations of Point Groups

bond angle
3.2: Valence Shell Electron-Pair Repulsion

Bromobenzene
13.1: What is Organometallic Chemistry?

C

ccp
12.3E: Structure - Zinc Blende (ZnS)

character (matrix)
6.7.2: Representations of Point Groups

character table
6.6: Character Tables

compression
8.1.2: The Jahn-Teller Effect

conductivity
12.2A: Electrical Conductivity and Resistivity

cubic closet packing
12.3E: Structure - Zinc Blende (ZnS)

D

dipole moment
3.2: Valence Shell Electron-Pair Repulsion
3.3: Molecular Polarity

Drago and Wayland's EC Model
5.6.1: Quantitative Measures of Hardness, Softness, and Acid-Base Interactions from a Hard Soft Acid-Base Principle perspective involve orbital energies and or apportioning acid-base bonding in terms of electrostatic and covalent factors

E

electronegativity (Mulliken)
5.6.1: Quantitative Measures of Hardness, Softness, and Acid-Base Interactions from a Hard Soft Acid-Base Principle perspective involve orbital energies and or apportioning acid-base bonding in terms of electrostatic and covalent factors

electronic configurations
8.1.2: The Jahn-Teller Effect

electrophile
13.1: What is Organometallic Chemistry?

elongation
8.1.2: The Jahn-Teller Effect

F

Face Centered Cubic
12.3A: Structure - Rock Salt (NaCl)

fcc structure
12.3A: Structure - Rock Salt (NaCl)

formal charge
3.1.1: Formal Charge

Frenkel defect
12.5B: Frenkel Defect

G

Gouy Method
14.14.4: Magnetic Susceptibility Measurements

H

high spin
8.1.2: The Jahn-Teller Effect

hydroboration
13.1: What is Organometallic Chemistry?

hydrogen bonding
3.4: Hydrogen Bonding

hypervalency
3.1: Lewis Electron-Dot Diagrams

hypovalency
3.1: Lewis Electron-Dot Diagrams

L

Lancashire
8.1.2: The Jahn-Teller Effect

Ligand Close Packing (LCP)
3.2.4: Ligand Close Packing

linear
3.2: Valence Shell Electron-Pair Repulsion

low spin
8.1.2: The Jahn-Teller Effect

M

Marcus Theory
11.6.1: Outer Sphere Electron Transfer

N

nephelauxetic ratio
9.3: Tanabe-Sugano Diagrams

Nephelauxetic Series
9.3: Tanabe-Sugano Diagrams

O

octahedral
3.2: Valence Shell Electron-Pair Repulsion

orbital mixing
4.2.2: Orbital Mixing

organometallic
13.1: What is Organometallic Chemistry?

organometallic chemistry
13.1: What is Organometallic Chemistry?

Outer Sphere Electron Transfer
11.6.1: Outer Sphere Electron Transfer

P

Pearson's absolute hardness
5.6.1: Quantitative Measures of Hardness, Softness, and Acid-Base Interactions from a Hard Soft Acid-Base Principle perspective involve orbital energies and or apportioning acid-base bonding in terms of electrostatic and covalent factors

philosopher's stone
1.2: History of Inorganic Chemistry

Polymorphism
12.9A: Polymorphism - Phase Changes in the Solid State

Q

quasilinear structure
12.3C: Structure - Fluorite (CaF_2)

R

Racah parameter
9.3: Tanabe-Sugano Diagrams

resistivity
12.2A: Electrical Conductivity and Resistivity

resonance
3.1.2: Resonance

resonance structures
3.1.2: Resonance

rock salt structure
12.3A: Structure - Rock Salt (NaCl)

rotation axis
6.7.2: Representations of Point Groups

S

SALC
6.9.4: Carbon Dioxide

Schottky defect
12.5A: Schottky Defect

Section 4.1
7.4: The Effect of the Metal Ion on d-Orbital Splitting

seesaw
3.2: Valence Shell Electron-Pair Repulsion

siemens (unit)
12.2A: Electrical Conductivity and Resistivity

sphalerite
12.3E: Structure - Zinc Blende (ZnS)

square pyramidal
3.2: Valence Shell Electron-Pair Repulsion

substitutional alloy
12.1A: Substitutional Alloys

symmetry elements
6.1: Symmetry Elements and Operations

symmetry operation
6.7.2: Representations of Point Groups

symmetry operations
6.1: Symmetry Elements and Operations

T

tetrahedral
3.2: Valence Shell Electron-Pair Repulsion
trigonal bipyramidal
3.2: Valence Shell Electron-Pair Repulsion
trigonal planar
3.2: Valence Shell Electron-Pair Repulsion
trigonal pyramidal
3.2: Valence Shell Electron-Pair Repulsion

V

valence shell electron pair repulsion theory
3.2: Valence Shell Electron-Pair Repulsion
VSEPR
3.2: Valence Shell Electron-Pair Repulsion

Z

zinc blend structure
12.3E: Structure - Zinc Blende (ZnS)

This page titled Index is shared under a license and was authored, remixed, and/or curated by LibreTexts.

GLOSSARY

S

Sample Word 1 | Sample Definition 1

This page titled Glossary is shared under a license and was authored, remixed, and/or curated by LibreTexts.

DETAILED LICENSING

Overview

Title: CHM 320: Advanced Inorganic Chemistry

Webpages: 250

Applicable Restrictions: Noncommercial

All licenses found:

- Undeclared: 86.4% (216 pages)
- CC BY-NC-SA 4.0: 11.6% (29 pages)
- CC BY-NC 4.0: 1.2% (3 pages)
- Public Domain: 0.4% (1 page)
- CC BY 4.0: 0.4% (1 page)

By Page

- CHM 320: Advanced Inorganic Chemistry - *Undeclared*
  - Front Matter - *Undeclared*
    - TitlePage - *Undeclared*
    - InfoPage - *Undeclared*
    - Table of Contents - *Undeclared*
    - Licensing - *Undeclared*
  - 1: Introduction to Inorganic Chemistry - *Undeclared*
    - 1.1: Inorganic vs Organic Chemistry - *Undeclared*
    - 1.2: History of Inorganic Chemistry - *CC BY-NC-SA 4.0*
    - 1.3: Perspectives - *Undeclared*
  - 2: Atomic Structure - *Undeclared*
    - 2.1: Historical Development of Atomic Theory - *Undeclared*
      - 2.1.1: The Periodic Table - *Undeclared*
      - 2.1.2: Discovery of Subatomic Particles and the Bohr Atom - *Undeclared*
    - 2.2: The Schrödinger equation, particle in a box, and atomic wavefunctions - *CC BY-NC-SA 4.0*
      - 2.2.1: Particle in a Box - *CC BY-NC-SA 4.0*
      - 2.2.2: Quantum Numbers and Atomic Wave Functions - *CC BY-NC-SA 4.0*
      - 2.2.3: Aufbau Principle - *Public Domain*
      - 2.2.4: Shielding - *CC BY-NC-SA 4.0*
    - 2.3: Periodic Properties of Atoms - *Undeclared*
      - 2.3.1: Ionization energy - *Undeclared*
      - 2.3.2: Electron Affinity - *Undeclared*
      - 2.3.3: Covalent and Ionic Radii - *Undeclared*
    - 2.4: Problems - *Undeclared*
  - 3: Simple Bonding Theory - *Undeclared*
    - 3.1: Lewis Electron-Dot Diagrams - *Undeclared*
      - 3.1.1: Formal Charge - *Undeclared*
      - 3.1.2: Resonance - *Undeclared*
      - 3.1.3: Breaking the octet rule with higher electron counts (hypervalent atoms) - *Undeclared*
      - 3.1.4: Lewis fails to predict unusual cases-Boron and Beryllium - *Undeclared*
    - 3.2: Valence Shell Electron-Pair Repulsion - *CC BY-NC-SA 4.0*
      - 3.2.1: Lone Pair Repulsion - *Undeclared*
      - 3.2.2: Multiple Bonds - *Undeclared*
      - 3.2.3: Electronegativity and Atomic Size Effects - *Undeclared*
      - 3.2.4: Ligand Close Packing - *Undeclared*
    - 3.3: Molecular Polarity - *Undeclared*
    - 3.4: Hydrogen Bonding - *Undeclared*
  - 4: Molecular Orbitals - *CC BY-NC-SA 4.0*
    - 4.1: Formation of Molecular Orbitals from Atomic Orbitals - *CC BY-NC-SA 4.0*
      - 4.1.1: Molecular Orbitals from s Orbitals - *CC BY-NC-SA 4.0*
      - 4.1.2: Molecular Orbitals from p Orbitals - *CC BY-NC-SA 4.0*
      - 4.1.3: Molecular orbitals from d orbitals - *CC BY-NC-SA 4.0*
      - 4.1.4: Nonbonding Orbitals and Other Factors - *CC BY-NC-SA 4.0*
    - 4.2: Homonuclear Diatomic Molecules - *CC BY-NC-SA 4.0*
      - 4.2.1: Molecular Orbitals - *CC BY-NC-SA 4.0*
      - 4.2.2: Orbital Mixing - *CC BY-NC-SA 4.0*
      - 4.2.3: Diatomic Molecules of the First and Second Periods - *CC BY-NC-SA 4.0*
      - 4.2.4: Photoelectron Spectroscopy - *CC BY-NC-SA 4.0*
    - 4.3: Heteronuclear Diatomic Molecules - *CC BY-*

NC-SA 4.0
- 4.3.1: Polar bonds - CC BY-NC-SA 4.0
- 4.3.2: Ionic Compounds and Molecular Orbitals - CC BY-NC-SA 4.0
- 4.P: Problems - CC BY-NC-SA 4.0

◦ 5: Coordination Chemistry I - Structure and Isomers - Undeclared
- 5.1: History - Undeclared
- 5.2: Nomenclature and Ligands - Undeclared
- 5.3: Isomerism - Undeclared
- 5.4: Coordination Numbers and Structures - Undeclared
- 5.5: Coordination Frameworks - Undeclared
- 5.6: Hard and Soft Acids and Bases - Undeclared
  - 5.6.1: Quantitative Measures of Hardness, Softness, and Acid-Base Interactions from a Hard Soft Acid-Base Principle perspective involve orbital energies and or apportioning acid-base bonding in terms of electrostatic and covalent factors - Undeclared
  - 5.6.2: Hard-Hard and Soft-Soft preferences may be explained and quantified in terms of electrostatic and covalent and electronic stabilization on the stability of Lewis acid-base adducts - Undeclared

◦ 6: Symmetry and Group Theory - Undeclared
- 6.1: Symmetry Elements and Operations - Undeclared
- 6.2: Successive Operations - Undeclared
- 6.3: Significance of Recognizing Symmetry Elements - Undeclared
- 6.4: Point Groups - Undeclared
  - 6.4.1: Groups of Low and High Symmetry - Undeclared
  - 6.4.2: Other Groups - Undeclared
- 6.5: Character Tables - An Introduction - Undeclared
- 6.6: Character Tables - Undeclared
- 6.7: Properties and Representations of Groups - Undeclared
  - 6.7.1: Matrices - Undeclared
  - 6.7.2: Representations of Point Groups - Undeclared
- 6.8: Examples and Applications of Symmetry - Undeclared
  - 6.8.1: Chirality - CC BY-NC 4.0
  - 6.8.2: Molecular Vibrations - Undeclared
  - 6.8A: Vibrational Spectroscopy - Undeclared
  - 6.8C: Vibrational Spectroscopy of Linear and Bent triatomic Molecules - Undeclared
- 6.9: Larger (Polyatomic) Molecules - CC BY-NC-SA 4.0
  - 6.9.1: CO_2 (Revisted with Projection Operators) - CC BY-NC-SA 4.0
  - 6.9.2: BF_3 - CC BY-NC-SA 4.0
  - 6.9.3: Bifluoride anion - CC BY-NC-SA 4.0
  - 6.9.4: Carbon Dioxide - CC BY-NC-SA 4.0
  - 6.9.5: H_2O - CC BY-NC-SA 4.0
  - 6.9.6: NH_3 - CC BY-NC-SA 4.0
- 6.10: MO Theory Applied to Polyatomic Molecules BH_3, NH_3, and CH_4 - Undeclared
  - 6.10A: BH_3 - Undeclared
  - 6.10B: NH_3 - Undeclared
  - 6.10C: CH_4 - Undeclared
  - 6.10D: A Comparison of MO and VB Bonding Models - Undeclared
- 6.P: Problems (under construction) - Undeclared

◦ 7: Ligand Field Theory (LFT) and Crystal Field Theory (CFT) of Octahedral Complexes - Undeclared
- 7.1: Introduction to Crystal Field Theory (Octahdral complexes) - Undeclared
- 7.2: Introduction to Ligand Field Theory (Octahedral complexes) - Undeclared
- 7.3: Ligand Field Stabilisation Energy (LFSE) - Undeclared
- 7.4: The Effect of the Metal Ion on d-Orbital Splitting - Undeclared
- 7.5: The Effect of Ligands and the Spectrochemical Series - Undeclared

◦ 8: LFT for Other Geometries / Spectroscopic Properties - Undeclared
- 8.1: The d-orbital splitting patterns for non-octahedral complexes - Undeclared
  - 8.1.1: Tetrahedral and Octahedral Geometries - Undeclared
  - 8.1.2: The Jahn-Teller Effect - Undeclared
  - 8.1.3: Summary of the three most common geometries - Undeclared
- 8.2: Absorption Spectra and Magnetic Properties - Undeclared
  - 8.2.1: Colors of Coordination Compounds (Electronic Absorption Spectra) - Undeclared
  - 8.2.2: Predicting UV-visible Absorption - Undeclared

◦ 9: Spectroscopic and Magnetic Properties - Undeclared
- 9.1: Quantum Numbers of Multielectron Atoms - CC BY 4.0
- 9.2: Electronic Spectra of Coordination Compounds - Undeclared
- 9.3: Tanabe-Sugano Diagrams - Undeclared
- 9.4: Magnetic Properties of Coordination Compounds - Undeclared
- 9.5: Magnetic Properties of Materials - Undeclared

◦ 10: Thermodynamics, Trends in Metal Complex Stability - Undeclared
- 10.1: Introduction to Substitution Reactions - Undeclared
- 10.2: Metal-Ligand Association Constants - CC BY-NC-SA 4.0

- 10.3: Trends in M-L stability (Thermodynamics) - *Undeclared*
- 11: Kinetics, Trends in Kinetic Lability - *Undeclared*
  - 11.1: Trends in Kinetic Lability - *Undeclared*
  - 11.2: The Kinetic Chelate Effect - *Undeclared*
  - 11.3: The Eigen-Wilkins Mechanism - *Undeclared*
  - 11.4: Mechanisms of Substitution - *Undeclared*
  - 11.5: The trans-effect - *Undeclared*
  - 11.6: Redox Mechanisms - *Undeclared*
    - 11.6.1: Outer Sphere Electron Transfer - *CC BY-NC 4.0*
    - 11.6.2: Inner Sphere Electron Transfer - *CC BY-NC 4.0*
- 12: Structures and Energetics of Metallic and Ionic solids - *Undeclared*
  - 12.1: Alloys and Intermetallic Compounds - *Undeclared*
    - 12.1A: Substitutional Alloys - *Undeclared*
    - 12.1B: Interstitial Alloys - *Undeclared*
    - 12.1C: Intermetallic Compounds - *Undeclared*
  - 12.2: Bonding in Metals and Semicondoctors - *Undeclared*
    - 12.2A: Electrical Conductivity and Resistivity - *Undeclared*
    - 12.2B: Band Theory of Metals and Insulators - *Undeclared*
    - 12.2C: The Fermi Level - *Undeclared*
    - 12.2D: Band Theory of Semiconductors - *Undeclared*
  - 12.3: Ionic Lattices - *Undeclared*
    - 12.3A: Structure - Rock Salt (NaCl) - *Undeclared*
    - 12.3B: Structure - Caesium Chloride (CsCl) - *Undeclared*
    - 12.3C: Structure - Fluorite (CaF_2) - *Undeclared*
    - 12.3D: Structure - Antifluorite - *Undeclared*
    - 12.3E: Structure - Zinc Blende (ZnS) - *Undeclared*
    - 12.3F: Structure - β-Cristobalite (SiO_2) - *Undeclared*
    - 12.3H: Structure - Rutile (TiO_2) - *Undeclared*
    - 12.3I: Structure - Layers (CdI_2 and $CdCl_2$) - *Undeclared*
    - 12.3J: Structure - Perovskite ($CaTiO_3$) - *Undeclared*
  - 12.4: Lattice Energy - The Born-Haber Cycle - *Undeclared*
  - 12.5: Defects in Solid State Lattices - *Undeclared*
    - 12.5.E: Defects in Solid State Lattices (Exercises) - *Undeclared*
    - 12.5A: Schottky Defect - *Undeclared*
    - 12.5B: Frenkel Defect - *Undeclared*
    - 12.5C: Experimental Observations of Schottky and Frenkel Defects - *Undeclared*
    - 12.5D: Non-Stoichiometric Compounds - *Undeclared*
    - 12.5E: Color Centers (F-Centers) - *Undeclared*
    - 12.5F: Thermodynamic Effects of Crystal Defects - *Undeclared*
  - 12.6: Introduction - *Undeclared*
  - 12.7: Packing of Spheres - *Undeclared*
    - 12.7A: Cubic and Hexagonal Closed Packing - *Undeclared*
    - 12.7B: The Unit Cell of HPC and CCP - *Undeclared*
      - 1.1: The Unit Cell - *Undeclared*
    - 12.7C: Interstitial Holes in HCP and CCP - *Undeclared*
    - 12.7D: Non-closed Packing- Simple Cubic and Body Centered Cubic - *Undeclared*
  - 12.8: The Packing of Spheres Model Applied to the Structures of Elements - *Undeclared*
    - 12.8A: Group 18 Elements in the Solid State - *Undeclared*
    - 12.8B: H_2 and F_2 Solids - *Undeclared*
    - 12.8C: Solid Metallic Elements - *Undeclared*
  - 12.9: Polymorphism in Metals - *Undeclared*
    - 12.9A: Polymorphism - Phase Changes in the Solid State - *Undeclared*
    - 12.9B: Phase Diagrams - *Undeclared*
  - 12.10: Metallic Radii - *Undeclared*
  - 12.11: Melting Points and Standard Enthalpies of Atomization of Metals - *Undeclared*
  - 12.12: Size of Ions - *Undeclared*
    - 12.12A: Ionic Radii - *Undeclared*
    - 12.12B: Periodic Trends in Ionic Radii - *Undeclared*
  - 12.13: Crystal Structure of Semiconductors - *Undeclared*
- 13: Introduction to Organometallic Complexes - *Undeclared*
  - 13.1: What is Organometallic Chemistry? - *Undeclared*
  - 13.2: Historical Background - *Undeclared*
  - 13.3: The 18 Electron Rule - *Undeclared*
  - 13.4: Reactions Involving Gain or Loss of Ligands - *Undeclared*
  - 13.5: Organometallic Catalysts - *Undeclared*
- 14: Experimental Techniques - *Undeclared*
  - 14.1: Introduction - *Undeclared*
  - 14.2: Separation and Purification Techniques - *Undeclared*
    - 14.2A: Gas Chromatography (GC) - *Undeclared*
    - 14.2B: Liquid Chromatography (LC) - *Undeclared*
    - 14.2C: High-Performance Liquid Chromatography (HPLC) - *Undeclared*
    - 14.2D: Recrystallization - *Undeclared*

- 14.3: Elemental Analysis - *Undeclared*
  - 14.3A: CHN Analysis by Combustion - *Undeclared*
  - 14.3B: Atomic Absorption Spectroscopy (AAS) - *Undeclared*
- 14.4: Computational Analysis - Thermogravimetry (TG) - *Undeclared*
- 14.5: Mass Spectrometry - *Undeclared*
  - 14.5A: Electron Ionization (EI) - *Undeclared*
  - 14.5B: Fast Atom Bombardment (FAB) - *Undeclared*
  - 14.5C: Matrix-Assisted Laser Desorption Ionization Time-of-Flight (MALDI-TOF) - *Undeclared*
  - 14.5D: Electrospray Ionization (ESI) - *Undeclared*
- 14.6: Infrared and Raman Spectroscopies - *Undeclared*
  - 14.6A: Energies and Wavenumbers of Molecular Vibrations - *Undeclared*
  - 14.6B: The Fourier Transform Infrared (FT-IR) Spectrometer and Sample Preparation - *Undeclared*
  - 14.6C: Diagnostic Absorptions - *Undeclared*
  - 14.6D: Deuterium/Hydrogen Exchange - *Undeclared*
  - 14.6E: Raman Spectroscopy - *Undeclared*
- 14.7: Electronic Spectroscopy - *Undeclared*
  - 14.7A: UV-VIS Absorption Spectroscopy - *Undeclared*
  - 14.7B: Types of Absorption - *Undeclared*
  - 14.7C: Absorbance and the Beer-Lambert Law - *Undeclared*
  - 14.7D: Emission Spectroscopy - *Undeclared*
- 14.8: Nuclear Magnetic Resonance (NMR) Spectroscopy - *Undeclared*
  - 14.8A: NMR Active Nuclei and Isotope Abundance - *Undeclared*
  - 14.8B: Which Nuclei are Suitable for NMR Spectroscopic Studies - *Undeclared*
  - 14.8C: Resonance Frequencies and Chemical Shifts - *Undeclared*
  - 14.8D: Chemical Shift Ranges - *Undeclared*
  - 14.8E: Solvents for Solution Studies - *Undeclared*
  - 14.8F: Integration of Signals and Signal Broadening - *Undeclared*
  - 14.8G: Homonuclear spin-spin coupling - $^{1}H - ^{1}H$ - *Undeclared*
  - 14.8H: Heteronuclear spin-spin coupling - $^{13}C - ^{1}H$ - *Undeclared*
  - 14.8I: Case Studies - *Undeclared*
  - 14.8J: Stereochemically Non-Rigid Species - *Undeclared*
  - 14.8K: Exchange Processes in Solution - *Undeclared*
- 14.9: Electron Paramagnetic Resonance (EPR) Spectroscopy - *Undeclared*
  - 14.9A: What is EPR Spectroscopy? - *Undeclared*
  - 14.9B: The Zeeman Electronic Effect - *Undeclared*
  - 14.9C: EPR Spectra - *Undeclared*
- 14.10: Mossbauer Spectroscopy - *Undeclared*
  - 14.10A: The Technique of Mossbauer Spectroscopy - *Undeclared*
  - 14.10B: What Can Isomer Shift Data Tell Us? - *Undeclared*
- 14.11: Structure Determination - Diffraction Methods - *Undeclared*
  - 14.11A: X-Ray Diffraction (XRD) - *Undeclared*
  - 14.11B: Single Crystal X-Ray Diffraction - *Undeclared*
  - 14.11C: Powder X-Ray Diffraction - *Undeclared*
  - 14.11D: Single Crystal Neutron Diffraction - *Undeclared*
  - 14.11E: Electron Diffraction - *Undeclared*
  - 14.11F: Low-Energy Electron Diffraction (LEED) - *Undeclared*
  - 14.11G: Structural Databases - *Undeclared*
- 14.12: Photoelectron Spectroscopy (PES, UPS, XPS, ESCA) - *Undeclared*
- 14.13: Computational Methods - *Undeclared*
  - 14.13A: Hartree-Fock Theory - *Undeclared*
  - 14.13B: Density Functional Theory - *Undeclared*
  - 14.13C: Hückel MO Theory - *Undeclared*
  - 14.13D: Molecular Mechanisms (MM) - *Undeclared*
- 14.14: Magnetism - *Undeclared*
  - 14.14.1: example magnetic moment data and their interpretation - *Undeclared*
  - 14.14.2: Magnetic Moments - *Undeclared*
  - 14.14.3: Magnetic Moments 1 - *Undeclared*
  - 14.14.4: Magnetic Susceptibility Measurements - *Undeclared*
  - 14.14.5: Magnetism - *Undeclared*

◦ Back Matter - *Undeclared*
- Tanabe Sugano Diagrams - *Undeclared*
- Index - *Undeclared*
- Glossary - *Undeclared*
- Detailed Licensing - *Undeclared*

This page titled CHM 320: Advanced Inorganic Chemistry is shared under a license and was authored, remixed, and/or curated by LibreTexts.